BRITISH JOURNAL OF
APPLIED PHYSICS

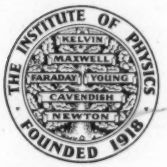

EDITOR

H. R. LANG

A.R.C.S., PH.D., F.INST.P.

Secretary of The Institute of Physics

VOLUME 7

including

Supplement No. 5

LONDON

THE INSTITUTE OF PHYSICS

BRITISH JOURNAL OF APPLIED PHYSICS

ADVISORY COMMITTEE

for year ending 30 September, 1956

T. E. ALLIBONE, PH.D., D.SC., M.I.E.E., F.INST.P., F.R.S., *Chairman*

C. B. ALLSOPP, PH.D., D.SC., F.INST.P., *Representing the British Institute of Radiology*

H. BARRELL, A.R.C.S., D.SC., F.INST.P.

W. BETTERIDGE, B.SC., PH.D., F.INST.P.

R. L. BROWN, M.A., F.INST.P.

W. H. J. CHILDS, PH.D., D.SC., F.INST.P., F.R.S.E., *Representing the Scottish Branch*

SIR JOHN COCKCROFT, K.C.B., C.B.E., PH.D., D.SC., F.INST.P., F.R.S., *President, The Institute of Physics*

B. M. CROWTHER, M.A., PH.D., F.INST.P.

MISS T. J. DILLON, M.SC., F.INST.P., *Representing the Education Group*

B. P. DUDDING, M.B.E., A.R.C.S., PH.D., F.INST.P., *Honorary Secretary, The Institute of Physics*

E. K. FRANKL, M.A., *Representing the Stress Analysis Group*

M. E. HAINE, M.SC., F.INST.P., *Representing the Electron Microscopy Group*

S. T. HENDERSON, M.A., PH.D., F.INST.P.

M. R. HOPKINS, M.SC., PH.D., F.INST.P., *Representing the South Wales Branch*

J. M. A. LENIHAN, M.SC., PH.D., F.INST.P.

R. MEREDITH, D.SC., F.INST.P., *Representing the Manchester and District Branch*

E. A. OWEN, M.A., M.SC., SC.D., D.SC., F.INST.P., *Representing the Liverpool and North Wales Branch*

T. LL. RICHARDS, B.SC., PH.D., F.I.M., F.INST.P., *Representing the Midland Branch*

G. D. ROBINSON, B.SC., PH.D., F.INST.P., *Representing the Royal Meteorological Society*

L. A. SAYCE, M.SC., PH.D., F.INST.P.

W. E. SCHALL, B.SC., F.INST.P., *Representing the Non-destructive Testing Group*

R. W. SILLARS, B.A., D.PHIL., A.M.I.E.E., F.INST.P.

E. G. STEWARD, B.SC., PH.D., A.INST.P., *Representing the X-ray Analysis Group*

E. C. STONER, B.A., PH.D., SC.D., F.INST.P., F.R.S.

A. M. TAYLOR, M.A., PH.D., F.INST.P., *Representing the London and Home Counties Branch*

R. S. TEBBLE, B.SC., PH.D., F.INST.P., *Representing the Yorkshire Branch*

N. THORLEY, B.SC., PH.D., F.INST.P., *Representing the North Eastern Branch*

S. TOLANSKY, PH.D., D.SC., F.INST.P., F.R.S., *Representing the Physical Society*

E. VAN SOMEREN, B.SC., F.INST.P., *Representing the Industrial Spectroscopy Group*

S. WHITEHEAD, PH.D., D.SC., M.I.E.E., F.INST.P. (died, May 1956), *Honorary Treasurer, The Institute of Physics*

R. G. WOOD, M.SC., A.M.I.E.E., F.INST.P.

D. A. WRIGHT, D.SC., F.INST.P., *Representing the Electronics Group and the Physical Society*

CONTENTS OF VOLUME 7

JANUARY 1956

PAGE

CONFERENCE REPORT

Summarized proceedings of a conference on stress analysis—Sheffield, September, 1955. By H. Spooner . . 1

ORIGINAL CONTRIBUTIONS

Specimen thickness and image resolution in electron microscopy. By V. E. Cosslett 10
The analysis of gases at low pressures. By M. A. Cayless 13
A study of Formvar replica process. By A. W. Agar and R. S. M. Revell 17
Caesium 137 for industrial radiography. By R. S. Morgan 25
The automatic recording of electron diffraction patterns applied to the study of evaporated copper layers. By R. B. Kehoe, R. C. Newman and D. W. Pashley . 29
Electrode deterioration in "keep-alive" discharges in transmit-receive switches. By D. Walsh, A. W. Bright and T. J. Bridges 31
A microwave resonant cavity method for measuring the resistivity of semi-conducting materials. By J. G. Linhart, I. M. Templeton and R. Dunsmuir . . 36
The corona resisting property of polytetrafluorethylene. By K. Sugita, S. Nagao and Y. Toriyama . . . 38

NOTES AND NEWS

New books 39
Notes and comments 42

FEBRUARY 1956

SPECIAL ARTICLE

The United Kingdom Atomic Energy Authority and its functions. By Sir John Cockcroft 43

ORIGINAL CONTRIBUTIONS

The laminar flow of streams of suspended particles. By T. V. Starkey 52
The inductance of two elliptic tubes. By E. E. Jones . 56
A photographic method of obtaining stress trajectories. By A. R. Morris 59
A modified replica technique and its application to the examination of etched single crystals of barium titanate. By D. S. Campbell and D. J. Stirland . . . 62
Collodion replicas from cross-sections of thin metallic strip and coatings. By D. J. Evans 65
A comparison of dry stripped, unbacked collodion and Formvar replicas. By D. J. Evans 66
The measurement, by nuclear resonance, of light water concentration in mixtures of light and heavy water. By A. M. J. Mitchell and G. Phillips 67
The thermal and electrical conductivities of deposited carbon. By A. R. G. Brown, W. Watt, R. W. Powell and R. P. Tye 73
Stress distribution in a tee junction of thick pipes. By H. Fessler and B. H. Lewin 76

NOTES AND NEWS

Correspondence:

Errors in the A.S.T.M. Index of X-ray powder diffraction patterns. From J. W. Hughes, I. E. Lewis and A. J. C. Wilson 80
New books 81
Notes and comments 84

MARCH 1956

SPECIAL ARTICLE

Rain—natural and artificial. By R. C. Sutcliffe . . 85

CONFERENCE REPORT

Summarized proceedings of a conference on electron microscopy—Glasgow, July, 1955. By C. E. Challice 89

ORIGINAL CONTRIBUTIONS

Origin and analysis of gas in electron tubes. By S. J. Stoll 94
Diffusion (or conduction) along a slightly tapering tube, and its application to the determination of diffusion coefficients. By A. Talbot and J. A. Kitchener . 96
The wall effect and the viscometry of suspensions. By A. D. Maude and R. L. Whitmore 98
Coplanar mesh storage. By G. R. Hoffman . . 102

NOTES AND NEWS

Correspondence:

The determination of base thickness in alloy junction transistors by etching. From J. Rolfe 109
Current distribution in an expanding spark channel. From J. M. Somerville and C. T. Grainger . . 109
Decomposition of $CaSO_4 . 2H_2O$ in the electron microscope. From J. H. Talbot 110
A replica technique for "reflexion" electron microscopy. From L. Holland 113
The square wave response method of analysing process control systems. From E. Persson; L. Mandel . 113
Ferrites in resonant cavities. From R. A. Waldron . 114

New books 115
Notes and comments 117

APRIL 1956

SPECIAL ARTICLE

Physics of the Sun. By Z. Kopal 119

ORIGINAL CONTRIBUTIONS

An apparatus for the accurate control of the peak X-ray energy of a 20 MeV betatron. By K. Phillips . . 129
Fields and stresses in dielectric media. By G. Power . 137
A new method for the measurement of rapid fluctuations of temperature. By R. Dehn 144
The measurement of the electrical resistivity of silicon. By R. H. Creamer 149
The Eberhard effect in X-ray powder photographs. By T. W. Baker 150

NOTES AND NEWS

Correspondence:

Ultra-violet polymerization of embedding monomers for thin sectioning. From A. Charles and J. Sikorski . 152

PAGE

Vapour lubrication of titanium and zirconium. From G. W. Rowe 152
Observations on the characteristics of the cold cathode ionization gauge. From J. H. Leck and A. Riddoch 153

New books 155

Notes and comments 158

MAY 1956

SPECIAL ARTICLE

The physical meaning of indentation and scratch hardness. By D. Tabor 159

ORIGINAL CONTRIBUTIONS

A re-determination of the equal-loudness relations for pure tones. By D. W. Robinson and R. S. Dadson . 166
The spectral quantum- and energy-efficiency of calcium tungstate X-ray intensifying screens. By R. H. Herz 182
The production of transparent profiles of dust particles as an aid to automatized particle counting. By R. J. Hamilton and B. A. Phelps 186
Measurement of the half-life of radon with a Curie-type ionization chamber. By P. C. Marin 188
A photoelastic method of two-dimensional separation of stresses along a line of symmetry by using the isochromatic fringes only. By S. P. Christodoulides . . 190

NOTES AND NEWS

New books 194

JUNE 1956

SPECIAL ARTICLES

Science and technology in industry. By Sir John Cockcroft 199
Stress waves in solids. By R. M. Davies 203

ORIGINAL CONTRIBUTIONS

The mechanism of pulse temperature rise on the surface of thermionic cathodes. By R. Dehn 210
Direct carbon replicas from metal surfaces. By E. Smith and J. Nutting 214
An extension of the circle and sphere theorems. By G. Power 218
Electron optics of X-ray tubes and the design of unbiased sharply-focusing cathodes. By A. R. Lang and D. A. G. Broad 221
Apparatus for the measurement of time of impact. By P. L. Kirby 227

NOTES AND NEWS

Correspondence:

The suitability of Araldite D resin in photoelastic investigations. From C. L. Amba Rao 229
A note on the polarization due to oblique reflexion at an aluminized or silvered mirror. From J. N. Hodgson 229

New books 230

Notes and comments 232

PAGE

JULY 1956

SPECIAL ARTICLE

The International Temperature Scale and a redefinition of the Kelvin Scale. By J. A. Hall 233

CONFERENCE REPORT

A symposium on magnetism—London, September, 1955. By A. C. Lynch and J. Watkins 236

ORIGINAL CONTRIBUTIONS

The tensile strength of coal. By C. D. Pomeroy and W. T. A. Morgans 243
Apparatus and techniques for the application of a water flow system to the study of aerodynamic systems. By E. F. Winter and J. H. Deterding 247
The "ploughing" contribution to friction. By R. T. Spurr 260
Klystron oscillator noise theory. By R. L. Bell . . . 262
The display of logarithmic Langmuir probe characteristics on a cathode-ray oscillograph. By A. R. Johnston . 266

NOTES AND NEWS

Correspondence:

Measurement of the electrical conductivity of the oxide-coated cathode. From T. B. Tomlinson and R. E. J. King 268

New books 269

Notes and comments 272

AUGUST 1956

SPECIAL ARTICLE

Physics in oceanography. By K. F. Bowden 273

ORIGINAL CONTRIBUTIONS

Dielectric properties of polar solutes in non-polar solvents at microwave frequencies. By D. E. Clark and S. N. Kumar 282
The expansion of mercury and fused silica between 0 and 300° C. By A. H. Cook 285
The tension in strings wrapped slantwise round cylinders when friction is proportional to a power of the normal reaction. By C. Mack 294
Space-charge limited current in insulating oil. By Tadashi Sato, Shigeo Nagao and Yotsuo Toriyama . . 297
The vibration of segmented beams. By J. P. Ellington 299
Applications of a transformer analogue computer. By J. R. Barker 303

NOTES AND NEWS

Correspondence:

Note on discharges from a flat thermionic cathode. From N. R. Daly and K. G. Emeleus 308
A photographic method of obtaining stress trajectories. From D. Vasarhelyi; A. R. Morris. 308

New books 309

Notes and comments 312

PAGE

SEPTEMBER 1956

SPECIAL ARTICLE

Crystallography and the phase rule. By A. R. UBBELOHDE 313

ORIGINAL CONTRIBUTIONS

Preparation of scattering foils of uranium by evaporation of the metal in high vacuum. By K. K. DAMODARAN 322
The viscosity of mixtures of gases at high temperatures. By M. J. KENNEY, R. J. SARJANT and M. W. THRING 324
Focal properties and chromatic and spherical aberrations of the three-electrode electron lens. By G. D. ARCHARD 330
The accuracy of particle size determination by cumulative sedimentation methods. By J. K. DONOGHUE 333
Uniform-field breakdown in air. By R. F. SAXE 336

NOTES AND NEWS

New books 341

Notes and comments 344

OCTOBER 1956

SPECIAL ARTICLE

Neutron radiography. By J. THEWLIS 345

ORIGINAL CONTRIBUTIONS

Reactions occurring during decomposition of alkaline earth carbonates on tungsten. By M. A. CAYLESS and B. N. WATTS 351
The dynamic magnetostriction of nickel–cobalt alloys. By C. A. CLARK 355
The use of the stereoscopic tilt device of the electron microscope in unit-cell determinations. By J. A. GARD 361
A possible source of error in the interpretation of electron diffraction patterns. By G. D. ARCHARD 367
The flow of air through beds of charcoal. By W. M. JONES 370
A replica technique for particle surfaces. By J. MARRIOTT 373
Defects in germanium crystals grown from the melt. By E. BILLIG 375
The properties of high-pressure steady-state discharges in hydrogen. By W. A. GAMBLING and H. EDELS 376

NOTES AND NEWS

Correspondence:

Large increase of light sensitivity at low temperatures for certain types of X-ray film. From K. LONSDALE and H. J. GRENVILLE-WELLS 380
Arc initiation in hydrogen. From F. W. CRAWFORD and H. EDELS 380

New books 381

Notes and comments 383

NOVEMBER 1956

CONFERENCE REPORT

Summarized proceedings of a conference on the structures of semi-crystalline and non-crystalline materials—London, November 1955. By R. E. FRANKLIN and R. L. GORDON 385

PAGE

ORIGINAL CONTRIBUTIONS

The suppression of screen grid emission by carbon. By J. A. CHAMPION 395
Multiplicity in the anode marks of sparks. By J. M. SOMERVILLE and C. T. GRAINGER 400
The frequency of vibration and the elastic stability of a fixed-free strip. By R. F. S. HEARMON 405
The fusing of wires with heavy surge currents. By A. E. BARRINGTON 408
The electric strength of hydrocarbon gases. By A. E. D. HEYLEN and T. J. LEWIS 411
Reduction of counting time in low activity assays. By H. A. HUGHES 415
The tensile strengths of viscous liquids under dynamic loading. By T. H. BULL 416

NOTES AND NEWS

Correspondence:

A photoelastic method of two-dimensional separation of stresses along a line of symmetry by using the isochromatic fringes only. From P. D. FLYNN and R. GUERNSEY; S. P. CHRISTODOULIDES 419
Ring conduction in the early stages of sparks. From J. M. SOMERVILLE and N. H. FLETCHER 419

New books 420

Notes and comments 424

DECEMBER 1956

CONFERENCE REPORT

Summarized proceedings of a conference on low temperature crystallography—Oxford, April, 1956. By D. W. J. CRUICKSHANK, E. MENDOZA and J. H. ROBERTSON 425

ORIGINAL CONTRIBUTIONS

A photoelastic method employing scattered light for the solution of plane stress problems. By W. SHELSON and I. W. SMITH 436
Flying spot counting and sizing of non-uniform particles. By H. W. LOEB 440
The elastic properties of dilute aqueous gels. By L. J. HASTEWELL and R. ROSCOE 441
Viscosity and action. By T. V. STARKEY 448
Vibrations of an end-loaded strip. By H. S. C. CHEN 450

NOTES AND NEWS

Correspondence:

The application of the centripetal effect in air to the design of a pump. From B. POPPER and M. REINER 452
Corner fractures in explosively loaded thin-walled steel cylinders. From S. SINGH 453

New books 455

Notes and comments 456

SUPPLEMENT No. 5

THE PHYSICS OF NUCLEAR REACTORS

SESSION 1. OPENING ADDRESS

Scientific problems in the development of nuclear power. By SIR JOHN COCKCROFT S 1

PAGE

SESSION 2. LECTURE

The physics of advanced reactors. By J. R. DIETRICH . S 9
DISCUSSION . . . . . S 24

SESSION 3. LECTURES

Experimental reactor physics. By P. W. MUMMERY . S 27
The zero-energy fast breeder reactor, ZEPHYR. By L. R. SHEPHERD . . . . . S 32
DISCUSSION . . . . . S 41

SESSION 4. EVENING LECTURE

Recent developments in nuclear theory. By Prof. R. E. PEIERLS. (Headings only) . . . . . S 42

SESSION 5. LECTURE

The effects of irradiation on the physical properties of solids. By A. H. COTTRELL . . . . . S 43
DISCUSSION . . . . . S 49

SESSION 6. DISCUSSION ON "ANCILLARY PROBLEMS OF REACTORS"

OPENING PAPERS
Shielding for reactors. By G. C. LAURENCE . . . S 54
The control of reactors. By A. J. SALMON . . . S 59
The instrumentation of reactors. By W. MACRAE . S 71
DISCUSSION . . . . . S 82

PAGE

SESSION 7. EVENING LECTURES

The role of chemistry in a nuclear energy project. By R. SPENCE . . . . . S 88
The role of metallurgy in a nuclear energy project. By L. ROTHERHAM . . . . . S 91

SESSION 8. DISCUSSION ON "RESEARCH REACTORS AND THEIR USES"

OPENING PAPERS
The Canadian research reactors and their uses. By W. B. LEWIS . . . . . S 96
The United Kingdom research reactors and their uses. By F. W. FENNING . . . . . S 100
DISCUSSION . . . . . S 103
EXHIBITS AND FILMS . . . . . S 107

SUBJECT INDEX TO THE PHYSICS OF NUCLEAR REACTORS . . . . . S 108

NAME INDEX TO THE PHYSICS OF NUCLEAR REACTORS . . . . . S 111

SUBJECT INDEX TO VOLUME 7

AUTHOR INDEX TO VOLUME 7

INDEX TO VOLUME 7

SUBJECT INDEX

Aberrations, chromatic and spherical, Focal properties and, of the three-electrode electron lens 330
Accuracy of particle size determination by cumulative sedimentation methods, The 333
A.C. power system studies, Terms used in 272
Action, Viscosity and 448
Aerodynamic systems, Apparatus and techniques for the application of a water flow system to the study of 247
Air,
  The application of the centripetal effect in, to the design of a pump 452
  The flow of, through beds of charcoal 370
  Uniform-field breakdown in 336
Alkaline earth carbonates on tungsten, Reactions occurring during decomposition of 351
Analogue computer, Applications of a transformer 303
Analogue, Resistance network 7
Analysing process control systems, The square wave response method of 113
Analysis of gases at low pressures, The 13
Anode marks of sparks, Multiplicity in the 400
Araldite D resin in photoelastic investigations, The suitability of 229
Arc initiation in hydrogen 380
Assays, Reduction of counting time in low activity 415
A.S.T.M. Index of X-ray powder diffraction patterns, Errors in the 80
Atomic Energy Authority, The United Kingdom, and its functions 43
Atomic energy research at Harwell, *erratum* 118

Barium titanate, A modified replica technique and its application to the examination of etched single crystals of 62
Beams, segmented, The vibration of 299
Beds of charcoal, The flow of air through 370
Betatron, An apparatus for the accurate control of the peak X-ray energy of a 20 MeV 129
Bibliography, Heat 384
Bibliography of information on servo-mechanisms and related subjects 118
Bimetallic contacts, corrosion at 272
Biological applications of electron microscopy 92
Books, New
  Abstracts of the literature on semiconducting and luminescent materials and their applications 420
  Advanced calculus; an introduction to classical analysis 196
  Advances in electronics and electron physics. Vol. 7 311
  Aérosols, Les 342
  Applications of spinor invariants in atomic physics 271
  Atomkraft 343
  Atomphysik, Vols. 1 and 2 41
  Boundary layer theory 198
  Building materials, their elasticity and inelasticity 39
  Control of nuclear reactors and power plants 310
  Creep and fracture of metals at high temperatures 310
  Diffusion in Metallen 115
  Dislocations et la croissance des cristaux, Les 157
  Dust is dangerous 39
  Electrolytic and chemical polishing of metals, in research and industry, The 423
  Elektronik des Einzelektrons 83
  Engineering fluid mechanics 422
  Flow of gases through porous media 423
  Foundations of quantum theory: a study in continuity and symmetry 157
Books, New (*continued*)
  General aspects of radio interference. British Standard Code of Practice CP 1006: 1955 115
  Geometrical optics 198
  Guidance, principles of guided missile design 195
  Handbook of chemistry and physics 309
  Harmonic analysis and the theory of probability 41
  High speed aerodynamics and jet propulsion: Vol. 1, *Thermodynamics and physics of matter* 197
  High vacuum technique 83
  Hydro-dynamics 381
  International electrotechnical vocabulary 343
  Introduction to electronic and analogue computers, An 157
  Introduction to experimental physics 40
  Introduction to reactor physics, An 231
  Introductory nuclear physics 230
  Ionized gases 455
  Kinetic theory of liquids 271
  Kovar 309
  Light calculations and measurements 81
  Machine translation of languages 155
  Magnetic materials in the electrical industry 40
  Mechanical properties of textile fibres 194
  Mesons and fields, Vol. 1, *Fields* 309
  Mesons and fields, Vol. 2 81
  Messen and Rechnen in der Physik 115
  Metallurgy of the rarer metals, No. 4, *Titanium* 231
  Metals reference book, Vols. 1 and 2 156
  Meteorological results of the Balaena *expedition*, 1946–7 341
  Methods of mathematical physics 382
  Micro-indentation hardness testing 271
  Microscopy of animal textile fibres (including methods for the complete analysis of fibre blends), The 269
  Microstructures of diamond surfaces 381
  Microwave spectroscopy 82
  Modern physics for the engineer 116
  Molecular beams 155, 421
  Molecular vibrations 343
  Multipole fields 115
  Neutron diffraction 40
  Noise reduction manual 156
  Notes on applied science, No. 10, *Noise measurement techniques* 41
  Notes on applied science, No. 11, *Wind effects on bridges and other flexible structures* 422
  Nuclear and radiochemistry 342
  Nuclear levels in the neighbourhood of the 1 $F_{7/2}$ *state* 40
  Nuclear magnetic resonance 194
  Numerical analysis 269
  Operational calculus—based on the two-sided Laplace Integral 81
  Photographische Objectiv (Die wissenschaftliche und angewandte Photografie), Das 155
  Physical techniques in biological research, Vol. 1, *Optical techniques* 270
  Physics of fully ionized gases 421
  Polar aurora, The 81
  Precision electrical measurements 82
  Present state of physics, The 196
  Proceedings of conference on effects of radiation on dielectric materials 310 erratum 424
  Proceedings of the Eastern Joint Computer Conference 41
  Proceedings of the eleventh general assembly of the International Scientific Radio Union (U.R.S.I.), Vol. 10, Part 2, *Radio and Troposphere* 423

For *The Physics of Nuclear Reactors* and cognate subjects *see also* separate index to the supplement

Books, New (*continued*)
Proceedings of the eleventh general assembly, Vol. 10, Part 5, *Radio-astronomy* 230
Proceedings of the fourth meeting of the mixed commission on the ionosphere 83
Proceedings of the international conference of theoretical physics, 1953, *Kyoto and Tokyo* 116
Progress in biophysics and biophysical chemistry 196
Progress in nuclear energy; Series 1, *Physics and mathematics*, Vol. 1 341
Progress in semiconductors 423
Radium therapy—its physical aspects and extensions with radioactive isotopes 311
Reactor handbook: materials 195
Reports on progress in physics, Vol. 18, 1955 39
Research reactors 231
Resonance in organic chemistry 342
Scattering and diffraction of radio waves 270
Schaltungstheorie und Messtechnik des Dezimeter und Zentimeter-Wellengebietes 195
Servomechanisms and regulating system design, Vol. 2 82
Small-angle scattering of X-rays 309
Solid state physics. Advances in research and application, Vol. 1 197
Spectrochemical abstracts, Vol. 4, 1946–1951 157
Spectroscopy at radio and microwave frequencies 197
Statistical mechanics of irreversible change 381
Structure Reports for 1942–44, Vol. 9 271
Survey in mechanics 381
Survey report on human factors in undersea warfare, A 196
Symposium on non-destructive testing of materials and structures, Vols. 1 and 2 341
Temperature: its measurement and control in science and industry, Vol. 2 455
Textbook of sound, A 455
Theoretische Metallkunde 423
Theory of combustion instability in liquid propellant rocket motors 382
Theory of games and linear programming, The 342
Theory of hydraulic stability, The 230
Theory of sound, Vols. 1 and 2 420
Transistor electronics 422
Transistors and other crystal valves 82
Transmission-line theory 270
Ultrasonic engineering 41
Vierpoltheorie und Frequenztransformation 310
Wool research, Vol. 2, *Physical properties* 311
X-rays; their origin, dosage, and practical application 422
Year book of The Physical Society, 1955 116
Breakdown, Uniform-field, in air 336
British Chemical Engineering 344
British
electrical products, Catalogue of 118
manufacturers, Register of 84
scientific instruments, Permanent display of 158
Standards Institution 424

Caesium 137 for industrial radiography 25
Calcium tungstate X-ray intensifying screens, The spectral quantum- and energy-efficiency of 182
Cameras, User specification for high-temperature X-ray powder diffraction 272
Carbon
, deposited, The thermal and electrical conductivities of 73
replicas from metal surfaces, Direct 214
The suppression of screen-grid emission by 395
Carbons, Structure of coals, cokes and 485
$CaSO_4.2H_2O$, Decomposition of, in the electron microscope 110
Castings, internal defects in, Terminology of, as revealed by radiography 383
Catalogue of British electrical products 118
Cathode
, flat thermionic, Note on discharges from a 308
, oxide-coated, Measurement of the electrical conductivity of the 268
-ray oscillograph, The display of logarithmic Langmuir probe characteristics on a 266
Cathodes, the design of unbiased sharply-focusing, Electron optics of X-ray tubes and 221
Cathodes, The mechanism of pulse temperature rise on the surface of thermionic 210
Cavities, Ferrites in resonant 114
Cavity, microwave resonant, method for measuring the resistivity of semi-conducting materials, A 36
Cell, unit-, determinations, The use of the stereoscopic tilt device of the electron microscope in 361
Centripetal effect in air to the design of a pump, The application of the 452
Characteristics of the cold cathode ionization gauge, Observations on the 153
Charcoal, The flow of air through beds of 370
Chemical applications of electron microscopy 91
Circle and sphere theorems, An extension of the 218
Coals, cokes and carbons, Structure of 385
Coal, The tensile strength of 243
Coatings, Collodion replicas from cross-sections of thin metallic strip and 65
Cobalt, nickel-alloys, The dynamic magnetostriction of 355
Cokes and carbons, Structure of coals 385
Cold cathode ionization gauge, Observations on the characteristics of the 153
Collodion and Formvar replicas, A comparison of dry stripped, unbacked 66
Collodion replicas from cross-sections of thin metallic strip and coatings 65
Computer, transformer analogue, Applications of a 303
Conduction, Diffusion or, along a slightly tapering tube, and its application to the determination of diffusion coefficients 96
Conduction in the early stages of sparks, Ring 419
Conductivities, thermal and electrical, of deposited carbon, The 73
Conductivity, electrical, of the oxide-coated cathode, Measurement of the 268
Conference on
electron microscopy, Glasgow, July, 1955, Summarized proceedings of a 89
engineering fastenings, Report of a 118
low temperature crystallography—Oxford, April, 1956, Summarized proceedings of a 425
magnetism and magnetic materials 158
stress analysis—Sheffield, September, 1955, Summarized proceedings of a 1
the physics of nuclear reactors 232
the structures of semi-crystalline and non-crystalline materials—London, November, 1955, Summarized proceedings of a 385
Congress of refrigeration, Proceedings of the ninth international 344
Congress of the International Union of Crystallography, Fourth general assembly and international 456
Contacts, bimetallic, Corrosion at 272
Convention, International ferrite 383
Co-operative Electrical Research 384
Coplanar mesh storage 102
Copper layers, evaporated, The automatic recording of electron diffraction patterns applied to the study of 29
Cores, Magnetic, for storage circuits 238
Corner fractures in explosively loaded thin-walled steel cylinders 453
Corona resisting property of polytetrafluorethylene, The 38
Corrosion at bimetallic contacts 272

For *The Physics of Nuclear Reactors* and cognate subjects *see also* separate index to the supplement

Counting
and sizing of non-uniform particles, Flying spot 440
automatized particle, The production of transparent profiles of dust particles as an aid to 186
time in low activity assays, Reduction of 415
Crystalline materials, semi- and non-, Summarized proceedings of a conference on the structures of,—London, November, 1955 385
Crystallography
and the phase rule 313
Fourth general assembly and international congress of the International Union of 456
Summarized proceedings of a conference on low temperature—Oxford, April, 1956 425
Crystals, etched single, of barium titanate, A modified replica technique and its application to the examination of 62
Crystals, germanium, grown from the melt, Defects in 375
Current distribution in an expanding spark channel 109
Current, Space-charge limited, in insulating oil 297
Currents, heavy surge, The fusing of wires with 408
Cylinders, explosively loaded thin-walled steel, Corner fractures in 453

Data, Nuclear reactor 117
Decomposition of $CaSO_4.2H_2O$ in the electron microscope 110
Defects in crystals of germanium grown from the melt 375
Delft, Work at 4
Dielectric media, Fields and stresses in 137
Dielectric properties of polar solutes in non-polar solvents at microwave frequencies 282
Diffraction, Neutron 241
Diffraction, X-ray 7
Diffusion (or conduction) along a slightly tapering tube, and its application to the determination of diffusion coefficients 96
Discharges
from a flat thermionic cathode, Note on 308
in hydrogen, The properties of high-pressure steady-state 376
"keep-alive", in transmit-receive switches, Electrode deterioration in 31
Disordered structures, Glasses, liquids and 389
Display of logarithmic Langmuir probe characteristics on a cathode-ray oscillograph, The 266
Dividing machines, Exhibition of 42
Documentation of molecular spectroscopy (D.M.S. system) 84
Dust particles, The production of transparent profiles of, as an aid to automatized particle counting 186
Dynamic
loading 5
loading, The tensile strengths of viscous liquids under 416
magnetostriction of nickel–cobalt alloys, The 355

Eberhard effect in X-ray powder photographs, The 150 *erratum* 312
Efficiency, The spectral quantum- and energy-, of calcium tungstate X-ray intensifying screens 182
Elastic properties of dilute aqueous gels, The 441
Electrical energy 424
Electrical
conductivities of deposited carbon, The thermal and 73
conductivity of the oxide-coated cathode, Measurement of the 268
products, Catalogue of British 118
resistivity of silicon, The measurement of the 149
Electric strength of hydrocarbon gases, The 411
Electrode deterioration in the "keep-alive" discharges in transmit-receive switches 31
Electron
diffraction patterns, A possible source of error in the interpretation of 367
Electron (*continued*)
diffraction patterns, The automatic recording of, applied to the study of evaporated copper layers 29
lens, Focal properties and chromatic and spherical aberrations of the three-electrode 330
microscope, Decomposition of $CaSO_4.2H_2O$ in the 110
microscope in unit-cell determinations, The use of the stereoscopic tilt device of the 361
microscopy, "reflexion", A replica technique for 113
microscopy, Specimen thickness and image resolution in 10
microscopy, Summarized proceedings of a conference on,—Glasgow, July, 1955 89
optics and general instrumentation 89
optics of X-ray tubes and the design of unbiased sharply-focusing cathodes 221
tubes, Origin and analysis of gas in 94
Electronics for spectroscopists 118
Elliptic tubes, The inductance of two 56
Emission, screen-grid, The suppression of, by carbon 395
End-loaded strip, Vibrations of an 450
Energy, X-ray, of a 20 MeV betatron, An apparatus for the accurate control of the peak 137
Engine vibration, Aircraft 5
Equal-loudness relations for pure tones, A re-determination of the 166
Error, A possible source of, in the interpretation of electron diffraction patterns 367
Errors in the A.S.T.M. Index of X-ray powder diffraction patterns 80
Estimation of the specific surface of a soil from mechanical analysis data, The *erratum* 384
Etched single crystals of barium titanate, A modified replica technique and its application to the examination of 62
Etching, The determination of base thickness in alloy junction transistors by 109
Evaporation of the metal in high vacuum, Preparation of scattering foils of uranium by 322
Exhibition of dividing machines 42
Exhibition of scientific instruments and apparatus, The Physical Society's annual 117
Expansion of mercury and fused silica between 0 and 300° C, The 285
Explosively loaded thin-walled steel cylinders, Corner fractures in 453

Fastenings, engineering, Report of a conference on 118
Ferrite convention, International 383
Ferrites
at microwave frequencies, Use of 237
in resonant cavities 114
Theory of the magnetism of 236
Fibres, Non-biological 391
Fields and stresses in dielectric media 137
Film, X-ray, Large increase of light sensitivity at low temperatures for certain types of 380
Flow
, laminar, of streams of suspended particles, The 52
of air through beds of charcoal, The 370
system, water, Apparatus and techniques for the application of a, to the study of aerodynamic systems 247
Fluctuations of temperature, rapid, A new method for the measurement of 144
Flying spot counting and sizing of non-uniform particles 440
Focal properties and chromatic and spherical aberrations of the three-electrode electron lens 330
Foils, scattering, of uranium, Preparation of, by evaporation of the metal in high vacuum 322
Formvar replicas, A comparison of dry stripped, unbacked collodion and 66
Formvar replica process, A study of 17

For *The Physics of Nuclear Reactors* and cognate subjects *see also* separate index to the supplement

Fractures, Corner, in explosively loaded thin-walled steel cylinders 453
Frequencies, microwave, Use of ferrites at 237
Frequency of vibration and the elastic stability of a fixed-free strip, The 405
Friction is proportional to a power of the normal reaction, The tension in strings wrapped slantwise round cylinders when 294
Friction, The "ploughing" contribution to 260
Fusing of wires with heavy surge currents, The 408

Gas in electron tubes, Origin and analysis of 94
Gases
  at high temperatures, The viscosity of mixtures of 324
  , hydrocarbon, The electric strength of 411
  , The analysis of, at low pressures 13
Gauge, ionization, Observations on the characteristics of the cold cathode 153
Gels, The elastic properties of dilute aqueous 441
Germanium crystals grown from the melt, Defects in 375
Glasses, liquids and disordered structures 389

Half-life of radon, Measurement of the, with a Curie-type ionization chamber 188
Hardness, scratch, The physical meaning of indentation and 159
Harwell, Atomic energy research at *erratum* 118
Heat bibliography 384
High-temperature strain gauges 7
High-speed photography 42
Hydrocarbon gases, The electric strength of 411
Hydrogen, Arc initiation in 380
Hydrogen, The properties of high-pressure steady-state discharges in 376

Impact, Apparatus for the measurement of time of 227
Indentation and scratch hardness, The physical meaning of 159
Inductance of two elliptic tubes, The 56
Industrial radiography, Caesium 137 for 25
Industry, Science and technology in 199 *erratum* 272
Institute of Physics,
  Elections to The 84, 158, 232, 344, 424
  Publications of The 158
  The 312
Instrumentation, general, Electron optics and 89
Instruments, scientific, British, Permanent display of 158
Insulating oil, Space-charge limited current in 297
Isochromatic fringes only, A photoelastic method of two-dimensional separation of stresses along a line of symmetry by using the 190, 419
International Temperature Scale and a redefinition of the Kelvin Scale, The 233
Interpretation of electron diffraction patterns, A possible source of error in the 367
Ionization chamber, Curie-type, Measurement of the half-life of radon with a 188
Ionization gauge, Observations on the characteristics of the cold cathode 153
Ionizing radiations, The protection of workers against 42

Journal of Fluid Mechanics 456
Journal of The British Nuclear Energy Conference 117

Kelvin Scale, The International Temperature Scale and a redefinition of the 233
Klystron oscillator noise theory 262

Laminar flow of streams of suspended particles, The 52
Langmuir probe characteristics, The display of logarithmic, on a cathode-ray oscillograph 266
Layers, evaporated copper, The automatic recording of electron diffraction patterns applied to the study of 29
Lens, three-electrode electron, Focal properties and chromatic and spherical aberrations of the 330
Light, scattered, A photoelastic method employing, for the solution of plane stress problems 436
Light sensitivity at low temperatures for certain types of X-ray film, Large increase of 380
Liquids and disordered structures, Glasses 389
Liquids, viscous, The tensile strengths of, under dynamic loading 416
Load cells, Strain gauge 6
Loading, Dynamic 5
Loading, dynamic, The tensile strengths of liquids under 416
Loudness, re-determination of the equal-, relations for pure tones, A 166
Low temperature
  crystallography, Summarized proceedings of a conference on —Oxford, April, 1956 425
  crystallography, Physical problems in 425
  , Nuclear magnetic resonance measurements at, as an aid to structure analysis 432
  , X-ray methods and measurements at 429
Lubrication, Vapour, of titanium and zirconium 152

Magnetic cores for storage circuits 238
Magnetic resonance, Symposium on 312
Magnetism
  and magnetic materials, Conference on 158
  , A symposium on—London, September, 1955 236
  of ferrites, Theory of the 236
Magnetization, Spontaneous: experimental methods 238
Magnetostriction, dynamic, of nickel-cobalt alloys, The 355
Magnets, micro-powder, Materials for 240
Manufacturers, British, Register of 84
Mercury and fused silica, The expansion of, between 0 and 300 C 285
Mesh storage, Coplanar 102
Metallic strip, thin, and coatings, Collodion replicas from cross-sections of 65
Metallurgical applications of electron microscopy 91
Metallurgical Reviews 383
Metal surfaces, Direct carbon replicas from 214
Meteorological Office annual report for 1954–5 117
Micro-powder magnets, Materials for 240
Microscopy and microradiography, X-ray, Symposium on 118
Mining 5
Mirror, A note on the polarization due to oblique reflexion at an aluminized or silvered 229
Molecular spectroscopy, Documentation of (D.M.S. system) 84
Monomers, embedding, Ultra-violet polymerization of, for thin sectioning 152

Neutron diffraction 241
Neutron radiography 345
Nickel–cobalt alloys, The dynamic magnetostriction of 355
Noise theory, Klystron oscillator 262
Non-biological fibres 391
Non-metallic materials for use at extreme temperatures 383
Nuclear Engineering 456
Nuclear Physics 117
Nuclear Power 232
Nuclear
  magnetic resonance measurements at low temperatures as an aid to structure analysis 432
  reactor data 117
  reactors, Conference on the physics of 232 S1–112
  resonance, The measurement, by nuclear, of light water concentration in mixtures of light and heavy water 67

For *The Physics of Nuclear Reactors* and cognate subjects *see also* separate index to the supplement

Oceanography, Physics in 273
Oscillator noise theory, Klystron 262
Oxide-coated cathode, Measurement of the electrical conductivity of the 268

Particle
  counting, automatized, The production of transparent profiles of dust particles as an aid to 186
  size determination by cumulative sedimentation methods, The accuracy of 333
  surfaces, A replica technique for 373
Particles,
  non-uniform, Flying spot counting and sizing of 440
  single-domain, Theory of 240
  The laminar flow of streams of suspended 52
Patents abridgements, Publication of 158
Phase rule, Crystallography and the 313
Photoelastic
  investigations, The suitability of Araldite D resin in 229
  method employing scattered light for the solution of plane stress problems, A 436
  method of two-dimensional separation of stresses along a line of symmetry by using the isochromatic fringes only, A 190, 419
Photoelasticity 8
Photographic method of obtaining stress trajectories, A 59, 308
Photographs, X-ray powder, The Eberhard effect in 150 *erratum* 312
Photography, High-speed 42
Physical Society's annual exhibition of scientific instruments and apparatus, The 117
Physics in oceanography 273
Physics of the Sun 119
Pipes, thick, Stress distribution in a tee junction of 76
Plastic yielding and residual stresses 1
"Ploughing" contribution to friction, The 260
Polarization due to oblique reflexion at an aluminized or silvered mirror, A note on the 229
Polimerization, Ultra-violet, of embedding monomers for thin sectioning 152
Polytetrafluorethylene, The corona resisting property of 38
Power system studies, a.c., Terms used in 272
Pressures, low, The analysis of gases at 13
Probe characteristics, The display of logarithmic Langmuir, on a cathode-ray oscillograph 266
Proceedings of the ninth international congress of refrigeration 344
Process control systems, The square wave response method of analysing 113
Profiles of dust particles, The production of transparent, as an aid to automatized particle counting 186
Protection of workers against ionizing radiations 42
Pulse temperature rise on the surface of thermionic cathodes, The mechanism of 210
Pump, The application of the centripetal effect in air to the design of a 452

Quality control and applied statistics abstracts 344

Radiations, ionizing, The protection of workers against 42
Radioactive products 383
Radiography, Neutron 345
Radiography, Terminology of internal defects in castings as revealed by 383
Radon, Measurement of the half-life of, with a Curie-type ionization chamber 188
Rain—natural and artificial 85
Reactions occurring during decomposition of alkaline earth carbonates on tungsten 351
Reactors, nuclear, Conference on the physics of 232 S1–112
Refrigeration meeting, International Institute of 232
Refrigeration, Proceedings of the ninth international congress of 344
Reflexion at an aluminized or silvered mirror, A note on the polarization due to oblique 229
"Reflexion" electron microscopy, A replica technique for 113
Register of British manufacturers 84
Replica
  process, Formvar, A study of 17
  technique, A modified, and its application to the examination of etched single crystals of barium titanate 62
  technique for particle surfaces, A 373
  technique for "reflexion" electron microscopy, A 113
Replicas,
  Collodion, from cross-sections of thin metallic strip and coatings 65
  comparison of dry stripped, unbacked collodion and Formvar 66
  Direct carbon, from metal surfaces 214
Resistance network analogue 7
Resistivity, electrical, of silicon, The measurement of the 149
Resistivity of semi-conducting materials, A microwave resonant cavity method for measuring the 36
Resolution, image, in electron microscopy, Specimen thickness and 10
Resonance, magnetic, Symposium on 312
Resonance, nuclear, The measurement, by, of light water concentration in mixtures of light and heavy water 67
Resonant cavities, Ferrites in 114
Resonant cavity method for measuring the resistivity of semi-conducting materials, A microwave 36
Ring conduction in the early stages of sparks 419

Scattering foils of uranium, Preparation of, by evaporation of the metal in high vacuum 322
Science and technology in industry 199 *erratum* 272
Scratch hardness, The physical meaning of indentation and 159
Screen-grid emission, The suppression of, by carbon 395
Screens, calcium tungstate X-ray intensifying, The spectral quantum- and energy-efficiency of 182
Sectioning, thin, Ultra-violet polymerization of embedding monomers for 152
Sedimentation methods, The accuracy of particle size determination by cumulative 333
Semi-conducting materials, A microwave resonant cavity method for measuring the resistivity of 36
Sensitivity, light, Large increase of, at low temperatures for certain types of X-ray film 380
Servomechanisms and related subjects, Bibliography of information on 118
Silica, fused, The expansion of mercury and, between 0 and 300° C 285
Silicon, The measurement of the electrical resistivity of 149
Sizing of non-uniform particles, Flying spot counting and 440
Soil, The estimation of the specific surface of a, from mechanical analysis data, *erratum* 384
Solids, Stress waves in 203
Solutes, polar, Dielectric properties of, in non-polar solvents at microwave frequencies 282
Soviet Physics 84
Space-charge limited current in insulating oil 297
Spark channel, expanding, Current distribution in an 109
Sparks, Multiplicity in the anode marks of 400
Sparks, Ring conduction in the early stages of 419
Specimen thickness and image resolution in electron microscopy 10
Spectroscopists, Electronics for 118
Spectroscopy, Documentation of molecular (D.M.S. system) 84
Sphere theorems, An extension of the circle and 218

For *The Physics of Nuclear Reactors* and cognate subjects *see also* separate index to the supplement

Square wave response method of analysing process control systems, The 113
Stability, elastic, The frequency vibration and the, of a fixed-free strip 405
Stereoscopic tilt device of the electron microscope in unit-cell determinations, The use of the 361
Storage circuits, Magnetic cores for 238
Storage, Coplanar mesh 102
Strain gauge load cells 6
Strain gauges, High temperature 7
Streams of suspended particles, The laminar flow of 52
Strength, The tensile, of coal 243
Stress
  analysis, Summarized proceedings of a conference on—Sheffield, September, 1955 1
  distribution in a tee junction of thick pipes 76
  problems, plane, A photoelastic method employing scattered light for the solution of 436
  trajectories, A photographic method of obtaining 59, 308
  waves in solids 203
Stresses
  , A photoelastic method of two-dimensional separation of, along a line of symmetry by using the isochromatic fringes only 190, 419
  in dielectric media, Fields and 137
  residual, Plastic yielding and 1
Strings wrapped slantwise round cylinders when friction is proportional to a power of the normal reaction, The tension in 294
Strip,
  end-loaded, Vibrations of an 450
  fixed-free, The frequency vibration and the elastic stability of a 405
  thin metallic, and coatings, Collodion replicas from cross-sections of 65
Structures of semi-crystalline and non-crystalline materials, Summarized proceedings of a conference on—London, November, 1955 385
Sun, Physics of the 119
Suppression of screen-grid emission by carbon, The 395
Surface of thermionic cathodes, The mechanism of pulse temperature rise on the 210
Surfaces, metal, Direct carbon replicas from 214
Surfaces, particle, A replica technique for 373
Suspensions, The wall effect and the viscometry of 98
Switches, transmit-receive, Electrode deterioration in "keep-alive" discharges in 31
Symposium
  on magnetic resonance 312
  on magnetism—London, September, 1955 236
  on X-ray microscopy and microradiography 118

Technology, Science and, in industry 199 *erratum* 272
Tee junction of thick pipes, Stress distribution in a 76
Temperature
  , rapid fluctuations of, a new method for the measurement of 144
  rise on the surface of thermionic cathodes, The mechanism of pulse 210
  scale, The International, and a redefinition of the Kelvin Scale 233
Temperatures, extreme, Non-metallic materials for use at ' 383
Tensile strengths of viscous liquids under dynamic loading, The 416
Tensile strength of coal, The 243
Tension in strings wrapped slantwise round cylinders when friction is proportional to a power of the normal reaction, The 294
Terminology of internal defects in castings as revealed by radiography 383
Terms used in a.c. power system studies 272
Thermal and electrical conductivities of deposited carbon, The 73
Thermal Syndicate Ltd., The Story of The 384
Thickness, base, in alloy junction transistors, The determination of, by etching 109
Time, counting, Reduction of, in low activity assays 415
Time of impact, Apparatus for the measurement of 227
Titanium and zirconium, Vapour lubrication of 152
Tones, pure, A re-determination of the equal-loudness relations for 166
Trajectories, stress, A photographic method of obtaining 59
Transformer analogue computer, Applications of a 303
Transistors, alloy junction, The determination of base thickness in, by etching 109
Tubes, electron, Origin and analysis of gas in 94
Tubes, elliptic, The inductance of two 56
Tungsten, Reactions occurring during decomposition of alkaline earth carbonates on 351

Ultra-violet polymerization of embedding monomers for thin sectioning 152
Uniform-field breakdown in air 336
Unit-cell determinations, The use of the stereoscopic tilt device on the electron microscope in 361
United Kingdom Atomic Energy Authority and its functions, The 43
Uranium, Preparation of scattering foils of, by evaporation of the metal in high vacuum 322
User specification for high-temperature X-ray powder diffraction cameras 272

Vacuum, high, Preparation of scattering foils of uranium by evaporation of the metal in 322
Vapour lubrication of titanium and zirconium 152
Vibration
  , Aircraft engine 5
  of segmented beams, The 299
  The frequency of, and the elastic stability of a fixed-free strip 405
Vibrations of an end-loaded strip 450
Viscometry of suspensions, The wall effect and the 98
Viscosity and action 448
Viscosity of mixtures of gases at high temperatures, The 324
Viscous liquids, The tensile strengths of, under dynamic loading 416

Wall effect and the viscometry of suspensions, The 98
Water flow system, Apparatus and techniques for the application of a, to the study of aerodynamic systems 247
Water, The measurement, by nuclear resonance, of light water concentration in mixtures of light and heavy 67
Waves, Stress, in solids 203
Wires, The fusing of, with heavy surge currents 408

X-ray
  diffraction 7
  energy, peak, of a 20 MeV betatron, An apparatus for the accurate control of the 129
  film, certain types of, Large increase of light sensitivity at low temperatures for 380
  intensifying screens, calcium tungstate, The spectral quantum- and energy-efficiency of 182
  methods and measurements at low temperatures 429
  microscopy and microradiography, Symposium on 118
  powder diffraction cameras, User specification for high-temperature 272
  powder diffraction patterns, Errors in the A.S.T.M. Index of 80
  powder photographs, The Eberhard effect in 150 *erratum* 312
  tubes, Electron optics of, and the design of unbiased sharply-focusing cathodes 221

Zirconium, Vapour lubrication of titanium and 152

For *The Physics of Nuclear Reactors* and cognate subjects *see also* separate index to the supplement

AUTHOR INDEX

Agar, A. W., and R. S. M. Revell, A study of Formvar replica process 17
Amba Rao, C. L., The suitability of Araldite D resin in photo-elastic investigations 229
Archard, G. D., A possible source of error in the interpretation of electron diffraction patterns 367
Focal properties and chromatic and spherical aberrations of the three-electrode electron lens 330

Baker, T. W., The Eberhard effect in X-ray powder photographs 150
Barker, J. R., Applications of a transformer analogue computer 303
Barrington, A. E., The fusing of wires with heavy surge currents 408
Bell, R. L., Klystron oscillator noise theory 262
Billig, E., Defects in germanium crystals grown from the melt 375
Bowden, K. F., Physics in oceanography 273
Bridges, T. J., *see under* Walsh, D.
Bright, A. W., *see under* Walsh, D.
Broad, D. A. G., *see under* Lang, A. R.
Brown, A. R. G., W. Watt, R. W. Powell and R. P. Tye, The thermal and electrical conductivities of deposited carbon 73
Bull, T. H., The tensile strengths of viscous liquids under dynamic loading 416

Campbell, D. S., and D. J. Stirland, A modified replica technique and its application to the examination of etched single crystals of barium titanate 62
Cayless, M. A., The analysis of gases at low pressures 13
Cayless, M. A., and B. N. Watts, Reactions occurring during decomposition of alkaline earth carbonates on tungsten 351
Challice, C. E., Summarized proceedings of a conference on electron microscopy—Glasgow, July, 1955 89
Champion, J. A., The suppression of screen-grid emission by carbon 395
Charles, A., and J. Sikorski, Ultra-violet polymerization of embedding monomers for thin sectioning 152
Chen, H. S. C., Vibrations of an end-loaded strip 450
Christodoulides, S. P., A photoelastic method of two-dimensional separation of stresses along a line of symmetry by using the isochromatic fringes only 190, 419
Clark, C. A., The dynamic magnetostriction of nickel–cobalt alloys 361
Clark, D. E., and S. N. Kumar, Dielectric properties of polar solutes in non-polar solvents at microwave frequencies 282
Cockcroft, Sir John, Science and technology in industry 199
The United Kingdom Atomic Energy Authority and its functions 43
Cook, A. H., The expansion of mercury and fused silica between 0 and 300° C 285
Cosslett, V. E., Specimen thickness and image resolution in electron microscopy 10
Crawford, F. W., and H. Edels, Arc initiation in hydrogen 380
Creamer, R. H., The measurement of the electrical resistivity of silicon 149
Cruickshank, D. W. J., E. Mendoza and J. H. Robertson, Summarized proceedings of a conference on low temperature crystallography—Oxford, April, 1956 425

Dadson, R. S., *see under* Robinson, D. W.
Daly, N. R., and K. G. Emeleus, Note on discharges from a flat thermionic cathode 308
Damodaran, K. K., Preparation of scattering foils of uranium by evaporation of the metal in high vacuum 322
Davies, R. M., Stress waves in solids 203
Dehn, R., A new method for the measurement of rapid fluctuations of temperature 144
The mechanism of pulse temperature rise on the surface of thermionic cathodes 210
Deterding, J. H., *see under* Winter, E. F.
Donoghue, J. K., The accuracy of particle size determination by cumulative sedimentation methods 333
Dunsmuir, R., *see under* Linhart, J. G.

Edels, H., *see under* Crawford, F. W.
Edels, H., *see under* Gambling, W. A.
Ellington, J. P., The vibration of segmented beams 299
Emeleus, K. G., *see under* Daly, N. R.
Evans, D. J., A comparison of dry stripped, unbacked collodion and Formvar replicas 66
Collodion replicas from cross-sections of thin metallic strip coatings 65

Fessler, H., and B. H. Lewin, Stress distribution in a tee junction of thick pipes 76
Fletcher, N. H., *see under* Somerville, J. M.
Flynn, P. D., and R. Guernsey, A photoelastic method of two-dimensional separation of stresses along a line of symmetry by using the isochromatic fringes only 419
Franklin, R. E., and R. L. Gordon, Summarized proceedings of a conference on the structures of semi-crystalline and non-crystalline materials—London, November, 1955 385

Gambling, W. A., and H. Edels, The properties of high-pressure steady-state discharges in hydrogen 376
Gard, J. A., The use of the stereoscopic tilt device of the electron microscope in unit-cell determinations 361
Grainger, C. T., *see under* Somerville, J. M.
Grenville-Wells, H. J., *see under* Lonsdale, K.
Gordon, R. L., *see under* Franklin, R. E.
Guernsey, R., *see under* Flynn, P. D.

Hall, J. A., The International Temperature Scale and a redefinition of the Kelvin Scale 233
Hamilton, R. J., and B. A. Phelps, The production of transparent profiles of dust particles as an aid to automatized particle counting 186
Hastewell, L. J., and R. Roscoe, The elastic properties of dilute aqueous gels 441
Hearmon, R. F. S., The frequency of vibration and the elastic stability of a fixed-free strip 405
Herz, R. H., The spectral quantum- and energy-efficiency of calcium tungstate X-ray intensifying screens 182
Heylen, A. E. D., and T. J. Lewis, The electric strength of hydrocarbon gases 411
Hodgson, J. N., A note on the polarization due to oblique reflexion at an aluminized or silvered mirror 229
Hoffman, G. R., Coplanar mesh storage 102
Holland, L., A replica technique for "reflexion" electron microscopy 113
Hughes, H. A., Reduction of counting time in low activity assays 415
Hughes, J. W., I. E. Lewis and A. J. C. Wilson, Errors in the A.S.T.M. Index of X-ray powder diffraction patterns 80

Johnston, A. R., The display of logarithmic Langmuir probe characteristics on a cathode-ray oscillograph 266
Jones, E. E., The inductance of two elliptic tubes 56
Jones, W. M., The flow of air through beds of charcoal 370

Kehoe, R. B., R. C. Newman and D. W. Pashley, The automatic recording of electron diffraction patterns applied to the study of evaporated copper layers 29
Kenney, M. J., R. J. Sarjant and M. W. Thring, The viscosity of mixtures of gases at high temperatures 324
King, R. E. J., *see under* Tomlinson, T. B.
Kirby, P. L., Apparatus for the measurement of time of impact 227
Kitchener, J. A., *see under* Talbot, A.
Kopal, Z., Physics of the sun. 119
Kumar, S. N., *see under* Clark, D. E.

For *The Physics of Nuclear Reactors* and cognate subjects *see also* separate index to the supplement

Lang, A. R., and D. A. G. Broad, Electron optics of X-ray tubes and the design of unbiased sharply-focusing cathodes 221
Leck, J. H., and A. Riddoch, Observations on the characteristics of the cold cathode ionization gauge 153
Lewin, B. H., *see under* Fessler, H.
Lewis, I. E., *see under* Hughes, J. W.
Lewis, T. J., *see under* Heylen, A. E. D.
Linhart, J. G., I. M. Templeton and R. Dunsmuir, A microwave resonant cavity method for measuring the resistivity of semiconducting materials 36
Loeb, H. W., Flying spot counting and sizing of non-uniform particles 440
Lonsdale, K., and H. J. Grenville-Wells, Large increase of light sensitivity at low temperatures for certain types of X-ray film 380
Lynch, A. C., and J. Watkins, A symposium on magnetism—London, September, 1955 236

Mack, C., The tension in strings wrapped slantwise round cylinders when friction is proportional to a power of the normal reaction 294
Mandel, L., The square wave response method of analysing process control systems 113
Marin, P. C., Measurement of the half-life of radon with a Curie-type ionization chamber 188
Marriott, J., A replica technique for particle surfaces 373
Maude, A. D., and R. L. Whitmore, The wall effect and the viscometry of suspensions 98
Mendoza, E., *see under* Cruickshank, D. W. J.
Mitchell, A. M. J., and G. Phillips, The measurement, by nuclear resonance, of light water concentration in mixtures of light and heavy water 67
Morgan, R. S., Caesium 137 for industrial radiography 25
Morgans, W. T. A., *see under* Pomeroy, C. D.
Morris, A. R., A photographic method of obtaining stress trajectories 59, 308

Nagao, Shigeo, *see under* Sato, Tadashi
Nagao, S., *see under* Sugita, K.
Newman, R. C., *see under* Kehoe, R. B.
Nutting, J., *see under* Smith, E.

Pashley, D. W., *see under* Kehoe, R. B.
Persson, E., The square wave response method of analysing process control systems 113
Phelps, B. A., *see under* Hamilton, R. J.
Phillips, G., *see under* Mitchell, A. M. J.
Phillips, K., An apparatus for the accurate control of the peak X-ray energy of a 20 MeV betatron 129
Pomeroy, C. D., and W. T. A. Morgans, The tensile strength of coal 243
Popper, B., and M. Reiner, The application of the centripetal effect in air to the design of a pump 452
Powell, R. W., *see under* Brown, A. R. G.
Power, G., An extension of the circle and sphere theorems 218
Fields and stresses in dielectric media 137

Reiner, M., *see under* Popper, B.
Revell, R. S. M., *see under* Agar, A. W.
Riddoch, A., *see under* Leck, J. H.
Robertson, J. H., *see under* Cruickshank, D. W. J.
Robinson, D. W., and R. S. Dadson, A redetermination of the equal-loudness relations for pure tones 166
Roew, G. W., Vapour lubrication of titanium and zirconium 152
Rolfe, J., The determination of base thickness in alloy junction transistors by etching 109
Roscoe, R., *see under* Hastewell, L. J.

Sarjant, R. J., *see under* Kenney, M. J.
Sato, Tadashi, Shigeo Nagao, and Yotsuo Toriyama, Space-charge limited current in insulating oil 297
Saxe, R. F., Uniform-field breakdown in air 336
Shelson, W., and I. W. Smith, A photoelastic method employing scattered light for the solution of plane stress problems 436
Sikorski, J., *see under* Charles, A.
Singh, S., Corner fractures in explosively loaded thin-walled steel cylinders 453
Smith, E., and J. Nutting, Direct carbon replicas from metal surfaces 214
Smith, I. W., *see under* Shelson, W.
Somerville, J. M., and C. T. Grainger, Current distribution in an expanding spark channel 109
Multiplicity in the anode marks of sparks 400
Somerville, J. M., and N. H. Fletcher, Ring conduction in the early stages of sparks 419
Spooner, H., Summarized proceedings of a conference on stress analysis—Sheffield, September, 1955 1
Spurr, R. T., The "ploughing" contribution to friction 260
Starkey, T. V., The laminar flow of streams of suspended particles 52
Viscosity and action 448
Stirland, D. J., *see under* Campbell, D. S.
Stoll, S. J., Origin and analysis of gas in electron tubes 94
Sugita, K., S. Nagao and Y. Toriyama, The corona resisting property of polytetrafluorethylene 38
Sutcliffe, R. C., Rain—natural, and artificial 85

Tabor, D., The physical meaning of indentation and scratch hardness 159
Talbot, A., and J. A. Kitchener, Diffusion (or conduction) along a slightly tapering tube, and its application to the determination of diffusion coefficients 96
Talbot, J. H., Decomposition of $CaSO_4 . 2H_2O$ in the electron microscope 110
Templeton, I. M., *see under* Linhart, J. G.
Thewlis, J., Neutron radiography 345
Thring, M. W., *see under* Kenney, M. J.
Tomlinson, T. B., and R. E. J. King, Measurement of the electrical conductivity of the oxide-coated cathode 268
Toriyama, Yotsuo, *see under* Sato, Tadashi
Toriyama, Y., *see under* Sugita, K.
Tye, R. P., *see under* Brown, A. R. G.

Ubbelohde, A. R., Crystallography and the phase rule 313

Vasarhelyi, D., A photographic method of obtaining stress trajectories 308

Watkins, J., *see under* Lynch, A. C.
Waldron, R. A., Ferrites in resonant cavities 114
Walsh, D., A. W. Bright and T. J. Bridges, Electrode deterioration in "keep-alive" discharges in transmit-receive switches 31
Watts, B. N., *see under* Cayless, M. A.
Watt, W., *see under* Brown, A. R. G.
Whitmore, R. L., *see under* Maude, A. D.
Wilson, A. J. C., *see under* Hughes, J. W.
Winter, E. F., and J. H. Deterding, Apparatus and techniques for the application of a water flow system to the study of aerodynamic systems 247

For *The Physics of Nuclear Reactors* and cognate subjects *see also* separate index to the supplement

PRINTED IN GREAT BRITAIN BY UNWIN BROTHERS LIMITED, WOKING AND LONDON

CONFERENCE REPORT

Summarized proceedings of a conference on stress analysis —Sheffield, September, 1955

The Ninth Annual Conference of the Stress Analysis Group of The Institute of Physics was held in the Stephenson Hall of the University of Sheffield on 28–30 September, 1955. Papers dealing amongst other things with design, plastic yielding, work at T.N.O. Delft, aircraft engine vibration, and photoelastic investigations, were read, and are summarized in this report.

OPENING LECTURE

DR. D. G. SOPWITH (Mechanical Engineering Research Laboratory, East Kilbride) delivered the opening lecture of the conference, relating some personal experiences in a paper entitled "The application of stress analysis to the design of some engineering components." He chose lifting gear and springs as illustrating components which were used reasonably successfully long before the stresses in them were really known.

The lifting gear problem originated in 1939–40 with the need for standardizing the design of these components. Two main stress analysis problems are involved, that of the curved beam, and that of multiple connectivity. An investigation of the curved beam problem shows that the Bach–Winkler theory, neglecting radial stresses, is adequate. The most efficient section turns out to be re-entrant, an impracticable shape, and in consequence a rounded triangular section is recommended. In the multiply connected body the bending moments have to be obtained by strain-energy methods.

The work on springs originated during the early years of the last war with some failures of gun springs. Dr. Sopwith discussed various approximate solutions for the stress in terms of the spring index C, $C = (b + a)/(b - a)$ where a and b are the inner and outer radii of the spring respectively. It was interesting to examine the efficiency of various spring configurations. The efficiency can be expressed either in terms of the energy stored per unit volume of the spring material or of the housing Table 1. An examination of existing practice showed a wide divergence in design practice.

Table 1. *Spring efficiencies*

		Weight efficiency τ_{ew}*				*Volume efficiency* τ_{ev}†			
Section		*c infinite (straight bar)*	$c = 10$	$c = 5$	$c = 3$	*c infinite (straight bar)*	$c = 10$	$c = 5$	$c = 3$
Circular		1·00	0·78	0·59	0·39	0	0·202	0·258	0·230
Rectangular	$m = 1$	0·62	0·48	0·38	0·27	0	0·160	0·211	0·203
	$m = 2$	0·53	0·51	0·45	0·29	0	0·170	0·251	0·220
	$m = 3$	0·54	0·50	0·44	0·30	0	0·167	0·244	0·225
	$m = 5$	0·58	0·50	0·40	0·29	0	0·160	0·223	0·219

* Efficiency based on volume of spring material. † Efficiency based on volume of spring housing.

Dr. Sopwith suggested that any design investigation should follow the same pattern.

(1) A survey of existing practice in design.
(2) Stress analysis to fill in the gaps in, or rationalize, existing knowledge. At this stage the working stresses should be considered.
(3) Preliminary design or the preparation of a basis for design.
(4) An experimental check on the design. The most discriminating check is invariably the fatigue test.
(5) Modification to the design in the light of the above check.
(6) Presentation of the results, if appropriate as a British Standard Specification, otherwise as a paper in easily usable form including a design chart or simple formulae.

The stress analyst's task is not finished until the results are presented in such a form that the designer can apply them directly to the problem in mind.

PLASTIC YIELDING AND RESIDUAL STRESSES

MR. H. LL. D. PUGH (Mechanical Engineering Research Laboratory, East Kilbride), read a paper entitled "Plastic yielding of metals." He said that before the time independent macroscopic plastic deformation of materials can be analysed and understood, it is necessary to elucidate the fundamental plastic properties of materials. This is done by observing their behaviour in critical experiments. In particular it is necessary to study the yielding of materials under combined stresses, the relation between stress and strain, the work hardening of the material, and the development of the yield locus with pre-strain.

(*a*) *Yield criterion.* Work on the behaviour of materials under combined stresses has led to the concept of the criterion of yielding which determines when a material will yield plastically. If the material is isotropic the criterion of yield will depend wholly on the magnitude and not on the direction of the stresses, and so the yield criterion can be expressed as some function of the principal stresses. Further, from the experimental observation that a pure hydrostatic pressure cannot cause a material to yield, it follows that the criterion of yield must be a function of the differences in principal stresses and renders untenable a number of suggested criteria. The criteria due to Tresca (maximum shear stress theory) and von Mises (maximum shear strain energy theory) still remain. It can be shown that the yield criterion can be represented in principal stress space by a cylinder whose generator is equally inclined to the three principal stress axes and whose section is termed the yield locus, being a

hexagon and a circle for the Tresca and von Mises criteria respectively.

In 1931 Taylor and Quinney[1] produced a classical paper on combined tension and torsion tests on specimens tested for isotropy. The results for copper and aluminium were closely represented by the von Mises criterion, and by a third criterion due to Bishop and Hill which had been calculated on the basis of their theory of crystal distortion. Although work up to the present suggests that there is no one criterion of yielding which accurately represents the behaviour of all materials, it is unfortunately true that, with a few exceptions, notably Taylor and Quinney and the work of Morrison, the work is marred because insufficient attention has been paid to the question of isotropy. Indeed, recent work by Pugh shows that even the tests by Taylor and Quinney do not in fact guarantee isotropy and so there is some doubt about the results of this classical work.

(*b*) *Stress strain relations.* Many experimental workers such as Alkins, Bridgman, etc., have shown that plastic deformation is not accompanied by permanent volume change, which is consistent with the fact that hydrostatic pressure produces no plastic deformation in an isotropic material. It therefore follows that the sum of the incremental plastic strains in a material is zero.

In order to relate stress and strain in the plastic range, two theories have been suggested. The deformation (or Hencky) theory relates the total plastic strain to the current state of stress through some modulus which may vary with work hardening, whilst the incremental (Levy–Mises) theory relates strain increment to stress by a constant which varies during the deformation. The total strains can therefore only be obtained by integration and are path dependent, but where the ratio of the stresses remains constant, the two theories are identical. It can be shown theoretically that the incremental theory is the only satisfactory one, and this has been confirmed experimentally by Morrison and Shepherd. However, since the deformation theory is easier to use in practice, it is of importance to determine the error introduced.

In 1926 Lode carried out combined tension-internal pressure tests on iron, copper and nickel. He introduced two variables

$$\mu = \frac{2\sigma_3 - \sigma_1 - \sigma_2}{\sigma_1 - \sigma_2}; \qquad \nu = \frac{2\epsilon_3 - \epsilon_1 - \epsilon_2}{\epsilon_1 - \epsilon_2}$$

and found a deviation from the Levy–Mises relation ($\mu = \nu$). Taylor and Quinney suspecting anisotropy in Lode's specimens repeated the test only to confirm this deviation. In view of the possibility of anisotropy in the Taylor and Quinney specimens, the question of equality of μ and ν still remains.

(*c*) *Strain hardening characteristic.* The strain hardening characteristic is easily represented for simple stress systems but for combined stresses it is necessary to derive some equivalent stress/equivalent strain relation, in which the yield locus is assumed to be independent of the strain path. Equivalent stresses based on both the Mises and Tresca yield criteria with corresponding equivalent strains have been used. Experimental work to determine their validity suggests that the octahedral representation gives fairly good agreement up to about 20% strain. Taylor suggested an alternative representation, namely that octahedral stress is a function of the plastic work done. This reduces to the octahedral representation when $\mu = \nu$ and when the principal axes of stress and strain increment coincide.

(*d*) *Development of yield locus.* The implication of the above is that the yield locus remains of the same form and merely increases in size for small strains. For large strains, however, anisotropy can be expected to develop and the yield locus may change in shape as well as size. The question of the nature and development of the yield locus with strain for various metals has been neglected and needs experimental investigation.

Combined stress apparatus. For experimental investigations in this field, a versatile apparatus, probably the first of its kind, has been designed and built in the Plasticity Division, Mechanical Engineering Research Laboratory. It is designed to subject thin tubular specimens to a perfectly general two-dimensional stress system by applying internal pressure, axial tension and torque. Nearly all previous work has used some combination of only two of these stresses. In this way, principal stresses of any value and acting in any direction relative to the axis of the tube can be applied. All the loads are provided by fluid pressures which are controlled and measured by specially designed beam pressure units. Circumferential strain is measured by using a coaxial cylinder condenser around the specimen whilst the axial strain and the twist are measured by the relative movement of a pointer attached to the specimen over a fine scale also attached to the specimen.

It is proposed to examine experimentally the criteria of yielding including that suggested by Bishop and Hill, the accuracy of the incremental stress strain relations and a determination of the error introduced by using the deformation theory, the equality of the Lode variables for an isotropic material, the strain hardening characteristic and its dependence on stress path, and finally the development of the yield locus with plastic strain.

MR. E. M. LOXLEY (Engineering Department, University of Sheffield) read a paper entitled "The measurement of residual stresses in cold-drawn tubes." Mr. Loxley said that despite the overwhelming amount of published information on residual stresses, the accurate determination of the residual stresses in a tubular component did not appear possible when the investigation at Sheffield was started, some five years ago. The difficulties are largely those of experimentation. Residual stresses can be determined by progressive release of internal strain with measurement of the resultant change in the dimensions of the body at each stage, or by X-ray and similar non-destructive methods. The present paper is concerned with the former procedures. Two alternative methods are available: direct strain release and measurement, widely known as the Sachs boring method,[2] or strain release and measurement of bending deflexion. The latter method has been evolved for cases in which the residual stress changes sign in passing from one surface to the other. The circumferential stress is evaluated from the measured change in diameter when a longitudinal slit is made through the tube wall. More information is obtained by applying the slitting procedure to specimens from which successive layers of material have been removed. The mathematical solution of this problem is due to Davidenkov.[3] The method is sound but cumbersome in application. A simpler analysis based on the bending theory of straight beams was later published by Sachs and Espey.[4] The method is much simpler in application but may lead to errors as high as 20% in exceptional cases. However, an amended analysis, similar to that of Davidenkov, but using the simple beam theory of Sachs and Espey, is both quick and accurate. It is limited to tubes where the

wall thickness/outside diameter ratio is not greater than 0·125.

Mr. Loxley then gave some account of the experimental procedures necessary to obtain results of reasonable accuracy. Layer removal in steel tubes is best achieved by pickling in a 15% nitric acid solution at 110° F with continuous agitation of the pickling solution. A sprayed coating of Neoprene was found satisfactory for protection of surfaces where removal was not wanted. The results obtained by direct strain release, and by bending deflexion measurements (Davidenkov analysis) are compared in Fig. 1. The tube

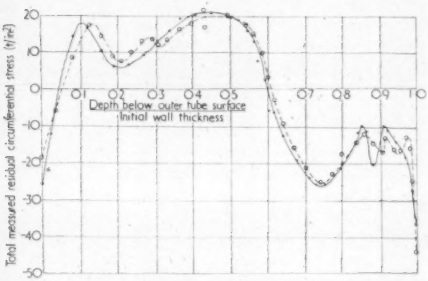

Fig. 1. Distribution curves of residual circumferential stress

— — — Mean distribution curve from bending deflexion tests (Davidenkov analysis).

——— Distribution curve for direct strain release tests (Sachs analysis).

was of mild steel, initial outside diameter 4·125 in., bore 3·500 in., drawn down to 3·374 in. outside diameter and 0·385 in. mean wall thickness. The die had a straight taper, 30° included angle.

In conclusion Mr. Loxley considered the influence of some of the variables involved in cold drawing normalized steel tubes. The maximum residual stress can in some cases approach the 0·5% proof stress of the material.

MESSRS. K. FIKRI and W. JOHNSON (Engineering Dept., University of Sheffield) read a paper entitled "The effect of tensile overstrain on the yield criterion for mild steel, brass and copper." The authors described investigations carried out on thin-wall tubes of mild steel, brass and copper. The tubes were machined from annealed 1·750 in. square bar and finished by grinding to 0·750 in. inside diameter, 0·1 in. wall thickness. They were not heat treated after manufacture. The tubes were subjected to 0, 5 and 10% tensile overstrain and then unloaded. The tubes were then tested under gradually increasing combined stresses, due to torsion and tension, until yielding occurred. In the majority of the experiments the method adopted was first to apply the torque and subsequently the tension. It is clear that in this way a non-radial stress path is followed. An alternative method maintaining a constant stress ratio, that is following a radial stress path, was attempted. This method greatly simplifies the extraction of μ and ν, the well-known Lode parameters.

The results show that despite tensile pre-strain to the extent of 10%, and sometimes 20%, the materials tested tend to adhere to the von Mises criterion of yield, and the Levy–Lode relationship $\mu = \nu = 1$, with reasonable accuracy. In addition the axes of stress and strain remain nearly coincident at yielding.

MR. J. F. WALLACE (Engineering Department, University of Sheffield) read a paper entitled "Extrusion under drop hammer impact." Mr. Wallace described experiments in which a cylindrical rod was produced from a cylindrical slug under the impact of tups weighing between 25 and 500 lb falling through 12 ft. Impact velocities reached a maximum of 360 in./s giving an extrusion time of 1–3 ms. There is a considerable reduction in the required extrusion pressure under the adiabatic conditions achieved at these velocities. The calibration of the strain gauges on the punch has been checked under impact loading by a consideration of the energy balance of impact.

MESSRS. J. B. HAWKYARD and P. FREEMAN (Engineering Department, University of Sheffield) read a paper entitled "Stress–strain characteristics of metal at high rates of strain." The paper described apparatus and experimental techniques by means of which the compressive stress–strain relations of various metals had been determined at rates of strain from 100 to 600 in./in. per s. The dynamical problem involved in the work is essentially that of a long cylinder striking a much shorter cylinder of reduced diameter resting on a rigid body. Ideally the force exerted on the specimen is constant during the time the stress wave travels the double length of the tup. In practice the yield force increases as a result of strain hardening and the increase in cross-sectional area of the specimen. The rate of straining, which again ideally remains constant during this period, is also affected by the reduction in specimen length. It is possible, however, to design a tup which produces an approximately constant strain rate for an appreciable period of a dynamic compression test. The tup used in the present tests was of brass, 3 in. diameter and 24 in. long, giving a stress wave transit time of about 0·3 ms.

The stress–strain curves were derived from simultaneous recordings of load and plastic strain of cylindrical specimens. The load was measured by three symmetrical longitudinal wire resistance gauges on the punch and recorded on the Y_1 plates of a double beam oscilloscope. The strain was measured

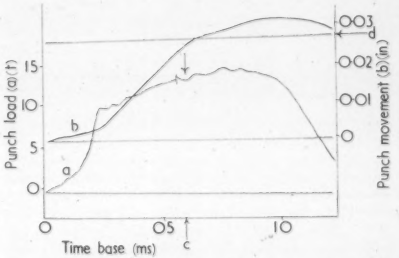

Fig. 2. Typical punch load displacement diagram
Tup of 50 lb drops through 21 in. on to $\frac{1}{8}$ in. specimen of aluminium alloy type AW10.

Curve *a*: punch load variation.
Curve *b*: punch movement variation.
Point *c*: return of stress wave from tup.
Point *d*: final punch position.

by a photoelectric displacement indicator. In this device the end of the punch acts as a shutter on the beam of light falling on the photoelectric cell. The change in voltage produced across a load resistor in series with the cell was fed *via* a cathode follower and low-gain amplifier to the Y_2 plates of the oscilloscope. Fig. 2 shows a typical recording during a dynamic test. It is seen that the punch velocity remains sensibly constant until the stress wave in the tup returns to the end in contact with the tools.

Preliminary tests demonstrated the necessity for standardizing the friction between the dies and the specimen. The most satisfactory lubricant for both static and dynamic testing was found to be a mixture of oleic acid, colloidal graphite and tallow. The dies were polished to a finish better than 1 μin. Tests were carried out on four materials—a 0·28% carbon steel, a 0·1% carbon steel, 99·7% aluminium and an aluminium alloy A.W.10 (a 0·75% magnesium, 1·0% silicon, aluminium alloy under the British Standards Institute STA 7 Schedule; the general engineering equivalent is B.S. HE 10 : 1476, or commercially Hiduminium 44).

The true stress–strain relation under static loading was obtained from results on a number of specimens of different thickness by the use of the so-called "friction hill" equation.

$$\bar{P} = Y[1 + (2\mu a/3\,h)]$$

where $\bar{P}$ is the mean pressure on the specimen, Y is the yield stress corresponding to the current compressive strain, μ is the coefficient of friction between the specimen and the die, a is the radius of the specimen, and h its height. Assuming that the friction hill equation could be applied to dynamic conditions, it was found that the dynamic coefficients of friction were of the same low order as the static coefficients. On this basis it was considered reasonable to take the ratio of the true yield stresses under dynamic and static conditions as equal to the ratio of the compressive stresses at a given strain. At a natural strain $\epsilon = 0{\cdot}05$ in./in. the ratio of dynamic to static yield stress for the 0·1% carbon steel is 1·85 at a strain rate of 600 in./in. per s and 1·70 at 300 in./in. per s. For the 0·28% carbon steel the ratio is 1·31 at 450 in./in. per s and 1·23 at 260 in./in. per s. The same ratio is found to be 1·45 for 99·7% aluminium at 500 in./in. per s and 1·05 for the aluminium alloy at 620 in./in. per s. These last results are consistent with the findings of other workers.

WORK AT DELFT

MR. R. G. BOITEN (Institut T.N.O. Voor Werktuigkundige Constructies, Delft, Holland) read a number of short papers describing the work of the institute. The first concerned "The photoelastic bench at T.N.O." The bench was completed eight years ago to the following specification. (1) The bench was to be of rigid construction, placed on anti-vibration mountings. (2) It was to have a large useful field. (3) All controls were to be handled from a movable desk. (4) It was to be adapted for both white and monochromatic light. (5) It was to be suitable for short-exposure photography. (6) It was to be of high accuracy and good optical quality.

The bench is of welded steel construction, in two sections, with a central movable carriage bearing the loading frame. The load is applied either pneumatically or by lead weight. The source of light is a high intensity open electric arc-lamp with a source size of 4 mm. Monochromatic light is obtained by means of a Schott interference filter of 100 Å band width, with a peak at 5440 Å. The single condenser-collimating lens, and the collecting lens, are of 5 feet focal length and corrected for chromatic aberration. The polarizer and analyser are 12 in. diameter polaroid sheets capable of simultaneous rotation by magslip transmission controlled from the operating desk. The quarter-wave plates are synthetic and of the same diameter as the polaroids. Pictures are normally taken with a miniature Leica camera using a 1/1000 s exposure time.

Mr. Boiten described a recent investigation of the stress distribution around a crack at the tensile side of a reinforced bar. The model material was cold-setting Araldite casting resin type D by Aero Research Ltd., Duxford, Cambridge. It was found that a second crack is unlikely to appear at a distance from the first crack less than the height of the bar. This was in accord with tests on full-scale concrete bars.

Mr. Boiten's second paper described work on "Prefabricated strain gauges." He said that the object of these gauges is to overcome a number of difficulties presented by standard wire resistance gauges, namely, (1) the difficulty of cementing and drying the gauges, particularly out of doors, (2) the delay of a day or so between gauge application and testing, (3) the difficulty of the water-proofing process, and (4) the fact that gauges can only be used once, with the inherent objection that the actual gauge used in a test cannot be independently calibrated.

The following technique has been found most successful. The gauge is cemented in the normal way to a piece of steel plate of 0·002 in. thickness and subsequently protected either by a rubber cap cemented to the steel, or by a synthetic rubber cover cured in position. The prefabricated gauge of about 20 mm gauge length, is cemented to the structure under investigation by an Amco cement type F.88. By heating the cemented joint to 50° C maximum bond strength can be achieved in one hour. The cement is unaffected by water and most organic solvents and, since it is relatively weak in tension, the gauge can be removed and used again, up to about five times. The gauge factor changes by less than 1·5% with successive calibrations.

Mr. Boiten's next paper was entitled "Pick-ups based on the use of strain gauges." Mr. Boiten described a comprehensive investigation into the dimensions and shape of measuring units for compressive forces, tensile forces, and pressures. This work is shortly to be published in Germany.

Mr. Boiten then described "A new type of brittle lacquer." The raw material is plumber's resin, which is distilled under vacuum at 200° C until no more volatile components are liberated. The resin is then poured out, cooled to a brittle mass, and split up into pea-size granules. Since the material is extremely hygroscopic it must be stored in a sealed container. The resin is sprayed with an ordinary gas–air torch. The air is passed through a mill, in which the resin granules are ground to a fine powder. This powder is blown into the flame. The end of the torch is held some 1½ in. from the surface to be coated, in the cool part of flame. As a result the test object is only moderately heated. After cooling, the sensitivity to strain is good, cracks appearing at strains of $3 - 5 \times 10^{-4}$ in./in.

In conclusion Mr. Boiten showed a 16 mm film demonstrating "The practical application of high-speed photography." The film was taken at camera speeds between 500 and 3000 pictures per second. It demonstrated, amongst other things, the behaviour of telephone contacts, arc-welding, the turning of steel and the investigation of a flame trap.

MINING

A paper by PROF. E. L. J. POTTS and MR. J. K. DIXON (School of Mines, King's College, Newcastle upon Tyne) on "The application of stress analysis to ground control in mining" was introduced by Mr. Dixon and read by DR. JENKINS. Mr. Dixon emphasized the importance of a better understanding of the stresses involved when considering ground control in mining. Loss of life and output from pressure bursts is still very serious. The material with which the mining engineer has to deal is neither homogeneous nor isotropic. It exhibits initial anelasticity, elastic hysteresis, creep and plastic flow. Sandstones and shales differ from coal in having very large values of the Poisson number (inverse of Poisson's ratio). Accordingly it is necessary to make a number of rather sweeping assumptions before simple photoelastic methods can be applied, but there is such a paucity of information on underground rock pressure that the approach is justified. Since many mining excavations are roadways which are long, narrow, and of uniform cross-section, the problem reduces to one in two dimensions. It is assumed that the only load is that due to the superincumbent strata. In practice this is of the order of 1 lb/in.^{2} per foot of stratum.

The present analysis is concerned with a rectangular roadway driven in a coal seam in laminated ground. In the model the laminations were separated by sheets of packing; the most satisfactory material was found to be polythene 0·006 in. thick. The importance of the ratio roadway width/lamination thickness was discussed. No fracture is likely if this ratio is much less than unity. The application of the results to the positioning of roof bolts was also discussed. In the past it has been quite common for these to be placed in regions of tension.

AIRCRAFT ENGINE VIBRATION

MR. D. A. DREW (Rolls-Royce Ltd., Derby) read a paper entitled "Measurements of aircraft engine vibration in flight." Mr. Drew said that for the study of engine vibration very great accuracy was often not vital, but the measuring system had to be capable of dealing with frequencies up to 15 kc/s. It is often only necessary to determine the running condition responsible for maximum stress and the frequency of the stress. An instrument capable of recording a frequency of 15 kc/s for 10 min must store 9×10^6 cycles. This is an almost impractical requirement in a photographic recorder, even if located on the ground. For long recordings there are clearly overwhelming advantages in favour of magnetic recording, especially if the equipment is to be airborne. The tape requires no processing after the record is made, and it can more readily be played back into electronic analysing equipment than a photographic record.

The simple, single-channel, telemetry system that had been used by Rolls-Royce Ltd., before satisfactory tape recorders suitable for carrying in a small aircraft were available, had already been described.[5] Since high performance tape transport mechanisms in a form suitable for mounting in an aircraft were now available, 5-channel airborne recorder equipment has now been developed by Rolls-Royce. The equipment is suitable at this stage for frequencies up to 7 kc/s, and twice this figure after a simple modification. This equipment, together with recordings of actual flight tests, was exhibited.

MISS B. M. RIMMER (Societé de Fabrication d'Instruments de Measure, Paris) read a paper entitled "Measurement of engine vibration in flight." Miss Rimmer described the use of continuous trace recording for the measurement of vibrations at frequencies up to 25 c/s. This type of recording is particularly suited to airborne measurements. Vibrations measured at a number of points together with quantities defining the flight conditions, e.g. height, airspeed, engine revolutions per minute, and jet-pipe temperature, may be inscribed on the same record against the same time base. Once the film is developed a rapid assessment of the value of the flight can be made and important sections identified and selected for detailed analysis. The equipment is small, easy to install and relatively inexpensive. Miss Rimmer described a number of types of recorder together with the relevant measuring elements and transducers.

MR. L. N. KATZ (Epsylon Research and Development Co. Ltd., St. Margarets, Middlesex) read a paper entitled "Mechanics in the design of tape recording systems." He said that longitudinal magnetization is standard in all modern tape recording equipment. This is achieved using a ring-type magnetic recording head, the tape being moved at a constant velocity past, and in contact with, the magnet gap. The crucial point of all such recording is the maintenance of good contact between the gap and the tape.

The two mechanical problems involved are concerned with the design and manufacture of, firstly, the magnetic recording gap and, secondly, the tape transport mechanism. The gap must be extremely accurate dimensionally, particularly for replay heads. This is difficult to achieve in the high permeability material of the head, which must not be subject to mechanical manipulation after annealing. On the other hand, it is a complex problem to devise a mechanism capable of moving the very elastic and fragile tape past the gap without introducing wow, flutter, drop-outs or noise due to variations in contact.

Mr. Katz described the present position in the search for the solution of these problems in high quality sound recording.

DYNAMIC LOADING

MR. S. MAHALINGHAM (Post Graduate School of Applied Mechanics, University of Sheffield) read a paper entitled "Dynamic loading of power transmission chains." The author said that some of the factors contributing to dynamic loading had recently been dealt with theoretically, but, to his knowledge, no attempt at an experimental investigation had yet been made. The most important factors contributing to dynamic loading are: (1) centrifugal tension, (2) polygonal action, (3) impact, (4) pitch errors, (5) vibration.

The present paper is concerned only with polygonal action. This is the periodic fluctuation in the speed of the chain arising from the fact that the chain around the sprocket forms a polygon rather than a circle. The magnitude of the dynamic effects of polygonal action depends in part on the inertia of the driven system.

In chain transmission the drive is transmitted from one sprocket to another through a series of four-bar linkages, each linkage operating for the period equal to that of tooth engagement. In general the speed ratio of the two sprockets is subject to periodic fluctuations. Morrison[6] has used the analysis of the four-bar linkage to study the variations in speed ratio resulting from polygonal action. In this analysis the chain is assumed to be a rigid bar. The elasticity of the chain has, however, a profound influence on the behaviour

of the system. The problem then appears to be one of forced vibration in which, beyond a certain critical speed, higher speeds produce lower dynamic loads. It turns out that the amplitude of the force in the chain is given by,

$$A = \frac{ak}{w}\left[\left(\frac{\cos\alpha}{N^2} - 1\right)^2 + \left(\frac{\sin\alpha}{N^2}\right)^2\right]^{\frac{1}{2}}\left(1 - \frac{\omega^2}{p^2}\right)^{-1}$$

where a is a constant, k is the stiffness of the chain, w is the number of teeth in the driving sprocket, α is the "phase difference" between the two sprockets corresponding to the fractional pitch in the tangent span, N is the speed ratio, p is the frequency of tooth engagement and ω is a function of K, N and I, the moment of inertia of the driven system.

The apparatus used for the experimental investigation was a "four-square" power circulator with equal sprockets driven by a 5 h.p. motor. Stresses were measured by two electrical resistance strain gauges attached to the outside of a link. Using an intermediate shaft carrying a mercury slip-ring it was possible to record stresses up to chain speeds of 3000 ft/min. The results obtained for two different values of the inertia of the driven system are shown in Fig. 3. The first peak in

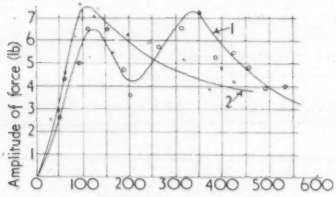

Fig. 3. Polygonal effect in chain drives

curve 1 corresponds to excitation by the second harmonic. The maximum chain speed used was 1200 ft/min at which speed it was found possible to identify and separate the impact loads from the oscillograph record.

MR. A. Y. ATTIA (Post Graduate School of Applied Mechanics, University of Sheffield) read a paper entitled "Dynamic loading of spur gear teeth." The speaker outlined the experimental method used to obtain the deflexion curve of the gear tooth under both static and dynamic loads and gave some preliminary results. No final conclusions have yet been reached. The main difficulty in the analytical approach is the derivation of the discontinuous equations resulting from the change in the number of teeth carrying the load along the path of contact. The actual load between any pair of teeth is made up of the nominal transmitted load, together with a dynamic increment dependent on the rotational speed of the gears, and an increment arising from the change of relative velocity of the mating gears, generally caused by errors in the tooth profile, inaccuracies of production, and elastic deformation under load.

The testing was carried out in a power circulating type of machine; two pairs of gears of the same velocity ratio were joined by two shafts to which torque was applied, loading one pair of gears against the other. The gears under test were of 5 in. pitch circle diameter, having 20 teeth of B.S. involute form, 20° pressure angle. They were made of type E.N. 39 case hardening steel. The deflexion of one tooth of the driven gear was measured using a 1000 Ω wire resistance strain gauge placed circumferentially and bridging the gap between a rectangular steel piece, soldered to one of the teeth of the driven gear, and a steel disk firmly secured to the body of the gear. The disk had a small rectangular slot at its outer diameter to accept the steel piece soldered to the tooth. Standard equipment was used to obtain records of the tooth deflexion.

Traces of tooth deflexion under varying loads at a rotational speed of 10 rev/min were obtained. At this speed there are no dynamic effects. The traces show to some extent how the load is distributed between the teeth in mesh and the effect of tooth errors on this distribution. Dynamic traces were then obtained which showed the effect of speed on tooth deflexion, and the positions of maximum impact loading by comparison with the earlier traces. These dynamic traces were repeated for a number of different mesh settings. Since this alters the amount, and distribution, of the resultant errors it is possible to study the effect of errors on the impact loading of the tooth. Finally the strain gauge was calibrated under static loads for different points of contact on the tooth profile.

From the results obtained it is expected that a tentative correlation of the impact stresses in gear teeth with speed and resultant error can be reached.

STRAIN GAUGE LOAD CELLS

MESSRS. H. GILL and G. W. ALDERTON (British Iron and Steel Research Association) read a paper entitled "Temperature compensation of strain gauge load cells." They said that, with demands on increased accuracy, the problem of adequate temperature compensation became increasingly difficult. In the strain gauge load cell temperature compensation is achieved by fixing gauges in pairs, one horizontal and one vertical. In this arrangement each gauge is both active and temperature compensating. For complete compensation

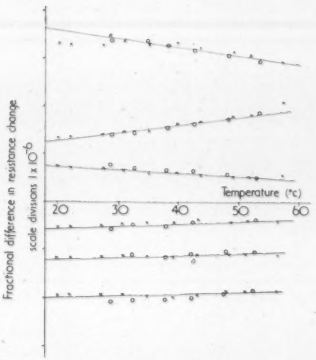

Fig. 4. Variation of fractional difference in resistance change with temperature for pairs of wire gauges

(Nichrome wire of nominal resistance 1 kΩ.)

× Increasing temperature.
⊙ Decreasing temperature.

it is necessary that three requirements should be fulfilled. The gauges should (1) have the same temperature coefficient, (2) suffer the same temperature change, (3) have the same gauge factor. Conditions (1) and (3) were usually met by using gauges from one manufacturer's batch, and condition (2) by placing pairs of gauges as close together as possible.

The present work was carried out in an attempt to explain the unexpected temperature dependent zero-drift of two

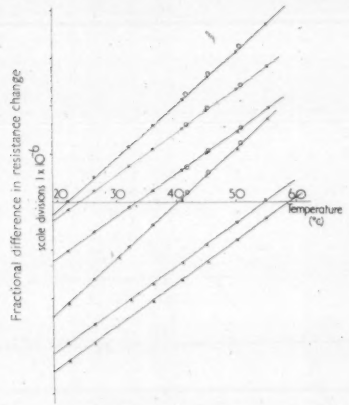

Fig. 5. Variation of fractional difference in resistance change with temperature for pairs of linear foil gauges

(50/50 copper–nickel of nominal resistance 50 Ω.)

× Increasing temperature.
○ Decreasing temperature.

150 ton load cells when rebuilt with foil gauges instead of the normal wire type. The results of tests on foil and wire gauges cemented in pairs on to steel blocks is shown in Figs. 4 and 5. The zero-drift of the cells using foil gauges is attributed to the wide variations in the individual temperature coefficients of this type of gauge. Manufacturing experience has shown

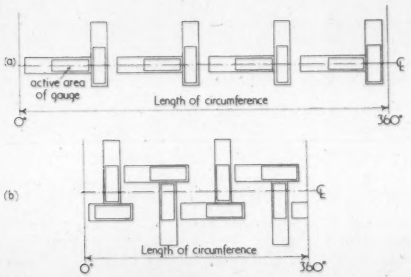

Fig. 6. Suitable gauge layouts for (*a*) cylinders, (*b*) small cells

that it is difficult to produce 0·0005 in. thick copper–nickel foil having consistent electrical properties throughout. Modified gauges have now been produced from a new type of foil 0·001 in. thick specially selected for this purpose. These gauges are similar to wire gauges as regards temperature coefficients.

The arrangement of the gauges on the cell was discussed; suitable arrays are shown in Fig. 6. These arrangements have proved successful in practice. In one case for a temperature difference of 5° C between the top and bottom of the cell, accompanied by a mean rise of 10° C, only 0·2% drift was recorded.

RESISTANCE NETWORK ANALOGUE

A paper by DR. G. LIEBMANN (Associated Electrical Industries Ltd., Research Laboratories, Aldermaston) entitled "Further investigations with the resistance-network analogue for solving plane stress problems" was read by MR. F. C. GAIR. The paper considered in more detail the questions of accuracy and boundary conditions in the resistance-network solution of plane stress problems. The details of the method, first introduced at Cambridge in 1953, have already been published.[7,8] Mr. Gair described the salient features of the analogue solution and explained the need for two networks "in cascade" for the solution of the biharmonic equation:

$$\nabla^4\chi = 0$$

arising in plane stress problems.

The method is much quicker than the relaxation procedure and a complete problem can be solved in two to three days. This does not include the time required for setting up the network which may be another two days. The latter is the main objection to the method; each new problem has to be tackled from scratch. Some attempts have been made to build up a universal network but, for relatively simple problems, it is better to build up a new network for each problem. It is characteristic of the method that the error is greatest at the boundary.

HIGH-TEMPERATURE STRAIN GAUGES

A discussion on a paper entitled "High-temperature strain gauges" by MR. L. BROOKE-EDWARDS (Baldwin-Lima-Hamilton Corp.) was introduced by MR. L. F. ATKINSON (Vauxhall Motors Ltd., Luton) and MR. W. H. RAY (Admiralty Engineering Laboratory, Middlesex). There are three distinct problems involved, namely, (1) the decision on the type of gauge to be used, whether it shall be of the wire resistance or etched foil type, a reluctance or capacitance gauge, (2) the lack of stability of the strain sensitive element at temperature, and (3) the choice of a suitable cement. There is still a great need for development work on ceramic and other cements.

X-RAY DIFFRACTION

MR. R. S. SHARPE (Engine Division, Bristol Aeroplane Co. Ltd., Bristol) read a paper entitled "Machining stresses in turbine blades." Mr. Sharpe referred to the rigorous inspection for material or structural defects in gas turbine engines and suggested that the inspection might be extended to cover residual surface and internal stresses. There is evidence that surface residual stresses in turbine blades are potentially dangerous in two distinct ways. Firstly, if they are tensile,

they may lower the safe operating stress of the blade. Secondly, they influence the kinetics of surface oxidation. The mechanism of selective oxidation is well known in many alloys. In the case of the Nimonic alloys by Henry Wiggin and Co. Ltd., Birmingham, used for turbine blades, it is the readiness to form a non-permeable protective surface oxide layer containing a preponderance of one or other of the constituent elements that in fact confers on them their heat resisting properties. However, when the surface layers are highly stressed initially, the loss of one or other of the elements occurs at an accelerated rate, and at a lower temperature, probably aided by recrystallization of the stressed layers. This constituent loss may seriously impair the mechanical strength of the blade.

Residual stresses can be divided into three types: (1) sub-granular lattice distortion; stresses which exist on a microscopic scale within the grains, (2) micro-residual stresses; constant in any one grain but varying from grain to grain, (3) macro-residual stresses; of constant value over a relatively large area of surface, with compensating stresses of opposite sign within the interior.

The effect of these three types of stress on the position and appearance of X-ray diffraction lines is shown in Fig. 7.

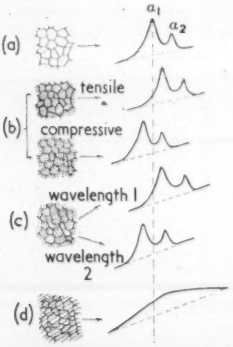

Fig. 7. Effects of stress on X-ray diffraction lines

(*a*) Stress free.
(*b*) Elastic macro-stresses.
(*c*) Residual micro-stresses (after plastic deformation).
(*d*) Localized lattice distortions (after machining).

Elastic macro-stresses result in a shift of the diffracted X-ray lines, the direction of the shift being determined by the sign of the stresses. When present on their own they can, under favourable conditions, be measured. Micro-stresses also result in a line shift but their interpretation is very much more difficult. Localized lattice distortions result in broadening of the diffraction lines. This type of stress is rarely divorced from the other two and in general there is a shift and a broadening of the diffraction line. The shift is usually entirely masked by the line broadening and the latter is the only effect which can really be measured. This is only one, and probably not the most important, aspect of the residual stress problem; to divorce it from the context of the overall stress situation can be very misleading.

Mr. Sharpe described the results of an X-ray diffraction investigation on Nimonic surfaces which had been given different machining treatments. These results are given in Fig. 8. It is of interest to note that there is reasonable correlation between the surface hardness, measured with a

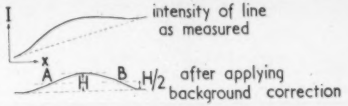

Fig. 8. Result of X-ray line breadth measurements of Nimonic surfaces with different surfaces

Machining operation	*Line breadth AB (radians/1000)*
Reamed surface	103
Turned surface	83
Plunge ground surface	63
Milled surface	62
Turned surface after polishing	58

diamond indenter under 1 kg load, and the lattice distortion as measured by X-ray diffraction line breadths, Fig. 9. The scatter in Fig. 9 can be explained by the differences in penetration of the hardness indenter, 10–14 μ, and of the X-ray beam, 3–4 μ. The inference that when one type of residual stress is high the others are also high can be misleading.

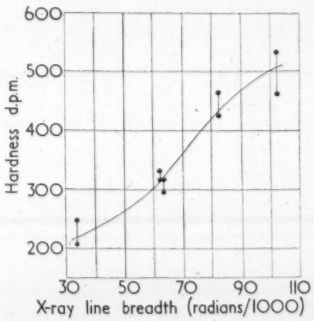

Fig. 9. Relation between surface hardness and X-ray line broadening for surfaces listed in Fig. 8

Grinding, which is more a cutting than a rubbing action, can result in quite small sub-granular distortion and large macro-stresses.

In conclusion Mr. Sharpe referred to the use of surface ultrasonic waves for residual stress determinations. This method has been discussed by Firestone.[9]

PHOTOELASTICITY

Messrs. H. Fessler and B. H. Lewin (Department of Mechanical Engineering, University of Nottingham) read a paper entitled "Branched pipes studied by frozen stresses in Araldite models." The frozen stress method of photoelastic analysis was employed to determine the stresses in the tee junction of a "semi-infinite" branch 1¼ in. outside diameter,

½ in. bore, to an "infinite" pipe 3 in. outside diameter, 1 in. bore. Stress free models 3½ in. diameter, 15 in. long were obtained by curing the Araldite casting resin B at 105 to 110° C and cooling the models at 1½° C per hour. "Thermocouples placed inside a closed cylinder showed that the oven had to be maintained at the freezing temperature for five hours for the model to attain oven temperature.

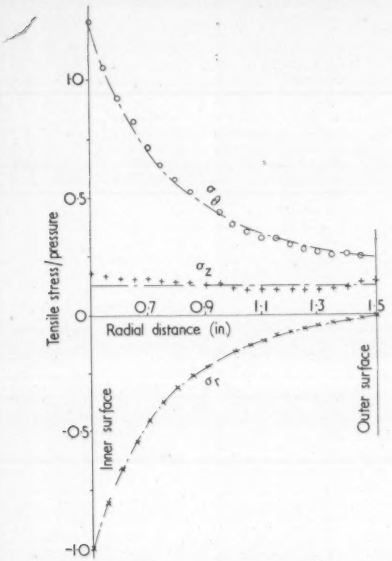

Fig. 10. Comparison of measured stresses with theoretical distribution in thick cylinder

Lines represent theoretical stress distribution.

Casting resin B was found suitable only for joints which could be firmly clamped during curing, or for those which could be formed by a "trough" filled with liquid resin. The addition of 50 to 55% of French chalk to casting resin B formed an effective cement which did not run out of the joint during curing, but joints of this type could not be made less than 0·002 in. thick. To avoid the stress disturbance caused by such a joint, the end of the branch piece was machined to the profile of the outside of the main pipe and cemented to it before machining the bores. This arrangement could be clamped, without causing distortion, and thin effective joints could be made with chalkless cement which did not disturb the fringe pattern.

The models were calibrated by equating the known internal pressure to the difference in radial stress between the outer and inner surfaces; the principal stresses were obtained for a radial line, remote from ends or juncture, by applying Frocht's shear difference method to cylindrical polar co-ordinates. Fig. 10 shows the agreement between these measured stresses and those obtained from thick cylinder theory. The use of a diamond impregnated cutting wheel enabled slices 0·015 in. thick to be cut.

It was found that time-edge stresses could be removed from models or slices by storage in air at 85° C, without disturbance to the frozen fringe pattern. This is valuable in allowing adequate time for a comprehensive analysis without the embarrassment of spurious edge stresses.

H. SPOONER

REFERENCES

(1) TAYLOR, G. I., and QUINNEY, H. *Phil. Trans, A*, **230**, p. 323 (1931).

(2) SACHS, G. *Z. Metallkunde*, **19**, p. 9 (1927).

(3) DAVIDENKOV, N. N. *Z. Metallkunde*, **24**, p. 25 (1932).

(4) SACHS, G., and ESPEY. *Iron Age*, **148** (12), p. 63, and **148** (13), p. 36 (1941).

(5) DREW, D. A. Lecture before the Stress Analysis Group of The Institute of Physics (March 1952).

(6) MORRISON, R. A. *Machine Design*, **24** (9), p. 159 (September 1952).

(7) LIEBMANN, G. *Nature* [*London*], **172**, p. 78 (1953).

(8) LIEBMANN, G. *Brit. J. Appl. Phys.*, **6**, p. 145 (1955).

(9) FIRESTONE, F. A. *Non-Destructive Testing*, **7** (2), p. 5 (1948).

Specimen thickness and image resolution in electron microscopy*

By V. E. Cosslett, Ph.D., F.Inst.P., Cavendish Laboratory, University of Cambridge

[*Paper received* 3 *August*, 1955]

The working rule that the resolution obtainable in the electron image of a biological specimen is of the order of one-tenth its thickness is quantitatively explained in terms of the energy loss of electrons scattered in the specimen and of the chromatic aberration of the objective lens. This limitation holds true down to the thinnest sections (100–200 Å) that can be cut at present. That they normally do not show a resolution approaching 20 Å is ascribed to lack of contrast. The use of a filter lens, rejecting all electrons that lose more than 10 V, would improve both contrast and resolution. Its use is even more important for rendering visible carbonaceous structures of size comparable with the instrumental resolving power. A lower accelerating voltage than currently used for electron microscopy is desirable for specimens of poor contrast.

Experience in this laboratory with electron microscopy of biological specimens (unsectioned) led the author to formulate the working rule that the practically attainable resolution was of the order of one-tenth the thickness of the specimen,[1] even though the resolving power of the electron microscope itself might be very much better. The thickness of specimen was such (1000 Å–1 μ) that a plausible explanation was given by the confusion caused by overlapping detail from different layers, the depth of focus being so great that all of the specimen is in focus at once.

It has recently become possible to cut very thin sections of tissues and experience with this new technique showed that the one-tenth rule still applied as specimen thickness decreased, certainly down to 200 Å, and when the structures observed were embedded in a solid material such as methacrylate. A more fundamental explanation was then sought and ultimately came out of a study of the theoretical work of von Borries (Ref. 2, pp. 168–185) and Lenz [3] on electron scattering in the conditions of electron microscopy. However, it follows most simply by relating the Thomson–Whiddington law,[4] for the rate of energy loss of electrons with penetration, to the chromatic aberration of the imaging system, and this approach will be used here.

Once it is established that the image resolution achieved in practice is tied to the specimen thickness, it becomes important to enquire if this remains true up to the instrumental limit of resolving power, i.e. whether sections no thicker than 50 Å have to be cut if 5 Å resolving power is to be utilized. In such thin layers electrons will suffer on the average less than one collision each, so that the question of contrast becomes fundamentally connected with resolution. For carbon, for which the inelastic scattering cross-section is much greater than the elastic, it appears that the one-tenth rule should hold true down to the best resolving power at present conceivable (5 Å). It follows that the resolution would be further improved, and the contrast considerably enhanced, if the inelastically scattered electrons were rejected from the imaging beam by some form of filter lens. Greater benefit is likely to result from such a development than from chromatic correction of the objective lens, which would bring all the inelastic electrons back into the true image point and thus worsen the contrast whilst only slightly improving the resolution, which is primarily limited by adventitious instabilities of instrumental origin.

* Based on a paper presented at a Conference of the Electron Microscopy Group of The Institute of Physics held at the University of Glasgow on 5 July, 1955.

CHROMATIC LOSS IN THE IMAGING ELECTRON BEAM

The Thomson–Whiddington law, based on experiments on the loss of energy of cathode rays in passing through matter, gives the most probable exit voltage V for electrons of initial voltage V_0 after passing through a thickness t of an element of density ρ, atomic number Z and atomic weight A:

$$V_0^2 - V^2 = a(\rho Z/A)t \qquad (1)$$

The "range" of the electrons is given by setting $V = 0$. The constant a has a value depending on the element and on the initial voltage V_0. For light elements and voltages of order 5×10^4 V, $a = 8 \times 10^{11}$. The exponent in equation (1) becomes less than 2 at very high voltages, but its value in the voltage range here considered has been confirmed by Terrill[5] and others. Equation (1) properly gives the most probable energy loss of the electron beam, whereas in fact there will be a finite spread of velocities. However, for the very thin layers of material considered here both the spread and the energy loss are small and approximately equal [cf Bethe[6]].

When the thickness traversed Δt is much less than the electron range, equation (1) may be written:

$$\Delta V = V_0 - V = a(\rho Z/A)\Delta t/(V_0 + V) \qquad (2)$$

leading to

$$\Delta V/V_0 = a(\rho Z/2AV_0^2)\Delta t \qquad (3)$$

For a carbon film, with $\rho = 2$ and $a = 8 \times 10^{11}$, this gives for a 60 kV beam:

$$\Delta V/V_0 = 110\,\Delta t \qquad (4)$$

An electron beam that has suffered this degree of chromatic loss, imaged by a lens of chromatic aberration constant C_c, will give a disk of confusion of radius δ_c in the Gaussian image plane:

$$\delta_c = C_c \alpha \Delta V/V_0 \qquad (5)$$

where α is the angular aperture of the objective lens. Combining equations (4) and (5) gives the aberration of the image, due to the chromatic defect alone, in terms of specimen thickness; taking $C_c = 2$ mm, $\alpha = 5 \times 10^{-3}$, corresponding to high resolution operation, we have

$$\delta_c = \Delta t/9 \qquad (6)$$

It is known that the greater part of the inelastically scattered electrons falls within an aperture of this order (Ref. 3, p. 180)

so that the chromatic loss is fully effective in producing loss of resolution in the image. Spherical aberration, residual astigmatism and instrumental instabilities together produce a total effect smaller than 10 Å in modern high performance electron microscopes. The chromatic effect will thus predominate for specimens thicker than 100 Å.

If, instead of the Thomson–Whiddington law, we use a relation which was derived from his own experimental work by Lenard[6] and which has been used by von Borries (Ref. 3, p. 205) in discussing chromatic loss in the specimen, the factor in equation (6) becomes $\frac{1}{1\cdot6}$ instead of $\frac{1}{6}$. On the other hand, the values calculated by Lea[7] from the Bethe theory of energy loss in single scattering[8] give the much larger value $\frac{1}{3}$. A value of order $\frac{1}{10}$ seems justified for our present purposes.

A density of 2, corresponding to graphite, has been assumed in deriving the numerical result of equation (6). Thin sections in fact are likely to have a density nearer to unity; if they are ashed in the electron beam it would be even lower, but this is normally prevented by careful beam control. For $\rho = 1$ the resolution factor would be $\frac{1}{20}$ in place of $\frac{1}{10}$. It is interesting to note that experiments on electron penetration (at 30 kV) in a plastic material by Ehrenberg and Franks[9] also lead to a figure of approximately $\frac{1}{20}$.

VERY THIN SPECIMENS

The experimental work on which the above argument rested was done with metal foils of thickness equal to an appreciable fraction of the electron range, so that conditions of multiple scattering obtained. The results should still be reliable for the conditions of plural scattering that obtain in the normal electron microscope specimen, since we are interested in the first place in the average loss of energy of the electrons. But extrapolation may not be justified for very thin specimens (less than 100 Å) in which the average chance that an electron will suffer a scattering act becomes less than unity. Even if such extrapolation can be justified, the quantitative effect of the inelastically scattered electrons on the image would need evaluation; they may or may not exceed in number the elastically scattered component, with a different effect on contrast and resolution in the two cases.

A convenient reference thickness is that amount of specimen material in which, on the average, every electron suffers a single scattering act. This critical thickness will depend on the nature of the element present, its density, the voltage of the incident beam and whether we are concerned with elastic or inelastic collisions. The inelastic critical thickness will be denoted by t_i and the elastic critical thickness by t_e; multiplied by the density of the specimen they correspond to the quantities *Bremsdicke* and *Aufhellungsdicke*, defined by von Borries (Ref. 3, pp. 173, 181). For most elements their values lie between 50 and 1000 Å for the range of voltage employed in electron microscopy. The values for three typical substances, carbon, chromium and gold are given in the table, evaluated from Lenz's corrected version[3] of the original treatment of von Borries.[10] The values for C assume $\rho = 1$.

Elastic (t_e) and inelastic (t_i) critical thicknesses at 60 kV

	Carbon	*Chromium*	*Gold*
t_e	1000 Å	120 Å	45 Å
t_i	200 Å	100 Å	110 Å

Whilst elastic scattering increases rapidly with Z, the inelastic varies very little; for carbon, inelastic acts greatly exceed elastic acts in frequency.

In the thinnest sections (200 Å) at present regularly preparable, therefore, every electron on the average will be scattered once and equation (6) may be taken as valid. With a resolution factor of $\frac{1}{20}$ the image resolution to be expected is 10 Å, whereas such a figure is rarely, if ever, reached with biological material in whatever form. The discrepancy may arise from at least three causes: (*a*) a disproportionate confusion due to electrons which have suffered more than the average energy loss; (*b*) other lens aberrations and instrumental instabilities; and (*c*) lack of contrast between the structures examined and the material in which they are embedded or on which they are mounted.

The fact that the imaging beam has a spread of voltage, instead of being reduced uniformly to a value V_0–ΔV, will give a peaked distribution to the electron intensity across the image point in place of the well-defined disk expected if monochromatic loss alone occurs. But in practice the image point will, in any case, have an approximately Airy distribution and the small voltage spread from a very thin specimen will not add appreciably to its half-width, which is probably the best measure of resolution. It has also been shown by Haine and Mulvey[11] that the effect of spherical aberration on the Airy distribution is less than originally supposed. In any case the limiting resolving power, as set by spherical aberration and residual astigmatism, will be much less than 10 Å in a high performance electron microscope. Provided that instrumental stability is properly assured, therefore, the failure to attain high resolution in biological preparations must be ascribed to lack of contrast.

CONTRAST

Contrast in the electron microscope image arises primarily from differential loss of electrons by scattering at object details of varying elementary composition or thickness. A small aperture in the objective admits the central part of the electron beam that has passed through the specimen, but traps all electrons that have suffered a deviation greater than the critical angle for optimum resolution, as determined by the spherical aberration constant of the lens and the electron wavelength. Such a contrast aperture will admit a large portion of the inelastically scattered component but stop most of the elastically scattered electrons, which are deviated through larger angles.

For elements of high atomic number, such as gold, the cross-section for elastic scattering is greater than that for inelastic, so that $t_e < t_i$ (see the table). Also t_e is absolutely as well as relatively small, so that a thin layer of heavy metal will scatter very efficiently and give high contrast images. The inelastic loss is small, so that chromatic aberration is inappreciable. Hence the successful use of metal shadowing for enhancing contrast in electron micrographs and the universal employment of small particles of heavy metals as test objects for high resolution.

For carbon, on the other hand, the elastic scattering is very much less whilst the inelastic component is only slightly less than for a heavy metal. The table shows that only about 20% of electrons will be elastically scattered in a thickness of 200 Å of carbonaceous material, in which on average every electron will be once scattered inelastically, so that contrast due to elastic scattering will be small. This agrees with the general experience that very thin sections show very poor contrast.

In practice contrast has been improved by three devices: (*a*) raising the electron beam intensity so as to remove some of the embedding material by evaporation or chemical action.

This is effective but may well destroy some of the finer details of the specimen itself; observation shows that the major features are not normally changed;

(*b*) staining the specimen with a heavy metal compound, which may also be the fixative, as with osmium tetroxide. This again is usually effective but may equally cause artefacts at the molecular level. Systematic investigation of stains for electron microscopy is so far almost entirely lacking;

(*c*) Employing an objective aperture of smaller diameter than the critical value. For instance, by reducing its size from the optimum 40 μ to 10 μ contrast can be appreciably improved. In the case of carbonaceous specimens this will be mainly due to the trapping of more of the inelastically scattered electrons. Since the critical aperture size is, by definition, that which gives the optimum compromise for resolving power as between spherical aberration and diffraction, this expedient inevitably leads to loss of resolution. Change from 40 μ to 10 μ aperture diameter will broaden the diffraction disk by four times.

A much greater improvement would be effected by the complete elimination from the imaging beam of the inelastically scattered electrons. Chromatic confusion would be removed, with increase in resolution, and each image point would receive fewer electrons, leading to better contrast. Suitable filter lenses have already been proposed by Boersch[12] and shown to function successfully in electron microscopy by himself[13] and by other authors,[14] but they have not yet been developed into practicable components for conditions of high resolution. The essential principle of a filter lens is to introduce a retarding field in the path of the beam such that all electrons which have suffered more than a prescribed loss in energy are rejected; for such electrons it acts as a mirror, for the more energetic as a lens. For the present purpose it would be enough to hold the filter electrode at some 10 V positive with respect to the cathode. The average loss in inelastic scattering is given by equation (4) as 6·5 V for a 200 Å film of carbon with $\rho = 1$; most scattered electrons would lose more than this since (on average) a fraction $1/e$ would not be scattered at all. This crude estimate assumes a continuous distribution of losses, but it is now known that a large part is played by discrete or "characteristic" loss, especially in thin films; for a survey of recent work, see Marton.[15] These losses are incurred without loss of direction, so that the non-chromatic component is accepted by apertures of the size employed in electron microscopy. In the case of carbon the loss spectrum shows a pronounced minimum at about 8 V, with the strongest "line" at 20 V. A filter lens rejecting all electrons for which $\Delta V > 10$ V would therefore have a great effect in improving electron micrographs of thin biological specimens.

Recent experiments by Gabor and Jull[16] have suggested that discrete losses are largely if not entirely absent from films thinner than about 60 Å. If so, then a filter lens would be of less effect as only electrons that had suffered ordinary inelastic loss would be available for rejection. On the other hand, experiments by Marton[17] show characteristic losses down to the thinnest films used, so that the question is still open. It may well be that non-metals show different behaviour from metals in this respect. In any case we are concerned here with carbonaceous specimens thicker than about 100 Å, particularly in the form of thin sections. The visibility of very small structures, of the order of 10 Å and less, involves a much smaller chromatic effect and depends largely on electron phase contrast effects, as recently discussed by Haine.[18] A rough estimate shows, however, that the chromatic contribution from a 10 Å particle of carbon is of the same order as the phase contrast effect, so that a filter lens would also be of value for resolving minute isolated details of biological specimens.

It may be noted that chromatic correction of the objective lens, which is theoretically possible,[19] and may be practically attainable,[20] would be of less value than a filter lens for the circumstances considered. A corrected lens would bring into the true image point all the inelastically scattered electrons that normally are spread over the disk of confusion. It would improve thereby the resolution, but the contrast would be distinctly less than if the inelastic component were completely removed from the imaging beam. It is assumed that a filter lens can be constructed which will remove them without impairing the resolving power of the instrument.

EFFECT OF VOLTAGE

It would appear from equation (3) that it would be advantageous to increase the beam voltage, since $\Delta V/V$ is inversely proportional to V_0^2. The average loss is reduced and the proportion of electrons suffering no loss is increased, so that with a specimen of thickness greater than the critical value t_i the resolution and clarity of the image should both increase with voltage. Observations to this effect in the earlier days of electron microscopy led to a demand for high accelerating voltages for biological work. Now that thin sections can be readily cut the need no longer exists, and, indeed, there is a case for lower voltage when specimens thinner than t_i can be prepared, especially in combination with a filter lens.

For very thin specimens, as already noted, the contribution of chromatic electrons to the aberration disk becomes small compared with the other factors limiting resolution, yet their contribution to contrast becomes of the greatest importance. In a particle of carbonaceous material 20 Å thick, for instance, 10% of the incident electrons suffer energy loss and only 2% are elastically scattered (see the table). In the absence of a filter lens, contrast is provided only by the elastic component scattered outside the aperture, and by phase effects. Contrast can be increased by reducing the voltage so as to increase scattering. In first approximation the elastic cross-section is proportional to $1/V$ and the inelastic to $(\log V)/V$.[3] Decreasing V thus increases both types of scattering, with the elastic component increasing slightly the faster. Contrast should thus improve with decrease in voltage, even in normal conditions of microscopy, as originally pointed out by von Borries and Ruska.[21] The use of a filter lens would give a much greater improvement still, since the inelastic component exceeds the elastic in carbonaceous specimens.

CONCLUSION

In the electron microscopy of biological specimens, largely carbonaceous in nature, it would be advantageous to employ a filter lens to reject the inelastically scattered electrons, which greatly outnumber the elastic component. With specimens 100–200 Å thick, this would improve both contrast and resolution; with much thinner specimens, approaching the limit of visibility, contrast would primarily gain and this limit would be moved closer to atomic dimensions. With such specimens a lower accelerating voltage would also benefit contrast.

REFERENCES

(1) COSSLETT, V. E. *Practical Electron Microscopy*, p. 198 (London: Butterworths Scientific Publications, 1951).

(2) VON BORRIES, B. *Die Uebermikroskopie* (Berlin: Saenger, 1949).

(3) LENZ, F. *Z. Naturforsch.*, **9a**, p. 185 (1954).

(4) WHIDDINGTON, R. *Proc. Roy. Soc. A*, **89**, p. 554 (1914).

(5) TERRILL, H. M. *Phys. Rev.*, **24**, p. 616 (1924).

(6) LENARD, P. *Quantitatives über Kathodenstrahlen aller Geschwindigkeiten* (Heidelberg: Winter, 1925).

(7) LEA, D. E. *Actions of Radiations on Living Cells*, p. 24 (Cambridge: The University Press, 1946).

(8) BETHE, H. *Handbuch der Physik*, **24** (i), p. 273 (1933).

(9) EHRENBERG, W., and FRANKS, J. *Proc. Phys. Soc.* [*London*] *B*, **66**, p. 1057 (1953).

(10) VON BORRIES, B. *Optik*, **3**, pp. 321–377 and 389–412 (1948).

(11) HAINE, M. E., and MULVEY, T. *J. Sci. Instrum.*, **31**, p. 326 (1954).

(12) BOERSCH, H. *Z. Naturforsch.*, **2a**, p. 615 (1947); *Optik*, **5**, p. 436 (1949).

(13) BOERSCH, H. *Z. Phys.*, **134**, p. 156 (1953).

(14) RANG, O. *Optik*, **11**, p. 328 (1954).

(15) MARTON, L. *Advances in Electronics and Electron Physics*, Vol. VII (New York: Academic Press). To be published.

(16) GABOR, D., and JULL, G. W. *Nature* [*London*] **175**, p. 718 (1955).

(17) MARTON, L. *Colloquium of the Centre National de la Recherche Scientifique, Toulouse*, April, 1955.

(18) HAINE, M. E. *Colloquium of the Centre National de la Recherche Scientifique, Toulouse*, April, 1955.

(19) SCHERZER, O. *Optik*, **2**, p. 114 (1947).

(20) ARCHARD, G. D. *Proc. Phys. Soc.* [*London*], *B*, **68**, p. 817 (1955).

(21) VON BORRIES, B., and RUSKA, E. *Z. Phys.*, **116**, p. 249 (1940).

The analysis of gases at low pressures

By M. A. CAYLESS, A.R.C.S., B.Sc., A.Inst.P., The British Thomson-Houston Co. Ltd., Rugby

[*Paper first received* 12 *September, and in final form* 12 *October*, 1955]

An apparatus for handling and analysing small quantities of gas at low pressures is described. To avoid contamination an all-glass construction is employed and manipulation is entirely over mercury. Gases and gas mixtures may be readily introduced into experimental vacuum devices in measured quantities of 1 μcm^3 and over at pressures as low as 10^{-6} mm of mercury. Evolved gases may be analysed at pressures between 10^{-3} and 1 mm of mercury using mainly physical properties such as vapour pressure, diffusion and absorption for indentification and separation. Normally an accuracy of about 2% of the total quantity is obtained when 5 μl. or more is available. A method is described of identifying much smaller quantities in certain circumstances.

In the study of electron emission, discharge phenomena and vacuum processing techniques, it is frequently necessary to have facilities for introducing and manipulating small measured quantities of gases or gas mixtures in the pressure range from a fraction of a micron to a few millimetres of mercury. Further, the analysis of the gases present in evacuated devices, such as electric lamps and electronic devices, and the gases evolved under vacuum conditions from the materials which go into their construction is often of great importance.

The apparatus to be described enables gases to be introduced into experimental devices which have been constructed and processed on the apparatus in the best vacuum conditions. Quantities of a few micron cubic centimetres upwards may be handled with ease at pressures of one tenth of a micron and above. Gases evolved may be analysed in quantities of between 5 and 100 μl. to an accuracy which is generally about 2% of the total quantity, though minority constituents can be determined much more accurately in certain circumstances.

APPARATUS

A schematic diagram of the apparatus is shown in Fig. 1.

On the right is shown the apparatus for introducing known gases at a pressure of a few millimetres, reducing the pressure to the micron range and admitting measured doses to the specimen. In the centre, between the two long cut-offs *B*1 and *B*2, are the pumping heads to which the specimen tubes are attached. To the left of *B*2 is the analysis system. Thus the apparatus is essentially a pumping head to which gases may be admitted *via B*1 or removed for analysis *via B*2.

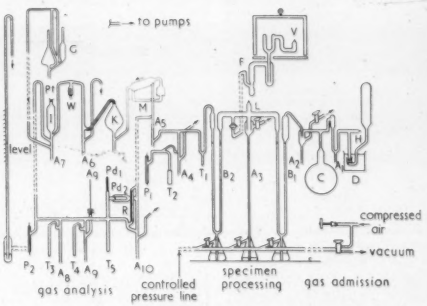

Fig. 1. Gas handling and analysis apparatus

The whole apparatus is constructed from C.9 borosilicate glass with no demountable joints of any kind, glass-to-metal seals being used for attaching all leads and metal parts. No stopcocks are used in positions where they would be in

**

prolonged contact with the gas, or where they would have to be turned during the actual manipulation of the gas, which is done entirely by mercury cut-offs as shown. Provision is made for evacuating the mercury reservoirs so that all the mercury columns may be lowered for a long pump for outgassing on first evacuating the apparatus. Provided this is done the elaborate gas traps described by some authors (e.g. Norton and Marshall[1]) are unnecessary, and no evidence of seepage up the columns has been found. A two-stage glass mercury vapour pump is used to evacuate the apparatus to below 10^{-5} mm of mercury and, when closed off by the cut-offs, it remains at a pressure below 10^{-4} mm of mercury for at least eight hours, and below 10^{-3} mm of mercury for at least a fortnight without baking or torching the apparatus; (this would be most undesirable because it would increase the absorption of the gases on the walls).

The apparatus is constructed from tubing of 5–7 mm bore for the most part, being attached at the points shown in Fig. 1 to a 2 cm diameter glass main pumping line which is attached to a rigid steel frame and which forms the structural backbone of the apparatus. The mercury flasks rest on a heavy gauge steel tray which is an integral part of the frame. Apart from one or two steadying clips to prevent vibration, and supports for the McLeod and Töpler bulbs there are no further clamps to the frame. This method of construction has proved successful in avoiding stress fractures which present quite a problem in an apparatus of this type.

The McLeod gauge *G*, which is the primary measuring instrument of the apparatus, has two bulbs, of 140 and 20 cm^3 trapped volume, and capillaries of 1·5 and 2·5 mm bore Veridia precision bore tubing by Chance Bros. Ltd. These are ground to prevent sticking as described by Rosenberg,[2,3] a procedure which we have found to be very effective. Readings are repeatable to 1% between 5 μ and 4 mm, and to a few per cent down to 1 μ.

The sintered glass plug *D* (Pyrex grade 4) is immersed in mercury so that known gases may be admitted from glass cylinders fitted with similar plugs, mounted in such a way that they may be brought into contact with *D* under the mercury as shown. The cut-off *A*1 acts as a manometer when raised and can be used to measure the amount of gas admitted at pressures from 1–30 mm of mercury. This pressure may be subsequently reduced some 300 times by expanding the gas into the 1·5 litre bulb *C*. This reduction may be repeated if desired to obtain still lower pressures by closing *A*1 and pumping out *C*. The chamber at the top of *B*1 may be varied in volume from 3 to 60 cm^3 by changing the mercury level, and by manipulation of *A*2 and *B*1, measured doses of gas may be admitted to the specimen head. Doses from 1 μ cm^3 to 1000 μl. are easily obtained. Convenient supplies of oxygen and hydrogen may often be obtained from the silver and palladium tubes mounted in the analysis apparatus.

When mercury vapour and a residual gas pressure of 10^{-4}–10^{-5} mm of mercury are no objection, the experimental specimen is conveniently attached to the low pressure head at *L*. Where mercury vapour must be excluded from the specimen and the highest vacua are required it is attached to the high vacuum head at *V*, where it may be baked and outgassed as required. A mercury vapour pump *F* is fitted between this and the main system to maintain the best vacuum conditions during treatment of the specimen. Pressures of 10^{-10} mm of mercury have been obtained and measured in this position.

An alternative use to which the pressure reduction apparatus may be put is for admitting gas for analysis at rather higher pressures than normal, i.e. up to about 20 mm of mercury. The contents of discharge tubes have been examined in this way. They are attached *via* a break seal to the extreme right tip *H* of the apparatus shown.

Gases to be analysed are passed through cut-off *B*2 into the apparatus on the left. Those which are condensible at liquid air temperatures are frozen out in the trap *T*1 and the remainder are pumped through a miniature mercury vapour pump into the apparatus beyond. This pump is of the horizontal type, the parallel jet leading into a parallel-sided tube 10 cm long and 6 mm diameter with 1 mm clearance. It has a speed commensurate with the dimensions of the tubes of the apparatus and will evacuate completely against a back pressure of a millimetre or more. Thus the analysis separates naturally into two parts: analysis of those gases frozen out in the liquid air trap ("condensibles") and those which are not ("non-condensibles").

The method of analysis employed is basically the familiar low pressure technique, which appears to have been first described by Langmuir,[4] in which the analysis is performed at pressures of 1–100 μ. So far as possible, purely physical processes, such as condensation and diffusion, are used to separate the constituents, supplemented by simple gaseous reactions. Since Langmuir, a number of authors have described methods of this type.[5–8] Others (notably Prescott and Morrison[9] and Shadduck and van Zee[10]) used rather different methods involving the use of prepared reagents. We have preferred to avoid these because of the uncertainty of the absorption errors which may be introduced. All these authors found that about 1 μl. is the smallest amount of gas which may be analysed in an apparatus of normal size (a few hundred cubic centimetres), with about 5 μl. for any quantitative accuracy. This is borne out by experience with the present apparatus and is largely the result of the limitations of the McLeod gauge as a quantative instrument.

ANALYSIS OF CONDENSIBLE GASES

These are separated by their vapour pressures in the manner first described by Campbell.[11] They are transferred to the tip *T*2 where they are confined by means of cut-off *A*4 in a volume of 20 cm^3 which contains a Pirani gauge *P*1. This consists of a straight platinum wire 0·0025 cm diameter and 10 cm long, mounted axially from tungsten leads in a 5 mm bore tube, following the general design of Rittner.[12] With the wire at a fixed temperature of 100° C in a balanced bridge, this gauge has an accurately linear calibration between 1 and 1000 μ when the square of the bridge voltage is plotted against the pressure.[11] The continual adjustment of the bridge required is more than outweighed by the ease of conversion to pressure readings afforded by the linear calibration and by the high sensitivity over the large range.

The tip *T*2 is surrounded by a copper block containing a copper-constantan thermocouple and is warmed up slowly and uniformly, taking about thirty minutes from liquid air to room temperature, the pressure being measured every thirty seconds. When taken in this way the vapour pressure curve shows a sharp kink as each gas is completely vaporized, as shown in Figs. 2 and 3. The rounding-off found by some authors (e.g. Ransley[4,8]) only occurs if the warming is done too rapidly. The most convenient method of warming is to pour off the liquid air, replace the flask, and then blow into it through a tube. This is easier and more controllable than the various electrical heaters tried. Carbon dioxide, sulphur dioxide and water are easily separated in this way, though the actual quantity of water present may only be estimated

because of wall absorption. Hydrocarbons and other mixtures which form solid solutions on freezing do not show as discontinuities in the curve, but reveal their presence by a gradual upward slope, as shown in Fig. 3.

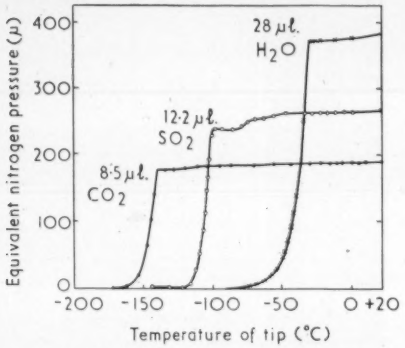

Fig. 2. Vapour pressure curves of condensed gases

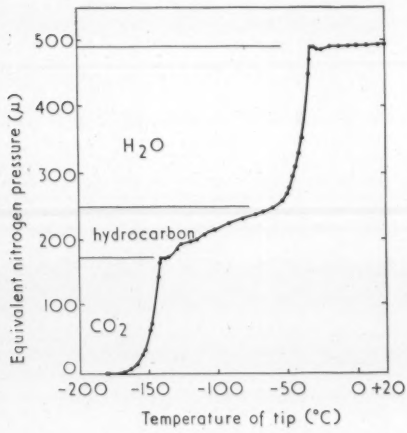

Fig. 3. Vapour pressure of condensed gases evolved from unclean nickel wire

Small quantities of one gas in the presence of another can be readily detected to about one part in a thousand if the minority gas has an appreciably lower vapour pressure. If the major constituent vapourizes first a minor constituent of higher vapour pressure may be readily detected if the former is first pumped off.

A refinement of this method is to pump off the gases as they vaporize through a constriction of suitable dimensions. In this way each gas gives rise to a peak, so that when the pressure is plotted against time, the area under the curve is proportional to the quantity of gas, provided suitable precautions are taken in measurement. This method has only been used to obtain semi-quantitative results, but the increased sensitivity and selectivity available is often valuable. Fig. 4 shows the condensible gases evolved from a heated soda-glass surface and separated in this way, the Pirani gauge being replaced by an ionization gauge in this case to further increase the sensitivity. Several components are seen in addition to the usual water and carbon dioxide.

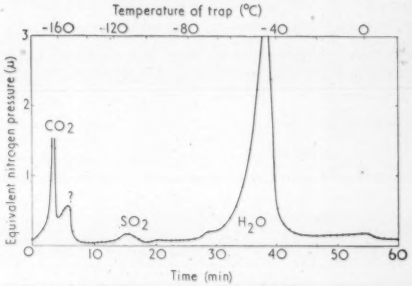

Fig. 4. Differential vapour pressure curve of gases evolved from heated soda glass

The system was continuously pumped at a speed of 5–10 l./min whilst the temperature was raised. The gas was evolved when about 500 cm² surface of C19 glass was heated at a uniform rate to 530° C during one hour.

ANALYSIS OF NON-CONDENSIBLE GASES

These are pumped into the apparatus to the left of *A*5 in Fig. 1 by the miniature mercury vapour pump *M* and the Töpler pump *K*. When *A*5 is closed this forms a closed circulatory system. Except that hydrogen is determined by diffusion through a palladium tube the method is essentially the same as that described by Kenty and Reuter.[7] We have preferred to use a Töpler pump in addition to the vapour pump because of the more precisely determined volume into which the gas is compressed, and because of the increased facilities which it provides for manipulating gases in the vacuum (such as making precise pressure adjustments). The connecting tube is short, and three strokes are usually sufficient.

Mixtures of hydrogen, carbon monoxide, oxygen and nitrogen have been successfully analysed in the pressure-range 10–100 μ to an accuracy of about 2%. Briefly, the gas is compressed into the known volume (328 cm³) between cut-offs *A*6 and *A*10, and the pressure measured on the McLeod gauge. Liquid air is placed around the tip *T*3, and any pressure reduction is due to carbon dioxide which was not completely frozen out in *T*1 (the vapour pressure is still quite appreciable at −180° C). Freezing acetone is kept round *T*5 as a precaution during the whole analysis to eliminate any water evolved from the walls during the heating operations. Hydrogen is then diffused out by heating the palladium tube *Pd*1 to 450° C with a small electric furnace. This takes about fifteen minutes if a gas mixture is present, though only a few seconds if hydrogen alone is present. If only a small quantity of hydrogen is expected the tube *Pd*2 may be

used, and the hydrogen collected by the pump *M* and measured separately.

After pumping the gas into the Töpler bulb, pure oxygen is admitted from the atmosphere by heating the thin silver tube *Ag* to about 800° C (see Ransley[6] and Taylor[14]). The mixture is then compressed into the region between *A6* and *A7*, whence it is further compressed to several millimetres in the ignition bulb *I* by raising the mercury in *A7*. Momentary heating of the 0·02 cm diameter platinum wire *Pt* to a dull red suffices to burn the carbon monoxide to carbon dioxide. This is repeated several times to ensure that practically all the gas trapped between *A6* and *A7* is burned. Cut-off *A7* is then lowered right down and the pressure measured, liquid air is applied to *T4*, and the carbon dioxide frozen out, giving the amount of carbon monoxide originally present. We have preferred this method (Kenty and Reuter's) to that of Ransley, in which the gas is not compressed, but burned at a filament during some fifteen minutes, to avoid the complication of the clean-up of oxygen at a platinum filament.[6]

The remaining gas is re-compressed into the space between *A6* and *A7* and the oxygen removed by flashing the tungsten filament *W* several times to about 1600° C for a second or so. The remainder is nitrogen (or inert gas) whilst the difference gives the amount of oxygen not consumed in the ignition, from which the original amount of oxygen can be found. The contents of the traps are measured at the end of the analysis as a cross-check.

The need to separate nitrogen from the inert gases does not often arise, but it may be accomplished by absorbing the former with a heated tantalum filament[13] or by combined Pirani and McLeod gauge readings and pumping speed measurements.[7] A Pirani gauge *P2* and a calibrated capillary *R* on *A10* have been incorporated for this purpose. Methane can be separated by Ransley's method,[6] which involves combustion with oxygen at two temperatures: 500° C to burn the carbon monoxide and 1150° C for the methane.

DISCUSSION

The apparatus has been used and found satisfactory for a variety of experiments, including investigations on the behaviour of cathodes in the presence of various gases, the analysis of the contents of discharge tubes, and the gases evolved from hot glasses and metals, electrodes under bombardment, and cathodes upon activation.

As an example of an analysis in which a variety of gases were present, the table shows the gases which were evolved on heating a 6 cm length of 0·1 cm diameter nickel wire to 850° C for 30 min. The wire was uncleaned and the results are compared with those of Jacobs and Wolk[15] who out-gassed uncleaned nickel cathode sleeves.

Gases evolved from nickel

	Present results %	*Jacobs and Wolk* %
Water	11	trace
Carbon dioxide	7	5·4
Other condensible gas	2	—
Oxygen	1	7·2
Hydrogen	34	41·6
Carbon monoxide	42	35·1
Nitrogen (residue)	3	11·1

The results are similar in showing the great preponderance of hydrogen and carbon monoxide. The value of 11% for water is a minimum value because of wall absorption losses. The apparatus of Jacobs and Wolk was not suitable for the detection of water, nor did they obtain a vapour-pressure curve, which reveals (Fig. 3) the presence of condensible gas (probably hydrocarbon from the unclean surface) other than carbon dioxide and water. It can be seen that the water and carbon dioxide points are clearly visible amongst this general background.

An obvious shortcoming of this method of analysis is in the determination of small amounts of oxygen which can easily be overlooked, or badly in error when a considerable amount has to be added for igniting carbon monoxide. There is no easy solution of this difficulty.

The only way of appreciably increasing the sensitivity of the apparatus so that it can analyse smaller quantities is to decrease the total volume. Kenty and Reuter[7] have described a miniature apparatus which will analyse samples of the order of 50 μ cm^3.

CONCLUSIONS

This apparatus has now been in continuous use in this Laboratory for the past eighteen months. It has shown itself to be trouble-free and has yielded reliable results under a variety of diverse conditions. The ease with which small quantities of gas mixtures of known composition can be introduced into vacuum or discharge devices, and the ability to analyse small quantities of gas, have proved of value in several research programmes into gas discharges and cathode problems.

ACKNOWLEDGEMENT

The author would like to thank his colleagues of the British Thomson-Houston Research Laboratory for many helpful discussions and assistance in the construction of the apparatus.

REFERENCES

(1) Norton, F. J., and Marshall, A. L. *Trans Amer. Inst. Min. Metall. Eng.*, **156**, p. 351 (1944).
(2) Rosenberg, P. *Rev. Sci. Instrum.*, **9**, p. 258 (1938).
(3) Rosenberg, P. *Rev. Sci. Instrum.*, **10**, p. 131 (1939).
(4) Langmuir, I. *J. Amer. Chem. Soc.*, **34**, p. 1310 (1912).
(5) Ryder, H. M. *J. Amer. Chem. Soc.*, **40**, p. 1636 (1918).
(6) Ransley, C. E. *Analyst*, **72**, p. 504 (1947).
(7) Kenty, C., and Reuter, F. W., Jr. *Rev. Sci. Instrum.*, **18**, p. 918 (1947).
(8) Dalton, R. H. *J. Amer. Chem. Soc.*, **57**, p. 2151 (1935).
(9) Prescott, C. H., and Morrison, J. *Industr. Engng Chem., Analyt. Ed.*, **11**, p. 230 (1939).
(10) Shadduck, H. A., and van Zee, A. *J. Amer. Ceram. Soc.*, **25**, p. 69 (1942).
(11) Campbell, N. R. *Proc. Phys. Soc.* [*London*], **33**, p. 287 (1921).
(12) Rittner, E. S. *Rev. Sci. Instrum.*, **17**, p. 113 (1946).
(13) Ransley, C. E. *G.E.C. J.*, **11**, p. 135 (1940).
(14) Taylor, J. B. *Rev. Sci. Instrum.*, **6**, p. 243 (1935).
(15) Jacobs, H., and Wolk, B. *Proc. Inst. Radio Engrs*, **37**, p. 1247 (1949).

A study of the Formvar replica process

By A. W. Agar, B.Sc., A.M.I.E.E., A.Inst.P.,* and R. S. M. Revell, B.Sc., A.Inst.P., Research Department, Metropolitan-Vickers Electrical Co. Ltd., Manchester

[*Paper first received* 20 *July, and in final form* 31 *October*, 1955]

A detailed study has been made of Formvar replicas of various depths of structure. Plain replicas, shadowed replicas and replicas shadowed on the back surface were prepared from each specimen and identical areas were photographed in the electron microscope. An interferometer microscope was used to measure the depths of structure on the metal specimens and on the back surfaces of the replicas. A reconstruction has thus been obtained of the shape of the replica cross-section under various conditions.

As a result of this work, it is concluded that an approximately true negative replica of the surface is only formed in the rare cases when the thickness of the film is more than double the depth of the structure. In spite of this, however, the Formvar replica is suitable for many classes of work and precautions can be taken to offset its deficiencies.

An explanation is given for the varied published estimates of plastic replica resolution, and the resolution under standard conditions is estimated.

The Formvar replica process still remains one of the simplest of the available replica methods and is very reliable. It is particularly easy to deduce the specimen structure from the contrasts observed in the electron microscope, and it gives very good correlation with the appearance of the surface under the optical microscope. It has, however, long been realized that the so-called negative plastic replica has not always a plane back surface, but that some structure sometimes penetrates to this surface. The subject has been discussed by several authors. Deacon and others,[1] Bailey and Vernon-Smith,[2] and Nutting and Cosslett[3] have all put forward suggested shapes for the back surface of Formvar replicas. Trotter[4] shadow-cast the back surface of a replica while it was still on the specimen, and showed some structure present on this surface. The above discussions, however, have been qualitative only, because the depth of the structure on the specimen and the thickness of the replica film were not measured.

A more quantitative investigation recently made by Deubner, Kimmel and Rollwagen[5] has come to our notice since this work was completed. Their investigation was made under rather specialized conditions and is discussed later.

In addition, the resolution of a plastic replica has been variously estimated to be between 100 and 500 Å or more, these estimates sometimes being made from replicas of very poor quality.

The work here reported was designed to elucidate the above problems with particular reference to the type of structure generally encountered in surface studies with the electron microscope.

EXPERIMENTAL METHOD

Interferometer microscope

Some information about the shape of a replica can be obtained by the careful study of electron micrographs of plain replicas, shadowed replicas and replicas shadowed on the back surface, all taken from the same area of a metal surface. This gives an accurate measure of horizontal distance, but not of height.

The height measurements were made with the aid of a reflexion interferometer microscope.[6] This microscope produces a fringe system across the normal image of the surface under examination, and has a resolution slightly better than that given by an ordinary 4 mm objective. This is much superior to the lateral resolution offered by most other interferometric methods, and is an essential requirement for the type of measurements recorded here.

Using monochromatic illumination of wavelength 5780 Å, a height difference of 1930 Å on the specimen results in a displacement of the fringe system by one fringe width. As a fairly close fringe spacing is necessary in order to obtain adequate delineation of the individual features, the microscope could not be used at its maximum sensitivity; however, sufficiently accurate height measurements were still possible. The necessary variations of fringe spacing and direction were obtained by the use of tilting stage.

Specimen

In order to obtain useful measurements on the metal structure, it was necessary that the features should be clearly resolved by a 4 mm objective. A suitably coarse structure (pearlite) was obtained from a plain 0·6% carbon steel which was austenized at 930° C for 30 min, and then isothermally transformed at 675° C for 15 min.

Four specimens of this steel were prepared by mechanical polishing and acid etching alternately until the flowed layer was removed. They were given final etches of 20, 10, 5 and 2 s respectively in 1% nital. These treatments resulted in heavy, normal, light and invisible etches respectively, as judged by an examination under the optical microscope, using normal illumination. After etching, the specimens were rinsed in distilled water, absolute alcohol and then dried in hot air.

The cleaved face of a calcite crystal was also used, as it provided a different type of structure for examination, and was especially suitable for the interferometric measurements.

EXPERIMENTAL PROGRAMME

The experiments had to be designed to give the height of various structural features, the average thickness of the replica film and the height of any structure penetrating to the back surface of the replicas of the various specimens. It was also desirable to relate the measurements on these replicas to their appearance in the electron microscope, and to that of the specimens themselves under the optical microscope, thus establishing the relevance of the results to the etching depths and replica techniques commonly used. The experiments were therefore based on the examination of

* Now at Research Laboratory, Associated Electrical Industries Ltd., Aldermaston, Berks.

identical areas of a given specimen under different conditions, as follows:

(*a*) Electron microscope examination of:
- (i) a negative Formvar replica, prepared as described below;
- (ii) a shadowed Formvar replica [using the replica from (i) after photography was complete];
- (iii) a replica shadowed on the back surface while it was still on the specimen surface. [After shadowing, the replica was then backed, stripped and mounted as for (i).]

(*b*) Interferometer microscope examination of:
- (i) a replica film on the specimen surface heavily coated with evaporated silver on its back surface;
- (ii) the specimen surface itself, also silvered.

Where structure was observed on the back surface of a replica, the interferometer experiment (i) was repeated with a thicker Formvar film on the specimen.

The success of the experiment clearly depends on the recognition, in each of the five different examinations, of the areas previously studied. For this purpose, the surfaces were scratched with a fine mesh of lines by means of a microhardness diamond, as previously described.[7] A loading of about 0·75 g for the metal specimens and about 0·25 g for the calcite crystal resulted in scratches which were always visible in the replica films, but which were not so deep as to cause tearing of the film.

REPLICA FILM THICKNESS

It is necessary to use uniform replica films of known thickness if the measurements of the structure height on the back of the film are to have any significance. Most methods of preparing plastic films result in wide variations of film thickness between different areas of the same film and between successive films. A simple method, which is described in detail elsewhere,[8] was developed for producing suitable films. In this, a Formvar solution of suitable strength was held in a separating funnel, the outlet tube of which was replaced by a length of capillary tubing. The specimen was immersed in the Formvar solution which was then allowed to drain away slowly through the capillary tube. It was found that the thickness of the film deposited on the vertical surface of the specimen was uniform to $\pm 10\%$ and was proportional to the solution concentration. The measurements also showed that the average thickness of replica films has generally been underestimated. A typical "thin" replica film, showing a blue coloration, is of the order of 700–1000 Å thick. Such a film certainly requires backing if it is to be removed without strain from an etched metal surface, and it is apparent that many replica films must be much thicker than this. Films 400 Å thick (a figure often quoted for the thickness of replicas) are practically colourless and too thin for use as replicas except on surfaces with a much lighter etch than is usually employed.

The replica films used in this investigation were all of average thickness 700 Å unless otherwise stated.

REPLICA TECHNIQUE

The Formvar replicas were backed with a thick layer of collodion and wet stripped by the modified backed replica process.[9] The solvent now employed for the collodion is ethyl acetate, as it evaporates much more quickly than amyl acetate.[10] Although it is still advisable to use the slower-acting amyl acetate in the washing baths when removing the backing film, the backed replica process is now speedy enough to satisfy the requirements of a standard technique for routine examinations. In a few cases where extreme speed is required, the dry-stripping technique may be used, but it has important limitations in comparison with the backed replica method which are discussed more fully later.

The replica films were positioned by the method described by Booker,[11] so that the identification scratch system lay across the large central aperture (350 μ diameter) of some special grids.

Since the experimental plan called for the removal of several replicas from the same specimen surface, a preliminary experiment was carried out in which nineteen replicas were removed from the same area of an etched chrome-molybdenum steel surface. Comparative micrographs showed the replicas to be completely reproducible until spots of corrosion began to appear on the specimen surface. Corrosion was reduced to a minimum by flooding the specimen with absolute alcohol as soon as the replica film had been detached, and by drying it in a hot air stream. This procedure was adopted for the present series of experiments, and no corrosion effects were noticed.

RESULTS

Structure on the back surface of the replica

The electron micrographs and the interferometric examination yielded the qualitative information on the structure penetrating a standard 700 Å replica film shown in Table 1: Some of these results are demonstrated in Figs. 1–6.

Fig. 1 shows an unshadowed Formvar replica of an area of specimen 2. Fig. 2 shows the replica shadowed on the structure surface, and Fig. 3 a replica film which was shadowed on the back surface before removal from the metal. These figures show that all the principal structural features appear on the back surface of the replica film. The most noticeable difference between Figs. 2 and 3 is the broadening of the lamellae and other narrow features on the back of the replica film. It will also be noted that, as expected, the fine-scale roughness of the metal surface has not penetrated the film. Fig. 4 is an enlargement from Fig. 3 which shows the shadows cast by the ends of some lamellae on to an adjacent grain

Table 1. *Effect of structure height on replica reproduction*

Specimen number	*Etch time (s)*	*Average structure height on specimen surface Å*	*Structure penetrating the replica film*
1	20 (heavy)	1600–2000	All details except finest.
2	10 (normal)	1000–1600	All details except finest.
3	5 (light)	500–800	Large grains only.
4	2 (invisible)	200–300	Very little; a few large grains just detectable by interferometry.

(the shadowing angle was $\cot^{-1} 2$). This gives a very clear picture of the shape of the back surface of the replica film in this region, and it will be seen that the curvatures are much more marked than has been previously supposed. Fig. 5 is a micrograph of the surface from the same area as Figs. 1, 2 and 3 taken on the interferometer microscope. Measurement of the fringe displacement over some lamellae and grain boundaries show them to range between 1200 and 1600 Å in height.

Replica on shallow structure

Fig. 6 shows a replica 700 Å thick from specimen 4, where the average height of the structure details is about 300 Å. No contour effects can be detected around the structure boundaries and no shadows appear on a replica shadowed on the back surface. [The term "contour effects" used in this paper refers to the artefacts arising from the curvature of the back surface of the replica over steep level changes in the specimen surface. The effect is shown in Fig. 11; the type of misinterpretations arising are illustrated by Bailey and Vernon-Smith[2] and Nutting and Cosslett.[3]] It may therefore be supposed to be a true negative replica. However, under the interferometer microscope, the back surface of such a replica over large grains was seen to be sometimes as much as 200 Å above the general level of the film. The discontinuity of the fringes at grain boundaries appeared to be quite sharp. However, taking account of the limited lateral resolution of the interferometer, this means no more than that the change of level takes place within a distance of perhaps $\frac{1}{2}\mu$; such a small slope could not be detected by any contrast change in a replica.

Measurements of structure height

Since all the main structural features of specimens 1 and 2 were evident on the back surface of the 700 Å replica film, an effort was made to obtain a nearer approach to a true negative replica from these more deeply etched specimens by using films of 1400 and 4000 Å thickness. Table 2 summarizes the measurements made on the various specimens with the aid of the interferometer microscope.

Two principal points of interest arise from these figures. Firstly, it is remarkable that with a 700 Å film on structure of a comparable depth, about 70% of this depth penetrates to the back surface of the replica. This means that the thickness variation is relatively small, and is particularly surprising in view of the high contrast of such a replica (Fig. 1).

Secondly, it is apparent that a true negative replica of structure such as lamellae can be obtained by a sufficiently thick replica film (a film 4000 Å thick is about sufficient for lamellae 1750 Å deep). However, extended areas of elevation or depression (such as metal grains) have quite remarkable powers of penetration. Thus, a grain 1340 Å high is still 840 Å high at the back surface of a 4000 Å film.

In this connexion, the measurements on the calcite crystal appear even more remarkable. As can be seen in Fig. 7, there are large parallel flat areas with abrupt changes of level at the cleavage steps. These steps are conveniently measured by the interferometer microscope, and results on two typical ones are tabulated below (Table 3).

Table 3. *Measurements on structure penetrating replica films on the calcite crystal*

Height of step on crystal surface (Å)	*Height on back of replica films (thickness T)* (Å)		
	$T = 700$ Å	$T = 1400$ Å	$T = 4000$ Å
3460	2960	2850	3000
520	460	340	340

It will be seen that this type of structure will persist through a replica film even eight times thicker than the structure height, and that there is some evidence for a slight increase in the step penetrating the 4000 Å replica.

Interference micrographs of the crystal surface and the back of the 1400 Å film are shown in Figs. 8 and 9 respectively. It will be seen that the fringes on the back of the thick replica film are starting to show some curvature, which indicates that the change in level is spread over perhaps $\frac{1}{2}\mu$ on either side of the actual step. The effect is even more marked in the fringes observed on the back of the 4000 Å film, so that in the case of these thicker films it is no longer realistic to call these level changes a "step."

Referring again to Fig. 7, which shows a standard film on a step 600 Å high, the apparent change in intensity between the different levels of the crystal surface is due to the contour effect resulting from the curvature of the back of the replica film. If this region of Fig. 7 is blanked out, it can be seen that the intensity of the image (and hence the film thickness) is sensibly constant over the two planes. This is in qualitative agreement with the interferometer results. It was further confirmed by microphotometer readings of the densities on the electron micrograph.

Table 2. *Measurements on structure penetrating replica films of different thickness*

Structure measured	*Height on specimen surface* (Å)	*Height on back of replica films (thickness T)* (Å)		
		$T = 700$ Å	$T = 1400$ Å	$T = 4000$ Å
Spec. 1, lamellae	1750	1270	870	<200
Spec. 1, grain edge	1360	960	840	840
Spec. 2, lamellae	1160	700	480	<200
Spec. 2, lamellae	960	620	270	Not detectable
Spec. 2, lamellae	770	520	Not detectable	Not detectable
Spec. 3, lamellae	700	480	—	—
Spec. 3, grain	720	530	—	—
Spec. 3, grain	500	340	—	—
Spec. 4, lamellae	300	Not detectable	—	—
Spec. 4, grain	300	200	—	—

Reconstruction of the shape of the replica film

The information obtained from the different micrographs of the same area of the specimen surface was combined to reconstruct the actual shape of the replica film.

The electron micrographs of the replicas shadowed on the structure surface and on the back surface gave the general lateral dimensions of the structure. The film thickness was known, and the interferometer micrographs provided the height measurements of the various structural features. In view of the limited resolution of the interferometer microscope, the extent of the curvature of the back surface of the replica was found by taking microphotometer readings on electron micrographs of the areas in question.

Typical replica cross-sections have been deduced for a crystal face with cleavage steps (Fig. 10), and a metal surface

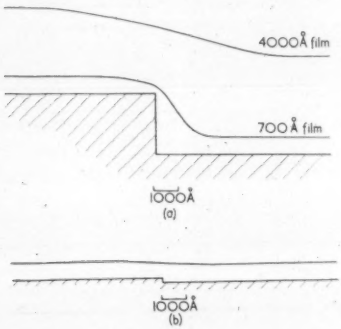

Fig. 10. Typical cross-sections of Formvar replicas on the calcite crystal

(*a*) Films 4000 and 700 Å thick over a step 2500 Å high.
(*b*) Film 700 Å thick over a step 200 Å high.

(*a*) with structure shallow compared with the replica thickness, (*b*) with structure comparable with replica thickness, and (*c*) with structure much deeper than replica thickness [Fig. 11 (*a*), (*b*), (*c*)].

In connexion with these reconstructions, it is important to note that the replica cross-section published by Deubner, Kimmell and Rollwagen[5] is not a scale drawing. No numerical values of step height are given, but from the interferometer picture published it seems to be of the order of 1000 Å. The "range of influence" of the replica (that region of the replica where the back surface is not plane) is quoted as 6–7 μ which is some 60–70 times greater than the step height. The slope of the back surface of the replica should, therefore, be negligibly small [less than on Fig. 11(*a*), for example].

The results of their investigations can strictly only be compared with our measurements on the calcite crystal, which has somewhat similar surface structure. Since no measurements of a comparable step (1000 Å) on the calcite were made, however, an extended metal grain in specimen 2 is taken as roughly equivalent to their specimen, for the purposes of comparison of results. Assuming, as seems likely, that the thickness of their replica was comparable with that of the standard film, it will be seen from Fig. 11(*b*) that we are roughly in agreement with their finding of a replica of nearly uniform thickness. However, it will also be seen that the "range of influence" of a standard replica film on such structure is only of the order of 1000 Å. This is well below the resolving limit of the interferometer microscope, which has a much superior lateral resolution to the multiple beam interference method. It seems likely that the discrepancy between their figure for the range of influence, and ours for the region of contour effects, is due to their use of the multiple beam interferometer for these measurements rather than electron micrographs.

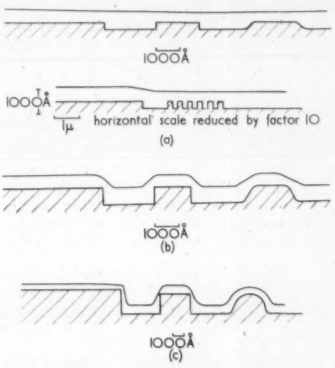

Fig. 11. Typical cross-sections of Formvar replicas. Films 700 Å thick on pearlite structures

(*a*) Structure 300 Å deep.
(*b*) Structure 700 Å deep.
(*c*) Structure 1600–2000 Å deep.

The use of multiple beam interferometry also limits the investigation to rather special types of structure, as very few metallurgical specimens have structure coarse enough to be resolved by this method.

DISCUSSION

Qualitative structure interpretation

Besides measurements of structure height, the interferometer microscope can provide useful correlation of the qualitative accuracy of the replica process. Fig. 12 shows a negative Formvar replica in which grains *A* and *B* should be noted. Grain *A* is relatively smooth, grain *B* has a mottled appearance and it clearly shows a grading of intensity along its edge adjacent to *A* from *X* to *Y*. The maximum intensity in the image, corresponding to maximum prominence in the specimen surface, is at *Y*. Fig. 13 is an interference micrograph of the metal surface. The fringes crossing *A* can be seen to be relatively straight and those crossing *B* are ragged. The fringe shift across the boundary *A*–*B* increases from *X* to *Y*, and thus confirms the interpretation of the replica photographed in the electron microscope. This property of the interferometer microscope of producing a "contour map" of the specimen is an important advantage over normal optical microscopy in examinations of this nature.

Resolution and film thickness

The work of Bradley,[12] on the evaporated carbon replica technique shows that the primary Formvar replica is capable of a surface resolution of perhaps 30 Å. This suggests that

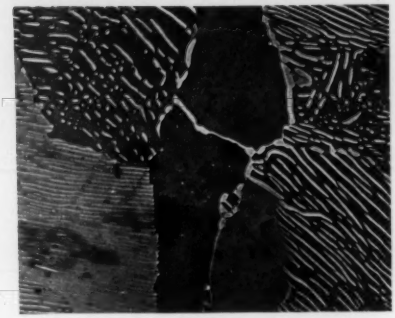

Fig. 1. Negative replica from specimen 2 (× 5000)

Fig. 2. Shadowcast replica of the same area as Fig. 1 (× 5000)

Fig. 3. Replica from the same area as Fig. 1, shadowcast on the back surface (× 5000)

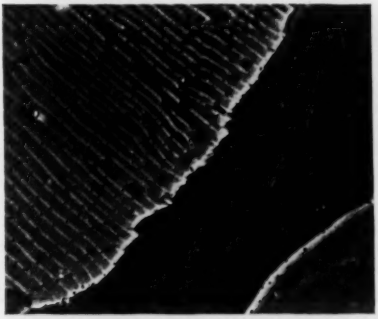

Fig. 4. Portion of Fig. 3 enlarged (× 12000)

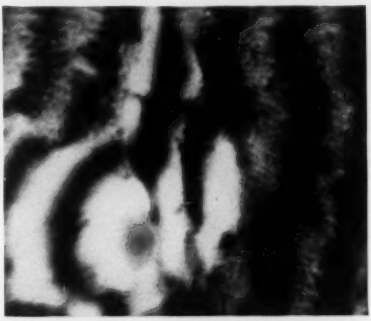

Fig. 5. Interferometer micrograph of the same area of the specimen surface as Fig. 1 (× 3500)

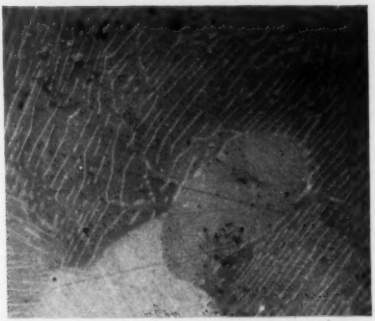

Fig. 6. Negative replica of specimen 4, very light etch (× 5000)

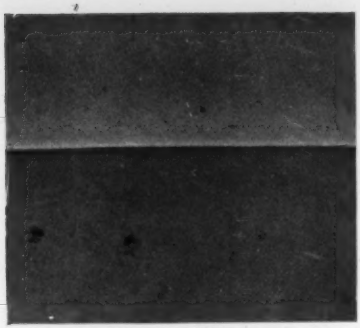

Fig. 7. Negative replica of cleaved calcite surface (× 7000)

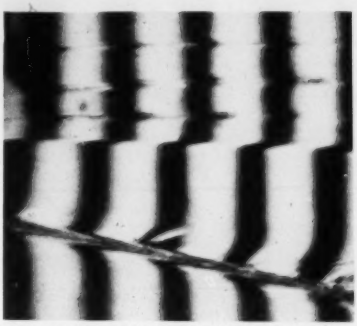

Fig. 8. Interferometer micrograph of silvered calcite surface, including the field of view of Fig. 7 (× 1200)

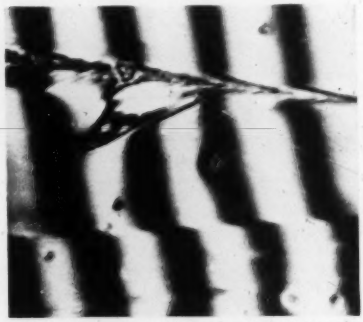

Fig. 9. Interferometer micrograph of the silvered back surface of a 1400 Å film on the specimen as in Fig. 8 (× 1200)

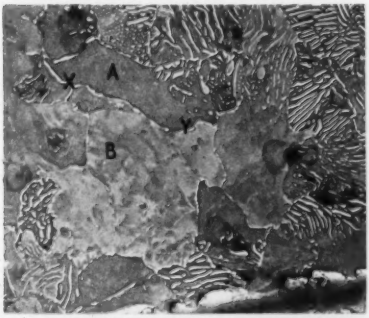

Fig. 12. Negative replica of heavily etched specimen (× 3000)

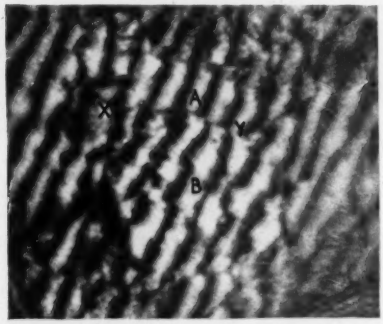

Fig. 13. Interferometer micrograph of the same area of surface as Fig. 12, showing excellent qualitative agreement on structure interpretation (× 3000)

Fig. 14. Negative replica of pit 1·5 μ deep in the calcite crystal (× 7000)

the molecular structure of the Formvar does not limit the resolution anything like as much as was formerly thought. An unshadowed replica as normally prepared never shows such a high resolving power, but this is only to be expected because of the low contrast of such small elevations or depressions in the replica surface. The 700 Å thick replica films used in this work were found to have a resolution of better than 200 Å. This implies that the minimum observable thickness difference for these films was also of this order, though it should be pointed out that the objective aperture used was considerably larger than the optimum size. In his discussion on contrast, Hall,[13] assuming that the background intensity was negligible in comparison with the intensity due to coherently scattered electrons, concluded that the minimum detectable thickness difference would be invariant with film thickness. This assumption is almost certainly not true for replica films of the thickness here used, and we found, in fact, a definite reduction in the resolution of a replica from a given specimen as the replica thickness was increased.

When a standard replica was shadowed, the measured resolution improved to better than 100 Å, and a reduction in replica thickness might be expected to improve the resolution still further.

These figures agree with those given by Deacon and others,[1] but are better than most other published estimates of plastic replica resolution. Most authors have assumed that the replica resolution was limited mainly by the molecular size of the plastic. We believe that the minimum size of fine detail reproduced faithfully in a structure surface of the replica is probably less than 25 Å, and that, in plastic replicas, the contrast of this order of detail is reduced below the detectable limit by excessive scatter in the bulk of the film. It is easy to explain the varied estimates of plastic replica resolution on this basis, as it then becomes principally a function of the thickness of the film employed. For example, the micrograph of a negative plastic replica, published by Heidenreich,[14] to which he assigns a resolution of 1000 Å, appears to show a very thick film on relatively fine structure and therefore one where the mass thickness differences are very small and the background scatter high.

In a discussion on inorganic replicas, Calbick[15] includes (for comparison purposes only) a figure of 500 Å as the "intrinsic resolution" for a plastic replica. This resolution is calculated with reference to the reproduction of a sharp edge in the original specimen, assuming a replica of uniform thickness. This condition is approximately satisfied by a Formvar replica, the thickness of which is comparable with or less than the depth of the structure on the specimen. The extent of the curvature on the back surface of the replica over such a feature, as measured in the present work, is also of the order of 500 Å. Thus, Calbick's "intrinsic resolution" concept applied to a plastic replica in this particular narrow sense is a measure of the region in which misinterpretation of the structure due to contour effects could occur.

Contrast in Formvar replicas

Referring again to Figs. 1 and 2, an obvious increase in contrast due to the shadowing of the replica can be seen. The tone differences between grains at different levels have been preserved, however, which indicates that contrast is still being derived in part from the Formvar film.

Comparison of these micrographs with those obtained by Trotter[4] indicates that the contrast which he attributed to differential deposition of chromium was probably, in fact, arising from the Formvar film. Heidenreich[14] considers that shadowed plastic replicas should be considered as inorganic replicas. This is a comparable assumption to that made by Trotter in his work, and would be true only if the shadowing were very heavy, the structure very shallow, or the Formvar much thinner than is used in practice. This can be shown by consideration of the equivalent mass thicknesses of the materials of a shadowed replica. A thickness change of 400 Å in the replica film (as for structure on specimen 2) is equivalent in electron scattering power to about 30 Å of gold. Thus, an image of a standard replica film with this depth of structure shadowed with 30 Å of gold will derive as much contrast from the film thickness variation as from the gold. Considerably smaller thickness variations would be detectable.

This investigation has shown that a plastic replica film does not vary greatly in thickness when the replica thickness is comparable with, or less than, the height of the structure being reproduced. In fact, as the structure height is increased in comparison with replica thickness, the film tends towards a skin type replica. This is well illustrated by Fig. 14, which shows a pit in the calcite crystal about $1 \cdot 5\ \mu$ deep, reproduced by a Formvar film 700 Å thick. The film at the bottom of the pit, though thicker than that over the crystal surface, is still thin enough to reveal fine structure at the bottom of the pit.

In spite of the marked departure of the replica from the ideal shape, the contrast on the electron micrograph (Figs. 1, 12 and 14) remains much as would be expected from this ideal. Clearly, the evidence of contrasts in the electron microscope must be interpreted with caution when deducing the shape of the object, particularly with those replicas which are assumed to be of uniform thickness (largely on the basis of such evidence). It may transpire, when exact measurements can be made, that they too depart materially from the ideal.

Comparison of results for wet- and dry-stripped Formvar replicas

(*a*) *Resolution.* This subject has been discussed in detail for dry-stripped replicas by Nutting and Cosslett.[3] They found that dry-stripped Formvar films of a given thickness could be removed from a fairly well-defined range of structure depths (as determined by etching time). Replicas detached from lightly-etched surfaces exhibited very low contrast, and their resolution was considered to be limited by the lack of contrast. Improvement of contrast was obtained by increasing the depth of etch, and the thickness of the replica film. It will be noted that this procedure runs counter to the trend for wet-stripped backed replicas, where the aim is to reduce the film thickness as much as possible. It has already been suggested that increasing the film thickness tends to reduce the effective resolution of the replica. Hence, the resolution limit of dry-stripped replicas may well be of the order of 400 Å as suggested by Nutting and Cosslett, but should not be confused with the fundamental limit of resolution of the plastic surface.

(*b*) *Replica stripping and straining.* On the subject of the stripping and straining of replicas, the present results can only be compared with a small part of the range of Nutting and Cosslett's experiments, as the maximum etching time for the specimens in this work was only twenty seconds. The only replica on which any strain lines were noted was a 700 Å replica on specimen 1 (etch 20 s), where structure of the order 2000 Å deep occurred. As far as can be ascertained, this would lie in the region "impossible to strip" on the curves published by Nutting and Cosslett. We did not find any conditions under which a backed replica could not be

detached from the specimen surface; this is hardly surprising in view of the considerable strength contributed by the backing film. We have not attempted to measure the thickness of the backing film, but it may be estimated to be not less than 5000 Å thick.

Elasticity of Formvar

Since Formvar replicas must reproduce deep structure faithfully when used as the primary replica in the evaporated carbon replica technique, it is of interest to record some observations on the physical properties of the Formvar.

A replica film was dried on to a glass slide, structure side down [a condition normally reached during the preparation technique for backed replicas[9]], and the back surface of the film was coated with evaporated silver and examined under the interferometer microscope. The identification scratches showing in the replica film were found to be above the general level of the back surface of the film. This observation may be explained by assuming that the replica was in close contact with the glass surface, and that the elevated features of the structure side of the replica were pressed flat against the glass, causing a corresponding rise in the back surface of the film. Such a replica film shows no sign of mechanical strain when mounted on a specimen grid and examined in the electron microscope. If shadowed, it is clear that the structural features are correctly reproduced. The Formvar must, therefore, have returned elastically to the shape in which it was cast.

The reproduction of the pit 1·5 μ deep (Fig. 14) by a replica film only 700 Å thick is a further demonstration of this elasticity, since there are no signs of mechanical strain of the film due to the stripping operation.

The ability of the Formvar replica to penetrate and reproduce very deep structure has previously been demonstrated by Bailey and Vernon-Smith.[2]

Properties of Formvar films on grids

The original intention in examining the back of a replica film on a glass slide under the interferometer microscope was to measure the structure penetrating the film after separation from the original specimen, to see if this was unchanged after the stripping. Since this proved impracticable, an attempt was made to examine the back surface of the replica after it had been mounted on a specimen grid. The reflectivity of the Formvar film surface was found to be insufficient to give the sharp fringes required to measure the structural features of the film, so a thick silver layer was evaporated on to it. It was then found, however, that the film in the centre of a grid square was up to thirty fringes (approximately 6 μ) below the level of the grid bars, and no fine detail could be seen. It was thought that this distortion was probably due to the silver layer, and this was confirmed by examination of the unsilvered film. A grid-mounted film was placed between a glass slide and a cover slip so that it could be examined free of any stress from the immersion oil. The reflexion was very weak, but the faint fringes obtained showed that the film in the grid openings was nearly flat, and that where irregularities existed, they rarely exceeded two fringes (about 3600 Å) in depth. For a 70 μ square grid aperture, a sag of 3600 Å can be produced by a stretching of the film of only about 0·014%.

These measurements show that the sagging and distortion of properly mounted Formvar films can be neglected in any practical application, such as a magnification calibration by grating replicas. It is also of importance to specimens which are shadow-cast, as it means that the shadowing angle is sensibly constant over the area of a grid square.

CONCLUSIONS

Comparisons of Formvar replicas with optical micrographs and interference micrographs of identical areas show excellent correlation of structure, and it is clear that these replicas are reliable and very suitable for many classes of work.

The study has shown that only in a very few practical cases is the plastic film a true negative replica of the surface, though this does occur when the replica film is about twice as thick as the structure height. It has been found that replica films are, in general, much thicker than most authors claim and it seems that films up to about 1000 Å in thickness are suitable for examination in a 75 kV beam without introducing excessive scatter. This suggests that for work where completely unambiguous interpretation is required, the structure height should not exceed about 500 Å. For metal specimens, this would correspond to a light etch by optical standards.

Although it would clearly be possible to obtain a nearly true negative replica of deep structure by choosing a replica film of suitable thickness, the gain in accuracy of interpretation at edges would be more than offset by the reduced resolution of the replica as a whole, owing to the excessive scatter it would cause. It will, in general, be preferable to use a replica film of normal thickness and to compare micrographs of the plain and shadowed replica to identify contour effects, or to apply the results described here for replica film shape to the interpretation.

In addition to the information of direct value to the Formvar replica process derived from this investigation, it has been shown that the use of the electron micrope in conjunction with the optical interference microscope is a powerful combination for investigations involving measurement of structure dimensions on surface. It has also shown how misleading may be the results obtained only from optical interference measurements at points where fringe discontinuities occur.

ACKNOWLEDGEMENTS

The authors wish to thank the Council of the Royal Microscopical Society for permission to reproduce Figs. 1, 2 and 3, Dr. Willis Jackson, Director of Research and Education, and Mr. B. G. Churcher, Manager of the Research Department, Metropolitan-Vickers Electrical Co. Ltd., for permission to publish this paper.

REFERENCES

(1) Deacon, B. M., Ellis, S. G., Cross, W. G., and Sennett, R. S. *J. Appl. Phys.*, **19**, p. 704 (1948).
(2) Bailey, G. L. J., and Vernon-Smith, S. *The Metallurgical Application of the Electron Microscope*, Monograph No. 8, p. 43 (London: The Institute of Metals, 1949).
(3) Nutting, J., and Cosslett, V. E. *The Metallurgical Application of the Electron Microscope*, Monograph No. 8, p. 65 (London: The Institute of Metals, 1949).
(4) Trotter, J. *Nature* [*London*], **164**, p. 227 (1949).
(5) Deubner, B., Kimmell, H., and Rollwagen, W. *Z. Angew. Phys.*, **5**, p. 284 (1953).
(6) Dyson, J. *Proc. Roy. Soc. A*, **216**, p. 493 (1952).
(7) Agar, A. W., and Revell, R. S. M. *Brit. J. Appl. Phys.*, **4**, p. 1 (1953).

(8) REVELL, R. S. M., and AGAR, A. W. *Brit. J. Appl. Phys.*, **6**, p. 23 (1955).
(9) AGAR, A. W., and REVELL, R. S. M. *Brit. J. Appl. Phys.*, **2**, p. 8 (1951).
(10) WILLIAMS, E. W., and O'NEILL, H. *J. Iron Steel Inst.*, **177**, p. 224 (1954).
(11) BOOKER, G. R. *Brit. J. Appl. Phys.*, **5**, p. 349 (1954).
(12) BRADLEY, D. E. *Proceedings of the International Conference on Electron Microscopy, London*, 1954. To be published.
(13) HALL, C. E. *Introduction to Electron Microscopy*, p. 287 (New York: McGraw-Hill Book Co. Inc., 1953).
(14) HELDENREICH, R. D. *Rev. Sci. Instrum.*, **23**, p. 583 (1952).
(15) CALBICK, J. *Bell Syst. Tech. J.*, **30**, p. 798 (1951).

Caesium 137 for industrial radiography

By R. S. MORGAN, B.Sc., A.Inst.P., Armament Research and Development Establishment, Woolwich, London

[*Paper first received* 25 *July, and in final form* 6 *October*, 1955]

The suitability of caesium 137 as a γ-ray emitter for the radiography of steel has been investigated. An exposure chart has been produced and penetrameter-sensitivities calculated from experimentally determined broad-beam and narrow-beam absorption curves. The broad-beam curve is approximately linear for steel thicknesses exceeding 0·8 in., and from its slope, it would be expected that caesium 137 would give radiographs similar in contrast to an X-ray tube operating at about 1·25 million volts peak. While caesium 137 is a useful source for the examination of steel in the thickness range 1·5 to 4·0 in., below 1·5 in. iridium 192 is superior. Within the range 1·5 to 3·0 in. the penetrameter sensitivity obtainable with caesium 137 reaches its optimum value and is better than that obtainable with either iridium 192 or cobalt 60. Protection data for sources of various strengths have been calculated from an experimentally determined attenuation-curve for lead.

The radioactive isotope of caesium, caesium 137 (^{137}Cs) is one of the most abundant fission products of the atomic pile. It is extracted by a chemical precipitation method and issued by the Radiochemical Centre, Amersham. In this investigation its suitability as a γ-ray emitter for the radiography of steel has been assessed.

PHYSICAL PROPERTIES

The accepted value of the half-life period of caesium 137 is 33 years, but a recent determination by Wiles and Tomlinson suggests a value of 26·6 years.[1] The γ-ray output is stated to be 0·35 röntgens per hour per curie at a distance of one metre from the source.[2]

The isotope decays by β-emission to an isomeric state of barium 137 and the γ-radiation from a caesium source originates from the decay of this barium isotope. The γ-emission is mono-energetic. A precision measurement of wavelength using a curved crystal γ-ray spectrometer of high sensitivity has given a value of $661{\cdot}60 \pm 0{\cdot}14$ keV for the quantum energy of the single spectrum line.[3]

The 250 mc 2×2 mm source used in this investigation contained 12% of additional activity arising from the presence of caesium 134. The effective γ-ray energy from caesium 134 is almost identical with that from caesium 137, but the radiation output per millicurie is 2·5 times that of caesium 137. Caesium 134 has a relatively short half-life period of 2·3 years. The sources issued more recently are, however, stated to contain a lower proportion of the 134 isotope, the amount being not greater than 4% of the caesium 137 strength.

EXPERIMENTAL INVESTIGATION

Exposure chart for steel. Exposure-curves have been produced for steel plates under broad-beam conditions such as normally arise in practical radiography. In Fig. 1 the curve for Ilford Industrial C film with lead screens, related to a source-strength of one curie, is shown together with curves obtained under similar conditions for iridium 192[5] and cobalt 60[4] for comparison.

The experimentally determined curve obtained with the nominally 250 mc source has been adjusted so that the curve as drawn in Fig. 1 refers to a source in which the activity of the 134 isotope has decayed to a negligible amount. Initially with a new source containing 4% of additional caesium 134

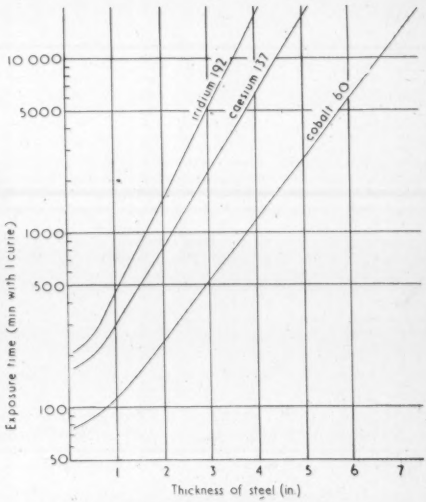

Fig. 1. Exposure chart for steel

Industrial C film; source-film-distance 20 in.; lead screens, 0·004 in. front, 0·020 in. back; film density, 2·0; development, D-19b, 5 min, 68° F.

Exposure-factors for different film densities: $D = 3{\cdot}0$, $\times 1{\cdot}6$; $D = 2{\cdot}5$, $\times 1{\cdot}3$; $D = 2{\cdot}0$, $\times 1{\cdot}0$; $D = 1{\cdot}5$, $\times 0{\cdot}7$.

Exposure-factors for different films: Ilford Industrial C, $\times 1{\cdot}0$; Kodak Crystallex, $\times 0{\cdot}5$; Ilford Industrial B, $\times 0{\cdot}3$; Ilford Industrial G, $\times 0{\cdot}12$.

activity, exposure times as given by Fig. 1 will be 10% too long. In a source about two years old, however, this will have fallen to 5%, and the error thus introduced will be considerably less than batch-to-batch variations and other fortuitous variables associated with the processing of X-ray films.

Derived information. (*a*) For a steel thickness exceeding 0·8 in. the curve becomes approximately straight, thus indicating exponential absorption.

(*b*) Above 0·8 in. of steel, the half-value thickness reduces to a constant value of 0·67 in. The effective absorption coefficient corresponding to this half-value thickness is 1·04 in.$^{-1}$ Comparison with previous experimental work[5] suggests that the same absorption coefficient would be obtained from an X-ray tube operating at about 1·25 MV. It is to be expected therefore that caesium 137 will give radiographs similar in quality to those obtained from an X-ray tube operating at this voltage.

(*c*) From the relative slopes of the curves in Fig. 1 it is to be anticipated that the contrast obtainable with caesium 137 would be superior to that obtainable with cobalt 60 and slightly inferior to that obtainable with iridium 192.

Penetrameter sensitivity. The step-penetrameter sensitivity may be calculated from the expression

$$\text{sensitivity} = \frac{\delta t}{t} = \frac{2{\cdot}303\delta D[1 + (I_S/I_D)]}{G_D \mu t}$$

where δt is the minimum detectable thickness, δD is the minimum discernible change in film density, taken to be 0·006,[6] G_D is the gradient of the film characteristic curve at density D, t is the thickness and μ is the true linear absorption coefficient.

The factor $[1 + (I_S/I_D)]$, where I_S/I_D is the ratio of the intensities of the scattered and direct radiations reaching a point on the film, is obtained from the broad-beam and narrow-beam exposure curves. To evaluate this factor, broad-beam and narrow-beam exposure-curves were determined experimentally. The narrow-beam curve also gives the value of μ. As would be expected with a mono-energetic source the narrow-beam curve is a straight line. The slope of this line gives a value of $\mu = 1{\cdot}49$ in.$^{-1}$, which corresponds to a quantum energy of 630 keV, in fair agreement with the accepted value. G_D was obtained by measuring the slope of the experimentally determined film characteristic curves.

Sensitivity curves calculated from this formula for film-densities of 1·0, 2·0 and 3·0 are plotted in Fig. 2. The percentage sensitivity improves with increasing thickness of steel to an optimum value in the region of 2·0 to 2·5 in. of steel and thereafter deteriorates slightly. Investigation beyond 3·5 in. was limited by the relatively low strength of the source. It will be observed that the higher the film-density, the better the sensitivity as is to be expected.

Sensitivity experiments based on the discernibility of long straight grooves in a steel plate enabled the accuracy of the theoretical curves to be checked. Steel plates were built up to different thicknesses with the grooves on the surface remote from the film, and exposed to give various film-densities on development. Reasonably good agreement was obtained between the calculated and experimental sensitivities as is shown in Table 1.

Table 1. *Step-penetrameter sensitivity*

Steel thickness (in.)	*Film density (Industrial B)*	*Step penetrameter sensitivity (%)*	
		Calculated	*Observed*
0·24	2·15	1·34	1·25
0·47	2·45	0·77	0·85
0·80	1·35	1·02	1·25
1·06	1·25	0·99	0·75
1·41	1·34	0·97	1·14
2·32	1·55	0·61	0·67
3·20	2·40	0·50	0·50
4·14	0·82	1·63	1·56

Comparison with iridium 192 *and cobalt* 60. Penetrameter-sensitivity curves serve as a basis for the assessment of the radiographic quality obtainable with their respective isotope sources. Comparison of the curves for caesium 137 and iridium 192 (Fig. 3) indicates that caesium 137 is a suitable source for the radiography of steel 1·5 to 4·0 in. thick. Within the range 1·5 to 3·0 in., its sensitivity, which reaches its optimum value at about 2·3 in. becomes better than that of iridium 192. Below about 1·5 in. of steel, iridium 192, which has a complex spectrum with strong γ-ray lines of quantum energy about 300 keV, is preferable, its optimum sensitivity occurring at about 1·4 in. In the range 3·0 to

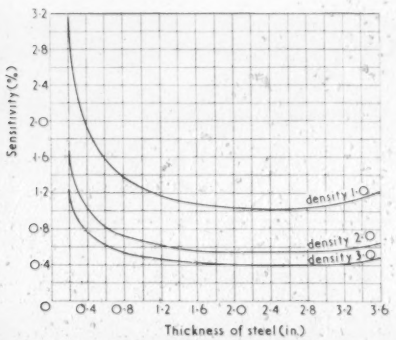

Fig. 2. Step-penetrameter sensitivity against steel thickness with ^{137}Cs radiation

Industrial B film; lead screens; development, D-19b, 5 min, 68° F.

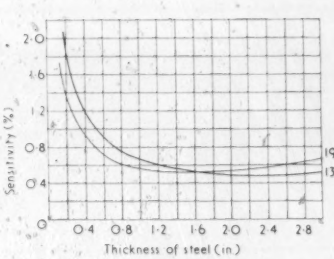

Fig. 3. Comparison of step-penetrameter sensitivities obtainable with ^{137}Cs and ^{192}Ir radiation

4·0 in. of steel, the sensitivities attainable with caesium 137 and cobalt 60 are comparable. Below 3·0 in. cobalt 60 has a correspondingly poorer sensitivity than either caesium 137 or iridium 192.

Latitude (range of specimen thickness). In radiography it is often necessary to examine specimens in which there is a considerable range in thickness. The maximum range of thickness which can be examined per exposure in a single radiograph is determined by the permissible density range. The maximum density, corresponding to the thinnest section, should be the highest which can be viewed. The minimum density, corresponding to the maximum thickness of metal, must be such that the sensitivity, which is a function of the film-gradient and therefore of the density, is not worse than 2·0% (a commonly accepted figure), or some other stipulated value.

The change of sensitivity with thickness has been calculated for steel specimens in which the smallest thickness is 0·5, 1·0 and 2·0 in. respectively. The films generally used for γ-radiography reach their maximum gradient at densities too high for practicable viewing. A density of 3·0 has, therefore, been chosen for the thinnest section. The calculated sensitivities for different thicknesses are plotted in Fig. 4.

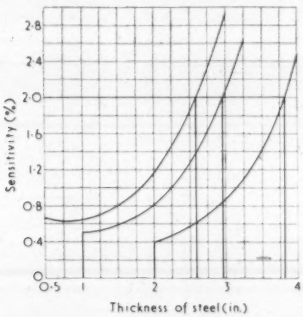

Fig. 4. Relation between thickness-latitude and sensitivity with ^{137}Cs radiation

The thickness-latitudes in the three examples chosen are 0·5 to 2·6 in., 1·0 to 3·0 in. and 2·0 to 3·8 in. If the sensitivity is not to be poorer than 1·0%, the range of thickness is less, but still quite useful. In the examples chosen the thickness latitudes are then 0·5 to 1·8 in., 1·0 to 2·25 in. and 2·0 to 3·15 in.

RADIATION PROTECTION

Broad-beam absorption measurements have been made for various thicknesses of lead and are shown in the form of an attenuation curve in Fig. 5. Absorption is exponential for thicknesses of lead exceeding 0·1 in. The half-value thickness measured under conditions of exponential absorption is 0·29 in. and the tenth-value thickness 0·96 in. of lead. The effective linear absorption coefficient is $2{\cdot}40\ \text{in.}^{-1}$. Due to the presence of a "shoulder" to the curve, the first half-value thickness is only 0·23 in.; this should be taken into account in designing protective containers and shielding.

Source containers. A knowledge of the attenuation-curve enables the thickness of lead required to reduce the radiation rate to a safe level to be calculated. The attenuation curve as experimentally determined applies to a source containing 12% of additional activity arising from caesium 134. Lead thicknesses thereby obtained will therefore afford protection from sources containing only 4% of additional 134 activity slightly in excess of that required.

The main hazard with portable containers is usually exposure of the hands, and if this can be reduced to a safe level, the rest of the body, in general, will also be safeguarded. The maximum permissible dose rate (M.P.D.R.) on the hands, 37·5 mr/h[7] is equivalent to a total dose of 1·5 r per working week of forty hours. No isotope container is handled continuously for a full working week, so the size and weight of the container may be considerably reduced by adopting a dose rate based on the maximum dose likely to be received during an average working week.[8,9] Experience over a number of years in the Armament Research and Development Establishment has confirmed that the dose rate of 1000 mr/h at the surface of the container suggested by Allen, Peiser and Rait[8] gives adequate protection in practice.

For caesium 137, the size and weight of a lead container, assuming a spherical shape with a central cavity of 0·25 in. radius to accommodate the source, have been calculated and are given in Table 2.

Table 2. *Comparison of source containers*

	M.P.D.R. (on hands)		1000 mr/h	
Source strength (c)	*Wall thickness (in.)*	*Weight (lb)*	*Wall thickness (in.)*	*Weight (lb)*
0·25	2·5	36	1·5	10
1	3·0	59	1·9	18
2	3·2	72	2·2	24
4	3·5	87	2·4	30
6	3·6	96	2·5	36

A considerable saving in weight is effected by the use of the higher dose rate suggested above. For example, a container for a 250 mc source designed to give the M.P.D.R. for the hands on the surface would safely accommodate 6 c, provided the maximum handling time associated with the higher surface dose rate is not exceeded.

A container designed to carry 6 c of caesium 137 would also accommodate the strongest iridium source likely to be used in industrial radiography, but would be suitable for only about 100 mc of cobalt 60.

Protection barriers. During radiographic exposures the source is wholly or partially unshielded. Where γ-ray sources are in regular use, protection is best achieved by confining radiography to a special room with reinforced walls. Barium concrete sandwiched between bricks provides a good and cheap protective wall. The thickness of wall necessary for protection from the direct beam of radiation emitted by a caesium source may be estimated from the "broad-beam" attenuation curve in steel, since for radiations above about 0·5 MeV the mass absorption coefficients of steel, concrete and brick are approximately equal. It is then permissible to take the ratio of the thicknesses as equal to the inverse ratio of the densities of steel and other material.

Where specimens have to be examined in position and space is limited, temporary lead shielding may be erected, if practi-

cable, in order to reduce the radiation to a safe level at a specified distance from the source. The lead shielding involved in this and similar problems may be determined by calculating the attenuation-factor and reading off the corresponding lead-thickness from the attenuation curve (Fig. 5).

The erection of lead or concrete barriers is, however, costly and unadaptable. Where ample space is available it is far simpler, cheaper and more convenient to rope off an area around the source beyond which the radiation is at a safe

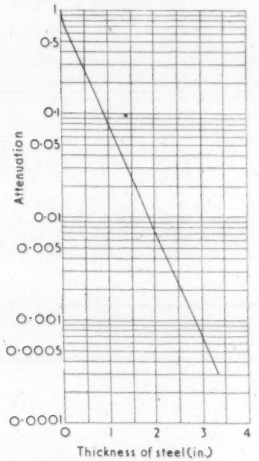

Fig. 5. Attenuation of ^{137}Cs radiation in lead

level. For an unprotected source, as used in panoramic exposures, the minimum safe distance is easily calculated by direct application of the inverse square law. For a 1 c source of caesium 137 the minimum safe distance for continuous whole body irradiation would be 22·4 ft.

It is frequently convenient to manipulate a source at the end of a rod. The length of rod necessary can be determined by using the same safety criterion as was suggested for source containers. The length of rods for various source strengths required to give a dose rate of 1000 mr/h at the hand is listed in Table 3.

Table 3. *Handling rods*

Source strength (c)	*Length of rod (ft) for 1000 mr/h*
0·25	1·0
1	1·9
2	2·7
4	3·9
6	4·8

With the larger sources, necessitating the use of long rods, the dose rate at the gonads becomes the determining factor in the design of rod. Using the rod for the 6 c source at arm's length, the dose rate at the gonads would be about 600 mr/h which would allow a maximum handling time of about 6 min per day. Using a dummy for setting up exposures, the active source need only be manipulated for a few seconds at any one time and this handling time limit, in many applications, would be more than adequate. The dose rate adopted, however, can easily be determined from an estimate of the number of exposures envisaged per working week.

The lengths of rod given in Table 3 have been calculated for a source of pure caesium 137 and some extra protection will be needed for the 134 component, if present. For a source containing 4% of additional 134 activity, these values and safe distances will need to be increased by a factor of 1·05.

CONCLUSIONS

Caesium 137 is a useful source for the radiography of steel up to 4 in. in thickness. The radiation from caesium 137 is intermediate in quality between that of iridium 192 and cobalt 60 being closer to iridium 192 than to cobalt 60. Below 1·5 in. of steel, iridium 192 gives better penetrameter sensitivity, while above 4·0 in., cobalt 60 is essential for penetration. In the range 1·5 to 3·0 in. where the radiographic sensitivity reaches its optimum value, caesium 137 gives better results than either iridium 192 or cobalt 60, and also has the advantage of a long half-life period. In the range 3·0 to 4·0 in., caesium 137 is as good as cobalt 60, but because of its lower output and specific activity, exposure-times are considerably longer. Protection, however, is correspondingly simplified. The specific activity obtainable with caesium 137 is at present 40 mc/mm^3 as compared with 70 mc/mm^3 for cobalt 60 and about 200 mc/mm^3 for iridium 192.[10]

ACKNOWLEDGEMENTS

The advice and guidance of the late Mr. C. Croxson and the help of Mr. R. Halmshaw are gratefully acknowledged. Thanks are due to Mr. B. N. Clack and Mr. P. E. Carter of the Radiochemical Centre, Amersham, for checking the physical data and providing up-to-date information on caesium 137. Crown copyright reserved. Reproduced with the permission of the Controller of H.M. Stationery Office.

REFERENCES

(1) WILES and TOMLINSON. *Phys. Rev.*, **99**, p. 188 (1955).

(2) *Data sheet for caesium* 137: (Amersham: Radiochemical Centre, 1954).

(3) MULLER, HOYT, KLEIN and DUMOND. *Phys. Rev.*, **88**, p. 775 (1952).

(4) HALMSHAW and KNAPP. Unpublished report 1954.

(5) HALMSHAW. *Brit. J. Appl. Phys.*, **5**, p. 238 (1954).

(6) NEEF. *Z. Techn. Phys.*, **6**, p. 208 (1925).

(7) Recommendations of the International Commission on Radiological Protection. *Brit. J. Radiol.*, **27**, p. 245 (1954).

(8) ALLEN, PEISER and RAIT. *Brit. J. Appl. Phys.*, **4**, p. 268 (1953).

(9) CROXSON. *Welding and Metal Fab.*, **22**, p. 15 (1954).

(10) Radiochemical Centre, Amersham, and Atomic Energy Research Establishment, Harwell: Private communications.

The automatic recording of electron diffraction patterns applied to the study of evaporated copper layers

By R. B. Kehoe, B.Sc., A.R.C.S., R. C. Newman, B.Sc., A.R.C.S.,* and D. W. Pashley, Ph.D., A.R.C.S., A.Inst.P.,
Department of Physics, Imperial College of Science and Technology, London

[*Paper first received* 25 *July, and in final form* 3 *October*, 1955]

An apparatus has been constructed which successively records complete electron diffraction patterns after preset time intervals. This has been used in conjunction with a reflexion specimen furnace of new design in the study of the growth of copper evaporated on to flat (111) silver surfaces.

Electron diffraction provides a unique tool for structural studies of very thin films. The scope of such studies can be extended considerably if observations are carried out while changes (e.g. growth and deformation processes) are actually taking place in the film. Trillat and Takahashi[1,2] have developed a technique which is applicable to the examination of randomly oriented polycrystalline aggregates. A slit is placed in front of a slowly moving photographic film, so that any changes along one diameter of the ring pattern are recorded. When combined with a specimen heater, this technique can be used to study such processes as the annealing and alloying of thin metallic films.

The above method is unsuitable for the study of the growth of thin oriented layers on single crystal surfaces. For such experiments it is necessary that the complete diffraction pattern be recorded at successive intervals of time. A motor driven film unit, which is described below, allows this to be carried out with a high degree of operational flexibility. Exposure times, intervals between exposures and film winding are made completely automatic by means of suitable control circuits. Since the mode of growth of an oriented layer, particularly in the case of metal deposits (see, for example, Bruck[3]), depends upon the temperature of the substrate, a specimen furnace has also been constructed. The main features of this furnace are: (i) a controllable specimen temperature; (ii) freedom from specimen contamination; (iii) provision for deposition of vapours on to heated reflexion specimens. Both units form attachments to an existing electron diffraction camera, the specimen chamber of which has previously been described.[4]

The first application of the apparatus is concerned with a preliminary study of the growth of oriented copper films on silver crystal surfaces. This extends previous work,[9] in which the substrate surfaces were maintained at room temperature. In this latter case the copper deposited in the form of well oriented plate-like crystallites during the growth of the first few ångströms in average thickness, after which randomly oriented copper was formed. The effect of using heated substrates is now investigated.

THE APPARATUS

The film holder. The film holder is built on to a flat brass plate which bolts directly on to the diffraction camera. The film passes under a masking frame fixed between two drums, each of which can hold up to 30 ft (120 exposures) of film 7 cm wide. The drum spindles pass out of the vacuum, and are fitted with exterior worm wheels. A horizontal worm drive is bolted on to the front of the brass plate, and can engage with either worm wheel. The worm drive is attached to a gear box which is directly coupled to an electric motor.

The film cannot be adequately outgassed while it is tightly wound on a drum. It is therefore driven slowly by the motor from one drum to the other in the evacuated camera; the time needed for this is about two hours. Subsequent evacuation of the camera after the film has been exposed to air for a short time is quite rapid, as the film absorbs moisture only slowly.

The motor is automatically controlled by an electronic device. The film is transported one frame between successive exposures, during which period the electron beam is deflected into a trap, by means of the magnetic field produced by two coils. The time interval between exposures is variable from six seconds to five minutes in steps, and the exposure period is continuously variable from one to thirty seconds. The speed of the motor is stabilized against mains voltage and load fluctuations by means of a feed-back circuit and is adjusted so that the correct length of film is wound on during the five seconds period for which the motor runs between exposures.

The film unit can be operated manually by disengaging the worm drive, and is readily interchangeable with a plate holder which carries five quarter plates.

The specimen furnace. The types of furnace suitable for reflection specimens, which have been described elsewhere,[5–8] are inadequate for the type of experiments projected. The water-cooling in the furnaces of Jackson and Quarrell[5] and of Gulbransen[6,7] is undesirable, while those of Jackson and Quarrell[5] and of Picard and Dornfeld[8] are unsuitable for insulating specimens. The furnace described below avoids many such complications, since it is thermally isolated in the camera. Furthermore the specimen is almost completely enclosed in a hot cavity, and so reaches a temperature equilibrium which is independent of its thermal properties.

A section of the heater is shown in Fig. 1. The cylindrical block *A* is fixed rigidly to a mica disk *M*, which in turn is fastened to the circular rack *R*. This mounting is mechanically rigid, and provides good thermal insulation. On to block *A* fit disks *B* and *C*, between which the specimen is held on a spring-loaded seating *F*. Above disk *C* is the heater section *D*. The heater element is wound in two concentric coils in opposite senses, so that with a d.c. supply the magnetic deflexion of the electron beam is negligible. A thin-walled sleeve *G* is fitted into the axial hole in the heater section *D*.

Parts *A*, *B*, *C* and *D* and the cover disk *E* are held together by two threaded rods which screw into *A*. The furnace is mounted with the circular rack *R* replacing that of the specimen table in the specimen holder already described.[4] The vertical electron beam, which is perpendicular to the plane of Fig. 1(*a*) reaches the specimen through a radial slot in *B* and *C* [see Fig. 1(*b*)]. The size and shape of these slots

* Now at Associated Electrical Industries Research Laboratories, Aldermaston, Berks.

is such that the azimuth angle can be varied through 120° and the grazing angle of incidence between 0 and 4°.

Evaporated metals, or other substances, can pass through the sleeve *G* to reach the surface of the specimen at normal incidence. For lightness, and in order to reduce heat loss by radiation, parts *A*, *D* and *E* are made of Duralumin.

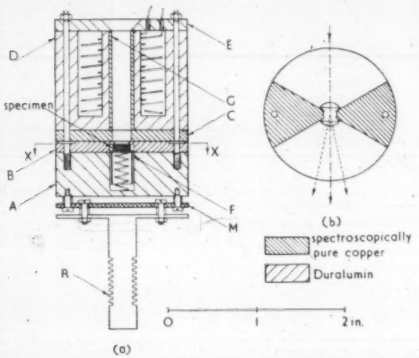

Fig. 1(*a*). The specimen furnace. (*b*) Section across *XX* of (*a*)

Parts *B*, *C* and *G* to which the specimen surface is exposed are made of spectroscopically pure copper. This reduces to a minimum the possibility of contamination of the specimen by impurities which may be expelled by parts of the furnace. The temperature of the specimen is measured by a copper–constantan thermocouple, the hot junction of which is clamped in block *A*.

THE GROWTH OF ORIENTED COPPER LAYERS

When copper is deposited on to a flat (111) surface of silver maintained at room temperature, oriented crystallites are formed.[9] The (111) planes of the copper are parallel to the (111) silver surface, with the [1$\bar{1}$0] copper direction lined up with the [1$\bar{1}$0] and [$\bar{1}$10] of silver [referred to as (111) double positioning]. When the average thickness of the layer is increased beyond about 10 Å, further copper deposits are randomly oriented. The initial nuclei of the deposit were estimated to be in the form of (111) plates, of thickness about 12 Å and width about 60 Å. This work is now extended to include growth of copper layers on heated (111) silver surfaces, which are prepared in the same manner as previously described.[9]

Experimental technique. Approximate thickness estimations have been made from the known total amount of copper evaporated from the tungsten spiral. The rate of deposition was maintained approximately constant in the range 0·5–5·0 Å/min. The growth of layers up to a mean thickness of about 200 Å has been studied. At the beginning of a run, exposures were recorded at half-minute intervals. Since it was possible to examine the diffraction pattern visually between successive exposures, the exposure interval was increased when the pattern was seen to be changing less rapidly. All automatic recording was carried out with the electron beam passing along the silver [1$\bar{1}$0] azimuth. In addition, a few photographs were recorded at the [2$\bar{1}\bar{1}$] azimuth. Experiments were carried out at the following substrate temperatures: 50, 80, 110, 170, 215 and 270° C.

Results. At all the elevated temperatures used complete orientation of the copper was observed for all thicknesses studied. This orientation consisted of (111) double positioning, although at higher temperatures there was a tendency towards single positioning (copper [1$\bar{1}$0] parallel to silver [1$\bar{1}$0] only). The general features observed on the diffraction patterns are illustrated in Fig. 2. Effects due to secondary

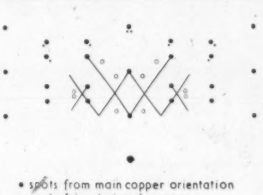

Fig. 2. Main diffraction features from copper deposited at 215° C. Silver [1$\bar{1}$0] azimuth. The continuous lines represent the [110] spines

scattering were also frequently observed; this involved both copper–copper and copper–silver double scattering.

At room temperature the intensity of the copper pattern increased very rapidly with small increases in the mean thickness of the deposit, immediately after the first appearance of the copper spots. This effect persisted at 50 and 80° C, but was progressively less noticeable for the higher temperatures. The patterns did not reveal any important changes in the structure of the copper film as the thickness was increased.

At 85° C, signs of twinning on all (111) planes appeared; at higher temperatures the twinning became stronger, and quite intense spots were observed at 215° C. At the highest temperature, however, no twinning occurred.

The size of the copper crystallites was very large at the higher temperatures; at 270° C they were visible under the optical microscope, and it was estimated that their lateral dimensions were of the order of 1 μ. With such large crystallites, the estimation of size and shape from the diffraction patterns is not possible, because of the low penetrating power of the electrons. All that can be stated is that the lateral dimensions of the crystallites increase from about 60 Å at 20° C to about 1 μ at 270° C. Since the diffracted spots from the copper deposited on to heated substrates showed no appreciable refraction effects, it is concluded that the upper surfaces of these crystallites were not as smooth as those of the oriented crystallites obtained at room temperature.

A prominent feature of the patterns obtained at the elevated temperatures was the appearance of fine structure (see Fig. 2). Firstly, thin lines or "spines" were observed along directions joining certain spots. The most prominent spines at the [1$\bar{1}$0] azimuth were along the [110] directions, and they occurred at temperatures of 170° C and above. At 110° C [001] spines were observed; weak [111] spines also occurred in some cases. At the [2$\bar{1}\bar{1}$] azimuth the spines were along the [120] and [102] directions. In addition to the spines, splitting of some diffraction spots into pairs or triplets occurred. Although this splitting might be associated with the spines, since the two features normally occurred together,

it was not sufficiently well defined to allow any conclusive measurements to be made.

The spines are similar to effects observed by others (see, for example, Uyeda[10]). Since they are very long and sharp, they presumably arise from some kind of fault or imperfection involving fairly large areas (say greater than a few hundred ångströms square) of almost single atomic planes, perpendicular to the spine directions. This is consistent with the fact that they are only observed from the larger crystallites.

The diffraction patterns were the same from patches of the surface which had not been bombarded by the electrons during the deposition, as from those which had been bombarded. It was therefore concluded that the incident electron beam did not influence the mode of growth of the copper.

The apparatus described above is expected to have applications to various studies of changes occurring on single crystal surfaces.

ACKNOWLEDGEMENTS

Two of the authors (R. B. K. and R. C. N.) are indebted to the University of London for Postgraduate Studentships, and the former also to the Department of Scientific and Industrial Research for a maintenance grant. The third author (D. W. P.) is an Imperial Chemical Industries Research Fellow of the University of London.

REFERENCES

(1) TRILLAT, J. J., and TAKAHASHI, N. *C.R. Acad. Sci.* [*Paris*], **236**, p. 790 (1953).
(2) TRILLAT, J. J., and TAKAHASHI, N. *Acta Cryst.*, **7**, p. 15 (1954).
(3) BRUCK, L. *Ann, Phys.* [*Leipzig*], **26**, p. 233 (1936).
(4) KEHOE, R. B., NEWMAN, R. C., and PASHLEY, D. W. *J. Sci. Instrum.*, **31**, p. 399 (1954).
(5) JACKSON, R., and QUARRELL, A. G. *Proc. Phys. Soc.* [*London*], **51**, p. 237 (1939).
(6) GULBRANSEN, E. A. *J. Appl. Phys.*, **16**, p. 718 (1945).
(7) GULBRANSEN, E. A. *Rev. Sci. Instrum.*, **18**, p. 546 (1947).
(8) PICARD, R. G., and DORNFELD, E. G. *Rev. Sci. Instrum.*, **25**, p. 158 (1954).
(9) NEWMAN, R. C., and PASHLEY, D. W. *Phil. Mag.*, **46**, p. 927 (1955).
(10) UYEDA, R. *Proc. Phys-Math. Soc. Japan*, **24**, p. 809 (1942).

Electrode deterioration in "keep-alive" discharges in transmit-receive switches

By D. WALSH, B.Sc., A.Inst.P., A. W. BRIGHT, B.Sc.(Eng.), Ph.D.,* and T. J. BRIDGES, B.Sc.(Eng.), Services Electronic Research Laboratory, Baldock, Herts

[*Paper first received* 3 *August, and in final form* 28 *September*, 1955]

An investigation of the behaviour of electrode materials in a discharge containing water vapour is described. Most common stable metals, as well as a semiconducting ceramic were tried. Some information is given on the increase of maintaining voltage and sputtering with time for both normal and abnormal glow discharges. Measurements of the rate of clean-up of water vapour in normal discharges have also been made.

The function of a transmit-receive (T.R.) switch is to isolate the crystal receiver of a radar set from the magnetron whilst the latter is transmitting. It thus enables a common aerial to be used for transmitting and receiving. The switch consists essentially of a gas-filled waveguide component with a geometry that causes the gas to ionize rapidly when a radio-frequency pulse is incident upon it. The gas used is normally one of the heavier noble gases (argon, krypton or xenon). In addition, the discharge must not persist long beyond the transmitter pulse, since short-range echoes have to pass to the receiver. The filling, therefore, includes a gas with a strong affinity for electrons. Water vapour is used for this purpose in practically all T.R. switches.

A T.R. switch as described above would permit an unacceptably high amount of energy to pass through it whilst the discharge was building up. This would be due to a "statistical" time lag in firing that is normally reduced by supplying free electrons to the discharge gap from a d.c. primer or keep-alive discharge. Since the T.R. switch must protect the receiver from nearby transmitters as well as the one with which it shares an aerial, the discharge is on all the time, and thus can have an important effect on the life as well as the performance of T.R. switches. Typical dispositions of keep-alive electrodes in T.R. switches are shown in Fig. 1.

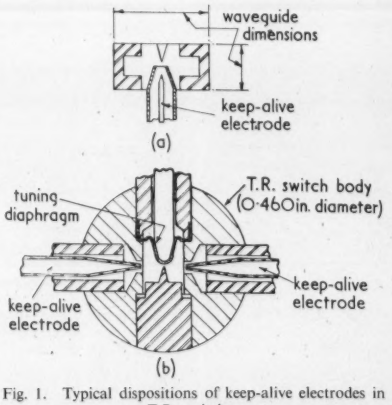

Fig. 1. Typical dispositions of keep-alive electrodes in T.R. switches

(*a*) Section of a single element of a 3 cm band broadband T.R. switch. (*b*) Section of an 8 mm band tunable T.R. switch (CV 2330).

* Now at Electrical Engineering Dept., Imperial College, London.

In fact, three of the main types of T.R. switch failure are caused or accelerated by the keep-alive discharge. They are:

(i) instabilities, such as glow-to-arc transitions, in the keep-alive discharge. These result in periods when the supply of free electrons is interrupted, permitting sufficient power to damage the crystal to pass through the T.R. switch;[1]

(ii) detuning of the switch cavity by sputtered material;

(iii) "clean-up" of water vapour, due to chemical reactions in the discharge.

The problem of improving keep-alive performance could obviously be approached in two ways, the investigation of alternative gas fillings or keep-alive materials. This paper deals with the latter approach. The investigation was made with test diodes similizing the d.c. condition of the discharge. In actual T.R. switches the radio-frequency discharge also plays an important part in switch failure especially hastening water vapour clean-up.

NORMAL AND ABNORMAL GLOW

In the low pressure glow discharge, the voltage drop across the discharge is sensibly independent of current over a certain range and is a function only of the gas and the electrode material. This is the "normal glow condition." As the current increases, the area of the glow at the cathode increases and the cathode current density remains constant. If the current increases still further, the glow covers the whole of the cathode and is unable to spread further. Consequently, the cathode current density increases as the discharge current increases. This is the "abnormal glow condition."

Transitions from glow to arc would obviously be more likely from the abnormal glow, in view of the greater possibility of local heating at the cathode. Also the sputtering rate of cathode material is roughly proportional to the cathode drop and is thought to be appreciably less in the normal than in the abnormal glow.[2]

It was thus convenient to divide the investigation into two parts, dealing with the abnormal and the normal glow conditions. It should be mentioned that most keep-alive electrodes in existing T.R. switches operate in the abnormal glow for two main reasons. By having a keep-alive electrode of restricted area, the discharge could be localized and placed close to the radio-frequency gap. As the discharge was more intense, the irradiation of the radio-frequency gap was more adequate.

ABNORMAL GLOW EXPERIMENTS

Electrode configuration. Two types of diode were used in these tests. Type *A* (Fig. 2) was similar to the keep-alive electrode in a T.R. cell. It consisted of a glass-sheathed metal rod, ground so that a circle of 0·010 in. diameter of metal was bared. Type *B* electrodes were used to compare qualitatively the sputtering rates of various cathode materials. The glass sheathing of the cathode was carried beyond the tip of the electrode and very small quantities of sputtered material could readily been seen on the surface of the glass.

Preliminary experiments. The effects to be investigated were the rise in discharge voltage and the sputtering of cathode material during the life of a discharge in argon and water vapour. Without the latter gas, there is no voltage rise and the sputtering rate is considerably reduced. For this reason, the sputtering that occurs in a T.R. switch due to the presence of a chemically active gas is often referred to as abnormal, or electrochemical sputtering.

The following preliminary experiments were performed:

(i) A tube with two sets of type *A* electrodes (Fig. 2) was filled with 25 mm of mercury of argon and 5 mm of mercury of water vapour. A current of 100 μA was passed through one for several hundred hours. The discharge voltage required was approximately doubled in this time. The second diode was tested at intervals, and showed no change in voltage. This demonstrated that the voltage rise was caused by an electrode effect and not by a change in gas composition.

(ii) X-ray analysis of the cathode surface showed that oxides of the cathode material were being formed.

(iii) To confirm that oxidation at the cathode occurs in a water vapour discharge, a diode was made with a clean 1 mm diameter copper rod as cathode. With an argon and water vapour filling, the copper oxidized in the discharge. At first interference colours appeared on the copper, then it progressively blackened along its length. Oxidation still occurred in such a diode when the gas filling was hydrogen and water vapour.

These experiments showed that the presence of water vapour caused oxidation at the cathode. It seemed likely that the two effects to be studied were associated with this oxidation reaction.

Rise in discharge voltage. The results of a series of experiments under standardized conditions are given in Table 1. Diodes of the first type were used. The diameter of the cathode material was 0·010 in., i.e. an area of 0·05 mm^2, its separation from the nickel anode being about 1 mm. The gas filling was 5 mm of mercury of water vapour and 20–25 mm of mercury of argon. They were run with a discharge current of 100 μA and the voltage was measured at this value. Table 1 gives results for one typical diode of each material.

There is a correlation between the voltage rise for a given material, and the heat of formation of its oxide. The more stable the oxide, the greater is the rise. In some cases the type of oxide produced was deduced from the colour of the deposit (see Table 1). When more than one material is present (in an alloy) it seems likely that the most stable oxide formed determines the voltage rise. In the case of alloys the correlation depends on this assumption. The main anomaly is nickel, which may be due to small impurities of silicon or manganese. Both of these have large heats of formation.

In view of this evidence and that of the preliminary experiments described above, it seems certain that the voltage rise effect is due to the formation of an oxide layer on the cathode. Two possible mechanisms are suggested, although little evidence is available for any.

(i) The oxide forms a high resistance on the cathode surface.

(ii) A high resistance film of oxide restricts the discharge cathode to a very small area. Sometimes bright metallic spots are seen on the cathode surface after running. These may be due to this effect.

Abnormal sputtering. Diodes of the second type described above were used to compare sputtering rates of different materials. The gas filling was the normal argon/water vapour mixture. The amount of sputtering after a standard run was estimated by observing the deposit on the inside of the glass sheath. A qualitative order of sputtering rates could then be prepared (Table 2). It will be seen that the order of the

Table 1. *Changes in discharge voltage during life*

Material	*Voltage for 100 μA discharge current (0 h)*	*Increase in voltage drop % after 20 h*	*100 h*	*500 h*	*Appearance and deduced chemical nature of deposit*	*Heat of formation of oxides (kg. cal/mole)*	
gold	300	0	−15	diode shorted	Finely divided metal	Au_2O_3	0
platinum	200	0	−10	−10	Dark grey spongy mass. Oxide finely divided metal	PtO	17
rhodium	300	−5	−10	−10	As platinum, but cathode surface bright rhodium		—
palladium	270	5	5	10	As platinum	PdO	21
copper	250	0	10	10	Black CuO		35
reduced titania	270	20	10	15	White whiskery patches on cathode stoichiometric TiO_2		—
iron	260	40	40	30	Red oxide Fe_2O_3		191
nickel iron	300	45	35	45	Black, NiO		58
nickel 42% iron 58%					Fe_3O_4		266
nicosel	310	55	85	90	Black	NiO	58
nickel 29% cobalt 17% iron 54%					(Chemical and X-ray analysis) NiO Fe_3O_4	Fe_3O_4	266
					CoO	CoO	57
nickel	260	70	110	130	Black NiO		58
					? Mn_2O_3		227
					? SiO_2		198
immaculate 5	260	120	160	160	Black Fe_3O_4		227
iron 53% chromium 24·5% nickel 21·5%					Cr_2O_3		267
aluminium	245	130	very unstable		Grey Al_2O_3		390

table is similar to that of Table 1 (the chief exception being gold). This suggests that the abnormal sputtering may be connected with formation of oxide. Aluminium is not shown in Table 2 since type *B* diodes of this material were very unstable and frequently extinguished.

Table 2. *Sputtering rates*

titania	abnormal sputtering rate least
*rhodium	
*platinum	
*palladium	
copper	
nimonic (temperature resistant steel)	
immaculate 5 (stainless steel)	
nicosel (usual keep-alive material)	
nickel	
gold	abnormal sputtering rate greatest

* See text.

Abnormal sputtering has been attributed to the occurrence of glow-arc transitions in the discharge.[3] Some experiments have been performed to confirm this theory. A cathode-ray oscillograph was connected to the keep-alive cathode. An instantaneous deflexion of the beam indicated the occurrence of an arc. Diodes of type *A* previously described were used in this arrangement.

With fillings of dry argon no arcs were observed with any cathode material. When the standard argon/water vapour mixture was used, arcs were seen with most materials. However, with materials that do not readily form oxides (platinum, rhodium, palladium, gold) abnormal sputtering, but not arcing, occurred.

These results confirm and indicate that:

(i) oxide formation is necessary to glow-arc transitions;

(ii) there is still a further mechanism required to account for all cases of abnormal sputtering. In particular, gold shows a high sputtering rate although arcs do not occur.

NORMAL GLOW

It was expected that the glow discharge in the normal glow would be less liable to instability than in the abnormal glow, because of the lower cathode current density. It was hoped that an electrode material would be found with which the glow discharge did not tend to wander over the cathode surface. With previous electrode materials having cathodes of unrestricted area, such instability did occur.

Experimental details. Two types of electrode assemblies were used. The first, type *C* (Fig. 2), consisted of a 1 mm diameter pointed electrode inside a mild steel conical anode. The second, type *D*, suitable for visual observation, consisted

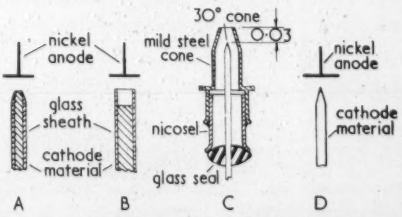

Fig. 2. The four types of experimental diodes

simply of a pointed cathode 1 mm in diameter with a flat circular anode, the tip of the cathode being 1 mm from the anode surface.

With these tests, two gas fillings were used. The first was an argon/water vapour mixture. It had been discovered[4] that the addition of ammonia to this mixture had the effect of reducing the rate of sputtering of the cathode. Some tests were therefore made in mixtures of argon, water vapour and ammonia. With argon and water vapour only it was possible to measure the amount of water vapour by a dewpoint method, and thus the change of partial pressure of water vapour with life could be recorded.

Oscillations. With all types of electrode material it was found that, during the first few minutes of running, the discharge tended to wander over the surface of the cathode, but eventually settled down at the tip. When the discharge had thus stabilized, the voltage/current characteristic showed that it was operating in the normal glow condition, the voltage drop across the discharge being sensibly independent of current.

When a cathode-ray oscillograph was connected across a small resistance in series with the 0·5 MΩ limiting resistance, oscillations of the discharge current were observed. These occurred over a limited range of currents and their frequency was a function of discharge current, increasing with increasing current up to a maximum of about 400 to 500 kc/s. There was no obvious connexion between the slope of the voltage/current characteristic and the onset of oscillations. Fig. 3 shows a typical example of the variation of the

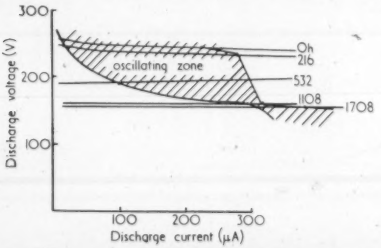

Fig. 3. Curve showing variation of current/voltage with life (rhodium tipped cathode)

Gas filling: argon at 8 mm of mercury, ammonia at 2 mm of mercury, water vapour at 2 mm of mercury

"oscillating zone" with life for a rhodium cathode. It was not thought that these oscillations could be simply explained by a "neon time base" type of mechanism. The appearance of the discharge itself changed when oscillations occurred, tending to become more diffuse. Although the external circuit has a considerable influence on the frequency of oscillations, it is possible that they may be due to some space charge mechanism of the sort which occurs in negative point corona discharged at atmospheric pressure, first noted by Trichel.[5]

Although several tests were made with various types of electrode in pure dry argon, no oscillations were ever observed. This again supports the view that oscillations are dependent upon the gas discharge rather than upon the external circuits.

Water vapour clean-up and voltage rise. It was known that in a discharge in a mixture of argon and water vapour, the water vapour tended to vanish after a certain number of hours running. This was thought to be due to the water vapour dissociating to give OH + H, the hydroxyl ion then reacting with the electrode to form an oxide. Electrodes of type *D* were used and cathodes of rhodium (both pure and rhodium plate), nicosel, copper, platinum, stainless steel and reduced titania were tried. The anode was of nickel. The gas filling was 8 mm argon and 4½ mm water vapour. The anode was outgassed by eddy current heating in vacuum before filling. During life, the partial pressure of water vapour was measured by the dewpoint method.

The results obtained are shown in the curves of Fig. 4 and Fig. 5. Fig. 5 shows that there was considerable clean-up of

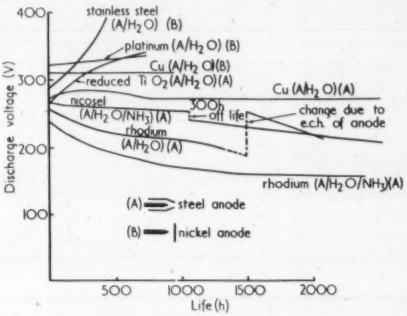

Fig. 4. Change in normal fall with life. Keep-alive current, 200 μA

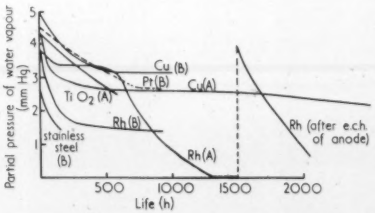

Fig. 5. Variation of partial pressure of water vapour with life. (Agon pressure, 8 mm of mercury)

water vapour in the first few hundred hours of running with all types of cathode. With a stainless steel cathode, the water vapour pressure fell from 3·4 mm to 2·2 mm in 16 hours. At the same time it was seen that the cathode became oxidized over the portion immediately exposed to the discharge. The areas of the anode facing the point was also oxidized. In addition there was a certain amount of cathode material deposited on the anode.

When a type *D* electrode assembly having a rhodium cathode and nickel anode was examined after a few hours running, there was a black deposit on the anode. Chemical analysis showed this to be nickel oxide and rhodium oxide. Similar deposits were found with the other electrode materials, the greatest deposit occurring with copper cathodes. The

mechanism of initial clean-up of water being due to dissociation followed by reaction of the dissociation products to form oxides seems reasonable.

There was then a second stage in which the rate of clean-up decreased until the partial pressure of water vapour remained constant. This period lasted for some 700 h with a copper cathode and 500 h with rhodium. It was found that the time required to reach this period of equilibrium was greater for the anodes of larger area (type *D*). This suggests that the anode had a considerable influence upon the rate of clean-up. It is possible that an equilibrium occurs when the anode is completely oxidized or completely covered by a sputtered oxidized layer. Further evidence is required on this point.

A third stage in the clean-up process was noted in two experiments. This occurred after the equilibrium period when the water vapour pressure was observed to decrease steadily. With a copper cathode this second decrease of pressure was merely from 2·60 mm to 2·15 mm in 2000 h. With rhodium, however, the water vapour changed from 3·4 mm at 570 h to complete clean-up at 1250 h. This third stage was reversible, as it was found on heating the anode of a rhodium tipped keep-alive diode that the water vapour pressure rose from zero to 2·9 mm. This was only slightly below the value noted during the equilibrium stage and suggests that some of the water vapour is adsorbed or absorbed by the electrodes.

The curves of Fig. 4 show how the voltage drop varied with life. The results were similar, in general, to those obtained in the tests described for abnormal glow conditions. It is of interest to note, however, that there was no appreciable change of voltage drop with a copper cathode, even after 3500 h running.

Interpretation of these results is difficult as the voltage drop depends both upon electrode material and gas filling. The effect of decreasing water vapour pressure is to decrease the voltage for a given current, this being an accepted method of measuring dewpoint. The influence of oxides and impurities at the cathode is less well understood. In general, there was no simple correlation between water vapour clean-up and the change of voltage drop with life. The characteristics of the various cathode materials are given in Table 3.

Table 3. *Summary of results in normal glow discharges*

Material	*Stability of position of discharge*	*Clean-up of H_2O*	*Sputtering of cathode material on anode*	*% change in voltage drop after 500 h*	*Remarks*
copper	stable	slow	considerable	0	Cannot be used in NH_3. Sputtering may be serious.
rhodium	stable	relatively high	medium	−17	Tip does not erode.
nicosel	unstable	—	medium	−3	Discharge wanders away from tip.
platinum	stable	continuous	medium	+5	Tip erodes considerably.
reduced titania	stable	continuous	small	+14	Mechanically difficult to use.
stainless steel	unstable	high	medium	+49	Discharge wanders away from tip. High voltage rise during life.

CONCLUSIONS

From the abnormal glow experiments it was evident that the most stable discharge would be obtained with electrodes which did not oxidize readily and which would not vaporize readily in the arc discharge. Metals of the platinum group have these characteristics, but have the disadvantage that the sputtered material is highly conducting and increases the effective cathode area after some time, so that the discharge eventually will be in the normal glow condition. The most suitable material was reduced titania, which had a small voltage rise and low sputtering. A test diode of this material ran for 1000 h with little change in electrical characteristics. Its use in practical devices is somewhat limited by difficulties in fabrication.

The main conclusion to be drawn from the normal glow experiments is that freedom from short circuits and glow-arc transitions during life can be obtained. As regards the clean-up of water vapour, it was clear that this would occur with all the cathode materials used. A stable discharge could be run in an argon/water vapour mixture using a rhodium cathode, but complete clean-up of water might be expected to occur after some 1000 h. With a copper cathode, a stable discharge would run for many thousands of hours with a relatively slow rate of water clean-up, but there would be considerable sputtering of material from the cathode. The choice between rhodium and copper must be decided from consideration of the relative importance of sputtering and water vapour clean-up to the particular application under consideration.

In general, the conclusions reached may be conveniently summarized thus:

(i) normal glow—long life, free from short circuits, but possibility of oscillations of the discharge;

(ii) abnormal glow—freedom from oscillations, but increased sputtering and a greater possibility of glow to arc transitions.

ACKNOWLEDGEMENT

This paper is published by permission of the Admiralty.

REFERENCES

(1) HAWKINS, P. O., BRIDGES, T. J., and WALSH, D. *Proc. Inst. Radio Engrs.*, **44** (March, 1956).

(2) COBINE, J. D. *Gaseous Conditions*, p. 230 (New York: McGraw-Hill Book Co. Inc., 1941).

(3) FRENCH, J. C. *J. Res. Nat. Bur. Stand.*, **45**, p. 310 (1950).

(4) HAWKINS, P. O. Private communication.

(5) TRICHEL, G. W. *Phys. Rev.*, **54**, p. 1078 (1938).

A microwave resonant cavity method for measuring the resistivity of semi-conducting materials

By J. G. LINHART, Ph.D., Dipl.Ing., I. M. TEMPLETON, M.A., D.Phil., and R. DUNSMUIR, M.Sc., Ph.D.,
Research Laboratories, British Thomson-Houston Co. Ltd., Rugby

[*Paper received* 25 *July*, 1955]

A method is described for measuring the resistivity of semi-conductors at centimetre wavelengths. A small spherical or cubic specimen is placed in a cavity resonating in the H_{011} mode, and the reduction in Q due to eddy-current loss in the specimen is measured. The theory given enables the resistivity of the material to be calculated. It is shown that resistivities in the range 0·005 to 10 Ω cm can be determined.

The technique for measurement of dielectric loss at centimetre wavelengths using resonant cavities is well established[1] and is particularly useful and simple with materials of high resistivity, for which the field penetration depth is substantially greater than any dimension of the test specimen.

It has been shown that a similar microwave cavity method can be applied to materials with lower resistivity, for example, in the range 10–0·005 Ωcm. In this case the power absorption is appropriately described in terms of eddy-currents and skin-effect. From the value of the power absorption one may calculate the resistivity of the given material.

Measurement of resistivity in this frequency range is of particular interest for semi-conductors such as silicon and germanium, with controlled "impurity" additions, as used in crystal valves.

Using d.c. or audio-frequencies, the conventional method of measuring the resistivity of semi-conducting materials uses current and potential probes.[2] Such measurements are often complicated by contact resistance and carrier injection. In many cases it is difficult to obtain specimens of size and shape suitable for these measurements.

At centimetre wavelengths on the other hand, using the resonant cavity technique, these difficulties do not arise because it is unnecessary to make metallic contact to the semi-conductor and because a small compact specimen can be used.

THE RESONANT CAVITY METHOD

A spherical specimen of test material is placed at the centre of a circular cylindrical cavity excited to resonance in the H_{011} mode. The magnetic field of this mode of oscillation is approximately uniform near the centre of the cavity.

The quality factor of the cavity is measured with (Q) and without (Q_0) the specimen, and the loss due to the specimen is determined in terms of a quality factor Q_s defined by

$$1/Q_s = (1/Q) - (1/Q_0) \tag{1}$$

For low resistivity materials and at centimetric wavelengths the losses are predominantly due to eddy-currents confined to the surface of the specimen. In this case the resistivity ρ of the material may be calculated from the measured Q_s using an expression which is derived below.

EDDY-CURRENT LOSS IN A SPHERE

Electromagnetic units are used throughout unless otherwise specified. Consider a spherical specimen (Fig. 1) placed in a homogeneous, alternating magnetic field

$$\bar{B} = \bar{z}B\exp(j\omega t)$$

This magnetic field induces azimuthal eddy currents in the sphere. The expression for the current density i_ϕ is well known[3] but rather complicated. Assuming that the skin-depth δ is much smaller than the radius a of the sphere the expression for i_ϕ is considerably simplified and becomes

$$i_\phi = -\frac{3}{8\pi}B\sqrt{(jp)}\frac{a}{r}[\exp - \sqrt{(jp)}(a-r)](\sin\theta)\exp(j\omega t) \tag{2}$$

where $p = (4\pi\omega\mu)/\rho = 2/\delta^2$ and ρ is the resistivity.

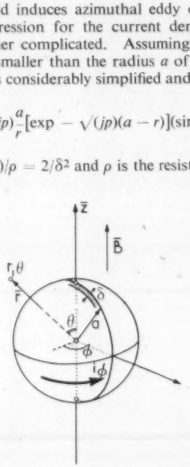

Fig. 1. Lossy sphere in a radio-frequency magnetic field

The power dissipated in a volume element $r^2dr d\phi \sin\theta d\theta$ is

$$dW = \tfrac{1}{2}\rho i i^* r^2 dr d\phi \sin\theta d\theta$$

$$dW = \frac{9}{32\pi}\omega\mu B^2a^2\left\{\exp\left[-\sqrt{(8\pi\omega\mu/\rho)}(a-r)\right]\right\}\sin^3\theta d\theta d\phi dr \tag{3}$$

The total power loss is obtained by integrating expression (3) over the volume of the sphere giving

$$W = 0{\cdot}15B^2a^2\sqrt{\rho\omega\mu}\ (\text{erg/s}) \tag{4}$$

For $\mu = 1$ and with ρ expressed in Ωcm we have

$$W = 0{\cdot}475 \times 10^4 B^2a^2\sqrt{\rho\omega\mu}\ (\text{erg/s}) \tag{4a}$$

A more accurate expression obtained by taking into account the second powers of δ/a is as follows

$$W = 0{\cdot}475 \times 10^4 B^2a^2\sqrt{\rho\omega}[1 + \sqrt{2}(\delta/a)] \tag{4b}$$

where $\delta = 0{\cdot}892 \times 10^4\sqrt{(\rho/\omega)}$ (cm)

CAVITY CONTAINING A LOSSY SPHERE

In applying the above formulae care must be taken that the magnetic field is reasonably uniform over the volume of the sphere. This condition is satisfied for the magnetic field of an H_{011} mode in a cylindrical cavity provided that the diameter of the specimen a is small compared with the resonant wavelength λ (Fig. 2). A criterion such as $a < \lambda/8$ gives satisfactory measurement accuracy.

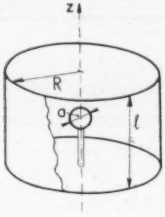

Fig. 2. Resonant cavity containing the specimen

The Q-factor of the cavity is

$$1/Q = (1/Q_0) + (1/Q_s)$$

where Q_0 is the Q-factor of the empty cavity and $1/Q_s$ represents the loss in the sample.

By definition

$$Q_s = \omega W_0/W \tag{5}$$

where W_0 is the stored energy of the H_{011} mode, and is given by:

$$W_0 = B^2 \frac{R^4}{1{\cdot}49 l}\left(1{\cdot}49\frac{l^2}{R^2} + 1\right)10^{-2} \text{ (erg)} \tag{6}$$

where R is the radius and l is the depth of the cavity (cm).

The resonant frequency $\omega/2\pi$ of the cavity oscillating in the H_{011} mode may be also expressed in terms of R and l.

$$\frac{\omega}{2\pi} = \frac{c}{2l}\sqrt{\left(1{\cdot}49\frac{l^2}{R^2} + 1\right)} \tag{7}$$

Substituting this into equation (6)

$$W_0 = B^2 \frac{R^4 l}{1{\cdot}49}\frac{\omega^2}{\pi^2 c^2}10^{-2} \text{ (erg)} \tag{8}$$

Using equations (4a), (5) and (8) the expression for Q_s becomes:

$$Q_s = 0{\cdot}159 \times 10^{-27}\frac{\omega^{5/2}}{\sqrt{\rho}}\frac{R^4 l}{a^2} \tag{9}$$

and therefore the resistivity is given by:

$$\rho = \left(0{\cdot}159 \times 10^{-27}\frac{\omega^{5/2}}{Q_s}\frac{R^4 l}{a^2}\right)^2 (\Omega\text{cm}) \tag{10}$$

A more accurate formula for ρ is obtained by using equation (4b) instead of (4a), thus,

$$\rho = \left\{\frac{\alpha}{Q_s}\left[1 - \left(\frac{1{\cdot}26 \times 10^4}{\sqrt{\omega}}\right)\left(\frac{\alpha}{Q_s}\right)\right]\right\}^2 (\Omega\text{cm}) \tag{10a}$$

where $\alpha = 0{\cdot}159 \times 10^{-27}(\omega^{5/2}R^4 l/a^2)$

EXPERIMENTAL ARRANGEMENTS

Measurements have been carried out at X-band on single crystal silicon material of d.c. resistivity approximately 0·1 Ωcm. A specimen of 0·5 cm diameter was supported centrally in a commercial wavemeter type cavity (Fig. 3), in a distrene cup with a stem of 0·2 cm diameter. This could be inserted axially through an 0·7 cm diameter hole in the end of the cavity, thus allowing specimens to be changed without dismantling the resonator. The base of the support was a push fit into the hole with a shoulder for longitudinal location. The distrene support alone caused less than 1% reduction in Q.

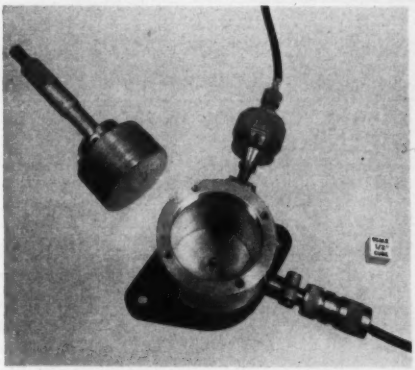

Fig. 3. Experimental arrangement

The cavity was 2·5 cm deep and 2·5 cm in radius. The radio-frequency source and detector were of the conventional type comprising a type CV. 323 reflex klystron oscillator (square wave modulated at 3 kc/s), a crystal detector and tuned 3 kc/s amplifier. The experimental results are given in the table.

Experimental results

	Resonance wavelength (cm)	*Resonance width (cm)*	*Q*
Cavity and stand alone:	3·162	0·00111	2850 (Q_0)
Cavity and stand + specimen:	3·144	0·00675	406 (Q)

From equation (1) it follows that the value for Q_s is 577 and thus the silicon resistivity ρ calculated from equation (10a) is

$$\rho = 0{\cdot}145\ \Omega\text{cm}$$

It is interesting to note that the measured resistivity at 3 cm wavelength is little different from that obtained by d.c. methods.

CONCLUSIONS

A resonant cavity technique has been developed for the measurement at centimetre wavelengths of resistivities within the range 0·005 to 10 Ωcm. These limits are due to the difficulty of measuring accurately Q-factors larger than 2500 and smaller than 50, and also to the failure of the approximate formulae for higher resistivities.

It is not necessary for the sample to be spherical if a shape correction factor is used in calculating the resistivity from

the measured Q_s factor. The shape factor has been determined for a cube sample of volume equal to that of the spherical (calibrating) sample. In this case

$$Q_s \text{ (sphere)} = 1{\cdot}20\ Q_s \text{ (cube)}$$

This shape factor is roughly equal to the inverse ratio of surface areas (1·24).

ACKNOWLEDGEMENT

This investigation was carried out under a contract placed by the Department of Physical Research, Admiralty, and thanks are given to the Admiralty for permission to publish. The authors are also indebted to their colleagues in the Laboratory for encouragement and assistance in this work.

REFERENCES

(1) HORNER, F., TAYLOR, T. A., DUNSMUIR, R., LAMB, F., and JACKSON, W. *J. Instn Elect. Engrs*, **93** (III), p. 53 (1946).
(2) VALDES, L. B. *Proc. Inst. Radio Engrs*, **42**, p. 420 (1954).
(3) SMYTHE, W. R. *Static and Dynamic Electricity*, p. 396 (New York: McGraw-Hill Book Co. Inc., 1939).

The corona resisting property of polytetrafluorethylene

By K. SUGITA, S. NAGAO, D.Sc. and Y. TORIYAMA, D.Eng., Engineering Faculty, Tohoku University, Sendai, Japan

[*Paper received* 23 *February, and in final form* 21 *June*, 1955]

The existence of pin-holes in the granular structure of polytetrafluorethylene tape (0·055 mm) is confirmed by microscopic examination. It was also shown by dielectric strength tests that the heat treatment to close these holes at about the transition temperature increases the mean breakdown voltage by some 20%, and reduces the spread in breakdown values from about 50% with untreated tape to about 20% with heat-treated tape.

Despite superior mechanical properties and good thermal and chemical resistance, polytetrafluorethylene (PTFE) tape shows poor corona resistance.[1,2] Tests have therefore been made on PTFE sheets 0·055 mm thick and 25 mm wide to determine the mechanism of breakdown by corona. In the first instance the PTFE sheets were placed between a point electrode and a glass sheet resting on a plane electrode. The point electrode (weight 87 g) was merely resting on the PTFE. Applying an alternating voltage, corona onset was observed at 5·0 kV (rms); at 12 kV (rms) there was a general glow around the needle and some radial sparks terminating in fixed blue spots. After 10 min at 12 kV (rms) the sheets were examined microscopically and many punctures were observed in positions corresponding to the blue spots observed when voltage was applied. If a photographic plate was placed between the PTFE sheet and the plane electrode, corona at 6 kV (rms) affected a central area and also many surrounding points, which correspond to the fixed blue points previously referred to. The photograph obtained after 1 min at 6 kV (rms) is shown in the figure.

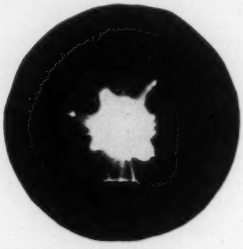

Photograph obtained after 1 min. at 6 kV by punctures of PTFE sheet

If the PTFE sheet is heated for a short time at about the transition temperature (327° C) and then cooled rapidly, it becomes semi-transparent. Then if a voltage is applied between point and plane electrodes there are fewer fixed blue spots than with the normal material and correspondingly few breakdown channels after the same time at 12 kV (rms).

Dielectric strength tests were also made between a sphere of 6 mm radius and a plane electrode in transformer oil and in air. The results given in the table show that heat treatment increases the mean breakdown voltage by some 20% and also reduces the spread in breakdown values from about 50% with untreated to about 20% with heat-treated PTFE. A possible explanation for these results is that there are many microscopic pin-holes in the untreated PTFE and that many of these holes are closed by heating at the transition temperature. Microscopic examination shows that there are several large pin-holes of one or more micron diameter per square centimetre in untreated PTFE. To test this hypothesis PTFE sheets were impregnated under vacuum in transformer oil and in silicone oil. It was then found that the mean value of the dielectric strength was increased but there was considerable divergence in the results. It appears, therefore, that the existence of pin-holes in the granular structure are not the only reason for the poor corona resistance of PTFE.

Effect of heat treatment on electric strength of 0·055 *mm thick PTFE sheet*

		Breakdown voltage [kV(rms)]	
		Untreated PTFE	*Heat-treated PTFE*
In oil	(a.c.)	5·6 ± 49%	6·6 ± 10%
In oil	(d.c.)	6·8 ± 21%	7·5 ± 16%
	Sphere: positive		
In oil	(d.c.)	5·3 ± 27%	7·9 ± 16%
	Sphere: negative		
In air	(a.c.)	3·2 ± 32·5%	4·0 ± 20%

ACKNOWLEDGEMENTS

The authors wish to express their thanks to Mr. K. Mase, Hitachi Company, for his kindness in offering the PTFE tape specimens.

REFERENCES

(1) PERKINS, J. R., and BRODHUN, C. G. Teflon as an electrical insulator. *Report of National Research Council of Canada on Electrical Insulation*, p. 31 (1949).
(2) MASON, J. H. *Proc. Instn Elect. Engrs*, **98**, Pt I, p. 44 (1951).

New books

Reports on progress in physics. Vol. 18, 1955. Edited by A. C. STICKLAND. (London: The Physical Society, 1955.) Pp. 477. Price 50*s*.

The ever-increasing volume of research and the opening up of many new fields of investigation make it quite impossible for any physicist to keep abreast of current developments by reading original papers, except those in his field of special interest. Thus good survey articles written by experts are becoming more and more a necessity. As its predecessors, the eighteenth volume of these reports provides excellent information on a variety of subjects in experimental and theoretical physics.

The article by G. H. Kinchin and R. S. Pease deals comprehensively with the displacement of atoms in solids by radiation, the processes of recovery and the experimental irradiation techniques. This is followed by an account of the experimental results. B. T. Price gives a survey of ionization by relativistic particles, summarizing the existing theories and comparing experimental data with the predictions. A discussion of the various methods for measuring strong magnetic field with particular emphasis on the application of magnetic resonance is given by J. L. Symonds. J. C. Gunn considers that the theory of radiation is now in a very complete state and his article consequently treats the subject with a certain degree of finality. He stresses the limitations imposed on radiation theory by extraneous interaction which can, however, be disregarded to a large extent. The general review of the field is supplemented by more detailed consideration of special problems exhibiting radiative corrections. There follow two articles on magnetostriction and electrostriction by E. W. Lee and H. F. Kay respectively. In the former the main emphasis is on the linear magnetostriction due to anisotropy which is the effect most easily and frequently observed. The effects arising from the exchange and demagnetizing energies are discussed in less detail. In the article on electrostriction the difference between this phenomenon and piezoelectricity is defined and the striction phenomena in single crystals and ceramic materials is dealt with separately. After giving a brief survey of demagnetization cooling, E. Ambler and R. P. Hudson discuss temperature determination and the properties of paramagnetic salts below 1° K. A description of various researches carried out below 1° K is followed by an account of recent developments such as two-stage and continuous cooling and the use of anisotropic salts. The article by K. D. Bowers and J. Owen on paramagnetic resonance is supplementing an earlier one (vol. 16) on the same subject by Bleaney and Stevens. The present report is a collection of data on crystalline solids containing ions of the transition groups. J. D. Craggs and C. A. McDowell have contributed an article on the effects of electron impact on complex molecules. A survey is given of experimental methods and techniques of measurement together with the results obtained.

The volume concludes with six short articles by R. E. Peierls, A. Salam, P. T. Matthews and G. Feldman which are based on a series of lectures given at a meeting of The Physical Society in Birmingham in December 1954. They give a survey of the field theory of elementary particles which is intended for the non-specialist reader.

K. MENDELSSOHN

Building materials, their elasticity and inelasticity. Edited by M. REINER, with the assistance of A. G. WARD. (Amsterdam: North-Holland Publishing Company, 1954.) Pp. xv + 560. Price 84*s*.

This book consists of a number of articles dealing with the elastic and the plastic properties of the materials commonly used in buildings, and the bearing of their properties on design and use. The materials include fresh and set concrete, metals, bitumen and tars, unfired clay, and the soil on which the buildings rest; and minor materials such as paint, mastics, flooring materials and putties. The whole is prefaced by an essay in theoretical rheology by M. Reiner. Many of the authors of the individual contributions are at the forefront of research on their chosen topic and write with authority and completeness, so that the book is of value to specialist workers seeking to review the elastic and plastic properties of building materials with which they are concerned.

Inevitably the book tends to reflect the character of the building industry, which has been given the appearance of unity by statisticians and planners, a unity which in reality it does not possess. The industry is itself a congeries of contractors, craftsmen, manufacturers of building materials, architects, engineers and many other specialists. In addition, research workers trained in many diverse scientific disciplines have concerned themselves in recent years with the problems of the industry. Similarly in the book the editors have failed to integrate completely the main themes—rheology, concrete technology, metal physics, soil mechanics; indeed, the otherwise excellent essay on soil mechanics uses a special notation. But at least the book is a step towards such integration, and its value rests in having brought authoritative accounts of the diverse studies within the same covers, thus enhancing the possibilities of cross-fertilization.

A. T. PICKLES

Dust is dangerous. By C. N. DAVIES, D.Sc., F.Inst.P. (London: Faber and Faber Ltd., 1955.) Pp. xvii + 116. Price 21*s*.

This excellent book "seeks to explain and classify the dangers of dust, and to set out general principles for assessing and dealing with dust problems." It does not deal to any extent with the science of dust, which, the author points out, is mainly physics, nor does it go into great detail about the engineering of preventive measures. Dr. Davies achieves his object with a clear, direct and unequivocal style which reveals a real mastery of the subject. His book can be commended to all who are concerned with dust problems (and most of us are whether we like it or not); few readers will fail to find something new in it.

The discussion on dust hazards to industrial workers in mine and factory shows how widespread and unsuspected the hazards may be. There are chapters on the new subject of radioactive dusts, on explosion dangers, and on dust in the home. Dust sampling instruments and the problem of how to use them to assess exposures are quite well covered, but it would be helpful if a distinction could be drawn between the devices which are commercially available and those which exist only in prototype stage. No mention is made of the new micro-pore filters which enable particles to be examined under high power microscopy on the surface of the filter membrane used for their collection. A particularly valuable

chapter of the book is that dealing with preventive measures, which correctly emphasizes the importance of tackling dust at its source.

The problem of dust in mines must inevitably occupy a prominent place in such a book as this, and here perhaps the reviewer may be permitted a few specific comments. It should be made clear (p. 52) that the figure given for the production of fine dust by coal cutting machinery relates to the "sawdust," which forms only a small part of the coal won by the machine. The reviewer knows of no "schemes afoot for the technically difficult extraction of highly diluted methane from the upcast shafts of coal mines," although experiments are in hand to burn it usefully in the diluted state, moreover the local extraction of methane in high concentration from the coal measures is already being successfully exploited (pp. 69–70). The purpose of cooling the air of mines is to provide a comfortable environment for men, not to cool the strata. This object is helped, not hindered, by the "film resistance" to heat transfer between rock and air (pp. 69–70). Finally, the author states that all coal conveying, etc., must be in return airways (p. 71). His argument is sound from the point of view of dust, but it ignores the other problem of gas which is usually considered to present a greater hazard and has determined the more frequent placing of haulage machinery in the intake roadways.

The book is well indexed and illustrated and only a few typographical errors were noted. A minor but irritating feature is the grouping of references by chapters at the end of the book so that it is necessary to turn back to find the number of the chapter that one is reading, before a reference can be found.

W. H. WALTON

Neutron diffraction. By G. E. BACON. (London: Oxford University Press, 1955.) Pp. ix + 299. Price 35*s*.

During the past ten years the technique of neutron diffraction has been developed to the point where results of great importance and significance have been published. Dr. Bacon is one of the relatively few who have had access to an intense beam of thermal neutrons, and he has contributed much original work in this field on both the theoretical and the experimental sides. This excellent textbook, which is the fourteenth volume in the series of monographs on the physics and chemistry of materials, gives a comprehensive account of principles, practice and achievements.

The main applications of neutron diffraction are firstly in the location of light atoms, and especially of hydrogen in crystals which also contain heavier atoms; secondly in problems, such as arise in alloy systems and in spinels, where distinction must be made between atoms of neighbouring atomic numbers; thirdly, and perhaps most important, in investigations of the structures of magnetic materials and especially of antiferromagnetic and ferrimagnetic compounds. It is clear that neutron diffraction studies are likely to provide new information about the forces in nuclei and about various types of magnetic atom, as well as about structural problems.

The book has a useful list of symbols, excellent indexes, and a valuable collection of references.

KATHLEEN LONSDALE

Nuclear levels in the neighbourhood of the 1 $F_{7/2}$ state. By R. H. NUSSBAUM. (Assen: Van Goreum and Comp., N.V., 1955.) Pp. 78. Price H.Fl. 7.90.

Experiments with beta- and gamma-ray spectrometers on the decay of eight nuclei with N or Z between 16 and 29 are described. A survey is made of the known energy levels of odd mass nuclei in this range and their properties are compared with the predictions of the shell model. There does not seem to be enough detailed evidence on these nuclei to make this comparison very useful at present.

J. O. NEWTON

Introduction to experimental physics. By W. B. FRETTER, Ph.D. (London: Blackie and Son Ltd., 1955.) Pp. viii + 349. Price 35*s*.

This is a good book with a somewhat unsuitable title. It is essentially a compilation from lectures given at the University of California on technical topics that are of special interest to research physicists at Berkeley. Since the fifty-two contributors include many of the physicists whose skill in technique has helped to make Berkeley one of the world's greatest centres of nuclear research, the book has much to offer to the young nuclear physicist. It also contains summaries of techniques current in such fields as low temperatures and X-ray diffraction, but these form a quite small part of the collection.

The book is to be recommended most strongly to the experimenter in nuclear physics who wants to know how things are done at Berkeley; strongly to the reader who wants an introduction to the techniques of nuclear physics; and doubtfully to the student who is looking for an introduction to experimental physics in general.

P. B. MOON

Magnetic materials in the electrical industry. By P. R. BARDELL, B.Sc., M.I.E.E., F.Inst.P. (London: Macdonald and Co. Ltd., 1955.) Pp. viii + 288. Price 32*s*. 6*d*.

Several recent books on magnetic materials, their properties and applications are available to students and research workers interested in the subject, and the present work is a valuable addition.

It is clear that the author is an authority on the applications of magnetic materials at power frequencies and in communication engineering. Thus the parts of the book dealing with measurements of properties of laminated magnetic materials and powder cores, as well as with applications of these substances, are excellent. The treatment of fundamental principles involved and technological knowledge required is very skilfully balanced to be of greatest possible use to the physicist who seeks for information on the application of magnetic substances.

Special mention must be made of the very full and sound treatment given to magnetic recording, where the available literature seems to be scattered and not of easy access. A short chapter is devoted to magnetic amplifiers, dealing with fundamental principles only, but representing a good introduction. A chapter on transducers is included which gives the basic theory in an easily understandable manner.

Thus there is much in this book to recommend it, but unfortunately there are a few grave inadequacies and omissions. The introductory chapter dealing with magnetic theory and with the properties and production of hard and soft magnetic materials might have been omitted. To give a few obvious examples, magnetic powder patterns are mentioned, but the names of R. M. Bozorth and H. J. Williams do not appear either in the text or in the references to the chapter. According to the author, quench hardened magnet steels are classed as austenitic. Magnadur has the formula $(BaO)_6Fe_2O_3$, and anisotropic permanent magnets are

magnetized during heat treatment. Ferrites are only mentioned, but not discussed in any manner corresponding to their usefulness.

The chapter on magnetic testing is sketchy and unsound.

The book is carelessly printed, printer's errors can be found on many pages and it appears that not enough care has been exercised in proof correction. On the other hand, the illustrations are well produced and are in all cases a valuable addition to the text. K. HOSELITZ

Atomphysik, Vols. 1 and 2. By KARL BECHERT. (Berlin: Walter de Gruyter and Co., 1955.) Pp. 120 and 109. Price DM 2.40 each.

With the appearance of these two volumes the presentation of atomic physics in the Sammlung Göschen has become complete. Volumes 3 and 4 were reviewed in 1954.*

In Volumes 1 and 2 the experimental foundations of atomic physics are presented in more or less the usual way but in a very concise and well-considered form. The presentation begins with the behaviour of gases and goes on to cathode rays, positive rays and mass spectroscopy. Particle counters and cloud chambers are briefly described, and the passage of fast particles through matter leads to Rutherford's experiments on α-particle scattering and the atomic nucleus. The last chapter deals with diffraction phenomena and dispersion. In Volume 4 quantum phenomena appear in earnest and the wave and corpuscular character of matter is discussed at length. Magnetic moments of atoms and sub-atomic particles take up one chapter, and the last two chapters are concerned with the interaction of fast particles with matter and the phenomena of cosmic radiation.

As in my previous review, I feel compelled to praise the compactness and precision of the writing. Mathematically, Volumes 1 and 2 are much easier than Volumes 3 and 4 in which quantum mechanics is presented. The compact writing has made it possible to include a surprising amount of material, and these four slender volumes should be particularly valuable to a lecturer (if he knows German) in preparing his course. O. R. FRISCH

Harmonic analysis and the theory of probability. By S. BOCHNER. (London: Cambridge University Press; California: University of California Press, 1955.) Pp. viii + 176. Price 35*s*.

Ever since harmonic analysis was invented by Fourier this method has played an important role in probability theory. One of the most significant modern improvements of the theory was brought about by the introduction of the "Fourier Transform" of a probability function, called "characteristic function." The author of the present book is one of the foremost experts in the field of Fourier transforms. He was recently able to generalize the notion of the characteristic function to stochastic processes, which are essentially infinite directed sequences of probability distributions generated one from another by certain transformations. For such sequences one can, under certain conditions, define a "characteristic functional" as a Fourier transform in an Euclidian space with an infinite number of dimensions. This is likely to become a valuable tool in the analysis of stochastic processes. The presentation of the theory is very abstract and requires familiarity with the theory of sets and other subjects of advanced analysis. Although certainly of great value to mathematicians it will hardly appeal to applied physicists who are concerned with the practical analysis of random phenomena. R. FÜRTH

Proceedings of the Eastern Joint Computer Conference. (New York: The American Institute of Electrical Engineers, 1955.) Pp. 92. Price $3.00.

Probably most readers are aware of the nature and purpose of electronic digital computers. Broadly speaking they fall into three classes. Firstly, the large scale fully automatic machines, represented in this country by the Ferranti Model MK I* and the English Electric DEUCE; secondly, the smaller machines based mainly on a magnetic drum storage system, e.g. the Elliott Brothers 401 and 402; and finally the semi-automatic computers built up from punched-card systems. This conference report deals with the last two kinds of machines, which might be described as little-big and big-little computers respectively. Several American machines are described and compared; applications, both scientific and commercial, are mentioned. Some machines are mainly of interest from the constructional point of view, notably the Bell Laboratories' TRADIC, a breadboard machine built largely from point contact transistors (incidentally the builders suggest that the future lies with junction transistors). Finally there are papers dealing with special components: these include high-speed punched-tape equipment, a high-speed printer, techniques for increasing the storage density of a magnetic drum system, and magnetic core storage circuits. R. A. BROOKER

Notes on applied science No. 10. Noise measurement techniques. (London: H.M. Stationery Office, 1955.) Pp. iv + 40. Price 2*s*.

The booklet is a guide to the choice of methods and techniques for determining the physical characteristics of noise based on the experience of the National Physical Laboratory. After briefly setting out the physical and subjective characteristics of noise the various methods of measurement are considered, namely, waveform recording and analysis into broad or narrow bands. The suitability of these methods for particular practical problems is discussed and appropriate measuring apparatus described, giving the performance of microphones and amplifiers and much detailed information on circuits and components. Output meters, level recorders, filters and analysers are all clearly explained in quantitative terms and advice is given on the checking of calibrations. On the subjective side, the new N.P.L. equal loudness contours and loudness scale are given. Appendices describe the N.P.L. mobile acoustical laboratory and give some useful references. The producers of the booklet are to be congratulated on condensing an enormous amount of useful practical information into 40 pages. A. J. KING

Ultrasonic engineering. By A. E. CRAWFORD. (London: Butterworths Scientific Publications, Ltd., 1955.) Pp. x + 344. Price 45*s*.

Judging by the number of books on ultrasonics which have appeared in recent years, interest in this branch of physics is by no means flagging. The author of this one has been concerned with the development of ultrasonic tools and high power equipment by one firm. Yet this is not just a "house" textbook; Mr. Crawford has devoted much space to other firms' equipment and added good bibliographies on all types of applications. The book is to be recommended to those who wish to know what apparatus is available in this field and what can be done with it. E. G. RICHARDSON

* *Brit. J. Appl. Phys.*, **5**, p. 456 (1954).

Notes and comments

Exhibition of dividing machines

Dividing machines are now used to engrave the graduations on linear and circular measuring scales used in instruments. However, until the middle of the eighteenth century measuring scales were divided by hand or by the use of a dividing plate. The first successful dividing engine was built in 1775 by Jesse Ramsden and divided circular scales mechanically. Improvements since then have yielded increased accuracy. To illustrate the evolution of the dividing machine eight circular dividing machines are being exhibited for a few months at The Science Museum. The earliest is dated 1778 and the latest 1955; two of them will be shown in operation.

The protection of workers against ionising radiations

We have received a copy of a very readable and informative sixty-six-page report presented by the International Labour Office to the Geneva Conference on the Peaceful Uses of Atomic Energy entitled *The protection of workers against ionising radiations*. It was prepared for the ILO by Mr. K. L. Goodall, H.M. Chemical Inspector of Factories, and covers the following subjects: Part I, the interests of the ILO in radiological protection; Part II, the history of radiation injuries, the nature and properties of the various ionising radiations and the injurious effects to which they can each give rise; Part III, standards of exposure; Part IV, the manifold uses of ionising radiations in medicine, agriculture and industry; Part V, the general and special precautions appropriate for radiation workers in atomic energy plants, factories, hospitals and research laboratories; Part VI, problems arising in uranium mining and processing; Part VII, the packing, labelling and transport of radioactive materials. A number of appendices include the ILO Model Radiation Code, a summary of the current ICRP recommendations on permissible doses and examples of suitable medical record forms for the clinical and haematological examination of radiation workers.

Copies of the report may be obtained from the International Labour Office in Geneva or from the United Kingdom Office at 38–39 Parliament Street, London, S.W.1, price 3*s.* 0*d.* (50 cents). It is also available in French and Spanish.

High-speed photography

A third international congress on high-speed photography is to be held in London from 10 to 15 September, 1956, at Government Offices, Horse Guards Avenue, London, under the sponsorship of the Department of Scientific and Industrial Research. An international exhibition of high-speed photographic equipment will also be mounted in the same building. It is the intention of the exhibition committee to bring together research and commercial exhibits which will be representative of the latest work in the following and other fields: flash light sources; inertialess shutters; mechanical–optical drum cameras; image sampling techniques; schlieren, interferometric stereoscopic colour photomicrography.

The exhibition committee invites exhibits and reserves the right to accept those exhibits most appropriate to the congress. Further details may be obtained from Department of Scientific and Industrial Research, Charles House, 5–11 Regent Street, London, S.W.1.

British Journal of Applied Physics

Original contributions accepted for publication in future issues of this Journal

An apparatus for the accurate control of the peak X-ray energy of a 20 MeV betatron. By K. Phillips.
Stress distribution in a tee junction of thick pipes. By H. Fessler and B. H. Lewin.
The laminar flow of streams of suspended particles. By T. V. Starkey.
Measurement of the half-life of radon with a Curie-type ionization chamber. By P. C. Marin.
A comparison of dry stripped unbacked collodion and Formvar replicas. By D. J. Evans.
Collodion replicas from cross-sections of thin metallic strip and coatings. By D. J. Evans.
Fields and stresses in dielectric media. By G. Power.
The measurement by nuclear resonance of light water concentration in mixtures of light and heavy water. By A. M. J. Mitchell and G. Phillips.
Photographic method of obtaining stress trajectories. By A. R. Morris.
The thermal and electrical conductivities of deposited carbon. By A. R. G. Brown, W. Watt, R. W. Powell and R. P. Tye.
Origin and analysis of gas in electron tubes. By S. J. Stoll.
Electron optics of X-ray tubes and the design of unbiased sharply-focusing cathodes. By A. R. Lang and D. A. G. Broad.
A modified replica technique and its application to the examination of etched single crystals of barium titanate. By D. S. Campbell and D. J. Stirland.
The inductance of two elliptic tubes. By E. E. Jones.

Journal of Scientific Instruments

Contents of the January issue

ORIGINAL CONTRIBUTIONS

Papers

A scintillation counter for the assay of radioactive gases. By D. R. Stranks.
Some aspects in the design of a torque magnetometer. By F. W. Harrison.
A servo-mechanism for the study of self-extinction of gaseous discharges in cavities in dielectrics. By E. C. Rogers, E. B. Page and V. G. Harriss.
Some parasitic deflexions in parallel spring movements. By R. V. Jones and I. R. Young.
The stability of thermistors. By A. Beck.
A mechanical binary-decimal converter. By M. Setterwall.
The use of polarized light for the measurement of small angular displacements. By A. J. Bartley.
A laboratory scale chill-casting vacuum induction furnace. By D. A. Craw and W. G. Henry.
Apparatus for the electronic presentation of optical diffraction patterns. By A. W. Hanson and A. Menarry.
A constant temperature solubility cell or reaction vessel for a Beckman quartz spectrophotometer. By D. N. Glew and R. E. Robertson.
A wide range Schlieren system. By H. Jeffree.

Laboratory and workshop notes

A simple desorption system for obtaining temperatures above that of liquid helium. By A. C. Rose-Innes and R. F. Broom.
A two-way tap for continuous operation. By F. A. Grimes.
A thyratron index and time-marking unit. By R. B. Morrison.
A method of preparing laminated copper. By K. Nelson.
A simple relay-operated timer. By L. R. Jenkin.
A magnetically operated vacuum valve. By R. M. Glaister.
An object holder for microscopic measurements. By H. Shapiro.
An adaptable mechanism for converting rotary motion into a succession of linear movements. By A. L. Sims.

NOTES AND NEWS

Correspondence

Transit time spread in electron multipliers. From T. D. S. Hamilton and G. T. Wright.
A capacitance-resistance hygrometer. From C. L. Cutting, A. C. Jason and J. L. Wood.

New instruments, materials and tools
Notes and comments

THIS JOURNAL is produced monthly by The Institute of Physics, in London. It deals with all branches of applied physics (including theory and technique).
All rights reserved. Responsibility for the statements contained herein attaches only to the writers.
EDITORIAL MATTER. Communications concerning editorial matter should be addressed to the Editor, The Institute of Physics, 47 Belgrave Square, London, S.W.1. (*Telephone:* Sloane 9806.) Prospective authors are invited to prepare their scripts in accordance with the *Notes on the preparation of contributions*. (Price 2*s.* 6*d.* including postage.)
REPRODUCTION. The Institute of Physics is a signatory to The Royal Society's Fair Copying Declaration. Details may be obtained upon application from The Royal Society, London, W.1.
ADVERTISEMENTS. Communications concerning advertisements should be addressed to the agents, Messrs. Walter Judd Ltd., 47 Gresham Street, London, E.C.2. (*Telephone:* Monarch 7644.)
CLAIMS FOR MISSING JOURNALS. Claims from regular subscribers to this *Journal* for missing numbers will only be considered if received within 60 days of the date of mailing plus normal outward time of transit and time for lodging the claim. Losses attributable to failure to notify a change of address or to similar omissions will not be considered.
SUBSCRIPTION RATES. A new volume commences each January. The charge is £4 per volume ($11.50 U.S.A.), including index (post paid), payable in advance. Single parts, so far as available, may be purchased at 8*s.* each ($1.15 U.S.A.), post paid, cash with order. Orders should be sent to The Institute of Physics, 47 Belgrave Square, London, S.W.1, or to any bookseller.

SPECIAL ARTICLE

The United Kingdom Atomic Energy Authority and its functions*

By Sir John Cockcroft, K.C.B., C.B.E., D.Sc., F.Inst.P., F.R.S., Atomic Energy Research Establishment, Harwell, Berkshire

The United Kingdom Atomic Energy Authority has three main groups: research, industrial and weapons. The Research Group carries out research and development directly relating to civilian application of atomic energy. The Industrial Group designs and operates factories for the production of uranium metal and the fissile materials uranium 235 and plutonium. It has also a design office for the design of pioneering type of nuclear power stations. The Industrial Group has also a Research and Development Branch which carries out experimental research into the operational problems of the factories and into specific development problems of new plant and nuclear power stations.

The nuclear power programme of the future requires the development of new types of power stations as successors to the gas-cooled graphite-moderated power stations which are now to be constructed by industry in successively improved marks. The Research and Industrial Groups together explore the different possible types of future power stations and are carrying out design studies on the most promising types. During the last year, for example, a design study on the pressurized-water reactor has been carried out in collaboration with industry and the Central Electricity Authority (C.E.A.). The comparative merits of this and other possible Stage-2 reactors are now being assessed.

At the same time longer-range work is carried out on still more advanced reactors such as the homogeneous reactor and the fast reactor. This work combines with zero-energy reactor physics studies and is followed by construction of an experimental reactor.

Each new reactor requires the development of specific technologies, particularly in the development of appropriate fuel elements and associated chemical-processing facilities for spent fuel elements. This development requires an intensive testing programme of reactor components, particularly fuel elements, and the Authority is now building three heavy-water research and fuel-element-testing reactors to speed up such testing. These reactors require associated heavily shielded and remote-handling facilities for examining the highly radioactive components. These expensive central facilities are likely to continue to be provided by the Authority. Also it seems likely that fuel-element fabrication and chemical-processing facilities will be held by the Authority. Industry will take an increasing share of the research and development work and construction work for reactors and nuclear power stations, and the pattern of co-operation is being worked out by experience.

The Research Group is responsible for the production and application of radioactive isotopes and radiation. These applications are growing rapidly, at a rate of about 25% a year, and it is expected soon to have very powerful sources of radiation available for industrial processes.

The Research Group also looks to the future and carries out research and long-term projects of importance to future developments.

The United Kingdom Atomic Energy Project was founded in 1946. It now consists of an Authority—the directing Board of the project—with three groups: the Research Group, the Industrial Group, and the Weapons Group. The first six years of its existence was devoted to building up the facilities and the supply of uranium and fissile material essential to atomic energy development. The Harwell airfield of the Royal Air Force was converted into a research establishment and two atomic piles and several nuclear accelerators were built there. A design organization was formed at Risley, near Warrington, Lancs, and factories were built to produce uranium metal, plutonium and uranium enriched in ^{235}U. The production of these materials was begun largely for military purposes, but the availability of plutonium and enriched uranium for research and development purposes has within the last year increased the facilities for civil development.

RESEARCH AND INDUSTRIAL GROUPS

During the last three years it has been possible to turn an increasing part of the effort of the Research and Industrial Groups towards the development of nuclear power. At present the Research Group has just over 500 scientific, technical and engineering staff working directly on power projects and associated nuclear technology. The Industrial Group has also an Applied Research Department, which has about 250 staff of these grades working on the programme.

The distribution of effort between the two groups is complementary. The Research Group is responsible for all basic nuclear requirements, such as the cross-sections of nuclei and the number of neutrons per fission of the important isotopes. It is also responsible for work in reactor physics, namely, the calculation and prediction of the nuclear properties of new types of reactors. It does this by building sub-critical or just critical assemblies of uranium and moderator for thermal reactors, or of plutonium or enriched uranium assemblies for fast reactors. The reactors DIMPLE,

* Being the opening address at the inaugural meeting of the British Nuclear Energy Conference, held in London on 30 November, 1955, and originally published in the first issue of the Journal of that Conference. The British Nuclear Energy Conference is a permanent consultative body formed by the Institutions of Civil, Mechanical, Electrical and Chemical Engineers and The Institute of Physics.

Further particulars about the Conference and its Journal are obtainable from the secretary of the Conference 1–7 Great George Street, London, S.W.1.

ZEPHYR and ZEUS are examples of so-called zero-energy reactors built for this essential task (Figs. 1–5).

The Research Group also designs and operates reactors built for research, development and testing. Thus the low-power GLEEP reactor operates on a 24-hour schedule testing the quality of the uranium metal and graphite for nuclear reactors. It also performs a few useful research jobs such as studying the effect of slow neutrons on biological systems. The BEPO research reactor operates at a power level of 8 MW and is used for engineering, metallurgical, chemical and other experiments, at a reasonable neutron intensity of 10^{12} neutrons per square centimetre per second. It also provides neutron beams for the physicist and is one of the main sources of radioisotopes for the world.

To meet the need for much higher neutron intensity of the order of 10^{14} neutrons per square centimetre per second two new heavy-water reactors, DIDO (Fig. 6) and PLUTO are being built at Harwell and a further PLUTO reactor at Dounreay, Caithness. These will be used for long periods for testing nuclear fuels and fuel elements to be used in future reactors. They are essential tools of the metallurgist and chemical engineer. The PLUTO reactor has been described as a fuel-element-testing reactor, since it will contain six to eight "loops" in which the fuels and fuel elements will be exposed to radiation at the operating temperatures expected in future reactors. The testing reactors will have associated with them facilities for examining the exposed fuel elements, which will become highly radioactive. Accordingly, buildings equipped with heavily shielded laboratories and remote-handling facilities are being provided.

Also being built is a so-called swimming-pool reactor for studying the design of shields for reactors. It will have fuel elements containing about 3 kg of highly enriched uranium and will operate at a normal power level of 100 kW.

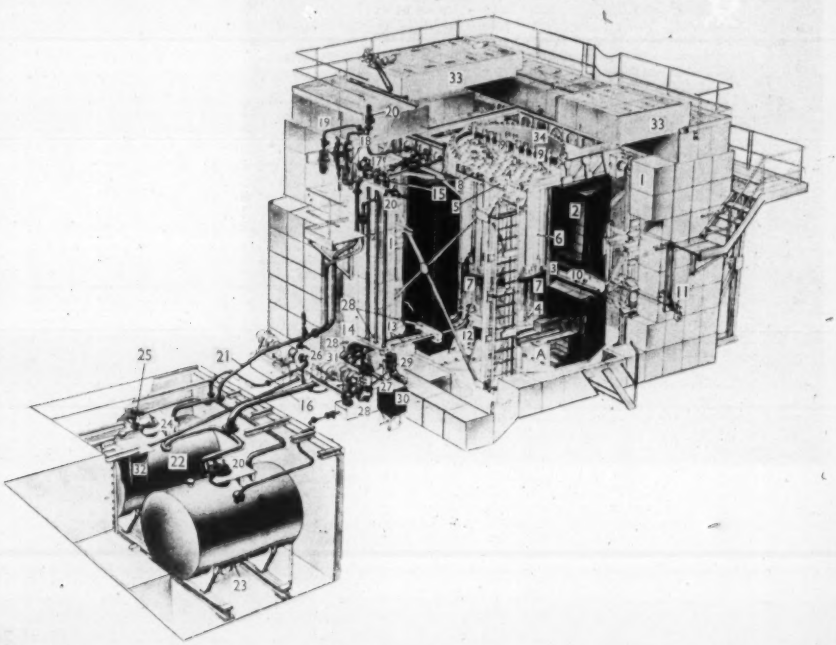

Fig. 1. DIMPLE (deuterium-moderated pile, low energy)

1, biological shield (concrete); 2, graphite reflector; removable section below "A"; 3, reactor tank, aluminium, containing heavy water; 4, lattice plates; 5, support beams; 6, uranium elements; 7, shut-off rod; 8, shut-off rod winding gear; 9, experimental search tubes; 10, flux-measuring ion chamber; 11, ion-chamber moving gear; 12, partial dump stand pile; 13, dump lines; 14, dump valves; 15, dump-valve operating head; 16, main dump line; 17, D_2O level transmitter; 18, safety valve (liquid-sealed U-tube); 19, breather drier; 20, drying connexion; 21, balance line; 22, dump tanks; 23, dump-tank balance line; 24, priming pump; 25, non-return valve; 26, transfer pump; 27, control pump; 28, leak shrouds; 29, controlled dump valves; 30, pump-motor control cabinet (for control pump); 31, D_2O sampling point; 32, D_2O leak tank; 33, travelling top shield, 34, removable tank top.

These central facilities must for some time to come be largely owned and operated by the Authority, just as the largest wind tunnels are owned and operated centrally in the world of aerodynamics.

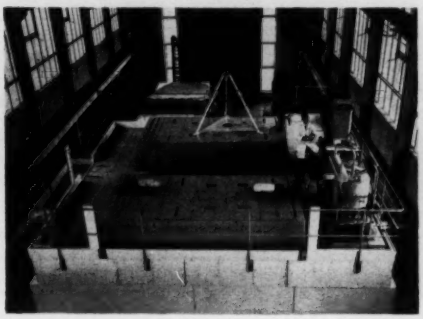

Fig. 2. DIMPLE (deuterium-moderated pile, low energy)

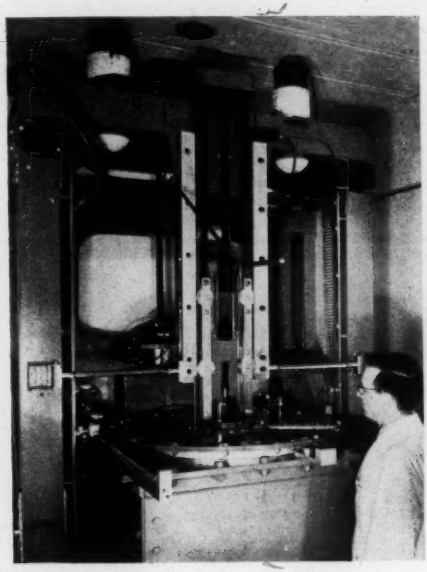

Fig. 3. ZEPHYR (zero-energy fast breeder reactor)

DEVELOPMENT OF REACTORS

The development of nuclear reactors passes through several well-defined stages. The first is the selection of a particular type for study out of the 900 or so possible "types." From this large number the nine types shown in Table 1 are engaging the main attention of designers today. The table shows that countries lacking access to appreciable quantities

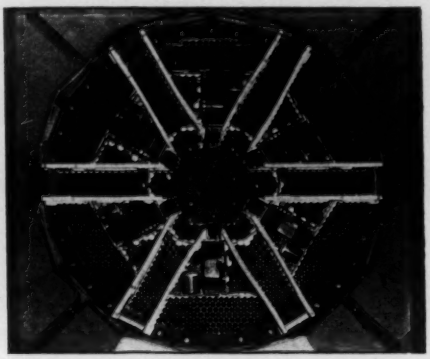

Fig. 4. View of core of ZEUS (zero-energy uranium system reactor) from above

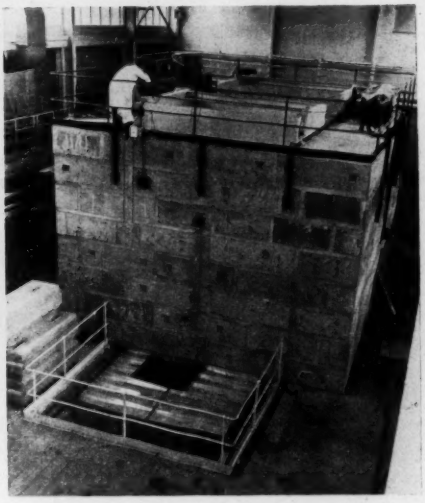

Fig. 5. ZEUS (zero-energy uranium system reactor)

of enriched uranium are limited to a choice of two reactors to start their programme: graphite-moderated gas-cooled, or heavy-water reactors. Since the United Kingdom was not producing large quantities of heavy water the United

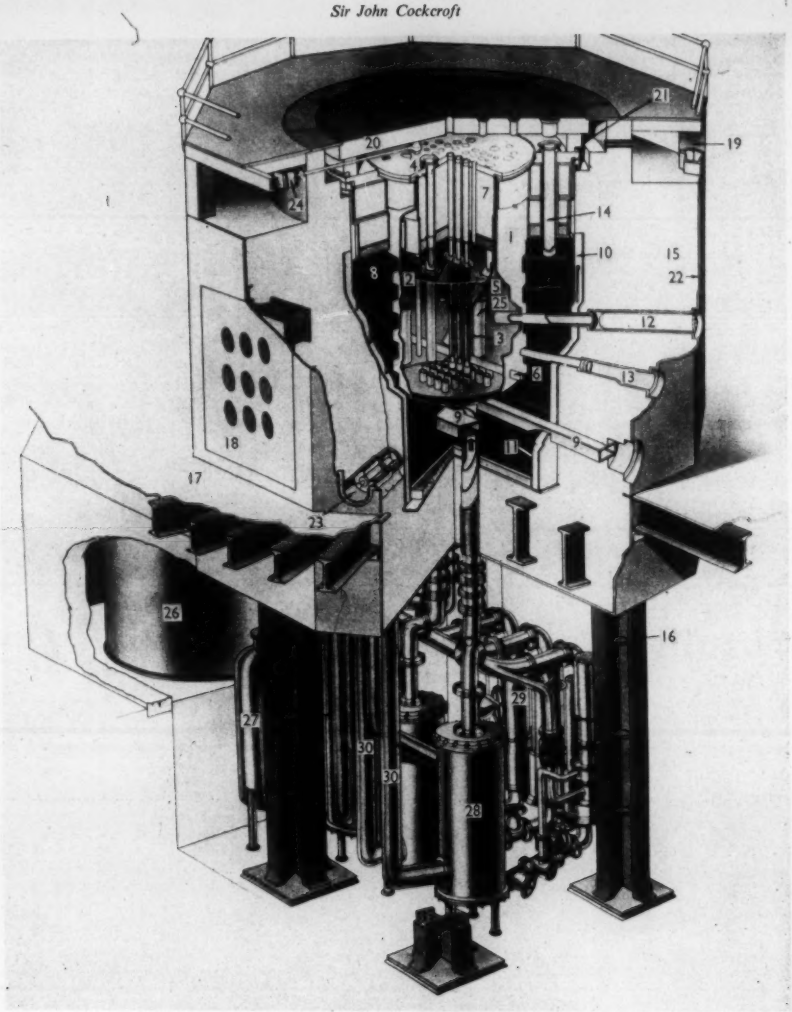

Fig. 6. Cut-away view of heavy-water reactor DIDO

1, reactor aluminium tank containing heavy water; 2, heavy-water level; 3, fuel element; 4, vertical experimental hole thimble; 5, six control signal arms; 6, experimental hole 4 × 2 in.; 7, top biological shield; 8, graphite reflector; 9, experimental holes 12 × 18 in.; 10, lead thermal shield (water-cooled); 11, reactor steel tank with boral sheet lining; 12, experimental hole entering heavy-water zone; 13, experimental hole entering graphite zone; 14, vertical experimental hole entering graphite zone; 15, concrete biological shield; 16, reactor supporting structure; 17, first floor; 18, thermal column; 19, hollow stanchions communicating with base of reactor; 20, 10 in. thick steel top plate; 21, duct for experimental services; 22, biological shield casing plates; 23, ion chamber; 24, fine control rod gear box; 25, heavy-water outlet pipe; 26, heavy-water storage tank; 27, heavy-water safety dump tank; 28, heavy-water heat-exchangers; 29, heavy-water main circulation pump; 30, secondary cooling water piping (to coolers).

Table 1. *Types of reactor*

Type	*Output (MW)*	*Coolant*	*Fuel*	*Country of construction*
Graphite-moderated	100–200	Gas	Natural uranium	U.K.
Graphite-moderated	100	Water	Enriched uranium, 2·5% ^{235}U	U.S.S.R.
Graphite-moderated	75	Sodium	Enriched uranium, 1·8% ^{235}U	U.S.A.
Pressurized water	75	H_2O	Enriched uranium, 1·6% ^{235}U	U.S.A.
Boiling H_2O	180	H_2O	Enriched uranium	U.S.A.
D_2O	10 (experimental)	D_2O	Natural uranium	Canada
Aqueous homogeneous	10 (experimental)		^{233}U	U.S.A.
Liquid-metal-fuelled homogeneous			^{233}U	
Fast breeder	60		Pu–^{238}U ^{235}U–^{238}U	U.S.A. U.K., U.S.A.

Kingdom Atomic Energy Authority (U.K.A.E.A.) programme began with the graphite-moderated gas-cooled reactor (Fig. 7).

The programme for the development of nuclear power in Britain was announced in a Government White Paper[1] published in 1955. This programme provided for the construction of twelve nuclear power stations for the Central Electricity Authority (C.E.A.) to be completed by 1965. The first of these are to be improved versions of the Calder Hall graphite-moderated reactors. The engineering features of the Calder Hall power station were described by Sir Christopher Hinton[2] at the Geneva Conference and the construction is shown in the Calder Hall film. The C.E.A. power stations are being designed by four groups of firms and it is not yet known what design output will be achieved, but it may be in the region of 150 MW per station. Forecasts of the cost of the power from a 150-MW unit of this kind were made by Jukes[3] of the U.K.A.E.A. at the Geneva Conference and are shown in Table 2.

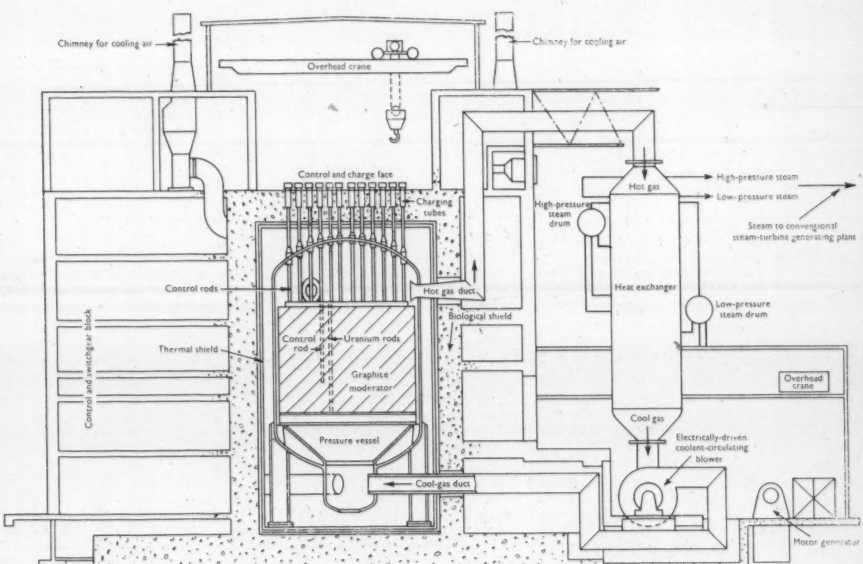

Fig. 7. A gas-cooled graphite-moderated power reactor

CHOICE OF REACTOR

An essential feature of the graphite-moderated reactors, which the White Paper[1] refers to as Stage-1 reactors, is that

Table 2. *Costs of gas-cooled graphite-moderated nuclear power stations* (150 *MW output*)

	Capital cost (£ *million*)	*Annual cost* (£ *million*)	*Cost of electricity at 80% load factor* (*pence per kWh*)
Capital and overhead costs			
Reactor items	7·5	0·68	
Other plant	11·3	0·69	
Total construction	18·8	1·37	
Cost of initial fuel charge at £20000 per ton uranium	5·0	0·20	
Total	23·8	1·57	0·36
Operating costs			
Site operating costs		0·26	
Cost of replacement cartridges at £20000 per ton uranium		1·46	
Total operating cost		1·72	0·40
Total gross cost		3·29	0·76 (= 9 mills)
Credit for plutonium at £5 and £10 a gramme net of processing costs		0·17 (= 2 mills)	0·33 (= 4 mills)
Net cost of electricity		0·59 (= 7 mills)	0·42 (= 5 mills)

they will produce plutonium as a by-product that can be stockpiled and used for more highly rated reactors requiring enriched fuel in Stage 2 or Stage 3 of the programme. The white paper envisaged a change to the more highly rated reactors of Stage 2 towards the end of the ten-year period. Five to ten times higher ratings—up to 5 electrical megawatts per ton of uranium—can probably be achieved by using water or liquid sodium as the heat-transfer medium.

Four reactors are being built in the United States which will be moderated by ordinary water. Three of these will be of the pressurized type (Fig. 8) in which the water is heated by uranium fuel elements generating a pressure of about 1 500 lb/in^2. The hot water then circulates through a heat exchanger. The electrical output from these three stations will be 75, 100 and 250 MW. The fourth station being built for the Nuclear Power Group will be of the boiling-water type in which steam will be generated in the reactor vessel itself and passed straight to a turbine. This station will develop 180 MW. Fig. 9 gives a comparison of the two types.

Boiling-water reactors have much lighter pressure vessels and components such as pumps. They have the possible disadvantage of radioactive contamination of the turbine. This does not, however, seem to have been a serious problem in the full-scale experimental boiling reactors which have operated successfully in the United States. The United States are also building a 75-MW power station using a sodium-graphite reactor as the heat source. This reactor can provide heat at a higher temperature than the water-moderated system so the thermodynamic efficiencies are likely to be well over 30%. These reactors also avoid the high pressures associated with the water-moderated systems and this is of importance from the safety point of view because of the difficulty of inspecting pressure vessels when they become radioactive.

The water-moderated reactors and the sodium-graphite reactors seem, therefore, to be the principal competitors for the second stage of the United States and United Kingdom programmes. In considering their relative merit, the overall "burn-up" of the uranium fuel which can be achieved must be taken into account. This depends on the conversion ratio of uranium 235 to plutonium in the system; the higher the conversion ratio, the more secondary fuel is produced, the longer the chain reaction can continue and the greater the utilization of uranium. The conversion ratio of the sodium-graphite reactor is likely to be rather worse than that of the water-moderated reactors. Another important factor is the type of fuel element used. Highly alloyed fuel elements are more expensive to fabricate and process. However it appears likely that water-moderated reactors will use uranium oxide fuel elements while sodium-graphite reactors will probably use unalloyed uranium metal since sodium is compatible with uranium metal. Engineering design considerations must also enter heavily into the consideration of relative merits. For example, the graphite core of the sodium-graphite reactor must consist of graphite blocks carried in zirconium sheet or otherwise rendered impervious to liquid sodium and it must be possible to replace defective graphite blocks.

For some time the U.K.A.E.A. have been carrying out a design study of a water-moderated reactor to produce enough heat for a power station of at least 150 MW output. The sodium-graphite system has also been studied by the U.K.A.E.A. At the present stage of study the economics of the two systems seem to be very evenly balanced and a choice will probably have to be made on technical and general engineering grounds.

Present feeling in the U.K.A.E.A. is that the best policy is to concentrate all their resources on one Stage-2 reactor.

The longer term Stage 3 of the programme aims at breeding, either by homogeneous reactors using the ^{233}U–Th fuel cycle, or the fast reactor using the ^{239}Pu–^{238}U fuel cycle. Although work is proceeding vigorously on Stage-3 reactors it is thought that the development period will be long, and a large-scale contribution to nuclear power from such breeders is likely to be in the 1970s rather than the 1960s. Fig. 10 shows the general arrangement of the Dounreay fast reactor.

PROCEDURE IN DEVELOPMENT OF A NEW REACTOR

The usual procedure in the development of a new reactor is to begin by a research or feasibility study of a reactor system. This involves reactor physics and some engineering studies

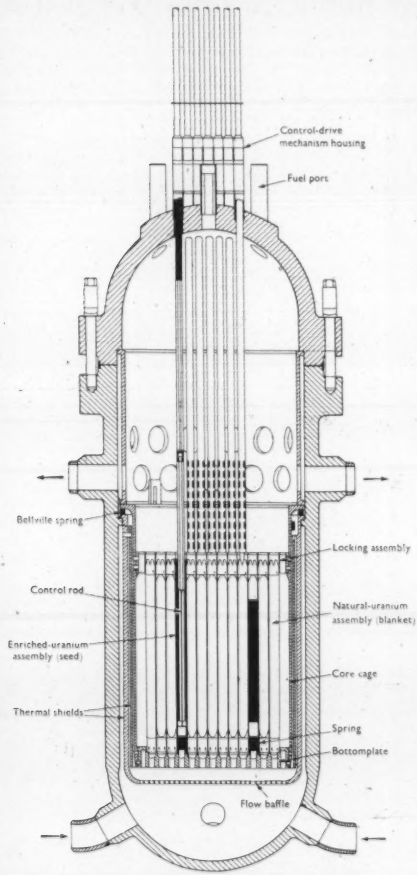

Fig. 8. Longitudinal section of reactor vessel of pressurized-water reactor

together with work by chemists, chemical engineers and metallurgists to make a preliminary assessment of the problems. If the reactor appears sufficiently promising, a design study is started. This requires a team of about fifteen engineers and draughtsmen, a reactor physics group to build sub-critical or zero-energy core assemblies, and chemists and metallurgists to study the chemical and fuel-element problems, for which loops must be built at this stage. The cost of the study may easily amount to £200 000 per annum. Preliminary design studies of this kind were carried out at Harwell for the Calder Hall reactor and a similar study has been proceeding on a pressurized-water reactor, LEO, as a possible candidate for Stage 2.

When a reactor is selected for design and construction, the Industrial Group design office takes over and the project is then co-ordinated and progressed by a design committee on which the Research Group is strongly represented. The Applied Research Department of the Industrial Group now takes a major responsibility for engineering development and for developing fuel elements and chemical-processing technology to meet the planned schedule of the project.

Industry is associated with each stage of reactor studies. At Harwell forty-two representatives of industrial organizations are taking part in reactor studies at the research or feasibility stage. Representatives of C.E.A. and two groups from industry have been helping with the design study of the pressurized-water reactor.

The Industrial Group is working closely with four industrial organizations on the design of the C.E.A. Stage-1 graphite-moderated power stations. The design proceeds independently in the separate organizations but regular co-ordinating meetings are held to discuss common problems and the contribution of the Authority to the development work.

The homogeneous reactor, which is part of the Stage-3 programme, is being studied with the help of chemical industry, since this reactor will be a highly specialized chemical plant with built-in facilities for continuous chemical processing of fuel.

Industry is also taking a major part in the design and construction of the new research reactors DIDO and PLUTO, and has already obtained an overseas order for a reactor of this type. Another industrial organization is prepared to build swimming-pool types of reactors. The export of such reactors will be limited by the availability of enriched fuel.

FUEL ELEMENTS

The production of uranium fuel and the processing of spent fuel is likely to continue to be the responsibility of the U.K.A.E.A. Development of fuel elements which will withstand the irradiation damage during the long "burn-up" period is probably the most difficult task in the whole programme. For some types of reactors heat extraction in a single cycle could reach 10 000 megawatt-days per ton—the equivalent of 30 000 tons of coal of 12 000 B.t.u./lb quality—before loss of reactivity would shut down the chain reaction. Radiation damage may well limit the actual "burn-up" to 30% of this, and this figure has been assumed in the White Paper. Uranium-metal fuel elements are distorted under thermal cycling owing to the peculiar metallurgical structure of uranium. The process of fission also contributes to distortion since the metal is traversed by large numbers of high-speed fission fragments, and fission gases build up large pressures. These effects can be mitigated by suitable temperature treatment leading to control of grain size and orientation. Judiciously adding small amounts of alloying material may also help, but in this case some degree of enrichment of fuel may be required.

Water reactors may use uranium-oxide fuel elements as their main charge since such elements are not attacked by hot water. Alternatively, the fuel elements must be alloyed or otherwise protected against corrosion.

Sodium-graphite reactors will be able to use uranium metal since this is compatible with liquid sodium. Whatever the type of fuel elements used they need prolonged testing in large numbers in the development period. The importance

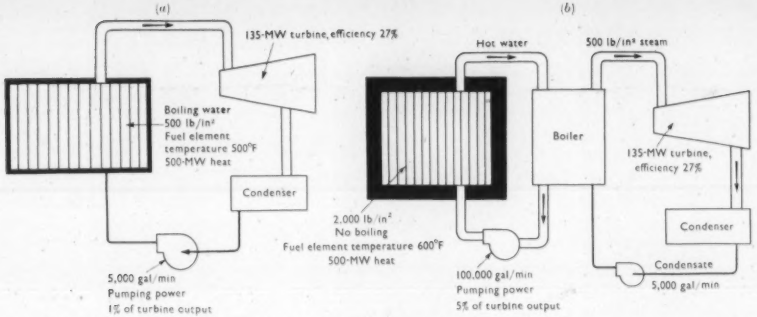

Fig. 9. Comparison of (*a*) boiling-water reactor with (*b*) conventional reactor and heat exchanger, supplying same steam requirements

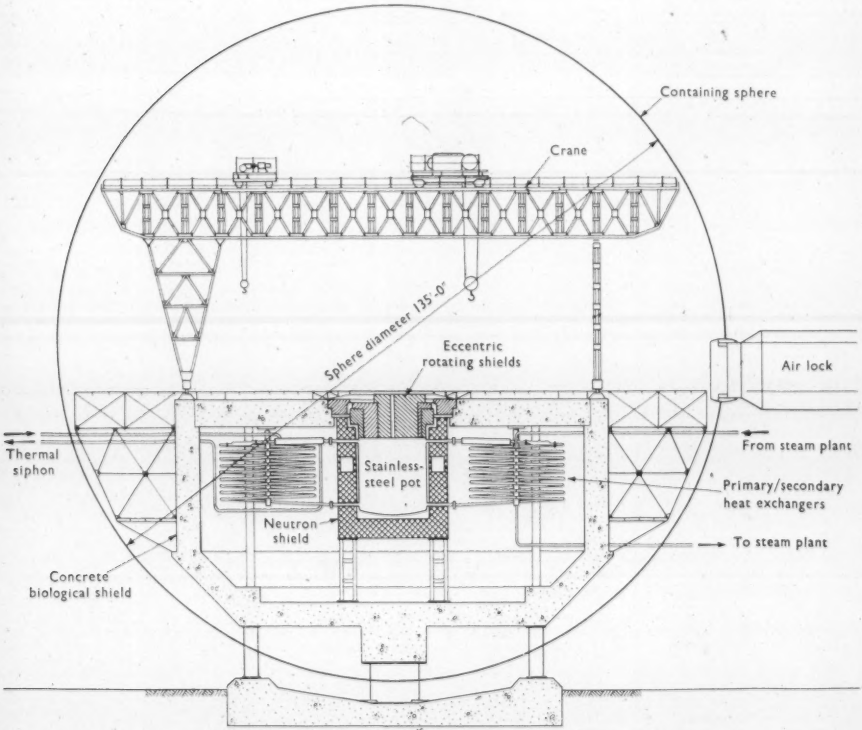

Fig. 10. General arrangement of the Dounreay fast reactor

of the testing reactors DIDO and PLUTO for such purposes has already been mentioned.

Fuel for light-water-moderated or sodium-graphite reactors must be enriched in ^{235}U or plutonium. Plutonium will be used to enrich the Stage-2 reactors, as soon as the Stage-1 reactors have produced enough. Thus plutonium-enriched fuel elements will also be required; perhaps plutonium oxide will prove to have properties as good as those of uranium oxide.

The processing of spent fuel elements is at present carried out at Windscale by the aqueous-solvent extraction process. The uranium metal rods, after a long cooling period, are dissolved in acid and the solution is then passed through long extraction columns and separated into plutonium, fission products and depleted uranium metal. Only a few pints of plutonium solution are produced for each ton of metal; it is purified and concentrated into metal billets. The fission products are concentrated by evaporation and stored in stainless-steel tanks; the depleted uranium metal is purified and sent back to the Springfield factory to be converted into uranium hexafluoride. This is sent to the diffusion plant, so that it can be restored to normal concentration or used for higher enrichment.

The details of the fuel-element design have a marked effect on the character of the chemical-separation operations. For example, highly alloyed fuel elements are not liked by the chemical plant operators since they complicate the separation and waste-disposal problems. Accordingly, the reactor designer must work closely with the chemical plant designer.

Experience has shown that costs of chemical processing fall rapidly with the increase in the scale of operations; it seems likely that the existing U.K.A.E.A. factory will be adequate to deal with the programme of nuclear power up to 1965. It is also expected that the U.K.A.E.A. will be able to provide natural uranium fuel for any reactors which may be exported in the decade 1960–70 and the Authority is willing to undertake the processing of spent fuel.

RADIOISOTOPES AND RADIOACTIVE WASTES

The Authority also produces radioactive isotopes and processes them into complex compounds at its Radiochemical Centre at Amersham. Production is now increasing at a rate of about 25% per annum (Fig. 11); the present annual value is about £400 000, and about 55% of the production is exported.

A future extension of this activity will be the separation, concentration and utilization of the radioactive wastes. The most important of these are radio-caesium and radio-strontium. Supplies of radio-caesium in kilocurie quantities are already being produced for use in hospital radiotherapy and a programme of production of 100 kc has been arranged. The Authority looks forward to the production of 100 kc sources for industrial applications. The possible field of applications of radiation to industrial processes is wide and a radiation-using industry may well develop. Applications to industrial processes such as the polymerization of ethylene to polyethylene and other plastics are now well known, but the commercial advantages compared with well tried high-temperature high-pressure processes are not clear. The improvement of the high-temperature properties of polyethylene is another well-known example. The production of halogenation and oxidation reactions and many organic reactions are being studied. A Technological Irradiation Group at Harwell assists industry to study these possibilities by providing at Harwell intense sources of radiation from fission products, reactors and accelerators. About thirty investigations are at present proceeding on behalf of industry, many of them with attached staff.

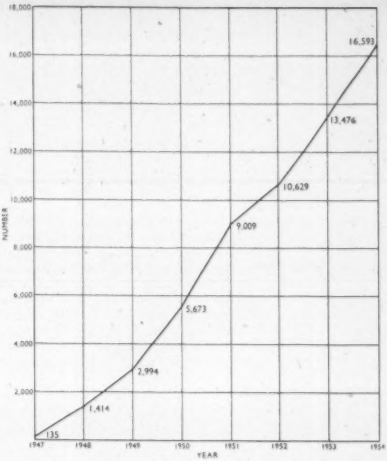

Fig. 11. Number of isotopes despatched from Harwell and Amersham in the period 1947–54

COLLABORATION

Other Government organizations. The Authority is responsible for collaboration with atomic energy organizations of other countries, and for maintenance of classification policies. Most of the information on nuclear power is now unclassified, but a limited degree of classification is retained on chemical-separation technology and some aspects of fuel-element and reactor technology. Further changes in declassification policy may well take place when the results of the Geneva Conference have been assessed.

The United States. The bilateral agreement for co-operation with the United States has been published. It provides for a wide exchange of information on the basic technology of nuclear engineering, together with arrangements for negotiating the exchange of more detailed information with United States industry.

The Commonwealth. Co-operation with Canada in reactor development is close, particularly on water-moderated reactors. The United Kingdom is assisting Australia in the construction of a DIDO type reactor and by the supply of research information for their development programme. Similar arrangements are being made with other Commonwealth countries and with some countries of Western Europe.

REFERENCES

(1) *A Programme of Nuclear Power.* Cmd. 9389 (London: H.M. Stationery Office, 1955).

(2) HINTON, C. *The graphite-moderated gas-cooled pile and its place in power production*, U.N. International Conference on the Peaceful Uses of Atomic Energy, Geneva, 1955 (Paper No. P/406).

(3) JUKES, J. A. *The cost of power and the value of plutonium from early nuclear power stations*, U.N. International Conference on the Peaceful Uses of Atomic Energy, Geneva, 1955 (Paper No. P/390).

The laminar flow of streams of suspended particles

By T. V. STARKEY, B.Sc., Ph.D., F.Inst.P., The Technical College of Monmouthshire, Crumlin, Mon.

[*Paper first received* 11 *May, and in final form* 25 *November*, 1955]

It was shown theoretically in a previous paper[1] that during the laminar flow of a suspension through a tube, and for least action, a suspended particle would follow a path adjacent to the tube axis. In general, therefore, a particle entering a tube non-axially would be expected to move with a component of translation normal to the streamlines and directed towards the axis. In the present paper this theory is developed and leads to the conclusion that for a particle at any given point in the tube this component increases with particle size. Experiments are described in which streams of coloured particles of mixed sizes suspended in water were admitted at a given point on the horizontal diameter of a tube placed horizontally, through which a steady flow of water was maintained. These coloured streams diverged on entry to the water and formed filaments in a horizontal plane. A study of the lateral movement of these filaments relative to one another, as the point of their admission to the tube and the rate of flow of water in the tube are varied, leads to the conclusion that lateral forces act on the suspended particles. Such forces, the magnitudes of which increase with particle size and with mean shear gradient, result from the motion of the particles in non-uniform velocity gradients. The motions observed lead directly to a simple flow mechanism, independent of particle configuration and orientation, which is shown to be qualitatively consistent with a number of well-established phenomena.

1. INTRODUCTION

In a previous paper[1] it was shown theoretically that an isolated particle in suspension and subject only to the action of hydrodynamic forces would move during the laminar flow of the suspension through a tube, so as ultimately to follow a streamline adjacent to the tube axis. A particle entering a tube non-axially would, therefore, move with a component of motion normal to the direction of flow and directed towards the axis.

If a streamline is defined as the path followed by an imaginary identifiable element of the continuous phase, the effect postulated involves a divergence between the tracks of the suspended particles and those of the imaginary elements just referred to. This immediately raises the question as to how the directions of streamlines can be defined in practice, a question which is seen to be particularly acute in view of the wide use which is made of the motions of small suspended or dissolved coloured particles for this purpose.

In consequence of this difficulty the theory outlined in the previous paper has been developed with the object of determining whether the extent of the suggested deviations of suspended particles from streamlines is likely to depend on particle size, since in this event it would be sufficient simply to demonstrate the deviations from one another of the paths of particles of different sizes which enter the tube at the same point, as a means of confirming the existence of deviations of the kind postulated. This extension of the theory is set out in Section 2.

In Section 2 experiments designed primarily to demonstrate the deviations predicted and to indicate the factors on which these depend are described and the results of these are discussed in the subsequent sections.

2. DEVELOPMENT OF THE THEORY

The results derived theoretically in the previous paper[1] involve the application of the principle of least action to the motion of a particle through a viscous fluid under shear. The applicability of this principle to such a non-conservative system is shown by Jeans.[2] The present section involves the further application of this same principle to the case of two particles.

Thus, let us consider the passage through a tube of two "ideal macromolecular vortices"[1] associated with particles of different sizes, and let us assume that on entry to the tube these vortices are at the same distance as each other from the tube axis. Let us also assume that, because of their different sizes, they follow different paths through the tube, and let us define these paths as such that the actions arising as a result of the passage of the vortices along them are the same as would arise if they respectively followed streamlines distant r_1 and r_2 from the tube axis. Let $r_1 > r_2$ and let the "form factors" of these ideal vortices be F_1 and F_2 where $F_1 > F_2$.

Let us consider in turn the two cases (*a*) in which the vortex of form factor F_1 that is, vortex No. 1, follows the equivalent path r_1 and that of form factor F_2, that is vortex No. 2, the equivalent path r_2, and (*b*) in which vortex No. 1 follows the equivalent path r_2 and vortex No. 2 the equivalent path r_1.

Case (*a*). As shown in the previous paper [equations (3) and (4) of Ref. 1] the separate actions arising as a result of the passage of the particles through the tube are respectively $F_1\eta l^2\omega_1^2/v_1^2$ and $F_2\eta l^2\omega_2^2/v_2^2$ where ω and v are respectively the angular and linear velocities on the streamlines to which the suffices refer, η the viscosity of the continuous phase and l the tube length.

The total action A_a in this case is therefore given by:

$$A_a = \eta l^2[(F_1\omega_1^2/v_1^2) + (F_2\omega_2^2/v_2^2)] \quad (1)$$

Case (*b*). In this case the total action A_b is similarly given by:

$$A_b = \eta l^2[(F_1\omega_2^2/v_2^2) + (F_2\omega_1^2/v_1^2)] \quad (2)$$

The difference between the actions in the two cases is therefore:

$$A_b - A_a = \eta l^2\{(F_1 - F_2)[(\omega_2^2/v_2^2) - (\omega_1^2/v_1^2)]\} \quad (3)$$

As $F_1 > F_2$ and $\omega_1/v_1 > \omega_2/v_2$ this difference is negative. That is, the action arising in case (*a*) is greater than that in case (*b*). From the principle of least action then, it must be concluded that if the vortices follow different paths that with the bigger form factor would follow the path nearer to the tube axis.

Next let us imagine the smaller particle with which F_2 is associated to become so small that it can be identified with an element of the continuous phase. The equivalent path r_1 consequently becomes, by definition, identical with the streamline through the point of entry of the particle to the tube. Moreover, this path must be for the particle in question that which involves least action.

Let us now suppose that the second vortex of form factor F_1 also follows this same path; and let the total action for the two particles in this case be A_c.

Then
$$A_c = \eta l^2[(F_1\omega_1^2/v_1^2) + (F_2\omega_1^2/v_1^2)] \quad (4)$$

or
$$A_c = \eta l^2\{[(F_1\omega_2^2/v_2^2) + (F_2\omega_1^2/v_1^2)] + [(F_1\omega_1^2/v_1^2) - (F_1\omega_2^2/v_2^2)]\} \quad (5)$$

i.e.
$$A_c = A_b + \eta l^2 F_1[(\omega_1^2/v_1^2) - (\omega_2^2/v_2^2)] \quad (6)$$

Therefore, since
$$\omega_1/v_1 > \omega_2/v_2, \quad A_c > A_b \quad (7)$$

The supposition that F_1 also travels along the same path is, therefore, not consistent with the requirement of least action; the particles must hence be assumed to travel along different paths, that with the bigger form factor following the path nearer to the axis.

3. APPARATUS AND METHOD

The apparatus used in the present experiments is basically similar to that employed by Reynolds in his well-known experiments on turbulence.[3] It consists of a rectangular plate glass tank of length about 100 cm, width 50 cm and depth 15 cm. A glass tube, of approximately 1·5 cm diameter, is fixed centrally inside the tank and lies parallel to the longest tank sides, its axis being horizontal. This tube passes through one end wall of the tank and is closed by a tap outside the tank. The other open end of the tube, which is flared, reaches to within a few centimetres of the opposite end of the tank.

A fine glass jet, carried by a micrometer head fixed to the end wall of the tank, is arranged with its orifice on the horizontal diameter of the tube at its flared end. By means of the micrometer the jet can be traversed slowly to and fro along this diameter, the axis of the jet remaining always parallel to the axis of the tube. The jet is connected through a flexible tube and tap to an adjustable constant head device.

For the purpose of the experiments the tank is filled nearly to its full depth with water, and during experiments a controllable low velocity stream of water under approximately constant head conditions passes to waste through the tube, the rates of flow used being of the order of 1 cm^3/s.

Dilute aqueous solutions of various dyestuffs are admitted, in turn, to the stream, being fed to it at a very small and constant pressure *via* the jet. This is arranged by adjusting the constant head device so that the direction of flow of the solutions is initially away from the jet exit. By increasing the head slowly until the direction of flow is just reversed it is possible to arrange for the solutions to enter the tube at a velocity approximately equal to the velocity of the water at the point of entry.

In the present series qualitative experiments only were made. These consisted of observing in turn the forms of the several coloured streams within the tube, under various conditions of shear gradient, and for various concentrations and points of entry of the solutions to the tube. Whilst the observations to be described were in all cases made from points vertically above the tube and consequently relate to the forms of the streams in a horizontal plane, observations were also made in directions normal to this so as to ensure that these forms even with the streams in the most extreme positions were never attributable to "fall out" and subsequent contact with the tube wall.

4. THE EXPERIMENTS

In the first instance experiments as described by Reynolds[3] were carried out. In these, very dilute solutions of eosin were used. By carefully controlling the rate of flow of the solutions extremely fine filaments of dyestuff could be obtained and these, as observed by Reynolds, were seen always to be initially convergent. With higher rates of flow of the dyestuff solution the "candle flame" form described by Reynolds was observed, and the filaments, although initially diverging from the jet, rapidly became convergent.

These experiments were followed by a series in which mixed solutions were employed. Throughout this series the solutions used were aqueous solutions of eosin and colloidal carbon black stabilized with gum, in relative proportions of the same order by weight and in concentrations of the order of one hundredth of one per cent (g/ml.). The following observations were made with these.

(i) With the jet off-centre, the dyestuff stream was observed to consist of two clearly defined filaments diverging from the jet orifice as indicated in the figure.

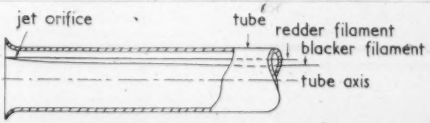

Horizontal axial section of part of flow tube showing filament forms

Both filaments were red in colour (presumably as a result of the adsorption of the eosin on the carbon particles), that nearer to the tube axis being darker than that which was more remote. The interspace between the filaments was also faintly tinted red, although this was not noticeable at the lower rates of flow of the solution nor at the higher rates of flow of the water.

(ii) As the jet was traversed across the horizontal diameter of the tube the separation of the two filaments from each other decreased progressively as the jet orifice approached the tube axis. With the jet on the axis the filaments formed a single stream. This broke up again into two distinct diverging filaments, the separation of which increased progressively as the jet was moved further towards the opposite end of the tube diameter.

(iii) With an increasing proportion of carbon black in the mixed solution the filament nearer to the tube axis became blacker. "Fall out," which was not noticeable at all in the filament more remote from the axis, where because of the slower translational velocity it would be expected to be most apparent, became progressively more noticeable in the other filament as the proportion of carbon black was increased.

(iv) With the jet at a fixed point off-centre, an increase in the rate of flow of the water through the tube was accompanied by an increase in the separation of the filaments from one another.

5. DISCUSSION OF RESULTS

The following summarizes the chief results of the experiments described above.

(i) With very dilute solutions of a single dyestuff the dyestuff streams were either initially convergent or rapidly became so after initial divergence.

(ii) With very dilute solutions of mixed solutes of widely diverging particle size the dyestuff streams were always divergent.

(iii) With eosin–carbon black mixtures the coloured streams consisted of diverging filaments, the carbon black being the nearer to the tube axis.

(iv) The separation between the filaments in the mixed streams increased as the point of entry of the solution was moved further from the tube axis.

(v) The separation between the filaments in the mixed streams increased as the rate of flow of the water was increased.

These results confirm the predictions of the theory outlined in Section 2, and lead directly to the conclusions that in very dilute solutions and suspensions particles entering a tube non-axially deviate from the streamlines on which they enter, moving towards those on which the velocity gradient is smaller, and that the extent of the deviations increases with particle size and rate of shear.

The translation of suspended particles with a component normal to the direction of flow requires the existence of forces directed towards the tube axis. It is proposed to consider here the origin of such forces.

In the simple theory outlined in the previous paper[1] it was assumed that the motion of the "ideal" vortex associated with an isolated particle, relative to the continuous phase, was wholly rotational. Since in the case under consideration the vortices move in a non-uniform velocity gradient this must be regarded as only approximately true. Under these conditions of non-uniform gradient, the forces transmitted to a suspended particle through the continuous phase must reduce to a couple together with a single resultant force acting in the direction of streaming. Suspended particles must, therefore, have components of translation relative to the continuous phase and in the direction but in the opposite sense to that of the flow. It is these components of translation, acting in conjunction with the rotation, that give rise to the lateral components of translation which form the subject of this paper. As will become apparent later the components of translation relative to the continuous phase are in general extremely small and consequently contribute only to a negligible extent to the total action.

As a basis for the analysis of this problem let us assume that the velocity gradients in which the ideal vortex associated with a suspended particle moves, are of "Poisseuille" form and, therefore, that the velocity varies parabolically with distance from the tube axis. This is equivalent to assuming that the resultant velocities at all points within the tube can be determined by adding vectorially components of velocity as in the continuous phase considered alone, to those associated with the real vortex.

Let us also assume that the component of translation in the position of the centre of the ideal vortex, relative to the continuous phase and in the direction of flow, is equal to the difference between the linear velocity of the continuous phase considered alone, and the arithmetic average of the extreme velocities of the continuous phase at the circumference of the ideal vortex. That is, denoting this velocity component by v_x,

$$v_x = P[R^2 - \tfrac{1}{4}(r_1 + r_2)^2]/4\eta l - P[R^2 - \tfrac{1}{4}(r_1^2 + r_2^2)]/4\eta l \quad (8)$$

where r_1 and r_2 are the radii of the streamlines at the ideal vortex extremities. The two terms on the right-hand side of equation (8) follow from the application of the expression for the streamline velocity in a Newtonian fluid, namely, $v = P(R^2 - r^2)/4\eta l$ where v is the velocity of the fluid at a distance r from the axis of a tube of radius R and length l, η the viscosity of the fluid and P the applied pressure difference.

On simplification the expression for v_x reduces to:

$$v_x = P(r_2 - r_1)^2/16\eta l \quad (9)$$

or, since $r_2 - r_1 = 2a$, a being the radius of the ideal vortex, to:

$$v_x = Pa^2/4\eta l \quad (10)$$

Since in general a is very small, v_x is also very small. For large particles and at high rates of shear, however, its consequences may be very considerable.

This component of translation relative to the continuous phase would, in combination with the rotation, give rise to a trajectory for the suspended particle fundamentally similar to that of a "sliced" golf ball. The deviations of particles from streamlines, as described in this paper, must then be essentially similar to the deviation of a spinning body from its line of projection.

The magnitude of the lateral force acting on a spinning body in a homogeneous current has been investigated analytically by Magnus.[4] For a rotating cylinder of radius a and height h, spinning with a uniform angular velocity ω and moving relative to a continuous phase of density ρ with a linear velocity v_x, the lateral force f_r is given by:

$$f_r = 2\pi\rho ha^2 v_x\omega \quad (11)$$

Substituting for v_x from equation (10), this becomes:

$$f_r = \pi\rho hPa^4\omega/2\eta l \quad (12)$$

or, once the nature of the continuous phase and its temperature have been fixed, by:

$$f_r = kha^4\omega P/l \quad (13)$$

where k is constant.

In accordance with equation (13), this force increases with the particle size, with the mean rate of shear of the suspension, and, since ω increases with r, with distance of the particle from the tube axis also. It is, therefore, qualitatively consistent in every particular with the experimental results summarized at the beginning of this section. Forces of this kind must, moreover, always exist where particles are

suspended in streams characterized by a non-uniform velocity gradient.

In terms of a concept developed in an earlier paper[1] these results may be summarized in the statement that the "flow factor" of suspended particles in a non-uniform velocity field decreases progressively towards a minimum value at a rate which increases with particle size and rate of shear.

6. SOME CONSEQUENCES OF THE RESULTS

The effect described in this paper can readily be made the basis for the qualitative description of a fairly large number of well-established phenomena. It is proposed, therefore, to discuss some of these.

(*a*) *Dependence of viscosity of suspensions, etc., on rate of shear.* Many observations have been made which show that the measured values of the viscosities of macromolecular solutions and suspensions decrease with increasing mean rate of shear, and several theories have been proposed to account for them.[5] The most widely accepted of these rely either on the assumption that the suspended particles are flexible or porous and that their configuration alters with rate of shear, or that they are anisodiametric and that the average state of their orientation toward the streamlines varies as the rate of shear is altered.[5]

In experiments carried out by Richardson and Tyler[6] the shear dependence of the viscosity of suspensions of rice starch in paraffin was studied quantitatively, and the results show a variation of viscosity with velocity gradient similar in type to that reported in a number of papers for macromolecular solutions. And yet, in this case, the assumptions referred to in the last paragraph would hardly appear to be applicable.

The results outlined in the present paper, however, suggest a mechanism dependent on the positions of the particles in the velocity field rather than on their configurations or orientations. This mechanism is hence independent of the flexibility, the porosity or the aspect ratios of the particles and would, therefore, appear to be generally applicable.

The existence of a component of translation normal to the direction of flow leads inevitably to the conclusion that in a dilute suspension flowing through a tube there is a continuous drift, however slight, of the particles towards the tube axis. Since the extent of this drift in a given tube must, in accordance with the results cited, increase with mean rate of shear, the mean distance of the particles from the tube axis must decrease as the mean shear gradient is increased. This, as a result of the slower rotations of particles and of their increased streaming velocities as they approach points nearer to the axis, would lead to a diminution of the viscosity of the suspension with increased shear gradient. Where the suspended particles are of various shapes or sizes it is to be expected, since the lateral components of translation increase with the form factors of the associated ideal vortices, that these particles which are distributed at random over the tube section on entry progressively sort themselves out so that the proportion of the "bigger" particles in the axial regions of the tube increases as the tube exit is approached. The random distribution of particles of all sizes on entry to a tube is thus gradually superseded by a size distribution pattern as the particles progress along the tube.

Since the magnitude of the lateral forces has been shown to increase with particle size the shear dependence of the intrinsic viscosity of solutions of high polymers would be expected to increase with the degree of polymerization. This appears to be the case.[5]

(*b*) *Variations in the measured value of the viscosity of a suspension from instrument to instrument.* Variations in the distribution of velocity gradients across the sections of different viscometers of the same type but having different dimensions, as well as variations with the type of the viscometer used, would lead to the well-established variations referred to in the above title as a consequence of the mechanism outlined in Section 6(*a*).

(*c*) *Erosion.* The lifting of the particles as required in the explanation of this process under steady motion conditions can be directly accounted for in terms of the forces discussed in Section 5.

(*d*) *Plug flow.* The very rapidly changing velocity gradients in the neighbourhood of the wall of a tube through which a substance exhibiting a yield value is being forced would give rise in the case of substances having a particulate structure, to a component of motion of the particles away from the wall and hence to the formation of a lubricating sheath between the central plug and the wall as required in the explanation of so-called plug flow.

(*e*) *Weissenberg effect.*[7] The lateral forces which act on the suspended particles in the direction of decreasing velocity gradient would lead directly to this effect and would account for the increase in its magnitude with mean rate of shear.

ACKNOWLEDGEMENTS

I wish to acknowledge my indebtedness to Mr. J. A. H. Roberts for his considerable help with the experimental work, to Mr. W. H. Jones (also of the College staff) who made the micrometer head and to Messrs. Pilkington Bros. (South Wales) Ltd., who presented the tank. I am grateful too for the interest shown in this work by other members of the College staff and by members of the research staff of Messrs. British Nylon Spinners, Ltd.

REFERENCES

(1) STARKEY, T. V. *Brit. J. Appl. Phys.*, **6**, p. 34 (1955).

(2) JEANS, J. H. *The Mathematical Theory of Electricity and Magnetism*, 5th ed., p. 492 (London: Cambridge University Press, 1951).

(3) REYNOLDS, O. *Phil. Trans*, **174**, p. 935 (1884).

(4) GRIMSEHL, E. *A Textbook of Physics*, Vol. 1, p. 389 (London: Blackie and Son, Ltd., 1946).

(5) IMMERGUT, E. H. and EIRICH, F. R. *Industr. Engng Chem.*, **45**, p. 2500 (1953).

(6) RICHARDSON, E. G., and TYLER, E. *Proc. Phys. Soc. [London]*, **45**, p. 142 (1933).

(7) WEISSENBERG, K. *Nature [London]*, **159**, p. 310 (1947); *Proc. 1st Intern. Congr. Rheol. (Scheveningen)*, p. 46 (1948).

The inductance of two elliptic tubes

By E. E. JONES, B.Sc., Ph.D., University of Nottingham

[*Paper first received* 26 *July, and in final form* 31 *October*, 1955]

The magnetic field of two conducting tubes of non-magnetic material is determined in terms of certain vector potential components. Each tube forms the annulus between two successive elliptic cylinders of the same confocal system, and equal and opposite steady currents flow along them. The inductance of the system is determined in terms of its geometry and some numerical results are recorded.

The inductance per unit length is one of the many important parameters of a cable transmitting electrical power, the steady state properties of the cable depending on its magnitude. At the lower frequencies the inductance per unit length influences the amount of voltage drop along the length of the cable, and at higher frequencies influences the distortion of the transmitted wave-form, as well as the attenuation along the length of the cable.

The investigation carried out on the determination of the inductance of tubular cables having concentric circular sections is extensive, and formulae and tables exist predicting these inductances.[1, 2] From the point of view of ease of manufacture, tubular cables of circular section have the most desirable shape; however, because of various design considerations instances may arise when a cable must have a cross-section other than circular. Cables formed from wire tubes of elliptical cross-sections are possibilities, these include the strip-conductor surrounded symmetrically by an oval conducting tube. An analytic investigation into the value of the inductance of an elliptic tubular system of conductors is therefore undertaken in this paper.

Inductance calculations for systems of conductors which have simple geometrical characteristics, e.g. conductors in the form of concentric circular cylinders, or cylinders of rectangular section external to each other, are usually deduced by applying Maxwell's principle of the geometric mean distance.[1] The calculations when the cylinder sections are not of these simple forms, e.g. when the sections are elliptical in profile, involve complicated integrals which are difficult and tedious to solve. However, when the conducting tubes have section profiles in the form of confocal ellipses, the method used in this paper determines the inductance in the form of a single expression dependent only on the geometry of the system, and as an intermediate step leads to the expressions for the magnetic field intensities in the whole of the space surrounding the conductors. It also has the advantage of indicating the approach to the solution of the more involved problem of conductors in the form of elliptic cylinders made of magnetic materials.

The latter problem is complicated by the difference in the permeabilities of the various media concerned, and application of the boundary equations at each interface leads, even in the comparatively simple case of two tubular conductors, to twenty-four simultaneous equations. Fortunately, in practice, when the conducting materials are non-ferromagnetic, e.g. copper and aluminium, their permeabilities are almost equal to that of free space, hence very little restriction is imposed in these cases by assuming that the permeabilities have the same constant value everywhere. The currents in the conductors are assumed to be steady and uniformly distributed over the sections of the conductors; the results deduced here are thus applicable to low frequency alternating return circuits, where the skin-effect is negligible.

The exact calculation of the inductance per unit length involves taking into account several disturbing factors, e.g. the skin-effect occurring at high frequencies, the proximity effect of the conductors forming the cable, as well as the effect of the presence of adjacent conductors and stray magnetic fields, all of which cause the current over the cross-section of the cable to be non-uniform in distribution. There also exists the effect due to the difference in permeabilities of the various media forming the cable, and their variation when the conducting material exhibits ferromagnetic characteristics. The approximate results for the inductance per unit length of any given tubular system that are deduced by assuming that the disturbances due to the above effects are negligible are accurate enough for practical purposes. These are particularly applicable for the analysis of power transmission cables, when the frequency is very low.

Mathematically the problem is simplified by transforming the right section of the tubular system containing the elliptic contours of the conductors into a plane where the corresponding contours are concentric circles. The boundary conditions at each contour are also transformed, and the magnetic field problem solved in this new plane. The units used are the rationalized m.k.s. or Giorgi system,[3] and wherever "log" is employed it signifies the natural logarithm.

Right sections of the two tubular conductors have profiles in the z-plane given by the curves $|\zeta| = t_s > 1, (s = 1, 2, 3, 4)$, in the net defined by the equation

$$z = c(\zeta + \zeta^{-1}) \tag{1}$$

where c, t_s are real constants, such that $t_{s+1} > t_s$, and $z = x + iy$, $\zeta = r \exp(i\theta)$. The curves are confocal ellipses with semi-major axes $u_s = c(t_s + t_s^{-1})$, and semi-minor axes $v_s = c(t_s - t_s^{-1})$, with $s = 1, 2, 3, 4$.

The transformation of equation (1) maps the complete z-plane into the region external to the unit circle $r = 1$ in the ζ-plane, and the ellipse with semi-axes u_s, v_s in the z-plane maps on to the circle $r = t_s$ in the ζ-plane. It also follows that the two sides of the line $-2c \leqslant x \leqslant 2c$ in the z-plane map on to the complete unit circle $r = 1$ in the ζ-plane.

If a steady current I flows with uniform density J_2 in one direction along the length of the cylinder confined by the surfaces corresponding to $t = t_1$, t_2 respectively, and flows with constant density J_4 in the opposite direction along the length of the cylinder confined between the surfaces corresponding to $t = t_3$, t_4 respectively, then by definition

$$\begin{aligned} I &= \pi c^2 J_2 (t_2^2 - t_2^{-2} - t_1^2 + t_1^{-2}) \\ &= -\pi c^2 J_4 (t_4^2 - t_4^{-2} - t_3^2 + t_3^{-2}) \end{aligned} \tag{2}$$

THE FIELD EQUATIONS

The magnetic field throughout all space can be defined in terms of a vector potential directed along the length of the system of tubes, having a magnitude $A_s(x, y), (s = 1, 2, 3, 4, 5)$,

in the region of the z-plane corresponding to $t_{s-1} \leqslant t \leqslant t_s$. The equations satisfied by A_s are

$$\nabla^2 A_s = -\mu J_s, (s = 1, \ldots, 5) \tag{3}$$

where μ is the specific inductive capacity of free space, and it is assumed that $J_1 = J_3 = J_5 = 0$. It is now possible to introduce complex potential functions w_s, $(s = 1, \ldots, 5)$, such that $w_s = \phi_s + iA_s$, where $\phi_s(x, y)$ is a harmonic function. If $\psi_s(x, y)$, $(s = 1, \ldots, 5)$, is another harmonic function, then in order that A_s is to satisfy equation (3), we choose

$$A_s = \psi_s - \tfrac{1}{4}\mu J_s z\bar{z}, (s = 1, \ldots, 5) \tag{4}$$

It is noticed that when $s = 1, 3, 5$, then A_s itself is a harmonic function. In general it follows that

$$w_s = w'_s - \tfrac{1}{4}i\mu J_s z\bar{z}, (s = 1, \ldots, 5) \tag{5}$$

where $w'_s = \phi_s + i\psi_s$, a harmonic function of z.

On the curve separating the sth region from the $(s + 1)$th region, the boundary conditions are

$$A_s = A_{s+1}, \partial A_s/\partial n = \partial A_{s+1}/\partial n. \tag{6}$$

These ensure that the magnetic vector potential and the tangential component of the magnetic intensity are separately continuous across the curve of separation of the media.

In terms of $\zeta_{ss} = t_s \exp(i\theta)$, from equation (4) the first condition becomes

$$\psi_s(\theta) - \tfrac{1}{4}\mu J_s z(\zeta_{ss})\bar{z}(\bar{\zeta}_{ss}) = \psi_{s+1}(\theta) - \tfrac{1}{4}\mu J_{s+1} z(\zeta_{ss})\bar{z}(\bar{\zeta}_{ss}) \tag{7}$$

Differentiating this expression with respect to θ, and using the Cauchy–Riemann conditions for analytic functions, given by $\partial\phi_s/\partial r = \partial\psi_s/r\partial\theta$, then equation (7) becomes

$$\partial\phi_s/\partial r = (\partial\phi_{s+1}/\partial r) + \tfrac{1}{4}i\mu(J_s - J_{s+1}) \times [\exp(i\theta)z'(\zeta_{ss})\bar{z}(\bar{\zeta}_{ss}) - \exp(-i\theta)z(\zeta_{ss})\bar{z}'(\bar{\zeta}_{ss})] \tag{8}$$

The second boundary condition can be written as $\partial A_s/\partial r = \partial A_{s+1}/\partial r$, hence from equation (4)

$$\partial\psi_s/\partial r = (\partial\psi_{s+1}/\partial r) + \tfrac{1}{4}\mu(J_s - J_{s+1}) \times [\exp(i\theta)z'(\zeta_{ss})\bar{z}(\bar{\zeta}_{ss}) + \exp(-i\theta)z(\zeta_{ss})\bar{z}'(\bar{\zeta}_{ss})] \tag{9}$$

But it is well known,[4] that

$$dw'_s/d\zeta = [(\partial\phi_s/\partial r) + (i\partial\psi_s/\partial r)]\exp(-i\theta)$$

Hence, writing

$$dw'_s/d\zeta = (dw'_{s+1}/d\zeta) + \tfrac{1}{2}i\mu(J_s - J_{s+1})z'(\zeta)\bar{z}(t_s^2\zeta^{-1}) \tag{10}$$

it is noticed that equation (10) is a relation involving ζ as the sole variable, which on the bounding curve, when $\zeta = \zeta_{ss}$, $\zeta_{ss}\bar{\zeta}_{ss} = t_s^2$, sums up both the boundary conditions of equations (8) and (9), and thus of equation (6).

On integrating equation (10) it follows that

$$w'_s = w'_{s+1} + \tfrac{1}{2}i\mu(J_s - J_{s+1})F_s + B_s + iC_s \tag{11}$$

where

$$F_s = \int^{\zeta} z'(\zeta)\bar{z}(t_s^2\zeta^{-1})d\zeta \tag{12}$$

and B_s, C_s are real constants.

With a transformation of the type given by equation (1),

$$F_s = c^2(t_s^2 - t_s^{-2})\log\zeta + \tfrac{1}{2}c^2(t_s^{-2}\zeta^2 + t_s^2\zeta^{-2}) \tag{13}$$

Also from equations (5) and (11),

$$w_s = w_{s+1} + \tfrac{1}{4}i\mu(J_s - J_{s+1})(2F_s - z\bar{z}) + B_s + iC_s \tag{14}$$

and if the imaginary part of this equation is to reproduce the first boundary condition of equation (6) when $r = t_s$, then it can readily be shown that

$$C_s = \tfrac{1}{4}\mu(J_s - J_{s+1})c^2[t_s^2 + t_s^{-2} - 2(t_s^2 - t_s^{-2})\log t_s] \tag{15}$$

Although B_s can similarly be determined, it is not required in the subsequent analysis.

THE COMPLEX POTENTIAL FUNCTIONS

From equation (14), by addition through all the values of s, it is seen that

$$w_1 = w_5 + \tfrac{1}{2}i\mu J_2(F_2 - F_1) + \tfrac{1}{2}i\mu J_4(F_4 - F_3) + \sum_{n=1}^{4}(B_n + iC_n) \tag{16}$$

At large distances from the system of tubes the perturbation effect due to the presence of the currents is small, then it may be assumed that

$$w_5 = ic^2\sum_{n=1}^{\infty} D_n\zeta^{-n} \tag{17}$$

where the D_n are arbitrary complex constants. In the region enclosed by the ellipse $t = t_1$, the field intensity must be finite and single-valued at all points. This is ensured by assuming

$$w_1 = ic^2\sum_{n=1}^{\infty} H_n(\zeta^n + \zeta^{-n}) + const \tag{18}$$

where the H_n are arbitrary complex constants.

The magnetic field intensity has components given by

$$\mu H_x = \partial A/\partial y, \mu H_y = -\partial A/\partial x$$

then

$$\mu(H_x - iH_y)_s = (dw'_s/dz) - \tfrac{1}{2}i\mu J_s\bar{z} \tag{19}$$

Since $dw_1/d\zeta$ has $dz/d\zeta$ as a factor, then dw_1/dz is finite in particular at the points $\zeta = \pm 1$, the zeros of $dz/d\zeta$, and consequently at all points inside the ellipse where w_1 is defined. Again, since $w_1(\zeta) = w_1(\zeta^{-1})$, the values of w_1 at near points one on each side of the line $-2c \leqslant x \leqslant 2c$ are identical; thus w_1 is continuous across the line joining the branch points of equation (1), and is therefore single-valued and continuous everywhere in the region in which it is defined. The same result holds for dw_1/dz, and therefore for the magnetic field intensity.

Substituting from equations (17) and (18) into equation (16), and equating coefficients of like functions of ζ, then $D_n = 0$ for all values of n; $H_n = 0$ for $n \neq 2$; and for $n = 2$,

$$H_n = \tfrac{1}{4}\mu[J_2(t_2^{-2} - t_1^{-2}) + J_4(t_4^{-2} - t_3^{-2})] \tag{20}$$

Hence $w_5 = 0$ for all $t \geqslant t_4$, and thus from equations (14) and (19), the resultant magnetic field intensity can be determined in all regions subtended by the tubular conductors.

In particular the imaginary parts of w_2 and w_4, with $\zeta = r\exp(i\theta)$, are given respectively by

$$A_2 = \sum_{n=2}^{4} C_n + \tfrac{1}{2}\mu J_2 c^2(t_1^2 - t_1^{-2})\log r + \tfrac{1}{4}\mu J_2 c^2(t_1^{-2}r^2 + t_1^2 r^{-2})\cos 2\theta - \tfrac{1}{4}\mu J_2 c^2(r^2 + r^{-2} + 2\cos 2\theta) + \tfrac{1}{4}\mu c^2[J_2(t_2^{-2} - t_1^{-2}) + J_4(t_4^{-2} - t_3^{-2})](r^2 + r^{-2})\cos 2\theta \tag{21}$$

and

$$A_4 = C_4 + \tfrac{1}{2}\mu J_4 c^2(t_4^2 - t_4^{-2})\log r + \tfrac{1}{4}\mu J_4 c^2(t_4^{-2}r^2 + t_4^2 r^{-2}) \times \cos 2\theta - \tfrac{1}{4}\mu J_4 c^2(r^2 + r^{-2} + 2\cos 2\theta) \tag{22}$$

where C_n, $(n = 2, 3, 4)$, are given by equation (15).

THE INDUCTANCE OF THE SYSTEM

The inductance L of the system per unit length of the tubes is given by

$$L = \frac{1}{IS_2}\int_{S_2} A_2 dS_2 - \frac{1}{IS_4}\int_{S_4} A_4 dS_4$$

where S_2, S_4 are the areas of the regions between the contours corresponding to t_1, t_2 and t_3, t_4 respectively.(5)

In terms of r and θ, the space metric deduced from equation (1) is given by

$$ds^2 = c^2(r^2 + r^{-2} - 2\cos 2\theta)[r^{-2}(dr)^2 + (d\theta)^2]$$

hence the element of area in the ζ-plane is

$$dS = c^2(r + r^{-3} - 2r^{-1}\cos 2\theta)drd\theta$$

The inductance can thus be evaluated from the relation

$$L = \frac{c^2}{IS_2}\int_0^{2\pi}\int_{t_1}^{t_2} A_2 dS - \frac{c^2}{IS_4}\int_0^{2\pi}\int_{t_3}^{t_4} A_4 dS \qquad (23)$$

The functions A_2 and A_4 are given by equations (21) and (22) respectively, and the simple integrals involved in equation (23) are readily evaluated. The result with the use of equation (2), and elimination of t_s in favour of the semi-axes of the ellipses, is

$$\frac{2\pi L}{\mu} = \log\frac{u_3 + v_3}{u_2 + v_2} + \frac{u_1 v_1}{2(u_2 v_2 - u_1 v_1)^2} \times \left(2u_1 v_1 \log\frac{u_2 + v_2}{u_1 + v_1} + u_1^2 - u_2^2\right) + \frac{u_4 v_4}{2(u_4 v_4 - u_3 v_3)^2} \times \left(2u_4 v_4 \log\frac{u_4 + v_4}{u_3 + v_3} + u_3^2 - u_4^2\right) \qquad (24)$$

This formula can also be used to determine the inductance of a wave-guide in the form of a concentric cable with a solid inner conductor, operating at very high frequencies. In this case the currents in the conductors exhibit a skin-effect, the current flowing only on the outer surface of the inner solid conductor, and on the inner surface of the outer conductor. Equation (24) in this limiting case takes the form

$$\frac{2\pi L}{\mu} = \log\frac{u_3 + v_3}{u_2 + v_2} - \frac{u_2 v^2}{2(u_2^2 + v_2^2)} + \frac{u_3 v_3}{2(u_3^2 + v_3^2)} \qquad (25)$$

where u_2, v_2 are the semi-major and semi-minor axes of the outer surface of the inner conductor, and u_3, v_3 are the corresponding semi-axes of the inner surface of the outer conductor. This extends the range of application of equation (24).

If $u_s = v_s$, $(s = 1, 2, 3, 4)$, the ellipses degenerate into circles, and the results deduced by Snow[2] can be verified, with an appropriate change in units.

NUMERICAL EXAMPLES

The specific inductive capacity $\mu = 4\pi \times 10^{-7}$ H/m, hence if $L = kL'$, and L is measured in μH/m then $k = 0{\cdot}2$, whereas if L is measured in μH/yd then $k = 0{\cdot}1829$. The function L' has a dimensionless form.

(i) As a first example the values of L' are determined when the conducting system is formed from two confocal elliptic tubes, the lengths of their semi-major axes being kept constant in the ratios 5 : 4 : 3 : 2. The semi-minor axis of the innermost ellipse varies from $v_1 = u_1$ to $v_1 = 0$, and thus the value of c also varies. But since $4c^2 = u_s^2 - v_s^2$, then for each value of v_1 the length c can be determined, and thus so can v_2, v_3 and v_4. The ratios v_s/u_s are recorded in Table 1, as well as the values of L'.

Table 1. *Two confocal tubes: variation of inductance with minor to major axis ratio of elliptic sections*

v_1/u_1	v_2/u_2	v_3/u_3	v_4/u_4	L'
1·000	1·000	1·000	1·000	0·480
0·800	0·917	0·954	0·971	0·518
0·600	0·846	0·917	0·947	0·560
0·400	0·792	0·889	0·930	0·605
0·200	0·757	0·872	0·920	0·651
0·000	0·745	0·866	0·917	0·697

Although no completely general conclusions can be drawn from the results of Table 1, it is noticed that when the lengths of the major-axes are kept constant, the inductance increases as the two tubes deviate from the circular form, and the increase is greater the flatter the tubes.

(ii) If the system of conductors is in the form of a concentric cable, with the innermost conductor having a section in the form of an ellipse of semi-axes u_2, v_2, and surrounded by a coaxial conductor bounded by two ellipses of semi-axes u_3, v_3, and u_4, v_4, respectively, then the inductance per unit length of the cable is deduced from equation (24) by allowing $v_1 \to 0$. The second term of this equation is then evanescent.

With the semi-axes u_4, u_3, u_2 in the ratios 4 : 3 : 2, then L' is given by Table 2 for variations $v_2 = u_2$ to $v_2 = 0$.

Table 2. *The concentric cable: variation of inductance with minor to major axis ratio of elliptic sections*

v_2/u_2	v_3/u_3	v_4/u_4	L'
1·000	1·000	1·000	0·766
0·800	0·917	0·954	0·836
0·600	0·846	0·917	0·923
0·400	0·792	0·889	1·031
0·200	0·757	0·872	1·169
0·000	0·745	0·866	1·346

Again, for constant lengths of the semi-major axes of the ellipses, the inductance per unit length of the system increases as the inner conductor and surrounding tubular conductor deviate further from the circular form of section. The increase is greater at smaller values of the semi-minor axes of the respective ellipses, i.e. the flatter the tube and core.

REFERENCES

(1) GROVER, F. W. *Inductance Calculations*, p. 17 (New York: D. Van Nostrand Co. Inc., 1946).

(2) SNOW, C. *Nat. Bur. Stand. Circular* 544, pp. 36, 39 (1954).

(3) STRATTON, J. A. *Electromagnetic Theory*, p. 16 (New York: McGraw-Hill Book Co. Inc., 1941).

(4) MACROBERT, T. M. *Functions of a Complex Variable*, 3rd ed., p. 294 (London: Macmillan and Co. Ltd., 1947).

(5) WEBER, E. *Electromagnetic Fields*, p. 57 (New York: J. Wiley and Sons, Inc., 1950).

A photographic method of obtaining stress trajectories

By A. R. Morris, M.Sc., National Physical Laboratory, South African Council for Scientific and Industrial Research, Pretoria, South Africa

[*Paper received* 17 *October*, 1955]

A method of superimposing a set of photographs of isoclinics is described. With each isoclinic photograph is included a grid, the lines of which are inclined at an angle corresponding to that isoclinic parameter. These grid lines, being everywhere tangential to the principal stress directions, enable the stress trajectories to be easily and accurately drawn.

It is by now a very well-known fact that photoelastic fringe photographs, although spectacular in appearance and capable of giving useful quantitative information, do not convey to the eye a direct mental picture of stress distribution. On the other hand, a well-drawn set of stress trajectories, apart from providing the starting point for methods of calculation, such as the step integration process, gives a display which is immediately intelligible to the layman. Like magnetic lines of force, stress trajectories show the directions of the principal stresses and, by their variations in lateral spacing, they suggest the variations in magnitude of stress.

Unfortunately the conventional method of drawing stress trajectories is a time-consuming process and the final shape of the pattern is very much subject to the artistic eye of the draughtsman. It would be very useful if these mechanical lines of force could be obtained by a direct photographic method. The method described in this paper cannot be truly claimed as fulfilling that requirement, but it does go part way in that direction.

What may now be called the classical method of drawing stress trajectories can be summarized as follows. If a photoelastic pattern is viewed with plane polarized white light, the isochromatic fringe pattern is coloured in that each fringe is a more or less complete spectrum. Superimposed on the fringe pattern will be seen a set of isoclinics which are dark areas, each being a locus of constant direction of stress. On an isoclinic the principal stresses are parallel to the planes of polarization of the polarizer and analyser. It is usual to project the pattern on to a sheet of paper on a board and the isoclinics are traced. That is to say, a line is drawn down the approximate centre of each isoclinic. A complete isoclinic pattern requires a number of such tracings for different settings of the polaroids through a total rotation of 90°. The stress trajectories are then drawn (on a sheet of tracing paper placed over the isoclinic pattern) in such a way that they always pass over any isoclinic at an angle equal to the setting of the polaroids at which that isoclinic was traced.

There are many practical methods of drawing stress trajectories, but they are all variations of that outlined above. Most textbooks on photoelasticity give geometrical constructions for improving the accuracy with which trajectories are derived from isoclinics, but they all rely on the lines being finally "smoothed in" artistically. Methods are available for improving the process of tracing the isoclinics, notably the method of Brown and Hickson[1] which uses a photoelectric photometer to detect the line of maximum darkness along an isoclinic.

Isoclinics can be photographed but photographs of isoclinics are usually only for illustrating textbooks to show the reader what an isoclinic looks like. The principle is to use panchromatic film heavily-exposed with a plane polarized white light pattern. As panchromatic film is sensitive to all colours, the coloured fringe system is completely blanked out and the black isoclinic system remains as in Fig. 1.

The photographic method of obtaining stress trajectories is in principle as follows. First, nine isoclinic photographs

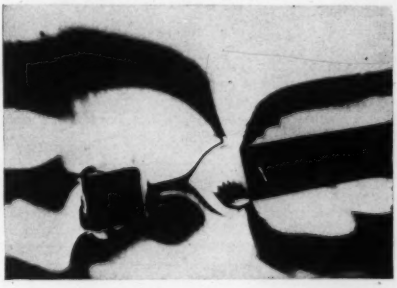

Fig. 1. The 30° isoclinic in part of a Catalin model containing a square hole and a rectangular slot. The model is in uniform compression from above and below

are taken on panchromatic film of a plane polarized white light photoelastic pattern with the polaroids at nine different settings, starting with the horizontal and going through 90°. Then a print is made with all the isoclinic photographs superimposed. During the printing process, a grid is included

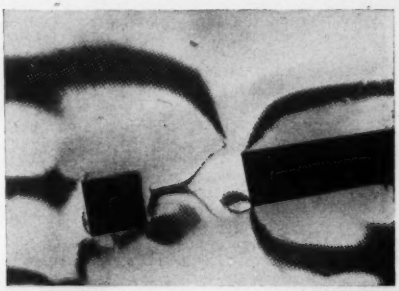

Fig. 2. The 30° isoclinic of the same model as in Fig. 1 printed through a 30° grid

with each negative to identify the isoclinic parameter and to give the very necessary indication of the directions of the principal stresses at every point. Fig. 1 shows the 30° isoclinic printed alone and Fig. 2 shows the same isoclinic printed with its 30° grid. The result of superimposing all nine isoclinic photographs is the basket-like pattern illustrated in Fig. 3.

Fig. 3. The complete pattern formed by printing all the isoclinics, each with its appropriate grid

This pattern is not a true stress trajectory system although the lines approximate to stress trajectories. Stress trajectories are continuous lines running right through the system; these lines are short disconnected stubs of lines. Stress trajectories have lateral spacing which varies from place to place as the magnitudes of the principal stresses vary; these lines have constant lateral spacing throughout as they are nothing but photographs of wire gauze. However, the lines in the photographic pattern obey the rule that they are always tangential to the true stress trajectories and they make the task of drawing trajectories remarkably easy and free from the ambiguities and uncertainties which are inseparable from the conventional methods of stress trajectory drawing.

PRACTICAL DETAILS

The system described above is simple in principle but, as may be expected of a photographic technique, its successful application depends very largely on the use of the correct photographic materials and methods. Panchromatic film is necessary to eliminate the isochromatic fringe pattern entirely, but it has been found that the ordinary panchromatic press films, such as Ilford H.P.3 and Kodak XX, are not suitable as they have insufficient contrast. The dark areas of the negatives are always thin enough to allow the grids to show through during the printing process and the isoclinic areas are never quite transparent enough. The ideal film for this purpose should have perfectly transparent celluloid areas where the isoclinics are and sooty black deposits elsewhere. Each negative needs to act like a mask which lets the grids show through only on the isoclinics.

Such a film is Ilford Ortho-line which is made for the blockmaking process in the printing trade and has long been known as an excellent film for photographing fringes. The first successful stress trajectory patterns were made using this film. Unfortunately, Ortho-line is not sensitive in the red region of the spectrum and therefore the red part of each fringe order appears almost transparent on the negatives and needs to be painted out before the printing of a combined positive can be attempted. Ilford Ltd. also make Panchro-line which is a slower film than Ortho-line, but has almost as high contrast. It requires no painting out of fringes as it is sensitive to the entire visible spectrum and is commonly used as a colour separation negative for three-colour printing. No doubt any high contrast panchromatic film made for a similar purpose could be used for photographing isoclinics.

The exposure time when photographing isoclinics is the most critical factor in the success of the method. Exposures must be long enough to eliminate the isochromatic fringe pattern entirely but not long enough to lose the isoclinics. The correct exposure for a particular polariscope will depend on the design of the instrument and the power of the light used. Using Catalin 800 models, exposures of slightly more than half-a-second up to two seconds have been found correct with Panchro-line film and a 150 W incandescent white light, used in an 8 in. diameter polaroid-and-lens type polariscope. Isoclinic patterns in glass have been obtained using exposures of up to three minutes with the same apparatus. Under-exposure allows the grids to show through the dark deposits on the film during printing, resulting in a characteristic speckled appearance of the print.

An interesting effect is observed when exposure times are progressively increased up to several seconds. At first sight the negatives appear to be no different from those which have had a half second exposure. The isoclinic areas are still perfectly transparent but, on measuring the widths of the isoclinics, it is found that they have become slightly narrower with the heavier exposures. On the more lightly exposed negatives, the transparent centre of each isoclinic is bordered by a grey margin which is in turn surrounded by the black of the remainder of the negative. When the exposure time is lengthened, this grey margin becomes black and the isoclinic is narrowed. Thus the effect of lengthening the time of exposure is an increase in the angular resolving power of the system, which for this purpose is defined as the smallest angular difference between two polaroid settings giving two separate non-overlapping isoclinics. However, there is a tendency for weak isoclinics to close up completely when the film is over-exposed so that the optimum results are obtained when the film has been exposed just enough to hide the last traces of the fringe pattern.

The grids needed for the printing process are simply made by spreading a piece of wire gauze on a piece of Ortho-line film, weighted down by a sheet of glass, and exposing to white light for about a second. Before exposing the film, great care must be taken to make sure that the wires of the gauze are laid out straight and inclined at the desired angle to the datum edge of the film. As Ortho-line is not sensitive to red light the gauze may be adjusted to the correct angle by the light of a red darkroom lamp, but it is very helpful if the gauze has been previously fastened to a frame in order to keep its wires straight. The original set of grids were thirty meshes to the inch on 4 × 5 in. film. Coarser meshes can also be used but the impression of continuity of the lines tends to be lost if the grids are too coarse. The angles chosen for the slopes of the grid lines were 0, 10, 20, 30, 40°. For the angles above 40° the same grids were used inverted. The 10° interval between the isoclinics was determined by the angular resolving power of the system.

A combined print from all the isoclinic negatives and a set of grids may be made directly when enlarging on photostat paper, provided that precautions are taken to ensure that all the isoclinic patterns coincide exactly on the print. It is also

possible to make a combined positive print on Ortho-line by a contact printing process similar to that described for the making of grids. From this positive, a negative may be made for printing copies. The success of the contact printing process depends on the correct positioning of the negatives in the camera so that, when they are superimposed, their images coincide exactly. If a negative has, by some chance, had its image slightly displaced, it can be corrected by trimming two of its edges with a razor blade so that, when these edges are made to coincide with the corresponding edges of the master negative, the images on the two negatives also coincide.

The master negative is an extra negative which contains only the outlines of the model and the zeros of the fringe pattern, such as isotropic points and neutral axes. The purpose of this extra negative, which is printed without a grid, is to show the fringe zeros, to sharpen the outline of the model and to eliminate the unsightly speckled appearance of the dark background (including any holes in the model) caused by the overlapping of all the grids. The master negative is made on Panchro-line with white light with the isoclinics eliminated either by using circular polarization or by the method mentioned by Koch and Szego[2] in which plane polarization is used and the negative exposed *twice*, rotating the polaroids through 45° between exposures.

Having completed the photography and obtained an enlarged photograph of a basket-work pattern such as that in Fig. 3, it is still necessary to carry out the very simple task of drawing the true stress trajectories as in Fig. 4. Place a

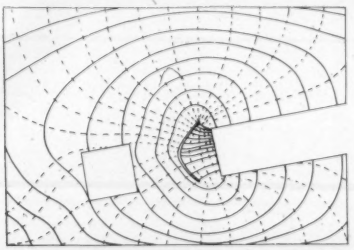

Fig. 4. The stress trajectory pattern drawn from the pattern in Fig. 3

sheet of tracing paper over the photograph and, to draw the lines, use as a guide a piece of copper wire which is thin enough to be bent easily and encased in a plastic sheath so as to be thick enough to be handled easily. When the wire has been bent so that the photograph grid lines are everywhere tangents to it, pin or weight the wire down and run a ruling pen or letter stencil pen along it. A French curve can also be used but the special advantage of the wire method is that the entire length of a stress trajectory can be seen at once and it gives an opportunity of adjusting the position of the line laterally, particularly if several wires are laid down simultaneously.

A defect, referred to as "white patches," may be found on some of the photographic patterns. They are usually found in the area bounded by the first order fringe and give rise to the inference that, since no isoclinics pass through these areas, the plastic does not obey the isoclinic law for very low orders. This is not strictly true as most traced isoclinic patterns show isoclinics intersecting at isotropic points, indicating that the isoclinics, though too faint to be photographed, are, nevertheless, visible to the eye of the person doing the tracing. Frocht[3] remarks that "isoclinics are rather vague in the neighbourhood of isotropic points and often their positions can be found only by producing or joining branches of the isoclinics on opposite sides of the isotropic points."

The extent of the white patch area is affected by the exposure time of the isoclinic negatives. Long exposures tend to close up weak isoclinics with an increase in white patch area. Great care should be exercised in adjusting the analyser so that it is correctly crossed with respect to the polarizer as incorrect alinement here also has an effect on the formation of white patches.

The quality of the plastic used for making models influences the formation of white patches as much as the photography, mottled plastic being especially objectionable in this respect. Perspex, a hard plastic, gives the clearest isoclinics and Perspex models show no white patches at all. However, Perspex is insensitive as regards fringes and in a Perspex model the zero order fringe usually occupies almost as much area as the white patch in a model made of Catalin 800. Columbia resin, another hard plastic, has been found to give white patches as bad as the comparatively soft plastic Catalin 800.

Working on the hypothesis that the isoclinic effect depends on strain in the plastic rather than stress, an experiment was performed as follows. A Catalin 800 model under load was heated by blowing hot air over it. As expected the fringe pattern showed increased orders everywhere as the material softened, but, contrary to expectations, the isoclinic pattern faded completely. This result suggests that the isochromatic effect depends on the lattice of higher melting-point material which undergoes greater strain as soon as the material softens, and the isoclinic effect depends on the lower melting point material which becomes less effective optically when it softens.

The model, when unloaded after it had cooled, showed both frozen-in fringes and isoclinics. Reloaded to about the same load as before, the isoclinics became so faint as to be almost extinct. It appears as though the isoclinics in a frozen stress pattern may be the result of the higher melting point lattice, in its strained condition, imposing a load on the remainder of the material. This load is then almost neutralized by an externally-applied load.

It has been noticed from the records kept during the development of this photographic method that the models photographed during the winter months produced hardly any white patches at all, compared with those done in the summer.

ACKNOWLEDGEMENTS

The work on which this paper is based was carried out in the National Physical Laboratory, Pretoria, and is published by permission of the South African Council for Scientific and Industrial Research.

REFERENCES

(1) Brown, A. F. C., and Hickson, V. M. *Brit. J. Appl. Phys.*, **I**, p. 39 (1950).

(2) Koch, W. M., and Szego, P. A. *J. Appl. Mech.*, **21** (2), p. 198 (1954).

(3) Frocht, M. M. *Photoelasticity*, Vol. 1, p. 192 (New York: J. Wiley and Sons, 1941).

A modified replica technique and its application to the examination of etched single crystals of barium titanate

By D. S. Campbell, B.Sc., and D. J. Stirland, B.Sc., The Plessey Co. Ltd., Caswell, Towcester, Northants

[*Paper received* 30 *September*, 1955]

A replica technique, combining the pre-shadowing and extraction methods, has been developed and applied to the study of etched surfaces of barium titanate single crystals. The results obtained are discussed in relationship to the structure of barium titanate.

A modified replica technique has been developed during an investigation of the surface structure of etched barium titanate. The method is a combination of the extraction replica technique and that of pre-shadowing and may have useful applications in other fields.

METHOD

The crystals to be examined were small, brittle, right-angled isosceles triangular plates of approximately 1 cm hypotenuse and 0·01 cm thick. Several standard replica methods[1] were used initially, but due to the fragility of the crystals fracturing invariably resulted. This was a serious disadvantage as it was desirable to retain the crystals for further experiments and any fracturing produced structure changes such as twinning.

The extraction technique used by Fisher,[2] and Nutting and Smith,[3] was attempted but had the disadvantage that portions of the surface adhered to the stripped replica and hence gave confused micrographs. Finally, a method combining the pre-shadowed technique[4] and the extraction technique was found to be satisfactory.

The crystals were placed in a platinum basket and etched by immersion in cold concentrated hydrochloric acid for periods of time varying from 1 to 10 min. They were then washed in distilled water followed by absolute alcohol, and finally dried in a warm air stream. The etched crystal was gently pressed on to adhesive cellulose tape with the surface under examination uppermost. It was then viewed under the optical microscope and suitably orientated for shadowing. After shadowing in a vacuum at an appropriate angle, using chromic oxide, the shadowed crystal was covered with a 1% solution of necoloidine in amyl acetate and held upright while the solvent evaporated. The coated crystal was next re-immersed in hydrochloric acid. After a few seconds the replica could be seen to be loosening on the crystal surface. It was then transferred to distilled water where the replica either floated off, or could be gently pulled off the surface. Finally, the replica was broken with a needle into suitably sized pieces which were picked up on copper support grids for examination in the usual way.

RESULTS

Barium titanate is tetragonal below the transition temperature of 120° C (Curie temperature), with one axis (*c*-axis) longer than the other two. The crystals grow with the crystal faces corresponding to {100} planes. They show spontaneous polarization below the Curie temperature along the *c*-axis.

Hooton and Merz[5] have shown that etching in concentrated hydrochloric acid reveals three different types of areas. These correspond with, firstly, a heavily etched area in which the positive end of the polarization vector is towards the surface, secondly, a less heavily etched area in which the polarization vector is parallel to the surface, and finally, a lightly etched area in which the negative end of the vector is towards the surface.

Figs. 1, 2 and 3 show optical and electron micrographs of various etched surfaces. The shadowed negative replica used for Fig. 2 was obtained by a dry-stripping method which resulted in the fracturing of the crystal, while Fig. 3 was obtained using the modified pre-shadowed technique. The increase in detail of the latter can be observed since, although the replica was from a crystal with a slightly different structure, the same etched time and magnification were used as for Fig. 2.

Figs. 4 and 5 show in more detail the effect of etching. Examination of these micrographs shows that, unlike most etching in which pitting is produced, the surface etches down leaving protuberances. These appear to be larger and more closely packed on the more heavily etched areas.

Figs. 7(*a*) and (*b*) are diagrams of a cross-section of the type of surface examined, before and after etching. The three different regions are shown, the positive polarization directions being represented by arrows. In Fig. 7(*b*) the

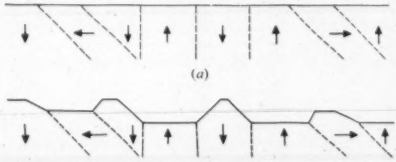

Fig. 7. (*a*) Cross-section of surface before etching. (*b*) Cross-section of surface after etching (simplified)

diagram is simplified in that the protuberances are omitted. Optically it can be shown that, with reference to the surface, the regions with the polarization parallel run through the crystal, as laminae, at 45°, and that the regions in which the polarization is normal run through the crystal at right angles.[5,6] The slopes on the surface arise from the different etch rates of the three regions. This is illustrated in more detail in Fig. 8(*a*) where E_1, E_2 and E_3 refer to the etch rates anti-parallel, normal and parallel to the positive polarization direction ($E_1 > E_2 > E_3$). It can be seen that the slope of *BC* results from the different etch rates E_2 and E_3 such that

$$\tan\theta = E_3/E_2$$

In the case of the laminae the etching produces different surface slopes at the two boundaries. This is illustrated for the two cases that can arise. In Fig. 8(*b*) the lamina is surrounded by a part of the crystal in which the positive polarization vector points away from the surface, and in Fig. 8(*c*) the vector points towards the surface. Hence when a lamina traverses both types of region, a slope such as *GH* will change inclination to become *NP*.

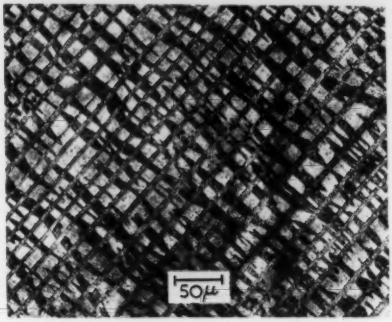

Fig. 1. Optical micrograph of crystal surface after 8 min etch

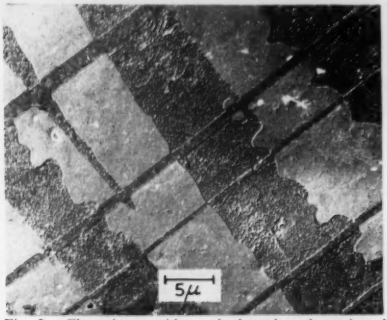

Fig. 2. Chromic oxide shadowed dry-stripped necoloidine replica of surface after 1 min etch

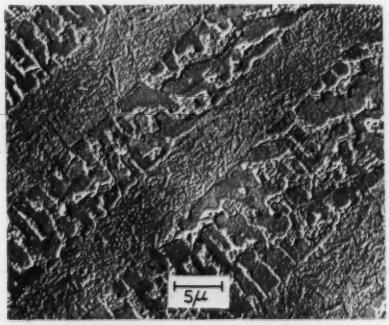

Fig. 3. Pre-shadowed necoloidine replica of surface after 1 min etch. Chromic oxide at 30°

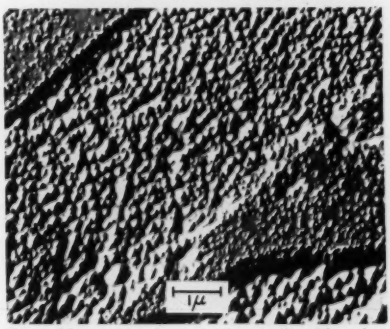

Fig. 4. Pre-shadowed necoloidine replica of surface after 1 min etch. Chromic oxide at 30°

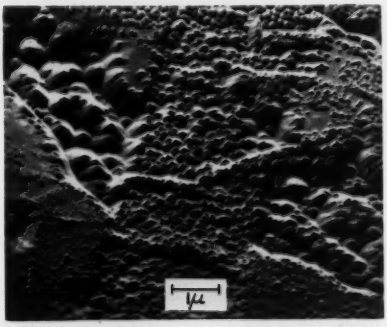

Fig. 5. Pre-shadowed necoloidine replica of surface after 1 min etch. Chromic oxide at 30°

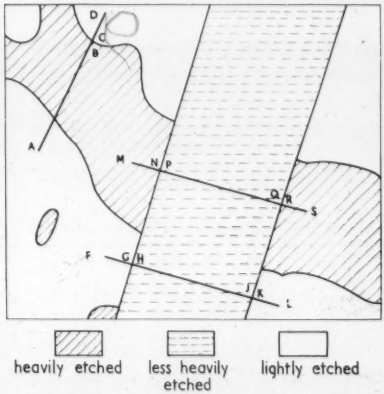

Fig. 6. Diagram of area shown in Fig. 5 (for explanation see text)

Collodion replicas from cross-sections of thin metallic strip and coatings

By D. J. Evans, M.Sc., A.Inst.P.

See page 65

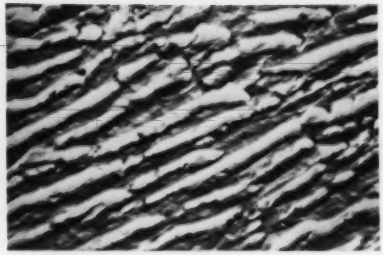

Fig. 1. Pearlite in 0·8% carbon steel. Collodion replica taken from a cross-section of 0·025 in. strip. (× 12000)

Fig. 2. Nickel electrodeposit 0·000 3 in. thick. Collodion replica taken from cross-section. (× 8000)

A comparison of dry stripped, unbacked collodion and Formvar replicas

By D. J. Evans, M.Sc., A.Inst.P.

See pages 66–67

(*a*)

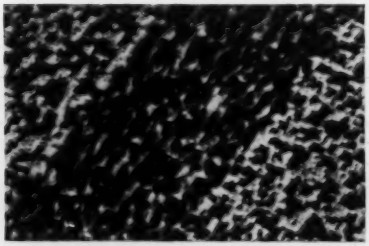

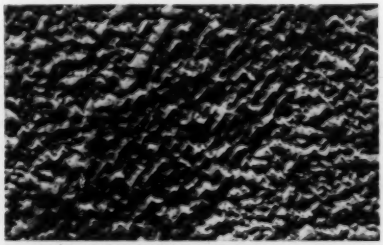

(*b*)

Fig. 1. Austenitic stainless steel twin crystal (× 8000). (*a*) Formvar; (*b*) collodion

(*a*)

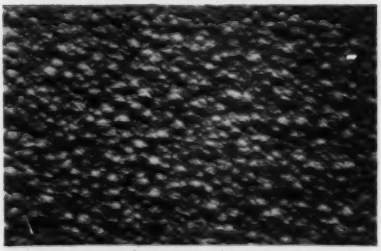

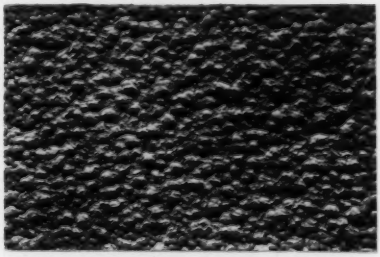

(*b*)

Fig. 2. Nickel electrodeposit as deposited (× 10000). (*a*) Formvar; (*b*) collodion

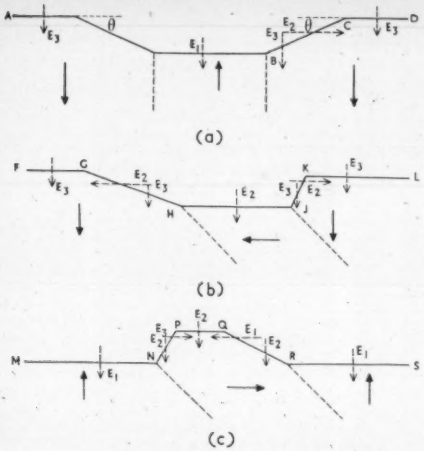

Fig. 8. Cross-section of parts of a surface after etching

Fig. 5 illustrates the three types of relative etching discussed in Figs. 8(*a*), (*b*) and (*c*). Fig. 6 is a diagram of the area shown in Fig. 5, *AD* representing the section of Fig. 8(*a*), *FL* that of Fig. 8(*b*) and *MS* that of Fig. 8(*c*).

From the micrographs, Figs. 4 and 5, an approximate estimate of the angles involved and hence the ratio of the etch rates could be obtained. These were

$$E_1 : E_3 \simeq 2 : 1$$
$$E_1 : E_2 \simeq 4 : 3$$

ACKNOWLEDGEMENTS

It is a pleasure for the authors to acknowledge the helpful discussions held with their colleagues at Caswell, in particular Mr. G. V. Smith. They would also like to thank The Plessey Co. Ltd. for permission to publish this paper.

REFERENCES

(1) COSSLETT, V. E. *Practical Electron Microscopy*, p. 213–241 (London: Butterworth Scientific Publications, 1951).
(2) FISHER, R. M. *Symposium on Techniques for Electron Metallography*, p. 49 (Philadelphia: American Society for Testing Materials Special Tech. Pub. No. 155, 1954).
(3) NUTTING, J., and SMITH, E. Private communication.
(4) AGAR, A. W., and REVELL, R. S. M. *Brit. J. Appl. Phys.*, **2**, p. 8 (1951).
(5) HOOTON, J. A., and MERZ, W. J. *Phys. Rev.*, **98**, p. 409 (1955).
(6) CAMPBELL, D. S. *Phil. Mag.*, **46**, p. 1261 (1955).

Collodion replicas from cross-sections of thin metallic strip and coatings

By D. J. EVANS, M.Sc., A.Inst.P., Department of Metallurgy, University College of Swansea

[*Paper first received* 19 *September, and in final form* 24 *October*, 1955]

The use of collodion as a replica material for obtaining electron micrographs of cross-sections of thin metallic strip and coatings is outlined.

In the application of electron microscopy to metallurgy, specimens such as metallic powders, wires, thin metallic strip and coatings may be termed specialized. Taylor[1] describes the use of the Formvar replica technique for the examination of etched sections of metal powder particles, whilst Nutting[2] describes a method of taking replicas from metal wires. The viewing of cross-sections of thin strip or coatings is often essential in optical metallography, and it is felt that a simple technique for obtaining electron micrographs of such sections might prove useful.

Ordinary metallographic mounting in Bakelite is found unsatisfactory since the replica film breaks at the specimen-Bakelite interface, but the following simple method of mounting is found to yield satisfactory replicas. A suitable length of strip is first cut into small pieces, each about $0{\cdot}75 \times 0{\cdot}5$ in. The pieces are placed side by side between two steel blocks of dimensions $1{\cdot}5 \times 0{\cdot}5 \times 0{\cdot}2$ in., the whole tightened by means of two bolts through the extremities of the steel blocks, and the specimen then polished and etched. Collodion yields satisfactory replicas, but it has been found impossible to strip Formvar films. Fig. 1 is an example which shows the structure of pearlite found in a 0·8% carbon steel strip 0·025 in. thick. Samples of silicon steel, stainless steel and nickel strip have also been investigated in this way, the thickness of strip varying from 0·03 in. for the nickel to 0·012 in. for the stainless steel.

A technique which is essentially similar to the above is also used for the examination of thin metallic coatings. The coating under investigation is considerably thinner than the substrate strip, so that prior to the cutting of the specimen and mounting between the two steel blocks, a buffer electroplating is first deposited on the specimen to prevent any disintegration or distortion of the edge of the coating during subsequent grinding and polishing. Collodion replicas are then dry stripped as in the case of the strip material. Thus Fig. 2 shows a nickel electrodeposited coating 0·0003 in. thick, with a portion of the substrate near the substrate coating interface, and also a part of the buffer plating, which in this instance is a nickel electrodeposit 0·003 in. thick.

ACKNOWLEDGEMENT

The author wishes to acknowledge with gratitude the experimental facilities made available by Prof. H. O'Neill, under whose general direction the work was performed.

REFERENCES

(1) TAYLOR, A. *Soft Magnetic Materials for Telecommunications Symposium*, Post Office Research Station, April 1952 (London: Pergamon Press Ltd., 1952).
(2) NUTTING, J. *Proceedings of the International Conference on Electron Microscopy, Delft*, 1949, *Nature* [*London*], **164**, p. 481 (1949).

A comparison of dry stripped, unbacked collodion and Formvar replicas

By D. J. Evans, M.Sc., A.Inst.P., Department of Metallurgy, University College of Swansea

[*Paper first received* 19 *September, and in final form* 24 *October*, 1955]

Dry stripped and unbacked Formvar and collodion replicas from identical areas of metallic specimens are compared, and differences other than comparative stability in the electron beam are apparent. The ease and rapidity of preparation of the collodion and also its increased resolution over Formvar commends its use for routine metallographic examinations.

The application of plastic replica techniques to the study of metal surfaces by electron microscopy is now well known. The simplicity and speed of the dry stripping process is a decided advantage, but certain investigators, e.g. Agar and Revell[1] and Williams[2,3] encounter serious difficulties in the actual stripping process. Both find it extremely difficult to detach unbacked Formvar films by this method, and nearly all the films which can be detached exhibit strain lines.

Plastic replicas may be formed with either Formvar or collodion, but most British workers appear to prefer Formvar, although collodion replicas are mentioned by many American writers including Wyckoff,[4] who has used them extensively. The main objection to collodion appears to be that it is less stable than Formvar in the electron beam and many investigators dismiss collodion with a mere brief reference to this instability. It is felt, therefore, that further information on the dry stripping process and a comparison of the properties of collodion and Formvar would be useful.

Agar and Revell[1] conclude that it is impossible to obtain satisfactory dry stripped replicas of Formvar when proper precautions to ensure cleanliness are taken, whilst Williams[2] appears to blame non-metallic inclusions present in his samples. Their replicas are obtained from a 0·5% solution of Formvar in chloroform and on repeating their technique with a variety of specimens it is found extremely difficult to obtain satisfactory replicas. However, in the present investigation, by increasing the Formvar concentration to a 1% solution in chloroform it is found a simple matter to strip the film, which then gives satisfactory electron micrographs (Figs. 1 and 2, p. 64). The ease with which a replica is freed must depend greatly on the nature of the surface of the object; it is to be expected that the parting is more difficult the rougher the surface. Also, the total thickness of the film must exceed the depth of relief to be copied, or the film will contain holes and lack the strength to withstand the stresses of detaching and mounting for examination. It is suggested that a 0·5% solution of Formvar is unsatisfactory in dry stripping unbacked films, except, perhaps, in the case of a smooth metal surface, where the depth of relief is small enough to allow the formation of sufficient excess thickness of replica above the relief, i.e. a metal surface sufficiently smooth to allow uniform and intimate contact between the free replica surface and the cellulose tape.

In the case of collodion it is found that replica films from a 0·5% solution of collodion in ethyl acetate can be stripped but are rather thin and tend to break up in the electron beam. However, a 1% solution of collodion is most useful, giving satisfactory electron micrographs with a wide variety of specimens. The tendency to break up in the electron beam is greatly diminished using this 1% solution and it is possible to make a representative survey of the specimen. In no instance has instability either prevented the taking of a photograph, or required the preparation of a second replica.

Williams[2,3] compares wet stripped Formvar and dry stripped collodion, but does not compare identical areas of specimen, relying instead on the comparison of typical areas. An attempt is made here to compare identical areas of a variety of specimens using dry stripped and unbacked Formvar and collodion replicas. A reference mark of some kind is essential if identical areas of a number of replicas are to be identified successfully in the electron microscope. The reference mark is made on the metal surface by drawing a sharp needle lightly along the surface. The replica is then formed on the metal surface in the usual way and the copper grid placed over the reference mark. A $\frac{1}{8}$ in. diameter hole is punched in the cellulose tape, the replica and grid breathed upon, the tape placed with a hole over the grid and the replica stripped. Placing of the copper grid on the replica surface before breathing upon the surface does not appear to affect the ease of stripping in any way. In general, it is found that the collodion adheres less strongly to the metal than does the Formvar, which is a distinct advantage. Movement of the Formvar film with respect to the grid occurs sometimes during the actual stripping, so that on subsequent examination of the replica the reference mark is frequently obscured by a grid bar, and several Formvar replicas are required before a favourable positioning of the reference mark occurs. Hyam and Nutting[5] in their comparison of optical and electron micrographs also encounter this rather troublesome difficulty with Formvar replicas. On no occasion is this difficulty encountered with the stripping of the collodion replicas.

Various specimens including plain carbon steels, alloy steels and electrodeposits were prepared to compare the various properties of collodion and Formvar, and Figs. 1 and 2 are a sample of some of the micrographs obtained. Perhaps the most striking feature is the difference in clarity of picture. Photographs of Formvar replicas sometimes appear to be out of focus and lack the finer detail shown with collodion, the improved resolution probably resulting from the collodion replicas being thinner than the Formvar. Again, it is found that Formvar replicas sometimes show strain lines which are absent in collodion replicas. Collodion replicas may be stripped from rougher surfaces than Formvar, and are considerably easier to prepare than the Formvar. Collodion is perhaps less stable than Formvar in the electron beam, but it is considered that this defect is outweighed by the above advantages.

In conclusion, it can be said that the ease and rapidity of preparation of these dry stripped plastic replicas over a wide range of metallurgical specimens commends their use for routine metallographic examinations.

ACKNOWLEDGEMENT

The author wishes to acknowledge with gratitude the experimental facilities made available by Prof. H. O'Neill, under whose general direction the work was performed.

REFERENCES

(1) AGAR, A. W., and REVELL, R. S. M. *Brit. J. Appl. Phys.*, **2**, p. 8 (1951).

(2) WILLIAMS, E. W. *M.Sc. Thesis*, University of Wales.

(3) WILLIAMS, E. W., and O'NEILL, H. *J. Iron Steel Inst.*, **177**, p. 224 (1954).

(4) WYCKOFF, R. W. G. *Electron Microscopy* (New York: Interscience Publishers Inc., 1949).

(5) HYAM, E. D., NUTTING, J. *Brit. J. Appl. Phys.*, **3**, p. 173 (1952).

The measurement, by nuclear resonance, of light water concentration in mixtures of light and heavy water

By A. M. J. MITCHELL, B.Sc., A.Inst.P., and G. PHILLIPS, M.Sc., Signals Research and Development Establishment, Christchurch, Hants

[*Paper first received* 19 *September, and in final form* 10 *November*, 1955]

Nuclear resonance absorption is induced in protons contained in mixtures of light and heavy water. The magnitude of the power absorption is used as a measure of the concentration of light water present and samples of known concentration are used to standardize the absorption.

Two techniques for inducing the absorption are described, one appropriate for H_2O concentrations in the range 7–100% and the other for low concentrations. In both cases the signal output from the equipment rises almost linearly with H_2O concentration. Using the first method, a signal-to-noise voltage ratio of twenty is obtained with a 7% concentration. A similar ratio is obtained from samples with 0·2% H_2O by using the second technique. The effect of flowing low concentration samples through the apparatus has been studied. The signal output falls with flow rate and at 40 ml/s is half that obtained at zero flow. Suggestions are made for improving the stability of the equipment and for reaching a quantitative theoretical understanding of the absorption signal shapes observed.

The phenomenon of nuclear magnetic resonance (N.M.R.) may be used to carry out non-destructive qualitative and quantitative analyses of certain substances. The N.M.R. effect may be induced in nuclei of finite spin and, by choosing the experimental conditions appropriately, only nuclei of chosen gyro-magnetic ratio are excited. This enables one to excite only the protons, for example, in a light/heavy water mixture. The number of chosen nuclei present may be deduced from the magnitude of the N.M.R. effect, but it is necessary to calibrate the effect by comparison with a standard sample of known nuclear population.

An investigation has been carried out to determine whether the N.M.R. effect could be used to design an equipment capable of continuously monitoring the amount of light water in a light/heavy water mixture. Such an equipment would find use for monitoring heavy water in nuclear reactors and in the manufacture of heavy water by enrichment from ordinary water.

THEORY OF THE METHOD

The theory of the N.M.R. techniques described here was first reported almost simultaneously by Bloch, Hansen and Packard[1] and Purcell, Torrey and Pound.[2] Since then several reviews of the subject have been published.[3–5]

Two basic schemes for detection of the N.M.R. effect were considered, the nuclear induction method[1] and the absorption method.[2] Both systems have the same theoretical sensitivity, but the absorption method as developed by Pound[5, 6] and Watkins[5, 7] offers a number of practical advantages. In this method the sample is contained in a coil forming part of the tank circuit of an oscillator. Nuclear resonance is detected by the drop in radio-frequency voltage across the coil as power is absorbed by the protons in the sample. Both the nuclear induction method and absorption methods which use radio-frequency bridges, require very careful construction if they are to be easily adjusted and yet be highly stable.

Primarily, the power absorbed at resonance by protons in a mixture of H_2O and D_2O depends on the excess number of protons per unit volume in the low energy level, namely $N\mu H/kT$, where N is the number of protons in unit volume, each of magnetic moment μ, H is the externally applied strong magnetic field, k is Boltzmann's constant and T the absolute temperature of the sample. Energy absorption occurs when the relationship $\omega = \gamma H$ is satisfied, where ω is the angular frequency of the applied radio-frequency field and γ the gyromagnetic ratio of the proton. The magnetic fields at individual protons differ slightly from the externally applied field H because of the fluctuating fields of neighbouring nuclei. Also, in practice, the externally applied field H is inhomogeneous and thus varies over the sample volume. In the authors' experiments, this latter effect is the more serious and leads to a broadening of the resonance. It is therefore desirable for H to be highly uniform over the sample volume. This becomes increasingly difficult for large samples and high fields so that the choice of sample size and H becomes a practical compromise. Although it is sometimes useful to increase absorption by lowering the sample temperature it was decided to work at room temperature and avoid the complexity of cooling equipment.

The change in resonance absorption as the concentration of H_2O in the mixture is changed is now considered. If, for

example, the concentration is reduced but the total volume of mixture is held constant, N falls proportionately. Reduction of concentration can also be expected to change the values of T_1 and T_2, the spin lattice and spin–spin relaxation times. In this application, changes in T_2 will be masked by inhomogeneity of H since the intrinsic line width is extremely small.[8] Anticipating results described later, T_1 increases with decreasing concentration. The value of T_1 limits the rate at which energy leaks from the spin system to the lattice and hence governs the rate at which energy is absorbed by the spins. One may therefore expect the absorption to vary somewhat more than linearly with concentration.

Finally, the amount of power absorbed depends on the particular way the resonance condition $\omega = \gamma H$ is brought about. Two methods have been used in which the radio-frequency ω is held constant and the main magnetic field H is varied through the resonant value. In the first method a single rapid passage through resonance is used, as previously reported.[9] In the second a slow passage through resonance is employed with a superimposed small amplitude 50 c/s modulation of the magnetic field.

Because of the difficulty of solving the Bloch differential equations[1] for these particular cases, particularly in allowing for inhomogeneity of the applied field H, the conditions for optimum signal have been found by trial.

APPARATUS

The apparatus comprises four main units: the magnet, the detecting head containing the sample, the absorption detector and the display system. A block diagram of the apparatus is shown in Fig. 1.

A 4700 G permanent magnet[10] is used to provide the main field H which has a uniformity of 2 parts in 10^5 over a volume $0{\cdot}5 \times 1{\cdot}0 \times 1{\cdot}0$ cm. The temperature coefficient of the field in the gap is $-2{\cdot}5 \times 10^{-4}$/°C. The field may be modulated by passing current of appropriate amplitude and waveform through two coils, mounted one on each pole tip of the magnet. The coils are fed from a modulation unit providing sawtooth current of adjustable repetition rate or a slow triangular waveform with superimposed 50 c/s ripple.

The mixtures of light and heavy water to be examined, were provided by the Atomic Energy Research Establishment. The light water used was purified at Harwell by an ion-exchange process and was not air-free. The heavy water was of approximately 99·8% purity. The concentration of heavy water in the mixtures was measured before dispatch to this laboratory by an infra-red absorption method, (HOD band at 3 μ), developed by Gaunt.[11] This method relies ultimately on comparison with a standard, the concentration of which is measured by a specific gravity technique. For experiments with static samples, sealed glass tubes approximately 11 mm outer diameter × 8 cm long containing known concentrations of heavy water were supplied. The apparatus for producing flowing samples is described later. In both cases the liquid under examination is contained in a glass tube upon which is wound a nine-turn radio-frequency coil of enamelled copper wire, approximately 1 cm length with $Q = 125$. This coil generates the necessary radio-frequency field in the sample and encloses a sample volume of the order 0·6 ml. The coil and sample are mounted in a 1 in. diameter cylindrical brass tube which acts as an electrical screen and also serves as a feeder to connect the radio-frequency coil to the absorption detector. The radio-frequency coil assembly is positioned in the magnet gap so that the axis of the coil is normal to the main field H. It is important that no materials containing protons are used in the construction of those parts of the assembly within the magnet gap and in the neighbourhood of the radio-frequency coil so that background signals are avoided. Glass and polytetrafluorethylene are therefore used as insulants. No absorption due to protons in the enamel on the copper wire was detected. Non-ferrous materials must be used to avoid distorting the magnetic field

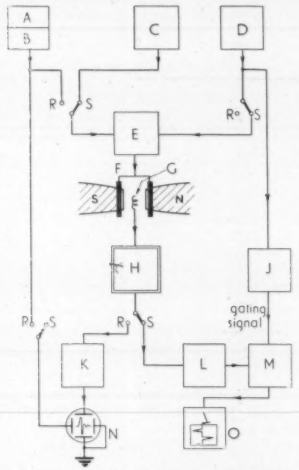

Fig. 1. Block diagram of nuclear magnetic apparatus (shown set for "slow passage")

A, trigger; *B*, cathode-ray oscillograph time base; *C*, triangular wave-form generator; *D*, 50 c/s sine wave; *E*, modulation unit; *F*, modulation coil; *G*, radio-frequency coil wound round sample; *H*, Watkins spectrometer; *J*, phase adjuster; *K*, audio-frequency amplifier; *L*, 40–60 c/s B.P. filter and audio-frequency amplifier; *M*, phase-sensitive detector; *N*, cathode-ray tube; *O*, pen recorder.

in the gap and no difficulties were experienced using brass for the assembly.

The detector comprises an "absorption" type spectrometer as described by Watkins.[7] The radio-frequency coil assembly forms the tuning coil of an oscillator running at 20 Mc/s. Absorption of radio-frequency energy by the sample, as the magnetic field H passes through the resonant value, causes an amplitude modulation of the voltage across the coil. This radio-frequency carrier is amplified and then amplitude demodulated. The modulation signal is finally amplified in a wide-band audio-frequency amplifier.

For the rapid passage experiments, the nuclear signal is amplified further and applied to the Y plates of a cathode-ray oscillograph. The X plates are driven by a voltage proportional to the sawtooth field modulation. In the slow passage experiments further amplification takes place in a narrow-band amplifier (40–60 c/s), followed by a phase-sensitive detector and pen recorder.

All the electronic equipment is operated from 240 V, 50 c/s mains with the exception of the heater voltage supply for the

spectrometer. This is derived from a 6 V storage battery, which is continuously float charged, in order to prevent the production of false signals by 50 c/s pick-up through heater-cathode coupling.

STATIC SAMPLE EXPERIMENTS

From the theory outlined above it can be seen that the rate of passage of radio-frequency energy into the spin system is limited by the rate at which energy can leak away to the lattice. The spin-lattice time constant T_1 is of the order three seconds for protons in distilled water. Preliminary experiments indicate it rises to about five seconds for protons in a 10% H_2O in D_2O mixture and to about ten seconds in an 0·3% H_2O mixture. Such values of T_1 are unfavourable for the detection of continuous absorption. If, however, the radio-frequency field is made effective for a short time only, an initial transient absorption of comparatively high value may be obtained.

This is the basis of the rapid sawtooth field modulation method. The spectrometer frequency is fixed and the main field is swept through the resonant values at a rate of the order 100 G/s. A sharp pulse of absorption occurs and typical results are shown in Fig. 2. A damped train of waves follows the pulse and arises from an interaction between the precessing nuclear moment and the applied radio-frequency field at frequency ω_0. As the value of the instantaneous field H passes through and beyond the resonant value $H_0 = \omega_0/\gamma$, the moment precesses at an instantaneous value $\omega = \gamma H$. The amplitude of the moment is also decaying to zero because the individual nuclei begin to go out of phase with a time constant T_2. If T_2 is sufficiently long, the moment will be large enough for beats to be seen between ω and ω_0.

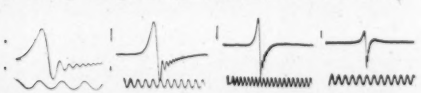

Fig. 2. Absorption pulse at high sweep rates for a static sample (50% H_2O in D_2O)

(*a*) Sweep rate, 570 G/s; timing trace frequency, 1000 c/s.
(*b*) Sweep rate, 190 G/s; timing trace frequency, 1000 c/s.
(*c*) Sweep rate, 54 G/s; timing trace frequency, 500 c/s.
(*d*) Sweep rate, 18 G/s; timing trace frequency, 100 c/s.

The sawtooth modulation is derived from the time-base of the cathode-ray oscillograph used to display the absorption. Having produced the pulse, the main field is returned rapidly to its initial off-resonance value by the time-base flyback, and held there. Somewhat less absorption occurs during the flyback because the sample has been partially saturated on the forward stroke and also because there is less time for energy to be absorbed during flyback.

By waiting at the off-resonance field value, time is allowed for the nuclei to relax back to the ground state from the high energy level to which they were driven by the radio-frequency field. It would be necessary to wait for a period of the order $10T_1$ in order to obtain maximum absorption with a second cycle of field modulation. In practice, it is desirable to induce absorption more frequently and in these experiments five recurrence rates were investigated, namely one sawtooth every 0·5, 1·0, 2·0, 5·0, 10·0 s. The sweep-rates were varied between 5·4 and 570 G/s. The variation of the peak-to-peak pulse amplitude (measured on a long-persistence cathode-ray oscillograph screen) with recurrence rate and sweep rate is shown in Fig. 3. The sample used was 50% H_2O in D_2O and the radio-frequency field applied was 0·013 G (half amplitude value).

The results indicate the effect of saturation in that maximum absorption occurs at low recurrence rates. At low sweep rates saturation is severe and full relaxation has not occurred

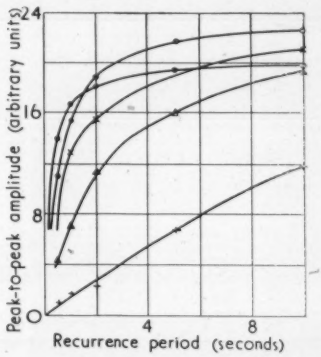

Fig. 3. Absorption pulse amplitude *versus* recurrence period for a range of sweep rates. (Static sample with 50% H_2O in D_2O)

Sweep rate (G/s): + = 5·4; △ = 18; ○ = 54; ● = 190; × = 570.

after ten seconds. At high sweep rates the time spent at resonance is inadequate for full absorption. For the particular value of radio-frequency field used, a recurrence rate of one sawtooth every two seconds with a sweep rate of 54 G/s was chosen as giving a strong signal at a useful recurrence rate. Although the absorption did not vary markedly with radio-frequency field it was found, as expected, that strong field gave smaller signals due to saturation. At smaller radio-frequency fields the background noise level of the spectrometer increased. With the conditions stated above the variation of signal amplitude against concentration of H_2O in the sample was investigated. The results are shown in Fig. 4. The signal amplitude rises almost linearly with H_2O concentration. At low concentrations spectrometer noise becomes appreciable, leading to a signal-to-noise ratio of three at 1% H_2O. Attempts were made to improve signal-to-noise ratio by using band-pass filters centred upon the dominant frequency of the absorption pulse. No significant improvement was obtained, possibly due to the broad band spectrum of the pulse.

It was then decided to investigate the possibility of improving signal-to-noise ratio by using a coherent detection system in which the absorption is modulated cyclically at an audio frequency. Narrow band amplification at the modulation frequency is used and the signal detected in a phase-sensitive detector gated at the modulation frequency. The detector output feeds a pen recorder of adjustable time constant. In order to modulate the absorption cyclically the main field is slowly varied in a linear manner, back and forth

through the resonant region. Superimposed on the main field is a 50 c/s sinusoidal ripple. A 50 c/s component of the absorption signal, in a chosen phase relationship to the ripple on the main field, is amplified in an audio-frequency amplifier with a 40–60 c/s pass band. After detection in the phase-sensitive detector the slowly varying signal is displayed on a pen recorder of 1·6 s time constant. Under certain conditions, in particular with substances of short T_1, the output should be the derivative of the absorption curve and appear as an S-shaped signal. In the authors' experiments the pen recorder traces were single sided. Qualitatively, this is probably due to main field inhomogeneities and long relaxation times. As mentioned above, conditions for optimum signal were approached experimentally by varying the sweep-rate of the main field, the amplitude of the 50 c/s ripple and the value of the radio-frequency field. For any particular set of these parameters it was necessary to seek the optimum phase relationship between a 50 c/s component of the nuclear signal and the 50 c/s ripple on the main field. This was effected by adjusting the phase of the 50 c/s gating signal fed to the phase-sensitive detector. In view of the sensitivity of this method attention was directed towards detecting concentrations of H_2O up to 0·5% and the above experimental conditions were optimized using an 0·3% H_2O sample. The optimum field sweep rate was 0·013 G/s with a 50 c/s ripple of 0·02 G peak-to-peak. The radio-frequency field was 0·0017 G (half amplitude value). A typical pen recorder trace under these conditions is shown in Fig. 5. The variation of trace amplitude with H_2O concentration was investigated using the range of samples available and a typical result is shown in Fig. 6.

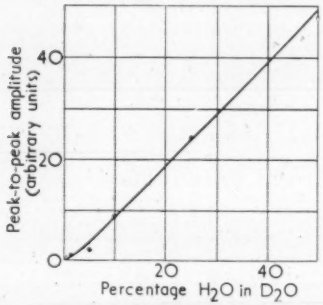

Fig. 4. Transient amplitude *versus* percentage H_2O in D_2O

Sweep rate 54 G/s, recurrence period 0·5 s, radio-frequency field 0·013 G—half amplitude value.

It will be noted that two of the eight points lie well above the curve which is a reasonable fit to the remainder. In these static sample experiments the radio-frequency coil is self-supporting and is designed to fit the sample tubes closely. It was noted that the two samples giving anomalous output were a very tight fit in the coil. The outside diameters of these two tubes were 11·3 ± 0·1 mm compared with 10·4 ± 0·3 mm for the remainder. The inside diameters were not checked, as it was not desired to destroy the samples, but it is reasonable to assume that the high output from the two anomalous samples was due to increased sample volume. Check tests with samples of similar concentration, housed in tubes of the correct diameter, confirmed this to be the case. The effect is mentioned here to illustrate the importance of controlling the size of sample tubes for accurate quatitative work.

In these experiments both the main field and the oscillator frequency are subject to drift due to thermal causes. By adjusting the oscillator frequency it was possible to ensure that absorption always occurred at the centre of the field sweep. If, however, drifts were not corrected absorption could occur close to the end of the field sweep so that one absorption followed closely on the next. The second absorption amplitude was less than the first and this was due to an inadequate time interval during which the protons relaxed back to their normal state. By an experiment of this type it was possible to estimate T_1 which was of the order of ten seconds for 0·3% H_2O in D_2O.

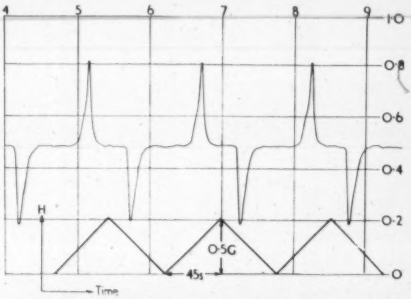

Fig. 5. Absorption signals from 0·3% H_2O in D_2O using slow field sweep modulated at 50 c/s

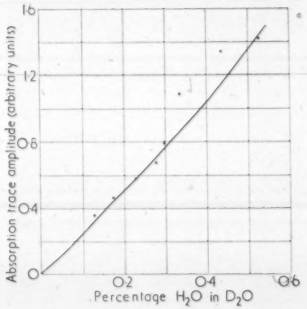

Fig. 6. Absorption trace amplitude *versus* percentage H_2O in D_2O (static samples)

FLOWING SAMPLE EXPERIMENTS

It was decided to investigate the nuclear resonance signals to be obtained from H_2O/D_2O mixtures flowing through the radio-frequency coil assembly. In particular, attention

was directed to the study of D_2O with low H_2O content as this was of immediate practical interest. A new radio-frequency coil assembly was constructed employing a cylindrical glass tank (Fig. 7) mounted in the magnet gap. Liquid enters the tank through the two side tubes and leaves through the central tube. A radio-frequency coil is wound on the central tube and is screened by a 1 in. diameter brass tube. As before, this tube also serves as a feeder to connect the coil to the absorption detector. Liquid is circulated through the tank by a pump unit and flow rates of up to 50 ml/s are available. The flow is controlled by a throttle valve or by varying the speed of the pump motor.

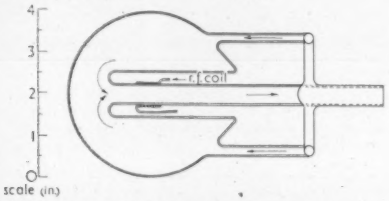

Fig. 7. Cross-section through glass tank

Ideally, it is desirable to expose the incoming liquid to the main magnetic field H for a time considerably in excess of T_1, before the liquid enters the radio-frequency field. If this condition is fulfilled the liquid becomes completely polarized and is thus in a condition to absorb the maximum possible power from the radio-frequency field. In practice, the tank volume is limited by the volume of the magnet gap and the volume of the screen around the radio-frequency coil. In the authors' design the "polarizing" volume of the tank is 230 ml, but it is doubtful whether the incoming liquid sweeps through this entire volume. It would have been preferable to arrange a series of baffles to ensure maximum utilization of the polarizing volume but this was impracticable with a glass tank. A non-ferrous metal tank might have been used, but in view of the expense of D_2O the authors wished to avoid possible sources of contamination.

The liquid under examination in the work reported here was D_2O with 0·3% H_2O. It was assumed that the N.M.R. absorption would vary with H_2O concentration in a similar way as for static samples and the main concern was with the effect of flowing the liquid through the radio-frequency coil. The technique used was to sweep the main field H back and forth through the resonant value at 0·013 G/s and to modulate the field with a 50 c/s ripple as before. In searching for the optimum signal amplitude at a particular flow rate, the radio-frequency field amplitude was held constant and the amplitude of the 50 c/s ripple varied.

At zero flow rate the signals were single-sided as in Fig. 5, but from 2·5–40 ml/s the signals were double-sided (Fig. 8). Qualitatively, this occurs because during resonance the saturated sample is being continuously replaced by freshly polarized liquid. The effect of the long relaxation time T_1 is thus minimized and a signal approaching the differential of the bell-shaped absorption signal would then be expected. The optimum field modulation amplitude for the flowing liquid was three times that for the static sample but was not critical. In Fig. 9 the signal trace amplitude is plotted against flow rate, for two values of the radio-frequency field. It will be noted that the signal falls off as the flow rate increases, in contrast to the increase in signal reported by Suryan.[12] Although his work was carried out using a different H modulation method and with liquids of shorter relaxation time, some increase in signal should be expected. The discrepancy can tentatively be explained by assuming that the

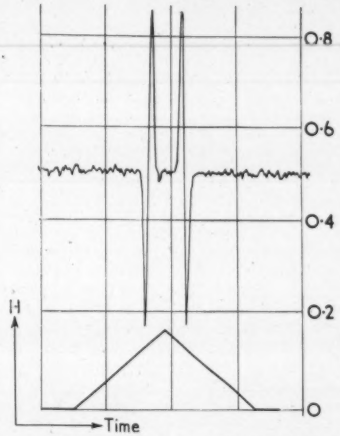

Fig. 8. Absorption signals from 0·3% H_2O using slow field sweep modulated at 50 c/s. Liquid flowing at 5 ml/s. (Pen recorder time constant reduced to $<0·1$s)

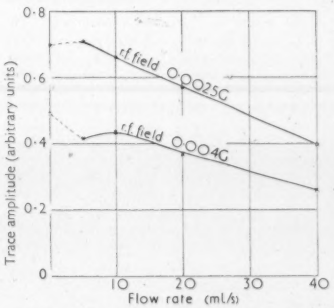

Fig. 9. Absorption trace amplitude *versus* rate of flow of 0·3% H_2O sample. (Traces at zero flow are single-sided; traces above 5 ml/s are double-sided)

design of tank used did not permit the complete polarization of the liquid before it entered the radio-frequency field. With the present tank, however, it is possible to sweep through the resonance more frequently and this is a practical advantage.

DISCUSSION

The techniques investigated cover the range of H_2O concentrations of practical interest (0·2–100% H_2O in D_2O)

with adequate sensitivity. Using the rapid transient method a static sample containing 1% H_2O gives proton signals with a signal-to-noise ratio of 3 : 1. This indicates the minimum detectable H_2O concentration and the method is suitable up to 100% H_2O. Static or flowing samples (up to 40 ml/s) containing 0·3% H_2O yield signals of at least 20 : 1 signal-to-noise ratio. Measurements have been made on samples from 0·13% to 0·53% H_2O concentration. The higher H_2O concentration was the maximum in which the authors were interested for a particular application, but does not represent a practical limit. Further work is required to improve the stability of the equipment but no great difficulty is expected on this account.

The largest effect to be controlled is the possible loss of signal due to magnet and/or oscillator drift. Control could be exercised by automatically adjusting the oscillator frequency or, less elaborately, by mounting the magnet in a lagged box. For accurate quantitative work it will be necessary to stabilize the gain of the equipment. This may be effected by the use of standard samples or by a calibrator of the type described by Watkins[5,7] which provides an artificial resonance signal.

It is also desirable to arrive at a quantitative understanding of the size and shape of the N.M.R. signals observed. In particular, the reason for single-sided signals when using the weakly modulated field technique requires more adequate explanation.

Reference has been made to the effects of the relaxation times T_1 and T_2, on the amplitude of the resultant nuclear signal. In practical applications of the techniques described here it will be important to ensure that an increase in signal amplitude is not due to the ingress of paramagnetic impurities into the liquid under examination.[13]

Finally, it is of interest to compare, briefly, the N.M.R. methods described above with other methods proposed for measuring H_2O concentration in D_2O. The fundamental method is that of density determination but no quick routine method is currently available nor does it seem applicable to continuous monitoring. Squires[14] describes a method in which the transmission of slow neutrons through an H_2O–D_2O mixture is compared with that through a standard. A source of thermal neutrons is required and a counting time of six minutes necessary for 0·02% accuracy in D_2O content. It is stated that the method could be adapted for continuous monitoring, but it seems unlikely that this method would be suitable for large concentrations of H_2O in D_2O. Mass spectrometric methods are lengthy and unsuited for continuous monitoring. The infra-red method of Gaunt[11] could probably be adapted for continuous monitoring, but is at present limited to the range 0–0·5% and 99–100% H_2O in D_2O.

Although further work is required to improve the stability of the equipment, the authors consider that the results obtained establish nuclear magnetic resonance as a promising tool for the measurement of H_2O in D_2O by methods which are applicable to both stationary and flowing samples and which are quick and non-destructive.

ACKNOWLEDGEMENTS

It is a pleasure to acknowledge the co-operation we have received from the Atomic Energy Research Establishment, Harwell. In particular we would like to thank P. Mummery for helpful discussions, D. Tyack for designing the pump unit used to circulate the D_2O and F. Seymour who made a number of the measurements during the later phases of the work. We also wish to acknowledge the contributions made by P. Cutler of this Establishment, who furnished the basic design of the electronic triangular waveform generator, and K. Roots and E. Richards who built and operated much of the N.M.R. equipment.

Crown copyright reserved. Reproduced by permission of the Controller, H.M. Stationery Office.

REFERENCES

(1) Bloch, F., Hansen, W. W., and Packard, M. *Phys. Rev.*, **69**, p. 127 (1946).

(2) Purcell, E. M., Torrey, H. C., and Pound, R. V. *Phys. Rev.*, **69**, p. 37 (1946).

(3) Pake, G. E. *Amer. J. Phys.*, **18**, pp. 438–52, pp. 473–486 (1950).

(4) Darrow, K. K. *Bell Syst. Tech. J.*, **32**, p. 74 (1953).

(5) Pound, R. V. *Progress in Nuclear Physics*, Vol. 2, p. 21 (London: Pergamon Press Ltd., 1952).

(6) Pound, R. V., and Knight, W. D. *Rev. Sci. Instrum.*, **21**, p. 219 (1950).

(7) Watkins, G. D. Doctoral Thesis, University of Harvard (May, 1952).

(8) Jacobson, B., Anderson, W. A., and Arnold, J. T. *Nature* [*London*], **173**, p. 772 (1954).

(9) Taylor, K. *Nature* [*London*], **172**, p. 722 (1953).

(10) Mitchell, A. M. J. *S.R.D.E. Technical Memorandum No. Res.*, 175 (1954).

(11) Gaunt, J. *A.E.R.E. Report* C/R 1264 (1953).

(12) Suryan, G. *Proc. Indian Acad. Sci., A*, **33**, p. 107 (1951).

(13) Bloembergen, N., Purcell, E. M., and Pound, R. V. *Phys. Rev.*, **73**, p. 679 (1948).

(14) Squires, G. L. *Proc. Phys. Soc.* [*London*], *A*, **67**, p. 520 (1954).

The thermal and electrical conductivities of deposited carbon

By A. R. G. Brown, M.Sc., and W. Watt, B.Sc., Royal Aircraft Establishment, Farnborough, Hants,
R. W. Powell Ph.D., D.Sc., F.Inst.P., and R. P. Tye, National Physical Laboratory, Teddington, Middlesex

[*Paper received* 29 *September*, 1955]

Details are given of a method used to deposit carbon from hydrocarbons at high temperatures for the production of small tubular specimens. The density had been found to vary systematically with the temperature of deposition, and the present work relates to measurements of thermal conductivity and electrical resistivity made over the range 20 to 200° C on commercial graphite and deposited carbons formed at temperatures of 1800, 1900, 2000 and 2100° C. The thermal conductivities of the specimens deposited at 2000 and 2100° C were found to be exceptionally high. At 50° C the value for material deposited at 2000° C was approximately 20% greater than that of copper; for material deposited at 2100° C it was approximately 40% greater than that of copper. These measurements were made in a direction parallel to the axis of the tube for which direction the deposited carbon showed a pronounced layered structure. This, and an associated high electrical resistance normal to its plane, made it difficult to determine the electrical resistivity of the sample deposited at 2100° C. The high thermal conductivity appears to result from the high lattice conductivity of this material, the electronic component being only of the order of 1%.

The dependence on temperature of deposition of the density of carbon deposited on to graphite rods from methane at sub-atmospheric pressures has already been reported.[1] The density varied from 1·2 g/cm^3 for material deposited at 1700° C to 2·23 g/cm^3 for that deposited at 2100° C, the X-ray lattice density of graphite being 2·26 g/cm^3. Further investigations have shown that these variations also occur with deposits produced from propane and hydrogen saturated with benzene. In view of these wide variations it was thought probable that other physical properties of the deposited carbons would show extensive changes. Accordingly, the method of deposition was modified to permit the production of more massive deposits, and some of the properties of these materials have now been investigated.

PREPARATION OF DEPOSITED CARBON

The deposition apparatus consisted of a large, water-cooled, metal vacuum chamber through the base of which were inserted two pairs of water-cooled copper electrodes, connected to a continuously variable step-down transformer. These electrodes were equipped with conical graphite contact blocks which, in turn, held graphite grips holding the rods on to which deposition took place. The vacuum chamber was equipped with a sighting hole for an optical pyrometer, gas inlet, vacuum and manometer connexions.

To form a deposit a $\frac{1}{4}$ in. rod of commercial graphite was inserted between the electrodes and the chamber pumped out. The base rod was then outgassed by heating to a temperature equal to, or in excess of, the deposition temperature to be employed, by the passage of a low voltage electric current, the gases evolved being continually pumped off. When the pressure was reduced to about 10 μ of mercury the rod was cooled down.

Pure dry hydrogen saturated with AR grade benzene was then admitted to the vacuum chamber, the rate of gas flow being adjusted to a suitable value, in this case 900 cm^3/min. A manostat was arranged to operate a magnetic valve separating the deposition vessel from the pumps, so that the pressure could be held at any desired value. In this way a continuous current of hydrogen benzene mixture was passed through the apparatus at an approximately constant rate. When pressure conditions had stabilized the specimen was heated to the deposition temperature, and maintained at temperature until sufficient carbon had been deposited. In the present experiments the partial pressure of benzene in the apparatus was 2·5 cm of mercury, the total pressure being approximately 60 cm of mercury.

After deposition the base rod was covered with a layer of deposited carbon which was slightly less thick at the ends than in the centre. Chemical analysis of material prepared in this manner returned 99·75 ± 0·2% C with undetectable ash on a 1 g sample. To permit measurements of thermal conductivity to be made such specimens were turned into cylindrical form, and the base rod machined away, leaving a hollow cylinder consisting solely of deposited carbon. It was not found possible to prepare such specimens with material deposited below 1800° C, as the low temperature deposits were very hard, brittle and difficult to machine, and invariably shattered during turning.

X-ray investigation showed that the deposited carbon consisted of layers of carbon atoms arranged as in graphite, alined so that the layers lay parallel to the surface of the original substrate, but were otherwise randomly oriented.[1] In the case of some deposits formed at 2100° C some (*hkl*) reflexions were obtained, indicating a graphitic orientation of some neighbouring layer planes. Hence, the structure is, in general, not that of graphite owing to lack of three-dimensional ordering. In the present work, the measurements of conductivity were made along the axes of the tubes, i.e. along the hexagonal layer planes.

The densities of the deposited carbons were determined by direct measurement of the weight and volume of the tubes, and the results are shown in Table 1.

Table 1. *Densities of test samples*

Temperature of deposition (° C)	*Density* (g/cm^3)
2100	2·15
2000	2·09
1900	1·75
1800	1·27
Commercial graphite	1·65

MEASUREMENT OF THERMAL CONDUCTIVITY AND ELECTRICAL RESISTIVITY

The samples of these four grades of deposited carbon, supplied to the National Physical Laboratory for measurements of thermal conductivity and electrical resistivity over

the range 50 to 200° C, were in the form of tubes approximately 4·5 cm long by 0·95 cm external diameter by 0·75 cm internal diameter. A similar tube of high purity commercial graphite was also included in the tests.

For the purposes of the thermal conductivity determination, each tube was joined to a bar of iron of about 15 cm length and 1·26 cm diameter and of known thermal conductivity. A sufficiently good contact was obtained by forcing the tube into a short, tightly-fitting brass collar and soldering this into a slightly over-size cavity in the upper end of the iron bar. A water-flow calorimeter was fitted to the lower end of the iron bar, and a heating unit was attached to the top of the specimen. The composite specimen was mounted centrally within a vertical guard tube and the interspace and axial hole packed with heat insulating powder. A steady temperature distribution was maintained, lateral interchange of heat being prevented by suitable adjustment of the temperature of the guard tube. The temperature gradients in the test specimen and the standard bar were obtained from the readings of three or four thermocouples attached at points along the lengths of each. The thermocouples used were of 40 s.w.g. Nichrome and constantan wires, the electromotive forces being measured on a potentiometer capable of reading to 1 μV. The heat flow in the test specimen was derived both from the gradient established in the standard bar and from a determination of the heat absorbed by the water-flow calorimeter. After applying a small correction for any out-of-match of the guard tube these observations enabled two estimates to be made for the energy flowing in an axial direction at the centre of the working section of the test sample. These two values usually agreed to within 1 or 2% of their mean value, Q J/s, which was used for deriving the thermal conductivity λ of the test material from the equation $\lambda = \dfrac{Q(x_1 - x_2)}{A(t_1 - t_2)}$, where A is the cross-sectional area of the tube in cm^2 and t_1, t_2 are the temperatures in °C of the tube as given by thermocouples at distances of x_1 and x_2 cm from one end. The range of mean temperatures covered in these experiments was from about 40 to 200° C. Observations were taken at successively higher steady temperatures and a final repeat measurement at about 50° C served to show that no significant changes had been caused by the heat treatment associated with the test.

The electrical resistivity determinations were later made over the same range of temperature. For this experiment a current of about 0·5 A was passed through the specimen and a standard resistance connected in series. Thermocouples spaced about 2 cm apart and attached to the centre section of the tube served as potential leads as well as providing means for measuring the temperature. The effect of thermal electromotive forces on the resistance readings was eliminated by reversal of the direction of the measuring current. An electric heater inserted in the axial hole of the specimen enabled its temperature to be raised so that the electrical resistivity determinations could also be made to temperatures of the order of 200° C.

This method proved satisfactory for the commercial graphite and the tubes deposited at 1800, 1900 and 2000° C, but considerable trouble was experienced in measuring the electrical resistivity of the material deposited at 2100° C. By making changes in the contact of the current electrodes or in the positions of the potential leads apparent values ranging from about 60 to 600 $\mu\Omega$ cm were obtained. The differences were attributed to the presence of relatively high electrical resistances in a direction normal to the axis of the tube, which tended to prevent the attainment of uniform current distribution over the cross-sectional area.

At this stage it was considered desirable to check whether the thermal measurements were influenced in a similar manner. The thermal conductivity determination on the tube deposited at 2100° C was therefore repeated. Whereas in the first determination the dispositions of the heat source and sink were such that most of the heat would enter and leave at the external surface of the tube, in this second experiment the contacts were also made on the inner surface of the tube.

Four instead of three thermocouples were now used to determine the temperature distribution along the central 2 cm length of the tube. Whereas in the electrical measurements on this tube a linear potential gradient was not obtainable over this length, a linear temperature gradient was again obtained and the thermal conductivity values derived from this second experiment agreed closely with those of the first over the full range of temperature.

Having completed these confirmatory thermal conductivity measurements, longitudinal slices were cut from the tube for the purpose of making further electrical resistivity measurements. The slice split on cutting to give an inner and outer curved strip, and this revealed a laminar structure in the deposited material. There was no difficulty in further subdividing the strips, the weak bond always being parallel to the curved surfaces of the tube.

Measurements with potential points located at corresponding positions on the inner and outer surfaces were made on the inner and outer strips first obtained. The apparent resistivities, as calculated in the usual way in terms of the current supplied and the cross-sectional area of the strip, were 83 and 317 $\mu\Omega$ cm for the inside slice and 256 and 266 $\mu\Omega$ cm for the outside slice. The inside slice was next further sub-divided to give three slices. Similar measurements on these, again giving the value for the potential points on the inner surface first, gave values of 206 and 228, 296 and 278, and 192 and 162 $\mu\Omega$ cm. These six values suggest a mean value of 227 $\mu\Omega$ cm for the inside slice compared with a mean of 261 $\mu\Omega$ cm for the outside slice, and an average value of 244 $\mu\Omega$ cm for this section of the tube.

Using the outside slice an attempt was then made to study the variation of the electrical resistivity with temperature, potential contacts being maintained on both inner and outer surfaces during this experiment so as to check that the current distribution had not been seriously altered during heating. From the potential measurements made on the inner surface a smooth curve was obtained, indicating resistivities at 100 and 200° C of 0·88 and 0·79 respectively of the resistivity at 20° C. A fall in resistivity was also indicated by the measurements on the outer surface, but the points were badly scattered suggesting that the distribution of current had been varying during the test.

For a repeat experiment another strip was cut from the tube and from an inner layer of this strip a rectangular bar, about 0·04 cm thick and 0·28 cm wide, was formed by rubbing on fine emergy paper. This time both sets of measurements gave smooth results lying on smooth curves and good repeat values were obtained on cooling. The resistivities at 100° C were 0·87 of the resistivity at 20° C in both cases, whilst at 200° C this ratio amounted to 0·79 for the inner surface and 0·80 for the outer.

The electrical resistivity values adopted for the specimen deposited at 2100° C, which can clearly be only approximate values, have been obtained by using the foregoing mean value at 20° C of 244 $\mu\Omega$ cm and the mean temperature coefficient furnished by this last experiment.

Table 2. *Results of thermal conductivity and electrical resistivity measurements*

Material	*Temperature*	*Thermal conductivity*	*Electrical resistivity* $\times 10^5$	*Lorenz ratio* $\times 10^7$
	(°C)	(J cm/s cm² °C)	(Ω cm²/cm)	(J Ω/s °K²)
Carbon deposited at 2100° C	20	—	$24{\cdot}_5$	—
	50	$5{\cdot}6$	23	40
	100	$5{\cdot}4$	$21{\cdot}_5$	31
	150	$5{\cdot}1_5$	20	$24{\cdot}_5$
	200	$4{\cdot}9$	$19{\cdot}_5$	20
Carbon deposited at 2000° C	20	—	38	—
	50	$4{\cdot}6$	36	51
	100	$4{\cdot}4_5$	33	$39{\cdot}_5$
	150	$4{\cdot}3_5$	$30{\cdot}_5$	$31{\cdot}_5$
	200	$4{\cdot}2_5$	29	26
Carbon deposited at 1900° C	20	—	$164{\cdot}_5$	—
	50	$0{\cdot}89$	$158{\cdot}_5$	$43{\cdot}_5$
	100	$0{\cdot}94$	147	37
	150	$0{\cdot}96$	137	31
	200	$0{\cdot}97$	127	26
Carbon deposited at 1800° C	20	—	323	—
	50	$0{\cdot}27_5$	317	27
	100	$0{\cdot}29$	$306{\cdot}_5$	24
	150	$0{\cdot}30_5$	296	$21{\cdot}_5$
	200	$0{\cdot}32$	286	$19{\cdot}_5$
Commercial graphite	20	—	$76{\cdot}_2$	—
	50	$0{\cdot}89$	$76{\cdot}_0$	21
	100	$0{\cdot}92$	$77{\cdot}_2$	19
	150	$0{\cdot}90_5$	$79{\cdot}_0$	17
	200	$0{\cdot}89_5$	$81{\cdot}_6$	$15{\cdot}_5$

Values obtained in this way are included in Table 2, together with values of the thermal conductivity of each sample and the electrical resistivity of the other samples which have been read from smooth curves drawn through the experimental points. Table 2 also contains values of the Lorenz ratio, the product of the thermal conductivity and electrical resistivity divided by the absolute temperature.

DISCUSSION OF RESULTS

The most outstanding result of the present investigation relates to the thermal conductivities of the carbons deposited at temperatures of 2000 and 2100° C. Over the range studied both samples have thermal conductivities exceeding that of any metal or, indeed, of any material previously measured, with the one possible exception of an earlier sample of the same kind. This was a sample described as pure graphite, which Pirani and Fehse[2] had prepared by heating a cellulose xanthogenate fibre in hydrocarbon at 2200 to 2500° C and subsequently heating the deposited material to about 3000° C. A thermal conductivity determination by a method of the Ingenhausz type, in which comparison was made with rods of copper, aluminium and nickel of similar dimensions, gave the surprising result that the graphite filament conducted heat better than the copper wire. For the specific electrical resistances of these graphites Pirani and Fehse quote room temperature values as low as $4{\cdot}7 \times 10^{-5}$ Ωcm, which suggests that their heat treated material may have possessed a somewhat larger thermal conductivity than the authors present sample, although no indication was given of the amount by which the thermal conductivity exceeded that of copper. One of the present authors has previously reported[3,4] that a sample of Ceylon graphite had a thermal conductivity of 1·01 cal. cm/s cm² °C (4·2 J cm/s cm² °C) at 20° C which just exceeded that of copper. In the case of the present samples, however, the thermal conductivity of copper has been exceeded by approaching 20% for

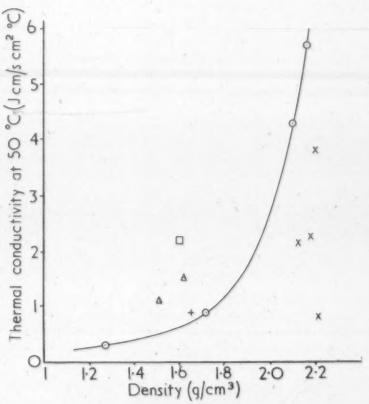

Variation of thermal conductivity at 50° C with density for samples of deposited carbons and graphites

Present work: ○ = Deposited carbons.
+ = Commercial graphite.
Previous work: × = Ceylon graphite.
△ = Acheson graphite.
□ = Hilger "H.S." graphite.

that deposited at 2000° C and over 40% for that deposited at 2100° C.

It will be observed that the thermal conductivities of these two samples decrease much more slowly with increase in temperature than did that of the Ceylon graphite. It would seem to follow from this that the temperature at which the thermal conductivity assumes a maximum value[5] is somewhat greater in the case of the present materials than for the Ceylon graphite. For the present sample of highly pure commercial graphite the maximum occurs at about 100° C, whereas for the carbons deposited at 1900 and 1800° C, if a maximum is obtained, it would seem to occur at a temperature beyond the range of the present experiments.

The accompanying figure shows the variation with density of the thermal conductivity at 50° C for the samples of deposited carbon. The experimental points are seen to lie on a smooth curve which is rather surprising in view of the layered structure of this material and its consequent anisotropy. The orientation of the layers would thus seem to be closely similar in all samples. The results for the present commercial graphite and for the graphites tested previously[4] do not, however, conform to this curve. The departures may be due in part to orientational effects.

The high values of the Lorenz ratio suggest that the major contribution to the thermal conductivity comes from the crystal lattice. Assuming that the electronic contribution can be calculated from the electrical conductivity, at 50° C the contribution from the electrons increases from 0·5% for the deposit formed at 2000° C to 0·9% for that formed at 1800° C and 1·2% for the commercial graphite. By 200° C the electronic contributions have increased so that these percentages become about 0·8, $1{\cdot}2_5$ and 1·6%.

ACKNOWLEDGEMENTS

This paper is published with the permission of the Directors of the Royal Aircraft Establishment and the National Physical Laboratory.

REFERENCES

(1) Brown, A. R. G., Hall, A. R., and Watt, W. *Nature* [*London*], **172**, p. 1145 (1953).
(2) Pirani, M., and Fehse, W. *Z. Elektrochemie*, **29**, p. 168 (1923).
(3) Griffiths, E., Powell, R. W., and Hickman, M. J. *J. Inst. Fuel*, **15**, p. 107 (1942).
(4) Powell, R. W. Institution of Mechanical Engineers, and the American Society of Mechanical Engineers, "General Discussion on Heat Transfer," p. 290 (1951).
(5) Berman, R. *Proc. Phys. Soc.* [*London*], *A*, **65**, p. 1029 (1952).

Stress distribution in a tee junction of thick pipes*

By H. Fessler, M.Sc.(Eng.), A.M.I.Mech.E., and B. H. Lewin, B.Sc.(Eng.), A.M.I.Mech.E., Department of Mechanical Engineering, University of Nottingham

[*Paper first received* 25 *October and in final form* 29 *November*, 1955]

The stress distribution on the inner surfaces of both pipes near their juncture, as caused by internal pressure, was determined by the "frozen stress" photoelastic technique. An approximate method of calculation (based on the theoretical solution for a hole in an infinite plate under uniform tension) was developed and a measure of agreement between the calculated and measured stresses was found.

Tee junctions in thick pipes are frequently needed where fluids at high pressure have to be transmitted. The interruption of the main pipe by the branch hole results in stresses greater than those encountered in the pipe without a hole. The exact theoretical solution of this problem was not attempted because the surfaces of main pipe and branch are most simply expressed in terms of *two* sets of cylindrical polar co-ordinates (see Fig. 1) and therefore impose complicated boundary conditions on any analytical solution.

Surface stresses near the junction of thin pipes have been determined experimentally by means of strain gauges. The frozen stress photoelastic technique is more convenient for the stress determination in thick pipe junctions because no high-pressure test rig is required and because the stresses can be measured very near to the edges of the pipes.

An approximate analytical solution was derived for the stresses in the main pipe near the branch hole and stresses calculated from this solution and compared with the measured stresses.

The model consisted of a cylinder 3 in. outside diameter, 1 in. bore, 15 in. long, to which a branch 1½ in. outside diameter, ½ in. bore, 6 in. long was cemented. The ends of the main cylinder were closed by hemispherical caps of ¼ in. wall thickness and the branch was connected to a pressure loading device.

As the investigation is concerned with the stress system due to the discontinuity of the junction only, it is necessary to ensure that the stress disturbances due to the end closures do not extend to this region. Measurements of the change of outside diameter were made, on the $\theta = 0$ and $\theta = 90°$ planes of the main pipe, and $\phi = 0$ and $\phi = 90°$ planes of the branch (see Fig. 1). It was found that regions existed in all three directions in which the diametral strains were constant and equal in the 0 and 90° planes. This showed that these regions were not influenced by discontinuities. The model can therefore be considered as equivalent to the junction of a semi-infinite branch to an infinite cylinder.

The frozen stress photoelastic technique[1] was employed with Araldite casting resin B[2] as the model material. Details of the experimental technique have been reported elsewhere.[3] The material was calibrated from separations of the stresses along radial lines through the main pipe and branch, at sections remote from discontinuities. The separations were carried out by applying Frocht's shear difference method[4] to cylindrical polar co-ordinates, the difference in radial

* Based on a paper presented to the Stress Analysis Group of The Institute of Physics in Sheffield on 30 September, 1955.

stress between the inner and outer surfaces being equated to the known internal pressure. The distribution of radial, hoop and axial stress at these sections agreed very closely with that predicted by Lamé's thick cylinder theory.[3]

Circumferential and axial slices of the main pipe and branch were cut and the stresses on the inner surfaces were obtained from them. These measured stresses were compared with stresses calculated as follows.

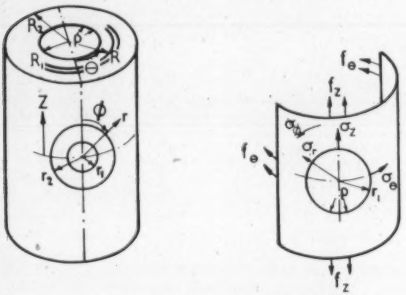

Fig. 1. Definition of directions and stresses

Successive cylindrical laminae of the main pipe were considered as infinite flat plates, each with a circular hole, under the action of two perpendicular tensions and an internal pressure p acting in the hole. The perpendicular tensions are the theoretical (Lamé) hoop and axial stresses f_0 and f_z, which would act on the particular lamina of the main pipe if the branch did not exist. With the nomenclature of Fig. 1, these stresses are

$$f_0 = p\frac{R_1^2}{R_2^2 - R_1^2}\left(1 + \frac{R_2^2}{R^2}\right) \tag{1}$$

$$f_z = p\frac{R_1^2}{R_2^2 - R_1^2} \tag{2}$$

The stresses near the hole due to f_0 and f_z may be determined from Kirsch's solution[5] for a circular hole in an infinite plate under uniform tension. Using the nomenclature of Fig. 1, the stresses due to f_z may be expressed as

$$\sigma_\phi = \frac{f_z}{2}\left[1 + \frac{r_1^2}{r^2} - \left(1 + \frac{3r_1^4}{r^4}\right)\cos 2\phi\right] \tag{3}$$

$$\sigma_r = \frac{f_z}{2}\left[1 - \frac{r_1^2}{r^2} + \left(1 - \frac{4r_1^2}{r^2} + \frac{3r_1^4}{r^4}\right)\cos 2\phi\right] \tag{4}$$

Similar expressions may be written for the stresses due to f_0.

Additional stresses occur due to the internal pressure p, which may be regarded as acting inside an infinitely thick cylinder of internal radius r_1.

The sum of the stresses due to the two perpendicular tensions and the pressure which act on the lamina, may be expressed by

$$\frac{\sigma_\phi}{p} = \frac{R_2^2R_1^2}{2(R_2^2 - R_1^2)}\left[\left(\frac{1}{R^2} + \frac{2}{R_2^2}\right) + \frac{r_1^2}{r^2}\left(\frac{1}{R^2} + \frac{2}{R_1^2}\right) + \frac{\cos 2\phi}{R^2}\left(1 + \frac{3r_1^4}{r^4}\right)\right] \tag{5}$$

$$\frac{\sigma_r}{p} = \frac{R_2^2R_1^2}{2(R_2^2 - R_1^2)}\left[\left(\frac{1}{R^2} + \frac{2}{R_2^2}\right) - \frac{r_1^2}{r^2}\left(\frac{1}{R^2} + \frac{2}{R_1^2}\right) - \frac{\cos 2\phi}{R^2}\left(1 - \frac{4r_1^2}{r^2} + \frac{3r_1^4}{r^4}\right)\right] \tag{6}$$

These equations are good approximations only when the bore of the branch is small compared with the bore of the main pipe. For larger branch holes the expressions must be modified. It is seen from Fig. 2 that different points in any

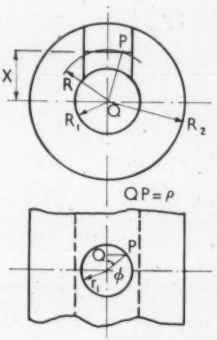

Fig. 2. Effect of curvature of laminae

circular section of the branch bore lie in different laminae and that, for all points except $\phi = 0$, the hoop stress in the main pipe is inclined to the plane of that circular section. The general expressions which incorporate the correct radius ρ instead of X and the component of the Lamé stress f_0 in the plane of the circular section are very cumbersome and the corrections are therefore only applied to the particular solutions which are presented.

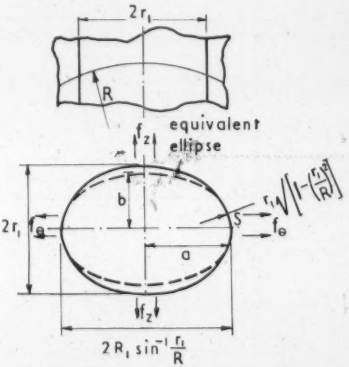

Fig. 3. Developed shape of branch hole

The fact that the hole due to the branch is not circular when the lamina is flattened necessitates a further modification. It has been shown for an elliptical hole[6] that, in an infinite plate under uniform tension, the ratio of the stress at S in Fig. 3 to the stress at the edge of a circular hole is unity for the stress f_0, and $\frac{1}{3}(1 + 2a/b)$ for the stress f_z. Instead of the oval hole in the lamina, an elliptical one of the same major axis and minimum radius of curvature was considered. It can be shown that the length of the developed hole is $2R \sin^{-1}(r_1/R)$ and that, where $\phi = 90°$, the radius of curvature of the distorted circle is $r_1(1 - r_1^2/R^2)^{\frac{1}{2}}$. The equation of the ellipse of such major axis and minimum radius of curvature can be shown to be

$$\frac{Y^2}{\left[R \sin^{-1}\left(\frac{r_1}{R}\right)\right]^2} + \frac{Z^2}{r_1\sqrt{(R^2 - r_1^2)}\sin^{-1}\left(\frac{r_1}{R}\right)} = 1$$

It follows from this, that

$$a/b = \sin^{-1}\left(\frac{r_1}{R}\right) \Big/ \frac{r_1}{R}\sqrt{(1 - r_1^2/R^2)}$$

but this correction for non-circularity applies along the line ($r = r_1$, $\phi = 90°$) only.

The straightened laminae are, strictly, flat plates pierced by a row of holes spaced $2\pi R$. In the case considered, the smallest value $2\pi R_1$ is six times the length of the oval holes. As far as stresses at the surface of the hole are concerned, it was therefore considered that the interaction of "neighbouring holes" could be neglected. This approximate analysis does not consider the shear and compressive stresses which occur between the laminae in the vicinity of the hole.

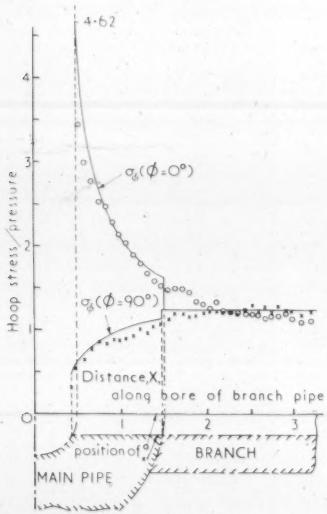

Fig. 4. Hoop stresses along branch bore. Lines show theoretical stresses, allowing for obliquity

The measured hoop stresses σ_ϕ along the branch bore ($r = r_1$) for the generators $\phi = 0$ and $\phi = 90°$ are plotted in Fig. 4. Substitution of $R = X$ in equation (5) gives

$$\frac{\sigma_\phi}{p} = \frac{R_2^2 + R_1^2}{R_2^2 - R_1^2} + \frac{3R_2^2R_1^2}{R_2^2 - R_1^2}\left(\frac{1}{X}\right)^2 \quad \text{for} \quad \phi = 0° \qquad (7)$$

and

$$\frac{\sigma_\phi}{p} = \frac{R_2^2 + R_1^2}{R_2^2 - R_1^2} - \frac{R_2^2R_1^2}{R_2^2 - R_1^2}\left(\frac{1}{X}\right)^2 \quad \text{for} \quad \phi = 90° \qquad (8)$$

No corrections need be applied to equation (7) but when obliquity and non-circularity have been allowed for equation (8) becomes

$$\frac{\sigma_\phi}{p} = \frac{R_2^2}{R_2^2 - R_1^2} + \frac{2R_1^2}{R_2^2 - R_1^2}\left[\left(\frac{X}{r_1} + \frac{r_1}{X}\right)\tan^{-1}\frac{r_1}{X}\right]^2 - \left(\frac{R_1^2X^2}{R_2^2 - R_1^2}\right)\left[\frac{R_2^2 + X^2 + r_1^2}{(X^2 + r_1^2)^2}\right] \qquad (8a)$$

The curves drawn in Fig. 4 were calculated from equations (7) and (8a). These equations can only be applied over the thickness of the main cylinder. This accounts for the discontinuities in the calculated curves. (The horizontal straight line represents the Lamé hoop stress on the inner surface of the branch.) It should be noted that the experimental points show that the stress disturbance due to the joint is small.

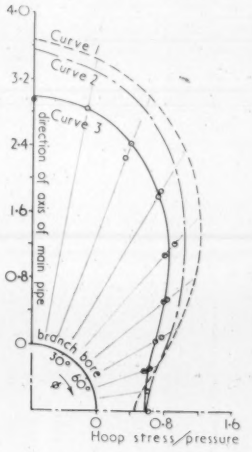

Fig. 5. Hoop stress in the circular section $X = 0{\cdot}59$ in. of branch bore

Curve 1: Theoretical, ignoring obliquity.
Curve 2: Theoretical, allowing for obliquity.
Curve 3: Experimental.

Fig. 5 shows the hoop stress distribution along the branch bore as measured on a plane close to the junction. Substitution of $r = r_1$ and $R = X$ in equation (5) gives

$$\frac{\sigma_\phi}{p} = \frac{R_2^2 + R_1^2}{R_2^2 - R_1^2} + \frac{R_2^2R_1^2}{R_2^2 - R_1^2}\left(\frac{1 + 2\cos 2\phi}{X^2}\right)$$

from which Curve 1 was plotted.

Curve 2 takes the obliquity of the stresses into account (but ignores non-circularity) and is plotted from

$$\frac{\sigma_\phi}{p} = \frac{R_1^2(1 - 2\cos 2\phi)}{R_2^2 - R_1^2} + \left(\frac{R_1^2}{R_2^2 - R_1^2}\right)\left[\frac{1 + 2\cos 2\phi}{1 + \left(\frac{r_1}{X}\sin\phi\right)^2}\right]\left[\frac{R_2^2}{X^2 + (r_1\sin\phi)^2} + 1\right] + 1$$

The experimental points shown were obtained from two adjacent quadrants and thus give a measure of the symmetry which was achieved.

Along the generator of the bore of the main cylinder which intersects the axis of the branch, $\phi = 0°$, $r = Z$, $R = R_1$. Substitution in equation (5) results in the expression

$$\frac{\sigma_\theta}{p} = \frac{R_2^2 + R_1^2}{R_2^2 - R_1^2} + \frac{3R_2^2}{2(R_2^2 - R_1^2)}\left(\frac{r_1}{Z}\right)^2 + \frac{3R_2^2}{2(R_2^2 - R_1^2)}\left(\frac{r_1}{Z}\right)^4$$

for the hoop stress and

$$\frac{\sigma_z}{p} = \frac{R_1^2}{R_2^2 - R_1^2} + \frac{R_2^2}{2(R_2^2 - R_1^2)}\left(\frac{r_1}{Z}\right)^2 - \frac{3R_2^2}{2(R_2^2 - R_1^2)}\left(\frac{r_1}{Z}\right)^4$$

for the meridional stress. No correction need be applied to these expressions and the curves in Fig. 6 were plotted from them.

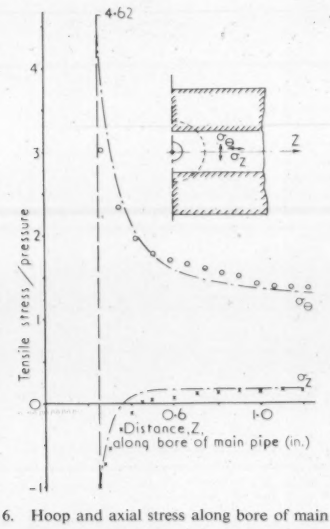

Fig. 6. Hoop and axial stress along bore of main pipe

The hoop stress along the bore of the main cylinder in the same circumferential plane as the axis of the branch is defined by $\phi = 90°$, $r = R_1\theta$, $R = R_1$ and $\sigma_r = \sigma_0$. Substitution in equation (6) results in

$$\frac{\sigma_0}{p} = \frac{R_2^2 + R_1^2}{R_2^2 - R_1^2} - \frac{7R_2^2}{2(R_2^2 - R_1^2)}\left(\frac{r_1}{R_1\theta}\right)^2 + \frac{3R_2^2}{2(R_2^2 - R_1^2)}\left(\frac{r_1}{R_1\theta}\right)^4$$

and allowance for the obliquity modifies this to

$$\frac{\sigma_0}{p} = \frac{R_2^2 + R_1^2}{R_2^2 - R_1^2} - \left(\frac{2{\cdot}5R_2^2 + R_1^2}{R_2^2 - R_1^2} + \frac{R_1^2}{R_1^2 + r_1^2}\right)\left(\frac{r_1}{R_1\theta}\right)^2 + \frac{3R_2^2}{2(R_2^2 - R_1^2)}\left(\frac{r_1}{R_1\theta}\right)^4$$

from which the theoretical curve in Fig. 7 was plotted.

It may be seen from Figs 4 to 7 that the theoretical values are good approximations along generators but that the peak

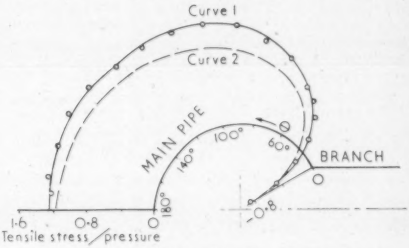

Fig. 7. Hoop stress in the circular section of main pipe bore which contains the axis of the branch

Curve 1: Actual hoop stress.
Curve 2: Theoretical hoop stress.

stresses predicted by the theory are too large. Curves drawn through the experimental points in Figs. 4 and 6 indicate a maximum value of stress/pressure of 3·50, compared with a calculated value of 4·62. These results may be expressed as stress concentration factors, defined as (peak stress)/(Lamé hoop stress in the bore of the pipe). The theoretical value of 3·70 is 32% greater than the measured value of 2·80.

ACKNOWLEDGEMENTS

The authors wish to thank Prof. J. A. Pope, who, as Head of the Departments of Civil and Mechanical Engineering at Nottingham University, provided facilities for this work.

REFERENCES

(1) FESSLER, H. *Proc. Instn Mech. Engrs*, **1B**, No. 12 (1953).

(2) SPOONER, H., and MCCONNEL, L. D. *Brit. J. Appl. Phys.*, **4**, p. 181 (1953).

(3) FESSLER, H., and LEWIN, B. H., in Proceedings of 9th Annual Conference of Stress Analysis Group, Institute of Physics, *Brit. J. Appl. Phys.*, **7**, p. 1 (1956).

(4) FROCHT, M. M. *Photoelasticity*, Vol. I, p. 252 (London: Chapman and Hall Ltd., 1941).

(5) DEN HARTOG, J. P. *Advanced strength of materials*, p. 193 (New York: McGraw-Hill Book Co., 1952).

(6) TIMOSHENKO, S. P., and GOODIER, J. N. *Theory of Elasticity*, p. 203 (New York Engineering Societies Monographs, 1951).

Correspondence

Errors in the A.S.T.M. Index of X-ray powder diffraction patterns

Early in 1953 the X-Ray Analysis Group of The Institute of Physics published[1,2] a request that A. J. C. Wilson should be notified of any errors which had been found in the A.S.T.M. Index of X-ray powder diffraction patterns. Over a hundred errors and comments have now been collected from twenty-six different sources. While it is expected that these will eventually be incorporated in the Index, it is thought advisable that they should be published now, so that regular users of the Index may be made aware of them earlier than would otherwise be the case. Some of the corrections, which were received soon after the original request for them, have already been incorporated in the set of Index cards issued in 1954, but are included for the benefit of those who possess only earlier sets.* Such corrections are appropriately indicated in the main table of errors. The various types of error which have been reported, and the percentage of the total represented by each type, are shown in the following table.

Analysis of errors

Type of error	*Percentage of total*
Incorrect naming or identification of substances (especially minerals)	22
Incorrect crystal structure, space group, or cell parameters	18
Incorrect or absent spacings or intensities	16
Misprints, including transcription errors from earlier cards, spelling mistakes, and omissions from the indexes to each set of cards	11
Incorrect structural or chemical formulae	9
Radiation given incorrectly	8†
Extraneous lines and specimen impurity	5
Loss of important lines by camera cut-off	5
Disagreement between cards	3
References given incorrectly	3

† The figure given here is probably not a true reflexion of the state of the Index. It is believed that there are many errors of this type that have not been notified, particularly in the First Supplement.

It will be observed that errors in actual powder patterns and in crystallographic data together make up 34% of the total, while errors in chemical formulae and mineral nomenclature, and misprints of varying importance, supply 42%. It is perhaps reassuring to note that camera cut-off does not appear to have introduced a serious source of error, and that few incorrect references have been reported.

The distribution of the errors among substances of various types is shown below:

	Inorganic			
Nature of substance	*Minerals*	*Non-minerals (except metals)*	*Metals*	*Organic*
Percentage of total errors	50	27	7‡	16

‡ Including nitrides, etc., of metallurgical interest.

* About 600 correction cards are included in the sixth set of cards, but there is practically no overlap between the corrections noted in our list and those incorporated in the sixth set; the compilations are independent.

The full list of corrections is too long for publication here, but will be circulated to members of the X-Ray Analysis Group of The Institute of Physics and to those who have purchased copies of the Index through the Institute; others who would find the list useful are invited to apply for a copy to one of the authors or to The Institute of Physics. In the list the substances appear in alphabetical order. In the first two columns of the list the reference numbers of the cards in the A.S.T.M. Index are given for each set in which the error occurs. The name of the substance follows, and then a brief summary of the correction or comment as received by the authors, whose occasional additional comments are added in square brackets. The source of the correction or comment is indicated by a number which refers to the list of acknowledgements.

The introduction into the Index of data obtained with counter diffractometers has given rise to discrepancies which, though perhaps not strictly errors, should certainly be pointed out here. An example[3] will indicate their nature.

The five strongest lines of the calcite pattern are:

(dÅ)	3·035	2·285	2·095	1·913	1·875
I/I_1 (camera, visual)	100	60	60	70	70
I/I_1 (counter)	100	18	18	17	17

Replacing the photographic pattern by the diffractometer pattern, as recommended in the fifth set of A.S.T.M. cards, thus introduces different second- and third-strongest lines. Such discrepancies frequently arise from the fact that the transparency factor (better, though less correctly, known as the absorption factor) is constant at μ^{-1} for the flat-plate specimen used in the diffractometer, but increases rather rapidly with θ for the cylindrical rod used in powder cameras.

Since the use of counter data in conjunction with patterns obtained with a camera, and *vice versa*, might lead to difficulties in identification because of this effect, the elimination of good camera data from the Index in favour of counter data appears to be premature except when the three strongest lines of the two patterns agree. An examination of the eliminations recommended in the fifth set of cards shows that some ninety substances (representing many more cards) show disagreements of the kind under discussion, and that for about sixty of these the spacings of the three strongest lines, as well as their intensities, differ in the camera and diffractometer data. A detailed list of these substances has been prepared, and is to be made available in the same way as the list described above. It should also be noted that it is not always indicated on a card that the data have been obtained with a diffractometer; such cards are appropriately indicated in the list.

The authors acknowledge with gratitude the assistance of the organizations and individuals who have supplied the information from which the full list of corrections has been compiled.

Viriamu Jones Laboratory,
University College, Cardiff.

J. W. Hughes
Isabel E. Lewis
A. J. C. Wilson

REFERENCES

(1) *J. Sci. Instrum.*, **30**, p. 64 (1953).
(2) *Brit. J. Appl. Phys.*, **4**, p. 32 (1953).
(3) Whittaker, E. J. W. Private communication.

New books

Operational calculus—based on the two-sided Laplace Integral (2nd Ed.). By BALTH VAN DER POL and H. BREMMER. (London: Cambridge University Press, 1955.) Pp. xiii + 415. Price 60*s*.

When the present writer reviewed the first edition of this book* he made the rather conservative prediction that "this book is likely to become and should become a classic." This prediction has been amply and properly fulfilled and the need for a second edition of a work comprising difficult and profound mathematics, however attractively presented, is evidence of the importanee, value and success of the authors' work. It is only necessary now to repeat that the book aims at presenting in a modern, more rigorous and comprehensive form the operational calculus so widely applied in physics and engineering. The changes in the second edition comprise some detailed corrections and improvements, but the new material, as stated in the new preface, is confined to paragraphs on rules for the treatment of correlation functions, a note on the theory of distributions and a note on the Wiener–Hopf technique for dealing with integral equations (of a kind which the principle of superposition can yield) where the difference kernel is valid only when the main variable is positive. The authors have not added some recent work to their interesting discussion of the delta or impulse function but, in any event, some of this appeared too late for inclusion. It is heartening to record the success of so excellent a book. S. WHITEHEAD

* *Brit. J. Appl. Phys.*, **2**, p. 57 (1951).

Mesons and fields, Vol. 2. By HANS A. BETHE and FREDERIC DE HOFFMANN. (Evanston, Illinois: Row, Peterson and Company, 1955.) Pp. ix + 446. Price 60*s*., $8.00.

In less than a decade a new and exciting branch of physics, that concerned with the π-meson, has been discovered and developed with considerable vigour by many physicists in laboratories around the world. (There are over 500 named references in this book.) To a newcomer into meson physics an up-to-date survey with an emphasis on the interplay between experimental and theoretical results will be a boon of first importance: the strictly mechanical benefit of less frequent visits to the *Physical Review* is not negligible. To those familiar with some branch of the physics of mesons a critical appraisal of the present position in other aspects of the subject such as meson-nucleon scattering, the theory of nuclear forces, meson production in gamma or proton collisions on nuclei or (the content of the last two sections) other mesons than the π-meson is most welcome.

Except for R. E. Marshak's book on *Meson physics* (1952) one has had to rely on surveys, such as those by Michel and Dalitz, which, though excellent, are no substitute for a textbook admittedly didactic as well as informative. Physicists are now satisfied that the π-meson is a spinless particle of odd parity, and, moreover, one which interacts symmetrically with nucleons thus enabling a classification into isotopic spin states to be of value. This enables Bethe and de Hoffmann to discuss the interpretation of experimental results with more assurance than Marshak was able to do. The largest contribution to detailed calculation which has arisen since Marshak's book, and which is reported in detail in the book being reviewed, has been in the use of Tamm's method of approximating to the field theoretical equations over and beyond strict perturbation theory. To the theorist it is true to say that this volume by itself will not enable him to start computing. The reviewer, who was privileged to spend last year at Bethe's laboratory at Cornell, is acquainted with Volume 1 in the form of a lecture course, and believes it will form an indispensable companion to Volume 2 for the theoretical physicist.

Bethe and de Hoffmann's book contains very few errors. Two minor points are that it is hard to see how a $\cos^2\theta$ distribution in the proton–proton production of the π^+-meson taken by itself makes it very unlikely that it is a scalar particle (page 13) and that a factor 1/3 is missing in the nuclear potential on page 301. The layout could have been better. A uniform reduction and presentation of graphs—compare those on pages 107 and 314 with those on pages 109 and 318 respectively—and a more attractive mathematical typography are two possible improvements. E. A. POWER

Light calculations and measurements. By H. A. E. KEITZ. (London: Cleaver Hume Press, Ltd., 1955.) Pp. xvi + 413. Price 52*s*. 6*d*.

This translation into English of Mr. Keitz's book, published in German in 1951, is very welcome. The first part, somewhat the larger, is theoretical and deals very clearly with the fundamentals of photometry, i.e. of light treated quantatively. The author has succeeded in his aim of bringing this well within the reach of those who follow A. P. Trotter in lamenting when "the problem takes refuge in an integral." The long chapter on the properties of optical systems is exceptionally good. The second part deals with the practical side, i.e. with all types of photometric measurement (other than spectrophotometry) and bears ample evidence of the author's extensive experience in this field.

The work of translation has been admirably done by Mr. G. Ducloux and the terminology is generally impeccable. There are remarkably few misprints or other errors, though it is strange that the name of Russell should have lost the final letter it rightly enjoyed in the German edition. It should be mentioned that the author has introduced, where appropriate, the Anglo-Saxon units in addition to the international ones. The paper and printing are excellent and the production is of a high standard. J. W. T. WALSH

The polar aurora. By CARL STÖRMER. (Oxford: The Clarendon Press, 1955.) Pp. xvii + 403. Price 55*s*.

In 1903 Professor Carl Störmer became interested in calculating the trajectories of charged particles moving under the influence of the Earth's magnetic field. His researches made him realize the great need for reliable information on the height and position of aurora. Though a mathematician, he decided to carry out the observational work required himself, and he developed and applied the method of parallactic photography with outstanding success. Having once embarked on observational work he did not confine himself to obtaining data relevant to his original theoretical investigations, but studied also other aspects of aurora. It is to be doubted if anyone has contributed more to our knowledge of the phenomenon.

The numerous papers on auroras which Professor Störmer has written during the past half century are not all readily available. For this reason alone this book is to be warmly welcomed for it gives a connected account of the material

in these papers. Professor Störmer rightly concerns himself mainly with presenting the important work he himself has done. He does not attempt to discuss the contributions of others critically. Instead he often merely gives suitable references or quotations. For example, in a chapter devoted to the origin of the primary auroral stream he simply refers the reader to *Geomagnetism* for the theory of Professors Chapman and Ferraro; reproduces an article in *Nature* on the theory of Dr. Martyn, and lets Professor Alfven summarize his own theory.

The extensive collection of observational data and the careful descriptions of events should be invaluable to all carrying out research on auroras; and much of the mathematics should be of interest in addition to students of cosmic rays. The book is a noteworthy addition to the literature on geophysics. D. R. BATES

Precision electrical measurements. Proceedings of a symposium held at the National Physical Laboratory on 17–20 November, 1954. (London: H.M. Stationery Office, 1955.) Pp. xxii + 349. Price 27*s.* 6*d.*

This volume contains twenty-six papers in full, arranged in five groups corresponding to the sessions of the symposium. Each group of papers is followed by a summarized version of the discussion held at the end of each session.

The scope of the papers ranges from descriptions of precision methods of measuring physical properties (e.g. dielectric constant) to general surveys of testing techniques, such as impulse testing. The papers include the appraisal of special properties of new materials, such as the microwave performance of magnetic dielectrics, and descriptions of present-day methods of attacking old problems, such as breakdown tests on high-voltage equipment.

This collection of papers is thus valuable both in describing refinements of established techniques and in opening the gateway to reliable testing at increasingly higher frequencies and voltages. Noteworthy among new test equipment is the precision dual admittance bridge for the range 3 Mc/s to 300 Mc/s described by D. Woods of the Ministry of Supply and developed as a result of a painstaking study of the potentialities of the twin-T circuit.

Taking the papers as a whole the word "precision" is applied in a somewhat elastic sense and physicists in both academic and industrial laboratories will find much of interest in their contents. P. R. BARDELL

Servomechanisms and regulating system design, Vol. 2. By HAROLD CHESTNUT and ROBERT W. MAYER. (London: Chapman and Hall Ltd., 1955.) Pp. xiii + 384. Price 68*s.*

This volume is mainly concerned with practical engineering solutions to the design of feedback control systems, based on the mathematical approach given in Volume 1. The first five chapters deal with particular aspects of linear systems: measurement techniques, input and noise characteristics, load characteristics and power requirements, passive "shaping" networks, and amplifier design. Each topic is illustrated by examples, mostly taken from aircraft tracking systems. The sixth chapter deals with a.c. servomechanisms, by means of an approximate treatment using the concepts developed for d.c. systems. The remaining chapters are concerned with systems of progressively greater non-linearity: first, treatment by linearization for small departures, then "describing function" and phase-plane methods, and lastly a discussion of intentional non-linearities for improving performance. Particular attention is given to the effects of saturation and backlash in a position control system.

Although this book offers no new analytical methods, it brings together most of the recent developments in the design theory of linear and quasi-linear feedback systems, with the exception of pole-zero methods and equivalent circuits for electrical machines. The emphasis on position control and the lack of reference to non-minimum-phase systems may reduce its usefulness to process control engineers, but for servomechanism design it can be recommended as a valuable reference work. N. REAM

Microwave spectroscopy. By C. H. TOWNES and A. L. SCHAWLOW. (London: McGraw-Hill Publishing Co. Ltd., 1955.) Pp. xviii + 698. Price 90*s.* 6*d.*

During the last ten years a very rapid development of microwave spectroscopy has taken place. The authors of the present book have endeavoured to give a thorough and critical treatment of the subject, intended mainly for those working in the field. They have succeeded, however, in presenting the material in such a way as to make certain sections of the book an excellent introduction for research students. The first four chapters deal with the spectroscopy of molecules (about 110 pp.); there follow chapters on atomic spectra (30 pp.), hyperfine structures (60 pp.), Stark and Zeeman effects (50 pp.), shapes and widths of spectral lines (40 pp.), with a separate chapter on the ammonia spectrum and related problems. Four further chapters (110 pp.) treat experimental methods and instruments and a final chapter deals with applications to chemical analysis. Most of the individual chapters can be read independently, a feature which greatly enhances the value of the book.

The authors have not intended to incorporate the microspectroscopy of solids into the book but have restricted themselves to gases. Even so they have to touch on a great variety of subjects, all of which have received useful information from microspectroscopy.

The treatment of the theoretical sections is exact, but, nevertheless, requires only knowledge of elementary quantum mechanics and of fairly simple mathematical tools. The usefulness of the book is greatly enhanced by a thorough bibliography and by a series of appendices (50 pp.) consisting of very extensive tables of quantities required in the discussion of microwave spectra. H. FRÖHLICH

Transistors and other crystal valves. By T. R. SCOTT. (London: Macdonald and Evans Ltd., 1955.) Pp. xvi + 258. Price 45*s.*

This book has been written for engineers who may have to use crystal valves, rather than for those engaged in developing and designing them. Up to the present, any engineer coming into the field for the first time has had to obtain the background by reading a large number of articles in many different journals, and there has been little to guide him as to which are the important ones. Mr. Scott's book removes this difficulty and any newcomer will find the book invaluable.

Since the subject is now very large, no single book can deal adequately with all aspects, and Mr. Scott has realized this. He has, however, presented an integrated account of the subject and has avoided going into details by giving adequate references.

Chapter 1 gives the history of the development of the crystal diode and transistor. Chapter 2 discusses the various

types of crystal imperfections that determine the characteristics of valves. Chapter 3 discusses the theory of *p–n* junctions, and the design of junction diodes and transistors, while Chapter 4 deals with point contact devices. The important questions of operating temperature, output and life are discussed in Chapter 5, while some typical applications are described in Chapter 6. Chapter 7 discusses the newest developments in transistors for high frequency operation and includes the "field effect" and *p–n–i–p* types. Compound semiconductors are discussed and their possibilities compared with germanium and silicon in Chapter 8, while Mr. Scott peeps into the future in Chapter 9.

Two appendices are included; Appendix A deals with the energy band structure of semiconductors and Appendix B with the techniques used for testing diodes and triodes and also with the measurement of resistivity, Hall effect and minority carrier life-time in materials. A most valuable bibliography of 277 references is included. E. G. JAMES

High vacuum technique. 3rd Ed. (revised). By J. YARWOOD. (London: Chapman and Hall Ltd., 1955.) Pp. viii + 208. Price 25*s*.

It is well known that all branches of high vacuum technology have made great strides in the last ten to fifteen years. This has led to the development of a range of vacuum equipment which is finding increased applications in industries covering a diverse field. It is therefore of particular interest to have a variety of books covering the subject of high vacuum technique from the introductory to the specialist standard.

The book under review aims at introducing "the latest developments in apparatus, to describe important industrial processes hitherto discussed only in scientific periodicals, and to bring together in one volume the diverse facts regarding the relevant properties and uses of materials encountered in all types of vacuum work." The new edition is a considerable extension of the previous edition and includes new topics such as gas ballast pumps, data on manufacturers' apparatus, new materials, etc.

It is unfortunate that the account is spoilt for the specialist who will notice and often be annoyed by the large number of superficial and inexact statements and omissions, some of which must be particularly misleading to the beginner. It is impossible to discuss all these, but here is a typical example. On pages 9 and 11 concerning gas ballast pumps we read "the vapour does not condense at all" and "all condensible vapours are removed from the system." For these statements to make sense they would have to be qualified by giving some idea of the vapour pressure of the vapours in question; for example a simple quantitative formula would show the connexion of this with ballast flow and pump temperature. Also, for the successful operation of gas ballast pumps, mention could have been made to the use of catch pots for the vapours condensed in the pipe lines. There is no mention of the use of condensers and pumping combinations in connexion with gas ballast pumps.

Some of the vacuum practice described would not be recommended by the reviewer. For example, on p. 58, painting porous metals with shellac is advocated. The diagram on p. 39 shows a pumping table with a large bell jar connected to a small diffusion pump by long narrow lines. Among the collection of more than 100 well reproduced and clear illustrations there are many showing obsolete equipment, but there is no sectional drawing of any really modern equipment such as large diffusion pump or sputtering plant. Other omissions are: air-cooled diffusion pumps, Apiezon C oil, the backing pressure technique on leak testing, pressure switches, "reactive" sputtering. The section on properties of materials is equally scrappy. We read that brass withstands temperatures up to 450° C without any warning about the evaporation of zinc when heated in vacuum. Again, there is no mention of some substances which have more recently found vacuum applications such as certain plastics: Nylon, polytetrafluoroethylene, Polythene, polyvinyl chloride. Vacuum technique is constantly developing and there is a definite need for a book for those who are new to the subject. Although this book is not up to date in every respect many will find in it a useful introduction.

W. STECKELMACHER

Elektronik des Einzelelektrons. By F. OLLENDORFF. (Vienna: Springer-Verlag, 1955.) Pp. xii + 643. Price 165*s*.

The author is well known for his excellent earlier books in which he applied the methods of rigorous mathematical analysis to a great variety of problems in electrical technology. In the present book a similar technique is used to describe, often in great detail or by a novel approach, the motion of electrons in electric and magnetic fields. The main topics covered are electron focusing and deflexion in cathode-ray tubes, the electron (and ion) paths in multipliers, magnetrons and mass spectrometers, electron lenses and their aberrations, a theory of the aurora, and accelerators for electrons at relativistic speeds, including a discussion of their stability conditions. The treatment is based on Hamilton's principle and perturbation methods, conformal transformations being widely used to obtain the field distributions, and a good mathematical background is required of the reader. Unfortunately, the notation deviates often from that used by other authors, and even a simple graph may require the careful study of many pages of mathematics to understand its meaning. In spite of its length and erudition, one feels that this book is not too well balanced. Emphasis is placed on those problems which lend themselves to a full investigation by analytical means, while many problems of current scientific interest or of practical importance receive little or no attention. For instance, 245 pages are devoted to electron lenses in general, but electron microscopy receives a single line. The motion of electrons in high-frequency fields is not mentioned except in connexion with accelerators. While Pierce guns are briefly treated, the problems associated with the formation of electron beams, or space charge effects, are not discussed. Perhaps the author has left these topics, and others like noise and electron emission phenomena, over for the next volume on "collective processes," although this has not been made clear. The book is excellently produced and will find readers among university teachers and specialists. G. LIEBMANN

Proceedings of the fourth meeting of the mixed commission on the ionosphere (Union Radio-Scientifique Internationale, 42 Rue des Minimes, Bruxelles, 1954). Pp. 238. Price 43*s*. (300 Belgian Fr. or $6).

This volume contains the papers presented in Brussels in August 1954 and the discussion on them. There were six sessions as follows: The International Geophysical Year; The E layer and associated problems in low-pressure physics; Geomagnetic distortion in region F2, its nature and origin; Ionospheric storms; Ionospheric movements; Sporadic E ionization.

The resolutions of the commission regarding future international work, particularly during The International Geophysical Year, are also included.

Notes and comments

Elections to The Institute of Physics

The following elections have been made by the Board of The Institute of Physics:

Fellows: R. T. W. Bingham, C. G. Cannon, A. H. Cockett, J. H. Davis, P. Hatfield, O. S. Heavens, G. M. Lewis, D. G. Marshall, G. B. Townsend.

Associates: E. W. V. Acton, T. S. Ainsworth, R. G. C. Arridge, A. J. F. Banks, R. W. Bicknell, H. Bridge, G. Brook, W. R. Caff, P. E. Ciddor, A. C. Copisarow, L. J. Davies, R. D. P. Davies, G. T. Davis, N. Dickinson, A. Dudley, T. P. Flanagan, K. G. W. J. Forshaw, W. Gemmell, J. A. F. Gidley, K. Greenwood, J. E. Hardy, E. M. Healey, C. Holden, A. D. Holt, G. D. Hubbard, D. Madoc-Jones, J. H. Mallard, B. E. Moody, K. W. Ogilvie, J. M. Owen, A. T. Partridge, L. G. Penhale, S. Raghavachari, H. M. Rosenberg, D. J. Shapland, E. I. Sherrard, G. W. R. Smith, H. J. Stokes, P. M. Stott, R. Stratton, A. W. S. Tarrant, N. B. Terry, E. B. Whittaker, O. Wilson, H. C. Wright.

Forty-three Graduates, forty-seven Students and six Subscribers were also elected.

Soviet Physics

The American Institute of Physics announces the publication of a new bi-monthly journal entitled *Soviet Physics*. This publication will report, in English, current Soviet research in physics as contained in the *Journal of Experimental and Theoretical Physics of the Academy of Sciences of the U.S.S.R.*

One volume is published annually. Volume 1 (1955) will contain three issues and subsequent volumes, beginning in January 1956 will contain six issues. The subscription rates are: Vol. 1 (1955), $16.00; Vol. 2 (1956), $32.00. (In U.S.A. and Canada these subscriptions are $15.00 and $30.00.)

Subscriptions should be addressed to the American Institute of Physics, 57 East 55th Street, New York 22, New York.

Documentation of molecular spectroscopy (D.M.S. system)

The question of documenting and publishing the work of spectroscopists has been much discussed during recent years. A number of systems, all of them using punched cards in one form or another and all of them documenting spectra in the infra-red range, have been published. The publication of a new system of documenting infra-red and Raman spectra is announced jointly by Butterworths Scientific Publications, 88 Kingsway, London, and Verlag Chemie, Weinheim/Bergstrasse, Germany. This new system (D.M.S.) claims several advantages over those hitherto published. It combines a survey of current literature with an expanding collection of spectra of purified substances in classified form. It does not require a sorting machine but yet may be used with one and incorporates a large amount of data on single cards. There are two identical editions, one in English and the other in German.

The D.M.S. system provides two kinds of cards. Literature cards provide information in abstract form from papers relevant to molecular spectroscopy, and spectra cards for every substance of which a spectrum of satisfactory quality is available. The spectrum will be reproduced with a linear wave-number scale and the card will also carry the structural formula, physical constants and other data. An important feature of the cards is the coded classification based on the structural units of the molecule which makes unnecessary any separate index.

It is expected to start the D.M.S. Service in 1956 with an initial batch of about 500 cards, and to issue about 2000 cards in the first year of operation. It is also expected that this figure of about 2000 cards annually will be maintained, the proportions being roughly 20% literature cards and 80% spectra cards. The substances to be examined have been carefully selected so as to cover a very wide range which will satisfy the requirements of both academic and industrial users in different applied fields.

Register of British manufacturers

The twenty-eighth edition (1956) of the FBI register of British manufacturers classifies the products and services of over 7000 firms who are members of the Federation of British Industries. The headings used are: products and services, addresses, trade associations, trade names and trade marks. In addition there are language glossaries in French, German and Spanish.

The register is published by Kelly's Directories Ltd., and Iliffe and Sons Ltd., Dorset House, Stamford Street, London, S.E.1. The price is 42*s*.

Journal of Scientific Instruments

Contents of the February issue

ORIGINAL CONTRIBUTIONS

Papers

The temperature calibration of a high temperature X-ray diffraction camera. By J. A. Brand and H. J. Goldschmidt.

A calorimeter for measuring energy absorption from pile radiation. By A. R. Anderson and R. J. Waite.

The principles and apparatus of the injection system of the Birmingham proton synchrotron. By C. A. Ramm.

An isothermal micro-calorimeter. By J. B. Stott.

A cell for kinetic measurements of gas evolution from systems irradiated by fast electron beams. By C. B. Amphlett and T. F. Williams.

Small angle X-ray diffraction unit. By C. R. Worthington.

A wide range, recording, logarithmic photometer circuit. By P. Hariharan and M. S. Bhalla.

A fast multiple coincidence circuit. By B. Collinge, A. W. Merrison and D. Eccleshall.

The effect of humidity on the stability of inductance standards. By G. H. Rayner and L. H. Ford.

Fundamental behaviour of sensitive springs. By R. Tomaschek.

Laboratory and workshop notes

A simple universal X-ray camera stand. By M. D. Karkhanavala.

A sensitive manostat. By H. Tompa.

A simple air lock for ionization gauges. By C. Barrow.

A portable β-γ radiation monitor. By B. W. Emmerson and S. P. Newbery.

A simple interval timer. By M. T. Lilburne and D. Shipley.

A four-point probe apparatus for measuring resistivity. By D. B. Gasson.

NOTES AND NEWS

Correspondence

Errors in the A.S.T.M. Index of X-ray powder diffraction patterns. From J. W. Hughes, Isabel E. Lewis and A. J. C. Wilson.

New instruments, materials and tools

Notes and comments

THIS JOURNAL is produced monthly by The Institute of Physics, in London. It deals with all branches of applied physics (including theory and technique).

All rights reserved. Responsibility for the statements contained herein attaches only to the writers.

EDITORIAL MATTER. Communications concerning editorial matter should be addressed to the Editor, The Institute of Physics, 47 Belgrave Square, London, S.W.1. (*Telephone:* Sloane 9806.) Prospective authors are invited to prepare their scripts in accordance with the *Notes on the preparation of contributions.* (Price 2*s*. 6*d*. including postage.)

REPRODUCTION. The Institute of Physics is a signatory to The Royal Society's Fair Copying Declaration. Details may be obtained upon application from The Royal Society, London, W.1.

ADVERTISEMENTS. Communications concerning advertisements should be addressed to the agents, Messrs. Walter Judd Ltd., 47 Gresham Street, London, E.C.2. (*Telephone:* Monarch 7644.)

CLAIMS FOR MISSING JOURNALS. Claims from regular subscribers to this *Journal* for missing numbers will only be considered if received within 60 days of the date of mailing plus normal outward time of transit and time for lodging the claim. Losses attributable to failure to notify a change of address or to similar omissions will not be considered.

SUBSCRIPTION RATES. A new volume commences each January. The charge is £4 per volume ($11.50 U.S.A.), including index (post paid), payable in advance. Single parts, so far as available, may be purchased at 8*s*. each ($1.15 U.S.A.), post paid, cash with order. Orders should be sent to The Institute of Physics, 47 Belgrave Square, London, S.W.1, or to any bookseller.

SPECIAL ARTICLE

Rain — natural and artificial*

By R. C. Sutcliffe, O.B.E., Ph.D., Meteorological Office, London, W.C.2

Mean precipitation of water over the earth's surface is about 90 cm per year. This is balanced by evaporation using about 20% of the total solar energy incident upon the earth and its atmosphere. The world patterns of precipitation and evaporation do not coincide; balance is maintained by transport in wind systems. The mechanisms for condensing the vapour require vertical motion and adiabatic cooling by expansion: by orographic ascent, vertical (static) instability and large-scale cyclonic (dynamical) instability. Supersaturation does not occur owing to the presence of minute nuclei in vast numbers. Cloud droplets have diameters of about 10 μ and number about 200/cm^3. Raindrops have diameters of about 1 mm, equivalent to about 10^6 cloud droplets. The process of combination may be by coalescence of droplets (warm rain) or by distillation from water droplets on to ice crystals at sub-freezing temperatures. The introduction of nuclei or ice crystals (silver iodide, common salt, solid carbon dioxide, etc.) into cloud may produce a little precipitation in special circumstances but no method of economic value is yet established. Interference with radiation, evaporation or the large-scale dynamics is conceivable but at present purely speculative.

Man is a fresh-water animal and his dependence on this element is complete. Nature, employing the heat energy from the sun, distils the elixir from the salty oceans, pours it lavishly over favoured parts of the dry land and there man makes his settlements. The challenge to understand, predict, utilize and control such miracles of nature gave rise to the science of physics but in this twentieth century the physicists in our universities have, whether or not they realize or wish it, become providers to the engineering industries to such an extent that it is possible to graduate with honours in physics and know less about the weather than did Aristotle.

If there are two reasons each sufficient to justify the pursuit of learning, that it be either interesting or useful, then, to whichever side one leans, there is in meteorology the reward one looks for, and in this short article, with no attempt to deal with any aspect thoroughly, the theme of rainfall is used to illustrate the diversity of problems which are set in this branch of science. We shall try briefly to trace events from evaporation to precipitation, there leaving the story to be completed by the oceanographers and hydrologists.

Rough estimates based on rainfall records put the annual mean amount over the earth's surface at some 90 cm. The reservoir of moisture, the vapour in the air, remains pretty constant from year to year at about the equivalent of 2·5 cm of water. We have then a rapid turnover with a very near balance year in, year out between evaporation and precipitation and an account should be rendered. It is not easy. Over the open oceans which cover so much of the earth we have very little direct information on rainfall and no direct measure of evaporation—so far the instrumentation has defeated us. The patching together of evidence is a matter of expert judgment and, surprising though it may seem, estimates of evaporation are perhaps more reliable on the whole than those of rainfall.

Two methods, both resting in part on theory, are available. By the aerodynamic method the mean vertical flux of vapour near the earth's surface is derived from turbulence theory and observed winds and humidities. By the energy balance method the heat used in evaporation is estimated. Making the best use of all the data and calculations and adjusting to a world balance, Jacobs[1] has prepared hemisphere maps: they are accurate within 10 or 20% perhaps and to get greater refinement will not be easy.

Referring again to energy, the average value of incoming solar radiation outside the earth's atmosphere is 0·5 cal cm^{-2} min^{-1} averaged over the earth's surface as a whole and this is about the most accurate quantity we know in the whole problem—within perhaps 2%. After that we must accept rough figures and say that 20% is absorbed in the atmosphere, about 40% reflected as earthlight (cf. moonlight) and about 40% absorbed at the surface, 20% being returned as sensible heat by conduction and infra-red radiation and 20% being used in evaporation. The evaporation of a layer of about 90 cm of water per year requires energy at the rate of 0·1 cal cm^{-2} min^{-1}, showing that the figures roughly fit but much more direct observing of radiation reaching the surface is needed to get precision into a world map.

The moisture obtained from the surface is ultimately released from cloud systems in the free atmosphere and must be carried there by vertical currents. The mechanism of turbulent vertical diffusion in the near-surface layer is tolerably well understood but for higher levels there is no adequate theory. There is a complex of vertical motions on all scales from small-scale turbulence to world-scale overturning and the relative importance of each in determining the three-dimensional vapour field at any time remains to be worked out—a difficult but approachable problem.

Secondly, inspection of the world charts of evaporation and precipitation reveals the need for large-scale horizontal transports; the latitude of maximum evaporation in the tropics is actually a minimum in precipitation. The mechanism of this transport has received some rather limited attention; it is partly by world-scale or continental-scale mean currents of the general circulation and partly by large-scale "turbulence"—on the scale of cyclones and anticyclones—with the emphasis varying with the geographical region. In the tropics relatively steady seasonal transports, in other latitudes irregular turbulent transport, are predominant. Much remains to be done to settle this matter and studies of the transport and horizontal divergence or convergence of water vapour over geographical regions are now just practicable in some areas where upper air data are available.

We pass now to the dynamical systems which lead to the production of rain-producing clouds and enter a different field of inquiry. While slow diffusion and transports are

* Based on a lecture delivered to the South Wales Branch of The Institute of Physics in Cardiff on 14 October, 1955.

effective in modifying the humidity field and radiation is effective in modifying temperature so that the conditions favouring saturation are built up gradually, it is recognized that the final stage leading to thick rain-producing clouds is of a different order; it requires relatively rapid ascent of the moist air through a height of some thousands of feet with the associated rapid cooling by adiabatic expansion. Vertical motions of this nature are provided mainly in three ways, distinct in principle and sometimes occurring separately but often, perhaps most often, in combination. These are: forced ascent over high ground (orographic ascent), quasi-vertical convective systems (static instability), and large-scale cyclonic systems (dynamical instability). A few remarks follow on each of these.

Forced ascent over higher ground in the path of the wind is a process which is intuitively acceptable, which certainly takes place and which largely accounts for the comparative raininess over mountains and the comparative dryness of districts to the lee. Only limited progress has, however, been made with the quantitative hydrodynamical problem of orographical air-flow and this only by perturbation solutions of the equations for streamline flow. Turbulent motion, which is usual, has not been treated analytically. A series of papers by Scorer[2] and a review by Corby[3] are valuable. Vertical stability and variation of wind with height are important factors. There is, of course, an extensive climatological literature on the observed rainfall over hilly or mountainous country, but it would be completely erroneous to deduce that the great excesses of rainfall over high ground normally represent pure orographic rainfall. The extra lift given to rain-bearing clouds produced by other processes and outbreaks of vertical instability triggered by the ascent are important but perhaps more significant still is the washing out of orographic cloud droplets (too small to fall by gravity themselves) by rain falling from higher levels. Rainfall over high ground in the British Isles is characterized by greater intensity rather than by longer duration when compared with that over lower ground in the vicinity.

Rain-forming systems of vertical convective instability—cumulonimbus systems—have been described and in a general way explained in text-books this half century. Air rising vertically cools by adiabatic expansion some $5\frac{1}{2}^{\circ}$ F per 1000 feet. Almost invariably, except near the earth's surface, the actual lapse rate is less than this so that air displaced upwards becomes colder than the environment, has negative buoyancy and sinks back: in brief there is vertical stability. If, however, the air rises sufficiently to become saturated and cloud condenses, the latent heat liberated may be sufficient to provide positive buoyancy and continued ascent even to the base of the stratosphere may occur in suitable air masses—with showers, perhaps thunderstorms. We cannot repeat here what is extensive text-book matter but we may justify a few comments. There is nothing more effective in rendering an air mass unstable in the vertical than general ascent, nothing more effective in promoting stability than subsidence above. Hence showery weather is associated with cyclonic conditions, absence of showers with anticyclones—the different scales of dynamical processes so interact. There remain many serious gaps in our knowledge. The dynamical treatment of convective cloud systems through their individually short lives of the order of an hour is in its very early stages; the statistical properties of size, number, life and frequency of vertical convection systems in an unstable air mass set a problem which remains almost untouched.

The remaining important rain-forming system is the familiar depression or cyclone, a quasi-horizontal dynamical system with slow ascent over large areas hundreds of miles in dimensions, with ascending velocities in the order of a few centimetres per second maintained for periods of the order of a day. It is now established that these are essentially the outcome of a form of dynamical instability in air currents with marked horizontal temperature gradients (baroclinic) on the large scale where the winds are largely controlled by the earth's rotation (quasi-geostrophic). Strictly, instability is a term appropriate only to a state of balance and the study of instability yields only the criteria for and the initial form of breakdown; the mature growth of the systems once initiated is a problem of hydrodynamical development and is extremely difficult owing to the complication and non-linearity of the differential equations. In very recent years this problem has been effectively opened up by combining mathematical-physical insight with numerical methods of integration using electronic calculators to the extent that calculation promises to displace experienced judgment in the forecasting of cyclone and anticyclone development. This truly exciting advance has received much attention in recent literature and it will be sufficient here to refer to an article by Sutton.[4] Again much remains to be done and especially so in connexion with rainfall. Theory and calculation so far yield very crude generalized patterns of rainfall and much refinement must be provided before they can displace extrapolation and judgment in the routine prediction of this element.

Reverting a moment to the world picture we must, knowing the dynamical mechanisms which produce rain, explain why these occur with so marked a geographical pattern providing rainy and dry zones. In the past it has been usual for text-book writers to avoid or to beg this fundamental question, to assume that the broad climatic pattern, the general circulation, is something existing as a background in its own right. Granted the sub-tropical high-pressure belt with trade winds converging towards the equator, it is not difficult to "explain" the convective rains. Nor, granted the westerlies poleward of the sub-tropics and the strong baroclinity of middle latitudes, is it difficult to "deduce" cyclonic rains. But the difficulty here is that the liberation of latent heat in the rain-forming systems is a major item in the thermodynamics of the world pattern itself; it is invalid to treat the rain-forming systems as perturbations or embroidery on a general circulation, the feed-back is so great that the ultimate solution to the world structure is largely the statistical effect of the embroidery in the same sense as the variation of wind with height near the earth's surface is as much the result as the cause of turbulence. As is usual in physical problems, step by step arguments which talk their way through complex differential relationships are treacherous and unconvincing and the time is now ripe for a big advance by formal mathematical-physical methods. It may soon be possible to put the statistical effects of vertical convection and baroclinic systems, together with radiation and other factors, into the shape of differential equations representing a first model of the world circulation and then to make a frontal attack on their numerical solution. This attack, should it prove successful, will open up still another field through the physical explanation of climate to that of climatic anomalies and so to the scientific formulation of the problem of long-range forecasting: whether this in turn will afford practically useful solutions is, however, another matter upon which it is hardly profitable to speculate until we know just what sort of problem it is.

Pursuing further the broad theme, we note that so far it has been tacitly assumed that when rising air becomes saturated

and further ascent leads to the condensation of excess moisture, this moisture will fall out as rain, or perhaps snow. Roughly speaking, the assumption is not grossly misleading for climatic or dynamical studies of rain-producing systems, but as a scientific principle nothing could be more naïve. When air temperature passes below the dew point value supersaturation is the direct result and in highly purified air this state can exist even to 400% supersaturation. This particular difficulty is, however, of no moment in meteorology for the atmosphere always contains impurities in the form of vast numbers of minute solid and liquid particles, more or less hygroscopic, and many of these will accumulate individual excess molecules, according to the vapour pressure at their surfaces; it is not necessary to await the chance process of multi-molecular combinations. The most important particles for the condensation process are believed to be of sea salt and of sulphur compounds, the latter derived from combustion processes, natural or man-made; their numbers and sizes vary very widely indeed, ranging from a few per cubic centimetre of diameter greater than 1 μ to perhaps 10^5 per cubic centimetre of diameter 0·1 μ or less, much depending on the source of the air mass. As at a certain stage the vapour pressure over the droplet decreases somewhat as the curvature decreases, the cloud formation is usually rather sudden and optically apparent. The number of cloud particles averages, say, 200 per cubic centimetre with a mean diameter of order 10 μ.

This natural provision for condensation eliminates one possible difficulty from the mechanism, but leads immediately to another and a more serious one. The cloud particles are so numerous that they could accommodate all the excess moisture obtained by prolonged cooling without growing to a size at which they would fall at any significant speed by gravity. Thus one could imagine circumstances in which cloud particles were suspended indefinitely in the atmosphere, as an aerosol, to be evaporated in due course when the air was again warmed at some stage in its life of continuous circulation. Were this behaviour characteristic of the atmosphere precipitation would nowhere exceed the intensity of a very light drizzle, the atmosphere would become nearly saturated everywhere and the evaporation from the surface would almost cease. This hypothetical state of affairs may be scientific fantasy, but by putting it forward we emphasize that the climatic character of the world is dependent on mechanisms which allow small drops somehow to combine, at the rate of a million to one, to form ordinary raindrops.

In meteorological literature earlier than that of the present generation this mechanism, although not understood, was tacitly assumed to present no major issue. Evidently rain did fall and presumably the water droplets must have a natural tendency to collide and combine in sufficient numbers to provide large drops; exactly how was not known. But when the problem of aerosols of water droplets was carefully analysed the difficulties of combination by collision appeared so formidable that Bergeron[5] was led to the conclusion that significant rainfall required the occurrence of the ice phase. Clouds must first reach levels where the temperature is below freezing point, they would then remain supercooled until at a few degrees lower some would freeze and the vapour would distil from the liquid to the solid phase, by virtue of the vapour pressure difference, allowing the ice crystals to grow, the water droplets to evaporate, and the rate of the process would be sufficient to produce large falling ice particles in a short time measured in minutes. It was of course realized that the early stages were the difficult ones; given particles of around 0·1 mm diameter their further growth by coalescence in relative vertical motion would be explicable, but it was somewhat startling to be confronted with the theory that without sub-freezing temperatures significant rainfall would be impossible.

The theory had its vogue and convincing evidence of what is now called "warm rain," that is rain from clouds whose tops were never at freezing temperatures, was slow to accumulate. Today, however, we have moved away from this extreme position; most authorities would agree that the ice phase is probably the trigger agent in many rain-forming clouds, but that the direct coalescence of water particles is sufficient given clouds of some thousands of feet in vertical extent, that this is the sole mechanism in much tropical rainfall and perhaps the main mechanism in many systems even where freezing at the higher levels is also present.

The most spectacular outcome of a great deal of research into the problems of the micro-physics of clouds is perhaps to demonstrate that the rain-forming mechanism has critical features which might permit of a degree of artificial control. Many clouds exist with sub-freezing temperatures without precipitating and without freezing: can the trigger action be introduced artificially before natural events supervene, so stimulating rainfall? Many deep water clouds not at freezing temperatures exist without precipitation: can the coalescence process be stimulated by introducing some larger particles? These questions, opening before the science of meteorology prospects of weather control, have attracted a great deal of both serious scientific attention and enterprising commercial activity, the latter certainly profitable to the contracting operator whatever the return to the customer.

I shall not here attempt to survey this wide subject in detail. It has been amply demonstrated that in some cases large cumulus clouds seeded from the air with pellets of solid carbon dioxide will react quickly, precipitation may fall and may reach the ground. Supercooled layer clouds also react in this way by leaving cleared lanes behind a seeding aircraft. Silver iodide crystals have had a similar result, by acting as freezing nuclei for supercooled water clouds. Larger water droplets sprinkled into clouds have been proved effective, common salt particles have been used with no certain effect.

There is absolutely no doubt about the practicability of precipitating clouds on the laboratory scale by various methods; there is no doubt about there being some effect on natural clouds seeded, at considerable cost, by aircraft. There is as yet no convincing evidence of methods of economic usefulness. A much publicized and commercially much used method is the release of silver iodide smokes from ground burners; relying on natural diffusion and convection the particles can be carried upwards into clouds where their effect is presumed to stimulate additional rainfall. The theory is just plausible enough to justify experiments but evidence to date is much clouded by unverified commercial claims and the question of whether surface seeding increases, decreases or leaves unaffected the natural rainfall remains to be decided. The assessment of experiments is itself a formidable statistical problem for the variability of natural rainfall, in time and place, is so large that only a marked effect regularly in the same direction could show through the background "noise." The difficulty of weighing satisfactorily all the claims made in other countries has prompted the Meteorological Office to start a series of experiments in this country. It is too much to hope that they will be finally decisive, but they will afford new evidence and give direct knowledge of the considerations which arise. A recent report[6] contains several interesting papers and many references. A review article by Browne, Palmer and Wormell[7] is valuable.

To recapitulate, rainfall has been examined as a major factor in world climate and in the physics of the general circulation, balancing evaporation through the medium of geographical transport. In lower latitudes this transport is largely carried out by large-scale general circulation currents, trade winds and monsoons, in middle and higher latitudes by the temporary circulations of cyclones and anticyclones—large-scale turbulence. The dynamical systems directly producing rain-cloud, vertical convective showers and cyclonic synoptic systems are, in broad terms, tolerably well understood, both being of an instability nature and so subject to critical conditions, the one concerning vertical (static) instability, the other quasi-horizontal baroclinic (dynamical) instability. They show well-marked geographical preferences. Saturation, due, in the latter stages, to dynamical cooling in ascending motion, leads to condensation, without significant supersaturation, in the form of vast numbers of minute droplets or crystals forming on salt or acid nuclei and producing an aerosol. The precipitation mechanism requires some combination mechanism and both freezing and direct coalescence are effective agencies under suitable critical conditions.

If one broadly considers in this light the possibilities of artificial control the most promising is that already studied, but very inconclusively, in the field of the micro-physics. There are many possibilities, not economically established. It is sometimes argued that seeding techniques have an inherent limitation in that no amount of such interference could do more than redistribute rainfall since evaporation by solar energy provides an overall control. This, however, is a fallacy of over-statement. The proportion of solar energy used in evaporation depends on the cloudiness and the relative humidity and a mechanism which accelerates precipitation would feed back to accelerate evaporation in some degree at least. Without a precipitating mechanism evaporation would automatically cease.

Other possibilities lie in stimulating the large-scale dynamical instabilities but energy considerations seem to rule this out. Evaporation might be modified by controlling incoming radiation, perhaps through reflecting dust layers introduced explosively into the stratosphere: the method is probably within reach in principle, but the effect on the world-wide redistribution of precipitation is at present quite unpredictable. Artificial modification of the sea surface by monomolecular layers has also aroused speculation; at present it is no more than this.

The problem of prediction, of rainfall forecasting, has long been partially solved for periods of the order of a day ahead by synoptic analysis and extrapolation of trends coupled with physical understanding of the processes. Their instability character presents a formidable barrier to any major improvement in accuracy, but numerical methods based on the hydrodynamics of large-scale motions promise some advance. Long-range predictions of the departure of rainfall from its climatic average are at present without any physical basis and the urgent need is for a basic theory of the general circulation of the atmosphere; this might not be long delayed.

One may end on a political note. Meteorology has long been acclaimed as an international science *par excellence* and its record of amicable world collaboration is an enviable one. Mankind has been content to regard weather as an act of God and to adapt itself to Providence while believing it not impious to attempt prediction; and on this basis neighbourly collaboration has been cordial. Weather control raises new aspects, for the circulation of the world's atmosphere is such that no large-scale modification of climate, however desirable in one part of the world, could fail to be disadvantageous if not disastrous to some community elsewhere. While pursuing research the peace-loving meteorologist may secretly hope that success will not come so quickly as to raise the prospect of yet another kind of warfare, wet or dry as well as hot or cold.

REFERENCES

(1) Jacobs, W. C. *Arch. Met. Geo. Bioklimatologie*, *A*, **2**, pp. 1–16 (1950).

(2) Scorer, R. S. *Quart. J. Roy. Met. Soc.*, **81**, pp. 340–350 (1955).

(3) Corby, G. A. *Quart. J. Roy. Met. Soc.*, **80**, pp. 491–521 (1954).

(4) Sutton, O. G. *Quart. J. Roy. Met. Soc.*, **80**, pp. 328–338 (1954).

(5) Bergeron, T. *Proc. Verb. Assoc. Met. U.G.G.I., Lisbon*, p. 156 (1933).

(6) International Symposium on Experimental Meteorology, Zürich, 1954. *Arch. Met. Geo. Bioklimatologie*, *A*, **8**, H.3 (1955).

(7) Browne, I. C., Palmer, H. P., and Wormell, T. W. *Quart. J. Roy. Met. Soc.*, **80**, pp. 291–327 (1954).

Summarized proceedings of a conference on electron microscopy — Glasgow, July, 1955

The Annual Conference of the Electron Microscopy Group of The Institute of Physics was held in the Department of Chemistry, University of Glasgow from 5 to 7 July, 1955. The papers presented are summarized in this report.

ELECTRON OPTICS AND GENERAL INSTRUMENTATION

The conference opened with a paper by DR. V. E. COSSLETT (Cavendish Laboratory, Cambridge) on the relation between image contrast and the thickness of the specimen. The working rule that the resolution obtainable from the normal type of specimen is of order one-tenth its thickness was based on experimental evidence. It has now been shown to be simply explained in terms of the chromatic aberration arising from energy loss of the beam in the specimen. The variation of the ratio resolution thickness with atomic number and with voltage was discussed, and conclusions were drawn as to specimen preparation requirements for very high resolution.

MR. M. E. HAINE (Associated Electrical Industries Ltd., Aldermaston) gave some further observations on image contrast and resolving power. The electron microscope specimen is primarily a phase object, and amplitude contrast arises because of loss in the scattered wave outside the objective aperture, and the magnitude of this is assessed by integration of the theoretical scattering distribution for single atoms. The possibilities of phase contrast have been pointed out by Gabor. The theoretical maximum value of phase contrast for a single atom would be high if the aperture were unlimited, whereas most of the scattered wave is lost outside the aperture. The maximum value of phase contrast which it should be possible to obtain is computed by integrating the scattered wave amplitude within the aperture. The magnitude is such as to allow any single atom to be visible in an instrument with a resolving power better than about 5 Å.

MR. R. W. HORNE (Cavendish Laboratory, Cambridge) then discussed some problems encountered in the preparation of specimens for high resolution microscopy. Using the double condenser lens system in the Siemens Elmiskop, the object contamination rate has been found to be of the order of 1 Å per second with an illuminating area of 15 μ. To check true structure from 6–10 Å on separate plates required rapid focusing and exposure technique. Carbon supporting films for biological objects were the only substrates found stable enough to resolve very small structure in unshadowed preparations. By digesting *spirillum serpens* with enzymes and staining with phospho tungstic acid, it was possible to resolve regular structures in the cell walls with a spacing of 80–100 Å. Flagella and basal granules appeared to remain intact after digestion, but slime layers surrounding the flagella obscured much of the structure present. The urgent need for staining and selective digestion techniques was stressed, together with the need for reducing the total object thickness in sections. Shadowcasting was found to be of little value in improving contrast at instrumental magnifications of 40 000–80 000 and was found to obscure much of the original object structure.

MR. HAINE then discussed the theoretical and practical possibilities for the intensification of the electron microscope image. It was shown that, if a time varying image is to be intensified, as would be desirable to follow the focusing process, etc., the information available in the electron image is already severely limited by quantum fluctuations. If a slow response is acceptable, focusing would then be carried out in "slow motion," a just worthwhile intensified image should result. Practical possibilities were discussed, and it was suggested that a scanned photo-conductor type system shows some promise.

Mr. Haine went on to describe a specimen stage for use with "reflexion" (grazing incidence) electron microscopy. The stage developed at Aldermaston has all the required degrees of freedom, i.e. vertical, horizontal, and also rotation. The stage fits into the standard EM3 instrument.

The length of electron microscope filament lives was discussed by MR. R. N. BLOOMER (Associated Electrical Industries Ltd., Aldermaston). The effect on the life of the filament of both vacuum and temperature were described in the light of exhaustive experiments on the subject.

MISS M. K. B. DAY (British Aluminium Co. Ltd., Gerrards Cross, Bucks) described two auxiliaries for the E.M.3 type electron microscope. Firstly she described some position indicators for specimen traverse controls. A pointer screwed into the rocking lever at the top of each traverse control indicates the number of complete revolutions through which the control has been turned, while a dial on the coupling of the control rod itself indicates the fractions of a revolution. Each dial is divided into twelve divisions marked *A* to *L* for the left-hand control and *M* to *X* for the right, so there is no confusion between the position references corresponding to the two controls. Also a tool for removing the objective aperture which had been found useful. A tool has been designed whose jaws grip the tube which carries the specimen cap and aperture disk in such a way that overcomes the risk of removing the specimen cap alone.

MR. J. A. GARD (University of Aberdeen) described a use of the tilting specimen stage in electron diffraction work. His procedure was outlined for improving the accuracy with which the "third row" lattice spacing can be determined. A series of electron diffraction patterns are recorded at different angles of tilt, one pattern being used as the datum for location of Laue zone centres in the other patterns. Calibration of the instrument factors, and of the stage tilt by an optical method was described.

MR. D. E. BRADLEY (Associated Electrical Industries Research Laboratories, Aldermaston) described some further variations in his carbon replication techniques. Firstly he described how one could use firmly mounted and backed replicas for reflexion electron microscopy. This is of particular use when the electron beam is likely to damage the fine structure of the specimen to be examined. A method of

obtaining replicas from biological materials was described, and also a method for examining selected areas of the specimen which had been identified by light microscopy. Excellent examples of the application of these techniques were produced.

MESSRS. PAGE, WATTS and EMERTON (Paper Research Association, Kenley) discussed the value of the solid replica method as a means of integrating fibre microscopy by permitting the same fibre to be studied in (*a*) the light microscope (with its relatively large field of view) using the metal shadowed plastic matrix, (*b*) the reflexion electron microscope (with its large depth of focus and its oblique viewpoint), and (*c*) the transmission electron microscope (with its high resolution) using transmission replicas taken from the solid replica.

MR. A. W. AGAR (Associated Electrical Industries Ltd., Aldermaston) in association with MR. BRADLEY discussed the resolution obtainable from replicas. The resolution claimed for different replica materials and processes cannot at present be compared because of the different bases on which the resolutions have been judged. They proposed that the criterion should be the limit of detection of small near-spherical particles on a smooth plane surface. A suitable model would be a dispersion of protein molecules mounted on a glass microscope slide; a graded test could be obtained by selecting suitable molecules. Working on the basis that the minimum detectable thickness difference in a replica film is the main limiting factor in its resolution, they concluded that the limiting resolution for Formvar replicas would be about 50 Å under ideal conditions and that for a thin evaporated carbon replica, the minimum detectable thickness difference would be about 10 Å.

MESSRS. G. R. BOOKER, R. S. M. REVELL and A. W. AGAR (Associated Electrical Industries Ltd., Aldermaston) reported on difficulties in stripping replicas from surfaces with particular reference to the "pre-shadowed" replica process. They pointed out that if a surface is scrupulously clean (e.g. heated *in vacuo*), then it becomes impossible to strip a replica from the surface. They tried the expedient of "controlled contamination" with borax or a proprietary substance obtainable in U.S.A. called Victawet (by Victor Chemical Works, Chicago). They found that, unless extreme care was exercised, however, these substances introduced structure on their own account, and that the criteria of thickness, etc., to prevent this happening varied with the surface under investigation. Thus the techniques were not of great value, except in the case of a single surface under extensive investigation.

MR. E. SMITH and DR. J. NUTTING (Metallurgy Laboratory, Cambridge) described some recent developments in the carbon replica technique. Two methods for the examination of metals using a directly evaporated carbon film have been developed. One is a replica process and the other an extraction replica method by which particles of a second phase can be extracted and examined in the positions they occupied in the metal, and identified by electron diffraction. In both methods the specimen is polished and etched for examination in the usual manner, a plastic cleaning replica taken, and a carbon film evaporated on to the surface to be examined. The film on the metal is then scored into small squares. To make a replica the film is removed by electropolishing in a suitable solution, washed in 50% nitric acid and then in water, and transferred to specimen grids for examination. For the extraction replica method the film is loosened from the surface in a suitable etchant and finally removed in water, washed and transferred to grids. By these methods, particles of vanadium carbide less than 100 Å in diameter have been identified in steels. The results are reproducible and the resolution is by far the best yet obtained with any replica method.

DR. K. C. A. SMITH (Engineering Laboratory, Cambridge) described some applications of the scanning electron microscope. Micrographs of a fairly wide range of specimens were shown and the possible advantages of this method of examination for certain specimens were demonstrated. A resolution of about 250 Å is obtainable and has been realized in micrographs of latex particles both in transmission and reflexion. The chief advantages of the method are the relatively small degree of foreshortening and the large angle of illumination. Shapes are rendered faithfully and detail is discernible in parts of the micrographs which would be in shadow in the normal reflexion technique. This is demonstrated in micrographs of etched germanium and particularly in the micrograph of an iconoscope mesh control screen. The method is suitable for surfaces of a rough or loose nature and the waxy surface of a meal worm grub was shown to illustrate this point. Another field of application is in the examination of biological material or fibres which are easily damaged by heating or ionization. The average specimen loading is only about $\frac{1}{4}$ W/cm^2 and micrographs of an amoeba and various fibres have been obtained without any perceptible structural change. The long working distance and large depth of field enable certain dynamic experiments to be carried out while under direct observations, and as a final example, micrographs of the forming and burn-out processes of a germanium-tungsten point contact rectifier were shown.

DR. W. C. NIXON (Cavendish Laboratory, Cambridge) then discussed high resolution X-ray projection microscopy. A resolution of 0·1 μ (1000 Å) has been reached with a shadow projection X-ray microscope by using a gold leaf X-ray target 0·1 μ thick supporting atmospheric pressure. Electron penetration and scattering in the thicker foil targets was the previous limit on resolving power and not astigmatism of the electron lens. A 0·1 μ thick heavy metal layer on beryllium as an X-ray microscope target will not give high resolution due to electron penetration and production of X-rays in the beryllium, unless the voltage of the beam is well below 10 kV. Electron induced contamination occurs on 1500 mesh/inch grids due to electrons penetrating this gold leaf target. X-ray micrograph of bull spermatozoa, shadowed latex particles and test grids have shown this resolution. Fresnel edge diffraction fringes 0·1 μ wide can be seen and the *minimum first fringe width* is suggested as a resolving power test for X-ray microscopes.

DR. L. JACOB (George Holt Physics Laboratory, University of Liverpool) described some problems arising in focusing electron beams in the energy range 30–70 V. It was pointed out that space-charge effects, potential depression and non-homocentricity of the beam require the lenses to handle beam diameters in excess of aberration limits. The examination of the distributions recorded for the focused paraxial regions showed unexpected behaviour in that the Gaussian form of the incident beam is no longer reproduced in the focused beam. This is particularly marked with magnetic lenses. With near symmetrical lenses of the electrostatic type, maximum and minimum values of effective beam width were obtained for the 30 V beams; these do not occur for beams of higher energy and may represent a manifestation of the standing wave pattern which, it is believed, exists across the emitter at the lowest energy. The peak current densities on the axis for both types of focusing at other energies are apparently the same. However, the power of the magnetic lens has to be increased by a factor of about

thirty over any expected thin-lens performance to achieve this. Comparison of magnetic lenses with aperture ratios 2/1 showed that for 60 V beams the smaller lens was the more efficient; an unexpected result which was interpreted in terms of the abnormal conditions for focus.

CHEMICAL APPLICATIONS

DR. D. H. WATSON (Chemistry Department, University of Glasgow) described some work on the growth characteristics of substituted paraffins. The work was designed to investigate the effect of side chains and large end groups on the crystal growth of long chain compounds. It was thus hoped to obtain information on the growth mechanism when dislocations are formed only with difficulty because of structural factors. The effect of side chains was investigated with 4-methyltritriacontane. The crystals are very irregular, show very few growth spirals and apparently grow by addition of monomolecular layers. The surface is folded and it is presumed that this is related to the bad lattice packing of the molecules which also accounts for the absence of dislocations. The folds restrict migration of molecules across the crystal surface and this explains the irregular crystallization. The effect of large end groups was studied using the long chain iodides containing thirty-one and forty-one carbon atoms. The first compound gives a very irregular crystallization with no dislocations since its crystal structure involves a very close concentration of end groups which prevents slip to give dislocations. The second compound has a less concentrated arrangement of the large end groups and gives fairly regular crystals showing monomolecular growth spirals and dislocations at the edge which are frequently multimolecular. The large end groups result in a slightly folded surface. The orientation of the folds can be related to the lattice geometry. Surface migration is again restricted and results in preferential growth in one direction. Growth frequently occurs on the multimolecular steps at the crystal edge without dissociation and this is also related to the restrictions imposed on surface migration by the folds.

DR. M. GORDON and DR. J. W. SHARPE (Royal Technical College, Glasgow) then reported on some electron microscope studies on synthetic rubber lattices. A new reaction-locus in chemical reactions of polymer dispersions was detected kinetically during a study of the hydrochlorination of rubber lattices. This locus consists of the region near the particle surface, which reacts rapidly with hydrogen chloride by a mechanism different from that operating in the bulk of the particles. In full confirmation of the theory, electron microscopic measurements of the particle sizes of various lattices, and hence of the specific surface, has been quantitatively correlated with the extent of the fast reaction. The technical importance of the existence of a surface locus, particularly in the pre-vulcanization of latex was stressed.

MR. P. H. HARRIS, in collaboration with MRS. I. M. HONEY (British Insulated Callender's Cables Ltd., London) described a replica technique for the examination of rubber surfaces. Replicas of rubber surfaces have been prepared by a two-stage replica technique using gum arabic for the first replica and a vacuum-deposited film of silica or carbon for the final replica. The first replica is prepared by drying a deep drop of gum arabic solution (gum arabic 5 g, glycerol 0·8 cm^3, water 10 cm^3) on the surface overnight in a desiccator. The resulting gum flake is removed from the rubber and a vacuum-deposited film of silica or carbon laid down on the working surface. The gum replica may be shadowcast prior to this operation. The gum is then removed by floating the flake on water, gum side down, to leave the final replica floating on the surface ready for mounting on specimen grids.

This technique has been used to study the structure of certain crepe rubbers and replicas of surfaces produced by tearing were compared with thin sections of such materials.

MR. J. CARTWRIGHT (Safety in Mines Research Establishment, Sheffield) described the results of studies, by microscopy, of airborne dusts in contrasting environments. The samples were collected with a thermal precipitator on membrane-coated coverglasses, counted optically, and then the membranes with the dust deposit were stripped and mounted for electron microscopy. The optical and electron microscope counts agreed in an overlap range between 0·5 and 2·0 μ and the mass concentrations calculated from the counts were of the same order of magnitude as smoke filter estimates from similar locations. Attempts to determine the composition of dust particles by electron diffraction were unsuccessful but promising results were obtained by other methods. The combustion temperature of different components of atmospheric pollution was determined by collecting samples on heat-stable membranes of alumina and examining identical fields before and after heating to temperatures up to 600° C. The amount of material soluble in hydrofluoric acid was estimated by examining fields before and after exposure to HF vapour.

METALLURGICAL APPLICATIONS

MR. P. H. HARRIS (British Insulated Callender's Cables Ltd., London) described a replica technique for the examination of wire surfaces. The wire is clamped between two small plates of 1/16 in. thick Perspex and heated by a suitable electric current until an impression of the wire is produced in the plastic. The wire is allowed to cool, the plates removed and a film of silica or carbon deposited on the working surfaces. This film is then backed by applying a deep drop of gum arabic solution (gum arabic 5 g, glycerol 0·8 cm^3, water 10 cm^3) and drying overnight in a desiccator. The Perspex is then removed by immersing in chloroform until complete penetration of the solvent is obtained, mounting the now swollen plate on gauze, gum side down, and washing with freshly distilled chloroform. The resulting gum flake bearing the vacuum deposited film is dried and floated on water, gum side down, when the gum rapidly goes into solution leaving the final replica floating on the surface ready for mounting on specimen grids. This technique may also be used for examining the identifying by electron diffraction contamination on wire surfaces, since any material removed from the surface by the Perspex plate is transferred to the final replica.

MISS M. K. B. DAY and MISS R. SMITH (British Aluminium Co. Ltd., Gerrards Cross, Bucks) described the effect of composition on the mode of precipitation in aluminium–copper–magnesium–zinc alloys. An anodic replica technique has been applied to the study of the structure of aluminium–copper-magnesium–zinc base alloys in the form of 0·036 in. thick sheet. Edge sections of the materials were mounted in small blocks of super-purity aluminium so that they could be electropolished and anodized without the edges of the sheets bevelling badly. Interesting differences were first detected in the amount and distribution of the magnesium–zinc bearing precipitate in aluminium–copper–magnesium–zinc base alloys containing chromium and manganese. This led to an investigation of the basic

aluminium–magnesium–zinc alloy and its quaternary variants containing chromium, copper or manganese. Their observations suggest that the larger quantity of precipitate present in the chromium bearing quinary alloy, and the susceptibility of this alloy to rate of cooling during quenching, is not due to the fact that chromium itself causes increased precipitation, but rather that manganese suppresses the heavy precipitation associated with the aluminium–copper-magnesium–zinc alloy to a far greater extent than chromium does.

Some studies on wear were described by Dr. D. Scott and Mr. H. M. Warren (Department of Scientific and Industrial Research, Glasgow). The effect on surfaces exposed to various degrees of abrasion were shown and discussed.

The tempering of alloy steels was discussed by Mr. R. G. Baker and Dr. J. Nutting (Metallurgy Laboratory, Cambridge). In studying the microstructure of secondary hardening alloy steels in the tempered condition, it is necessary to be able to resolve carbide particles of less than about 300 Å in diameter. A critical review was given of various types of replica, which can be used in the examination of steel, with special reference to the fidelity of the methods, and reproducibility of the results. Two carbide extraction replica techniques were described, and the results obtained compared with those obtained using other replica methods. The application of the extraction replica, in the identification of carbides by electron diffraction methods, was described also.

BIOLOGICAL APPLICATIONS

Dr. K. Little (Medical Research Council, Harwell) described the examination by electron microscope of hard dental tissues. Photographs were shown of sections of normal and carious dentine, and of chemically treated enamel, which were cut with an ordinary glass knife. The appearance of the chemically treated enamel is the same as that of early enamel caries. Some artefacts caused by the preparations were discussed, including an appearance of the dentine tubules which might cause thicker sections examined by polarized light to be misinterpreted.

Some studies on the electron microscopy of pancreas cells were described by Dr. C. E. Challice (Wright–Fleming Institute, London) and Dr. D. Lacy (St. Bartholomew's Hospital Medical College, London). An attempt was made to follow the secretion cycle in the acinous cells, in which it was proposed that the pro-zymogen granules develop from fragmented mitochondria in the region of the Golgi apparatus. The Golgi apparatus consists of a system of membranes separating two, or sometimes three, substances of different opacity as seen in the electron microscope.

Some observations made on ultra-thin sections of nerve cells were reported by Dr. I. M. Dawson, Mr. J. Hossack and Prof. G. M. Wyburn (University of Glasgow). Thin sections of spinal ganglia of normal adult rabbits were examined. The axon was observed in the cytoplasm of the capsule cells which are separated from the nerve cells by a lipid sheath. Nissl's substance occurs as discreet aggregates in "light" cells and dispersed throughout the cytoplasm in "dark" cells. The unit structures of Nissl's substance are seen as granules of size range 50–200 Å. Small mitochondria and a network of fine filaments of 20–50 Å diameter were observed in the nerve cell cytoplasm and the axoplasm. The nuclear membrane has been resolved into a multilayered structure, with a number of *c* 1000 Å nodes distributed on it. The authors suggested that the nuclear membrane may undergo a phasic alteration in structure and that the nodes are present during active nucleocytoplasmic transport.

Dr. E. M. Brieger and Dr. A. M. Glauert (Papworth Hospital and Strangeways Research Laboratory, Cambridge) gave a preliminary report on their work on the intracellular inclusions in organ cultures of normal and tuberculous tissues. The development of tubercle bacilli within infected cells was followed in organ cultures of lungs removed from guinea pigs infected with virulent bovine bacilli. In this type of tissue culture fragments of organs are maintained *in vitro* for some days. A single culture is small and can be fixed as a whole in buffered osmic acid. Ultra-thin sections were cut on a Porter–Blum type microtome. In the electron microscope the cultures were seen to be well preserved. After six days' growth the cells in the infected cultures contained dense cytoplasmic inclusions of 0·5 to 1·0 μ diameter. Some of these inclusions had a dense core and a surrounding spiral structure and others were vacuolated with only an outer ring of dense material. No bacilli were seen in the cultures at this stage and comparative studies with the light microscope showed that only a few bacilli were present. However, staining revealed the presence of large numbers of gram-positive granules which presumably corresponded with the inclusions seen in the electron microscope. Cells in normal, uninfected organ cultures contained larger, more highly vacuolated inclusions which were recognizably different from those seen in the infected cells. It is hoped that further work will throw light on the nature of the inclusions in the infected cells.

Focusing the electron microscope when ultra-thin sections are used is a problem which has been encountered in a number of laboratories. Dr. T. H. Flewett and Miss P. Tymms (School of Medicine, Leeds) described how a gold sol could be used to deposit an object of suitable contrast for focusing when these specimens are examined.

Dr. C. E. Challice and Dr. W. H. Hughes (Wright–Fleming Institute, London) said that they had modified the method of preparation of bacteria for thin sectioning described by Brieger and Glauert at last year's conference. By far the best method was to grow the bacteria in a "poured" plate, and to cut out a cube and treat it as if it were a block of tissue. When this was not possible a sandwich could be made by pouring a thin layer of agar on to the surface on which the bacteria were growing and when the agar had set a cube was cut from the plate and treated thereafter as if it were a block of tissue. Miss A. M. Glauert (Strangeways Research Laboratory, Cambridge) said that they had tried this but that they had found that the sandwich separated during the embedding procedure. The advantage of the method was that the bacteria were not exposed to such a high temperature.

Miss P. Tymms and Dr. G. Eaves (School of Medicine, Leeds) described a modification they had made in the preparation of red blood cell ghosts for electron microscopy, which they had found to be an improvement over the method of Hillier.

Dr. Nagelschmidt (Safety in Mines Research Establishment, Sheffield) described the results of studies of dusts isolated from pneumoconiotic human lungs. Dusts were recovered by ashing the lung tissue at 380° C followed by extraction of the lung ash by dilute acid. Enzyme digestion and hydrogen peroxide treatment were used to destroy lung tissue when ashing had to be avoided. Examples were given of recoveries of monomineralic dusts showing characteristic features that could be recognized by electron microscopy. A comparison between the airborne dust and the recovery

from a man who died of lung fibrosis after working for twenty years in a kaolin producing plant showed no evidence of chemical attack of the kaolin platelets by lung fluid. Examples were given of lung residues from asbestos and kieselguhr workers.

DR. R. REED and MISS M. J. WOOD (Department of Leather Industries, University of Leeds) and DR. M. K. KEECH (Department of Medicine, University of Leeds) described some recent electron microscopic studies of skin collagen. A batch of human dermal collagen (aged 9 years) was prepared free from interfibrillary material. The collagen fibrils were then treated with chemical reagents of various pH values at 37° C for similar periods of time. With all the reagents used, irrespective of pH value, small cigar-shaped elements were observed. These fitted together in a spiral arrangement along with the fibrils. With alkaline solutions, small filamentous structures were released from the fibrils, and their length increased with the pH value of the reagent. With periodic acid at pH value 5·0 and with certain alkaline buffer solutions, the collagen fibrils transformed into structures closely resembling elastin from elastic tissue and from certain pathological conditions of collagen. The significance of these findings for medical and leather science was briefly outlined.

DR. I. M. DAWSON and MR. T. A. HAMOR (Chemistry Department, University of Glasgow) reported on an investigation into the structure of cellulose fibres. Cellulose degraded with sulphuric acid and washed was examined shadowcast and particulate material of various thicknesses down to the microscope resolution limit and of length from 500–5000 Å. Efforts to cut sections of sisal fibres were not very successful, probably due to the non-cellulose material present. Efforts were made to remove these non-cellulose products but this caused some degradation at the same time. Sections were obtained of this material longitudinally, transversely and obliquely. Longitudinally a number of layers are displayed about 1 μ in length and transversely these are shown as concentric rings of width 1400 Å. The particles of the sulphuric acid degradation have so far appeared only in sections of material which have undergone considerable degradation.

Tissue fractionated by differential centrifugation and examined by electron microscopy was the subject of a report by MR. M. S. C. BIRBECK and MR. E. REID (Royal Cancer Hospital, London). It was possible by examining sections of the pellets to distinguish features such as mitochondrial cristae. Difficulties in the technique were discussed.

Electron microscopy of hair follicle was described by DR. N. A. BARNICOT, MR. M. S. C. BIRBECK and DR. E. H. MERCER (Royal Cancer Hospital, London). The preparation of sections of the hair follicle for the purpose of studying the formation of keratin and of pigment was described. Follicles, obtained by plucking from the human head, were fixed in 1% osmium tetroxide buffered at 7·4 embedded and sectioned in the standard manner. The keratin forming cells of the presumptive cortex and cuticle and the pigment forming cells, the melanocytes, were readily distinguished in micrographs of these sections. In their cytoplasmic organization the melanocytes resemble other secretory type cells in possessing a polarity: a cluster of ergastoplasmic membranes occurring predominantly at the end of the cell nearest the papilla and at the other end a specialized region where the pigment granules are formed. This specialized region seems analogous in function to the Golgi region of other cells and is characterized by the presence of many vacuoles in which the melania accumulates. Sections of partly formed granules in these vacuoles and of granules isolated from hair itself often revealed that the melanin was laid down in successive lamellae. In the keratin cells there is no organized ergastoplasm but many free dense particles of the type described by Palade. The keratin fibrils could be traced from their first appearance as fine filaments (approximately 100 Å diameter) to their final condensation in the dense fully hardened fibre. Large macrofibrils (1000–2000 Å) form early in the cells and seem to grow by the addition of the finer filaments. Higher in the follicle there is some evidence of a denser amorphous material cementing the larger fibrils together.

Some similar studies by DR. G. E. ROGERS and MR. R. W. HORNE (Anatomy School and Cavendish Laboratory, Cambridge) were then described. The hair root of the human hair follicle in the active growth phase has been studied in ultra-thin sections using the Siemens Elmiskop microscope. Several morphological features of developing cortical cells, cuticle and sheath cells and melanocytes have been observed. Early oriented keratin fibrils less than 100 Å in width occur in the cytoplasm of presumptive corticle cells. The changes in number, size and distribution that they undergo during hair growth have been followed. Some small mitochondria are also found but no endoplasmic reticulum. The individual microfibrils can be distinguished in cross-sections of macrofibrils. The microfibrils on the outer rim of each macrofibril are denser to electrons than those in the bulk. In contrast to the cortex the keratin in the scale cells is granular and not fibrillar. During hair growth the granules increase in size and number and accumulate on the outer edge of the scale cells adjacent to the cell membrane and correspond to the so-called exocuticle layer. Fine fibrils and granules of a further keratin are produced by the cells of the inner sheath. Melanocyte cytoplasm contains numerous small mitochondria, endoplasmic reticulum, agranular reticulum, and melanin granules in various stages of development. Melanin granules at high resolution possess internal lamellae.

C. E. CHALLICE

Origin and analysis of gas in electron tubes

By S. J. Stoll, B.S., Diamond Ordnance Fuze Laboratories, Washington, D.C., U.S.A.

[*Paper received* 10 *October*, 1955]

It is shown that the gas liberated in an electron tube, during electron bombardment of the anode, originates in the oxide-coated cathode. This gas was found, by spectrographic analysis, to be nearly all carbon monoxide. The significance and relative effects of tube processing on tube gas are shown.

One of the problems associated with all vacuum tubes which use an oxide cathode is the residual tube gas. The gas with which we are concerned here is liberated when tube parts are bombarded by electrons. It affects tube performance, and in many cases results in a defective tube. The standard practice relies on a getter to remove this so-called residual gas during tube ageing: this takes place after the tube is processed and sealed off the vacuum system. This gas is believed, by some investigators, to be a combination of gas inherent in tube parts (which cannot be removed by eddy current heating) and gas adsorbed as a result of getter flashing and tube seal-off. Wagener[1] pointed out that, "if a metal has been degassed even by an intense eddy current heating, additional gases are always set free by subsequent electron bombardment." This gas of which Wagener writes is inherent in the anode. However, our experiments indicate that if any inherent gas is liberated during electron bombardment of the anode, the amount is negligible compared with the amount of gas liberated as a result of factors related in this paper.

The objective of this work on tube gas was to determine the nature and origin of the gas, and to find the most efficient method of eliminating the gas. The tubes used in the experiments were miniature triodes. Carbonized nickel and bright nickel anodes were used; similar results were obtained. Directly heated cathodes were used, each consisting of a tungsten ribbon, coated with a triple carbonate (Ba–Sr–Ca)CO_3. Later, $BaCO_3$ (single carbonate) cathodes were used; these produced similar results.

The vacuum system used in this work had a forepump and an oil diffusion pump. A Westinghouse metal vacuum valve was located between the tubes on test and the oil diffusion pump; this was used to control pumping speed. An ionization gauge was located on the tube side, and a cold trap was located on the pump side of the metal valve.

DISCUSSION OF EXPERIMENTS

The work on tube gas is summarized in three parts:

(i) the origin of the gas; (ii) the nature of the gas; (iii) tube processing and gas.

(i) *The origin of the gas.* It was found that thorough outgassing of the anode by eddy current heating (before conversion of the cathode carbonates to the oxides) did not eliminate gas which appeared later when the anode was bombarded by electrons. Therefore, it was suspected that the anode was adsorbing a relatively large amount of gas, evolved during the conversion of the cathode. An experimental tube was sealed on to the vacuum system and baked out at 350° C for half an hour. The anode was then outgassed by high frequency induction heating (750° C) until the ionization gauge indicated a pressure below 10^{-5} mm of mercury. The cathode temperature was then raised slowly until colour became visible. No rise in pressure was detected by the ionization gauge. This indicated that the cathode binder was broken down during tube bake-out, and eliminated the binder as a possible source of tube gas. The cathode temperature was further increased until a small amount of cathode conversion occurred. This produced an increase in gas pressure. The cathode heating voltage was then shut off and the system pumped out until the pressure was below 10^{-5} mm of mercury. The anode was reheated by eddy currents to a temperature slightly lower than the initial 750° C out-gassing temperature. This lower temperature was to insure that any rise in pressure would not be due to gas originally in the anode. A pressure increase was detected on the ionization gauge. The anode was kept hot until the pressure was below 10^{-5} mm of mercury, and then allowed to cool. Once again the cathode was partly converted, the gas pressure allowed to drop, and the anode reheated. Another pressure increase was detected. This procedure was repeated several times until the cathode was completely converted. The number of cycles required to complete cathode conversion depended upon the amount of conversion that took place on each cycle. After the cathode was converted, drawing anode current did not result in further liberation of gas.

This experiment indicated that a considerable amount of gas was adsorbed by the anode during cathode conversion. Subsequently, this gas was removed by reheating the anode. Since anodes that had not been reheated after cathode conversion invariably liberated gas when bombarded by electrons, it can be stated that this gas had its origin in the oxide-coated cathode.

(ii) *The nature of the gas.* Several experimental triodes were sealed on to the vacuum system, given a normal bake-out, and thoroughly outgassed by eddy current heating. The cathodes were not converted. The tubes were sealed off, with several inches of glass tubulation remaining on each tube. The tubes were taken to the National Bureau of Standards' Mass Spectrometry Laboratory for investigation.

Using a low vapour pressure wax, an experimental tube was sealed into the manifold of the vacuum system associated with the mass spectrometer. After a good vacuum was obtained, the tube was cracked open to the vacuum system. The cathode was then converted, and the conversion gas pumped out. Next, the manifold was isolated from the vacuum pumps, so that gas liberated from the tube would enter the mass spectrometer for analysis. Fifteen milliamperes of anode current were drawn for two minutes. The gas liberated from the anode, as a result of electron bombardment, flowed into the mass spectrometer. A spectrographic analysis showed an appreciable amount of carbon monoxide, water vapour, and hydrogen. After five minutes, a second analysis was made of the same sample, and it was found

that the amount of water vapour and hydrogen had increased considerably. When the system was pumping, the amount of water vapour detected by the mass spectrometer was low. When the tube was isolated from the pumps and the cold trap, the amount detected increased with time. It is probable that some of this water vapour reacted with barium in the experimental tube to form hydrogen, according to the reaction,

$$Ba + 2H_2O \rightarrow Ba(OH)_2 + H_2 \uparrow$$

The amount of hydrogen increased as the exposure time increased. Berdennikowa,[2] Clausing (as quoted by de Bohr[3]) and Jenkins and Newton[4] used this action of water vapour on barium to produce hydrogen. When the tube was sealed off the system, an analysis of the background gas of the mass spectrometer (with the manifold isolated from the pumps) revealed that the amount of water vapour increased with time, while the amount of hydrogen remained essentially the same.

A different technique was developed, in order to minimize the Ba–H_2O reaction so as to make its effect negligible. The experimental tube was sealed on to a 50 cm^3 glass bulb which in turn was sealed on to the vacuum system. The tube was baked at 350° C for half an hour and the anode heated by eddy currents until the gas pressure reading corresponded to a pressure below 10^{-5} mm of mercury. The cathode was converted and the tube and flask sealed off as a unit. The getter was not flashed. To liberate gas from the anode, 15 mA of anode current were drawn for one minute. The 50 cm^3 bulb was then sealed off from the tube, with several inches of glass tubulation remaining on the bulb. It had been determined earlier that the sealing-off points were thoroughly outgassed.

The bulb was sealed on to the vacuum system, adjacent to the mass spectrometer, so as to bypass the original manifold and most of the glass tubing. This was done in an attempt to reduce the source of water vapour. By collecting the sample in the glass bulb, the source of barium was eliminated. After the system pumped down, the tube was isolated from the pumps, the bulb tubulation cracked open, and the sample analysed. Eight samples were run in this manner; a background analysis preceded each sample. During the water vapour analysis, the time element was important, since the amount of water vapour increased with time. After the tube was isolated from the pumps, the period of time which elapsed before obtaining a water vapour reading was made the same for both background and sample. Spectrographic analysis of the sample showed a relatively large amount of carbon monoxide. Very small amounts of hydrogen, water vapour and carbon dioxide were detected. It could not be determined whether these three gases came from the sample or were in the background of the mass spectrometer. Nevertheless, the important observation was that nearly all the gas in the sample was carbon monoxide.

During cathode conversion, an appreciable amount of conversion gas, which is known to be principally carbon dioxide, was adsorbed by the anode. Gehrts,[5] Becker,[6] and Jenkins and Newton[4] proved the existence of free barium on electrodes adjacent to the oxide cathode. As a result of electron bombardment of the anode, it is probable that carbon dioxide and barium reacted to form carbon monoxide, according to the reaction,

$$Ba + CO_2 \rightarrow BaO + CO \uparrow$$

Prescott and Morrison[7] made use of this reaction in determining the amount of free alkaline earth metal in an oxide cathode; the free alkaline earth metal was determined by oxidation with carbon dioxide and analysis of the gaseous reaction products.

(iii) *Tube processing and gas.* Several experimental tubes were sealed on to the vacuum system in order to determine the effect of tube processing on tube gas. A test schedule was developed, referred to as schedule *A*, which was applied to the tubes (while pumping) after standard bake-out, eddy current heating, and cathode conversion. The schedule was as follows. The tube was biased at $-7\frac{1}{2}$ V and the anode current raised to 10, 15, and 20 mA respectively, two minutes for each step. The gas liberated from the anode, as a result of electron bombardment, was detected on the ionization gauge. The gas pressure, calibrated in microamperes on the ionization gauge, was recorded every ten seconds. This pressure was plotted on the figure as a function of time. The curves show the relative effects of tube processing on tube gas.

Three methods were used in processing the tubes prior to application of schedule *A*. Method 1 consisted of baking a tube for half an hour at 350° C, and heating the anode by high frequency induction, at a temperature of 750° C, until the ionization gauge read below 1 μA. With the tube cool, the cathode was converted. The figure shows that a tube processed by this method liberated a relatively large amount of gas during electron bombardment of the anode. The different curves for Method 1 represent tubes of a slightly different construction. These tubes were tested under the same conditions, but varied in temperature. The hottest tubes liberated the most gas. Also, heating or cooling a tube externally during electron bombardment of the anode resulted in an increase or decrease, respectively, in the amount of gas liberated.

Method 2 was the same as method 1 except that the anode was reheated after cathode conversion to a temperature of 650° C in order to drive off gas which was adsorbed during the conversion process. However, in doing so, some of the gas was readsorbed by the cathode. The anode and cathode were reheated several times, alternately, in order to get rid of most of the gas. The figure shows that tubes processed

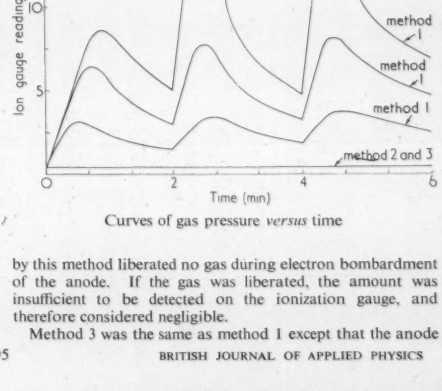

Curves of gas pressure *versus* time

by this method liberated no gas during electron bombardment of the anode. If the gas was liberated, the amount was insufficient to be detected on the ionization gauge, and therefore considered negligible.

Method 3 was the same as method 1 except that the anode

was kept hot during cathode conversion. After eddy current heating, the anode temperature was lowered to 650° C and the cathode converted. The anode temperature during cathode conversion was lower than the initial outgassing temperature to ensure that no gas was being liberated at the anode while the cathode was being converted. When this precaution was not taken, poisoning of the cathode occurred in some tubes, thus affecting cathode emission. Keeping the anode hot prevented it from adsorbing carbon dioxide; as a result no carbon monoxide was liberated during electron bombardment (schedule *A*). Method 3 produced the same results as method 2. However, method 3 is preferred, since it prevents carbon dioxide from being adsorbed at the anode and eliminates the necessity of removing it after cathode conversion.

It may be noted that an attempt was made to remove carbon monoxide from the anode of an experimental tube by ageing the tube on the vacuum system. After applying processing method 1, the anode current was set at 10 mA for twenty minutes. At the end of this period the anode was still liberating gas, as detected on the ionization gauge. The anode current was raised to 15 mA causing a rise in gas pressure. After twenty more minutes, gas was still detected. This emphasizes the difficulty experienced in attempting to remove all of this gas by getter action, as done in tubes after they are sealed off the vacuum system. Although proper ageing of a tube gets rid of much of the gas, the effectiveness of the getter is reduced, and the tube may become gassy during normal operation.

CONCLUSION

The investigation of the nature of the gas liberated at the anode of an electron tube during electron bombardment revealed that this gas is carbon monoxide. It is believed that the cool anode surface adsorbs carbon dioxide and barium during cathode conversion; as a result of electron bombardment, the carbon dioxide and barium react to form carbon monoxide. The most efficient processing method that was used to eliminate this gas involved keeping the anode hot during cathode conversion. The anode temperature should be at least 600° C and should be maintained until the carbon dioxide is pumped out. The tubes require no aging and are relatively free of gas.

The experiments were repeated on several standard test diodes. Similar results were obtained and the same conclusions apply.

ACKNOWLEDGEMENTS

The author wishes to thank Mr. J. M. Stinchfield for his encouragement and helpful advice during the course of the work, which forms part of the electron tube research programme of the Diamond Ordnance Fuze Laboratories. Acknowledgement is also due to the staff of the N. B. S. Mass Spectrometry Laboratory for their work on the gas analysis.

REFERENCES

(1) WAGENER. *The Oxide Coated Cathode*, Vol. 1, p. 68 (London: Chapman and Hall Ltd., 1951).

(2) BERDENNIKOWA. *Phys. Z. Sowjet.*, **2**, p. 77 (1932).

(3) DE BOER. *Electron Emission and Adsorption Phenomena*, p. 349 (London: Cambridge University Press, 1935).

(4) JENKINS and NEWTON. *J. Sci. Instrum.*, **26**, p. 172 (1949).

(5) GEHRTS. *Z. Techn. Phys.*, **11**, p. 246 (1930).

(6) BECKER. *Phys. Rev.*, **34**, p. 1323 (1929).

(7) PRESCOTT and MORRISON. *J. Amer. Chem. Soc.*, **60**, p. 3047 (1938).

Diffusion (or conduction) along a slightly tapering tube, and its application to the determination of diffusion coefficients

By A. TALBOT, Ph.D. and J. A. KITCHENER, Ph.D., Imperial College of Science and Technology, London, S.W.7

[*Paper received* 21 *December*, 1955]

The diffusion equation has been solved for the case of diffusion from a slightly tapering tube into an infinite medium of zero concentration. The theory provides a means of correcting results obtained for diffusion coefficients in the capillary tube method of Anderson and Saddington, when the tube is not of uniform bore throughout its length. This is frequently the case when silica capillary tubes have to be used (as for high-melting substances) and the correction is often significant.

INTRODUCTION; CYLINDRICAL TUBES

A very convenient method of determining diffusion coefficients of substances in liquids—particularly when radioactive tracers can be employed—is that described by Anderson and Saddington.[1] The liquid "labelled" with radio-tracer is introduced into a uniform capillary tube (about 1 mm in internal diameter and of length, l, about 2 cm). One end of the tube is closed, and the other end is placed in a vessel of the same liquid without radio-tracer [Fig. 1(*a*)].

After a timed interval (t seconds) the tube is removed, and the fraction of radioactive tracer remaining in the tube (ρ) is determined. The diffusion coefficient (D) of the labelled substance can then be calculated from the following relationship

$$\rho = \frac{8}{\pi^2}\left[\exp(-\theta) + \frac{1}{9}\exp(-9\theta) + \frac{1}{25}\exp(-25\theta) + \ldots\right] \quad (1)$$

where $\theta = \pi^2 Dt/4l^2$. This is the well-known solution of Fick's law for the case of diffusion from a cylindrical column, initially at uniform concentration C, one end being maintained at $C = 0$ from time $t = 0$[2].

Equation (1) can be solved for D graphically. Alternatively, the following approximation formula (2) is suggested;

it is correct to four significant figures when $\rho < 2/3$. Putting $\pi^2\rho/8 = x$,

$$\theta = -\ln x + q/p + rq^2/2p^3 \qquad (2)$$

where

$$p = 1 + x^8 + x^{24}$$

$$q = \frac{1}{9}x^8 + \frac{1}{25}x^{24}$$

$$r = 1 + 9x^8 + 25x^{24}$$

SLIGHTLY TAPERING TUBES

In applying the method of Anderson and Saddington to fused salts at high temperatures,[3] the difficulty was encountered that fused silica capillary tubes had to be used and, unlike those of glass, they cannot be obtained with accurately uniform bore. It was therefore necessary to examine the bore of each tube, reject tubes which showed excessive irregularity, and apply a correction for those having a slight taper. The solution of the diffusion (or conduction) problem for a slightly tapering tube could not be found in the literature and is therefore given here.

Assume tapering as shown in Fig. 1(*b*), and specify the degree of taper by $\mu = (d_2 - d_1)/d_1$; μ may be positive or negative.

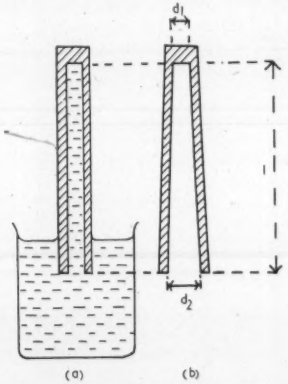

Fig. 1. (*a*) Principle of the method of Anderson and Saddington. (*b*) Definition of the taper (see text)

Provided μ is small (e.g. of the order of 0·01) the problem can be treated as one of *radial* diffusion. Then by standard methods, one obtains

$$\rho = \frac{6(1+\mu)^2}{3+3\mu+\mu^2} \sum_{n=1}^{\infty} \frac{1}{\alpha_n^2} \frac{(\alpha_n^2+\mu^2)}{(\alpha_n^2+\mu^2+\mu)} \exp(-D\alpha_n^2 t/l^2) \quad (3)$$

where $\alpha_1, \alpha_2, \alpha_3 \ldots \alpha_n$ are roots of $\tan\alpha = -\alpha/\mu$.

Very closely $\alpha_n = (n - \frac{1}{2})\pi + \mu/(n - \frac{1}{2})\pi$

and, to the first order in μ, $\alpha_n^2 = (n - \frac{1}{2})^2\pi^2 + 2\mu$.

Thus, altogether, to the first order in μ,

$$\rho = \sum_{n=1}^{\infty} \frac{8}{(2n-1)^2\pi^2} [1 + (k_n - \lambda\theta)\mu] \exp[-(2n-1)^2\theta] \quad (4)$$

where $\theta = Dt\pi^2/4l^2$, $\lambda = 8/\pi^2$, and $k_n = 1 - 3\lambda/2(2n-1)^2$, i.e. $\lambda = 0{\cdot}81057$, $k_1 = -0{\cdot}21585$, $k_2 = 0{\cdot}86491$, $k_3 = 0{\cdot}95137$. Thus, putting $x = \pi^2\rho/8$ as before, θ must satisfy

$$[1 + (k_1 - \lambda\theta)\mu]\exp(-\theta) + \frac{1}{9}[1 + (k_2 - \lambda\theta)\mu]\exp(-9\theta) + \ldots + \frac{1}{25}[1 + (k_3 - \lambda\theta)\mu]\exp(-25\theta) + \ldots = x \quad (5)$$

For the case of no taper, $\mu = 0$, equation (5) reduces to equation (1).

For the general case, use of equation (1) to calculate θ (or D) would give an erroneous value, say θ_0 (or D_0), which could be corrected by using the following approximation, valid for μ of order 0·01:

$$\theta = \theta_0\left[1 - \mu \cdot \frac{\lambda(1+q) - s/\theta_0}{p}\right] \qquad (6)$$

where $s = k_1 + \frac{1}{9}k_2x^8 + \frac{1}{25}k_3x^{24}$ (and p and q are defined above).

Consequently, experimental data calculated on the basis of equation (1) can be corrected for taper by applying a fractional reduction amounting to $k\mu$, where k stands for $(1/p)[\lambda(1+q) - s/\theta_0]$, and roughly

$$k \simeq (0{\cdot}807 - 0{\cdot}60x^8) + (0{\cdot}212 - 0{\cdot}25x^8)/\theta_0$$

In practical diffusion experiments, one would normally work with ρ between about $\frac{3}{4}$ and $\frac{1}{2}$; the corresponding values of k are then between 1·4 and 1·2, as seen from the following table.

x	ρ	θ_0	k
0·6	0·486	0·5127	1·21
0·65	0·527	0·4342	1·26
0·7	0·567	0·3628	1·32
0·75	0·608	0·2978	1·37
0·8	0·649	0·2395	1·42

It follows, therefore, that if D is required to an accuracy of, say, 1%, any taper in the capillary tube must be determined with a somewhat greater accuracy, and the correction $k\mu$ can then be applied. The correction is frequently significant when silica capillary tubes are employed.

REFERENCES

(1) ANDERSON and SADDINGTON. *J. Chem. Soc.* (*Suppl.* No. 2), pp. *S* 381–6 (1949).

(2) CARSLAW and JAEGER. *Conduction of Heat in Solids*, p. 79 (London: Oxford University Press, 1947).

(3) BORUCKA, KITCHENER and BOCKRIS. To be published.

The wall effect and the viscometry of suspensions

By A. D. MAUDE, B.Sc., and R. L. WHITMORE, B.Sc., Ph.D., A.Inst.P., Dept. of Mining and Fuels, University of Nottingham

[*Paper first received* 3 *May*, 1955, *and in final form* 5 *January*, 1956]

When the viscosity of a suspension of spherical particles uniformly distributed in a simple liquid is measured in a capillary tube viscometer, a wall effect, which is not found with coaxial rotating cylinder viscometers, is observed. The paper suggests that it may be caused by a redistribution of a portion of the suspension particles on entering the tube of the viscometer, leading to a reduction in both the concentration and viscosity of the suspension near to the walls of the tube. The diminution in concentration is measured experimentally and found to yield a value for the wall effect which is in agreement with that obtained from viscosity measurements. The reason for the redistribution of the particles at the tube inlet is discussed.

It has been found experimentally by a number of investigators[1-3] that when the viscosity of a dispersed suspension of hard spheres is measured in a capillary tube viscometer, the value which is obtained is dependent upon the diameter of the tube, increasing with increasing tube diameter. The phenomenon, which has been referred to as the σ-effect, suggests that slip takes place between the wall and the suspension, the system behaving as though there were a layer of pure fluid adjacent to the wall. From viscosity measurements in tubes of different diameters, the thickness of the hypothetical layer can be calculated[1-3] but there is no evidence that the layer does in fact exist; indeed cine-films of the flow of suspensions of spheres down a narrow tube show particles moving in contact with the walls.[2] From a theoretical investigation of the interaction between a plane surface and a parallel-moving sphere, Vand[4] deduced that the discontinuity at the plane interface would modify the viscosity measurement in the same way as a layer of pure liquid at the wall, and he obtained a value for its thickness which was in good agreement with his experimental value.[1] However, his reasoning leads to the conclusion that this wall effect must be present in all types of viscometers, whilst measurements made on the viscosity of suspensions in rotating cylinder viscometers have failed to disclose any wall effect, the measured viscosity being independent of the width of the annulus.[5-7] Thus it appears that Vand's theory of wall interaction is unacceptable in its present form and a new approach is necessary to explain the observed effects.

THEORETICAL

Before examining the influence of the walls of a viscometer upon the viscosity of a suspension as measured by it, conditions prevailing in the bulk of a suspension undergoing shear must be considered. Two subsidiary propositions relating to the properties of suspensions in the absence of wall effects will first be introduced, and it will then be shown that if they are applied to elements of suspensions adjacent to the containing wall of a viscometer the experimentally observed phenomena mentioned above may be satisfactorily explained.

PROPOSITION 1. *The apparent viscosity of a suspension of spheres when sheared between parallel-moving planes is independent of the distribution of particles in a direction normal to the plane of shear.*

A dispersed, non-settling suspension of hard spherical particles will be considered to be uniformly sheared parallel to the plane $z = 0$ when a constant force F per unit area is transmitted tangentally across any plane $z =$ constant. This is the formal definition of uniform shear used in this paper. If η is the viscosity of the suspension, and v its velocity parallel to the plane of shear which is a function of z only, then

$$F = \eta(dv/dz) \tag{1}$$

The viscosity of such a suspension is related empirically to the viscosity of the pure fluid η_0, and its volume concentration c, by

$$\eta = \eta_0/(1 - Kc) \tag{2}$$

where K is a constant.[8] This has been found to hold for suspensions in bulk up to 30% concentration, and it will be assumed here to hold even for thin layers.

Substituting for η from equation (2) into equation (1) and integrating we get

$$(v)_{z=h} = \frac{F}{\eta_0}\int_0^h (1 - Kc)dz$$

$$= Fh(1 - K\bar{c})/\eta_0 \tag{3}$$

where $\bar{c} = \frac{1}{h}\int_0^h cdz$, is the average concentration of the suspension, assuming that c is a function of z only. Equation (3) can be written in the form

$$(v)_{z=h} = Fh/\eta' \tag{4}$$

and η' can be interpreted as the apparent viscosity of the suspension as actually measured by a viscometer, because such a measurement is based on the determination of the value of Fh/v. If $c = 0$, then $\eta' = \eta_0$, the viscosity of the pure fluid.

One practical result of the proposition is that if, in any viscometer in which conditions approximate to those of uniform shear, the concentration of spherical particles should become non-uniform across the sheared suspension, the experimental value obtained for the viscosity should be unaffected. In a coaxial rotating cylinder viscometer, any redistribution of the particles of a suspension cannot alter the average concentration, so that the proposition should hold, provided that the annular gap over which the shear is applied is small compared with the radii of the cylinders.

PROPOSITION 2. *If a suspension of spheres flows through a capillary tube viscometer, a small inward radial displacement of particles within the tube will reduce the average concentration of particles in the viscometer, and hence the apparent viscosity of the suspension.*

The average concentration within a capillary tube down which a suspension is flowing depends not only upon the

relative volumes of solid and liquid entering the tube, but also on the relative times for which the two components remain within the tube. If, for example, all the particles were moved into the centre of a tube down which a suspension was flowing with parabolic velocity distribution, they would travel at a greater velocity than the average velocity of the fluid. As they would stay in the tube for a shorter time than the liquid, the concentration within the tube would be lower than that of the suspension before it entered or after it left the tube. In general, the concentration can only change if particles are moved in the liquid from a region with one velocity to another one with a different velocity.

We may calculate the concentration in a tube from the continuity condition that the number of spherical particles crossing the right cross-section of any tube of flow is constant, provided that none pass through its walls. That is

$$\int_A v_p c dA = \text{constant} \qquad (5)$$

where A is the right cross-section of a tube of flow i.e. a cylinder bounded by streamlines of flow, and v_p is the velocity of a suspension sphere which is taken to be the same as the velocity of the liquid which would occupy the position of the centre of the particle if the particle were replaced by liquid.

Suppose that a suspension of spheres is flowing down the tube of a capillary tube viscometer. Consider the right cross-sections, a and b, of two thin tubes of flow the cross-sections of which are of the same area δA and are coplanar. Compare the two cases, firstly when n_a and n_b particles per unit volume cross a and b respectively, and secondly when a number of particles has been displaced so that they cross b instead of a. If the reduction in particles per unit volume passing a is l, and the increase in particles per unit volume passing b is m then, for reasons given above, l need not equal m.

In fact, from the continuity equation (5), if the velocities of flow across the areas are v_a and v_b respectively

$$\delta A n_a v_a + \delta A n_b v_b = \delta A(n_a - l)v_a + \delta A(n_b + m)v_b$$
$$= \delta A n_a v_a + \delta A n_b v_b - \delta A(v_a l - v_b m)$$

Therefore, $$l v_a = m v_b$$

This assumes that the displacement has not significantly altered v_a or v_b.

The total number of particles per unit volume crossing these two areas without the transfer is $n_a + n_b$, and the number crossing with the transfer is

$$n_a - l + n_b + m = n_a + n_b - l(1 - v_a/v_b)$$

If v_a is less than v_b there is a reduction in the total number of spheres in the two thin tubes and hence in the concentration of the suspension. If a large number of such displacements take place, the total reduction will be the sum of the component reductions.

It follows that as long as particles are moved from slower to faster flowing portions of the fluid the concentration averaged over the portions of the tube from which and to which the particles have moved, will be less than if no such move had taken place. Furthermore, the reduction will be confined to areas of the tube in which the move takes place.

In a capillary tube viscometer, any inward, radial displacement of particles must be to a region of greater velocity and will always reduce the average concentration. If the displacement is small, conditions will approximate to those of uniform shear and, from Proposition 1, the average viscosity must also be reduced, as viscosity and concentration increase and decrease together.

HYPOTHESIS

It is now postulated that the wall effect, the existence of which has been established in capillary tube viscometers, is due to an inward, radial displacement of particles, confined to a region near the wall and brought about by some interaction between the particles and the wall. It is also postulated that the amount of the displacement is a function of the particle diameter and not the tube diameter. The cause of the displacement will be discussed later when it will be shown that it can be expected.

It has been shown in Proposition 2 that such a displacement causes a reduction in the apparent viscosity in a layer adjacent to the wall. As the thickness of this layer depends upon the particle rather than the tube size, its importance increases as the diameter of the tube is reduced, explaining the observed effect that the measured viscosity of a suspension decreases with decreasing tube diameter.

In a coaxial rotating cylinder viscometer however, movement of the particles from the walls cannot affect the average concentration, and hence it cannot alter the value of the viscosity which the experimenter obtains (Proposition 1).

Thus the hypothesis explains the original dilemma that a wall-effect has been observed in capillary, but not in coaxial rotating cylinder viscometers.

Workers who have measured the viscosity of a suspension of spheres in capillary tubes and found that the measured viscosity decreased with decreasing tube diameter have expressed their results in the form of a width D of an annulus adjacent to the wall, the viscosity of which is that of the pure fluid. The central core was assumed to contain a suspension of the same concentration and viscosity as that entering the capillary tube. With a few simplifying assumptions it is possible to relate the change of concentration to be expected as a consequence of the present hypothesis to a similar model.

Consider an annular cylinder, the outer wall of which coincides with the wall of the capillary tube and is wide enough to cover the region in which particles have been radially displaced. If the width of the annulus is small compared with the radius of the tube, it may be assumed that the contained suspension is uniformally sheared because approximately equal forces will be transmitted across the cylindrical surfaces concentric with the tube. Since, from Proposition 1, the apparent viscosity of a suspension under uniform shear is independent of the distribution of the particles perpendicular to the plane of shear, the apparent viscosity of the suspension within this annulus will depend only on the average concentration within it. If it is assumed that the transverse movement of the particles does not materially alter the velocity distribution in the annulus, then the annulus can be considered to consist of two sub-annulii, one adjacent to the wall and containing pure fluid, and a second, concentric, adjacent, inner annulus containing suspension of concentration c_0. The average concentration in the tube can then be considered as due to a central core of suspension of the same concentration as that entering the tube and an annulus of width D adjacent to the wall containing pure fluid.

It was assumed in the hypothesis that D is a function of the particle radius r, and does not depend on the tube radius R. From dimensional reasoning D must be proportional to r.

Thus if $D = sr$, where s is a constant, the area of cross-section of the tube containing no particles is

$$\pi R^2 - \pi(R - D)^2 \simeq 2\pi Rsr$$

as $R \gg r$

Therefore the proportion of the area containing no particles is $2sr/R$. This must equal the proportional drop in concentration $(c_0 - c_1)/c_0$, so that

$$s = R(c_0 - c_1)/2rc_0 \qquad (6)$$

where c_1 is the average concentration within the tube.

Thus from measurements of the concentration of a suspension entering or leaving the tube, and contained within it, together with the radii of the tube and the suspension spheres, a value for s may be obtained which can be compared with that obtained by other workers from viscosity measurements. Hence the hypothesis can be tested numerically.

EXPERIMENTAL

An experiment was devised to measure the actual concentration in a tube of a suspension of spheres flowing down it.

The suspension consisted of closely-sized polystyrene spheres immersed in a mixture of glycerol and water, having the same density as the spheres. The particles were obtained by dry-sieving unsized polystyrene spheres. The 150–170 B.S.S. mesh fraction was then sieved separately in water, dried and density-separated by adding it to solutions of lead nitrate of known density to give spheres of a narrow size and density range. Details of the spheres are given in Table 1, and the figure shows a photomicrograph of a sample of them.

Table 1. *Spheres used in experiment*

Size range	0·089–0·104 mm
Average diameter	0·0965 mm
Density range	1·0543–1·0572 g/ml.
Average density	1·0553 g/ml.

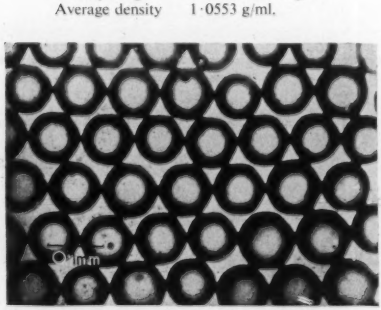

Photomicrograph of polystyrene spheres

The glycerol/water suspending fluid was adjusted to a density of 1·0550 g/ml. and had a viscosity of 1·931 cP, the measurements being made at 20° C ± 0·1.

It was found that after a sample of the suspension had stood for about half an hour flocculation was just discernible under the microscope. However, as all subsequent measurements were made within ninety seconds of stirring the suspensions, it is most unlikely that the results were affected by this phenomenon.

The apparatus consisted of a conical glass funnel, 75 mm in diameter and of approximately 100 ml. capacity, through the outlet of which projected a capillary tube, 595 mm in length and 1·876 mm in diameter. The upper end of the capillary tube, which projected some 25 mm into the funnel, terminated in a bell mouth of 15 mm diameter and the top lip was ground flat. By dropping a microscope cover-glass over the inlet, the capillary tube could be cut off from the conical funnel.

A volume of 100 ml. of suspension having a suitable concentration was made up in a beaker and poured into the funnel. After at least 40 ml. had flowed out of the capillary tube, a sample of approximately 10 ml. was collected in a weighed sintered-glass filter. The flow was then stopped by pressing a finger against the outlet and a microscope cover-glass placed over the inlet. Suspension remaining in the funnel was poured into a beaker and the suspension contained in the capillary tube and on the under side of the cover-glass washed into a second weighed sintered-glass filter. The first filter was weighed so that the volume of suspension present could be calculated, and both samples washed, dried and weighed. The Reynolds number in the tube at no time exceeded 310 and during the experiment the temperature was controlled to 19·5° C ± 0·5.

RESULTS

The results, calculated from equation (6) are given in Table 2.

Table 2. *Calculated results*

Volume of suspension leaving tube (ml.)	*Volume concentration of suspension leaving tube (c_0) (%)*	*Volume concentration of suspension in tube* (c_1) (%)*	s
8·46	20·51	18·92	0·74
9·16	20·70	19·47	0·57
10·18	20·93	19·65	0·59
15·60	16·66	15·38	0·74

* Calculated on the assumption that the bell-mouth was full of suspension at concentration c_0, and the capillary tube of suspension at concentration c_1

Volume of tube and bell-mouth = 1·831 ml.
Volume of tube only = 1·626 ml.

Measurements of the wall effect from viscosity determinations made on suspensions in tubes of different diameters have been reported by Vand[1], Higginbotham[2] and Oliver[3].

Vand, who used B.S. Ostwald viscometers, corrected the concentration of the suspension added to the instrument for spheres sticking to the glass envelope and taking no part in the flow. He also corrected the concentration for the absence of sphere centres within one radius of the wall of the instrument. However, it has been pointed out[2] that any redistribution of spheres in the vessel feeding the capillary tube should not alter the average concentration of suspensions entering the tube. Oliver[3] considered that any redistribution of sphere centres in the tube, as postulated by Vand, should not affect the average concentration, although it might give rise to some apparent wall effect. Until there is complete understanding of conditions near the wall of a tube, it would not appear to be permissible to allow for them by a correction of the type used by Vand. Recalculating his results after correcting only for spheres sticking to the glass envelope, a value of s varying from 0·34 at 5% to 1·36 at 30% volume concentration, with an average value of 0·89 over the range is obtained.

Both Higginbotham and Oliver, using the same capillary viscometer as each other, found that s was practically independent of the concentration, Higginbotham's value being 0·67 and Oliver's 0·69. They may be compared with the average value of 0·66 obtained above from concentration measurements in a tube.

DISCUSSION

Vand's conclusion,[1] that no sphere centre may lie at a distance less than r from the wall of a containing vessel has already been mentioned. It follows that when a suspension enters a capillary tube some particles will be forced radially inward, and it is this movement which may be identified with the displacement postulated in the hypothesis. It will be noted that the interaction is mechanical, and not hydrodynamic, in origin. It will also be noted that whilst the primary effect is a mechanical displacement of some spheres by the wall, it will be complicated by a number of other factors. The actual movement of the spheres and the counterflow of fluid may produce a net movement of other spheres, but it is not obvious in which direction this movement will be. Further, spheres, the centres of which lie between r and $3r$ from the wall, must be moved further and more often radially inwards as they overtake particles touching the wall than they are moved outwards in overtaking particles which are nearer to the centre of the tube. However, in order to obtain an approximation to the amount of movement, and hence the drop in concentration to be expected, it is assumed that all spheres displaced directly by the wall move inwards and travel with their centres at a distance r from the wall, and that no other particles are moved across the direction of flow.

Again assuming that the shear near the wall is uniform and that the transverse movement of the particles does not appreciably alter the velocity profile near to the wall, the velocity of flow down the tube is given by $v = Lz$, where L is constant, and z, the distance radially inward from the wall, is small. If the spheres were not forced inwards, the concentration in any small volume of the tube would be c_0 and the continuity integral over the region near to the wall would be

$$\int v_p c dA = \int_0^{z=r} c_0 Lz d(pz) \qquad (7)$$

$$= \tfrac{1}{2} c_0 L p r^2$$

where p is the circumference of any cylinder concentric with the tube and is assumed constant with respect to z as z is small. If there are n particles per unit length within this annulus, we may write $V'n/pr$ for c_0 if V' is the volume of one particle.

When all the particles have been moved to the surface $z = r$ they will have a velocity Lr, and if there are now n' particles per unit length

$$\int v_p c dA = Lrn'V' \qquad (8)$$

since the limit of cdA is $n'V'$ in this case. Comparing this with the value obtained if no interaction had taken place, equation (7), and using equation (5), we get

$$n' = \tfrac{1}{2} n$$

Thus the average concentration of displaced spheres is halved and is equivalent to a layer of thickness $\frac{1}{2}r$ containing no sphere centres, together with a layer of thickness $\frac{1}{2}r$ containing the original concentration of spheres. Hence $s = 0{\cdot}5$.

Two further facts which have been ignored in the above calculation will affect the value. Firstly, the velocity profile near to the wall will not be unaffected by the displacement. The rate of shear of the wall layer will increase, and so s will be somewhat larger than 0·5. Also the concentration at a distance r from the wall may rise to more than 30%, so that equation (2) is no longer applicable. When these effects and the possibility of further displacement of particles not in immediate contact with the wall are considered, the experimental figure of about 0·7 is not unreasonable.

If the density of the suspension particles differs from that of the suspending fluid, the curvature of the flow lines at the tube entrance might be expected to expose the spheres to inertial forces. For a downward-settling suspension the usual inward movement of particles would be accentuated, leading to a further diminution in the concentration and an increased value of s. For an upward-settling suspension the inward movement of liquid would be accentuated at the expense of the spheres, leading to an increase in average concentration and a decrease in the value of s. Oliver[3] made viscosity measurements on suspensions of these types and obtained values of s varying from 0·8 for downward-settling suspensions to 0·36 for upward-settling types. These results are in qualitative agreement with the theory.

CONCLUSIONS

The hypothesis, that when a suspension of spheres enters the tube of a capillary viscometer a mechanical interaction between the walls and the particles causes them to be displaced radially inwards, leads to the conclusion that there must be a reduction in the average concentration of spheres in the tube and hence in the measured viscosity. When the concentration within a tube was measured it was, in fact, found to be appreciably lower than that of the suspension leaving the tube. Moreover the magnitude of the wall effect calculated from the change in concentration agreed closely with that reported by other workers from viscosity measurements made on similar suspensions in capillary viscometers. Thus the qualitative truth of the hypothesis appears to be established. An exact quantitative calculation of the particle displacements to be expected at a tube inlet has not been possible but an approximate solution leads to a minimum average particle displacement of $0{\cdot}5r$ (where r is the radius of the spheres) compared with $0{\cdot}7r$ for the experimental determination.

Under the conditions of shear satisfied approximately by the coaxial rotating cylinder viscometer it can be shown that any displacement of spheres across the annulus which may take place should not alter the measured viscosity because the average concentration is unchanged. Experimental viscosity measurements reported elsewhere by other workers support this conclusion.

It is important to consider whether the observed wall effects may, in part, be due to causes other than a drop in concentration of the suspension. A hydrodynamic interaction at the interface between the wall and the suspension might, for example, be present. In a coaxial rotating cylinder viscometer a wall effect of any kind should appear as a change in the measured viscosity of a suspension with the width of the sheared annulus. Experimental results so far reported do not record any systematic change of this kind and it must be assumed that if, in fact, other wall interactions are present they are so small that they have not been detected.

ACKNOWLEDGEMENTS

The authors are particularly indebted to Dr. E. E. Jones for his help in arranging the paper. Their thanks are also due to British Resin Products Ltd., for their gifts of plastic materials, to Prof. F. B. Hinsley for valuable discussions and to the Scientific Department of the National Coal Board for financing the work.

REFERENCES

(1) VAND, V. *J. Phys. Coll. Chem.*, **52**, p. 300 (1948).
(2) HIGGINBOTHAM, G. *Ph.D. Thesis* (University of Birmingham, 1951).
(3) OLIVER, D. R. *Ph.D. Thesis* (University of Birmingham, 1954).
(4) VAND, V. *J. Phys. Coll. Chem.*, **52**, p. 277 (1948).
(5) EVESON, G. F., WHITMORE, R. L., and WARD, S. G. *Nature* [*London*], **166**, p. 1074 (1950).
(6) EVESON, G. F., WARD, S. G., and WHITMORE, R. L. *Disc. Faraday Soc.*, **11**, p. 11 (1951).
(7) SWEENY, K. H., and GECKLER, R. D. *J. Appl. Phys.*, **25**, p. 1135 (1954).
(8) OLIVER, D. R., and WARD, S. G. *Nature* [*London*], **171**, p. 396 (1953).

Coplanar mesh storage

By G. R. HOFFMAN, B.Sc., Ph.D., Electrical Engineering Department, University of Manchester

[*Paper first received* 16 *May, and in final form* 5 *September*, 1955]

The paper describes a cathode-ray tube capable of storing an array of binary digits on a special target surface. The target surface incorporates a mesh which is sensibly coplanar with the storage surface and, therefore, simple to manufacture by evaporation. An attempt was made to develop a storage system that would combine the advantages of mesh storage with the simplicity of control of the Williams–Kilburn system in two steps, namely, transfer of control to the bright-up mechanism and the elimination of transient voltages on the mesh. The store for comparable spot size has a greater packing density than the normal non-mesh cathode-ray tube store, and at low speed operation the output signal is controllable both in amplitude and sign. The limits of the output signal amplitude are discussed and methods of improving the speed of operation and output amplitude are described.

There are basically two types of storage tubes at present developed for computing machines. One uses the more normal construction of conventional cathode-ray tubes,[1,2] and the other has more complex structures incorporating a mesh close to the storage surface.[3,4,5] Both types can be used to retain binary digits stored on the target surface as a charge pattern, by rewriting the information periodically (regeneration), and, in the case of the mesh tube, if another electron gun floods the storage surface with low velocity electrons the information can be held without regeneration.[4,13] For the tubes which follow normal methods of cathode-ray tube construction the stored charge pattern depends on the redistribution electrons.[1,2,6,7] It follows that for these tubes the difference in potential between the bombarded areas of screen surface is governed fundamentally by the velocity distribution of the secondary electrons. As a large fraction of the secondary electrons is emitted with velocities corresponding to less than two or three volts (Fig. 1), the differences in potential of the charged areas are correspondingly small.[8,9,10] This limits the amplitude of the signal which can subsequently be picked up by an electrostatically coupled plate, when the area is re-bombarded with primary electrons. In the other type of storage tube, a mesh is placed between the source of primary electrons and the storage surface, then, providing the mesh is sufficiently close to the surface, the stable potential of the bombarded area is a function principally of the mesh potential.[3–5,11,14] This mesh potential may be varied, and the resultant differences of potential between storage areas can be made large. In turn this enables larger signal amplitudes to be picked up by a similar electrostatically coupled plate. Alternatively, the plate may be changed in potential, the mesh earthed, and either a separate collector used or the storage signals taken from the modulated plate.

In the Williams–Kilburn store (the normal cathode-ray tube store), the binary information in the storage surface was

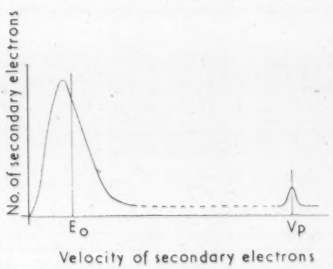

Fig. 1. Velocity distribution of secondary electrons

maintained or changed by control of the bright-up pulses during one digit period; the other potentials applied to the deflexion plates and focus anode were periodic. This gave the minimum possible interference to the sensitive amplifier from sources other than the bombarded storage area. The mesh type stores, however, required large voltage changes in the vicinity of the sensitive signal amplifier, resulting in

large transients occurring non-periodically which had to be separated from the storage signals.

It was therefore decided to attempt the development of a storage system that would combine the advantages of mesh storage with the simplicity of control of the Williams–Kilburn system. Two steps are required, namely, transfer of control to the bright-up mechanism and elimination of transient voltages on the mesh.

In order to obtain the maximum advantage from the experiments it was decided that a new type of mesh should be used which was sensibly coplanar with the storage surface and therefore simple to manufacture by evaporation.

THE COPLANAR MESH

An important advantage of the mesh is its ability to restrict the scatter of the redistribution electrons from the bombarded area. This feature improves the read round ratio[6] of the store. To ensure the maximum influence on the potential of the bombarded areas, it is essential for the mesh to be as near as possible to the insulator surface and, further, for the electron transparency to be high. Normal mesh storage tubes need meshes of high transparency which have to be accurately supported very close to the storage surface. The manufacture of the meshes is expensive and their location difficult. In the storage tubes described below, however, a coplanar mesh was used and all the successful mesh structures in both the demountable vacuum system and sealed-off assemblies were of silver evaporated on to either mica, or phosphor supported by glass.

There are three major capacities involved in the composite storage structure. These are illustrated in Fig. 2. For satisfactory operation the following conditions must be satisfied:

(i) $C_a > C_c$. When the mesh potential V_m is varied, the potential of the storage spot will change by $\propto V_m \times [C_c/(C_a + C_c)]$. It is essential that this change is small, as the greatest change of potential is wanted when the storage spot is bombarded with electrons.

(ii) Capacitance C_b should be small; it increases the input capacitance of the amplifier and also transfers the unwanted mesh voltage variations to the amplifier input circuits.

(iii) Capacitance C_a should be large. The limit is a function of the beam density available. It is desirable that the storage area be allowed to change more than 3 V in potential, otherwise outputs will be no greater than normal type cathode-ray tube signals.

(iv) Capacitance C_c should be small, so that the total capacitance of the storage area is reduced, enabling the changing of potential of the spot to be as rapid as possible.

The capacitance C_a can be controlled by choosing the appropriate dielectric thickness. The capacitance C_b is dependent both on the dielectric thickness and the surface area of the mesh grid, the latter being made as small as possible. The capacity between the spot and mesh (C_c) is also dependent on the surface area of the mesh grid, and will be small if C_b is small.

In addition to the above considerations there are three further requirements for the storage surface, namely:

(*a*) it is necessary to have at least three conducting bars to any one spot diameter. Otherwise the amplitude of the storage signal will vary depending on the position of the spot relative to the mesh bar;

(*b*) ideally, the width of the conducting material forming the bars would be infinitesimal, so as to retain as much storage area as possible. In practice, the ratio of conducting material to storage area of 1 : 10 was used;

(*c*) the thickness of the conducting bars must be sufficient to provide adequate conduction to avoid potential drop along the bars due to capacity loading. This was limited in practice by the evaporation technique as large thicknesses peel off the insulator surface.

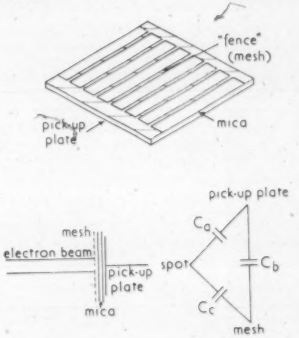

Fig. 2. The mesh structure

THE AVOIDANCE OF TRANSIENT EFFECTS

One method of avoiding the blocking action of the mesh waveform has been described in the literature.[4] In this case the beam current was modulated at high frequency. The storage signals caused by the charging or discharging of the storage spots were modulated at this frequency, and a tuned amplifier connected to the pick-up plate increased the signals to a level where their phase could be detected by a phase-sensitive rectifier. The mesh voltage depended on the digit information required at any storage location and the large transients had to be greatly reduced by the first tuned circuit

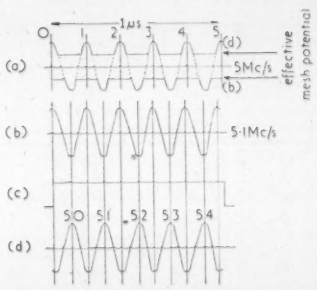

Fig. 3. Beat frequency radio-frequency storage
(*a*) mesh; (*b*) cathode; (*c*) grid bright-up; (*d*) cathode.

of the amplifier. It will be appreciated that the phase shift of the tuned amplifier must be stable, since it is the phase that carries the sign of the information.

In the system now described a sinusoidal voltage of 5 Mc/s was applied to the mesh and a sinusoidal voltage of 5·1 Mc/s applied to the cathode (Fig. 3). A bright-up waveform was applied to the cathode-ray tube grid for 1 μs when the cathode modulation and mesh modulation were substantially in phase. A second 1 μs bright-up period 5 μs later could be included or not at will during the periods when the modulations were substantially antiphase, because of the ordinary beat frequency effect. For the first pulse the radio frequency on the cathode allowed beam current to flow only during part of alternate half-cycles (5·1 Mc/s), i.e. beam current only occurred when the mesh was negative. The second bright-up pulse caused beam current during positive half-cycles of the mesh waveform. The storage area under bombardment could therefore be left charged either positively or negatively depending on the presence or absence of the second bright-up pulse, Fig. 4. On subsequent bombardment

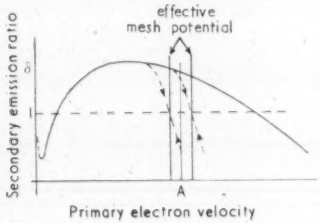

Fig. 4. Secondary emission ratio *versus* primary electron velocity

with the initial pulse, a storage signal was obtained from the pick-up plate, its sign dependent on the potential of the storage area. This formed the basis for the storage of binary digits.

EXPERIMENTAL INVESTIGATION

Cathode-ray tube storage characteristics. The important characteristics of cathode-ray tube storage systems are as follows:

(i) the ability to erase and rewrite in one operation on a particular storage location, under specified conditions (i.e. beam current density, pulse duration, location capacity, etc.);

(ii) packing density
(iii) read round ratio } comparable conditions;

(iv) as a general consideration the signals should be of adequate amplitude, and the signals representing 0 or 1 clearly distinguished.

To obtain information about these characteristics, circuitry of familiar computing type was built. As in the previous cathode-ray tube store,[1] the total time available was divided into periods of 80 μs, allowing 10 μs per digit, labelled "scan" and "action" periods. During eight "scan" periods an eight by eight television type raster of spots could be produced on the storage tube target surface [Fig. 5(*a*)]. During the "action" periods any particular line could be chosen with manually operated switches. This chosen line would normally be bombarded every alternate 80 μs, whilst its immediate neighbours were bombarded every 1280 μs. In effect the "action" line could be bombarded nine times before the adjacent line was scanned again.

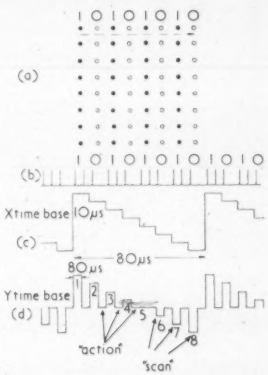

Fig. 5. Storage raster and time base waveforms
(*a*) raster; (*b*) grid bright-up; (*c*) *X* time base; (*d*) *Y* time base.

The appropriate storage location was always bombarded with a 1 μs pulse timed to coincide when the mesh and cathode modulations were in phase. A second pulse 5 μs later (corresponding to cathode-mesh antiphase) could be introduced when required in selected storage locations as follows:

(i) on any scan line;
(ii) on any number of scan lines (not any particular arrangement);
(iii) on any column;
(iv) on any number of columns (not any particular arrangement);
(v) the configuration set up along a line by using the column controls could be applied during one or more action periods.

X time base. The *X* time base was of the stepped variety, such that the beam paused at each storage location for most of the 10 μs [Fig. 5(*c*)]. This enabled the second bright-up pulse of a pair to bombard the screen in a similar position to the first pulse.

Y time base. The *Y* time base had similar facilities to the *X* time base, with the additional "action," "scan" operation mentioned previously[1] [Fig. 5(*d*)].

EXPERIMENTAL RESULTS

Bombardment of one storage location. When one storage location is bombarded continually by both pulses, i.e. dash configuration, the storage surface is left relatively negative or positive in potential, as the first and second bright-up pulses

occur when the mesh and cathode waveforms are substantially in phase and antiphase respectively. Subsequently, the initial pulse will cause the storage area to change from a positive to a negative potential, resulting in a negative signal at the pick-up plate. The second pulse which changes the potential of the storage surface from negative to positive gives a positive signal at the pick-up plate. This is shown in Fig. 6(*b*). The experimental outputs correspond well to the predicted outputs. If, however, "dash" pulses occurred only once every four digit periods, Fig. 6(*c*), the positive pulses were almost double the amplitude of the following negative pulse. Other negative pulses were also present [Fig. 6(*e*)]. The predicted output is as Fig. 6(*d*) where an output is obtained only when the storage surface should change in potential. The results indicate that potential equilibrium of the storage location had not been obtained in one bombardment. A simple diagrammatic explanation is shown in Fig. 6(*f*), where the general level of the screen surface potential is shown displaced from the mean value. For the

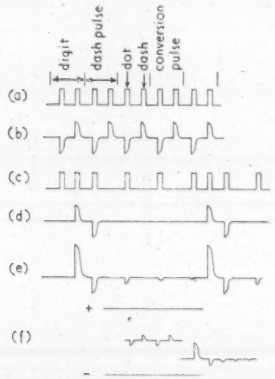

Fig. 6. Output signals from radio-frequency store. Bombardment of one spot.

(*a*) cathode-ray tube grid; (*b*) signal output, predicted and actual; (*c*) cathode-ray tube grid; (*d*) predicted signal output; (*e*) observed signal output; (*f*) shift of mean potential level.

signals occurring less frequently (positive signals) the secondary electrons from the storage location would experience a stronger field initially attracting the electrons to the mesh having a larger output signal. The following negative pulses of reducing amplitude indicate that a new equilibrium potential level is gradually attained. This was checked on alternative equipment which operated at 50 c/s and it was found that 4 μs were needed to obtain the maximum output signals with comparable beam current conditions.

The complete raster. The complete raster of storage locations was then bombarded sequentially. Symmetrical distributions of information displayed on the storage surface gave output signals exactly as expected. The more interesting distributions and output signals are shown in Fig. 7. In one case only the seventh storage location and the "scan" period was bombarded by the second "dash" conversion pulse. Regarding scan line No. 4, the output signal obtained is for the dash pulse at the seventh storage location. This is a negative pulse followed by a positive pulse. During the following "action" period No. 5, no output is obtained at the seventh location as the potential of the storage surface has not been changed. In the next period, scan No. 5, again the dot pulse on the seventh location is absent but the dash conversion pulse gives a positive output signal. The following action period No. 5 gives a negative output on the dot pulse, leaving the area negatively charged. The actual observed signals are shown and correspond to those predicted. However, a spurious negative signal (one-third of the normal amplitude) occurred in the following "action" line.

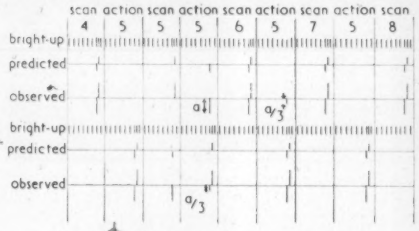

Fig. 7. Radio-frequency mesh raster outputs

In the other case the reverse was arranged so that the "action" line only contained the dash pulse at the seventh storage location. The predicted and observed signals are shown. A similar spurious one-third amplitude signal was also observed. It was apparent that the stability of the individual storage location was not being obtained with a single bombardment; some modification was therefore necessary.

The possibility of changing the stored information in one attempt. In order to stabilize a storage location in one attempt (i.e. one bright-up pulse) we may:

(i) reduce the individual storage location capacity. An optimum capacity is essentially a compromise between various requirements, namely, (*a*) the storage areas do not change potential appreciably during mesh voltage variations unless bombarded with electrons; (*b*) the input capacity connected across the amplifier input terminals should be as low as possible;

(ii) increase the beam current density. The beam current density is a complicated function of many parameters and can be increased by more efficient electron gun design, higher activation resulting in more emission from the cathode, etc. Magnetic focusing would increase the current density but the broader beam travelling along the tube before focusing into a very fine spot would, however, possibly need magnetic deflexion to prevent excessive defocusing at the edges of the raster.[12] Magnetic deflexion would make it difficult to select a particular location in a short enough time. A few experiments were made, and selection was certainly possible when heavy feedback was applied to the current waveform in the deflexion coils. "Ringing" of the coils produced excessive spurious signals at the pick-up plate. These no doubt could be reduced by adequate screening;

(iii) increase the bright-up duration.

Higher beam current density. To satisfy condition (ii) a special long anode fine focus gun was used in a demonstrable system. The heater was over-run to provide maximum cathode current. A storage pattern of the type described in the section on the complete raster was used, and similar output pulses were obtained with a slightly defocused spot. On focusing the electron beam (thereby increasing the beam density), the spurious one-third amplitude pulses completely disappeared, indicating that the new information had been written in one attempt.

Increase of bright-up duration. Condition (iii) was limited by two considerations, firstly by the duration of a digit period, which is limited to 10 μs to provide high-speed operation of the store, and secondly the need for the mesh and beam current modulations to be substantially in or out of phase during bright-up periods. It was decided to investigate the second condition in more detail. Initially the beam current intensity modulated at 5·1 Mc/s was allowed to fall continuously on to the target surface. The mesh as before was subject to a 5 Mc/s waveform. The amplified signal

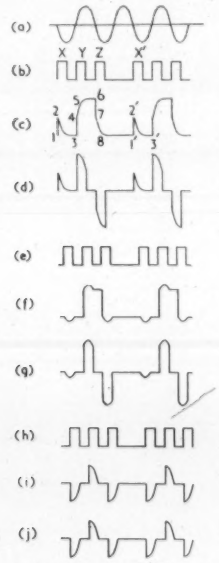

Fig. 8. Predicted waveforms for a single spot

(*a*) effective mesh potential, 100 kc/s; (*b*) bright-up pulses; (*c*) predicted integrated output signal; (*d*) clamped output signal; (*e*) bright-up pulses; (*f*) predicted integrated output signal; (*g*) clamped output signal; (*h*) bright-up pulses; (*i*) predicted integrated output signals; (*j*) clamped signals.

output was integrated, and as the 5 Mc/s mesh waveform had been filtered from the signal, the resultant output, a 100 kc/s sine wave, was a measure of the potential existing at the dielectric surface. Increasing the beam density by increasing the beam current or focusing the beam, the output sine wave could be advanced in phase, confirming that the ability of the storage surface to follow the difference frequency was a function of the beam current density.

The beam current was then interrupted by pulses of 2·5 μs width applied to the cathode-ray tube grid. Thus with dash conversion pulses, the bright-up waveform appeared as a 50 : 50 square wave. No longer could the mesh voltage waveform and the beam current modulation be considered substantially in or out of phase and the resultant storage potentials had to be reconsidered as follows. If it is assumed that the storage location attains its equilibrium potential on electron bombardment, then the prediction of the output signals is simplified.

The predicted output signals for a 1, 0, 1, 0 configuration bombarding a single storage area are shown in Fig. 8. Fig. 8(*a*) shows the difference frequency component of 100 kc/s which is the output which would be obtained if radio frequency were applied to the cathode and mesh, and the grid of the cathode-ray tube was on continuously. This output was a measure of the potential of the storage location. Several outputs are now considered, each associated with a particular timing relationship between applied bright-up pulses and the 100 kc/s difference component.

Consider the predicted integrated output from Fig. 8(*b*). At the end of pulse *X* the storage area is left charged at the maximum negative potential. At the start of pulse *Y* the stable amplitude of the storage element is zero; initially, therefore, we get a positive step 3–4 representing the discharge of the element to zero [Fig. 9(*c*)]. During the *Y* pulse the signal follows the 100 kc/s sine wave as 4–5, so that at the end of pulse *Y*, the storage area is left charged at the full positive potential. When the pulse *Z* starts, again the stable amplitude of the storage element is zero, so a negative edge is obtained (6–7). The output then follows the sine wave 7–8, leaving the storage area charged at the maximum negative potential. At the beginning of the first pulse *X'*, the stable amplitude of the storage element is zero so that a positive edge 1'–2' occurs and the output follows the sine wave as the element moves down to the maximum negative potential 2'–3'; beyond this point the cycle is repetitive.

The waveform shown in Fig. 8(*d*) represents the clamped version of the integrated output signal, the clamp being released during the bright-up periods.

If the phase of the bright-up pulses relative to the difference frequency is as shown in Fig. 8(*e*), then the predicted output waveform is as Fig. 8(*f*). A clamped version of this waveform is shown at Fig. 8(*g*). Similarly the waveforms shown in Fig. 8(*i*) and (*j*) show the integrated and clamped versions caused by the phasing of the bright-up pulses [Fig. 8(*h*)].

Signals for a complete raster can be predicted in a similar manner. Fig. 9 illustrates the predicted integrated and clamped outputs for various phasings of the grid bright-up waveform relative to the difference frequency. There are detail differences between the complete raster and the single spot bombardment.

To use these signals in a store, it is essential to detect the state of the storage area during the period of the initial pulse, so that the second pulse, the dash conversion pulse, can be either present or suppressed. The 0 or 1 information can then be continuously regenerated and thus retained indefinitely in the storage screen surface. It will be seen that the signal shown in Fig. 9(*c*) satisfies these criteria, the 1 state giving a negative signal and the 0 state a positive signal on the initial bright-up pulse. The signal shown in Fig. 9(*e*) gives negative signals on the initial bright-up pulse for both the 1 and 0 state but with a large amplitude discrimination. Fig. 10 shows an actual integrated and clamped signal output traced

from a monitor screen for a 1, 0, 1, etc., raster of spots, and corresponds well to the condition shown in Fig. 9(*e*). The signal shown in Fig. 9(*g*) gives negative signals of the same

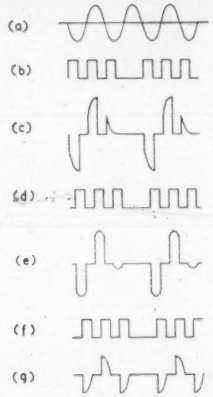

Fig. 9. Predicted waveforms for a raster of spots (Integrating amplifier with clamp)

(*a*) effective mesh potential, 100 kc/s; (*b*) bright-up pulses; (*c*) predicted output signal integrated and clamped; (*d*) bright-up pulses; (*e*) predicted output signal integrated and clamped; (*f*) bright-up pulses; (*g*) predicted output-signal integrated and clamped.

amplitude for both 1 and 0 during the initial bright-up pulse and could not be used in a regenerative store.

Clearly the maximum discrimination is obtained for the signal shown in Fig. 9(*c*) where the signals are of opposite sign. More complex configurations of stored charge patterns

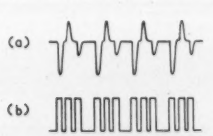

Fig. 10. Single spot bombardment

(*a*) amplifier output signals integrated and clamped; (*b*) bright-up pulses.

similar to Fig. 7 [using the (*b*) phasing] have been investigated, and Fig. 11, an oscilloscope tracing, is an example where a dash pulse is on the seventh storage location on every action line, the remainder of the storage locations being bombarded with a dot pulse.

In Fig. 11 only the action lines are displayed. The superimposed positive signals of the dot pulses in the action line can be clearly seen. The dash pulse in the seventh location is a negative signal followed by a positive signal similar to a 1 pulse in Fig. 9(*c*). An additional positive pulse occurs only once per complete repetition cycle owing to seventh location bombardment by a single dot pulse during the preceding scan period leaving the storage spot at a negative potential. The following initial pulse on the seventh location gives a positive output signal. The small size of this positive pulse indicates that the dot pulse in the preceding scan period is not reaching an equilibrium negative potential. The eighth dot pulse on the action line was enhanced in amplitude owing to inefficient clamping of the integrated output signal between it and the previous dash conversion pulse.

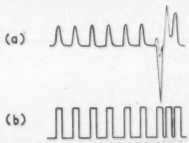

Fig. 11. Raster bombardment. Dash pulse on seventh storage location of "action" line only

(*a*) amplifier output signals integrated and clamped; (*b*) bright-up pulses.

The packing density and read round ratio. Mesh storage systems use only one spot position on the storage surface per digit. The binary information 1 or 0 is stored as positive or negative potential levels on the insulator surface, the levels controlled by the mesh potential during electron bombardment. The non-mesh system[1,2] which depend on redistribution electrons from adjacent spots need two spot positions to record a 1 state. Clearly space has to be left even if a 0 is recorded. The alternative focus-defocus and slight shift also require areas larger than the diameter of a single spot.

As the storage areas are brought closer together, the redistribution electrons caused by bombardment of one spot begin to interfere with storage or adjacent spots. In the case of mesh storage tubes the effect of redistribution electrons is reduced by the presence of the mesh. The main interference of all kinds is most pronounced from the presence of the action line which bombards the chosen line many times more frequently than the adjacent scan lines.

Direct comparison with a normal cathode-ray tube store was difficult as most of the experiments were performed with a spot diameter of the order of 1 mm and an eight-line raster, whereas the normal cathode-ray tube store has a spot diameter less than $\frac{1}{2}$ mm; further there are thirty-two lines on the normal store with a correspondingly higher number of action periods per complete cycle. A few tests were made in which the raster size was reduced progressively until the interference was no longer tolerable. It was estimated that the coplanar mesh storage tube would permit a digit packing density at least twice that used in redistribution type stores.

CONCLUSION

Two-state information can be stored as a charge pattern on the surface of a special target. This target consisted of a sheet of mica on to which a coplanar conducting mesh (fence) had been evaporated. It operated essentially as a mesh type store, except that the coplanar mesh was, by virtue of its construction and location, a more economic proposition than a normal closely spaced structure. Signals indicating the presence of a 1 or 0 were of opposite sign. The writing of a 1 or 0 was controlled by the timing of the cathode-ray tube grid bright-up pulses alone. This meant that transient voltages were eliminated in the vicinity of the sensitive

amplifier input. The packing density was greater than normal cathode-ray tube stores because the area required to store one digit is defined by one minimum spot diameter, and because the mesh reduces the spread of secondary electrons from adjacent spots.

In a normal type cathode-ray tube store, the amplitude of the signal, or rather the "depth of the well," was fixed by the velocity distribution of the emitted secondaries. This was not the case in the coplanar mesh store; the amplitude of the signals could be varied as the mesh waveform amplitude was changed, provided sufficient bright-up time was allowed.

The speed of operation of a Williams–Kilburn store is limited by the redistribution electrons which need a 4 μs interval to set up stable conditions at the storage spot. In mesh tubes this limitation does not apply. The limit of speed is set by the available beam density. It appears, however, that with the beam density readily available the rather high capacity of the mesh storage surface offsets this advantage, and a large increase in speed is not readily available. It might, however, be achieved by redesign of the storage surface and the development of better electron guns.

ACKNOWLEDGEMENT

The author wishes to acknowledge his indebtedness to Prof. F. C. Williams, Dr. T. Kilburn and Dr. C. N. W. Litting for their advice and encouragement.

REFERENCES

(1) Williams, F. C., and Kilburn, T. *Proc. Instn Elect. Engrs*, **96** (III), p. 81 (1949).

(2) Williams, F. C., Kilburn, T., Litting, C. N. W., Edwards, D. B. G., and Hoffman, G. R. *Proc. Instn Elect. Engrs*, **100** (II), p. 523 (1953).

(3) Jensen, A. S., Smith, J. P., Mesner, M. H., and Thory, L. E. *R.C.A. Rev.*, **9**, pp. 112–135 (1948).

(4) Dodd, S. H., Klenperer, H., and Youtz, P. *Elect. Engng*, **69**, pp. 990–995 (1950).

(5) Forrester, J. W. *Symposium of Large Scale Calculating Machinery*, pp. 125–129 (Cambridge, Mass.: Harvard University Press, 1948).

(6) Parker, C. V. *Proc. Inst. Radio Engrs*, **39**, p. 900 (1951).

(7) Holt, A. W., and Write, J. H. *Progress Report on Electrostatic Storage*, Report No. 1082 (Washington: National Bureau of Standards, 1951).

(8) Heydt, H. L. *Rev. Sci. Instrum.*, **21**, p. 639 (1950).

(9) McKay, K. G. *J. Appl. Phys.*, **22**, p. 89 (1951).

(10) Litting, C. N. W. *J. Appl. Phys.*, **5**, pp. 219–293 (1954).

(11) Harrington, J. V. *J. Appl. Phys.*, **21**, p. 1048 (1950).

(12) Moss, H. *J. Brit. Instn Radio Engrs*, **6**, No. 3, p. 99 (1946).

(13) Haeff, A. V. *Electronics*, **20**, pp. 80–83 (1947).

(14) Schagen, P. *Phillips Res. Rep.*, **6**, p. 135 (1951).

APPENDIX

Manufacture of the coplanar mesh. Freshly cleaved mica was used as the insulator surface for the mesh storage experiments. Fig. 12 shows the mask used to shield part of the mica during evaporation of the silver "fence." The main

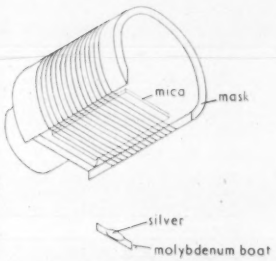

Fig. 12. The mask

structure was made of steel. A fine thread was cut into the surface of the metal and a copper wire was wound into the grooves. The thickness of the wire chosen was such that the mark to space ratio was 10 : 1. Silver was evaporated under vacuum from an electrically heated molybdenum boat. The mask wires were lined up with the length of the boat to minimize penumbra effect. In use, the mark to space ratio improved as the number of evaporation processes increased, owing to the deposition of silver on the surface of the copper wires.

In the sealed-off tubes, trouble was experienced due to globulation of the silver bars when the target surface was heated in a nitrogen atmosphere during the glass pinch sealing. This difficulty was overcome by depositing a thick layer of silver which, even after globulation, was still continuously conducting because the globules were in electrical contact. Unfortunately too thick a layer tended to peel off the mica. To ensure that the "fence" was conducting after sealing in, the surface was preheated, globulated, and the resistance measured before the sealing process. Great care was essential to ensure good contacts to both the "fence" and the evaporated "pick-up plate." Poor contacts deteriorated considerably during the sealing-in processes.

Correspondence

The determination of base thickness in alloy junction transistors by etching

During a study of factors influencing the geometry of indium *p–n* alloy junctions in germanium, it was found that a short C.P.4 etch[1] (of the order of 20 s) precisely indicated the *p–n* junction formed. Fig. 1 (p. 112) shows the etched surface of a junction which was mounted in sealing wax and ground down until a cross-section through the middle of the junction was obtained. The *p–n* junction is shown by a fine line, which at higher magnification was seen to be a sharp step, about 5 μ high. Impure (indium-saturated) germanium was in this case etched more slowly than pure germanium, an unexpected result which is probably an electrochemical effect due to the presence of metallic indium. The step is sharp since there is a concentration change from about 10^{20} to 10^{15} impurity atoms/cm^3 occurring over a distance of about 250 Å.

An extension of this method has been applied to alloy junction transistors. Indium at the collector and emitter was dissolved off with mercury and nitric acid. The transistor was then mounted under pressure in a thermoplastic material, and ground and polished so that a cross-section through the middle of the transistor was exposed. Fig. 2 (p. 112) shows the result obtained on a germanium *p–n–p* transistor by a 30 s C.P.4 etch, where the emitter and (larger) collector junction are clearly visible. After indium had been removed, it was always found that impure germanium was more quickly etched than pure germanium, in agreement with the observation of Rösner.[2] Also, a slightly longer etching time was needed to show up the junctions.

The effective base thickness of the transistor shown in Fig. 2 has been measured by Mr. R. L. Rouse of this Laboratory, using the diffusion capacity method.[3] After correction for the space-charge layer of the collector (calculated from the resistivity of the *n*-type material and the collector voltage), a value of $2{\cdot}3 \pm 0{\cdot}05 \times 10^{-3}$ in. was obtained. The dimensions of the base region, obtained from the photomicrograph shown in Fig. 2, were used to calculate an effective base thickness by a method similar to that of Kansas,[4] assuming that the collector is flat and the emitter dished. The calculated effective base thickness was $2{\cdot}4 \pm 0{\cdot}1 \times 10^{-3}$ in. which is in reasonable agreement with the electrical measurements, and confirms that the lines observed correspond to *p–n* junctions.

A similar effect has been observed here with aluminium *p–n* alloy junctions in silicon, and recently Fowler and Levesque[5] have measured the base thickness of grown *n–p–n* silicon crystals by a combination of C.P.4 and electrolytic etching.

The author is grateful to Mr. R. L. Rouse for supplying a transistor of known base thickness, Dr. N. C. Welsh for advice on mounting and polishing techniques, and Dr. E. Billig for suggesting the problem. Thanks are due to Dr. T. E. Allibone and the Admiralty for permission to publish this paper.

Research Laboratory, J. ROLFE
Associated Electrical Industries, Ltd.,
Aldermaston, Berks.

REFERENCES

(1) HAYNES, J. R., and SHOCKLEY, W. *Phys. Rev.*, **81**, p. 835 (1951).
(2) RÖSNER, O. *Z. Metallkunde*, **46**, p. 225 (1955).
(3) HEROLD, E. W. *Brit. J. Appl. Phys.*, **5**, p. 115 (1954).
(4) KANSAS, R. *Proc. Inst. Radio Engrs*, **41**, p. 1712 (1953).
(5) FOWLER, A., and LEVESQUE, P. *J. Appl. Phys.*, **26**, p. 641 (1955).

Current distribution in an expanding spark channel

During the course of a study of the multiplicity which has been observed[1] in the anode marks left by transient high current discharges in air at atmospheric pressure when the rate of rise of current is very large (approximately 10^8 A/s), we have encountered a phenomenon which appears to give some information about the distribution of current throughout the spark channel during its initial period of expansion.

When we began to make systematic measurements of anode mark multiplicity we found that it depended markedly on the state of the anode surface and, in order to obtain consistent and reproducible results, it was necessary to control this surface state. To do this, the anode surface was first thoroughly cleaned and then a number of monolayers of barium stearate were deposited on it by the well-known Langmuir–Blodgett[2] process. It was then found that the degree of multiplicity of the anode mark depended chiefly on the initial rate of rise of the current and on the number of layers of barium stearate, and that it depended only to a very minor extent on other variables such as the anode material, the spark length or the total current.

When about fifteen or twenty layers of barium stearate are present on the anode surface, multiplicity is considerably enhanced and, if the time during which the current is allowed to flow is varied and the corresponding changes in the typical anode mark pattern are observed, it is possible to draw some inferences about the distribution of current in the channel at various times. The figure (p. 111) shows a series of photographs of anode marks left by arcs of different durations. In each case the current rose to a maximum of 36 A in about 0·2 μs, thereafter remaining constant for a time which could be varied and which is indicated under each photograph. It will be noticed that the spots forming the mark of the 2 μs arc are more or less uniform in distribution and size, with a tendency already noticeable for the outer spots to be larger than the inner ones. In the next mark the outer spots are decidedly larger, and in the mark of the 8 μs arc the outer spots have enlarged further and joined into a nearly complete ring around the still small central spots. By 20 μs the outer spots have melted further, and perhaps moved back, and the inner spots have been obliterated by the melting. The last two photographs of the sequence show the further development of the mark with time, all trace of the original multiple structure finally being lost.

These photographs, which are typical and are of uniform magnification, suggest that after about 2 μs most of the energy, and presumably most of the current, flows into the anode in a ring near the outside of the channel, and that this state of affairs persists for perhaps 10 μs, after which the current becomes more uniformly distributed or perhaps concentrates again towards the centre. Apparently, during or immediately after the passage of the initial shock wave described by Drabkina[3] and others[4–7] which leaves a low density at the centre of the channel, conditions are more favourable to

conduction of high currents near the outer boundary of the channel than in the centre. This might be due to the transfer of the initial ionization outwards with the shock wave or to the limit imposed on the central conductivity by the low density existing there. It might be thought that skin effect would contribute appreciably to this peripheral current distribution, but a simple calculation suggests that its influence would be small, and observations with a current pulse rising much more slowly (in 1 μs), although showing a change in multiplicity, do not show any marked change from the general behaviour described above.

After the initial expansion, gas molecules and ions will move back into the central low density region and equilibrium will be established. As this takes place the current distribution changes as indicated by the last three photographs.

The variation with time of the current distribution suggested by these observations is strikingly similar to the variation in light intensity from a hydrogen spark channel described by Craig and Craggs.[8] Similar concentration of intensity towards the channel periphery has not, however, been reported for any gas except hydrogen.

A more detailed account of this work, including a fuller account of the influence of rate of current rise and of anode surface layer thickness on anode mark multiplicity, will be published in the future.

University of New England, New South Wales, Australia.

J. M. Somerville
C. T. Grainger

REFERENCES

(1) Somerville, J. M., Blevin, W. R., and Fletcher, N. H. *Proc. Phys. Soc.* [*London*] *B*, **65**, p. 963 (1952).
(2) Langmuir, I. *Proc. Roy. Soc. A*, **170**, p. 1 (1939).
(3) Drabkina, S. I. *J. Exp. Theor. Phys. USSR*, **21**, p. 473 (1951).
(4) Abramson, I. S., and Gegechkori, N. M. *J. Exp. Theor. Phys. USSR*, **21**, p. 484 (1951).
(5) Gegechkori, N. M. *J. Exp. Theor. Phys. USSR*, **21**, p. 493 (1951).
(6) Boyle, W. S. *J. Appl. Phys.*, **26**, p. 584 (1955).
(7) Olsen, H. L., Edmonson, R. B., and Gayhart, E. L. *J. Appl. Phys.*, **23**, p. 1157 (1952).
(8) Craig, R. D., and Craggs, J. D. *Proc. Phys. Soc.* [*London*] *B*, **66**, p. 500 (1953).

Decomposition of $CaSO_4 . 2H_2O$ in the electron microscope

Changes in the appearance and chemical composition of certain inorganic compounds, as the result of exposure to the electron beam in an electron microscope, have been reported by Burton, Sennett and Ellis* and by Fischer.†

Similar changes have been observed to take place in samples of Witwatersrand mine dusts when examined in the electron microscope. Calcium sulphate was suspected to be one of the principal constituents of these dusts. In order to detect the presence of this substance by electron diffraction, it became important to determine the changes produced in calcium sulphate by exposure to the electron beam.

Specimens of chemically pure $CaSO_4 . 2H_2O$ were prepared by making a solution of this substance in water, placing one drop on a specimen grid covered with a collodion film, and removing the excess with filter paper. The specimens were finally dried in the high vacuum of the electron microscope.

Electron micrographs and selected area electron diffraction patterns were recorded, care being taken not to subject the specimen to more than the minimum beam intensity. A typical electron diffraction pattern is shown in Fig. 1(*a*) (p. 111). The beam intensity was then increased until a point was reached where intense activity in the specimen was observed. After a few seconds the specimen was observed to become more transparent and the activity to become less intense. After reducing the beam intensity, electron micrographs and diffraction patterns were again recorded. A typical electron diffraction pattern is shown in Fig. 1(*b*) (p. 111).

The interplanar spacings and intensities obtained from measurements on the diffraction patterns taken before and after exposure to the high beam intensity are shown in Tables 1 and 2 respectively. Spacings of intensities for the X-ray diffraction patterns of $CaSO_4$, CaS and CaO obtained from the A.S.T.M. card index are given for comparison. The intensities are expressed as percentages of the intensity of the strongest line.

Table 1. *Interplanar spacings and intensities before exposure to a high beam intensity*

Observed		*A.S.T.M. index for* $CaSO_4$	
$I/I_0 \times 100$	*d*	$I/I_0 \times 100$	*d*
100	3·48	100	3·49
10	3·12	3	3·11
100	2·86	70	2·85
10	2·45	7	2·46
20	2·33	30	2·32
20	2·21	30	2·20
10	2·09	10	2·08
10	1·98	10	1·99
10	1·93	4	1·93
20	1·86	30	1·86
10	1·74	20	1·74

Table 2. *Interplanar spacings and intensities after exposure to a high beam intensity. Note decomposition into CaS and CaO*

Observed		*A.S.T.M. index*			
		CaS		*CaO*	
$I/I_0 \times 100$	*d*	$I/I_0 \times 100$	*d*	$I/I_0 \times 100$	*d*
30	2·86	100	2·84		
60	2·76			60	2·76
100	2·39			100	2·39
30	2·00	100	2·00		
80	1·70			60	1·69
10	1·63	50	1·63		
20	1·44	20	1·42	20	1·45
20	1·37			20	1·38
10	1·26	60	1·27		
10	1·20			10	1·20
10	1·15	30	1·16		
10	1·09			7	1·10
30	1·07			30	1·07
20	0·97			13	0·98

It appears that the $CaSO_4 . 2H_2O$ loses its water to become anhydrous $CaSO_4$ after insertion in the microscope, probably

* Burton, E. F., Sennett, R. S., and Ellis, S. G. *Nature* [*London*], **160**, p. 565 (1947).
† Fischer, R. B. *J. Appl. Phys.*, **25**, p. 894 (1954).

Current distribution in an expanding spark channel

From J. M. SOMERVILLE and C. T. GRAINGER

(*See pages* 109–110)

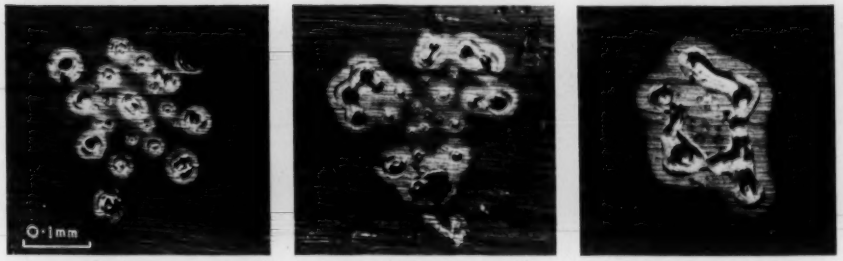

2 μs 4 μs 8μs

20 μs 30 μs 50 μs

Anode marks left on a contaminated palladium anode by transient arcs of increasing duration

---

Decomposition of $CaSO_4 \cdot 2H_2O$ in the electron microscope

From J. H. TALBOT

(*See pages* 110–113)

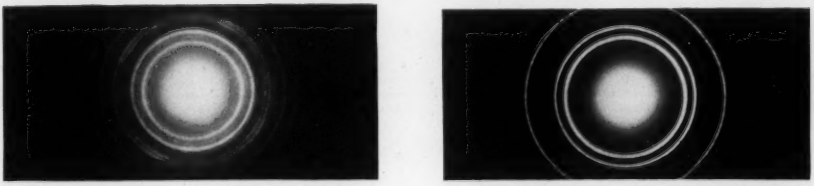

(*a*) (*b*)

Fig. 1. Electron diffraction patterns of calcium sulphate (*a*) before exposure to high beam intensity, and (*b*) after exposure to high beam intensity ($L\lambda = 3{\cdot}36 \times 10^{-8}$ cm^2)

The determination of base thickness in alloy junction transistors by etching

From J. ROLFE

(*See page* 109)

Fig. 1. Indium *p–n* alloy junction in germanium, 20 s C.P.4 etch. Magnification × 75

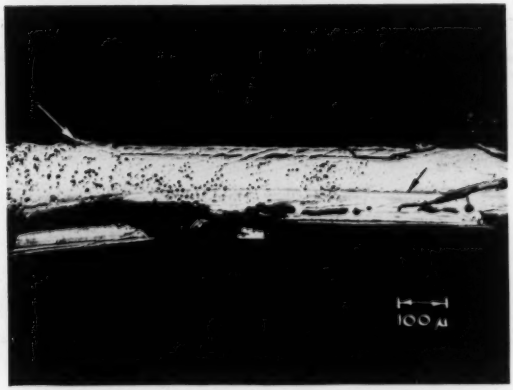

Fig. 2. Cross-section through germanium *p–n–p* transistor, 30 s C.P.4 etch. Emitter (upper) junction and collector (lower) junction indicated by arrows

on account of the high vacuum. Intense electron bombardment causes further decomposition into CaS and CaO, with an accompanying increase in the transparency of the specimen.

Transvaal and Orange Free State Chamber of Mines, Johannesburg, South Africa. J. H. TALBOT

A replica technique for "reflexion" electron microscopy

I read with interest the paper by Mr. Bradley on the method of preparing electro-deposited replicas for reflexion microscopy published on p. 191 of the June 1955 issue of this *Journal*. We have not in our laboratory had experience of the particular application that Mr. Bradley describes, but have produced electro-formed copper negatives from silver-coated plastic articles. In his paper Mr. Bradley lists a number of reasons why the electro-deposited film may penetrate the base conducting coating and form a deposit between the silver and the substrate. Whilst we do not disagree with his views, we have found that unsatisfactory electro-forming of plastics generally occurs when the base is plasticized. For example, when electro-depositing on either cellulose acetate (containing plasticizers) or cellulose nitrate (containing castor oil) we have found that there was a tendency for the plasticizer to seep through pores in the evaporated metal film. Further, that the adhesion of the evaporated coating varied over the plastic surface depending on the degree to which plasticizer had migrated to the surface. When the article was electro-deposited it was possible for the electro-deposit to form under the metal film or fail to form in regions where the plasticizer had seeped through the film.

We have found it useful to remove plasticizer from the surface of a plastic master by washing in a detergent prior to evaporating silver, followed by a second cleaning with a detergent prior to electro-plating. In one application we were concerned with preparing electro-deposited negatives of gramophone master disks which had been made from a lacquer coating of a heavily plasticized material. Only when the master was processed in the manner described above was it possible to produce recordings free from noise. Although the vacuum deposition technique is no longer used for metallizing lacquered master disks, the experience we have gained may be of value to those concerned in producing replicas for microscopy.

Research Laboratory, Edwards High Vacuum Ltd., Crawley, Sussex. L. HOLLAND

The square wave response method of analysing process control systems

In the previous volume of this *Journal*[1] Dr. L. Mandel presented a very interesting paper in which he showed that the frequency response for a process may be easily derived from measurements with a square wave input by making certain approximations. The errors were not evaluated analytically but determined on a system consisting of a single exponential stage, where the approximations were considered weakest. However, there was a certain discrepancy in the calculated amplitudes at medium frequencies in spite of the fact that in some cases more than six terms were used in the approximating series. Although the accuracy is good for high-order systems it may be of interest to point out that merely a slightly different definition of the amplitude of the output will increase the accuracy considerably for low order systems.

In the paper one of the parameters measured in the output was the maximum amplitude P (Fig. 1). In the text below equation (10) the assumption was made that the maximum

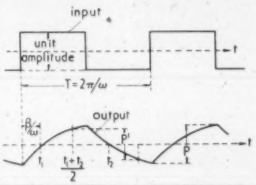

Fig. 1. Definition of symbols

amplitude occurred in the middle of the interval $t_1 - t_2$ between two zero points. This apparently is true at very low and very high frequencies but not at intermediate frequencies, where the approximation also turned out to be less good for the first-order system. This observation suggests that one should define the amplitude as the value P' of the output at the time $\frac{1}{2}(t_1 + t_2)$ (see Fig. 1) instead of the maximum value P. The new definition will make the above-mentioned assumption unnecessary and tend to decrease the errors at intermediate frequencies.

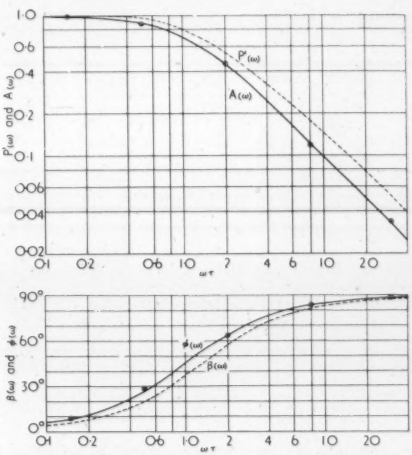

Fig. 2. Sinusoidal response curves (full curves) and values calculated from the series (circles) for a single time-lag

In the case of a single time-lag with the time constant τ P' as a function of ω is calculated from the following equation:

$$P'(\omega) = 1 - \exp(-\pi/2\omega\tau) \qquad (1)$$

$\beta(\omega)$ is given by equation (17) in Dr. Mandel's paper

$$\beta(\omega) = \omega\tau \log\left[\frac{2}{1 + \exp(-\pi/\omega\tau)}\right] \qquad (2)$$

These quantities are plotted in Fig. 2 as broken curves and the sinusoidal response as full curves. Some points on the sinusoidal response curves calculated with four terms of the approximative series (12) and (13) in Dr. Mandel's paper but with P' inserted instead of P are shown by circles in Fig. 2.

The calculation shows that the method proposed in Dr. Mandel's paper yields very good accuracy even for a single capacity system if the amplitude is measured as suggested above. However it should be pointed out that for processes where disturbances are present, some means of measuring mean values over a long period of time has to be used in order to get good accuracy,[2,3] and that for systems with an oscillatory response, the proposed method may possibly give greater errors than for the single time-lag system investigated.

Allmänna Svenska Elektriska Aktiebolaget, E. PERSSON
Västerås, Sweden.

I should like to thank Mr. E. Persson for his very interesting and constructive comments on my paper. The parameter P—the maximum response amplitude—was introduced for the practical reason that it is easy to measure. This is not without importance when one is confronted with a typical chart record of a process response curve containing the usual superimposed fluctuations. The popularity of the frequency response as compared with the step response method of analysis is no doubt largely due to the ease with which the relevant information can be extracted from the response curves. The introduction of P led to approximate formulae, whose accuracy decreased with the order of the system under investigation. The approximations were, however, justified by the very reasonable accuracy obtainable even with a second-order system.

It is nevertheless most gratifying to learn that a slightly redefined amplitude P', which leaves all the equations unaltered, leads to very good accuracy even with a first-order system. Mr. Persson's computed curves for a single transfer stage are impressive and his parameter P' would certainly be the one to use for processes that are not too much troubled by disturbances.

Department of Physics, L. MANDEL
Imperial College of Science and Technology,
London, S.W.7.

REFERENCES

(1) MANDEL, L. *Brit. J. Appl. Phys.*, **6**, p. 291 (1955).
(2) ALMSTRÖM, K., and GARDE, A. "Investigation by frequency analysis of the Swedish network," Cigré-report No 315, part 3, pp. 23–36 (1950).
(3) GARDE, A., and PERSSON, E. "Experimental frequency analysis of servo elements," *Asea Journal*, **23** (12), pp. 163–166 (1950).

Ferrites in resonant cavities

Several authors[1–5] have published formulas for the frequency shift on introducing a sphere of ferrite into a resonant cavity. In all cases, the assumption has been made that the field in the ferrite can be taken as approximately equal to the unperturbed field, and the formulas are found to be of the form

$$\delta\omega/\omega = (\mu - 1 \pm \alpha)(A/3)(V_1/V_0) \qquad (1)$$

where V_1 is the volume of the ferrite, V_0 is the volume of the cavity, A is a numerical constant depending on the cavity dimensions and mode of oscillation, and μ and α are the diagonal and off-diagonal elements, respectively, of the (relative) permeability tensor. The plus and minus signs are to be taken for the right- and left-circularly polarized modes, respectively.

Using Polder's formulae for μ and α[6], $(\mu + \alpha)$ becomes infinite for an applied field H given by

$$H = H_0 + (4\pi I/3) \qquad (2)$$

where I is the saturation magnetization and H_0 is defined by

$$\gamma H_0 = \omega_0 \qquad (3)$$

Here ω_0 is the frequency at which ferromagnetic resonance occurs in the cavity, when the polarizing field is H_0, and γ is the gyromagnetic ratio. It will be seen from equation (2) that H is the value of applied field for which the internal field becomes equal to H_0. It is to be noted here that, for the right-circularly polarized mode, infinite frequency shift is predicted by equation (1) when the applied field is given by equation (2). But, as pointed out by Polder,[6] ferromagnetic resonance occurs, for a sphere, at a frequency γH_0, when the applied field is H_0.

The reason for the discrepancy is that the assumption made above is only valid if $\mu \simeq 1$ and $\alpha \ll 1$, i.e. when the polarizing field differs considerably from H_0; the conclusions drawn about the behaviour of the frequency shift for polarizing fields of the order of H_0 are not justified.

The present writer has performed the perturbation calculation, using the calculated value of the field in the ferrite, and the frequency shift is now found to be

$$\frac{\delta\omega}{\omega} = \frac{\mu - 1 \pm \alpha}{\mu + 2 \pm \alpha} A \frac{V_1}{V_0} \qquad (4)$$

If α is put equal to zero, this reduces to the well-known formula for an isotropic magnetic material. It will be seen that infinite frequency shift is predicted for $\alpha = (\mu + 2)$ for the left-circularly polarized mode, and for $\alpha = -(\mu + 2)$ for the right-circularly polarized mode. The case $\alpha = (\mu + 2)$ does not occur, while $\alpha = -(\mu + 2)$ when the applied field is equal to H_0. Thus the left-circularly polarized mode should never show an infinite frequency shift, while the right-circularly polarized mode should do so at $H = H_0$. This behaviour has been observed.[3]

Details of this calculation will be published elsewhere in due course.

Marconi's Wireless Telegraph Co. Ltd., R. A. WALDRON
Chelmsford,
Essex.

REFERENCES

(1) SPENCER, E. G., LE CRAW, R. C., and REGGIA, F. *J. Appl. Phys.*, **26**, pp. 354–5 (1955).
(2) SPENCER, E. G., LE CRAW, R. C., and REGGIA, F. *Convention Record of the Institution of Radio Engineers*, Part 8, pp. 113–21 (1955).
(3) ARTMAN, J. O., and TANNENWALD, P. E. *Phys. Rev.*, **91**, pp. 1014–15 (1953).
(4) ARTMAN, J. O., and TANNENWALD, P. E. *J. Appl. Phys.*, **26**, pp. 1124–32 (1955).
(5) LAX, B., and BERK, A. D. *Convention Record of the Institution of Radio Engineers*, Part 10, pp. 70–74 (1953).
(6) POLDER, D. *Phil. Mag.*, **40**, pp. 99–115 (1949).

Note added in proof. The attention of the writer has been called to a letter by J. H. Rowen and W. von Aulock [*Phys. Rev.*, **96**, pp. 1151–3 (1954)], in which an equivalent formula to equation (4) is stated without proof.

New books

General aspects of radio interference. British Standard Code of Practice CP 1006: 1955 (London: British Standards Institution). Price 10*s*.

The population of this country regards radio and television as normal, almost essential, services. Interference to them is a national problem. More restricted, but intrinsically more important, are the safety services such as navigational aids for ships and aircraft. The Wireless Telegraphy Act of 1949 gives the Postmaster General powers to make regulations which will restrict the use of interfering apparatus. He has made regulations under this act with respect to ignition systems, refrigerators and small motors. To avoid hardship and ensure practicability in a subject about which the average person knows very little, statutory regulations must be hedged about with safeguards. Furthermore this country is lucky in enjoying high broadcast field-strengths which reduce the severity of interference. Thus progress in reducing interference requires a great background of technical information and advice directed towards those capable of using it. Part is supplied by publications and the reports of bodies such as the G.P.O., B.B.C. and E.R.A. Part is supplied by British Standards which show how to measure interference and the limits to which it should be abated in various instances. In addition to the foregoing, there is need to explain as simply but as comprehensively as possible how interference can be reduced. This is appropriate not to regulations or to standards or to specialized technical reports but to a code of practice. The present code of practice covers the ordinary wavelengths for sound broadcasting and the television wavelengths 41 Mc/s to 68 Mc/s in Band I. Experience is inadequate in Bands II and III, consideration of which is deferred to a later revision. The code covers most types of interfering appliance, but excludes ignition systems and apparatus which normally and essentially generate radio frequency energy, such as transmitters, receivers, industrial, scientific and medical equipment using radio frequencies.

The code briefly describes how interference is generated and transmitted and how different kinds can be recognized. It deals with action which can be taken at the receiving site but most of the code is devoted to the different ways in which the interference may be abated at the source. The code draws attention to the need for the proper design and maintenance of electrical installations. A surprisingly large number of complaints arise from inadequate maintenance. The sharing of the responsibility for interference abatement between the listener or viewer and the user of appliances is emphasized. The code is well written and attractively illustrated. It is timely and valuable: it ought to be widely disseminated.

S. WHITEHEAD

Diffusion in Metallen. 2nd Ed. By W. SEITH in collaboration with TH. HEUMANN. (Berlin: Springer-Verlag, 1955.) Pp. vi + 306. Price *DM*39.

This book is a second and extended edition of the text first published in 1940. Despite the gap caused by the war there has been a healthy and accelerating development in this interesting and technically significant field. The time is past, in the reviewer's opinion, when a single monograph can, without being overlong, do adequate justice to the subject of diffusion in condensed phases. The present account, in agreement with this view, is confined to material transport phenomena in metallic phases. The arrangement is good, and the following typical sectional headings give an idea of the development.

A section on Fick's laws and on definitions is followed by a discussion of experimental methods, some of which are of post-war origin. A chapter summarizing the experimental data, and especially Table 1, will be found a very useful reference source. Some other topics in order are: general theory of place change processes; concentration dependence of diffusion coefficients, D; measurements of D when there is a volume change; relations between D for self-diffusion and diffusion of foreign atoms in binary mixed crystals; partial diffusion coefficients; course of diffusion in multiphase systems; direction-sensitivity of D in non-isotropic crystals; surface and grain-boundary diffusion. Among other sections are some which discuss processes closely related to diffusion, such as sintering, technical applications, and transport in alloys.

Certain of the sections and chapters are rather sketchy. For example, that on diffusion of gases in metals is so limited that it might well have been omitted. The section on surface diffusion is also rather limited, perhaps in part because the textual matter has been drawn only from metallic systems. The same might be said of the discussion on sintering. There is, however, no doubt that this monograph fills a gap, that it is up to date in most of what is discussed, and that it provides a very useful reference source and commentary in the selected field.

R. M. BARRER

Multipole fields. By M. E. ROSE. (London: Chapman and Hall Ltd., 1955). Pp. viii + 99. Price 40*s*.

Workers in theoretical atomic and nuclear physics have been making increasingly wide use of an angular momentum description of phenomena. This is due in no small part to the development of powerful analytical tools, based on group theory. These enable problems which appear highly complex to be reduced to manageable forms, and the results to be expressed in terms of simple algebraic functions which have been tabulated extensively. Dr. Rose has been long associated with this work, and the present volume is a valuable addition to the literature, although of interest primarily to the theoretician. It is confined to a description of electromagnetic interactions, but the extension to other fields, such as β-decay, is fairly obvious.

After a preliminary discussion of the Maxwell equations and angular momentum operators, the concepts of spherical tensors are introduced. These are applied in detail to the problems of internal conversion and γ-ray emission. Not least in value is a discussion of gauge invariance, and an appendix devoted to sign conventions. It is, however, to be regretted that no mention was made of the Hermitian conjugate properties of the tensor operators used.

G. R. SATCHLER

Messen und Rechnen in der Physik. By ULRICH STILLE. (Braunschweig: Friedr. Vieweg and Sohn., 1955.) Pp. viii + 416. Price *DM*54.

Dr. Stille's book is a very thorough and detailed compendium of the dimensions and systems of physical quantities. The main part of the book is taken up with an analysis of the various systems and the derivation of quantities in these systems as well as with critical discussions of their relative merits and disadvantages. The material is grouped into

sections on mechanics, heat, electricity and magnetism and sound and light respectively. There follow two chapters on standards and physical constants and finally thirty-five conversion tables for the various systems and units. The author has gone far beyond providing merely a reference book, but has made a detailed study of the subject involving the historical development. His book is more likely to appeal to the student of physical units and systems than to their average user. The book may well justify the author's hope that by a clear exposition which covers the whole field of physics future discussions on systems and units may be simplified.

K. MENDELSSOHN

Modern physics for the engineer. Edited by LOUIS N. RIDENOUR. (New York: McGraw-Hill Book Company, Inc., 1954.) Pp. xix + 499. Price 53*s.* 6*d.*

Publishers usually tend to regard without enthusiasm books based on lecture courses. The publishers, showing commendable perspicacity, heard of this lecture course, and sought it as a book. Roy Weller's introduction must have allayed any doubts that may have remained concerning the project. Two of his comments bear on the aim and value of such a lecture course and book: "new ideas seldom occur to thoroughly compartmented people" and "Before the war the delay experienced between scientific discovery . . . and common application in engineering was, in many cases, nearly a generation." The titles of the three parts into which the book is divided should spell the end of "compartmentation" for the attentive reader: they are "The laws of nature," "Man's physical environment" and "Information and its communication." The coverage is remarkable yet each of the eighteen chapters is by an acknowledged expert, and gives a stimulating, succinct account of the subject, and sometimes a quite fascinating one, as is that of Seitz on the physics of the solid state. In addition to this last, Part 1 comprises chapters on relativity, atomic structure, magnetism, microwave spectroscopy, nuclear structure, electronuclear machines, elementary particles, and the active elements and nuclear power. The chapters naturally cannot give a working knowledge of the subject; that is not their purpose. They give an overall picture which is so presented as to leave the reader with an appetite for more. In this connexion it is curious that there is so little uniformity in the matter of references, or suggestions for further reading. Some chapters offer no help at all in this respect, while others not only list texts for further reading, but give detailed references in the text to individual papers as well, which would have been a desirable conclusion to all the chapters.

The section on our physical environment comprises chapters on astrophysics, high pressure phenomena and their bearing on geophysics, the sea bed, thunderstorms and lightning, and transient phenomena in supersonic flow. Though "astrophysics" had to be treated in under forty pages since the section title is "Man's physical environment" one would have expected room to be found for the fairly recent and surprising discoveries concerning the sun's outer atmosphere, and surely a word or two at least on radio astronomy. The writer hopes that some of the engineers addressed asked Professor Loeb to explain how it comes about that "1- to 4-kV/cm gradient is necessary to keep the current of 5 to 600 A flowing down the channel" of the lightning leader stroke, and would himself like to know the answer.

Chapters on electrons and waves, semiconductor electronics, communication theory and computing machines complete the book, the last being an excellent account of this important field, which commendably spares two valuable pages in homage to Babbage. The engineers addressed must have found the course a stimulating experience. The writer can speak for three physicists who have found the reading of the book, or parts of it, likewise stimulating. It is well and clearly illustrated, and a pleasure to handle.

C. E. R. BRUCE

Proceedings of the international conference of theoretical physics, 1953 Kyoto and Tokyo. (Tokyo: Science Council of Japan, 1955.) Pp. xxviii + 942. Price $10.00.

The scope of this detailed record is unusually wide: part 1 is concerned with field theory and elementary particles; part 2 with nuclear physics; part 3 with statistical mechanics; part 4 with molecules and solids; part 5 with liquid helium and superconductivity.

About 120 substantial contributions were made and there is a full record of the subsequent discussion. Some contributions are essentially original papers which would have been published anyway. The special value of this volume is that it contains many expert surveys of the important fields of work and that there is a high level of discussion and criticism. So many papers in theoretical physics are being published at present that no research worker can read more than a fraction of the total, much less assess its significance. Thus we depend more and more on survey articles and on conferences to get a general picture of progress in physics and to appreciate the nature of the outstanding problems. This makes it very useful to have a detailed report available.

Production of the record of the conference proceedings evidently required much careful reporting and editorial work by many Japanese physicists, who are to be congratulated on its appearance. The presentation and printing are good.

K. J. LECOUTEUR

Year book of The Physical Society, 1955. (London: The Physical Society.) Pp. 92. Price 10*s.*

This year book contains the special lectures delivered before the Society (67 pages), obituaries, the formal proceedings of meetings, annual report of Council and accounts for 1954. The special lectures open with the Presidential address entitled "Progress and problems in physics today," by Professor H. S. W. Massey. The first part of this very readable address describes a selection of remarkable achievements in recent research in physics which illustrate the very advanced state of technique today, and the second part is concerned with some of the serious problems raised by this rapid expansion of research in physics. Professor P. M. S. Blackett's 1954 Rutherford Memorial lecture is concerned with the ways in which the study of Rutherford's career can help in present-day problems. Professor E. C. Stoner's Guthrie lecture is on magnetism in retrospect and prospect and is a valuable addition to the literature. The Thomas Young oration by Dr. W. S. Stiles describes and discusses a new determination of the colour-matching functions and is well worthy of previous orations in this series. Among the obituary notices are to be found personal reminiscences of G. F. C. Searle and Albert Einstein by people who knew them well. Altogether the book is good value for the money even though only a few pages could interest any one reader in these days of specialization; the official records can only be of interest to those few members who are interested in these things.

H. R. LANG

Notes and comments

Journal of The British Nuclear Energy Conference

The first issue of the *Journal of The British Nuclear Energy Conference* has just been published. The Conference, as already announced in these columns, is the permanent organization through which the Institutions of Civil, Mechanical, Electrical and Chemical Engineers and The Institute of Physics collaborate in "advancing and disseminating knowledge concerning the application of nuclear energy and ancillary subjects."

The issue of the Journal before us has an attractively designed cover carrying the crests of the five constituent bodies of the Conference and measures 8½ by 11 in.; it has 52 pages of text and 40 pages of advertisements. It contains the lectures and papers presented at the opening Symposium held in London on 30 November last and the discussion on these contributions. They were: "The United Kingdom Atomic Energy Authority and its functions" by Sir John Cockcroft, "The place of nuclear energy in United Kingdom power development" by V. A. Pask and J. C. Duckworth, "Health and safety in a nuclear power industry" by A. S. McLean and W. G. Marley, and "The use of research reactors in nuclear power development" by H. G. Grout.

The subscription rate to this well produced Journal is £3 p.a. for non-members of the constituent bodies and £1 10*s*. p.a. for members of the constituent bodies. Orders and subscriptions should be sent to the Secretary, The British Nuclear Energy Conference, 1–7 Great George Street, London, S.W.1.

Nuclear Physics

We have received the first issue of a new monthly periodical entitled *Nuclear Physics*, edited by Professor L. Rosenfeld of the University of Manchester, and published by the North-Holland Publishing Company, Amsterdam.

One of the objects of this new venture is to provide for quick publication of original work "in such a form that it may be easily available to workers in the same field and come to their notice without the necessity of scanning huge piles of periodicals of the most varied description." In his editorial notice Professor Rosenfeld says "the new journal will be devoted to the experimental and theoretical study of atomic nuclei, not excluding those lines of research which may be expected to throw light on the nature of the nuclear forces, i.e. on the one hand the quantum theory of fields, on the other the investigation of the 'elementary' particles. This is, of course, no rigid delimitation of the scope of the journal; it may well become advisable to modify it from time to time.

"The emphasis will be laid on the publication of original papers, including extended reports of completed research as well as shorter notes announcing new results or presenting remarks and suggestions. An effort will be made to provide, whenever this may appear useful, longer review articles or shorter reports dealing with questions of topical interest. Moreover, as occasion arises, the journal will publish book reviews and news items of interest for nuclear physicists."

The issue before us measures 6¾ × 9½ in. and runs to 72 pages of text. The titles of the original papers are: Studies with the scintillation spectrometer; Interpretation of (*d*, *t*) angular distributions; Renormalization and mass levels; Formulation mathématique du modèle de Gell-Mann; Observations of the energy spectrum of the cosmic radiation below ground; there is also a progress report entitled "New results on elementary particles at the Pisa Conference (12–18 June, 1955)" and a book review.

The subscription rate for the volume of 700 pages is 106*s*. and postage 8*s*. Orders should be sent to the publishers at P.O. Box 103, Amsterdam, or to any subscription agent.

Nuclear reactor data

We have received a *Catalogue of nuclear reactors* 1955 AECL No. 220 (CRR-590) prepared by Atomic Energy of Canada Ltd., Chalk River Project, with the co-operation of the Atomic Energy Research Establishment, Harwell, England. The following data is given so far as it is available: neutron speed (thermal, intermediate or fast), fuel configuration (heterogeneous, homogeneous), kind of moderator, purpose (research, plutonium production, propulsion, power), thermal power, neutron flux (at the speed implied by the first item above; maximum value unless otherwise noted). Construction details of each reactor are also given when this has been published. Copies of the catalogue can be obtained from H.M. Stationery Office, price 4*s*. 6*d*. net.

The Raytheon Manufacturing Company of Waltham 54, Massachusetts, U.S.A., has issued a seventeen-page brochure the principal feature of which is a series of charts giving some fifty characteristics of each of the nearly one hundred reactors built or under construction in different parts of the world. The compilation was greatly aided by the declassification of information at the recent Geneva Conference. The reactors are classified into the following groups: pressurized water; boiling water; swimming pool; homogeneous; heavy water; graphite; sodium graphite; liquid-metal cooled; liquid fuel; fast breeder. Copies of this brochure are available from the firm for *bona fide* enquirers, at a nominal charge.

The Physical Society's annual exhibition of scientific instruments and apparatus

The Physical Society announces that its fortieth annual exhibition will be held at the Royal Horticultural Society's Old and New Halls, Westminster, London, S.W.1, from 14–17 May, 1956 (inclusive).

Tickets for *any one* of the following days are available from the Physical Society, 1 Lowther Gardens, Prince Consort Road, London, S.W.7:

Monday, 14 May	2 p.m. to 8 p.m.
Tuesday, 15 May	10 a.m. to 8 p.m.
Wednesday, 16 May	10 a.m. to 8 p.m.
Thursday, 17 May	10 a.m. to 5 p.m.

Members of The Institute of Physics may obtain tickets from the Institute's office. The handbook of scientific instruments and apparatus published in connexion with the exhibition will be available at the beginning of April, price 6*s*.; by post 7*s*. 3*d*.

Meteorological Office annual report for 1954–5

The annual report of the Director of the Meteorological Office for the year ending 31 March, 1955 (H.M. Stationery Office, price 2*s*. 6*d*. including postage) describes the work which has been maintained and includes an account of the research programme. Considerable progress has been made in the study of "numerical weather forecasting" in which an electronic computer is used to produce maps of the pressure field twenty-four hours ahead by step-by-step integration of the equations of motion. Another important investigation which is being undertaken is a long series of carefully controlled trials of the possibility of increasing rainfall by seeding suitable clouds with silver iodide particles released from ground generators.

Development was continued of instruments mentioned in

previous reports, such as the radar sonde equipment and aircraft instruments which are intended to give meteorological information well into the stratosphere.

Symposium on X-ray microscopy and microradiography

A symposium, sponsored by the International Union of Pure and Applied Physics, will be held in the Cavendish Laboratory, Cambridge, from 16–21 August next. Its scope will include all microscopic methods which employ X-rays and sessions are planned on the reflexion, contact and projection methods. Sessions will also be devoted to applications in biology, medicine, metallurgy and other fields, including industrial applications.

Further details may be obtained from Dr. W. C. Nixon, Cavendish Laboratory, Cambridge.

Electronics for spectroscopists

If the demand justifies it, the Photoelectric Spectrometry Group will publish the proceedings of two summer schools in electronics for spectroscopists held at University College, Southampton. These were concerned with theoretical aspects of electronics associated with photoelectric instruments, including ultra-violet and infra-red spectrometers, a.c. and d.c. amplifiers, stabilized power supplies, circuit design and fault-finding in addition to notes on noise, semi-conductors, feedback and other features.

Those interested are invited to write for further details to Mr. K. A. MacDonald, c/o Unicam Instruments Ltd., Arbury Works, Cambridge.

Bibliography of information on servomechanisms and related subjects

The second addendum to the *Bibliography of information on servomechanisms and related subjects* has now been received. The bibliography was first issued in 1950 and was prepared for the Interdepartmental technical committee on servomechanisms (see *J. Sci. Instrum.*, **25**, pp. 224 and 368, 1948). Limited supplies of the addenda and the bibliography are available from the Ministry of Supply, TPA3/TIB (M) Servo Library, 140 Leysdown Road, Mottingham, London, S.E.9.

Report of a conference on engineering fastenings

Copies are available of the report of a conference held in New York in April 1955 between America, Britain and Canada on the unification of engineering standards. Its purpose was to smooth out some of the many small but highly important differences which still exist between British and North American practice in the design and manufacture of engineering fastenings. The wide range of subjects discussed is well shown by the following summary of the agenda, which also constitutes the main headings in the contents list of the published report: gauging of unified screw threads; unified screw threads; unified bolts and nuts; acme threads; microscope objective threads; gas cylinder outlet threads; terminology; surface finish; limits and fits; miniature ball bearings; informal discussion on the general subject of gauging.

The eighty-seven page report has been published on behalf of the conference by the American Society of Mechanical Engineers. Limited supplies are available at 10*s.* per copy from the British Standards Institution, 2 Park Street, London, W.1.

Catalogue of British electrical products

The third edition (1955–56) of the BEAMA catalogue classifies the electrical equipment manufactured by firms which are members of the British Electrical and Allied Manufacturers' Association into three sections: (i) electrical power plant, (ii) electrical equipment in industry, transport and communications, (iii) domestic and commercial electrical appliances, lighting, accessories and installation material. Other sections are a buyers' guide, a trade directory, an index to the catalogue and a glossary in five languages: English, French, German, Portuguese and Spanish.

Further details may be obtained from The British Electrical and Allied Manufacturers' Association, 36–38 Kingsway, London, W.C.2.

Erratum

In the fourth paragraph of the review of *Atomic energy research at Harwell*, on p. 340 of the September 1955 issue of this Journal, reference is made to "the use of the plane grating in divergent light"; this should have read ". . . convergent light."

Journal of Scientific Instruments

Contents of March issue

ORIGINAL CONTRIBUTIONS

Papers

An attachment for high-temperature single-crystal X-ray work. By L. S. Dent and H. F. W. Taylor.
An ultrasonic apparatus for recording the height of water waves in model ship tanks. By E. G. Richardson.
Devices for automatic potentiometric titration. By R. Audran and D. T. R. Dighton.
Some notes on the design and performance of X-ray proportional counters. By A. R. Lang.
An analysis of injection phenomena in the Birmingham proton synchrotron. By C. A. Ramm, R. F. Coe and T. B. Vaughan.
A precision high-temperature specimen chamber for an X-ray diffractometer. By G. K. Williamson and A. Moore.
A continuous-flow rotational viscometer for use with downward-settling suspensions. By G. F. Eveson and E. W. Hall.
A simple fast-recycling cloud chamber. By J. Walker, G. Tagliaferri, J. C. Bower and D. W. Hadley.
A simple theory for solid-backed bolometers. By L. M. Roberts and S. J. Fray.
A personal γ-radiation monitor with audible warning device. By D. Allenden and I. W. Collip.

Laboratory and workshop notes

Large liquid-filled plastic lenses. By J. W. Telford and N. S. Thorndike.
Measurement of the damping of metal bar specimens in mechanical resonance. By H. Pursey and E. C. Pyatt.
A simple method of controlling the temperature of a prism. By K. P. Norris.

NOTES AND NEWS

Correspondence

Correction of millimetre mercury barometers. From D. Ambrose and P. H. Bigg.
A liquid scintillator containing nitrogen. From J. R. Prescott.

New instruments, materials and tools
Notes and comments

THIS JOURNAL is produced monthly by The Institute of Physics, in London. It deals with all branches of applied physics (including theory and technique).
All rights reserved. Responsibility for the statements contained herein attaches only to the writers.
EDITORIAL MATTER. Communications concerning editorial matter should be addressed to the Editor, The Institute of Physics, 47 Belgrave Square, London, S.W.1. (*Telephone:* Sloane 9806.) Prospective authors are invited to prepare their scripts in accordance with the *Notes on the preparation of contributions*. (Price 2*s.* 6*d.* including postage.)
REPRODUCTION. The Institute of Physics is a signatory to The Royal Society's Fair Copying Declaration. Details may be obtained upon application from The Royal Society, London, W.1.
ADVERTISEMENTS. Communications concerning advertisements should be addressed to the agents, Messrs. Walter Judd Ltd., 47 Gresham Street, London, E.C.2. (*Telephone:* Monarch 7644.)
CLAIMS FOR MISSING JOURNALS. Claims from regular subscribers to this *Journal* for missing numbers will only be considered if received within 60 days of the date of mailing plus normal outward time of transit and time for lodging the claim. Losses attributable to failure to notify a change of address or to similar omissions will not be considered.
SUBSCRIPTION RATES. A new volume commences each January. The charge is £4 per volume ($11.50 U.S.A.), including index (post paid), payable in advance. Single parts, so far as available, may be purchased at 8*s.* each ($1.15 U.S.A.), post paid, cash with order. Orders should be sent to The Institute of Physics, 47 Belgrave Square, London, S.W.1, or to any bookseller.

Physics of the Sun*

Prof. ZDENĚK KOPAL, D.Sc., Department of Astronomy, University of Manchester

The first part of this paper reviews the fundamental observed data bearing on the physics of the Sun—in particular, its size, mass, and luminosity. In the second part, an outline of the equilibrium model of solar interior is given. It is pointed out that the forces determining its structure are primarily gravitational, and that most of its interior is likely to be in radiative equilibrium. High internal temperature (attaining some 14×10^6° K at the centre) brings about far-reaching ionization which, in turn, permits solar matter to behave like a perfect gas even at a central density of 90 g/cm^3, and causes part of the radiant energy leaking slowly outwards to have the nature of soft X-rays. The third part reviews the principal nuclear reactions capable of transforming hydrogen into helium under conditions which prevail in the solar interior, and whose exothermic nature provides the source of energy which causes the Sun to shine. It is pointed out that a high temperature-dependence of such reactions restricts the actual energy production essentially to central portions of the Sun; and high opacity of its internal matter is bound to keep this central thermonuclear reactor of the solar system burning at an exceedingly steady rate. The concluding section of this paper reviews the physics and chemistry of the solar visible surface and of its atmosphere. It is pointed out that most phenomena observed in these regions involve but minute transport of mass; but, unlike in the interior, the forces governing them are electromagnetic rather than gravitational. The survey ends with a brief description of the solar corona, whose physical structure is dominated by a temperature of the order of 10^6° K. Dynamically the corona is a fleeting, unstable phenomenon constantly dissolving and being replenished; but the source of the energy necessary for the maintenance of so high a temperature remains one of the great unsolved puzzles of solar physics.

BASIC DATA

Our Sun—the nearest star which we can view at a relatively close range and to which we owe our life and existence—is a body vastly different in mass and size from our terrestrial abode. Its mean distance from us (as deduced in different ways from observations of the asteroid Eros in 1930–31) is known to be 149 530 000 km—light will traverse it in just under 500 s—with an uncertainty of the order of 7000 km. The mass of the Sun, necessary to swing the Earth, at its distance, around it in the period of one year, results as $1{\cdot}9866 \times 10^{33}$ g. The diameter of apparent solar disk at the mean distance is 1919·3 seconds of arc and corresponds to a radius of 695 700 km. The Sun is, therefore, 332 500 times heavier than the Earth, and 109 times larger by size (its mean distance to the Earth equals approximately 215 solar radii); its mean density of 1·408 g cm^3 being somewhat higher than that of ordinary water. The effective temperature of visible solar surface is in the neighbourhood of 5800° K. In addition, a quantitative analysis of the solar spectrum reveals that the matter forming the atmosphere of the Sun consists predominantly of hydrogen (i.e., about 81·76% of hydrogen, 18·17% of helium and a hydrogen-metal ratio of about 10 000 : 1), and it is reasonable to suppose that similar proportions may hold good in its interior as well. The central problem of solar astrophysics consists of investigating the extent to which all these fundamental and seemingly unrelated data are but different aspects of the same consistent model, and make sense in terms of the established laws of physics. What is the actual number of independent parameters which define the broad structure of the Sun? Is, in particular, an agglomeration of common matter, consisting of light elements and equal in mass to that of the Sun, bound to be distended to the observed solar size; and does it have to shine as a star? The principal aim of this article is to attempt to answer these questions as far as they can be done by an astronomer at the present time.

The most conspicuous physical characteristic of the Sun is its radiation. The spectral composition of sunlight reaching the surface of the Earth at the bottom of the atmospheric ocean ranges from approximately 2900 Å in the ultra-violet to 10 μ in the infra-red; the radiation of wavelengths shorter than 2900 Å being cut off by ozone absorption in the upper atmosphere, while the infra-red spectrum of the Sun beyond 10 μ is virtually obliterated by overlapping absorption bands of atmospheric water vapour and carbon dioxide. In the past ten years the ozone barrier has been pierced with the aid of high-altitude rockets carrying spectrographs, and the infra-red barrier has been by-passed by radio-astronomical methods. From high-altitude rockets the spectrum of the Sun has now been photographed down to the region of the hydrogen Lyman series (and studied indirectly—by photoluminescence of phosphorous salts exposed to sunlight—all the way to the domain of soft X-rays). The existing radio telescopes have recorded solar noise at wavelengths as long as 40 m.

The total amount of radiant energy reaching us from the Sun in all frequencies can be obtained by an integration of the observed distribution of intensity throughout the spectrum, duly corrected for the transmission losses in our atmosphere. In doing so we find that, beyond the limit at which the atmospheric absorption begins to make itself felt, each square centimetre of an area exposed normally to sunlight received an amount of energy equal to $2{\cdot}00 \pm 0{\cdot}04$ cal/min, or $1{\cdot}39 \times 10^6$ erg/s. This fundamental value is usually referred to as the "solar constant" and, as its name suggests, exhibits little, if any, significant fluctuation with the time. Of this total of 2 cal. cm^{-2}. min^{-1} the extreme ultra-violet and X-ray spectrum ($\lambda < 3500$ Å) accounts for approximately 0·085 cal. cm.$^{-2}$ min^{-1} and the extreme infra-red and radio spectrum ($\lambda > 2{\cdot}4$ μ) adds 0·076 cal. cm.$^{-2}$ min^{-1}. The bulk (i.e., 1·841 cal. cm.$^{-2}$ min^{-1}) of solar heat reaches us through

* Based on the lecture given at the inaugural meeting of the Liverpool and North Wales Branch of The Institute of Physics in Liverpool on 19 May, 1955.

the medium of ordinary optical frequencies between 3500 and 24000 Å.

The mean distance of the Earth from the Sun is 149 530 000 km and if each square centimetre of the surface of a sphere of this radius, with the Sun at its centre, is to receive an equal amount of heat, the total energy emission L of the Sun must be equal to $1{\cdot}39 \times 10^6 \times 4\pi\,(1{\cdot}4953 \times 10^{13}\,\mathrm{cm})^2 = 3{\cdot}93 \times 10^{33}$ erg/s. Now the radius R of the Sun is known to be 695 700 km, and its surface, therefore, $6{\cdot}08 \times 10^{22}$ cm^2. A comparison of this latter figure with the above value of L discloses that, in order to account for the observed value of solar constant, a flux of energy of $6{\cdot}46 \times 10^{10}$ erg/s must constantly be streaming through each square centimetre of visible solar surface. Perhaps, the reader might be inclined to say that this is because the solar surface is very hot—in fact, approximately 5800° K. But such an argument would merely be putting the cart before the horse. The Sun does not radiate $6{\cdot}46 \times 10^{10}$ erg. cm.$^{-2}$ s^{-1} because its surface (the photosphere) has a temperature of 5800° K; but rather its photosphere is maintained at 5800° K because $6{\cdot}46 \times 10^{10}$ ergs are streaming each second through every square centimetre of it under the impulse of the internal temperature gradient. If we wish to investigate the source of the tremendous solar power, we must work our way upstream into the interior.

SOLAR INTERIOR

How can we hope to be able to penetrate the internal structure of the Sun and to probe the mechanism of its "engine room"? Does, in fact, an agglomeration of matter of the order of magnitude of the Sun's mass (i.e., 10^{33} g) *have* to emit the light we observe; and if so, what must be the characteristics of its outward flux in order to keep the mass of the Sun distended to its present size? At first sight, the utter remoteness of the subject of our inquiry may seem to render a quest for appropriate answers rather hopeless; but, on closer scrutiny, our problem will turn out to be relatively easy. For even though the interior of the Sun is as well shielded from direct view as any region in Nature, it is possible, in principle, by scientific reasoning to learn much about its prevailing physical conditions: i.e., to work out by mathematical methods how fast the density and pressure increase as we go down into the Sun, and how fast the temperature must increase to withstand this pressure.

The problems confronting the astronomer in this connexion bear a close comparison with the tasks of a terrestrial architect or engineer when he has to work out the stresses inside the foundations of a new building, or the strength of an aircraft fuselage at the blueprint stage. In order to find his answer the terrestrial engineer does not have to bore holes into the structures of his design to measure their strength, but can (and does) compute it by a recourse to mathematical equations expressing (or approximating to) the behaviour of his objects under stress. The "astrophysical engineer" concerned with the internal structure of the Sun (or stars) does likewise; and we may add that as the behaviour of gas at very high temperature is, in general, much simpler than that of solid matter under terrestrial conditions, the tasks confronting our astrophysical engineer are relatively simple in comparison with a majority of problems encountered by his terrestrial colleague in his daily life. The differential equations governing the internal constitution of the Sun are certainly simple in comparison with those controlling the supersonic flight of a gun projectile, or aircraft flutter!

In order to convince the reader that this is actually the case, let us produce the equations of solar structure for the reader's inspection. First, if the Sun is to be in hydrostatic equilibrium and if P, ρ denote the (total) pressure and density at a distance r from the centre of a self-gravitating gas sphere, it follows that

$$\frac{dP}{dr} = -G\frac{m}{r^2}\rho \tag{1}$$

where G denotes the constant of gravitation and m, the mass interior to r which is, in turn, governed by the subsidiary equation

$$\frac{dm}{dr} = 4\pi\rho r^2 \tag{2}$$

These *two* equations connect *three* dependent variables, P, ρ and m, and do not, therefore, complete the specification of our problem. In order to do so, we must adjoin to them an "equation of state" whose form will depend on the mechanism of internal energy transfer. Now under physical conditions prevailing throughout most part of the solar interior (with possible exception of a small region surrounding the centre, or a shallow layer just below the visible surface) the heat is transmitted almost entirely by *radiation*—its flow being induced by prevailing temperature gradient (or, in more specific terms, by a gradient of the radiation pressure), and obstructed by the opacity of stellar material. In an equilibrium configuration both forces must again balance each other at any point; and their equalization leads to a differential equation of state, of the form

$$\frac{d}{dr}\left(\tfrac{1}{3}aT^4\right) = -\frac{\kappa\rho}{c}\frac{L}{4\pi r^2} \tag{3}$$

where T denotes the temperature, $L/4\pi r^2$ the flux of energy per unit area, κ the mass-absorption coefficient of solar matter, a the Stefan constant, and c the velocity of light. The function $L(r)$ is, in turn, defined by another subsidiary equation of the form

$$\frac{dL}{dr} = 4\pi\rho r^2\epsilon \tag{4}$$

where ϵ denotes the amount of energy generation per unit mass of solar matter which causes the Sun to shine.

The foregoing relations (1)–(4) represent a set of four simultaneous differential equations for five dependent variables P, ρ, T, m and L as functions of r. Since, however, P is known to be related with ρ and T by means of the equation

$$P = \frac{R}{\mu}\rho T + \frac{1}{3}aT^4 \tag{5}$$

where μ denotes the molecular weight of solar material and R denotes the gas constant, the simultaneous system (1)–(5) is now determinate and its particular solutions can be obtained —numerically or otherwise—for any specified set of boundary conditions. The radiation pressure term aT^4 in equation (5) is almost negligible under solar conditions. At the centre of the Sun, $P = P_c$, $\rho = \rho_c$ and $T = T_c$, while $L(0) = m(0) = 0$. At the surface $r = R$, $L(R)$ is identical with the observed solar luminosity of $L = 3{\cdot}93 \times 10^{33}$ erg/s, and $m(R)$ to its total mass of $M = 1{\cdot}985 \times 10^{33}$ g, but $P(R) = \rho(R) = 0$. (Theoretically, equation (5) should then yield also $T(R) = 0$, while the surface temperature of the Sun is known to be finite. The reason is the partial transparency of solar surface layers, which permits us to see down to a level at which a temperature of the order of 5800° K has already been attained.) The

values of L and M are, therefore, known from the observations, while we wish to find those of P_c and ρ_c (or T_c). The problem for computation consists then of finding such initial values of P_c and ρ_c which, by the process of continuation will eventually render both P and ρ to vanish for the same value of $r = R$.

Equations (1)–(5) contain (apart from a number of physical constants) three variable coefficients—namely: μ, κ and ϵ—whose functional relationship with the dependent variables of our problem must be established before the solution can proceed. Of this trio, the molecular weight, μ depends on the composition of the solar material, predominantly hydrogen and helium, and its degree of ionization. The extent of ionization can be computed for any given mixture as a function of the prevailing physical conditions (i.e., density and temperature) by standard methods of statistical mechanics. In particular, the molecular weight of completely ionized hydrogen is $\frac{1}{2}$; of completely ionized helium, $1\frac{1}{3}$; and for heavy elements it will be essentially equal to $A/(Z + 1)$, where A is the atomic weight and Z is the atomic number. It is, moreover, a well-known rule that the atomic number of an element is about half its atomic weight, so that the mean molecular weight of an ionized mixture of heavy elements is unlikely to exceed 2 by an appreciable amount. Therefore, whatever the actual composition of solar matter, its molecular weight in the interior will be constrained by prevailing ionization to vary between 0·5 and 2 and the large preponderance of hydrogen is likely to depress μ to very nearly its lower limit.

In order to determine the opacity κ—the hindering factor in the outward flow of radiation—we have to turn to physical theories of the absorption processes in ionized media. What kind of radiation is to be absorbed? At the temperature of some millions of degrees to which most part of solar matter will be found to be exposed, the prevalent radiation will be of the nature of soft X-rays, and it is the absorption coefficient of matter for light of this kind that we have to study. In laboratory experiments the X-ray absorption coefficient (or that part of it related to the photoelectric effect) is found to depend strongly on the wavelength of incident radiation—or, in thermodynamic equilibrium, on temperature of the exposed matter—but not on its density. The extraordinarily high intensity of radiation in solar interior will, however, completely alter the picture. In laboratory experiments radiation produced by an X-ray tube meets complete atoms, and these will absorb suitable quanta whenever the opportunity comes. Each atom is an absorbing mechanism for itself and works independently of other atoms, hence, the density exerts no influence on absorption coefficient per unit mass. Inside the Sun, however, the radiation meets atoms whose absorbing capacity is much reduced on account of the high ionization, so that the amount of energy which an atom can absorb per unit time depends primarily on the facility of regaining some of the lost electrons. The frequency of resetting of the absorbing mechanism of ionized atoms by electron capture is directly proportional to the number of free electrons per unit volume—i.e., the ratio of ρ/μ. Since, in highly ionized material containing heavy elements, the number of ions per unit volume is much smaller than the number of free electrons, this latter number should be sensibly proportional to ρ/μ. The absorption of light in the solar interior should, therefore, be also roughly proportional to the density.

Eddington[1] and Milne[2] were the first to calculate the stellar opacity coefficient on the basis of Kramers'[3] classical theory and assumed the electronic transitions to take place in Coulomb fields of atomic nuclei. Gaunt,[4] Strömgren,[5] Morse[6] and others have later investigated the problem from the standpoint of quantum mechanics, and their results essentially confirmed (for absorbing media relatively low density) the earlier developments on classical lines. The absorption of radiation in solar interior takes place through three different processes: (*a*) the bound-free transitions (photoelectric effect), (*b*) free-free transitions, and (*c*) electron scattering. Except for the outermost layers of the solar interior, the bound-free continua of hydrogen and helium contribute but little to general opacity and their effect is much smaller than that of their free-free continua, of electron scattering, or the absorption by a small sprinkling of heavy elements present. In the central regions of the Sun, the effects of electron scattering, free-free transitions in the field of hydrogen and helium nuclei, and the absorption by heavy elements are comparable in magnitude. On the whole, the general opacity in solar interior is of the order of 1 to 10 in absolute units, and decreases inwards. Ionized gases inside the Sun are, therefore, voracious devourers of energy and produce a fog far thicker than the best Manchester tradition: the "visibility" would be at best a fraction of a yard.

SOLAR ENERGY SOURCES

An inquiry as to the nature of the function ϵ governing the energy production in the interior of the Sun will lead us to confront the central problem of solar physics. Astronomical observations reveal that the Sun is emitting a flow of energy of $3{\cdot}93 \times 10^{33}$ erg/s; and geological evidence indicates that this flow must have remained roughly constant for at least 500 million years in the past. If so, however, the total amount of energy released by the Sun must be of the order of at least 6×10^{49} erg/s—and possible several times as large. Any mechanical source (contraction) or ordinary chemical reaction (burning) is manifestly inadequate to provide an energy supply of the requisite order of magnitude; if the Sun were a heap of coal weighing 2×10^7 tons, its burning would not keep it shining at the observed rate for more than 6000 years. Gravitational contraction could defray the energy losses for about 50 million years; but even this time is adequate to account for but a small fraction of the minimum age of the Sun. The only source equal to the required demand is the energy stored in the structure of atomic nuclei; investigations of the past ten or fifteen years have at last elucidated to a considerable extent this fascinating problem of theoretical astrophysics, and enabled us to identify this energy source in some detail.

As hydrogen is the Sun's most plentiful (and combustible) nuclear fuel, it is logical to begin by inquiring what may happen during so commonplace an event in the solar interior as a close encounter of two fast protons. Since the ^{2}He nucleus does not exist, two protons cannot combine with emission of radiation alone. However, during the short time of close proximity of two colliding protons a beta-decay can take place in accordance with the equation

$$^1\mathrm{H} + {}^1\mathrm{H} = {}^2\mathrm{H} + \beta^+ + \text{neutrino} \qquad (6)$$

leading to the production of a deuteron, positron, and a neutrino. The rate of reaction of this process under solar conditions was first calculated by Bethe and Critchfield[7] (1938) and, more recently, by Salpeter[8] (1951); it is found to be so low that the mean half-life of a proton in central regions of the Sun is of the order 10^{10} years. So low a rate (which is no doubt responsible for the fact that this synthesis has as yet never been observed in the laboratory) would—in the

absence of any more effective way of hydrogen burning—make the life time of the Sun a quantity of the same order of magnitude. As the mass of a proton is, however, only $1{\cdot}672 \times 10^{-24}$ g, the total solar mass of $1{\cdot}9866 \times 10^{33}$ g should contain some 10^{57} protons—so that, in spite of a half-life of the order of 3×10^{17} s some 10^{40} of them are likely to react in the manner indicated by equation (6) each second!

In the central regions of the Sun a deuteron, once formed, will react almost immediately with another proton in accordance with the equation

$$^2\mathrm{H} + {}^1\mathrm{H} = {}^3\mathrm{He} + \gamma\text{-radiation} \qquad (7)$$

whose mean half-life is of the order of some 10 s. The ^{3}He nucleus thus formed may react with another ^{3}He nucleus, or with ^{4}He.* Fowler and Lauritsen[9] have found that, under conditions prevailing in the central regions of the Sun, the probability of the reaction with ^{3}He is more than 100 times greater than that of reaction with ^{4}He. The next step is, therefore, practically always

$$^3\mathrm{He} + {}^3\mathrm{He} = {}^4\mathrm{He} + 2{}^1\mathrm{H} \qquad (8)$$

leading to the production of an α-particle (which is completely stable under solar conditions), and returning two protons into the fray.

The net result of the cycle as represented by equations (6)–(8) is, therefore, a production of one ^{4}He nucleus, two positrons, and two neutrinos from four protons. The two positrons, once formed, will annihilate almost immediately two electrons with the consequent emission of a γ-quantum, and the latter will be rapidly transformed into local thermal energy. The neutrinos released by the β-decay (6) do not react with solar matter, and escape from the Sun without adding to its luminosity. But a formation of an α-particle from four protons is an exothermic process *par excellence*. The atomic weight of ^{1}H is known to be $1{\cdot}008\,131 + 0{\cdot}000\,003$; and that of ^{4}He is $4{\cdot}003\,86 + 0{\cdot}000\,03$. Hence, $4{}^1\mathrm{H} - {}^4\mathrm{He} = 0{\cdot}028\,66$, and the energy released by this formation is equal to $0{\cdot}028\,66 \times 1{\cdot}673 \times 10^{-24}\,c^2 = 4{\cdot}32 \times 10^{-5}$ ergs per reaction (corresponding to 28 MeV). This energy has to be diminished by about 5% because of the escape of neutrinos. But even so, as there are some 10^{40} protons in the Sun ready to enter the cycle (6)–(8) any second, the total energy production should be of the order of $4{\cdot}3 \times 10^{-5} \times 10^{40} \simeq 4 \times 10^{35}$ erg/s, which is more than 100 times the rate actually observed. We surmise, therefore, that only a relatively small fraction of solar protons (in central regions) are reacting in this way at any time.

It should be noted that the proton–proton cycle as summarized by the foregoing reactions (6)–(8) does not represent the only process by which hydrogen can be converted into helium with the consequent release of energy. Another set of reactions, known as the carbon–nitrogen cycle, can accomplish the same purpose even more effectively, but at somewhat more extreme conditions than those met in the Sun. A decade ago, the carbon–nitrogen cycle (discovered by Bethe[10] in 1939) was thought to be the principal source of solar energy; but more recent information on the rates of nuclear transformations envisaged by it led to the conclusion that it is primarily operative in more massive stars, and of subordinate importance as far as the Sun is concerned.

How does the rate of energy production by the proton–proton cycle vary with the density and temperature? The speed of the whole cycle will be obviously controlled by that of its "bottleneck" reaction, which is (6) on all scores. The rate of this latter reaction is, in turn, essentially equal to the product of the effective cross-section of the target times the probability that the impinging proton will penetrate the Coulomb barrier of its mate. Owing to the simplicity of the interacting particles, both these expressions can be formulated theoretically without undue risk; and it can be shown

$$\text{that} \qquad \epsilon = 481 \rho X^2 \left(\frac{3380}{T^{1/3}}\right) \exp\left(-\frac{3380}{T^{1/3}}\right) \text{erg/g. s} \qquad (9)$$

where X denotes the proportional hydrogen content of solar matter. This is very approximately the expression which should be inserted in equation (4) before the system (1)–(5) can be integrated. An analysis of this expression reveals that the rate of energy production by the nuclear reactions (6)–(8) is very sensitive to prevailing temperature, and increases roughly with a fairly high power of T. As the temperature in the Sun is bound to increase inwards, the temperature-dependence of equation (9) alone should lead us to expect that the actual energy generation inside the Sun will be confined mainly to its central hottest region.

In looking over our system of equations governing solar structure, a few qualifying words concerning the extent of their reliability or importance may be added. Of the system (1)–(4) the first equation of hydrostatic equilibrium is the most important of them all, as it expresses the equality of two quantities which are numerically very large and require detailed balancing. Equation (3) of radiative equilibrium is less important in this respect, due to the high opacity of stellar matter. A breakdown of hydrostatic equilibrium in the Sun would lead to consequences which would be felt on the Earth as a matter of hours, and probably prove fatal to the well-being of us all. On the other hand, a breakdown of the radiative equilibrium would not be felt till after a relatively long time, and its consequences would set in so slowly that life on this Earth would have a good chance of gradual adjustment to new conditions.

In writing down equation (1) we deprived it of all time-dependent terms, which means that a body built up in accordance with it could not rotate, or possess any internal circulation currents. In actual fact, the Sun does rotate about an axis in a period little shorter than a month, but the centrifugal force thus produced is so small in comparison with gravity that it exerts little influence on the internal structure. The same is true of the effects of internal circulatory currents. The electromagnetic forces, important as they may be in outer parts of the Sun, are probably likewise negligible in comparison with gravity in the interior.

As regards a formulation of the expressions for μ, κ and ϵ, those of μ and ϵ are probably quite reliable and subject to relatively little uncertainty. The same cannot, unfortunately, be said as yet of our knowledge of the absorption coefficient κ, because of its dependence on even a small admixture of heavy elements, and also because the Coulomb approximation underlying Kramers' theory of it may be seriously in error at high densities. In particular, the opacity of ionized hydrogen gas compressed to densities between 10 and 100 g/cm^3, and such gas constitutes the bulk of solar matter, is subject as yet to considerable uncertainty; it is this uncertainty which is preventing our astrophysical engineers from feeling confident about the details of their investigations.

Within the scheme of these approximations, numerical integrations of the equations of solar structure have been

* Further proton capture is no longer possible, since ^{4}Li is unstable (by particle disintegration).

carried out by many investigators, and the latest outcome reveals that if a mass of gas of $1{\cdot}9866 \times 10^{33}$ g is to be distended to the present solar size and to emit the observed amount of energy, its central physical characteristics are: $P_c = 1{\cdot}72 \times 10^{17} \pm 0{\cdot}08$ dyn/cm^2, $\rho_c = 90 \pm 4$ g/cm^3, and $T_c = 13{\cdot}7 \pm 0{\cdot}2 \times 10^6$ °K—the uncertainty of these values arising mainly from our incomplete knowledge of the opacity of ionized hydrogen at high densities. The pressure at the Sun's centre attains, therefore, $1{\cdot}7 \times 10^{11}$ atm; and the density turns out to be approximately five times as large as that of solid gold (the mean density of the Sun being $1{\cdot}408$ g/cm^3). Is it legitimate, under these circumstances, to expect solar matter to behave as perfect gas (as is implied in our equations 1–5)? The answer is indeed in the affirmative; and the clue is the high ionization of the matter. Under the conditions we found in solar interior, all light atoms will be totally ionized, and the specific volume of their splinters becomes so small that matter consisting of them would behave as perfect gas at densities, not only of the order of 100 g/cm^3, but even if they were 10 or 100 times higher.

As to the chemical composition of solar material (provided that the latter is well mixed), the Sun at present appears to consist of $75 \pm 1\%$ of hydrogen, $24 \pm 1\%$ of helium; while all other heavier elements combined do not seem to account for more than about $0{\cdot}75\%$ of the solar mass and are thus present in amounts which a terrestrial chemist would be inclined to regard as impurities. The mean molecular weight μ of solar matter is, accordingly, in the neighbourhood of $0{\cdot}59$. The Sun manifestly contains, therefore, still ample stores of hydrogen fuel to keep it shining for an astronomically long future—much longer no doubt than its whole past, checkered as it may be by such extraordinary events as the formation of its planetary family. Radioactive dating of the terrestrial rocks reveals that the solid crust of the Earth must be at least 4000 million years old, and the Sun can scarcely be younger. If, therefore, in the course of 4×10^9 years the Sun has managed to keep our Earth comfortably warm at an expenditure of not more than one-quarter of its initial hydrogen supply (or even less if its original composition contained an appreciable admixture of helium), we really do not have to worry about the future in this respect! (It should be remarked here that strictly speaking, our evidence of geological climates does not extend to more than some 500 million years in the past, but it is unlikely that the preceding aeons witnessed much else than what we know.)

Owing to the high temperature-dependence of thermonuclear reactions in solar interior, an overwhelming part of the energy which keeps the Sun shining is liberated in a relatively small region surrounding the centre; its rate of production being so high there that this region may be in a virtually "boiling" state—i.e., convective equilibrium. The radiation there is probably inadequate to cope alone with the transfer of all energy liberated at the source, and heat is being transported outwards by material currents. In the region in which this is true equation (3) breaks down, and is to be replaced by the polytropic equation of state

$$P = K\rho^{\gamma}, \tag{10}$$

where K is a constant and γ, the effective ratio of specific heats, is likely to be very close to $1\frac{1}{3}$.

This part of the deep interior is the veritable "engine room" of the Sun and the seat of its power; all the rest of the solar superstructure (by far the largest part by volume) serves only as its shield, and its density and temperature distribution is effectively controlled by the central plant. As the energy of the latter is liberated by nuclear fire burning the hydrogen fuel into helium ashes, this part of the interior has often been compared with a permanent hydrogen bomb, prevented from bursting by the tremendous weight of the "casing." This analogy is, however, rather misleading; for the principal reactions causing an explosion of a thermonuclear bomb (i.e., reactions involving two deuterons or tritium) are insignificant in the Sun. It is much more accurate to compare the Sun's deep interior with a slowly smouldering thermonuclear reactor, so set that any adjustments in its controls can—fortunately for us—take place only at an exceedingly slow rate (owing to the very low probability of the $^1H - {}^1H$ reaction). The Sun has, therefore, solved effectively the technical problem of continuous energy production by controlled thermonuclear reactions and on a vast scale before the Earth was born; and when the terrestrial technicians are in a position to emulate this feat, we may really find ourselves on the threshold of a millennium.

There is, however, no doubt that Nature has concealed this critical part of solar mechanism from external inspection most effectively behind an enormous and truly infernal barrier which the new-born energy stream must slowly penetrate before eventually embarking on its journey through space. Read this account of the physical conditions prevailing in the solar interior as described by the late Sir Arthur Eddington,[11] to whom stellar interiors were his second habitat: . . . . . "Dishevelled atoms tear along at 50 miles a second with only a few tatters left of their elaborate cloaks of electrons torn from them in the scrimmage. The lost electrons are speeding a hundred times faster to find new resting-places. Look out! there is nearly a collision as an electron approaches an atomic nucleus; but putting on speed it sweeps round it in a sharp curve. A thousand narrow shaves happen to the electron in 10^{-10} of a second; sometimes there is a sideslip at the curve, but the electron still goes on with increased or decreased energy. Then comes a worse slip than usual; the electron is fairly caught and attached to the atom, and its career of freedom is at an end. But only for an instant. Barely has the atom arranged the new scalp on its girdle when a quantum of light runs into it. With a great explosion the electron sucks up the energy of the ray and darts off again for further adventures. Elsewhere two of the atoms are meeting full tilt and rebounding, with further disaster to their scanty remains of vesture.

"As we watch the scene we ask ourselves, can this be the stately drama of stellar evolution? It is more like the jolly, crockery-smashing turn of a music hall, or the hair-breadth escapades on the films. The knockabout comedy of atomic physics is not very considerate to our aesthetic ideals, and this 'music of the spheres' has almost a suggestion of—jazz. But it is all a question of time-scale. The motions of the electrons in stellar interiors are as harmonious as those of the stars but in a different scale of space and time, and the music of the spheres is being played on a keyboard 50 octaves higher . . .

"And what is the result of all this bustle? Very little. The atoms and electrons for all their hurry never get anywhere; they only change places. Just as many electrons are repaired as they are smashed; just as many bundles of light are sent out as they are absorbed; just as many electrons are captured as are exploded away. The light waves are the only part of the population which do actually accomplish something. Although apparently darting in all directions indiscriminately, they do on the average make a slow progress outwards. There is no outward progress of the atoms and electrons; gravitation sees to that. But the encaged light wave leaks out slowly as through a sieve. It hurries from one atom to

another, forwards, backwards, now absorbed, now flung out again in a new direction, losing its identity, but living again in its successor. It changes at the lower temperature from X-rays to light-rays, being altered a little at each re-birth. It will thread the maze for hundreds of years, until, at last, it finds itself so near the boundary that it can dart outside and travel forward in peace." And perhaps, we may add, it will be intercepted on its way through space by a tiny solid speck known as the Earth, to tell its inhabitants that the Sun is shining.

SOLAR SURFACE AND OUTER LAYERS

Emerging from the inferno of solar interior to its visible surface, we shall no doubt find ourselves confronted by the question: if the Sun is a body which is gaseous throughout, how can the limb of the visible solar disk appear perfectly sharp? Its abruptness depends, in principle, on the distribution of density, temperature and opacity (i.e., ionization) in surface layers; and their compound action turns out to govern the optical depth of solar surface layers in such a way that a transition from (practically) perfect transparency to complete opacity to light of ordinary optical frequencies takes place within a layer of approximately 100 km deep (which, at the mean solar distance, appears at an angle of less than $0{\cdot}14''$). The density in this region is of the order of 10^{-7} g/cm^3, and the pressure, around 10^5 bars. It is, moreover, in these layers that the principal features of the absorption spectrum of the Sun are formed.

Qualitative studies of this spectrum by countless investigators over a period of many years have revealed the presence, in the Sun, of almost all known chemical elements of the periodic table—with the exception of Cs, Re, Tl, Bi, or of heavy radioactive elements of atomic weights in excess of 210. Technetium, whose presence in the solar atmosphere was reported by Charlotte Moore-Sitterly[12] in 1951, raises an interesting problem. The half-life of its stablest known isotope, ^{99}Tc, is less than 10^6 years, which is but a fleeting moment in comparison with the Sun's age. Unless some more stable isotope exists in Nature, the observed lines of Tc must be due to atoms created relatively recently and manifestly not by thermonuclear reactions. Another group of elements (consisting of inert gases heavier than helium, the halogens, Se, Te, Hg) have not so far been identified for lack of ultimate lines in the accessible part of the spectrum.

One of the most interesting spectroscopic episodes of recent years was the discovery, in solar atmosphere, of the negative hydrogen ion (H^-). We may remember that once before in the annals of science a new element was discovered in the spectrum of the Sun before it was eventually found on the Earth: namely, in 1868, when Janssen and Lockyer detected the lines of helium in the flash-spectrum of the total solar eclipse. Seventy years later, history repeated itself, and a new chemical element was added to our knowledge: a negative hydrogen ion (i.e., a proton attended by two electrons) unknown from the laboratory, but one which can exist in finite concentration under the conditions prevailing in the solar atmosphere, and which revealed its presence there, not by line emission, but by its continuous absorption.

Another even more recent and exciting result concerns the relativistic red shift, or rather its absence, in the solar spectrum. As is well known, according to the general theory of relativity all light emitted in a gravitational field should be shifted to the red by an amount depending on the local potential; and in the solar spectrum this effect should be sufficiently large to be observable. Now recent systematic and careful measurements of the wavelengths of solar lines at Potsdam and at Oxford have revealed that this phenomenon was conspicuous by its absence: such shifts as are observed amount to but a small fraction of those predicted by the theory of relativity and, moreover, increase from centre to limb in a manner indicative of a volume rather than surface effect. The repercussions of this fact strike very deep indeed; and it is possible that its consequences may play the same role with regard to the general relativity as the negative outcome of Michelson–Morley experiment did for classical mechanics sixty and seventy years ago. The failure of the physicists to face up squarely to this fact can be explained by an apparent unwillingness to do so of the astronomers themselves. Thus Otto Struve,[13] a leading American astronomer, wrote recently in this connexion: "Most astrophysicists believe that the general theory of relativity is so fully confirmed by other evidence . . . that the relativistic velocity of $+0{\cdot}6$ km/s *must* exist in the Sun's light. If it does not appear in the observations, then perhaps the best explanation is still . . . that systematic motions in the solar atmosphere conceal the relativity effect." It seems that the lessons of the history of science are easily all forgotten only a few generations later. Would it be pertinent to recall in this connexion what happened to all the intra-mercurian planets postulated in the 19th century to reconcile classical mechanics with the observed advance of Mercury's perihelion?

Quantitative studies of the spectrum of the Sun reveal that its semi-transparent outer layers consist of a chemically almost pure mixture of hydrogen and helium. The actual hydrogen : helium ratio is as yet somewhat uncertain due to observational reasons (although it is probably close to 82 : 18 by volume); but both together account for at least $99{\cdot}9\%$ of the entire solar atmosphere, the remaining $0{\cdot}1\%$ of its contents being formed by all other elements lumped together roughly in proportion of their average cosmic abundances (which diminish rapidly with increasing atomic number).

The actual visible surface of the Sun as seen or photographed with the aid of a telescope is not smooth, but *granular* (see Fig. 1). On closer scrutiny, it is found to consist of myriads of distinct bright spots separated by darker irregular lanes reminiscent at a glance of a field of rice grains. The apparent dimensions of the individual granulae are of the order of a few seconds of arc, corresponding to a few thousand kilometres (i.e., to the dimensions of terrestrial continents). The granular structure is, moreover, not constant, but subject to rapid and perpetual change. Indeed, the mean life-time of the individual granulae is of the order of only a few minutes, in the course of which the whole detailed structure of the solar photosphere is constantly re-created.

The physical significance of these granulae is revealed by radial-velocity observations, disclosing that matter in them is constantly rising or sinking with velocities of the order of several hundred metres per second. They are apparently nothing else but "tops" of convection currents produced by turbulent flow in semi-transparent layers of the Sun. This convection may be produced (or stimulated) by a large-scale ionization of hydrogen, which should set in immediately beneath the visible surface and bring about a sudden decrease of the effective ratio of specific heats. Hydrogen ionization should, however, be practically complete at a depth of some 5000 km, while certain anomalies in the observed relative abundances of elements of the lithium group suggest that the surface convection "pumps" may be operating down to the depths at which temperatures of the order of $10^{6\circ}$ K are attained. Whatever the actual extent of solar surface convection may be, the granulae themselves may be loosely

compared with the cumulus "clouds of good weather" in the terrestrial atmosphere; except that this solar analogy covers constantly the entire visible surface, and whatever their bearing on solar weather forecasting, one prediction will never fail to be true: wherever they are, it will be always very hot: in fact, about 6000° K.

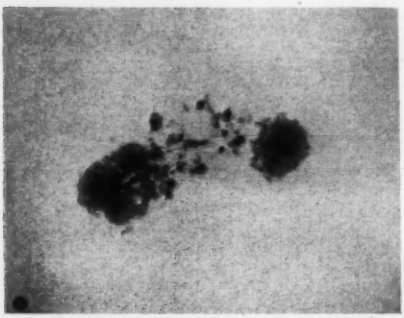

Fig. 1. Great sun-spot group photographed on 8 February, 1917, at Mount Wilson Observatory. The dark disk in the corner represents the proportional size of the Earth

The granular solar surface exhibits, at times, conspicuous features popularly known as sun-spots. If ordinary granulation can be likened to "clouds of good weather," sun-spots are solar cyclones—external manifestations of gigantic

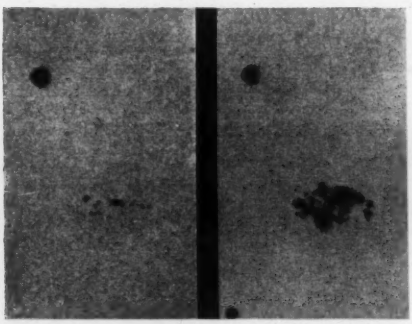

Fig. 2. Development of a sun-spot within 24 hours (18–19 August, 1916) as photographed at Mount Wilson. The dark disk at the bottom represents the proportional size of the Earth

storms in the solar atmosphere, whose central regions are cooler (by about 2000° K at their centre) than their surroundings. Such storms may break out over a period of hours (see, for example, Fig. 2) and extend over areas many times as large as the whole surface of the Earth (such spots may be visible to the naked eye without the aid of a telescope). Sometimes they may vanish just as rapidly as they have been formed and, at other times, they may hover in unchanged form and position for many weeks. Any forecasting of the behaviour of solar cyclones is, therefore, fraught with considerable risks.

The most conspicuous physical characteristics of sun-spots are their tremendous magnetic fields. The disturbed areas of solar surface exhibit magnetic fields of several thousand gauss, which may be homogeneous over areas of several hundred million square miles. The presence of such fields is revealed by the Zeeman splitting (in amounts proportional to the field's strength) of spectral lines into two circularly-polarized components near the Sun's centre, and three plane-polarized components near the limb (see Fig. 3)—observations

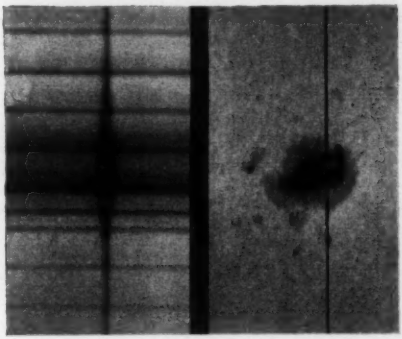

Fig. 3. Iron triplet, wavelength 6173 Å in the spectrum of a sun-spot on 9 March, 1916, showing circular polarization of the light; the red and violet components of the line were transmitted through the same strip of quarter-wave mica. Slit placed as shown on direct photograph on the right. The horizontal lines intersecting the photograph on the left represent divisions between segments of a special polarizing filter that will extinguish, first the left, and next the right, component of the magnetically split line (Mount Wilson Observatory photograph)

indicating that the magnetic field of a spot tends to be perpendicular to the surface. Such fields may sometimes betray the location of an incipient solar cyclone beneath the photosphere before it actually bursts through to the visible surface. The currents required to maintain the magnetic fields associated with large spots are of the order of 10^{12} amperes. How to explain the origin of such enormous currents in the Sun, or to account for their maintenance over long periods of time? No detailed satisfactory theory has as yet appeared to answer these questions, but at least some indications of such answers have emerged from intensive work of recent years. The outer portions of solar cyclones are likely to whirl less rapidly than the inner ones. The electrons in an ionized gas will, moreover, move faster than the ions and travel farther between collisions. The electrons moving outwards will possess greater rotational speeds than the inward-moving electrons which replace them. The difference between the two streams will then cause a current of electrons to flow in the direction

of the spot's rotation, and this current may be responsible for the observed magnetic fields.

Much more is, however, known from observations about sun-spots than current theories can satisfactorily explain. It is customary for spots to occur in pairs of opposite magnetic polarity (cf. Fig. 4), and this polarity is reversed in pairs occurring at opposite solar latitudes. Moreover, observations carried out over many years have revealed that sun-spots are no accidental surface features; but their number, location and magnetic polarity fluctuate regularly in an eleven-year cycle. These facts suggest that cyclones in the solar atmosphere are most likely only surface manifestations of deep-seated disturbances of the interior; a clue to their behaviour, when discovered, will probably take us back again to the solar "engine room" from which we started.

On bidding farewell to the Sun's interior and surface phenomena, our return to the Earth will require traversing outer solar layers—the chromosphere and the corona—which envelop the Sun to a considerable distance and slowly peter out into interplanetary gas. In spite of their great distension (the corona can be followed during a total eclipse up to distances of several solar radii from its centre), the total mass of the outer layers of the Sun is of the order of 10^{-16} that of the Sun's mass as a whole—i.e., actually a very tiny fraction of the mass of our own Earth.

Seldom has so small a mass given rise to phenomena so beautiful and intriguing as those exhibited by the solar corona (see Fig. 5). For centuries the corona has been observable only during the rare events of total eclipses of the Sun, which expose its ethereal beauty to direct sight for an average of 2·9 minutes per year somewhere on the surface of the Earth; and it was not until in the past 25 years that the development of special observing techniques (the coronograph) enabled us to study certain aspects of the corona in full daylight. The principal reason for the difficulty in observing the solar corona out of eclipse is its low relative luminosity; for its light contributes but 1 part in 500 000 to the integrated sunlight. The total light of the corona is comparable with that of full moon, and stems from several sources. Its principal part (i.e., at least 90% of it) is white light, exhibiting a purely continuous spectrum which is an exact replica of that of the solar photosphere, but with no trace of absorption lines (the K-corona). This light is, moreover, partly polarized and this fact gives away its origin: it is nothing else but sunlight scattered by free electrons in outer solar layers. The corona must, however, be electrically neutral, and the negative charges of free electrons must be balanced by positive charges of the ions. These latter emit a line spectrum; some 26 such lines have been observed between 3300–11 000 Å, contributing about 1% to the total light of the corona (the E-corona). Their origin was for a long time a mystery; for it was not until 1942 that Edlén[14] identified them with lines of certain common metals (Ca, Ni, Fe) whose atoms have lost nine to fourteen electrons. In particular, the famous green coronal line (5303 Å) turned out to be due to Fe XIV; and the red line (6374 Å) to Fe X. This latter is the only line of the coronal spectrum which appears to have been observed also in the absorption spectrum of the Sun. The K- and E-components of the corona are the only ones of solar origin. In addition, a part of the light of outer corona exhibits a spectrum which is a true replica of the solar spectrum with all its absorption lines, and shows no trace of polarization (the F-corona). This last part of coronal light is now known to be produced by a diffusion of sunlight on particles of interplanetary dust between the Sun and the Earth.

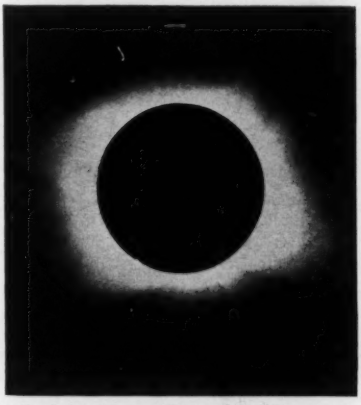

Fig. 5. Solar corona photographed during the total eclipse of 22 January, 1898, at Sahdol (India) by the Greenwich Expedition (Christie)

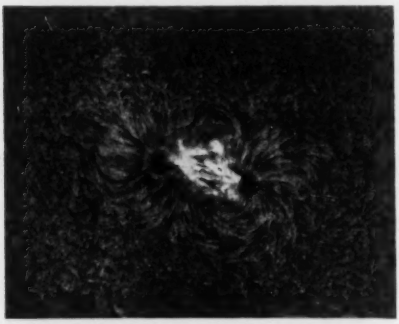

Fig. 4. Bi-polar spot group, photographed on 30 August, 1924, at Mount Wilson in the light of Hα

The ensemble of the observational evidence reveals that the internal temperature of the corona must be extremely high—in fact, between 1 and 2 million °K. Several lines of independent evidence converge to this conclusion. First, the obliteration of Fraunhofer lines in the spectrum of the K-corona alone (caused by thermal agitation of its electron gas) requires a temperature in excess of 10^5 ° K. The observed thermal broadening of the emission lines points to temperatures of the order of $1{\cdot}8 \times 10^6$ ° K; the observed degree of ionization requires at least 9×10^5 ° K, it may help us to recall that the excitation potential of the coronal green line (5303 Å) is 355 V; and that of 5694 Å, due (probably) to Ca XV, may be as high as 814 V. The observed brightness of the (quiet) Sun at wavelengths of the order of 1 metre corresponds to a temperature of about 8×10^5 ° K while

the density gradients observed in solar corona require temperatures between $1{\cdot}2$–$1{\cdot}6 \times 10^6$ °K for their stability. (It should be kept in mind that coronal electron gas is wellnigh opaque to radio waves. All observations of the Sun in wavelengths in excess of some 50 cm are, therefore, observations of the solar corona.) All these independent avenues converge, therefore, to the view that the temperature of the corona must be of the order of 10^6 °K; and a relatively high admixture of free electrons ensures, moreover, that most part of the corona will be very nearly isothermal.

Outwardly, in contrast with the hurly-burly of the solar interior, the corona is in a state of majestic calm, in keeping with its ethereal beauty. It shares the solar axial rotation, but its internal motions are ordinarily slow (of the order of a few kilometres per second). These motions are, moreover, likely to be governed by electromagnetic, rather than gravitational, forces. The characteristic plume-like structure of its electron-gas streamers (see again Fig. 5) is, incidentally, our only (but sufficient) proof so far that the Sun as a whole possesses a general magnetic field. In contrast with tremendous local fields associated with sun-spots, this general field appears to possess the strength of only a fraction of one gauss. The supreme problem of coronal physics, namely, the identification of the source of energy capable of maintaining the corona at its temperature of $1 - 2 \times 10^6$ °K remains, however, as yet unresolved. Although outside energy sources (external matter falling on the Sun) may add their contribution, it appears probable now that the bulk of heat is being fed into the corona from below. Details of the appropriate energy transfer remain, however, still largely to be worked out.

It is easy to understand that the vast expanse of solar

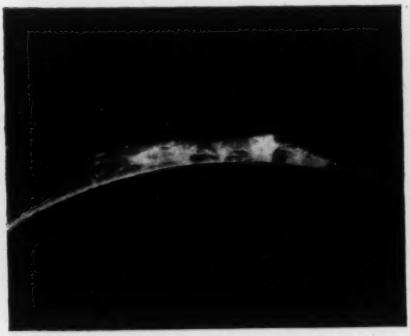

Fig. 6. A quiescent solar prominence visible at Sun's limb during total eclipse of 30 August, 1905 (Royal Observatory, Greenwich)

corona, consisting of gas so rarefied and hot, is unlikely to be in secular equilibrium, but intercommunicates constantly with both the main mass of the Sun below, and the interplanetary space above. Its main instruments of this intercommunication are *solar prominences*. A full-grown prominence is a gaseous sheet (blade-like structure) ranging from 10^6 to 10^9 km in size, and weighing anything between 10^6 to 10^9 tons. The density of gas forming the prominences is about 100, and its temperature about 1/100, times that of

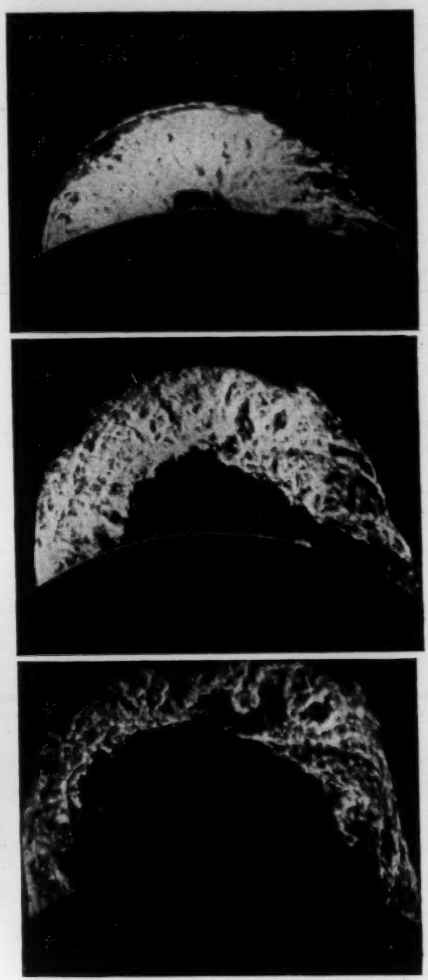

Figs. 7–9. The great eruptive prominence (the largest observed so far) photographed on 4 June, 1946, at the High Altitude Observatory, Climax, Colorado, by W. O. Roberts, in full daylight, with the aid of a coronograph, through a polarizing filter centred at Hα. The rapid development of this giant prominence can be gathered from the fact that the three photographs are separated by intervals of only 33 and 15 minutes, respectively. In final stages of its development this prominence became as large as the Sun itself

the surrounding corona. The prominences as a class appear, therefore, to be roughly in equilibrium with the surrounding corona, and may represent the loci of condensation of coronal matter, comparable with the "cold trap" of a vacuum equipment for condensation of vapours. The solar analogy of this process requires the "heat of condensation" to be drained away by radiation in the Lyman continuum; and if so, the optical depth of the prominence to be very small for wavelength less than 912 Å. This may explain why prominences occur preferentially in the form of gas sheets. Quiescent prominences (see Fig. 6) are, therefore, probably accreting and channelling matter which steadily falls down. Eruptive prominences (see Figs. 7–9) moving frequently at supersonic speeds in excess of that of escape from the gravitational field of the Sun, are carrying mass away. Taking account of the average frequency of eruptive prominences, we surmise that the Sun may be constantly losing in this way approximately 2×10^9 grammes of mass per second (which is but 4×10^{-4} of the mass lost by radiation at the same time, so that the relative importance of corpuscular emission appears to be fairly negligible). On the other hand, comparable amounts of mass may be accreted by the Sun on its journey through interstellar gas. The correct balance between accretion and evaporation is as yet impossible to estimate with any accuracy; but owing to the smallness of the masses involved its evolutionary consequences are likely to make themselves felt only after astronomically long periods of time.

A continuous loss of coronal mass at a rate of 2×10^9 g/s entails, however, one additional interesting consequence. As the total mass of the corona has been estimated to 5×10^{17} g, all of it should be lost by evaporation within a few years. The coronal matter which you may see at a given total eclipse of the Sun is, therefore, unlikely to be there when you chance to see another eclipse; all of it has probably evaporated away in the meantime. It will, however, have been replenished by accretion from above as well as from below, and the sublime beauty of the white silvery web surrounding the eclipsed solar disk will be no less enthralling for the exchange.

With these considerations we wish to conclude our brief survey of the physics of the Sun. The reader should judge for himself the extent to which we have been able to answer the principal questions raised at the outset of our inquiry. Many important problems remain still to be clarified, and a vast amount of detail worked out. Yet it is perhaps not too much to assert that to-day, by the middle of the 20th century, we possess sufficient understanding of the principal features of solar structure to enable us to put on rational basis that part of astrophysical engineering which is characterized by the term of "solar-terrestrial relations." These relations are indeed manifold and of great practical importance to such terrestrial occupations as agriculture, weather forecasting, communication engineering, or even power engineering. The amount of the energy given away by the central thermonuclear reactor of the solar system throughout the ages is so vast that its utilization, in diverse forms, has been the principal preoccupation of mankind from time immemorial, and exploitation of fossil solar energy stored in coal or oil is still the backbone of our civilized life. May we conclude by expressing the hope that terrestrial engineering may progress in the future sufficiently to master the utilization and distribution of incident solar energy for industrial or domestic use?

REFERENCES

(1) EDDINGTON, A. S. *Monthly Not. Roy. Astron. Soc.*, **84**, p. 104 (1924).
(2) MILNE, E. A. *Phil. Mag.*, **47** (6), p. 209 (1924); *Monthly Not. Roy. Astron. Soc.*, **85**, p. 750 (1925).
(3) KRAMERS, H. A. *Phil. Mag.*, **46** (6), p. 836 (1923).
(4) GAUNT, J. A. *Phil. Trans.*, *A*, **229**, p. 163 (1930).
(5) STRÖMGREN, B. *Z. Astrophys.*, **4**, p. 118 (1932); **7**, p. 222 (1933).
(6) MORSE, P. M. *Astrophys. J.*, **92**, p. 27 (1940).
(7) BETHE, H., and CRITCHFIELD, C. H. *Phys. Rev.*, **54**, p. 248 (1938).
(8) SALPETER, E. E. *Phys. Rev.*, **88**, p. 547 (1951); *Astrophys. J.*, **115**, p. 326 (1951).
(9) FOWLER, W. A. *Phys. Rev.*, **81**, p. 655 (1951); FOWLER, W. A., and LAURITSEN, C. C. *Phys. Rev.*, **76**, p. 314 (1949).
(10) BETHE, H. *Phys. Rev.*, **55**, p. 434 (1939).
(11) EDDINGTON, A. S. *The Internal Constitution of the Stars*, pp. 18–20 (London: Cambridge University Press, 1930), or his *Stars and Atoms*, pp. 29–30 (London: Oxford University Press, 1927) (free quotation).
(12) MOORE-SITTERLY, C. *Science*, **114**, p. 59 (1951).
(13) STRUVE, O. *Sky and Telescope*, **13**, p. 227 (1954).
(14) EDLÉN, B. *Z. Astrophys.*, **22**, p. 30 (1942).

An apparatus for the accurate control of the peak X-ray energy of a 20 MeV betatron

By K. PHILLIPS, M.Sc., A.M.I.E.E., Research Department, Metropolitan-Vickers Electrical Co. Ltd., Manchester 17

[*Paper first received* 27 *September, and in final form* 29 *November*, 1955]

Two methods on the accurate control of the electron energy of a 20 MeV betatron are described in detail. In one method a current transformer supplies a reference voltage in phase with the current in the betatron magnet coils to a trigger and potentiometer control unit. The second method uses a peaking transformer which is connected in series with the betatron magnet coils and supplies a pulse to a differentiating amplifier. The time of firing of the peaking transformer during the acceleration cycle is controlled by means of a high-current, low-voltage stabilizer. The same trigger circuit and expander modulator are used in both methods. A detailed comparison of the performance of the two methods is made and their advantages and limitations are discussed.

Recently, experimental evidence[1-4] has been found which suggests the probable existence of narrow multiple resonances superimposed on the giant resonances in photo-nuclear reactions. If this is the case then high energy electron accelerators, such as betatrons and synchrotrons will be still further used in the study of nuclear spectroscopy. Previously Van de Graaff generators and cyclotrons, which produce accurately controlled monochromatic beams of heavy particles, have been the main tools in the study and cataloguing of nuclear energy levels. With the advent of accurately controlled high-energy X-ray sources this state of affairs is likely to change. With this in mind a programme of work has been undertaken on a 20 MeV betatron to investigate methods of energy control, and it is the purpose of this paper to discuss the overall design and construction of such an apparatus. These methods are not restricted to 20 MeV machines but can be applied to accelerators of higher energy.

In a betatron the electrons are injected into the toroid at low energy and are accelerated over one-quarter cycle of the alternating magnetic field. As the magnetic flux through the electron orbit increases the electrons experience a tangential force and their gain in energy per revolution is equivalent to the voltage that would be induced in a loop of wire placed at the orbit. The kinetic energy of the electrons is determined by the magnetic field and the orbit radius. At peak energy or earlier, if desired, the electron orbit can be expanded, causing the electrons to produce X-rays by striking a target. This expansion of the orbit is accomplished by passing a high current pulse through two single turn coils in series, one above and one below the toroid.

The maximum X-ray energy is dependent on the exciting current passing through the magnet coils provided the expansion of the orbit takes place at the maximum value of the magnetic field. X-rays of lower peak energy can be obtained by expanding the orbit earlier in the acceleration cycle.

The magnet excitation circuit of the betatron used in these experiments is shown in Fig. 1. A 150 c/s supply is taken from a tripling transformer to a 30 kVA step-up transformer which supplies 16 kV to the magnet coils and tuning condensers. The magnet current can be controlled manually over a limited range by means of a simple buck-boost circuit. This method is of no use for accurate work and finer control of the energy can be obtained by disturbing the orbit at a predetermined magnetic field. Electronic methods of doing this have been developed and reported by McElhinney and others[5] and Katz and others.[6] Both these methods involve the use of a resistance-condenser integrator which produces a voltage proportional to the instantaneous electron energy. The energy of the electrons can be fixed by adjusting the bias on a trigger circuit. By consideration of the basic excitation circuit it can be seen that this method of obtaining an alternating reference voltage is suitable only when the supply frequency is constant. In the United States and Canada most

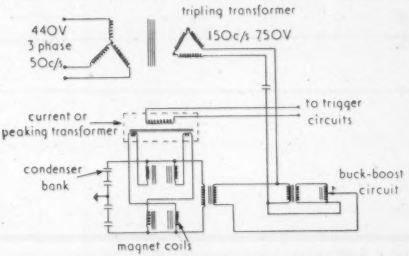

Fig. 1. The betatron excitation circuit showing the current transformer (or peaking transformer)

of the supplies are frequency controlled to better than 1 part in 10^5 c/s. In countries where the electrical generating plant is overloaded the mains frequency cannot be stabilized and variations depending on the demand may result in changes of up to $\pm 5\%$ in the frequency. An alternative method of obtaining a reference voltage uses a current transformer connected in series with the betatron magnet coils. This transformer produces a signal voltage proportional to the instantaneous electron energy and is independent of any frequency variations.

Three methods of accurate energy control were considered initially. The first was purely electronic using a current transformer to provide the reference voltage. The second method utilizes a series peaking transformer which can be biased, so as to fire at any part of the acceleration cycle, by means of a stable d.c. low-voltage power unit. A series peaking transformer consists of a saturable core excited by means of the betatron magnet current. It is not to be confused with the small peaking strips which are often used in the gaps of accelerator magnets for the purpose of producing sharp timing pulses. In the latter case a bias of only a few microseconds is required. The possibility of using a peaker

strip for energy control was considered but this would necessitate the use of a d.c. bias field of up to 3000 oersteds in opposition to the main guide field. Any coil capable of doing this would be large and the bias field would most likely interfere with the injection process.

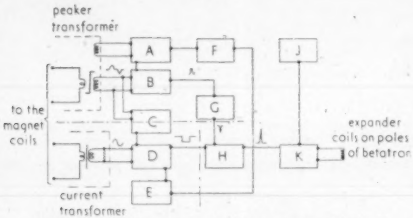

Fig. 2(*a*). Block diagram of the energy control circuit

A, low voltage stabilized d.c. supply; *B*, cathode follower; *C*, stabilized negative d.c. supply; *D*, double triode trigger unit; *E*, stabilized positive d.c. supply; *F*, megavolt meter; *G*, differentiating amplifier; *H*, trigger unit; *J*, monitoring cathode-ray oscillograph; *K*, expander modulator.

One reason why peaking transformers have been avoided by previous investigators is possibly due to the fact that if a sharp output pulse is required it is necessary to use a large number of ampere turns which need a correspondingly larger

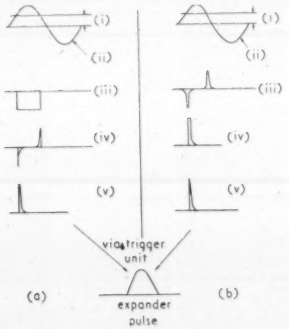

Fig. 2(*b*). Waveform comparison of the two methods

(*a*) current transformer method
(i) variable reference voltage
(ii) voltage wave in phase with magnet current
(iii) double triode trigger output
(iv) differentiated
(v) driver pulse

(*b*) peaking transformer method
(i) variable reference bias current
(ii) magnet current
(iii) series peaking transformer output
(iv) differentiating amplifier output
(v) driver pulse

bias. The chief advantage of a peaking transformer, however, is that there is very little jitter since the output depends on the saturation of the transformer core. If a sharp pulse can be produced so that it is locked to the peaking pulse and always coincides with its maximum voltage then a large number of ampere turns can be avoided. It has been found possible to do this with a differentiating amplifier. A block diagram showing the various sections of both methods of energy control and waveforms at various points in the circuits are shown in Fig. 2.

The third method, which at first sight seemed to show considerable promise as a method of energy control, is to employ a paramagnetic resonance technique. This is very similar to the well-known nuclear magnetic resonance which is often used for the stabilization of d.c. magnetic fields. Instead of using dielectric properties of an hydrogenous material, a crystalline organic compound such as diphenyl-trinitrophenyl hydrazol $(C_6H_5)_2N\text{-}NC_6H_2(NO_2)_3$ could be employed. This substance has a loosely bound electron with a relaxation time of the order of 10^{-10} s which should be small enough to handle varying fields of the order of 3×10^6 oersteds/s. The resonant wavelength λ is related to the magnetic field by the relationship $H\lambda = 10\,700$ oersted cm. Therefore for a maximum field of 3000 oersteds the frequency would be approximately 10 kMc/s, the half-width of the resonance being about 1·5 oersteds. The resonator and crystal would have to be located in the fringing field with a corresponding reduction in dH/dt and H. The main difficulty with this method is that a high-stability oscillator with a very wide frequency range is necessary and, owing to the technical problems in the construction of such an oscillator, it was decided to postpone the detailed investigation of this method.

For the purpose of monitoring the different waveforms a triggered cathode ray oscilloscope was included in the energy control unit. The oscilloscope has a conventional thyratron time base with several different sweep speeds down to 0·2 μs; the circuit details will not be described here.

THE CURRENT TRANSFORMER

In order to produce a reference voltage which faithfully represents the current flowing through the magnet coils it is important to reduce any phase shift in the current transformer to a minimum. A current transformer was constructed with

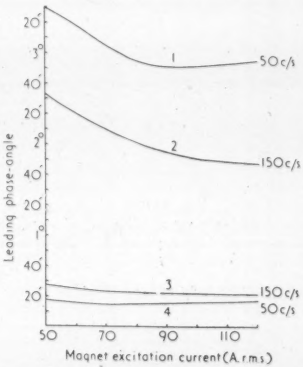

Fig. 3. Phase angle/magnet current characteristics of reference transformers

Curves 1 and 2: silicon–iron laminations (0·014 in. thick).
Curves 3 and 4: Mumetal laminations (0·015 in. thick).

silicon iron stampings and a turns ratio of 1 : 2500 with a load of 10 000 Ω across its secondary. The phase-shift, load-current characteristics are shown in Fig. 3 for frequencies of 50 and 150 c/s. The output voltage leads the magnet current by several degrees dropping steadily as the magnet excitation is increased from 70 to 120 A. This phase shift was certainly too large for any absolute energy measurements but even so, this current transformer was quite useful for certain relative determinations.

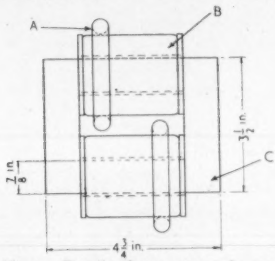

Fig. 4. Details of current transformer

A, two turns of 19 × 0·064 in. (vulcanized india rubber), 120 A cable (1 turn on each limb); *B*, secondary winding 5000 turns, 0·0076 in. diameter Lewmex covered wire (by The London Electric Wire Co. Ltd.) on each spool (connected in series); *C*, 0·015 in. thick Mumetal stampings (L and L), 1¼ in. thick stack.

These relatively large phase shifts were attributed to the poor quality of the silicon iron stampings and a second transformer with the same turns ratio but having a core of 0·015 in. thick Mumetal stampings was constructed. The detailed design of this transformer is given in Fig. 4. It is interesting to note that if the primary winding consisted of two turns of cable wound round one leg of the core, then the output voltage lagged the primary current. By splitting the primary turns, and arranging one turn round each of the separate legs of the core the phase shift was a leading one and was also considerably reduced. The two lower curves of Fig. 3 refer to the Mumetal core. This effect is probably due to the smaller magnetic leakage obtained by distributing the primary winding. Another possible variation was the alteration of the effective turns ratio with excitation current. It was found that this could be made almost constant provided a suitable load resistance was used. The final load consisted of nine 10 kΩ, 20 W wire-wound resistances connected in series parallel and mounted in an oil tank. A temperature coefficient of less than 1 part in 10^4 per °C helped to reduce any variation due to heating of resistances on load or to variations in the ambient temperature.

PULSE GENERATOR CIRCUITS

The problem of accurate energy control, after obtaining a proportional reproduction of the betatron excitation current, is reducible to that of producing a short electrical pulse having a small random jitter and which can also be accurately positioned at any point on the input sine wave. One method which has been used employs a circuit known as a "multiar." This was originally developed by Williams and Moody[7] as an accurate range marker in radar and its use as a method of energy control was suggested by Goward and others.[8] An improved multiar circuit was patented by

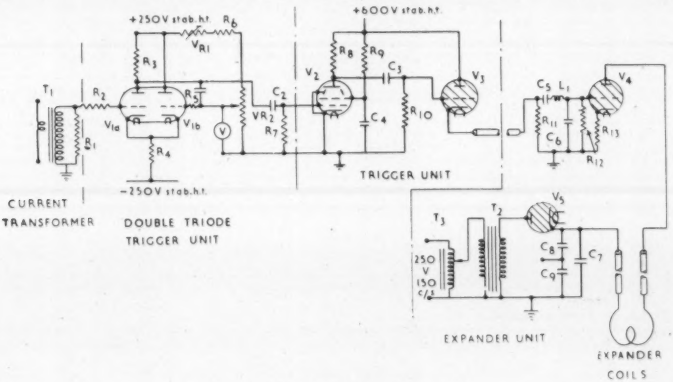

Fig. 5. Circuit for electronic method

R_1 = 9 kΩ w.w., 1800 W (9 × 200 W in series parallel)
R_2 = 100 kΩ w.w., 3 W
R_3 = 2 kΩ w.w., 5 W
R_4 = 168 kΩ w.w., 5 W
R_5 = 100 kΩ w.w., 5 W
R_6 = 150 kΩ w.w., 5 W
R_7 = 100 kΩ w.w., 5 W
R_8 = 10 kΩ w.w., 5 W
R_9 = 10 kΩ w.w., 5 W
R_{10} = 470 kΩ, ½ W
R_{11} = 100, ½ W
R_{12} = 47 kΩ, ½ W
R_{13} = 0·1 Ω, 50 W (Carbon pellet non-inductive resistor)
VR_1 = 50 kΩ, 5 W (Preset potentiometer)
VR_2 = 100 kΩ, 5 W [Helical potentiometer (10 turn)]
C_1 = 0·1 μF, 350 V
C_2 = 470 pF
C_3 = 0·05 μF
C_4 = 0·1 μF
C_5 = 0·05 μF
C_6 = 220 pF
C_7 = 0·125 μF, 5 kV
C_8 = 100 pF, 4 kV
C_9 = 0·005 μF
T_1 = Current transformers: primary 2 turns, 100 A cable; secondary 2 coils of 5000 turns of 0·0076 in. diameter wire
T_2 = Auto transformer: primary 230 V; secondary 3·5 kV, 300 mA
T_3 = Variac type 100 L
L_1 = R.F. choke 200 mH
V_1 = ECC34
V_2 = 6F17
V_3 = BT79
V_4 = BT83
V_5 = RG3–250

Carruthers.[9] The controlling 150 c/s sine wave is fed *via* a small pulse transformer on to a diode. The diode only conducts when the instantaneous voltage reaches a predetermined value fixed by a stabilized bias supply. This completes the feedback circuit for a pentode, the grid of which is driven rapidly negative, producing a complete oscillation which results in a positive square pulse having an amplitude of about 200 V at the anode.

An alternative pulse generator which seemed to have certain advantages over a multiar circuit is based on a Schmitt[10] trigger circuit, see Fig. 5. Improvements and modification to this circuit have been carried out by Scoles.[11] The positive bias provided by the energy control potentiometer (100 kΩ helipot), see Fig. 5, makes the second triode V_{1b} conduct and by its cathode follower action it causes V_{1a} to be cut off. The alternating 150 c/s reference voltage obtained from the current transformer is applied to the grid of the first valve V_{1a} which begins to conduct when the voltage on the grid reaches the same value as the voltage on the cathode, thus causing the anode voltage to fall. In turn the grid of V_{1b} is driven negative through the coupling condenser C_1 thus cumulatively cutting off V_{1b}. This results in a rapidly rising negative pulse on the anode V_{1a}. With a 150 c/s, 100 V input, this circuit provides pulses with a rise time of approximately 1 μs. The advantage of this type of circuit is that the positive feedback can be used to reduce the effective grid base of V_{1a} by adjusting its anode load. An analysis of a similar circuit has been given by Williams[12] who shows that the most rapid switchover is obtained if the anode load of V_{1a} is equal to $4/g$ where g is the mean slope of each valve. This shortening of the effective grid base reduces the delay and also some of the uncertainties in the time of firing. The output from the double-triode is differentiated and inverted by V_2 and the resulting positive component is used to trigger a BT79 hydrogen thyratron, V_3, which fires into a 100 Ω terminating resistance at the end of 20 ft of coaxial cable. This is used as a trigger supply for the expander unit.

The expander modulator, V_4, consists of a BT83 hydrogen thyratron which discharges a 0·125 μF capacitor, through the expander coils giving a 4 μs half sine wave pulse. The capacitor is charged from a 3 kV transformer through V_5, a mercury-vapour diode type RG5-250. The primary of the transformer is fed from an autotransformer connected to a 250 V, 150 c/s supply which is taken from coils wound round the pole pieces. The expander coils consist of one turn of polyvinyl chloride insulated (70/0·0076 in.) wire on each pole piece. The pulse current through the coils can be observed across a 0·1 Ω carbon pellet resistance in series, whilst the charging voltage can be measured on the potential divider.

THE SERIES PEAKING TRANSFORMER METHOD

Design and construction. The series peaking transformer consists of a suitable magnetic core upon which is wound an excitation coil. This coil is connected in series with a betatron magnet coil and produces a flux which saturates the core. If a second pick-up coil is wound on the core a voltage is produced which is nearly zero when the core is saturated. Just before the current reaches zero the flux density in the core begins to change from saturation in one direction to saturation in the opposite direction as shown in Fig. 6. The core changes from low permeability (saturation) to high permeability (unsaturated). As the saturation is reduced the voltage on the pick-up coil begins to rise rapidly reaching a maximum near zero current and then falling off as the core begins to saturate again. The position relative to the a.c. excitation current wave of zero flux in the core can be adjusted by means of a d.c. bias coil wound so that its flux opposes that in the main excitation winding.

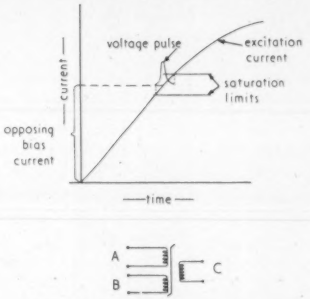

Fig. 6. The relationship between excitation current, bias current and output voltage for a series peaking transformer *A*, excitation winding; *B*, main d.c. bias winding; *C*, voltage coil and d.c. bias.

For the simple case of no bias current the magnetizing force H for a current I passing through zero is given by

$$H = \frac{4\pi}{10}\frac{N}{l}I$$

where N is the number of primary turns and l is the mean magnetic path of the core. The peak voltage produced in the secondary pick-up coil is

$$v = nA\frac{dB}{dt} \times 10^{-8}\ \text{V}$$

where B is the flux density in the core when unsaturated, A is the cross-section of the core and n is the number of turns on pick-up coil. Now $B = f(H)$, hence

$$v = nA\frac{d}{dt}\left[f\left(\frac{4\pi}{10}\frac{NI}{l}\right)\right] \times 10^{-8}\ \text{V}$$

In order to design a peaking transformer it is necessary to know the form and the characteristic $f(H)$. A tangent function for this was assumed by Wilkinson,[13] but this leads to only a rough approximation for the voltage and pulse length obtainable for a given core and turns ratio. A more recent article by Sim[14] describes a method in which four experimental constants K_{1-4} for a given core sample are used. Since the design is generally limited by the availability of standard cores and laminations it was found better to carry out simple tests on the cores, measuring the variation of the pulse length and voltage amplitude for various values of excitation current. This method seems all the more desirable when it is realized that large differences between the *B–H* characteristics of nickel–iron alloy cores can arise due to their "different histories." Some simple experiments with Mumetal, Rhometal and Radiometal laminations (by Telegraph Construction and Maintenance Co., Ltd.) soon revealed that Mumetal was by far the best core material, resulting in a narrower pulse with greater amplitude for a given rate of rise of primary current. Since

the rate of change of current dI/dt is fixed for a given magnet current, frequency and excitation, N and A are the only variables. It is not advisable to make the cross-sectional area of the core too large as this will increase the width of the output pulse. The value of N is also limited since in order to bias the pulse to any point throughout the accelera-

wave moves into the core it can be shown that a lower limit for the width of the output pulse is of the order of

$$a\left(\frac{\rho}{4\pi B_s}\cdot\frac{dH}{dt}\right)^{-\frac{1}{2}}$$

where ρ is the resistivity of the core material, $2a$ is the thick-

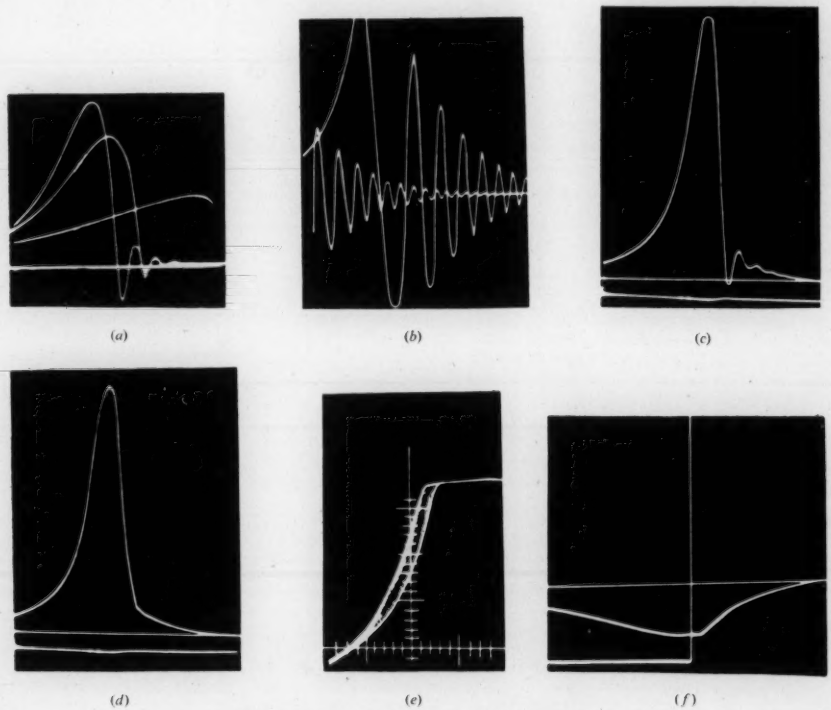

(*a*) (*b*) (*c*)

(*d*) (*e*) (*f*)

Fig. 7. Oscillograms illustrating performance of peaking transformer method

(*a*) Peaking transformer pulse fed into 20 ft of coaxial cable with load resistances of 10, 5 and 1 kΩ.
(*b*) Peaking transformer pulse fed into 20 ft of coaxial cable.
(*c*) Peaking transformer pulse 50 μs wide at half amplitude.
(*d*) Peaking transformer pulse fed into 20 ft of coaxial cable *via* a cathode follower.
(*e*) Time jitter on two double triode trigger unit output pulses using one pulse to trigger the cathode-ray oscillograph.
(*f*) Peaking transformer pulse with front of differentiating amplifier pulse superimposed.

tion period it is necessary to oppose the primary flux with the same number of ampere turns. As it is difficult to stabilize more than 1 A d.c. a figure of 100 ampere turns for the primary excitation was chosen, i.e. 1 turn primary and 141 turns on the bias winding.

By consideration of the velocity at which the saturation

ness of the laminations, and B_s is the saturation flux. This expression indicates that the laminations should be as thin as possible. This is a factor which is generally ignored although the values of K in Sim's paper must depend on the lamination thickness.

A toroidal core of 0·002 in. thick Mumetal, $\frac{3}{8}$ in. square

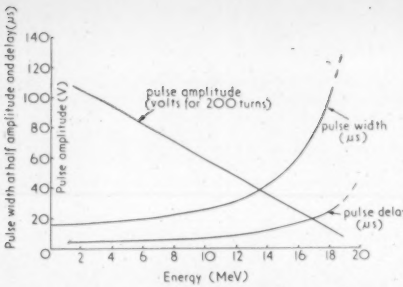
Pulse width at half amplitude and delay (μs)
Pulse amplitude (V)
pulse amplitude (volts for 200 turns)
pulse width (μs)
pulse delay (μs)
Energy (MeV)

Fig. 8. Characteristics of the series peaking transformer showing the variation of pulse delay, pulse width and amplitude with instantaneous energy in MeV (i.e. rate of change of excitation dI/dt)

cross-section, with an inside diameter of 1¼ in. was used for the final peaking transformer. The main excitation winding consists of 10 turns of polyvinyl chloride insulated wire connected in parallel, which helps to distribute the excitation flux around the core. The main bias winding consists of 140 turns of No. 19 s.w.g. double cotton covered eureka wire also distributed around the core. A second winding of 200 turns 37 s.w.g. enamelled copper wire was used as a secondary pick-up winding and as a separate bias winding in opposition to the other bias.

Method of biasing. Since the self capacitance of a large number of secondary turns has a similar effect to a capacitative load on the transformer, it was considered advisable to use a minimum number of turns and a correspondingly larger bias current. This meant a high-current, low-voltage stabilized supply rather than the conventional high-voltage and low-current power unit. There have been numerous articles describing various circuits for low voltage stabilizers. The most suitable for this purpose seems to be the one due to Attree[15] who suggested the use of a 2 kc/s multivibrator controlled by a series modulator valve (12E1) with its grid

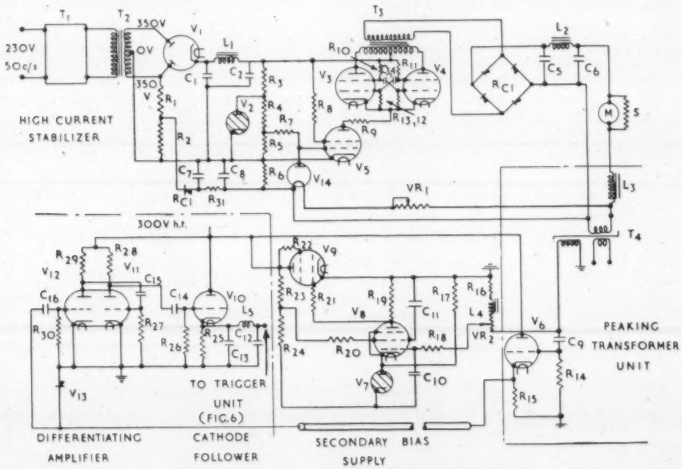

Fig. 9. Circuit for peaking transformer method

R_1 = 220 kΩ w.w.
R_2 = 22 kΩ w.w.
R_3 = 1 MΩ
R_4 = 1 MΩ
R_5 = 1 MΩ
R_6 = 100 kΩ w.w.
R_7 = 47 MΩ
R_8 = 10 kΩ
R_9 = 47 Ω w.w.
R_{10} = 10 kΩ
R_{11} = 10 kΩ
R_{12} = 470 kΩ
R_{13} = 470 kΩ
R_{14} = 1 MΩ
R_{15} = 10 kΩ
R_{16} = 1 kΩ
R_{17} = 33 kΩ w.w.
R_{18} = 47 kΩ
R_{19} = 100 kΩ w.w.
R_{20} = 100 kΩ
R_{21} = 100 kΩ
R_{22} = 2·2 kΩ
R_{23} = 10 kΩ w.w.
R_{24} = 22 kΩ w.w.
R_{25} = 10 kΩ
R_{26} = 1 MΩ
R_{27} = 1 MΩ
R_{28} = 100 kΩ
R_{29} = 100 kΩ
R_{30} = 1 MΩ
R_{31} = 15 kΩ w.w.
VR_1 = 100 kΩ helipot
VR_2 = 250 kΩ

C_1 = 8 μF, 350 V
C_2 = 16 μF, 350 V
C_3 = 470 pF, 350 V
C_4 = 470 pF, 350 V
C_5 = 32 μF, 15 V
C_6 = 2000 μF, 15 V
C_7 = 8 μF, 150 V
C_8 = 8 μF, 150 V
C_9 = 0·01 μF, 350 V
C_{10} = 0·1 μF, 500 V
C_{11} = 0·1 μF, 500 V
C_{12} = 220 pF, 600 V
C_{13} = 220 pF, 600 V
C_{14} = 470 pF, 350 V
C_{15} = 10 μF, 500 V
C_{16} = 220 pF, 600 V

V_1 = 5Z4G
V_2 = QS 70/20
V_3 = 6V6
V_4 = 6V6
V_5 = 12E1
V_6 = 6F12
V_7 = QS 70/20
V_8 = 6F12
V_9 = 12E1
V_{10} = 6F12
V_{11} = ECC35
V_{12} = ECC35
V_{13} = CG1-C
V_{14} = IT4

T_1 = Constant voltage transformer
T_2 = Main transformer: primary 230 V; secondary 350–0–350 V, and filament supplies

T_3 = Output transformer: primary 1600 turns, 37 s.w.g. enamel wire; secondary 40 turns, 20 s.w.g. enamel wire; core 40 T stampings Radiometal 1 in. stack (Telcon)

T_4 = Peaking transformer: primary 20 turns, 2 sets of 10 turns in parallel; secondary 200 turns, 37 s.w.g. enamel wire (distributed); 140 turns, 19 s.w.g. double cotton covered eureka wire (distributed)

L_1 = 25 H, 100 mA (d.c.)
L_2 = 0·1 H, 1 A (d.c.) {500 turns, 20 s.w.g. enamel wire on ¾ in. stack of 101T Radiometal stampings (Telcon), 0·005 in. gap}
L_3 = 1 H, 1 A (d.c.)
L_4 = 10 H, 200 mA (d.c.)
L_5 = 200 μH (r.f.)

RC_1 = Bridge rectifier 4 A, 20 V (r.m.s.)
RC_2 = Half-wave rectifier 20 mA, 20 V
M, S = Meter 0–100 μA, shunted to 1 A

voltage supply stabilized by means of a QS 70/20 gas discharge tube. Two 6V6 valves are used as the multivibrator with their anodes connected to a push-pull radio frequency transformer. A 250 Ω helical potentiometer in series with the filament of a diode-connected 1T4 valve was used for the control of the output voltage. The 2 kc/s supply is rectified by a selenium bridge rectifier and smoothed. The peaking transformer bias winding is fed through a 1 H choke (0·25 Ω) preventing the power unit acting as a short circuit to the peaking pulse.

Unfortunately the stabilizer output voltage does not fall to zero when the resistance of the control Helipot (VR1) is zero. In order to make the peaking transformer fire down to zero excitation current, it is necessary to provide an opposing bias which will cancel out the resulting residual flux. This secondary bias can also be used to eliminate any delays in the firing of the transformer by overbiasing. The maximum bias current required was about 20 mA and a conventional type of series stabilizer, shown in Fig. 9, was used to provide this.

Performance. It is usual to assume that the peak voltage of the output pulse occurs at zero flux. This is not always true as the shape of the pulse is generally modified by the shape of the *B–H* characteristics. The result is an output pulse which has a slowly rising front and a sharp trailing edge with a consequent delay in the voltage peak, see Fig. 7(*c*). This delay is dependent on the secondary load of the peaking transformer and must be kept to a minimum. Generally, if the load impedance is much greater than the impedance of the transformer then the pulse has only a short delay. In the present case the load impedance is that of the grid of a valve. The main factor affecting pulse shape is due to the capacitance of the 20 ft of coaxial cable from the peaking transformer, which is situated near the betatron magnet. The effect of this cable is to cause high-frequency oscillations on the trailing edge of the pulse, as shown in the oscillograms in Fig. 7(*b*). This problem of the pulse delay has been treated in detail by Harmer[16] for various types of load. The delays of the peaking transformer for loads of 10, 5 and 1 kΩ respectively, are shown in the oscillogram of Fig. 7(*a*). The delays in the present peaking transformer were measured by comparison with a fixed reference pulse and the results are shown in Fig. 8 for different energy values. In order to avoid the effect due to the cable capacitance the peaking pulse was fed into a cathode follower circuit mounted near the peaking transformer. This scheme eliminated the high-frequency oscillations, see Fig. 7(*d*).

Since amplitude and width of the peaking transformer pulse varies with its position in the acceleration cycle due to the change in dI/dt, some difficulty arises in sharpening the pulse so that a suitable trigger pulse can be passed on to the expander unit. Conventional methods such as blocking oscillators, etc., usually depend on the leading edge of the pulse. If these methods are used, the time at which the expander thyratron is triggered will not coincide with the peak of the pulse or with the point of zero flux. It should be possible to introduce some delay in the trigger pulse and it may be advantageous to use the leading edge of the peaking pulse in order to eliminate some of the delays inherent in the peaking transformer. This method, however, is complicated by the fact that the pulse amplitude also varies with the rate of change of flux. An attempt was made to produce a trigger pulse occurring only at the maximum of the peaking pulse. This was done by means of the double-triode differentiating amplifier shown in Fig. 9. An oscillogram of the peaking pulse with the front of the trigger output pulse superimposed is given in Fig. 7(*f*). There is some slight delay in the differentiating amplifier which varies with pulse width, but this seems to be small compared with the delay of the peaking transformer pulse. As the peaking transformer pulse changes slowly near its maximum it is difficult to measure this delay accurately and therefore it was included in the total delay of the peaking transformer shown in Fig. 8, and also in Table 2.

A megavoltmeter was also incorporated in the energy control unit. The indicating instrument was a milliammeter (0–1 mA), suitably shunted, and connected in series with the high-current bias winding of the peaking transformer, see Fig. 9. For the electronic method the indicator was simply an electrostatic voltmeter connected across the d.c. bias Helipot, see Fig. 5. The megavoltmeter cannot be relied upon to give an accuracy in the peak energy of X-rays of better than 0·25 MeV and it is used purely as an indicator.

COMPARISON OF PERFORMANCE OF THE TWO METHODS

A series of comparative tests has been carried out on the two methods of energy control and various features such as time jitter, delay and drift of the circuits have been measured. Jitter measurement in electronic circuits is never a simple matter, especially when the impulse reference voltage is a slowly varying voltage, such as a 150 c/s sine wave, since no accurate reference marker is available. If a fast cathode-ray oscilloscope is used and triggered from the alternating reference voltage, there will be the added complication of time-base jitter. The best technique found here was to construct two identical circuits and have them fed from the same alternating reference voltage and high-tension supplies. One output pulse can be used to trigger a high-speed cathode-ray oscilloscope, whilst the other can be displayed on a suitable time base. This method measures the total random jitter of one circuit with respect to the other and the effective jitter of one can be taken to be 0·707 times the total random jitter. Certain precautions have to be taken since it is possible to lock the two trigger circuits together, and this makes the jitter appear very small. On the other hand if the pulses are nearly locked together, they might jump into lock and out again making it seem as if the jitter is very large. By

Table 1. *Results obtained using the electronic method*

Circuit component	*Jitter*	*Delay*	*Drift*
Current transformer	—	25′ leading phase angle about −6 μs	No detectable change in phase angle and an effective turns-ratio stability of better than 1 part in 10^3.
ECC34	±1 μs over range 0 to 19·5 MeV	2·0 μs	Stable to better than 1 part in 2000 after initial warm up of power packs.
Inverter 6F17	±0·1 μs	2·0 μs	
BT79 hydrogen thyratron	±0·05 μs	0·5 μs	
BT83 hydrogen thyratron	±0·05 μs	0·5 μs	
Total	±1·2 μs (0·025 MeV)	1 μs lead	

inserting a 20 mH r.f. choke in the high-tension supplies to each unit with a 0·1 μF by-pass condenser connected to earth and also isolating the filament to the separate circuits, a true measure of the jitter was obtained. A good test is to adjust the observed pulse to various positions on the fast time base, by means of the bias potentiometer. Then if the measured jitter varies with the position of the pulse in time, there is likely to be interaction between the two circuits. For the present circuits, the jitter is approximately 1 μs over most of the acceleration cycle, see Fig. 7(*e*). However, near the peak of the voltage sine wave, the jitter was found to be as much as 10 μs, due to the very small rate of change of voltage. Some of the results of the jitter, delay and drift of the pulse units are summarized in Tables 1 and 2 for both methods. A further source of error resulting in a non-linear energy scale is due to the energy gain of the accelerated electrons from the flux produced by the expander pulse. It

Table 2. *Results obtained using the peaking transformer method*

Circuit component	*Jitter*	*Delay*	*Drift*
Peaking transformer	0·1 μs for an unbiased peaker. Dependent on the ripple of bias supply which is less than 1 mV hence jitter is less than $\pm$0·3 μs	Variation of delay with MeV is shown in Fig. 8. This can be corrected by means of opposing bias to an accuracy of $\pm$1 μs	After initial warm up, power supply (with constant voltage transformer T_1) output change by 0·01% for change of 20 V in mains voltage.
Differentiating amplifier and cathode follower	$\pm$0·1 μs	Included in the peaking transformer delay	
BT79	$\pm$0·05 μs	0·5 μs	
BT83	$\pm$0·05 μs	0·5 μs	
Total	$\pm$0·5 μs jitter (0·01 MeV)	Up to 2 μs delay	

has been estimated by McElhinney and others[5] to be of the order of 0·02 MeV. Combining this error with the delays, the error in the linear energy scale is approximately 0·05 MeV in both methods. The energy jitter of the peaking transformer method ($\pm$0·01 MeV) is smaller than the jitter in the electronic method ($\pm$0·025 MeV). Nevertheless the latter method is more convenient to use since it requires only one control potentiometer and no corrections have to be made for delays which are inherent in the peaking transformer. For very accurate control over a limited energy range the peaking transformer method is likely to prove superior.

Both methods suffer from the disadvantage that in the region of 19·5–20 MeV they become rather inaccurate. In the case of the electronic method this is due to the small rate of change of voltage applied to the double triode trigger unit, thus causing jitter of the output pulse. With the peaking transformer, the output pulse becomes so long and small in amplitude that it fails to trigger the differentiating amplifier. One simple way of avoiding this is to increase the magnet excitation so that the peak energy of the machine is a little higher than the maximum energy required. This disadvantage is not encountered with the integrator method as there is a 90° phase shift between the magnet excitation current and the reference voltage. In this case, however, the same difficulties will exist in the lower energy region up to about 0·5 MeV.

CONCLUSIONS

It has been shown that it is possible to control accurately the electron energy of a 20 MeV betatron by two different methods. The first method uses a current transformer to supply a reference voltage in phase with the current in the betatron magnet coils to a trigger and potentiometer control unit. The second method uses a peaking transformer connected in series with the betatron magnet coils and supplies a pulse to a differentiating amplifier.

The peaking transformer scheme is shown to be capable of controlling the electron beam energy to within $\pm$0·01 MeV and the current transformer method will control the energy to within $\pm$0·025 MeV. This latter method is the more convenient to use in practice though the former method is superior for very accurate control of energy over a limited range.

Both methods become rather inaccurate near the peak energy of a given machine (in this case in the region 19 to 20 MeV) because of the slow rate of change of flux with time at the peak of the excitation current wave.

ACKNOWLEDGEMENTS

The author wishes to thank Mr. G. Gaskin, who helped in the wiring and testing. Also Messrs. S. W. Redfearn and E. A. Finlay for discussions on the design of the current and peaking transformers; Mr. F. R. Perry for his comments on the work; Dr. Willis Jackson, Director of Research and Education, and Mr. B. G. Churcher, Manager of the Research Department, Metropolitan-Vickers Electrical Co. Ltd., for permission to publish this paper.

REFERENCES

(1) Goward, F. K., and Wilkins, J. J. *Proc. Phys. Soc., A*, **65**, p. 671 (1952).
(2) Phillips, K. *Phil. Mag.*, **44**, p. 53 (1953).
(3) Goldenberg, J., and Katz, L. *Phys. Rev.*, **95**, p. 471 (1954).
(4) Katz, L., Haslam, R. N. H., Horsley, J., Cameron, A. G. W., and Montilbetti, R. *Phys. Rev.*, **95**, p. 464 (1954).
(5) McElhinney, J., Hanson, A. O., Becker, R. A., Duffield, R. B., and Diven, B. C. *Phys. Rev.*, **75**, p. 542 (1949).
(6) Katz, L., McNamara, A. G., Forsythe, P. A., Haslam, R. N. H., and Johns, H. E. *Canad. J. Res., A*, **28**, p. 113 (1950).
(7) Williams, F. C., and Moody, N. F. *J. Instn Elect. Engrs*, **93**, IIIA, p. 1188 (1946).
(8) Goward, F. K., Lawson, J. D., Wilkins, J. J., and Carruthers, R. *J. Instn Elect. Engrs*, **97**, I, p. 320 (1950).
(9) Carruthers, R. British Patent 662341 (1950).
(10) Schmitt, O. H. *J. Sci. Instrum.*, **15**, p. 24 (1938).
(11) Scoles, G. J. British Patents 621752, 621872, 614219, 633772, 629907, 635643, 697879, 722428, 731159.
(12) Williams, F. C. *J. Instn Elect. Engrs*, **93**, IIIA, p. 289 (1946).
(13) Wilkinson, K. J. R. *J. Instn Elect. Engrs*, **93**, IIIA, p. 1090 (1946).
(14) Sim, A. C. *Wireless Engr*, **30**, p. 90 (1953).
(15) Attree, V. H. *Electronic Engng*, **25**, p. 71 (1953).
(16) Harmer, J. D. *B.T.-H. Res. Lab. Report* No. L. 4125 (1952).

Fields and stresses in dielectric media

By G. Power, M.A., Ph.D., University of Nottingham

[*Paper first received* 11 *August, and in final form* 18 *November*, 1955]

The Maxwell stresses are here considered and are used to obtain, in two dimensions, expressions for the mechanical forces experienced at the boundary of an isotropic dielectric owing to the presence of an electric field. Special dielectric boundary shapes are discussed, and the method of conformal transformation is employed in order to satisfy more easily the boundary conditions that are imposed on the fields. A number of cases are studied in detail, and experimental verification is obtained by use of the electrolytic tank.

1. THE MAXWELL STRESSES

By considering a surface S drawn in the ether, enclosing any amount of electrostatic charge, regarded as being made up of volume electrification (surface charges can be treated as limiting cases), Maxwell deduced that the system of stresses

$$\left.\begin{aligned} P_{xx} &= \frac{1}{8\pi}\left[\left(\frac{\partial\phi}{\partial x}\right)^2 - \left(\frac{\partial\phi}{\partial y}\right)^2 - \left(\frac{\partial\phi}{\partial z}\right)^2\right], \\ P_{yy} &= \frac{1}{8\pi}\left[\left(\frac{\partial\phi}{\partial y}\right)^2 - \left(\frac{\partial\phi}{\partial z}\right)^2 - \left(\frac{\partial\phi}{\partial x}\right)^2\right], \\ P_{zz} &= \frac{1}{8\pi}\left[\left(\frac{\partial\phi}{\partial z}\right)^2 - \left(\frac{\partial\phi}{\partial x}\right)^2 - \left(\frac{\partial\phi}{\partial y}\right)^2\right], \\ P_{xy} &= \frac{1}{4\pi}\frac{\partial\phi}{\partial x}\frac{\partial\phi}{\partial y}, \quad P_{yz} = \frac{1}{4\pi}\frac{\partial\phi}{\partial y}\frac{\partial\phi}{\partial z}, \quad P_{zx} = \frac{1}{4\pi}\frac{\partial\phi}{\partial z}\frac{\partial\phi}{\partial x} \end{aligned}\right\} \quad (1)$$

accounted satisfactorily for the mechanical action on all matter inside S, ϕ being the single-valued potential at a point due to the whole electrification. The existence of the Maxwell stresses has been doubted by many authors, some of whom go so far as to state that these stresses are simply mathematical fictions which can be used conveniently in the solution of certain electrical problems. Care has certainly to be exercised whenever the question of energy is involved, as the following paragraph illustrates.

The empirical laws of electrostatics show that if energy is distributed throughout space as a continuous function with volume density

$$\frac{1}{8\pi}\left[\left(\frac{\partial\phi}{\partial x}\right)^2 + \left(\frac{\partial\phi}{\partial y}\right)^2 + \left(\frac{\partial\phi}{\partial z}\right)^2\right],$$

the total energy will prove to be the same as the total energy of electrification. This result does not depend in any way on the Maxwell stresses. Moreover, since it is not made very clear how these stresses act, it is of interest to see if they can account for the energy of electrification when the ether is regarded as an elastic solid. With the usual notation, the elastic strain-energy stored per unit volume of material is

$$W = \tfrac{1}{2}(P_{xx}e_{xx} + P_{yy}e_{yy} + P_{zz}e_{zz} + P_{yz}e_{yz} + P_{zx}e_{zx} + P_{xy}e_{xy})$$

where, in the case of isotropic materials, the strain and stress components are related by equations of the form

$$e_{xx} = \frac{1}{E}[P_{xx} - \sigma(P_{yy} + P_{zz})], \text{ etc.}$$

$$e_{yz} = \frac{2(1+\sigma)}{E}P_{yz}, \text{ etc.}$$

E, σ being respectively Young's modulus and Poisson's ratio.

The expression for the strain-energy per unit volume can thus be written as

$$W = \frac{1+\sigma}{2E}\left[P_{xx}^2 + P_{yy}^2 + P_{zz}^2 + 2(P_{yz}^2 + P_{zx}^2 + P_{xy}^2) - \frac{\sigma}{(1+\sigma)}(P_{xx} + P_{yy} + P_{zz})^2\right]$$

and using the stresses (1), it is easily seen that W is proportional to

$$\left[\left(\frac{\partial\phi}{\partial x}\right)^2 + \left(\frac{\partial\phi}{\partial y}\right)^2 + \left(\frac{\partial\phi}{\partial z}\right)^2\right]^2$$

The Maxwell stresses thus fail completely to account for the energy of electrification on the assumption that the ether behaves like an isotropic elastic solid.

The same difficulties are met with when dealing with dielectric media. Neglecting the effects of electrostriction, the Maxwell stresses for a dielectric are

$$\left.\begin{aligned} P_{xx} &= \frac{k}{8\pi}\left[\left(\frac{\partial\phi}{\partial x}\right)^2 - \left(\frac{\partial\phi}{\partial y}\right)^2 - \left(\frac{\partial\phi}{\partial z}\right)^2\right], \text{ etc.} \\ P_{xy} &= \frac{k}{4\pi}\frac{\partial\phi}{\partial x}\frac{\partial\phi}{\partial y}, \text{ etc.} \end{aligned}\right\} \quad (2)$$

where k is the dielectric constant. Under certain conditions the stresses (2) can be used quite adequately to give the mechanical forces experienced at the boundary of a dielectric when in the presence of an electric field. In the work that follows the Maxwell stresses (2) are employed to deduce certain formulae for these mechanical forces, taking care to state when the solutions obtained are valid.

For the remaining part of this paper we shall be concerned with two-dimensional fields, and we start by considering a nested system of homogeneous isotropic dielectric cylinders having a cross-section of general shape. Let the perturbed electric fields in the various media be expressed in the terms of complex potential functions. We examine the stress on the contour of the interface separating the medium (s) of dielectric constant k_s from the medium ($s+1$) of dielectric constant k_{s+1}. Take the origin of co-ordinates inside the contour, and define the complex potential of the field in the medium ($s+1$) by $w_{s+1} = \phi_{s+1} + i\psi_{s+1}$ with the usual notation. Due to this field the interface c will experience a force whose rectangular components per unit length of the cylinder are

$$X_{s+1} = \int_c (P_{xx}dy - P_{xy}dx), \quad Y_{s+1} = \int_c (P_{yx}dy - P_{yy}dx),$$

where $$P_{xx} = \frac{k_{s+1}}{8\pi}\left[\left(\frac{\partial\phi_{s+1}}{\partial x}\right)^2 - \left(\frac{\partial\phi_{s+1}}{\partial y}\right)^2\right],$$

$$P_{yy} = \frac{k_{s+1}}{8\pi}\left[\left(\frac{\partial\phi_{s+1}}{\partial y}\right)^2 - \left(\frac{\partial\phi_{s+1}}{\partial x}\right)^2\right],$$

$$P_{xy} = P_{yx} = \frac{k_{s+1}}{4\pi}\frac{\partial\phi_{s+1}}{\partial x}\frac{\partial\phi_{s+1}}{\partial y}.$$

The complex force Z_{s+1} is thus

$$Z_{s+1} = Y_{s+1} + iX_{s+1} = \frac{k_{s+1}}{8\pi}\int_c \left(\frac{dw_{s+1}}{dz}\right)^2 dz \qquad (3)$$

In a similar manner, Γ_{s+1} the anti-clockwise moment about the origin of co-ordinates of the mechanical forces due to w_{s+1} is given by

$$\Gamma_{s+1} = \mathscr{R}\frac{k_{s+1}}{8\pi}\int_c \left(\frac{dw_{s+1}}{dz}\right)^2 z dz \qquad (4)$$

The total complex force $Z_{s,s+1}$ and couple $\Gamma_{s,s+1}$ on the boundary c are thus given by

$$\begin{aligned} Z_{s,s+1} &= Z_{s+1} - Z_s, \\ \Gamma_{s,s+1} &= \Gamma_{s+1} - \Gamma_s \end{aligned} \qquad (5)$$

where Z_s and Γ_s have an expression similar to equations (3) and (4) above.

It is to be emphasized that these results do not include the tendency of the dielectric material to change its shape. To take account of this effect proves in general to be impossible for solid media, but it is demonstrated that if the medium $(s+1)$ is fluid, electrostriction is accounted for by omitting the last term on the right-hand side of equations (5); that is to say, the complex force and couple become

$$\begin{aligned} Z_{s,s+1} &= Z_{s+1}, \\ \Gamma_{s,s+1} &= \Gamma_{s+1} \end{aligned} \qquad (5a)$$

We note that, in any case, for the many problems in which there are no singularities inside the contour c, Z_s and Γ_s both vanish, and so we are led to the same contour integrals whether we consider equations (5) or (5*a*).

It is frequently much easier to obtain the fields in the various media by using a conformal transformation in which the contours of the interfaces take a simplified form, straight lines for example, or circles. Let now $z = f(\zeta)$ be such a conformal transformation so that the contour c in the z-plane becomes the contour c_1 in the ζ-plane, then equations (3) and (4) become

$$Z_{s+1} = \frac{k_{s+1}}{8\pi}\int_{c_1}\left(\frac{dw_{s+1}}{d\zeta}\right)^2 \frac{d\zeta}{df/d\zeta} \qquad (6)$$

$$\Gamma_{s+1} = \mathscr{R}\frac{k_{s+1}}{8\pi}\int_{c_1}\left(\frac{dw_{s+1}}{d\zeta}\right)^2 \frac{f(\zeta)}{df/d\zeta}d\zeta \qquad (7)$$

The transformation $z = \sum_{n=0}^{\infty} A_n \exp\left[i(n-1)\zeta\right]$. Consider now the transformation

$$z = \sum_{n=0}^{\infty} A_n \exp\left[i(n-1)\zeta\right], \quad \zeta = \xi + i\eta \qquad (8)$$

where the coefficients A_n may be complex, and where the boundary between the media (s), $(s+1)$ is $\eta = 0$. With this transformation the points at infinity correspond, and since for large η

$$z \simeq A_0(\exp\eta)(\cos\xi - i\sin\xi)$$

we see that ξ varies from 2π to 0 as the contour of the boundary is described in an anti-clockwise direction.

Suppose that the field in $(s+1)$ is given by the complex potential

$$w_{s+1} = \sum_{n=1}^{p} a_n \exp(-ni\zeta) + \sum_{n=1}^{p} b_n \exp(ni\zeta).$$

It is easy to see that

$$\left[\sum_{n=1}^{p} na_n \exp(-ni\zeta)\right]^2 = \sum_{n=2}^{2p} c_n \exp(-ni\zeta),$$

where $$c_n = \sum_{r=1}^{p} r(n-r)a_r a_{n-r},$$

$$\left[\sum_{n=1}^{p} nb_n \exp(ni\zeta)\right]^2 = \sum_{n=2}^{2p} d_n \exp(ni\zeta),$$

where $$d_n = \sum_{r=1}^{p} r(n-r)b_r b_{n-r},$$

and $$\left[\sum_{n=1}^{p} na_n \exp(-ni\zeta)\right]\left[\sum_{n=1}^{p} nb_n \exp(ni\zeta)\right]$$

$$= f_0 + \sum_{n=1}^{p-1}\left[f_n \exp(ni\zeta) + g_n \exp(-ni\zeta)\right],$$

where $$f_0 = \sum_{r=1}^{p} r^2 a_r b_r, \quad f_n = \sum_{r=1}^{p-n} r(n+r)a_r b_{n+r},$$

and $$g_n = \sum_{r=1}^{p-n} r(n+r)b_r a_{n+r}.$$

Also we have

$$\frac{dw_{s+1}}{d\zeta} = -i\sum_{n=1}^{p} na_n \exp(-ni\zeta) + i\sum_{n=1}^{p} nb_n \exp(ni\zeta),$$

and $$\frac{dz}{d\zeta} = i\sum_{n=0}^{\infty}(n-1)A_n \exp\left[i(n-1)\zeta\right],$$

so that

$$\frac{1}{dz/d\zeta} = \frac{i\exp(i\zeta)}{A_0}\left[1 - \frac{A_2}{A_0}\exp(2i\zeta) - \right.$$

$$\left. - \frac{2A_3}{A_0}\exp(3i\zeta) - \ldots - \frac{(n-1)A_n}{A_0}\exp(ni\zeta) - \ldots\right]^{-1},$$

and for large ζ, this becomes $i\sum_{n=1}^{\infty} H_n \exp(ni\zeta)$, where

$$H_1 = 1/A_0, \; H_2 = 0, \; H_3 = 2A_3/A_0^2, \; H_4 = (3A_0A_4 + A_2^2)/A_0^3,$$

$$H_5 = 4(A_0A_5 + A_2A_3)/A_0^3,$$

$$H_6 = (5A_0^2A_6 + 4A_0A_3^2 + 6A_0A_2A_4 + A_2^3)/A_0^4, \text{ and so on.}$$

We assume here that the singularities of the transformation are inside the contour, so that $dz/d\zeta$ is never zero and hence dw_{s+1}/dz is never infinite in the medium $(s+1)$.

In the ζ-plane, the contour of the curve along which we integrate is PQ as shown in Fig. 1.

Now the contour integral (6) taken around $PQRS$ is zero,

and the integrals along QR and SP cancel, so that the required value is the integral along $\overleftarrow{RS}$ where η now may be taken to be large and constant. We thus obtain

$$Z_{s+1} = \frac{ik_{s+1}}{8\pi}\int_0^{2\pi}\left[\sum_{n=1}^{\infty} H_n \exp(ni\zeta)\right]$$
$$\left\{\sum_{n=2}^{2p}[c_n \exp(-ni\zeta) + d_n \exp(ni\zeta)] - \right.$$
$$\left. - 2f_0 - 2\sum_{n=1}^{p-1}[f_n \exp(ni\zeta) + g_n \exp(-ni\zeta)]\right\} d\zeta$$
$$= \frac{ik_{s+1}}{4}\left(\sum_{n=2}^{2p} H_n c_n - 2\sum_{n=1}^{p-1} H_n g_n\right) \qquad (9)$$

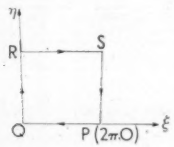

Fig. 1

To evaluate the couple Γ_{s+1} from equation (7) we have

$$\frac{z}{dz/d\zeta} = i\left[\sum_{n=1}^{\infty} H_n \exp(ni\zeta)\right]\left\{\sum_{n=0}^{\infty} A_n \exp[i(n-1)\zeta]\right\}$$
$$= i\sum_{n=0}^{\infty} K_n \exp(ni\zeta),$$

where $K_n = \sum_{r=0}^{n} A_r H_{n-r+1}$, and integrating round $PQRS$ as before we are led to

$$\Gamma_{s+1} = \mathscr{R}\frac{ik_{s+1}}{4}\left(\sum_{n=2}^{2p} K_n c_n - 2\sum_{n=1}^{p-1} K_n g_n - 2K_0 f_0\right) \qquad (10)$$

A method is indicated in the next section for finding the coefficients b_n in terms of the known a_n.

2. THE ELECTRIC FIELDS

In obtaining the formulae (9) and (10), we have assumed the singularities of transformation to be inside the profile. If there are such singularities in the medium (s), say, the complex potential w_s must be single-valued throughout the region and dw_s/dz must not become infinite at any point of the region. (Note that if the bounding surface is a conductor and that if the singularities of transformation are inside this surface, then no difficulty arises.) Also the conditions to be satisfied at the boundary of the two media (s), $(s+1)$ are

$$\mathscr{R}(w_s) = \mathscr{R}(w_{s+1}); \quad k_s\mathscr{I}(w_s) = k_{s+1}\mathscr{I}(w_{s+1}) \qquad (11)$$

Conducting cylinder. Suppose, as a special case, that in the transformation (8), $\eta = 0$ corresponds to the profile of a conducting cylinder placed in an undisturbed field the complex potential of which is Ω_0. The perturbed field can be found as follows. Divide Ω_0 into two parts $F_1(\zeta)$ and $F_2(\zeta)$, where $F_1(\zeta)$ tends to zero at infinity and hence $\bar{F}_1(\zeta)$ diverges there, and where $F_2(\zeta)$ diverges at infinity and so $\bar{F}_2(\zeta)$ tends to zero there. The required complex potential is then given by

$$\Omega = F_2(\zeta) - \bar{F}_2(\zeta) \qquad (12)$$

since $\Omega \to \Omega_0$ at a great distance from the conductor and it is purely imaginary on the boundary $\eta = 0$. For example, suppose that this conducting cylinder is placed in the field

$$\Omega_0 = \sum_{n=1}^{4}\delta_n z^n$$
$$= \sum_{n=1}^{4} m_n \exp(-ni\zeta) + f[\exp(i\zeta)],$$

where $f[\exp(i\zeta)]$ is a function of positive exponential functions, and

$$m_1 = \delta_1 A_0 + 2\delta_2 A_0 A_1 + 3\delta_3 A_0 A_1 (A_0 + A_1) +$$
$$+ 4\delta_4 A_0 (A_0^2 A_3 + 3A_0 A_1 A_2 + A_1^3),$$
$$m_2 = \delta_2 A_0^2 + 3\delta_3 A_0^2 A_1 + 2\delta_4 A_0^2 (2A_0 A_2 + 3A_1^2),$$
$$m_3 = \delta_3 A_0^3 + 4\delta_4 A_0^3 A_1,$$
$$m_4 = \delta_4 A_0^4.$$

Equation (12) gives

$$\Omega = \sum_{n=1}^{4}[m_n \exp(-ni\zeta) - \overline{m}_n \exp(ni\zeta)]$$

and the mechanical force Z and couple Γ can be determined from formulae (9) and (10).

More generally, if $z = f(\zeta)$ defines a system of co-ordinates (ξ, η) in which the cross-section C of an uncharged conducting cylinder is given by $\eta = \eta_0$ then on the cylinder C,

$$\overline{\zeta} = \zeta - 2i\eta_0.$$

Thus the complex potential

$$w = F(\zeta) - \bar{F}(\zeta - 2i\eta_0)$$

is purely imaginary on C.

Suppose now that C is placed in the undisturbed field Ω_0. If we can arrange to split $\Omega_0(\zeta)$ into two functions $F_1(\zeta)$, $F_2(\zeta)$, so that $F_1(\zeta)$ contains only terms which tend to zero at infinity, and $\bar{F}_2(\zeta - 2i\eta_0)$ also tends to zero at infinity, then the perturbed complex potential is given by

$$\Omega = F_2(\zeta) - \bar{F}_2(\zeta - 2i\eta_0)$$

As an example, suppose C is given by the parametric equations

$$x = f_1(t), \quad y = f_2(t),$$

then

$$z = f_1(\zeta - i\eta_0) + if_2(\zeta - i\eta_0)$$

is a co-ordinate system of the required type.

It must be remembered, however, that the principle given above is of general application (for conducting cylinders only), and need not be confined to parametrically represented co-ordinate systems.

Conducting cylinder with dielectric sheath. Using transformation (8), let now a system consist of the conductor $\eta = 0$ embedded in a sheath of dielectric, constant k_2, and let this be surrounded by an infinite dielectric, constant k_3, the boundary between the two dielectrics being $\eta = \beta$. If this system is set in the general field

$$w = \sum_{n=1}^{p} E_n z^n = \sum_{n=1}^{p} a_n \exp(-ni\zeta) + g[\exp(i\zeta)],$$

where the function $g[\exp(i\zeta)]$ contains only positive powers of $\exp(i\zeta)$, then application of equations (11), (12) shows that the fields in the dielectrics k_2, k_3 are, respectively,

$$w_2 = \sum_{n=1}^{p} \frac{2k_3 \exp(2n\beta)}{[(k_2+k_3)\exp(2n\beta)+(k_2-k_3)]} [a_n \exp(-ni\zeta) - \bar{a}_n \exp(ni\zeta)],$$

$$w_3 = \sum_{n=1}^{p} a_n \exp(-ni\zeta) - \sum_{n=1}^{p} \left[\frac{(k_2-k_3)\exp(2n\beta)+(k_2+k_3)}{(k_2+k_3)\exp(2n\beta)+(k_2-k_3)}\right] [a_n \exp(2n\beta)\exp(ni\zeta)]$$

In particular, confocal elliptic boundaries are obtained by taking the first two terms of the general transformation in the form $z = c\exp(i\zeta) + c\exp(-i\zeta) = 2c\cos\zeta$. However, such boundaries are discussed in detail in the next section by using a rather different transformation.

3. THE TRANSFORMATION $z = \zeta + (\zeta^{-p}/p)$

We will now consider a dielectric cylinder, constant k, the boundary S of which in the z-plane becomes the circle given by $|\zeta| = a(>1)$ when the conformal transformation $z = \zeta + (\zeta^{-p}/p)$ is applied, p being a positive integer. This transformation is of general interest, and gives an elliptical dielectric boundary in the z-plane for the case $p = 1$. We note that for large $|\zeta|$, $z \simeq \zeta$, and that the critical values occur when $dz/d\zeta = 0$, that is at the points on the unit circle in the ζ-plane where $\zeta^{p+1} = 1$.

Suppose now that this dielectric cylinder, surrounded by air, is placed in the general field the undisturbed complex potential of which is $g(z) \equiv \sum_{n=1}^{\infty} E_n z^n$ which becomes $\sum_{n=1}^{\infty} F_n \zeta^n + f(\zeta)$ in the ζ-plane where $f(\zeta)$ contains only negative powers of ζ. The complex potential for the disturbed field inside the dielectric will be a regular function of z, and only the external perturbed field will contribute to the mechanical force and couple. This external field will have a complex potential of the form

$$w_0 = \sum_{n=1}^{\infty} F_n \zeta^n + \sum_{n=1}^{\infty} C_n \zeta^{-n} \tag{13}$$

The complex force is given by equation (6) which becomes

$$Y + iX = \frac{1}{8\pi i}\int_c \left(\sum_{n=1}^{\infty} nF_n\zeta^{n-1} - \sum_{n=1}^{\infty} nC_n\zeta^{-n-1}\right)^2 \frac{\zeta^{p+1}d\zeta}{(\zeta^{p+1}-1)} \tag{14}$$

There are poles at $\zeta = 0$, $\zeta = \omega_r$, where ω_r is any root of $\zeta^{p+1} = 0$. Evaluating the contour integral (14) we obtain

$$\begin{aligned} Y + iX = {} & \frac{i}{4(p+1)}\sum_{r=1}^{p+1}\omega_r\left(\sum_{n=1}^{\infty} nF_n\omega_r^{n-1} - \sum_{n=1}^{\infty} nC_n\omega_r^{-n-1}\right)^2 - \\ & - \frac{i}{4}\sum n^2C_n^2 \text{ for all } n \text{ where } \frac{2n-p}{(p+1)} \text{ is a positive integer or zero} \\ & - \frac{i}{2}\sum_{m>n}\sum mnC_mC_n \text{ for all } m, n \text{ where } \frac{m+n-p}{(p+1)} \text{ is a positive integer or zero} \\ & + \frac{i}{2}\sum_{m>n}\sum mnC_mF_n \text{ for all } m, n \text{ where } \frac{m-n-p}{(p+1)} \text{ is a positive integer or zero} \end{aligned} \tag{15}$$

Similarly, the couple is given by

$$\begin{aligned} \Gamma = {} & \mathscr{R}\frac{1}{8\pi i}\int_c \left(\sum_{n=1}^{\infty} nF_n\zeta^{n-1} - \sum_{n=1}^{\infty} nC_n\zeta^{-n-1}\right)^2 \frac{\zeta[\zeta^{p+1}+(1/p)]}{(\zeta^{p+1}-1)}\,d\zeta \\ = {} & \mathscr{R}\frac{i}{4p}\sum_{r=1}^{p+1}\frac{1}{(\omega_r)^{p-1}}\left(\sum_{n=1}^{\infty} n\omega_r^{n-1}F_n - \sum_{n=1}^{\infty} nC_n\omega_r^{-n-1}\right)^2 + \\ & + \mathscr{R}\frac{i}{2p}\sum_{n=1}^{\infty} n^2F_nC_n \\ & - \mathscr{R}\frac{i}{4}\sum n^2C_n^2 \text{ for all } n, \text{ where } \frac{2n-p-1}{(p+1)} \text{ is a positive integer or zero} \\ & - \mathscr{R}\frac{i}{4p}\sum n^2C_n^2 \text{ for all } n, \text{ where } \frac{2n}{(p+1)} \text{ is a positive integer} \\ & - \mathscr{R}\frac{i}{2}\sum_{m>n}\sum mnC_mC_n \text{ for all } m, n, \text{ where } \frac{m+n-p-1}{(p+1)} \text{ is a positive integer or zero} \\ & - \mathscr{R}\frac{i}{2p}\sum_{m>n}\sum mnC_mC_n \text{ for all } m, n, \text{ where } \frac{m+n}{(p+1)} \text{ is a positive integer} \\ & + \mathscr{R}\frac{i}{2}\sum_{m>n}\sum mnC_mF_n \text{ for all } m, n, \text{ where } \frac{m-n-p-1}{(p+1)} \text{ is a positive integer or zero} \\ & + \mathscr{R}\frac{i}{2p}\sum_{m>n}\sum mnC_mF_n \text{ for all } m, n, \text{ where } \frac{m-n}{(p+1)} \text{ is a positive integer.} \end{aligned} \tag{16}$$

The coefficients C_n are obtained by applying the boundary conditions given by equations (11). In general these coefficients are not found exactly, as an infinite set of equations is involved, but approximations can usually be obtained quite simply. An exact solution, however, can be obtained for the case $p = 1$. An exact solution can also be obtained when a current flows along the generators of a cylinder having the curve S as cross-section, whilst the dielectric constant is the same both inside and outside S. This latter type of problem, however, will not be dealt with here.

Elliptic dielectric cylinder. We will now discuss the case $p = 1$ in more detail, taking as our transformation $z = (c/2)(\zeta + 1/\zeta)$. The external field is given by equation (13) whilst the internal complex potential, which can be expanded in a series of positive powers of z, may be written

$$w_i = \sum_{n=1}^{\infty} A_n\left(\zeta^n + \frac{1}{\zeta^n}\right) \tag{17}$$

Applying the boundary conditions

$$\mathscr{R}(w_i) = \mathscr{R}(w_0); \quad k\mathscr{I}(w_i) = \mathscr{I}(w_0), \text{ when } |\zeta| = a,$$

we obtain

$$C_n = [a^{4n}F_n(1-\mu^2) + a^{2n}\mu F_n(1-a^{4n})]/(a^{4n}-\mu^2) \tag{18}$$

where $\mu = (k-1)/(k+1)$.

The complex force and couple now become

$$Y + iX = \frac{i}{c}\sum_{r=2}^{\infty}\sum_{s=1}^{\infty} rsF_r(F_s - C_s), \quad r > s, \quad r - s \text{ odd},$$

and

$$\Gamma = \mathscr{R}\left[\frac{i}{2}\sum_{n=1}^{\infty} n^2F_n(F_n - C_n) + i\sum_{r=3}^{\infty}\sum_{s=1}^{\infty} rsF_r(F_s - C_s), \quad r > s, \ r - s \text{ even}\right] \quad (19)$$

where from equation (18)

$$F_s - C_s = (a^{4s} - 1)(F_s\mu^2 + \bar{F}_s\mu a^{2s})/(a^{4s} - \mu^2)$$

As a particular example let us take the unperturbed field to be

$$g(z) = Uz\exp(-i\alpha) + Vz^2\exp(-i\beta)$$

where U and V are real. The complex force becomes

$$Y + iX = \frac{imn(m+n)(k-1)UV\exp(-i\beta)[(mk+n)\cos\alpha + i(m+kn)\sin\alpha]}{2(m+kn)(mk+n)}$$

and the couple becomes

$$\Gamma = \frac{U^2(m^2-n^2)(k-1)^2mn\sin 2\alpha}{8(km+n)(kn+m)} + \frac{V^2mn(m^2-n^2)(m^4-n^4)(k-1)^2\sin 2\beta}{4[k(m^2+n^2)+2mn][(m^2+n^2)+2kmn]} \quad (20)$$

where m, n are the semi-axes of the ellipse and $c^2 = m^2 - n^2$, $a^2 = (m+n)/(m-n)$.

Equations (20) reduce to the well-known results for a uniform field when $V = 0$.

Elliptic dielectric cylinder with confocal dielectric sheath. This method can readily be extended to the case of an elliptic dielectric cylinder with a confocal dielectric sheath. Let the boundary of the inner elliptic cylinder, of dielectric constant k_1, transform into $|\zeta| = b$, and let the boundary of the outer confocal elliptic cylinder become $|\zeta| = a$. Between the cylinders is dielectric material of constant k_2, whilst outside the second cylinder is material of constant k_3, in which there is a field, the unperturbed potential of which is $g(z) = \sum_{n=1}^{\infty} E_nz^n$. On applying the transformation

$$z = (c/2)(\zeta + 1/\zeta),$$

$g(z)$ becomes $\sum_{n=1}^{\infty} F_n\zeta^n + f(\zeta)$ as before, so

that the perturbed complex potentials may be taken as

$$w_1 = \sum_{n=1}^{\infty} a_{1,n}\left(\zeta^n + \frac{1}{\bar{\zeta}^n}\right), \quad |\zeta| \leqslant b,$$

$$w_2 = \sum_{n=1}^{\infty} a_{2,n}\zeta^n + \sum_{n=1}^{\infty} b_{2,n}\zeta^{-n}, \quad b \leqslant |\zeta| \leqslant a,$$

$$w_3 = \sum_{n=1}^{\infty} F_n\zeta^n + \sum_{n=1}^{\infty} b_{3,n}\zeta^{-n}, \quad a \leqslant |\zeta|.$$

The boundary conditions are now

$$\mathscr{R}(w_1) = \mathscr{R}(w_2); \quad k_1\mathscr{I}(w_1) = k_2\mathscr{I}(w_2) \text{ when } |\zeta| = b,$$

$$\mathscr{R}(w_2) = \mathscr{R}(w_3); \quad k_2\mathscr{I}(w_2) = k_3\mathscr{I}(w_3) \text{ when } |\zeta| = a,$$

and these lead to

$$\left.\begin{aligned}
&(b^{4n}\alpha_n^2 - \beta_n^2)a_{1,n} = 4k_3k_2a^{2n}b^{2n}(b^{2n}\alpha_nF_n - \beta_n\bar{F}_n)\\
&(b^{4n}\alpha_n^2 - \beta_n^2)a_{2,n} = 2k_3a^{2n}\{[b^{4n}(k_2+k_1)\alpha_n - (k_2-k_1)\beta_n]F_n - [b^{2n}(k_2+k_1)\beta_n - b^{2n}(k_2-k_1)\alpha_n]\bar{F}_n\},\\
&(b^{4n}\alpha_n^2 - \beta_n^2)b_{2,n} = 2k_3a^{2n}b^{2n}\{[b^{4n}(k_2-k_1)\alpha_n - (k_2+k_1)\beta_n]\bar{F}_n - [b^{2n}(k_2-k_1)\beta_n - b^{2n}(k_2+k_1)\alpha_n]F_n\},\\
&(b^{4n}\alpha_n^2 - \beta_n^2)b_{3,n} = \{b^{4n}a^{2n}[a^{2n}(k_2+k_1)(k_3-k_2) + b^{2n}(k_2-k_1)(k_3+k_2)]\alpha_n - a^{2n}[a^{2n}(k_3-k_2)(k_2-k_1) + b^{2n}(k_2+k_1)(k_3+k_2)]\beta_n\}F_n - \{a^{2n}b^{2n}[a^{2n}(k_3-k_2)(k_2+k_1) + b^{2n}(k_3+k_2)(k_2-k_1)]\beta_n - a^{2n}b^{2n}[a^{2n}(k_3-k_2)(k_2-k_1) + b^{2n}(k_3+k_2)(k_2+k_1)]\alpha_n\}\bar{F}_n,
\end{aligned}\right\} \quad (21)$$

where

$$\alpha_n = a^{2n}(k_3+k_2)(k_2+k_1) + b^{2n}(k_3-k_2)(k_2-k_1),$$
$$\beta_n = a^{2n}(k_3+k_2)(k_2-k_1) + b^{2n}(k_3-k_2)(k_2+k_1).$$

The force and couple on the boundaries can now be calculated by applying previous results.

By letting $k_3 \to \infty$, we obtain the case of an elliptic conducting cylinder with confocal dielectric sheath. A solution to this particular problem was obtained in the previous section using a different method.

Internal line-charge. In an earlier paper[1] a general mathematical method has been given which is applicable to certain types of electrode systems. In particular, formulae were obtained for the perturbation effects of an elliptic dielectric cylinder of constant k on the field owing to a line-charge of strength m per unit length placed inside the cylinder. The external and internal fields are given in the form

$$\left.\begin{aligned}
w_0 = &-\frac{4m}{(1+k)}\left[\sum_{p=0}^{\infty}\mu^p\log\left(\zeta - \frac{\zeta_0}{a^{2p}}\right)\left(\zeta - \frac{1}{a^{2p}\zeta_0}\right) + \sum_{q=1}^{\infty}{}'\mu^q\log\left(\zeta - \frac{\bar{\zeta}_0}{a^{2q}}\right)\left(\zeta - \frac{1}{a^{2q}\zeta_0}\right)\right] + 2m\log\zeta,\\
w_i = &-\frac{2m}{k}\left\{\sum_{p=0}^{\infty}\mu^p\log\left(\zeta - \frac{1}{a^{2p}\zeta_0}\right) + \sum_{p=0}^{\infty}\mu^{p+1}\log\left[\zeta - \frac{\bar{\zeta}_0}{a^{2(p+1)}}\right]\left[\zeta - \frac{a^{2(p+1)}}{\bar{\zeta}_0}\right]\right.\\
&\left.[\zeta - a^{2(p+1)}\bar{\zeta}_0] + \sum_{q=1}^{\infty}{}'\mu^q\log\left(\zeta - \frac{1}{a^{2q}\zeta_0}\right) + \sum_{q=1}^{\infty}{}'\mu^{q+1}\log\left[\zeta - \frac{\zeta_0}{a^{2(q+1)}}\right]\left[\zeta - \frac{a^{2(q+1)}}{\zeta_0}\right]\right.\\
&\left.[\zeta - a^{2(q+1)}\zeta_0]\right\} - \frac{2m}{k}\log(\zeta - \zeta_0) + 2m\log\zeta,
\end{aligned}\right\} \quad (22)$$

where Σ refers to even powers, Σ' to odd powers, $\mu = (k-1)/(k+1)$, and ζ_0 is the point in the ζ-plane corresponding to the point z_0 in the z-plane, at which the line-charge is situated.

The complex force and couple are given by equations (6) and (7), where the contour c around which we integrate is the circle $|\zeta| = a$, and only the internal field will contribute. Remembering the sign of the force components, we have

$$Y + iX = -\frac{k}{8\pi}\int_c \left(\frac{dw_i}{d\zeta}\right)^2 \frac{d\zeta}{dz/d\zeta},$$

so that

$$Y + iX = -\frac{k}{8\pi}\int_c \frac{8m^2\zeta^2}{k^2c(\zeta^2-1)}\left[\sum_{p=0}^{\infty}\frac{\mu^p}{\left(\zeta-\frac{1}{a^{2p}\overline{\zeta}_0}\right)} + \right.$$
$$+\sum_{p=0}^{\infty}\mu^{p+1}\left\{\frac{1}{\left[\zeta-\frac{\overline{\zeta}_0}{a^{2(p+1)}}\right]}+\frac{1}{\left[\zeta-\frac{a^{2(p+1)}}{\overline{\zeta}_0}\right]}+\right.$$
$$\left.+\frac{1}{\left[\zeta-a^{2(p+1)}\overline{\zeta}_0\right]}\right\}+\sum_{q=1}^{\infty}{}'\frac{\mu^q}{\left(\zeta-\frac{1}{a^{2q}\overline{\zeta}_0}\right)}+$$
$$+\sum_{q=1}^{\infty}\mu^{q+1}\left\{\frac{1}{\left[\zeta-\frac{\zeta_0}{a^{2(q+1)}}\right]}+\frac{1}{\left[\zeta-\frac{a^{2(q+1)}}{\zeta_0}\right]}+\right.$$
$$\left.\left.+\frac{1}{\left[\zeta-a^{2(q+1)}\zeta_0\right]}\right\}+\frac{1}{(\zeta-\zeta_0)}-\frac{k}{\zeta}\right]^2 d\zeta.$$

The singularities in the integral that lie outside c occur at $\zeta = a^{2p+2}/\overline{\zeta}_0$, $\zeta = a^{2p+2}\overline{\zeta}_0$, $\zeta = a^{2q}/\zeta_0$, $\zeta = a^{2q+2}\zeta_0$.

Let us surround c and all these external singularities by a circle s of large radius, and let γ be a typical small contour surrounding one of the external singularities.

Now we have

$$\frac{k}{8\pi}\int_c [\quad]d\zeta = \frac{k}{8\pi}\int_s [\quad]d\zeta - \Sigma\frac{k}{8\pi}\int_\gamma [\quad]d\zeta,$$

where the summation sign refers to the small contours γ. By expanding in powers of $1/\zeta$ we easily see that the integral around s is zero, so that

$$Y + iX = \frac{4m^2i}{kc}\left\{\sum_{p=0}^{\infty}\mu^{p+1}\left[\chi_{a^{2p+2}/\overline{\zeta}_0}\left(\frac{a^{2p+2}}{\overline{\zeta}_0}\right)+\right.\right.$$
$$\left.+\chi_{a^{2p+2}\overline{\zeta}_0}(a^{2p+2}\overline{\zeta}_0)\right]+\sum_{q=1}^{\infty}{}'\mu^{q+1}\left[\chi_{a^{2q+2}/\overline{\zeta}_0}\left(\frac{a^{2q+2}}{\zeta_0}\right)+\right.$$
$$\left.\left.+\chi_{a^{2q+2}\zeta_0}(a^{2q+2}\zeta_0)\right]\right\} \quad (23)$$

where $\chi_{a^{2q+2}/\overline{\zeta}_0}(a^{2p+2}/\overline{\zeta}_0)$ is obtained by setting $\zeta = a^{2p+2}/\overline{\zeta}_0$ in the function obtained by omitting the term $1/(\zeta - a^{2p+2}/\overline{\zeta}_0)$ from

$$\frac{\zeta^2}{(\zeta^2-1)}\left\{\sum_{p=0}^{\infty}\frac{\mu^p}{\left(\zeta-\frac{1}{a^{2p}\overline{\zeta}_0}\right)}+\sum_{p=0}^{\infty}\mu^{p+1}\left[\frac{1}{\left(\zeta-\frac{\overline{\zeta}_0}{a^{2p+2}}\right)}+\right.\right.$$
$$\left.+\frac{1}{\left(\zeta-\frac{a^{2p+2}}{\overline{\zeta}_0}\right)}+\frac{1}{(\zeta-a^{2p+2}\overline{\zeta}_0)}\right]+$$
$$+\sum_{q=1}^{\infty}\frac{\mu^q}{\left(\zeta-\frac{1}{a^{2q}\overline{\zeta}_0}\right)}+\sum_{q=1}^{\infty}{}'\mu^{q+1}\left[\frac{1}{\left(\zeta-\frac{\zeta_0}{a^{2q+2}}\right)}+\right.$$
$$\left.\left.+\frac{1}{\left(\zeta-\frac{a^{2q+2}}{\zeta_0}\right)}+\frac{1}{(\zeta-a^{2q+2}\zeta_0)}\right]+\frac{1}{(\zeta-\zeta_0)}-\frac{k}{\zeta}\right\}$$

and then subtracting

$$\left[\mu^{p+1}\zeta_i/(\zeta^2-1)^2\right]_{\zeta=a^{2p+2}/\overline{\zeta}_0}$$

In a similar manner we can show that the anti-clockwise couple is given by

$$\Gamma = \mathscr{R}\frac{2im^2}{k}\left\{\sum_{p=0}^{\infty}\mu^{p+1}\left[\Theta_{a^{2p+2}/\overline{\zeta}_0}\left(\frac{a^{2p+2}}{\zeta_0}\right)+\right.\right.$$
$$\left.+\Theta_{a^{2p+2}\overline{\zeta}_0}(a^{2p+2}\overline{\zeta}_0)\right]+\sum_{q=1}^{\infty}{}'\mu^{q+1}\left[\Theta_{a^{2q+2}/\zeta_0}\left(\frac{a^{2q+2}}{\zeta_0}\right)+\right.$$
$$\left.\left.+\Theta_{a^{2q+2}\zeta_0}(a^{2q+2}\zeta_0)\right]\right\} \quad (24)$$

where $\Theta_{a^{2p+2}/\overline{\zeta}_0}(a^{2p+2}/\overline{\zeta}_0)$ is obtained by setting $\zeta = a^{2p+2}/\overline{\zeta}_0$ in the function obtained by omitting the term

$$1\Big/\left(\zeta-\frac{a^{2p+2}}{\overline{\zeta}_0}\right)$$

from

$$\frac{\zeta(\zeta^2+1)}{(\zeta^2-1)}\left\{\sum_{p=0}^{\infty}\frac{\mu^p}{\left(\zeta-\frac{1}{a^{2p}\zeta_0}\right)}+\sum_{p=0}^{\infty}\mu^{p+1}\left[\frac{1}{\left(\zeta-\frac{\overline{\zeta}_0}{a^{2q+2}}\right)}+\right.\right.$$
$$\left.+\frac{1}{\left(\zeta-\frac{a^{2p+2}}{\overline{\zeta}_0}\right)}+\frac{1}{(\zeta-a^{2p+2}\overline{\zeta}_0)}\right]+$$
$$+\sum_{q=1}^{\infty}\frac{\mu^q}{\left(\zeta-\frac{1}{a^{2q}\overline{\zeta}_0}\right)}+\sum_{q=1}^{\infty}{}'\mu^{q+1}\left[\frac{1}{\left(\zeta-\frac{\zeta_0}{a^{2q+2}}\right)}+\right.$$
$$\left.\left.+\frac{1}{\left(\zeta-\frac{a^{2q+2}}{\zeta_0}\right)}+\frac{1}{(\zeta-a^{2q+2}\zeta_0)}\right]+\frac{1}{(\zeta-\zeta_0)}-\frac{k}{\zeta}\right\}$$

and then subtracting

$$\left[\mu^{p+1}\frac{(\zeta^2+1)}{(\zeta^2-1)^2}\right]_{\zeta=a^{2p+2}/\overline{\zeta}_0}$$

General field and external line-charge. The same method[1] can obviously be employed more generally to find the effect of an elliptic cylinder when it is placed in the general field $g(z) \equiv \sum_{n=1}^{\infty} E_n z^n$, which we have been previously considering. The complex potentials outside and inside the elliptic cylinder of dielectric constant k are found to be respectively

$$\left.\begin{aligned} w_0 &= h(\zeta) - \overline{h}\left(\frac{a^2}{\zeta}\right)+\\ &+\frac{4k}{(1+k)^2}\left[\sum_{p=0}^{\infty}\mu^p h\left(\frac{1}{a^{2p}\zeta}\right)+\sum_{q=1}^{\infty}{}'\mu^q\overline{h}\left(\frac{1}{a^{2q}\zeta}\right)\right] \end{aligned}\right\} \quad (25)$$

and

$$\left.\begin{aligned} w_i &= \frac{2}{(1+k)}\left\{\sum_{p=0}^{\infty}\mu^p\left[h\left(\frac{\zeta}{a^{2p}}\right)+\overline{h}\left(\frac{1}{a^{2p}\zeta}\right)\right]+\right.\\ &\left.+\sum_{q=1}^{\infty}{}'\mu^q\left[\overline{h}\left(\frac{\zeta}{a^{2q}}\right)+h\left(\frac{1}{a^{2q}\zeta}\right)\right]\right\} \end{aligned}\right\}$$

where $h(\zeta) = \sum_{n=1}^{\infty} F_n \zeta^n$. For an external line-charge m placed at $z = z_0$ outside the elliptic cylinder

$$g(z) = -2m \log (z - z_0)$$
$$= -2m \log \{(\zeta - \zeta_0)[\zeta - (1/\zeta_0)]\}/\zeta$$

apart from an additive constant. The terms $-2m \log \left(\zeta - \frac{1}{\zeta_0}\right)$, $2m \log \zeta$, refer to line charges inside the region $|\zeta| < 1$ which corresponds to a different sheet on the Riemann surface, and are not considered. Thus we take

$$h(\zeta) = -2m \log (\zeta - \zeta_0)$$

and equation (25) gives the fields

$$\left.\begin{aligned} w_0 = {} & -2m \log (\zeta - \zeta_0) + 2m\mu \log \left(\frac{a^2}{\zeta} - \bar{\zeta}_0\right) + \\ & + \frac{4k}{(1+k)^2}\left\{\sum_{p=0}^{\infty} \mu^p \left[-2m \log \left(\frac{1}{a^{2p}\zeta} - \zeta_0\right)\right] + \right. \\ & \left. + \sum_{q=1}^{\infty}{}' \mu^q \left[-2m \log \left(\frac{1}{a^{2q}\zeta} - \bar{\zeta}_0\right)\right]\right\} \end{aligned}\right\}$$

and

$$\left.\begin{aligned} w_i = {} & \frac{2}{(1+k)}\left\{\sum_{p=0}^{\infty} \mu^p \left[-2m \log \left(\frac{\zeta}{a^{2p}} - \zeta_0\right) - \right.\right. \\ & \left. - 2m \log \left(\frac{1}{a^{2p}\zeta} - \zeta_0\right)\right] + \\ & + \sum_{q=1}^{\infty}{}' \mu^q \left[-2m \log \left(\frac{\zeta}{a^{2q}} - \bar{\zeta}_0\right) - \right. \\ & \left.\left. - 2m \log \left(\frac{1}{a^{2q}\zeta} - \bar{\zeta}_0\right)\right]\right\} \end{aligned}\right\} \quad (26)$$

where $\mu = (k-1)/(k+1)$.

Provided that $a^2|\zeta_0|$ is reasonably large (say greater than ten), the equations (26), which contain infinite series, can be easily seen to approximate to

$$\left.\begin{aligned} -\frac{w_0}{2m} = {} & \log (\zeta - \zeta_0) - \frac{(k-1)}{(k+1)} \log \left(\zeta - \frac{a^2}{\bar{\zeta}_0}\right) + \\ & + \frac{4k}{(k+1)^2} \log \left(\zeta - \frac{1}{\bar{\zeta}_0}\right) + \\ & + \frac{4k(k-1)}{(k+1)^3} \log \left(\zeta - \frac{1}{a^2\bar{\zeta}_0}\right) - \\ & - \left[1 - \frac{2k(k-1)^2}{(k+1)^3}\right] \log \zeta, \\ -\frac{(k+1)}{4m} w_i = {} & \log (\zeta - \zeta_0) + \log \left(\zeta - \frac{1}{\zeta_0}\right) + \\ & + \frac{(k-1)}{(k+1)}\left[\log (\zeta - a^2\bar{\zeta}_0) + \log \left(\zeta - \frac{1}{a^2\bar{\zeta}_0}\right)\right] + \\ & + \frac{(k-1)^2}{(k+1)^2}\left[\log (\zeta - a^4\zeta_0) + \log \left(\zeta - \frac{1}{a^4\zeta_0}\right)\right] - \\ & - \frac{(k+1)}{2}\left[1 - \frac{(k-1)^3}{(k+1)^3}\right] \log \zeta \end{aligned}\right\} \quad (27)$$

apart from an additive constant. That is to say, the fields can be regarded as approximately equivalent to a finite set of line charges at appropriate points.

SUMMARY OF SECTIONS 1–3

Briefly summarizing, we see in Section 1, that by assuming the Maxwell stresses, we are led to formulae of the Blasius type for the mechanical forces experienced at the interface of two different isotropic dielectric media due to the presence of an electric field. The evaluation of these formulae becomes quite easy if we can conformally transform the contour of the interface into elementary forms like the straight line or circle. In Section 2, boundary conditions are discussed, and a simple general method is given for the case of a conducting cylinder. Finally, in Section 3, we consider the boundary shape of general interest given by the transformation $z = \zeta + \frac{1}{p}\zeta^{-p}$, $|\zeta| =$ constant, where p is a positive integer, showing how the boundary conditions can be satisfied. The particular value $p = 1$ gives the important case of an elliptical contour, and this is discussed in great detail, formulae for both the perturbed fields and the mechanical forces being obtained for a wide range of problems. General formulae for the dielectric slab, dielectric annulus, parabolic dielectric cylinder and other cases can be deduced.

4. EXPERIMENTAL WORK

It is of interest to ascertain how the perturbed fields we have obtained theoretically agree with experimental work, and to see if we can reasonably approximate the infinite series solutions to the first few terms as in formulae (27). This is done most simply, if rather conventionally (see Fig. 2), by means of a small shallow electrolytic tank filled with water, in which the electrodes, made of copper, are immersed.

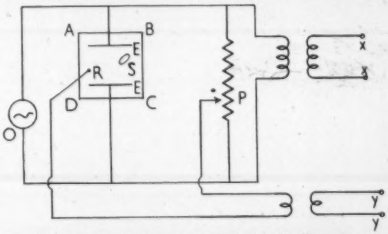

Fig. 2. Electrolytic tank and circuit diagram

ABCD, electrolytic tank; *S*, Perspex shape; *E*, electrodes; *R*, probe, attached to adjustable scale; *P*, calibrated potentiometer, divided into ten equal steps; *O*, oscillator which steps up alternating current to about 1000 c/s; *XX*, *YY*, terminals of oscilloscope, which gives horizontal trace when *R*, *P* are at same potential.

These electrodes are used to simulate the unperturbed field. A short piece of wire, insulated over its whole length except for a short piece at the end, is used as a probe to indicate the local potential. To reproduce the effect of different dielectric materials, the depth of water is varied in the ratio of the dielectric constants. This variation of depth is achieved by fixing to the bottom of the tank a piece of Perspex of uniform thickness cut to the desired shape, and then adjusting the amount of water in the tank to give the ratio required. The depth of water is arranged so that loss due to evaporation is negligible over the time required to take a set of readings.

The following boundary shapes and fields have been considered[2]:

(α) dielectric elliptic cylinder in a uniform field;

(β) dielectric elliptic cylinder with an external line charge;

(γ) dielectric elliptic cylinder and confocal sheath in a uniform field;

(δ) dielectric cylinder $z = \zeta + (1/3\zeta^3)$, $|\zeta| =$ constant in a non-uniform field;

(ϵ) dielectric slab in a non-uniform field.

Since the experimental technique is quite straightforward, no further details need be given here; it is enough to mention that in all cases reasonably good agreement with theoretical results has been obtained.

It is also of interest to note that this same technique can be applied to give the entire field, however complicated the boundary shape may be. For difficult contours it is usually impossible to obtain the perturbed fields theoretically, but functions may be *assumed* which can be made to agree with the plotted fields as closely as desired. By substituting these empirical formulae in the results of Section 1, the mechanical forces on the interface will be determined in all probability to a fair degree of accuracy.

REFERENCES

(1) POWER, G. *Brit. J. Appl. Phys.*, **6**, p. 245 (1955).

(2) POWER, G. *Ph.D. Thesis*, University of Nottingham (1954).

A new method for the measurement of rapid fluctuations of temperature*

By R. DEHN, M.Sc., A.R.C.S., A.Inst.P., The General Electric Co., Ltd., Wembley, Middlesex

[*Paper received* 14 *November*, 1955]

The method described uses a photomultiplier in conjunction with an infra-red image converter to measure changes in surface temperature of the cathode of an oscillating magnetron during microsecond pulses.

These instantaneous changes in temperature are displayed as pulses on the screen of a cathode-ray oscillograph. The procedure is given of calibrating the apparatus against an optical pyrometer. Changes as small as 2° C in 800–900° C have been detected (solid angle equals $2{\cdot}5 \times 10^{-3}$ steradians).

In connexion with a programme of research on the operation of high- and medium-power pulsed magnetrons it became desirable to measure instantaneous temperature changes on the cathode surface of an oscillating magnetron. The pulse length was generally of the order of 1 μs. Hence, in order to obtain any useful information the resolving time of the whole measuring system had to be at least 10^{-7} s, probably less. In view of this requirement most conventional temperature sensitive detectors were at once ruled out, leaving photoelectric devices of the vacuum-photoemissive type as the only choice.

DEVELOPMENT OF APPARATUS

Attention was turned, therefore, to the properties of photomultipliers and their possible use as radiation detectors. Their cathode sensitivity is usually of the same order as for a simple vacuum photocell, and the gain of a nine- or ten-stage multiplier due to secondary electron multiplication is generally about 10^6. This corresponds to overall sensitivities of 10 to 40 A/lm, making possible the detection of very low light intensities.[1–4] The superiority of a photomultiplier over a simple photocell followed by a high-gain amplifier lies almost entirely in the much shorter resolving time of the photomultiplier.[1] It is frequently used in scintillation counters where extremely rapid response is required. In this connexion resolving times of the order of 10^{-9} s or less are generally quoted for electrostatically focused types[5] and not more than 10^{-8} s for the unfocused type.[6] The high frequency response is only limited because of the statistical spread in electron transit time across the multiplier.[1,7] The absolute value of the transit time which may be as much as 3×10^{-8} s[8] does not affect the time resolution.

The spectral response of photomultipliers was the next important consideration.[1,9] The operating temperature of an oxide cathode lies between 800 and 900° C. At these temperatures nearly all the radiation is in the infra-red region. The response of photomultipliers, on the other hand, lies mainly in the visible and near ultra-violet region of the spectrum. Hence an extension of the normal spectral range of a photomultiplier appeared desirable. The infra-red sensitive image converter seemed to present an obvious answer.[10]

The image converter used throughout this investigation was of German origin, first developed during the war for night operations.[11] The resolving time of the image converters is of the same order as that of photomultipliers[12] but this does not take account of any delay due to the fluorescent screen. It appeared at first that the comparatively long time constant of the ordinary willemite screen would present a serious difficulty. It was, however, found quite possible to obtain the required time resolution because of the very low light intensity and hence low levels of excitation involved. Nevertheless, the image converter screen was the weakest link in the chain as far as time resolution was concerned, and an image converter with a specially fast screen,[10] would have been preferable but was not available at the time.

The photomultiplier (type 1.P.21 by The Radio Corporation of America) and the image converter were placed inside a light-tight enclosure with the photomultiplier separately screened against electrostatic interference by coarse wire mesh. This, and the provision of filters in the high tension supply leads, was necessitated by the close proximity of a high-power modulator required for operating the pulsed magnetron.

The final arrangement is shown in Fig. 1. Only one filter is shown but altogether ten were used, one in each lead, nine dynodes and one cathode, the anode being returned to earth *via* an anode load of 10 kΩ.

The gain of a photomultiplier is extremely sensitive to changes in dynode voltage.[1,2,13] For this reason the power supply was designed to use dry batteries as a float, with current being provided by a conventional mains transformer and rectifier. The circuit diagram of the complete photomultiplier power supply is shown in Fig. 2. This power supply worked quite satisfactorily giving a very constant voltage since no current was drawn from the batteries themselves. The overall photomultiplier voltage was variable in eleven equal steps from 1080 to 750 V. For each position

* G.E.C. communication No. 657.

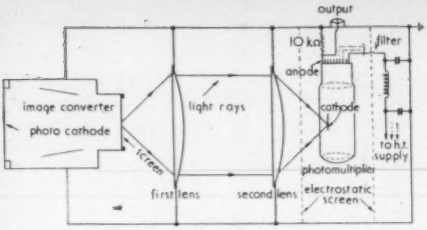

Fig. 1. Image converter and photomultiplier enclosure

X-band waveguide was soldered to the aperture in order to prevent any radio frequency leakage from the main guide. Two short focal length lenses were arranged to focus the image of the magnetron cathode on to the photocathode of the image converter. The amount of light so received was found to be adequate, although the equivalent solid angle was only $2{\cdot}5 \times 10^{-3}$ steradians.

The photomultiplier output was amplified by means of a special pulse amplifier of 5–10 Mc/s bandwidth and approximately 50 dB gain. The output signal from this amplifier was then displayed on a cathode-ray oscillograph. The total time base sweep was 5 μs triggered by the initiator of the high-power modulator [Fig. 3(*a*)].

With the magnetron operating and direct current applied to the image converter a pulse was observed on the cathode-ray

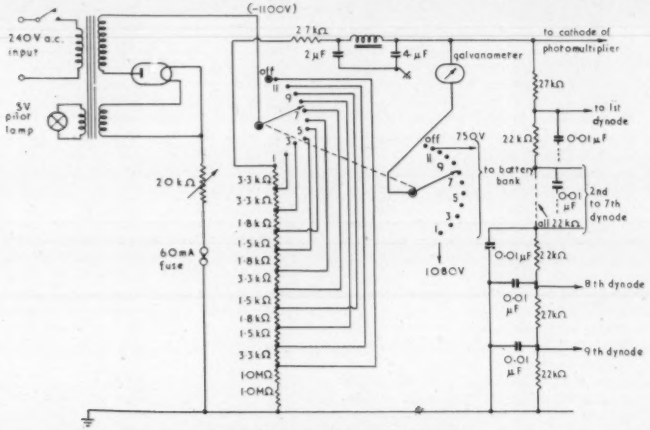

Fig. 2. Photomultiplier power supply

the variable 20 kΩ resistor was adjusted for zero deflexion on the galvanometer. The stepped voltage divider for selecting the required overall voltage had to be arranged in the seemingly irregular manner shown to make this adjustment possible over the whole range, despite varying photomultiplier current. The dynode potential divider applied a fixed proportion of the total voltage to each dynode. As indicated by the resistance values (Fig. 2) equal voltages were applied to all but the first and last dynodes. These two were each operated with a 20% higher voltage, with respect to cathode, than the other dynodes. The reason for increasing the first dynode potential is improved collection efficiency, whereas the last dynode was operated at a higher potential to minimize the possibility of space charge limitation, and hence non-linearity, during peak currents.[1,13]

The complete equipment was then arranged for the observation of the cathode of an operating magnetron. The magnetron, a medium power pulsed S-band type, had a small circular observation window of 0·6 cm diameter in its output system through which the cathode could be viewed. To allow the maximum amount of light to fall on the image converter a rectangular aperture, $2{\cdot}5 \times 1{\cdot}2$ cm, was cut into a right-angled bend placed in the main waveguide system as closely as possible to the magnetron. A short length of

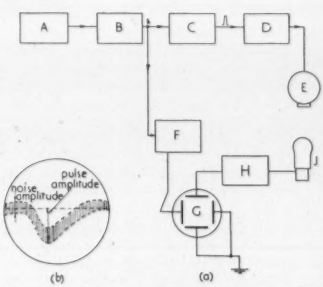

Fig. 3(*a*). Block diagram of apparatus, modulator and display unit

A, oscillator; *B*, initiator (pulse former); *C*, amplifier and shaper; *D*, final modulator; *E*, magnetron; *F*, cathode-ray oscillograph time base; *G*, cathode-ray tube; *H*, pulse amplifier; *J*, photomultiplier.

(*b*) Typical display

oscillograph which disappeared when the image converter supply was switched off. This suggested that the observed pulse was due to a genuine brightness change of the cathode surface and not due to noise or interference from the modulator. There was however a considerable amount of background noise due to the high level of steady illumination reaching the image converter from the magnetron cathode [Fig. 3(*b*)].

As far as is known the arrangement described represents an entirely new type of measuring technique. It seemed essential, therefore, before commencing systematic measurements, to ensure that the observed response of the apparatus was, in fact, due wholly to a genuine pulse temperature rise of the cathode surface, and not to some additional, or unrelated, effect.

One of the most important of such effects is the ionization glow always observed in the immediate vicinity of the cathode of an operating magnetron. This is due to residual gas, mainly carbon dioxide, and is confined almost entirely to the blue part of the spectrum. This glow appears only during the actual pulse and must, therefore, be prevented from reaching the image converter. This was effected simply by placing an orange filter between the image converter and the magnetron cathode, actually between the two lenses. The filter was a Kodak gelatine filter, Wratten No. 22, with a lower wavelength cut-off at 5200 Å. Although the absolute sensitivity of the equipment was reduced a little by the filter, the relative sensitivity, that is the sensitivity to small changes in temperature, may, in fact, increase, depending on the mean temperature. The reason for such a possible increase lies in the properties of the energy/wavelength distribution curve for blackbody radiation.[14] By introducing this filter the response of the whole equipment was confined entirely to the wavelength range 5200–14 000 Å.

The sensitivity of the apparatus to small temperature changes was very high, a 1% change in temperature would cause a 10 to 20% change in the output signal.

Having thus eliminated any interference due to ionization glow, attention was next drawn to the possibility of soft X-rays from the magnetron exciting the photocathode of the image converter. The possibility of X-ray interference could not *a priori* be ruled out, although photoemissive cathodes are inherently very inefficient detectors of direct X-rays.[9] The absence of any X-ray effect was proved in a very simple manner: a thin sheet of black paper was interposed first between magnetron and image converter, then between the latter and the photomultiplier. This reduced the output signal to zero in both cases, whereas the paper used would have been easily penetrated even by very soft X-rays.

Occasionally a faint fluorescence of the dome-shaped glass output window of the magnetron was observed. Possible interference from this source was eliminated by so positioning an opaque mask with a very small central aperture on the fluorescent screen of the image converter that no direct light other than that from the focused image of the actual magnetron cathode remained visible.

The test for electrostatic or similar non-optical interference consisted simply of switching off the image converter supply during operation. This again resulted in zero output signal showing that no spurious signals were picked up directly by the photomultiplier or its associated circuits.

In order to measure the direct current output from the photomultiplier as an indication of mean illumination level, and as part of the calibration procedure (see next section) a special "backing-off" circuit was devised in order to maintain high differential sensitivity over the entire range. This circuit is shown in Fig. 4. The voltmeter was a conventional multi-range instrument, the galvanometer was a 25 μA moving coil meter of 3840 Ω internal resistance. The two potentiometers served as coarse and fine controls respectively in adjusting for zero current through the galvanometer. The voltmeter then read directly the photomultiplier output voltage into an infinite impedance, i.e. the potential drop across the 10 kΩ anode load. Alternatively the galvanometer could be used to detect small changes in mean level anywhere within the range of the photomultiplier.

With the aid of this arrangement two further tests were carried out. The first one was to check the response linearity of the whole equipment with pulsed light input. It is obviously most important that the pulse response remains linear for wide variations in mean light level, so that the output pulse amplitude may be assumed proportional to the pulse temperature rise irrespective of mean cathode temperature. The magnetron was replaced by a neon tube and filament lamp so arranged that their images appeared superimposed on the same area of the image converter screen. In each case the lamp was adjusted for a convenient photomultiplier output (d.c.), and the neon tube was pulsed from the modulator at constant voltage to give an output pulse on the cathode-ray oscillograph. The lamp brightness was then varied, and it was observed that the amplitude of the output pulse was independent of the lamp brightness, i.e. the mean level, over a very wide range of both neon brightness, i.e. signal amplitude, and mean level. Readings were taken at several image converter voltages, and departures from linearity were observed only below 11 kV. This was almost certainly due to space charge limitation in the image converter. Since a supply voltage of about 15 kV was used in practice this non-linearity below 11 kV is of no importance. The results are tabulated below. Each of the six sets corresponds to a fixed amplitude pulse applied to the neon tube.

Results of linearity test

Set	*Photomultiplier output (d.c.)* (*V*)	*Image converter voltage* (*kV*)	*Noise amplitude* (*V*)	*Pulses per second*	*Output amplitude* (*V*)
1	0·0	14·6	0·0	500	100
1	0·63	14·6	17·0	500	100
2	0·0	14·6	0·0	1000	80
2	1·19	14·6	23·0	1000	80
3	0·0	14·6	0·0	1000	60
3	0·51	14·6	15·0	1000	62
3	1·00	14·6	21·0	1000	60
3	1·54	14·6	24·5	1000	60
3	3·40	14·6	41·0	1000	60
4	0·0	14·6	0·0	1000	28
4	2·05	14·6	30·0	1000	28
5	0·0	11·0	0·0	1000	48
5	1·68	11·0	26·0	1000	47
6	0·0	8·0	0·0	1000	50
6	1·61	8·0	25·0	1000	33

Finally the origin of noise was investigated mainly to enable conditions to be chosen for maximum signal/noise ratio. As already mentioned, the noise output from the amplifier increased with increasing mean cathode temperature. This made accurate measurement of the pulse amplitude difficult [see Fig. 3(*b*)].

In order to test whether this noise originated mainly in the image converter or in the photomultiplier a small metal filament lamp was placed inside the light-tight enclosure between the image converter and the photomultiplier. Otherwise the apparatus was set up as usual and focused on to a magnetron cathode. The supply voltage of the image

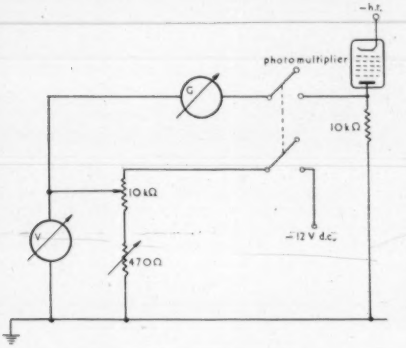

Fig. 4. Backing-off circuit for measuring the d.c. output from the photomultiplier

converter was then gradually reduced, and the brightness of the lamp increased so as to keep the photomultiplier d.c. output constant. At the same time the noise amplitude was measured on the cathode-ray oscillograph. The magnetron cathode temperature was constant and the valve was inoperative. Under these conditions the noise amplitude

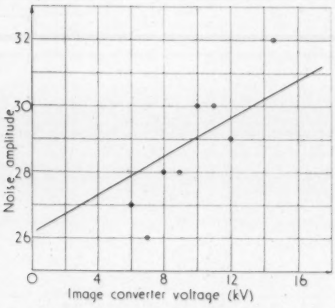

Fig. 5. Total noise as a function of image converter voltage (constant illumination)

decreased very slightly as the image converter voltage was reduced. A plot of noise amplitude against image converter voltage is shown in Fig. 5.

Hence it was concluded that a small amount of noise was probably contributed by the image converter but that most of it (nearly 90%) originated in the photomultiplier.

A fairly large number of signal/noise ratio measurements were then undertaken in order to find the optimum operating conditions for both image converter and photomultiplier, and also to select the best of three similar multipliers available. The signal/noise ratio in this connexion was defined as the ratio of d.c. photomultiplier output to noise amplitude observed on the cathode-ray oscillograph (maximum amplifier gain) for any given level of steady illumination.

CALIBRATION PROCEDURE

With the equipment in place the cathode could not be observed directly, and it was necessary, therefore, to have some "resetting-parameter" which bore a simple functional relationship to the cathode temperature. The filament voltage was an obvious choice but not convenient because in the operating magnetron, cathode and filament are at a high negative potential with respect to ground (anode). So the voltage across the primary winding of the filament transformer V_{pf} was chosen. The first step of the calibration procedure consisted of measuring the cathode temperature by means of an optical pyrometer and plotting this against V_{pf}. The photomultiplier enclosure was then placed in position, and by means of the backing-off circuit already described the photomultiplier output voltage V_0 was obtained as a function of V_{pf}. By eliminating V_{pf} between these two functions a calibration curve could be plotted of cathode temperature against V_0. This then formed the basis for subsequent determinations of pulse temperature rise for the given cathode. Voltage V_{pf} served throughout as a guide to the mean cathode temperature, particularly for an inoperative valve. Voltage V_0 was used for accurate settings, and for finding the mean cathode temperature of an operating valve which, due to back-bombardment, is always higher than that of the inoperative valve for a given filament voltage. Generally the mean of several calibrations was used and, in practice, it was immaterial whether the temperature/V_0 calibration just described was obtained before or after the actual determination of the pulse temperature rise. For each such determination the magnetron was run under the desired operating conditions, until observation of the d.c. photomultiplier output V_0 indicated that the mean cathode temperature was remaining constant. The photomultiplier output was then connected to the amplifier and cathode-ray oscillograph [Fig. 3(*a*)], and the amplitude a_0 of the observed pulse was measured on the cathode-ray oscillograph. The pulse amplifier was non-linear, i.e. its gain was a function of the amplitude of the applied signal. Hence the amplifier gain had to be measured for each observation. This was done by applying a suitable voltage pulse of amplitude a_1 from the modulator *via* a potential divider of accurately known ratio r to the input of the amplifier. The output was again observed on the cathode-ray oscillograph, amplitude a_2. The amplitude of the voltage pulse was adjusted until a_2 was exactly equal to a_0. The voltage pulse was then connected directly to the cathode-ray oscillograph and a_1 was measured. The value of $a_1 r$ was then equal to the amplitude of the input signal previously applied to the amplifier from the photomultiplier. After correcting for the input impedance of the amplifier (approximately 3000 Ω) which was effectively in parallel with the anode load, the equivalent increment in output voltage from the photomultiplier was obtained corresponding to the pulse temperature rise. By using the calibration curve of cathode temperature against V_0 this voltage increment was translated into a temperature increment, thus giving the desired value for the pulse temperature rise.

A typical calibration curve is shown in Fig. 6. Altogether quite a large number of such curves were obtained for the different cathodes used, and in each case the curve was found to approximate very closely to a function of the form:

$$T = a + bV_0 + c \log_e V_0 \qquad (1)$$

the arbitrary constants a, b, c, differing slightly in each case. Their order of magnitude, with V in millivolts, was: a between 400 and 500° C, b between 10^{-2} and 2×10^{-2} °C/mV and c between 40 and 60° C. For example, the function corresponding to Fig. 6 can be approximately represented by:

$$T = 467 + 2 \times 10^{-2} V_0 + 52 \log_e V_0$$

The great advantage of this particular function is the very simple form of its first derivative, so that numerical calculation of small increments becomes particularly easy. If δV is the observed change in V_0, then δT, the required pulse temperature rise, is given by:

$$\delta T = [b + (c/V_0)]\delta V \qquad (2)$$

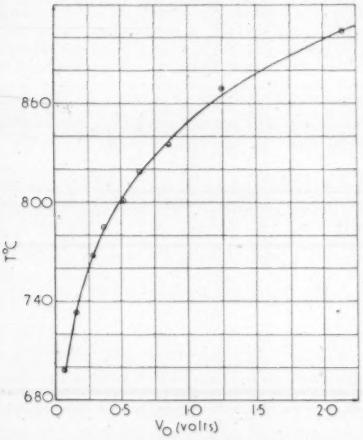

Fig. 6. Calibration curve of cathode temperature/photomultiplier output

This expression is only valid, of course, if the increments are small enough for all higher terms in the Taylor expansion to be negligible. This was nearly always true in practice. Where occasionally a larger value was observed δT was read directly from the calibration curve.

ESTIMATION OF ERRORS

By calculating the standard deviations of several determinations of the pulse temperature rise under identical operating conditions, an approximate estimate of the overall accuracy of the measurements became possible. While in one or two cases possible errors were as high as 26% or as low as 1%, the average was between 8 and 12%. The inherent accuracy of the method is limited mainly because of the presence of a considerable amount of noise [compare Fig. 3(*b*)]. On the other hand, temperature changes as small as 1 or 2° C have been detected when the mean temperature was between 800 and 900° C. This shows the high sensitivity of the method employed, and in view of the difficulties inherent in this type of measurement the performance of the apparatus was considered satisfactory. A full report on the results obtained with this apparatus and discussion of their significance is being published elsewhere.[15]

ACKNOWLEDGEMENT

The author is indebted to the Admiralty for permission to publish this paper.

REFERENCES

(1) RODDA, S. *Photoelectric Multipliers* (London: MacDonald and Co., 1953).
(2) ENGSTROM, R. W. *J. Opt. Soc. Amer.*, **37**, p. 420 (1947).
(3) ALLEN, J. S. *Proc. Inst. Radio Engrs*, **38**, p. 347 (1950).
(4) BOESCHOTEN, F., MILATZ, J. M. W., and SMIT, C. *Physica*, **20**, p. 139 (1954).
(5) POST, R. F. *Nucleonics*, **10**, p. 56 (1952).
(6) ALLEN, J. S., and ENGELDER, T. C. *Rev. Sci. Instrum.*, **22**, p. 401 (1951).
(7) MALTER, L. *Proc. Inst. Radio Engrs*, **29**, p. 587 (1941).
(8) SMITH, R. V. *Phys. Rev.*, **98**, p. 1170 (1955).
(9) ZWORYKIN, V. K., and RAMBERG, E. G. *Photoelectricity and its Applications* (New York: John Wiley and Sons, Inc., 1949).
(10) HOLIDAY, E. R., and WILD, W. *J. Sci. Instrum.*, **28**, p. 282 (1951).
(11) ECKART, F. *Ann. Phys.* [*Leipzig*], **14**, p. 1 (1954).
(12) JENKINS, J. A., and CHIPPENDALE, R. A. *J. Brit. Instn Radio Engrs*, **11**, p. 505 (1951).
(13) WILSON, R. *J. Sci. Instrum.*, **30**, p. 472 (1953).
(14) BENFORD, F. *G.E. Rev.*, **46**, pp. 377 and 433 (1943).
(15) DEHN, R. *Brit. J. Appl. Phys.* To be published.

The measurement of the electrical resistivity of silicon*

By R. H. Creamer, M.Sc., A.Inst.P., The General Electric Co., Ltd., Wembley, Middlesex.

[*Paper received* 19 *December*, 1955]

A modified four-probe method is described which employs probes made from wires containing a donor or acceptor type impurity for *n*- or *p*-type silicon respectively. By discharging a condenser between the probes, low resistance stable contacts are obtained which allow a steady current to flow in the specimen and permit the potential to be measured with a standard potentiometer. Resistivity measurements by the normal method and by the four-probe method are compared; the latter measurements give an accuracy of about ±7% for resistivities up to several hundred ohm centimetres.

Routine measurement of the resistivity of germanium ingots may be conveniently performed by means of a modified Wenner four-probe method,[1] and the work[2] on its merits and limitations makes it unnecessary to give further details here. The method is not directly applicable to silicon ingots, except for resistivities less than about 5 Ω cm, due to unstable contact resistances at the probes giving rise to a fluctuating current in the specimen. Furthermore, the very high values of contact resistance render it difficult to devise simple equipment to obviate these effects, and recourse must often be made to the normal potential probe method[3] despite its restricted specimen geometry and objectionable soldered or plated current leads. This paper describes a method of reducing the contact resistances in the four-probe method in a manner which allows a stable current to be carried by the current probes.

The initial experimental work employed the normal method of measuring electrical resistivity, namely, rectangular bars of silicon were provided with plated current contacts and potential probes were used to determine the voltage gradient when a known current was flowing. Two probes were then used as current leads on these specimens of known resistivity, and the effect on the contact resistances of: (i) pressure loading on the probes; (ii) electrical forming of the probes; (iii) varying the material of the probes; and (iv) the surface treatment of the silicon, was examined.

Increasing the pressure on the probes reduced the contact resistance but the effect was not sufficient to enable wire probes (approximately 0·3 mm diameter) to make satisfactory current-carrying leads. It was observed, however, that discharging a condenser between probes made from wires containing a donor or acceptor type impurity—with *n*- or *p*-type silicon respectively—gave low resistance stable contacts which allowed a steady current to pass through the specimen. This may be interpreted as being due to the alloying or diffusion of the probe impurity in the immediate vicinity of the probe contact and the resulting low resistivity silicon under the probe possessing a reduced contact resistance, i.e. reduced rectification effect.

In order to minimize minority carrier injection it was found desirable to give the surface of the silicon a light sand-blasting, this treatment being known to give a high surface recombination velocity.

These results were incorporated in a four-probe apparatus which had facilities for electroforming between any pair of probes, and for measuring the apparent resistance R_c, at a fixed voltage of about 10 V. Probe spacings of approximately 0·10 cm were used with 0·03 cm diameter phosphor-bronze and Duralumin wires as probe materials for *n*- and *p*-type silicon respectively. The ends of the wires were electrolytically etched to give pointed contacts. In general, the value of R_c for any pair of probes was reduced to less than 50 000 Ω by successive application of the electroforming discharge; this value being found to permit a stable current to be passed between the current probes and, incidentally, to allow the electromotive force between the potential probes to be measured with a standard laboratory potentiometer.

Resistivity measurements with the modified four-probe

Resistivity measurements by the normal and the four-probe methods

	Normal method		*Four-probe method*		
Specimen reference	*Measured resistivity (Ω cm)*	*Standard error*	*Probe treatment*	*Measured resistivity (Ω cm)*	*Standard error*
1	2·88	0·02	nil	2·86	0·09
(*n*-type)			electroformed	2·84	0·03
2	8·00	0·08	nil	7·80	0·56
(*p*-type)			electroformed	8·00	0·11
3	26·80	0·16	nil	†	†
(*n*-type)			electroformed	26·00	0·37
4	150·0	3·5	nil	†	†
(*n*-type)			electroformed	157	4
5(*a*)*	229	8	nil	†	†
(*n*-type)			electroformed	222	25
5(*b*)*	1627	87	nil	†	†
(*n*-type)			electroformed	1650	225

* Non-uniform resistivity along specimens.

† Fluctuating current in specimen.

* G.E.C. communication No. 648.

method were compared with the results obtained by the normal method on the same specimens. Typical examples of the resistivities obtained by the two methods are given in the table.

It can be seen that the measurement of resistivities up to the order of a few hundred Ω cm by this four-probe method gives reliable results with an accuracy of about ±7%. Measurements are also possible for resistivities up to several thousand Ω cm, although the accuracy deteriorates at these high values.

REFERENCES

(1) BRUCKSHAW, J. M. *Proc. Geog. Assoc.*, **59**, p. 113 (1948).
(2) VALDES, L. *Proc. Inst. Radio Engrs*, **42**, p. 420 (1954).
(3) VALDES, L. *Bell. Lab. Record*, **23**, p. 308 (1955).

The Eberhard effect in X-ray powder photographs

By T. W. BAKER, B.Sc., Grad.Inst.P., Atomic Energy Research Establishment, Harwell, Berks.

[*Paper received* 1 *December*, 1955]

The Eberhard effect is briefly described and observed spurious doublets in X-ray powder photograph positives are attributed to this cause. It is also considered that high angle doublets used for accurate lattice parameter measurement will suffer displacement due to this effect, and an example of this is quoted. The effect will also introduce intensity discrepancies in lines that are close together.

THE EBERHARD EFFECT

The Eberhard effect is an important factor affecting the fidelity of photographically recorded sound, and the accuracy of the photographic image in astrophysical and photometric investigations, but it does not seem to have been brought to the notice of crystallographers that the effect can lead to the misinterpretation of X-ray powder photographs. For this reason it is dealt with in some detail in this paper. The thick emulsion of X-ray film is particularly susceptible to the phenomenon.

Eberhard[1,2] exposed photographic plates behind a screen in which were circular openings of diameters varying from 0·3 to 30 mm. He found that the densities of the developed plates were not uniform, but the smaller images were denser than the larger, as if the smallest had received from one and a half times to twice the exposure of the largest. The term "Eberhard effect" has now come to include those phenomena which depend on the fact that the blackening of an area of a photographic plate is affected by the blackening of those parts immediately adjacent. It has its basis in the physical factors that are concerned in the development process. The silver bromide grains suspended in the photographic layer form a colloidal medium of appreciable thickness in which liquids move according to the laws of diffusion. During the development process not only is the developer considerably weakened in a heavily exposed region, but reduction products are formed which significantly retard further development. The formation of these appears to be most marked in the case of organic developers.

The case of a photographic plate with a heavily exposed portion separated from a completely unexposed part by a sharp boundary, and having a slight general fog level, is represented diagrammatically in Figs. 1 and 2. Unused developer diffuses from the unexposed portion to the exposed portion causing the exposed region to be darker at the border than elsewhere. This has been given the name "border effect". Reduction products diffuse in the opposite direction, preventing the development of the fog level in the region in close proximity to the junction. This is known as the "fringe effect" and the resulting white zone is referred to in general photography as the "Mackie line."

If the reaction products are on the surface of the emulsion the Eberhard effect can be minimized by agitation. Agitation may, however, be unsuccessful if the reduction products are confined chiefly within the depth of the emulsion layer. Some confusion exists in the literature concerning the effect, but a good résumé is given by Junkes.[3]

Fig. 1. Diagram of the diffusion trends in a photographic film at the boundary of a sharp image
←– – → reduction products; ——→ developer.

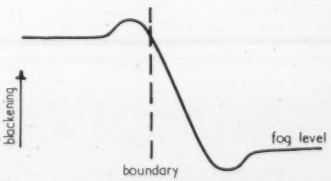

Fig. 2. Diagram of the blackening behaviour at the boundary of a sharp image on a fogged plate

SPURIOUS DOUBLETS

The author's interest in the Eberhard effect arose in connexion with the publication of work concerning the effects of irradiation on polymers. Positive prints were made of powder photographs of polythene. On the print it was noticed that the strongest line gave the appearance of a doublet, there being a faint dark line along its centre. The printing process was repeated, using several other films on

[*Note added in proof*: The Eberhard effect has received brief mention as a factor to be borne in mind by H. R. Herz in *X-ray Diffraction by Polycrystalline Materials*, (London: The Institute of Physics, 1955).]

which the X-ray exposure had been varied, and on each of them the strongest line had a dark line along its centre. No other line showed this phenomenon, nor was the doublet formation observable on the films themselves. A microphotometer trace of the film did not resolve the suspected doublet, but this was by no means conclusive evidence, since the instrument is less sensitive than the eye in this respect. Although from considerations of the energy absorbed it seemed unlikely that the dark line was caused by solarization of the negative, this was tested for by increased exposures and found not to be the case.

In view of the evidence, and the lack of any other satisfactory explanation, the idea that the doublet was due to a splitting of the polythene reflexion began to gain acceptance, it being assumed that the contrast properties of photographic papers brought out changes in the line's intensity not originally visible to the eye. The observed doublet had Bragg spacings of 4·04 and 4·23 Å, and further credence was given to its validity by the report of Pierce, Tordella, and Bryant,[4] of the latter spacing in a second crystalline modification of polythene.

At this stage the printing process itself was tested. A line was prepared on a piece of X-ray film in the following manner. Two pieces of black paper were fitted into a printing frame to form a slit with well-defined edges. This was printed on to X-ray films by means of a single filament lamp set several feet away, so ensuring that, if not entirely dark, the blackening was at least darkest at the centre. Prints were made of this line using a range of exposure times and papers of various contrasts. On several of these a white line was obtained with a dark line down its centre, particularly from batches consisting of well exposed negatives and prints. Further prints were made of the polythene and also of other powder patterns such as that of quartz. Under suitable conditions of exposure and paper all the lines could be printed with a dark line down the centre. It was thus clearly established that the apparent doublet in the polythene pattern was spurious, and was, in fact, due to the printing process.

The phenomenon can be satisfactorily explained as being due to the Eberhard effect, and the case of the specific problem, that of the printing of a dark line, is represented diagrammatically in Fig. 3. Here there are two boundaries separated

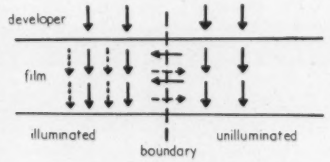

Fig. 3. Diagram of the blackening behaviour producing the spurious doublet

by an unexposed region. Along each boundary is the white under-developed zone, and in the centre is the developed fog level. The result is to give a white line with a darker line along its centre, which is precisely the appearance of a close doublet. In the case of polythene where one line is much stronger than the others, and so received the exposure necessary to bring up the effect, an optimum condition for confusion exists. As far as is known this is the first occasion in which a doublet has been produced by the Eberhard effect.

The doublet was in some aspects reminiscent of an optical illusion. That it was not illusory was shown in two ways: it could be photographed and enlarged; and instead of printing on paper, a print could be made on film which could then be projected. In both these cases, although the geometrical conditions for the optical illusion no longer existed, the doublet was still discernible. The similarity in appearance of the doublet to an optical illusion is not surprising, since the Eberhard effect is the photographic analogue of the optical illusion.

LINE DISPLACEMENTS

A further important consequence of the Eberhard effect is that it can cause two neighbouring lines to be displaced, since each lies within the fringe effect of the other. Kostinsky[5,6] observed the apparent repulsion of two star images—an effect which bears his name. Thewlis[7] has also observed discrepancies which could be due to this cause. In an accurate determination of the unit-cell dimensions of Li^6F and Li^7F he made allowance for the errors in reading the positions of the $K\alpha_1$ and $K\alpha_2$ reflexions, which arose from the proximity of these reflexions, and which were the greater the greater the proximity. The effect guarded against consisted of an apparent displacement of the $K\alpha_1$ and $K\alpha_2$ reflexions from each other, the observed θ-value for $K\alpha_1$ being too high and that for $K\alpha_2$ too small. He carried out independent Nelson–Riley extrapolations for the $K\alpha_1$, $K\alpha_2$ and $K\beta$ reflexions, and found the slopes of the three lines different, with that for the $K\beta$ reflexions intermediate between the other two. This is precisely the result to be expected from this cause. The writer has obtained similar results, though in less precise determinations. The effect will also cause a discrepancy in the intensity of lines that are close enough together.

ACKNOWLEDGEMENTS

Thanks are due to Mr. C. J. Harris for help with the experimental work.

REFERENCES

(1) EBERHARD, G. *Phys. Z.*, **13**, pp. 288–292 (1912).
(2) EBERHARD, G. *Publ. Astrophys. Obs. Potsdam*, **26**, pp. 45–55 (1926).
(3) JUNKES, J. *Z. Wiss. Photogr.*, **36**, pp. 217–234 (1937).
(4) PIERCE, R. H., JR., TORDELLA, J. P., and BRYANT, W. D. M. *J. Amer. Chem. Soc.*, **74**, p. 282 (1952).
(5) KOSTINSKY, S., and TIMOFEEFF, L. *Mitteilg. Pulkowo* (I), **11**, pp. 149–150 (1906).
(6) KOSTINSKY, S. *Mitteilg. Pulkowo* (II), **14**, pp. 17–28, (1907).
(7) THEWLIS, J. *Acta Cryst.*, **8**, p. 36 (1955).

Correspondence

Ultra-violet polymerization of embedding monomers for thin sectioning

In electron microscopy the established embedding technique for thin sectioning of biological materials is to infiltrate with pure or mixed esters of methacrylic acid, and subsequently to polymerize the monomer by heating with a catalyst.(1) An alternative method of polymerization, using ultra-violet radiation, has been described in a number of publications.(2) However, despite our adherence to the experimental procedures described, we found great difficulty in consistently polymerizing the monomer with ultra-violet radiation. Subsequently we became aware that this difficulty was widely experienced, and that some laboratories had discarded the method on account of its unreliability. We therefore thought it would be of help to others if the following methods, which polymerize more reliably than the heat method and completely eliminate objectionable bubble formation, were published.

We have used, on various occasions, the *iso*-butyl, *n*-butyl, ethyl or methyl esters of methacrylic acid, or mixtures of these esters. We found that reproducible polymerization could be obtained without a catalyst only when the monomers were freed from inhibitor by distillation in an atmosphere of nitrogen, as suggested to us by Dr. G. W. Madaras. This method is particularly useful because it enables a check to be made on any artifacts that may have been caused by the catalyst.

Using the same monomers but removing the inhibitor in the more usual way, by alkali extraction followed by several washings with distilled water, we have found it necessary to use a catalyst. At the suggestion of Imperial Chemical Industries Ltd. we tried using phenyl-benzoyl carbinol (benzoin) as catalyst and found it very satisfactory.

The catalyst works well in the pale-yellow powder form in which it is normally supplied, but, in view of possible variations in the amount of impurities in different batches of catalyst, thus impairing the reproducibility, and in order to guard against the possible source of artifacts in our samples, we have preferred to use the white crystals. These were prepared as follows: 10 g of the yellow powder were dissolved in 125 ml. acetone. The solution was filtered and the benzoin precipitated by adding 100 ml. distilled water. After chilling, the crystals were separated in a Buchner funnel, washed with 50% acetone followed by distilled water, and dried over calcium chloride in a vacuum desiccator.

As a source of ultra-violet radiation we used a 125 W high-pressure mercury discharge lamp. This was provided with a removable envelope of Wood's glass. Thus either unfiltered radiation or Wood's light, 95% of which has a wavelength of 3650 Å, could be obtained.

With 1% benzoin the monomer could be polymerized in 2 h if held about 10 in. from the source. If such a monomer is first pre-polymerized to a syrup by holding it in a thin glass tube about 6 in. from the source for 15–20 min, and frequently stirred, the syrup, if subsequently placed in a capsule 10 in. from the source, will harden in an hour. Such rapid polymerization gives a brittle polymer from which, however, the thinnest of "silver" sections(3) can be cut. The intensity of radiation under these conditions causes the benzoin to impart a light green-yellow colour to the polymer, which we do not find objectionable. If pre-polymerized plugs are required in the capsule for specimen orientation, it is advisable to form them from the thick syrup.

Because of the strains set up in the specimen by rapid polymerization, we have preferred to polymerize more slowly by placing tissue samples in monomer containing 0·5% benzoin, and exposing to Wood's light at a distance of 24–30 in. for about 8 h. This gives a colourless polymer, and a tougher one than is obtained by rapid polymerization.

We wish to thank Mr. J. Hope for his valuable help.

Department of Dermatology, A. CHARLES
General Infirmary and
Department of Biomolecular Structure,
The University,
Leeds.

Textile Physics Laboratory, J. SIKORSKI
Department of Textile Industries,
The University,
Leeds.

Note added in proof. It is recommended that the benzoin-catalyzed polymerization be used only for embedding robust materials such as textile fibres.

REFERENCES

(1) NEWMAN, S. B., BORYSKO, E., and SWERDLOW, M. *Science*, **110**, p. 66 (1949).
(2) MASSEY, B. W., *J. Stain Technology*, **28**, p. 19 (1953).
(3) EAVES, G., and FLEWETT, T. H. *Exp. Cell. Res.*, **6**, p. 159 (1954).

Vapour lubrication of titanium and zirconium

Titanium surfaces are usually covered with a thin oxide film which is chemically inert and makes boundary lubrication difficult. The film itself provides little protection from sliding damage and the coefficient of friction measured between two titanium sliders is fairly high, about $\mu = 0{\cdot}5$ under most ordinary conditions.

When the sliders are thoroughly cleaned by heating in a high vacuum ($10^{-3} - 10^{-4}$ microns of mercury) until some of the surface metal has evaporated away, the friction is much higher. Values of $\mu = 1{\cdot}5$ have been recorded *in vacuo* at room temperature both for spectroscopically standardized metal and for commercial titanium, while at temperatures above 300° C the friction rises rapidly to much higher values. It is probable that complete seizure is prevented only by the absorbed gases held in the metal lattice. High friction coefficients of this order may be obtained in engineering practice, for example during high-speed lathe turning,(1) when the chip rubs on the tool face before appreciable atmospheric contamination has occurred.

The influence of different vapours may be studied directly by admitting them to the vacuum tank containing denuded titanium sliders. Oxygen, water vapour and the vapours of caproic and lauric acids show very little effect either separately or in combination ($\mu = 1{\cdot}0$). This is in contrast to the

behaviour of copper sliders, which seize when denuded but are readily lubricated by a fatty-acid vapour in the presence of oxygen and water vapour ($\mu = 0{\cdot}3$), but the result is in agreement with the conclusion of Rabinowicz and Kingsbury[2] and others, that fatty acids are poor lubricants for titanium.

Vapour lubrication of titanium is, however, possible. Bowden[3] has shown that a lamellar coating of molybdenum disulphide formed by direct attack with hydrogen sulphide will give a low friction between molybdenum sliders in air, even at 300–400° C. The dihalides of titanium have a similar structure as shown by X-ray diffraction and it appears that a lamellar coating of titanium di-iodide is produced when pure iodine crystals are exposed *in vacuo* to the denuded titanium friction specimens. This is accompanied by an immediate fall in friction from $\mu = 1{\cdot}5$ to $\mu = 0{\cdot}3$. The figure shows that the friction remains low even at 400° C. Above this temperature the di-iodide decomposes into tetra-iodide which is volatile leaving clean metal surfaces again.

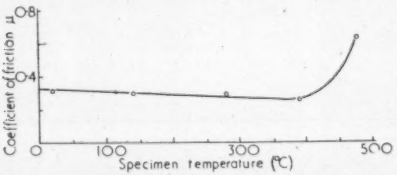

The friction between two titanium cylinders which have been outgassed by heating in high vacuum to 1250° C and then exposed to iodine vapour at a pressure of about 100 microns of mercury during the friction measurements

Zirconium also forms lamellar halides and behaves in a very similar way. After the specimens have been heated at 1200° C in a high vacuum, the coefficient of friction, measured at room temperature, is about 1·5. This may be reduced to 0·35 in iodine vapour and to 0·30 in chlorine vapour.

Comparison may be made with molybdenum disulphide under the same conditions. After outgassing at 1400° C the coefficient of friction between molybdenum sliders is about 2·0. Hydrogen sulphide vapour causes an immediate fall to $\mu = 0{\cdot}9$, but the full effect is produced only by heating the metal to about 850° C in the vapour. A tenacious film is then obtained which gives a low friction, $\mu = 0{\cdot}2$, at all temperatures up to about 900° C, above which the disulphide decomposes.

A few experiments were made in air, since most of the published results on titanium have been obtained from measurements in ordinary atmosphere. Titanium di-iodide is unfortunately not commercially available, but it was found that powdered iodine crystals gave a reasonably good lubrication between two titanium sliders, $\mu = 0{\cdot}15$ at a load of 1 kg. Cadmium iodide has the same structure as titanium di-iodide and if finely powdered shows $\mu = 0{\cdot}11$, but when vigorously rubbed into the surface gives a very good lubrication, $\mu = 0{\cdot}04$. This agrees well with the result recently obtained by Peterson and Johnson.[4]

We thank Tube Investments Ltd. for permission to publish this note.

Tube Investments Research Laboratories, Hinxton Hall, Cambridge.

G. W. ROWE

REFERENCES

(1) BOWDEN, F. P., and TABOR, D. *J. Inst. Petrol.*, **40** (369), pp. 243–253 (1954).
(2) RABINOWICZ, E., and KINGSBURY, E. P. *Met. Prog.*, **67/5**, p. 112 (1955).
(3) BOWDEN, F. P. *Research*, **3**, p. 383 (1950).
(4) PETERSON, M. B., and JOHNSON, R. L. *Lubrication Engineering*, **11**, p. 297 (1955).

Observations on the characteristics of the cold cathode ionization gauge

The calibration of a cylindrical anode cold cathode ionization gauge (Penning gauge) has been made in the pressure range 10^{-5} to 10^{-9} mm of mercury. Hence the lower limit of the pressure range over which this gauge has been calibrated has been extended considerably below the lowest previously recorded, i.e. 10^{-7} mm of mercury by Evans and Burmaster in 1950.[1] The gauge used here is the same in principle as that described by Penning and Nienhuis[2] in 1949. Careful measurements have been made at the upper end of the scale (10^{-5} to 10^{-6} mm of mercury) in order to find the stability of the discharge during the first 200 hours operation of a new electrode assembly. The behaviour in the region below 10^{-7} mm of mercury was investigated because extremely low ultimate pressures (when estimated by extrapolating the normal current-pressure characteristic) had made the validity of this extrapolation doubtful.

A Bayard–Alpert[3] type hot cathode ionization gauge has been used as the reference gauge in all these experiments. No accurate calibration of this gauge has been made to better than $\pm 5\%$ so that the accuracy of the results cannot be great. This is not important, however; the reliability and reproducibility of the readings are of much greater value.

The Penning gauge, with nickel electrodes, an anode approximately 1 in. long and 1 in. in diameter and a spacing between the cathode disks—also a 1 in. diameter—and the anode of $\frac{1}{16}$ in., was similar in design to that used in previous measurements of gas adsorption.[4] The glass envelope of this gauge was connected to the Bayard–Alpert gauge by a wide bore glass tube, the conductance for nitrogen being 10 l./s. The pumping plant comprised a mechanical pump and two mercury diffusion pumps connected in cascade, two liquid air traps separating the gauges from the pumps. The effective pumping speed at the gauges was estimated to be approximately 1 l./s for nitrogen. The pressure in the gauge envelopes was controlled by leaking gas into the main vacuum system from an auxiliary reservoir through a porous plug. With this continuous flow arrangement the gas pressure could be varied between 10^{-9} and 10^{-5} mm of mercury. For convenience of operation air was used in all the experimental work.

The Penning discharge was started for the first time after the glass work had been baked to a temperature of 400° C for an hour in order to give an ultimate pressure of better than 10^{-6} mm of mercury as indicated by the Bayard–Alpert gauge. Initially the discharge, operating with 2000 V anode-cathode potential and a magnetic field of 600 G caused appreciable desorption of gas, but this fell to a negligible value after operation for one hour. After ten hours' operation at 2000 V, when the discharge current had fallen to 5 μA from the initial value of 100 μA, the calibration characteristics, for voltages up to about 3800 V, were measured for air. The curves obtained, with current as a function of (*a*) voltage at constant pressure, and (*b*) pressure at constant voltage are shown in Fig. 1.

After obtaining the above calibration the discharge voltage was increased to 4000 V. The ultimate pressure reading immediately rose to 100 μA but subsequently fell steadily, to 1 μA after a further 200 hours at 4000 V. During this time the gauge sensitivity (current/unit pressure) also fell until after 200 hours stability was reached at the values shown by

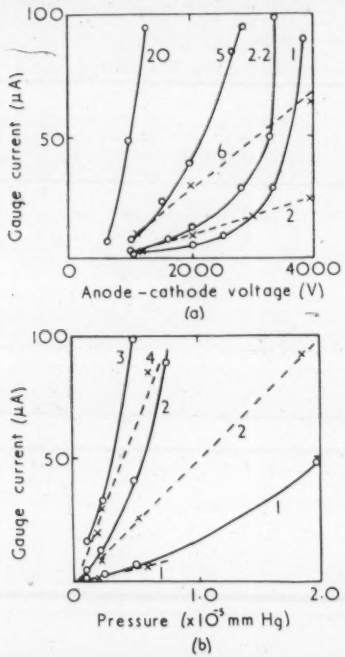

Fig. 1. The calibration curves of the Penning gauge obtained for air

(*a*) Current as a function of voltage at constant pressure. (The gas pressure, in units of 10^{-6} mm of mercury, is marked on each curve.)

(*b*) Current as a function of pressure at constant voltage. (The values of the voltage in kilovolts are marked on each curve.)

○—○—○ calibration curves after 10 hours' operation.
×—×—× calibration curves after 200 hours' operation.

the chain-dotted curves in Fig. 1. These calibration curves, showing the discharge current to be proportional to (*a*) voltage at constant pressure, and (*b*) pressure at constant voltage remained stable for the remainder of the experimental work. They are in fact typical of many calibration curves, all points lying on the same straight lines to $\pm 5\%$.

By means of further extensive baking at 400° C the ultimate pressure was reduced to the order of 10^{-9} mm of mercury to enable the Penning gauge to be calibrated in the range 10^{-9} to 10^{-7} mm of mercury. The current-pressure characteristics in this range are shown in Fig. 2. A very sharp discontinuity is observed at a pressure slightly below 10^{-8} mm of mercury. These curves are typical of many made both at 1000 and 2000 V and also at higher voltages, i.e. 3000 or 4000 V. In each case the same characteristics were obtained for both increasing and decreasing pressure, and further, they were not changed by varying the magnetic field through the range

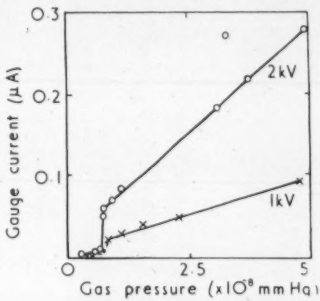

Fig. 2. Calibration curves of the Penning gauge in the low pressure range for air

500 to 1000 G. Because of difficulties in these experiments of controlling the pressure and interpreting ionization gauge readings below 10^{-8} mm of mercury accurate results were not obtained below this pressure. It could be established, however, that the discharge current increased with increasing pressure in this low pressure region.

There was no interaction between the Bayard–Alpert gauge and the cold cathode discharge. The discharge current was not changed significantly by switching off the hot cathode gauge and further, the discontinuity occurred between the same current limits when this gauge was "off." The leakage current in the Penning gauge was negligible even compared to discharge currents of 0·01 μA. In each test the anode-cathode current fell to less than 10^{-5} μA on removal of the magnet from the assembly, i.e. a leakage current of not more than 1% of the smallest discharge current.

The first part of the experiment showed a complete change in the sensitivity during the first 200 hours' gauge operation. Outgassing from the Penning gauge was insignificant during all the calibration measurements so there could be no error due to pressure differences between the two gauges. The changes in the characteristics must be caused, therefore, by some change in the nature of the electrodes themselves; for example, the rate of production of secondary electrons from the cathode under positive ion bombardment. After some hundreds of hours' operation, the cathode surfaces always show a black deposit which is almost certainly carbon.[5] This surface layer probably reduces the secondary emission by a considerable factor. (Lempicki[6] has shown recently that a carbon deposit lowers the secondary emission coefficient for 2000 V electrons by more than a factor of two.) It has been observed both in this series and in other experiments that after allowing the gauge pressure to rise to one atmosphere for twenty-four hours the sensitivity returns to its low stable value within a few hours of starting the discharge. This complete change probably accounts for the conflicting characteristics published by different workers. Conn and Daglish[7] and Hayashi,[8] for example, have published non-linear calibration curves in complete conflict with those of

Penning and Nienhuis.[2] Conn and Daglish's results correspond to those obtained here after ten hours' operation whilst Penning and Nienhuis obtained a linear calibration, as after 200 hours in these experiments.

The calibration at low pressure is interesting as it shows a complete change in the discharge mechanism at a pressure of the order of 10^{-8} mm of mercury. In the experiments at the lowest pressures the discharge could not be extinguished by reducing the pressure, even to 2×10^{-9} mm of mercury with only 1000 V applied.

The writers wish to thank Prof. Craggs and Prof. Meek of the University of Liverpool for the continuous interest that they have taken in this work.

Department of Electrical Engineering, University of Liverpool.

J. H. LECK
A. RIDDOCH

REFERENCES

(1) EVANS, E. C., and BURMASTER, K. E. *Proc. Inst. Radio Engrs*, **38**, p. 651 (1950).
(2) PENNING, F. M., and NIENHUIS, K. *Philips Tech. Rev.*, **11**, p. 116 (1949).
(3) BAYARD, R. T., and ALPERT, D. *Rev. Sci. Instrum.*, **21**, p. 571 (1950).
(4) LECK, J. H. *J. Sci. Instrum.*, **30**, p. 271 (1953).
(5) ENNOS, A. E. *Brit. J. Appl. Phys.*, **4**, p. 101 (1953); **5**, p. 27 (1954).
(6) LEMPICKI, A. *J. Sci. Instrum.*, **32**, p. 221 (1955).
(7) CONN, G. K. T., and DAGLISH, H. N. *Vacuum*, **3**, p. 24 (1953).
(8) HAYASHI, C., and others. *Rev. Sci. Instrum.*, **20**, p. 524 (1949).

New books

Machine translation of languages. Edited by W. N. LOCKE and A. D. BOOTH. (London: Chapman and Hall, Ltd., 1955). Pp. xii + 243. Price 48*s*.

The feasibility, and even more the desirability, of language translation by means of computer-type devices is likely to remain a matter of dispute for some time to come. Under these circumstances the collection of fourteen essays and articles, edited by W. N. Locke of M.I.T. and A. D. Booth of Birkbeck College, London, provides a useful guide for all those who are interested not only in the general problem itself but also in its present position. The type of translation which can be attempted, language of information which has been stripped of its beauty, elegance and emotion, is clearly defined in the foreword by Warren Weaver whose original memorandum on machine translation is included among the essays. It seems clear that the technical means at present in existence may already be sufficient to effect translation of simple scientific and technical texts, and this in itself is an interesting reflexion on the success of computers. Whether the new Tower of Anti-Babel will ever be worth building is another question.

K. MENDELSSOHN

Molecular beams. By K. F. SMITH. (London: Methuen and Co. Ltd., 1955.) Pp. viii + 131. Price 8*s*. 6*d*.

This small book is in lieu of a second edition of the monograph with the same title by R. Fraser which was first published in 1937. There have been many most important developments in the field since then and the new book lays special emphasis on the resonance technique which has been so extraordinarily fruitful. On perusing this slim volume one cannot help but admire the skill with which the author has covered such a wide ground without loss of clarity or readability.

The first three chapters are concerned with the physics of molecular beams in general. Nothing of importance seems to have been left out when techniques of detection are discussed while the usefulness of atomic beams for high resolution spectroscopy is particularly well described. The wave nature of molecular beams is adequately discussed in the third chapter.

The magnetic deflexion of atomic and molecular beams is introduced by an account of the classical experiments of Stern and Gerlach. This includes discussion of the use of deflexion methods for assessment of nuclear as well as atomic moments—in this connexion it is worth remembering that the anomalous magnetic moment of the proton was first observed by Estermann, Frisch and Stern as long ago as 1933 by a deflexion method. This was surely a triumph of technique in a field which has always been characterized by magnificent technique. This has been made even more evident by the remarkable success of the resonance technique first introduced by Rabi in 1937—the discovery of the electric quadrupole moment of the deuteron, of the Lamb shift between the $2s_{\frac{1}{2}}$ and $2p_{\frac{1}{2}}$ level of hydrogen and of the anomalous magnetic moment of the electron represent some of the greatest achievements of experimental physics. The accuracy attainable is incredibly high and the range of phenomena which can be covered is very wide. Chapter 5 provides an orderly account of the principles, technique and achievement of the method with economy and clarity.

The concluding chapter deals with the companion subject of the electric deflexion of molecular beams. This has been less extensively pursued but has already provided interesting information about molecular properties.

It will now be realized how fully the major aspects of molecular beam studies are covered in the book. There is no doubt that it satisfies the purposes for which the series is intended. It is both stimulating and informative and should be most valuable, not only to advanced students, but to lecturers on nuclear physics.

H. S. W. MASSEY

Das photographische Objectiv (Die wissenschaftliche und angewandte Photografie). By J. FLÜGGE. (Vienna: Springer-Verlag, 1955.) Pp. xiii + 373. Price 117*s*. 6*d*.

This is the first volume of the 2nd Edition of the original *Handbuch der wissenschaftlischen und angewandten Photographie*, the first edition of which appeared during the late twenties and early thirties. The new edition is organized completely afresh under the Chief Editorship of Dr. K. Michel. This first volume which deals with photographic lenses differs in approach from the corresponding volume of the first edition; the whole volume having been written by a single author (Flügge) has much greater unity than its predecessor. An idea of the scope of the book may be gained from the chapter headings which, apart from the introduction and appendix are: basis of geometrical optics, imperfections of image formation in monochromatic light, the theory of image aberrations of the third order, chromatic aberration

in image formation, image formation from the point of view of wave optics, the limitation of rays in the photographic objective and their importance, raw materials in optics, systematics of photographic lenses, filters, testing and measuring methods.

The book is written on a sound theoretical basis and the author is not afraid of mathematics and detailed calculations, but the aim of the book is to be thoroughly practical. For example, a detailed example of ray tracing is given, at this point turning the book into a textbook. The first edition contained a detailed description of all types of lenses. This has here been simplified to a description of the general types. The appendix contains notes on lens surface treatment and an analysis of image aberrations of a few typical lenses. As a detailed example of this, calculations and data are presented for a certain lens, i.e. the Schneider Xenon $1 : 2{\cdot}0\ f = 5$ cm.

The book is very well produced and I have not seen any obvious misprints. One regrettable omission is that of Herzberger's method of spot diagrams which, in the United States of America at least, is regarded as one of the most valuable methods for describing the behaviour of lenses in practice.

W. F. BERG

Metals reference book, Vols. 1 and 2. 2nd Ed. By C. J. SMITHELLS. (London: Butterworths Scientific Publications, 1955.) Pp. xiii + 967. Price £8 8*s*. 0*d*. per set.

The increasing output of scientific work is rapidly leading to a condition in which knowledge is accumulating faster than it can be assimilated. One method of help is the publication of reference books in which the most probable values of numerical data are collected or summarized. The present two volumes, which are priced at £8 8*s*. 0*d*. and are not sold singly, are the second edition of an ambitious attempt to summarize the data and some of the methods of metallurgical science and industry. The scope of the book is very wide—it includes sections on first aid, mathematical formulae, physical and chemical constants, spectroscopy, crystallography, equilibrium diagrams, gas-metal systems, diffusion, thermochemical data, physical and mechanical properties, thermoelectric properties, electrical properties and electronics, lubricants, friction, foundry data, refractories, fuels, electrometallurgy, and welding.

The present reviewer is in full sympathy with the object of the book, but feels that a clear warning must be given against the dangers of using it uncritically as a source of reference for numerical data. Some sections and articles are excellent, and every reader can learn much from the book, the value of which would be increased by a better indexing system. In assessing the book for reference purposes, the reviewer can only examine the sections with whose subject matter he is familiar, and when tested in this way the number of faults is disturbing. The fundamental physical constants on p. 44 are taken from the work of Birge,* and no notice has been taken of the later reviews which have led to slight changes in some of the accepted values. Some of the atomic weights given on p. 43 are different from those on the folder between pp. 96 and 97, and the reader is left without a reference which will enable him to choose—it is one of the weaknesses of the book that some data are given without references, although the sources of others are indicated. There appears to be no clear description of the change in the International Temperature Scale in 1948, and numerous small discrepancies occur between temperatures above 1000° C. Apart from this, there are three separate tables (pp. 576, 614, 636) giving the melting and boiling points of the elements and some values are very different in the different tables.

The section on crystal chemistry is most unfortunate. For the elements (p. 194) only one structure is given for strontium, no structure for δ-iron, and the structures given for γ- and δ-manganese are wrong, whilst the name Basinski appears as Bannister. The decision not to use the terms "body-centred" and "face-centred" is unfortunate, and the use of the Strukturbericht symbols alone is sometimes misleading—thus zinc (p. 197) is described as having the A 3 structure, and the reader who seeks the meaning of this on p. 212 finds A 3 described as "(Mg type)", and as the axial ratios are not given, the difference between the Zn and Mg structures may not be appreciated unless the c/a values are calculated. For the more complicated structures the giving of the atomic co-ordinates with no descriptions or diagrams appears of little value. Admittedly, the data will permit the construction of a model, but of those readers who are sufficiently interested to do this, the great majority will require references to original sources, which are often not given. The order of arrangement of the constituent atoms described on p. 193 is confusing, and different readers do not agree as to its interpretation, although all agree that the appearance of $MnCu_2Al$ and Cu_2MnIn in Table I cannot be reconciled with any reading of the rules.

The section on equilibrium diagrams has been much improved, but the failure to observe a strictly alphabetical order of the system is unfortunate, and may easily lead the busy reader to conclude erroneously that no work has been done on a particular system; thus the Ni–Th diagram is two pages before that for Ni–Sn. The references in this section are also faulty.

It is only right for the reviewer to say that in spite of its weaknesses, the compilation of the book is a very considerable achievement, and that any reader who consults it, either for general interest, or in connexion with a particular problem, will be certain to find much of interest in one way or another. But it is clear that in some sections, the numerical data must be verified before they are used seriously.

W. HUME-ROTHERY

Noise reduction manual. By P. H. GEIGER (Michigan, U.S.A.: Michigan University Press; London: Oxford University Press, 1955.) Pp. 167. Price 32*s*. 6*d*.

It is clearly stated in the foreword that "an elaborate acoustical reference work is not intended," but rather "a volume devoted to noise problems from a definitely practical viewpoint." In this aim the author has certainly succeeded, although it is very difficult to decide just how much of the underlying theory to include and in some places a little more would have been very helpful in appreciating the importance of some factors. Chapters 1 and 2 introduce the subject, dealing with procedures to be followed and the units to be used. Chapter 3 gives some useful information on the variation of absorption coefficient of porous materials with frequency and thickness of absorbent layer. However, the statement that "a good sound absorber is a poor sound insulator" must be qualified. Porous materials can give attenuations of 30 dB/ft, rising with frequency, and at high frequencies can give more attenuation per pound than solid partitions. It would be more informative to introduce frequency into the transmission loss equation 3.2 rather than to give the average over 125 to 2000 c/s.

Fig. 3.6 should be in terms of "sound level" not "loudness level." The fact that sound attenuating ducts are discussed

* BIRGE, R. T. *Rev. Mod. Phys.*, **13**, p. 233 (1941).

on pp. 54–9 should be noted on pp. 50 and 52. Some guidance on the frequency of the "beam effect," p. 57, would be helpful, e.g. width $> 2\lambda$. The author has obviously made a special study of the damping of vibrating plates and Chapter 4 deals very thoroughly with this subject, particularly from the point of view of the automobile manufacturers.

Chapter 5 is a useful treatment of vibration isolation by resilient mountings. Simple formulae for vertical natural frequency and for attenuation of vibration are given, but it would have been well to give a little more quantitative information on the "somewhat greater" dynamic stiffness of some materials. A warning is very necessary here to avoid an increase in vibration by resonance instead of a decrease. Wave effects in rubber 1 in. thick occur at 900 c/s which is very much less than the figure of 6000 c/s given on p. 119. Fig. 5.20 shows the double resonance encountered with resilient mountings on a resonant foundation. However, the higher frequency approaches that of the foundation, not that of the mass of the machine and the stiffness of the foundation, as the stiffness of the mountings is reduced towards zero. The last chapter gives some useful tips in regard to measuring instruments and techniques.

A. J. KING

Les dislocations et la croissance des cristaux. By W. DEKEYSER and S. AMELINCKX. (Masson et Cie, Editeurs, Libraires de l'Académie de Médecine, 120 Boulevard Saint-Germain, Paris, 6e.) Pp. viii + 184. Price 2000 *f*.

This book, written by two experts in the field, covers most aspects of crystal growth by the screw dislocation mechanism, with particular emphasis on the geometrical features of the phenomenon. It includes a non-mathematical description of the geometry of dislocations, an account of the theories of crystal growth and a comprehensive discussion of the phenomena observed. Polytypism, the interaction of growth spirals and the effect of movement of the dislocations are discussed in detail. A chapter is devoted to a useful review of the methods of observation, including interferometric techniques.

The text is clear and concise and many of the geometrical features are explained elegantly with the aid of diagrams. The authors are to be congratulated on giving an excellent overall account of this subject, and the printers for the excellence of the reproduction of many of the beautiful photographs.

P. B. HIRSCH

Spectrochemical abstracts. Vol. 4. 1946–1951. By E. H. S. VAN SOMEREN and F. LACHMAN. (London: Hilger and Watts Ltd., 1955.) Pp. 179. Price 30*s*.

Papers dealing with spectrochemical analysis—defined by the authors as "emission spectroscopy in its analytical applications"—appear in a wide range of specialist journals, not all of which would come within the scope of any one of the major abstracting organizations. A collection of spectrochemical abstracts, particularly when arranged and indexed to meet the special needs of the spectrochemist, is thus of considerable value to workers in the field.

The present volume is the fourth of a series which has covered the literature from 1933 onwards, the general arrangements being as in earlier volumes, namely, Part 1 contains an alphabetical author index with literature references whilst Part 2 gives the actual abstracts classified, according to subject. The main divisions of Part 2 are substances analysed (subdivided into six classes), apparatus, methods, source theory, reviews, wavelength tables, books. A very useful feature for the practising spectroscopist is the separate "index to elements observed as minor constituents of samples." It is features such as this which give the book its special place in the spectroscopist's library.

Compared with earlier volumes the size has increased appreciably, the price has risen approximately as the square of the number of abstracts included and the lapse between the period surveyed and the date of publication has increased to an alarming extent—now nearly four years compared with eighteen months for Vol. 3. This last feature calls for special attention in future volumes.

B. S. COOPER

An introduction to electronic analogue computers. By C. A. A. WASS (London: Pergamon Press Ltd., 1955.) Pp. vii + 237. Price 40*s*.

The author of this book comes from the home of Tridac, one of the world's largest electronic analogue computers, and he is fully competent to write on this subject. It is the first British textbook to deal exclusively with electronic analogue computers. The introduction differentiates between the roles played by analogue and digital computers and in the former class defines the terms differential analyser, simulator, and analogue computer.

The functional bricks required to build a computer are discussed, followed by details of the various methods using feedback by which the desired functions are derived. The most important unit, the d.c. amplifier, is dealt with at length and in detail including circuitry parameters. Examples are given of the arrangement of computer elements for solving specific problems. Other chapters deal with the use of computers and with descriptions of existing machines, including Tridac.

This is an excellent book which does not assume a high degree of knowledge in the electronic field. There is much to please anyone who wants to know what analogue computers really are and what they can do. It will also be of use to designers and users of these machines.

JOHN C. WEST

Foundations of quantum theory: a study in continuity and symmetry. By A. LANDÉ. (New Haven, Conn., U.S.A.: Yale University Press. London: Oxford University Press, 1955.) Pp. viii + 106. Price 32*s*.

The author, who had already made notable contributions to atomic spectroscopy in the early twenties before quantum mechanics was discovered, has given us in this book the fruit of his philosophic reflexions on the basic assumptions of quantum mechanics. The usual machinery of complex probability-amplitudes is nowadays familiar to every student of atomic physics—but why, asks Professor Landé, does Nature work in this curious way? Not everyone will agree with the answers he offers, and some may even doubt whether the question admits of an answer; but physicists interested in the philosophical aspects of science will certainly find it stimulating to be invited to think afresh about principles that are nowadays commonly taken for granted.

J. M. C. SCOTT

Notes and comments

Elections to The Institute of Physics

The following elections have been made by the Board of The Institute of Physics:

Fellows: A. Abou-El-Azm, G. Black, R. J. Clayton, R. F. Darling, A. E. Harper, J. C. Jones, G. E. Swindell, A. J. Woodall.

Associates: G. W. Alderton, H. L. Allsopp, L. W. Brown, K. M. Burrows, I. Butterworth, T. Cartledge, C. D. Clark, R. E. Copland, J. M. Dewey, R. G. Eades, A. S. Edmonson, G. A. Fagan, D. Fishman, P. E. Francois, E. E. N. Gouw, F. J. Grove, Hon Yung-Sen, Ho Peng Yoke, D. P. Howlett, J. O. Hughes, A. J. Hymans, G. M. Jeffrey, T. G. Jones, B. J. MacDonald, G. L. MacDonald, W. K. Mansfield, G. V. Marr, G. H. Millard, G. B. Mummery, S. E. Orchard, G. S. Rose, J. E. Samson, Panchanan Sen, Sunil Kumar Sen, D. Shaw, G. Slattery, W. R. Stamp, A. G. Stanley, G. R. Taylor, D. P. C. Thackeray, Achyut Parashuram Thatte, R. A. Ward, D. Wilkie, W. M. Williams, P. D. Wilmot, A. W. Wolfendale, B. H. Woodcock.

Forty-eight Graduates, twenty-eight Students and eleven Subscribers were also elected.

Publications of The Institute of Physics

A revised version of The Institute of Physics' list of publications is available. It includes brief details of the books published during the past few years in the Institute's Physics in industry series and Monographs for students series. Details are also given of the Institute's two monthly journals and the supplements already issued. In addition, it contains information on the charts, nets and index cards which are available from the Institute for the use of X-ray crystallographers.

Copies are available, without charge, from The Institute of Physics, 47 Belgrave Square, London, S.W.1.

Permanent display of British scientific instruments

On 9 February last there was opened at SIMA House, 20 Queen Anne Street, London, W.1, a display of selected items from the products of the member firms of the Scientific Instrument Manufacturers' Association of Great Britain Ltd. The object of the display is to provide a centre where overseas visitors can see a representative selection of instruments, and an extensive catalogue library is being assembled to aid enquirers. The centre will also serve as a common meeting ground for makers and users of instruments in this country. Since it is impossible to give space to all members at the same time, a rota system has been worked out which will give every member a chance to exhibit, and will also ensure that the character of the display will change frequently.

Publication of patents abridgements

The volumes containing abridgements of the patent specifications accepted during the war years are now on sale. Thus there is a complete range of volumes up to and including the 640,001–660,000 series which contains specifications accepted and published prior to November 1951. Abridgements of specifications accepted and published prior to August 1955 are also on sale in sheet form.

The abridgements in bound and sheet form can be obtained from the Sale Branch, Patent Office, 25 Southampton Buildings, Chancery Lane, London, W.C.2, at prices varying from £1 1*s.* 0*d.* to £1 10*s.* 0*d.* per group.

Conference on magnetism and magnetic materials

A conference on magnetism and magnetic materials will be held in Boston, U.S.A., on 16–18 October, 1956. It is sponsored by the American Institute of Electrical Engineers in co-operation with The American Physical Society, The American Institute of Mining and Metallurgical Engineers, and The Institute of Radio Engineers. Contributions are invited and authors should submit titles of proposed papers by 15 June and abstracts by 1 August, 1956. Further details may be obtained from T. O. Paine, Measurements Laboratory, General Electric Company, 40 Federal Street, West Lynn, Mass., U.S.A.

Journal of Scientific Instruments

Contents of the April issue

ORIGINAL CONTRIBUTIONS

Papers

A magnetic spectrometer. By D. J. Prowse and W. M. Gibson.
A water vapour recorder for equatorial use. By C. G. Webb and A. Rajaratnam.
An automatic scanner for nuclear emulsions. By S. J. Goldsack and H. B. van der Raay.
A versatile X-ray diffractometer for single-crystal and powder studies. By A. R. Lang.
Application of the electrostatic precipitator to the measurement of radioactive aerosols. By B. A. Bergstedt.
An improved helium liquifier and cryostat. By D. F. Brewer and D. O. Edwards.
A magnetic analyser for high energy particles. By A. Lovati and H. Tyrén.
An instrument for measuring respiratory rates and volumes. By W. Nisbet.
A logarithmic megohmmeter. By P. Hariharan and M. S. Bhalla.

Laboratory and workshop notes

Simple high-pressure closures and electrodes. By D. Gugan.
A simple gas valve. By J. Fuller.
A sensitive null-point manometer. By J. P. Berry.
Miniature diffraction cameras for micro-focus X-ray units. By J. B. Finean.

NOTES AND NEWS

Correspondence

Rotating electrode unit for measurements of the electric strength of insulating liquids. From A. Powell and K. H. Stark.
Modifications of photomultiplier characteristics by dynode voltage control. From D. S. Hobbs; E. M. Deeley.
A simple apparatus for recording the variation of Hall coefficient with temperature. From E. H. Putley.
New instruments, materials and tools
Manufacturers' publications
Notes and comments

THIS JOURNAL is produced monthly by The Institute of Physics, in London. It deals with all branches of applied physics (including theory and technique).
All rights reserved. Responsibility for the statements contained herein attaches only to the writers.
EDITORIAL MATTER. Communications concerning editorial matter should be addressed to the Editor, The Institute of Physics, 47 Belgrave Square, London, S.W.1. (*Telephone:* Sloane 9806.) Prospective authors are invited to prepare their scripts in accordance with the *Notes on the preparation of contributions*. (Price 2*s.* 6*d.* including postage.)
REPRODUCTION. The Institute of Physics is a signatory to The Royal Society's Fair Copying Declaration. Details may be obtained upon application from The Royal Society, London, W.1.
ADVERTISEMENTS. Communications concerning advertisements should be addressed to the agents, Messrs. Walter Judd Ltd., 47 Gresham Street, London, E.C.2. (*Telephone:* Monarch 7644.)
CLAIMS FOR MISSING JOURNALS. Claims from regular subscribers to this *Journal* for missing numbers will only be considered if received within 60 days of the date of mailing plus normal outward time of transit and time for lodging the claim. Losses attributable to failure to notify a change of address or to similar omissions will not be considered.
SUBSCRIPTION RATES. A new volume commences each January. The charge is £4 per volume ($11.50 U.S.A.), including index (post paid), payable in advance. Single parts, so far as available, may be purchased at 8*s.* each ($1.15 U.S.A.), post paid, cash with order. Orders should be sent to The Institute of Physics, 47 Belgrave Square, London, S.W.1, or to any bookseller.

SPECIAL ARTICLE

The physical meaning of indentation and scratch hardness*

By D. TABOR, Ph.D., A.R.C.S.,† Research Laboratory on the Physics and Chemistry of Surfaces, Department of Physical Chemistry, Cambridge

A study of the plastic deformation of metals by hard indenters shows that the indentation hardness is essentially a measure of the plastic yield stress of the metal. With pyramidal (and conical) indenters the hardness, because of geometric similarity, is independent of the size of the indentation. With spherical indenters this is not so, the hardness increasing with size of indentation. From the increase in hardness with load, a semi-quantitative estimate may be made of the work-hardening characteristics of the metal.

In the scratching and indentation of brittle solids such as minerals it is shown that the high hydrostatic pressures developed around the deformed region are often sufficient to inhibit brittle fracture. Under these conditions the deformation is primarily plastic. For this reason there is fairly good correlation between indentation and scratch hardness since both are essentially a measure of the plastic and not the brittle properties of the solid. From this approach it is possible to provide a physical basis for Mohs' scratch-hardness scale and to show that, excluding diamond, there is a reasonable "equality of intervals" between each number on the scale.

For the last fifty years or more engineers and metallurgists have been making hardness measurements of metals as a means of assessing their mechanical properties. Lapidaries and mineralogists have been carrying out scratch hardness tests for several hundred years, primarily as a means of identifying the gems and minerals with which they have to deal. In this article we shall discuss briefly the physical meaning of these two main classes of hardness measurement.

INDENTATION HARDNESS

The hardness of a metal is generally expressed in terms of its resistance to local deformation. Usually a hard indenter is pressed into the surface of the metal with a known load and the size of the resulting indentation is measured: a soft material giving a large indentation, a hard material a small one. Quantitatively the mean pressure between the indenter and the metal may be used as a measure of the hardness, typical values in kilogrammes per square millimetre being 4 for lead, 6 for tin, 50 for annealed copper, 95 for brass, 150 for mild steel, 900 for ball race steel, 1500 for tungsten carbide. The indentations made in these tests are discernible as permanent impressions in the metal, so that the indentation test must be primarily a measure of the plastic properties of the metal. It is true that some change in the shape and size of the indentation occurs when the indenter is removed[1] but the overriding effect is the plastic flow of the metal around the indenter. This implies that the mean pressure over the indenter is in some way connected with the plastic rather than the elastic properties of the metal. In what follows we shall show that this is indeed the case.

The deformation properties of metals under uniaxial tension or compression.

We consider here the simplest type of deformation process: the tension or compression of a cylindrical bar of metal along its axis. In the tensile experiment the extension may be defined as the fractional increase in length dl in relation to the initial length l_0; the ratio dl/l_0 is known as the linear strain ϵ. It may also be described in somewhat more basic terms as the natural logarithm of the ratio of the extended to the initial length: the quantity $\ln (l/l_0)$ is known as the logarithmic strain ϵ^* and for small strains is not very different from the linear strain. The chief difference is that linear strains are not strictly additive; for if a bar is extended by 20% and is then stretched by 20% of its extended length the final linear strain is not 40% but 44%. The logarithmic strains are additive: in the above example the first extension gives $\epsilon_1^* = \ln (l_1/l_0) = \ln (1{\cdot}2)$ and the second extension gives $\epsilon_2^* = \ln (l_2/l_1) = \ln (1{\cdot}2)$. The final logarithmic strain is $\epsilon^* = \ln (l_2/l_0) = \ln [(l_2/l_1)(l_1/l_0)] = \ln (l_2/l_1) + \ln (l_1/l_0) = \epsilon_1^* + \epsilon_2^*$. For small strains, however, the difference is not generally important. In carrying out the tensile experiment we shall express the stress as the tensile force at any instant divided by the cross-section of the specimen at that instant; this is the true stress Y as distinct from the engineering stress in which the force is divided by the initial cross-section of the specimen.

The results obtained when the true stress Y is plotted against the linear strain ϵ are shown in Fig. 1. Over the range OA the deformation is elastic and on removing the stress no detectable deformation remains. The slope of OA is the Young's modulus of the metal. If the specimen is stretched too far the stress-strain curve deviates from the elastic curve and on removing the stress some residual deformation remains; this is referred to as plastic, in contrast to elastic, deformation. In general the stress Y producing plastic deformation increases as the amount of strain ϵ is increased. This is associated with the general observation that as metals are worked or deformed they grow harder and stronger. The increase of Y with ϵ over a limited portion of the stress-strain curve can be represented by a relation of the form

$$Y = b\epsilon^x \qquad (1)$$

where b is a constant for the metal and x is a work-hardening index usually ranging from a value 0 for metals which do not work-harden to about 0·6 for annealed metals which are capable of undergoing very marked work-hardening. A

* Based on a lecture delivered to The Institute of Physics' Conference on Non-destructive Testing, Glasgow, June 1955.

† At present International Fellow (1955–6), Stanford Research Institute, California.

similar behaviour is observed if the metal specimen is compressed uniaxially between "frictionless" anvils. It must be emphasized that equation (1) is a very crude relation for it is clear that the plastic deformation curve does not start from the origin (Y is not zero for $\epsilon = 0$ in the plastic range) and Y does not increase indefinitely with increasing strain; there is an asymptotic trend in Y at high values of ϵ. However, for our purposes the simple relation is adequate.

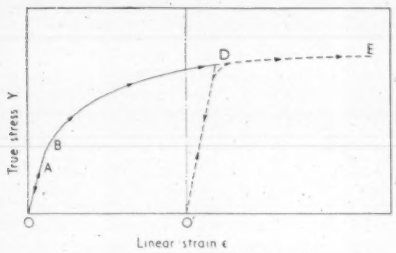

Fig. 1. Stress-strain curve for a metal under tension. Along OA the stress is proportional to the strain (elastic deformation). At B plastic deformation commences and the yield-stress increases as deformation proceeds. At D if the stress is removed the specimen contracts elastically along DO' and OO' is the residual plastic deformation. If O' is treated as the new origin and a stress is reapplied the stress-strain curve follows the path $O'DE$. The yield stress along DE shows little increase as plastic deformation continues

If an indentation experiment is carried out on a metal with a stress-strain curve similar to that shown in Fig. 1 the deformation associated with the plastic indentation process will increase Y by varying amounts around the indentation. Before we can understand how to cope with this it is clearly desirable to consider the indentation behaviour of a metal which is not work-hardened by the indentation process itself. We may obtain such a material by deforming the metal shown in Fig. 1 heavily up to, say, the point D and then removing the applied stress. The specimen recovers elastically to the point $0'$ where $00'$ is the amount of permanent or plastic deformation. If this work-hardened specimen is now subjected to a renewed tensile test with the point $0'$ as the new origin, the stress-strain curve follows the dotted curve $O'DE$, i.e. the yield stress Y along DE is almost constant. If an indentation is made in such a material the indentation process will have a negligible effect on Y. Consequently we may expect a relation between the indentation hardness and Y.

Indentation of materials of constant yield stress.

A material obtained in the above way is a good approximation to the ideal plastic material with which theoreticians deal in analysing plastic deformation. Although in an ideal plastic material the uniaxial stress to produce plastic yielding is a constant, Y, this does not mean that the stress between the indentation and the indenter (when a plastic impression is formed) is also Y. The value Y only applies to the case of simple tension or compression in one direction. The stresses around an indentation are not of this nature. It is true that they can be resolved into a series of pure tensile and pure compressive stresses, but these are by no means all along the same direction. They are inclined to one another in a very involved way. It is therefore necessary to know how an ideal plastic material will deform under combined stresses. One hint to the solution of this problem is provided by the observation that hydrostatic pressure itself plays no part in producing plastic flow. If, for example, a cylindrical specimen that would yield plastically under a uniaxial tensile (or compressive) stress Y is subjected to a hydrostatic pressure of amount Y or $2Y$ or $3Y$ no plastic flow occurs: a superposed uniaxial tensile (or compressive) stress Y must still be applied if plastic flow is to take place. This has led to the view that plastic flow is determined by a shear-stress criterion (Tresca, Mohr, Guest) or by a criterion of maximum shear-strain energy (Huber, von Mises). This approach makes it possible to deal with the behaviour of materials under combined stresses. It was first applied to the problem of indentation over thirty years ago by Prandtl[2] and independently by Hencky[3] a few years later. Their analysis is too involved to be given here[4] but we may summarize their conclusion descriptively by saying that nearly two-thirds of the mean pressure of contact is in the form of a hydrostatic pressure and plays no part in producing plastic flow: only one-third remains effective for this purpose. If P is the mean pressure between the indenter and the indentation, then $1/3P \simeq Y$ or

$$P \simeq 3Y \qquad (2)$$

Vickers hardness of materials of constant yield stress.

In metallurgical hardness measurements one of the most common types of indenters used in this country is the Vickers indenter. This is a square-based pyramid made of diamond in which the angle between the opposite faces is 136° (Fig. 2).

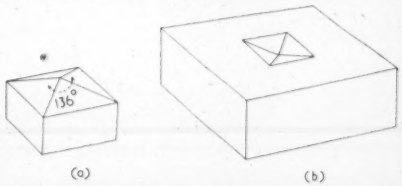

Fig. 2. Standard Vickers diamond pyramid indenter (*a*) and the indentation it produces (*b*)

Plasticity theory suggests that the mean yield-pressure will depend somewhat on the angle of the indenter, but the relation between P and Y will be close to that given in the above equation. This conclusion may be examined by work-hardening metals as far as convenient, until a portion of the stress-strain curve is reached where Y is substantially constant. Vickers indentations may then be made and the mean pressure P over the indentations calculated. This is given by

P = load/projected area of indentation

Table 1. *Relation between yield-stress Y and indentation pressure P (Vickers Indenter)*

Metal	Y (kg/mm²)	P (kg/mm²)	P/Y
tellurium-lead	2·1	6·7	3·2
aluminium	12·3	39·5	3·2
copper	27	88	3·3
mild steel	70	227	3·2

Typical results are given in Table 1[6]; it will be seen that for a wide range of materials $P = 3{\cdot}2Y$. Since the Vickers hardness number H_v is defined as the ratio of the load to the *pyramidal* area of indentation, H_v is less than P by a numerical factor depending on the shape of the pyramid. For the standard Vickers indenter this factor is 0·9272. Consequently

$$H_v = 0{\cdot}9272 \times 3{\cdot}2Y \simeq 3Y$$

Hence the Vickers hardness number of an ideal plastic material is roughly three times its yield-stress. This astonishingly simple relation, which follows directly from the work of Prandtl and Hencky, appears to have been overlooked in hardness literature for almost thirty years. Although many other factors are involved, it remains the basic relation between the indentation hardness and the bulk properties of a metal. Further, since an ideal plastic material under tensile conditions passes its maximum nominal tensile stress T_u as soon as plastic yielding begins, Y is essentially the same as T_u. Hence to a close approximation $T_u = 0{\cdot}33\,H_v$. In engineering circles the ultimate tensile stress is usually expressed in tons per square inch, whilst the Vickers hardness number is expressed in kilogrammes per square millimetre. This reduces the conversion factor by 1·57; consequently

$$T_u\,(\text{tons/in}^2) \simeq 0{\cdot}21\,H_v\,(\text{kg/mm}^2) \qquad (3)$$

This relation is widely used as a means of determining ultimate tensile strengths from hardness measurements for fully work-hardened materials.

Principle of geometric similarity.

The principle of geometric similarity is of considerable value in understanding a number of aspects of hardness measurements. Here we shall consider three applications: microhardness, the Vickers hardness of materials which work-harden and the Rockwell hardness test. The principle states that if two indentations are made of the same geometric shape, then, whatever their size the strain distribution and the stress distribution around the indentations will be geometrically similar. This is valid whether the material is fully work-hardened or undergoes work-hardening as a result of the indentation process, but it is only valid if the grain-size is so small that the material can be considered as being uniform and homogeneous. In its simplest terms the principle implies that a large indentation is essentially a magnified picture of a small indentation, the strains and hence the stresses being the same at any geometrically similar region. Consequently the indentation yield pressure P, which is the mean pressure acting on the indenter, will be the same whatever the size of the indentation. It follows that for a pyramidal (or conical) indenter the hardness is independent of the size of the indentation. This is well borne out in Vickers hardness measurements where the hardness is generally found to be independent of the load.

Microhardness measurements.

This principle has a direct bearing on microhardness measurements involving the use of a pyramidal indenter. It is often found that at small loads the hardness is greater than at large loads. This is not due to a breakdown of the law of geometric similarity. It arises from the fact that the surface layers of the specimen are harder than the substrate, and that for sufficiently small loads the hardness values approach the true hardness of the surface layer, while for large loads and deep indentations the hardness approaches the bulk hardness of the substrate.

At light loads it is sometimes found that the hardness appears to decrease. In some cases this may be due to the presence of a thin surface layer of softer material but with metals this state of affairs is very unusual. Recently Wilson[5] has shown that even with homogeneous materials an apparent decrease in hardness may be observed at very light loads as a result of vibration; these vibrations make the indentation larger than it would be under perfectly static conditions and so result in low hardness values. In Wilson's experiments, which were carried out on an apparatus where the loading mechanism is mounted on the stage of a standard optical microscope, it was found that even if all extraneous vibrations were eliminated, mechanical vibrations produced by the light source itself were sufficient to produce misleading results of this type. If the light source is maintained while the indentation is made, indentations below a load of 10 g are greater in size than they should be. If the light source is switched off during the actual loading operation and switched on only when the indentation is being measured uniform results are obtained. This is shown in Fig. 3 for measurements carried

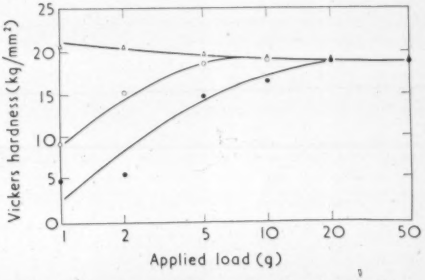

Fig. 3. Variation of Vickers hardness with load of an electrolytically polished annealed aluminium specimen.[5] When all vibration is eliminated the hardness is almost independent of the load. When mechanical vibration, due to the light source, is present the indentations at loads below 10 g are larger than they should be and the hardness appears to drop rapidly

△ no illumination.
○ carbon arc.
• mercury lamp.

out on the surface of annealed aluminium which has been electrolytically polished. When appropriate precautions are taken the hardness is practically constant over the whole load range: when vibrations, due to the light source, are present the hardness appears to fall markedly below a load of about 10 g. These observations emphasize the value of applying physical principles when "mysterious" hardness properties are observed.

Vickers hardness of materials which work-hardens.

With a material which can work-harden, the indentation process itself will produce work-hardening, that is, it will produce an increase in the yield stress Y. With the Vickers pyramidal indenter the plastic strains produced will vary from point to point so that Y will also vary from point to

point. A detailed analytical solution of the problem is not possible but we may provide a very simple analysis in the following way.[6] We assume that there is a representative value of the yield-stress Y_r which is related to the observed Vickers hardness by the relation $H_v = cY_r$, where c again has the value of about 3. By an empirical method it is found that the indentation produces an average or representative strain ϵ_r (corresponding to Y_r) equivalent to an 8% tensile strain. Hence if on the known tensile stress-strain curve of the metal we determine the yield-stress for an additional 8% strain, the Vickers hardness value will be three times this value. Because of the principle of geometric similarity, this additional strain will be the same whatever the size of the indentation. It also turns out that the additional strain is roughly constant whatever the initial state of work-hardening of the specimen. This is shown in Table 2 for annealed copper and steel specimens which were work-hardened by various strains ϵ_0 and had their Vickers hardness measured. The yield-stress at a strain of $(\epsilon_0 + 8)\%$ was determined from their stress-strain curves and compared with the observed Vickers hardness values. The agreement between the last two columns is fairly good. It is, of course, clear from what has been said in the introduction that the addition of linear strains is not strictly valid. However, the error involved is not serious and the satisfactory nature of the agreement indicates that the basic assumptions are reasonably valid.

Table 2. *Relation between yield-stress Y and Vickers hardness number, for metals which are work-hardened by the indentation process*

Metal	*Initial deformation* $\epsilon_0\%$	Y (kg/mm²) *at strain of* $(\epsilon_0 + 8)\%$	cY	*Observed Vickers hardness number*
			$c = 2{\cdot}9$	
mild steel	0	55	159	156
	6	62	176	177
	10	66	190	187
	13	67	194	193
	25	73	211	209
			$c = 3{\cdot}0$	
annealed copper	0	15	45	39
	6	20	60	58
	12·5	23·3	70	69
	17·5	25	75	76
	25	26·6	80	81

These results show that hardness values obtained with the Vickers indenter provide a measure of the plastic yield-stress of the metal as augmented by the indentation process itself.

Conical indenters in the Rockwell test.

In industrial practice, particularly in America, hardness measurements are often made with a Rockwell tester which measures, on a dial gauge, the depth of penetration under a standard load. In many of these tests a conical indenter with a minute hemispherical tip is used. If we ignore the complications introduced by the tip we may consider the indenter and the indentations to be conical in shape and geometrically similar whatever their size. The mean pressure P is therefore independent of the load. Hence if d is the diameter of the indentation formed, and a constant load is used in testing various metals, $P = k_1/d^2$. The depth of penetration t is $(d/2)\cot\theta$ where θ is the semi-angle of the cone. Consequently $t = k_2 P^{-\frac{1}{2}}$. This means that the depth is smaller for larger values of P, that is, for harder materials. In order to provide a scale in which large scale readings are associated with harder materials the depth-measuring dial-gauge is run "backwards," that is the depth of penetration is subtracted from a fixed zero value, say C. The observed Rockwell depth R_c is then

$$R_c = C - t = C - k_2 P^{-\frac{1}{2}}$$

The apical angle of the cone is not widely different from that of the Vickers pyramidal indenter and the indentation pressure is roughly the same in both cases. We may therefore put P equal to the Vickers hardness H_v and so obtain a relation between the Rockwell R_c scale and the Vickers hardness values.

$$R_c = C - k_2(H_v)^{-\frac{1}{2}} \qquad (4)$$

A typical calibration curve is given in Fig. 4. In view of the simplifying assumptions made the agreement is surprisingly good.

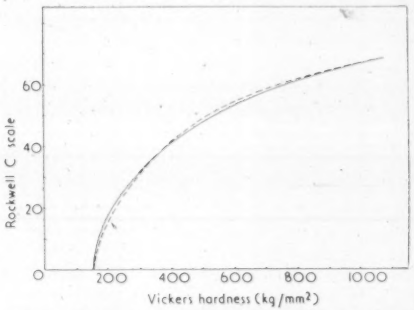

Fig. 4. Comparison of Rockwell C hardness values and Vickers hardness

—— experimental results, – – – curve calculated according to the theoretical relation $R_c = 110\,[1 - 12{\cdot}4\,(H_v)^{-\frac{1}{2}}]$.

Brinell hardness measurements.

An older type of hardness measurement due to Brinell involves the use of a hard spherical indenter. This is usually a standard steel ball such as is used in ball bearings and has the advantage of being both cheap and accurate in dimensions. When a spherical indenter is pressed into the surface of a fully work-hardened metal the indentation pressure is again roughly three times the yield stress of the metal so that Brinell hardness numbers and Vickers hardness numbers have very nearly the same value.

When, however, indentations are made in a metal which work-hardens there is a marked difference in behaviour between the spherical and the pyramidal indenter. This is because indentations of various sizes formed with a given spherical indenter are not geometrically similar. In contrast to the pyramidal or conical indentations, a large indentation produced by a given sphere involves greater plastic strains than a small indentation, a larger increase in the effective yield stress and hence an appreciable increase in the observed hardness. Thus the hardness is larger the bigger the indentation. Although this means that the Brinell hardness is *not* a single valued quantity its variation with load provides additional information about the properties of the metal.

Let us assume that the mean pressure P over the indentation is related to some representative value of the yield stress Y_r by a relation of the type $P = cY_r$ where c again has a value of about 3. If d is the chordal diameter of the indentation and D the diameter of the indenter the shape of the indentation is determined by the dimensionless parameters d/D. Thus the strains must be determined by this parameter. These will vary from point to point but we may again assume that there exists a representative strain ϵ_r corresponding to Y_r. A detailed study[6] shows that to a first approximation ϵ_r is a linear function of d/D. If then we assume that the stress-strain curve of the metal is given by equation (1) the representative yield stress Y_r is given by

$$Y_r = b(kd/D)^x$$

Hence the mean pressure P which we have put equal to cY_r can be written

$$P = P_0(d/D)^x \tag{5}$$

where P_0 is a suitable constant. This means that the variation of the mean pressure with size of indentation provides a means of determining the work hardening index x. Amongst practising metallurgists this is usually achieved by means of an experimental analysis originally proposed by Meyer. A spherical indenter (of fixed diameter) is pressed into the surface with a load W and the diameter d of the indentation measured. The experiment is repeated with various loads and log W is plotted against log d. The result is approximately a straight line implying that W is proportional to d^n where n is a constant. This constant is called the Meyer index and is found to have a value which ranges from 2 for fully work-hardened materials to about 2·6 for fully annealed materials. Since $P = W4/\pi d^2$ it follows from equation (5) that

$$W = Ad^{2+x}/D^x \tag{6}$$

where A is a suitable constant. Thus according to this analysis the Meyer index n is to be identified with the quantity $2 + x$. This conclusion is supported by results obtained with a wide variety of metals in different states of work-hardening (see Table 3, data from O'Neill[7]). It should, of course, be borne in mind that this analysis assumes the validity of the power-law relation between stress and strain. As was pointed out earlier this is only a crude relation and has only a limited range of applicability. Nevertheless the agreement obtained is sufficiently good to show that the basic assumptions are reasonably sound.

Table 3. *Relation between Meyer index n and work-hardening index x, showing comparison between $n - 2$ and x*

Metal	*Typical values of Meyer index, n*	$n - 2$	*Work-hardening index, x*
mild steel A	2·25	0·25	0·259
yellow brass	2·44	0·44	0·404
yellow brass, cold drawn	2·10	0·10	0·194
copper L	2·45	0·45	0·414
steel 1A	2·25	0·25	0·24
steel 6A	2·28	0·28	0·18
nickel, annealed	2·50	0·50	0·43
nickel, rolled	2·14	0·14	0·07
aluminium, annealed	2·20	0·20	0·15

It follows that hardness measurements with spherical indenters, and the Meyer analysis to which they can be subjected, can provide a fairly direct measure of the ability of a metal to undergo work-hardening. This is an important property of a metal for it is closely connected with its ductility.

SCRATCH HARDNESS OF MINERALS

We now deal with the type of scratch hardness test that was first put on a quantitative basis by the famous Austrian mineralogist Mohs[8] over 130 years ago. Mohs proposed a scale of ten minerals in increasing order of scratch hardness such that each mineral will scratch the one on the scale below it, but will not scratch the one above it. Mohs was fully aware of the difficulty of constructing such a scale and went to considerable trouble to select his minerals to provide equal intervals between each pair. He finally proposed as his ten basic minerals: 1 talc, 2 gypsum, 3 calcite, 4 fluorite, 5 apatite, 6 orthoclase, 7 quartz, 8 topaz, 9 corundum, 10 diamond.

He realized that the gap between corundum and diamond was larger than it should have been but seemed satisfied with the remainder of the scale. However Mohs nowhere explains his criterion of equality of intervals and at first sight it would seem that such a scale might be so arbitrary as to have no basic physical significance. However, as we shall see in what follows, there is a sound physical basis on which equal intervals can be constructed and that the Mohs scale follows it surprisingly well.

Deformation properties of minerals.

When minerals are deformed, as in indentation or scratching, it might seem that the main factors determining their behaviour are their brittle properties. Recent experiments from two different fields suggest, however, that this in general is not so. Thus Bridgman,[9] using his high-pressure equipment has shown that under sufficiently high hydrostatic pressures brittle materials may be prevented from fracturing, so that any deformation which they undergo under these conditions is essentially plastic. This may be demonstrated in a very simple way in the laboratory with a block of rock-salt.[10] If a cube of rock-salt is subjected to tension in air it fractures after undergoing a very small extension. If it is compressed it shatters after very little compression. If, however, a thin slab of rock-salt is placed between rigid plattens and compressed, a very different behaviour results. The slab of rock-salt can be readily compressed to one-half its thickness and will emerge as a complete piece apart from some crumbling at the edges. The reason becomes clear if the plattens are made of glass so that the rock-salt can be studied during the compression. It is then observed that at the initial stages some cracking occurs but that these are healed-up as compression continues. The finite friction between the rock-salt and the platten produces a very large hydrostatic pressure within the specimen and this is sufficient to inhibit brittle fracture over most of the crystal. The deformation is primarily plastic and using a reasonable value for the friction between crystal and platten the true plastic stress-strain curve of rock-salt may be deduced.

Secondly, if a Vickers indenter is pressed into the surface of a rock-salt crystal under moderate loads, a very well defined plastic indentation is formed with very little cracking around the edges. As we saw earlier the stresses around an indenter are equivalent to a hydrostatic pressure on which is superposed a shear-stress. With rock-salt the local hydrostatic pressure prevents brittle fracture and the indentation is

primarily plastic. Further the local yield-pressure turns out to be roughly three times the yield stress as determined in the compression experiments.

A very large number of materials which are normally considered brittle give satisfactory indentations even though some cracking occurs. A very simple experiment may, for example, be carried out with glass,[11] viewing the indentation process through the glass as it occurs. For loads which are not large enough to cause gross cracking it is found that a clearly defined plastic indentation is formed as the load is applied but that when the indenter is removed cracks spread out from the corners of the indentation. If the indenter is replaced and the load reapplied the cracks close up. It is clear that, in this case at least, the indentation process is a plastic one and that the cracking plays only a subsidiary part. It would seem that in many cases, when a well defined indentation is formed, the mean pressure or indentation hardness provides a measure of the plastic rather than the brittle properties of the material.

These conclusions raise an interesting issue—the size effect. According to our earlier discussion we should expect, on grounds of geometric similarity, that if a small plastic indentation can be formed in a brittle material, it should also be possible to form a large plastic indentation. With rock-salt this is found to be so, if the specimen is large enough to accommodate the elastic stresses developed in the material surrounding the indentation. For example, with a single crystal of rock-salt approximately 2 cm cube it is possible to form a Vickers indentation 4 or 5 mm in diameter without shattering the specimen. With many other brittle materials, including glass, this is not possible. With glass this may be because the surface layers are in a different condition from the bulk substrate. With other minerals it may be that there are gross inhomogeneities in larger specimens. These explanations are tentative and further work on this is desirable.

The friction and scratching of minerals.

A detailed study of the friction of brittle solids shows that here again although some fragmentation may occur, the deformation is dominated by the plastic properties of the material. For example with rock-salt a well-defined grooved friction track is formed in the surface of the crystal. Micro-hardness measurements within the track show that work-hardening, corresponding to a strain of over 100% has occurred. If the main process were one of brittle fracture there would be negligible work-hardening of the material. The fact that it occurs to such an extent emphasizes the plastic nature of the sliding process. The reason is essentially the same as that discussed above. The conditions around any individual contact region are similar to those around a static indenter and the high hydrostatic pressures inhibit brittle fracture.

The process of scratching appears to be very similar except that in addition to the frictional process there is superposed a cutting action. Here again the local pressures enable the material to flow plastically and even with brittle materials there is often evidence of a fine chip or shaving. This may be observed with glass at such slow speeds of sliding that frictional heating can be considered unimportant.

It follows from this discussion that both the scratching process and the indentation process are determined primarily by the plastic properties of the material. We may therefore expect to find some correlation between the Mohs hardness and the indentation hardness of minerals. This correlation does in fact exist as is shown in Fig. 5, which is based on data published by Taylor,[12] Krushchov,[13] Winchell[14] and Knoop and others.[15] Some of the indentation measurements in this figure were made with the standard Vickers indenter; others with the Knoop indenter.[15] This indenter produces an elongated pyramidal indentation (see Fig. 6) and with metals gives roughly the same hardness values as the Vickers

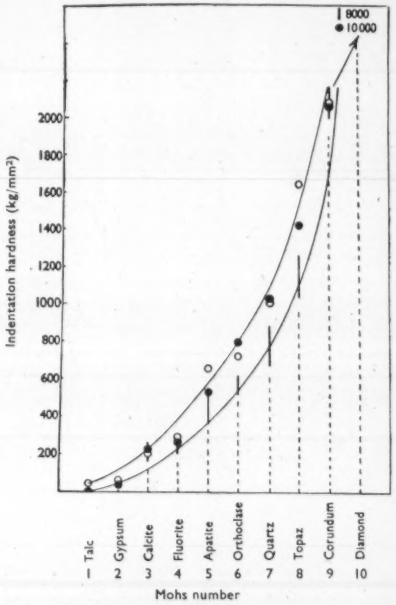

(Reproduced from *Endeavour*)

Fig. 5. Relation between indentation hardness values and Mohs hardness numbers

Vickers indenter: ○ results from Taylor[12]; ● results from Khrushchov.[13]

Knoop indenter: | results from Winchell[14] and Knoop and others.[15]

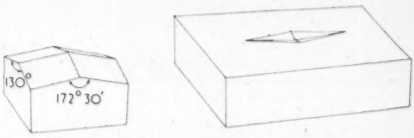

Fig. 6. Knoop indenter (*a*) and the type of indentation produced (*b*). The indentation is in the form of an elongated pyramidal impression its length being seven times its width. The Knoop indenter often gives more satisfactory impressions in brittle materials than the Vickers indenter

indenter. It is seen that both types of indenters also give roughly the same hardness values on minerals. From Fig. 5 the general trend is clearly revealed. The indentation hardness rises monotonically with increasing steps for each increment on the Mohs scale.

The scratch hardness of metals.

If we assume that the scratch hardness of brittle materials is determined primarily by their plastic properties we may greatly simplify the study of scratch hardness by using metals instead of minerals and other brittle solids. A simple experiment along the following lines[11] at once reveals the basic characteristics of a scratch-hardness scale. By suitable heat-treatment, a strip of metal is rendered soft at one end and hard at the other, with a fairly uniform increase in indentation hardness along its length. Another metal specimen of uniform intermediate hardness is prepared with a sharp point at one end, and the point is dragged over the strip from the soft to the hard end. It is then found that, over the soft portion of the strip, the friction is high and the motion intermittent, and a fine chip or shaving is produced. The behaviour remains much the same as the point approaches the harder end, until at a critical hardness of the surface the friction suddenly drops to a low value and the surface damage becomes negligible. Scratching has ceased.

Applying this experimental procedure as a general criterion of scratching, it is found that a point of indentation hardness H_p will scratch a surface of indentation hardness H_s only if $H_p \geqslant 1{\cdot}2\ H_s$. The reason for this is not clear, for it does not appear to depend very critically on the shape of the point. Assuming, however, that scratching just occurs when $H_p = 1{\cdot}2\ H_s$, we may construct a hardness scale in which every unit is $1{\cdot}2$ times as hard as the preceding one. The scratch-hardness number M is then related to the indentation hardness H by a relation of the form

$$H = k(1{\cdot}2)^M$$

Taking logarithms of both sides we have

$$\log H = M \log 1{\cdot}2 + \text{constant}. \qquad (7)$$

Thus a plot of $\log H$ against M should give a straight line of slope $1{\cdot}2$. In practice we may wish to avoid the change of an overlapping of the units by increasing the ratio to something greater than $1{\cdot}2$. Provided this new ratio is kept constant the general characteristic will still be a linear relation between $\log H$ and M.

Relation between Mohs hardness and indentation hardness of minerals.

The results obtained by Winchell and by Taylor, shown in Fig. 5, have been replotted in Fig. 7 as $\log H$ against M. It is seen that, if diamond be excluded, the relation $\log H = kM$ is surprisingly well obeyed, the value of k being roughly $\log 1{\cdot}6$ instead of $\log 1{\cdot}2$. This suggests that each interval on the Mohs scratch hardness scale could be subdivided into 2 or 3 finer steps: but a finer subdivision would not be possible since it would involve steps in which the hardness difference ($H_p < 1{\cdot}2\ H_s$) would not be sufficient to produce well defined scratching.

The value of k on the Mohs hardness scale corresponds to a ratio of indentation hardness between each Mohs unit of about $1{\cdot}6$. Thus the Mohs hardness scale gives scratch hardness values which correspond to fairly well-defined indentation hardness values, each increment on the Mohs scale corresponding roughly to a 60% increase in indentation hardness.

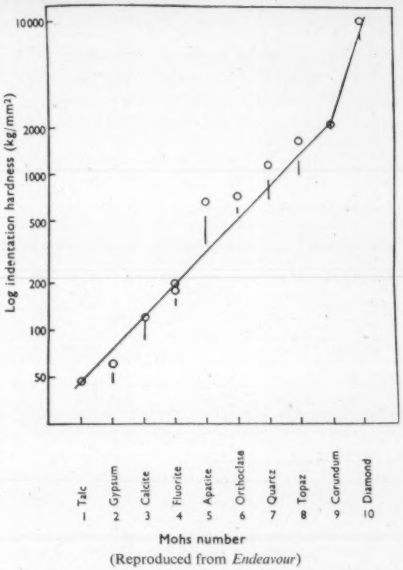

(Reproduced from *Endeavour*)

Fig. 7. Relation between Mohs hardness number M and the logarithm of the indentation hardness number H. ○ results of Taylor[12]; | results from Winchell[14] and Knoop and others.[15] Excluding diamond, it is seen that M is roughly proportional to $\log H$. Each Mohs interval corresponds to an increase in indentation hardness by a factor of about $1{\cdot}6$

CONCLUSION

The purpose of this survey is to show that there is, basically, nothing mysterious about hardness measurements and that they may be given a simple physical explanation. Several sweeping assumptions have been made and a number of over-simplifications introduced. Nevertheless the broad conclusion seems to be well substantiated: indentation-hardness and scratch-hardness measurements of metals and of minerals are essentially a measure of the plastic yield properties of the material under examination.

REFERENCES

(1) BELK, T. A. *Sheet Metal Industries*, **31**, p. 757 (1954).
(2) PRANDTL, L. *Nachr. Ges. Wiss. Göttingen*, p. 74 (1920).
(3) HENCKY, H. *Z. Angew. Math. Mech.*, **3**, p. 250 (1923).
(4) HILL, R. *The Mathematical Theory of Plasticity* (Oxford: Clarendon Press, 1950).
(5) WILSON, R. *Ph.D. Dissertation*, University of Cambridge (1952).
(6) TABOR, D. *The Hardness of Metals* (Oxford: Clarendon Press, 1951).

(7) O'NEILL, H. *The Hardness of Metals and its Measurement* (London: Chapman and Hall Ltd., 1934).

(8) MOHS, F. *Grundriss der Mineralogie* (1824). English translation by W. Haidinger, *Treatise on Mineralogy* (Edinburgh: Constable and Co., Ltd., 1825).

(9) BRIDGMAN, P. W. *Studies in Large Plastic Flow and Fracture* (London: McGraw-Hill Publishing Co., Ltd., 1952).

(10) KING, R. F., and TABOR, D. *Proc. Roy. Soc. A*, **223**, p. 225 (1954).

(11) TABOR, D. *Proc. Phys. Soc.* [*London*] *B*, **67**, p. 249 (1954).

(12) TAYLOR, E. W. *Miner. Mag.*, **28**, p. 718 (1949).

(13) KHRUSHCHOV, M. M. *Zavod. Labor.*, **15**, p. 243 (1949).

(14) WINCHELL, H. *Amer. Min.*, **30**, p. 583 (1945).

(15) KNOOP, F., PETERS, C. G., and EMERSON, W. B. *J. Res. Nat. Bur. Stand.*, **23**, p. 39 (1939).

ORIGINAL CONTRIBUTIONS

A re-determination of the equal-loudness relations for pure tones

By D. W. ROBINSON, B.Sc., A.C.G.I., A.M.I.E.E., and R. S. DADSON, M.A., National Physical Laboratory, Teddington, Middlesex

[*Paper received* 17 *January*, 1956]

The paper describes a new determination of the equal-loudness relations for pure tones in free-field conditions which has been carried out at the National Physical Laboratory as a result of requests from organizations interested in various aspects of the acoustics of hearing. The equal-loudness contours are of considerable importance in this field, being fundamental to a proper understanding of aural judgments of the loudness of sounds of all kinds. They are also concerned in numerous practical applications in the study of noise.

The first set of contours for free-field conditions was given by Fletcher and Munson in 1933, and a second determination was carried out by Churcher and King in 1937, but these two investigations showed considerable discrepancies over parts of the auditory diagram. The present work has been carried out on a more extensive scale, using a large team of otologically normal persons, and new techniques have been introduced enabling reliable measurements to be made over a wider range of intensity than has hitherto been possible.

The new results cover a range of frequency of from 25 to 15 000 c/s and of sound pressure level up to about 130 dB relative to 0·000 2 dyn/cm^2. The data show a greater degree of regularity than the former results, and allow the equivalent loudness of a pure tone of any frequency to be expressed by formulae quadratic in the sound pressure level, the coefficients varying smoothly with frequency. The results include a new determination of the normal threshold of hearing in free field, which is highly consistent with the equal-loudness contours. At frequencies above 1000 c/s account needs to be taken of variations due to the age of the observers, which become of particular importance at the upper end of the frequency range.

The new results have indicated the causes of some of the discordant features in the earlier determinations and it is hoped that the work will facilitate agreement on a standard set of equal-loudness contours. On account of its relevance to noise measurement, some extension to equal-loudness relations for bands of noise is being undertaken.

In the study of many aspects of subjective acoustics, and especially in the study of noise, the concept of the "loudness" of a sound is of fundamental importance. It is, of course, clear that loudness is not the only subjective attribute of a complex sound which may be of concern, though it is frequently the primary factor. Experience has shown that equal-loudness judgments are considerably less subject to extraneous psychological factors than are the less tangible qualities such as, for example, "annoyance." Moreover there is a fairly direct correspondence between loudness and the physical properties of the stimulus, which provides a firm basis for a consistent scheme of measurement.

Sounds may be analysed in various ways, but for most purposes analysis into a frequency spectrum, either of individual components or a distribution in terms of frequency bands, is the most convenient. It thus comes about that the loudness relations for pure tones of different frequencies, and as an extension of this the corresponding relations for distributed sound in particular frequency bands, are not only of great interest in themselves but are of basic importance in many applications. Such diverse problems as the study of the behaviour of the ear to complex sounds, and the procedure by which it arrives at a characteristic loudness sensation, the selection of frequency weighting networks for objective noise meters, and the development of methods for computing the loudness levels of complex sounds from objectively measured spectrum analyses, all rest at some stage or other on a knowledge of the equal-loudness relations for pure tones or other simple sounds. The relations are also involved in many aspects of the communication and reproduction of speech and other sounds.

The earliest measurements of the equal-loudness relations for pure tones were those of Kingsbury,[1] but as these were restricted to telephone listening conditions they will not be considered further here. The present paper describes a new determination of the equal-loudness relations for pure tones which has recently been carried out at the National Physical Laboratory. The investigation relates to free-field conditions of listening, under which conditions there have been two previous determinations, namely that of Fletcher and Munson

in 1933[2] and Churcher and King in 1937.[3] It has long been apparent that it would be most valuable to have a single set of equal-loudness contours acceptable to all workers in the field. The two previous determinations, however, showed considerable discrepancies over parts of the auditory diagram of such a nature and magnitude that it would have been difficult to derive from them a standard set of contours. It was largely as a result of discussions on this situation at the Committee on Noise Measurement of the British Standards Institution that it was decided that a new investigation should be carried out at the National Physical Laboratory. This had the principal aims of resolving the discrepancies in the previous work and of providing a new and more comprehensive set of data, as a contribution to future standardization. The number of subjects tested is considerably greater than hitherto, and several new techniques have been introduced in order to cover the widest possible range of intensity and frequency.

The equal-loudness relations must for completeness be associated with a threshold curve appropriate to the same conditions of listening, and this forms a natural "zero" for the whole set of curves. The investigation has therefore included a re-determination of the threshold of hearing in free field which shows a high degree of consistency with the equal-loudness relations at supraliminal levels.

Some extensions of this work, to include equal-loudness relations for sound distributed in particular frequency bands, is being undertaken and will be published separately in due course. The main object of this work is to clarify and further develop methods of computing the loudness levels of complex sounds from their spectrum analyses, which seems to be a particularly promising method for use in noise measurement problems.

DESCRIPTION OF EXPERIMENTAL PROCEDURE

(*a*) *General.* In view of the main object of this investigation, namely, to provide data which might assist in arriving at standardization of the equal-loudness contours, it was decided to maintain continuity with the practice in earlier determinations and with the definition of equivalent loudness[4] by carrying out the measurements under the same reference conditions. The sounds were presented to the listeners in the form of free progressive plane waves of sinusoidal waveform, with the observers listening binaurally and directly facing the oncoming wave. The advantages of these somewhat artificial conditions are the simplicity and freedom from ambiguity with which they can be specified. On the other hand, the accurate realization of the reference conditions over the wide frequency and intensity range of normal hearing involves some instrumental difficulties and limitations. The measurements have been carried beyond the range covered by the previous investigations[2,3] by the use of special reproducing arrangements. Except for the highest frequencies, the tests range from threshold to sound pressure levels of about 130 dB, and in frequency from 25 to 15 000 c/s. Altogether the investigation was in progress for nearly four years.

(*b*) *Selection of observers.* A random sample of observers from the entire population would include persons of various degrees of otological abnormality in addition to the great majority having normal hearing. The study and classification of abnormal hearing is, however, the province of the otologist and would form a separate investigation. The present experiments were deliberately restricted to persons of normal, in the sense of unimpaired, hearing. To this end the prospective subjects were submitted to an otological examination to ensure that no one was included having symptoms or signs of ear disease, or wax in the external auditory canals. Only subjects judged as normal at this examination were accepted for the tests. This basis of selection conforms to the usage adopted in a recent British Standard[5] for the threshold of hearing by earphone listening. The observers were selected from the available personnel of the Laboratory to be representative of both sexes and of a wide distribution of adult ages. So far as was known, the observers had not been subjected to prolonged periods of excessive noise such as might have caused permanent loss of hearing.

Experience at the National Physical Laboratory in various kinds of loudness estimation has indicated that stable results are generally obtainable with a homogeneous group of about thirty observers. To obtain truly representative results, however, a larger test group is necessary, particularly in those tests where the age is an important factor. On these grounds it was considered desirable to employ a substantially larger number of subjects than those who took part in the earlier determinations.

The present results are based primarily on the judgments of a team of ninety persons, forty-five of each sex, with ages ranging from sixteen to sixty-three years. This group participated in about thirty tests. In addition, a second team, consisting of seventeen men and thirteen women of average age about thirty years and all distinct from the members of the larger group, took part in over a hundred tests. Their results were barely distinguishable from those of larger group.

(*c*) *Description of apparatus.* The extensive frequency and intensity range of normal hearing necessitated the use of several distinct experimental arrangements. Except for the lowest frequencies the subjects were seated on the axis of and directly facing various sound sources in a lagged room, a headrest or sighting wires being provided to fix the head position. Measurements of the ambient noise level in the test room showed that it was lower than the normal threshold of hearing.

A large part of the investigation was carried out with conventional cone-type loudspeakers. In order to reach high intensity levels these arrangements were supplemented by the use of a powerful reflex horn loudspeaker.

As the investigation was intended to relate to strictly pure tones, various devices were employed to reduce the harmonic distortion and circuit noise. The harmonic distortion of the tones used in tests at moderate levels was generally of the order −50 dB relative to the fundamental. In order to allow for extreme conditions, experiments were made to determine the degree of harmonic distortion which was acceptable without influencing the equal-loudness judgments. These are described in Appendix 1. The results of these tests were taken into account in setting an upper limit to the sound levels at which the different loudspeakers were operated.

For the higher frequencies, a plane array of twenty-eight 2½ in. cone speakers was designed, and this was used in conjunction with the reflex horn, the latter providing the 1000 c/s tone. The twenty-eight loudspeakers were electrically equalized in sensitivity and phase and so connected that a better approximation to a plane wave front was realized than could have been obtained from conventional sources of comparable power. For some work at 15 000 c/s at high intensities a resonant barium titanate transducer in the form of a cylinder of diameter 4·7 cm was employed.

At the lowest frequencies it would be very difficult to obtain the high intensities required with direct radiators in a free-

space room. Since one of the objects of the investigation was to extend the range of the equal-loudness contours in the low-frequency region while maintaining progressive plane-wave conditions the difficulty was met by the use of a duct. This was of the same general form as that described by Dadson and Butcher[6] which is in use at the National Physical Laboratory for low-frequency microphone calibration. The duct was of a hard-walled construction with a square cross-section 60 × 60 cm, and overall length 6·8 m of which 5·2 m were occupied by an absorbent termination consisting of a double fibre glass wedge. The driving unit employed was an 18 in. cone-type loudspeaker with a modified coil assembly. The subject's head and shoulders were accommodated in the free section of the duct, with arrangements for easy access. Reflexion from the absorbent wedge and the obstruction to the sound wave caused by the body of the subject were found to be negligible for frequencies from 25 to 200 c/s, and sound pressure levels up to 130 dB could be obtained without appreciable harmonic distortion. The duct was not suitable for the transmission of plane waves at 1000 c/s; accordingly intermediate reference tones of 200 c/s or 50 c/s were employed. Some of the apparatus used is shown in the photographs, Figs. 1, 2 and 3.

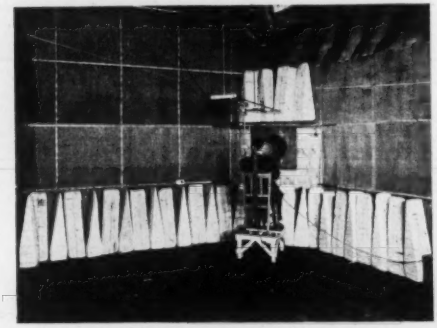

(*a*)

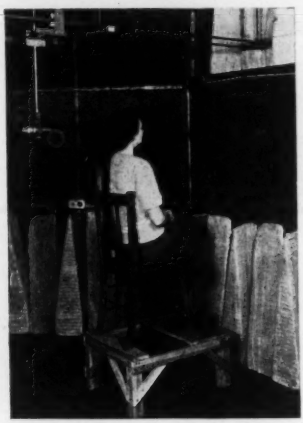

(*b*)

Fig. 1. - Views of anechoic room showing conventional cone loudspeaker

(*d*) *Methods for equal-loudness comparisons.* The great majority of the equal-loudness tests have been carried out by the constant-stimulus (CS) method, in which the subject has the sole task of making judgments of loudness inequality but is otherwise passive. Reasons for preferring this method have been described by Robinson in a previous paper.[7] For the most part comparisons were made between a pure tone of constant intensity and frequency and a pure tone of 1000 c/s at intensity levels which were varied at random. The fixed and variable tones were occasionally interchanged and the distinction which should be drawn between tests carried out in these two ways will be discussed later. A number of comparisons between tones other than 1000 c/s were also made, in part to demonstrate the invariance of the equal-loudness relations but also in cases where instrumental limitations precluded reproduction of the 1000 c/s tone under the reference conditions. In the constant-stimulus tests, the time-sequence patterns *AOBOAOB* and *BOAOBOA* were employed, where *A* represents the fixed stimulus, *B* the randomized variable stimulus and *O* a period of silence. The order of presentation of these sequences was randomized as well as the level of *B*. The duration of *A*, *B* and *O* was based on the available evidence as to the time taken to reach full sensation,[8] periods of from 1 to 3 s being used depending on the comparison frequencies. The growth and decay of the tones were retarded by an electronic switch in order to eliminate the disturbing click which is heard with rapid transients. The switching was complete in 0·15 s. The *B* tone was varied over a wide range of sound pressure level so as to include, with an adequate margin, the transition levels of all observers. There are considerable instrumental difficulties in providing signals variable over a range consistent with these requirements, while allowing adequate signal-to-

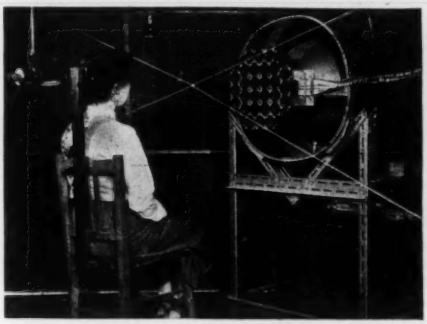

Fig. 2. Compound loudspeaker unit, The high-frequency unit is mounted on a high-efficiency reflex horn type, the latter providing the 1000 c/s tone

noise ratio, particularly in tests at high intensities. For very quiet *A*-tones a complication of another kind arises. If the *A*-tone is fixed at a sensation level within the dispersion of the threshold levels, the equal-loudness test must fail for some fraction of the observers. Fortunately, the dispersion of threshold values for otologically normal observers is not very great. At levels down to 20 phons no data were lost in this way. At levels in the region of 10 phons, however, which have been included by previous experimenters, appreciable errors would have arisen from the dispersion of the threshold and the resulting loss of data. It was considered that such tests would have been misleading and in the present work the equal-loudness comparisons were not usually taken below 20 phons.

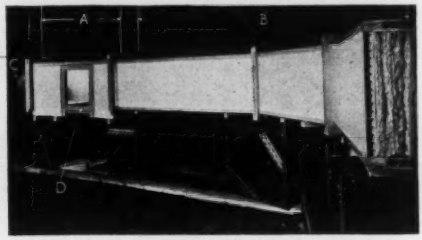

(*a*)

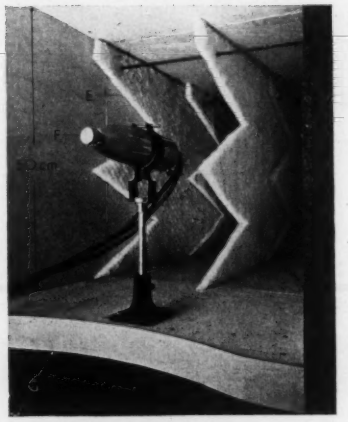

(*b*)

Fig. 3. Low-frequency duct

(*a*) General exterior view. *A*, working section; *B*, absorbent section; *C*, sound source; *D*, double door for access to listening position. (*b*) Detail of absorbent wedge structure looking towards remote end of duct. *E*, commencement of absorbent termination; *F*, standard microphone at the listening position; *G*, adjustable aperture to suit body dimension of listener.

In order to extend the upper limit of intensity at which tests by the normal CS procedure are possible, use was made of a variant of the constant-stimulus procedure which has been described by Robinson.[7] In this method the fractions of observers judging tone *A* louder than tone *B* for a fixed level of *A* and a very few levels (usually 2 or 3) of tone *B* not far removed from the expected average transition level of the group are recorded, and from these values it is possible to deduce the correct transition point of the group. Generally only one level of *B* was presented at each testing session. It has been found that a modest change of perhaps 5 dB in the level of the *B*-tone produces a critical change in the fraction of judgments. The modified CS method has the double advantage over the usual procedure of extending the practical limit of intensity set by the apparatus and of producing results of comparable reliability in less time. The method was accordingly also used to a limited extent for some comparisons at moderate levels and the opportunity was taken in these cases to test the results against the more usual procedure. Success depends on a fairly accurate prediction of the result by the experimenter but this, of course, in no way influences the observers.

(*e*) *Interpretation of the equal-loudness test records.* The result of each equal-loudness test was obtained by the operator in the form of a chart showing the judgment recorded at each intensity level of the variable tone. These levels were presented at random, as already mentioned, and were recorded in the form shown in Fig. 4, which gives extracts from two typical test records of a constant-stimulus equal-loudness comparison. In the first example the pattern is symmetrical and the transition value corresponds evidently to the attenuation setting 16·5. A substantial proportion of the results conformed to simple patterns such as this, but some of the tests yielded a blurred pattern of which the second example is typical. In such cases the transition value is not obvious, but various formal processes may be adopted as a means of consistent interpretation. For instance, assigning α to the probability that tone *A* is louder and hence $(1 - \alpha)$ to the probability that *B* is louder, the judgments recorded may be regarded as quantized estimates of α or $(1 - \alpha)$ restricted to the values 0 and 1. By computing the attenuation value corresponding to $\alpha = \frac{1}{2}$, one arrives at a consistent interpretation of the data. As a result of applying these methods to a large number of transition patterns occurring in the tests, it was found, as regards averages over thirty or so test results, that they could be replaced by a simpler process. This consisted of averaging the mid-points of the ranges of uncertainty in the upper and lower rows of judgments. For example, in the second illustration the upper row is uncertain from 12 to 20 and the lower row from 13 to 23. The transition value $(16 + 18)/2 = 17$ was therefore assigned.

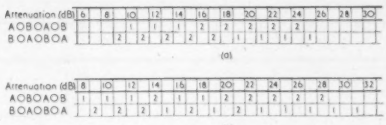
Attenuation (dB) 6 8 10 12 14 16 18 20 22 24 26 28 30
A O B O A O B
B O A O B O A
(a)
Attenuation (dB) 8 10 12 14 16 18 20 22 24 26 28 30 32
A O B O A O B
B O A O B O A
(b)

Fig. 4. Typical records from equal-loudness test by constant-stimulus method

1 signifies first tone heard was louder; i.e. tone A in upper rows, tone B in lower.
2 signifies second tone heard was louder.

Having arrived at these values, the next step is to deduce from them the normal equal-loudness relations for the group. The actual method adopted to represent the group data by a single figure is to some extent arbitrary and a number of different methods were explored to determine which could best be regarded as typical.

One of the ways of treating the data, which has the advantage of being independent of the form of the distributions and of the units employed, is to determine the median value for the group. In order to avoid the quantization error resulting from observations at whole decibel intervals, the position of the central value is better determined by drawing a freehand curve through the cumulative distribution plotted on probability paper and reading off the 50% point. Both the individual transition levels, and the totals of votes cast for, say, "tone *A* louder" at each attenuation step, could be treated in this way and the results were usually indistinguishable.

In the majority of the tests, the results conformed fairly closely to the normal error law provided the levels of attenuation were expressed in logarithmic units. In such cases the process for extracting the median value could be formalized by the method of probit analysis. The median values shown in the tables in Appendix 2 were mainly obtained in this way, including all cases of tests carried out by the modified CS procedure.

With the exception of the modified CS tests, values for the mode and mean of the distributions were also obtained, the attenuation steps being expressed in decibels. These values are also included in the table of test results. It is, of course, always possible to evaluate the mean but the result was occasionally influenced to an appreciable extent by lack of symmetry in the tails of the distribution, especially if the dispersion was large. The determination of modal values often required some care and numerical processes were devised for smoothing the histograms as an aid to consistent interpretation. In a few cases the mode was rather indeterminate or even, apparently, double-valued, and could not be estimated with accuracy. As the tables of test results show, the various processes rarely led to values differing by more than 1 phon. Moreover, any differences occurring were unsystematic in trend.

It should be noted that the ways just described for obtaining a value representative of the group suggest themselves as a natural consequence of a particular experimental procedure, namely the comparison of a constant test tone with a reference tone (usually 1000 c/s) of variable intensity. From a theoretical standpoint, there is no reason to accord the 1000 c/s tone this special place, although this is undoubtedly convenient for the purposes of definition and in practice. The equal-loudness relations ought to be valid for comparisons conducted between any pair of tones, either of which might be the one varied during the experiment. It is shown in Appendix 3 that a symmetrical treatment of the data can be defined which is independent of the use of a conventional reference tone, but it has been found experimentally that the more usual statistical procedures already discussed give results which are not materially different.

To summarize, the results adopted for incorporation in the tables and curves of equal-loudness are, in general, the modal values for the group of observers, corresponding to the usage in the definition of the phon.[4] In a few cases where the mode was ill-defined, for example, the tests at the higher frequencies where the necessary separation into age-groups resulted in smaller numbers of observers per group, the mean value is adopted. The results of tests by the modified CS method are expressed as the median value, obtained by probit analysis.

(*f*) *Method of determining the threshold of hearing.* The threshold curve may be regarded as a special member of the equal-loudness contours corresponding to just-zero loudness. It is appropriate at this point to anticipate the results and to note that the threshold values, though determined in a substantially different way, are entirely consistent with the equal-loudness data and, moreover, could have been predicted from them with considerable accuracy.

The method adopted for the determination of the minimum audible field was to switch the tone on and off at irregular intervals of a few seconds while decreasing by 2 dB steps from a clearly audible level until the observer no longer signalled in synchronism. In the neighbourhood of the minimum audible level the tone was presented several times at each step, and was recorded as audible if signalled for more than half the appropriate periods and as inaudible otherwise. The level was then raised in 2 dB steps from a level below threshold until the observer again responded. This frequently occurred on the same step recorded as minimum audible on the descent. The procedure was next repeated at levels staggered 1 dB with respect to the first set.

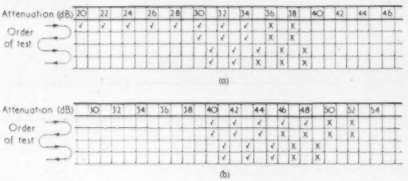

Fig. 5. Typical test records from a threshold determination

Two specimen test records are shown in Fig. 5, and serve to illustrate methods of assessing the threshold level. The ticks and crosses represent "audible" and "inaudible" as just defined. In practice only the steps in the immediate vicinity of the limen would have been presented more than once, for instance, steps 34 to 36 in Fig. 5(*a*). At least two criteria may be adopted to define the threshold, depending on whether an optimistic or pessimistic view is taken of contradictory judgments. Referring to Fig 5(*a*), the top two lines indicate a result between 34 and 36, while the bottom two lines point to a value very close to 35. On the other hand, step 35 has not always been heard. An optimistic estimate of 35 would be assigned in this case. In Fig. 5(*b*), 48 has been heard in the first descent but the subject has then "lost the thread" and only responded reliably at 44 on the ascent. In the second part of the test, the indications are in favour of a value close to 46 which would be the value assigned. On a more conservative view the threshold could be defined as the mean of the four least levels reliably heard, yielding 34 and 45·5 for the two illustrations respectively. The difference between these bases of assessments is commonly 0, 0·5 or 1·0 dB, and the difference averaged over all the threshold test records was 0·7 dB of which 0·5 is due to the use of 1 dB steps. For the purposes of this paper the lower levels have been adopted, but since each frequency is affected to a similar extent, it makes practically no difference to the equal-loudness relations which criterion is used.

RESULTS

(*a*) *General.* The experimental results are shown in Figs. 6 and 7, in which the co-ordinates are sound pressure level in decibels relative to 0·0002 dyn/cm² and equivalent loudness in phons, and in Fig. 8 which shows them in the form of equal-loudness contours. Comparisons between tones other than 1000 c/s have been converted to phons by means of the smooth curve at the appropriate frequency; this applies to the data for 25 and 33·3 c/s, the upper levels at 50 c/s, and to miscellaneous points on the curves for 100, 200 and 10 000 c/s. For completeness, the full experimental results have been collected and are tabulated in Appendix 2.

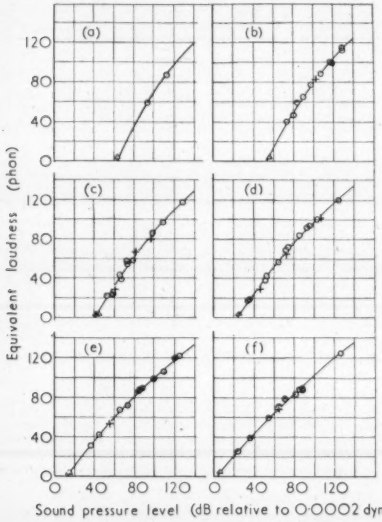

Fig. 6. Equal-loudness relations for pure tones below 1000 c/s

+, team A (ninety subjects); ○, team B (thirty subjects); △, combined team (threshold determination).
(*a*) 25 c/s, (*b*) 33⅓ c/s, (*c*) 50 c/s, (*d*) 100 c/s, (*e*) 200 c/s, (*f*) 500 c/s.

It would have been expected from previous work that the equal-loudness relations at the higher frequencies would show a fairly complicated dependence on the age of the observers. In the present work the effects of age were found to be negligible below and including 1000 c/s. Above 1000 c/s it is necessary to divide the observers into age groups in order to obtain a consistent picture of the equal-loudness relations. The curves show an increasing separation as the frequency is raised; the separation between the age groups is greatest at the threshold level and progressively diminishes as the intensity is raised. These effects are illustrated in various ways in Figs. 7, 8 and 9. Figs. 6 and 7 show the equal-loudness relations for each of the principal test frequencies, the results above 1000 c/s having been divided into successive decades of age. These curves show clearly that the maximum spread due to age occurs at the lowest levels of intensity and illustrate the converging tendency of the curves as the level is raised.

Analysis of the results has shown that the variations with age may be represented with considerable accuracy by

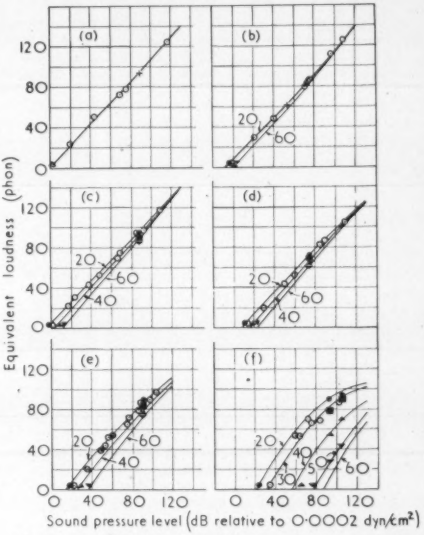

Fig. 7. Equal-loudness relations for pure tones above 1000 c/s

○, team B (average age about thirty years).
+ { ●, team A (average age about twenty years).
■, team A (average age about thirty years).
▲, team A (average age about forty years).
▼, team A (average age about fifty years). }
● ○ ▲ ▼, combined team (threshold determinations).
(*a*) 2000 c/s, (*b*) 3000 c/s, (*c*) 5000 c/s, (*d*) 7000 c/s, (*e*) 10 000 c/s, (*f*) 15 000 c/s.

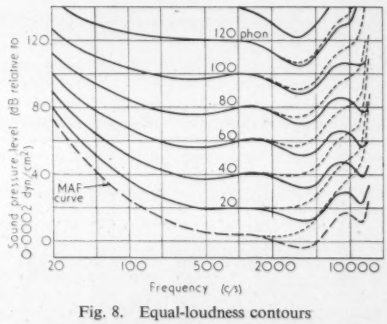

Fig. 8. Equal-loudness contours

—— age twenty years; - - - - age sixty years.

formulae involving two parameters, one of which is a function only of the age and the other a function only of the frequency. The formulae and tables of these parameters are given in Appendix 4, and were used in deducing the final forms of the equal-loudness relations. The equal-loudness contours are shown in Fig. 8 in which the results for age groups centred round twenty to sixty years have been separated in order to illustrate the trend of the results. The threshold level is shown in detail in Fig. 9 for successive age groups at ten year intervals. The dependence of the results on age shows many interesting points of detail which will be further considered in another publication.

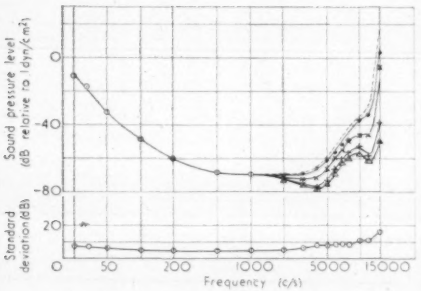

Fig. 9. Minimum audible field. (Binaural, listener facing source)

Ages: – – – – 60 years; —●— 50 years; —×— 40 years; —+— 30 years; —△— 20 years.

It will be apparent from Fig. 7(*f*) that the age effects at 15 000 c/s are so large as to be a dominant factor and this gave rise to considerable difficulty in the treatment of the data. At frequencies higher than 15 000 c/s the dispersion would probably be greatly increased, and it is doubtful whether group data could be defined without using a very large number of subjects and a disproportionate expenditure of effort.

The data have also been analysed to see whether there was any substantial difference between the results for men and women. In most of the comparisons little difference was found in the loudness judgments of men and women but this was not always the case. Over the lower half of the frequency range there were occasional differences which, however, showed no signs of any systematic effect. Above 4000 c/s some larger differences were observed of the order ± 2 dB from the mean which appeared to exhibit a systematic trend with frequency, and which may be connected with differences in the diffraction effects of male and female heads. The general trend with frequency is consistent with a change in the diffraction pattern corresponding to a reduction of linear dimension, of the order 10%, of female as compared with male heads. In view of the comparatively small magnitude of the effect, however, it has been ignored in drawing the equal-loudness contours which relate to the average of the male and female data. It may be noted that Dadson and King,[9] commenting on the minimum audible pressure for telephone listening, stated that there was no significant difference between the sexes in that case. Thus, with the possible exception of effects due to external geometry, it is fairly safe to conclude that males and females respond equally to a given sound pressure.

(*b*) *Equal-loudness relations.* Referring to Figs. 6 and 7 it will be seen that in most cases the experimental results fall almost on straight lines and in no case require more than quadratic dependence on the sound pressure level to represent them. This has enabled the full results of the equal-loudness investigation to be expressed in relatively compact tables, giving, for normal observers, the equivalent loudness of a pure tone of given frequency and sound pressure level corresponding to ages from eighteen to sixty years. These tables are given in Appendix 4. The equal-loudness relations found in the present investigation, particularly for the tones of low frequencies, differ considerably from the corresponding results in earlier work and are a good deal more regular in form. This point is illustrated in Figs. 6 and 12 and is discussed in more detail in a later section.

As mentioned above, the equal-loudness relations for tones above 1000 c/s show an increasing tendency to divide into age groups. At any one frequency the curves for different age groups tend to converge as the intensity level is raised, indicating that the rate of growth of loudness with intensity is augmented for those subjects whose threshold level is raised, a phenomenon which is analogous to that known in the clinical literature[10,11] as "recruitment." Bearing in mind that the subjects were classed as otologically normal this effect seems to be present to some extent, apparently in binaural form, among older subjects generally.

(*c*) *The equal-loudness contours.* Fig. 8 shows the results in the form of equal-loudness contours and is simply the data of Figs. 6 and 7 presented in another way. For clarity only the curves for twenty and sixty years of age are drawn. The ordinate scale has been referred to a datum level of 0·0002 dyn/cm^2. The lowest contour is the minimum audible field, the value being 4·2 dB relative to 0·0002 dyn/cm^2 at 1000 c/s, or in round numbers, -70 dB relative to 1 dyn/cm^2. A zero-phon contour, passing through 0·0002 dyn/cm^2 at 1000 c/s has not been shown as it would seem misleading to indicate a contour audible to only 12% of the population, or even fewer for the higher frequencies.

The general form of the contours resembles those of the preceding investigations, although there are several differences which will be discussed in a later section. A new feature of the results is the dip in the contours in the region 400–500 c/s. In order to confirm this feature a supplementary series of tests was carried out, using frequencies of 333·3, 500 and 750 c/s, those at 500 c/s being repeated with several different loudspeakers, in different test rooms, and at two different listening distances, namely 1 and 2 m. All these confirmed the existence of the dip and its magnitude which is greatest for moderate levels of the intensity. The general appearance of the contours in the upper part of the frequency range where they are influenced by diffraction effects resembles the earlier results, though there are differences in detail.

(*d*) *Dispersion of the results.* The variance of an equal-loudness judgment is composed of three clearly defined components in addition to the residual errors of objective origin including instrumental error. A number of the tests were repeated under identical conditions, both with the object of assessing the relative importance of the various errors and of determining the extent of any interaction between them. These tests showed that the largest component is the variance between persons and the next largest the variance of repeated results by one observer representing on the average 89% and 9% respectively of the total variance. There is also a small component of variance due to the order of presentation,

which is discussed in the next paragraph. In high frequency comparisons the variance between the results for different persons can be further resolved by separating the subjects into age groups. The "crude" (i.e. total) standard deviations of the various tests are included in the tables of test results (Appendix 2) and their dependence on frequency separation is illustrated in Fig. 10. It may be noted that in this figure the standard deviations have been expressed in phons which gives a more realistic comparison between the different tests.

In the threshold determinations, the tests at 50, 200, 3000 and 7000 c/s were repeated at intervals of several months, and a similar analysis shows again the largest part (80%) of the total variance is due to the differences between individuals.

(*e*) *Assessment of accuracy.* The overall accuracy of the equal-loudness relations can be assessed from the data contained in Fig. 10. For example, for moderate frequency

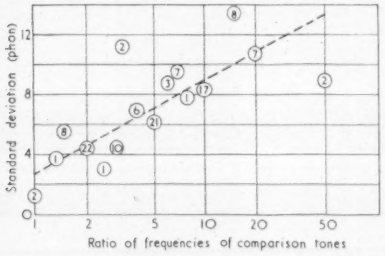

Fig. 10. Standard deviation in equal-loudness tests as a function of the frequency separation of the comparison tones. Number of tests shown in circles

separations, standard deviations of the order of 5 phons were obtained. Bearing in mind the numbers of observers involved, this is equivalent to a standard error of rather less than 1 phon. This figure is subject to appreciable improvement for moderate levels of the intensity due to the fact that the equal-loudness relations Figs. 6 and 7—which are no doubt inherently smooth curves—rely on data distributed over a considerable range of the variables. Using the method developed by Hayes and Vickers,[12] the accuracy of the curves over 85% of the intensity range covered by the measurements was found to be improved approximately two-fold compared with that of the individual values plotted. In addition, since the threshold determinations are based on the maximum number of observers employed and were, moreover, repeated at a number of frequencies, the error of the threshold measurements is already comparatively small. To summarize, over most of the intensity range, and all but the highest frequencies, the standard error of the equal-loudness relations is about 0·4 to 0·9 phon, depending on the frequency separation, the values rising to 1·0 to 1·5 phon for extreme upper levels of the intensity.

CONSISTENCY TESTS FOR THE EQUAL-LOUDNESS RELATIONS

Three types of consistency test were carried out in order to provide evidence as to the degree of coherence of the data as a whole. These were as follows:

(*a*) changing the order of presentation of the two comparison tones;
(*b*) interchanging the fixed and variable tones;
(*c*) triangular comparisons of the type $A - B$, $B - C$, $C - A$.

(*a*) The extent to which a change of order affected the judgments was readily obtained from the test records, illustrated in Fig. 4. Briefly, the results showed a small but persistent tendency to a surplus of "2" judgments in the vicinity of the equal-loudness point, that is to say the observers nearly all show a bias towards overestimation of loudness of the second tone heard, without, of course, being aware of this tendency. The extent of the "order" effect does not seem to depend on the nature of the comparison sounds but is somewhat dependent on the intensity level. It is interesting to note that the "order" effect was also observed in an experiment using two tones of the same frequency (1000 c/s). Between 30 and 100 phons, the "order" effect increases on the average from 0·6 to 1·3 dB. The effect does not appear in the results as presented, however, an average having been taken in all cases.

(*b*) For complete coherence of the data the average judgments recorded in any particular comparison should not depend on which of the two tones is fixed and which is variable. This point has already been mentioned in connexion with the statistical handling of the data. A number of tests, for the pairs of frequencies 50–1000, 50–200 and 33·3–50 c/s, were carried out both ways in order to investigate this effect. As regards individual observers, it was demonstrated that an interchange of the fixed and variable tones was immaterial; for example, in a two-stage comparison 50–1000–50 c/s, thirty observers returned to the initial value to within 1 dB on the average, in spite of a large dispersion at the intermediate stage. Similar tests carried out using the mean values for the group indicated a similar consistency of the order 1 dB, and in no case was it found necessary to take account of the order of the variables in treating the results.

(*c*) The third, and most crucial, test of consistency amounts to a verification of the proposition that sounds which are separately judged equal in loudness to the same reference sound are themselves judged equally loud. That this is substantially true was shown in a number of triangular comparisons, using tones of 50–100–1000 c/s, 33·3–50–200 c/s, 200–500–1000 c/s, 200–1000–10 000 c/s and 1000–3000–10 000 c/s. These triangular comparisons showed on the average a consistency of 1·5 phons, which is comparable with the standard error of the observations involved. The relevant determinations are listed in the tables in Appendix 2, especially Table 6.

The consistency revealed by these tests justifies their amalgamation with the remainder of the data in order to arrive at the final equal-loudness relations.

DISCUSSION

It is useful at this stage to compare the results of the present investigation with those previously available, due to Fletcher and Munson and Churcher and King. An attempt is made below to discuss the possible origin of the various discrepancies.

Considering in the first place the data on minimum audible field (MAF) (see Fig. 11) it is necessary to take note not only of the threshold curves given by the former authors but also

of their actual experimental points. Fletcher and Munson preferred to show a conventional minimum contour passing through a round value, namely 10^{-16} W/cm^2 or roughly 0·0002 dyn/cm^2 at 1000 c/s, while recognizing that this represented hearing some 3 to 4 dB more sensitive than the average for their observers. It appears, however, that the contour so chosen does not lie uniformly below Fletcher and Munson's experimental threshold values but ascends to meet them at the low frequencies. Churcher and King also do not appear to have drawn their zero-phon contour through their threshold results. For example, their threshold level for 54 c/s (38·5 dB) is in very close agreement with the present work but the Churcher–King contour for zero phon passes 11·5 dB above this value. It has already been shown that in the present results the threshold values fall naturally on an extension of the equal-loudness relations which is not the case in Churcher and King's results, as may be seen in Fig. 12(*a*). It would appear that these authors preferred to rely on the equal-loudness results, extrapolating these to a nominal threshold value. This procedure involves placing reliance on equal-loudness judgments conducted at a level of only 10 dB above 0·0002 dyn/cm^2, the objections to which have already been mentioned.

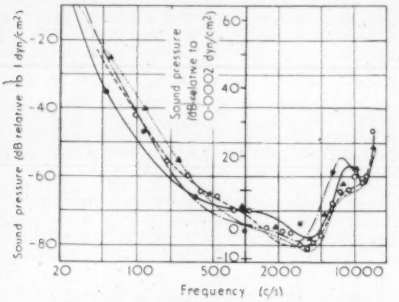

Fig. 11. Comparison of minimum audible field data

———, minimum audible field at age twenty years (this paper).
- - - - -, Fletcher and Munson zero phon contour; ▲, threshold values.
— · —, Churcher and King zero phon contour; ●, threshold values.
– – –, Sivian and White smoothed MAF curve: ○, experimental values (average: twenty-four years).

As regards the high frequency end of the scale there appears to be general agreement as to the incidence of the fluctuations due to diffraction effects but some discrepancy in the general levels. Direct comparison with the earlier results is not, however, possible in the absence of information regarding the age of the subjects. The only direct comparison which is available at high frequencies is between the present work and that of Sivian and White,[13] the age of whose observers is known. In this case, once again excepting the low-frequency region, there is fairly good agreement.

To summarize, the principal difference between the present work and the previous investigations as regards the threshold levels, consists in a lowering of the threshold of the order 10 dB at the low frequency end combined with a rise of 4 dB at 1000 c/s. There remain ambiguities at the high frequencies, the resolution of which would require information about the age of the observers in previous investigations.

Recent results due to Dadson and King[9] make it possible to relate the present work on MAF with their results for monaural minimum audible pressure (MAP) by telephone listening (see Fig. 13). It is interesting to note that the

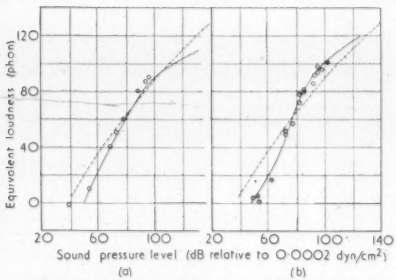

Fig. 12. Comparison of equal-loudness relations

(*a*) 54 c/s Churcher and King

○, experimental data; ———, smooth curve adopted by Churcher and King; – – – –, this paper.

(*b*) 60 and 62·5 c/s. Fletcher and Munson

○, experimental data; ———, smooth curve adopted by Fletcher and Munson; – – –, this paper.

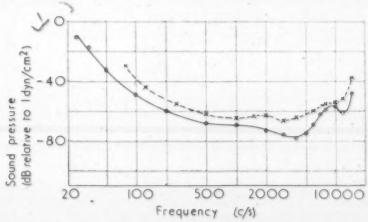

Fig. 13. Threshold of normal hearing for the age group eighteen to twenty-five years

———○———, N.P.L. minimum audible field (binaural).
– – – × – – –, minimum audible pressure (monaural) (B.S. 2497: 1954).

difference between the MAF and MAP values, often referred to as the "missing 6 dB," is very consistent* with the corresponding *difference* in the work of Sivian and White, although the absolute values obtained by the American workers are not in agreement with the British results in the low-frequency region. The cause of the latter is not entirely clear but is probably of objective origin. It may be remarked that the present work, as well as that of Dadson and King, was carried out in exceptionally silent conditions. It is possible, therefore, that the elevation of the threshold level and the

* The average elevation of the MAP relative to the MAF over the frequency range 80–6000 c/s is 10·2 dB for Sivian and White's data and 9·2 dB in the case of the N.P.L. results.

corresponding crowding of the lower level contours at the low frequencies in the previous investigations may be explainable on the basis of masking by ambient noise.

Considering next the data for equal loudness over the remainder of the auditory diagram, the main differences between the present and previous work may first be illustrated by reference to the equal-loudness relations. The differences are most apparent at the low frequencies where the present investigation leads to curves which are considerably more regular in form (see Fig. 12). In particular, the inflected form of equal-loudness relations shown by the work of Fletcher and Munson receives no support. This increased regularity of the equal-loudness relations is reflected in the more uniform distribution of the equal-loudness contours in the low-frequency area, which may be seen by comparing Figs. 8 and 14. There is an interesting difference between

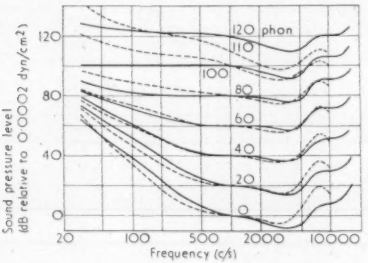

Fig. 14. Equal-loudness contours (previous determinations)

– – – –, Churcher and King; ———, Fletcher and Munson.

the results of Fletcher and Munson and the present work for frequencies above 6000 c/s. Whereas Fletcher and Munson show the loudness level increasing with the intensity level at an increasing rate, the present results show the opposite tendency. This tendency is present in all age groups and suggests some kind of saturation in the processes determining the sensation of loudness at high frequencies.

CONCLUSIONS

A new determination of the equal-loudness relations for pure tones has been carried out at the National Physical Laboratory using a large team of otologically normal observers. The measurements have extended over the frequency range 25 to 15000 c/s and up to some 130 dB above 0·0002 dyn/cm^2. The objects of the work were to attempt to reconcile the discrepancies between previous determinations, to extend the range of intensity as far as possible and to provide data which may assist in arriving at a standard set of contours. The work includes a re-determination of the threshold of hearing for free-field listening.

The great majority of the equal-loudness tests were conducted by the constant-stimulus method, in which the observers' task is confined solely to judgments of inequality of loudness in relation to pairs of pure tones, one of fixed intensity and the other variable in random steps. New techniques were used in order to realize the reference free-field conditions at the extremities of the frequency and intensity range.

The relations connecting sound pressure level expressed in decibels with equivalent loudness in phons are accurately expressible by formulae quadratic in the sound pressure level. These formulae are expressed by means of parameters which are functions of the frequency, the sensation level of the tone, and the age of the observers. This has enabled compact tables to be prepared for the equivalent loudness of a pure tone over the range of measurement.

At each of the frequencies concerned, the threshold measurements proved to be highly consistent with the equal-loudness relations.

At frequencies above 1000 c/s, the age of the observers is an important factor, becoming dominant at 15000 c/s. At the latter frequency the equal-loudness relations suggest a kind of saturation effect in the process of audition. An effect analogous to bilateral recruitment also seems to occur to some degree in normal observers of the higher age groups at high frequencies.

Comparing the results with the previous data, the equal-loudness relations show a considerably greater degree of regularity. At the low frequencies a lower threshold level has been found, and in the region around 500 c/s there is a depression in the contours, which has been carefully investigated. This was not shown in the earlier determinations.

The dispersion of the measurements corresponds generally with a standard deviation of the order of 5 phons, depending somewhat on the separation of the comparison frequencies. The major component of the variance, which arises from the differences between individuals, considerably exceeds the uncertainties of repetition by any given observer. Bearing in mind the number of persons tested, the accuracy of the smoothed equal-loudness relations is estimated to be of the order ± 1 phon over the greater part of the auditory diagram. At the extreme upper frequencies only, a more conservative figure should be assigned.

The minimum audible field values are found to bear a close resemblance to the corresponding minimum audible pressures by earphone listening recently determined at the N.P.L., but lie uniformly below them. This generally confirms the well-known phenomenon loosely called the "missing 6 dB." It is interesting to note that the minimum audible field at 1000 c/s was found to be -70 dB relative to 1 dyn/cm^2 in agreement with the experimental data of Fletcher and Munson and of Sivian and White. Fletcher and Munson, however, adopted a conventional zero of 10^{-16} W/cm^2 (roughly 0·0002 dyn/cm^2) at 1000 c/s as the reference datum for their equal-loudness contours, this convention having subsequently been sanctioned in the definition of the phon. The present results show that a contour through the latter value would lie outside the range of audibility of the great majority of normal observers.

ACKNOWLEDGEMENTS

The authors wish to acknowledge the patient co-operation of the staff of the N.P.L. who took part in the subjective tests. Acknowledgement is due to Mrs. G. W. Tucker who carried out many of the tests, to Mr. C. W. Clenshaw of the Mathematics Division for assistance in the preparation of the tables, and to Mr. G. Bradfield of the Physics Division who kindly supplied the transducer used for some work at 15000 c/s. Thanks are also due to Mr. T. Cawthorne and Mr. R. M. Harvey of King's College Hospital, London, who

kindly arranged the otological examination of the subjects. The work described was carried out as part of the research programme of the N.P.L., and the paper is published by permission of the Director of the Laboratory.

REFERENCES

(1) KINGSBURY, B. A. *Phys. Rev.*, **29**, p. 588 (1927).

(2) FLETCHER, H., and MUNSON, W. A. *J. Acoust. Soc. Amer.*, **5**, p. 82 (1933).

(3) CHURCHER, B. G., and KING, A. J. *J. Instn Elect. Engrs*, **81**, p. 57 (1937).

(4) *Brit. Stand.* 661: 1955. Clause 3013.

(5) *Brit. Stand.* 2497: 1954.

(6) DADSON, R. S., and BUTCHER, E. G. *Acustica*, **4**, p. 103 (1954).

(7) ROBINSON, D. W. *Acustica*, **3**, p. 317 (1953).

(8) MUNSON, W. A. *J. Acoust. Soc. Amer.*, **19**, p. 584 (1947).

(9) DADSON, R. S., and KING, J. H. *J. Laryng. and Otology*, **46**, p. 366 (1952).

(10) DIX, M. R., HALLPIKE, C. S., and HOOD, J. D. *Proc. Roy. Soc. Med.*, **41**, p. 516 (1948).

(11) DENES, P., and NAUNTON, R. F. *J. Laryng. and Otology*, **64**, p. 375 (1950).

(12) HAYES, J. G., and VICKERS, T. *Phil. Mag.*, **42**, p. 1387 (1951).

(13) SIVIAN, L. J., and WHITE, S. D. *J. Acoust. Soc. Amer.*, **4**, p. 288 (1933).

(14) GATES, B. G. Discussion to Ref. 3.

APPENDIX 1

A note on the permissible harmonic distortion in pure-tone equal-loudness measurements

Harmonic distortion is most likely to be a source of error in the low-frequency region, partly on account of the difficulty in producing a sinusoidal sound waveform and partly because the acuity of hearing is considerably reinforced for the harmonics relative to the fundamental.

Several experiments were carried out with tones of fundamental frequency 25, 33·3, 40, 50, 200 and 1000 c/s to determine the permissible level of harmonic distortion at various intensity levels. Two methods were used:

(*a*) Constant-stimulus loudness comparisons between a reference tone and a tone of the same fundamental frequency containing a controlled admixture of harmonic components, giving a quantitative estimate of the loudness increment due to the added components.

(*b*) A qualitative form of test in which the observer indicated his awareness or otherwise of any effect on the total loudness due to the presence of overtones. The method used was to inject into the sound source an input at a frequency very slightly removed from that of the harmonic already existing and so adjusted in amplitude that it alternately reinforced and cancelled it.

The results showed that for tones of moderate intensity level the loudness was not significantly influenced by harmonic components at a level of −40 dB or lower relative to the fundamental. Applying the method of loudness summation due to Gates,[14] combined with the equal-loudness curves in this paper, to the results obtained by method (*a*), it was found that the increment of loudness due to the presence of harmonics could be calculated with considerable accuracy from the sound pressure levels of the components.

At high intensities, quite high levels of harmonic distortion may be tolerated without effect on the total loudness, which is presumably due to the already considerable effect of aural harmonics. For example, in the case of a 33·3 c/s tone operated at a sound pressure level of 130 dB, and using method (*b*), observers were unable to detect the presence of a third harmonic component only 20 dB below the fundamental.

Method (*b*) was particularly useful in connexion with the low-frequency duct in order to determine the maximum sound levels at which the experiments could be carried on. Provided observers could not detect the fluctuations as the harmonic component cancelled and reinforced the injected signal it was concluded that no error in the loudness comparison was occurring, whatever might be the indicated level of the harmonic.

In the threshold measurements it was only necessary to ensure that each harmonic was well below the normal threshold for the harmonic concerned. This condition was met throughout, the margin being still adequate at 25 c/s.

APPENDIX 2

Experimental results

The results of the experiments are given in Tables 1–7. All values are rounded to the nearest 0·5 dB. In general, the mean, modal and median values are quoted. In some cases the modal value could not be estimated with accuracy, and has been omitted. In experiments conducted by the modified CS procedure, only the median value can be determined. In tests at frequencies above 1000 c/s the effect of age is shown by the results for groups of average age twenty, thirty, forty and fifty years. In these cases the standard deviations are net values, the variation due to age having been allowed for.

Table 1. *Minimum audible field; frequencies up to* 1000 *c/s*

Frequency (c/s)	*MAF (dB relative to 1 dyn/cm²)*			*Standard deviation of observations (dB)*
	Mean	*Mode*	*Median*	
25	−10·5	−11	−10·5	8
33·3	−17·5	−17·5	−17·5	7
50	−31	−32	−31	6·5
50	−32	−32·5	−32·5	6
100	−49	−49	−49	5
200	−59	−59·5	−59	4·5
200	−59·5	−59·5	−59·5	4·5
500	−68·5	−68·5	−69	4·5
1000	−69·5	−70	−70	4·5

Table 2. *Minimum audible field; frequencies above* 1000 *c/s*

Frequency (c/s)	*MAF (dB relative to 1 dyn/cm²) (mean value)* — *Average age of observers (years)* 20	30	40	50	*Standard deviation of observations within groups (dB)*
2000	−73·5	−72·5	−72	−69·5	5
3000	−75·5	−74·5	−73·5	−70·5	6
3000	−75	−74	−72·5	−68·5	6·5
4000	−79	−78	−73	−65·5	8
5000	−75	−74	−66	−61·5	8
6000	−69·5	−67	−59·5	−57·5	8·5
7000	−63·5	−60	−55	−50	10·5
7000	−62	−61·5	−53	−54·5	9·5
8000	−60·5	−56	−50	−50·5	8·5
10000	−57·5	−53	−46	−38·5	11·5
12000	−61	−58·5	−46	−37·5	11·5
15000	−49·5	−39	− 5	+ 2·5	17
Number of observers per group	51	38	17	14	

Table 3. *Direct phon determinations; tones below* 1000 *c/s*

Test tone — *Frequency (c/s)*	*Sound pressure level (dB relative to 0·0002 dyn/cm²)*	*Equivalent loudness (phons)* — *Mean*	*Mode*	*Median*	*Standard deviation of observations (phons)*
50	52	21·5	22	21·5	5·5
	60	32	28	30·5	10·5
	65	44	—	44·5	13
	65	44·5	—	44	15
	72·5	55·5	57·5	57	13·5
	80	65·5	67·5	66·5	9
100	32·5	17	17·5	17·5	5
	45·5	29·5	28·5	28·5	6·5
	50·5	39	38	38	7·5
	70·5	65·5	65·5	65·5	7
	73	—	—	72 *	6·5
	85·5	81·5	84	83	7·5
	95·5	92·5	94·5	93·5	6·5
	103	—	—	100 *	7
200	36	30	30·5	30	4·5
	45	42·5	42	42	5·5
	55·5	52	52·5	52·5	6
	65	66·5	67·5	67	5·5
	72	—	—	70·5*	5·5
	86	88	88·5	88·5	5·5
	86	88	88	88	5
	99·5	97·5	98·5	99	4·5
	109	—	—	106·5*	3
	120	—	—	120·5*	5·5
	124	—	—	122·5*	12·5
333	61	62·5	62	62	5
500	24	25	25	24·5	4
	34·5	38	38·5	38	3
	54	59	58·5	59	4
	64·5	70	69·5	69·5	4
	64·5	68·5	68·5	68·5	4
	70·5	—	—	79 *	3·5
	81	83·5	—	83·5	3
	85	88	88·5	88	2·5
	86	89	88·5	88·5	2·5
	86	89	88·5	88·5	4
	127	—	—	124·5*	3
750	53·5	59·5	59·5	59·5	3·5

* Determinations by modified CS procedure. Standard deviations in these cases are estimated values.

Table 4. *Direct phon determinations; tones above* 1000 *c/s*

Test tone		*Equivalent loudness (phons)*						
Frequency (c/s)	*Sound pressure level (dB relative to 0·0002 dyn/cm²)*	*Mean value* Age 20	30	40	50	*Mode* Age 30	*Median* Age 30	*Standard deviation of observations (phons)*
1 500	74·5	—	75·5	—	—	75·5	75·5	3·5
2 000	20·5	—	24·5	—	—	24·5	24·5	4·5
	45·5	—	49	—	—	49·5	49·5	5
	70·5	—	72·5	—	—	72·5	72·5	4·5
	75·5	—	—	—	—	—	76	6
	90	92·5	93	92	93	—	—	4
	118	—	—	—	—	—	124	7
3 000	22	—	29	—	—	29	29	4
	42	—	48	—	—	47·5	48	5·5
	55	—	61	—	—	60·5	61	5
	55	63	62	59·5	62	—	—	4·5
	73	—	—	—	—	—	79·5*	4
	74·5	—	—	—	—	—	82 *	4
	75	—	83·5	—	—	84·5	84	5
	75	—	84	—	—	84	84	4
	97·5	—	—	—	—	—	111 *	4
	110	—	—	—	—	—	124·5*	—
5 000	16·5	—	—	—	—	—	22·5*	5
	23	—	31	—	—	30·5	31	6
	37·5	—	—	—	—	—	42·5*	4·5
	48	—	51	—	—	52·5	51·5	8·5
	66·5	—	—	—	—	—	69·5*	7·5
	68	—	72·5	—	—	75·5	73·5	8
	85·5	—	—	—	—	—	93 *	4·5
	87	91·5	90	85	86	—	—	6
	92	—	96·5	—	—	96·5	96·5	6·5
	109	—	—	—	—	—	117 *	8
7 000	30	—	—	—	—	—	18·5*	9
	50	—	42·5	—	—	42	42	8·5
	60	—	—	—	—	—	51·5*	8
	75	70·5	69	60·5	59·5	—	—	10·5
	84·5	—	79·5	—	—	82·5	80	6·5
	89·5	—	—	—	—	—	86·5*	9·5
	109	—	—	—	—	—	104 *	—
10 000	34·5	—	—	—	—	—	19·5*	9·5
	49·5	—	42·5	—	—	38·5	41	9
	53·5	—	—	—	—	—	43·5*	10
	58·5	—	51·5	—	—	53	52	13
	74	—	—	—	—	—	65 *	9
	89	—	85	—	—	87	86·5	11
	89	82·5	78·5	70	68·5	—	—	12·5
	97·5	—	90·5	—	—	89	90·5	9·5
	103	—	—	—	—	—	96·5*	6·5
15 000	59·5	—	50·5	—	—	54	53	13
	64	—	51	—	—	53·5	52	15
	72·5	—	64	—	—	69	67	10
	76·5	—	68	—	—	65·5	67	13
	83·5	—	—	—	—	—	67·5*	11·5
	94	89	77	53·5	26·5	—	—	20
	103·5	—	—	—	—	—	86 *	11·5
	105	93	89·5	70	43·5	—	—	13

* See footnote to Table 3.

Table 5. *Phon determinations by "average-error" method*

Test tone: Frequency (c/s)	Sound pressure level (dB relative to 0·0002 dyn/cm²)	Equivalent loudness (phons)	Standard deviation of observations (phons)
100	32·5	18	5·5
	52·5	44	10
	72·5	70	7·5
	92·5	92	5

Table 6. *Indirect determinations*

Test tone: Frequency (c/s)	Test tone: Sound pressure level (dB relative to 0·0002 dyn/cm²)	Reference tone equal in loudness to test tone: Frequency (c/s)	Sound pressure level (dB relative to 0·0002 dyn/cm²): Mean	Mode	Median	Standard deviation of observations (dB)	Equivalent loudness (phons)†
25	94·5	50	77	76·5	77	5	57·5
	113·5	200	85	85·5	85	7·5	87
33·3	72·5	50	64·5	64·5	64·5	6·5	37·5
	84	50	77·5	77·5	77·5	5	59
	99	50	92	92	92	4	78
	116·5	50	111·5	111·5	111·5	3·5	101
	129	50	—	—	125·5*	2	116
	80·5	200	49·5	—	49·5	10·5	48
	118	200	99	—	98·5	7	100
	129	200	—	—	113 *	7	113
50	72·5	100	62·5	—	64	7·5	53·5
	58	200	33	30·5	32·5	7·5	25
	78	200	57·5	58	56·5	8	58
	96·5	200	79	79·5	79	6·5	81
	97·5	200	83	84	83·5	5·5	86
	107·5	200	94·5	95	95	6·5	96·5
	127·5	200	—	—	118·5*	4·5	117·5
100	65	200	57·5	58	57·5	4·5	57·5
	106	200	100·5	101	100·5	3·5	102
	124·5	200	—	—	121	2·5	119·5
200	86	500	85	85	85·5	3	88·5
10 000	55·5	3000	45	—	45	11·5	50
	75	3000	64·5	—	66	9	71·5

* See footnote to Table 3. † The loudness in phons is calculated from the tables in Appendix 4, using the modal value of the equally-loud reference tone where available.

Table 7. *Experiments with interchange of fixed and variable tones*

The entries in this table should be compared with those for 33·3 c/s in Table 6 and for 50 c/s in Table 3

Fixed tone: Frequency (c/s)	Fixed tone: Sound pressure level (dB relative to 0·0002 dyn/cm²)	Variable tone, equal in loudness to fixed tone: Frequency (c/s)	Sound pressure level (dB relative to 0·0002 dyn/cm²): Mean	Mode	Median	Standard deviation of observations (dB)	Equivalent loudness (phons)*
50	81·5	33·3	89·5	90	89·5	4	64·5
	96·5	33·3	102·5	102·5	103	4·5	83·5
	100·5	33·3	107	107	107	4	88·5
1000	39·5	50	67	65·5	66	6	39·5

* The loudness in phons is calculated from the tables in Appendix 4 for the fixed tone in each case.

APPENDIX 3

The effect of interchanging the fixed and variable stimuli in comparisons between two tones and a method for treating the results in a symmetrical manner

It has been mentioned in connexion with the tests of consistency that, so far as individual observers are concerned, it was found to be immaterial which tone was varied in equal-loudness tests: there is a unique correspondence between the two sound pressure levels for the condition of equal-loudness. Thus, expressing the sound pressure level of one tone as a function of that of the other, an equal-loudness relation can be defined for each individual. Many of these relations were drawn out and showed that, though they are fairly diverse in position, slope, and curvature as between one individual and another, the curve for each observer is well-defined and smooth.

To illustrate the problem of determining the symmetrical form of the equal-loudness relation for a group in terms of the individual data already mentioned in connexion with the statistical treatment of the results, it will be sufficient to represent the individual loudness relations by linear functions of the sound pressure levels. In practice, the form of the functions is more nearly quadratic, but this fact, while introducing a complication, does not change the argument in principle. It should be emphasized that the following discussion is based on an algebraic rather than a statistical consideration. We may write, for each individual,

$$y = ax + b \qquad (1)$$

where x is the sound pressure level of one tone and y the sound pressure level of a tone at another frequency judged by that individual to be equally loud to the first and a and b are constants for the individual but have statistical distributions over the group, the nature of which is immaterial to the discussion. In determinations of phon values, we identify y with the 1000 c/s tone and x with the fixed tone, and the equal-loudness relation for the group as customarily defined is

$$y = \bar{a}x + \bar{b} \qquad (2)$$

in which the barred symbols represent some form of average.

However, let us suppose that the test procedure had been reversed, so that fixed 1000 c/s tones (y) were equated in loudness by adjustment of the other tone. Since the loudness relations (1) are fixed for each observer, they may also be written $x = (1/a)y - (b/a)$, and the results of the reversed tests for the group would be $x = \overline{(1/a)}\,y - \overline{(b/a)}$ or

$$y = [1/\overline{(1/a)}]x + [\overline{(b/a)}/\overline{(1/a)}] \qquad (3)$$

From the theoretical standpoint, equations (2) and (3) ought to represent the same function. It is easy to prove, however, that this condition is not satisfied if the averaging process indicated by the bar symbol corresponds to any of the usual statistical operations for measurement of central tendency such as the mean, mode or median processes.

Viewed as a geometrical problem in the x, y plane, it may be seen that the desired operation represented by the bar symbol must depend only on the ensemble of lines in equation (1) and not on the co-ordinate frame to which they are referred. In particular, the operation must be invariant with respect to translation of the co-ordinate frame since this is equivalent merely to changing the zero level to which the sound pressures are referred. This condition of invariance is satisfied if the bar symbol is identified as the operation defining a line having the orientation

$$(1/n)\sum_{r=1}^{n}\theta_r$$

where

$\theta_r = \arctan a_r$, and which passes through the point (x_0, y_0) such that the sum of squares of normals from (x_0, y_0) on to the ensemble of lines in equation (1) is minimal; r is a running index for the different members of the group.

This method was applied to groups of thirty individual equal-loudness relations for the frequency pairs 33·3/1000, 100/1000, and 200/1000 c/s and the resulting functions were compared with the pairs of relations corresponding to equations (2) and (3) with the bar symbol taken, by way of example, to signify the arithmetic mean. The differences were found never to exceed 1 dB and, except at the extremities of the intensity range, the difference was only a small fraction of 1 dB. These examples, especially the first, apply to comparisons between fairly remote frequencies for which the distributions of the parameters of the individual curves had a considerable dispersion. It was therefore concluded that no appreciable error is caused by treating the loudness judgments in this investigation by the more usual statistical methods, and no distinction needs to be made in practice between the fixed and variable stimuli.

APPENDIX 4

Tables of normal threshold of hearing (MAF) and equivalent loudness

(*a*) *Equivalent loudness of pure tones.* The equal loudness relations for pure tones for normal subjects of age twenty years are expressed by the formulae

$$y_{20} = a + bx + cx^2$$

where y_{20} = equivalent loudness in phons

x = sound pressure level of pure tone of frequency f(c/s), expressed in dB relative to 0·0002 dyn/cm²

and a, b and c are functions of the frequency f.

Values of a, b and c are given in Table 8. For most accurate use, second differences should be employed when interpolating in the table. The spacing of frequencies has, however, been so chosen that equivalent loudness values may be derived to the nearest phon by linear interpolation. Owing to changes of sign in the second differences, the values of y in such cases should, in general, be rounded up except for frequencies in the range 1000–4000 c/s where they should be rounded down. The experimental results for frequencies from 33·3 to 1000 c/s cover the intensity range from threshold to about 130 dB, and for the higher frequencies to about 110 dB. The accuracy of y calculated for values of x within these ranges is of the order 1 phon, except possibly above 10 000 c/s. The estimated accuracy for $x = 140$ (from 33·3 to 1000 c/s) or for $x = 120$ (from 3000 to 10 000 c/s) is about 2 phons, these values representing an extrapolation of some 10 dB beyond the experimental data. Values in the table for $f = 20$ c/s are extrapolated.

(*b*) *Effect of age on the threshold of hearing of normal subjects.* The threshold level t_n, expressed in decibels, for normal subjects of age n is given by $t_n = t_{20} + \beta\gamma$ where t_{20} is the threshold of hearing (MAF) for normal subjects of age twenty years, β is a function only of the frequency, and γ a function only of the age.

Values of t_{20} are given in Table 8 and values of β and γ in Tables 9 and 10 respectively. The value of γ is arbitrarily chosen to be zero for age twenty.

The tabulated values of t_{20} correspond to the twenty-year MAF curve shown in Fig. 9. This figure also illustrates the accuracy with which the $\beta\gamma$ correction fits the experimental data.

Table 8. *Equivalent loudness parameters*

Frequency (c/s)	a	b	c	t	b'	Frequency (c/s)
20	−217·2	3·669	−0·009 27	+74·3	2·291	20
25	−167·2	3·145	782	65·0	2·128	25
30	−135·7	2·801	677	58·1	2·014	30
35	−113·2	2·538	589	52·7	1·917	35
40	− 96·3	2·326	514	48·4	1·828	40
45	− 83·2	2·155	454	44·8	1·748	45
50	− 73·0	2·021	408	41·7	1·681	50
55	− 65·1	1·917	371	39·1	1·627	55
60	− 58·7	1·835	−0·003 43	+36·8	1·583	60
60	− 58·7	1·835	−0·003 43	+36·8	1·583	60
70	− 49·1	1·722	305	32·9	1·521	70
80	− 42·5	1·652	285	29·8	1·482	80
90	− 37·4	1·603	275	27·2	1·453	90
100	− 33·5	1·570	−0·002 68	+25·1	1·435	100
100	− 33·5	1·570	−0·002 68	+25·1	1·435	100
120	− 27·0	1·512	260	21·4	1·401	120
140	− 22·7	1·473	255	18·9	1·377	140
160	− 19·4	1·444	249	16·8	1·360	160
180	− 16·9	1·422	245	15·2	1·348	180
200	− 14·7	1·404	−0·002 41	+13·8	1·337	200
200	− 14·7	1·404	−0·002 41	+13·8	1·337	200
250	− 10·8	1·362	230	11·2	1·310	250
300	− 8·1	1·325	218	9·4	1·284	300
350	− 6·1	1·290	204	8·1	1·257	350
400	− 4·7	1·259	−0·001 88	+ 7·2	1·232	400
400	− 4·7	1·259	−0·001 88	+ 7·2	1·232	400
600	− 1·8	1·155	116	5·2	1·143	600
800	− 0·5	1·064	−0·000 48	4·4	1·060	800
1 000	0	1	0	+ 4·2	1	1 000
1 000	0	1	0	+ 4·2	1	1 000
1 500	+ 1·4	0·944	+0·000 60	+ 3·0	0·948	1 500
2 000	+ 3·3	0·924	100	+ 1·0	0·926	2 000
2 500	+ 5·3	0·928	118	− 1·2	0·922	2 500
3 000	+ 6·9	0·937	120	− 2·9	0·930	3 000
3 500	+ 7·9	0·946	113	− 3·9	0·937	3 500
4 000	+ 7·9	0·954	098	− 3·9	0·946	4 000
4 500	+ 7·1	0·963	080	− 3·0	0·958	4 500
5 000	+ 5·3	0·973	+0·000 59	− 1·1	0·972	5 000
5 000	+ 5·3	0·973	+0·000 59	− 1·1	0·972	5 000
6 000	− 0·5	1·011	+0·000 14	+ 4·6	1·012	6 000
7 000	− 7·5	1·075	−0·000 35	10·9	1·067	7 000
8 000	− 13·3	1·159	89	15·3	1·132	8 000
9 000	− 16·5	1·242	145	17·0	1·193	9 000
10 000	− 16·8	1·314	203	16·4	1·247	10 000
11 000	− 14·8	1·377	269	14·2	1·301	11 000
12 000	− 12·7	1·450	350	12·0	1·366	12 000
13 000	− 13·9	1·566	454	12·0	1·457	13 000
14 000	− 22·7	1·777	591	16·0	1·588	14 000
15 000	− 43·0	2·146	−0·007 72	+24·1	1·774	15 000

Table 9. *Threshold parameter (age)*

Age	γ	Age	γ	Age	γ	Age	γ
18	−0·9	30	5·9	40	19·9	50	32·7
20	0·0	32	7·6	42	23·8	52	34·0
22	+1·0	34	9·7	44	26·9	54	35·3
24	2·0	36	12·2	46	29·2	56	36·4
26	3·2	38	15·7	48	31·1	58	37·4
28	4·4					60	38·3

Table 10. *Threshold parameter (frequency)*

Frequency (c/s)	β	Frequency (c/s)	β	Frequency (c/s)	β
0	0	5500	0·41	11 000	0·71
500	0	6 000	0·41	11 500	0·78
1000	0	6 500	0·41	12 000	0·85
1500	0·02	7 000	0·40	12 500	0·94
2000	0·06	7 500	0·41	13 000	1·05
2500	0·13	8 000	0·43	13 500	1·17
3000	0·20	8 500	0·45	14 000	1·32
3500	0·26	9 000	0·49	14 500	1·49
4000	0·32	9 500	0·54	15 000	1·72
4500	0·37	10 000	0·59		
5000	0·40	10 500	0·65		

(*c*) *Effect of age on the equivalent loudness at levels above threshold.* The threshold shift has already been given in paragraph (*b*) as the product ($\beta\gamma$) of two independent parameters. The dependence on age of the equal-loudness relations at levels above the threshold naturally requires a more complicated expression. In the first place it must take account of the form of the equal-loudness relations themselves, and, as already stated, these are quadratic functions of the sound pressure level. Secondly, allowance must be made for the converging tendency of the equal-loudness relations for different age groups at the higher levels of intensity. It has been found that this part of the variation due to age is adequately represented by a quantity diminishing in a linear manner with the sound pressure level. From these considerations we arrive at the following approximate formula for the variation of the equivalent loudness with age of pure tones in the frequency range above 1000 c/s. The reduction of equivalent loudness in phons Δy corresponding to age n relative to the value for age twenty is given by

$$\Delta y = y_{20} - y_n = \beta\gamma(b' + c\beta\gamma)\,(140 + t_{20} - x)/(140 - \beta\gamma)$$

In this formula, β, γ, c, t_{20} and x have the same significance as above and $b' = b + 2ct_{20}$. For convenience in computing the age corrections, values of b' are included in Table 8.

The spectral quantum- and energy-efficiency of calcium tungstate X-ray intensifying screens*

By R. H. Herz, Dr.Phil.Nat., F.R.P.S., F.Inst.P., Kodak Ltd., Harrow, Middlesex

[*Paper received* 9 *February*, 1956]

The intensifying action of calcium tungstate screens in combination with X-ray film has been investigated over a wide range of X-ray wavelengths equivalent to X-rays generated with energies of between 40–1200 kV. By means of the evaluation of the quantum- and energy-efficiencies of screen and film an understanding of their behaviour, i.e. their utilization of energy within this range of quantum energies, is obtained.

Calcium tungstate screens are used extensively in medical and industrial radiography, but surprisingly little information is available on how and why their intensifying action varies with the quality of radiation over a wide range of X-ray wavelengths. The need for such information has become greater since hard X-rays and γ-rays from radio-isotopes are now so widely applied. Often the intensifying action obtainable is masked by the decreased speed to blue light of the film material, caused by low-intensity reciprocity failure. This occurs particularly at short wavelengths where high intensities of X-radiation cannot usually be obtained. Hence photographic effects with screens can be truly assessed only if the reciprocity failure of the film is taken into consideration.

In order to understand the behaviour of X-ray intensifying screens, i.e. their utilization of energy over a wide range of X-ray wavelengths, it was necessary to investigate the more fundamental aspect of this problem, namely the quantum- and energy-efficiency of the screens.

The variation of the intensifying action with X-ray wavelength has been investigated by Tasker[1] for a variety of types of screen down to a wavelength of 0·1 Å (corresponding to 200 kV X-rays filtered by 2 mm copper + 2 mm aluminium). Coltman, Ebbighausen and Altar,[2] who have made a thorough investigation of the spectral emission, total light output and light absorption within calcium tungstate screens, have also reported on the energy-efficiency of screens, considering, however, one X-ray wavelength only. Eggert and Schopper[3] have carried out investigations on the quantum- and energy-efficiency of screens at three wavelengths within the region of soft X-rays. According to their results both the quantum- and energy-efficiency of screens decrease sharply over the wavelength range from 1·54 to 0·29 Å.

The last result was the starting point of the present investigation, which had as its object the reconciliation of this decrease with the well-known increase of the intensifying action towards wavelengths still shorter than those considered by Eggert and Schopper. In fact, it was of primary interest to know whether the increase of the intensifying action is only apparent and mainly caused by the drop of the direct X-ray film speed at shorter wavelengths, or whether the efficiency of the screen is indeed increased within this range of wavelengths.

In the following, the experimental procedure for the evaluation of the intensifying action of the screens and their energy-efficiency will be described, and the later sections will discuss the results and consider further the utilization of X-ray energy in the photographic process.

CHANGE OF INTENSIFYING FACTOR WITH WAVELENGTH

(*a*) *Sources of radiation and the determination of their quality.* The range of X-ray wavelengths comprising radiations from 40–1200 kV was covered by means of two X-ray units and two γ-ray emitting radio-isotopes. The two X-ray units generated X-rays at energies up to 130 and 200 kV respectively, and the isotopes used were iridium 192 (0·60, 0·58, 0·29, 0·13 MeV) and cobalt 60 (1·33, 1·17 MeV). With these sources of radiation the complete range of qualities of radiation of wavelengths from 0·275–0·01 Å was covered by using copper filters of various thicknesses. The determination of quality was carried out by measurements of the half-value layers in millimetres of copper ($h.v.l._{Cu}$) which were converted into linear absorption coefficients (μ_{Cu}) by means of the relationship:

$$\mu_{Cu} = \log_e 2/(h.v.l._{Cu}) \qquad (1)$$

The equivalent wavelengths corresponding to given linear absorption coefficients were taken from experimental data available in the literature. In Table 1, the energies of the various sources of radiation in kV or MeV (isotope), the filtration, $h.v.l._{Cu}$ and equivalent wavelengths λ (in Å) are quoted. In several cases wavelengths were obtained by interpolation from other measured *h.v.l*'s used in previous work.[4]

Table 1. *Qualities of radiation*

kV or isotope p	*Filtration* (mm Cu)	*h.v.l* (mm Cu)	*Equivalent wave-length* λ (Å)
70	0·51	0·21	0·275
90	1·0	0·42	0·22
125	1·9	1·0	0·155
130	2·0	1·15	0·145
165	2·0	1·47	0·133
140	5·3	1·82	0·12
197	4·0	2·33	0·104
140	12·7	2·45	0·100
197	8·0	2·75	0·095
197	10·0	3·14	0·088
197	20·0	3·65	0·082
197	3·5 mm Pb	4·4	0·072
^{192}Ir	20 mm Cu	9·7	0·024
(0·60, 0·58, 0·29, 0·13 MeV)			
^{60}Co	0	15·1	0·01
(1·33, 1·17 MeV)			

(*b*) *Evaluation of intensifying factors.* In order to survey the intensifying action of calcium tungstate screens over the wide range of X-ray wavelengths used in practice, the intensifying factor, i.e. the ratio of the X-ray exposures required to obtain a density of 1·0 above fog without and with screen, was measured for nine different *h.v.l*'s using Kodak Blue Brand X-ray film and a pair of Kodak Ultra Speed intensifying screens (calcium tungstate). Characteristic curves were prepared for each *h.v.l.* with screen and direct X-ray exposure, and the intensifying factors were determined

* Kodak communication No. 1776H.

in the usual manner from the displacement of the screen curve along the log E axis, compared with the non-screen curve, at a density of 1·0 above fog. The films were processed throughout in Kodak D19b developer at 68° F for 6 min.

Since the exposure times required by the sources available at various *h.v.l*'s varied from a fraction of a second to several minutes, the measured intensifying factors have been corrected for the reciprocity failure (to light) of Blue Brand X-ray film. No corrections were required for the direct X-ray exposures, as these obey the reciprocity law. In this way it was possible to calculate the intensifying factors when the sources were such as to require exposures of one second, one minute, one hour and twelve hours respectively. The results of these measurements are shown in Fig. 1, which

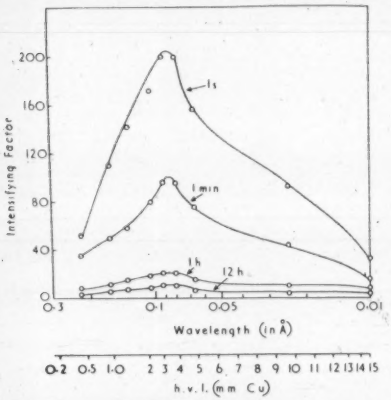

Fig. 1. Intensifying factor at a density of 1·0 above fog as a function of wavelength and of *h.v.l.* Double-coated Kodak Blue Brand X-ray film

illustrates the relationship between intensifying factors and *h.v.l.* (in millimetres of copper) and equivalent wavelengths, for one second, one minute, one hour and twelve hours exposure time. There is a considerable drop in intensifying factor as exposure time is increased, but for all times of exposure the intensifying factor increases up to a maximum at a *h.v.l.* of about 3 mm copper, and then decreases as higher values of *h.v.l.* are approached.

The intensifying factors shown in Fig. 1 refer to a density of 1·0 above fog. A density of 1·0 was chosen because it is close to the optimum density level in medical and industrial radiography.

For experimental convenience the wavelength dependence of the intensifying factor was analysed with a single front screen and a single-coated Blue Brand X-ray film exposed at a density of 0·2 above fog.

ANALYSIS OF THE INTENSIFYING FACTOR

The important factors which determine the intensifying factor (*IF*) can be derived as follows.

If the X-ray energy incident on the screen is X_s, A_s the proportion absorbed by the screen, and Ω the energy-efficiency of the screen, i.e. the ratio of light emitted (in energy units) to the X-rays absorbed (also in energy units), then the amount of light L emitted is given by

$$L = X_s A_s \Omega$$

If X_f is the energy of X-rays incident on the film, A_f the proportion of this absorbed by the film, i.e. the ratio of X-ray energy absorbed X_a to that incident X_f, the amount of X-ray energy available to produce a photographic effect is $X_f A_f$.

If X_f is now the X-ray exposure required to produce a certain density by direct impingement on the film, and X_s the X-ray exposure required to produce the same density when a screen is used, the intensifying factor (*IF*) for that density is defined as X_f/X_s, whence

$$IF = X_f/(L/A_s\Omega)$$

where L is now the light exposure required to produce the standard density. The most informative way of proceeding is to replace X_f by X_a/A_f, and re-write the equation as

$$IF = \Omega(A_s/A_f)\,(X_a/L) \qquad (2)$$

The energy efficiency Ω of the screen is independent of the X-ray exposure for a given wavelength, or nearly so, and so also is the ratio A_s/A_f (percentage absorption of X-ray energy by the screen divided by percentage absorption by the film), in any given case. The ratio (X_a/L) is likely to vary with the reference density, because the relation between density and X-ray exposure is not the same as the relation between density and light exposure. The light energy absorbed is proportional to that incident and the constant of proportionality approaches unity, because the absorption coefficient of the film is relatively high for blue light and because the high reflectivity of the screen will force back into the film any light which might otherwise escape absorption by reflexion from the film. We may therefore take X_a/L as the ratio of the X-ray energy absorbed to the light energy absorbed in the film when both exposures produce a standard density. It is a measure of the ratio of photographic efficiencies.

In measuring these quantities, Ω, A_s/A_f, X_a/L, use was made of a combination of a front screen with a single-coated Blue Brand X-ray film, prepared by removing one coating from a normal double-coated film. During the exposure the screen and film were so arranged that the radiation passed first through the screen and then through the film as in the ordinary use of a front screen.

In order to arrive at the three quantities mentioned above, the following steps were taken in succession.

(i) The number of roentgens necessary to obtain a density of 0·2 above fog with and without screen was measured at each wavelength by means of an ionization chamber. The number of roentgens required for the screen was then corrected so as to be valid for one second exposure time, taking into consideration the known reciprocity failure of the film in use.

(ii) The energies incident (E_{inc}) on film and on screen in erg per cm^2 per roentgen were calculated for each wavelength by the relation[5,6]

$$E_{inc} = 0{\cdot}11/(\tau + \sigma_a)\ \text{air} \qquad (3)$$

where τ is the photoelectric absorption coefficient and σ_a is the true absorption coefficient associated with Compton recoil electrons. (τ and σ_a are wavelength dependent quantities.)

(iii) The absorption by the screen was measured ionometrically and was also calculated at a number of points, as shown in Fig. 2. The break in the computed curve (*b*) arises from the selective absorption of tungsten at 0·178 Å. Taking into account the fact that the radiation in the experimental

measurements was not monochromatic, which has the effect of smoothing out the experimental curve (*a*) somewhat, the agreement is considered satisfactory.

Similar absorption measurements have been carried out on film. These measurements were described by D. Bromley and the author[6] and the results have been used in this work.

The energy of light emitted by the screen was assumed to be equal to the incident light energy required by the film to produce a density of 0·2 above fog. At an exposure time of one second, the number of light quanta was measured by Dr. Farnell of these laboratories (private communication), and was found to be $7{\cdot}85 \times 10^8$ quanta/cm^2 for radiation of 4360 Å. This radiation is very close to the maximum in the spectral emission curve of the screen, which remains constant as the wavelength of the exciting X-radiation is changed, as has been shown by M. B. Hodgson[7] and G. F. Knipe (private communication). Since the energy of a single light quantum at 4360 Å is $4{\cdot}6 \times 10^{-12}$ erg, the light energy emitted by the screen to obtain a density of 0·2 above fog is

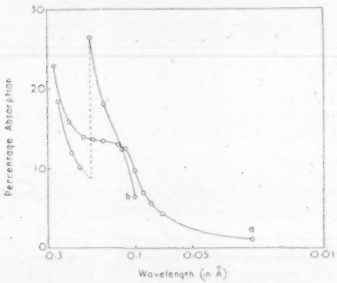

Fig. 2. Percentage absorption of front screen as a function of X-ray wavelength, curve (*a*) experimental, (*b*) calculated

$$7{\cdot}85 \times 10^8 \times 4{\cdot}6 \times 10^{-12} = 3{\cdot}6 \times 10^{-3}\ \text{erg/cm}^2$$

The results of the various computations are illustrated in Fig. 3 which shows the three quantities Ω, A_s/A_f and X_a/L respectively.

The addition of the log values of these three quantities leads to the curve marked by filled-in circles, which gives the intensifying factor for a single front screen and single-coated film for a density of 0·2 above fog. This curve approximates very closely to the top curve of Fig. 1, if the latter is replotted on a logarithmic scale, making allowance for the difference in exposure required to give a density of 0·2 instead of 1·0. This shows that the use of a pair of screens with a double-coated film results in practically the same wavelength dependence as a single screen with single-coated film.

From the analysis (see Fig. 3) it is found that the change of the intensifying factor with wavelength is predominantly influenced by the relative absorptions of screen and film and to a rather lesser extent by the relative photographic efficiencies of the film for X-rays and light respectively. The energy efficiency (Ω) of the screen is almost constant over the whole range of wavelengths and is of the order of 1–2%; i.e. only 1–2% of the absorbed X-ray energy is converted into photographically useful light energy by the screen.

Losses of light due to absorption or scattering within the screen have not been considered, since the chief object of this investigation was to find the general trend of the behaviour of screens with the varying quality of radiation.

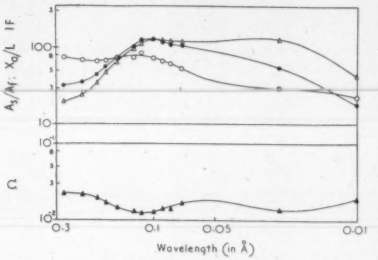

Fig. 3. (Ω) Energy-efficiency of front screen as a function of wavelength ▲——▲

(A_s/A_f) Ratio of percentage absorption of X-ray energy by screen to that by film. △——△.

(X_a/L) Ratio of (X-ray energy absorbed by film)/(light energy absorbed by film) to obtain a density of 0·2 above fog. ○——○.

$(IF) = \Omega(A_s/A_f)(X_a/L)$. ●——●.

THE UTILIZATION OF X-RAY AND LIGHT ENERGY

(*a*) *Quantum-efficiency of the screen.* In the course of this investigation it appeared to be of interest to study quantitatively the conversion of the absorbed X-ray quanta of increasing energy in the screen into light quanta. For this purpose, the quantum efficiency of the screen (Φ) as a function of wavelength is plotted in Fig. 4; Φ is defined as the ratio:

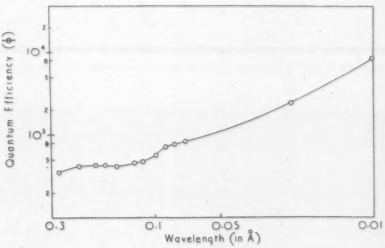

Fig. 4. Quantum efficiency of front screen as a function of wavelength

(number of light quanta emitted by screen)/(number of X-ray quanta absorbed by screen). The number of X-ray quanta absorbed by the screen were found from the data on the incident energies E_{inc} the percentage absorption values for the screen and the quantum-energies ($h\nu$) at each wavelength, i.e. by

$$(E_{inc} \times \%\ \text{absorption})/h\nu$$

It is seen from Fig. 4 that Φ increases with increasing quantum-energy. About 23 times as many light quanta are emitted per absorbed quantum at 1·2 MeV than in the soft X-ray

region. The explanation of the increase is thought to be similar to the explanation of the increasing quantum efficiency with shorter wavelengths for non-screen X-ray film; i.e. with the increasing range of electrons released in the screen more and more fluorescent centres are excited to fluorescence.

(*b*) *The utilization of the light and X-ray energy incident on film.* Another aspect of interest is the rather strikingly low photographic efficiency of direct X-ray exposures, particularly at high quantum energies, compared with that of light exposures. This effect, already known qualitatively, is shown in Fig. 5, where the ratio (X-ray energy incident on film)/(light

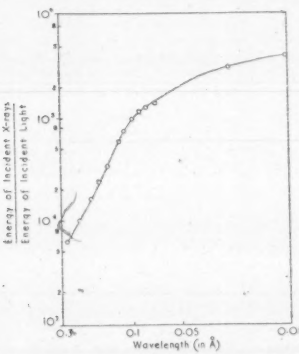

Fig. 5. Ratio (energy of incident X-rays)/(energy of incident light), for a standard density of 0·2 above fog, as a function of wavelength

energy incident on film), for a standard density of 0·2 above fog, is plotted against wavelength. This ratio increases from 6000 to 400 000 between $\lambda = 0{\cdot}275$ Å and 0·01 Å; the incident X-ray energy, even in the most favourable case with soft X-rays, is found to be 6000 times greater than the light energy necessary to produce the same density.

This is explained partly by the fact that the incident light energy is almost completely absorbed by the photographic emulsion, whereas only a fraction of the incident X-ray energy can be absorbed by the emulsion and this fraction decreases the shorter the wavelength applied. Also a very large amount of X-ray energy is wasted, since the X-ray energy is inevitably delivered in quanta each carrying much more energy than is necessary to make the grain developable, as is shown by the comparatively few quanta necessary when exposure is made by visible light.

TEST WITH SOFT RADIATION FROM 0·28–0·56 Å

A few exposures with still softer radiations than those mentioned so far were made in order to check the values obtained by Eggert and Schopper[3] referred to in the introduction. The wavelengths and *h.v.l*'s used for this test are set out in Table 2. Since in Eggert and Schopper's work the radiation apparently passed first through the film and then through the screen, this arrangement has been used for this test only. Eggert and Schopper used monochromatic radiation and their films and screens were of makes different from those used in these experiments. However, a comparison of the results on quantum (Φ) and energy-efficiency (Ω) shows a fair agreement in spite of the differences mentioned above, as is seen from the value quoted in Table 3.

It is almost certainly fortuitous that the two sets of values of Φ and Ω are practically equal at $\lambda = 0{\cdot}56$ Å. The fact that Eggert and Schopper's values decrease with decreasing wavelength while those of the author increase, may be caused by the use of monochromatic and heterogeneous radiation respectively.

Table 2. *Radiations used in test*

λ (Å)	*h.v.l.* (mm Cu)
0·56	0·03
0·46	0·05
0·36	0·1
0·28	0·2

Table 3. *Comparison of quantum-efficiencies and energy-efficiencies according to Eggert and Schopper[3] and to Herz*

	Quantum-efficiency (Φ)		*Energy-efficiency* (Ω)	
λ (Å)	*Eggert and Schopper*	*Herz*	*Eggert and Schopper*	*Herz*
0·56	157	154	2×10^{-2}	2×10^{-2}
0·29	93	—	$6{\cdot}1\times10^{-3}$	—
0·28	—	272	—	$1{\cdot}7\times10^{-2}$

CONCLUSIONS

It has been shown that the variation of the intensifying factor of calcium tungstate screens with wavelength is predominantly caused by the relative absorptions and photographic energy efficiencies of film when used with light or X-rays. The advantage of the screen lies chiefly in its ability to absorb a greater proportion of the incident radiation than the film; this advantage varies from 20 to 130 times, according to wavelength. The light energy produced by the screen is about 60 times as efficient as the same quantity of X-ray energy. The effect of the high photographic efficiency of the light energy produced by the screen is, however, opposed by the loss of energy, about 98–99%, occurring in the conversion of X-ray energy into light energy of the screen.

The accuracy of these investigations is limited and difficult to assess, as it is influenced by various factors, including errors in ionization measurements over a wide range of wavelengths, and in the measurements of the number of light quanta necessary to obtain a given density, and the fact that the spectral light emission of the screen was simulated by using a light emission of a single wavelength to produce the same density. In spite of these and other shortcomings it is believed that the general trend of the results is correct.

ACKNOWLEDGEMENTS

The author wishes to express his appreciation to Mr. J. Boardman, who has carried out the bulk of the experimental work of this investigation, and to Dr. Farnell for valuable discussions.

REFERENCES

(1) TASKER, H. S. *Photogr. J.*, *B*, **85**, p. 75 (1945).
(2) COLTMAN, J. W., EBBIGHAUSEN, E. G., and ALTAR, W. *J. Appl. Phys.*, **18**, p. 530 (1947).
(3) EGGERT, J., and SCHOPPER, E. *Ann. Phys.* [*Leipzig*], **6**, p. 270 (1948).
(4) HERZ, R. H. *Photogr. J.*, *B*, **89**, p. 89 (1949).
(5) MAYNEORD, W. V. *Brit. J. Radiol.*, **13**, p. 235 (1940).
(6) BROMLEY, D., and HERZ, R. H. *Proc. Phys. Soc.* [*London*] *B*, **63**, p. 90 (1950).
(7) HODGSON, M. B. *Phys. Rev.*, **12**, p. 431 (1918).

The production of transparent profiles of dust particles as an aid to automatized particle counting

By R. J. Hamilton, B.Sc., A.Inst.P., and B. A. Phelps, B.Sc., National Coal Board, Mining Research Establishment, Isleworth, Middlesex

[*Paper received* 30 *January*, 1956]

The technique of "shadowing" by metal evaporation in a vacuum has been adapted to the production of plane "negative" images of dust deposits on microscope slides at natural size by vacuum evaporation of metal at right angles to the slide, and subsequent removal of the dust. The slide receives a precise impression of the geometric projections of the particles. The correspondence of image and object is exact. The thickness of the deposited film can be suited to the contrast requirements of an automatic particle counter; further, the film lies in one plane and is only a few hundred Ångström units thick. Many of the optical problems arising from the association of automatic counting techniques with high power light microscopy, namely, depth of focus and variable contrast between particles and background and between different parts of single particles, are avoided by substituting the shadow for the original specimen, as suggested by Whitaker.[7]

It has recently become clear that, before automatized particle counting techniques can be applied to the evaluation of dust samples in the size ranges below 5 μ, attention must be given to the problems arising from the association of such techniques with high power light microscopy.[1]

These problems arise from the following causes: (i) the small depth of focus of high power objectives and the close approach to the limit of optical resolution; (ii) the commonly poor and sometimes false contrast between the finest particles and the background, and between different parts of single particles; (iii) the small quantity of light passed by the objective.

The depth of focus of a 1·8 mm focal length, 1·25 numerical aperture objective, as commonly used for the visual counting of such particles, is 0·4 μ (being approximately inversely proportional to the numerical aperture). This depth of focus is much less than the diameter of many of the dust particles, so that the focus setting of the microscope is dependent on particle size and must be continually readjusted during the appraisal of a specimen. Only gross elaborations could provide such adjustments in automatic devices. An increase in focal depth could only be achieved at the expense of resolving power, which is about 0·2 μ for the objective quoted and thus already comparable with the particle size.

The use of a "split beam" optical system to provide a guard spot accentuates the difficulties caused by depth of focus and resolution limitations. Many materials in thin section are almost transparent. This is particularly noticeable in the case of siliceous rock dust particles which can behave as miniature lenses, appearing to have bright centres (often brighter than the background) and dark edges. The results of these effects will be shown as different scanning levels and multiple counts. The restriction in the quantity of light passed by high power objectives leads to a low signal-to-noise ratio in the counting machine.

An adaptation of the metal shadowing technique already well established in electron microscopy[2] for the production of images of three-dimensional appearance, appeared to have distinct possibilities of solving some, at least, of these optical problems, owing to the ability of a beam of metal atoms propagated in a vacuum to form sharp shadow images of minute objects.

DESCRIPTION OF THE TECHNIQUE

Samples of airborne dusts collected both on microscope cover slips and on microscope slides have been treated. Briefly, the technique consists of the vacuum evaporation of a thin metal film on to the particle-covered surface of the glass followed by the removal of the particles, thus leaving behind transparent profiles, the holes corresponding to the "shadows" cast by the particles. The "shadowing" is carried out normally to the slide so that the holes are images of the projected cross-sections of the particles. The technique is applicable only to samples in which the particles are deposited directly on to a solid base without the use of an adhesive material.

Either of two microscope illumination methods can be used with the resulting specimens. Firstly, normal transmitted light, in which case the particles appear as bright areas on a dark ground, and secondly reflected light, in which case the particles appear as dark areas on a bright ground.

In practice the use of bright images on a dark ground has much in its favour for automatic particle counting purposes. With such specimens, the detecting photocells are quiescent for the background, and provide positive pulses when particles are scanned.

The evaporation process. The metal evaporation process was carried out in a standard Edwards vacuum coating unit (model 12E). Three metals have been used, gold, silver and aluminium, but there seems to be no reason why this range should not be extended if necessary.

The techniques used with the three metals have been described in detail by Williams and Wyckoff.[3] The evaporation of both gold and silver was carried out from a small conical spiral of tungsten wire coated with alundum paste and flashed to form a small crucible. The metal was placed in the crucible and melted in a vacuum by passing a current of about 50 A through the tungsten wire. The evaporating surface was 2·5 mm or less in diameter. Aluminium was evaporated from a hairpin-shaped tungsten filament. High purity aluminium wire was hung on the angle of the filament and a bead formed by heating in a vacuum. With all metals, the evaporation was carried out at a pressure of about 10^{-4} mm of mercury.

In practice, it has been found that the operator can best judge the optical density of the deposited film by watching the brightness of the glowing filament through the darkening film. The filament is white hot during the evaporation process.

For use with automatized counting machines, an attenuation of 90% or more of the incident light seems to be desirable. This is attainable, as shown by Bond,[4] with gold, silver and aluminium films of 270, 220 and 120 Å thickness respectively.

Cover slips and slides have been "shadowed" at a distance of 15 cm from the source. At this distance a source of maximum dimension 2·5 mm gives negligible distortion of small particle sizes. In order that a number of samples can be treated simultaneously, a tubular framework has been constructed, forming an arc of a circle centred upon the metal source and facing downwards to avoid adventitious deposition of atmospheric dust on the specimens.

Using the apparatus described, eight slides or pairs of cover glasses can be treated simultaneously in approximately thirty minutes. The number of specimens in a loading could, if desired, be increased considerably without much trouble.

Removal of particles after shadowing. The particles on the coated slips or slides are most readily removed by a jet of compressed air directed at a very shallow angle to the surface of the glass. It is possible by the use of this method to obtain virtually complete removal of particles without damage to the film. No breakage of cover slips has been caused in this laboratory by the compressed air, although there is possibly a risk of this if they are not supported rigidly.

Under certain conditions it may be more desirable to use a liquid to remove the particles from the coated slides. Except in the case of soluble particles (e.g. methylene blue spheres) such a technique is less efficient than the compressed air method, although quite satisfactory results have been obtained by the use of very dilute solutions of wetting agents (e.g. Teepol) in water applied as a gentle jet over the slide surface. Particularly with gold films, the dust particles, after being moved from their original positions, tend to adhere to the metal when the "liquid cleaning" technique is used and are sometimes very difficult to move further. The application of a high voltage gas discharge for a few seconds after the evaporation process greatly reduces this tendency of the particles to adhere to the metal during the "washing." The equipment for this standard cleaning process of "ionic bombardment" is normally incorporated in vacuum coating units.

Cover slip and slide mounting. It is desirable after treatment to protect the metal film by mounting it so that it lies between slide and cover slip. A standard microscope mounting medium is used, great care being taken when the film is on a cover slip to ensure that cover slip and slide are parallel.

RESULTS

Three photomicrographs are presented of a thermal precipitator rock dust sample, obtained using a 2·2 mm oil-immersion objective. Fig. 1 shows the untreated sample, Fig. 2, after shadowing and by reflected light, and Fig. 3, after shadowing and by transmitted light.

Fig. 1 illustrates clearly the depth of focus problem, since the small particles only are in focus, and readjustment of the microscope would be required for clear delineation of the larger particles. In addition, the misleading and inadequate contrast between particles and background is demonstrated.

The shadowed preparation, Figs. 2 and 3, on the other hand, shows the almost complete relief afforded by this technique from the problems of depth of focus and contrast; formerly ill-defined areas, in the case of larger particles, appearing sharply defined and of uniformly high contrast. It will be clear that these two-dimensional reproductions form ideal specimens for fixed focus counting devices.

Many shadowed dust samples have been prepared for, and used with, two automatic particle counters, the Mullard type 599 instrument in this laboratory, and the Casella particle counter in the British Coal Utilisation Research Association laboratories. With the former instrument, which relies on an optical beam splitting method for the production of "main" and "guard" scanning spots, the performance with shadowed specimens has proved to be incomparably better than with the untreated dust samples. It is true to say that the only limitations with the shadowed slides are those set by the instrument itself, due, in particular, to the small

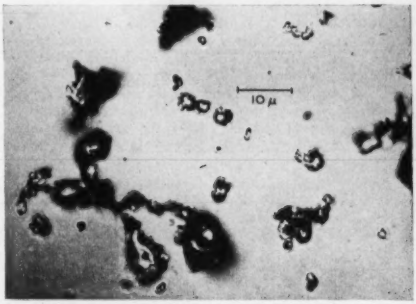

Fig. 1. Rock dust untreated (2 mm objective)

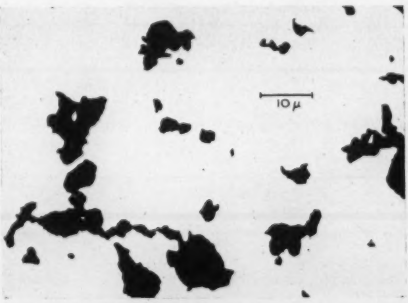

Fig. 2. Shadowed specimen viewed by reflected light

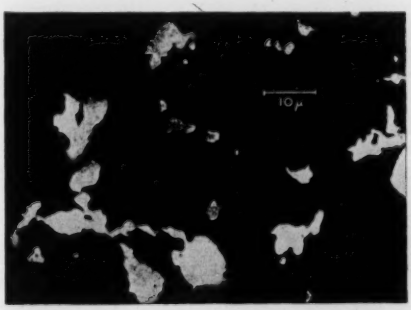

Fig. 3. Shadowed specimen viewed by transmitted light

amount of light available at the highest magnifications. Hawksley[5] has reported a greatly improved performance from the Casella counter also with shadowed specimens, and a reduction in the lower size limit of countable particles below the figure of 5 μ he has quoted[6] for the instrument on conventional dust samples.

ACKNOWLEDGEMENTS

Mr. A Whitaker, Director of Extra Mural Studies in the National Coal Board, is responsible for the original suggestion to use the technique,[7] and the authors are also indebted to Mr. P. G. W. Hawksley for his collaboration.

This paper describes work carried out as part of the Research Programme of the Mining Research Establishment and is published by permission of Dr. W. Idris Jones, Director General of Research in the Scientific Department of the National Coal Board. The views expressed are those of the authors and not necessarily those of the Board.

REFERENCES

(1) WALTON, W. H. *Brit. J. Appl. Phys.*, **5**, *Suppl.* 3, p. S 121 (1954).
(2) MULLER, H. O. *Kolloid. Z.*, **99**, p. 6 (1942).
(3) WILLIAMS, R. C., and WYCKOFF, R. W. G. *J. Appl. Phys.*, **17**, p. 23 (1946).
(4) BOND, W. L. *J. Opt. Soc. Amer.*, **44**, p. 429 (1954).
(5) HAWKSLEY, P. G. W. Private communication (1955).
(6) HAWKSLEY, P. G. W., BLACKETT, J. H., MEYER, E. W., and FITZSIMMONS, A. E. *Brit. J. Appl. Phys.*, **5**, *Suppl.* 3, p. S 165 (1954).
(7) WHITAKER, A. Brit. Prov. Pat. Appl. No. 23135/54 (9 August, 1954).

Measurement of the half-life of radon with a Curie-type ionization chamber

By P. C. MARIN, Clarendon Laboratory, Oxford*

[*Paper received* 17 *October*, 1955]

An improved version of the Curie-type ionization chamber enables an accurate comparison to be made of the ionization currents produced by γ-rays. The ionization current produced by 1 mc of radium can be measured with an accuracy of 0·02%. The linearity of response of this instrument has been investigated for radon sources up to 250 mc, with an argon gas filling. The half-life of radon measured in this way was found to be 3·8229 $\pm$ 0·000 27 days.

An ionization chamber of the type designed by Madame Curie[1] in 1912 was used in this laboratory by Bishop and Wilson[2] for the measurement of the decay constants of ^{24}Na, ^{72}Ga, ^{140}La. The ionization current of the decaying source is compared to that produced by a standard radium source. The voltage it develops by flowing through a high resistor is measured by a zero method using an amplifying valve.

For the purpose of making a photo-neutron standard, it was found necessary to compare radiothorium sources of respectively 0·5 mc and 50 mc or larger with an accuracy of better than 0·1%.

Thus the ionization current of the 0·5 mc source should be known to an accuracy of better than 0·1%. The non-linearity of the apparatus over such a wide range of source strength should be much smaller than 0·1%.

1. DESCRIPTION OF THE INSTRUMENT

The apparatus used (Fig. 1) is basically the same as the one described by Bishop and Wilson.[2] (In particular all the geometrical dimensions have been conserved.) However, several improvements have been made to improve the standards of accuracy and reliability.

The new lead top of the chamber is made from rolled lead. Its thickness (10·02 mm at the centre) is uniform to better than 0·05 mm over a circle of 30 cm diameter and 0·1 mm over all the surface. Its homogeneity was investigated by X-ray and γ-ray techniques and found to be uniform within the experimental errors (2%).

The chamber is sealed off and can be filled with gases other than air through taps (all at a pressure of one atmosphere). The amplifying valve and the resistance are enclosed in an evacuated tank to reduce drifts due to variations of temperature.

The potentiometer which supplies the bias voltage of the grid was calibrated to 0·01%. All the various units except the potentiometer and the galvanometer are housed in a large metal box having thin walls for screening against electrical interference.

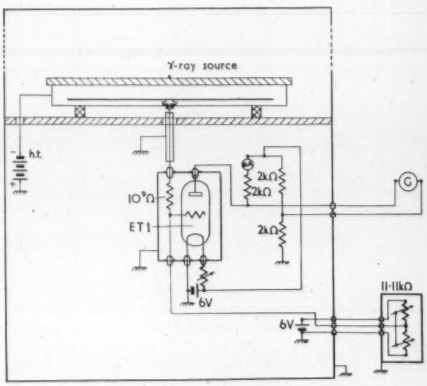

Fig. 1. Schematic diagram of the detection system

* Now at the Laboratoire de Physique de l'Ecole Normale Supérieure, 24 rue Lhomond, Paris 5ème.

2. LINEARITY TESTS

The resistances used for measuring the ionization current were carbon resistances made by Welwyn and Co (high stability pyromatic resistances). They are claimed to be linear to better than 0·002%, for voltages less than 5 V. If no ion recombination takes place inside the chamber, the instrument should then be perfectly linear.

Linearity tests were made in the following way. Two sources of radon adsorbed on charcoal, of very nearly equal strength and small dimensions (1 mm diameter) were used. The ionization current of each source—I_1 and I_2—and of both sources—I_{1+2}—were measured. The ratio $R = (I_1 + I_2 - I_{1+2})/(I_1 + I_2)$ gives a measure of the non-linearity of the instrument.

When filled with air, large deviations from linearity were observed up to 0·7% for a strength of each source of 100 mc. This value is much larger than the expected one.

The discrepancy was traced to a small ionization current collected *outside* the chamber and was decreased as much as possible: firstly by reducing the length of the connecting lead to the electrometer valve and by using a screened lead; secondly by filling the chamber with argon which has a larger stopping power than air, for secondary electrons (1·5 times). Any residual non-linearity due to an ionization current collected outside the chamber is correspondingly reduced.

Table 1 shows the non-linearity as a function of the source strength S_{1+2}, expressed as a percentage for an argon filling and a collecting voltage of 500 V. The non-linearity, if any, is extremely small.

that. This means that the relative error on the current I is approximately constant in the range 300 to 4·5 mc, a result which differs quite markedly from the ones at lower strengths (see next section).

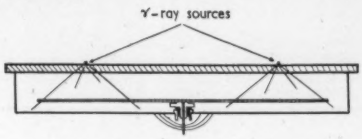

Fig. 2. Diagram of the Curie chamber

A probable explanation for this is that for sources strengths above a few millicuries the largest part of the error comes from the small changes in position of the sources on the top of the chamber. On the contrary for sources strengths below 1 mc, statistical fluctuations of the current contribute for most part of the error, which increases towards the small intensities.

The figures for the three measurements are:

$$T_1 = 91{\cdot}774 \pm 0{\cdot}012 \text{ h}$$
$$T_2 = 91{\cdot}731 \pm 0{\cdot}017 \text{ h}$$
$$T_3 = 91{\cdot}758 \pm 0{\cdot}010 \text{ h}$$

Combining the three values and the errors as usual gives: $T = 91{\cdot}749 \pm 0{\cdot}007$ hours or $3{\cdot}8229 \pm 0{\cdot}000\,27$ days.

Table 1. *Variation of the non-linearity by $\Delta I/I$ with the source strength*

$S_1 + S_2$ in mc	294	261	252	222	171	120	106	75
$\Delta I/I$ in %	+0·035	−0·063	−0·001	−0·047	+0·040	−0·062	−0·055	−0·055
$S_1 + S_2$ in mc	57	30·4	13·5	11·3	9·4	3·5	2·4	1·7
$\Delta I/I$ in %	+0·126	+0·058	+0·047	−0·030	+0·103	−0·027	+0·010	+0·076

3. HALF-LIFE OF RADON

The half-life of radon was measured by following the decay of the three currents for 454 h. They were compared to the ionization current produced by a radium standard of 250 mc. Both sources S_1 and S_2 decayed from 150 mc down to 4·5 mc and S_{1+2} from 300 mc to 9 mc.

Table 2. *Average deviation of the measured values from the least squares fit, for each curve*

	Log I_1	Log I_2	Log I_{1+2}
$\overline{di^2}$ for $0 < t < 216$ h	$0{\cdot}154 \times 10^{-6}$	$0{\cdot}207 \times 10^{-6}$	$0{\cdot}051 \times 10^{-6}$
$\overline{di^2}$ for $216 < t < 454$ h	$0{\cdot}016 \times 10^{-6}$	$0{\cdot}257 \times 10^{-6}$	$0{\cdot}157 \times 10^{-6}$

The half-life was computed by the least squares method. The same weight was given to each point on the logarithmic plot. This can be justified from the measurements in the following way. If one calls the differences $d_i = y_0 - y$, between the measured values, and the least squares fit, the values of d_i do not show any definite sign of increase towards the small intensities as can be seen from Table 2. On this table the average $\overline{di^2}$ have been worked out for the first and the second half of the three curves. A weight of $1/I$ for the logarithmic plot would be justified by a 5 to 1 ratio between the two values. The average increase, if any, is much smaller than

The error quoted above is the probable error. These results are in good agreement with the previous results of Curie and Chamié,[3] 3·823 ± 0·002 days, and Bothe,[4] 3·825 ± 0·003 days.

4. ACCURACY IN THE COMPARISON OF γ-RAY SOURCE

As examples the measurements are given in Table 3 of the ratio of a 50 mc source of RdTh to a 6·4 one and of a 6·4 mc to a 0·67 mc source.

Table 3. *Measurements of ratios of source strengths*

$R = I_{50mC}/I_{6\cdot4mC}$	δR	$R = I_{6\cdot4mC}/I_{0\cdot67mC}$	δR
7·818	$2{\cdot}8 \times 10^{-3}$	9·569	$8{\cdot}6 \times 10^{-3}$
7·815	0·2	9·554	6·4
7·816	0·8	9·553	7·4
7·814	1·2	9·557	3·4
7·816	0·8	9·554	6·4
7·817	1·8	9·564	3·4
7·812	3·2	9·574	13·6
7·814	1·2	9·558	2·4
Average: 7·815[2]		Average: 9·560[4]	
Standard deviation	$\epsilon = 2{\cdot}4 \times 10^{-4}$	Standard deviation	$\epsilon = 8{\cdot}1 \times 10^{-4}$

The standard deviations have been worked out and show that the degrees of accuracy which are obtainable in making several intercomparisons of sources are 10^{-4} in the first case, and 2 or 3×10^{-4} in the second case.

ACKNOWLEDGEMENTS

I would like to express my thanks to Prof. H. Halban and to Dr. G. R. Bishop for their advice during this work, to Mr. V. Round for his help in building the chamber, to Mr. Gregory (U.K. Atomic Energy Authority, Harwell) for the machining of the lead top and to Mr. Derbyshire (U.K. Atomic Energy Authority, Harwell) for the X-ray and the γ-ray tests of its uniformity.

REFERENCES

(1) CURIE. *J. Phys. Radium*, Ser. 5, **11**, p. 795 (1912).
(2) WILSON, R., and BISHOP, G. R. *Proc. Phys. Soc. [London]*, **62**, p. 457 (1949).
(3) CURIE, I., and CHAMIÉ, C. *J. Phys. Radium*, **5**, p 238 (1924).
(4) BOTHE, W. *Z. Phys.*, **16**, p. 266 (1923).

A photoelastic method of two-dimensional separation of stresses along a line of symmetry by using the isochromatic fringes only

By S. P. CHRISTODOULIDES, B.Sc., Ph.D., A.M.I.C.E., Dipl.Phys-Maths.,* University College, London

[*Paper received* 22 *August*, 1955]

Examination of the general equations of equilibrium in curvilinear co-ordinates for a two-dimensional model shows that when these are applied to points on an axis of symmetry, the isochromatics and their orthogonals being taken as axes of co-ordinates, an equation of the same form as the Lamé–Maxwell equations is obtained, and this leads to a method of separating the stresses on an axis of symmetry by the use of the isochromatic fringes only.

The equations of equilibrium, or body-stress equations, in two-dimensional stress systems, are used both in theoretical and experimental investigations. The simple forms in which these equations are usually obtained are those referring to Cartesian co-ordinates, and polar co-ordinates.

Another case of the equations applied in experimental elasticity, particularly in photoelasticity, are the equations known as the Lamé–Maxwell equations. These refer to the envelopes of the principal stresses, often called the principal stress trajectories.

In each of these cases the equations of equilibrium are referred to a system of orthogonal co-ordinates. General expressions are established below in which the equations of equilibrium are referred to any system of orthogonal curvilinear co-ordinates. All other forms of equations can be derived from these general expressions.

THE GENERAL FORM OF THE BODY-STRESS EQUATIONS

It can be shown that the body-stress equations can be expressed in complex potentials by one equation,[1] i.e.

$$\frac{\partial \Phi}{\partial z} + \frac{\partial(\Theta - 2\rho V)}{\partial \bar{z}} = 0 \qquad (1)$$

(see Fig. 1).

where x, y are the Cartesian co-ordinates of the point M; $\widehat{xx}$, $\widehat{yy}$, $\widehat{xy}$ the stresses referred to these axes: $z = x + iy$; $\bar{z} = x - iy$; $\Phi = \frac{1}{2}(\widehat{xx} - \widehat{yy} + 2i\widehat{xy})$; $\Theta = \widehat{xx} + \widehat{yy}$; $\rho =$ density; $V =$ body force potential.

Since:

$$\partial z = \partial s \exp\left[i(\tfrac{1}{2}\pi + \theta)\right] = i\partial s \exp(i\theta), \text{ on the } s\text{-curve}$$

$$\partial z = \partial n \exp(i\theta), \text{ on the } n\text{-curve}$$

$$\partial z/\partial s = i \exp(i\theta); \quad \partial z/\partial n = \exp(i\theta) \qquad (2)$$

hence:

$$\left.\begin{aligned} \frac{\partial}{\partial n} &= \exp(i\theta)\frac{\partial}{\partial z} + \exp(-i\theta)\frac{\partial}{\partial \bar{z}} \\ \frac{\partial}{\partial s} &= i\exp(i\theta)\frac{\partial}{\partial z} - i\exp(-i\theta)\frac{\partial}{\partial \bar{z}} \end{aligned}\right\} \qquad (3)$$

or:

$$\frac{\partial}{\partial \bar{z}} = \tfrac{1}{2}\exp(i\theta)\left(\frac{\partial}{\partial n} + i\frac{\partial}{\partial s}\right) \qquad (4)$$

$$\frac{\partial}{\partial z} = \tfrac{1}{2}\exp(-i\theta)\left(\frac{\partial}{\partial n} - i\frac{\partial}{\partial s}\right) \qquad (5)$$

so equation (1) becomes:

$$\exp(-i\theta)\left(\frac{\partial}{\partial n} - i\frac{\partial}{\partial s}\right)\Phi + \\ + \exp(i\theta)\left(\frac{\partial}{\partial n} + i\frac{\partial}{\partial s}\right)(\Theta - 2\rho V) = 0 \qquad (6)$$

Let the xMy-axes be turned through an angle θ in a counter-clockwise direction, until they coincide with the nMs-axes. If the new stress-combinations are Φ_0, Θ_0,

$$\left.\begin{aligned} \Phi_0 &= \widehat{nn} - \widehat{ss} + 2i\widehat{ns} = \Phi\exp(-2i\theta) \\ \Theta_0 &= \widehat{nn} + \widehat{ss} = \Theta \end{aligned}\right\} \qquad (7)$$

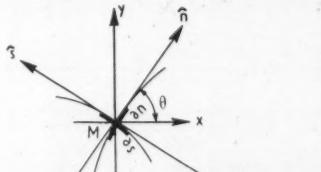

Fig. 1

* Now at Ove Arup and Partners, London, W.1

Equation (6) then becomes:

$$\exp(-i\theta)\left(\frac{\partial}{\partial n} - i\frac{\partial}{\partial s}\right)\Phi_0 \exp(2i\theta) + \\ + \exp(i\theta)\left(\frac{\partial}{\partial n} + i\frac{\partial}{\partial s}\right)(\Theta_0 - 2\rho V) = 0 \quad (8)$$

By taking $\exp(2i\theta)$ through the operators in the brackets, simplifying, re-arranging, and equating the real and imaginary parts to zero, we have:

$$\left.\begin{aligned} \frac{\partial}{\partial n}(\widehat{nn} - \rho V) + \frac{\widehat{nn} - \widehat{ss}}{\rho_s} + \frac{\partial \widehat{ns}}{\partial s} - \frac{2\widehat{ns}}{\rho_n} = 0 \\ \frac{\partial}{\partial s}(\widehat{ss} - \rho V) + \frac{\widehat{nn} - \widehat{ss}}{\rho_n} + \frac{\partial \widehat{ns}}{\partial n} + \frac{2\widehat{ns}}{\rho_s} = 0 \end{aligned}\right\} \quad (9)$$

where $\rho_n = \partial n/\partial\theta$, $\rho_s = \partial s/\partial\theta$, the radii of curvature of the n- and s-curves respectively.

Equations (9) are the general form of the equations of equilibrium referred to orthogonal curvilinear co-ordinates.

For no body force $V = 0$, and equations (9) become:

$$\left.\begin{aligned} \frac{\partial \widehat{nn}}{\partial n} + \frac{\partial \widehat{ns}}{\partial s} + \frac{\widehat{nn} - \widehat{ss}}{\rho_s} - \frac{2\widehat{ns}}{\rho_n} = 0 \\ \frac{\partial \widehat{ss}}{\partial s} + \frac{\partial \widehat{ns}}{\partial n} + \frac{\widehat{nn} - \widehat{ss}}{\rho_n} + \frac{2\widehat{ns}}{\rho_s} = 0 \end{aligned}\right\} \quad (10)$$

PARTICULAR CASES

(*a*) *Equations of equilibrium in Cartesian co-ordinates.* If $\hat{n}$, $\hat{s}$ are the directions of x, and y in the Cartesian system,

$$\rho_n = \rho_s = \infty$$

and equations (10) become:

$$\left.\begin{aligned} (\partial \widehat{xx}/\partial x) + (\partial \widehat{xy}/\partial y) = 0 \\ (\partial \widehat{yy}/\partial y) + (\partial \widehat{yx}/\partial x) = 0 \end{aligned}\right\} \quad (11)$$

These are the well-known equations of equilibrium in Cartesian co-ordinates.[2]

(*b*) *Equations of equilibrium in polar co-ordinates.* Here the n-curve is a straight line (Fig. 2), and the s-curve a circle of radius r.

Since $\widehat{nn} = \widehat{rr}$, $\widehat{ss} = \widehat{\theta\theta}$

$\widehat{ns} = \widehat{r\theta}$

and $\rho_n = \infty$, $\rho_s = r$, $ds = rd\theta$

equations (10) become:

$$\left.\begin{aligned} \frac{\partial \widehat{rr}}{\partial r} + \frac{\widehat{rr} - \widehat{\theta\theta}}{r} + \frac{\partial \widehat{r\theta}}{r\partial\theta} = 0 \\ \frac{\partial \widehat{\theta\theta}}{r\partial\theta} + \frac{2\widehat{r\theta}}{r} + \frac{\partial \widehat{r\theta}}{\partial r} = 0 \end{aligned}\right\} \quad (12)$$

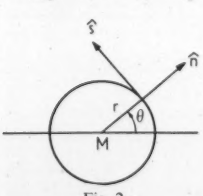

Fig. 2

Equations (12) are the equations of equilibrium in polar co-ordinates.[3]

(*c*) *Lamé–Maxwell equations.* If the n-, and s-curves are the principal stress trajectories, $\widehat{ns} = 0$, and equations (10) become:

$$\left.\begin{aligned} \frac{\partial \widehat{nn}}{\partial n} + \frac{\widehat{nn} - \widehat{ss}}{\rho_s} = 0 \\ \frac{\partial \widehat{ss}}{\partial s} + \frac{\widehat{nn} - \widehat{ss}}{\rho_n} = 0 \end{aligned}\right\} \quad (13)$$

These are the Lamé–Maxwell equations.[2]

THE GENERAL EQUATIONS IN TERMS OF THE PRINCIPAL STRESSES

Let P, Q be the principal stresses (Fig. 3), at a point M.

Taking $P + Q = T$

$P - Q = R$

$\phi = \theta - \alpha$

it is found that

$$\left.\begin{aligned} \widehat{nn} = \frac{T + R\cos 2\phi}{2}; \quad \widehat{ss} = \frac{T - R\cos 2\phi}{2} \\ \widehat{ns} = \frac{-R\sin 2\phi}{2}; \quad \widehat{nn} - \widehat{ss} = R\cos 2\phi \end{aligned}\right\} \quad (14)$$

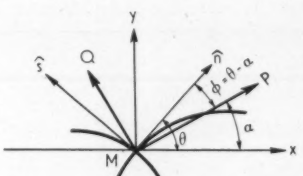

Fig. 3

Substituting these expressions in (10), and re-arranging, we have:

$$\left.\begin{aligned} \frac{\partial T}{\partial n} + \cos 2\phi\frac{\partial R}{\partial n} - \sin 2\phi\frac{\partial R}{\partial s} + \\ + 2R\left(\cos 2\phi\frac{\partial \alpha}{\partial s} + \sin 2\phi\frac{\partial \alpha}{\partial n}\right) = 0 \\ \frac{\partial T}{\partial s} - \cos 2\phi\frac{\partial R}{\partial s} - \sin 2\phi\frac{\partial R}{\partial n} - \\ - 2R\left(\sin 2\phi\frac{\partial \alpha}{\partial s} - \cos 2\phi\frac{\partial \alpha}{\partial n}\right) = 0 \end{aligned}\right\} \quad (15)$$

Equations (15) are the equations of equilibrium referred to orthogonal curvilinear co-ordinates and expressed in terms of the principal stresses.

The following particular cases where the photoelastic curves are used, are given below. It is known that by photoelastic observations the isoclinics and isochromatics can be obtained.

An isoclinic is the locus of points at which the principal stresses are parallel to a given direction, i.e. arg. Φ = constant.

An isochromatic is the locus of points at which the principal stress differences are equal to a given constant, or mod. Φ = constant.

(*a*) If the isoclinics are taken as *s*-curves, then $\partial\alpha/\partial s = 0$, and equations (15) become:

$$\left.\begin{aligned}\frac{\partial T}{\partial n} + \cos 2\phi\,\frac{\partial R}{\partial n} - \sin 2\phi\,\frac{\partial R}{\partial s} + 2R\sin 2\phi\,\frac{\partial \alpha}{\partial n} = 0\\ \frac{\partial T}{\partial s} - \cos 2\phi\,\frac{\partial R}{\partial s} - \sin 2\phi\,\frac{\partial R}{\partial n} + 2R\cos 2\phi\,\frac{\partial \alpha}{\partial n} = 0\end{aligned}\right\} \quad (16)$$

If a model has a line of symmetry, the latter coincides with the 0°, or 90° isoclinic. Along this line $\phi = 0$, $\theta = \alpha$ (see Fig. 4).

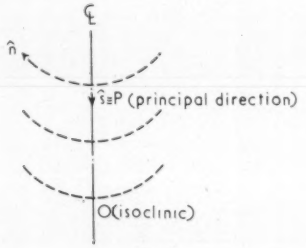

Fig. 4

Equations (16) then simplify to:

$$\left.\begin{aligned}\frac{\partial T}{\partial n} + \frac{\partial R}{\partial n} = 0\\ \frac{\partial T}{\partial s} - \frac{\partial R}{\partial s} + 2R\,\frac{\partial \alpha}{\partial n} = 0\end{aligned}\right\} \quad (17)$$

The first of equations (17) is an identity. The second one simplifies to:

$$\frac{\partial Q}{\partial s} + (P - Q)\,\frac{\partial \alpha}{\partial n} = 0 \quad (18)$$

where $\partial n/\partial\alpha = \partial n/\partial\theta =$ the radius of curvature of the curves orthogonal to the 0° isoclinic.

It can be seen that equation (18) is of the same form as the Lamé–Maxwell equations (13); therefore, at any point on a line of symmetry, the principal stress trajectory and the orthogonal curve to the isoclinic at the point have the same curvature.

(*b*) If the isochromatics are taken as the *s*-curves, then $\partial R/\partial s = 0$, and equations (15) become:

$$\left.\begin{aligned}\frac{\partial T}{\partial n} + \cos 2\phi\,\frac{\partial R}{\partial n} + 2R\left(\cos 2\phi\,\frac{\partial \alpha}{\partial s} + \sin 2\phi\,\frac{\partial \alpha}{\partial n}\right) = 0\\ \frac{\partial T}{\partial s} - \sin 2\phi\,\frac{\partial R}{\partial n} - 2R\left(\sin 2\phi\,\frac{\partial \alpha}{\partial s} - \cos 2\phi\,\frac{\partial \alpha}{\partial n}\right) = 0\end{aligned}\right\} \quad (19)$$

In a model with a line of symmetry, the latter is an orthogonal curve to the isochromatics (see Fig. 5).

In this case, it can be shown that the second of equations (19) simplifies to an identity, and the first one to the equation:

$$\frac{\partial P}{\partial n} + (P - Q)\,\frac{\partial \alpha}{\partial s} = 0 \quad (20)$$

Here, $\partial s/\partial\alpha = \partial s/\partial\theta =$ the radius of curvature of the isochromatics.

A comparison of equation (20) with the Lamé–Maxwell equations (13) shows that the two equations are of the same form and that at any point on a line of symmetry, the principal stress trajectory and the isochromatic at the point have the same curvature.

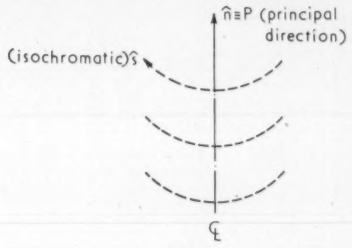

Fig. 5

SEPARATION OF STRESSES ALONG A LINE OF SYMMETRY

In two-dimensional photoelastic work, the values of the principal stress differences, and the principal directions can be observed.

To obtain the separate principal stresses along a line of symmetry, it is normal practice in photoelasticity, at present, to use the Lamé–Maxwell equations and carry out a step-by-step integration. In this case the principal stress trajectories are used, and the integration is started from a point on the line of symmetry where one principal stress is known.

Alternative methods can be deduced from equations (18) and (20). The use of equation (18) would involve the values of the relative retardation and the curvature of the orthogonal curves to the isoclinics; the use of equation (20) would involve the values of the relative retardation and the curvature of the isochromatics. Of the two sets of curves, the isochromatics are obtained directly as smooth curves and their curvature may in many cases be measured with reasonable accuracy from a photograph.

A simple practical method of measuring the curvature of the photographed isochromatics is by using a logarithmic curve (see Fig. 6 in which numbers denote the radii of curvature in centimetres).

At any point on a logarithmic curve the angle between the tangent and the polar ray is constant, say α.

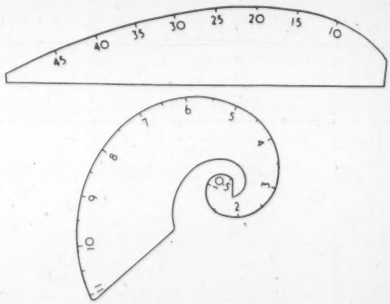

Fig. 6

Separation of stresses by using the isochromatics

Measurements obtained from photograph (Fig. 8)

Distance from straight line boundary (cm)	*Fringe value* $(Q - P)$ *(wavelengths)*	*Radius of curvature of isochromatics* (ρ) (cm)	$(Q - P)/\rho$ *(wavelengths)*
0·75	2	4·5	−0·44
1·85	3	4·0	−0·75
2·70	4	9·0	+0·44
3·15	5	4·5	+1·11
3·42	6	4·0	+1·50
3·62	7	3·75	+1·87

Integration by equation $(\partial P/\partial n) + (P - Q)(\partial x/\partial s) = 0$

Distance from straight line boundary (cm)	$Q - P/\rho$ *ordinate read off graph*	*Multiplier*		*Product*	*Sum*	*Area*	*Total area* $= P$ *(wavelengths)*	$Q - P$ *(wavelengths)*	Q *(wavelengths)*
0	0	1	Simpson's rule	0			0	1·6	1·6
0·5	−0·22	4		−0·88			(−0·15)	1·8	1·65
1·0	−0·63	1		−0·63	−1·51	$\times\frac{1}{3} \times 0{\cdot}5 = -0{\cdot}25$	−0·25	2·1	1·85
1·5	−0·80	4		−3·20			(−0·62)	2·7	2·08
2·0	−0·55	1		−0·55	−4·38	$\times\frac{1}{3} \times 0{\cdot}5 = -0{\cdot}73$	−0·98	3·1	2·12
2·0	−0·55	1		−0·55					
2·4	0	1		0	−0·55	$\times\frac{1}{2} \times 0{\cdot}4 = -0{\cdot}11$	−1·09	3·5	2·41
2·4	0	1		0					
3·0	0·80	1		0·80	0·80	$\times\frac{1}{2} \times 0{\cdot}6 = 0{\cdot}24$	−0·85	4·5	3·65
3·5	1·65	1		1·65	2·45	$\times\frac{1}{2} \times 0{\cdot}5 = 0{\cdot}61$	−0·24	6·3	6·06
3·7	2·0	1		2·0	3·65	$\times\frac{1}{2} \times 0{\cdot}2 = 0{\cdot}36$	+0·12 (closing error)	7·3	7·42

Where Simpson's rule has not been used, the areas of figures were calculated either as for triangles or trapeziums.
Numbers in brackets are values obtained from graph on Fig. 8.
Negative values are for compression, positive values are for tension.

If r, θ are the polar co-ordinates, s the length of arc of the logarithmic curve measured from a point such that for $r = 0$, $s = 0$, and K a constant, then

$$r = K \exp(\theta \cot \alpha)$$

$$\rho = r/\sin \alpha$$

and $$s = r/\cos \alpha$$

Therefore $$\rho = s \cot \alpha$$

i.e. the radius of curvature is proportional to the arc.

Fig. 6 shows two celluloid templates cut to the shape of logarithmic curves for measuring radii of curvature from 0·5 to 50 cm.

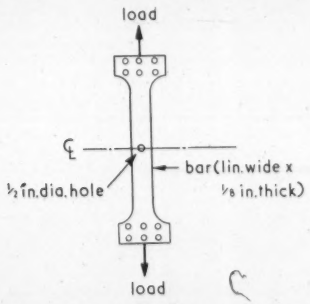

Fig. 7

Example. Fig. 7 shows a model made of Araldite B, hot setting resin loaded cold in tension as shown. A photograph of the isochromatics in dark field is given on Fig. 8. Integration is carried out along the centre line.

The measurements taken on this photograph and the calculations for obtaining the values of the principal stresses

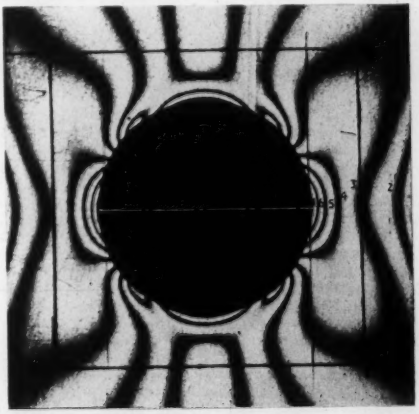

Fig. 8

P and Q are given in the table. The graphs for the principal stress difference $Q - P$, the ratio $(Q - P)/\rho$, where ρ is the radius of curvature of the isochromatic, and the principal stresses are given on Fig. 9.

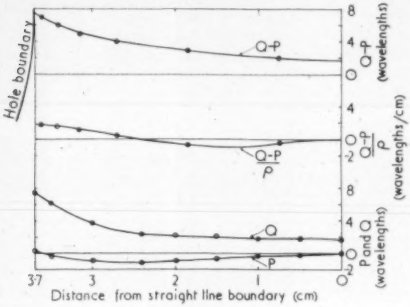

Fig. 9

The radii of curvature of the isochromatics were measured by using the celluloid templates, shown in Fig. 6. For these measurements to be made accurately the following considerations were found to be necessary.

The radius of curvature of the isochromatics may change rapidly as they move away from the line of symmetry and care must be taken to match the curvature of the template and the isochromatic curve for the shortest possible length of the curve.

Since, however, the radius of curvature is the same for the stress trajectories and the isochromatics on a line of symmetry, the known values of the radius of curvature for the stress trajectories on the free boundaries can be used.

CONCLUSIONS

When the general equations of equilibrium are referred to the isoclinics and their orthogonal trajectories, or the isochromatics and their orthogonal trajectories or the principal stress trajectories, they are of the same form on a line of symmetry.

From this similar form, it is deduced that the radius of curvature is the same for any of the curves: the orthogonal to the isoclinics, the isochromatics, and one of the principal stress trajectories, at any point on a line of symmetry. Therefore, in the case of a model with a line of symmetry, the principal stresses can be separated by taking a photograph of the isochromatic pattern and integrating along the line of symmetry by using the above form of equation.

ACKNOWLEDGEMENTS

The author wishes to express his thanks to Colonel H. T. Jessop and Mr. A. C. Stevenson for their encouragement and help without which this work could not have been possible.

REFERENCES

(1) STEVENSON, A. C. *Proc. Roy. Soc. A*, **184**, p. 129 (1945).
(2) JESSOP, H. T., and HARRIS, F. C. *Photoelasticity* (London: Cleaver-Hume Press Ltd., 1949).
(3) TIMOSHENKO, S. *Theory of Elasticity* (New York: McGraw-Hill Book Co., 1934).

NOTES AND NEWS

New books

Mechanical properties of textile fibres. Edited by R. MEREDITH. (Amsterdam: North Holland Publishing Co., 1956.) Pp. xiii + 333. Price 61*s*.

This addition to the series of monographs on the rheological behaviour of materials is particularly welcome. It covers in a comprehensive manner the whole range of fibres. As would be expected, large sections are devoted to cellulosic fibres and the natural protein fibres, the latter being dealt with by L. Peters and H. J. Woods, but the more recent synthetic materials also receive adequate attention.

The aspects of mechanical properties which are treated include relaxation and creep phenomena, stress-strain characteristics, tensile strength, dynamic properties, resilience and permanent set. The treatment is not limited to the presentation of experimental data, but includes an account of the principal theoretical methods which have been proposed for the interpretation and correlation of the observations.

There are a few misprints, and the X-ray diffraction photograph of stretched rubber is mistakenly stated to correspond to 70% stretch. Apart from these small points, however, the book is well produced and can be recommended to research workers and others who are interested in fibre properties.

L. R. G. TRELOAR

Nuclear magnetic resonance. By E. R. ANDREW. (London: Cambridge University Press, 1955.) Pp. xi + 265. Price 35*s*.

Transitions between the energy levels of a nuclear magnetic moment can be induced by suitable radio-frequency fields, and a study of these transitions may give information not only of nuclear properties but also of the nuclear environment, i.e. of the presence and movement of other magnetic atoms.

Since the first observations of this phenomena a decade ago some hundreds of papers have been published on it and Prof. Andrew's book is as much a textbook on an established subject as it is a monograph. He describes in a clear and pleasant manner the basic concepts necessary, experimental methods, and the type of information obtained concerning nuclear properties and the atomic or molecular structure and kinetics of a wide variety of substances. The emphasis throughout is on methods of experiment and interpretation of results, the finer theoretical details being relegated to appendices or mentioned with a reference to the original paper. The bibliography is therefore an essential part of the book, and is fairly complete, containing some five hundred items published up to the middle of 1954.

Since the book deserves to be read by a wide variety of

workers it is unfortunate that the price is higher than is usual in this series. J. H. MITCHELL

Guidance, principles of guided missile design. By A. S. LOCKE. (New York: D. Van Nostrand Co. Inc.; London: Macmillan and Co. Ltd., 1956.) Pp. xvii + 729. Price 90*s*.

This book is one of a series of volumes on principles of guided missile design and contains some 700 pages arranged in twenty chapters. A good deal of the material has been contributed by specialists in the topics which are dealt with.

The author of this book starts under a severe handicap in that much of the material that he would no doubt like to use is subject to security restrictions. The book therefore deals with the principles involved in missile guidance. A large number of topics have necessarily to be covered in such a work. Included are chapters on radio propagation, on infra-red transmission and detection, on servo theory, radar techniques, missile aerodynamics, and on the measurement of missile motion by gyroscopes and accelerometers. Other chapters deal with guidance systems, tactical considerations, launching, and flight-path kinematics.

It is not possible to give a thorough treatment to such a vast range of subjects in a single volume. One of the principal criticisms of the book is that the treatment of the various subjects is uneven. For instance, the chapter on servo theory contains a fairly detailed mathematical treatment, while only a simple descriptive account is given in the chapter on gyroscopes and accelerometers. It is difficult to see what point there is in including a chapter on mathematical groundwork. It is not possible to deal adequately with the Laplace transform method of solving integro-differential equations, with complex variable theory, and with probability theory in less than fifty pages, and most of this mathematics is not needed to understand the remainder of the book. The chapter which deals with radar techniques is sketchy and covers a tremendous range of subjects in some eighty pages. Despite these criticisms some topics are treated very well, the chapters on infra-red technique and on flight-path kinematics being worthy of special mention.

As an introduction to missile guidance, the book is undoubtedly a valuable contribution. It contains a great deal of information which has not hitherto been available in a single volume, and will be welcomed by many engaged on guided missile work. It does not wholly succeed, however, in its object of giving a balanced account of the principles involved in missile guidance. R. A. G. DUNKLEY

Schaltungstheorie und Messtechnik des Dezimeter und Zentimeter-Wellengebietes. By A. WEISSFLOCH. (Basel: Verlag Birkhauser, 1955.) Pp. 308. Price DM33.50.

The book contains four chapters covering (1) the theory of linear transformations; (2) transmission line theory, waveguide theory and measurement techniques; (3) $2n$-terminal ($n > 2$) networks; (4) matching. The first chapter, being of fundamental importance for the rest of the book, covers almost exactly one third of its volume.

It is well known in research that two entirely different lines of approach, the analytical and the experimental, are always possible and real success can be expected when they are combined together in a judicious manner. The author leans heavily towards the analytical methods and the book will mainly appeal to those who have a particular flair for this type of approach.

The first chapter is devoted to the dicussion of the bi-linear transformation $w = (az + b)/(cz + d)$ examples being taken exclusively from the theory of four-terminal networks. This forms the theoretical basis for the rest of the book where some more elementary problems in the transmission line theory and wave-guide theory are treated. The corresponding measurement techniques in the microwave range are explained adequately in principle. The practical side of the measurement is not discussed. The last two chapters, mainly dealing with cable and waveguide junctions, resonators, microwave filters and broad-band matching, tend to be rather condensed and even sketchy. In the opinion of the reviewer the book would have profited greatly by a considerable enlargement of these two chapters and consequent inclusion of more up-to-date material, especially in the field of multiple junctions and their broad-band behaviour. The fact that the manuscript was ready as early as 1946 resulted possibly in an understandable bias against the more recent work in this field.

On the whole the book is very stimulating as a mental *tour de force* in unifying all the aspects of the network theory under the aegis of bi-linear transformations, but it contains little of essential interest to the engineer or physicist interested in the day-to-day problems in the design of microwave circuits.

The typography of the book is exemplary. It is to be regretted, however, that the author considered it necessary to change the standard notation in several places. The use of Gothic characters for vector or complex quantities in preference to heavy type is well established in the German scientific literature, but it seems difficult to see why $\mathfrak{z} = R + jX$ should be written $\mathfrak{R} = R + jX$ or even worse, why $\mathfrak{y} = G + jB$ should be written $\mathfrak{G} = G + jY$(!) Surely, these two definitions, one would have thought, hardly needed an alteration. It is also to be regretted that a propagation constant of $\beta + j\alpha/2l$ is used instead of $\alpha + j\beta$ which is at least one of the established conventions, except probably for the microwave valve work, where $\alpha - j\beta$ is generally preferred. Another departure, a little less distracting, is the author's choice of the numeral 1 for the output terminals, and numeral 2 for the input terminals of all four terminal networks.

Summing up, the book is probably of value to many research workers as a stimulating literature and it should be found in most libraries of various research laboratories, but it could hardly be recommended for a private library, which by necessity must be of a more limited and essential nature. P. A. LINDSAY

Reactor handbook: materials. Edited by J. F. HOGERTON and R. C. GRASS. Prepared by the U.S. Atomic Energy Commission. (London: McGraw-Hill Publishing Co. Ltd., 1955.) Pp. 614. Price 79*s*.

This volume deals with the properties of a wide range of reactor materials, ranging from fuels through moderators, structural and control materials to the most commonly used shielding material, concrete. The nuclear properties required of a material to be used for any of these different functions are dealt with in detail in other volumes of the reactor handbook. Here, information is provided for the reactor designer on extraction, fabrication, mechanical properties, corrosion and health hazards, in an impressive survey of work carried out by the U.S. Atomic Energy Commission. The security regulations prevailing at the time of publication did not permit any extensive discussion of the effects of radiation on the properties of the materials, but most of the other relevant aspects are covered in detail.

The difficult task of selection has been successfully accomplished. Thus, while attention is naturally centred on materials such as zirconium, which owe their rapid develop-

ment largely to their use in reactor applications, a considerable amount of space is devoted to the properties of better known materials, such as stainless steels, which are widely used in reactor construction; exotic carbides and hydrides are covered, but do not displace concrete.

G. H. KINCHIN

Advanced calculus; an introduction to classical analysis. By L. BRAND. (London: Chapman and Hall, Ltd.; New York: John Wiley and Sons Inc., 1955.) Pp. xii + 574. Price 68*s*.

This book, written by the Head of the Department of Mathematics in the University of Cincinnati, is correctly described by its sub-title. With a special emphasis on fundamental concepts, and a keen regard for rigour, it is a book for students of advanced mathematics.

The first chapter opens with the definition of a group, and like the beginning of some other books on the calculus is forbidding and can be skipped on a first reading. There follows a logical and lucid treatment of functions of a real variable, including the usual work on convergence, continuity, differentiation and integration. There is a useful chapter on vector algebra and calculus, providing an introduction to grad, div and curl, which is linked with later chapters on line and multiple integrals. Another chapter is devoted to functions of a complex variable, including some contour integration, and there is a final chapter on Fourier series, which are treated entirely from a mathematical point of view, there being no mention of the theory of heat, presumably as differential equations are regarded as outside the scope of the book.

It is good to see included, however, iterative solutions of equations, some discussion of various approximations and errors. It is an attractive addition to mathematical textbooks.

The printing and binding of the book are examples of the prevailing high American standards.

J. TOPPING

The present state of physics. Arranged by F. S. BRACKETT. (Washington: American Association for the Advancement of Science, 1954.) Pp. vi + 265. Price 60*s*.

This volume is the record of a symposium presented at the New York meeting of the American Association for the Advancement of Science on 30 December, 1949. It is difficult to understand why publication has been delayed for five years and no reason is given by Dr. Karl Lark-Horovitz in his preface. A symposium of this nature must inevitably be compared with such publications as *Reviews of modern physics* and the *Progress reports* of The Physical Society of London. The publishers of annual reviews in any subject would certainly fail to satisfy the scientific public for such matter if the long delay already noted became common practice. In physics, as in most scientific subjects at the present time, progress is so rapid that delayed accounts such as those under review can only be of value as a record of progress, possibly enhanced by the unusual nature or quality of particular contributions. There are certainly articles in this volume that teachers of physics will be glad to have.

The symposium attempted to cover the subjects elementary particles, physics of the solid state, chemical physics and biophysics, and is in no sense comprehensive, even within the prescribed limits. The section on elementary particles includes an article by Kusch on the magnetic moment of the electron; an account of cosmic ray experiments at high altitude by Ney, and one on developments in cosmic radiation physics between 1945–50 by Street. On the physics of the solid state Lark-Horovitz contributes a very useful and substantial article on the new electronics; this is followed by Bardeen's discussion of the flow of electrons and holes in semi-conductors and an interesting account by von Hippel of barium titanate ferroelectrics. The structure of polymers (P. J. W. Debye) and implications of the chemical kinetics of some biological systems (Lumry and Eyring) form the rather curious choice of subject matter for the chemical physics section. Biophysics is represented by Brink who writes on "the physical and chemical properties of axons related to conduction of nerve impulses"; and by Johnson who discusses bioluminescence and the theory of reaction rate control in living systems.

Most physicists will find something of value and interest in the volume, which nevertheless strikes the reviewer as being of rather uneven quality. The contributions on the physics of the solid state are probably the most generally useful; those on elementary particles the ones that have dated most rapidly.

J. T. RANDALL

A survey report on human factors in undersea warfare. Prepared by the Panel on Psychology and Physiology. (Washington: Committee on Undersea Warfare, National Research Council, 1949.) Pp. x + 541. Price (with supplement) 21*s*. 6*d*.

Despite its title this book contains a very large amount of applied physics. It consists of a series of reviews, each with a bibliography and written by members of American University staffs, of the accumulated knowledge in various fields relating to maintenance of efficiency in submarine crews; but much of the information is directly applicable to ordinary industrial practice. The reports are in nine groups, the first five of which at least should interest physicists concerned with design and lay-out of apparatus and equipment. These are headed respectively "General visual problems," "Design and arrangement of operating equipment," "Auditory problems," "Communication" and "Habitability, physiological factors." The other four are more concerned with psychology. The individual titles range over topics such as "How we see: a summary of basic principles," "The design and use of optical instruments," "Visibility on radar scopes," "Human factors in panel design," "Auditory signals," and "Temperature and humidity in relation to the thermal interchange between the human body and the environment." The reviewer has read this book with considerable pleasure and recommends it not only to physicists concerned with industrial efficiency but also as a source book to any who work in the borderline fields of physics and medicine or biology.

C. B. ALLSOPP

Progress in biophysics and biophysical chemistry; Vol. 6. Edited by J. A. V. BUTLER. (London; Pergamon Press Ltd., 1956.) Pp. viii + 274. Price 60*s*.

This volume, in common with the previous ones, includes chapters on unrelated topics, some of which are of doubtful claim to be "biophysics." Three chapters: "Protamines and nucleoprotamines," by Felix, Fischer and Krekels; "The structure of chromosomes," by Ambrose; and "Biology and biophysical properties of transforming principles," by Zamenhof, fall in that domain common to biochemistry and genetics where the structure of deoxyribose nucleic acid and proteins are studied by all possible means. For the uninitiated the last of the three subjects above is concerned with the substance, probably a deoxyribose nucleic acid, which can transform some strains of bacteria to different strains; as shown, for example, by presence or absence of a polysaccharide capsule. Once the transformation has been effected it is inherited by the daughter cells so the factor must have acquired the property of self-replication. The terminology in this field needs attention to avoid phrases like

"... the transforming phenomenon will be considered merely as a detector of activity of the transforming principle."

There is a section on "The Donnan equilibrium," by Overbeek, which should interest physical chemists and electrophysiologists. The departure from ideal behaviour in a system including colloid particles of high charge is discussed. Deviations are worse at low concentrations than at high, and the field round each colloid particle may be so high that the first-order approximation of the Debye–Hückel treatment is inapplicable. As ions of sign opposite to that of the colloid are held in the local field their mobility is reduced; this affects the magnitude of the junction potential between the colloid suspension and a solution in contact with it, as for example between a micro-electrode and a cell interior.

The other three sections are concerned with the nervous system. Castillo and Katz give a detailed account of the properties of the chemically mediated system which transmits an impulse from nerve to muscle in "Biophysical aspects of neuro-muscular transmission." The nerve ending liberates quanta of transmitter substance, in the resting state these are spontaneously discharged in a random way, whereas stimulation leads to simultaneous discharge of many quanta. The reproductions of the oscilloscope records are not up to the standard of the other illustrations. In "Models for biological excitation processes" Franck discusses the thermodynamics of open systems, which is probably more useful than consideration of highly artificial models. Finally De Vries in "Physical aspects of the sense organs" shows examples of the application of physical laws in the explanation of the mechanisms of perception. Here again random discharges (in the sensitive cells of the ear) receive attention.

I found much to interest me in this volume; it is, however, not economic for the biochemist to acquire three chapters of nerve biophysics or for the biophysicist to have the biochemical sections. One must conclude that the book is destined mainly for libraries.

E. J. HARRIS

Spectroscopy at radio and microwave frequencies. By D. J. E. INGRAM. (London: Butterworths Scientific Publications, 1955.) Pp. xi + 332. Price 45*s*.

In the last ten years radio-frequency spectroscopy has grown into an important and flourishing branch of physics. The development of very sensitive techniques has made it possible not only to detect the tiny absorptions involved in nuclear magnetic resonance but to observe the finer details of the absorption line shape, while oscillators extending the radio-frequency range to wavelengths of a few millimetres have opened the way to the radio-frequency spectroscopy of gases and the investigation of paramagnetic and ferromagnetic resonance. Dr. Ingram's book is to be welcomed as a successful effort to present this new material at a comparatively elementary level, suitable for the student and for the research worker contemplating the use of these new methods.

An extended account of microwave techniques as applied in spectroscopic work is followed by summaries of the different types of experiment. Some of these topics, notably gaseous spectroscopy, are treated very briefly, as is to be expected in view of the wide field covered. The book concludes with a particularly interesting chapter on the application of radio-frequency methods to such problems as chemical analysis, investigations of the structure of solids, and the detection of free radicals. Among the illustrations, photographs of oscilloscope traces taken in actual experiments give a good idea of the types of results obtainable.

A. H. COOKE

High speed aerodynamics and jet propulsion: Vol. 1. Thermodynamics and physics of matter. Edited by F. D. ROSSINI. (London: Oxford University Press; Princeton: Princeton University Press, 1955.) Pp. xviii + 812. Price 100*s*.

This book presents collectively the work of several authors with the principal purpose of providing a basis of thermodynamics and its application to the physics of matter, as an introduction to the further study of the problems of high speed aerodynamics and jet propulsion. These terms of reference have been interpreted very widely and the book contains some material, such as solid state physics, which can be regarded as someway removed from this object. The contents of the book are divided into ten sections, some original, others condensed versions of the same authors' material presented elsewhere. Thus Section A on the fundamentals of thermodynamics by Rossini is completely taken from his own book, Section C by Beattie on thermodynamics properties of real gases and mixtures of real gases is a modified version of parts of the book by Beattie and Stockmayer, Section D and a part of Section B on statistical mechanics and transport properties of gases from an earlier publication of Hirschfelder, Curtiss and Bird. Most of the original material in this book was written in 1951–2.

The introductory section by Rossini is clear and full, presenting familiar material in its simplest mathematical form. The contribution by Beattie in Section C is particularly useful, containing a summary of the various equations of state that have been proposed and providing numerous equations from which particular thermodynamic properties of pure gases and mixtures can be calculated.

In general the book will be useful as a reference book, though it may not specifically fulfil its primary intention. It is expensive to be considered as a textbook for students, and indeed certain sections of the book are better covered by existing texts. A point of considerable merit is that overlapping, often common in books with several authors is hardly to be found. Its presentation is attractive, the references and bibliography are numerous and are clearly and completely given.

D. SMITH

Solid state physics. Advances in research and application. Vol. 1. Edited by F. SEITZ and D. TURNBULL. (New York: Academic Press Inc., 1955.) Pp. xii + 469. Price $10.00, 80*s*.

The fragmentation of science, so obvious between the main divisions of the subject, is also taking place on a much finer scale. Even in such a compact field as solid state physics separate disciplines and terminologies are growing up round the main topics, for example, electron theory, semi-conductors, superconductivity, dislocations, radiation damage, magnetic resonance, and alloy phases; so that few people have the ability to command more than one of them fully. Attempts to counter this disintegration deserve utmost encouragement. Solid state physicists will therefore be most grateful to Professor Seitz and Dr. Turnbull for their initiative in starting a new series of books which will attempt to unify solid state physics by providing comprehensive reviews, side by side, of all its main topics. It is hoped to bring out two volumes a year and, judging from this first one, each will contain about six articles some 25 000 words in length written by specialists. Most of the articles in this first volume deal with the electron theory of solids, and are particularly valuable because of the most detailed way in which modern techniques in electron theory, e.g. the quantum defect method, electron plasma theory, orthogonalized plane waves, are expounded. The editors are to be congratulated

on having made such a promising start to their series. The articles in this volume are: "Methods of the one-electron theory of solids" by J. R. Reitz, "Qualitative analysis of the cohesion in metals" by E. P. Wigner and F. Seitz, "The quantum defect method" by F. S. Ham, "The theory of order-disorder transitions in metals" by T. Muto and Y. Takagi, "Valence semi-conductors, germanium and silicon" by H. Y. Fan, "Electron interaction in metals" by D. Pines.

A. H. COTTRELL

Geometrical optics. By L. C. MARTIN. (London: Sir Isaac Pitman and Sons Ltd., 1955.) Pp. xii + 215. Price 22*s*. 6*d*.

As one would expect of the author of the well-known book *Technical Optics*, this new textbook for university physics students is excellent. It pays the reader the compliment of not shirking difficulties for, although the mathematics is not difficult, the treatment of geometrical optics is reasonably logical and rigorous and thereby justifies the claim in the preface that the subject has an intellectual discipline of its own. Starting from consideration of a refracting surface so formed that all rays from a given object point converge to a single point, the discussion proceeds to show that, in general, good imagery can be secured only for a small aperture and over a small field. A general treatment can be applied, therefore, only to the paraxial region, but within this region the treatment may be based on the laws of refraction or on purely geometrical notions of collinear correspondence. Subsequent chapters deal with optical instruments, the connexion between physical and geometrical optics (particularly the connexion between waves and rays), the observation and recording of images and photometry. The final chapter on aberrations explains by purely geometrical arguments (deriving from Hamilton) how the different kinds of aberration arise. To me, the book has two not very important defects. I do not like to be referred so often to books on physical optics in chapter 4 and would have preferred to see sufficient physical optics included to have avoided this. Also the initial discussion of collinear correspondence is a little awkward.

E. W. H. SELWYN

Boundary layer theory. By H. SCHLICHTING, translated by J. KESTIN. (London: Pergamon Press Ltd., 1955.) Pp. xx + 535. Price 105*s*.

It is just over 50 years since Ludwig Prandtl made amenable to mathematical analysis the flow of water and air around solid bodies. He took into account the force of friction in the thin boundary layer which surrounds a solid body that is immersed in a streaming fluid of low viscosity, appreciating that it was in these restricted regions only that the effects of friction were essential. He studied the effect of the boundary layer on the general flow in its neighbourhood. Today work is going on over a very wide range of Reynolds numbers, be it in wind tunnels or with jet propelled craft or other means of propulsion.

Dr. Schlichting was trained by a man with a genius for simple, clearly conceived experiments. This is reflected in this book which, although intended for engineers, makes fascinating and enjoyable reading for physicists. There are many examples of everyday life to drive home a point of an abstruse nature. The evening mist over a damp meadow in a gentle breeze is chosen as an illustration of the influence of stabilizing forces on the origin of turbulence, or the streaming of sweet water over salt water in the Kattegat.

A large number of beautifully clear diagrams and excellent photographs (Schlieren photographs of shock waves for example) enliven the text. A great deal of attention is devoted to the transition from laminar to turbulent motion on a macroscopic scale without reference to molecular turbulence.

The bibliography is very comprehensive and is valuable for reference purposes.

If there is one regret, it is that the style is a little heavy, and the translator presumably adhered too rigidly to the original text. This is a minor criticism of this masterly survey of a subject of considerable complexity.

The publishers are to be congratulated on a very well produced book.

R. SCHNURMANN

Journal of Scientific Instruments

Contents of the May issue

ORIGINAL CONTRIBUTIONS

Papers

A large optical slit mechanism employing spring movements. By R. V. Jones.
A remotely-controlled traversing yawmeter for boundary-layer exploration. By D. W. Bryer.
Two designs for a paramagnetic oxygen meter. By A. Hobson and R. H. Kay.
A Pirani gauge for operation up to a pressure of 10 mm of mercury. By J. H. Leck and C. S. Martin.
A modified bridge earthing device. By B. Berger.
An oxygen-quenched Geiger-Müller counter. By D. Srdoč.
An input amplifier for a pulse-height analyser. By A. Folkierski.
A remote control apparatus for the movement of dosage measuring or similar equipment to indicated positions. By B. J. Perry and N. H. Pierce.
Fine grain development in xerography. By K. A. Metcalfe and R. J. Wright.
A switch-dial potential divider. By W. K. Clothier.

Laboratory and workshop notes

A simple water failure guard for diffusion pumps and condensers. By G. Houghton.
The direct evaluation of psychrometric data from dry- and wet-bulb recorders. By I. F. Long.
Transfer of movement into a vacuum by means of twisting a copper tube. By H. von Ubisch.
A furnace over-temperature protection device. By R. F. Newman.
A beam splitter with illumination control. By P. M. Forsyth and R. W. G. Hunt.

NOTES AND NEWS

Correspondence

An automatic cathode-ray oscilloscope beam brightening device for transient recordings. From O. H. Davie; J. Wood.
A monitored Geiger-counter X-ray powder diffractometer with automatic recording. From J. W. Hughes and E. R. Pike.
Calibration of a stroboscopic light. From T. F. Ford and T. G. Alexander.

New books

New instruments, materials and tools

Manufacturers' publications

THIS JOURNAL is produced monthly by The Institute of Physics, in London. It deals with all branches of applied physics (including theory and technique).

All rights reserved. Responsibility for the statements contained herein attaches only to the writers.

EDITORIAL MATTER. Communications concerning editorial matter should be addressed to the Editor, The Institute of Physics, 47 Belgrave Square, London, S.W.1. (*Telephone:* Sloane 9806.) Prospective authors are invited to prepare their scripts in accordance with the *Notes on the preparation of contributions*. (Price 2*s*. 6*d*. including postage.)

REPRODUCTION. The Institute of Physics is a signatory to The Royal Society's Fair Copying Declaration. Details may be obtained upon application from The Royal Society, London, W.1.

ADVERTISEMENTS. Communications concerning advertisements should be addressed to the agents, Messrs. Walter Judd Ltd., 47 Gresham Street, London, E.C.2. (*Telephone:* Monarch 7644.)

CLAIMS FOR MISSING JOURNALS. Claims from regular subscribers to this *Journal* for missing numbers will only be considered if received within 60 days of the date of mailing plus normal outward time of transit and time for lodging the claim. Losses attributable to failure to notify a change of address or to similar omissions will not be considered.

SUBSCRIPTION RATES. A new volume commences each January. The charge is £4 per volume ($11.50 U.S.A.), including index (post paid), payable in advance. Single parts, so far as available, may be purchased at 8*s*. each ($1.15 U.S.A.), post paid, cash with order. Orders should be sent to The Institute of Physics, 47 Belgrave Square, London, S.W.1, or to any bookseller.

Science and technology in industry*

By Sir John Cockcroft, K.C.B., C.B.E., D.Sc., F.Inst.P., F.R.S.,
Atomic Energy Research Establishment, Harwell, Berkshire

The lecture describes some of the more important contributions of science and technology to industrial development during the last ten years. Mention is made of radar, transistors, digital computers, electronic instruments, and the nuclear power and chemical industries.

The expenditure devoted to research and development in the United Kingdom is analysed and the future requirements for scientists and technologists are discussed.

The early industries in this and other countries were based on craft skills, arts and inventions rather than science. Examples of this are the textile, metallurgical, ceramic and early engineering industries. The electrical industry and chemical industry founded in the last century were, on the other hand, based firmly on the discoveries of science. In the present century applied science and technology is playing a rapidly increasing part in the development of industry. It is important now to be aware of these trends so that we can make provision during the next decade to train the scientists and technologists who will be needed if we are to maintain our place in the world.

Applications of science and technology

I will first remind you of some outstanding examples of the way in which new industries have recently been founded by science and technology. Radar and allied technology developed during the war years is my first example. I remember very well seeing the first 10 cm wavelength magnetron developing a pulsed power of 10 kW connected up to a vacuum pump in a hut on the downs of St. Albans Head in Dorset in the middle of 1940. This was a technical revolution increasing a thousand-fold the power available for short-wave radar. This magnetron had been devised by academic physicists working in Professor Oliphant's laboratory in the University of Birmingham. Within a few months it had been applied to centimetre radar sets installed in destroyers and corvettes for the war at sea. I remember also seeing in 1941 the first 3 cm radar set looking out for a submarine in Swanage Bay under the direction of Professor Skinner. During the next four years at least 2000 scientists and technologists in Government establishments and industry worked to apply this centimetre radar development to a whole range of objectives. Today every ship of any size has its 3 cm radar set; every airport has rotating scanners controlling traffic and other radar sets to talk down planes through haze and fog. Without it the modern density of air traffic would be impossible. The annual output of the U.K. electronic industry in radar and allied devices is now about £60 million per annum, of which about 20% is exported.

The development of computers is another interesting example. The digital computer may be said to have been born when Dr. Wynn-Williams in the Cavendish Laboratory about 1929 developed the scale-of-two counter. I remember how indebted we were in our then state of penury to the British Thomson-Houston Co. Ltd. for presenting two thyratrons for this work. From this small beginning scale-of-two counters multiplied and spread into most laboratories of the world, whilst after the war high-speed digital computers based on scale-of-two operation were developed. An important example was the work of Professor F. C. Williams in the University of Manchester which led to the Ferranti high-speed digital computer. This computer can work at least a million times faster than a mathematician equipped with a slide rule or tables of logarithms and can solve problems which no mathematician can solve in finite time. The development of this computer was made possible by the catalytic investment of the National Research and Development Corporation. Up to the present, nine of these computers have been made; their use, which started in Government research establishments, will soon be spreading through industry and the universities. Other U.K. examples are the Ace and Deuce computers resulting from the work of the National Physical Laboratory's Mathematical Division and the General Electric Co. Ltd. The expenditure on research and development on computers in Britain since the war has been about £1·4 million.

If we look at the other side of the Atlantic the expenditure on digital computers and automatic control has been about $250 million. The number of types of U.S. computers is now legion. A single computer, the I.B.M. type 704, commands an annual rent of £250 000. Over $1000 million of capital is being invested in electronic computers or data processers and the U.S. computer output seems to be more than one hundred times the U.K. output. There are already 100 000 computer engineers and technicians employed in the U.S. and these numbers are rapidly increasing.

Why is it that the use of high-speed computers is spreading so rapidly? The answer is that there are many fields of work which are only made possible by their use. One example is the hydrogen bomb. The testimony in the Oppenheimer case showed that its development was only made possible by the use of high-speed computing facilities—so complex are the processes occurring. In our work on reactors for civil purposes we find also that the difficult calculations can only be done with any reasonable accuracy by the use of computers like the Ferranti or Ace. The large atomic particle accelerators now being constructed to accelerate protons to energies of 25 000 million volts requires the orbits of these particles to be contained within a 8 × 16 cm vacuum tube during 500 000 revolutions, during which time they travel several hundred thousand miles. Perturbations due to very small irregularities in the guiding magnetic fields can easily induce oscillations which throw the particles out of the orbits. All this must be computed, requiring months of work even by the high-speed machines. As a result of this we can

* Based on a public lecture delivered by the President of The Institute of Physics at a one-day conference on "Physics in industry" arranged by the South Wales Branch of the Institute in Cardiff on Friday, 13 April, 1956.

proceed to build the 25 billion volt European machine at Geneva costing £7 million with a reasonable degree of faith that it will work.

Other applications of the computer are to accounting and management where they are expected in the United States to revolutionize managerial methods. Essentially they enable the detailed operation of an organization to be analysed and fed extremely rapidly to the management. Thus the Monsanto Company is receiving detailed cost figures on each of its products every month instead of once a year. Aviation companies are getting results of prototype flight tests within days instead of weeks, which means that the information keeps pace with the tests instead of lagging behind it. Tests on guided missiles produce a vast amount of data through telemetering; only a computer enables this to be analysed rapidly enough to be useful. The Industrial Group of the U.K.A.E.A. is now using an I.B.M. to keep continuous records and control of its stocks and to control costs of operation. One is in use at Harwell for the analysis of scientific data.

Another impressive example of electronic development is the transistor valve. This is a remarkable example of the application of fundamental solid state physics carried out by Dr. Shockley and his colleagues at the Bell Telephone Laboratories in New York. The semi-conductors germanium and silicon are produced in single-crystal form in extremely high degrees of purity—impurity contents have to be less than one part per million. To this pure germanium or silicon is added very small amounts of controlled impurities such as arsenic in specific regions of the crystal. These impurities are diffused into the crystal and form layers which are extremely sharply defined geometrically. With suitable geometry and electrodes the crystal valve can be either a diode or a triode and rectifiers, amplifiers, oscillators become possible. The amplifier or oscillator is characterized by a very low voltage and low overall power input. Already the oscillators and amplifiers can deal with frequencies up to 100 Mc/s so they can cover most of the range of radio communications. The manufacture of transistors now exceeds a million a year and before long they are likely to outnumber thermionic tubes.

The very low power and voltage requirements of the transistor will enable new kinds of electronic equipment to be developed—thus it seems likely that in the telephone industry switching operations which at present are a combination of relay and thermionic devices will soon be entirely "transistorized" thus greatly reducing maintenance. Matchbox hearing aids and cigarette case radio receivers have already been produced in large numbers, and the transistor hearing aid sales reached a value of about a million dollars per annum in the U.S. a year or two ago. All this has developed from the fundamental work of Dr. Shockley and his colleagues backed up later by the enormous applied research and development effort of the Bell Laboratory.

Another electronic example is the development of instruments for use in atomic energy and the application of radioactive isotopes produced in atomic piles. A simple example of this is the thickness gauge. A radioactive source such as strontium 90 emits high-speed electrons which travel through sheet metal as it comes out of a rolling mill. An instrument on the other side measures the intensity and since this diminishes with increasing thickness the sheet thickness can be continuously monitored and controlled. It is also possible to measure and control the thickness of a coating such as tin on tin plate by measuring the electrons scattering back from the tin layer. In this way the thickness of tin can be controlled to a few hundred thousandth parts of an inch.

Another example is an electronic analytical tool known as the "square-wave polaragraph," invented by Dr. Barker at Harwell. This instrument can measure continuously impurity contents of liquids down to one part in a hundred million. It now has important control functions in chemical operations.

Instruments of this and many other types have been developed by electronic staff of the Harwell establishment during the last ten years in close collaboration with industry. A walk through the stands of the British Scientific Instrument Manufacturers' Association at the Geneva Conference showed a very impressive display of instruments resulting from this collaboration. About 450 different types of instruments have resulted and the annual output is now worth about £10 million. This has resulted from development work—costing perhaps £250 000 a year—a multiplication factor of 40.

The development of nuclear power is a still more impressive example. In this country we now have probably about 1000 scientists and technologists working on nuclear power development. In the United States the number of scientists and technologists is ten times greater.

The first result of the British effort will be the Calder Hall power station to be opened by H.M. the Queen next October. In this power station the usual coal-fired furnace is replaced by two nuclear reactors. These reactors consist of a huge pressure drum, 37 ft in diameter, containing a core of bricks of very pure graphite. In vertical channels in the graphite bricks hang rods of uranium metal about 1 in. in diameter sheathed in a light alloy. Control rods hang in other vertical channels. These move into and out of the core to control the chain reaction in the uranium. When the chain reaction is proceeding, heat is developed in the uranium metal rods. This is transferred from the hot rods to four steam generators by circulating carbon dioxide gas under a pressure of 7 atm. The steam passes to a conventional turbo-generating station and about 70 MW of electricity will be produced. We are building four of these Mark 1 power stations and by 1960 they should be contributing about 300 MW of electricity to the National Grid. These are to be followed by twelve further Central Electricity Authority power stations which should develop at least 2000 MW of electricity by 1965. The Government plan provides for spending about £300 million on this development by 1965. From 1965 to 1975 the construction of nuclear power stations should proceed at a much greater pace and the annual installation may well rise to 2000 MW—requiring an annual expenditure of about £200 million.

Important new developments in industry are likely to arise from the application of high-intensity, short-wave radiation, which is now becoming available from two sources. The first source of radiation is the electron linear accelerator which was developed by A.E.R.E. and is now being produced by industry. The mean beam power in the latest accelerator is 2 kW. The second source is from the waste products—the fission products which will automatically be produced in ton quantities from nuclear power stations within the next few years. Recently a group has been formed at the Atomic Energy Research Establishment, to investigate the possible applications of the vast amount of radiation which will become available. Already important successes have been achieved in widely different fields. Mutations of seeds has resulted in hitherto unknown variants of plants, entirely new physical properties have been achieved by the radiation of plastics, a number of products have been sterilized which are of great commercial interest and chemical changes have been stimulated which may result in development of new products.

The United States Atomic Energy Commissioner, Dr. Willard F. Libby, has estimated that, in that country, $200 million could be saved per year by using radiations in the field of agriculture alone. The main part of the savings results from variants of farm products which are resistant to diseases. Soon, 600 researchers will be employed in the United States on the preservation of food by radiation. Looking a few years ahead one can foresee a great number of commercially suitable applications which will either make a product considerably cheaper or better or will be instrumental in producing entirely new products.

In this country some success has been achieved in the sterilization of hospital blankets and also in the sterilization of pharmaceuticals by γ-radiations. More recently, research work has been started on the safe sterilization of virus which is extremely difficult to achieve by orthodox methods without harming the anti-genicity of the resulting vaccine.

It is contemplated that the new Technological Irradiation Group will be the centre for the development work for many applications of ionizing radiations to industry. This group will be diversified and will consist not only of physicists, chemists and engineers, but also of biologists, all of whom will work closely with other existing organizations. A number of radiation facilities are being set up. The first of these will be a powerful electron linear accelerator; later this year there will be at least one assembly of spent fuel rods from our DIDO reactor providing a radiation source equivalent to two million grams of radium. They will also have two 10 kc sources, of which one will be cobalt 60 and the other caesium 137 and eight smaller cobalt 60 units. To allow the new group to expand it is being set up at a separate site some nine miles from Harwell. I believe that its development will make a very important contribution to industry in this country in the near future, and it may well be comparable to the power programme in its importance.

The chemical industry provides another good example of the application of science and technology. Its achievement in the production of new products such as nylons, plastics, synthetic rubber, silicones are very well known. The President of the U.S. Dupont Company in an article in *Fortune* (May 1955) gave some very interesting figures of the growth in the number of scientists employed by the chemical industry in the United States. During the last twenty years they have increased from 6500 to 35 000—they double in numbers in somewhat under ten years. The Dupont Company have good records of their expenditure on research and development since 1921 and also for construction expenditure during the same period. During the whole of this period the ratio has been about one to three. That is for every dollar spent in their research and development they have sooner or later spent three dollars for new plants, products and processes. This ratio has remained constant during a period when research expenditure has increased from $1 to 60 million a year. In this country Imperial Chemical Industries Ltd. employ a research staff of 1700 graduates and 2800 technicians and their annual expenditure on research and development is £9 million. Their expenditure on new plant, processes and products in 1955 was over £30 million. Their annual output is worth £400 million. Terylene and titanium are good examples of their recent new products.

The antibiotics and allied industry is another post-war growth which developed from the work of two or three academic scientists, particularly Sir Alexander Fleming and Sir Howard Florey in British Laboratories; followed by intensive applied research and development in the U.S. We are all now more and more indebted to the wonder drugs, penicillin, streptomycin, aureomycin and the sulphur drugs. Other important products are the anti-malarials, the insect repellents, the insecticides and selective weed killers. Compounds such as B_{12} together with antibiotics are now used in a large way in farming to promote the fattening of livestock. A single U.K. company employs about a hundred graduate staff and a single compound such as Cortisone has cost half a million pounds to develop.

In the metallurgical industry in Britain a little over 2000 scientists and technologists are engaged in research and development, half of these being graduates. My personal knowledge extends only to the development of the newer metals important in atomic energy—uranium, plutonium, thorium, zirconium, beryllium, niobium. We have developed methods for the extraction and fabrication of these metals with the help of industry. We have found it necessary to build pilot plants, usually with the help of industry. A typical pilot plant may cost £70 000 to construct and £50 000 per annum to operate. This must go on for a period of three or four years. It may then lead to the construction of a full-scale plant with an output in the region of 100 tons per annum with an annual value of perhaps £1 million.

Research and development may easily lead to economies in extraction and fabrication of uranium amounting to between £1000 and £2000 a ton, so in a future nuclear power programme which demands tonnages of uranium of over 1000 a year, savings of several million pounds a year may result from a comparatively modest research and development effort.

An interesting recent example of metallurgical research and development at Harwell has been the production of fuel elements for our new research reactor DIDO. The fuel elements consist of enriched uranium alloyed with aluminium and sheathed in aluminium sheets to prevent corrosion by the water of the reactor. Billets of the enriched uranium are first of all melted in a vacuum furnace with aluminium to form an alloy. The alloy billet is then covered with sheets of aluminium and passed through a rolling mill forming a strip a few millimetres thick, the sheath being automatically pressure welded on to the alloy. The resulting plates are then X-rayed to show the distribution of the alloy. They are then cut and bent to shape and a number are brazed together with channels between to form a complete fuel element.

The aircraft industry has been based very heavily on scientific research and technological development. The industry relies heavily on the Royal Aircraft Establishment at Farnborough for its basic knowledge and for the operation of very expensive facilities such as high-speed wind tunnels. The annual expenditure in the industry on research and development approached £100 million, of which more than half is Government money. Its annual intake of graduates is very high—over 200.

The extent of the trade resulting from the development of a successful aircraft is shown by the sales of the Viscounts which now exceed £100 million, whilst the total annual export of the industry is about £100 million.

If we look at the position in other and older industries such as railways, shipbuilding and the automobile industry, science appears to play a much smaller role. A recent report of the Committee on Scientific Manpower stated that in one year three shipbuilding firms recruited no graduates but over 200 apprentices; five motor firms recruited thirteen science graduates and 270 apprentices. The annual expenditure on research and development of railways, shipbuilding and automobiles is £350 000, £200 000 and £3 million respectively.

These lower figures are characteristic of industries relying very much on traditional methods changing only by small steps from one model to the next. They prefer to recruit their technicians and technologists at 16 or 17 years of age and bring them up by way of the shop floor and the local technical college.

EXPENDITURE AND MANPOWER DEVOTED TO RESEARCH AND DEVELOPMENT IN U.K.

If we now look at the overall picture there are a number of important questions which might be asked. First of all, how does our total expenditure on research and development compare with our most important competitor—the United States?

Exact figures for total expenditure and scientific manpower engaged in research are difficult to obtain. Government expenditure on scientific research and development in 1956–57 has been estimated to be about £235 million. Research expenditure by industry for its own purposes was probably over £40 million. This compares with an expenditure in the United States of about $5 billion. If we take the "real value" of the dollar to be five to the pound this means that the United States are spending about four or five times as much as we are on research and development so that the expenditure per head of population is not very different. They have a rather greater ratio, about six to one, in the number of graduate scientists and technologists in the working populations.

We might next inquire how this expenditure is divided between fundamental research, civil applied research and defence research. Exact figures are again not available but our research expenditure is probably divided roughly as follows:

	expenditure	*graduates engaged*
Fundamental research, universities	£5 ± 2 million	4000
Fundamental research, Government and semi-Government	£5 ± 1 million	1000
Civil applied research	over £60 million	40000
Defence research	about £200 million	

It seems then that expenditure on fundamental research is less than 5% of the total and the numbers engaged on fundamental research are about 10% of the total graduates engaged on research. The corresponding U.S. proportion of expenditure is 7%. We do *not* therefore seem to be devoting too much of our effort to the basic research from which all applied research springs.

THE EDUCATION OF SCIENTISTS AND TECHNOLOGISTS

We might ask ourselves next how the demand for scientists and technologists is likely to grow during the next ten years. The Committee on Scientific Manpower recently reported that industry is at present only getting about 75% of the graduates it needs. There are also large shortages of graduate science teachers in the schools. The committee is inquiring now into the probable increase of demand for graduate scientists and technologists in the next decade and its report will certainly be awaited with interest. In the meantime it is interesting to note a forecast made by the President of M.I.T. in his recent annual address. He predicted that the requirements for scientists and technologists in the United States would double again in the next decade—as it has doubled during the previous two decades. A similar forecast for their own needs has been made by two of the largest employers of scientists and technologists in Britain. These forecasts seem to be very reasonable in view of the increasing complexity of the newer industrial developments.

What sort of training will this next generation of applied scientists require? I will again quote from the President of M.I.T.'s address. "As our advancing technology becomes more complex and sophisticated it requires scientists and engineers and managers of more advanced education and analytical powers. There are areas of technology so new and rapidly advancing that only men with self-acquired fundamental and versatile understanding or with recent education in the new technologies are able to master and keep pace with them. Employers want more scientists and engineers but they don't feel that they are meeting the need by employing inferior or narrowly educated ones. They want men, particularly young engineers, with the power to deal with the technologies of tomorrow and not today or yesterday."

These views have been strongly supported by Dr. Mervyn Kelly, Director of the Bell Telephone Laboratories of New York, the largest scientific and technological institute in the world, in a recent informal talk in this country. Dr. Kelly feels the education of engineers must in future have a higher scientific background. My own experience of atomic energy development has shown that our rapid advances have been made possible by the high scientific and technical quality of our graduate staff backed by the support of equal numbers of technicians.

We must also see to it that our young engineers and scientists are educated in an environment which will produce the future leaders of industry. Leadership requires not only good technical knowledge and judgment but the personal qualities which inspire others. In my view the best way to achieve this is first to maintain a good standard of general education up to and including the sixth form level and then for students to live for at least part of their university life in colleges or halls of residence where all the faculties of a university are mixed. The clubs and societies of the undergraduate world are the best form of general education at that period of life.

Let us now look at our achievements in producing technologists. Our annual output of graduate technologists is at present about 2800 and of scientists about 5200. The 2800 graduate engineers compares with an output of 23000 in the United States and 53000 in Russia. So Russia is now turning out about eighteen times our number of graduate engineers and about ten times our number of scientists. The training of the Russian graduates in science is severe—they receive 5800 hours of full-time instruction in a course of five and a half years—so they are fully equivalent to our graduates.

At a lower level the U.S.S.R. produces annually about 78000 technicians from the *Technicums*—these compare with our 9000 a year Higher National Certificate and Diploma students. The Russians have given good evidence of their capacity in the fields of atomic energy and jet aircraft as well as in academic studies in the most important fields of modern physics. The power of the U.S.S.R. in a world where military power is stalemated may well in future depend more on its big battalions of technologists than the classical methods of power politics.

What are we doing to improve our relative position? The recent Government White Paper (Cmd. 9703) has stated that

it is the intention of the Government to expand still further the provision for technological education in universities. I would like to express a personal hope that it will be possible to double the number of university graduates in technology during the next decade.

The Government is also to spend £100 million in expanding and improving twenty-four regional technical colleges to enable them to organize sandwich courses of instruction over a period of five years. This course will lead to a new award—"the Hives award." It is hoped that these arrangements will enable the stream of good talent amongst the "early school leavers" to be tapped. In the White Paper it is hoped that it will be possible to produce an additional 2500 technologists a year in this way.

By 1962 the birthrate bulge will increase the number of children of college age by 40%; there is also evidence of an increasing proportion of sixth form students and university entrants taking science. If we take advantage of all these factors there is a good chance of providing the additional scientists and technologists we need.

Stress waves in solids*

By Prof. R. M. Davies, Ph.D., D.Sc., F.Inst.P., Department of Physics, University College of Wales, Aberystwyth

The aim of this paper is to discuss, in fairly elementary fashion, the topic of the transmission of transient stress pulses of short duration in solids, together with the associated problem of the measurement of pressures subject to very rapid changes. The pressure bar method, devised by Betram Hopkinson, forms one of the basic experiments in the field and it is described in some detail. An analysis of the limitations of the method leads to a discussion of the change of form of stress wave pulses as they recede from the origin, and the main features of the distortion are discussed when the pulses are propagated in (*a*) elastic solids, (*b*) visco-elastic solids, and (*c*) solids stressed beyond the elastic limit.

1. Introduction

One important aspect of the study of stress waves is the investigation of the propagation of transient pulses of short duration which are initiated when a solid is subjected to impulsive loading. This type of loading occurs very frequently in practice and, as typical examples, one may take a solid subjected to the action of an explosive charge or to some form of impact. The time-scale of the phenomena and the maximum values of the stresses will depend on a number of factors. Taking T.N.T. as an example of an explosive, the pressure at the detonation front in the explosive rises almost instantaneously from zero to values of the order of 1500 tons/in^2 (2×10^{11} dynes/cm^2); the subsequent variation of the pressure with time depends on the size and shape of the charge and on the conditions at its boundaries. As an example of an impact, one may take a solid struck normally by a lead bullet. The stress at the area of impact and its variation with time is a function of the velocity and calibre of the bullet and of its size and shape. A commercial bullet of 0·22 in. (0·56 cm) calibre, travelling with a velocity of 1200 ft/s ($3{\cdot}65 \times 10^4$ cm/s), gives rise to a stress which rises from zero to a maximum value of the order of 100 tons/in^2. ($\sim 1{\cdot}5 \times 10^{10}$ dynes/cm^2) in a time of the order of 5 μs; the stress is maintained at this value for about 15 μs and it subsequently falls to zero in another 10 μs.

The accurate measurement of pressures (or stresses) of this order of magnitude which are, at the same time, subject to very rapid changes, is a matter of some difficulty. One of the most satisfactory methods is the ingenious pressure bar experiment which was devised in 1913–14 by Bertram Hopkinson[1] when he was Professor of Mechanism and Applied Mechanics at Cambridge. Later, the experiment was developed at Woolwich into a routine method for proving explosives and some of this work has been described by Robertson[2] and by Landon and Quinney.[3]

Hopkinson's experiment does not seem to have attracted much interest except in circles dealing with explosives and it is well worth describing and discussing because of its simplicity and its fundamental importance in stress wave measurements.

2. Hopkinson's pressure bar experiment

Hopkinson's experiment consisted in applying the unknown pressure normally to one end (the "pressure" end) of a cylindrical steel bar (the "pressure bar"), several feet long and about an inch in diameter; the bar was suspended as a ballistic pendulum. The second end (the "measuring" end) of the pressure bar was ground plane and lapped; detachable end-pieces (the "time-pieces") of steel, of the same diameter as the bar, were also ground plane and lapped and they were then wrung to the measuring end of the bar with a smear of grease, or, alternatively, by magnetizing the bar and the time-piece. The pressure acting on the pressure end of the bar is assumed to give rise to a pulse of longitudinal stress waves which is propagated along the bar without change of form with a constant velocity $c_0 = \sqrt{(E/\rho)}$, where ρ is the density of the material of the bar and E is Young's modulus.

When the pulse approaches the measuring end of the bar, it is transmitted unchanged through the joint between the pressure bar and the time-piece, since the pulse is one of compression and a joint of this type can withstand compression. The pulse then reaches the free end of the time-piece where it is reflected as a pulse of extension which travels back to the joint. From this time onwards, the net stress at the joint is the resultant of the pressure due to the incident pulse and the tension due to the reflected pulse. Ultimately the tension will exceed the pressure, and when this occurs the time-piece becomes detached from the bar, since the

* Based on a lecture given before the North-Eastern Branch of The Institute of Physics in Newcastle upon Tyne on 24 November, 1954.

joint cannot sustain a net tension. Furthermore, at this instant, the time-piece will have trapped a certain amount of momentum and it will fly away from the bar with a velocity which is measured by a ballistic pendulum. The remainder of the momentum of the pulse is deduced from the throw of the pressure bar.

Let the curve $OB''C''$ in Fig. 1(*a*) represent the relationship between the pressure, p, and the time, t', in the pulse applied to the pressure end of the bar. Let $QRST$ in Fig. 1(*b*) represent the section of the pressure bar at the measuring end, RPS being the free end of the time-piece. Let the axis of the bar be taken as the axis of x. If σ_i is the stress in the incident pulse of compression in the bar (σ_i being taken as positive for compression), the (σ_i, x) curve at any instant can be deduced from the (p, t') curve of Fig. 1(*a*) in the usual way.

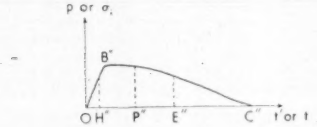

(a)

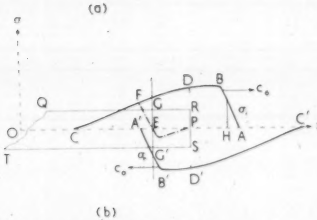

(b)

Fig. 1. The Hopkinson pressure bar. (*a*) The relationship between the pressure, p, applied to the pressure end of the bar and time, t', or between the stress, σ_i, in the pulse in the bar and time, t. (*b*) The reflexion of a pulse at the free end, RS, of a time-piece, PE

Let ABC in Fig. 1(*b*) represent the (σ_i, x) relationship at a time t reckoned from the arrival of the leading edge of the pulse at P. Let σ_r be the stress in the reflected pulse. The (σ_r', x) curve at time t is derived from the (σ_i, x) curve by satisfying the condition that the resultant stress over the free end RPS always vanishes. The (σ_r, x) curve constructed in this way is represented by $A'B'C'$. The (σ_i, x) and the (σ_r, x) curves may be regarded as moving to the right and to the left respectively with the velocity c_0.

The resultant stress distribution in the bar at time t is obtained by superposing the stresses σ_i and σ_r, giving the dotted-line curve PEF in the region PA' where the two pulses overlap, and the curve FC outside this region. The resultant stress $(\sigma_i + \sigma_r)$ vanishes at the point E where the two ordinates EG, EG' are equal. At time $(t + \epsilon_1)$, where ϵ_1 is a very small quantity, ABC will have moved to the right through a distance $\epsilon_1 c_0$ and $A'B'C'$ to the left through the same distance; the resultant stress at E will therefore be a tension. If EP represents a time-piece, E being the joint with the pressure bar, it follows that at time $(t + \epsilon_1)$, EP will have become detached and that it will have trapped momentum corresponding to the portion $EPDG$ of the incident pulse and to the portion $PD'G'E$ of the reflected pulse. Although the signs of the stresses σ_i and σ_r are opposite, the signs of the momenta associated with the two pulses are the same, since the velocities of the pulses are in opposite directions. The total momentum trapped in the time-piece is therefore equal to the momentum of the incident pulse between the limits H and E, where H is the point on Ox in the forward portion of the pulse where the ordinate is equal to EG or EG'. If L is the length of the time-piece, $HE = 2L$.

Reverting to Fig. 1(*a*) and regarding the curve now as showing the relationship between σ_i and t, where t is reckoned from the instant at which the leading edge of the pulse reaches P, let H'', P'' and E'' be the points corresponding to H, P and E in Fig. 1(*b*); $OH'' = AH/c_0$, $H''P'' = HP/c_0$, etc.

If A is the area of cross-section of the pressure bar, the total thrust over the cross-section when it is traversed by the incident pulse is $A\sigma_i$ and the momentum of an elementary interval $t, t + dt$ of the curve of Fig. 1(*a*) is $A\sigma_i dt$. The total momentum trapped by the time-piece EP of Fig. 1(*b*) is therefore

$$A\int_{H''}^{E''} \sigma_i dt = A\int_{H''}^{E''} p\, dt'; \quad H''E'' = 2L/c_0$$

If U is the velocity of projection of the time-piece, the momentum is also equal to ρALU; hence

$$\int_{H''}^{E''} p\, dt' = \rho LU; \quad H''E'' = 2L/c_0 \qquad (1)$$

By using time-pieces of different lengths, it is possible thus to determine the area under the (p, t') curve over varying time intervals. In general, it is not possible to deduce the precise form of the curve itself since the times corresponding to the beginning (or the end) of the various intervals are not known, but the duration and the maximum value, $\hat{p}$, of the applied pressure can always be found. The duration is $2L_0/c_0$ where L_0 is the length of the time-piece which just catches the whole of the momentum, leaving the bar at rest. To determine $\hat{p}$, a very short time-piece is used so that the time-interval $2L/c_0$ brackets the instant of maximum stress; the momentum trapped in the time-piece is $2A\hat{p}L/c_0 = \rho ALU_0$ where U_0 is the velocity of projection. Thus $\hat{p} = \frac{1}{2}\rho c_0 U_0$.

To check the accuracy of the method, Hopkinson carried out a series of experiments in which lead bullets were fired normally at the end of a pressure bar. If the impact stress is large enough, the bullet will behave as a pellet of fluid and it becomes possible to calculate the duration of the impact and the variation of the impact stress with time. Let U_B be the velocity of the bullet and L_B its length. The duration, T_B, of impact is equal to the time taken by the bullet to traverse its own length, i.e. $T_B = L_B/U_B$. Let ρ_B be the density of the material of a bullet and A_B the area of cross-section of the bullet in contact with the end of the bar at a given instant. The mass of the material flowing with velocity U_B towards the area of impact per second is $\rho_B A_B U_B$, and, if the material comes to rest after impact, the rate of destruction of momentum, i.e. the total thrust, F_B, over the area of impact is $\rho_B A_B U_B^2$ and the stress is $\rho_B U_B^2$. The variation of F_B with time can be calculated from the values of ρ_B, U_B and the radius of the cross-section of the bullet at various points on the axis.

To verify that the impact stress is usually much larger than the strength of lead in compression, consider a bullet with

initial velocity $U_B = 1000$ ft/s $= 3{\cdot}05 \times 10^4$ cm/s; $\rho_B = 11{\cdot}34$ g/cm^3, giving $\rho_B U_B^2 = 1{\cdot}06 \times 10^{10}$ dynes/cm$^2 = 68{\cdot}3$ tons/in.^{2} which is much greater than the strength of lead ($\sim$2 tons/in.^{2}).

The maximum value, $\hat{F}_B$, of the total thrust, F_B, corresponds to the area of the calibre, $\hat{A}_B$, say, of the bullet, and, in Hopkinson's experiments, the calculated and observed values of $\hat{F}_B$ and T_B were compared. It was found that the agreement was of the order of 2–7% and the discrepancy, in the case of T_B at any rate, was attributed to the fact that the bullet was really not absolutely fluid, particularly in the later stages of the impact.

The two main advantages of the Hopkinson bar are: (*a*) It allows measurements to be made at a reasonable distance from an explosion or a bullet impact and so decreases the risk of damage to apparatus. (*b*) Ordinary mechanical gauges can seldom be used for rapidly varying transient stresses such as those considered here; in some instances, their natural periods of oscillation are too large; in others, their use perturbs the quantity which it is desired to measure. In the Hopkinson bar, the errors due to these causes are at a minimum.

The method is, however, subject to certain disadvantages and limitations:

(*a*) As shown already, it cannot give the exact relationship between pressure and time.

(*b*) The inevitable adhesion between the time-pieces and the bar leads to inaccuracy, particularly when measuring small pressures and those which vary slowly with time.

(*c*) It is assumed that the stresses nowhere exceed the elastic limit; in point of fact, this factor sets an upper limit to the pressure which can be measured. With tool steel of high quality and reasonable homogeneity, the upper limit is of the order of 60 tons/in.^{2}.

(*d*) The distribution of the stress over a cross-section of the bar is assumed to be uniform. This assumption is wide of the truth near the pressure end of the bar if the applied pressure is confined to a small area of the surface, as in a bullet impact. As the distance from the pressure end increases, the stress distribution becomes more uniform and in a series of experiments,[3] in which the time-pieces of Hopkinson's experiment were replaced by steel ball-bearings, it was shown that the stress and the displacement are reasonably uniform when the pulse has travelled a distance equal to four or five times the diameter of the bar from the area of impact.

(*e*) Finally, the theory assumes that the pulse is propagated along the bar without distortion and that the stresses on the time-piece are due to a single pulse. The latter implies that the time-piece has parted company with the pressure bar before the pulse returns to the measuring end after reflexion at the pressure end; it follows that the maximum duration of the pulse which can be accommodated in a bar of length L_a is $2L_a/c_0$. This condition is not difficult to satisfy, but there still remains the question as to whether the pulse is distorted in its passage along the bar.

In order to overcome the two first-named disadvantages of the original method and in order to study the propagation of pulses, an electrical version of the Hopkinson bar was developed.[4] In the new method, a plain bar, i.e. one without time-pieces, was used and, in essence, the experiment consisted in measuring electrically the variation with time t of either the longitudinal displacement, ξ, of the measuring end of the bar, or, alternatively, the radial displacement, ζ, of its cylindrical surface. It follows from the elementary theory of the propagation of extensional waves in cylindrical bars that the stress σ is given by the equations

$$\sigma = \tfrac{1}{2}\rho c_0 \dot{\xi} \tag{2}$$

and

$$\sigma = E\zeta/\nu a \tag{3}$$

where a is the radius of the bar and ν is the value of Poisson's ratio. Thus the variation of σ with time t can be deduced if it is possible to determine the (ξ, t) or the (ζ, t) curve by experiment; in the former case, it is, of course, necessary to differentiate the observed curve. The displacements ξ and ζ were measured by condenser gauges of suitable design.

These experiments showed that pressure bars about 2 ft long and 1 and 0·5 in. diameter could be used to measure pressures which lasted for about 20 and 10 μs respectively with an accuracy of 2 or 3%. To explain some features of the experimental results, a theoretical study of the propagation of waves in circular cylinders was carried out and this showed that, owing to dispersion, a stress pulse was modified in its passage along the bar, the shorter waves lagging behind the longer ones. The theory provided a satisfactory explanation of certain anomalies in the experimental results which were incompatible with the elementary theory.

3. DISTORTION OF STRESS WAVE PULSES

The distortion of pulses as they recede from the origin is the rule rather than the exception. The phenomenon occurs not only in the comparatively simple case of elastic waves, but also in the more complex cases of waves in visco-elastic media, in which frictional stresses act in addition to elastic stresses, and in plastic waves, where the stresses and strains exceed the elastic limit.

In a bounded elastic solid, the velocity of an infinite train of monochromatic stress waves is usually a function of the wavelength (or frequency), i.e. dispersion is present (Section 4). Any pulse may be resolved into a spectrum of Fourier components which differ in their wavelengths and which will therefore travel with different velocities, but with undiminished amplitude, when dispersion is present; it follows that the relative phases of these components will vary with the distance from the origin and the pulse will suffer distortion as it recedes.

In waves in visco-elastic media (Section 5), dispersion and attenuation are present, i.e. the velocity of an infinite train of monochromatic waves is a function of the wavelength, and, in addition, the amplitude of such a train decreases exponentially with the distance from the origin, the rate of decrease being usually a function of the wavelength. In this case, not only is there a change in the relative phases of the Fourier components of a pulse as it travels away from the origin, but there is also a change in the relative amplitudes, resulting in a more complex form of distortion.

One common feature of the theory of elastic and visco-elastic waves is that the stresses, strains or displacements are assumed to be so small that the equations of motion are linear. When the amplitudes become finite, the (stress, strain) relationship extends into the plastic region and the equations of motion become non-linear. Under these circumstances, there is a close analogy with the Earnshaw–Riemann equations for the propagation of waves of finite amplitude in a compressible fluid as was pointed out by G. I. Taylor[5] in his pioneer work on plastic waves. In fluids, an arbitrary disturbance builds up into a shock front, but for most solids the (stress, strain) relationships are such that an arbitrary

disturbance degenerates as it recedes from the origin (Section 6).

4. THE DISPERSION OF ELASTIC WAVES

The elementary theory of the propagation of elastic waves in beams and bars leads to the well-known result that extensional (or longitudinal) waves are propagated with a constant velocity $c_0 = \sqrt{(E/\rho)}$. This theory, however, neglects the effect of the lateral inertia of the bar and it breaks down when the lateral dimensions of the bar are not negligible in comparison with the wavelengths of the stress waves. Not all forms of cross-section are amenable to exact mathematical treatment, but, when the bar is in the form of a circular cylinder, it is possible to use the appropriate form of the exact equations of elasticity (the Pochhammer–Chree equations) to calculate the velocity, c, of monochromatic waves of wavelength Λ [see e.g. ref. (4)]. This investigation shows that the non-dimensional ratio, c/c_0, is a function of the non-dimensional variables a/Λ and ν, where a is the radius of the cylinder and ν is Poisson's ratio. Alternatively, the variable a/Λ can be replaced by the non-dimensional ratio an/c_0 where $n(=c/\Lambda)$ is the frequency of a wave of velocity c and wavelength Λ, and the variation of c/c_0 with an/c_0 for steel, for which $\nu = 0{\cdot}29$ is shown in Fig. 2, curve (a). [The equation giving c/c_0 as a function of an/c_0 (or a/Λ) has an infinite number of roots, corresponding to various modes of propagation which differ in the number of nodal cylinders which are present. The curve (a) shown in Fig. 2 relates to the fundamental mode, without a nodal cylinder or with one such cylinder.] To give some idea of the orders of magnitude, a scale giving the values of c for steel, assuming $c_0 = 5{\cdot}23 \times 10^5$ cm/s, is shown on the right of the diagram and a scale giving the values of n for a steel rod, 1 in. diameter ($a = 1{\cdot}27$ cm) is shown on the upper scale of abscissae. The diagram shows that the curve is horizontal, with $c = c_0$, for small values of an/c_0; this region corresponds to the dispersionless propagation of the elementary theory. As an/c_0 increases, c/c_0 decreases, rapidly at first and then much more slowly, and, for large values of an/c_0, c asymptotically approaches the velocity, c_s, of Rayleigh surface waves; when $\nu = 0{\cdot}29$, $c_s/c_0 = 0{\cdot}5764$.

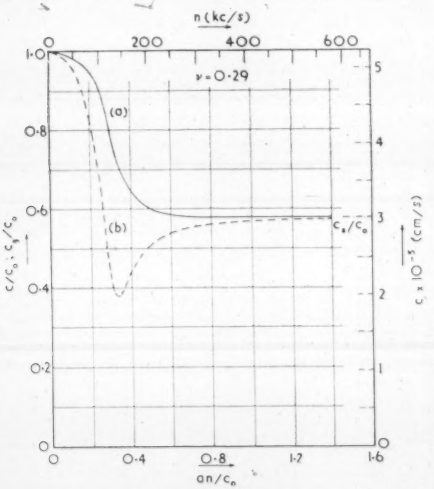

Fig. 2. Dispersion curves for sinusoidal elastic waves of frequency n in a cylindrical rod of radius a. Curve (a): phase velocity, c. Curve (b): group velocity, c_g

$c_0 = \sqrt{(E/\rho)}$; c_s = velocity of Rayleigh surface waves. The ordinates of the right-hand scale refer to steel, assuming $c_0 = 5{\cdot}23 \times 10^5$ cm/s. The upper abscissa scale relates to a steel cylinder, 1 in. diameter ($a = 1{\cdot}27$ cm) and $c_0 = 5{\cdot}23 \times 10^5$ cm/s.

The velocity c in Fig. 2, curve (a), is a phase velocity. In dispersive media, the group velocity, i.e. the velocity of propagation of a wave packet composed of waves whose wavelengths do not differ greatly from a certain fixed value, is more important than the phase velocity. If c_g is the group velocity,

$$c_g = c\left(1 - \frac{n}{c}\frac{dc}{dn}\right)^{-1} \quad \text{or} \quad \frac{c_g}{c_0} = \frac{c}{c_0}\left[1 - \left(\frac{c_0}{c}\right)\left(\frac{an}{c_0}\right)\frac{d(c/c_0)}{d(an/c_0)}\right]^{-1} \tag{4}$$

The values of c_g/c_0 for different values of an/c_0 can be derived by differentiating curve (a) in Fig. 2 and using equation (4); the variation of c_g/c_0 with an/c_0 is shown in curve (b) of Fig. 2. A significant feature of this curve is the minimum value, $c_g/c_0 = 0{\cdot}38$, which occurs when $an/c_0 = 0{\cdot}322$.

From the group velocity curve, it is possible to make certain generalizations about the propagation of a pulse in a cylindrical bar. To avoid the effects of reflexions, consider a bar of infinite length with its axis along Ox. Suppose the bar is stressed initially so that the stress is zero everywhere except at the cross-section $x = 0$, where it is infinite. The spectrum of a distribution of this type will include all possible wavelengths. Suppose the distribution is released at time $t = 0$; consider the sequence of events at a point P of abscissa x at time t. From Kelvin's method of stationary phase, it follows that waves of most wavelengths will interfere destructively (in the sense in which the phrase is used in optics) at P at time t; there will, however, be a group of waves whose wavelengths are such that they reinforce at P at time t and these waves must satisfy the condition that the phase $2\pi(x - ct)/\Lambda$ is stationary. This is easily shown to be equivalent to the condition $x - c_g t = 0$.

From curve (b) of Fig. 2, the maximum value of the group velocity is c_0; the leading edge of the pulse will therefore arrive at P at time $t_0 = x/c_0$ and, since $c_g/c_0 = 1$ corresponds to small values of an/c_0, the initial disturbance will be composed of waves of very low frequency. The minimum value of the group velocity is $0{\cdot}38\ c_0$ and the trailing edge of the disturbance will therefore reach P at time $t_1 = x/0{\cdot}38\ c_0 = 2{\cdot}63\ x/c_0$. It follows that, in traversing the distance x, a pulse, originally of infinitely short duration, is distorted into a disturbance of duration $t_1 - t_0 = 1{\cdot}63 \times x/c_0$; the duration of the disturbance thus increases linearly with the distance x from the origin.

In Section 2, it was pointed out that a pulse which originated in a limited area gave rise to a non-uniform distribution of stress over the cross-section, unless it had travelled a distance of about $8a$ from the origin. Putting $x = 8a$ in the above expression for $(t_1 - t_0)$, we obtain an approximate value for

the minimum duration, Δ, of the pulse which can be produced in a bar of radius a:

$$\Delta \simeq 13\, a/c_0 \qquad (5)$$

For steel, $c_0 \simeq 5 \times 10^5$ cm/s, giving $\Delta \simeq 26\, a\ \mu$s, implying that in a bar 1 in. diameter ($a = 1{\cdot}27$ cm), $\Delta \simeq 33\ \mu$s.

In using this result, it must be remembered that it is based on experiments with a bar 2·5 in. diameter, struck by a bullet of 0·22 in. calibre. If the ratio of the area of the bar to the area over which the pressure is applied is increased, the value of Δ will also increase, and vice versa.

The mean frequency, n_p, of the small group of waves which produces the predominant effect at P at time t can be derived easily from curve (b) of Fig. 2. It is again convenient to think in terms of non-dimensional variables and to imagine $n_p a/c_0$ plotted as ordinate against t/t_0 as abscissa. Now $t/t_0 = c_0/c_g$, whilst $n_p a/c_0$ is simply the value of an/c_0 corresponding to the chosen value of c_g/c_0. Thus the only differences between the ($n_p a/c_0$, t/t_0) curve and curve (b) of Fig. 2 are that the ordinate and abscissae scales are interchanged and that c_g/c_0 in the latter is replaced by c_0/c_g.

One interesting feature is that in the range $1 \geqslant c_g/c_0 \geqslant c_s/c_0$, i.e. the range $1 \geqslant c_g/c_0 \geqslant 0{\cdot}5764$ or, in terms of t/t_0, $1 \leqslant t/t_0 \leqslant 1{\cdot}735$, $n_p a/c_0$ is a single-valued function of t/t_0, whereas it is a double valued function in the range $1{\cdot}735 \leqslant t/t_0 \leqslant 2{\cdot}64$. This implies that, in the former range, the disturbance will consist of a single dominant group whose frequency increases as t/t_0 increases; in the second range of t/t_0, two dominant groups, differing in frequency and wavelength, will arrive simultaneously at the point considered.

In general, one would expect the (strain, time) or the (displacement, time) curve at a given point to consist of a pulse which may be regarded as a distorted form of the original pulse, followed by a tail, or coda, of high frequency oscillations. Experiments confirm this view and analysis of experimental data gives results which are in good agreement with the calculated values of n_p [see item (2) of Short Bibliography, Fig. 14].

Similar considerations apply to almost every type of wave in bounded solids of practically every geometrical form and dispersion appears almost invariably when the propagation of the waves is investigated using the exact equations of motion of elastic solids. It is, however, interesting to note that there exist two cases of dispersionless propagation: bodily and surface waves in a homogeneous, semi-infinite solid and torsional waves in a circular cylinder.

5. VISCO-ELASTIC WAVES

The characteristic property of a visco-elastic solid is that frictional or viscous stresses are operative, in addition to elastic or Hookean stresses. In general, the viscous stresses are a function of the time and space derivatives of the displacement; in a number of solids, it is sufficient to consider the first derivatives only and the relation between the stress σ and the strain ϵ for the so-called "standard linear solid" is of the form

$$A\sigma + B\frac{d\sigma}{dt} = C\epsilon + D\frac{d\epsilon}{dt} \qquad (6)$$

where A, B, C and D are constants for a given solid. The terms involving the time-derivatives of σ and ϵ represent the viscous forces and when they vanish, equation (6) reduces to the usual Hookean equation. For the majority of metals, the viscous stresses are small compared with the Hookean stresses, but they become very important in materials like rubber and plastics which exhibit large time-effects when they are stressed or unstressed.

If we consider a one-dimensional system, the type of dispersion discussed in the preceding section will be absent and it is possible to derive the equation of wave motion in the solid. If the space-variable is x, the displacement, u, at a point abscissa x at time t, in a solid whose elements obey equation (6), may be shown to be given by the equation

$$\rho\left(A\frac{\partial^2 u}{\partial t^2} + B\frac{\partial^3 u}{\partial t^3}\right) = C\frac{\partial^2 u}{\partial x^2} + D\frac{\partial^3 u}{\partial x^2 \partial t} \qquad (7)$$

where ρ is the density of the solid.

For a sinusoidal wave of frequency $\omega/2\pi$, travelling in the positive direction of x, the solution is of the form

$$u = u_0\, e^{-\gamma x} \sin \omega\left(t - \frac{x}{c}\right) \qquad (8)$$

where c is the phase velocity, and u_0 and γ are constants. u_0 represents the initial amplitude and the factor $e^{-\gamma x}$ shows that the wave is attenuated exponentially as it moves away from the origin.

When the value of u in equation (8) is substituted in equation (7), there results a complicated algebraic equation from which one can derive the phase velocity c and the attenuation coefficient γ. It is found that c and γ, together with the group velocity, c_g, are functions, not only of the constants, ρ, A, B, C and D of the material, but also of the frequency $\omega/2\pi$. It follows that dispersion is present, accompanied by attenuation which is a function of frequency, or wavelength.

By way of illustration, consider a solid for which the constant C in equations (6) and (7) vanishes. Such a solid is usually called a Maxwell[6] solid and it is often represented either by an electrical model, or by a mechanical model consisting of a spring of modulus E, in series with a dashpot, with which a coefficient of viscosity, η, is associated. (See inset in Fig. 3.) The (stress, strain) relationship for an element of a Maxwell solid is

$$\sigma + \frac{\eta}{E}\frac{d\sigma}{dt} = \eta\frac{d\epsilon}{dt}$$

or, introducing a constant $\beta = \eta/E$, which has the dimension of time and is called the time of relaxation,

$$\sigma + \beta\frac{d\sigma}{dt} = \beta E\frac{d\epsilon}{dt} \qquad (9)$$

Some insight into the features of the propagation of sinusoidal waves in a Maxwell solid may be obtained by considering the behaviour of an element when it is subjected to a stress which varies harmonically with time. Let $\sigma = \hat{\sigma}\, e^{i\omega t}$, where $\hat{\sigma}$ is the amplitude of the stress, $\omega/2\pi$ the frequency and i the imaginary. Substituting in equation (9), it is found that

$$\epsilon = \frac{\sigma}{E}\left(\frac{1 + i\beta\omega}{i\beta\omega}\right) = \frac{\sigma}{E}\left(1 - \frac{i}{\beta\omega}\right)$$

The amplitude, $\hat{\epsilon}$, of the resulting strain is therefore

$$\hat{\epsilon} = \frac{\hat{\sigma}}{E}\sqrt{\left(1 + \frac{1}{\beta^2\omega^2}\right)}$$

and the strain ϵ lags behind the applied stress σ by the angle $\theta = \tan^{-1}(1/\beta\omega)$.

When $\beta\omega \gg 1$, $\hat{\epsilon} = \hat{\sigma}/E$ and $\theta = 0$; the element behaves elastically and viscous effects are negligible, as one would

expect, since $\beta\omega \gg 1$ implies that $\eta\omega/E \gg 1$, i.e. the dashpot behaves as a rigid connexion and the strain of the spring per unit stress is very large. Under these conditions, the phase velocity, c, of stress waves in the solid will depend only on E and $c = c_0 = \sqrt{(E/\rho)}$.

If, on the other hand, $\beta\omega \ll 1$, $\hat{\epsilon} = \hat{\sigma}/E\beta\omega = \hat{\sigma}/\eta\omega$ and $\theta = \pi/2$, implying that dissipative effects predominate; the spring now behaves as a rigid connexion and the sole effect of the applied stress is to shear the liquid in the dashpot. Since there are no restoring forces in the medium, waves cannot be propagated, and, effectively, $c = 0$.

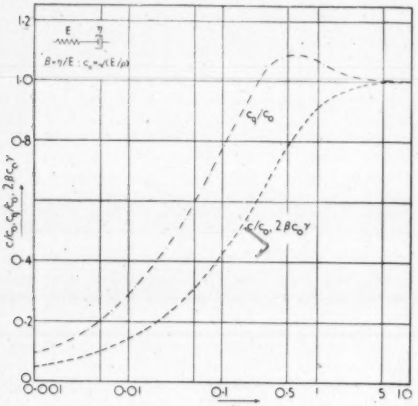

Fig. 3. Maxwell solid. The variation of phase velocity, c, group velocity, c_g, and attenuation coefficient, γ, with frequency, $\omega/2\pi$, for sinusoidal waves

A detailed investigation [see Short Bibliography (2), p. 116] confirms these deductions and the relationship between the non-dimensional variables c/c_0, $2\beta c_0\gamma$, c_g/c_0 plotted as ordinates against $\beta\omega$ as abscissa is shown in Fig. 3. When $\beta\omega = 0$, $c = c_g = \gamma = 0$. As the frequency increases (or the wavelength decreases), c/c_0, c_g/c_0 and $2\beta c_0\gamma$ are seen to increase and, when $\beta\omega$ becomes very large, they approach the value unity asymptotically.

6. PLASTIC WAVES

The theory of the propagation of waves in metal wires, when the stress exceeds the yield stress, was developed independently by Taylor[5] and by von Kármán[7] during the last war. Even in the simple case of one-dimensional extensional waves, the velocity, c_p, of a plastic wave of loading is a function of the stress or the strain. If σ^* is the "nominal" or "engineering" stress, i.e. the ratio of the total force over a cross-section to the original, unstressed area of the section, and if ϵ is the strain, i.e. the fractional increase in length of an element, c_p is given by the equation

$$c_p = \sqrt{\left(\frac{1}{\rho}\frac{d\sigma^*}{d\epsilon}\right)} \qquad (10)$$

ρ being the density of the material.

In the elastic region, $d\sigma^*/d\epsilon$ is constant and equal to Young's modulus, E; equation (10) then reduces to the familiar equation $c_0 = \sqrt{(E/\rho)}$.

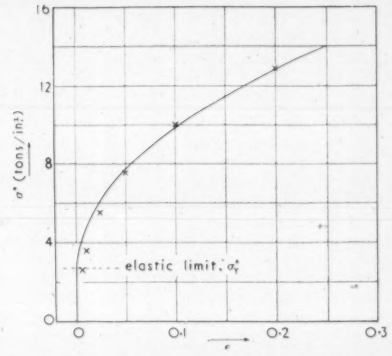

Fig. 4. The variation of nominal stress, σ^*, with strain, ϵ, for copper, based on Taylor's[8] parabolic relationship, $\sigma(\text{dynes/cm}^2) = 5{\cdot}52 \times 10^9 \times \sqrt{[\ln(1+\epsilon)]}$, where $\sigma =$ true stress

$\times$ are values deduced from Taylor's equation.
$E = 12{\cdot}75 \times 10^{11}$ dynes/cm^2 = 8258 tons/in.^{2}.
Assumed value of elastic limit, $\sigma_Y^* = 2{\cdot}83$ tons/in.^{2}. Strain at elastic limit = $3{\cdot}43 \times 10^{-4}$.

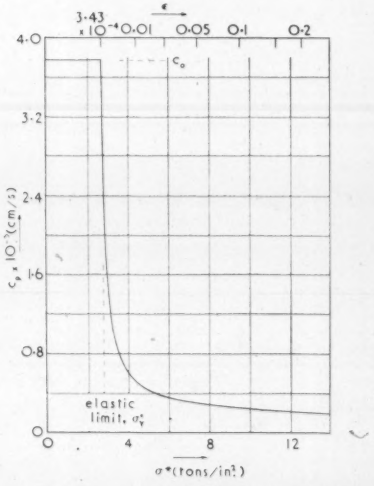

Fig. 5. The velocity, c_p, of plastic waves in copper as a function of nominal stress, σ^*, and strain, ϵ, deduced from the (σ^*, ϵ) curve of Fig. 4. $\rho = 8{\cdot}93$ gm/cm^3; $c_0 = 37{\cdot}78 \times 10^4$ cm/s

In the case of most metals, $d\sigma^*/d\epsilon$ decreases as ϵ increases, when σ^* exceeds the stress σ_Y^* at the elastic limit; plastic waves will usually travel with a lower velocity than elastic waves and, in the plastic region, the velocity of propagation will decrease as the stress and the strain increase.

Figs. 4 and 5, which refer to annealed polycrystalline copper, will serve for the purpose of illustration. Fig. 4 shows the relationship between σ^* and ϵ. The yield stress σ_Y^* has been taken as 2·83 tons/in.^{2} ($4{\cdot}37 \times 10^8$ dynes/cm^2) and the value of E as 8258 tons/in.^{2} ($12{\cdot}75 \times 10^{11}$ dynes/cm^2); the strain corresponding to σ_Y^* is $3{\cdot}43 \times 10^{-4}$. In the plastic region, the curve has been based on Taylor's[8] parabolic relationship between σ, the true stress (i.e. the ratio of the total force to the instantaneous value of the cross-sectional area) in dynes/cm^2 and strain ϵ under statical loading:

$$\sigma = 5{\cdot}52 \times 10^9 \sqrt{[\ln(1+\epsilon)]} \qquad (11)$$

The crosses in Fig. 4 represent values which have been calculated from this equation.

Assuming that the curve of Fig. 4 holds also for dynamical loading, Fig. 5 shows the relationship between c_p and σ^* (or ϵ) deduced by means of equation (10). For copper, $\rho = 8{\cdot}93$ gm/cm^3 and the velocity, c_0, of stress waves in the elastic region is $37{\cdot}78 \times 10^4$ cm/s. The striking feature of the curve is the sudden drop in the value of the velocity which occurs when σ^* just exceeds σ_Y^*.

The effect of this variation of velocity on the propagation of a pulse has been discussed by Taylor[9] who considers a semi-infinite wire, the longitudinal velocity of one end of which is suddenly increased from zero to a finite, constant value. If the stress exceeds σ_Y^*, the stress pulse travelling away from the impelled end will consist of a steep front, at which the stress jumps from zero to σ_Y^*, followed by a region in which the stress is constant and equal to σ_Y^*. At the rear of this region, the stress increases until it attains a limiting value determined by the value of the velocity of the impelled end and by the form of the (σ^*, ϵ) curve of the material of the wire. The length of the pulse increases as it travels away from the origin.

SHORT BIBLIOGRAPHY

(1) DAVIES, R. M. *Appl. Mech. Rev.*, **6**, p. 1 (1953).

(2) DAVIES, R. M. *Surveys in Mechanics*: *G. I. Taylor* 70*th Anniversary Volume* (Ed. by G. K. Batchelor and R. M. Davies). Article "Stress Waves in Solids," pp. 64–138 (London: Cambridge University Press, 1956).

(3) KOLSKY, H. *Stress Waves in Solids* (Oxford: Clarendon Press, 1953).

(4) RINEHART, J. S., and PEARSON, J. *Behaviour of Metals under Impulsive Loads* (Cleveland, Ohio: American Society for Metals, 1954).

(5) SCHOCH, A. *Ergebn. Exact. Naturw.*, **23**, p. 127 (1950).

REFERENCES

(1) HOPKINSON, B. *Phil. Trans A*, **213**, p. 437 (1914) [Reprinted in Hopkinson, B. *Scientific Papers* (London: Cambridge University Press, 1921)].

(2) ROBERTSON, R. *Trans Chem. Soc.*, **119**, p. 1 (1921).

(3) LANDON, J. W., and QUINNEY, H. *Proc. Roy. Soc. A*, **103**, p. 622 (1923).

(4) DAVIES, R. M. *Phil. Trans A*, **240**, p. 375 (1948).

(5) TAYLOR, G. I. Confidential Ministry of Supply Report, R.C. 70 (1940). To be published in G. I. Taylor *Scientific Papers*, Vol. 1 (London: Cambridge University Press, 1956).

(6) MAXWELL, J. C. *Phil. Trans*, **157**, p. 49 (1867) [Republished in 1890: *Scientific Papers*, Vol. 2 (London: Cambridge University Press)].

(7) VON KÁRMÁN, TH. Confidential U.S. Report (1942). Later published in shortened form by VON KÁRMÁN, TH., and DUWEZ, P. *J. Appl. Phys.*, **21**, p. 987 (1950).

(8) TAYLOR, G. I. *Proc. Roy. Soc. A*, **145**, p. 388 (1934).

(9) TAYLOR, G. I. *J. Instn Civ. Engrs*, **26**, p. 486 (1946).

The mechanism of pulse temperature rise on the surface of thermionic cathodes*

By R. DEHN, M.Sc., A.R.C.S., A.Inst.P., The General Electric Co. Ltd., Wembley, Middlesex

[*Paper first received* 19 *December*, 1955, *and in final form* 10 *February*, 1956]

During the operation of high- and medium-power pulsed magnetrons, spontaneous fluctuations were observed in the surface temperature of the cathode, during the application of the pulse. On investigation of this effect it appeared that the pulse temperature rise was not due to electron bombardment of the cathode as previously assumed. It seems probable that the effect is caused by resistive heating as current passes through a thin layer of high resistivity at the cathode surface. The existence of such a layer is confirmed by the findings of other investigators.

While the present investigation has been undertaken in connexion with a research programme on the operation of high- and medium-power pulsed magnetrons, many of the results are applicable to thermionic emitters in general, principally to those of the oxide-coated type.

During magnetron operation, a small proportion—usually about 5–10%—of the input power is dissipated in cathode heating by electron back-bombardment. The increase in *mean* cathode temperature is easily measured with an optical pyrometer, and the increase in filament power required to produce the same temperature rise in the inoperative magnetron is used as an indication of the mean back-bombardment power.

In a pulsed magnetron, the observed mean temperature rise is the integrated effect of the instantaneous temperature rise, since power is only supplied during the pulse. The pulse length throughout this work has been 1 μs, except in a few cases where it was 2 μs. Repetition rates have varied from 10 to 1000 pulses/s with 500 pulses/s as the usual figure. During the pulse, the temperature of the cathode surface may rise well above the mean temperature, particularly if a very thin layer is considered. Such a temperature rise would affect both operation and life of the cathode.

Previous attempts have been made to calculate this instantaneous or pulse temperature rise theoretically, or to estimate it from measurements of the mean temperature rise.[1–3] All such attempts suffer from a wide margin of uncertainty in the values of the physical constants of the cathode surface, particularly specific heat and thermal conductivity. Some means for measuring the pulse rise of temperature directly was therefore sought.

APPARATUS

Full details of the apparatus developed for this purpose and of the experimental technique have already been published.[4] The same paper also deals at some length with the time resolution obtained, and with the elimination of effects other than genuine temperature fluctuations on the cathode surface. It is sufficient here to say that some of the visible and infra-red radiation from the magnetron cathode was focused on to the photo-cathode of an infra-red image converter. The light from the fluorescent screen of the image converter was in turn received by a photomultiplier. The photomultiplier output was amplified and displayed on the screen of a cathode-ray oscillograph. From the amplitude of the observed pulse it was possible to calculate the instantaneous temperature rise of the cathode surface.

A simplified block diagram of the arrangement is shown in Fig. 1. This apparatus enabled temperature changes as small as 1 or 2° C at a mean cathode temperature of between 800 and 900° C to be detected, with a time resolution of the order of 10^{-7} s.

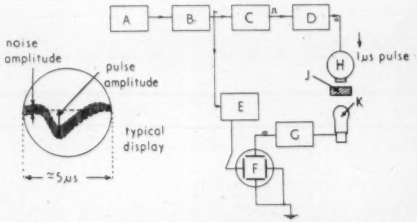

Fig. 1. Block diagram of apparatus, modulator and display

A, oscillator; *B*, initiator (pulse former); *C*, amplifier and shaper; *D*, final modulator; *E*, cathode-ray oscillograph time-base; *F*, cathode-ray tube; *G*, pulse amplifier; *H*, magnetron; *J*, image converter; *K*, photomultiplier.

EXPERIMENTAL RESULTS

Six different valves were studied, all medium power pulsed magnetrons for operation at *S*-band frequency. The difference between the valves was only in their structural details, i.e. "side-arm" or "packaged" type, the number of resonators comprising the anode block, and the type of cathode employed; these characteristics are shown in Table 1. The active (i.e. coated) area of all cathodes was 7·54 cm^2. The pulse length was 1 μs, unless otherwise stated.

Table 1. *Details of magnetrons examined*

Valve number	*Construction*	*Resonators*	*Cathode*
1	side-arm	14	oxide-coated
2	packaged	12	oxide-coated
3	packaged	12	nickel-mush
4	packaged	12	nickel-mush
5	side-arm	14	oxide-coated
6	side-arm	12	oxide-coated

* G.E.C. Communication No. 656.

Table 2 shows a typical set of readings obtained with valve No. 1. This was a trial run only to obtain some idea of the order of magnitude of the pulse temperature rise, T_p, and no endeavour was made to keep any particular operating parameters, such as power or mean cathode temperature, constant.

Table 2. *Typical set of readings*

Anode voltage (kV)	*Anode current* (A)	*Pulses/s*	*Efficiency* (%)	W_b (W)	*Mean cathode temperature* (°C)	T_p (°C)
16·0	20·0	500	61	21·7	657	59
20·0	20·0	500	55	30·4	699	25
16·8	40·0	500	42	41·2	757	18
16·0	20·0	1000	53	46·7	778	10
20·0	30·0	500	50	48·4	786	20
16·8	40·0	500	51	45·5	850	6·5
21·0	40·0	500	43	65·2	867	9·5
20·0	30·0	500	50–60	52·0	882	12

It seemed that T_p depended on several of the variables, so that conditions were more carefully controlled in later experiments. In particular, the mean back-bombardment power W_b was obviously not the chief controlling factor here, since apparently T_p has a tendency to decrease with increasing W_b. However, in view of the other varying parameters, no physical significance was attached to this.

Three further sets of readings were taken on valves Nos. 1 and 2 under conditions of either constant cathode temperature or constant input power. The value of T_p was found to be of the same order of magnitude as before, i.e. a few degrees to a few tens of degrees, depending mainly on mean cathode temperature. In one particular experiment the effective loading of the magnetron—and hence the back-bombardment power W_b—was varied by means of an external mismatcher keeping all other operating conditions constant. In this and all other experiments, except one, the correlation between W_b and T_p was negligible at any given mean cathode temperature.

These results made it clear that back-bombardment was not the main cause of the observed pulse temperature rise, as had originally been supposed. Moreover, any theoretical attempt to account for the pulse temperature rise in terms of electron back-bombardment fails to explain the considerable dependence of T_p on the mean cathode temperature. In applying, for example, Collins's theory of pulse temperature rise[1] one would have to assume that the specific heat and thermal conductivity of the cathode coating are themselves functions of temperature. On this basis, however, the results obtained could only be brought into agreement with theory by assuming an impossibly large variation with temperature of the thermal properties of the coating. In fact, the thermal conductivity and/or specific heat would have to vary by a factor of five or six to one, for a temperature change of about 200° C (650–850° C). It seems that variations of such magnitude must almost certainly be ruled out.

A question which arose out of these considerations was whether any pulse temperature rise would still be observed in the absence of cathode back-bombardment. In practice back-bombardment may be completely eliminated by applying a normal voltage pulse but no magnetic field to the magnetron. No radio-frequency oscillations can then build up, and there is consequently no back-bombardment. The magnetron, in fact, operates as a diode, saturated or unsaturated, depending on the applied voltage and on the cathode temperature.

Valves Nos. 1 and 2 were therefore run as diodes at 500 pulses/s. Owing to the complete absence of back-bombardment, the mean temperature rise was practically negligible. It was certainly too small to be measured, corresponding to a mean power in the cathode of less than 1 W. It was probably caused by the I^2R loss resulting from the passage of current through the resistance of the cathode, as observed by other workers.[1,3] The results showed that the observed T_p was at least of the same order as for the normally operated magnetron (from a few degrees to over 60° C). In addition, it was noted that T_p increased rapidly throughout with increasing anode potential, particularly after saturation had been reached. These results further confirmed that the electron back-bombardment, which takes place in the normally operated magnetron and which is responsible for a considerable increase in *mean* cathode temperature, is not the main cause for the observed *pulse* temperature rise of the cathode surface.

The extent to which T_p would depend on the nature of the cathode surface itself was next examined. Valves Nos. 1 and 2 were fitted with an ordinary oxide-coated cathode (BaO.SrO). The cathodes of valves Nos. 3 and 4, on the other hand, were of the "mush" type, i.e. sintered nickel mush impregnated with the active oxides. Valve No. 3 was run as a diode, up to an anode voltage of 30 kV and peak anode current of 16 A. No pulse temperature rise, nor any increase of mean temperature, was observed. It was estimated that if any pulse rise did exist at all it would be less than 1° C.

Valve No. 4 was then run as a normal magnetron, up to a maximum peak power input of 1·6 MW. The mean back-bombardment power was then 55·8 W. Still no pulse rise was observed. Thus it would seem that some property peculiar to the mush type of cathode prevents T_p from reaching observable magnitudes in both diode and magnetron operation. In addition, these results with the mush cathode furnish independent evidence that the pulse rise observed in the case of oxide-coated cathodes is not due to some spurious effect, e.g. fluorescence at the surface.

Valve No. 1 was then operated under constant conditions as a magnetron, varying the pulse repetition rate at several fixed mean cathode temperatures. It was thought possible that the repetition rate might have some effect on T_p.

The results showed that even over the very wide range of from 10 to 500 pulses/s T_p was practically independent of repetition rate, at any given mean cathode temperature. The average of all measured T_p values was then computed for each mean cathode temperature.

It was found that the points could be closely fitted to a straight line when $\log T_p$ was plotted against $1/T$, where T is the mean cathode temperature in °K (Fig. 2).

The results so far obtained showed fairly conclusively that:

(i) T_p decreased with increasing mean cathode temperature, probably according to the law: $\log T_p = (a/T) + b$, where T is the mean cathode temperature in degrees absolute, and a and b are constants;

(ii) there was no significant correlation between T_p and W_b;

(iii) no pulse rise was observed for a nickel-mush cathode under any conditions;

(iv) when valves were operated as diodes, i.e. with no magnetic field, thus eliminating all back-bombardment, T_p was found to be of the same order as for normal magnetron operation. In particular, points (i) and (iii) were found to apply in the case of diode, as well as magnetron, operation;

(v) there was apparently no dependence of T_p on pulse repetition rate.

A possible interpretation of these facts could be that the observed T_p is almost entirely due to I^2R heating as electrons are emitted from the cathode surface. The emissive surface is a type of semiconductor, and as such its resistance decreases exponentially with increasing temperature, accounting for point (i) above. For oxide-coated cathodes the variation of coating resistivity with temperature has been investigated by several workers.[5–11] They all quote the same general relation connecting coating resistance and temperature:

$$K = K_0 \exp(-Q/kT) \tag{1}$$

where K is the electrical conductivity, K_0 is a constant, k is Boltzmann's constant in eV/°K, T is the absolute temperature and Q is an activation energy, called an internal work function by some writers.[8] Others[6] identify this energy with Richardson's thermionic work function ϕ for well-activated cathodes at high temperatures.

Equation (1) can easily be re-written in terms of coating resistance rather than conductivity:

$$R = R_0 \exp(Q/kT) \tag{2}$$

where R is the resistivity and R_0 a constant. If it is assumed that the observed pulse temperature rise is proportional to I^2R, where R is the coating resistivity and I is the emission current density, one can write:

$$T_p = aI^2R + b$$

where a and b are constants. Neglecting b, which is zero if T_p is caused solely by the I^2R heating effect, and substituting for R from equation (2) gives the relation:

$$\log_e(T_p) = (Q/kT) + C \tag{3}$$

where C is another constant. It is because of this relationship that such importance was attached to the plot shown in Fig. 2. Hence, if the proposed hypothesis is correct, the slope of a plot such as that of Fig. 2 should yield a value of the activation energy of the cathode (in electron volts) of the same order as, or slightly smaller than, the thermionic work function. For Fig. 2 the value of $Q = 1{\cdot}01$. This is of the same order of magnitude as the work function normally quoted in this connexion for oxide cathodes.[8,12]

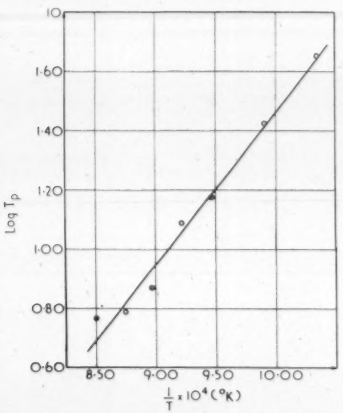

Fig. 2. Plot of log (pulse temperature rise) against reciprocal of absolute temperature

The absence of any observable pulse rise in the case of valves fitted with the mush cathode could presumably be accounted for by the proposed hypothesis on the grounds of the very much lower resistivity of this type of cathode.

The next step consisted of more detailed examination of the T_p/mean cathode temperature relationship for both magnetron and diode operation, and investigation of a possible contribution to the total observed T_p by other factors.

Two further valves (Nos. 5 and 6) were examined in addition. Another eight sets of measurements entirely confirmed the previous findings, and results will not be quoted in detail. In many cases log T_p was plotted against $1/T$ (as in Fig. 2) for both magnetron and diode operation. Fig. 3

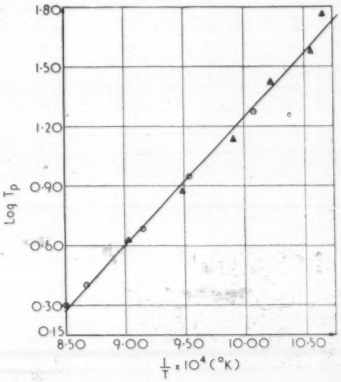

Fig. 3. Plot as in Fig. 2, but for two sets combined

shows one such plot prepared from two separate series of observations covering a total mean cathode temperature from 664 to 904° C in two partially overlapping ranges. Although the two sets were obtained on different occasions the respective results are seen to be in close agreement.

DISCUSSION OF RESULTS

The most important fact arising out of all the results is the evident confirmation of the relationship suggested earlier [equation (3)] between the pulse temperature rise and the mean cathode temperature, i.e.

$$\log T_p = (Q/kT) + C \tag{3}$$

In all cases where the operating conditions were kept constant and only the mean cathode temperature was varied it was found that the above relationship was obeyed very closely for both magnetron and diode operation.

Further, in using this relationship to calculate the activation energy of the cathode, the values obtained were of the right order of magnitude. For valve No. 1 this value was 1·01 eV,

for valve No. 5 the mean of three sets was $0{\cdot}82 \pm 0{\cdot}04$ eV, and for valve No. 6 the mean of three sets was $1{\cdot}39 \pm 0{\cdot}16$ eV. The agreement between results for the same valve seems adequate in view of the limited accuracy of the measurement. The rather larger variations for different valves are most easily explained in terms of variation of the work function or activation energy with age, and with slight differences in processing of the different cathodes. All the valves used were experimental types where variations, particularly in cathode characteristics, are generally to be expected.

The evidence of these results, therefore, suggests that the observed pulse temperature rise is a linear function of the resistivity of the cathode coating in the case of oxide-coated cathodes. The resistivity of the mush-type cathode (valves Nos. 3 and 4) is naturally much lower and no pulse rise was observed under any conditions for this type of cathode.

The next point to be explained is the apparent failure of the electron back-bombardment of the cathode to cause any appreciable pulse temperature rise in the case of magnetron operation. It might be asked why, if this pulse rise is due to resistive heating of the oxide coating, no such heating is caused by the current due to the back-bombarding electrons. Moreover, these electrons represent enough total energy to cause quite a considerable mean temperature rise, while under diode operation the I^2R heating caused practically no increase in the mean cathode temperature. It seems that this apparent difficulty can be explained by assuming the existence of a thin, highly resistive, surface layer. It is known from the study of secondary emission[13–15] that for nearly all secondary emitters the secondary emission coefficient reaches a maximum if the energy of the primary electrons is somewhere between 500 and 1000 eV. If this energy is exceeded the secondary emission coefficient decreases because of the increasing depth of penetration of the primary electrons. Now the average energy of the back-bombarding electrons in a magnetron of the type here used is of the order of several kV at least. Hence these electrons will penetrate to a depth of about 3–5 μ into the surface layer. Most of their energy, therefore, will be dissipated a little below the cathode surface causing the observed mean temperature rise without at the same time producing any appreciable pulse temperature rise. This pulse rise will then be largely due to the I^2R heating caused by the passage through the surface of the *net* current emitted. The fact that this current in the operating magnetron consists largely of secondary electrons does not affect the issue. The I^2R heating alone causes only a very small mean temperature rise which, as already mentioned, was observed under diode conditions, i.e. in the absence of any back-bombardment.

It was thought at first that if the pulse rise was due to the I^2R heating effect in accordance with the foregoing discussion that in plotting $\log T_p$ against T^{-1} the additive constant should be proportional to $\log I_a$ if the remaining operating conditions were kept constant. That is:

$$\begin{aligned}\log T_p &= \log (CI_a^2R)\\ &= \log CI_a^2 + \log R\\ &= \log CI_a^2 + (Q/kT), \text{ by equation (3)}\end{aligned}$$

where C is an arbitrary constant. Also, where in addition the cathode temperature was kept constant, T_p should be proportional to I_a^2. This was not confirmed by experiment, and no simple relationship between anode current and T_p was found, but this does not necessarily invalidate the proposed theory. The dependence of T_p on current as suggested above assumes that R, the coating resistance, is constant at any given temperature. This, however, is not the case. The coating resistance does, in fact, vary with current in a fairly complicated manner as shown by Coomes, Wright and others.[2,3,7,9,11,16,17] Some of these[7] stipulate an accelerating field at the cathode surface, i.e. operation under temperature limited conditions, whereas others[3,16] have observed variations of coating resistance with current even under space charge limited conditions. In at least one case[17] this variation was measured by means of an embedded probe. This would explain the apparent lack of correlation between T_p and the anode current, for both diode and magnetron operation.

By assuming normal values for the coating resistance,[3,5–9] specific heat and density,[18,19] it is easy to calculate T_p for a given pulse length, current density and layer thickness, assuming no heat losses during the pulse.

Considering unit area of coating, and neglecting the $I\phi$ cooling-effect which is always less than 6% of the I^2R heating for these experiments:

$$I^2Rt = dc\rho T_p \times 4{\cdot}18$$

where I = current density, R = resistance of unit area of coating of thickness d, t = pulse length, c = specific heat, ρ = density, and T_p = pulse temperature rise. Calculation shows[20] that in order to obtain the observed T_p the layer thickness must be of the order of 1–2 μ, whereas the thickness of the usual sprayed oxide coating is about 100 μ. This then lends further support to the proposed existence of a thin, highly resistive, surface layer. Such a layer, at the current densities used in pulsed operation, would lead to voltage gradients of the order of several hundred kV/cm. Normally such high gradients would almost certainly cause dielectric breakdown. This question of breakdown has been discussed by Wright in some detail.[5] It is known that the breakdown field becomes a function of thickness at very small thicknesses of insulator, increasing rapidly with decreasing thickness. Hence for a thin layer, such as is considered here, even the high potential gradients mentioned may not necessarily cause dielectric breakdown. Furthermore, even if such breakdown did occasionally occur it is doubtful whether this would be noticeable in practice because of the very thin layer involved. The possibility of dielectric breakdown does not, therefore, appear to constitute a serious objection to the proposed theory.

Results obtained by a number of other workers supply independent evidence for the existence of a high resistance surface layer.[3,6,8,9,16,17,21–25]

CONCLUSIONS

Thus it seems reasonable to suppose that the pulse temperature rise is almost entirely due to the heating effect caused by the passage of current through a thin high resistance surface layer.

Further investigation could profitably be directed towards the study of variations of T_p with composition and age of oxide-coated cathodes.

In addition, the main difficulty of the proposed theory of pulse temperature rise is the stipulation that the back-bombarding electrons penetrate deeply enough into the coating not to cause any appreciable pulse rise of the surface. This could be checked by constructing a special tube allowing the controlled bombardment of oxide-coated and possibly other targets with electrons, the velocity of which could be varied over a very wide range. The value of T_p should then be measured as a function of the velocity of the bombarding

electrons. Such experiments would help in further establishing the proposed theory and in removing some of its present difficulties.

ACKNOWLEDGEMENTS

The author is indebted to the Admiralty for permission to publish this paper.

REFERENCES

(1) COLLINS, G. B. *Microwave Magnetrons*, M.I.T. Rad. Lab. Ser., No. 6 (New York: McGraw-Hill Book Co. Inc., 1948).
(2) FINEMAN, A., and EISENSTEIN, A. *J. Appl. Phys.*, **17**, p. 663 (1946).
(3) COOMES, E. A. *J. Appl. Phys.*, **17**, p. 647 (1946).
(4) DEHN, R. *Brit. J. Appl. Phys.*, **7**, p. 144 (1956).
(5) WRIGHT, D. A. *Proc. Roy. Soc. A*, **190**, p. 394 (1947).
(6) LOOSJES, R., and VINK, H. J. *Philips Res. Rep.*, **4**, p. 449 (1949).
(7) WRIGHT, D. A., and WOODS, J. *Proc. Phys. Soc. [London] B*, **65**, p. 134 (1952).
(8) LOVETT, C. M. *Proc. Phys. Soc. [London] B*, **67**, p. 387 (1954).
(9) TOMLINSON, T. B. *J. Appl. Phys.*, **25**, p. 720 (1954).
(10) HANNAY, N. B., MACNAIR, D., and WHITE, A. H. *J. Appl. Phys.*, **20**, p. 669 (1949).
(11) EISENSTEIN, A. *J. Appl. Phys.*, **20**, p. 776 (1949).
(12) WRIGHT, D. A. *Proc. Instn Elect. Engrs*, **100 (III)**, p. 125 (1953).
(13) RODDA, S. *Photoelectric Multipliers* (London: MacDonald and Co., 1953).
(14) ALLEN, J. S. *Proc. Inst. Radio Engrs*, **38**, p. 347 (1950).
(15) BENEKING, H. *Z. angew. Phys.*, **4**, p. 258 (1952).
(16) DANFORTH, W. E., and GOLDWATER, D. L. *J. Appl. Phys.*, **20**, p. 163 (1949).
(17) NEERGARD, L. S. *R.C.A. Rev.*, **13**, p. 464 (1952).
(18) PENGELLY, A. E. S. *Brit. J. Appl. Phys.*, **6**, p. 18 (1955).
(19) HERRMANN, G., and WAGENER, S. *The Oxide-Coated Cathode* (London: Chapman and Hall Ltd., 1951).
(20) WARD, H. L. H. Private communication.
(21) EISENSTEIN, A. *J. Appl. Phys.*, **17**, p. 654 (1946).
(22) LOOSJES, R., and VINK, H. J. *Vide*, **5**, p. 731 (1950).
(23) LOOSJES, R., and JANSEN, C. G. J. *Vide*, **7**, p. 1131 (1952).
(24) JANSEN, C. G. J., and LOOSJES, R. *Philips Res. Rep.*, **8**, p. 21 (1953).
(25) JANSEN, C. G. J., LOOSJES, R., and COMPAAN, K. *Philips Res. Rep.*, **9**, p. 241 (1954).

Direct carbon replicas from metal surfaces

By E. SMITH, B.A., and J. NUTTING, M.A., B.Sc., Ph.D., Department of Metallurgy, University of Cambridge

[*Paper received* 23 *January*, 1956]

Two methods have been developed for the removal of carbon replica films directly evaporated on to etched metal surfaces. These involve either electropolishing or chemically etching after deposition of the carbon. The film removed by electropolishing gives a replica of high resolution, whilst with the etching technique extraction replicas may be prepared from multiphase alloys and the extracted phases identified by electron diffraction. Some examples of the application of the techniques to carbon and alloy steels are given.

The chief disadvantages of the carbon replica method developed by Bradley[1] for the examination of metal surfaces are that it is a two-stage process and that in some cases the results are not reproducible. With the Formvar-carbon technique the resolution may be limited by the Formvar replica rather than the carbon replica which, it is thought, has a much higher resolving power. The lack of reproducibility is probably due to artefacts which arise when dissolving the Formvar from the carbon, and the effects are particularly marked when examining tempered alloy steels in which the structures are very fine.

Clearly it would be more desirable to evaporate carbon directly on to the etched metal surface and strip the film so produced to provide a suitable replica. Diehl, Mader and Seeger[2] have been able to strip directly-evaporated carbon films from electropolished aluminium, nickel and copper, by backing the replica with a plastic film which is subsequently dissolved away. However, with etched metal surfaces the film is often so adherent that it is very difficult to remove with the backing technique. If the film is removed it usually curls or breaks into very small pieces during separation from the backing film. Methods are described below which have been developed for removing evaporated carbon films from etched metal surfaces, thus producing replicas of excellent resolving power. It has also been possible to use the technique for preparing carbon extraction replicas from multi-phase alloys.

EXPERIMENTAL METHOD

Apart from complete solution of the specimen, two methods for the removal of the carbon film have been devised. The easiest and most universal method is by electropolishing, whilst as an alternative method for preparing extraction replicas chemical etching may be used. The stages in the processes are as follows.

(*a*) The metal surface is polished and etched so that the structure is readily visible under the optical microscope.

(*b*) A cleaning replica of Formvar is applied and dry-stripped from the surface in the usual manner. The purpose of the cleaning replica is to remove any loose particles of unattacked phases or etch products.

(*c*) A thin carbon film is evaporated on to the metal surface to be examined using the method developed by Bradley.[1] It has been found that good results are obtained if the point of one carbon rod is very sharp whilst the other is flattened or slightly hollowed. (A rotary pencil sharpener has been found to give an ideal type of point.) A suitable film is

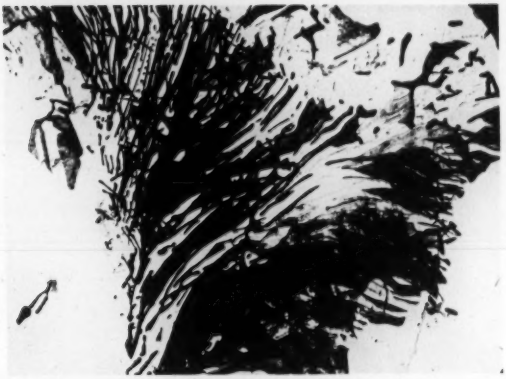

Fig. 1. Cementite lamellae from a 0·4% carbon, 1% chromium steel normalized from 850° C. The carbon extraction replica removed by etching and electro-polishing (×7500)

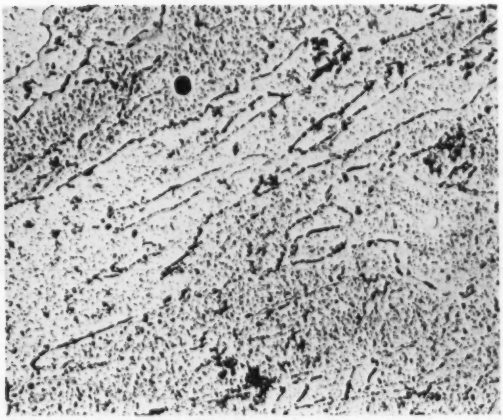

Fig. 2. Fine particles of vanadium carbide in a 0·2% carbon, 1% chromium, 0·65% vanadium steel. Oil quenched from 1050° C and tempered for half an hour at 700° C. The carbon extraction replica was removed from the specimen by etching (×30 000)

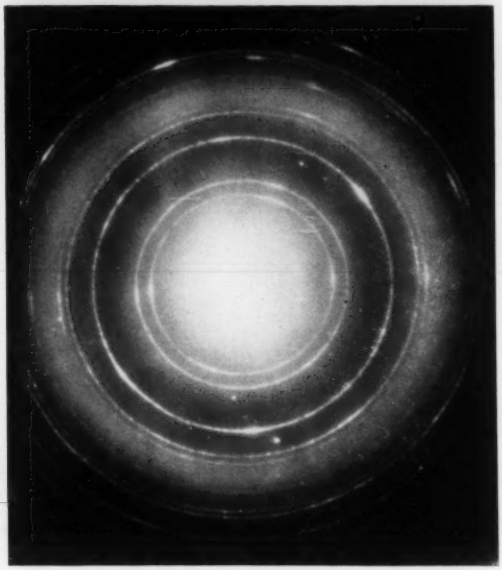

Fig. 3. Electron diffraction pattern of vanadium carbide from an extraction replica similar to that shown in Fig. 2

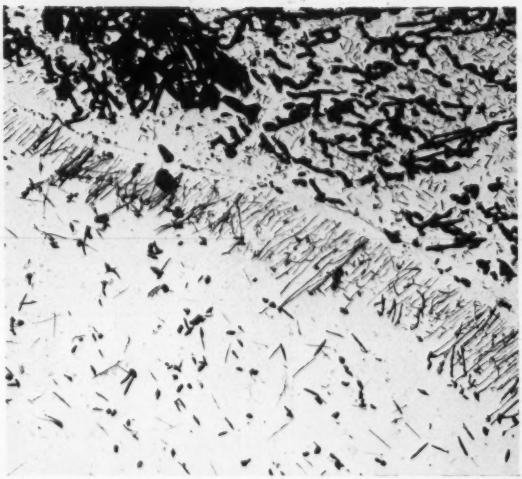

Fig. 4. Carbon extraction replica from a 2·25% chromium, 1% molybdenum steel, showing needle-like molybdenum carbides, and bainitic iron–chromium carbides. The replica was removed from the specimen by etching (×15 000)

obtained by evaporating the carbon for two seconds at a potential of 30 V which gives a current of about 30 A.

(*d*) The carbon film may be stripped by electropolishing in the solution normally used for the metal being examined. To aid removal, the film is scored into small squares whilst it is still on the specimen. During electropolishing the squares of film float into the electrolyte, from which they are collected and then washed. As it is difficult to collect all the film squares, the electrolyte must be filtered before being re-used. Filtering may be avoided by not scribing the film and stripping only a part of it during electropolishing. The final stripping can then be effected by transferring the specimen and film to water, when the surface tension forces at the air/water interface result in complete removal of the film on to the water surface. During this treatment the film sometimes breaks into small pieces, but these are usually large enough to cover specimen mounting grids.

To strip replicas from plain carbon and alloy steels the electropolishing solution used was 10% nitric acid in ethyl alcohol. With a current density of 1–1·5 A/cm^2, the film was removed after about fifteen seconds. The current density is lower than that normally used for electropolishing, since if the current density is too high the gases evolved may break up the replica. After stripping from the steel the replicas were washed in 30–40% nitric acid in water for at least ten minutes, and finally for about five minutes in distilled water. They were then collected on mounting grids and dried.

The method of removal by etching is more difficult. It has, however, been found to be suitable for the examination of finely dispersed multiphase alloys, but it is not satisfactory for structures containing large closely-packed particles, e.g. pearlitic steels. The great advantage of the method is that any particles of secondary phases loosened from the alloys by etching remain attached to the replica, and they can therefore be photographed in the positions they occupied in the alloy, whilst in many cases it is possible to identify the particles by their electron diffraction patterns.

The specimens are prepared and the carbon films evaporated on to the surface as before. The film is loosened from the metal by chemical etching in a suitable reagent, and removed from the metal surface by transferring to water as before. The film is then washed in distilled water and collected on grids ready for examination in the electron microscope. If electron diffraction photographs are to be taken of the extracted particles, it is essential to wash for only a short time and to examine the replicas as soon as they are dry, otherwise oxidation of the particle surfaces may occur.

To remove replicas from multiphase alloys containing large particles of secondary phases a combination of the etching and electropolishing techniques has been found to be successful. Carbon is evaporated on to the specimen surface in the usual way and then the specimen is etched for a short time but not sufficient to strip the replica. The film can then be removed from the specimen surface by electropolishing. Using this method it is possible to extract the carbide lamellae from pearlitic steels.

RESULTS

Both the replica and the extraction replica methods have been used to examine plain carbon and alloy steels after various heat treatments. It has been possible to extract pearlite colonies from normalized and annealed steels. The electron micrographs show the pearlite to be of a feathery nature, and to consist mainly of "combs" rather than plates. An example is shown in Fig. 1.

The most striking results have been found when examining quenched and tempered alloy steels. In a chromium–molybdenum–vanadium steel, particles of less than 100 Å diameter have been found and identified as vanadium carbide from their electron diffraction pattern (see Figs. 2 and 3).

The arcing of the rings on the diffraction pattern shown in Fig. 3 is thought to result from the larger particles which are formed preferentially at the grain boundaries of acicular grains. In the field from which the diffraction pattern was obtained the grain boundaries lie in one preferred direction and therefore the carbides formed at these boundaries exhibit a type of preferred orientation.

In a chromium–molybdenum steel which had been normalized and then tempered, an unusual type of precipitation of molybdenum carbide Mo_2C has been found. It appears from Fig. 4 that bainitic iron–chromium carbides are precipitated first and that subsequently Mo_2C, having a needle-like shape, forms as a fringe along some of the ferrite-bainite boundaries.

The replica method has also been found to be suitable for the examination of slip lines in steels, and replicas have also been obtained from copper and electro-deposited chromium.

CONCLUSIONS

The advantages of these carbon replica methods are as follows.

(*a*) The carbon film is thin (about 100 Å), it has no self structure and it does not burn in the electron beam.

(*b*) The methods are essentially single-stage techniques and the results are more reproducible than with the two-stage Formvar-carbon technique.

(*c*) Since the film is not mechanically stripped the depth of etch on the specimen is not so critical as it is for the successful removal of plastic replicas.

(*d*) By preparing carbon extraction replicas from multiphase alloys it is possible to examine the actual particles of the secondary phases, and since the diffraction pattern of the carbon film is very diffuse, the diffraction patterns from the secondary phases are in no way obscured.

(*e*) The resolving power of the replicas is much better than with a single-stage Formvar replica and is better than 50 Å.

The chief disadvantage is that only one replica can be taken from a prepared surface; for further replicas the specimen has to be repolished and etched. However, as consistently good results are obtained with the first replica it is seldom necessary to take a second replica.

ACKNOWLEDGEMENTS

The authors would like to thank Prof. G. W. Austin for his interest and encouragement, and Mr. R. G. Baker, of the Department of Metallurgy, University of Cambridge, who has helped in the development of the techniques and supplied the electron micrograph shown in Fig. 4. The diffraction pattern shown in Fig. 3 was obtained by Mr. R. W. Horne, of the Cavendish Laboratory, University of Cambridge.

This work forms a part of the programme of the High Temperature Steels Committee of the British Iron and Steel Research Association and the authors would like to thank the Association for their financial support.

REFERENCES

(1) BRADLEY, D. E. *Brit. J. Appl. Phys.*, **5**, p. 165 (1954); *J. Inst. Metals*, **83**, p. 35 (1954).

(2) DIEHL, J., MADER, S., and SEEGER, A. *Z. Metall.*, **46**, pp. 650–657 (1955).

An extension of the circle and sphere theorems

By G. Power, M.A., Ph.D., University of Nottingham.

[*Paper received* 15 *November*, 1955]

The circle and sphere theorems are here extended to include certain other boundaries along which either the electric potential or the current function takes a constant value. This greatly facilitates the solution of problems previously treated by *ad hoc* methods, especially in two dimensions where use of the method of conformal transformation can also be made. Illustrative examples are given, showing how these theorems can be applied even when fairly difficult boundary shapes are involved.

TWO-DIMENSIONAL FIELDS

The circle theorem was first enunciated by Milne-Thomson[1] in a hydrodynamical context in order to facilitate the solutions of problems which previously had to be treated by *ad hoc* methods. A corresponding theorem[2] can be stated for electrical theory in the following manner. If a circular cylinder of radius a, filled with homogeneous dielectric of specific inductive capacity k_i, is placed with its centre at the origin of co-ordinates in a two-dimensional field, whose complex potential is $f(z)$ in a homogeneous dielectric, constant k_0, having no singularities inside or on $|z| = a$, then the complex potentials outside and inside the cylinder are respectively given by

$$w_0 = f(z) + \left(\frac{k_0 - k_i}{k_0 + k_i}\right) f\left(\frac{a^2}{z}\right), \quad w_i = \frac{2k_0}{k_0 + k_i} f(z) \qquad (1)$$

with the usual notation. It is assumed that there are no other finite boundaries.

The results for fields caused entirely by internal singularities[2, 3] takes a form similar to equation (1). For the case when $|z| = a$ is a conducting surface we let $k_i \to \infty$, giving $w_0 = f(z) - f(a^2/z)$, and for the hydrodynamical case let $k_i \to 0$, obtaining $w_0 = f(z) + f(a^2/z)$. The introduction of further finite boundaries will, in general, violate the above results, and the problem then proves to be complicated. The object of this investigation is to find what barriers may be inserted in order that the circle theorem may still hold. This opens up the possibility of a simple solution to problems involving fairly difficult boundary shapes.

Let $f(z) = \phi(x, y) + i\psi(x, y)$, so that $\phi(x, y)$ is the electric potential, and $\psi(x, y)$ is the current function. It is easy to see that

$$f\left(\frac{a^2}{z}\right) = \phi\left(\frac{a^2x}{x^2 + y^2}, \frac{a^2y}{x^2 + y^2}\right) - i\psi\left(\frac{a^2x}{x^2 + y^2}, \frac{a^2y}{x^2 + y^2}\right)$$

and so the fields w_0, w_i can be split up into their real and imaginary parts.

Suppose C is a boundary which is introduced into the original field. The type of boundary here envisaged is one that has some physical importance, that is to say, it is either a conductor on which the electric potential is constant, or else it is a curve along which the current function is to have a constant value (the latter case has hydrodynamical significance also). To be specific, we will assume that C, defined by $x(t)$, $y(t)$, for a given range of parameter t, is a conductor; so that along this curve the real part of w_0 is constant. Using equations (1), we see that outside the dielectric cylinder

$$\phi[x(t), y(t)] + \left(\frac{k_0 - k_i}{k_0 - k_i}\right)\phi\left[\frac{a^2x(t)}{x(t)^2 + y(t)^2}, \frac{a^2y(t)}{x(t)^2 + y(t)^2}\right] = \text{constant}.$$

But in the original field C is a curve of constant electric potential. It follows that

$$\phi\left[\frac{a^2x(t)}{x(t)^2 + y(t)^2}, \frac{a^2y(t)}{x(t)^2 + y(t)^2}\right] = \text{constant} \qquad (2)$$

for the given range of t. This means that in the original field, the inverse of C with regard to the circle $|z| = a$ must also be an equipotential. It may be that the conducting boundary extends into the region $|z| < a$, but this does not matter as w_i is simply a multiple of the original field. Clearly the condition that inverse curves must be equipotentials imposes a strict limit on the original field $f(z)$. But if it so happens that C is mapped into itself when inverted with regard to $|z| = a$, then the results (1) hold for all fields $f(z)$ having a conducting boundary coincident with C.

Precisely the same results hold when C is a curve along which the current function $\psi(x, y)$ is constant. If C inverts into itself the equations (1) will hold for all fields; otherwise we must impose the restriction that both C and its inverse are curves of constant current function in the original field $f(z)$. This theorem is of importance in hydrodynamics[6] in which case $k_i = 0$ and there is only an external flow. The results for fields caused entirely by singularities inside $|z| = a$ are exactly the same.

Examples of curves that invert into themselves can easily be given. For instance we may take any arc of a circle orthogonal to $|z| = a$ between points P and Q, provided P and Q are inverse points, that is to say provided the chord PQ passes through the origin of co-ordinates; and in particular the line joining inverse points is a possible curve.

Applications.

(α) The complex potential

$$w = E\left\{\cos\alpha[(z - \beta)(z - a^2/\beta)]^{\frac{1}{2}} - i\sin\alpha[z - \tfrac{1}{2}(\beta + a^2/\beta)^{\frac{1}{2}}]\right\} \qquad (3)$$

represents the perturbation of a uniform electric field of strength E in air making an angle α with the real axis, when there is a conducting plate placed along this axis between the points $z = \beta$, $z = a^2/\beta$ (β real). This conductor satisfies the necessary and sufficient conditions for the use of the circle theorem (1) when the uniform dielectric cylinder $|z| = a$, of constant k, is inserted, so that we get the perturbed fields

$$\left.\begin{aligned} w_0 &= E\left\{\cos\alpha\left[1 + \frac{a}{z}\frac{(1-k)}{(1+k)}\right][(z - \beta)(z - a^2/\beta)]^{\frac{1}{2}} - \right. \\ &\qquad \left. - \frac{i\sin\alpha}{(1+k)}\left[\frac{z^2(1+k) - a^2(1-k)}{z} - k(\beta + a^2/\beta)^{\frac{1}{2}}\right]\right\} \\ w_i &= \frac{2E}{(1+k)}\left\{\cos\alpha[(z - \beta)(z - a^2/\beta)]^{\frac{1}{2}} - \right. \\ &\qquad \left. - i\sin\alpha[z - \tfrac{1}{2}(\beta + a^2/\beta)^{\frac{1}{2}}]\right\} \end{aligned}\right\} \qquad (4)$$

By letting $k \to \infty$ in equations (4), we get the case of an uncharged conducting circular cylinder with a radial spike placed in a uniform field, the complex potential of the perturbed flow being

$$w_0 = E\left\{\cos\alpha\left(1 - \frac{a}{z}\right)[(z-\beta)(z - a^2/\beta)]^{\frac{1}{2}} - \right.$$
$$\left. - i\sin\alpha\left[\left(z + \frac{a^2}{z}\right) - \left(\beta + \frac{a^2}{\beta}\right)^{\frac{1}{2}}\right]\right\} \quad (5)$$

(β) Applications of equations (1) shows that when the circular uncharged conducting cylinder $|z - c| = b$, (c real and positive), is placed in air in the general field whose complex potential is $f(z)$, we obtain the perturbed field

$$g(z) = f(z) - f\left(\frac{b^2}{z-c} + c\right) \quad (6)$$

If now the uniform dielectric cylinder $|z| = a$, constant k, is set in the field given by equation (6), use of equations (1) can be made once more provided the circles $|z - c| = b$ and $|z| = a$ are orthogonal, in which case $c^2 = a^2 + b^2$. The disturbed fields are then

$$\left.\begin{aligned} w_0 &= f(z) - \left(\frac{1-k}{1+k}\right)\left\{f\left[\frac{a^2(c-z)}{(a^2-cz)}\right] - \right. \\ &\qquad \left. - f\left(\frac{a^2}{z}\right)\right\} - f\left(\frac{cz-a^2}{z-c}\right) \\ w_i &= \frac{2}{1+k}\left[f(z) - f\left(\frac{zc-a^2}{z-c}\right)\right] \end{aligned}\right\} \quad (7)$$

By letting $k \to \infty$, we get the complex potential of the field obtained when an uncharged conducting cylinder, whose cross-section is formed by the parts (external to each other) of two orthogonal circles radii a, b, is placed in the general field $f(z)$. This is

$$w_0 = f(z) + f\left[\frac{a^2(c-z)}{(a^2-cz)}\right] - f\left(\frac{a^2}{z}\right) - f\left(\frac{cz-a^2}{z-c}\right) \quad (8)$$

For the case of a uniform field, we put $f(z) = E\exp(-i\alpha)z$, and equation (8) becomes

$$w_0 = E\left\{\exp(-i\alpha)\left[z - \frac{a^2b^2}{c^2(z-a^2/c)}\right] - \right.$$
$$\left. - \exp(i\alpha)\left(\frac{a^2}{z} + \frac{b^2}{z-c}\right)\right\} \quad (9)$$

apart from an additive constant, where $c^2 = a^2 + b^2$.

This method can obviously be extended to the case of a cylindrical conductor whose cross-section is the outer boundary of three mutually orthogonal circles.

Many other problems (both electrical and hydrodynamical) can be solved directly in a similar manner and the use of conformal transformation will extend the range almost indefinitely.

THREE-DIMENSIONAL FIELDS

The theorem in three dimensions which corresponds to the circle theorem can be stated as follows.[4] If a uniform dielectric sphere of radius a dielectric constant k_i, is placed with its centre at the origin of co-ordinates in a medium of constant k_0 in which there is a general field whose unperturbed electric potential function is $\phi(x, y, z)$, having no field singularities inside or on $r = a$ then the perturbed potentials inside and outside the sphere are respectively

$$\left.\begin{aligned} \phi_i &= \frac{2}{(1+k)}\phi(x,y,z) + \\ &\quad + \frac{(k-1)}{(k+1)^2}\int_0^1 t^{-k/(k+1)}\phi(xt, yt, zt)dt, \\ \phi_0 &= \phi(x,y,z) - \frac{(k-1)}{(k+1)}\frac{a}{r}\phi(x_1,y_1,z_1) + \\ &\quad + \frac{(k-1)}{(k+1)^2}\frac{a}{r}\int_0^1 t^{-k/(k+1)}\phi(x_1t, y_1t, z_1t)dt \end{aligned}\right\} \quad (10)$$

where

$$x_1 = \frac{a^2x}{r^2},\ y_1 = \frac{a^2y}{r^2},\ z_1 = \frac{a^2z}{r^2},\ r^2 = x^2 + y^2 + z^2$$
$$\text{and } k = k_i/k_0.$$

The results for fields caused by internal singularities takes a similar form. Again we assume that there are no other finite boundaries.

$$\text{If } \phi(x,y,z) = h_0(x,y,z) + \ldots + h_n(x,y,z) + \ldots \quad (11)$$

where $h_s(x, y, z)$ is a harmonic degree s, we see from equations (10) that

$$\left.\begin{aligned} \phi_i &= \sum_{n=0}^{\infty}\left[\frac{2n+1}{n(k+1)+1}\right]h_n(x,y,z), \\ \phi_0 &= \phi(x,y,z) - \sum_{n=0}^{\infty}\left[\frac{n(k-1)}{n(k+1)+1}\right]\frac{a}{r}h_n(x_1,y_1,z_1) \end{aligned}\right\} \quad (12)$$

Suppose S is a conducting surface defined by $x(t)$, $y(t)$, $z(t)$ for a certain range of the parameter t, placed in the original field then $\phi[x(t), y(t), z(t)]$ is constant for the given range of t, so that

$$\sum_{n=0}^{\infty}\left[\frac{2n+1}{n(k+1)+1}\right]h_n[x(t), y(t), z(t)] = \text{constant}$$

must be an equipotential surface when $r < a$, and

$$\frac{a}{r}\sum_{n=0}^{\infty}\left[\frac{n(k-1)}{n(k+1)+1}\right]h_n[x_1(t), y_1(t), z_1(t)] = \text{constant}$$

must be an equipotential when $r > a$.

We notice that direct use can be made of the sphere theorem for certain problems involving cones whose vertices are at the origin of co-ordinates or for planes which cut the sphere orthogonally. Examples with these types of boundary are given later.

For the case of a conducting sphere we let $k \to \infty$, and then equations (10) give

$$\phi_0 = \phi(x,y,z) - \frac{a}{r}\phi(x_1,y_1,z_1) \quad (13)$$

It now appears that if S is *any* surface at zero potential which inverts into itself with regard to the sphere, then equation (13) is satisfied on the surface S, and a result similar to that for the circle theorem is achieved. This is also true in the case of a dielectric sphere provided $\phi(x, y, z)$ contains harmonics of a single order, that is to say, the series (11) consists of one term only. If the series (11) contains more than one term and we wish to use the theorem involving a dielectric sphere, we have to restrict the conducting surfaces to cones and planes as mentioned above. Fields caused entirely by

internal singularities can be dealt with in exactly the same way.

The corresponding hydrodynamical problem can be solved in a similar manner when the fluid flow is axisymmetric. It has been shown[5] that if the spherical boundary $r = a$ is placed in an axisymmetric flow whose undisturbed Stokes' stream function $\psi(r, \theta)$ is given in terms of the spherical polar co-ordinates (r, θ), θ being measured from the axis of symmetry, then the perturbed stream function is

$$\psi_0 = \psi(r, \theta) - \frac{r}{a}\psi\left(\frac{a^2}{r}, \theta\right) \tag{14}$$

Thus equation (14) is satisfied along a surface S when S is an axisymmetric boundary of the original flow along which the Stokes' stream function is zero, provided S inverts into itself with regard to the sphere.

Many illustrations of this use of the sphere theorem can be given, but examples will naturally be of more limited value than in the two-dimensional case as there is no method analogous to that of conformal transformation.

Applications.

(α) The potential due to a charged infinite conducting wedge, exterior angle α is given by

$$V = C(r \sin\theta)^{\pi/\alpha} \cos \pi\phi/\alpha \tag{15}$$

using spherical polar co-ordinates (r, θ, ϕ), where the faces of the wedge are $\phi = \pm \alpha/2$. This is easily seen to satisfy Laplace's equation and give $V = 0$ on the wedge.

If now a solid dielectric sphere of radius a, constant k, has a sector removed so that it fits this wedge with its surface meeting the wedge faces orthogonally, then application of the sphere theorem can be made. The potentials inside and outside the sphere now become

$$\left.\begin{aligned} V_i &= \frac{C(\alpha + 2\pi)}{\alpha + \pi(k+1)} (r \sin\theta)^{\pi/\alpha} \cos \pi\phi/\alpha \\ \text{and} \\ V_0 &= C\left[r^{\pi/\alpha} - \frac{\pi(k-1)a^{\pi/\alpha}}{\alpha + \pi(k+1)}\left(\frac{a}{r}\right)^{(\pi/\alpha)+1}\right](\sin\theta)^{\pi/\alpha} \cos \pi\phi/\alpha \end{aligned}\right\} \tag{16}$$

(β) A conducting surface is in the form of a cone of semi-vertical angle $\cos^{-1}\mu_0$, whose vertex is at the origin of co-ordinates. If a charge m is placed on the axis of the cone at distance d from the vertex, then the potential of the axisymmetric field is known to be

$$\left.\begin{aligned} &\phi = \sum_n A_n r^n P_n(\mu) \quad \text{when } r < d \\ \text{and} \quad &\phi = \sum_n A_n \frac{d^{2n+1}}{r^{n+1}} P_n(\mu) \quad \text{when } r > d \\ \text{where} \quad &A_n = -2m \Big/ \left\{ d^{n+1} \left[(1-\mu^2) \frac{dP_n}{dn} \frac{dP_n}{d\mu} \right]_{\mu=\mu_0} \right\} \end{aligned}\right\} \tag{17}$$

θ being measured from the axis of the cone, and the summation extending to all numbers integral or fractional for which $P_n(\mu_0) = 0$.

Our theory shows that if part of the dielectric sphere $r = a$ $(a < d)$, constant k, is now introduced inside the cone then the potential inside the dielectric becomes

$$\phi_i = \sum_n \left[\frac{2n+1}{n(k+1)+1}\right] A_n r^n P_n(\mu) \tag{18}$$

The potential outside the sphere is given by

$$\left.\begin{aligned} \phi_0 = \sum_n \left\{ r^n - \left[\frac{n(k-1)}{n(k+1)+1}\right]\left[\frac{a^{2n+1}}{r^{n+1}}\right] \right\} A_n P_n(\mu) \end{aligned}\right\} \tag{19}$$

when $r < d$, and

$$\left.\begin{aligned} \phi_0 = \sum_n \left\{ \frac{d^{2n+1}}{r^{n+1}} - \left[\frac{n(k-1)}{n(k+1)+1}\right] \left[\frac{a^{2n+1}}{r^{n+1}}\right] \right\} A_n P_n(\mu) \end{aligned}\right\}$$

when $r > d$.

(γ) Application of equation (13) shows that when the spherical conductor $(x-c)^2 + y^2 + z^2 = b^2$ is placed in the field whose undisturbed potential is $\phi(x, y, z)$, we obtain the field whose potential is

$$\phi_b = \phi(x, y, z) - \frac{b}{r_1}\phi\left[\frac{b^2(x-c)}{r_1^2} + c, \frac{b^2 y}{r_1^2}, \frac{b^2 z}{r_1^2}\right] \tag{20}$$

where $r_1^2 = (x-c)^2 + y^2 + z^2$.

If now the spherical conductor $x^2 + y^2 + z^2 = a^2$ is placed in the field given by equation (20), we can apply equation (13) once more, provided the two spherical conductors of radii a and b are orthogonal. The potential function then becomes

$$\begin{aligned} \phi_{ab} = \phi(x, y, z) &- \frac{b}{r_1}\phi\left[\frac{b^2(x-c)}{r_1^2} + c, \frac{b^2 y}{r_1^2}, \frac{b^2 z}{r_1^2}\right] - \\ &- \frac{a}{r_2}\phi\left(\frac{a^2 x}{r_2^2}, \frac{a^2 y}{r_2^2}, \frac{a^2 z}{r_2^2}\right) + \\ &+ \frac{ab}{r_2 R}\phi\left[\frac{b^2\left(\frac{a^2 x}{r_2^2} - c\right)}{R^2} + c, \frac{b^2 a^2 y}{r_2^2 R^2}, \frac{b^2 a^2 z}{r_2^2 R^2}\right] \end{aligned} \tag{21}$$

where $r_2^2 = x^2 + y^2 + z^2$, $R^2 = \left(\frac{a^2 x}{r_2^2} - c\right)^2 + \frac{a^4 y^2}{r_2^4} + \frac{a^4 z^2}{r_2^4}$, $c^2 = a^2 + b^2$

This gives the perturbed field when a conductor formed by the parts (external to each other) of two orthogonal spheres is placed in the general field whose undisturbed potential is $\phi(x, y, z)$.

The method here employed can be extended to the case of a conductor whose boundary is the outer part of three or more mutually orthogonal spheres.

(δ) The potential function due to an uncharged circular conducting disk of radius b with its centre at the origin of co-ordinates whose normal makes an angle α with an electric field E, which was uniform before the introduction of the disk, is known to be

$$V = E\left[\frac{2\rho}{\pi}\left(\tan^{-1}\zeta + \frac{\zeta}{\zeta^2+1}\right)\sin\alpha\cos\phi + z\cos\alpha\right] \tag{22}$$

where z is measured perpendicular to the plane of the disk,

$$x = \rho\cos\phi,\ y = \rho\sin\phi, \text{ and } \frac{z^2}{\zeta^2} + \frac{\rho^2}{\zeta^2+1} = b^2.$$

If a spherical conductor of radius a with centre at the point $x = p$, $y = q$, $z = 0$ is now introduced, use may be made of equation (13), where the potential is given by

equation (22), provided $p^2 + q^2 = a^2 + b^2$. This leads to the disturbed potential

$$V_0 = E\left[\frac{2\rho}{\pi}\left(\tan^{-1}\zeta + \frac{\zeta}{\zeta^2+1}\right)\sin\alpha\cos\phi - \right.$$
$$- \frac{2a\rho_1}{r\pi}\left(\tan^{-1}\zeta_1 + \frac{\zeta_1}{\zeta_1^2+1}\right)\sin\alpha\cos\phi_1 +$$
$$\left. + \left(1 - \frac{a^3}{r^3}\right)z\cos\alpha\right] \quad (23)$$

where

$$\frac{a^2(x-p)}{r^2} + p = \rho_1\cos\phi_1, \quad \frac{a^2(y-q)}{r^2} + q = \rho_1\sin\phi_1,$$
$$\frac{a^4z^2}{r^4\zeta_1^2} + \frac{\rho_1^2}{\zeta_1^2+1} = b^2, r^2 = (x-p)^2 + (y-q)^2 + z^2$$

Equation (23) thus gives the potential function when an uncharged conductor in the form of a sphere with a plane fin is placed in a field E, which was uniform before the conductor was introduced.

REFERENCES

(1) MILNE-THOMSON, L. M. *Proc. Cambridge Phil. Soc.*, **36** p. 246 (1940).

(2) POWER, G. *Math. Gaz.*, **37**, p. 220 (1953).

(3) POWER, G. *Brit. J. Appl. Phys.*, **6**, p. 245 (1955).

(4) POWER, G. *Amer. Math. Monthly*, **58**, p. 249 (1951).

(5) BUTLER, S. F. J. *Proc. Cambridge Phil. Soc.*, **49**, p. 169 (1953).

(6) LEVIN, E. *Quart. Appl. Math.*, **12**, p. 315 (1954).

Electron optics of X-ray tubes and the design of unbiased sharply-focusing cathodes

By A. R. LANG, M.Sc., Ph.D., A.Inst.P.,* and D. A. G. BROAD, Cavendish Laboratory, University of Cambridge

[*Paper received* 19 *October*, 1955]

Using an accurate rubber model, electron trajectories produced by both conventional and various special X-ray tube cathode systems have been studied. Excellent agreement between predicted and observed focal patterns was obtained, in contrast to the results of electrolytic trough measurements reported by Thorp. In conventional cathode systems the effects of space charge were shown to be negligible. A simple unbiased cathode assembly was designed which gave a sharply bounded focal line of width 1 mm.

X-ray tube focal-spot requirements vary in stringency according to the particular diffraction technique employed. As long as X-ray beam collimation is effected by a system of pinholes or slits and the whole collimator is filled with radiation, a broad and diffuse focus results only in waste of X-rays and does not impair resolution. However, with cameras designed to use the size of focal spot itself to limit the apparent source dimensions, an arrangement preferable from the point of view of efficient use of X-ray energy, the focus size and intensity distribution must be strictly controlled. In single-crystal work with conventional collimators and sharply-reflecting small crystals the shape of all diffraction spots is largely determined by the focus structure, and of back reflexions even in the case of large crystals. Hence a diffuse or markedly banded focal structure severely handicaps intensity measurements. In the powder diffractometer the arrangement employing a line focus as the source of divergent X-rays, oriented parallel to the diffractometer axis and situated on the Brentano focusing circle, is necessary for obtaining adequate intensity and resolution. It follows that a sharp focus is essential for high angular resolution, and a focal pattern possessing broad wings can cause undesirable tails in the diffraction-line profiles.

The present paper gives an account of an investigation of X-ray tube electron optics, using a rubber model as analogue. This led to the design of an improved cathode system. The cathode was fitted to an older Metropolitan-Vickers Raymax X-ray tube, and it produced a sharply-defined X-ray source for use with a counter diffractometer.[1]

Initially, attempts were made to improve the Raymax focus by adjustments of the conventional coiled filament and focusing hood, but though in the best position it was found possible to obtain a fairly strong peak about 1 mm wide, a considerable fraction of the X-ray energy was then distributed in a "penumbra" about 6 mm wide. The coiled filament was replaced by a single wire filament to give a line source. The overall focal dimensions were thereby reduced, but the patterns obtained were still very unsatisfactory and varied in a remarkable way with changes in position of the focusing hood relative to the filament. In order to achieve a suitable filament geometry it became clear that detailed study was necessary of the mode of formation of focal patterns.

THE RÔLE OF SPACE CHARGE

Beese[2] and, more recently, Thorp[3,4] give an account of the focal patterns obtained in X-ray tubes with electrode systems similar to that of the Raymax. A complex picture is presented, and the problem of fully interpreting the observed patterns or of producing a focus to specified dimensions appears as one of considerable intractability. Using an electrolytic trough, Thorp has constructed equipotentials and electron trajectories for various filament settings. Whilst these explain generally the mode of formation of the patterns and their intensity distribution, predicted focal dimensions are found always to be considerably less than those observed

* Now at Harvard University, Massachusetts, U.S.A.

experimentally, in some cases by an order of magnitude. To explain this discrepancy Thorp suggests that space-charge effects are active, but gives no record of having tested this hypothesis. Now it should not be expected that space charge plays an important rôle in shaping the focal patterns when the values of electric fields and specific emission of the filament are compared with those of other types of vacuum tube. In any case, space charge effects cannot be large. Hence if the field equation $\nabla^2 V = 0$ has to be modified to $\nabla^2 V = 4\pi\rho$ [ρ representing the (negative) space charge] it may be assumed that ρ is sufficiently small for the perturbation of trajectories to depend approximately linearly upon ρ, and ρ may be taken as proportional to the total X-ray tube current. Thus the magnitude of space-charge effects may be estimated extremely simply by observing if any change in focal pattern occurs when the tube current is varied. Fig. 1 shows the results of such experiments for three different types of filament

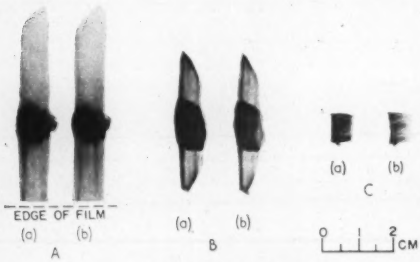

Fig. 1. Focal patterns with (*a*) high tube-current and (*b*) low tube-current. Vertical scale actual focus size.

assembly. In each case the filament axis lies horizontal, and the direction of view makes an angle of about 6° with the target face, so an ideal 10 × 1 mm focus would appear square. A distance of the film from the pinhole giving a magnification of ×12 was chosen so as to make clear the fine structure in the focal patterns. No correction for pinhole size was necessary, a sufficiently small hole being used. Patterns *A* were obtained with the standard Raymax coiled filament, the distance from filament to front surface of focusing hood being set rather larger than the usual value in order to give a sharp central peak to the focus. For *A*(*a*), the tube current is 10 mA and for *A*(*b*) it is $\frac{1}{3}$ mA, exposure times being 2 and 60 s respectively. The X-ray tube voltage is 40 kV in all cases. Though the current is varied by a factor of 30 : 1, *no change at all in the pattern can be detected.* A line filament backed with a plate at cathode potential gives the patterns *B*(*a*) (10 mA and 2 s exposure) and *B*(*b*) ($\frac{1}{3}$ mA and 100 s exposure). With a 50 : 1 ratio of current strengths still no variation in focal pattern is observed. Patterns *C*(*a*) (10 mA and 2 s exposure) and *C*(*b*) ($\frac{1}{3}$ mA and 100 s exposure) were obtained with a filament assembly (described more fully below) consisting of a line filament placed behind a narrow slot cut in a plate, the filament itself being backed by another plate. Here for the first time some variation of pattern is observed, doubtless due to the weaker field conditions prevailing in the "box" containing the filament. It will be seen that with the higher current the outer double bands coalesce, but the effect on overall dimensions is negligible and on intensity distribution quite small. As a result of these experiments it may be confidently asserted that space-charge effects can be neglected in describing the mechanism of focal-pattern production in cathode systems of the Raymax type, and the explanation of the discrepancy between Thorp's predictions and observations must be sought elsewhere. This fortunate simplification shows that a suitable analogue method of representing the condition $\nabla^2 V = 0$ should be most helpful in studying the generation of focal patterns.

THE RUBBER MODEL

A good general description of the rubber model has been given by Kleynen.[5] The basis of its application to X-ray tube design may be briefly indicated as follows. A weightless, perfectly elastic membrane, stretched so as to be in uniform tension, will take up a form such that at every point the radii of curvature in two mutually perpendicular directions are equal and opposite. If three-dimensional co-ordinates are chosen with the membrane lying approximately in the x–y plane, and the slope of the membrane with this plane is everywhere limited so that $(dz/dx)^2$ and $(dz/dy)^2$ are small compared with unity, then the above condition may be written $(d^2z/dx^2) + (d^2z/dy^2) = 0$. Now the type of electrode system which it is here required to investigate can be regarded as effectively two-dimensional, if influences of the ends of the filament and of the focusing hood are neglected. The field equation in a median plane perpendicular to the filament is then $(d^2V/dx^2) + (d^2V/dy^2) = 0$. The similar form of this equation with that of the membrane surface shows that the height of the membrane above the x–y plane, z, will form an analogue representation of the potential V when boundary conditions of x and y are chosen geometrically similar to the electrode configuration, and boundary elevation z made proportional to electrode potential. A point mass sliding over the membrane under the force of gravity follows a trajectory identical with that of a charged particle of appropriate sign in the electrostatic field. Trajectories are independent of the scale of the model, provided the slope is kept small. In practice, small rolling balls replace sliding point masses and the effects of rolling friction and rotational inertia of the ball have to be taken into account. But with a good experimental technique and a favourable type of electrode system to study, the rubber model is capable of considerable accuracy. Satisfactory performance of the model depends upon careful attention to a number of details in its method of operation. Some of these points will now be briefly noted, with specific relevance to the design of model used by the authors.[1]

The membrane is a sheet of surgical latex rubber, selected for smooth surface. It must be held under uniform tension. A square grid is therefore pencilled on the surface before stretching and care is exercised to see that it does not become distorted. Closely spaced brass pins round the periphery of the model engage holes near the edge of the rubber sheet to secure it in position. If the holes are cleanly cut there is no tendency to tear, even under considerable tension, but care is needed when attaching or removing the sheet. The tension is chosen so as to be sufficient to avoid sagging of the sheet under its own weight or that of a ball on its surface, but not too great as to approach the limit of proportionality between tension and extension. The rubber must be protected from grease, heating and sunlight.

The whole model is supported on a rigidly constructed frame of Dexion light-alloy angle. The focusing hood is represented by a suitably shaped wooden block, and the filament by a brass rod of appropriate diameter adjustable

both in height and position within the focusing hood. The cathode model rests on three screws and is made accurately level before each experiment.

The component of the model requiring most care in design is the ball-launching mechanism which is placed above the filament and releases small steel balls in any required direction. It has to define closely the initial direction of the ball, but it must subject it to no constraint after release. The ball must be poised accurately on the periphery of the filament and no impulse must be given to it at the instant of release. To fulfil these conditions a magnetic method of release was developed which would neither accelerate nor retard the ball at the beginning of its trajectory. In the course of experiments the filament is frequently changed in position. An optical method was therefore devised which enabled the ball launcher to be quickly and accurately centred above the filament.

The positions of impact of balls upon the anode are recorded very simply. The anode itself is a sheet of Perspex. On its front surface lies a strip of tracing paper covered by a strip of carbon paper. To the back of the anode is attached a scale. Balls strike the anode through the carbon paper, and make a distinct dot on the tracing paper which can be seen through the Perspex. The position of impact is read with the aid of the scale, and it may be plotted directly on a graph.

The difference in level between cathode and anode is made as great as possible without introducing errors due to too large a slope, in order that gradients may be sufficiently defined in the low field region inside the focusing hood. It was experimentally verified that trajectories were not dependent upon this difference in level. The effect of positive or negative bias on the focusing hood may be investigated by raising or lowering the filament by the appropriate amount relative to the overall filament-to-anode height-difference.

A number of tests were made with balls of various sizes, from which it was concluded that $\frac{1}{4}$ in. diameter balls were quite suitable. The ideal ball would be inhomogeneous, having a dense core surrounded by a light shell. Thus very suitable balls for the model could be made with a heavy metal core and an outer shell of Teflon, the low coefficient of friction of the latter substance being especially advantageous.

The assumption is always made that in the absence of a retarding field the emission from the filament is isotropic. Also, on the scale used in this model, the finite emission velocities of the electrons would produce no change in focal pattern. As the model satisfactorily accounts for the observed X-ray tube focal patterns it may be concluded that effects due to emission velocities can be neglected. This may no longer be the case when very fine foci are considered, as is shown in the work of Ehrenberg and Spear.[6]

In its final form, operation of the model was convenient and quick and the trajectories had very satisfactory reproducibility.

INTERPRETATION AND SYNTHESIS OF FOCAL PATTERNS

Both biased and unbiased cathode systems were studied with the model, but attention was devoted principally to the latter type, since the chief aim of the work was to make improvements on the standard older Raymax cathode assembly, which was not designed to be biased.

The general run of the equipotentials in the vicinity of the filament under various bias conditions is shown in Fig. 2(*a*)–(*d*). The maps have not been derived from actual potential-plotting experiments, and they serve only to portray field conditions as visually estimated from the model. Observation of the model in action revealed in a most striking way how the various types of focal pattern were generated, and a situation previously regarded as complex soon became understood. Permanent records of trajectories could have been obtained by photography, but time was not spent in this direction because of the need to find rapidly a solution to the pressing problem of focus improvement.

In Fig. 2 contour values are in arbitrary units and are drawn at closer intervals in the low field regions. The width w of the slot in the focusing hood is equal to the distance between

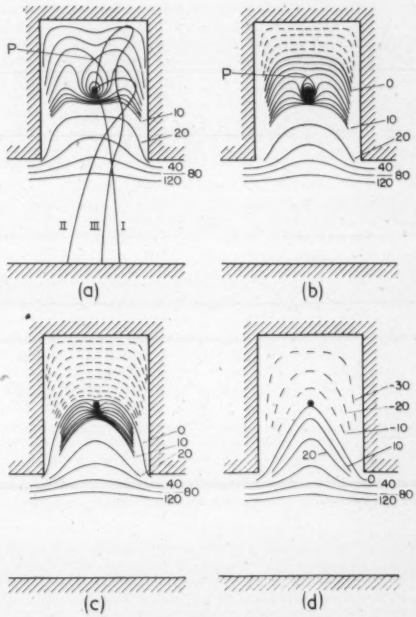

Fig. 2. Approximate equipotential maps, (*a*) zero bias, (*b*)–(*d*) increasing negative bias

hood and anode. In the model this slot is closed at the rear whereas in the X-ray tube assembly the cathode stem is relatively much more remote from the filament. However, experiments showed that as long as the closed end of the slot was not nearer to the filament than a distance about equal to the slot width, its exact position had a negligible effect on focal patterns. The filament axis is set back from the mouth of the focusing hood a distance equal to two-thirds of the slot width. This dimension will be denoted by s. Referring to Fig. 2(*a*) (zero bias) it will be seen that the field to the rear of the filament is low and very non-uniform, and there is a neutral point at *P*.

The electron trajectories observed with zero bias can be considered to fall into one of three types. These modes are sketched in Fig. 2(*a*), and may be described in simplified

terms as follows. Forward going electrons, i.e. those initially making angles not greater than about 60° with a line drawn directly from filament to target, follow a path such as I, and strike the target at a distance from the central axis which varies rapidly with changes in *s*. Regarded as a simple cylindrical lens, the system has strong positive aberration. Electrons having emission angles between about 60° and 135° fall into mode II. They travel out nearly as far as the walls of the slot, then swing forward, cross over the axis and strike the target with marked aberration. These electrons form what is often termed the "penumbra" of the focal pattern. The maximum width of the "penumbra" does not vary rapidly with the setting *s*. Mode III represents the electrons emitted rearwards: their trajectories are the most complex and depend fairly sensitively upon the value of *s*.

Fig. 2(*b*) represents the conditions when slight negative bias is applied to the focusing hood. The negative equipotentials are drawn dashed. As the bias is increased the zero equipotential approaches the filament, and the neutral point *P* maintains a position approximately half-way between the filament and the zero equipotential. The excursions rearwards and sideways of the electrons in modes II and III are now considerably reduced since they cannot move out further than the zero equipotential. The trajectories of forward-going electrons are not much affected, except in so far as the effective focal length of the system is somewhat modified by application of bias. This demonstrates the experimentally observed feature that comparatively slight biasing noticeably reduces the "penumbra" of the focal pattern without much altering the central part of the pattern.

On further increase of bias the condition is reached, shown in Fig. 2(*c*), when the zero equipotential just touches the rear of the filament. There is now no accelerating field away from the filament in the rearward direction and emission from the back of the filament is suppressed. When a much greater bias voltage is applied, amounting to several per cent of the overall cathode-anode potential difference, field conditions are as shown in Fig. 2(*d*). Electron emission is suppressed from all but a narrow frontal strip of the filament surface, and the potential surface in front of the filament takes the form of a narrow, sloping trough. These two factors operate together to produce a narrow focus largely independent of the shape and position of the focusing hood. However, this arrangement has two serious disadvantages. Firstly, as only a small fraction, possibly one twentieth or less, of the filament surface can emit electrons, the specific emission from this area must be correspondingly increased if the total X-ray beam current is not to be reduced. This increased specific emission entails an increase of filament temperature and tungsten evaporation rate, with consequent reduction of filament life. Secondly, the relatively high bias voltage required necessitates careful insulation of the filament from the focusing hood, making it difficult to design a compact cathode assembly. The desirability of adopting means to obtain a sharp focus free from the above disadvantageous conditions is thus evident.

Now referring back to Fig. 2(*b*), it can be seen that field conditions round the filament will not be altered if a suitably shaped electrode at earth potential is placed in the position of the zero equipotential and the bias on the focusing hood then removed. A flat "reflector" plate was placed behind the filament in the X-ray tube, and various simple shapes of electrodes were tried on the model. In both cases a considerable reduction in overall width of focal pattern was obtained. The limit to this replacement method is, of course, reached under the conditions of Fig. 2(*c*) when the zero equipotential first touches the filament. In fact, in a cathode system such as that of the older Raymax, which lacks means for positioning components accurately, it is not advisable to try to keep a reflector plate too close behind the filament. For application to an unbiased system with considerable dimensional tolerances, an electrode assembly using other than a continuous reflector plate was adopted as the simplest method of ensuring a good focus. On the other hand, when bias is available, fine foci can easily be obtained with a single plate of suitable shape fairly close behind the filament, held at a bias a small fraction of that needed on the standard focusing hood to achieve the same results. Suitable shaping of this plate can modify the field so that emission is suppressed from as little of the filament surface as possible.

Some representative electron trajectory-plots are shown in Fig. 3(*a*)–(*d*). These were obtained using the model described above. In the method adopted for depicting the results, emission angle is plotted as an ordinate against impact position on the target as abscissa. Below the abscissa-scale of the model the appropriate scale for the Raymax is added: 15 cm on the model is equivalent to 0·8 cm on the Raymax. In both cases the focusing-hood slot-width is equal to the hood-anode distance. For each filament setting on the model twenty-four emission angles were studied, at fifteen-degree intervals. Usually three balls were released at each position. Individual impact positions are shown in the figure, from which the reproducibility of the measurements may be judged. A continuous line is drawn through these experimental points. The form of this line is characteristic of each filament setting. On the assumption that the number of electrons emitted in a given angular range is independent of angle, the intensity distribution across the focus should be inversely proportional to the rate of variation of impact position with change of emission angle. Except when this rate of variation is high, the length of the curve through the experimental points falling between two abscissae can be taken as proportional to the intensity between them. Hence to construct synthetic patterns, the curves in Fig. 3 were redrawn on a very large scale and the curve-length lying in an abscissa interval was recorded as a column of appropriate height. One justification of this procedure is the close resemblance of the synthesized and observed intensity distributions.

Fig. 3(*a*)–(*d*) form a sequence of increasing values of the distance *s* of filament axis from the front of the focusing hood. Fig. 3(*b*) and (*c*) show how, at values of s/w approximately equal to $\frac{2}{3}$, the separation of the inner focal bands varies more rapidly with *s* than that of the outer bands. With increased values of s/w [Fig. 3(*d*)], the inner focal bands coalesce to form a narrow central band, just as is observed experimentally. The model also shows that, though this central band remains sharp as s/w is further increased, its intensity diminishes as the range of electron emission angles contributing to it decreases. In Fig. 3(*d*) the curve shows a discontinuity at an emission angle of 180°, and hence there is some uncertainty regarding the contribution to the pattern of rearward-going electrons. On the other hand, with a low value of s/w as shown in Fig. 3(*a*), the rearward-going electrons are fairly well focused, and hence it is these which are responsible for the broad central peak experimentally obtained under such conditions.

It was not possible to measure filament positions accurately in the Raymax cathode, nor alter this position when once the filament had been installed. Hence it was not practicable to record a complete series of focal patterns to compare with the synthesized patterns. The focal pattern reproduced to scale in Fig. 4 represents a value of s/w intermediate between those

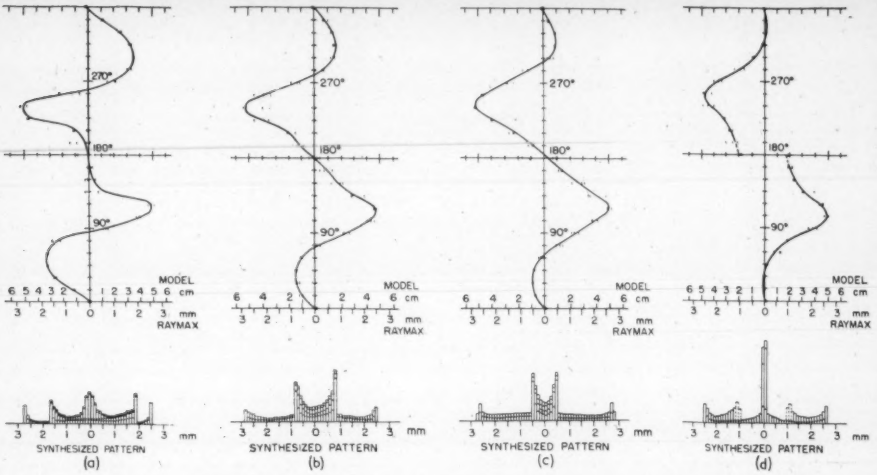

Fig. 3. Electron trajectories and synthesized focal patterns, (*a*) $s/w = 0{\cdot}5$, (*b*) $s/w = 0{\cdot}67$, (*c*) $s/w = 0{\cdot}73$, (*d*) $s/w = 0{\cdot}87$

of the synthesized patterns in Fig. 3(*b*) and (*c*). The agreement with the synthesized patterns as regards intensity distribution and overall dimensions is quite satisfactory. This is in contrast with the marked lack of agreement between observed and predicted patterns obtained by Thorp.[3,4]

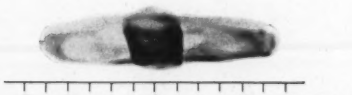

Fig. 4. Observed focal pattern with $s/w \simeq 0{\cdot}7$

THE SHARP-FOCUS CATHODE SYSTEM

Practical considerations dictated the choice of cathode system finally adopted. It was required to combine sharp focusing properties with reasonable ease of fitting to the Raymax. Though the rubber model indicated that a good focus would be obtained with a single, suitably curved, reflector plate behind the filament, experiments were not pursued very far on these lines. Clearly, the required result will be obtained if sideways and rearwards emitted electrons can either be suppressed or constrained to move in the forward direction. The disadvantages of suppressed emission have been pointed out above. The method of constraint was adopted in the following way. If the filament be placed in a small box open only towards the anode, or behind a plate with a narrow slot in it, electrons can issue only in the forward direction. Experiments on the model with a number of different arrangements showed that very satisfactory results could be obtained with the system shown in section in Fig. 5, which consists simply of a reflector plate behind the filament, and a plate with a slot in front of the filament. The electron-trajectory plot and synthesized focal pattern, with the electrodes in their best positions, are shown. Though there is a discontinuity at an emission angle of 180°, the model suggests that a double band is formed at the edges of the pattern. This double band is observed in the Raymax at low beam currents and, as shown in Fig. 5, there is again good agreement between observed and predicted patterns. At higher beam currents this double structure coalesces to form a single band: compare patterns *C*(*a*) and *C*(*b*) of Fig. 1. In this system, unlike the standard Raymax or those shown in Fig. 3, space-charge effects do modify slightly the observed pattern.

Fig. 6 shows a partly-sectioned perspective diagram of the sharp-focus cathode assembly. A part-section in the horizontal plane of the unmodified and modified Raymax tube-head is shown in Fig. 7. For use with the counter diffractometer the tube window has been enlarged so that the lower limit of target viewing-angle is defined by the target shadow. The cathode modifications are as follows. The conventional horizontal coil filament *F* is replaced by a vertical single-wire filament *F'*. Close behind the filament is a thin metal "reflector" *R*, whilst in front of the filament is a circular plate *G* with a vertical slot cut in it. This plate is held off the focusing hood by three screws, one of which (*T*) is shown. The reflector is formed out of tantalum sheet and is supported by one of the filament-supporting legs. It is fitted at the same time as the filament is inserted. The slotted plate is made of Inconel 0·018 in. thick, the slot being 0·44 in. long and about 0·088 in. wide. Three holes, 8 B.A. tapped, spaced approximately 120° apart, match three holes in the focusing hood through which pass the supporting screws. In assembly, the focusing hood is screwed on to the cathode stem in the usual way, and then the position of the slotted

plate is adjusted by means of the screws. The holes in the focusing hood are slightly less than clearance size and hence grip the shanks of the screws. This ensures that the slotted plate does not shake forward. The distance from focusing hood to anode and the width of the focusing hood both equal 8 mm. The front of the slotted plate lies 7 mm behind the front of the focusing hood, and the filament axis and reflector plate lie respectively 1 and 1·5 mm behind the front of the slotted plate.

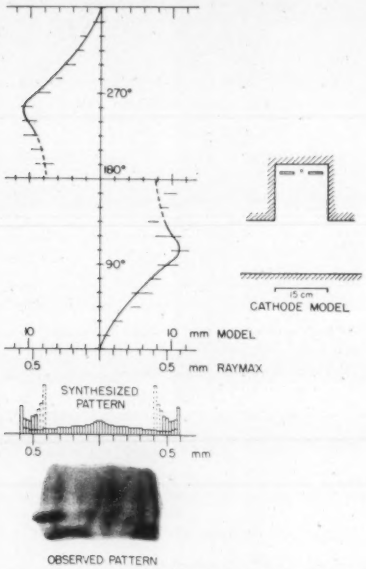

Fig. 5. Electron trajectories and comparison of observed and synthesized focal pattern with sharp-focus cathode system

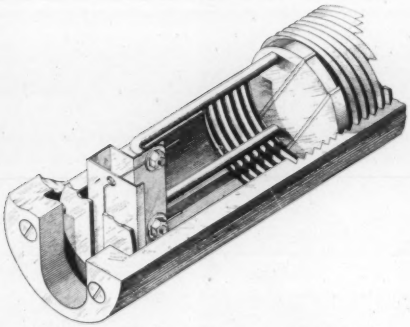

Fig. 6. Perspective sketch of sharp-focus cathode design

It is sometimes stated that use of a single-wire filament rather than a coiled filament in the X-ray tube will give insufficient life. However, the specific emission at a tube current of 15 mA is only 10^{-3} A/cm^2 for the filament used in this assembly, and a lifetime of hundreds of hours should be expected in a good vacuum. The first filament installed in the assembly did, in fact, last until after the authors' work with the Raymax was finished. Hence no opportunity arose to correct some defects in the original set-up. These were, firstly, an axial mis-setting of the filament with respect to the slotted plate which caused a concentration of intensity at one end of the focal line, and, secondly, a notch accidentally cut in one side of the slot which, as will be seen from Fig. 5, acted as a lens to produce an abnormally high local intensity at the corresponding point in the focus.

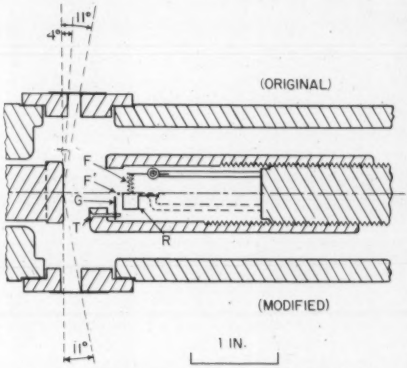

Fig. 7. Part section of X-ray tube head

The filament assembly here described can be fitted without difficulty to a standard Raymax X-ray tube, though care is required in the positional adjustments. It provides a focus of sharply limited dimensions without the use of bias. As designed the focus was 1 mm in width, and it showed no great variation of intensity across this width. Use of a somewhat wider or narrower slotted plate would give correspondingly wider or narrower foci. Hence, within certain limits, the focal dimensions can be chosen at will.

ACKNOWLEDGEMENTS

The interest of Sir Lawrence Bragg and Dr. W. H. Taylor in this work is gratefully acknowledged. One of the authors (A. R. L.) is indebted to the British Electrical and Allied Industries Research Association for financial support.

REFERENCES

(1) Lang, A. R. *Ph.D. Diss.*, University of Cambridge, 1952.
(2) Beese, N. C. *Rev. Sci. Instrum.*, **8**, p. 258 (1937).
(3) Thorp, J. S. *J. Sci. Instrum.*, **26**, p. 201 (1949).
(4) Thorp, J. S. *Brit. J. Appl. Phys.*, **1**, p. 144 (1950).
(5) Kleynen, P. H. J. A. *Philips Tech. Rev.*, **2**, p. 338 (1937).
(6) Ehrenberg, W., and Spear, W. E. *Proc. Phys. Soc. [London] B*, **64**, p. 67 (1951).

Apparatus for the measurement of time of impact

By P. L. Kirby, M.Sc., A.Inst.P.,* J. A. Jobling and Co. Ltd., Sunderland

[*Paper first received* 4 *November*, 1955, *and in final form* 21 *February*, 1956]

Apparatus is described whereby the time of impact of a freely falling sphere on a horizontal surface is measured electrically without direct connexion to the sphere. The time of impact of an 8 mm steel sphere on a solid Pyrex glass slab is 18 μs at room temperature and is the same within $\pm 10\%$ at 700° C. Over this range of temperatures the absorption of fractional impact energy increases considerably and rebound is zero at about 1000° C.

In an attempt to raise the maximum temperature at which measurements of elastic and anelastic properties of glass can be made, the time-order of the necessary deformation was reduced by the use of an impact technique. A range of temperatures was to be explored in which the glass would exhibit a considerable amount of viscous flow, and the material had therefore to be in the form of a block contained in a crucible and presenting the upper horizontal surface for impact. A small elastic sphere, which would incur only small anelastic energy loss during impact, was used to initiate the transient deformation in the glass. The measurements of hysteretic energy loss during this deformation were deduced simply from the relative heights of free fall and rebound of a steel ball.

Before deductions can be made from the measurements of energy absorption concerning the viscoelastic processes in the glass which are responsible for the effect, a knowledge is required of the time of contact during impact. The duration of impact is approximately equivalent to one half-cycle of a continuous cyclic deformation process. It is expected that in the latter case, maximum absorption of energy would occur when the frequency (ν) and the viscoelastic relaxation time (τ) are related by the equation $2\pi\nu = \tau^{-1}$. It therefore follows that if the time of contact is T, then the maximum absorption of energy during impact will occur when

$$T = \frac{1}{2\nu} = \pi\tau \qquad (1)$$

Methods have been described[1,2,3] whereby the time of contact during impact between two metal spheres or between one sphere and a plane surface has been measured. During such an impact the time of contact is usually very short and electrical methods of measurement,* with the resulting information displayed on a cathode-ray oscillograph, have been particularly successful. These methods have generally involved the flow of current across the interface and have therefore necessitated the attachment of a fine conducting wire to any sphere involved in the impact. This is no inconvenience if the sphere is also suspended by means of this wire, as is the case when two such spheres are suspended and allowed to collide or when a sphere, moving as a simple pendulum, impinges on a flat vertical surface. In the present case, however, direct electrical connexion to the steel ball would have interfered with its free fall. This difficulty was overcome by the use of the following apparatus.

The glass specimen consisted of a solid glass block which had been cast into a steel crucible lying on a dense refractory base and contained in an electric furnace (Fig. 1). The surface of the glass was polished and coated with a silver-based conducting medium giving electrical continuity to the steel crucible. The latter system was regarded as the earthed electrode of a capacitor, the other element of which consisted of a metal ring (diameter about 15 mm) mounted 5 mm above the glass surface. The electrode system formed part of a bridge in a capacity sensitive circuit and the standing capacity was balanced to give zero output. The steel ball (8 mm diameter) was suspended by an electromagnet and allowed to fall freely through the ring and bounce on the

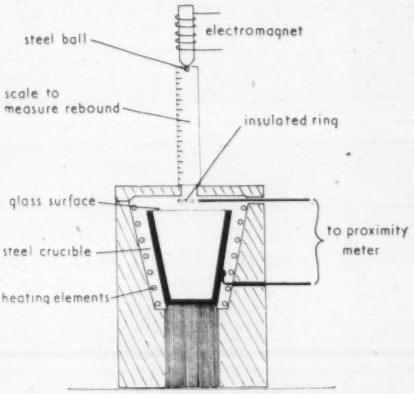

Fig. 1. Apparatus used in the study of the resilience of glass from 20 to 900° C

glass surface. Large capacity variations occurred when the ball approached the glass, but during the actual time of contact, there was no change in capacity and thereafter, during the rebound, the capacity decreased. A proximity meter (model PM.2 by Fielden Electronics Ltd.) was successfully adapted for use in this work, and when the output was displayed on a time base a trace of the type shown in Fig. 2 was obtained. Multiple bounces involving repeated entry of the ball into the electrode system were prevented by moving a plate (operated by a long insulated rod to avoid hand-capacity effects) across the orifice after the rebound.

Ideally the resulting trace should have sloping sides, indicating the approach and recession of the ball and the glass block, but should have an absolutely flat-topped peak during the period of contact when the sphere is stationary. Minor elastic deformations of the sphere would not be apparent on this scale. In practice, and particularly when the time of contact was short, the trace lost its ideal shape and a somewhat arbitrary estimate of the duration of contact had to be made. The apparatus was, however, satisfactory

* Now at Welwyn Electrical Laboratories, Bedlington, Northumberland.

for the present purpose as two traces could be compared and any *change* in time of contact could be detected to a high degree of accuracy.

The fractional energy absorption $\Delta E/E$ is obtained from the heights of fall (h_1) and rebound (h_2) which are measured

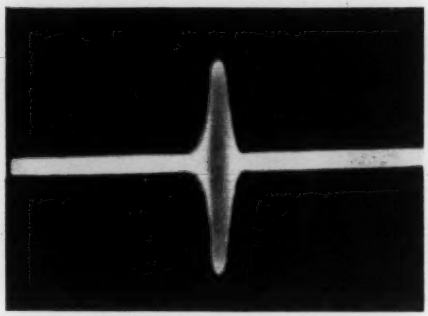

Fig. 2. Oscilloscope trace showing capacity variations during impact of a steel ball on a Pyrex glass block

by visual estimation on the vertical scale. It can be shown that

$$\Delta E/E = (h_1 - h_2)/h_1 \qquad (2)$$

and the variation of this term for Pyrex glass over a wide range of temperatures is shown in Fig. 3. It is interesting to

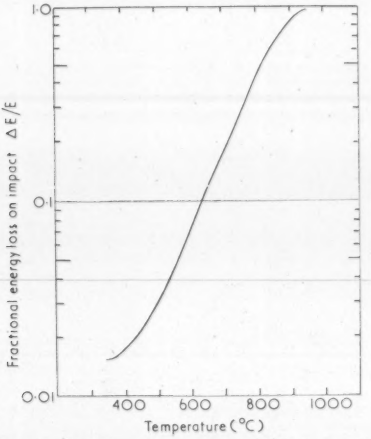

Fig. 3. Variation with temperature of the fractional energy absorbed during impact between an 8 mm steel ball and a block of Pyrex glass. Velocity of impact = 170 cm/s; time of contact 0 to 700° C = 18 μs

note that an appreciable rebound occurs at temperatures at which the glass is capable of appreciable viscous flow. The relative rebound does not fall below 25% until a temperature of 900° C is reached (the conventionally adopted softening point for this glass, arbitrarily defined by a viscosity of $10^{7\cdot6}$ P, is about 820° C). The curve in Fig. 3 shows that energy absorption is practically complete and there is no rebound at a temperature of about 1000° C. At this temperature, therefore, the anelastic processes involved appear to be represented by a relaxation period which is related to the period of contact by equation (1).

At room temperature the measured value for the time of contact between an 8 mm steel ball striking the glass with a velocity of 170 cm/s was 18 ± 3 μs and from careful comparison of a number of traces it was estimated that no change within ±10% occurred at temperatures up to 700° C. At higher temperatures the rebound was not sufficient to bring the sphere above the entrance to the furnace. Multiple bounces therefore occurred which obscured the trace under examination. The carrier frequency of the proximity meter was approximately 500 kc/s, giving adequate resolution when measuring periods of the order of 20 μs.

It is believed that the factor controlling the period of contact is the time for the full traverse of elastic waves in the smaller of the two bodies (in this case the steel ball). As the latter is always at room temperature, and falls into the furnace for a very short period, it is not to be expected that the contact period would vary with variation in the anelastic condition of the glass. It is likely that the value for the time of contact quoted is applicable above the highest temperature at which measurement was possible (700° C) up to the maximum temperature at which estimates of the rebound height could be made.

Two techniques were adopted to obtain satisfactory records of the capacity variations. The output from the proximity meter was taken from immediately after the radio frequency stages and before detection, thus avoiding any distortion associated with the low-frequency stages. This output was applied directly to the *Y*-amplifiers of an oscilloscope (model 1049 by A. C. Cossor Ltd.) and also to an auxiliary amplifier with a gain of approximately 1000. The latter was connected to the synchronizing or triggering terminal, thus ensuring that the trace began as soon as any small capacity change occurred, and enabled a picture of the development of the full capacity change incurred during impact to be obtained. Eventually most of the records were obtained by a second method using a free-running time base. In this case a template across the tube normally obscured the trace from view until, when an impact occurred, the waveform rose above the template and was recorded photographically. A number of exposures were made to ensure that one was obtained with the waveform at a suitable position along the time base. This method avoids the difficulty of triggering a single-shot high velocity trace.

REFERENCES

(1) TABOR, D. *The Hardness of Metals*, p. 133 (Oxford: Clarendon Press, 1951).

(2) TILLETT, J. P. A. *Proc. Phys. Soc.* [*London*] *B*, **67**, p. 677 (1954).

(3) MULLINS, L. *Trans Instn Rubber Industr.*, **22**, p. 235 (1947).

Correspondence

The suitability of Araldite D resin in photoelastic investigations

The results of the investigation of the mechanical and stress optical properties of a resin, Araldite D by Ciba Ltd., with different concentrations of hardener are presented in this note. This resin can be cast into any complicated shape at room temperature without the application of heat, while Araldite B needs heat for setting. The two main disadvantages of Araldite B are that thermal stresses are introduced and that impurities are present in the resin.* Though the figure of merit as defined by Leven (namely, Young's modulus divided by material fringe constant) is higher for Araldite B, yet Araldite D scores over Araldite B in some other respects.

Stress optical properties of Araldite resins

Material	*Young's modulus E at about 30° C (lb/in²)*	*Fringe constant f (lb/in² tension per in. per fringe)*	*Figure of merit as defined by Leven E/f*	*Remarks*
Araldite D with 10% hardener	$3{\cdot}75 \times 10^5$	65	5780	
Araldite D with 9% hardener	$2{\cdot}80 \times 10^5$	44	6360	Considerable scatter in fringe constant.
Araldite D with 8% hardener	$2{\cdot}70 \times 10^5$	33	8200	Considerable optical creep.
Araldite B with 25–30% of hardener	$4{\cdot}20 \times 10^5$‡	59‡	7120	Heat is needed for setting—thermal stresses—inclusion of extraneous matter.

‡ Agrees with the values given by Spooner and McConnel.*

Araldite D is suitable for freezing stresses for three-dimensional photoelastic work which are not disturbed by careful machining, filing and sawing. The resin acts as a very powerful adhesive; this property can be utilized in problems of composite structures and complicated built-up shapes like crankshafts, etc. Initial stresses are absent at the glued joints which are as strong as the parent material itself. Further, the stress-birefringence relationship is linear up to the point of fracture. By varying the percentage of hardener the Young's modulus of the cast resin can be varied. This is sometimes valuable in non-homogeneous structures. Other factors in favour of Araldite D as a photoelastic model material are absence of prominent creep and rind effect, the ability to remove initial stresses by annealing in a liquid paraffin bath at about 100° C and the ease with which it can be machined and drilled without chipping (unlike Columbia Resin 39). The strain is proportional to stress up to a stress of 2500 lb/in² and up to ten minutes of loading.

The results reported in the table are the result of a number of experiments conducted by the writer. The fringe constant and Young's modulus, etc., at higher temperatures are not yet calculated for want of necessary equipment. This photoelastic resin can also be cast on to the highly polished component itself and the optical effect in the layer, when the component is loaded, can be observed by the reflexion type of photoelastic polariscope. Further, fillers can also be added and it may be worth while to carry out investigations for the use of this resin as a brittle lacquer.

The author is indebted to Mr. R. Krishna Murthy for helping him in conducting all the above experiments and to Ciba Dyes Ltd., Bombay, and to their representative, Mr. U. S. Umesh, for furnishing all the available information. After carrying out the work independently, it was brought to the author's notice that Araldite Casting Resin D is sold under the denomination CN 502 in U.S.A. and some work on the above resin by four authors has been reported recently.†

Indian Institute of Science, Bangalore, 3, India.

C. L. AMBA RAO

* SPOONER, H., and MCCONNEL, L. D. *Brit. J. Appl. Phys.*, **4**, pp. 181–184 (1953).

† D'AGOSTINO, J., DRUCKER, D. C., LIU, C. K., and MYLONAS, C. *Proc. Soc. Exper. Stress Anal.*, **12**, pp. 123–129 (1955).

A note on the polarization due to oblique reflexion at an aluminized or silvered mirror

A rough estimate of the polarization caused by an oblique reflexion at an aluminized or silvered mirror is often useful in designing optical apparatus. The purpose of this note is to present a simple, approximate formula [equation (2)], which gives the degree of polarization P in terms of the normal reflectivity R_0 and the angle of incidence θ. The formula has an error less than 10% for aluminized or silvered mirrors in the visible spectrum, when $\theta \leqslant 45°$.

Suppose that unpolarized light of unit intensity falls on a mirror at an angle of incidence θ. Let R_p and R_s be the reflected intensities with the electric vector parallel and perpendicular, respectively, to the plane of incidence. Then P is defined by:

$$P = (R_s - R_p)/(R_s + R_p) \qquad (1)$$

If the mirror has reflectivity R_0 for $\theta = 0$, then P is given approximately by:

$$P \simeq \tfrac{1}{2}(1 - R_0) \sin\theta \tan\theta \qquad (2)$$

For a typical aluminized mirror, $R_0 \simeq 0{\cdot}90$ in the visible spectrum. Using this value in equation (2), one finds:

θ	0	15°	30°	45°
P	0	0·3	1·5	$3{\cdot}5 \times 10^{-2}$

Derivation: Fresnel's laws of reflexion give:

$$\frac{R_p}{R_s} = \left|\frac{\cos(\theta + \phi)}{\cos(\theta - \phi)}\right|^2 \qquad (3)$$

where ϕ is determined by:

$$\sin\theta = (n - ik)\sin\phi \tag{4}$$

$(n - ik)$ is the complex refractive index of the reflecting layer.

Let $$(n_1 - ik_1)^2 = (n - ik)^2 - \sin^2\theta \tag{5}$$

Then from equations (4) and (5):

$$(n - ik)\cos\phi = (n_1 - ik_1) \tag{6}$$

A transformation of equation (3) gives:

$$\frac{R_p}{R_s} = \frac{\cos\theta\cos\phi - \sin\theta\sin\phi^2}{\cos\theta\cos\phi + \sin\theta\sin\phi} \tag{7}$$

Sin ϕ and cos ϕ can be eliminated from equation (7), using equations (4) and (6), to give:

$$P = \frac{R_s - R_p}{R_s + R_p} = \frac{2n_1\sin\theta\tan\theta}{n_1^2 + k_1^2 + \sin^2\theta\tan^2\theta} \tag{8}$$

From equation (5):

$$(n_1 - ik_1) = (n - ik)\sqrt{\left[1 - \frac{(n + ik)^2}{(n^2 + k^2)^2}\sin^2\theta\right]}$$

Expanding by the binomial theorem and neglecting terms in $\sin^4\theta$:

$$\left.\begin{aligned} n_1 &\simeq n\left[1 - \frac{1}{2}\left(\frac{\sin^2\theta}{n^2 + k^2}\right)\right] \\ k_1 &\simeq k\left[1 + \frac{1}{2}\left(\frac{\sin^2\theta}{n^2 + k^2}\right)\right] \end{aligned}\right\} \tag{9}$$

The normal reflectivity R_0 is given in terms of n and k by:

$$1 - R_0 = \frac{4n}{(n + 1)^2 + k^2} \simeq \frac{4n}{n^2 + k^2} \tag{10}$$

if $$(2n + 1) \ll n^2 + k^2$$

If also $\tan^2\theta \ll n^2 + k^2$, then:

$$P \simeq \tfrac{1}{2}(1 - R_0)\sin\theta\tan\theta \tag{11}$$

Values of n and k for aluminium and silver films have been given by Schulz.* As an example, the values for an aluminium film at a wavelength of $0{\cdot}8\ \mu$ are: $n = 2{\cdot}0$, $k = 7{\cdot}1$, $R_0 = 0{\cdot}86$. Using these values and $\theta = 45°$, the accurate formulae (8) and (9) give $P = 0{\cdot}051$, while formula (2) gives $P = 0{\cdot}048$.

Physics Department, J. N. HODGSON
University College of North Staffordshire.

* SCHULZ, L. G. *J. Opt. Soc. Amer.*, **44**, p. 357 (1954).

New books

Introductory nuclear physics. 2nd ed. By D. HALLIDAY. (New York: John Wiley and Sons Inc.; London: Chapman and Hall Ltd., 1955.) Pp. ix + 493. Price 60*s*.

The occasion of the publication of a second edition of this book has been used to introduce a number of changes, in both matter and manner, designed to bring the contents up to date, and to present them in a logical fashion. A new chapter, "Elements of quantum mechanics," has been added and there are thirteen appendices, mostly dealing with the derivation of formulae. The reviewer is pleased to note that the negatron is no longer listed as a fundamental particle, although the word is still used on occasion in the text, and he is again surprised at the omission of all reference to radiation damage, a subject which is so important in reactor technology, and so full of theoretical interest. Nevertheless, there can be no doubt about the usefulness of the new edition. No serious misprints were noted, but it is to be hoped that recognition of Cockcroft and Walton's Nobel laureate will be acknowledged in future impressions in Table 1: "Some milestones in nuclear physics." Both the production and make-up of the book are excellent. J. THEWLIS

Proceedings of the eleventh general assembly, Vol. 10, Part 5, Radio-astronomy. (Brussels: International Scientific Radio Union, 1955.) Pp. 113. Price 18*s*.

For the general physicist reader, the interesting parts of this volume are not in the legislations of the sub-commissions on standards and nomenclature (pp. 1–19 and 107–114), but rather in the intervening major portion summarizing the last three years' research at Sydney, Jodrell Bank, Cambridge, Leyden, and the other lesser-known centres in Europe and America. Russia, now playing a large part in many astronomical meetings, appears to be absent from this report.

Physicists in many unrelated fields may well discover enviously a science growing up free from the sin of departmental insularity. For example, there is here the contribution from Jodrell Bank on the physics of meteors, which may catalyse the synthesis of many scattered astronomical and geophysical projects. Another British contribution towards bridging gaps, mentioned in this volume, is the Cambridge work on extragalactic radio sources; from Ryle's recent Halley Lecture this is likely to bring radio observation with some vigour into the controversies of cosmology.

Solar physics is as well represented as it should be in this volume, and likewise the mapping of the galaxy by the 21 cm radiation of hydrogen which was mentioned in reviewing an earlier volume of this series. MARTIN JOHNSON

The theory of hydrodynamic stability. By C. C. LIN. (London: Cambridge University Press, 1955.) Pp. xi + 155. Price 22*s*. 6*d*.

The theory of hydrodynamic stability has had a long and troubled history. Although the subject is yet far from complete no one is more entitled than the author of this monograph to say that "a more permanent outline of the subject has emerged through recent advances." The text of the monograph together with its extensive list of references gives a very complete picture of the present state of the craft and can be thoroughly recommended if for no other reason than the absence of comparable rivals. Fortunately the reasons for possessing it are more positive than this but your reviewer would take issue with the author over the exasperating number of forward references. The editor of a standard work on fluid mechanics took great pride and many pains in avoiding forward references altogether and one has only to read the present monograph to see his wisdom. Each time the present author appears to be grasping

the nettles in his subject the inevitable forward reference appears and in fact I strongly recommend the reader to tackle the final chapter early in his reading of the book.

The book is primarily concerned with the stability of the motion of homogeneous viscous fluid with respect to infinitesimal disturbances. The fundamental problems discussed are the flow between rotating cylinders and the flow in pipes and channels, the last-named including the case when the walls are in relative motion. In addition, the discussion ranges through chapters on the general theory of hydrodynamic stability and boundary layers to astrophysical and geophysical applications. The same word of warning to the uninitiated is perhaps as necessary in the review as in the monograph itself; the problem of transition to turbulence which is quite a different one is not discussed in detail in this monograph.

Criticism of arrangement on one side, this book is one which anyone interested in fluid mechanics will be glad to possess.

L. HOWARTH

Research reactors. Published for U.S. Atomic Energy Commission by McGraw-Hill Book Co., New York, 1956. Pp. 460. Price 49*s*.

This book contains very full descriptions of four general types of research reactor now in use or planned in the U.S.A. The homogeneous, aqueous-type reactor for fluxes up to $1{\cdot}7 \times 10^{12}$ n cm^{-2} s^{-1}, the heterogeneous, solid fuel element, natural water moderated reactor for fluxes up to 5×10^{14} and the heterogeneous, solid fuel element, heavy-water moderated reactor giving 2×10^{13} n cm^{-2} s^{-1} are the examples of ^{235}U enriched fuel reactors. The Brookhaven graphite-moderated reactor giving 6×10^{12} n cm^{-2} s^{-1} is described as an example of the natural-uranium-fuelled type of reactor.

Though much of the material has appeared in separate reports before, it is of great value to have it all collected in one volume. This permits a ready comparison of different approaches to a given problem and a comparison of the costs of solving the problem. The detail included in this book is sufficient to warrant study by the experienced reactor physicist, engineer or instrument man. By suitable omissions, the newcomer in the reactor field who merely wants to compare the pros and cons of the different types of reactor in use will also find he is well catered for.

To look for faults, I suspect that some statements as of fact are merely reflexions of hope. This remark I illustrate by doubting whether boral does in fact attenuate thermal neutron intensity by a factor of 100000 and asking how important the high water content is to the fast neutron shielding power of the BNL concrete. But the triviality of these examples shows how insignificant these faults are in the book.

F. W. FENNING

Metallurgy of the rarer metals No. 4 Titanium. By McQUILLAN and McQUILLAN. (London: Butterworths Scientific Publications, 1956.) Pp. xix + 466. Price 56*s*.

With commendable speed the publishers have added a fourth volume to this recently begun and valuable series dealing with the metallurgy of the less familiar metals. Titanium in combined form is abundant in nature and concentrations of titanium minerals of sufficient size to warrant commercial mining are found in many parts of the world. Moreover, it is clear that alloys based on titanium offer an attractive combination of high strength, lightness and corrosion resistance and that they can be wrought and subsequently fabricated without undue difficulty. The principal factor now opposing the large-scale use of the metal in important sectors of the engineering industries is the extreme reactivity of the metal when molten, particularly towards oxygen, which necessitates difficult and at present costly extraction and alloy-melting procedures and imposes problems also in the reclamation of scrap.

Less than ten years ago there was virtually no commercial supply of titanium or its alloys. This year world production will be of the order of ten thousand tons. The scientific and technological background of knowledge about every aspect of titanium has increased, and continues to grow, in comparable manner. It must be difficult to make a balanced appraisal of this mass of information, most of which has appeared in print since about 1949. Yet the two authors of this book, who have themselves made distinguished contributions to titanium technology, successfully achieve their aim to present a unified picture of the basic properties of titanium metal and its alloys, and of the principles involved in all aspects of their production and processing on an industrial scale. What is more, they succeed in presenting their material in a style which this reviewer found to be pleasantly readable.

G. L. J. BAILEY

An introduction to reactor physics. By D. J. LITTLER and J. F. RAFFLE. (London: Pergamon Press Ltd., 1955.) Pp. viii + 196. Price 25*s*.

This book is based on the authors' lectures at the Atomic Energy Research Establishment's Reactor School to the engineers and physicists now designing the gas-cooled thermal reactors which are part of the United Kingdom's programme for nuclear power. Thus it tends to deal mainly with that type of reactor. Sufficient information is given in the book to understand some of the main problems involved in designing thermal reactors of other types. However it would be improved by an extension of scope so that it includes the important concepts of enriched fuel, fuel cycles and fast reactors. Also some discussion of reactivity changes with time and flux-flattening would be worth while.

With regard to details the present edition suffers from a mild attack of misprints and mis-statements, some definitely misleading (the writer is indebted to one of the authors for indicating some of the latter to him before he was involved in this review). For example, the cross-sections in the discussion on conversion factor should be modified, for with the microscopic cross-sections as defined the final expression for the factor is incorrect. Similarly, the Fermi age of a neutron is not the time which has elapsed since it was born as a fission neutron. The section on shielding could usefully be extended, two pages is surely insufficient even though specialized texts on this topic are being prepared. A rearrangement of the chapters on chain reactions and neutron diffusion is indicated, at present the reproduction constants are discussed in the chapter on neutron diffusion. The book is well indexed, the printing is good, it fulfils a need, the price is reasonable and the authors are to be congratulated on a lucid presentation. It is a worth-while investment for persons interested in reactor physics. As the book was written before the Geneva Conference, it is to be hoped that the United Kingdom Atomic Energy Authority will encourage the authors to provide a revised edition which includes the latest nuclear constants and involves an enlargement of scope as outlined above. The book will then be an excellent introduction to reactor physics.

A. SALMON

Notes and comments

Elections to The Institute of Physics

The following elections have been made by the Board of The Institute of Physics:

Fellows: E. Billig, W. Cochran, L. Cohen, P. G. Deo, J. E. Gould, D. K. McCleery, A. Nightingale, E. Nightingale, K. K. Schiller, M. W. Townsend, C. G. Webb.

Associates: R. E. Adlington, T. Ashton, R. Axe, K. H. Barker, C. J. Bennett, H. D. Blakelock, I. Brodie, E. W. Carpenter, D. G. Cole, W. E. Copsey, A. M. Davies, T. A. Duerden, M. J. Dumbleton, J. B. Earnshaw, G. F. Filbey, R. Forester, T. L. Goodfellow, D. J. Hine, D. R. Holmes, W. R. Inch, A. C. Jason, A. P. H. Jennings, H. Minshall, D. P. Morris, K. E. Parks, W. A. J. Preece, G. B. Redmond, J. G. Rider, R. C. Ritchie, D. A. Robins, S. C. Roy, A. Sanson, C. H. Sturley, D. Tittensor, W. Traub, A. J. F. Trott, H. V. Wainwright, O. M. White, G. R. Wignall, H. R. Wilson, J. O. Wood, M. M. Woolfson.

Eighteen Graduates, five Students and five Subscribers were also elected.

Conference on the physics of nuclear reactors

The Institute of Physics is arranging a conference in London on "The physics of nuclear reactors" from 3 to 6 July, 1956, which its President (Sir John Cockcroft) will open with an address on the scientific problems in the generation of nuclear power. The primary purpose of the conference is to inform members of the Institute, particularly those engaged in industry, of recent developments in reactor physics and cognate subjects, and to make known to them the problems awaiting solution. As it is likely that an increasing number of physicists will find themselves concerned with these subjects the Board of the Institute desires to assist its members to keep abreast of developments. A limited number of non-members will be able to attend the conference; application forms and further details may be obtained from the Secretary, The Institute of Physics, 47 Belgrave Square, London, S.W.1.

Nuclear Power

We announce the establishment of a further periodical devoted to the application of nuclear physics and wish the Editor, Mr. W. Davidson, and his colleagues success. The new periodical is called *Nuclear Power* and is a monthly magazine published by Rowse Muir Publications Ltd., of 3 Percy Street, London, W.1. The subscriptions are £2 2*s*. 0*d*. in the United Kingdom, £3 3*s*. 0*d*. overseas, and $8.0 in the United States and Canada (including postage). This first issue has forty-four pages of text, measuring $8\frac{1}{2} \times 11\frac{1}{4}$ in., and is produced in a modernish style, which may appeal to some readers. For instance, the first eight pages are printed on mauve paper; they carry a leader entitled "The Eisenhower deal" and a series of new items under the general heading "Nuclear Power Worldview." Then follows an excellent survey of known processes of heavy water production methods, an account of a gamma dose-rate meter now in commercial production, a write-up of a British firm's radiation research, L. M. Wyatt's account of the production of reactor fuel elements from the ore to uranium metal, the first of a series on reactor physics by J. F. Hill of the Reactor School at Harwell, and some brief items under such headings as "survey of equipment," "names in the news" and "abstract of patents." The first of a series of detachable data sheets "microscopic cross-sections of elements for thermal neutrons" is included. Very brief abstracts of all the articles in English, French, German, Spanish and Russian are added.

International Institute of Refrigeration meeting

A joint meeting of Commissions 1 and 2 of the International Institute of Refrigeration will take place at Louvain from 4–7 September, 1956. The general topics to be discussed are:

1. Methods for the detection at very low temperatures of traces of impurities in metals, semiconductors and other solids (magnetic susceptibility, electrical resistance, electronic resonance, heat conductivity, etc.).

2. Heat conductivity and viscosity coefficients of gas and liquid mixtures at low temperatures.

3. Relationship between insulating materials and the gas or vapour included.

4. Hygrometry.

Further details may be obtained from Prof. I. van Itterbeek, Naamsestraat 73, Louvain, Belgium.

Journal of Scientific Instruments

Contents of the June issue

ORIGINAL CONTRIBUTIONS

Papers

A proportional counter tube for X-ray diffraction analysis. By A. R. B. Skertchly.
Calorimetry by the method of mixtures. By D. W. Plester, S. E. Rogers and A. R. Ubbelohde.
The measurement of frictional forces at vibrating contacts. By J. S. Halliday.
A wavelength discrimination spectrometer. By C. R. Forshaw.
An X-ray absorptiometer for the determination of tetraethyl lead in petrol. By J. F. Brown and R. J. Weir.
A simple monitor circuit for a spectrographic a.c. arc source. By D. F. T. Roberts and E. H. S. van Someren.
A semi-automatic pen-recorder chart analyser. By C. W. Spencer and G. H. Bazzard.
A calorimetric method of determining the energy output of radioactive materials. By A. G. White.
A general purpose electromagnet. By W. Sucksmith and S. P. Anderson.
Fringe spacing in interference microscopes. By F. R. Tolmon and J. G. Wood.

Laboratory and workshop notes

A simple visual method of accurately positioning a specimen relative to an X-ray beam. By P. J. Holmes and P. D. Fochs.
An illuminator for detecting air lines in glass tubing. By S. J. Morrison and S. M. Phillipson.
Thin film abrasion tester. By J. C. Kelly.
A two-circle Geiger counter mounting. By R. Bones.
A high vacuum magnetic mercury cut-off. By R. A. W. Haul and E. R. Swart.
A control valve for corrosive liquids. By J. Hodkinson.

NOTES AND NEWS

Correspondence

Conduction-cooled vapour traps. From V. A. Heathcote.
Angle-spring hinges. From R. V. Jones.
An adaptable mechanism for converting rotary motion into a succession of linear movements. From P. Grodzinski.

New instruments, materials and tools
Notes and comments

THIS JOURNAL is produced monthly by The Institute of Physics, in London. It deals with all branches of applied physics (including theory and technique).
All rights reserved. Responsibility for the statements contained herein attaches only to the writers.
EDITORIAL MATTER. Communications concerning editorial matter should be addressed to the Editor, The Institute of Physics, 47 Belgrave Square, London, S.W.1. (*Telephone:* Sloane 9806.) Prospective authors are invited to prepare their scripts in accordance with the *Notes on the preparation of contributions*. (Price 2*s*. 6*d*. including postage.)
REPRODUCTION. The Institute of Physics is a signatory to The Royal Society's Fair Copying Declaration. Details may be obtained upon application from The Royal Society, London, W.1.
ADVERTISEMENTS. Communications concerning advertisements should be addressed to the agents, Messrs. Walter Judd Ltd., 47 Gresham Street, London, E.C.2. (*Telephone:* Monarch 7644.)
CLAIMS FOR MISSING JOURNALS. Claims from regular subscribers to this *Journal* for missing numbers will only be considered if received within 60 days of the date of mailing plus normal outward time of transit and time for lodging the claim. Losses attributable to failure to notify a change of address or to similar omissions will not be considered.
SUBSCRIPTION RATES. A new volume commences each January. The charge is £4 per volume ($11.50 U.S.A.), including index (post paid), payable in advance. Single parts, so far as available, may be purchased at 8*s*. each ($1.15 U.S.A.), post paid, cash with order. Orders should be sent to The Institute of Physics, 47 Belgrave Square, London, S.W.1, or to any bookseller.

SPECIAL ARTICLE

The International Temperature Scale and a redefinition of the Kelvin Scale

By J. A. HALL, B.Sc., A.R.C.S., F.Inst.P., National Physical Laboratory, Teddington, Middlesex

The Tenth General Conference of Weights and Measures has accepted a redefinition of the Kelvin (absolute) temperature scale in terms of one fixed point, the triple point of water, to which a value of 273·16° K has been assigned. The International Temperature Scale continues to be defined in terms of 100° between the ice point (0·0100° C below the triple point of water) and the steam point. The relationship between the scales, and the approved designations are set out in a table. Work is being carried out with a view to future improvement of the international scale. It is hoped that it may be found possible to extend the range covered by the resistance thermometer both above and below its present limits of 630·5° C and −182·97° C, the latter temperature being the present lower limit of the international scale. If the resistance thermometer scale can be carried up to 1063° C (the freezing point of gold), it will be possible to eliminate the thermocouple as a standard instrument and so improve both the continuity and reproducibility of the scale.

The purposes for which an accurate knowledge of temperature is required may be classified broadly as theoretical or practical. Thermodynamical calculations are typical of the first class, of which the distinguishing feature is that the measurements must be related to the absolute (thermodynamic) scale of temperature. In the second class we have those measurements of temperature which are required in order to define some other physical property, such as specific heat, density, length or electrical resistance. Here the need is for an accurately realizable scale, and knowledge of the thermodynamic temperature is unnecessary.

It was in order to satisfy the practical requirements that the various national standardizing laboratories, in association with the Bureau International des Poids et Mesures, agreed on an International Temperature Scale, which was adopted in 1927 by the Seventh General Conference of Weights and Measures. In 1937 the Comité Consultatif de Thermométrie was formed to advise the International Committee of Weights and Measures on all matters connected with temperature, and the main business of this committee has been the maintenance and revision of the international scale. So far, there has been one major revision of the scale, in 1948.[1] At the meeting of the comité consultatif in 1954, the main topic of discussion was the relationship between the international scale and the thermodynamic scale.

The original aim of the international scale was to provide a practical scale of temperature reproducible to very high accuracy, and as nearly as possible identical with the Thermodynamic Celsius Scale. That is to say, it should be identical with the Thermodynamic Celsius Scale to within the limits of accuracy of measurement with the gas thermometer, but it should offer the higher reproducibility obtainable with such instruments as the platinum resistance thermometer, not in themselves capable of defining an absolute scale. This position has now been slightly modified in consequence of a redefinition of the thermodynamic scale, proposed by the comité consultatif in July 1954,[2] and accepted by the Tenth General Conference of Weights and Measures in October of that year.

THE KELVIN SCALE WITH ONE FIXED POINT

Joule and Thomson (Lord Kelvin)[3] had pointed out in 1854 that only one fixed point was necessary to define the absolute scale, and they suggested that when the value of the absolute zero on the Celsius (centigrade) scale was known to a sufficient accuracy (they considered 0·1° C would be adequate), then the scale should be defined by assigning that value to the ice point on the thermodynamic scale. In 1874, Mendeleev[4] made an alternative suggestion, in which he proposed a new scale having 1000° as the value of the ice point, thus making no attempt to correlate the thermodynamic and Celsius scales.

The value of the absolute zero on the Celsius scale has now been known to 0·1° for many years, but our requirements in temperature measurement are no longer satisfied by such an accuracy. The interval between 0 and 100° C can be reproduced to about 0·001° C, so that to define the degree to the same precision, it would be necessary to fix the value of the ice point on the absolute scale to 0·0027°, which is well outside present-day possibilities. However, in 1939, Giauque[5] suggested that the time had come to adopt Kelvin's proposal, and he proposed that the best-known value of the ice point on the absolute scale should be adopted permanently.

At that time the Physikalisch-Technische Reichsanstalt put forward the suggestion that the triple point of water should be used instead of the ice point as one of the primary fixed points on the International Temperature Scale. Both this and Giauque's proposal were before the comité consultatif in 1939 but were deferred for further study. At the same time, the committee passed a resolution that they considered the most likely value for the ice point on the Kelvin scale was $273{\cdot}15 \pm 0{\cdot}02$° K.

The next meeting of the comité consultatif took place in 1948, and, as already reported,[1] it was agreed to define the zero of the international scale as 0·0100° C below the triple point of water. Later, in 1954, it was agreed to call this temperature the "ice point" and to reserve the expression "melting point of ice" for the temperature physically realized by the equilibrium between water and ice. Detailed discussion of Giauque's proposal revealed two points of view. The suggested method of defining the scale had obvious advantages for workers at low temperatures, and, indeed, for all those making gas-thermometer measurements, for which an observation at the steam point would no longer be necessary. On the other hand, the proposal was less attractive to the metrologist, anxious to define temperatures as accurately as possible, but not concerned with their values on the absolute scale. His needs are best met by the Celsius scale with a

degree which can be reproduced to an accuracy of 1 in 100 000 (that is to say, 0·001° C in the fundamental interval from 0 to 100° C) and a zero reproducible to 0·0001° C. The degree on the proposed absolute scale cannot as yet be known to better than 1 in 27 000, since different workers' values for the ice point on the thermodynamic scale vary by more than 0·01°, but for theoretical work in thermodynamics only absolute temperatures are of interest, and a reproducibility of better than 1 in 27 000 in the size of the degree is, at the present time, quite illusory.

In 1948 there was a sharp difference of opinion on the comité consultatif as to whether the value 273·16° K or 273·17° K should be accepted for the triple point of water (0·0100° C), but in the resolution which they put forward to the International Committee of Weights and Measures, the figure of 273·16° was given. The international committee, however, declined to ratify this figure, and the 1948 resolution, as finally adopted, appeared thus:

> The comité consultatif accepts the principle of a thermodynamic scale having only a single fixed point, provided at present by the triple point of pure water, of which the absolute value will be fixed later.
>
> The introduction of this new scale does not affect in any way the use of the international scale, which remains the recommended practical scale.
>
> In the present state of the accuracy of measurement, the new scale is identical with the thermodynamic Celsius scale.

The comité consultatif met again in 1952, but decided that they were in no better position to recommend a value for the ice point on the absolute scale, so that things remained in the same state until the meetings which were held in 1954. At these meetings[2] all the available data were reviewed, memoranda from Germany, Japan, the Netherlands and the United States being considered. The decisive factor turned out to be two recalculations of the old Physikalisch-Technische Reichsanstalt results which had been carried out independently by H. van Dijk of Leiden and J. Otto of the Physikalisch-Technische Bundesanstalt, both of which led to a value of 273·149° K for the ice point instead of the original figure of 273·158° K. In consequence of this revision, there were three values in the neighbourhood of 273·15° K (Leiden, P.T.R. and the Tokyo Institute of Technology), and one in the neighbourhood of 273·17° K (Massachusetts Institute of Technology), and it became possible to secure agreement on a value of 273·15° K (273·16° K for the triple point of water). The fact that various existing thermodynamical tables were based on a value of 273·16° K for the ice point was considered, but it was pointed out that such tables would still be usable without change, since a relative error of about 1/30 000 would in all cases be negligible. The following resolution was then adopted, and it was subsequently accepted by the international committee and the Tenth General Conference of Weights and Measures:

> The Comité Consultatif de Thermométrie recommends that the thermodynamic scale should henceforth be defined by means of one fundamental fixed point, the triple point of water.
>
> After having considered carefully all the numerical results obtained up to the present time, the Comité Consultatif de Thermométrie considers that the best value for the temperature of the triple point of water is 273·16° K on the thermodynamic scale in use up to the present.
>
> In consequence, it recommends that the temperature of the triple point of water should be given, on the thermodynamic scale with one fundamental fixed point, the numerical value of 273·16° K exactly.

THE RELATIONSHIP BETWEEN THE INTERNATIONAL AND KELVIN SCALES

Since, in accordance with the resolution of 1948, the international scale is not to be affected, we now have two scales, independently defined: the thermodynamic scale based on the interval between the absolute zero and the triple point of water (273·16°) and the international scale, based on the interval between the ice and steam points (100°). However, for certain purposes, such as the extrapolation of the international scale above 1063° C by means of Planck's law, we need an "absolute" scale related to the international scale, and this can be obtained by adding 273·15° to the temperature expressed in °C (International, 1948). Each scale, therefore, can be expressed in either of two forms, as indicated in the table, where the arrows indicate the direction of transition from the scale originally defined to the scale derived from it by a shift of zero. In this way, it seems that both theoretical and practical needs have been met.

INTERNATIONAL SCALE

International temperature	→	*International Kelvin temperature*
t		$T_{int} = t + 273{\cdot}15$ exactly
Identification		*Identification*
°C (Int. 1948)		°K (Int. 1948)
degree Celsius (International 1948)		degree Kelvin (International 1948)

THERMODYNAMIC SCALE

Thermodynamic Celsius temperature	←	*Thermodynamic temperature*
$t_{th} = T - 273{\cdot}15$ exactly		T
Identification		*Identification*
°C (therm.)		°K
degree Celsius (thermodynamic)		degree Kelvin

At the present time the degrees of the two scales are indistinguishable in size, but they must, in fact, be slightly different, and, as time goes on, the difference will no doubt become appreciable. It will then be necessary to decide whether to let the situation remain, or whether to bring the two scales into line. This could obviously be done if we regard the steam point as a "primary" point instead of a "fundamental" point on the International Temperature Scale, and so give ourselves the liberty of changing its value slightly as was done with the silver point in 1948.

NEW WORK ON THE INTERNATIONAL TEMPERATURE SCALE

The change in the definition of the thermodynamic scale involves a slight inconsistency in the introduction to the 1948 edition of the International Temperature Scale, but the international committee decided not to make minor changes in the text at the present time, as there is likely to be a more considerable revision in 1960. Another small change in the text which has been deferred relates to the radiation part of the scale (above 1063° C). In 1952 the comité consultatif decided to recommend a wording which did not limit the wavelength to be used for the radiation measurements to one in the visible region. The question is not of immediate

importance, as measurements are normally made visually with an optical pyrometer, but it is likely to become so as photoelectric methods for realizing the scale are developed.

The work on which it has been decided to concentrate with a view to a revision of the scale in 1960 may be divided into two parts. The first of these concerns the possibility of extending the scale below the oxygen point—at any rate down to the boiling point of hydrogen. At temperatures below the oxygen point the differences between different samples of platinum used as resistance thermometers become much more serious than at higher temperatures. This is because the "residual resistance" to which the resistance of the thermometer approaches as it nears the absolute zero of temperature varies very much with the chemical purity and physical condition of the wire. Various platinum thermometers have been calibrated as individual instruments down to the hydrogen point, but insufficient work has been done to establish any general law. Attempts are now being made to accumulate the necessary data.

The second region of the scale which is to be intensively studied is that lying between the sulphur point (444·600° C) and the gold point (1063° C). At present, this part of the scale is divided into two parts: up to 630·5° C it is obtained by extrapolation of the resistance thermometer law based on the ice, steam and sulphur points, while above that temperature it depends on the platinum/10% rhodium–platinum thermocouple, using a quadratic equation based on observations at the antimony, silver and gold points. There is thus an inevitable discontinuity at 630·5° C, though this was minimized in 1948 by changing the accepted value of the silver point from 960·5 to 960·8° C.

Resistance thermometers were used for measurements up to the gold point at the Physikalisch-Technische Reichsanstalt and the National Physical Laboratory some twenty-five years ago, and further measurements have been made recently at the Mendeleev Institute of Metrology in Leningrad. The results of all these investigations show a satisfactory degree of concordance, and lead to a value of about 960·9° C for the silver point if the equations are adjusted to make the thermometers read 1063° C at the gold point. Simple extrapolation of a quadratic law from the sulphur point leads to a value of about 1062° C for the gold point.

In view of the encouraging nature of these results, it has been decided to investigate thoroughly the possibility of extending the resistance thermometer scale up to 1063° C. For this purpose it is necessary to decide what fixed points should be used for the calibration, what values should be assigned to them, what interpolation formulae should be used and what should be the specification for a resistance thermometer to be used over this range of temperature.

As regards the first of these points, some interesting work has been done by McLaren and others at the laboratory of the National Research Council at Ottawa, on the freezing point of zinc.[2],[6] Using eight resistance thermometers, seven of which had been calibrated at the National Bureau of Standards and one at the National Physical Laboratory, values ranging from 419·499 to 419·509° C were obtained. The mean of the results given by the N.B.S. calibrated thermometers, made by C. H. Meyers, was 419·504° C, while the N.P.L. calibrated thermometer, made by H. Tinsley and Co. Ltd., gave 419·508° C. On the other hand, the Mendeleev Institute[2] report a value of 419·59 ± 0·03° C for their resistance thermometer measurements of the zinc point. Though their measurements were made on a different sample of zinc, it seems rather unlikely that either sample should be sufficiently impure to account for such a large difference, which suggests rather that imperfections in the realization of the scale itself (in effect that of the sulphur boiling point) in different laboratories may account for discrepancies of several hundredths of a degree in this region. This work at once raises the question as to whether the freezing point of zinc would be a better fixed point for the international scale than the boiling point of sulphur, and the reproducibility of the two points is to be the subject of further study.

Discrepancies between the values of Planck's second radiation constant, c_2, obtained from radiation measurements and those obtained from atomic constants, have, in recent years, caused some doubt to be cast on the reliability of the value of 1063° C which is at present accepted for the gold point. New gas thermometer determinations of the gold point have therefore been undertaken at the Physikalisch-Technische Bundesanstalt,[7] and it is hoped to achieve an accuracy of a few tenths of a degree. The work will be extended to the other fixed points required for the International Temperature Scale. High-temperature gas thermometry is also in hand at the Mendeleev Institute and at the University of Tokyo. Oishi, Awano and Mochizuki, of Tokyo, have already reported values of 961·28° C for the silver point and 1063·69° C for the gold point.[8]

All resistance thermometers which have been used hitherto at high temperatures have had one thing in common: the sensitive element has been too large to provide a convenient standard for use in the calibration of other instruments. For example, the thermometer should be usable for measuring the temperature of a small black-body enclosure at 1063° C in order to link with the optical pyrometer scale at this temperature. In order to secure uniform temperature conditions, such a black body cannot conveniently be large; a typical example is about 25 mm long, and, so far, no high-temperature resistance thermometer bulb has been made as short as this. Stability of zero at high temperatures is most easily achieved by the use of heavy wire (0·5 mm diameter for example), but this leads to a rather massive coil, even when the resistance is kept down to a few tenths of an ohm at 0° C. On the other hand, the zeros of thermometers using wire of 0·1 mm diameter have been found to rise by about 0·01° C after 6 hours at the gold point. Evidently there is need for judicious compromise in order to achieve the best design, if resistance thermometers are to take over the duty of standards up to 1063° C.

Attempts are being made at the Physikalisch-Technische Bundesanstalt and at the National Physical Laboratory to extend the radiation scale below the gold point, taking advantage of the highly-sensitive detectors which are now available for measurements in the infra-red region of the spectrum. If this work achieves sufficient accuracy, it will afford a valuable overlap of the resistance thermometer and radiation scales.

To sum up, the work of the Comité Consultatif de Thermométrie in 1954 provided a redefinition of the Thermodynamic Temperature Scale and laid down a programme of research which, when completed, should make it possible to provide a practical scale covering the important region between 20 and 90° K, and (to quote a resolution of the committee) "to revise the International Temperature Scale in the region between the sulphur and gold points in order to obtain better reproducibility, good continuity and a better agreement with the thermodynamic scale."

REFERENCES

(1) HALL, J. A., and BARBER, C. R. *Brit. J. Appl. Phys.*, **1**, p. 81 (1950).

(2) Comité int. des Poids et Mesures. *Procès-verbaux des Séances de* 1954, **24** (1955).
(3) JOULE, J. P., and THOMSON, W. *Phil. Trans*, **144**, p. 351 (1854).
(4) LOUGUININE, W. *Bull. Soc. Chim. Paris*, **21**, p. 302 (1874).
(5) GIAUQUE, W. F. *Nature [London]*, **143**, p. 623 (1939).
(6) PRESTON-THOMAS, H. *Temperature, its Measurement and Control in Science and Industry*, Vol. 2, p. 169 (New York: Reinhold Publishing Corporation, 1955).
(7) MOSER, H., p. 103 of reference (6).
(8) OISHI, J., AWANO, M., and MOCHIZUKI, T. *J. Phys. Soc. Japan*, **11**, p. 311 (1956).

CONFERENCE REPORT

A symposium on magnetism—London, September, 1955

The Electronics Group of The Institute of Physics held an informal symposium on recent developments in magnetism on 23 and 24 September, 1955.

Speakers from university, government and industrial research groups took part in the conference and the subjects discussed ranged from some latest advances in theoretical studies, to the application of magnetic materials to computor systems.

THEORY OF THE MAGNETISM OF FERRITES

Dr. E. W. GORTER (Philips Research Laboratories, Eindhoven) gave an introduction to the physics of the ferrite group of materials. These have the general formula $MeFe_2O_4$, where Me is one of a group of divalent metals or perhaps a mixture of two or more of them.[1] They have a spinel type of structure (as shown in Fig. 1), having a close-packed array of oxygen

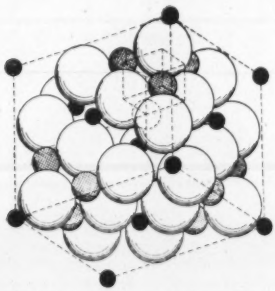

(Reproduced from *Reports on Progress in Physics*)

Fig. 1. The spinel crystal structure (after Verwey and Heilman)

Circles represent: open, oxygen anion; shaded, octahedral cation; solid, tetrahedral cation.

ions with the metal ions located between them in two different types of site. In the complete unit cell, which contains eight formula groups and therefore thirty-two oxygen ions, there are eight metal ions each surrounded by four nearest neighbours (tetrahedral or *A* sites) and sixteen ions each surrounded by six nearest neighbours (octahedral or *B* sites). The so-called normal structure has the divalent ion in the *A* site and the two trivalent ions in the *B* sites; the inverse structure also occurs, in which the divalent ion and one of the trivalent ions are in the *B* sites and the other trivalent ion in the *A* site.

A particularly interesting property of the ferrites is the saturation magnetic moment at low temperatures. The characteristic feature of ferrites is that this moment, which can conveniently be expressed in Bohr magnetons per formula group, is found to be less than the total of unpaired spins known (from measurements on paramagnetic salts) to be present. Dr. Gorter gave four reasons why this should occur, and why the total moment for the formula group may be fractional (as it often is).

First and most important: Néel[2] introduced the idea of two sub-lattices, consisting of the ions in the *A* and *B* sites respectively, in which three different interactions are possible, namely, *A–A*, *B–B*, and *A–B*. Néel suggested that the *A–B* interaction is predominantly negative, producing an anti-parallel orientation, so that the resultant magnetic moment of the two-lattice material is the difference between the moments of the two separate sub-lattices. He gave the name "ferrimagnetism" to this effect. Most of the observed values are greater (though only by a fraction of a Bohr magneton) than those calculated according to this model.

Although in zinc ferrite the *B–B* interaction is evidently negative, since the material is non-magnetic, this is not necessarily the case in double ferrites such as nickel-zinc ferrite. Such materials may have higher moments than the single ferrites, though not so high as if the *B–B* interaction were entirely positive.

Second, the distribution, between the *A* and *B* sites, of the di- and tri-valent ions may be neither exactly "normal" nor exactly "inverse," but intermediate between them; and, further, it may vary with temperature. In magnesium ferrite at ordinary temperatures a few of the magnesium ions are in *A* sites and most in *B*; at high temperatures the distribution becomes one-third in *A* and two-thirds in *B* sites. Quenching from high temperatures freezes the latter arrangement, and the quenched material has a higher moment than the annealed one. At temperatures somewhat below the Curie point there is already some tendency towards this distribution, and the curve for saturation moment against temperature is thus distorted because it does not all relate to identical material.

Third, the magnetic moment of the ions may not be an integral number of Bohr magnetons. Spin-orbit coupling can increase the total beyond that due to spins alone. This is the explanation for the value of 2·3 Bohr magnetons observed for nickel ferrite, which must have a completely inverse structure because the magnetic moment is unaltered by quenching.

Fourth, the equilibrium positions of the moments may not

be exactly antiparallel, and the angles between them may be dependent on temperature. It was thought by Néel that antiparallel ordering of the moments was necessary for the energy to be a minimum. Subsequently, Yafet and Kittel have shown that in some cases a lower value of the energy is obtained when the moments are not parallel but are at a small angle to one another.

These four concepts allow the prediction of various types of anomalous saturation/temperature curves, even including some which cross the horizontal axis and thus refer to materials which are non-magnetic at one particular temperature well below the Curie point. Dr. Gorter demonstrated the odd behaviour of one such material, a mixed lithium-ferrite-lithium-chromite; a bar of this material, swinging in a magnetic field, turned through 180° when heated.

The relative strengths of the types of interaction can be inferred from the observed moments of ferrites. The strongest negative interaction is the *A–B*, in which there is an oxygen ion in the direct line between the metal ions. The *B–B* super-exchange interaction, in which the directions of the metal ions as seen from the oxygen ion are perpendicular, is weak. These findings are in agreement with the theoretical descriptions of super-exchange interaction given first by Kramers[3] and more recently by Anderson.[4]

Dr. Gorter, replying to Dr. STREET, said that the antiferromagnetic arrangement of the iron in zinc ferrite had been confirmed by unpublished tests using neutron diffraction. Replying to Dr. MCCAIG, he saw no likelihood of finding ferrites with a higher saturation than that of manganese-zinc ferrite.

USE OF FERRITES AT MICROWAVE FREQUENCIES

Mr. J. WATKINS (G.E.C. Research Laboratories, Wembley) described some effects produced by electromagnetic fields at microwave frequencies acting on ferrites.

With the advent of low-loss ferrite materials, many properties exhibited by magnetic materials at microwave frequencies and previously masked by eddy-current effects can now be studied by conventional microwave techniques. Two such properties are the Faraday rotation[5,6] and the transverse phase-shift.

The Faraday effect, as shown in Fig. 2, is the rotation of the plane of polarization of a wave in passing through a magnetic material subjected to a static magnetic field along the direction of propagation. The rotation is independent of the sense of propagation; that is, waves travelling with or against the direction of the static field have their planes rotated in the same direction in space. The phase-shift effect occurs when a magnetic material in a wave-guide is subjected to a transverse magnetic field; the phase and attenuation differ for the two directions of propagation.

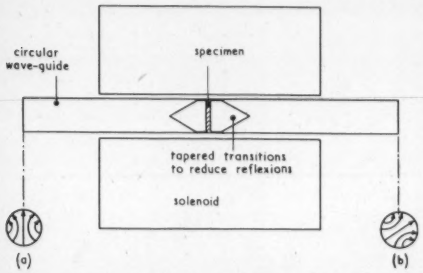

Fig. 2. Apparatus for the measurement of the Faraday effect in wave-guides

(*a*) Cross-section of guide showing electric vectors of TE_{11} mode. (*b*) Cross-section of guide showing rotation of electric vectors of TE_{11} mode.

The basis of these effects can be traced to the behaviour of the ionic spins constituting the magnetism shown by a material. These spins precess around the direction of a magnetic field which is either externally applied or exists spontaneously in the material. The behaviour is analogous to that of spinning tops consisting of negatively-charged spheres spinning about a diameter and possessing a magnetic moment and a moment of momentum (which, if the usual conventions are used, are in opposite directions). In the static field, the magnetic moment precesses round the field direction, and does so until the damping by frictional forces brings the directions into coincidence. If, to such a system with its magnetic moment lying along the *z*-axis, an oscillatory field of frequency equal to that of the precession is applied along the *y*-axis, the magnetic moment in attempting to precess around the resultant field direction will diverge more and more until it reaches a limit set by damping. A field 90° out of phase with that in the *y*-direction is induced in the *x*-direction. Calculations show that the permeability takes on a tensor character, and the following equations hold:

$$\begin{aligned} b_x &= \mu H_x - jKH_y \\ b_y &= jKH_x + \mu H_y \\ b_z &= H_z \\ \mu &= \mu' - j\mu'' \\ K &= K' - jK'' \end{aligned}$$

where μ', μ'', K', K'' are separate functions of H_z, α, M_z, and ω, and where H_z is the applied field, α is the damping constant, M_z is the saturation magnetization, and $\omega/2\pi$ is the frequency of the applied field. Because the terms containing jK have different signs, reciprocity does not hold.

The Faraday and phase-shift effects can be explained by assuming the plane-polarized wave to be resolved into two circularly-polarized waves having different propagation constants, one containing a term in $(\mu - K)$ and the other a term in $(\mu + K)$. Because the velocities of the waves are different, the plane of polarization of the resultant wave is progressively rotated.

The phase-shift effect arises when the mode configuration of the incident wave is such that its field has as a component a circularly-polarized wave in the region occupied by the magnetic material. Consider a slab of ferrite mounted asymmetrically in a wave-guide supporting a TE_{10} mode, and subjected to a transverse static field: it is subjected to a negatively-circularly-polarized wave when energy flows in one direction and a positively-circularly-polarized wave when the energy flow is reversed. Because the two propagation constants differ, the attenuation and phase shift are different for the two directions of propagation.

In reply to Mr. C. E. RICHARDS, who asked what properties at low frequencies would indicate good properties at microwave frequencies, Mr. Watkins said it was essential to keep the eddy-current loss low; this could be done by starting with an iron-deficient ferrite which would approach stoichiometric composition during firing. Further, the materials should be free from internal flaws. Dr. GORTER agreed that flaws must be avoided, and suggested the introduction of trivalent manganese to achieve a high resistivity. He added that in applications where external static fields are used it is

important that the permeability should be high. Dr. BLACKMAN asked what correlation existed between the resistivities at high and low frequencies; the answer, from both Mr. Watkins and Dr. Gorter, was "very little."

Dr. LAVERICK suggested that the physical picture of the precessing moments would be different when the applied field was small, but Mr. Watkins could not be persuaded to agree.

MAGNETIC CORES FOR STORAGE CIRCUITS

Mr. B. G. PARKIN (Post Office Research Station, Dollis Hill, London) read a paper on memory cores. These cores are used in computers and similar devices for the storage of information,[8] and they must be made from material having an approximately rectangular hysteresis loop with a coercivity preferably not more than 1 oersted.[7] As "memory" devices their main advantage is that they consume no power in maintaining the information, and their main disadvantage is that the information is lost after it has been read out unless special steps are taken to restore it. Mr. Parkin showed a few examples of the circuits in which these devices are used.

Both metals and ferrites can be obtained with suitable shapes of hysteresis loop. In both cases single crystals would have such a loop, but are obtainable only with the greatest difficulty; the problem is to produce a polycrystalline material having similar properties. One solution is to use alloys such as 50/50 nickel-iron, alined by heavy cold-rolling followed by a particular annealing treatment. Another method is to use an alloy such as 65/35 nickel-iron, annealed in a magnetic field while the temperature is reduced from 600 to 300° C; there are rival theories to account for the resulting alinement, one theory based on the relief of magnetostrictive stress and the other (now seeming the more probable) on atomic ordering along an axis in the direction of the applied field. Rectangular loops have also been reported for the American 4–79 Permalloy when it is rolled to fractions of a thousandth of an inch in thickness, but details of the process are not available. Another method recently suggested is the depositing of evaporated metal to form thin films, applying a magnetic field while doing so.

Ferrites having roughly rectangular loops are available, but the methods used to produce them are largely empirical. Most ferrites have negative magnetostriction, and in any such material mechanical compression makes the loop more rectangular; internal stress may therefore be the essential point.

An important parameter is the "response time." This is the time in which the magnetization of such a core can be reversed, which determines the operating speed of a computer using these cores. It is, of course, dependent on the field applied. The classical eddy-current theory for a uniform material of coercivity H_c leads to a time τ equal to

$$\pi B_m d^2/[\rho(H_m - H_c)]$$

where B_m is the flux in a field H_m, d is the thickness of the material, ρ is the resistivity, and H_m is the applied field. In practice, however, the time is longer than this because of the strong local eddy currents associated with domain-wall movements and because of the damping effect of spin relaxations. In ferrites the spin relaxation effect predominates and fixes the response time for any given applied field.

For one type of storage circuit (the "matrix") the field available for switching is necessarily less than twice the coercive field. Ferrites have a coercive field of the order of 1 oersted, roughly ten times that for a metal, and can therefore be subjected to a greater driving field in this type of circuit. Other things being equal, they should switch more quickly, as in fact they do. For other types of circuit (including the "shift register"), in which the switching field is not limited in this way, some types of metal tape, if thin enough, can be switched faster than ferrites, for example, in 1 μs in a field of 1 oersted.

Mr. Parkin thought that engineers had achieved a number of results not yet explainable by physicists, a challenge taken up by Dr. GORTER, who outlined the conditions for producing rectangular loops in polycrystalline ferrites. These loops, he said, occur when there is only one source of anisotropy, which may, for example, be mechanical stress in a material of low crystal anisotropy or high crystal anisotropy in a material of low magnetostriction. Other conditions to be met are low porosity and, in the interests of high resistivity, the presence of some trivalent manganese. Theory may suggest a remanence which is 0·87 of the saturation; a slightly higher ratio is found in practice between the remanence and the maximum working flux.

SPONTANEOUS MAGNETIZATION: EXPERIMENTAL METHODS

Dr. STREET (University of Sheffield) described the experimental methods developed by the team working at the University of Sheffield.[9] He distinguished spontaneous magnetization from the so-called saturation magnetization which usually means the macroscopic average over a number of domains. The spontaneous magnetization σ varies with the temperature because thermal agitation opposes the alinement due to exchange forces, and σ becomes zero at the Curie point. The form of the σ/θ curve (where θ is the temperature) gives information about the coupling forces between the carriers of the magnetic moment; the best-known application of this information is in the study of ferrimagnetism.

A complication in the measurement of spontaneous magnetization is that it is field-dependent. At low temperatures the effect is small, but just below the Curie point it is of first-order importance. At the lower temperatures the value for $H = 0$ can be deduced by extrapolating the isothermal σ/H curve, but near the Curie point this no longer defines the required value clearly. The problem is to find an alternative method of extrapolating to the value σ_0 corresponding to $H = 0$; there are two main methods, magnetic and magnetothermal.

The "magnetic" method is based on the assumption (which can be derived from the Weiss theory) that σ is a function only of the variable H/θ. It follows that the curve for H against θ, with σ constant, is a straight line, which can be extrapolated to $H = 0$. This extends the range of temperature in which measurements can be made, but again the lines become curved as the Curie point is approached closely. This behaviour is illustrated in Fig. 3.

The "magnetothermal" method depends on measurement of the temperature rise when the field applied to a specimen is decreased to zero. Again assuming the Weiss theory to hold, the temperature rise $\Delta\theta$ is given by

$$\Delta\theta = \text{constant } (\sigma_H^2 - \sigma_0^2)$$

so that σ_0 for any given temperature can be found by plotting $\Delta\theta$ against σ_H^2 (which must be measured in a separate experiment) and extrapolating to $\Delta\theta = 0$, as shown in Fig. 4.

From the σ_0 values obtained by either method, the Curie point is found by plotting σ_0^2 against θ (this gives a more

nearly straight line than σ_0 against θ) and extrapolating to $\sigma_0^2 = 0$.

The simplest experimental technique for measuring over a wide range of temperatures is to determine the mechanical force on a specimen in a non-uniform field, using a Sucksmith ring-balance. A gradient uniform over a reasonably large region can be obtained by using stepped pole-pieces or by providing current-carrying conductors in an otherwise uniform field. The apparatus can most easily be calibrated by using it to measure a specimen of known σ.

For the magnetothermal method, σ is measured as just described. The temperature rise is measured by embedding

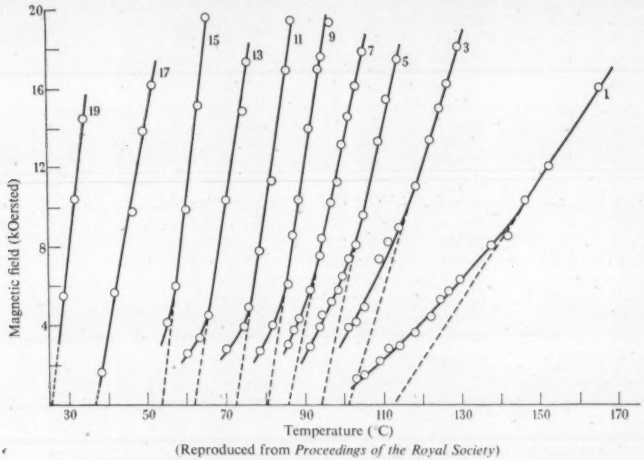

(Reproduced from *Proceedings of the Royal Society*)

Fig. 3. Curves of constant magnetization. The dependence of the magnetic field on the temperature for constant values of the specific magnetization, indicated by the numbers adjacent to each curve

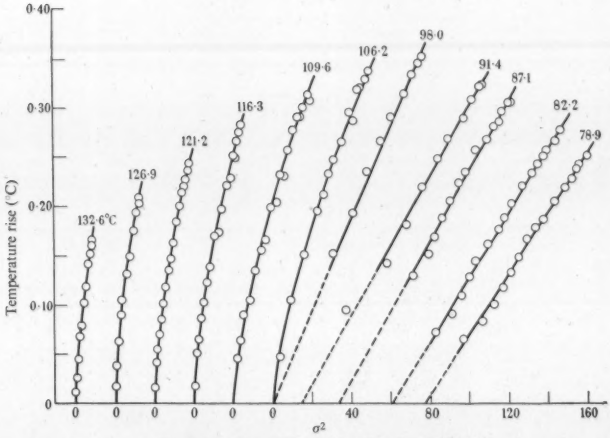

(Reproduced from *Proceedings of the Royal Society*)

Fig. 4. The dependence of the magneto-caloric temperature rise on σ^2 immediately below and above the Curie point

a thermocouple in the specimen; by using it to drive a galvanometer-type amplifier with negative feedback, a sensitivity of up to 1000 mm/° C, still with good linearity, can be obtained, and this is quite adequate. Care is needed to avoid inductive pick-up on the thermocouple leads and the conduction of heat along them.

The sensitivity obtained with galvanometer amplifiers has made possible, for the first time, comparisons between the results obtained by the two methods. As an example, for a 26/74 copper-nickel alloy, the two methods led to Curie temperatures of 93·3 and 97° C; the difference illustrates the uncertainties in extrapolation. When the complete curve for σ against θ is drawn, this difference is scarcely noticeable, but both methods are precise enough to show that the curve is not exactly that predicted by the Weiss theory. The magneto-thermal measurements for this alloy above its Curie point are also inconsistent with the Weiss theory. A magnesium-zinc ferrite, however, obeyed the theory above the Curie point while being anomalous below it.

Dr. Street concluded that for most purposes the measurements in a nonuniform field are adequate, if handled in the manner described, but that the more difficult magnetothermal method may sometimes have to be used to avoid ambiguities. To make a measurement was easy; to be sure what had been measured might be difficult.

In answer to Dr. Gorter, he thought that the magneto-thermal method should be useful for studying ferrimagnetic materials. Dr. Rhodes, interested in the variation of σ with H, was referred to some forthcoming work by Wooler.

MATERIALS FOR MICRO-POWDER MAGNETS

The next two papers were concerned with the magnetic properties of aggregates of small particles. Neel[10] and Kittel[11] have predicted that a particle of less than a certain size (of the order of 100 Å) would consist of a single domain. In such a particle magnetization proceeds entirely by rotation of the magnetic moment against forces due to anisotropy and magnetostrictive strains. Such a particle has a high coercivity: for a spherical particle of pure iron, it is 150 oersted and for acicular particles it is much higher. The interaction between particles in an aggregate reduces this figure, and Néel has suggested that the coercivity of a compacted powder could be expressed as

$$H_c = H_{c0}(1 - p)$$

where H_{c0} is the coercivity at infinite dilution and p the packing factor of the powder.

Dr. N. C. Tombs (G.E.C. Research Laboratories, Wembley) described the preparation of single-domain particles suitable for compacting into permanent magnets. Because of the interaction between compacted particles, the coercivities obtainable with spherical particles are not very high; a compact with a density of 4 would have a coercivity of only 72 oersteds. He had therefore tried to produce acicular particles, for which the theory predicts a coercivity of up to 500 oersteds even after compacting.

Very small particles of iron can be made by reducing ferrous formate or carbonate. Aggregates of such particles have coercivities larger than those predicted from the shapes of the particles; this suggests that the crystallites within the particles cannot be symmetrical. It is better, however, to start with acicular crystals of some iron compound, and to try to preserve their shape while the material is reduced to iron. A suitable starting material is hydrated iron oxide, $\alpha - Fe_2O_3.H_2O$, which can be prepared by passing a regulated stream of air through an aqueous solution of ferrous sulphate containing pieces of iron and maintained at a controlled temperature. The iron oxide is precipitated and can be collected by filtering. When Dr. Tombs first used this process the resulting crystals were not acicular, but later, for no apparent reason, acicular forms appeared and the earlier forms were not seen again. There are many organic compounds which can exist in two forms, of which only one at a time appears in any particular laboratory, but there are few inorganic compounds known to behave in this way. It is presumably a question of the presence of appropriate seed crystals.

X-ray examination of the iron-oxide powders suggested that the particles were, at this stage, single crystals. Electron micrographs show that when these acicular particles are reduced to iron (at carefully-controlled temperatures and in a regulated stream of dry hydrogen), the shape of the particles is gradually lost, and eventually a nodular mass of relatively symmetrical particles is obtained. Compacts of these particles have coercivities much smaller than those predicted for markedly acicular forms, but nevertheless high enough—about 200 oersteds—to be useful. The $(BH)_{max}$ product for these magnets is somewhat less than that for barium ferrite, but the ratio of B to H is so different in the two materials that they may both be found useful in particular applications.

In reply to Dr. Wohlfarth, Dr. Tombs said that the acicular form could be retained throughout the conversion of $\alpha - Fe_2O_3$ to Fe_3O_4 and to $\gamma - Fe_2O_3$, but the coercivity of the material so made, while high enough for sound-recording tapes, was too low for a permanent magnet.

Dr. McCaig suggested reduction in carbon monoxide or atomic hydrogen. Dr. Tombs said that carbon monoxide had been tried, but the results were not encouraging, perhaps because the gas had been impure; atomic hydrogen had not been tried, but would probably cause local overheating and consequent excessive crystal growth.

Dr. Hoselitz pointed out that some of the original oxide particles in Dr. Tombs's electron micrographs were well above the critical size for iron, and asked why such powders had been used. Dr. Tombs replied that the observed changes were similar whatever the initial size, and the process was more clearly shown in the pictures which he had chosen to illustrate his talk.

Mr. Rooksby emphasized the need to distinguish between crystals and particles, since the two were synonymous only in single-crystal particles.

THEORY OF SINGLE-DOMAIN PARTICLES

Dr. E. P. Wohlfarth (Imperial College of Science and Technology, London) then gave a theoretical account of the magnetic properties of aggregates of single-domain particles, including some recent developments in his own work.

As stated above, magnetization processes in these particles are opposed by the effects of magnetocrystalline anisotropy, strain, and shape effects. If shape anisotropy acts alone, for example, the theory for an aggregate of randomly-directed prolate ellipsoids leads to

$$H_c = 0{\cdot}479\,(N_1 - N_2)I_0$$

where H_c is the coercivity, N_1 and N_2 the demagnetizing factors for the prolate ellipsoid, and I_0 the saturation magnetization. This formula predicts a maximum value of about 5000 oersteds for the coercivity of an iron powder where there is no compacting. Similarly, magnetocrystalline anisotropy acting alone, in an aggregate in which the easy

directions for the various crystals are randomly directed, leads to

$$H_c = 0{\cdot}479\ (2K/I_0)$$

where K is the anisotropy constant. Powders of cobalt, as this formula would suggest, have coercivities of several thousand oersteds, and those of manganese bismuthide have even higher values.

A recent development is to allow for a distribution of particle shapes. A shape factor m is defined as the ratio of the major to the minor axis of a prolate ellipsoid. If all values of m are equally probable, the theory shows that those particles for which m is large will control the properties of the aggregate; if the distribution of m follows half a Gaussian curve with $m = 1$ (a sphere) as the most probable shape, then with a reasonable value of the standard deviation it is possible to arrive at the result $H_c/I_0 = 0{\cdot}5$ as obtained by Weil for a number of micropowders. (Because of the method of defining m, the half of the curve for which $m < 1$ has no physical meaning.) If instead of a continuous distribution there are two phases of different coercivities, the theory shows that the observed coercivity will be governed chiefly by that of the "softer" constituent. This result agrees with a more general statement made by Gerlach, but only approximately with the experimental results obtained by Meiklejohn.

Néel's formula for the effect of interaction of particles, already quoted, has been shown by Weil to hold for many (though not all) powders, which is surprising in view of the assumptions which were made in deducing it. Recent work has led to the more precise formula

$$H_c = H_{c0} - I_0(Ap + Bp^{5/3} + \ldots)$$

where $A, B, \ldots$ depend on the orientations and geometrical arrangement of the particles. Some recent experiments on iron oxide powders have also suggested that Néel's formula does not hold. Calculations have also been made of the variation of remanence with previously-applied field to be expected in γ-ferric oxide powders of (1) prolate spheroids all of one shape and randomly oriented, and (2) particles whose shape factors have a Gaussian distribution. The curve corresponding to the second case is shown in Fig. 5.

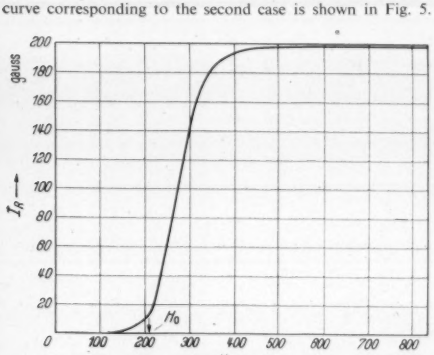

(Reproduced from *Research*)

Fig. 5. Remanent magnetization I_R as a function of previously applied field strength, H for non-acicular $\gamma - Fe_2O_3$ powders

It has all the characteristics needed in a good magnetic-recording tape: low remanence below a certain critical field (or, in the language of magnetic recording, low "print-through"), a rapid increase above the critical field (therefore high sensitivity), and linear increase above the critical field (or low distortion).

Finally Dr. Wohlfarth mentioned the study of haematite powders. Their variation of remanence with previously-applied field is important in the study of rock magnetism and calculations of such curves have been made. Dispersed haematite is one of the basic constituents of rocks and is unusual for a magnetic material in having a very low saturation magnetization ($I_0 \simeq 1$ gauss against 400 gauss for γ-ferric-oxide).

Other important effects which have an effect on the properties of micropowders are the dependence of the magnetization on the time interval between the application of the field and the measurement of the magnetization, and the change in the coercivity of the aggregate when the particles exceed the critical size. In the last effect it appears that the coercivity is inversely proportional to the size of the particles, but the theoretical work is difficult.

Dr. TOMBS doubted whether α-ferric-oxide was ferromagnetic. X-ray analysis showed that haematite had no small inclusions of ferrosoferric oxide, and as a consequence there should be no ferro- or ferri-magnetic phases present. He asked whether flake-shaped particles of a strongly paramagnetic material, such as the micaceous haematite, would produce an effect such as that observed. Dr. Wohlfarth thought that the shape of haematite particles could not produce any noticeable effect.

Dr. HOSELITZ asked whether the presence of a crystal boundary within a particle influenced the coercivity; Dr. Wohlfarth said that although this would certainly have an effect it had not as yet been studied. Dr. MCCAIG, who wanted to apply the theory to matrix-precipitated permanent magnets in which there is a mixture of hard and soft components, asked what value of saturation to use in the calculations; Dr. GORTER and Dr. STREET drew attention to Nesbitt's work on plate-shaped inclusions.

Dr. Wohlfarth emphasized that the results he had given applied only to particles so small that they contained no domain walls. The properties of particles containing a single wall were being studied, but no results were available yet.

NEUTRON DIFFRACTION

Dr. G. E. BACON (Atomic Energy Research Establishment, Harwell, Berks.) discussed the application of neutron diffraction in studies of magnetism, pointing out that these studies and the location of light atoms in crystals were the two main applications of the technique.[12] The work belongs entirely to the past ten years, and only three years ago it would have been possible to review the whole of it in a single lecture.

The main difficulty is the weakness of the available neutron beams. The nuclear pile provides neutrons having a Maxwellian distribution of energies, and a sufficiently monochromatic beam has to be selected from them; this process reduces the number of available neutrons from about a million per second leaving the collimator to about a million per minute reflected from the monochromator. This intensity is less by a factor of about 10^5 than those of the monochromatic beams used for X-ray diffraction. The peak of the energy distribution in the original beam corresponds to a wavelength of 1·7 Å.

In general the intensity of neutrons scattered from atomic nuclei varies irregularly with atomic number. But, superposed on the ordinary scattering, ferromagnetic and antiferromagnetic substances give diffracted beams from which the ordering of the atomic magnetic moments can be inferred. The detail of the pattern depends on the atomic positions and also on the magnitude and direction of the magnetic moments.

The first and most striking example of the use of neutron diffraction was in the detection of the structure associated with the antiferromagnetism of manganous oxide; the ordering of the magnetic moments in this material, and the relative directions of neighbouring ones, were shown. The detail of the structure is not uniquely determined, however, and alternatives have been put forward.

Ferrimagnetism has been demonstrated in many ferrites, and the inversed-spinel structure is made clear. The typical pattern for a ferrite is a few strong magnetic diffractions superposed on the nuclear ones; the two can be distinguished either by varying the temperature (with results as shown in Fig. 6) or by applying a magnetic field.

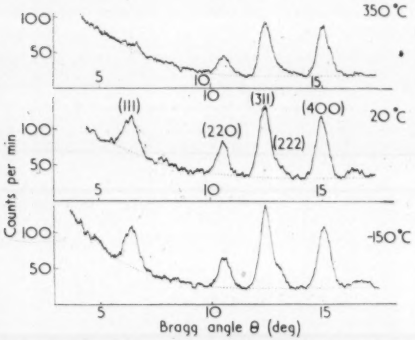

Fig. 6. Neutron diffraction patterns of $MgFe_2O_4$ above and below the Curie temperature

The possibility of ferrimagnetism or antiferromagnetism in the transition elements has been investigated. Chromium has thus been shown to be sometimes antiferromagnetic, but manganese (which would be particularly interesting) unfortunately gives a complicated pattern and the results seem to be anomalous. Neutron diffraction has also been used to study alloys, and is particularly useful here because it detects individual magnetic moments instead of averaging them (as does the ordinary measurement of saturation). Ordered and disordered forms of Ni_3Mn and Ni_3Fe have been studied.

The types of diffraction so far referred to are the result of elastic scattering. Neutrons are also liable to inelastic scattering, analogous to the diffuse scattering of X-rays but much more marked because the energy of a neutron is only 10^{-5} of that of an X-ray quantum of the same wavelength, and is thus of the same order as a quantum of thermal energy of the crystal lattice. This type of inelastic scattering occurs in all materials, but in magnetic materials there is a further effect detectable: the magnetic moments are disturbed by inelastic collisions, and "magnetic-spin waves" are propagated through the material. These waves can be detected by the further inelastic scattering which they cause. This scattering can be distinguished from other effects by the application of a magnetic field. The observed variation of field-sensitive scattering with angle has suggested that the outer electrons vibrate with three-quarters of the nuclear amplitude; it has not been reconciled with the collective-electron theory. Little work, however, has yet been done on inelastic scattering; more powerful neutron sources are desirable for it.

There remains enormous scope for the use of neutron diffraction in magnetic studies. The limit to it is set at present by the availability of neutron sources—and thus of nuclear piles—for experimental use. The nuclear pile is commonly regarded primarily as a source of power for generating electricity, but there are other and quite distinct uses for it which are unlikely to be fully developed until piles become available in private firms, universities, and research institutions.

In reply to Dr. GORTER, whose specimen of manganese chromite had given anomalous results when sent for neutron-diffraction tests, Dr. Bacon explained that most measurements are made with polycrystalline material, whereas single crystals are needed for unambiguous results. The patterns for a powder may be consistent with a suggested structure, but they cannot usually prove it to be the only possible structure. Subject to this limitation, the use of powder, or sintered masses, is justifiable; and Dr. TOMBS pointed out that single crystals of ferrites, if obtainable at all, could not be guaranteed to have the same composition as the polycrystalline material which is usually of practical interest at present.

A. C. LYNCH
J. WATKINS

REFERENCES

Some of the following references were quoted by the speakers; others, however, have been added by the present writers as a guide to further information.

(1) SNOEK, J. L. *J. Phys. Radium*, **12**, p. 229 (1951).
(2) NÉEL, L. *Ann. Phys.* [*Paris*], **3**, p. 137 (1948).
(3) KRAMERS, H. A. *Physica*, **1**, p. 182 (1934).
(4) ANDERSON, P. *Phys. Rev.*, **79**, p. 350 (1950).
(5) ROBERTS, F. F. *J. Phys. Radium*, **12**, p. 305 (1951).
(6) HOGAN, C. L. *B.S.T.J.*, **31**, p. 1 (1952).
(7) BOZORTH, R. M. *Ferromagnetism*, pp. 127–133, 497 (New York: D. Van Nostrand Co. Inc., 1951).
(8) BOOTH, A. D., and BOOTH, K. H. V. *Automatic Digital Calculators*, pp. 86, 97, 106, 124 (London: Butterworths Scientific Publications 1953).
(9) OLIVER, D. J., and SUCKSMITH, W. *Proc. Roy. Soc. A*, **219**, p. 1 (1953).
(10) NÉEL, L. *C.R. Acad. Sci.* [*Paris*], **224**, p. 1550 (1947).
(11) KITTEL, C. *Rev. Mod. Phys.*, **21**, p. 541 (1949).
(12) WILKINSON, M. K. *Amer. J. Phys.*, **22**, p. 263 (1954).

The tensile strength of coal

By C. D. Pomeroy, B.Sc., A.Inst.P., and W. T. A. Morgans, B.A., National Coal Board, Mining Research Establishment, Isleworth, Middlesex

[*Paper first received* 25 *January, and in final form* 1 *March*, 1956]

Apparatus is described which has been developed for the measurement of the tensile strength of coal by bending thin strips. Measurements on four coals show that the strength depends on the type of coal and on the direction of loading relative to the bedding planes.

One coal has been studied in some detail and the tensile strength is shown to decrease with increasing size of specimen. The effect is attributed to the increased probability of finding in larger specimens a weakness which imparts a low strength. It is estimated that for a given size of specimen the tensile strength is of the order of one-tenth of the compressive strength.

Further, it has been found possible to rejoin broken strips of this coal so that up to ten successive tensile tests can be performed on a single strip, thus enabling the distribution of the weaknesses to be studied. In general, there is an increment of strength between successive breakages, and after ten breaks the tensile strength is roughly double the value obtained at the first break. This method of studying distribution of strength does not appear to have been used previously, although it is likely to have applications to many other brittle materials.

No systematic measurement of the tensile strength of coal has previously been reported. This is not surprising, since any measurement must be made on regularly-shaped specimens and these are neither easily nor quickly produced. In consequence the "strength" of coal has been described mainly by empirical tests,[1–5] or at best by compression tests on cubes.[6–13] It is not immediately clear that there need be a close correlation between the tensile and compressive strengths of coal, which is far from homogeneous and is also permeated by cracks and other weaknesses. Large cracks may be so orientated as to make the tensile strength of a specimen very small, but the effect on compressive strength may not be so extreme since compressive loads may tend to close up cracks, thus reducing their effect on the strength. Consequently, it is important to obtain a measure of the tensile strength if coal is to be adequately described as a physical material.

Further, most practical methods of mining exploit the inherent weaknesses in a manner which produces tensile breakage. Examples are: (i) the wedge action of a plough, (ii) explosive breakage, and (iii) hydraulic bursting.

Despite the importance of tensile strength, practically no quantitative data on the subject are available and the apparatus which is described in this paper was developed as a first step towards remedying this omission. A technique is also described which enables repeated tensile tests to be carried out on the same sample, giving not only the initial tensile strength but also information on the distribution of weaknesses found in coal.

EXPERIMENTAL TECHNIQUE

The tensile strength was measured using a technique frequently adopted for brittle materials in which a specimen in the form of a long strip of rectangular cross-section is subjected to a gradually increasing bending moment. Application of simple beam theory enables the tensile strength to be estimated from the maximum bending moment sustained by the strip.

The tensile testing machine was designed to accommodate specimens with a minimum length of 4 in., a maximum width of 1·25 in. and a maximum thickness of 0·375 in. and to break specimens having a tensile strength of the order of 1 000 lb/in.[2]

Bending of the strips is achieved by means of four equal line loads applied perpendicularly to the length of the strip and symmetrically disposed with respect to its centre (i.e. the familiar four-point load system). The apparatus consists basically of a light steel beam *A*, Fig. 1, which pivots on a hardened steel knife-edge *B* placed at a point dividing the beam approximately in the ratio 1 : 2. The longer portion

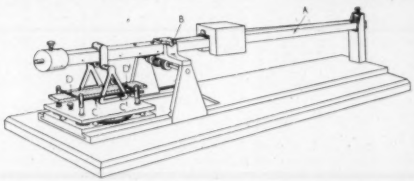

Fig. 1. Tensile testing apparatus (specimen shown shaded)

of the beam is graduated and carries a weight which can be driven slowly along the beam. A triangular saddle hangs freely from a ball-seating on the shorter arm, the lower end of the saddle carrying two parallel horizontal rollers CC^1, about 1·5 in. apart, lying perpendicular to the beam. To the base of the machine are fitted two more parallel horizontal rollers DD^1, 3·5 in. apart and symmetrically placed with respect to the triangular saddle. The height of these can be adjusted by means of a screw mechanism operating on both rollers simultaneously. The beam is constrained to move within a very small angle by means of a pair of stops placed at the end of the longer arm of the beam, the lower stop being a micro-switch forming part of the motor circuit.

By varying the mass of the travelling weight and the distance of the saddle from the knife-edge, several ranges of bending moment are obtainable, the maximum range being 0–6 lb in. and the minimum range 0–0·4 lb in., the sensitivity for each range being better than 0·2% of the maximum.

The strip of coal under test is placed in the saddle so that it rests on the two rollers CC^1 and passes under the two rollers DD^1. A steadily increasing bending moment is applied to the coal until failure occurs, at which point the beam

rotates through a small angle, contacts the micro-switch and stops the weight. From the distance moved by the weight, the maximum bending moment, and hence the maximum tensile stress sustained by the coal, is calculated.

In later experiments the saddle was fitted with a small optical extensometer indicating the vertical movement of the centre of the coal strip relative to the two inner rollers, and this is used to estimate Young's modulus for the coal. The results of these experiments will be published later.

PREPARATION OF SAMPLES

A lump of run-of-mine coal is cemented by plaster of Paris in a jig which can be rotated through a right-angle in both the horizontal and vertical planes. This enables rectangular blocks to be made by taking cuts with thin slitting wheels made of resin-bonded carborundum.

The smallest specimen obtainable depends largely on the degree of cracking in the coal so that the size range of specimens tested varied from one coal to another. The comparisons between coals are therefore complicated for it is known that the size of specimen affects the compressive strength of coal[11] and it is likely that a comparable relationship holds for tensile failure. This problem is considered in more detail later.

PRELIMINARY MEASUREMENTS

The initial measurements were made on four coals of very different type.

(i) Llandebie, an extremely hard anthracite. Coal Rank Code No. 100*a*.
(ii) Deep Duffryn, a fairly strong Welsh steam coal. Coal Rank Code No. 201.
(iii) Cwm "Mildred," a very friable Welsh coking coal. Coal Rank Code No. 301.
(iv) Barnsley Hards, a hard coal of low rank. Coal Rank Code No. 801.

Of these the Barnsley coal could be machined accurately to thicknesses less than 0·1 in. with considerable success but the other coals presented serious machining difficulties. The anthracite was hard and strong over much of its volume but it contained frequent flaws across which the tensile strength was virtually zero. The steam and coking coals were much weaker than the others, with weaknesses which permeated the general structure of the material. This made sample preparation extremely difficult at thicknesses of less than 0·375 in. for the most friable of the coals and even at this size strips broke very easily during handling.

For each coal two series of strips were cut with the bedding planes parallel and at right angles to the longitudinal axis respectively. In the former case the bedding planes lay parallel to the greatest surface of the strip. The results of the measurements are given in Table 1. (For purposes of comparison, typical values of the compressive strength of 1 in. cubes of the same coals are also given.)

These measurements were not made in sufficient numbers for useful estimates of the standard deviation to be made, and since the size of specimen was not constant, the results are not strictly comparable. However, the differences in strength between the various coals are so large that it is unlikely that the conclusions will be affected.

There is strong evidence that the effects of the bedding plane directions are different for Barnsley Hards than for both the anthracite and the Deep Duffryn steam coal. Barnsley Hards is weaker when the bedding planes are at right angles to the length of the specimen, whereas the other coals are weaker when these planes are parallel to the longitudinal axis.

A comparable difference between these coals has been observed in compression tests on cubes.[14] Barnsley Hards is stronger when the bedding planes are at right angles to the direction of loading, whereas anthracite is stronger when the bedding planes are parallel to that direction. There was no statistically-significant difference in the compressive strengths of the Deep Duffryn coal. If a compressive stress is regarded as setting up tensile stresses in a direction at right angles to the compressive stress, it can be seen that the behaviour of these coals in tension and compression is self-consistent.

SUCCESSIVE MEASUREMENTS ON A SINGLE SPECIMEN

Strips of Barnsley Hards cut at right angles to the bedding planes frequently broke along a visible discontinuity, for example, along a major crack or a fusain band, whilst the remainder of the strip appeared more uniformly strong. In order to measure the strength distribution along these strips the breaks were mended with Durofix, the strips being later retested so that breakage was effected at the second weakest part of the strip. These further breaks were rejoined and in this way successive strength measurements were made on each strip until five breaks had been made at distinct points along their lengths.

The results of these tests are given in Table 2, each mean value being based on eight specimens. The mean strength increases with the number of breaks, the significance of the increase between consecutive breaks being indicated by the paired *t* test.[15]

After the fifth break the joints were found to be unreliable, and alternative adhesives were tried. Of these Araldite 103 was found most satisfactory and further measurements using this adhesive are described later.

Table 1. *Measurements on various coals*

Coal	*Volatiles %*	*Size of specimen (approx.) (in.)*	*Tensile strength (lb/in.²)*		*Mean compressive strength (lb/in.²) of 1 in. cube*	
			Across bedding planes	*Along bedding planes*	*Across bedding planes*	*Along bedding planes*
Llandebie anthracite	7·5	$4 \times \frac{1}{4} \times \frac{1}{4}$	880 (6)	360 (8)	3600	5000
Deep Duffryn steam coal	13	$4 \times 1 \times \frac{3}{8}$	170 (6)	80 (7)	2200	1800
Cwm Mildred coking coal	25	$4 \times \frac{3}{4} \times \frac{3}{8}$	—	30 (6)	1000	1000
Barnsley Hards	40	$4 \times 1 \times \frac{1}{4}$	70 (15)	—	8100	5100
		$4 \times 1 \times \frac{1}{10}$	—	820 (20)	—	—

The numbers of samples tested for each mean quoted are given in brackets.

Table 2. *Successive breakage of strips of Barnsley Hards*

(Bedding planes at right angles to the longitudinal axis)

Break number	*Mean tensile strength* (lb/in.²)	*Standard error* (lb/in.²)
1	71	±11
2	132	±11
3	144	±11
4	163	±11
5	158	±14

t_{ij} is the value of Student's t derived from a paired t test of the significance of the difference between the ith and jth breaks.

$$t_{12} = 3{\cdot}29^{*}$$
$$t_{23} = 1{\cdot}29$$
$$t_{34} = 2{\cdot}06$$
$$t_{45} = -0{\cdot}30$$
$$t_{24} = 3{\cdot}51^{*}$$

* Significant at the 1% level.

DETAILED MEASUREMENTS OF REPEATED BREAKAGE

Strips of the same thickness but of six different widths were cut from the same lump of Barnsley Hards, the bedding planes lying parallel to the longitudinal axis. The strips were broken and repaired consecutively until each strip had undergone up to ten distinct breaks. In practice, it was not always possible to measure the strength ten times. This was particularly so for the smaller specimens since on breakage they frequently fell from the saddle of the apparatus and shattered beyond repair. This affected the mean strengths quite appreciably in some instances and consequently the results are given in two ways. In Table 3 the means of all the measurements are given, together with the number of results included in each mean value. In Fig. 2 the increase in strength with break number is shown for only those strips which were broken the full ten times. Paired t tests[15] show that in the majority of cases there was a statistically-significant increase in strength between two successive breakages on strips of the same size.

It will be seen that the tensile strength of the strips after they had been repaired nine times was, on average, almost double the initial value and, of greater importance, the strength was still increasing with little evidence of a steady value being reached.

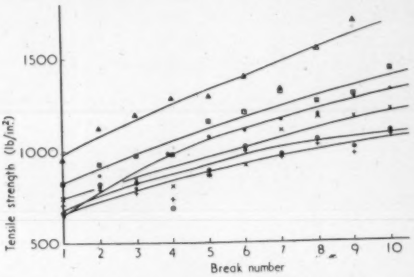

Fig. 2. Successive tensile measurements on strips of Barnsley Hards

Width of strips

△ = 0·09 in. ● = 0·58 in.
□ = 0·25 in. ○ = 0·92 in.
× = 0·41 in. + = 1·25 in.

Although there was considerable variation between nominally similar strips, there was a significant relationship between the strength and the size of the strips and this persisted even after the ninth and tenth breakages (Fig. 3).

It was suspected that the large increase in strength with decreasing size of specimen might be due to faulty sampling. Since more small samples were broken than large ones during their manufacture it is possible that the weakest of the small strips were rejected even before they were brought to test, only those samples which were unrepresentatively strong being tested and so giving an elevated mean strength.

Table 3. *Successive tensile breakage of strips of Barnsley Hards (all results)*

(Bedding planes parallel to the longitudinal axis)

Width (in.)	*Tensile strength* (lb/in.²) *Break* 1	2	3	4	5	6	7	8	9	10
0·090	1020	1230	1180	1320	1380	1400	1470	1540	1720	2050
	(23)	(20)	(14)	(11)	(11)	(10)	(9)	(7)	(6)	(3)
0·245	830	950	910	980	1150	1200	1320	1280	1320	1460
	(22)	(20)	(16)	(14)	(12)	(12)	(11)	(11)	(11)	(11)
0·415	760	850	870	800	860	1000	1160	1240	1200	1250
	(29)	(29)	(27)	(27)	(25)	(23)	(23)	(23)	(22)	(22)
0·582	680	870	820	990	1050	1110	1190	1240	1300	1340
	(24)	(22)	(22)	(22)	(22)	(22)	(22)	(21)	(20)	(19)
0·914	630	800	820	690	900	1020	1000	1060	1020	1120
	(23)	(20)	(19)	(19)	(18)	(18)	(18)	(18)	(17)	(17)
1·255	690	790	760	730	870	1010	980	1040	980	1090
	(8)	(6)	(6)	(6)	(6)	(6)	(6)	(6)	(6)	(6)

The number of measurements used for each average value quoted is given in brackets.

***

If, however, coal were to consist of a relatively homogeneous basic material which contains a small number of visible discontinuities, it is conceivable that a specimen would have a low tensile strength until all of these discontinuities were eliminated and would then have an approximately constant

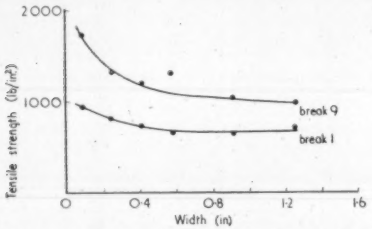

Fig. 3. Graph showing the relationship between tensile strength and width for specimens of Barnsley Hards

and a higher strength. This would be reached more quickly for the small specimens since these are likely to contain fewer gross weaknesses and, further, the most cracked of these specimens are likely to have been broken during manufacture and rejected. In fact, no such constant strength has been observed (Fig. 2) and there is, in general, an increment in strength between successive breaks for all sizes of specimen and, moreover, the most rapid increase in strength is recorded for the smallest sizes.

It is likely, therefore, that coal is ramified with weaknesses of various magnitudes so that once the largest has been eliminated the next largest confers only slightly greater strength and so on. Further, a large specimen is more likely to contain a gross weakness than a small one and so have a lower strength. This will be true of the second, third, fourth breaks and so on, so that the smaller strips will always tend to be stronger even when they have been tested many times. Ultimately the strength of the samples must converge to some maximum which is independent of the size of the sample, but there is no evidence of this happening during the ten successive measurements made on each strip in the experiment.

CONCLUSIONS

These experiments have shown wide differences in the tensile strengths of various coals, the differences being more marked than the comparable differences in the compressive strengths of the same coals.

It is extremely difficult to define a "tensile strength of coal" since any measurement is dependent primarily on the most acute weakness, and this implies that the strength is dependent also on the size of the specimen. Moreover, the scatter of the measurements is large even for nominally similar strips of the same coal. Consequently a very large number of measurements is essential if the coal is to be adequately described.

A technique of repairing broken specimens, which enables about ten successive breaks to be made on individual samples, has helped to overcome this difficulty. The measurements have tended to show that the Barnsley Hards used in these experiments does not consist of homogeneous coal interspersed with a few major weaknesses, but contains weaknesses which are of various magnitudes such that once the largest is eliminated the second largest, on average, confers only slightly greater strength, and so on. There is no evidence of a critical weakness frequency in this coal, such as might be anticipated if the vertical family of cracks ("cleats") occurred at roughly constant intervals. The results suggest that visible cracks such as these are merely the upper limit of the weaknesses and situated between them there may be cracks which are not visible but which, nevertheless, impart a wide range of strength, even down virtually to zero.

ACKNOWLEDGEMENTS

The success of this work depended to a large extent on the skill with which Mr. C. L. Rogers produced the strips of coal, and on the patience of Mr. P. Jarman and Mr. D. Hobbs who repaired the breaks and made many of the measurements.

This paper forms part of the programme of research of the Mining Research Establishment and is published by permission of Dr. W. Idris Jones, Director-General of Research in the Scientific Department of the National Coal Board. The views expressed are those of the authors, and not necessarily those of the Board.

REFERENCES

(1) NICHOLLS, J. H. H. *Canad. Dept. Mines, Investigation of Fuels and Fuel Testing Bull.*, No. 644, p. 20 (1924).

(2) PROTODYAKONOV, M. M. *Ugol*, **25**, p. 20 (1950); *Izv. Akad. Nauk. SSSR, Otdel. Tekh. Nauk*, No. 2, p. 283 (1953).

(3) WUERKER, R. G. *Min. Engng, N.Y.*, **5**, p. 1108 (1953).

(4) GURUSWAMY, S. *J. Sci. Industr. Res. B*, **11**, p. 482 (1952); **10**, p. 304 (1951).

(5) BROWN, R. L. *Fuel*, **27**, p. 82 (1948).

(6) HEYWOOD, H. *J. Inst. Fuel*, **9**, p. 94 (1935); *Coll. Guardian*, **151**, pp. 898, 941 (1935).

(7) TALBOT, A. N. *Year Book Illinois State Geol. Survey, Bull.*, No. 4, p. 199 (1906).

(8) DANIELS, J., and MOORE, L. D. *Engng Min. J.*, **84**, p. 263 (1907).

(9) RICE, G. S. *U.S. Bureau of Mines Bull.*, No. 303 (1929).

(10) PENMAN, D. *Coll. Guardian*, **143**, p. 700 (1931).

(11) MILLARD, D. J., NEWMAN, P. C., and PHILLIPS, J. W. *Proc. Phys. Soc. [London] B*, **68**, p. 723 (1955).

(12) LAWALL, C. S., and HOLLAND, C. T. *West Virginia Univ. Engng Exp. Res. Sta. Bull.*, No. 17 (1937).

(13) PULKRABEK, J. *Mitt. Kohlenforsch Inst. Prag.*, **3**, p. 155 (1937).

(14) POMEROY, C. D. Unpublished work.

(15) WEATHERBURN, C. E. *A First Course in Mathematical Statistics*, p. 186 (London: Cambridge University Press, 1949).

Apparatus and techniques for the application of a water flow system to the study of aerodynamic systems

By E. F. WINTER, B.Sc., and J. H. DETERDING, M.A., "Shell" Research Ltd., Thornton Research Centre, Chester

[*Paper first received* 21 *November*, 1955, *and in final form* 8 *February*, 1956]

The study of fluid flow in such gaseous systems as combustion chambers and furnaces is of value in the design and subsequent operation of the equipment. Useful information may be obtained from flow visualization in these systems under constant density conditions, even though in practice considerable density changes occur. Hydraulic models are then found to have distinct advantages over air models.

Apparatus has been developed by means of which the flow of water may be studied in transparent models of the simulated air systems. The flow is rendered visible by plastic tracers, of similar density to water, which are illuminated by continuous filament lamps, long-duration electronic flash lamps or vapour discharge lamps, according to the information required. Selected parts of the flow field may be observed by means of a narrow, flat beam of light directed through the appropriate section of the model. Semi-quantitative records of flow components may be derived from photographs obtained with the flash illumination. Individual tracers may be observed by selective illumination involving an ultra-violet light source and fluorescent tracers.

The subject is treated from a wholly practical point of view. Details of the apparatus and techniques are given, with examples of some of the types of information obtainable, and the elementary requirements for similarity with aerodynamic systems are stated.

INTRODUCTION

In the design and operation of equipment involving the flow of gases, the aerodynamic factors are often of major importance and a detailed study of the behaviour of the fluid is useful. The particular field with which the authors have been concerned is that of systems for continuous combustion in, for example, gas turbines and boilers, where the aerodynamic conditions are often critical in determining the performance of the system.

In this type of equipment, studies of flow in the presence of flame are somewhat difficult to carry out. Investigations by one of the authors, however, which are outside the scope of the present paper, have shown that in typical practical combustion systems the flow pattern without combustion is usually very closely related to that occurring under normal operating conditions. It is therefore possible to obtain useful information from a study of the "cold" flow conditions only.

Flow patterns may be observed, of course, in actual combustion chambers in which cold air provides the working fluid. Several techniques have been developed for the observation of the flow in such a system, notably by the use of various types of Pitot instrument, or by the "freezing" of cotton filaments treated with quick-drying lacquers; but those applicable to highly turbulent flow are generally rather time-consuming or suffer other disadvantages. On the other hand, direct flow visualization in a hydraulic model by means of visible tracers is generally a simpler and more convenient procedure and may be expected to give adequate agreement with the cold flow case, where no thermal gradients exist, provided that the conditions of physical similarity are met. This method possesses several advantages over both the "indirect" techniques (e.g. Pitot probing) and the application of direct visualization in an actual gas flow. These advantages may be summarized as follows:

(*a*) *Advantages of direct visualization*

(i) Simultaneous observation of the whole flow field is possible, therefore local details are noted which might be missed by other methods.

(ii) Observations are made at the time that the flow pattern exists, so that the time delay is reduced between successive observations of a system undergoing modification.

(iii) The obstructions to flow which result from the use of probing instruments are eliminated.

(*b*) *Advantages of the water flow method for the simulation of gas flows*

(i) Similarity at a given linear scale is obtainable at much lower velocities in water than in gas, so that observation and recording are facilitated.

(ii) It is possible to provide tracers of a density similar to that of the fluid, so that a high degree of accuracy is possible with tracers of a convenient size for observation.

(iii) The optical clarity through a transparent model is generally greater in water than in air.

This paper describes the construction at Thornton Research Centre of a hydraulic model apparatus and associated equipment for the study of flow in combustion systems. The techniques employed for the visualization and recording of flow phenomena are described in detail and the exactness of the similarity is discussed. The paper is written entirely from a practical point of view, with the intention of demonstrating the means by which this extremely useful method of flow visualization may be adapted to yield both qualitative and quantitative results. The system described is the result of considerable development, and it is hoped that the practical details given will be of value to other investigators who may wish to apply the method to their own problems.

DESCRIPTION OF HYDRAULIC SYSTEM

The apparatus installed at Thornton for water model studies (Fig. 1) is arranged as a continuous-flow, closed-circuit system, motivated by a centrifugal pump of 24 000 gal/h rated capacity at 15 lb/in.^{2} gauge. Since the loss of head through the models is usually rather small compared with the head available, the maximum flow rate in fact obtainable is of the order of 30 000 gal/h. Ducting of 6 in. diameter galvanized steel conveys the water, *via* a bronze Venturi meter with static pressure tappings and a bronze sluice-type control valve, to the model section. Provision is made for separately metering the flow, if necessary, to different parts of the model under test and the individual ducts at this point

are provided with butterfly-type valves and with velocity-head measuring probes calibrated for mass flow measurement. Inverted water U-tubes are used to indicate the meter pressures, those for the velocity-head meters being of the inclined type for greater accuracy.

The Perspex models are mounted horizontally and are immersed externally in a water-filled, rectangular, glass-walled tank. The tank is essential to prevent optical distortion when models with curved or non-vertical walls are being viewed and also eliminates the problem of condensation on the outside of the models.

From the model, the water flows through a single 6 in. diameter brass duct into an elevated cylindrical tank, which has virtually a free liquid surface and from which the inlet to the pump is fed. The inlet to this tank is eccentric to the cylindrical axis so as to provide a swirling motion and thereby effect adequate mixing of the water with any solid tracers which may be circulating. This tank, which forms a convenient place for the addition of solid tracing material, has superseded an open rectangular tank used in an early version of the apparatus. When the original tank was used, difficulty was experienced in maintaining a uniform dispersion of solid tracers in the circulating water, owing to a tendency for the particles to settle in the more stagnant parts of the tank. This difficulty has been completely overcome by the cylindrical tank with a tangential entry, shown in Fig. 1. The continuous mixing which occurs in this tank ensures a remarkably uniform concentration of tracers in the model.

The cylindrical tank has also overcome the difficulties associated with the inevitable introduction of gas bubbles into the system when fresh water is introduced. A supply of softened mains water is used which, when introduced into the system, normally contains an appreciable quantity of dissolved gases. During circulation, the water undergoes pressure changes which result in the release of gas bubbles upstream of the model, for example at the Venturi meter, at the valves and at bends and changes of section. The water also picks up any air which is not displaced from the system and carries it into the model as a dispersion of bubbles. The presence of such bubbles can render the water opaque and prevent the projection of a straight beam of light through the model. When the original open tank was used, it was found that the arrangement contributed appreciably to the problems of bubble evolution owing to the entrainment of air at the very turbulent surface of the water in the tank. In the present cylindrical tank, the undesirable entrainment of air into the system is prevented by the presence of an immersed plate, shown in Fig. 1. This plate ensures that there is substantially no direct contact in this tank between the circulating water and the air above it, and therefore entrainment of air is prevented. In particular, since a swirling motion is employed for assisting the tracer distribution, care has been exercised to exclude air from the core of the vortex at high rates of flow. The elevated position of the tank, together with air vents at the highest points in the Venturi line, assists the evacuation of air from the system when fresh water is introduced. The tank also acts as an outlet for gases released in the system if the water is circulated for a few minutes at a low rate of flow, e.g. about 1000 gal/h; at this condition a large pressure drop at the main valve encourages bubble evolution and the swirl in the tank is insufficient to prevent the rise of the bubbles to the surface. Twenty minutes has been found to be an adequate period for the substantial elimination of troublesome gas bubbles after the system has been newly filled. A few ounces of Teepol in the circulating water assists the dispersion of bubbles from the walls of the system. The inside surfaces of the models are also normally wetted with Teepol before the system is filled with water.

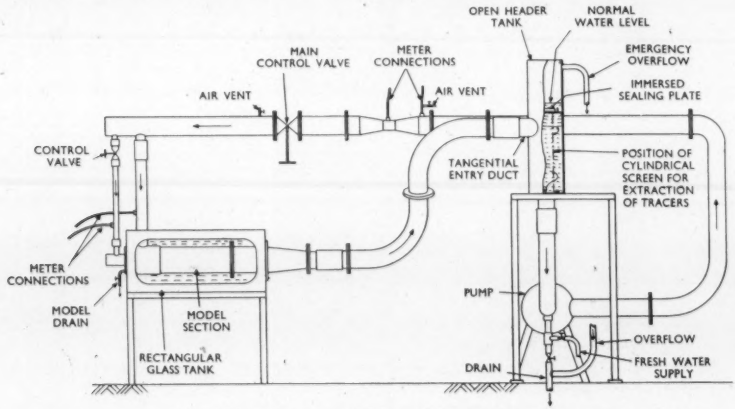

Fig. 1. Thornton hydraulic flow apparatus

A cylindrical gauze screen can be inserted into the tank for preventing the continued circulation of solid tracers; this is held in place over the outlet from the tank by the weight of the immersed plate and its position is indicated in Fig. 1.

If necessary, solid tracers circulating with the water may be selectively screened from either of the two feed lines normally used with the model by means of a gauze screen, arranged as a flap valve at the junction of these lines (Fig. 2).

The softened water used in the apparatus is normally slightly alkaline (pH 7·6) and contains small amounts of

various impurities including sulphates, calcium carbonate and chlorides. This water has exhibited a corrosive action on certain metals, notably aluminium and magnesium metals and alloys, resulting not only in the deterioration of items made in these materials, but also in the dispersion of the corrosion products in the water and consequent increase of the opacity.

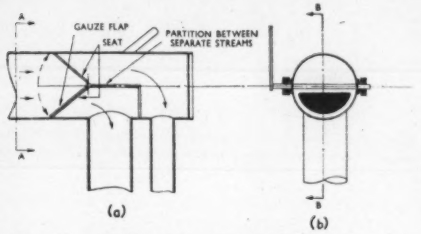

Fig. 2. Arrangement for selective screening of solid tracers from the water stream

(*a*) View on *BB*.
(*b*) View on *AA*.

On a few occasions some electrolytic action has also been observed between adjacent dissimilar metals at the model entry. A satisfactory solution has been reached by the use of brass for most of the non-transparent parts of the apparatus, except for some of the heavier ducting, which is in galvanized steel. Slight deterioration of the water occurs, but the increasing cloudiness presents no problem over a period of several days. Changing the water twice a week suffices to maintain adequate clarity at the model.

The observation section, situated within the rectangular glass tank, is occupied either by a Perspex model of an actual combustion system or by one of two simple Perspex "tunnels" in which experimental configurations of air directors may be mounted. One of these tunnels takes the form of an 8 in. diameter cylinder, in which complete three-dimensional air directors are tested, while the other is of rectangular section, measuring $8 \times 2 \times 8$ in. long, into which two-dimensional models can be fitted.

TRACERS FOR FLOW VISUALIZATION

For the observation of flow by the methods to be described, it is necessary for the fluid to carry with it a visible tracing material. Ideally, the tracers should comply with the following specification:

(*a*) they should remain as discrete bodies;
(*b*) they should have the same specific gravity as the fluid;
(*c*) they should be of spherical shape;
(*d*) they should be sufficiently small to follow the flow in fairly fine detail while being sufficiently large for satisfactory observation;
(*e*) they should possess the optical property of high proportional reflexion or re-radiation of light normal to the incident beam.

Air bubbles provide a simple means of indicating the flow pattern and have been used widely in previous work of this kind (for example, by Howes and Philip[1]). They suffer, however, from several disadvantages. Optically, air bubbles in water are unsatisfactory in that a considerable proportion of the incident light striking such a bubble is only slightly deflected and the proportion which emanates from the bubble in directions normal to the incident beam is rather low. Some improvement in this condition occurs along surfaces inclined at an angle of 20° or more to the normal, but the distorted view of a flow pattern obtained at such an angle of observation may not always be acceptable. A more serious failing of air bubbles is that, dynamically, they cannot be expected to give more than a very rough idea of the flow pattern in a system in which mass accelerations are of a high order, especially when the fluid velocities are of a rather low order. The relative buoyancy of the air bubbles causes their levitation to the regions of lower pressure, so that they tend to move, for example, to the axis of a rotating system. It has, moreover, been found difficult to produce continuously a dispersed stream of air bubbles of a suitable size for visualization, without also introducing a high proportion of very small bubbles, which contribute to a general scattering of the illumination with consequent obscuration of the flow pattern. A certain amount of the air introduced in this way also goes into solution in the water and causes the evolution of clouds of very fine bubbles as the water recirculates, resulting again in some optical obscuration. Air bubbles have therefore found a very limited use in the present apparatus, but there have, nevertheless, been a few exceptional cases when they could be employed with adequate accuracy and even showed advantages over other tracers. An investigation of the spread of an initially straight, highly turbulent jet was an example where tracing by fine air bubbles was completely effective.

Solid tracers which have been used or proposed for use in hydraulic models include aluminium,[1,2,3] treated sawdust, iron ore and Bakelite.[4] With the exception of some sawdusts these materials introduce gravitational errors in tracing flow paths. Moreover, with the exception of specially prepared aluminium, these materials are not readily observed by reflected light and are therefore not suitable when a selected section of a general flow is required to be observed.

In addition to the solid substances mentioned above, a number of plastic materials have been developed which have suitable properties for use as flow tracers. Various hydrocarbon polymers such as polystyrene, polyethylene and polyisobutylene were considered for the present work. Spherical pellets of these materials are obtainable and it has been found that the polystyrene spheres are generally suitable. The specific gravity of pure polystyrene is a little above unity, but the spheres obtained for this work were not completely homogeneous and the fortuitous inclusion of minute gas bubbles resulted in the overall specific gravity of the particles being spread over a narrow range from slightly below to slightly above unity. Actual measured values for particles selected at random varied from 0·93 to 1·053, the majority being between 0·98 and 1·02. The deviation from unity is considered to be sufficiently small for the consequent deviation of the tracers from the flow paths of the water to be insignificant in many of the models which have been studied. When greater accuracy has been desired, the particles in the specific gravity range 0·98–1·02 have been separated by flotation in suitable liquid blends and used exclusively. Apart from this, it has not been considered necessary to attempt to match accurately the densities of the fluid and tracers used, but methods of achieving this have been used successfully by Roberson,[5] who has used salt water adjusted to the density of fairly pure polystyrene and by Werlé,[6] who has mentioned the treatment of polystyrene with acetone to reduce the density.

Polystyrene varies in its degree of transparency depending

on its purity and texture. The particles which have been used successfully as tracers had a high degree of opacity and were white in appearance. When this type of particle is illuminated, a fairly high proportion of the light emerges normal to the incident beam and the particles may be seen very clearly in this direction.

This material has the additional advantage over some of the alternative tracing materials (e.g. aluminium) of immunity from chemical attack by the water or by the impurities which may be contained in the water.

For use in the model investigations, solid tracers of good sphericity and of a limited size range are required. Polystyrene particles of suitable size were selected from the random batches obtained by means of wire gauze sieves. The particles which have been used in this work have generally been between 0·4 and 1 mm in diameter. Particles of poor sphericity were eliminated by means of a simple sorting device, in which the particles were bounced, in rapid succession, from an inclined chute along a narrow horizontal plane, from which the non-spherical particles deviated before reaching a collecting tray at the far end.

Some consideration has also been given to white waxes, which can be raised in density by means of suitable fillers, and which then have the desirable properties for use as tracers possessed by polystyrene. A successful technique for producing solid wax spheres of the required size would, however, be required. Molten wax spray techniques produce hollow particles, which therefore cannot be controlled in respect of their specific weight.

Almost all the work carried out on the present apparatus has been done with the polystyrene tracers, illuminated by either the tungsten filament lamp or the electronic flash tubes described later. In addition, it has been necessary, for certain types of work, to provide fluorescent tracers which can be used in conjunction with the ultra-violet lighting, which will also be described, for the selective photography of individual tracers. For this purpose, solid tracers have been coated with G.E.C. luminescent powder type E (yellow), with the aid of I.C.I. luminescent paint medium No. 123–537. Polystyrene particles have again been used, since they are readily available in a suitable form and take the coating satisfactorily.

EQUIPMENT FOR ILLUMINATION AND PHOTOGRAPHY OF FLOW SYSTEMS

It has been found necessary to design and construct equipment for studying the flow by direct observation and also for recording the details photographically. The equipment developed for the illumination of the flow field is based on that used by Howes and Philip[1] and provides a choice of a continuous filament light source or an electronic flash unit. In addition provision is made for the use of an ultra-violet light source for special observations requiring the selective illumination of tracers.

Continuous lighting. The lighting unit for continuous illumination consists of a 230 V, 2 kW tubular line filament projection lamp by Edison Swan Electric Co. Ltd. This lamp has a diameter of 3½ in. and an approximate overall length of 17 in. with an 8 in. long coiled filament supported in a straight line within the glass tubular bulb.

The lamp is held in an adjustable carrier, which is positively located in a lamp housing by means of cone and V-groove positioning devices and a single screw retainer. It has been found unnecessary to provide any optical equipment for rendering the light beam parallel; a satisfactory beam is obtained by projection through a pair of adjustable apertures. Once the lamp and carrier have been adjusted in relation to the apertures on the housing no further adjustment is normally required after subsequent removal from the housing. The design of this lamp housing incorporates a cooling fan which operates whenever the mains supply to the lamp is switched on. The housing is provided with terminal plugs for the connexion of the mains (and alternatively for the extra high tension supply for the flash tubes, see below).

Sliding tubular members are used for the carriage of the air-cooled lamp house. The latter is normally mounted beneath the model tank for the projection of a beam of light vertically through the tank, although provision is made for transferring the complete carriage assembly to the vertical part of the frame (Fig. 3) for the horizontal projection of the light beam if this should become necessary.

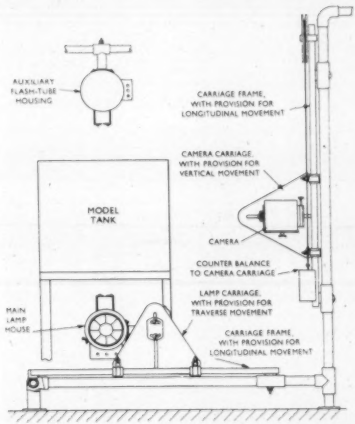
AUXILIARY FLASH-TUBE HOUSING
CARRIAGE FRAME WITH PROVISION FOR LONGITUDINAL MOVEMENT
CAMERA CARRIAGE WITH PROVISION FOR VERTICAL MOVEMENT
MODEL TANK
CAMERA
COUNTER BALANCE TO CAMERA CARRIAGE
LAMP CARRIAGE WITH PROVISION FOR TRAVERSE MOVEMENT
MAIN LAMP HOUSE
CARRIAGE FRAME WITH PROVISION FOR LONGITUDINAL MOVEMENT

Fig. 3. Arrangement of optical equipment

The power supply for the filament lamp is controlled by means of a Variac controller, which permits the lamp to be under-run during most of the visual and setting up operations, thus materially lengthening the life of the filament and increasing the reliability of the equipment.

Flash illumination. The lighting units for providing the flash type of illumination consist of a pair of linear quartz flash tubes (type LSD 17 by Mullard Ltd.). These tubes have an effective length similar to that of the filament lamp, and each tube will discharge up to 1000 J per flash if required, giving a peak light output of 100 Mlm; the electronic circuit built for use with these tubes actually provides about 700 J. The two tubes are arranged to flash consecutively from opposite sides of the model tank. A single tube has been found inadequate for providing reasonably constant illumination of the flow across the larger models used (i.e. models of about 8 in. depth).

One flash tube is mounted beneath the model in the same housing as is used for the filament lamp. The second tube is mounted above the model tank in a housing similar to the first except for the omission of the cooling fan. It is considerably lighter in weight than the air-cooled housing and is supported simply from tubular a single member. In

conjunction with the flash tubes a simple optical system is used, for the sole purpose of increasing the proportion of light emitted through the slits, which consists of a cylindrical mirror of polished steel and a cylindrical plastic lens mounted on the tube carrier. The gain resulting from this system is estimated as between 20 and 50%, mainly due to the use of the lens.

The use of two flash tubes for the illumination of a common section through the model involves considerable care in the positioning of the lamp housings. It is necessary for the tubes to be correctly alined relative to the apertures of the lamp housings and to each other so that they illuminate the same section of the model. When the tungsten lamp is used, of course, the position of the beam may easily be adjusted by visual observation. The flash duration is too short for this method to be employed for the general alinement of the tubes, although it is just possible to observe the position at which the beam intersects an opaque section of the model, as a check on the position of that part of the beam. The method employed for initially setting the beam position has been to use a straight steel rule passing through the apertures and to aline the tube and slots with the rule held vertically. By means of a source of continuous illumination within the lamphouse, the lamp assembly could then be adjusted to bring the slots into line with the requisite section when observed through the model. The horizontal rails carrying the two lamp housings have thus been calibrated to show the positions of alinement for different vertical sections through the model. Once carried out, the adjustments could be regarded as permanent, needing only a brief check of the point of intersection of the flash on each new model mounted in the system.

Power supply for high intensity flash tubes. The power circuit for the flash tubes is a specially built system which allows a choice of flash durations over a suitable range. A duration of about 5 ms has proved suitable for most of the model work carried out. Fig. 4 shows the power supply, control and safety circuits for the operation of the flash tubes.

The flash occurs when the condenser C_2, charged to about 2·5 kV, is discharged through the tube. The anode of the tube is earthed, and the discharge is initiated when a high

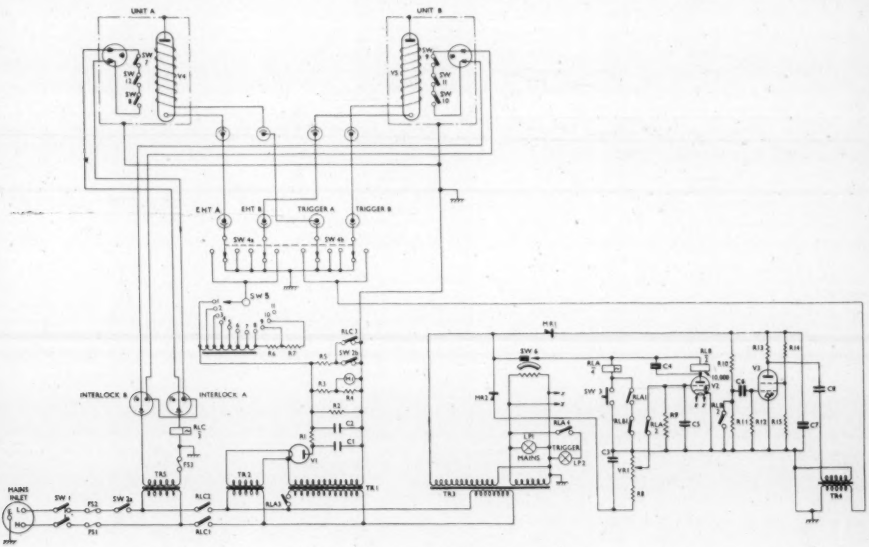

Fig. 4. High intensity flash tube circuit

R_1 = 10 kΩ w.w., 20 W
R_2 = 3 MΩ (3 × 1 MΩ carbon, 2 W series)
R_3 = 37·7 MΩ (5 × 6·8 MΩ + 2·2 MΩ + 1·5 MΩ carbon, 1 W series)
R_4 = 560 kΩ h.s. carbon, 1 W
R_5 = 1·57 kΩ (3 × 4·7 kΩ carbon, 2 W parallel)
R_6 = 12·5 Ω (2 × 25 Ω w.w., 20 W parallel)
R_7 = 23·5 Ω Nichrome strip
R_8 = 47 kΩ carbon, 1 W
R_9 = 4·7 MΩ h.s. carbon, 1 W
R_{10} = 220 kΩ carbon, ½ W
R_{11} = 100 kΩ carbon, ½ W
R_{12}, R_{13} = 220 kΩ carbon, ½ W
R_{14} = 100 kΩ carbon, ½ W
R_{15} = 22 kΩ carbon, ½ W

C_1 = 1 μF, 5 kV
C_2 = 8 × 28 μF, 2·5 kV TCC Hikonel
C_3 = 2 μF, 350 V
C_4 = 0·5 μF, 350 V
C_5 = 2 μF, 350 V
C_6 = 0·5 μF, 350 V
C_7 = 2 μF, 350 V
C_8 = 8 μF, 350 V

V_1 = U27
V_2 = GDT 4b
V_3 = NSP 1
V_4, V_5 = LSD 17

TR_1 = 250 V, 50 c/s primary: 1800 V secondary
TR_2 = 250 V, 50 c/s primary: 4 V, 1 A secondary*
TR_3 = 250 V, 50 c/s primary: 250 V, 60 mA secondary, 4 V, 4·1 A secondary
TR_4 = ignition coil
TR_5 = 250 V, 50 c/s primary: 12 V secondary

SW_1 = double pole on/off switch
SW_{2a}, SW_{2b} = safety plug (made-up) switch
SW_3 = trigger push button
SW_{4a}, SW_{4b} = high voltage (made-up) switch
SW_5 = 11-way switch
SW_6 = thermal delay switch
SW_7–SW_{12} = Burgess miniature micro-switches (interlock)

FS_1, FS_2 = 2 A
FS_3 = 1 A

MR_1, MR_2 = Sentercel H 18. 25. 1 W
M_1 = 100 μA (scaled 0 to 4000 V)

RLA = Londex 50 c/s
RLB = P.O. type 3000 10 kΩ
RLC = Londex 50 c/s modified

L_1 = 2 H tapped†
LP_1, LP_2 = 6 V, 2 W
VR_1 = 50 kΩ

* High voltage insulation between windings.
† Low resistance high voltage winding.

voltage positive pulse is applied to a trigger electrode consisting of a few widely-spaced turns of bare wire wound on the flash tube. A delay circuit in the trigger voltage supply ensures that the condenser C_2, which is rated for intermittent operation, is not charged continuously. Duration of the flash may be varied in ten steps from approximately 500 μs to 6 ms by connecting inductance and resistance in series with the tube by means of a switch SW_5.

Either of the two discharge tubes, V_4 and V_5, may be flashed according to the setting of the special rotary switch SW_4, which makes appropriate connexions to the cathode and trigger electrode of the selected tube. Comprehensive safety circuits are provided as protection against the lethal voltage which, in operation, occurs at the cathode. Details of the safety devices and of the trigger operation are given in the Appendix.

Ultra-violet lighting. The units for providing ultra-violet illumination contain six 125 W discharge lamps (Philips ultra-violet filter mercury lamps, type MBW/U). These are mounted in two housings, each of which holds three lamps. The housings are provided with ventilation holes, and with reflectors to give increased illumination; they are fixed close to the glass tank, one above and the other below it. The power supply for each lamp is obtained from the mains through a circuit containing a choke (Philips low power factor ballast) and condenser (Philips 8 μF capacitor).

Photographic equipment. A camera of simple box construction has been specially built for use with the above apparatus. Preliminary experiments showed that the most satisfactory photographs, with either the continuous or flash system of illumination, were obtained on Ilford HP-3 film developed in Promicrol (by May and Baker Ltd.) and that a lens aperture of $f/4$ was the largest required. It was therefore decided to use standard roll film, 2$\frac{1}{4}$ in. wide, which was considered suitable for enlargement to a convenient size for examination of details without undue trouble from graininess. It was, in fact, found that the normal degree of graininess prevented satisfactory enlargement of small tracers beyond about eight diameters and caused inconvenience if 35 mm film were used.

The camera, built at Thornton, consists essentially of a roll film adaptor and a lens and shutter assembly from an existing camera. The lens is a 10·5 cm, $f/3{\cdot}5$ Voigtländer Skopar unit and is mounted on an ordinary Compur-type shutter operating over a standard speed range. An accurately-made box, in Paxolin, provides a fixed focal position to suit the length of model normally observed. Fig. 3 shows how the camera is mounted on the frame which also carries the lamp housings. The positions of the carriages for the camera and the lamp can readily be interchanged should a record on a horizontal plane be required, but this facility is rarely used.

An electrically-driven rotating disk, with suitably spaced slots, is available for mounting in front of the lens as a more accurate exposure timing device than the Compur shutter. Used in conjunction with the continuous light source, the disk provides a means of fairly precise measurement of tracer velocities.

TECHNIQUES USED FOR THE STUDY OF FLOW SYSTEMS

The visualization of steady flow patterns in the rectangular tunnel, and in three-dimensional systems where motion in one of the dimensions is insignificant compared with the other two, is a straightforward problem. This is achieved by the use of a narrow, flat beam of light projected through the longitudinal section or axis of the model, i.e. so that the dimension in which the motion is zero is normal to the plane of the beam. Only the tracers which pass through the beam are illuminated, so that in the case of a three-dimensional model a two-dimensional section of the flow pattern can be observed without obscurement by the surrounding flow. The traces observed then represent in direction the true motion of the fluid. A time base can be applied by means of either the flash unit or a camera shutter, as described below, by which means velocities may also be determined.

Much of the work carried out on this apparatus, however, has involved the study of flow in gas turbine combustion systems of a type in which the motion is essentially three-dimensional and has, in fact, velocity components of similar order within and transverse to the observed planes at every plane of section. Moreover, the systems studied have been highly turbulent and consequently have not generally presented instantaneous flow conditions which could be directly related to a statistical mean flow pattern. In these respects, the appearance of the flow pattern has been considerably more complicated than that of systems in which the motion is practically two-dimensional. Into the latter category fall many well known aero-gas-turbine combustion chambers in which axial swirl, if present at all, plays mainly a rather local role and does not persist to an important degree, and also the steel furnaces and process plant examined by Newby,[7] Halliday and Phillip.[8] The flow systems examined have often included strong rotational components transverse to the components observed and have consequently produced flow patterns which do not approach the two-dimensional state, even on planes through the axis of symmetry of the system.

In the established types of cylindrical gas turbine combustion chamber, it is of particular interest to study the axial and radial components of flow in a plane through the longitudinal axis of the chamber, since the pattern of these components, that is the two-dimensional pattern which remains when swirl is neglected, is closely related to the geometry of the mixing and flame-holding patterns. This is the case, even in systems where the swirl components have velocities similar to or greater than the combined radial and axial flow components, since the swirling motion is usually employed as a means of distributing the energy of the stream

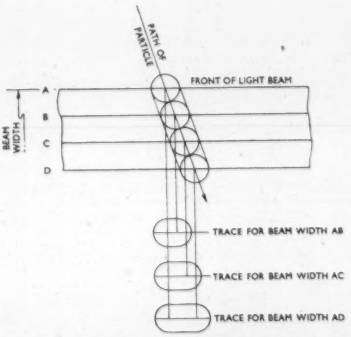

Fig. 5. The effect of beam width on the trace of particles moving through the beam

in such a manner as to create a desired radial-axial mixing mechanism rather than as an intrinsic mixing mechanism. It is possible for the flow components in the central plane of a model to be visualized by means of a flat beam of light of suitable width, provided that the following limitations of the technique are appreciated.

The use of the flat beam technique in a three-dimensional flow requires a certain amount of care if a reasonable degree

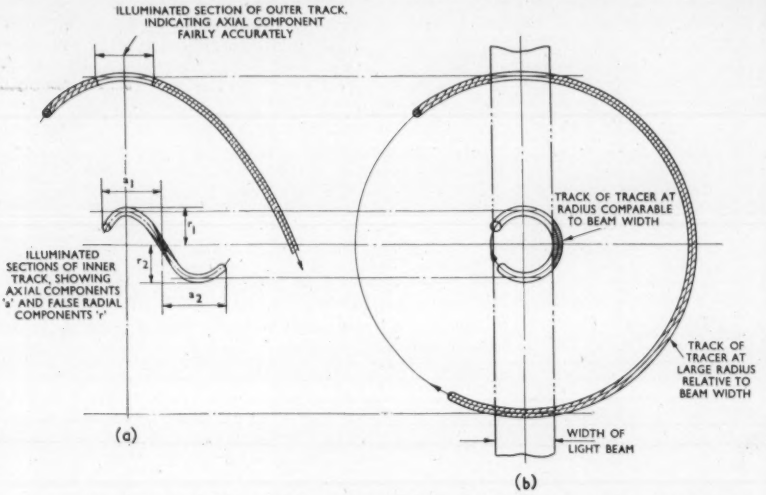
ILLUMINATED SECTION OF OUTER TRACK, INDICATING AXIAL COMPONENT FAIRLY ACCURATELY
a_1
r_1
r_2
a_2
ILLUMINATED SECTIONS OF INNER TRACK, SHOWING AXIAL COMPONENTS 'a' AND FALSE RADIAL COMPONENTS 'r'
TRACK OF TRACER AT RADIUS COMPARABLE TO BEAM WIDTH
TRACK OF TRACER AT LARGE RADIUS RELATIVE TO BEAM WIDTH
WIDTH OF LIGHT BEAM
(a)
(b)

Fig. 6. Visualization of helical motion by means of flat beam of light. The appearance of false radial motion near the axis of the model

(*a*) View of particle tracks from normal position, perpendicular to flat beam of light. (Beam contains axis of model.)
(*b*) Section perpendicular to axis of model showing rotational motion and intersection of particle tracks with beam.

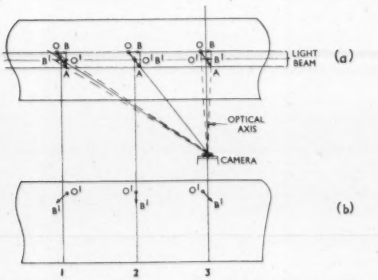

Fig. 7. Optical illusions in the observation of three-dimensional motion by two-dimensional techniques

(1) Position at which apparent direction of axial component is opposite to actual direction.
(2) Position at which axial motion appears to disappear.
(3) Substantially true observation of axial component.

(*a*) Plan of a trace, *OA*, observed from three relative camera positions. *OB* is the true axial component, *O'B'* is the apparent axial component for each camera position.
(*b*) Side elevation of apparent trace, *O'B'* observed from each of the three camera positions. The trace observed on the optical axis represents approximately the true trace for the components of motion in the centre plane of the beam.

of exactitude is to be attained. Clearly, the beam must be of sufficient width for the tracers to perform an observable degree of radial-axial motion during their passage through it, otherwise their traces, observed at right angles to the surface of the beam, will appear only as dots (Fig. 5). However, when it is required that the velocity of tracers be recorded in terms of the trace lengths for a known photographic exposure, it is necessary for the beam width to exceed the tangential distances travelled by the tracers during the exposure time. If this is not so, the traces will clearly be limited by the beam width instead of the exposure time. On the other hand, an excessively wide beam may lead to errors in the determination of the flow components. For example, towards the centre of a rotating flow the swirl component may appear as though it were a radial component, as shown in Fig. 6. This effect may give quite a false idea of the flow pattern and, of course, a similar effect will arise if the light beam is not alined exactly through the axis of the model.

An illusion may also occur, resulting in a false impression of flow, if the tracers are observed from a single viewpoint or photographed by means of a single camera. When a swirl component exists only the traces which occur on the optical axis of the camera, or of the eye of the viewer, will be registered correctly. Those which are observed at an angle to this axis will not be seen exactly as when viewed normally to the plane of illumination owing to the greater angle subtended by the swirl component. Fig. 7 shows how this effect may even result in the illusion that the axial motion at a position

in the fluid is opposite to its true direction. The thickness of the light beam has no influence on this phenomenon, which depends only on the angle at which the fluid traverses the beam and the angle of observation. Ideally, therefore, the traces should be recorded by a succession of normal photographs of adjacent narrow strips of the field. In practice, however, it has been found that a reasonably wide field may be covered by a single photograph, provided that a fairly large camera-object distance is employed. In the models dealt with, a field of 20° subtended angle has been considered a suitable limit within which adequate accuracy may be attained. At a camera-object distance of 40 in. this has allowed the photography of a 14 in. field.

The electronic flash unit has proved to be particularly useful in the photography of complex flow patterns, since it is possible for the direction of travel of each tracer to be determined. This depends upon the intensity/time characteristic of this type of flash. The light output builds up rapidly to a maximum and falls exponentially to zero (Fig. 8). The initial illumination of a tracer is therefore relatively strong and progressively weakens as the tracer moves across the field. The trace therefore disappears rather gradually in the direction of motion and is seen as a comet-shaped object as indicated in Fig. 8. The narrow end of the trace thus points in the direction of motion, as in Fig. 9. This property of the flash technique has been previously exploited by other workers.[1]

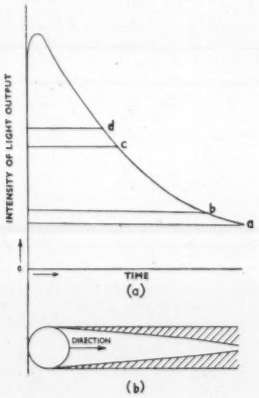

Fig. 8. Illumination of tracers by electronic flash

(*a*) Variation in flash intensity.
(*b*) Approximate appearance of tracer. Shaded area represents region where the light reflected normally has fallen below an arbitrary intensity.

Approximate local velocities may be found from measurements of the trace lengths. At a given setting of the timing control for the flash circuit, the flash duration has a constant value. It has been found, however, that it is not generally possible to calibrate the flash duration so that a constant relationship holds between the recorded trace length and the fluid velocity. The reason for this can be appreciated when consideration is given to the photographic factors involved. The level of illumination recorded depends on the sensitivity of the photographic emulsion at a given lens aperture. It also depends on the processing of the film, and, if prints are made from the negative, the sensitivity and processing of the printing material contribute a further effect. The lower limit of recorded illumination may thus be at some level above

Fig. 9. Typical flash photograph of polystyrene tracers in a model of a combustion chamber

zero as shown in Fig. 8. Variations in any of the above factors, such as the slight differences between emulsions on different lengths of nominally similar film, or differences in the freshness of the developing solution, will alter the level of the recorded illumination. If this level is on the lower part of the curve of Fig. 8, the effect of a small change of level on the effective exposure time will be considerable, as shown by the lines *a* and *b*. The proportional effect on exposure time becomes less as the overall sensitivity of the record is reduced (lines *c* and *d*), but an appreciable error may still be involved.

A further effect on the photographic record arises from the variable motion of the fluid, as a result of which tracers at different parts of the system move with different velocities. This results in different degrees of total illumination per unit trace length, since the total illumination (intensity × time) is the same for the complete illuminated trace of each tracer which is wholly in the light field during the flash period. The effective exposure time of the faster tracers is, therefore, less than that of the slower ones.

It is clear from the above that an independent calibration of the flash duration, for example by the flash illumination of photographic paper through a moving slit, is not likely to be a reliable basis for the analysis of the velocity field. Moreover, a calibration of any kind cannot reliably be applied to records made on different lengths of film although the error may be reduced to insignificance if exceptional care is taken in the reproduction of the processing conditions of successive films. The most accurate method of determining the time base consists of the photography of tracers, moving with known velocity, simultaneously with the photography of the experimental flow field. This may often be achieved by including in the photograph a portion of a transparent inlet section upstream of the model proper.

It has generally been found that the effect of tracer velocity on the effective exposure time has been rather small, since the apparent cut-off of illumination has been at a reasonably steep part of the curve (such as line *c* in Fig. 8). A variation

of exposure must also arise, of course, from the fall in intensity of the light across the model, but since the beam diverges significantly in one plane only, the effect is less than would otherwise be expected. The use of two lamps, on opposite sides of the model, further assists in equalizing the exposures across the model. Errors arising from these two effects in the present models have not been serious as long as they were not unduly increased by the addition of the more easily avoided errors due to faulty calibration or optical distortion.

Photographic records may also be obtained by the use of the 2 kW continuous light sources in conjunction with a timing shutter. The Compur shutter of the camera may be used for this purpose, or, more accurately, the timing may be achieved by the use of the spinning disk shutter. In either case, records may be obtained of the velocity components and of the paths of fluid elements, but not of the direction of travel along these paths. Attempts have been made to achieve comet-shaped traces by means of triangular slots in the shutter disk, but the idea was not a complete success. Because of this failing of the shutter method of exposure, flash illumination only has been used for the photography of the flow components in planes, but the flat continuous beam is of considerable use for the visual study of these components.

Flow components in planes are visualized by means of tracers circulating continuously with the water (in a volume concentration of about 0·1%). It is sometimes useful, however, to observe the motion of individual particles through the model, i.e. to study the flow from the Lagrangian rather than the Eulerian point of view. For this purpose, a wide continuous beam of light is employed for the illumination of the complete field of flow. Polystyrene particles are injected singly at a selected position in the model or in the inlet section by means of the simple plunger-operated injector shown in Fig. 10. Photographs of the traces of these particles through the model may be obtained up to a total exposure time per frame of 2 s at $f/8$; longer exposures than this result in fogging of the film by the scattered light from the model and from the gas bubbles present in the water, with consequent obscuration of the polystyrene traces. The

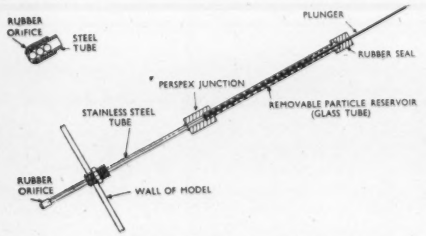

Fig. 10. Device for the introduction of single polystyrene tracers. Inset shows detail of end of tube. The tubes are of 0·10 in. bore and the particles are sifted to between 0·075 and 0·095 in. diameter

length of path photographed can be extended by the use of the disk shutter, which results in exposures of evenly spaced short lengths of traces and which also provides a useful time base. Photographs obtained by this method are shown in Fig. 11. A further extension in the permissible exposure time has been obtained by the technique of selective illumination of the tracers, which are provided with a fluorescent coating, by ultra-violet light from the bank of mercury discharge lamps. The tracers are then photographed on Ilford HP. 3 film through a Wratten K. 2 filter, which efficiently transmits the re-radiated light while transmitting

Fig. 11. Path of a single tracer in a model of a combustion system

only a small fraction of the initial radiation from the lamps. An adequate record of the path of the tracer can thus be obtained over a total time of ten seconds or longer, while the outline of the model is recorded faintly and does not obscure the field.

When an extensive three-dimensional path of this type is observed or photographed from a single point, an illusory view of the perspective of the motion is obtained. The use of stereoscopic records can eliminate this inaccuracy and photographs have been obtained with a stereo-camera of some of the three-dimensional fluid paths occurring in swirling systems. The method permits the accurate analysis of the recorded motion, provided that a measuring stereoscope is available for the interpretation of the negatives.

INTERPRETATION AND PRESENTATION OF PHOTOGRAPHS OF TURBULENT FLOW

Where a virtually two-dimensional motion exists, a photograph of an illuminated section containing the components of motion gives a fairly clear idea of the state of flow. Examples are given in Figs. 12 and 13. Such photographs, however, become increasingly obscure as the degree of turbulence and motion in the third dimension increases and it then becomes necessary to consider the interpretation of the photographic records.

Turbulent motion implies a disorderly, changing state. Fluids in turbulent flow follow a continually changing motion referred to both time and space. Fluid elements which move in a connected manner at one instant become apparently unrelated at the next instant and individual stream tubes rapidly lose their identity.

In highly turbulent three-dimensional flow, therefore, it is not possible to observe at any one instant a flow pattern which represents the "basic" or "statistical mean" flow of the system. In fact, the combination of random flow directions over any part of the field may appear to have no relation whatever to the basic flow. Moreover, successive instantaneous observations of the same basic pattern will give quite different detailed results.

These facts will be demonstrated for the case of a particular flow system, that in the burning zone of a swirl-type combustion chamber with the flame tube configuration shown in Fig. 14. The basic pattern was studied in terms of the components in a longitudinal plane by means of the flat-beam system of illumination. In Fig. 14, the basic flow pattern in this plane is shown, in direction but not in magnitude,

Fig. 12. Photograph of a two-dimensional flow pattern

Fig. 13. Photograph of flow through a simple air-director model

obtained by the method described later. If a flash photograph is taken of the tracers in this same flow field at some particular instant, however, the result is likely to be a rather haphazard combination of local flow features. Fig. 15 is a photograph of an example of instantaneous conditions which occurred within the basic flow pattern of Fig. 14. It is clear that no such single photograph would permit the derivation of the diagram of Fig. 14, although this diagram represents for precisely the same conditions the statistical mean flow pattern described by fluid elements over a period of time.

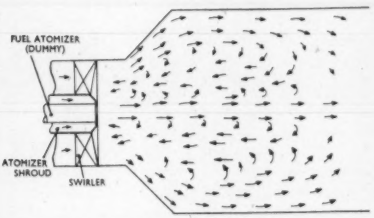

Fig. 14. Flow pattern in a combustion chamber (directional components in central plane)

At positions where the turbulence is less intense, some consistent relation between the instantaneous tracer motion and the basic pattern is obvious, for example, along the flame-tube wall. Over most of the field in this particular system, however, a large degree of random turbulence exists and the local fluctuations of both direction and velocity are large. Under these conditions, the visual impression of the flow is one of complete chaos, as illustrated in Fig. 16 by a photograph of the above flow field made by means of a rather long total exposure ($\frac{1}{2}$ s) with the continuous lighting.

Despite the apparent disorder observed, the turbulence occurs about a definite mean flow pattern which is spatially stationary. If the motion at a particular point in the field is recorded by a large number of photographs over a period of time, the flow vectors form a group which generally indicates a preferred direction of flow. A typical group of this kind is shown in Fig. 17(*a*). In such cases, it is possible to determine an approximate mean vector, for example, by averaging co-ordinates in two mutually perpendicular directions. This procedure may be carried out for suitably-spaced positions over the flow field until a complete mean pattern has been built up, as shown in Fig. 18(*a*). At positions in the field where the shear flow occurs with zero resultant velocity, the vector groups appear as in Fig. 17(*b*). For comparison with the diagram of mean vector flow [Fig. 18(*a*)] a diagram is shown [Fig. 18(*b*)] in which groups of some of the actual vectors recorded are plotted. (Where the recorded vectors lay very close together, or were coincident, every vector could not, of course, be shown in the diagram.)

This method has been employed generally for the derivation of flow patterns from the water model results, although it has been found that in flow patterns which are substantially two-dimensional a sufficient degree of orderliness frequently occurs for the flow to be plotted qualitatively by direct inspection of a single set of tracers. The initial set of vector groups is plotted by tracing the images projected from the negatives on to a sheet of paper on which a suitable grid has been drawn.

Fig. 15. Instantaneous flash photograph of the flow field of which the basic pattern is shown in Fig. 14

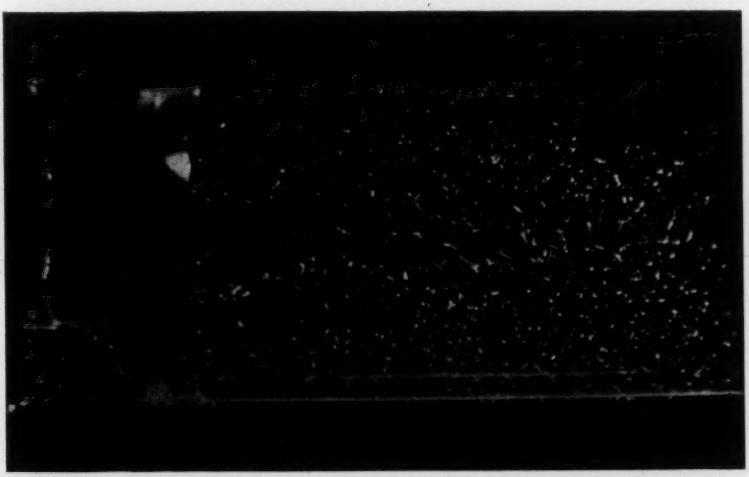

Fig. 16. Record of flow with continuous illumination; exposure $\frac{1}{2}$ s

SIMILARITY CONSIDERATIONS

It is appropriate in a practical paper of this kind to mention very briefly the question of dynamic similarity as it applies to the water flow method.

The physical properties of the fluid which influence flow in relation to a particular geometric system include compressibility, surface tension, specific weight and viscosity. The model in which the flow is observed need conform only to the requirement of geometric similarity, i.e. the various linear dimensions defining the model must be in the same ratio to each other as the corresponding dimensions in the original apparatus.

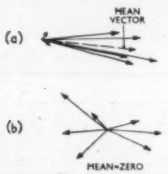

Fig. 17. Instantaneous vectors in turbulent flow

The above fluid properties may be used in conjunction with the model scale to express dimensionless parameters which govern the flow under various circumstances. For example, the Reynolds number, $\rho vL/\mu$, is a controlling parameter when viscous forces are important and the Froude number, v^2/Lg, is the equivalent parameter for flow controlled by gravitational forces. Other parameters apply when mass forces, surface tension or compressibility influence the fluid motion. (For notation used see below.)

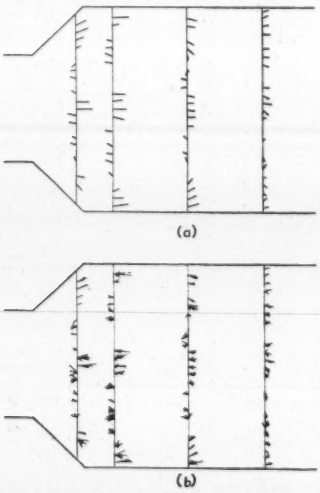

Fig. 18. Vectors of flow components in a plane at the centre of a cylindrical flame tube

(*a*) mean vectors;
(*b*) instantaneous vectors over a period of time.

In the present case of high-speed flow within a full-running system, it is clear that gravitational and surface tension effects can be considered unimportant. If compressibility effects may be neglected, the Reynolds number (the ratio of inertia to viscous forces) therefore remains as a possibly important criterion of similarity. This factor also may be unimportant in the control of the fluid motion if the rate of flow is high and the influence of viscosity consequently small. This state of affairs certainly exists in the bulk of the flow field of a gas turbine combustion chamber at normal operating conditions, and it is only at a few particular parts of such a system that the local Reynolds numbers might fall to somewhere near the critical value.

It therefore seems probable that a general similarity of flow may be achieved without regard for the strict equality of the characterization factors, provided that the flow is everywhere in a state of fully developed turbulence, and this has in fact been confirmed experimentally by model work carried out at this laboratory.

Because of the occasional occurrence of locally critical flows in the models examined, the practice has been adopted during all this work of simulating the Reynolds number of the full-scale system fairly exactly. The relationships involved when the flow of water in a model is used to simulate the flow of air in a full-scale system are as follows:

$$(\rho vL/\mu)_W = (\rho vL/\mu)_A \tag{1}$$

Therefore
$$v_W = v_A(L_A/L_W)\,(\nu_W/\nu_A) \tag{2}$$

or
$$v_R = \nu_R/L_R \tag{2a}$$

Also since
$$Q_R = (\rho vL^2)_R$$
$$Q_W = Q_A(\mu_W/\mu_A)\,(L_W/L_A) \tag{3}$$

or
$$Q_R = \mu_R L_R \tag{3a}$$

These simple formulae allow either a suitable velocity, or the mass flow, to be adjusted to suit the change of model scale and the change of working fluid.

For the time scale, which permits the assessment, for example, of the residence time of fluid elements in a system from observations in a model, the obvious relationship

$$T_R = L_R/v_R$$

may be used. This may be expressed in a more fundamental form when the Reynolds number ratio is unity by the substitution

$$v_R = \nu_R/L_R$$

so that
$$T_R = (L^2/Re\nu)_R$$

Therefore
$$T_R = L_R^2/\nu_R \tag{4}$$

Where rotating flow exists, the angular velocity relationship may be easily derived, since the dimensions of ω are $1/T$:

$$\omega_R = 1/T_R = \nu_R/L_R^2 \tag{5}$$

Provided, therefore, that the Reynolds numbers are identical, the above formulae allow the characteristics of the flow in a given system to be determined from observations of the corresponding characteristics in a model.

The effect of compressibility has so far not been considered. It may be reasonably accepted that compressibility effects on the flow in straight jets and enclosed streams in the absence of heat release are negligibly small at the velocities existing in the type of equipment which has been studied. When rotation exists, the pressure gradients which are then estab-

lished will affect the mass distribution in the system containing air but will have virtually no influence on mass distribution in the model containing water. Calculations of the radial pressure distribution due to axial swirl in systems examined have shown that in all cases the air density variation has been of such an order (about 1%) that it may reasonably be neglected in the study of major flow phenomena, although it may have a detectable influence on local details of flow.

As already stated, the water system is suitable only for the exact simulation of constant density conditions and must be used in conjunction with other means when applied to the study of combustion systems. Nevertheless, an adequate degree of similarity has been observed between combustion chambers with and without heat release in many cases.

Notation and dimensional units

g = gravitational constant $\equiv L/T^2$
L = linear dimension
M = mass
Q = mass flow rate $\equiv M/T$
Re = Reynolds number ($\rho vL/\mu$), dimensionless
T = time
v = velocity $\equiv L/T$
μ = dynamic viscosity $\equiv M/LT$
ν = kinematic viscosity (μ/ρ) $\equiv L^2/T$
ρ = density $\equiv M/L^3$
ω = angular velocity $\equiv 1/T$

Suffixes

A = air
W = water
R = ratio of value for water to value for air

FIELDS OF APPLICATION OF THE WATER FLOW METHOD

The method described here has been applied to numerous problems in combustion systems, including studies of the strength and position of recirculating flows set up by air directors, the mixing of adjacent streams, the velocity distributions existing in various parts of a system, the effectiveness of skin-cooling jets, the residence times of particles in burning zones, and particular cases of aerodynamic instability.

In other fields, the method can be applied to the study and development of flow systems in many types of chemical and mechanical engineering processes and is suitable generally for the study of low-speed aerodynamic problems.

CONCLUSIONS

The apparatus and techniques described have proved to be reliable and convenient for the study of flow problems. Both qualitative and quantitative records of flow phenomena can be obtained by their use. The water method has been very successful in investigations of combustion equipment, notwithstanding the limitation of constant fluid density, and it has obvious applications in other fields.

It is the hope of the authors that this detailed account of their experiences in the development of the equipment in use at the Thornton Research Centre will be of assistance to others who wish to use a similar technique.

ACKNOWLEDGEMENT

The authors would like to express their thanks to the Directors of "Shell" Research Ltd. for permission to publish this article, and to their colleagues at Thornton Research Centre, who have contributed to the work described.

It is also desired to acknowledge that the use of plastic tracers in this work was suggested by Dr. E. C. Roberson of the National Gas Turbine Establishment, and that the stereophotographic work was carried out with the advice and assistance of Dr. E. A. Miskin of University College, London.

REFERENCES

(1) Howes, R. S., and Philip, A. R. *J. Iron Steel Inst.*, **162**, p. 392 (1949).
(2) Triebnigg, H. *MTZ*, **13** (10), p. 237 (1952).
(3) Fage, A., and Preston, J. H. *J. Roy. Aero. Soc.*, **45**, p. 364 (1941).
(4) Chesters, J. H., and Philip, A. R. *J. Iron Steel Inst.*, **162**, p. 385 (1949).
(5) Roberson, E. C. Private communication.
(6) Werlé, H. *La Recherche Aéronautique*, **33**, p. 3 (1953).
(7) Newby, M. P. *J. Iron Steel Inst.*, **162**, p. 452 (1949).
(8) Halliday, I. M. D., and Philip, A. R. *J. Iron Steel Inst.*, **162**, p. 401 (1949).

APPENDIX

Operation of high intensity flash tube circuit (Fig. 4)

(*a*) *Safety devices.* The safety switch (SW_{2a} and SW_{2b}) and the interlock circuit, comprising a relay (RLC) and six microswitches (SW_7–SW_{12}) are used to ensure the safe operation of the flash tubes.

The safety switch takes the form of a plug which is removed when work is in progress on the lamps. Switch SW_{2a} removes the mains voltage from the primaries of transformers TR_1, TR_2, TR_3 and TR_5; switch SW_{2b} discharges the condenser C_2 *via* the resistance R_5. The interlock circuit contains the relay RLC, and until this is energized RLC_1 and RLC_2 are open, removing mains voltage from the primaries of transformers TR_1, and TR_2 and TR_3, and the special high-voltage contact RLC_3 is closed discharging the condenser C_2. The relay RLC is energized only when the mains switch SW_1 is closed, the safety plug SW_2 is in position, and the six switches SW_7–SW_{12} are closed. The latter consist of microswitches which are only all closed when the extra high tension plugs and the trigger plugs are in position, and when the covers of the flash tube housings are closed. When this interlock circuit is completed the relay RLC is energized and the contacts RLC_1 and RLC_2 are closed, while the contact RLC_3 is opened.

The lamp housings are earthed *via* the power supply chassis, and the covers are also earthed by connexion to the housings with flexible metal braiding.

(*b*) *Trigger operation.* When the safety circuits are completed, the flash may be operated by depressing the trigger push-button SW_3, which initiates the following sequence:

1. Relay RLA operates:
   (i) closing hold-in contact RLA_1;
   (ii) closing RLA_4 and lighting the trigger pilot lamp LP_2;
   (iii) closing RLA_3 and applying mains voltage to the primary of TR_1 so that condenser C_2 commences to charge through rectifying valve V_1;
   (iv) opening RLA_2.

2. When RLA_2 opens, the fixed bias on the grid of the gas triode V_2 is removed, and condenser C_5 commences to discharge through resistance R_9. After a delay of about

thirty seconds (determined by the setting of VR_1), which allows condenser C_2 to charge up to its full high voltage, V_2 fires and relay RLB operates:

(i) opening RLB_1 and releasing relay RLA;
(ii) closing RLB_2.

3. Closure of RLB_2 applies a negative pulse to the control grid of the cold cathode tetrode V_3, as a result of which the anode to cathode path immediately becomes conducting, and condenser C_8 discharges through the primary of the ignition coil TR_4. This produces in the secondary a damped oscillatory transient with an initial highly positive peak which, applied to the trigger electrode, flashes the discharge tube.

4. Release of relay RLA restores the negative bias to V_2 so that the a.c. energized relay RLB is released, and, after a short interval for recharging C_8, the circuit conditions prior to operation of SW_3 are resumed.

A two-minute thermal delay switch SW_6 prevents application of anode voltage to the gas triode V_2 until its heater has warmed up.

The "ploughing" contribution to friction

By R. T. Spurr, B.Sc., Ph.D., Ferodo Ltd., Chapel-en-le-Frith, Stockport, Cheshire

When a hard surface is slid over a softer surface part of the frictional resistance is due to the force required to plough asperities of the harder surface through the softer. It is shown how this ploughing contribution to friction can be obtained for hard steel balls and wedges sliding on soft metals.

Bowden, Moore and Tabor[1] have suggested that when a hard surface slides over a softer surface the resistance to sliding can be divided into two parts, one part due to friction arising from adhesion and the other part due to the force required to plough the asperities on the harder surface through the softer surface. In terms of coefficients of friction $\mu = \mu_F + \mu_P$ where μ_F is the component due to friction as such, and μ_P is the ploughing component.

In the work described below, expressions have been derived which enable the ploughing component to be calculated for two types of asperity, namely, spheres and wedges, and it is shown that calculated and experimental values of μ_P for spheres and wedges sliding on brass and other metals are in good agreement.

EXPERIMENTAL DETAILS

Metal plates were made to slide at low speeds against a steel ball or wedge in a Denison test machine using the arrangement illustrated in Fig. 1. The plates which were about $\frac{1}{2}$ in. thick, were polished to at least a 00 emery finish and all surfaces were degreased before each measurement.

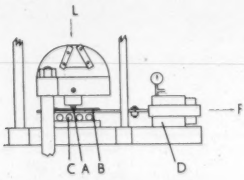

Fig. 1. Friction apparatus

A, steel ball; *B*, specimen; *C*, rollers; *D*, air cylinder.

The tangential force F required to bring about steady sliding and the width d of the track ploughed by the ball were measured for normal loads L ranging from 50 to 600 kg. Two runs were made at each load, a different track being used for each measurement. The steel balls were of $\frac{1}{4}$ in. diameter and had a hardness of about 1000 kg/mm^2. Plates of the following metals and hardnesses were used:

Material	*Brass*	*A*	*B*	*C*	*Aluminium*	*Copper*
Vickers hardness number (V.H.N.) (kg/mm^2)		76	110	106	35	42

The wedges were made by grinding flats at angles θ (Fig. 4) varying from 0° to 35° on the ends of lengths of $\frac{3}{8}$ in. square tool steel. The wedges, mounted transversely to the direction of sliding, were slid against a degreased brass plate of V.H.N. 120 kg/mm^2 under normal loads of 250 to 1000 kg.

In a third set of experiments, instead of sliding a hard wedge against a soft surface, lead cylinders (about $\frac{3}{8}$ in. in diameter) were slid against $\frac{1}{2}$ in. wide lengths of hardened gauge steel on the upper surfaces of which were machined half-wedges about $\frac{1}{10}$ in. long and of 5°, 10°, 20° and 30° angles. The normal loads used covered the range 10–60 kg.

RESULTS AND DISCUSSIONS

It was found that with the steel balls d^2 was proportional to the load for each specimen and subsidiary experiments on another apparatus showed that this proportionality extended down to at least 1 kg normal load. If during sliding the normal load is carried by the front half of the ball and A_L is the horizontal projected area of such contact then $L = A_L p_m$. The "flow pressure" p_m obtained from this equation agreed within 3% with the Meyer hardness calculated from the measured Vickers hardness number of the brass specimens. If (following Bowden and others[1]) the force F_p required to plough the ball through the metal is assumed to be given by an analogous equation $F_p = A_s p_m$, where A_s is the cross-sectional area of the ploughed groove, then the contribution of the ploughing component to the total measured coefficient of friction will be $\mu_p = F_p/L = A_s/A_L \simeq (4/3\pi)(d/D)$ where D is the diameter of the ball. The value of μ_p can therefore be calculated for any load and ball diameter if either the

hardness of the surface or the width d of the track can be measured. When the normal load is small, d and μ_p are small and for loads of 1 kg, μ_p ($\simeq 0{\cdot}004$ for $\frac{1}{2}$ in. balls on brass) can be neglected and so the adhesive friction component μ_F (assumed to be independent of load) can be measured by sliding steel balls along the specimens under light loads. We then have $\mu \simeq \mu 1\,\text{kg} + (4/3\pi)(d/D)$. The results for brass are shown in Fig. 2 where the smooth curves represent

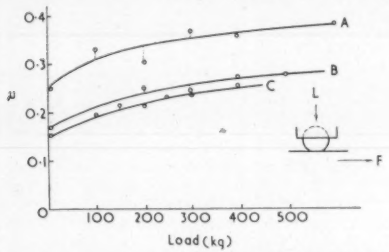

Fig. 2. Values of μ of a steel ball sliding over brass plates A, B and C plotted against the load

$\mu = \mu 1\,\text{kg} + (4/3\pi)(d/D)$ plotted against load and small circles represent the experimental values of μ obtained on the Denison machine. Similar agreement between calculated and experimental values of μ was obtained with the aluminium and copper plates (Fig. 3), except at loads above about 300 kg when the soft metals tended to pile up ahead of the ball. The μ_F values were obtained by sliding the steel balls against the metal surfaces under loads of 1 kg in a simple apparatus described elsewhere.[2]

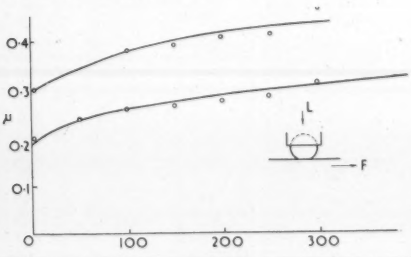

Fig. 3. Values of μ of a steel ball sliding over an aluminium plate (upper curve) and a copper plate (lower curve) plotted against the load

If the ploughing member is a wedge of angle θ then obviously $\mu_p = As/AL = \tan\theta$ provided p_m is independent of the geometry of the deformation, and $\mu = \mu_F + \tan\theta$. In Fig. 4 (lower plot) the values of μ (which was independent of load) obtained when wedges were slid over brass are plotted against the tangent of the wedge angles. The value of μ when $\tan\theta = 0$ was obtained by sliding steel balls over the specimen under light loads. It can be seen that $\mu = \mu_F + \tan\theta$. Similar results were obtained when wooden wedges were slid over beeswax.

Finally, in an inversion of the wedge experiments, lead specimens were slid against steel surfaces on which small wedges had been machined to determine whether the ploughing component for a soft surface sliding against a hard surface covered with small wedges could be evaluated in the same way as that for single hard wedges sliding on a soft smooth surface. Fig. 4 (upper plot) shows that the equation

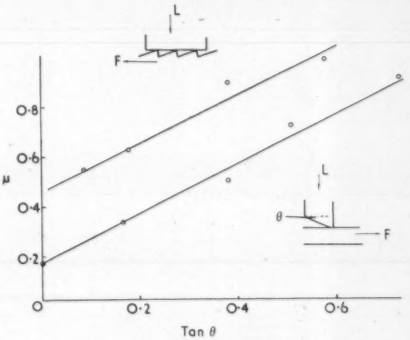

Fig. 4. Values of μ plotted against wedge angle θ
Upper curve: lead specimen sliding on wedges.
Lower curve: single wedge sliding on brass.

$\mu = \mu_F + \tan\theta$ still applies. Ernst and Merchant[3] also put $\mu = \mu_F + \tan\theta$ but their $\tan\theta$ term appears to arise from Coulomb friction and not as a result of plastic deformation.

ACKNOWLEDGEMENTS

The author wishes to thank the staff of the Technical Division of Ferodo for assistance and criticism, in particular Mr. Newcomb who helped with the experimental work, and the directors of Ferodo Ltd. for permission to publish this paper.

REFERENCES

(1) BOWDEN, F. P., MOORE, A. J., and TABOR, D. *J. Appl. Phys.*, **14**, p. 80 (1943).

(2) SPURR, R. T. *Brit. J. Appl. Phys.*, **6**, p. 402 (1955).

(3) ERNST, H., and MERCHANT, M. E. *Conf. Friction and Surface Finish*, p. 76 (Massachusetts Institute of Technology, 1940).

Klystron oscillator noise theory

By R. L. BELL, Ph.D., Services Electronics Research Laboratory, Baldock, Herts.

[*Paper first received* 22 *November*, 1955, *and in final form* 27 *March*, 1956]

Results are presented of calculations on the amplitude and frequency fluctuations generated in a floating-drift-tube klystron oscillator by thermal noise in the cavity and current and velocity noise on the electron beam. Current fluctuations at the oscillation and harmonic frequencies are found to be the main source of frequency and amplitude modulation noise. At the very lowest modulation frequencies flicker noise in the beam will take over as the source of a.m. noise. The predominant f.m. source in this region is uncertain. Methods of reducing the noise are pointed out.

1. INTRODUCTION

This paper presents some results of noise calculations on the floating-drift-tube klystron oscillator. An account of other characteristics of this device may be found in Ref. 1. The object of the present work was to obtain a credible estimate of the random frequency and amplitude modulation spectra of a typical klystron oscillator due to basic sources like shot noise in the beam. The results are available for comparison with the corresponding characteristics of magnetron oscillators.[2,3]

Owing to limitations of space, the argument is omitted and the results merely stated. Copies of the full calculations are available on application to the author. A complete *List of signs and symbols* is given as an Appendix, where additional explanations may be found on points only briefly covered in the text.

A brief description of the method of calculation is given in Section 2. The usual Webster approximations are made regarding the oscillation amplitude, leading to the familiar Bessel-function expression for the efficiency. This approach provides the non-linearity requisite to produce a stable point of oscillation from which transient departures in phase and amplitude can occur. As the additional complication introduced by considering space-charge debunching effects would have made the calculation unmanageable, space-charge has been ignored. However, the resulting model represents closely a case accessible to experiment, and so to experimental verification. It happens also to be a fair approximation for some practical oscillators.

The sources considered are velocity and current fluctuations in the beam at video, signal and harmonic frequencies, and Johnson noise in the cavity and load.

The quantities of practical interest are the modulation spectral density for the random frequency modulation and the power spectrum of the amplitude modulation sidebands. Generally these are only required for modulation frequencies of the order of or less than the half-bandwidth of the radio-frequency circuitry, and this condition is used to simplify the analysis. Only the case of oscillation at the resonant frequency of the cavity, i.e. in the region of maximum efficiency, has been worked out in full. Some (qualitative) consideration is given to other cases in Section 5.

2. SKETCH OF CALCULATION

Noise problems of the type to be discussed are essentially linear and reduce to finding the transfer functions which when multiplied by the relevant input spectrum give the required modulation spectrum. This can be done by a small-signal discrete-frequency analysis.

Accordingly one assumes a small current or velocity signal on the electron beam of arbitrary frequency, interacting with the steady-state oscillation of the klystron. A Fourier analysis of the beam current where it passes the second gap yields a series of modulation products. The modulation products occur in pairs, one pair falling closer in frequency to the fundamental than to the second harmonic of the oscillation, another closer to the second harmonic than the fundamental or the third, and so on. Because all oscillators of the type considered have to some extent a selective feedback mechanism, one need deal only with the effects of feeding back one of these pairs, namely that nearest the carrier. Applying these two sidebands to the input gap, it is found that within the pass band of the feedback loop they produce only each other. One concludes that this is a possible steady-state condition for the oscillator.

Simultaneous equations relating the sidebands to the carrier and to each other can be set up for this state. Their solutions give the sideband magnitudes and phases arising from the original modulation.

In order to render the expressions manageable after this point, the possible frequencies for the modulating currents and voltages are restricted to bands near zero, the carrier frequency and harmonic frequencies of the carrier. All these bands generate outputs which can be described in terms of low-frequency amplitude and phase modulation of the carrier.

Combining the sidebands and comparison of the phase of the combination with that of the carrier indicate which component of the modulation may be classed as amplitude and which as phase.

If very low-frequency modulations only are considered, the a.m. and f.m. intensities can be derived directly from the steady-state equation for the carrier alone, by allowing one parameter in that equation (beam voltage or current) to vary sufficiently slowly. The results can be compared with particular cases derived by the indirect method outlined above. The agreement obtained by the two different methods in these special cases has promoted confidence in the more general calculation.

3. RESULTS ON AMPLITUDE MODULATION

3.1 *Velocity noise.* The method of Section 2 yields the result that the sideband power-spectral-density around the carrier frequency due to a.m. by velocity noise in the m^{th} harmonic frequency band is

$$w(f_0 + \Delta f) = \frac{P_0 S^2 Z_1^2}{8u_0^2 Z_2^2} s_1(mf_0) \qquad (1)$$

where P_0 is the output carrier power, frequency f_0, S the transit angle between the gaps, u_0 the beam velocity and s_1 the power spectrum of the velocity fluctuations near the frequency mf_0. More precisely, s_1 is the average of the spectral densities at $mf_0 + \Delta f$ and $mf_0 - \Delta f$, if these are different.

Furthermore

$$Z_1 = \overline{\beta_2[J_{m+1}(x) + (-)^m J_{m-1}(x)]} \tag{2}$$

where β_2 is the output gap coupling factor, the J's are Bessel functions and the argument x is the bunching parameter. The bar indicates an average taken over the beam cross-section.

$$Z_2 = \overline{\beta_2 x J_2(x)} \tag{3}$$

The power spectrum s_1 for velocity fluctuations is of the form

$$2e\Delta\overline{u^2}/i_0 \tag{4}$$

where e is the electronic charge, i_0 the beam current and $\Delta\overline{u^2}$ the variance of the statistical spread in the electron velocities. The spectrum $w(f)$ may be written as kT_1, in terms of an equivalent background noise temperature T_1, where k is Boltzmann's constant. Inserting expression (4) in equation (1),

$$T_1 = \frac{eP_0S^2Z_1^2}{4ki_0u_0^2Z_2^2}\,\Delta\overline{u^2} \tag{5}$$

Setting $m = 0$ (video frequency velocity fluctuations), $Z_1 = 0$, i.e. there is no a.m. noise. Actually this is not strictly true since the exact values of the arguments in equation (2) differ slightly from x and from each other. However, the contribution from this source is still negligible. Using $m = 1$,

$$Z_1 = \overline{\beta_2[J_2(x) - J_0(x)]} \tag{6}$$

and there is, in general, a contribution to the a.m. noise near the carrier. Similarly for $m > 1$.

3.2 *Current noise.* The sideband noise temperature due to current fluctuations in the m^{th} harmonic band is

$$T_2 = \frac{P_0Z_3^2}{8ki_0^2Z_2^2}\,s_2(mf_0) \tag{7}$$

The power spectrum of the current fluctuations s_2 may be written

$$s_2 = 2ei_0\Gamma^2 \tag{8}$$

Furthermore

$$Z_3 = \overline{\beta_2[J_{m+1}(x) - (-)^m J_{m-1}(x)]} \tag{9}$$

There are two important exceptions to equation (7). The first is the case of video-frequency current noise, $m = 0$, when equation (7) should be divided by a factor 2. This also applies to velocity noise, where, however, it is unimportant since the velocity noise effect vanishes for $m = 0$. It arises from the fact that a given sideband has only one source of excitation in the video case, but two sources, one on either side of the carrier or harmonic frequency, in every other case.

The second exception is the carrier-frequency current noise which, in addition to exciting the oscillator in the normal way *via* modulation products at the second gap, also excites it directly *via* the first gap. The background noise temperature in this case [using equation (8)] is

$$T_3 = eP_0\Gamma^2Z_4^2/4i_0kZ_2^2 \tag{10}$$

$$Z_4^2 = \beta_1^2 + \beta_2^2[J_0(x) + J_2(x)]^2 \tag{11}$$

β_1 is the gap coupling factor for the first gap.

3.3. *Current-velocity noise.* Any correlation between current and velocity noise in the region of the first gap will contribute to the a.m. noise temperature by the amount

$$T_4 = \frac{Z_1Z_3P_0S}{8_ki_0u_0Z_2^2}\,s_{12}(mf_0) \tag{12}$$

where s_{12} is the cross power spectral density for the current and velocity fluctuations. It lies in the range

$$0 < s_{12} < 2\sqrt{s_1s_2} \tag{13}$$

This contribution will generally be negligible. Equation (12) fails to hold for $m = 0$. This is immaterial since at the same time $Z_1 \simeq 0$.

3.4 *Thermal noise.* Johnson noise from the radio-frequency circuitry in the neighbourhood of the carrier frequency will be amplified by the action of the oscillator, assuming a modified temperature given by

$$T_5 = P_0T_cG/2i_0^2Z_2^2 \tag{14}$$

where G is the real part of the driving-point circuit admittance seen from the second gap, and T_c is its equivalent temperature, which may be different from room temperature.

3.5 *Partition effects.* Non-uniform coupling of the electron stream to the radio-frequency gaps introduces a source of noise of the "partition" variety, affecting the results on current noise. Owing to this effect the expression (10) is modified to

$$T_6 = \frac{eP_0}{4i_0kZ_2^2}\,Z_5^2 \tag{15}$$

where in the case of radio-frequency shot noise

$$Z_5^2 = \overline{Z_4^2} - \overline{Z_4}^2(1 - \Gamma^2) \tag{16}$$

The bars indicate averages over the beam cross-section. For other cases replace Z_4 by Z_3 in equation (16); Γ is the space charge smoothing factor for the shot noise alone. For $\Gamma = 0$ (full smoothing)

$$Z_5^2 = \overline{(Z_4 - \overline{Z_4})^2} \tag{17}$$

Clearly a separate source of noise is generated, independent of the shot noise. It depends only on the non-uniform coupling of the carrier oscillation to the beam, and is not attributable directly to any high-frequency property of the noise. Thus there is a contribution to partition noise from the video-frequency band, $m = 0$.

Similar consideration of the velocity effects reveals no similar source in this case, but only that the relevant velocity spready $\Delta\overline{u^2}$ is an averaged difference between instantaneous velocities at a point, and the mean velocity at that point, in distinction to the total velocity spread of the beam, which might be much larger.

The absence of a partition effect is not surprising when we remember that the derivation assumes no possible smoothing mechanism for the velocity noise. For, putting $\Gamma = 1$ in equation (16) we get

$$Z_5^2 = \overline{Z_4^2}$$

and the effect is equivalent to full shot noise, i.e. the partition noise has disappeared. As we have assumed full velocity noise, a partition effect cannot appear.

4. RESULTS ON FREQUENCY MODULATION

The f.m. results are given in terms of the intensity of the modulation spectrum, denoted below by σ. The dimensions of this quality are (seconds)$^{-1}$, more graphically described as (cycles per second)^2/cycle per second, meaning, the mean square frequency deviation of the carrier attributable to each cycle per second of modulation bandwidth.

4.1 *Velocity noise.* Velocity fluctuations in the m^{th} harmonic band generate f.m. fluctuations given by

$$\sigma_1 = 2\,\frac{S^2 f_0^2 Z_3^2}{4Q^2 u_0^2 Z_6^2}\, s_1(mf_0) \tag{18}$$

where Q is the loaded Q-factor of the cavity and

$$Z_6 = \overline{2\beta_2 J_1(x)} \tag{19}$$

Z_3 and s_1 are given by expressions (9) and (4) respectively. The quotient Z_3/Z_6 is unity for $m = 0$ (video frequency noise) and converges eventually on zero for increasing m (order of harmonic). The initial factor 2 in equation (15) should be dropped when $m = 0$, for reasons already explained.

4.2 *Current noise.* Taking into account partition effects, the modulation spectral density due to current fluctuations in the m^{th} harmonic band is

$$\sigma_2 = \frac{e f_0^2}{i_0 Z_6^2 Q^2}\left[\overline{Z_1^2} - (1-\Gamma^2)\overline{Z_1}^2\right] \tag{20}$$

In the case of $m = 1$, to Z_1 as given by equation (2) must be added a term accounting for excitation *via* the first gap, i.e. Z_1 in equation (20) must be replaced by Z_7 given by

$$Z_7^2 = \beta_1^2 + Z_1^2 \tag{21}$$

In the case of $m = 0$, $Z_1 = 0$, i.e. there is no f.m. noise due to video-frequency current fluctuations. While this is true for the assumed on-tune operation, current pushing may contribute extensively to f.m. noise in other circumstances. This is discussed in Section 5.

Returning to equation (20), if the coupling to the beam at the oscillation frequency is uniform,

$$\sigma_2 = \frac{e f_0^2 Z_1^2 \Gamma_m^2}{i_0 Q^2 Z_6^2} \tag{22}$$

where Γ_m is the usual space-charge reduction factor for the current fluctuations in the m^{th} harmonic band.

4.3 *Current-velocity noise.* Correlation between velocity and current fluctuations will give rise to an f.m. spectral density of the order of

$$\sigma_3 = \frac{S f_0^2}{2 i_0 u_0 Q^2}\,\frac{Z_1 Z_3}{Z_6^2}\, s_{12} \tag{23}$$

Partition effects, for which there will be no correlation, have been omitted.

4.4. *Thermal noise.* The f.m. spectrum due to thermal fluctuations in the cavity and load is

$$\sigma_4 = 2 f_0^2 k T_c G / Q^2 i_0^2 Z_6^2 \tag{24}$$

5. OFF-TUNE OPERATION

The results given above apply only to the case where the beam voltage is such that the oscillation frequency coincides with the natural resonant frequency of the cavity. Qualitatively it can be seen that at other voltages only two new phenomena are likely to emerge, namely, frequency-pushing by current fluctuations and amplitude modulation by voltage fluctuations, both at video-frequencies. These are the cases for which $Z_1 = 0$ in the on-tune case. As for the old sources, the frequency-pushing and amplitude-modulation slopes may vary somewhat over the voltage "mode," but not, in the range of acceptable efficiencies, by orders of magnitude.

The importance of the two new sources may well reside in the possibility of greatly enhanced fluctuations at video-frequencies due to flicker effects. Their interest may thus be confined to very low modulation frequencies. Although the occurrence of enhanced velocity fluctuations at flicker frequencies has not, so far as the author is aware, been demonstrated, it seems reasonable to infer that the mechanisms responsible for flicker noise may also generate large-scale velocity fluctuations.

The case of video-frequency modulation can, as previously pointed out, be calculated directly from the unmodulated oscillation conditions by differentiating with respect to one or other of the operating parameters.

Considering the beam-current pushing, one gets, very approximately,

$$df_0/di_0 = \Delta f_0/i_0 \tag{25}$$

where Δf_0 is the amount by which the oscillation frequency differs from the natural cavity frequency. The value of Δf_0 is proportional to $V - V_0$ where V is the beam voltage and V_0 its value for maximum efficiency. Thus near the middle of the mode the curve of df_0/di_0 *versus* $V - V_0$ is a straight line through the origin.

Because of reactive beam loading at the separate gaps, also proportional to the beam current, the line is displaced, passing to the right or left of the origin according to whether the beam loading reactance is positive or negative. As this reactance is not very sensitive to beam voltage the new line is roughly parallel to the old.

The resulting f.m. modulation intensity is

$$\sigma_5 = (df_0/di_0)^2 2ei_0\Gamma_5^2 \tag{26}$$

where Γ_5^2 is the "reduction factor" for the current flicker noise. As explained above, σ_5 has a zero at one point in the voltage mode.

Similar considerations lead to an approximate expression for the a.m. noise temperature due to velocity fluctuations near the centre of the mode. It is

$$T_7 = \frac{P_0 S^2 \cot^2 S}{4ku_0^2}\, s_1(f) \tag{27}$$

where s_1 is the video-frequency velocity fluctuation spectrum. Equation (27) is zero just at the centre of the mode, where $\cot S = 0$.

6. DISCUSSION

Comparing expressions (13) and (10) we see that the background noise powers due to current noise and thermal noise are in the ratio

$$ei_0\Gamma^2 Z_4^2 / 2kT_0 G \tag{28}$$

or roughly of the order of the noise factor of the valve used as an amplifier, without feedback. As this is likely to be high, thermal noise is negligible.

Comparing now the current noise with velocity noise, the ratio of equations (5) to (7) is

$$S^2 \Delta\overline{i^2} Z_1^2 / u_0^2 \Gamma^2 Z_3^2 \tag{29}$$

As Z_1 and Z_3 will typically be of the same order, this ratio is likely to be low in a power oscillator, with a short drift time S, unless Γ^2 is small (good smoothing), since the spread in beam energy $\Delta\overline{u^2}$ is normally very small.

As a high degree of smoothing cannot be expected in fundamental and harmonic bands simultaneously, it seems likely that the main source of a.m. noise will be current fluctuations either at radio-frequency or in a harmonic band. In view of expressions (12) and (13), correlation effects between current and velocity noise must also be small compared with the current effect alone. Similar conclusions are found for the f.m. fluctuations.

The a.m. noise results contain the expression $Z_2(x)$ in the denominator. As this tends to zero rapidly for small bunching parameters x, the a.m. noise can be expected to increase as the amplitude of the oscillation decreases. Taking, for example, equation (10), the numerator vanishes as x^2, whereas the denominator vanishes as x^6. Quiet operation is obtained by promoting a high degree of bunching.

The f.m. results, on the other hand, all contain the factor f_0/Q, the loaded bandwidth of the radio-frequency cavity. At the same time the transit angle S appears only in the expressions for velocity noise, which is negligible. To build a low noise oscillator with the large pushing figure that may be required in particular applications therefore requires a long drift length and a lightly loaded cavity. As these are also the characteristics of low-power oscillators, an oscillator-amplifier combination is likely to be quieter than a power oscillator.

As the a.m. and f.m. fluctuations over most of the video spectrum have the same sources, correlation between them should be observable. At the lowest modulation frequencies, beam-current flicker noise will become the principal a.m. source, and may also contribute to the frequency modulation. On the other hand, flicker type velocity fluctuations may arise, possibly correlated with the beam current fluctuations, also contribution to the f.m. noise. Thus there may or may not be any correlation between the low-frequency a.m. and f.m. noise.

7. CONCLUSIONS

It has been shown that towards the middle and the higher end of the video-frequency spectrum the principal sources of amplitude and frequency modulation are shot and partition noise in the beam at oscillation and harmonic frequencies. The background noise temperature generated by the amplitude modulation is given by equations (7) to (11) and by equation (15). The frequency modulation spectral density is given by equation (20). It is defined at the beginning of Section 4.

There should exist a measurable degree of correlation between the a.m. and f.m. fluctuations.

Velocity fluctuations and thermal noise in the cavity are negligible as sources at these modulation frequencies.

At sufficiently low frequencies the modulation spectra will show a rise characteristic of flicker effect. The a.m. noise is then given by equation (7) and the f.m. noise by equations (18) or (26), depending on the extent to which the velocity fluctuations exhibit flicker noise.

ACKNOWLEDGEMENT

Acknowledgement is due to the Board of Admiralty for permission to publish this paper.

REFERENCES

(1) CHODOROW, M., and FAN, S. P. *Proc. Instn Radio Engrs*, **41**, p. 25 (1953).
(2) STEWART, J. L. *J. Appl. Phys.*, **26**, p. 409 (1955).
(3) GOTTSCHALK, W. M. *Trans Inst. Radio Engrs. Prof. Group on Electron Devices* ED-1, No. 4, pp. 91–98 (1954).

APPENDIX

List of symbols

$\overline{\quad}$ (bar), spatial average value. Some of the functions used vary in value from point to point over the cross-section of the electron beam, as, for example, the d.c. current density in the beam. The bar over an expression indicates that an average value of the expression over the beam cross-section is to be used, the average being evaluated using the d.c. beam current density as a weighting function.

β_1, gap coupling factor for the buncher gap. This is the ratio between the maximum energy (in electron volts) acquired by an electron in crossing the gap and the peak radio-frequency voltage across the gap.

β_2, coupling factor for the catcher gap.

Γ_{12345}, shot noise "space charge reduction factor" [see equation (8)].

$\Delta\overline{u^2}$, the mean square deviation from the mean of electron velocities in the unmodulated beam.

Δf, the frequency spacing of the noise sideband under consideration from the carrier frequency.

Δf_0, the amount by which the mean oscillation frequency differs from the natural resonance frequency of the cavity.

σ_{12345}, f.m. spectral density. See Section (4) for definition.

e, electronic charge.

f_0, mean oscillation frequency.

G, real part of driving-point admittance seen from the catcher gap in the absence of the beam (but including beam loading admittances).

i_0, d.c. beam current.

$J_m(x)$, Bessel function of the first kind, order m.

k, Boltzmann's constant.

m, order of harmonic (0 corresponds to video-frequency band, 1 to carrier-frequency band, 2 to second harmonic band, etc.).

P_0, carrier power delivered to load.

Q, loaded Q factor of radio-frequency cavity.

S, transit angle (radians) from centre of buncher to centre of catcher gap for an unmodulated electron.

$s_1(f)$, power spectrum for beam velocity fluctuations. s_1 is the contribution from unit frequency bandwidth about f to the total mean square velocity fluctuation.

$s_2(f)$, power spectrum for beam current fluctuations (see s_1).

$s_{12}(f)$, cross power spectrum for current and velocity fluctuations. A measure of the correlation between them.

T_c, equivalent noise temperature of conductance G. Available noise power from G is kT_c per unit bandwidth.

T_{123456}, equivalent background noise temperatures for a.m. noise sidebands. Noise power delivered to load is kT per unit bandwidth.

u_0, mean electron velocity in unmodulated beam.

V, beam voltage.

V_0, beam voltage for oscillation at natural resonance frequency of cavity.

$w(f)$, a.m. noise sideband power spectrum. Noise power delivered to load is $w(f)$ per unit bandwidth.

x, bunching parameter $= \frac{1}{2}S\alpha_1\beta_1$, where α_1 is the ratio of peak radio-frequency voltage across the buncher gap to the d.c. beam voltage, and S and β_1 are given above.

Z_1, see equation (2).

Z_2, see equation (3).

Z_3, see equation (9).

Z_4, see equation (11).

Z_5, see equation (17).

Z_6, see equation (19).

Z_7, see equation (21).

The display of logarithmic Langmuir probe characteristics on a cathode-ray oscillograph

By A. R. Johnston, B.Sc., Ph.D., Physics Department, The Queen's University of Belfast

[*Paper received* 8 *February*, 1956]

A new method for displaying Langmuir probe characteristics on a persistent screen cathode-ray oscillograph is described. The cathode-ray oscillograph traces are recorded on microfilm. A comparison is given of the values of some discharge parameters obtained by this method and those found by measuring the probe current with a galvanometer.

The electron temperature, electron density and space potential in the plasma of a low-pressure electrical discharge can be measured from the graph of the logarithm of the electron current to a probe *versus* the probe potential relative to either electrode of the discharge.[1] Near space potential, the positive ion current to the probe is small compared with the electron current. Measurements of the plasma parameters can then be made by plotting the logarithm of the total probe current against the probe potential, over a range of about 20–30 dB with respect to the current at space potential.

A method whereby semi-logarithmic probe characteristics were displayed on a cathode-ray oscillograph is illustrated in Fig. 1. A resistance R was placed in series with the probe P, and the voltage drop across R, which is proportional to the probe current, was applied to the input of a d.c. logarithmic amplifier A. This amplifier was similar to one described by Taylor.[2] The logarithmic characteristic of the amplifier was obtained by using two type W61 variable-mu valves and a type 6AG7 sharp cut-off pentode in parallel. The voltage across R was attenuated by approximately one-tenth at the input to the second type W61 valve. The characteristic of A is shown in Fig. 2. The input voltage required by A is rather large, hence large values were used for R (up to 0·5 MΩ variable by steps of approximately 10 kΩ).

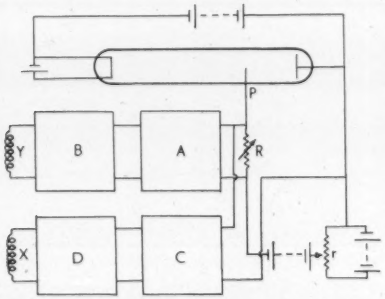

Fig. 1. Block circuit diagram illustrating the method of displaying semi-logarithmic probe characteristics on a cathode-ray oscillograph screen

A, logarithmic stage of the *Y* amplifier; *C*, differential cathode follower; *B*, *D*, linear d.c. amplifiers. Details of the discharge tube circuits (stabilizing resistance, etc.) are not shown, being standard.

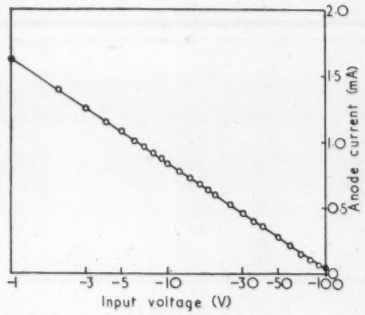

Fig. 2. The anode current *versus* input voltage of the amplifier *A*

The output of A was fed through a linear d.c. amplifier B to the Y-coils of a type 5FP7 magnetic deflexion oscillograph. The sensitivity of the latter was increased by reducing the normal anode-voltage to 400 V, giving full-scale deflexion in the vertical direction for 10 mA in the Y-coils. The amplifier

A could be adjusted to give an output of 10 mA, but as this reduced the input-voltage range over which the characteristic was logarithmic to 34 dB, the arrangement with an intermediate d.c. amplifier was preferred.

The potential difference between probe and anode, never more than 40 V, was recorded through the current in the *X*-coil, with maximum current of 30 mA for full-scale deflexion, through a differential cathode follower *C* and a linear d.c. amplifier *D*. The grid current at the input of *C* was negligible compared with the probe currents.

The probe potential was altered by varying the potentiometer resistance *r* (Fig. 1) manually. The time required to produce a single trace on the cathode-ray oscillograph with calibration spots was of the order of 15 s. The trace was photographed on 35 mm film, keeping the camera shutter open during this time. A typical characteristic enlarged from one of these is shown in Fig. 3.

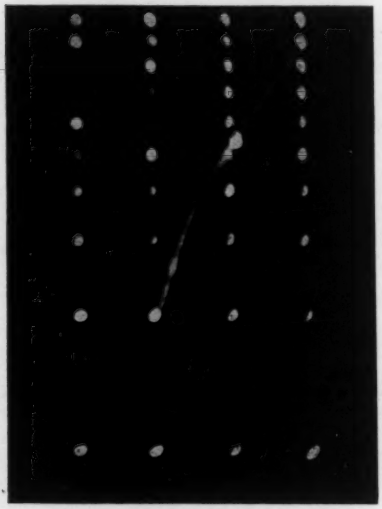

Fig. 3. A typical oscillogram

The large spot width is due to the low anode voltage on the cathode-ray oscillograph. The field of the vertical deflecting coils was not uniform at the edges of the screen. These two factors limit the accuracy with which the space potentials can be measured from the oscillograms. Both vertical and horizontal calibration marks correspond to 5 V intervals.

To check the accuracy of the method, probe characteristics were recorded using both a galvanometer and the cathode-ray oscillograph circuit under, as nearly as possible, identical discharge conditions. Some characteristics obtained with the galvanometer are shown in Fig. 4 as full lines; the circles are taken from the corresponding cathode-ray oscillograph traces.

Within the accuracy of the measurements, which is 10% or rather better, it is seen that the electron temperatures obtained by the two methods are the same. Curve (4) of Fig. 4 shows that a difference of 0·5 V can occur between the measured space potentials. This difference is due to the width of the cathode-ray oscillograph trace with the particular oscillograph employed and might be reduced.

The circuit described has been used in this laboratory to obtain rapid surveys of conditions in the plasma of hot cathode discharges which it is impracticable to run steadily for long periods, and, in particular, to obtain electron temperature measurements in them.

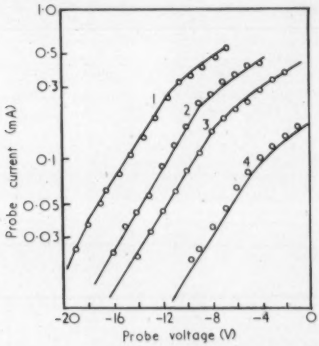

Fig. 4. The full lines are characteristics obtained using the galvanometer. The circles represent experimental points taken from the oscillograms for the corresponding characteristics. The voltage scales have been staggered to prevent overlapping of the curves. The discharge conditions for the characteristics are:

curve (1) anode voltage = 45 V, anode current = 75 mA;
curve (2) anode voltage = 29 V, anode current = 60 mA;
curve (3) anode voltage = 27 V, anode current = 40 mA;
curve (4) anode voltage = 25 V, anode current = 20 mA.

The probe was a 2 mm square of molybdenum in the positive column of a hot-cathode discharge through mercury vapour at a temperature of 19° C, in a tube 17·6 cm² in cross-section, and 50 cm long.

ACKNOWLEDGEMENTS

The author wishes to thank Prof. Emeleus for his advice and assistance during this work.

REFERENCES

(1) LANGMUIR, I., and MOTT SMITH, H. M. *Gen. Elect. Rev.*, **27**, p. 810 (1924).

(2) TAYLOR, J. R. *Electronics*, **10**, p. 24 (1937).

Correspondence

Measurement of the electrical conductivity of the oxide-coated cathode

During the course of an investigation into the dependence of the conductivity of the oxide-coated cathode upon the porosity of the coating, a simple experimental arrangement has been developed which we believe to be superior to other devices used for this purpose. The method of a probe wire embedded in the coating[1,2] has the disadvantage that the concentration of field near the surface of the fine probe wire causes a major part of the probe-cathode resistance to be concentrated in this small region. The actual conductivity is therefore difficult to assess. At high currents local heating in this region may cause errors in temperature. In addition, such local heating will cause thermal expansion of the probe wire which may crack open the coating. The method of using two conductivity wires in a coating on a ceramic base[3] avoids some of these difficulties but provides no means of measuring temperature in the important range below that of an optical pyrometer. Another method uses two button-type cathodes, under a pressure contact.[4] In our experience, the thermal expansion of the support rods in such a device introduces considerable design problems. Tungsten helical springs may be used for supports, but these must be balanced and wound in an opposite sense or the cathode buttons will be subjected to a torque which will tend to fracture the coating material placed between the buttons. Such springs will lose their temper when used at high temperatures so that the pressure is reduced and the buttons may pull apart when cooled.

Direct thermionic emission can occur through cracks or other fractures in the coating, and therefore results derived from systems liable to mechanical stress are not reliable at high temperatures. Other indirect methods[5,6] of determining conductivity are restricted to the temperatures at which emission is appreciable.

The present device is of the two-cathode type but mechanical difficulties are avoided by heating the assembly by means of 1 Mc/s eddy currents. The assembly, contained in a Pyrex envelope, consists of two similar annular nickel disks, between which the coating is sandwiched (Fig. 1). The average coating thickness is 150 μ. Contacts are made to the disks by means of thin foil strips so that no differential expansion or torque is introduced.

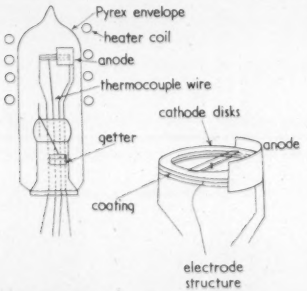

Fig. 1. The experimental tube

For the conductivity measurements a voltage was applied between the two disks. For the emission measurements use was made of an anode in the shape of part of a cylinder coaxial with the disks, and the emission was measured from the outer edge of the coating with the two disks connected together to form the cathode. Temperature was measured by means of a thermocouple. A preliminary series of measurements showed that the temperature distribution over the disks was quite uniform provided that they were symmetrically placed on the axis of a simple helical work coil of the radio-frequency heater.

The current-voltage characteristics of a well-activated triple (BaSrCa) oxide coating on O nickel core disks were measured in the range ± 20 V by an a.c. method using oscilloscope display. The changes of activation which would occur during a point-by-point d.c. plot were thus avoided. The radio-frequency heater magnetic field had no significant effect on the conductivity or emission currents. This was tested by observing the current-voltage characteristics both before and immediately after switching off the field; there was no noticeable change other than a smooth decay as the temperature fell. The conductivity given by the slope of the central part of the characteristic was measured also by an a.c. bridge method using an applied signal voltage of less than 0·1 mV r.m.s. The variation with temperature of the conductivity of a typical coating is shown in Fig. 2; the curve

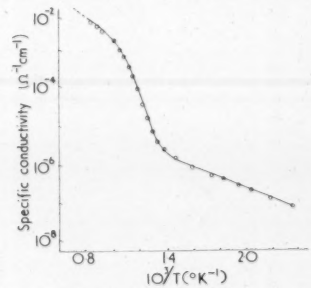

Fig. 2. Typical plot of the conductivity of (BaSrCa) oxide as a function of temperature

is similar to those observed previously by other methods. From such curves, the conductivity due to emission in the pores is deduced. In the tubes examined to date, this conductivity depends on pore size to an extent at least as great as that predicted by Hensley.[7]

From 300–600° K the current-voltage characteristics are approximately linear, but above 600° K (the cross-over temperature) a change occurs which is coincident with the change to a higher slope in the $\log \sigma$ *versus* $1/T$ curve of Fig. 2 because of the commencement of thermionic emission

in the pores of the material. The characteristics are now non-linear and symmetrical, but in the whole voltage range above ± 3 V approximately (corresponding to a field strength of 200 V/cm) there is a linear region of reduced slope. Above 600° K, the ratio of the slope at zero current to this final slope increases with temperature; this ratio is almost constant for a short temperature range below 1000° K and begins to decrease again above 1000° K. For a dense coating a maximum ratio of 5 : 1 has been obtained; for more porous specimens the maximum ratio was somewhat higher.

Similar results have been reported previously by one of us,[2] but then a maximum ratio of only 2 : 1 was obtained. A simple theory based on that ratio was presented but this theory must now be modified in the light of the new results. A complicated model would be required to give a detailed explanation of all our observations; however, it seems likely that the change in slope of the current-voltage characteristics is essentially due to saturation of the emission which occurs in the pores of the coating.

We wish to thank Prof. E. E. Zepler for valuable criticism and discussion, and we are also indebted to the Research Laboratories of the General Electric Co. Ltd. for presenting a number of carbonate mixtures used in this and other work for deriving oxide coatings.

University of Southampton. T. B. TOMLINSON
R. E. J. KING

REFERENCES

(1) WRIGHT, D. A. *Proc. Roy. Soc. A*, **190**, p. 394 (1947).
(2) TOMLINSON, T. B. *J. Appl. Phys.*, **25**, pp. 720–724 (1954).
(3) HANNAY, MACNAIR and WHITE. *J. Appl. Phys.*, **20**, p. 669 (1949).
(4) LOOSJES, R., and VINK, H. J. *Philips Res. Rep.*, **4**, p. 449 (1949).
(5) COOMES, E. H. *J. Appl. Phys.*, **17**, p. 647 (1946).
(6) EISENSTEIN, A. *Phys. Rev.*, **71**, p. 473 (1947).
(7) HENSLEY, E. B. *J. Appl. Phys.*, **23**, p. 1122 (1952).

New books

The microscopy of animal textile fibres (including methods for the complete analysis of fibre blends). By A. B. WILDMAN. (Leeds: Wool Industries Research Association, 1954.) Pp. viii + 209. Price 42*s*.

As might be expected in a volume published by the Wool Industries Research Association the emphasis in this one is essentially on the practical. The main body of the book is divided into two parts, one dealing with techniques (including an account of the methods used for the production of the many beautiful micrographs with which it is illustrated) and the other with results. An animal fibre (wool, hair, bristle, etc.) may be readily distinguished from other natural or man-made fibres by observation of its cuticle (an external sheath of flattish overlapping scales which envelops the body or cortex of the fibre) and its medulla (a core of spongy texture which is sometimes present). The principal object of the book is to study the scale edge pattern and the type of medulla, in the hope that this might help in the more difficult problem of distinguishing between varieties or types of animal fibre, and as an essay in systematics this is undoubtedly an advance on anything which has been attempted hitherto in this field. It is, of course, only too easy to pick holes in a system which is frankly qualitative, but since it is claimed that this one allows a fibre to be "easily and correctly placed," it is not unreasonable to mention difficulties which one reader, at least, has found. The weakness of the method is best illustrated by the definitions of "close," "distant" and "near" on p. 55: "Where successive scale margins are obviously very close together they are known as *close*," and so on. In fact, however, it may be said that any shortcomings in the verbal systematization are more than outweighed by the advantages of having gathered together in one place a selection of micrographs which Dr. Wildman's standing guarantees to be authentic and as representative as possible of the types of fibre considered. Their general excellence is only marred by the distortion seen in some of the rolled impressions, whose appearance suggests that some longitudinal movement of the fibre must have accompanied the rolling, and by the curious lack of quantitative significance in some of the legends, for example, that of Fig. 55, where fibres of diameter 20 μ and 65 μ are reasonably said to be fine and coarse, respectively, whereas the fibre giving the rolled impression is described as coarse, although its perimeter (measured by the micron scale provided) is only 47 μ.

The book is intended "to help those interested in fibre microscopy as applied to textile and allied industries"; if this refers to unskilled or semi-skilled workers in industrial testing laboratories the inclusion of descriptions of sampling techniques, and perhaps even the economic-geographical details of the habitat and productivity of the various animals may be justifiable; those whose interests in fibre structure are more than superficial would, perhaps, have welcomed instead more comprehensive first and last chapters (dealing, respectively, with growth in the follicle and fine details of the structure). Incidentally, the title of the book should strictly have been modified by the insertion of "optical" before "microscopy."

H. J. WOODS

Numerical analysis. By Z. KOPAL (London: Chapman and Hall Ltd., 1955.) Pp. xiv + 556. Price 63*s*.

By present day standards this is a large book for one author, partly because of a somewhat expansive style of writing, but also because the treatment is more detailed than in other recent books on the same subject. The book is based on lectures given by the author to students of science and engineering at the Massachusetts Institute of Technology. He hopes that it will serve both as an advanced text-book for undergraduates and as a research handbook. While it undoubtedly qualifies as the latter, the reviewer doubts whether there are many undergraduates in British Universities who have either the time or the money to spend on such an extensive work of this kind. It is not a book for beginners, but it can be strongly recommended to those who already have some knowledge of numerical analysis and who wish to read more deeply.

The full title is *Numerical analysis with emphasis on the application of numerical techniques to problems of infinitesimal calculus in single variable* and so we find nothing about algebraic equations of higher degree or about simultaneous algebraic equations, and, of course, partial differential equations are missing. After an historical introduction there

is a chapter on interpolation, followed by chapters on numerical differentiation and the solution of ordinary differential equations. Many formulae for numerical integration are derived and some are subsequently applied to the solution of integral and integro-differential equations. Throughout the book methods and the use of formulae are illustrated by numerical examples. At the end of each chapter are numerous examples for the reader to attempt; some are straightforward but others are almost research problems. Another valuable feature is that each chapter concludes with biographical and historical notes which serve as a guide to further study. Special mention should be made of Chapter 5 which deals with two-point boundary and eigen value problems by algebraic methods as distinct from the more familiar analytical methods of the Rayleigh–Ritz type considered in Chapter 6. No other English book describes the algebraic approach.

Apart from the occasional misprint which must be expected in a book of this kind, the standard of production is excellent. Sometimes the author's emphasis seems a little inconsistent. Thus, for example, in Chapter 5 he devotes forty-four pages to methods using ordinates but only seven to finite-difference methods though he feels the latter to be more useful. Also several techniques are relegated to appendices though they are stated to be either more powerful or of wider application than some discussed in the main text. However, these are minor criticisms of a valuable and scholarly work written in an engaging style.

J. CRANK

Transmission-line theory. By R. W. P. KING. (London: McGraw-Hill Publishing Co. Ltd., 1956.) Pp. xii + 509. Price 90*s*.

The object of this book was to provide a fundamental introduction to the study of wave guides, cavities and antennas. Briefly the scope of the book is as follows.

Chap. 1. The equations of an infinite line are derived both by means of a conventional lumped circuit approach, and also rigidly using potential functions, for a number of important cross-sections.

Chap. 2 deals very thoroughly with the terminated line and introduces the Cartesian circle diagram and Smith chart.

Chap. 3 is headed "Impedance and admittance" and treats a very wide variety of transmission line circuits, including the hybrid junction.

Chap. 4 deals with current, voltage distributions; power transfer, resonance curves, etc.

Chap. 5 considers discontinuities and non-uniformities in transmission lines.

Chap. 6 is unusual in a book of this kind and concerns transmission-line oscillators and coupled sections of transmission lines.

The general style of the book is analytical and though no advanced mathematics is used some of the analysis is quite long and difficult. Potential functions are used throughout and field theory is not mentioned. The work is characterized by rigour and precision of definition and it is most gratifying to see the degree of approximation categorically stated rather than implied by the usual "large compared to wavelength" remark. A number of problems are given for each chapter.

A very large number of circuits of practical importance are dealt with and the book should prove valuable for reference purposes, though in this connexion the frequent back references are a handicap and an accessible list of symbols would have proved helpful. The reviewer was pleased to note a number of British names in the comprehensive list of references (159), the index too is excellent.

The general finish of the book is what one now expects from a McGraw-Hill publication though unfortunately it is accompanied perhaps inevitably by a very high price.

P. D. DUNN

Scattering and diffraction of radio waves. By J. R. MENTZER. (London: Pergamon Press Ltd., 1955.) Pp. viii + 134. Price 30*s*.

This is the seventh monograph in the series "Electronics and waves" published under the general editorship of D. W. Fry and designed to report on the most recent research and state of theory in certain branches of electronics and applied physics.

In this volume stress is laid on the mathematical treatment of scattering and diffraction as applied to the calculation of radar cross-section of obstacles such as a cylinder, a sphere, a cone and a thin plate. The treatment of the diffraction and scattering problems involved is full and thorough, but it assumes a good grounding on the part of the reader in electromagnetic theory. By avoiding repetition of basic mathematical principles which can be found in any good mathematical text, the monograph is kept short and to the point. The point, however, is somewhat narrow and limits the book's usefulness to those workers intimately connected with the subject-matter. Whether they require such a text is another matter. The last chapter deals with the technique of measurement of radar cross-section and is followed by a useful bibliography of forty-five items.

The book is excellently produced, the print, figures and layout of formulae, etc., being easy to follow and pleasing to the eye. It is a valuable addition to a reference library.

M. H. N. POTOK

Physical techniques in biological research. Vol. 1. Optical techniques. Edited by G. OSTER and A. W. POLLISTER. (New York: Academic Press Inc., 1955.) Pp. xi + 564. Price $13.50.

There is an increasing tendency to attack the exciting problems arising in biology with ideas and techniques derived from physics and physical chemistry. This is the first of three volumes which contain descriptions written by specialists (the authorship is international) of a large number of physical techniques that have been found useful. The theoretical basis of each technique is outlined in a simple manner, together with practical details of the technique and necessary instrumentation, and examples illustrating their application are included. Mathematical treatment, where it is necessarily employed, is elementary, formulae of any complexity being quoted.

Chapter 1 (J. L. Rosenberg) deals with photochemistry and luminescence and contains a physical description of the quantum basis of light absorption and the various ways in which an excited molecule can lose its absorbed energy. A clear description of the light scattering method for determining the relative molecular weights of large molecules is given by G. Oster. Chapter 3 (C. F. Hiskey) contains a good account of the fundamental principles of absorption spectrophotometry necessary for an understanding of this method of measurement. There follow chapters on ultra-violet (J. F. Scott) and infra-red (C. Clark) absorption spectroscopy, both of which contain a good deal of information of practical value to the working spectroscopist. A valuable feature of

these articles is their extensive list of references to the literature and to sources of spectral absorption data. Chapter 6 (L. C. Martin) is a most useful practical and theoretical introduction to the critical adjustment and use of the ordinary light microscope. The article by H. Osterberg on phase and interference microscopy describes the simple vector theory of phase contrast. The section on the measurement of phase difference by interference microscopy appears to be over-complicated and the description of the adjustment of an interference microscope (p. 407) is certainly misleading. G. Oster describes clearly the nature and production of polarized light and the origin and measurement of birefringence and dichroism. Finally, there is an interestingly written account of electron microscopy (V. E. Cosslett) which contains a most valuable collection of details for the intending microscopist. Indeed, the collection of useful practical details and hints for making successful experiments is a feature of the volume.

Volume 1 is well produced, but does not lack misprints; one glaring example being the statement (p. 102) that a sheet of Polaroid cannot absorb more than 50% of the energy from an incident polarized light beam.

It is noted that the second volume will deal with the non-optical techniques (but will include X-ray diffraction) and that the third volume will deal more specifically with cells and tissues. While part of the material in this volume is to be found elsewhere, in the increasing number of reviews that are being written on physical techniques, it contains a comprehensive collection of data which will be a valuable compact source of reference.

H. G. DAVIES

Applications of spinor invariants in atomic physics. By H. C. BRINKMAN. (Amsterdam: North-Holland Publishing Co., 1956.) Pp. 72. Price 22*s*.

The method of spinor invariants introduced by Kramers in 1930 allows investigation of the transformation properties of one or many electron systems under co-ordinate rotations without appeal to group theory. Applications include the classification of states by their angular momenta, a detailed discussion of electron spin, electron–electron interactions, spin orbit interactions and spectral line intensities. The book is mathematical and reasonably concise but the method seems more limited and more intricate than the normal group–theoretical approach.

W. M. LOMER

Structure Reports for 1942–1944. Vol. 9. General editor: A. J. C. WILSON. Section editors: N. C. BAENZIGER, J. M. BIJVOET and J. MONTEATH ROBERTSON. (Utrecht: N.V. A. Oosthoek's Uitgevers Mij, 1956.) Pp. viii + 448. Price £6 6*s*. 0*d*.

The appearance of this volume brings in sight the end of another stage in the project which is to provide a complete series of informative and critical reports on all published structural data; for to close the gap between the cessation of *Strukturbericht* with volume 7 for 1939 and the initiation of *Structure Reports* with volume 11 for 1947–8, we now need only one more volume (8, for 1940–1).

The present volume maintains the high standard of the series. It is surely an indication of expert planning that the only considerable new feature in this, the fifth volume to appear, is the inclusion of a new index for carbon compounds with a classification based on the numbers (first) of carbon atoms and (second) of hydrogen atoms in the molecule. On sampling the text, the reviewer formed the impression of an increase in the amount of cross-referencing by the Editors; no doubt this is to be expected when coping with the arrears. Perhaps the reviewer was unlucky in detecting printing errors in four out of ten pages scrutinized in detail as a test for accuracy: p. 63, line 11 from bottom, words "change pattern" should be transposed; p. 64, references in text to numbering of diagrams on the same page are wrong; p. 263, under heading "Pyroxenes" the year of N. F. M. Henry's paper in *Miner. Mag.* should be 1942, not 1932; p. 416, reference 1 should read ". . . I. Woodward, . . ." (not F. Woodward)—unimportant errors, admittedly, but too numerous!

It is always easy to find fault with the work of others. In spite of minor criticisms, however, it is clear that each new volume adds to the indebtedness of all concerned with the use of structural data; many of these users would be the first to acknowledge how much their own work has been helped forward by the painstaking efforts of the Editors. More volumes, please, as soon as possible!

W. H. TAYLOR

Micro-indentation hardness testing. By B. W. MOTT. (London: Butterworth's Scientific Publications, 1956.) Pp. viii + 272. Price 42*s*.

In the late 1930's metallurgists started using diamond hardness indenters with extremely small testing loads for the determination of the hardness of thin deposits, brittle materials and even individual constituents of a micro-structure. A considerable literature has grown up since then which is comprehensively reviewed in this very welcome book primarily intended for metallurgists, but including some references to micro-indentation hardness testing of non-metallic materials.

The initial chapters describe the basic concepts and the available equipment, and the factors affecting the values recorded. Full discussions on the application of micro-indentation methods to metals and non-metallic materials leads to a final interesting short chapter on future developments, in which the author gives his views on the probable developments in the instruments and in their field of application.

The book is well produced and illustrated and many references are given. Clearly it will be of great value in many laboratories and should be widely used. The only criticism the reviewer wishes to offer is on the somewhat inadequate index which omits all reference to authors. The fact that the 500 or so references are listed together at the end does not eliminate the need for an author index as the references are listed in the order in which they are quoted. This, however, is a small criticism of an excellent book.

G. L. BAILEY

Kinetic theory of liquids. By J. FRENKEL (New York: Dover Publications, Inc., 1955.) Pp. xi + 488. Price $3.95.

This is a serviceable reprint of the original, published in 1943, under conditions scarcely encouraging for a work of this nature. The author's main thesis is that a special kind of "carry-over" of properties exists in the neighbourhood of the melting point. Thus, "rigidity-order" in liquids passes over into "fluidity-disorder" in solids, a typical kinetic process.

The contents include a discussion of crystal characteristics, fusion, heat motion, orientation problems, surface phenomena, phase transitions, solutions and high polymers. In following these principles, a bridge has been thrown across the gulf that divides classical physics from the more recent quantum developments so far as solid-liquid transitions are concerned. The whole is clearly set out in a convenient format.

F. I. G. RAWLINS

Notes and comments

User specification for high-temperature X-ray powder diffraction cameras

The user specifications which are prepared by the Equipment Sub-committee of the X-ray Analysis Group of The Institute of Physics are intended to record and make generally known those details of design which crystallographers consider essential in any instrument which they may use.

The existing user specification for high-temperature X-ray powder diffraction cameras was first published in 1950 and a revision is now being considered. Suggestions on any aspect of the design of this type of camera are invited, and should be sent to the Honorary Secretary of the Equipment Sub-Committee (Dr. E. G. Steward, Research Laboratories, The General Electric Co. Ltd., Wembley, Middlesex).

Terms used in a.c. power system studies

A thirty-page British Standard has been published with the title *Guide to terms used in a.c. power system studies* (B.S. 2658: 1956). It has been based on proposals submitted by the British Electrical and Allied Industries Research Association. Since it is intended as a guide rather than merely as a glossary the definitions and explanations have been made more detailed and descriptive than is usual in a British Standard glossary. Where a term is defined in both a previously published glossary and in this guide the later definition is recommended.

The contents cover the following: load response terms, stability terms, synchronous machines, symmetrical components, governor characteristics, transformers, lines and cables. Letter symbols for many quantities appear in the text and are collected for reference after the list of contents.

It is intended to review the guide after a year. A revised edition will then be issued which will include any changes found desirable. Copies may be obtained, price 6*s*., from the British Standards Institution, 2 Park Street, London, W.1.

Corrosion at bimetallic contacts

A booklet entitled *Corrosion and its prevention at bimetallic contacts* has been published by H.M. Stationery Office on behalf of the Corrosion and Electrodeposition Committee of the Inter-service Metallurgical Research Council (Admiralty and Ministry of Supply). It attempts to provide up-to-date and reliable information on the subject, primarily for the benefit of designers in government departments and government contractors although it should be of considerable interest and value to all who are, or should be, concerned with metallic corrosion.

The text provides general information about the conditions in which bimetallic contacts are most likely to lead to troublesome corrosion and also about the means of mitigating such effects. This should be read in conjunction with a table which indicates the relative corrosion of a range of metals when brought into mutual contact and bridged by water containing an electrolyte. The metals listed in the table are arranged in two groups. The first is similar to the "schedule of potentials" included in many documents; the second group comprises chromium, stainless steel, titanium and aluminium, all of which develop highly protective oxide films. It is the metals in this second group that cause difficulty in attempting to predict the behaviour of bimetallic contacts from a schedule of potentials.

Copies of the booklet are available from H.M. Stationery Office, price 1*s*. 6*d*.

Errata

In the article which appeared on p. 199 of our June issue, right-hand column, the reference to the development of the Ace and Deuce computers *should have read* "resulting from the work of the N.P.L. Mathematics Division and the English Electric Co., Ltd."

Journal of Scientific Instruments

Contents of the July issue

SPECIAL ARTICLE

The language of instrument calibration and performance. By K. M. Greenland.

ORIGINAL CONTRIBUTIONS

Papers

A method for rapid analysis of very small gas samples. By H. E. Lewis and O. C. J. Lippold.

A simple differential pulse height analyser. By E. C. Park.

A sensitive and stable nuclear induction head. By E. A. Richards, G. Phillips and W. K. Campe.

A constant-volume, membrane, interferometric microrespirometer. By B. M. Turner.

An instrument for the automatic recording of hysteresis loops. By D. C. Gall and J. D. Watson.

The omegatron as a leak detector. By R. L. Bell.

An apparatus for producing air of controlled relative humidity for hygrometer calibration and testing. By L. A. Cram.

A high pressure methane ionization chamber. By F. J. M. Farley.

Laboratory and workshop notes

Adaptation of a gas and water union to high vacuum circuits. By A. D. Cassell and D. A. Hockly.

A parallel-spring cross-movement for an optical bench. By R. V. Jones.

The use of a ball-point recording system on the Dines anemometer. By E. A. Cohen.

A light interrupter of continuously variable on-off ratio. By T. P. Brody.

A dual-purpose specimen spinner for transmission and reflexion X-ray diffraction. By P. N. Bestelink and D. R. Holmes.

A tapered plug vacuum valve. By H. R. Moore.

The infra-red spectrometer as a non-dispersive instrument. By R. Burt and G. J. Minkoff.

NOTES AND NEWS

Correspondence

A capacitance-resistance hygrometer. From J. MacDowall; C. L. Cutting, A. C. Jason and J. L. Wood.

New books

New instruments, materials and tools

Notes and comments

THIS JOURNAL is produced monthly by The Institute of Physics, in London. It deals with all branches of applied physics (including theory and technique).

All rights reserved. Responsibility for the statements contained herein attaches only to the writers.

EDITORIAL MATTER. Communications concerning editorial matter should be addressed to the Editor, The Institute of Physics, 47 Belgrave Square, London, S.W.1. (*Telephone:* Sloane 9806.) Prospective authors are invited to prepare their scripts in accordance with the *Notes on the preparation of contributions*. (Price 2*s*. 6*d*. including postage.)

REPRODUCTION. The Institute of Physics is a signatory to The Royal Society's Fair Copying Declaration. Details may be obtained upon application from The Royal Society, London, W.1.

ADVERTISEMENTS. Communications concerning advertisements should be addressed to the agents, Messrs. Walter Judd Ltd., 47 Gresham Street, London, E.C.2. (*Telephone:* Monarch 7644.)

CLAIMS FOR MISSING JOURNALS. Claims from regular subscribers to this *Journal* for missing numbers will only be considered if received within 60 days of the date of mailing plus normal outward time of transit and time for lodging the claim. Losses attributable to failure to notify a change of address or to similar omissions will not be considered.

SUBSCRIPTION RATES. A new volume commences each January. The charge is £4 per volume ($11.50 U.S.A.), including index (post paid), payable in advance. Single parts, so far as available, may be purchased at 8*s*. each ($1.15 U.S.A.), post paid, cash with order. Orders should be sent to The Institute of Physics, 47 Belgrave Square, London, S.W.1, or to any bookseller.

Physics in oceanography*

By K. F. Bowden, M.Sc., F.Inst.P., Oceanography Department, University of Liverpool

The physics of the oceans is a subject in which considerable progress has been made in recent years, largely because of the increasing application of new techniques. Some examples of the development or adaptation of physical methods for research at sea are described, with some of the results they have given in problems such as those of waves, storm surges and ocean currents.

INTRODUCTION

Oceanography has been defined as the study of the oceans in all their aspects. The subject is so wide and varied, however, that it has come to be divided into branches such as marine biology, physical oceanography, chemical oceanography, and so on. The name marine physics is preferred to physical oceanography by some workers in this branch of the subject and it has the advantage of indicating that it deals with the techniques and theories of physics as applied to the study of the sea. This article describes some examples of the progress made within the last ten years or so, due to the increasing use of physical ideas and techniques.

WAVES

Sea waves are considered to be so familiar to everyone that descriptions of waves of sound, light, heat or radio are often given in terms of waves of the sea. More than a century ago, mathematical treatments had been given of idealized systems of waves, such as an infinite train of waves of similar form or the waves radiating from an initial, localized disturbance. For many years, however, little progress was made in relating the theories to the irregular and ceaselessly changing appearance of the waves in a rough sea. The experimental study of waves was greatly stimulated during the last war by the need to be able to forecast waves on landing beaches, and the investigations then started are still being followed up.

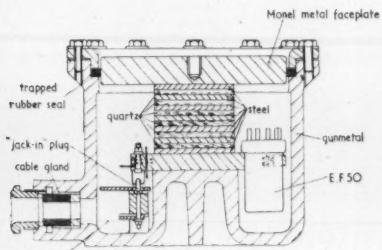

[Reproduced from *Dock and Harbour Authority*]

Fig. 1. Piezo-electric wave recorder

The first need of a study of waves is to be able to record them so that they can be accurately measured and analysed. In shallow water, one obvious method is to photograph the waves passing a graduated pole, and this has been used, but a more convenient method is by a pressure gauge laid on the bottom. Such a gauge may be up to a mile or so from the beach and connected by cable to the recording apparatus on the shore. One example of this type of gauge is the piezo-electric wave recorder, shown in Fig. 1. This instrument is, in fact, a very low frequency quartz hydrophone, consisting of slices of quartz crystal sandwiched between steel plates. The sea pressure acts directly on the faceplate and is transmitted to the quartz. The electric charges which appear on opposite faces of the quartz produce a varying voltage proportional to the wave pressure. After one stage of amplification in the sea unit itself, the signals are sent along a cable to the shore where they are amplified further and recorded. One of the prototypes of this wave recorder, which was designed by an Oceanographic Group at the Admiralty Research Laboratory, was laid at Perranporth in Cornwall and worked satisfactorily for over five years.

As an alternative to the pressure instruments, another form of wave recorder for use in shallow water consists essentially of an echo-sounder, laid on the bottom and transmitting upwards, so providing a continuous record of the waves passing over it. These and other types of wave recorder have been described by Tucker.[1]

The recording of waves from a ship in the ocean sea is a more difficult problem than recording near the shore, because of the absence of a fixed level of reference. Apart from visual estimates of wave height, length and period, methods using buoys or drogues released from the side of the ship have been used. Such methods are not very satisfactory, however, and it is difficult to lay and recover instruments from a ship in a rough sea. In 1951, members of the staff of the National Institute of Oceanography designed a ship-borne wave recorder, which is completely contained in the ship itself.[2] The principle of this instrument is shown in Fig. 2. The height of the sea surface above a fixed level is measured in

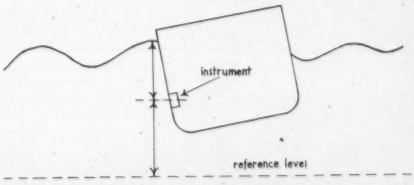

[Reproduced from *Dock and Harbour Authority*]

Fig. 2. Ship-borne wave recorder

* Based on a lecture given to the Manchester and District Branch of The Institute of Physics on 14 October, 1955.

two stages. The first part of the instrument, mounted on the side of the hull, about 10 ft below the normal water-line, is a pressure recorder which measures the rise and fall of water against the ship's side. The displacement of this point on the ship's side, relative to a fixed horizontal surface, is measured by an accelerometer which responds to the vertical acceleration of the point at any instant. The movement of the accelerometer mass is converted to an electrical output which is integrated twice thus giving the vertical displacement of the point above a fixed but arbitrary level.

In the actual instrument, the pressure element and the accelerometer, supported in gimbals, are contained in the same housing, and a pair of such units is used, bolted to the hull on opposite sides of the ship. The electronic apparatus, which integrates the output from each accelerometer and adds it to the pressure signal, is fitted in a convenient position elsewhere in the ship. The original instrument of this type was used in R.R.S. "Discovery II" and, during the first voyage with it in the North Atlantic, the growth of waves from calm conditions up to heights of 30 ft was recorded. Since February, 1953, a ship-borne wave recorder has been in regular use in the "Weather Explorer," one of the British weather ships in the North Atlantic. The highest waves recorded have been just over 50 ft high, whereas in six years' recording off the coast of Cornwall, in a depth of 80 ft, the highest wave recorded was 35 ft. Analysis of the wave spectra has shown significant differences between waves in the open ocean and those reaching the coast. For the same conditions of wind strength and fetch, the waves recorded in the open ocean were greater in height and shorter in period.[3] Ship-borne wave recorders have recently been fitted in three U.S. ships, the R.V. "Atlantis" of Woods Hole Oceanographic Institution and two other ships for research on ship motion due to waves.

Any wave record contains a superposition of waves of many different periods and an important step was the development of a method of analysing the record into constituent waves of a series of periods, i.e. a wave spectrum. Fig. 3

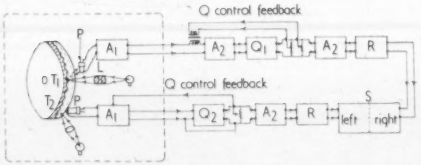

[Reproduced by permission of Admiralty Research Laboratory]

Fig. 3. Harmonic wave analyser

A_1, first amplifier; A_2, amplifier; L, cylindrical lens; P, photocell; Q_1, high Q resonator; Q_2, low Q resonator; R, rectifier; S, pen recorder; T_1, main pick-up; T_2, time-trace pick-up.

shows the principle of the harmonic wave analyser developed for this purpose. The record, in the form of a black and white profile on a strip of photographic paper, 8 ft long and 5 in. wide, representing about 20 min of wave record, is wrapped around a flywheel, whose speed is run up to a certain value and then reduced gradually. The record is illuminated by a line of light and the light scattered from the record, which is proportional to the displacement due to the wave, is picked up by a photocell. The electrical output from the cell is passed through a sharply-tuned resonant circuit. When the wheel is rotating at high speed, the alternating signals due to the longest waves present in the record are in resonance and are recorded. As the speed is reduced, waves of successively shorter periods resonate and so a spectrum of the waves is plotted. The scale of periods is provided by a second recording channel which scans the time trace. Fig. 4(*a*) shows a small portion of a wave record and Fig. 4(*b*) shows the wave spectrum of the whole record given by the analyser. In this spectrum a band of long period swell from a distant storm is seen separated from the shorter waves generated by local winds.

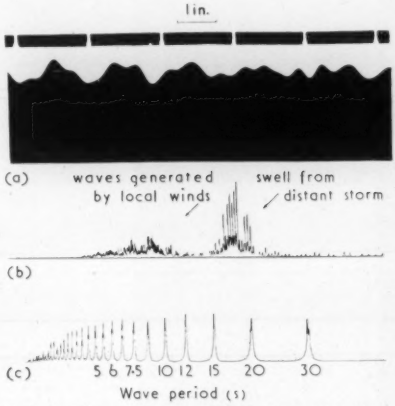

[Reproduced by permission of Admiralty Research Laboratory]

Fig. 4. Harmonic analysis of wave record

(*a*) Sample of wave record and time trace.
(*b*) Analysis of wave record.
(*c*) Analysis of time trace.

A study of wave spectra has been of great value in relating recorded waves and swell to the winds in the storm areas where they were generated. In this way methods of forecasting waves from the meteorological data may be developed and some light thrown on the physical processes of wave generation. Examples of this are given by the work of Barber and Ursell[5] and of Darbyshire.[6]

The question of wave generation is bound up with that of the stress of the wind on the sea surface. The full-scale study of these effects has been assisted by model experiments. In one such set of experiments, Keulegan,[7] at the Bureau of Standards in Washington, found that adding soap or detergent to the water prevented the formation of waves at wind speeds which would normally be high enough to produce them. At the same time the tangential stress of the wind, as shown by the surface slope which it produced on water in a closed channel, was reduced. These results were confirmed on a larger scale by Van Dorn,[8] working on a model yacht pond near San Diego, California. Results such as these suggest that the stress of the wind on the sea surface is made up of two parts: a "skin friction" which is always acting and a "form drag," which depends on the waviness of the surface and can be suppressed under certain conditions. Unlike most cases in aerodynamics, the form drag arises from a form

which is not rigid, but is moving relative to the water and continually changing its shape.

STORM SURGES

When the movement of water under the action of the wind is restricted by coasts, the piling-up of water which results may give rise to storm surges, such as those which have caused severe damage around the coasts of the North Sea on a number of occasions. In the absence of disturbances due to wind stresses or the direct effect of barometric pressure, the tidal rise and fall of water along a coast can be predicted with a high degree of accuracy; the heights of high water and low water to within a few tenths of a foot and the times into the North Sea. At the same time, an anticyclone was developing over the Atlantic, so that a very steep pressure gradient was set up in the rear of the depression, resulting in the most severe northerly gale ever recorded in the British Isles. Fig. 5(*a*) shows the meteorological chart for midnight on 31 January–1 February, and Fig. 5(*b*) shows the lines of equal disturbance of sea level, in units of $\frac{1}{10}$ ft, at the same time. The lines of equal disturbance are approximately perpendicular to the wind direction. The greatest surge height occurred from East Anglia across to the mouths of the Scheldt. South-west of this the level fell somewhat, due to the escape of water through the Straits of Dover, which acted as a partial safety valve. Subsequently the level fell on the English side but continued to rise for several hours on the

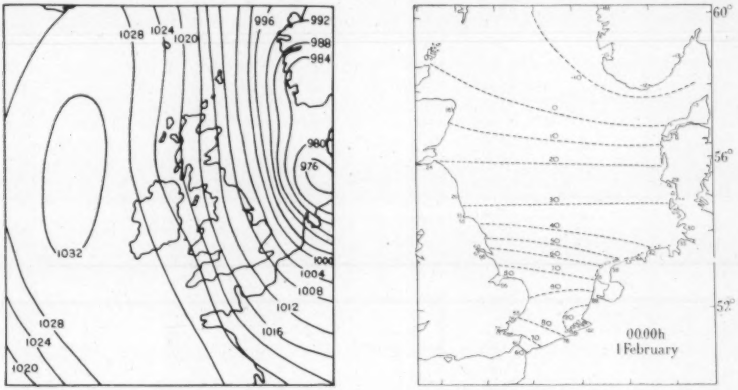

(*a*) (*b*)

[Reproduced from *Philosophical Transactions of The Royal Society*]

Fig. 5. Meteorological chart (*a*) and sea level disturbance chart (*b*) at 00.00 h on 1 February, 1953. Pressure is in mb and sea level disturbance in units of $\frac{1}{10}$ ft

to within a few minutes. At times, however, meteorological effects cause the sea level to deviate considerably from the predicted values, and a study of these effects is one of the most important aspects of tidal research today. In Britain this is being undertaken mainly at the Liverpool Tidal Institute. An example is provided by Rossiter's[9] analysis of the surge of 31 January–1 February, 1953, which caused the disastrous floods in eastern England and in Holland.

The surge height is defined as the height by which the actual water level exceeds the predicted level, and is found by eliminating the predicted values from the levels recorded by tide gauges. The course of the surge was found in this way for a number of places around the coasts of the North Sea. The peak of the surge occurred progressively later as one travelled southwards along the east coast of Great Britain. In East Anglia and south-east England, the sea level rose very rapidly shortly before midnight on 31 January. The maximum peak height of the surge, about 9 ft, occurred at King's Lynn.

The meteorological depression responsible for the surge passed about half-way between the north of Scotland and the Faroes, travelling eastwards, and then turned south-eastwards Dutch coast. The influence of the earth's rotation which, in the northern hemisphere, causes the level to rise to the right of a current, was apparent in the progress of the surge. While water was being driven southwards into the North Sea the levels were higher on the British coast but when, with a slackening of the wind, the excess water began to flow out again the level was higher on the coasts of Holland and Denmark.

In the problem of predicting storm surges in given meteorological conditions, considerable progress can be made empirically. It is probable that in the long run, however, further advances will depend on a better understanding of the dynamics of their generation and propagation. In this, physical problems arise such as the stress of the wind on the sea surface, the frictional stress between the water and the sea bed and the interaction of the tide and the surge.

WIND-PRODUCED CURRENTS

It is not only in such exceptional conditions as storm surges that oceanographers are interested in water movements and how they are influenced by wind. Fisheries research workers,

for example, wish to know the effects of water movements averaged over a period of, say, a month, and the methods of measurement should be robust enough to continue to work regardless of bad weather conditions. Shortly before the last war, observations were started from a number of light-vessels in the North Sea, with the vertical log current meter, designed by Carruthers.[10] This instrument has a stoutly constructed rotor, consisting of six anemometer-type cups, which is turned by the current and is suspended by a length of chain which also communicates its rotation to a counting mechanism. This is contained in a wooden box, supported on a boom projecting from the side of the ship. The direction of the current is measured separately by a logship which is allowed to stream with the current at the end of a rope, the direction of the rope being measured by a simple device. Since the main object of the investigation was to eliminate the tidal currents, the readings of the instrument were taken and analysed so as to give the direction and speed of the residual flow, averaged over a mean lunar day of 24 h 50 min.

Observations from light-vessels with the vertical log current meter were re-started in 1950, and at the time of the surge of 31 January–1 February, 1953, were in operation from eight light-vessels in the North Sea and Straits of Dover. In normal conditions, water enters the North Sea from the north and flows down the east coast of Britain. Flow from the English Channel, through the Straits of Dover, joins this and the combined flow turns north-eastwards along the Belgian and Dutch coasts. At the "Varne" light-vessel, which is in a strategic position near the centre of the Straits of Dover, observations over several years have shown that the mean rate of flow from the Channel towards the North Sea is 3·5 sea miles/day (approx. 0·15 knot).

The residual flow for several days covering the surge of 31 January–1 February, 1953, was given by Lawford,[11] from

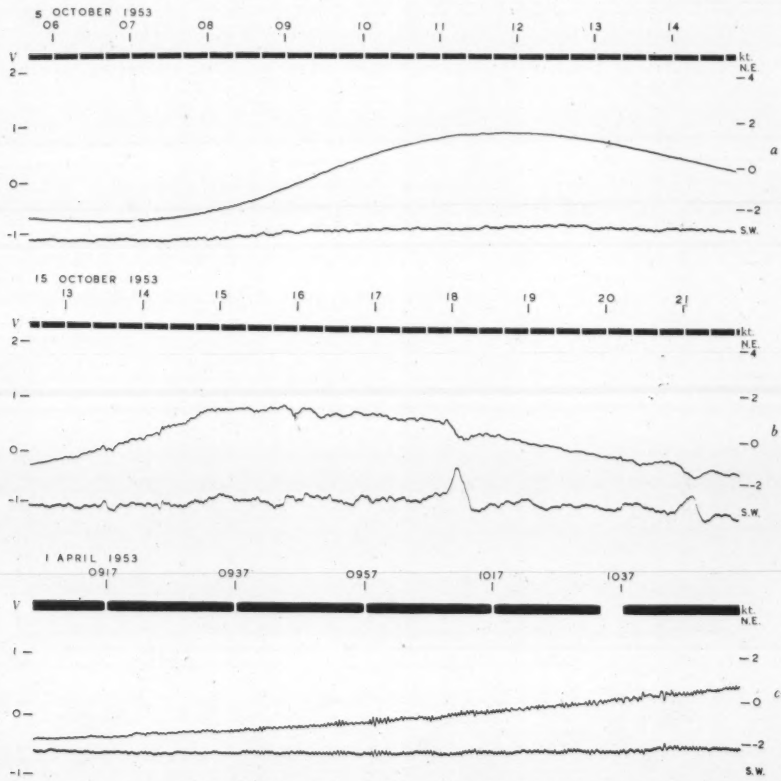

[Reproduced from *Philosophical Transactions of The Royal Society*]

Fig. 6. Typical records from St. Margaret's Bay—Sangatte cable

an analysis of the vertical log records. Owing to the method of measurement, the mean current over a lunar day was given, which was undoubtedly less than the peak current during the surge. From the "Varne" results, the flow on 1 February was 28·4 sea miles/day towards the south-west, and the south-westerly flow continued, although at a reduced speed, for several days. An increased south-westerly flow was also found at the "Galloper" light-vessel (off the Thames estuary), from 1 February onwards. At the "Terschelling Bank" off the north coast of Holland, there was an increased flow in an approximately easterly direction, reaching 37·7 sea miles/day on 31 January. These water movements, indicated by the vertical log data, are consistent with the changes in sea level in the Southern Bight of the North Sea, as shown by Rossiter's analysis.

There is a method of measuring the flow of water through a channel which was first suggested 120 years ago but has only come into practical use in the last few years. In 1832 Faraday, very soon after his discovery of electromagnetic induction, pointed out that water flowing in a channel would act as a moving conductor cutting the vertical lines of force of the earth's magnetic field, and would have an e.m.f. induced in it. He gave the Straits of Dover as an example, stating that the e.m.f. would change sign when the tidal currents changed direction. Faraday himself tried to observe this effect in the River Thames by suspending copper electrodes from Waterloo Bridge, but without any decisive result, due, no doubt, to electrochemical effects at the electrodes. The method has been used recently in a study of the currents in the Straits of Dover, following the observations of Cherry and Stovold[12] who, in the course of their work of restoring telephone communications between England and the Continent after the war, recorded tidal e.m.f.'s on four submarine cables.

If the water is moving along a channel with velocity V and Z is the vertical component of the earth's magnetic field, the induced e.m.f. E is directed across the channel, at right angles to V and Z. The magnitude of E is given by

$$E = VZL \times 10^{-8} \text{ volt}$$

where V is in centimetres per second, Z in gauss and L is the width of the channel in centimetres. Because of the

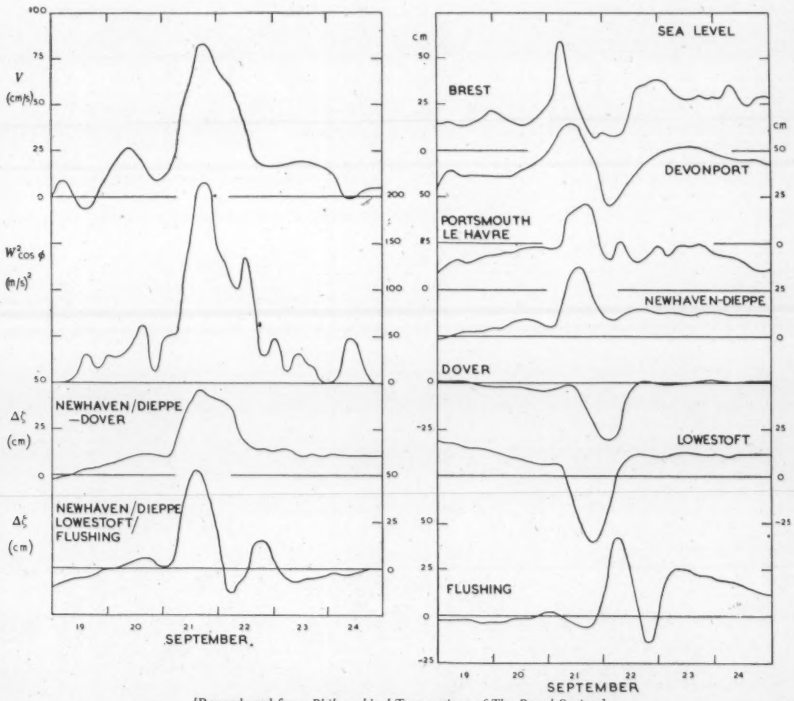

[Reproduced from *Philosophical Transactions of The Royal Society*]

Fig. 7. Curves of current V through the Straits of Dover, wind function $W^2 \cos \phi$, difference in sea level $\Delta\zeta$ and sea level ζ at various positions, 19 to 24 September, 1953

return flow of electric current through the sea bed, the potential difference measured between two electrodes on either side of the channel is less than E, however, by a factor depending on the specific resistivities of the water and the sea bed and the dimensions of the channel.

The cable used in the investigation in the Straits of Dover[13] crosses from St. Margaret's Bay, near Dover, to Sangatte, near Calais, a distance of 20 sea miles. It was found unnecessary to use special electrodes, the outer conductor of the coaxial cable being in electrical contact with the sea water and serving the purpose. On the French side the inner and outer conductors were connected together, while on the English side the potential difference was recorded by a galvanometer connected between the conductors.

Fig. 6 shows some typical records obtained in this way. The time scale is shown at the top, with time marks every 20 min. The voltage scale is shown on the left and the velocity scale in knots on the right. The top record is an almost perfect one and the tidal variation stands out clearly. The second record is taken under similar recording conditions but on a "disturbed day," the fluctuations being due to earth currents associated with geomagnetic disturbances. The lower trace shows the potential difference measured at the same time on a cable running inland from St. Margaret's Bay to Canterbury. The bottom record was taken at a higher paper speed and shows short period fluctuations, with periods of the order of 10 to 20 s. The calibration of the records in terms of knots per volt was determined by making use of previous measurements of tidal currents at a number of stations in the Straits.

To investigate the wind-produced currents, the tidal currents may be eliminated by the same method as that used in separating storm surges from the readings of tide gauge records. Fig. 7 shows curves obtained in this way for the period 19 to 24 September, 1953. The first curve on the left shows the current V, reaching a peak of 85 cm/s at 18 h on 21 September. The second curve shows values of $W^2 \cos \phi$, where W is the recorded wind speed at Lympne, the Meteorological Office station about 12 miles west of Dover, and ϕ is the angle between the wind vector and the north-easterly direction. On the assumption that the tangential stress of the wind is proportional to W^2 and in the same direction as the wind itself, the component of stress along the channel should be proportional to $W^2 \cos \phi$. This quantity reaches a peak almost simultaneously with V on 21 September. The third curve gives $\Delta\zeta$, the difference in sea level between a line from Newhaven to Dieppe and a line through Dover, i.e. the downward slope of the sea surface in the eastern end of the Channel, while the fourth curve gives the difference in level between two sections at approximately equal distances on either side of the Straits. The curves on the right show the changes in sea level at several ports in the English Channel and North Sea. This is an example of strong north-east-going flow, associated with a surge which travelled up the Channel, but had little effect on the elevation beyond the Straits of Dover. Other examples have been analysed in the same way, including a case of strong south-west-going flow which reached a peak of nearly 100 cm/s (2 knots) on 3 January, 1954, associated with a surge in the North Sea which raised the sea level at Lowestoft by 140 cm (4½ ft).

The cable method of measuring flow has been used in other places, a notable example being across the Straits of Florida from Key West to Havana,[14] thus crossing the Florida Current which flows from the Gulf of Mexico into the Atlantic Ocean, where it forms the beginning of the Gulf Stream. In this case the permanent current, with an average surface speed of 3 knots, is the dominant feature and the tidal currents are comparatively weak. The transport of water by the Florida Current, its variation from month to month, and its relation to variation in winds have been studied by this method.

OCEAN CURRENTS

Another application of the electromagnetic method has enabled currents in the open ocean to be measured by towing a pair of electrodes behind a ship.[15] A potential difference is produced which is proportional to the velocity of the drift at right angles to the line joining the electrodes, i.e. at right angles to the course of the ship through the water. By making measurements on two courses at right angles, the resultant velocity of the surface water may be determined. The potential difference is small, about 2 mV per knot when the distance between the electrodes is 100 yd, but with non-polarizing electrodes and suitable recording instruments the velocity can be measured with sufficient accuracy.

It is not immediately obvious that the electrodes should measure the potential difference due to the motion of the water while they are themselves drifting with it. In fact an electromotive force will be induced in the leads to the electrodes as well, and it is the difference between this electromotive force and the potential difference in the water which is actually measured. The potential difference in the water depends on the return flow of electric current through the sea bed and through the still water below the ocean current, when this does not extend to the bottom. For a given velocity of current, the measured potential difference will be greatest when the current extends only to a depth which is small compared with the total depth of water. This is usually true of the major currents of the surface layers, such as the Gulf Stream.

The method of towed electrodes is one of the new techniques introduced in recent years for the study of ocean currents. Another is the Bathythermograph, a diving thermometer which can be used from a moving ship to give a record of temperature against depth down to 900 ft.[16] The temperature measuring element is a copper spiral capillary tube, filled with xylene and connected to a Bourdon tube. A rise of temperature causes an increase of pressure in the xylene, resulting in a movement of the free end of the Bourdon tube and the stylus attached to it. The stylus marks a smoked glass slide, which is held in a holder attached to a metal bellows. As the Bathythermograph dives deeper, the hydrostatic pressure causes the bellows to contract against a steel spring and the slide-holder is moved in a direction at right angles to the movement of the stylus, so that a graph of temperature against depth is drawn.

Another instrumental tool which American oceanographers have found very useful in their investigation of the Gulf Stream is Loran, the navigational aid by which a ship can determine its position by measuring the time intervals between the arrival of radio pulses transmitted at fixed intervals from two pairs of stations. By this means the position of a ship can be fixed with greater accuracy and more frequently than by astronomical fixes. One application of this is to improve the method of determining surface currents by the drift which they impart to the ship. The ship may then be manœuvred, if desired, so as to investigate some special feature, such as the edge of a current or the axis of strongest flow.

The value of rapid temperature surveys of the surface layer by Bathythermograph is that they can give indications

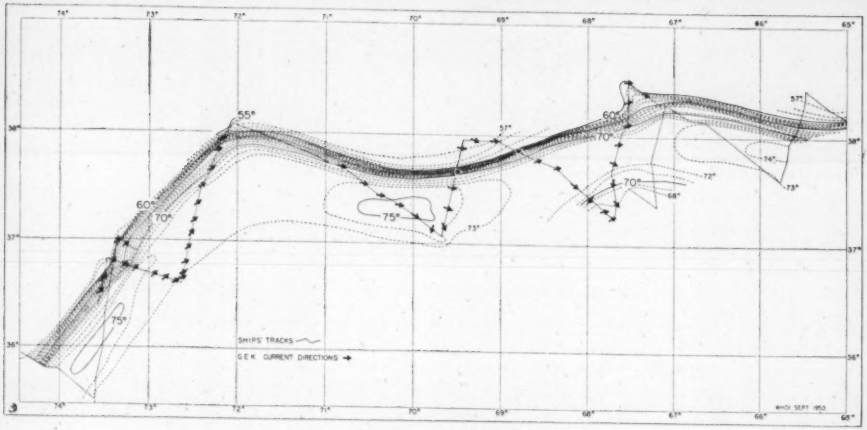

[Reproduced from *Tellus*]

Fig. 8. Mean temperature (° F), in the upper 200 metre layer of the Gulf Stream, 8 June, 1950

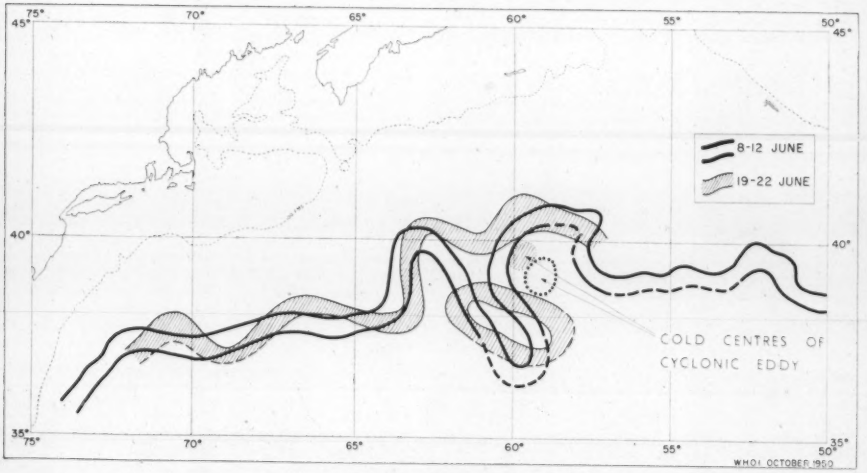

[Reproduced from *Tellus*]

Fig. 9. Positions of the "warm core" of the Gulf Stream during the first and last periods of "Operation Cabot," June, 1950

of the course of a current and its changes. It has been known for many years that the Gulf Stream marked the transition from the warm water of the Sargasso Sea on the south-east to cold water on the north-west. Since Benjamin Franklin, in 1775, initiated the regular measurement of sea temperature as a means of tracking the course of the Gulf Stream, many observations of surface temperatures have been collected from merchant ships making regular crossings of the area. By taking temperatures at various depths, as is done from research ships, and also taking samples of water to determine its salinity, the distribution of density can be found and from this the currents can be calculated. The method is analogous to that used in meteorology for calculating the direction and speed of wind from the barometric pressure as plotted on a weather chart.

Fig. 8 shows the course of the Gulf Stream as indicated by the mean temperature in the upper 200 metres on 8 June, 1950. This chart is one of a number representing the combined operations of six ships, five from U.S.A. and one from Canada, which took part in the most ambitious expedition in the Gulf Stream yet undertaken.[17] The strongest part of the Stream lies in the region of sharp change of temperature, shown by the closeness of the isotherms. This and other surveys have shown that the velocity in the swiftest part of the Gulf Stream is generally between 4 and 5 knots, but such velocities are confined to a band only 10 to 15 miles wide near the inshore edge of the current. Counter-currents with velocities up to 3 to 4 knots occur quite near the main current.

Fig. 9 shows the change in position of a portion of the Gulf Stream between the beginning and end of "Operation Cabot," the name given to the six-ship survey. The wave-like meanders in the current changed considerably during the interval, and one large loop is seen to have become completely cut off from the main stream and formed a detached eddy.

TURBULENCE

Figs. 8 and 9 give an example of the fine structure which is present in a major current system, such as the Gulf Stream, and the changes which are continually taking place. It is, in fact, an example of turbulent flow on a large scale. Fluctuations of a similar type are characteristic of all scales of motion in the sea and have a profound effect on the dynamics of currents, the exchange of heat energy or salt content between different water masses and other processes. Turning from the largest scale to a small-scale problem, an investigation of turbulence in a tidal current may be mentioned. The aim was to record the actual fluctuations in velocity, which are evidence of the eddying motion associated with the turbulent flow and are related to the frictional stresses in the water. Most current meters, including those of the propeller type, measure the average current over a period of several minutes or longer. To record turbulence, an instrument capable of responding to rapid fluctuations is required and a current meter was designed for the purpose by Doodson.[18] As seen in Fig. 10, this meter has a pressure wheel, similar to a propeller, but instead of revolving continuously, it rotates against springs so that the arc through which it turns is proportional to the speed of the current. The movement is communicated to the arm of a potentiometer and a voltage proportional to the velocity is transmitted up the cable to the recorder on board the boat. The instrument responds to all fluctuations with periods from approximately 2 s upwards.

There are several difficulties to be overcome in measuring the turbulent fluctuations. If the current meter is suspended from an anchored boat, the rolling of the boat or swinging of the meter on its cable may cause spurious variations in the measurements. When surface waves are present, the alternating velocities associated with them may be appreciable to a considerable depth. A successful series of measurements were made, however, in the Mersey estuary,[19] by supporting the current meter in a stand, within 6 ft of the bottom, as shown in Fig. 10. The lower frame could be adjusted in height according to the nature of the bottom, so that the vertical feet sank in as far as the frame. In a subsequent set of experiments, two current meters were used, supported in the same stand but with various separations, in order to compare the fluctuations at two neighbouring positions and so obtain an idea of the scale of the turbulence.[20] A typical record of simultaneous fluctuations at the two meters is shown in Fig. 11.

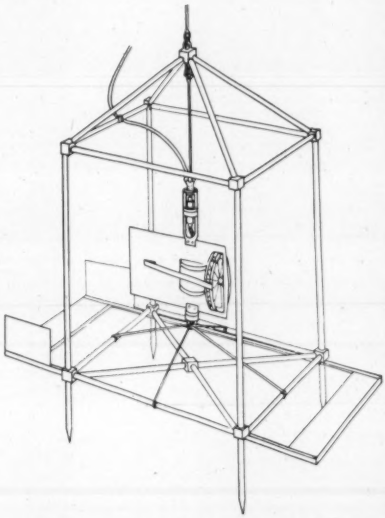

[Reproduced from *Proceedings of The Royal Society*]

Fig. 10. Stand for supporting the Doodson current meter

The analysis of these records follows similar lines to that of records of turbulence in a wind tunnel or in the atmosphere and consists mainly of computing various correlation coefficients, which may be interpreted in terms of the scale of the turbulence, or the range of sizes of eddies present. A recent development has been the use of an electromagnetic flow meter, supported on a tripod on the bottom, to record the vertical component of the turbulent velocity simultaneously with the horizontal component. The cross-correlation of these two components provides a direct measurement of the Reynolds' stresses in the water due to the shearing flow near the bottom.

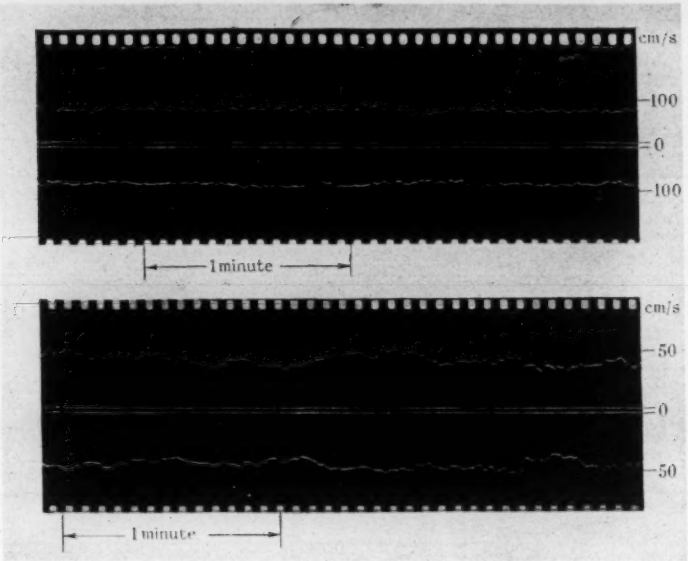

[Reproduced from *Proceedings of The Royal Society*]

Fig. 11. Two examples of simultaneous recordings by two current meters: (*a*) meters 7·3 and 9·0 metres below the surface; (*b*) meters separated horizontally by 75 cm, height 1·2 metres above the bottom

CONCLUSION

In a survey such as this it is necessary to select only a few topics of research for discussion. There are a number of other subjects, such as the acoustic properties of the sea, the transmission of light or the geophysical study of the sea bed, which would have been equally worthy of mention. No reference has been made, except in passing, to commercial developments like radio aids to navigation, echo-sounding, radar or underwater television, which have had their influence on methods of research at sea and have led to several special developments.

REFERENCES

(1) TUCKER, M. J. *Dock and Harbour Authority*, **34**, p. 207 (1953).

(2) TUCKER, M. J. *Nature* [*London*], **170**, p. 657 (1952).

(3) DARBYSHIRE, J. *Marine Observer*, **25**, p. 114 (1955).

(4) BARBER, N. F., URSELL, F., DARBYSHIRE, J., and TUCKER, M. J. *Nature* [*London*], **158**, p. 329 (1946).

(5) BARBER, N. F., and URSELL, F. *Phil. Trans A*, **240**, p. 527 (1948).

(6) DARBYSHIRE, J. *Proc. Roy. Soc. A*, **215**, p. 299 (1952).

(7) KEULEGAN, G. H. *J. Res. Nat. Bur. Stand.*, **46**, p. 358 (1951).

(8) VAN DORN, W. G. *J. Mar. Res.*, **12**, p. 249 (1953).

(9) ROSSITER, J. R. *Phil. Trans A*, **246**, p. 371 (1954).

(10) CARRUTHERS, J. N. *J. Cons. Int. Explor. Mer.*, **10**, p. 151 (1935).

(11) LAWFORD, A. L. *Weather*, **9**, p. 67 (1954).

(12) CHERRY, D. W., and STOVOLD, A. T. *Nature* [*London*], **157**, p. 766 (1946).

(13) BOWDEN, K. F. *Phil. Trans A*, **248**, p. 517 (1956).

(14) WERTHEIM, G. K. *Trans Amer. Geophys. Un.*, **35**, p. 872 (1954).

(15) VON ARX, W. S. *J. Inst. Nav.*, **4**, p. 117 (1951).

(16) SPILHAUS, A. F. *J. Mar. Res.*, **3**, p. 51 (1940).

(17) FUGLISTER, F. C., and WORTHINGTON, L. V. *Tellus*, **3**, p. 1 (1951).

(18) DOODSON, A. T. *Hydrogr. Rev.*, **17** (1), p. 79 (1940).

(19) BOWDEN, K. F., and PROUDMAN, J. *Proc. Roy. Soc. A*, **199**, p. 311 (1949).

(20) BOWDEN, K. F., and FAIRBAIRN, L. A. *Phil. Trans, A*, **244**, p. 335 (1952).

Dielectric properties of polar solutes in non-polar solvents at microwave frequencies

By D. E. CLARK, Ph.D., A.Inst.P., and S. N. KUMAR, B.Sc., The Northern Polytechnic, London, N.7

[*Paper first received* 11 *November*, 1955, *and in final form* 24 *February*, 1956]

The dielectric loss and permittivity of solutions of polar molecules in non-polar solvents have been measured at frequencies $9{\cdot}2 \times 10^9$ c/s and $3{\cdot}5 \times 10^{10}$ c/s. At the lower frequency independent determinations of absorption and wavelength were made on solutions of benzophenone over the temperature range 10 to 30° C. At the higher frequency the solute investigated was nitromethane and the temperature range was 10 to 40° C. Values of dipole moments obtained were 2·95 Debye units and 2·85 Debye units for benzophenone and nitromethane respectively.

It is well known that dipole moments of polar molecules may be determined by investigating the absorption characteristics of solutions of these molecules in non-polar solvents. Such measurements have been made with test sets operating at various spot frequencies covering the dispersive region (see, for example, Jackson and Powles[1]). Whiffen and Thompson[2] have also used the method of temperature variation. The present set of observations were made using temperature variation at fixed frequency and the results are compared with those of other authors using frequency variation.

1. MEASUREMENTS AT $9{\cdot}2 \times 10^9$ c/s

1.1. *General.* To determine the dielectric properties at this frequency, the fundamental measurements made were those for determining λ_g and α, the wavelength and attenuation constant, respectively, in the solution filling a length of waveguide. All measurements were made with H_{01} mode waves of fixed frequency ($9{\cdot}232 \times 10^9$ c/s) in rectangular waveguides, the oscillations being produced by a klystron oscillator operated from a stabilized power supply. Investigations were made on solutions of benzophenone in benzene and carbon tetrachloride.

1.2. *Determination of* λ_g. The following waveguide components, all horizontally mounted, were connected together in the order given: klystron oscillator, variable attenuator, wavemeter, test cell containing solution, variable short circuit. The test cell was a 34·5 cm length of brass waveguide sealed at each end by thin mica windows.

To determine λ_g a fixed probe was inserted into the test cell near one end and a movable probe near the other, the position of the latter being adjusted till the separation of the two probes was $\frac{1}{2}n\lambda_g$, an integral number of guide half wavelengths. The temperature of the solution was controlled by water circulating through a brass tube surrounding the test cell.

1.3. *Determination of* α. For this measurement the test cell was mounted vertically, with the end remote from the oscillator uppermost. It was preceded by a standing wave detector. The upper end of the cell was connected to a short section of waveguide containing a probe unit, and this section was terminated by a matched load. The rectified outputs from both the standing wave detector and the probe unit were measured by a direct-reading potentiometer balanced with a sensitive galvanometer.

When filling the cell the level of the solution at 15° C was adjusted to be 1 cm from the top of the cell, thereby ensuring no loss of liquid through thermal expansion at the highest temperature reached.

If E_{mx} and E_{mn} are the maximum and minimum values of the electric field in the standing wave detector, and E the field at the probe in the section following the test cell, then the mean power flow density at the input of the cell is:

$$P_1 = K_1 E_{mn} E_{mx} \tag{1}$$

and the mean power flow density at the output of the cell is:

$$P_2 = K_2 E^2 \tag{2}$$

where K_1 and K_2 are constants.

If P_1^+ is the forward power flow density at the nearer end of the cell, P_2^+ the forward power flow density at the further end and ρ the voltage reflexion coefficient at the further end, we have

$$P_2 = P_2^+(1 - |\rho|^2) = P_1^+[\exp(-2\alpha l)](1 - |\rho|^2)$$

l being the length of the liquid column.

But $$P_1 = P_1^+[1 - |\rho|^2 \exp(-4\alpha l)]$$

Hence $$\frac{P_1}{P_2} = \frac{1 - |\rho|^2 \exp(-4\alpha l)}{\exp(-2\alpha l)(1 - |\rho|^2)} \tag{3}$$

Combining equations (1), (2) and (3).

$$\frac{K_1 E_{mn} E_{mx}}{k_2 E^2} = \frac{1 - |\rho|^2 \exp(-4\alpha l)}{[\exp(-2\alpha l)](1 - |\rho|^2)} \tag{4}$$

Denoting corresponding quantities when the cell is empty by a suffix (0), we have:

$$\frac{P_{01}}{P_{02}} = \frac{k_1}{k_2}\frac{E_{0mn}E_{0mx}}{E_0^2} = 1 \tag{5}$$

Combining equations (4) and (5) and putting $E = E_0$ we have:

$$\frac{E_{mn}E_{mx}}{E_{0mn}E_{0mx}} = \frac{1 - |\rho|^2 \exp(-4\alpha l)}{[\exp(-2\alpha l)](1 - |\rho|^2)}$$

Hence

$$\exp(-2\alpha l) = \frac{-\sigma(1 - |\rho|^2) + \sqrt{[\sigma^2(1 - |\rho|^2) + 4|\rho|^2]}}{2|\rho|^2} \tag{6}$$

where $$\sigma \equiv (E_{mn}E_{mx}/E_{0mn}E_{0mx})$$

α was evaluated from equation (6).

Table 1. *Solutions of benzophenone in benzene.* (*Frequency* 9 2317 × 10^9 *c/s*)

Temperature (°C) \ Concentration	*benzene*		0·25 g *in* 100 cm³		0·5 g *in* 100 cm³		0·75 g *in* 100 cm³		1 g *in* 100 cm³	
	ε	tan δ × 10^3	ε	tan δ × 10^3	ε	tan δ × 10^3	ε	tan δ × 10^3	ε	tan δ × 10^3
10	2·298	1·33	2·308	3·41	2·318	6·885	2·327	10·32	2·336	13·70
15	2·293	1·32	2·304	3·415	2·315	6·84	2·322	10·35	2·332	13·67
20	2·289	1·31	2·2995	3·335	2·308	6·67	2·319	10·02	2·327	13·36
25	2·284	1·29	2·294	3·22	2·304	6·44	2·313	9·71	2·322	12·89
30	2·278	1·28	2·289	3·11	2·299	6·20	2·307	9·37	2·317	12·37

Table 2. *Solutions of benzophenone in carbon tetrachloride.* (*Frequency* 9·2317 × 10^9 *c/s*)

Temperature (°C) \ Concentration	*carbon tetrachloride*		0·25 g *in* 100 cm³		0·5 g *in* 100 cm³		0·75 g *in* 100 cm³		1 g *in* 100 cm³	
	ε	tan δ × 10^3	ε	tan δ × 10^3	ε	tan δ × 10^3	ε	tan δ × 10^3	ε	tan δ × 10^3
10	2·244	0·98	2·253	2·96	2·261	6·05	2·270	9·02	2·279	12·00
20	2·234	0·95	2·242	3·09	$2·251_5$	6·16	2·261	9·24	2·269	12·38
30	2·224	0·92	2·233	2·97	$2·240_5$	5·94	2·249	8·93	2·258	11·87

Table 3. *Solutions of nitromethane in benzene.* (*Frequency* 3·465 × 10^{10} *c/s*)

Temperature (°C) \ Concentration	*benzene*		0·1 cm³ *in* 100 cm³		0·15 cm³ *in* 100 cm³		0·22 cm³ *in* 100 cm³		0·3 cm³ *in* 100 cm³	
	ε	tan δ × 10^3	ε	tan δ × 10^3	ε	tan δ × 10^3	ε	tan δ × 10^3	ε	tan δ × 10^3
10	2·2895	1·44	2·298	4·33	2·302	6·48	2·306	8·76	2·313	13·20
20	2·287	1·55	2·295	4·22	2·299	6·37	2·303	8·58	2·310	12·82
30	2·284	1·61	2·292	3·92	2·295	5·78	2·300	7·95	2·306	11·73
40	2·282	1·65	2·287	3·36	2·291	5·08	2·296	6·85	2·302	10·25

Table 4. *Solutions of nitromethane in carbon tetrachloride.* (*Frequency* 3·465 × 10^{10} *c/s*)

Temperature (°C) \ Concentration	*carbon tetrachloride*		0·10 cm³ *in* 100 cm³		0·15 cm³ *in* 100 cm³		0·22 cm³ *in* 100 cm³		0·3 cm³ *in* 100 cm³	
	ε	tan δ × 10^3	ε	tan δ × 10^3	ε	tan δ × 10^3	ε	tan δ × 10^3	ε	tan δ × 10^3
10	2·234	1·26	2·243	3·91	2·250	5·84	2·254	7·77	2·261	11·66
20	2·232	1·26	2·240	4·04	2·244	6·05	2·250	8·06	2·257	12·09
30	2·229	1·27	2·236	4·04	2·240	6·06	2·245	8·09	2·253	12·10
40	2·226	1·27	2·233	3·91	2·237	5·80	2·241	7·82	2·250	11·70

Table 5. *Benzophenone in benzene*

Author	*Ref.*	μ × 10^{18} e.s.u.	*Relaxation time* τ × 10^{12} s	*Temperature* (°C)	*Method of measurement*
Holzmüller	7	2·95	16·1	24	Thermal method at 8 × 10^7 c/s.
Jackson and Powles	1	3·04	16·4	19	Over a spectrum of frequency passing through abs. maximum.
Whiffen and Thompson	2	2·88	22	19	Two-frequency method.
Cripwell and Sutherland	4	2·81	18·1	18·5	Two-frequency method.
Present work		2·95	15·88	20	Temperature variation around $T \tan \delta$ maximum.

Table 6. *Nitromethane in benzene*

Author	*Ref.*	μ × 10^{18} e.s.u.	*Relaxation time* τ × 10^{12} s	*Temperature* (°C)	*Method of measurement*
Whiffen and Thompson	2	2·87	3·9	19	Two-frequency method.
Cripwell and Sutherland	4	2·81	4·36	18·5	Two-frequency method.
Present work		$2·85_5$	4·24	20	Temperature variation around $T \tan \delta$ maximum.

The crystal in the standing wave detector was calibrated by the standard method of observing crystal current for various positions of the probe when the guide is terminated by a short-circuiting plate, sinusoidal spatial distribution of the field being assumed.

1.4. *Results at* $9{\cdot}2 \times 10^9$ *c/s.* The results at this frequency are given in Tables 1 and 2, where ϵ is the permittivity and $\tan\delta$ is the incremental loss tangent, the concentration being expressed in grammes of solute to 100 cm^3 of solution at 18° C.

Over the restricted temperature range involved, the variation of $T\tan\delta$ with T may be expressed by an equation of the type

$$T\tan\delta = a + bT + cT^2 \tag{7}$$

The maximum value of $T\tan\delta$ was calculated by least squares and the dipole moment, μ, of the solute determined from the relation:

$$\mu = \frac{\sqrt{\epsilon}}{(\epsilon+2)}\sqrt{\left[\frac{27k(T\tan\delta)_{mx}}{4\pi NC}\right]} \tag{8}$$

where K is Boltzmann's constant, N is Avogadro's number, C is the concentration in moles per cm^3, and T is the temperature in degrees absolute.

The relaxation time, τ, at any temperature may be determined from the relation:

$$T\tan\delta/(T\tan\delta)_{mx} = 2\omega\tau/(1+\omega^2\tau^2) \tag{9}$$

Equations (8) and (9) follow from the Debye equation[3]:

$$\tan\delta = \frac{(\epsilon+2)^2}{\varepsilon}\frac{4\pi}{27}\frac{\mu^2}{KT}NC\frac{\omega\tau}{1+\omega^2\tau^2} \tag{10}$$

The values of dipole moment and relaxation time for benzophenone thus determined from Table 1 are:

$$\mu = 2{\cdot}95 \text{ Debye units}$$

$$\tau \text{ (in benzene)} = 15{\cdot}88 \times 10^{-12} \text{ s at } 20^\circ \text{ C.}$$

The $T\tan\delta/T$ curves for the carbon tetrachloride solutions are broader and have smaller peak values than the corresponding curves for benzene solutions, thus indicating a probable distribution of relaxation times for the former solutions.

2. MEASUREMENTS AT $3{\cdot}5 \times 10^{10}$ C/S

2.1. *General.* Investigations were made on solutions of nitromethane in benzene and carbon tetrachloride. Results of previous investigators[4] at other frequencies indicate that an absorption peak might be expected within the temperature range 10–40° C at the frequency $3{\cdot}65 \times 10^{10}$ c/s. Such an absorption peak was observed.

2.2. *Experimental procedure.* This method of measurement was similar to that described in Sections 1.2 and 1.3. The figure indicates the components used for the determination of the attenuation constant of a solution. The power received by the crystal X_3 was determined when the cell was filled with solution and again when empty, the forward power flow, as indicated by the directional coupler D, being maintained constant. To determine the power flow density at the input surface of the cell, the reflexion coefficient at that surface was

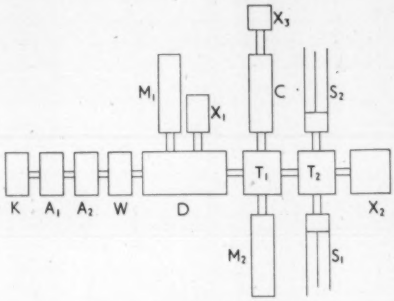

Apparatus used at $3{\cdot}5 \times 10$ c/s

K, klystron oscillator; A_1, level setting attenuator; A_2, rotary attenuator; *W*, wavemeter; *D*, directional coupler; M_1, M_2, matched loads; S_1, S_2, variable short circuits; T_1, T_2, hybrid tee junctions; X_1, X_2, X_3, crystals; *C* test cell.

obtained by replacing M_2 by a variable short circuit and proceeding in the manner described in Refs. (5) and (6).

The values of ϵ and $\tan\delta$ are given in Tables 3 and 4.

2.3. *Results at* $3{\cdot}5 \times 10^{10}$ *c/s.* The values for dipole moment and relaxation time for nitromethane are given below.

Nitromethane (using benzene): $\mu = 2{\cdot}85_5$ Debye units, $\tau = 4{\cdot}24 \times 10^{-12}$ s at 20° C;
nitromethane (using carbon tetrachloride): $\mu = 2{\cdot}83$ Debye units, $\tau = 6{\cdot}05 \times 10^{-12}$ s at 20° C.

3. COMPARISON OF RESULTS WITH PUBLISHED VALUES

Tables 5 and 6 enable a comparison to be made between the present set of observations and those published by other authors.

REFERENCES

(1) JACKSON and POWLES. *Trans Faraday Soc. A*, **42**, p. 101 (1946).

(2) WHIFFEN and THOMPSON. *Trans Faraday Soc. A*, **42**, p. 114 (1946).

(3) DEBYE. *Phys. Z.*, **35**, p. 101 (1934).

(4) CRIPWELL and SUTHERLAND. *Trans Faraday Soc. A*, **42**, p. 149 (1946).

(5) ROBERTS and VON HIPPEL. *Phys. Rev.*, **57**, p. 1056(*a*) (1940).

(6) BELJERS and VON LINDT. *Phillips Res. Rep.*, **6**, p. 96 (1951).

(7) HOLZMÜLLER. *Phys. Z.*, **38**, p. 574 (1937).

The expansion of mercury and fused silica between 0 and 300° C

By A. H. Cook, M.A., Ph.D., National Physical Laboratory, Teddington, Middlesex

[*Paper received* 7 *December*, 1955]

The determinations of the thermal expansion of mercury and fused silica have been reviewed. In principle the absolute hydrostatic balancing method is a more satisfactory way of measuring the expansion of mercury than deducing it from the expansion relative to a fused silica bulb, but a discussion of the determinations shows that despite the variability of the expansion of fused silica from specimen to specimen, systematic errors affecting the absolute determinations make them less reliable than the relative measurements of Harlow[14] and Beattie and others.[11] It is recommended that for the most accurate work, the expansion formula given by the latter authors should be used instead of that given by Sears.[27] The present uncertainty of the change of volume with temperature is about one or two parts in a million of the volume at 0° C for temperatures from 0 to 300° C, and may be as much as one part in ten thousand at other temperatures.

1. INTRODUCTION

The density of mercury at 20° C is at present being measured at the National Physical Laboratory and it is hoped that the final result will be correct to one part in a million, but to compare this value with others obtained at 0° C, as well as to deduce accurate values of the density at other temperatures, the change of density from 0 to 20° C must be known to better than one part in a million of the density. Accordingly the existing measurements of the expansion of mercury from 0 to 300° C have been reviewed, and since the most accurate determinations of the expansion of mercury seem to be those made relative to fused silica vessels, the measurements of the expansion of fused silica have also been examined.

The expansion of mercury has been measured absolutely, by the method of hydrostatically balanced columns, and relatively, by comparison with a container of known cubical expansion. In the absolute method,[1,2] the pressure exerted by mercury in a cold column is compared with that exerted by mercury in a hot column. To increase the pressure difference to be measured, Callendar and Moss[3] and Chappuis[4] used, respectively, six and seven pairs of hot and cold tubes connected in series, with the upper ends of the first cold and final hot tube connected to gauge tubes placed close together so that the difference in height of the mercury in them could be measured. The absolute method has the advantage that the measured expansion is independent of that of the container, but in applying it in practice two serious difficulties arise. The first is that, the columns being one or two metres tall, the oil or water baths containing them are large and it is difficult to keep the column temperatures uniform or to be sure that they are correctly measured. The second difficulty is that of defining and measuring the heights of the hot and cold mercury columns, these having no free surfaces.

Relative measurements, on the other hand, are less satisfactory in principle, but in practice much better results have been obtained. The mercury is contained in a vessel of which the volume is not usually more than one litre and which can be immersed in a well-stirred bath of convenient size having a steady well-defined, uniform temperature, while the relative expansion, found by weighing the mercury expelled from the vessel, can be determined to much better than one-millionth of the total volume. Results for relative expansion are therefore usually excellent, but to convert them to values of absolute expansion the cubical expansion of the vessel has to be known and this may introduce considerable uncertainty unless it is carefully investigated.

Recent workers have used silica vessels. The expansion of silica is small and the volume changes after a thermal cycle are negligible, but the coefficient of expansion at room temperature depends on the heat treatment to which the material has been subjected;[5] for instance, the expansion from 0 to 100° C may vary by over 5 %, that is, by more than 8 p.p.m. (parts per million) of the volume of 0° C. Thus, to obtain values for the absolute expansion of mercury that shall be correct to 1 p.p.m. of the initial volume, even over the range from 0 to 20° C, it seems essential to measure the expansion of the silica on a piece of the same material used to make the expansion vessel and to subject it to the same heat treatment. Even so, the cubical expansion may not be three

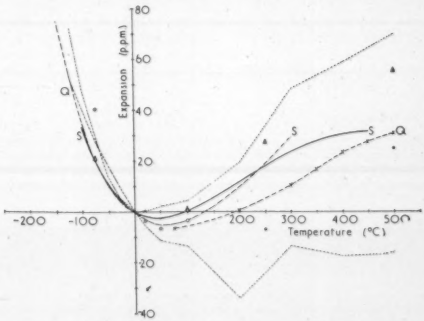

Fig. 1. Measurements of the expansion of fused silica where the expansion in parts per million is expressed as a difference from 0·5 t p.p.m. where t is temperature (°C)

——————— = formula of Beattie and others[11];
– · – · – · – = Callendar's formula;
– × — × — × – = Randall (above 75° C);
— · — · — = Valentiner and Wallot (below 20° C);
) = limits of Souder and Hidnert's results;
• = Holborn and Henning;
○ = Scheel (Heräus specimen);
△ = Scheel (Zeiss specimen);
S = fused silica;
Q = fused quartz.

Not all measurements between 0 and 100° C are shown.

times the measured linear expansion because of possible residual stress anisotropy.

These comments apply with greater force to determinations made with glass vessels for which the expansion is much larger than that of fused silica, the variation with heat treatment is probably also larger, and secular changes in volume and thermal hysteresis occur.

2. THE EXPANSION OF FUSED SILICA

The results of the observations made since 1903 are collected in Table 1 and shown graphically in Fig. 1. The comparator method, using a bar from 50 to 100 cm long and obtaining the change in length by comparison with a fixed length using micrometer microscopes; relative comparator methods in which the difference in length between two bars or tubes about 50 cm long is measured over a range of temperature, the one bar or tube being of a material of known coefficient; the absolute interferometer method in which the specimen, in the form of a ring of about 1 cm thickness, is the spacer in a Fizeau interferometer; and the relative interferometer method in which the difference in length between the specimen and a ring of known expansion is measured in a Fizeau interferometer.

Table 1. *Measurements of the linear expansion of fused quartz and silica*

(Values of mean coefficients from 0 to t°C* in units of 10^{-8}/°C.)

Author	*Chappuis*[28] §	*Holborn and Henning*[22] †		*Henning*[30]	*Scheel*[9, 32]	*Scheel*[12, 33]	*Scheel and Heuse*[34, 35]	*Randall*[10]	*N.P.L.*‖	*Callendar*¶	*Valentiner and Wallot*[36]	*Souder and Hidnert*[12]		*Beattie and others*[31]
Date	1903	1903		1907	1904, 1907	1907, 1921	1914	1910	1952	1913	1914	1926		1941
Method†	*I. R.*	*C, R.*			*I, R.*	*I, A.*		*I, A.*	*C, A.*	*I.*	*I, A.*	*C, A.*		*I, A.*
Material‡		*Heräus, Q.*			*Heräus, Q.* (2 *specimens*)	*Zeiss, Q.*		*Heräus, Q.*	*Thermal Syndicate*	*Thermal Syndicate*	*Zeiss, Q.*	17 *specimens extreme values*		*G.E.C., S.*
t: −250						−30·3								
−200		−31·0			−26·0	−14·2								
−150											0·2			2·4
−125											7·8	−8·0	+7·2	10·1
−100											15·4	+2·1	9·8	17·0
− 75					3·8	22·1					23·0	12·3	12·4	23·3
− 50											30·5	22·4	15·0	28·9
− 25											38·1	32·6	17·6	33·9
0	38·5				27·0	37·5			40·1	28·6	45·7	42·7	20·2	38·2
+ 20	40·8				30·8	41·2			41·7	33·6	51·8	50·8	22·3	41·2
+ 25	41·3								42·1	34·8				41·9
+ 50	44·3				36·7					39·6		54·7	28·0	45·1
+ 75	47·1							41·2		43·4				47·9
+100					46·5	50·7				46·6		54·4	36·8	50·2
+150										51·4				53·7
+200								50·3		54·9		59·8	38·2	55·9
+250			47·2			60·9				57·6				57·2
+300								53·5		59·8		66·1	45·6	57·9
+350								54·8						57·9
+400								55·8				64·7	45·7	57·6
+450								56·1						57·0
+500			55·0			61·1		56·2				64·0	46·7	

* Values are generally taken from authors' formulae but are entered only for the temperatures at or near which observations were made.

† *I*, interferometer method; *C*, linear comparator method; *A*, absolute; *R*, relative.

‡ *Q*, fused quartz; *S*, fused silica.

§ Source of material not reported.

‖ The figures are the results of N.P.L. observations on a line standard of fused silica made by the Silica Syndicate [Kaye[37]] Donaldson's[38] relative observations were made on this bar.

¶ Full details of Callendar's method do not seem to have been published. It is not stated at what temperatures the observations were made.

method used by each observer is given in the table; features of the methods are considered below. Vitreous silica is made in two ways, by fusing together crystals of quartz (fused quartz) or by local fusion of quartz sand (fused silica), the two forms being indicated by *Q* and *S* in Table 1. The principal maker of fused quartz was Heräus, who may also have made samples supplied by Zeiss, and most of the fused silica samples appear to have come from the Thermal Syndicate, previously the Silica Syndicate. There is no evidence in the results collected in Table 1 that the two forms expand differently, apart from differences due to annealing. Since Sosman[6] has reviewed the observations up to 1927, the present discussion concentrates on observations made since 1927 and on points which he did not consider.

Four methods have been used for measuring the coefficient of linear expansion of silica: the absolute line standard

The absolute comparator method is satisfactory over a small temperature range near room temperature but outside such a range the observations become inconvenient and distortion of the supports may tilt the bar; in general, any such tilt will make the measured change of length too small. The relative comparator methods, especially those of Holborn and Day[7] and of Blackie[8] and Douglas and Isard[5] are free of such troubles but the expansion of the reference bar has still to be measured.

The ends of the ring spacer for the interferometer methods have usually been relieved so that contact is made with each optical flat of the interferometer only along three short radial lines (see Scheel).[9, 40] It has been found, especially at high temperatures, that the separation of the optical flats at a given temperature does not repeat very well when the system is in air and Randall,[10] who ascribed this to variable air

films at the contacts, obtained much better results on evacuating the system; however, the observations of Beattie and others[11] still showed discontinuities which may be due to contact uncertainties even though the specimens were immersed in helium at a pressure of only 2 mm of mercury. Some observers have found that errors may occur in absolute measurements due to tilting of the specimen so that the optical flats are no longer perpendicular to the axis of the optical system of the interferometer; the measured expansion would then be too small.

The large scatter of the observations in Table 1 may be due in part to experimental error. The observations of Souder and Hidnert[12] are particularly open to criticism: in one arrangement of their apparatus the silica bar is supported horizontally in an oven and thin wires, which are led through grooves in the ends of the bar and loaded with weights so that they hang vertically, are observed with micrometer microscopes some distance below the bar and their separation found by comparison with a line standard. The main disadvantage of this arrangement is that any distortion of the bar or tilt due to distortion of the supports will produce an error which will usually make the measured expansion too small. The observed dilations of different specimens are not very consistent but, in general, the measured coefficients of expansion are lower than those obtained by many other observers.

However, some of the scatter is undoubtedly due to differences between specimens (see, for example, Blackie[8]). Douglas and Isard[5] have published curves showing the expansion of samples where the structure of the material is in equilibrium at various temperatures between 900 and 1400° C and it can be seen, for instance, that the mean coefficient of expansion between 0 and 100° C of a sample in equilibrium at 1000° C is about 5% greater than that of a sample in equilibrium at 1300° C. (Other curves show that a specimen may have to be held for a very long time at a given temperature before it attains equilibrium, for example, 250 h at 900° C.) At temperatures above about 400° C, the material in equilibrium at the higher temperature should show the greater expansion and although most of the observations given in Table 1 are not extended to high enough temperatures to check this, the differences between the results of Scheel and others[32,33,34,35] and Beattie and others appear to change sign at about 100° C. There is also an indication that the difference between the expansion of Callendar's material and Beattie's behaves as suggested by Douglas and Isard's results, for the mean coefficients are equal at about 250° C and thereafter the expansion of Callendar's material is the greater. This point is discussed further below (Section 3). The expansion of Randall's material probably exceeds that of Beattie's above 500° C.

Evidently absolute values of the expansion of mercury obtained from values relative to silica will not be reliable unless the expansion of the actual vessel is measured. Only Beattie and others[11] have done this and theirs are therefore the only measurements of the expansion of silica that will be considered further. They used a Fizeau interferometer to measure the expansion of a ring specimen absolutely from 0 to 450° C, immersing the apparatus in helium at a pressure of 2 mm of mercury and making the temperature changes in one continuous experiment without dismantling the apparatus. The observations showed unexplained discontinuities and the authors determined the expansion curve by grouping the observations in ten series separated by these discontinuities and adding an arbitrary constant to all the observations of a particular series so that the mean residual of the series from the fitted curve was made zero. Unfortunately, the authors do not say how large the discontinuities were. The standard deviation of a single observation is 0·84 p.p.m. (Beattie and others[11] give the r.m.s. deviation) and since the number of observations at any temperature varies from one to nine, the average being just less than four, the standard deviation of the mean value of the observed length at any temperature is about 0·45 p.p.m. and the standard deviation of any length calculated from the fitted curve will be slightly less. The corresponding standard deviation of the volume of this specimen at any temperature between 0 and 450° C as calculated from the curve will probably be between 1 and 1·5 p.p.m.

3. RELATIVE MEASUREMENTS OF THE EXPANSION OF MERCURY

There are four sets of observations with fused silica bulbs:

Harlow[13], measurements at 0, 100 and 184° C with two cylindrical bulbs;
Harlow[14], measurements at eight temperatures from 0 to 300° C with the 1911 bulbs and a spherical bulb;
James[15], measurements at 0 and 100° C only;
Beattie and others[11] measurements at ten temperatures from 0 to 350° C with two cylindrical bulbs.

The bulbs used by Beattie and others had already been used in gas thermometer studies and, as in those studies, they were immersed in an oil bath controlled thermostatically by comparison with a platinum resistance thermometer. The relative expansion of mercury was found from the mass of mercury expelled from the bulb. The standard deviation of a single measurement of the relative volume in a given bulb at a given temperature is about 0·7 p.p.m., and that of the mean value of the relative volume from all measurements with a given bulb at a given temperature is about 0·5 p.p.m. The difference between the relative expansions in the two bulbs should therefore have a standard deviation of $\sqrt{2} \times 0{\cdot}5$ p.p.m. of the volume of any temperature. The observed difference, 1×10^{-8}/° C, exceeds twice the above expected standard deviation at temperatures greater than 140° C, which shows that the cubical expansions of the two bulbs differ at the higher temperatures (Beattie and others show that the effect is not due to air in the bulbs) and indicates that neither may be exactly equal to three times the measured linear expansion of the ring specimen.

Callendar[16] has pointed out that the coefficient of volume expansion may not be equal to three times the coefficient of linear expansion measured in a particular direction, especially if that direction is along the axis of a cylindrical specimen which may have developed stress anisotropy while being drawn. He compared the axial and radial linear coefficients of ring specimens and at first concluded that they differed,[39,40] but finally decided that it was best to multiply the linear coefficient by three.[41] The matter has not since been re-examined and any such differences between the coefficients could lead to different cubical coefficients for the two bulbs used by Beattie and others, coefficients which would also not be equal to three times the measured axial linear coefficient of the ring specimen.

The authors state that the ring was cut from one of the two bulbs after the mercury observations had been completed and it seems from their account that it was then further annealed. If so, its expansion may have changed slightly and this possibility should be allowed for in assessing the overall uncertainty of the measured expansion of mercury.

At temperatures below 140° C, differences between the two bulbs are not significant relative to the errors of the relative expansion measurements, and it will be sufficient to take the standard deviation of bulb volume calculated from the linear coefficient of the ring specimen to be 1·5 p.p.m. At higher temperatures the differences between the relative expansions show the uncertainty to be greater and a standard deviation of 2 p.p.m. is adopted.

The temperatures were measured to about 0·001° C and were usually constant to 0·002° C,[17] corresponding to 0·4 p.p.m. of the density of mercury. The effects of temperature errors are, to a large extent, included in the uncertainties of the relative expansion measurements.

The standard deviations of the volumes observed by Harlow[14] in his relative measurements vary from about 0·2 to 1·5 p.p.m., comparable with those of Beattie and others. Harlow states that he measured his temperatures to 0·002° C and that during a run they were usually constant to 0·01° C (2 p.p.m. of the volume). Again, the effects of uncertainties in temperature are probably largely included in the scatter of the relative volumes.

The major uncertainty in Harlow's absolute results is how closely the silica expansion formulae he used represents the volumes of his bulbs. Harlow originally used a formula that Callendar[41] derived from observations by himself and Eagle on material obtained from the Silica Syndicate, who also supplied Harlow's bulbs, but later, Harlow[18] reviewed the data on the expansion of silica and adopted a formula which incorporated the results of other workers, such as Scheel. Two considerations indicate that Callendar's formula better represents the expansion of Harlow's bulbs. It has been seen that the expansion of silica is very dependent on the heat treatment the material has undergone, and since the material used by Callendar was obtained from the same source as Harlow's bulbs and therefore was made in the same way (by the local fusion of sand) and was probably given similar heat treatment, it is likely that it would have an expansion more nearly that of Harlow's bulbs than material obtained by other experimenters from different sources and possibly given different heat treatments. This argument is to some extent supported by the relative mercury expansions measured with Harlow's three bulbs which were obtained, apparently, from the Silica Syndicate at different times. The relative expansions from 0 to 100° C agree to within 1 p.p.m. of the volume and it is plausible that Callendar's silica tubes, obtained from the same firm, would have an expansion agreeing with that of the bulbs to about the same order.

The other consideration depends on the fact that the relative expansions determined by Harlow and by Beattie and others have uncertainties, about 1 p.p.m., that are much less than the scatter of the expansion of different samples of quartz. It therefore seems legitimate to infer the expansion of Harlow's bulbs from his own relative measurements and the absolute expansion found by Beattie and others, and to use the

Table 2. *Comparison of coefficients of relative expansion of mercury in silica vessels and of coefficients of expansion of fused silica.*

(*A*) *Coefficients of relative expansion of mercury in silica; unit:* 10^{-8}/° C.

Temperature (° C)	Mean coefficient of cubical expansion: Harlow	Standard deviation	Beattie and others	Standard deviation	(Harlow–Beattie)
25	(18 058)		18 037·3	2·0	+20·7
30	18 060	1·4	(18 039)		+21·0
50	18 068	1·0	18 049·9	1·0	+18·1
75	18 081	0·2	18 068·2	0·7	+12·8
100	18 102	0·3	18 091·7	0·5	+10·3
140	18 150	1·0	(18 143)		+ 7·0
150	(18 165)		18 156·9	0·3	+ 8·1
184	18 219	0·3	(18 214)		+ 5·0
200	18 248	0·4	18 246·6	0·3	+ 1·4
250	18 356	0·4	18 360·2	0·2	− 4·2
300	18 487	0·4	18 498·2	0·2	−11·2

(Bracketed values are interpolated.)

(*B*) *Coefficients of expansion of fused silica; unit:* 10^{-8}/° C.

Temperature (° C)	Mean coefficient of linear expansion: Callendar and Eagle	Beattie and others	$\delta = \frac{2}{(1-2)}$	-3δ
25	34·8	41·9	−7·1	+21·3
30	35·8	42·6	−6·8	+20·4
50	39·6	45·1	−5·5	+16·5
75	43·4	47·9	−4·5	+13·5
100	46·6	50·2	−3·6	+10·8
140	50·5	53·1	−2·6	+ 7·8
150	51·4	53·7	−2·3	+ 6·9
184	53·9	55·3	−1·4	+ 5·2
200	54·9	55·9	−1·0	+ 3·0
250	57·6	57·2	+0·4	− 1·2
300	59·8	57·8	+2·0	− 6·0

{Callendar and Eagle's values are calculated from the formula

$$[78{\cdot}0 - 8650/(t + 175)] \times 10^{-8}/°\text{C (Harlow}^{(14)})\}$$

expansion so inferred to discriminate between Callendar's formula for the expansion of Harlow's bulbs and Harlow's later formula of 1929. The data are given in Table 2. It will be seen from the comparison of the relative expansions that Harlow's bulbs expand less than those of Beattie and others below 200° C but expand more above that temperature. This is what is to be expected if Harlow's material was in equilibrium at a higher temperature than that of Beattie and others. The differences between the silica expansions measured by Callendar and Eagle and by Beattie and others agree very closely with the differences between the relative expansions of mercury and, like them, vanish between 200 and 250° C. Harlow's silica formula of 1929, on the other hand, is not consistent with the differences between the relative expansions.

Callendar's formula, quoted by Harlow,[14] is therefore used in calculating the expansion of mercury from the expansion relative to Harlow's bulbs. According to the material of Table 2, the r.m.s. difference between the cubical expansion of Harlow's bulbs and that given by Callendar's formula is about 2×10^{-8}/°C. This includes the effects of the errors of Beattie and others and Callendar. The differences are both positive and negative and it is likely that a standard deviation of 2×10^{-8}/° C fairly represents the uncertainty in applying Callendar's formula to Harlow's bulbs.

The results of Harlow and of Beattie and others are collected in Table 3. The coefficients are those actually observed, not calculated from fitted curves. The standard deviations

It will be seen from Table 3 that below 200° C, the two sets of results are in excellent agreement and have comparable uncertainties. The discrepancies at 200 and 250° C are consistent with the assigned standard deviations, but that at 300° C is rather large. In view of the scatter of the various observations and the uncertainty of the expansion of Harlow's bulbs, the good agreement below 200° C may be to some extent fortuitous and it would be unwise to assume that the expansion of mercury at any temperature is known to better than 1 p.p.m. of the volume.

James[15] made most of his measurements at temperatures below 0° C, and above 0° C he only observed at 100° C. He used Wheeler's[19] summary values for the expansion of silica to obtain the absolute expansion of mercury and his value for the mean coefficient from 0 to 100° C adds nothing to the data of Harlow and Beattie and others since he did not measure the expansion of his own bulb.

Below 0° C, James's results differ considerably from extrapolated values calculated from Beattie's quartic formula:

	Mean coefficient, 10^{-8}/°C	
Temperature range (°C)	*James*	*Beattie (extrapolated)*
−20 to 0	18059	18131
−30 to 0	18030	18125
−37 to 0	17988	18122

The expansion of mercury has also been measured relative to various glass vessels. Chappuis[20] used a *verre dur* vessel

Table 3. *The expansion of mercury from measurements relative to fused silica bulbs.*

(Coefficients are mean coefficients of volume expansion from 0 to t °C.)

	Harlow				Beattie and others				Harlow–Beattie		
		Standard deviation				Standard deviation					
Temperature (°C)	*Mean coefficient* 10^{-8}/°C	*Relative expansion* 10^{-8}/°C	*Silica expansion* 10^{-8}/°C	*Overall* 10^{-8}/°C	*Mean coefficient* 10^{-8}/°C	*Relative expansion* 10^{-8}/°C	*Silica expansion* 10^{-8}/°C	*Overall* 10^{-8}/°C	*Difference of coefficient* 10^{-8}/°C	$\frac{\delta V}{V}$ *p.p.m.*	*Standard deviation of* $\delta V/V$ *p.p.m.*
25					18163·6	2·0	6·0	6·5			
30	18168	3·3	2	3·7	(18167·7)				(+0·3	+ 0·1)	
50	18188	2·0	2	2·8	18186·5	1·0	3·0	3·3	+1·5	+ 0·75	2·1
75	18214	1·3	2	2·4	18213·8	0·6	2·0	2·1	+0·2	+ 0·15	2·4
100	18245	1·0	2	2·2	18245·0	0·5	1·5	1·6	0·0	0·0	2·7
140	18306	0·7	2	2·1	(18305·5)				(+0·5	+ 0·7)	
150					18322·3	0·3	1·0	1·0			
184	18387	0·6	2	2·1	(18386·5)				(+0·5	+ 0·9)	
200	18419	0·5	2	2·0	18420·5	0·2	1·0	1·0	−1·5	− 3·0	4·6
250	18537	0·4	2	2·0	18539·8	0·2	0·8	0·8	−2·8	− 7·0	5·5
300	18677	0·3	2	2·0	18681·4	0·2	0·7	0·7	−4·4	−13·2	6·3
350					18853·0	0·1	0·6	0·6			

(Bracketed values are interpolated, not experimental figures.)

are of the mean values at a given temperature; the ways in which they are determined have already been discussed and the values are summarized below:

(*a*) of relative expansion:
Harlow: 1 p.p.m. of the volume.
Beattie and others: 0·5 p.p.m. of the volume.

(*b*) of the cubical expansion of silica:
Harlow: 2×10^{-8}/°C.
Beattie and others: 1·5 p.p.m. of the volume at 150° C and below,
2 p.p.m. of the volume at 200° C and above.

and Thiesen, Scheel and Sell[21] used vessels of Jena glass. Because these glasses expand so much more than fused silica and because their constitutions are more complex, their coefficients of expansion probably vary more with heat treatment and from specimen to specimen; in addition, glass vessels may show greater stress anisotropy than ones of fused silica. The results of Thiesen, Scheel and Sell appear to substantiate these remarks. These observers used five dilatometers of three different sorts of Jena glass, the coefficients of expansion of which they determined for "similar" pieces of glass and obtained the following results for the mean coefficient or expansion of mercury between 0 and 100° C:

Dilatometer	Glass	Mean coefficient (10^{-8}/°C)
1	Jena 16^{III}	18 232·7
2	Jena 16^{III}	18 209·1
3	T	18 193·4
4	T	18 194·4
5	Jena 59^{III}	18 257·0

The difference between the coefficients obtained with the two dilatometers of 16^{III} should be particularly noted. The observations were made only at 0 and 100° C.

Chappuis's results are more reliable in that he made his vessel by sealing the ends of a glass tube, 1 m long, the linear expansion of which he had already measured absolutely, but it is possible that the working of the glass to seal it may have changed the properties so that the expansion when sealed was not the same as that measured. Chappuis used this bulb for measurements on the expansion of water at the same time as he made other observations on water with a platinum iridium vessel[22] and the water densities from the glass vessel are systematically higher than those from the platinum–iridium vessel by about 0·1 t p.p.m. (t is temperature, °C), the latter agreeing rather better with the water densities measured by Thiesen, Scheel and Diesselhorst[23,24] using the absolute method. Chappuis measured the expansion of mercury at temperatures between 0 and 40° C and at 100° C.

Chappuis and Thiesen, Scheel and Sell have also deduced values of the expansion at temperatures between 0 and 100° C from the departures of mercury-in-glass thermometers from the hydrogen scale and Hoffmann and Meissner[25] extended such observations to 500° C, using two Jena glass thermometers, one, evacuated, from 100 to 300° C and the second, nitrogen-filled, from 200 to 500° C. The expansion of the glass over the temperature range and that of mercury from 0 to 100° C have to be assumed; the bore of the capillary must be accurately calibrated and corrections must be applied for the compressibilities of mercury and glass and, with the nitrogen-filled thermometers, for the gas pressure.

The results of all these relative determinations are collected in Table 4. They are of negligible weight compared with the results of Beattie and others and Harlow.

5. ABSOLUTE MEASUREMENTS OF THE EXPANSION OF MERCURY

The apparatus with multiple hot and cold columns is shown diagrammatically in Fig. 2. Suppose there are n hot and n cold columns of height h_{1i} and h_{0i} respectively and that the base of each column is at a height x_{1i} or x_{0i} above an arbitrary

Table 4. *The expansion of mercury from measurements relative to* verre dur *and Jena glasses*

Mean coefficients, unit: 10^{-8}/°C

(*A*) *Range* 0 *to* 100° *C*

	Chappuis, verre dur		Thiesen, Scheel and Sell		
Temperature range (°C)	Dilatometer	Thermometer scale	Dilatometer	Thermometer scale	Beattie and others
−20 to 0		18 154			18 131
−10 to 0		18 153			18 137
0 to 10	18 167	18 157		18 194	18 151
20	18 168	18 162		18 195	18 159
30	18 170	18 169		18 197	18 168
40	18 176	18 177		18 200	18 177
50		18 186		18 205	18 186
60		18 198		18 210	18 197
70		18 210		18 217	18 208
80		18 224		18 225	18 220
90		18 238		18 239	18 232
100	18 254		18 245		18 245

(*B*) *Range* 100 *to* 500° *C*

Temperature range (°C)	Hoffmann and Meissner thermometer scale	Beattie and others
0 to 150	18 321	18 322
200	18 406	18 420
250	18 513	18 539
300	18 638	18 683
350	18 787	18 853
400	18 963	
450	19 164	
500	19 392	

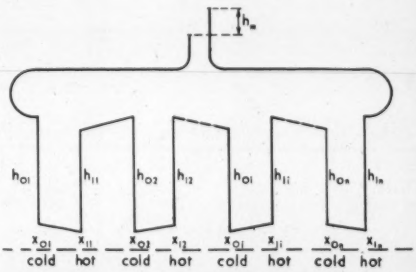

Fig. 2. Diagram of the arrangement of hot and cold columns for the absolute measurement of the expansion of mercury

horizontal plane. Let the density of the mercury in each hot column be ρ_1 and in each cold column, ρ_0, and in the manometer ρm; also let the density of the mercury in the connexions between the bottoms of the columns be ρ_{a1} and between the tops, ρ_{a2}

Let $\rho_0 h_{0i} - \rho_1 h_{1i} = \delta(\rho h)_i$,

$h_{0i} - h_{1i} = \delta h_i$ and $x_{0i} - x_{1i} = \delta x_i$

Then it may be shown that in hydrostatic equilibrium,

$$\Sigma\delta(\rho h)_i = \rho_m h_m + \rho_{a2}\Sigma\delta h_i + (\rho_{a2} - \rho_{a1})\Sigma\delta x_i \qquad (1)$$

[This equation is still true if the density in each hot column (or each cold column) is not the same; the densities may then be denoted by ρ_{1i} and ρ_{0i} and

$$\delta(\rho h)_i = \rho_{0i} h_{0i} - \rho_{1i} h_{1i}$$

However, there is no reason to suppose that such inequalities will in general lead to systematic errors, so they will be ignored.]

$$\delta(\rho h)_i = h_{1i}(\rho_0 - \rho_1) + \delta h_i \rho_0$$

and so $$\frac{\rho_0 - \rho_1}{\rho_0}\Sigma h_{1i} = \frac{\rho_m}{\rho_0} h_m + \frac{\rho_{a2} - \rho_0}{\rho_0}\Sigma\delta h_i + \frac{\rho_{a2} - \rho_{a1}}{\rho_0}\Sigma\delta x_i \qquad (2)$$

This equation shows first that if $(\rho_1 - \rho_0)$ is to be measured to one part in a million of ρ_0, then h_m must be measured to one part in a million of Σh_{1i}; if, for example, Σh_{1i} is 10 m, h_m must be measured to 10 μ. Very considerable precautions have to be taken to measure h_m so accurately, in particular, the manometer tube bore must be wide enough to make the effects of irregular contact angle unimportant, and refraction errors through the glass wall of the manometer tube must be carefully examined.

Secondly, for the same accuracy in $(\rho_1 - \rho_0)$, Σh_{1i} must be measured to $\rho_0/(\rho_1 - \rho_0)$ parts per million. For example, at 100° C, $(\rho_1 - \rho_0)$ is about 0·02 ρ_0 and so Σh_{1i} must be correct to 50 p.p.m., or 50 μ on each column 1 m long. The vertical tubes were connected to each other and to the gauge tubes by tubes of about 1 mm bore fitted into the ends of the vertical tubes and emerging from the sides of the baths. Callendar and Moss[3] pointed out that one essential condition for precise definition of vertical tube length is that the connecting tubes should be accurately horizontal in the zone where the temperature changes from the bath temperature to ambient, for otherwise the temperature gradient will set up a pressure gradient. Chappuis[4] adopted the same arrangement and, like Callendar and Moss, took the height of the vertical column to be the vertical distance between the axes of the bores of the top and bottom horizontal connecting tubes. In practice, it is necessary to measure to parts of the external surfaces of the tubes and then assume that the axis of the bore is the axis of the external surface, but neither Callendar and Moss nor Chappuis state that they measured the positions of the bores of the tubes. It is also necessary to assume that the axial pressure in a horizontal tube is equal to the mean pressure, but it is unlikely that this assumption is far wrong for tubes for such small bore.

The differences of the lengths of the hot and cold columns only appear in a fairly small correction term, with coefficient $(\rho_{a2} - \rho_0)/\rho_0$, while the differences between the heights of the bottoms of the columns only appear in an even smaller term with coefficient $(\rho_{a2} - \rho_{a1})/\rho_0$. The temperature of the cold column is unlikely to differ by more than 10° C from ambient so that the former coefficient will generally be of the order of 0·002 or less, while the upper and lower ambient temperatures are unlikely to differ by more than about 2° C and the value of $(\rho_{a2} - \rho_{a1})/\rho_0$ should not exceed 0·0004.

The main points to bear in mind in considering absolute measurements are, accordingly, the accuracy of the manometer measurements, the accuracy of the definition and measurement of the column lengths, and the uniformity of the bath temperatures and the accuracy with which they are measured. Of the two multiple-column experiments, only Chappuis's experiments[4] will be discussed since the results of Callendar and Moss[3] show large and erratic differences from the values of Beattie and others and no likely reason for these discrepancies is apparent.

Chappuis used seven pairs of columns 1 m long and 1·4 mm internal diameter. (He found that the mercury reached hydrostatic equilibrium too slowly in tubes of 1 mm diameter such as Callendar and Moss used.) The baths were filled with oil and were heated electrically. Details of the arrangements for stirring are not given. Two mercury-in-glass thermometers were inserted horizontally into each bath at one-quarter and three-quarters of the height and were contained in closed copper tubes so that they were not immersed directly in the oil but were surrounded by air inside the copper tubes. These arrangements may have led to the thermometer readings being systematically low at temperatures above ambient. The thermometers are not now available but the observations of Hall[26] suggest that the scales may have departed by up to 0·01° C from the International temperature scale, particularly in the neighbourhood of 50° C.

Chappuis reduced his results by a least-squares adjustment but as it is not clear how the mean coefficients from 0° C to temperatures above 10° C (ambient temperature) depend on the mean coefficient from 0 to 10° C, the results have been re-computed. The fundamental equation used by Chappuis is:

$$\frac{H_2}{V_2} = \frac{H_1}{V_1} - \frac{h_m}{V_m} + \frac{H_2 - H_1}{V_a} \qquad (3)$$

where H_1 is the total height of the columns at 10° C; H_2 is the total height of the other columns (either hotter or colder); h_m is the manometer height; V_1 is equal to $(1 + \alpha_1 t_1)$, where α_1 is the mean coefficient of expansion from 0° C to t_1, the temperature of the 10° C column; V_2, V_m and V_a are similarly equal to $(1 + \alpha_2 t_2)$, $(1 + \alpha_m t_m)$ and $(1 + \alpha_a t_a)$, where t_2 is the temperature of column 2, t_m that of the manometer, and t_a that of the connecting tubes; equation (3) is equivalent to equation (2) if the lower ends of the columns all lie in the same horizontal plane.

Trial values V' were inserted in equation (3). If $V = V' + v$,

$$v_2 - \frac{H_2}{H_1}v_1 = \frac{h_m}{H_1}\frac{V_1' V_2'}{V_m'} - \frac{H_2 - H_1}{H_1}\frac{V_1' V_2'}{V_a'} - \left(V_2' - V_1'\frac{H_2}{H_1}\right)' \qquad (4)$$

The results of Beattie and others[11] have been used for the trial values, principally because they are well tabulated.

Chappuis calculated his 100° C temperatures from the barometric pressure using tables compiled by Wiebe but for the present re-computation, these temperatures were recal-

culated by means of the formula used for the International temperature scale of 1948:

$$t_p = 100 + 28{\cdot}012\left(\frac{p}{p_0} - 1\right) - 11{\cdot}64\left(\frac{p}{p_0} - 1\right)^2 + 7{\cdot}1\left(\frac{p}{p_0} - 1\right)^3$$

They are then about 7×10^{-3} °C lower than Chappuis's temperatures.

The values of $(v_2 - H_2v_1/H_1)$ are listed in Table 5, mean values being given against the nominal temperature. At 100° C the difference from Beattie and others is hardly significant and the separate determinations are very consistent. The mean value of $(v_2 - H_2v_1/H_1)$ at all other temperatures is 8·1 p.p.m., the standard deviation about the mean being 3 p.p.m., while the departures from the mean show no systematic dependence on temperature.

Table 5. *Absolute measurement of the expansion of mercury by Chappuis*

(Chappuis's data have been recomputed to give residuals, equal to $(v_2 - H_2v_1/H_1)$ (see text) from the expansion formula of Beattie and others.[11] The temperatures near 100° C have also been recomputed from the barometric pressure.)

Nominal temperature (°C)	*Number of observations*	*Standard deviation of single observation* (*p.p.m. of volume*)	*Difference from Beattie and others* $(v_2 - H_2v_1/H_1)$ (*p.p.m. of volume*)
100 1st set	5	0·9	+ 0·2
2nd set	4	1·1	+ 1·4
75	5	3·7	+10·0
60	4	3·5	+ 7·6
50	4	0·7	+ 4·0
36	4	2·7	+ 5·8
25	4	1·7	+12·6
0	4	4·5	+ 8·8

Now V, the true relative volume of mercury, and V', the trial value are both functions of temperature which, by definition, are equal to unity at 0° C, and v, therefore, is a function of temperature which vanishes at 0° C, so that if the small difference between H_1 and H_2 is ignored, $(v_2 - H_2v_1/H_1)$ should vanish when t_2 and t_1 are equal and in general should be nearly proportional to $(t_2 - t_1)$. This is the behaviour that would have been shown by the observed values of $(v_2 - H_2v_1/H_1)$ if Chappuis's experiment had given a valid determination of the expansion, and the fact that the observed values are independent of temperature shows that the observations are inconsistent with equation (3).

Equation (4) may be written as

$$(v_2 - v_1H_2/H_1) = h_m/H_1 - (\alpha_2't_2 - \alpha_1't_1) + (h_m/H_1)(\alpha_2't_2 + \alpha_1't_1 - \alpha_m't_m) - (\delta H/H_1)(\alpha_2't_2 - \alpha_a't_a) \quad (5)$$

where α_2', α_1', . . ., denote trial values.

The various terms are considered in order of magnitude: h_m is the observed manometer height, nearly proportional to $(t_2 - t_1)$ and h_m/H_1 is about 2×10^{-4}/° C; $(\alpha_2't_2 - \alpha_1't_1)$ is the assumed expansion, and nearly equal to h_m/H_1; t_1 and t_m were very nearly equal so that the third term is almost $(h_m/H_1)\alpha_2't_2$, that is, proportional to $t_2(t_2 - t_1)$ and of the order of 4×10^{-8}/(° C)², finally, $\delta H/H_1$ is approximately proportional to $(t_2 - t_1)$ and of the order of 10^{-5}/° C so that the fourth term is of the order of $2 \cdot 10^{-9}$/(° C)².

Thus there are only two errors which could lead to temperature independent values of $(v_2 - H_2v_1/H_1)$; a constant error of about 60 μ in h_m or a constant error of about 0·04° C in $(t_2 - t_1)$, and these two errors would affect respectively the first and second terms of equation (5). Whatever the error is, it appears to vanish at 100° C and it is therefore related to differences of method at 100° C and at the lower temperatures; a constant error in t_1 cannot therefore be responsible.

At the lower temperatures, t_2 was measured by mercury-in-glass thermometers as explained above; an error of 0·04° C in t_2, whatever the value of t_2, is improbable, for errors due to poor mixing of the baths may increase the scatter of the results but would probably increase with temperature.

The measurement of h_m, the manometer height, must therefore be considered. The positions of the mercury menisci were defined by the direct and reflected images of a pin point held a few microns above the mercury surface and viewed in the telescope of a cathetometer. At 100° C, two telescopes were fixed to the cathetometer column, one for each limb of the manometer and were used to compare the position of each meniscus with a calibrated line standard set up close to the manometer. At the lower temperatures, however, the separation of the two menisci was not great enough for two telescopes to be fitted to the cathetometer without fouling, and accordingly the mercury in the manometer tube connected to the 10° C column was kept at a constant height by being connected to a large reservoir, this reference height being measured by comparison with the line standard at the beginning, in the middle, and at the end of a series of observations at a given temperature. The behaviour of the discrepancies in Table 5 strongly suggests that there was some error in the measurement of the reference level but it is difficult to see how it can have arisen although Chappuis did find, in a separate experiment, errors of up to 20 μ in the measured manometer levels due to wall refraction and contact angle variations (the scatter of observations at a given temperature is rather less). On the other hand, on bringing both sets of columns to 0° C, he found the manometer difference to be less than 1 μ.

The large differences of the two absolute measurements from each other and from Beattie's results show that in any future absolute measurement, much attention will have to be paid to systematic errors, particularly to the definition and measurement of the lengths of the columns and to the measurement of the pressure difference.

6. CONCLUSIONS

In deciding on values to adopt for the expansion of mercury, the results of the absolute measurements must evidently be

ignored because of the systematic errors with which they appear to be affected. Similarly, relative measurements in glass vessels are rejected since the expansion of the vessel cannot be determined sufficiently accurately, while high-temperature values deduced from the departures of mercury-in-glass thermometer scales from the International temperature scale are, in addition, subject to uncertainties in the pressure corrections. The only results which can be considered to be correct to within a few parts in a million of the volume are those of Harlow and of Beattie and others. These two series agree to within the probable standard deviation of their difference over the whole range from 0 to 300° C but, pending further observations, it seems best to adopt Beattie's results as definitive since there is less doubt about the expansion of the silica vessels used. The results below 0° C[15, 20] and above 350° C[25] depart considerably from extrapolated values calculated with Beattie's quartic formula and the expansion of mercury outside the range 0 to 300° C is uncertain by about 100×10^{-8}/°C.

The quartic formula given by Sears[27] has often been used in the reduction of the most precise barometric measurements to a standard temperature. It was calculated after Harlow's results had been announced but combined with Harlow's material other data now considered to be less reliable, and therefore, although satisfactory for reductions through temperature differences of a few degrees, it should not be used when the most accurate values are required over a wide range of temperature.

Beattie and others[11] fitted the following formula to their observations between 0 and 300° C:

$$10^8(V_t - V_0)/tV_0 = 18\,144{\cdot}01 + 70{\cdot}16 \times 10^{-2}t + 28{\cdot}625 \times 10^{-4}t^2 + 2{\cdot}617 \times 10^{-6}t^3$$

[t in °C Int. (1927)]

They have tabulated the mean coefficient, relative volumes, density and other quantities calculated from this formula. Volumes or densities obtained from the formula or tables should have standard deviations of between one and two parts in one million.

ACKNOWLEDGEMENTS

I have had helpful discussions with Mr. J. A. Hall and Mr. P. H. Bigg on the subject of this paper.

The investigation forms part of the research programme of the National Physical Laboratory and this paper is published by permission of the Director of the Laboratory.

REFERENCES

(1) DULONG, P. L., and PETIT, A. T. *Ann. Chim. Phys.*, **7**, p. 127 (1818).

(2) REGNAULT, V. *Mem Acad. Sci. Paris*, **21**, p. 205 (1847).

(3) CALLENDAR, H. L., and MOSS, H. *Phil. Trans. A*, **211**, pp. 1–32 (1911).

(4) CHAPPUIS, P. *Trav. Bur. Int. Poids Mes.*, **16**, pp. 7–31 (1917).

(5) DOUGLAS, R. W., and ISARD, J. O. *J. Soc. Glass. Technol.*, **35**, pp. 206–225 (1951).

(6) SOSMAN, R. B. *Properties of Silica* (New York: Chemical Catalog. Co. Inc., 1927).

(7) HOLBORN, L., and DAY, A. *Ann. Phys.* [*Leipzig*], **2**, pp. 505–545 (1900).

(8) BLACKIE, A. *Trans Faraday Soc.*, **7**, pp. 158–165 (1911).

(9) SCHEEL, K. *Wiss. Abh. Phys.-Tech. Reichsanst.*, **4**, pp. 35–60 (1904).
Verh. Dtsch. Phys. Ges., **5**, pp. 119–123 (1903).

(10) RANDALL, H. M. *Phys. Rev.*, **30**, p. 216 (1910).

(11) BEATTIE, J. A., BLAISDELL, B. E., KAYE, J., GERRY, H. T., and JOHNSON, C. A. *Proc. Amer. Acad. Arts Sci.*, **74**, pp. 371–388 (1941).

(12) SOUDER, W., and HIDNERT, P. *Sci. Pap. U.S. Bur. Stand.*, **21**, pp. 1–23 (1926).

(13) HARLOW, F. J. *Proc. Phys. Soc.* [*London*], **24**, pp. 30–39 (1911).

(14) HARLOW, F. J. *Proc. Phys. Soc.* [*London*], **26**, pp. 85–96 (1913).

(15) JAMES, C. B. *Trans Roy. Soc. Canada* (III), **8**, pp. 51–58 (1914).

(16) CALLENDAR, H. L. *Phil. Mag.*, **23**, pp. 998–1000 (1912).

(17) BEATTIE, J. A. *Proc. Amer. Acad. Arts Sci.*, **69**, pp. 389–405 (1934).

(18) HARLOW, F. J. *Phil. Mag.*, **7**, pp. 674–685 (1929).

(19) WHEELER, N. E. *Trans Roy. Soc. Canada* (III), **8**, pp.139–156 (1914).

(20) CHAPPUIS, P. *Trav. Bur. Int. Poids Mes.*, **13**, pp. 1–31 (1907).

(21) THIESEN, M., SCHEEL, K., and SELL, L. *Wiss. Abh. Phys.-Tech. Reichsanst.*, **2**, 75–184 (1895).

(22) CHAPPUIS, P. *Trav. Bur. Int. Poids Mes.*, **13**, D 1–40 (1907).

(23) THIESEN, M., SCHEEL, K., and DIESSELHORST, H. *Wiss. Abh. Phys.-Tech. Reichsanst.*, **3**, 1–70 (1900).

(24) THIESEN, M., SCHEEL, K., and DIESSELHORST, H. *Wiss. Abh. Phys.-Tech. Reichsanst.*, **4**, pp. 1–32 (1918).

(25) HOFFMAN, F., and MEISSNER, W. *Z. Instrum. Kde.*, **39**, pp. 212–224 (1919).

(26) HALL, J. A. *Phil. Trans, A*, **229**, pp. 1–48 (1929).

(27) SEARS, J. E. (Jun.). *Proc. Phys. Soc.* [*London*], **26**, p. 96 (1913).

(28) CHAPPUIS, P. *Com. Int. Poids Mes.*, **2**, p. 75 (1903).

(29) HOLBORN, L., and HENNING, F. *Ann. Phys.* [*Leipzig*], **10**, pp. 446–8 (1903).

(30) HENNING, F. *Ann. Phys.* [*Leipzig*], **22**, pp. 631–9 (1907).

(31) SCHEEL, K. *Verh. Dtsch. Phys. Ges.*, **9**, pp. 3–23 (1907).

(32) SCHEEL, K. *Verh. Dtsch. Phys. Ges.*, **9**, pp. 718–741 (1907).

(33) SCHEEL, K. *Z. Phys.*, **5**, pp. 167–172 (1921).

(34) SCHEEL, K., and HEUSE, W. *Verh. Dtsch. Phys. Ges.*, **14**, pp. 139–144 (1912).

(35) SCHEEL, K., and HEUSE, W. *Verh. Dtsch. Phys. Ges.*, **16**, pp. 1–3 (1914).

(36) VALENTINER, S., and WALLOT, J. *Verh. Dtsch. Phys. Ges.*, **16**, pp. 757–764 (1914).

(37) KAYE, G. W. C. *Proc. Roy. Soc. A*, **85**, 430 (1911).

(38) DONALDSON, H. *Proc. Phys. Soc.* [*London*], **24**, pp. 186–194 (1911).

(39) CALLENDAR, H. L. *Proc. Phys. Soc.* [*London*], **24**, pp. 195–200 (1911).

(40) CALLENDAR, H. L. *Z. Instrum. Kde.*, **32**, pp. 194–5 (1912).

(41) CALLENDAR, H. L. *Nature* [*London*], **92**, 467 (1913).

The tension in strings wrapped slantwise round cylinders when friction is proportional to a power of the normal reaction

By C. MACK, M.A., A.Inst.P., British Cotton Industry Research Association, Shirley Institute, Manchester

[*Paper received* 16 *February*, 1956]

It is now well established that for many, if not most, pairs of materials in contact friction is proportional to a power, smaller than unity, of the normal reaction. The relations between tension, normal reaction, curvature and certain angles are found for a string wrapped slantwise round a cylinder of general cross-section for friction obeying this law: (i) when friction acts tangentially to the string path, and (ii) when it acts parallel to the cylinder axis.

1. INTRODUCTION

This paper extends the results given in an earlier paper[1] [which will be subsequently referred to as (*A*)] for the tension in strings wrapped slantwise round cylinders when friction obeys Amonton's law*

$$F = \mu N \tag{1}$$

where F is the frictional force and N the normal reaction. However, while (*A*) was being written Bowden and Young[2] showed in a particular case that the law

$$F = aN^n \tag{2}$$

where a and n are independent of N was a much better fit to their observed data than law (1). Following this, other investigators[3–6] have shown that law (2) holds for a wide range of pairs of materials in contact including most cases in which one material is a textile. (It should be noted that a and n depend on the materials and also, to some extent, on the geometrical configuration.) For example, Lyne[7] has found that for cellulose acetate yarn on polished chrome steel n was 0·8 and a colleague has found that for low-twist multifilament Nylon yarn running at 120 cm/s against glass rod n was 0·735.[8]

Since most strings and ropes are made of textile materials and there are many practical cases of strings passing slantwise round objects which are, or are approximately, cylinders, it is the aim of this paper to establish formulae for the resultant variation in tension which occurs when law (2) holds. It is shown that for circular cylinders these formulae are simple and exact (though in one case a previously untabulated function is involved but a table is provided). For cylinders of general cross-section an integral appears in the formulae which can be evaluated for a number of special types of cross-section, but not generally. However, a good approximate formula can be used or a good approximation to the given cross-section made by taking the nearest special type which can be integrated. A noticeable feature of all these formulae is the explicit appearance of the radius of curvature.

For strings lying over a general type of body it is not possible to provide useful general formulae and it is possibly best in dealing with such cases in practice to approximate to the body by a cylinder of suitable cross-section and perhaps repeat this approximation once or twice over different lengths of the string.

2. STRING MOVING ALONG A STATIONARY PATH

Using the same notation as in (*A*), i.e. taking OZ as the cylinder axis and at a typical point $P \equiv x, y, z$ on the string path let T be the tension, N the normal reaction per unit length, S the length along the string path, ζ the angle made by the tangent to the string at P with OZ, ψ the angle made by the tangent to the transverse cross-section of the cylinder at P with OX and ρ the radius of curvature of this cross-section at that point (see figure).

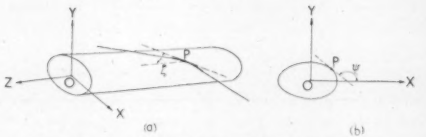

(*a*) String passing slantwise over a cylinder.
(*b*) Cylinder cross-section.

For string moving along its own path friction acts tangentially everywhere and it is shown below that in this case:

$$\left.\begin{aligned} &\text{(i)}\ N = (T\sin^2\zeta)/\rho; \\ &\text{(ii)}\ \zeta \text{ is everywhere constant on the string;} \\ &\text{(iii)}\ T_1^{1-n} - T_0^{1-n} = [a(1-n)\sin^{2n-1}\zeta]\int_{\psi=0}^{\psi=\psi_1} \rho^{1-n}d\psi. \end{aligned}\right\} \tag{3}$$

Proof. By considering the forces on an element of the string at P and in particular their components parallel to the plane OXY it can be seen that the forces normal to this element are in equilibrium if

$$T\sin\zeta d\psi = Nds \tag{4}$$

By projection on the plane OXY [or from equation (12) of (*A*)], we see that

$$\sin\zeta ds = \rho d\psi \tag{5}$$

and hence result (i) follows. Furthermore this result holds whatever the magnitude and direction of friction, provided that it is tangential to the cylinder.

However friction, in the present case, acts tangentially to the string and taking components of forces on an element in the direction of this tangent it is seen that

$$(dT/ds) + aN^n = 0 \tag{6}$$

Considering components parallel to OZ it is seen that

$$[d(Tdz/ds)/ds] + aN^n(dz/ds) = 0 \tag{7}$$

From equations (6) and (7) it follows that

$$T(d^2z/ds^2) = 0 \tag{8}$$

and hence $\cos\zeta \equiv dz/ds$ = constant, whence point (ii) follows.

* Sometimes known as Coulomb's law; however, Amonton's work was published much before Coulomb's.

From results (i) and (ii) and equations (5) and (6) it follows that

$$dT/T^n = (a \sin^{2n-1}\zeta)\rho^{1-n}d\psi \qquad (9)$$

Whence, by result (ii), result (iii) follows after integration.

Special types of cross-section

(*a*) *Circular cylinder.* Here ρ is a constant r, say, and result (iii) becomes

$$T_1^{1-n} - T_0^{1-n} = [a(1-n)\sin^{2n-1}\zeta]\, r^{1-n}(\psi_1 - \psi_0) \qquad (10)$$

the special case of this when $\zeta = \pi/2$ has been given by Howell.[3]

(*b*) *General cross-section.* Here the integral $\int \rho^{1-n}\,d\psi$ has to be evaluated and this can be done if ρ is expressed as a function of ψ, though the integral may not be expressible in terms of tabulated functions. A good approximation useful in many circumstances is the following, which can be deduced by expanding ρ^{1-n} as a Taylor's expansion in ψ,

$$\int_{\psi_0}^{\psi_1} \rho^{1-n}\,d\psi = \frac{(\rho_1^{1-n} + \rho_0^{1-n})(\psi_1 - \psi_0)}{2} - \frac{(1-n)(\psi_1 - \psi_0)^3}{6\rho_0^n}\left[\left(\frac{d^2\rho}{d\psi^2}\right)_0 - \frac{n}{\rho_0}\left(\frac{d\rho}{d\psi}\right)_0^2\right] \qquad (11)$$

the terms in $(\psi_1 - \psi_0)^3$, etc., often being negligible.

Alternatively one can approximate to a given cross-section by taking ρ to be the nearest function of ψ for which the integral and x and y can be simply evaluated in terms of ψ; and the following results[9] are useful in this respect:

$$x = \int \rho\cos\psi d\psi, \quad y = \int \rho\sin\psi d\psi \qquad (12)$$

We now give examples in which $\int \rho^{1-n}\,d\psi$, x and y are integrable in tabulated functions [in some cases, in terms of the function S_m defined in (*d*) and tabulated in Section 3].

(*c*) $\rho = A\psi + B$. Here

$$\int \rho^{1-n}\,d\psi = (A\psi + B)^{2-n}/[(2-n)A],$$

$$x = (A\psi + B)\sin\psi + A\cos\psi,$$
$$y = -(A\psi + B)\cos\psi + A\sin\psi \qquad (13)$$

(*d*) $\rho = C\sin(\alpha\psi)$. Here

$$\int \rho^{1-n}\,d\psi = (C^{1-n}/\alpha)S_{1-n}(\alpha\psi),$$

where

$$\int_0^{\psi} \sin^m\psi d\psi \equiv S_m(\psi)$$

$$x = \text{constant} - \frac{C}{2}\left\{\frac{\cos[(\alpha+1)\psi]}{\alpha+1} + \frac{\cos[(\alpha-1)\psi]}{\alpha-1}\right\}$$

$$y = \text{constant} + \frac{C}{2}\left\{\frac{\sin[(\alpha-1)\psi]}{\alpha-1} - \frac{\sin[(\alpha+1)\psi]}{\alpha+1}\right\} \qquad (14)$$

The particular case $\alpha = 1$ $\left\{\text{when } \cos[(\alpha-1)\psi]/(\alpha-1) \text{ is}\right.$ taken as constant and $\left.\sin[(\alpha-1)\psi]/(\alpha-1) \text{ as } \psi\right\}$ is the cycloid, and the general case gives an epi- or hypo-cycloid (see Edwards[9] paragraph 401 onwards).

Table of $S_m(\theta) \equiv \int_0^{\theta} \sin^m\theta\,d\theta$

(S_m is given in thousandths of a unit, θ in degrees)

m;	0	0·5	0·10	0·15	0·20	0·25	0·30
θ							
0	0	0	0	0	0	0	0
2	35	28	23	18	15	12	10
4	70	58	49	41	34	29	24
6	105	89	76	65	56	48	41
8	140	121	104	90	78	68	59
10	175	152	133	117	103	90	79
12	209	184	163	144	128	113	101
14	244	217	193	172	153	137	123
16	279	249	223	200	180	162	146
18	314	282	254	229	207	188	170
20	349	315	285	259	235	214	195
22	384	348	317	289	264	241	221
24	419	382	349	319	293	269	247
26	454	415	381	350	322	297	274
28	488	449	413	381	352	326	302
30	524	482	445	412	382	355	330
32	559	516	478	444	413	384	359
34	593	550	511	476	444	414	388
36	628	584	544	508	475	445	417
38	663	618	577	540	506	475	447
40	698	652	610	573	538	507	474
42	733	686	644	605	570	538	508
44	768	721	678	638	603	570	539
46	803	755	711	672	635	602	571
48	838	789	745	705	668	634	603
50	873	824	779	738	701	666	635
52	908	858	813	772	734	699	667
54	942	893	847	806	767	732	700
56	977	927	881	839	801	765	733
58	1012	962	916	873	835	799	766
60	1047	996	950	908	869	833	799
62	1082	1031	985	942	903	866	833
64	1117	1066	1019	976	937	900	866
66	1152	1101	1054	1011	971	934	900
68	1187	1135	1088	1045	1005	968	934
70	1222	1170	1123	1080	1040	1003	968
72	1257	1205	1158	1114	1074	1037	1003
74	1292	1240	1192	1149	1109	1072	1037
76	1326	1275	1227	1184	1143	1106	1072
78	1361	1309	1262	1218	1178	1141	1106
80	1396	1344	1297	1253	1213	1176	1141
82	1431	1379	1332	1288	1248	1210	1176
84	1466	1414	1367	1323	1283	1245	1211
86	1501	1449	1401	1358	1317	1280	1246
88	1536	1484	1436	1393	1352	1315	1281
90	1571	1519	1471	1428	1387	1350	1315

(*e*) $\rho = D \sin^{\eta} \psi$. Here

$$\int \rho^{1-n} d\psi = D^{1-n} S_{\eta(1-n)}(\psi),$$
$$x = (D \sin^{\eta+1} \psi)/(\eta + 1),\ y = S_{\eta+1}(\psi) \quad (15)$$

(*f*) *Elliptical cross-section.* Here a non-integrable expression occurs but the problem is best treated by using a different parameter from ψ as follows:

$$x = a \cos \phi, \quad y = b \sin \phi, \quad \tan \psi = -(b \cot \phi)/a,$$
$$\rho = [a^2 - (a^2 - b^2) \cos^2 \phi]^{3/2}/(ab) \quad (16)$$

Hence

$$\int \rho^{1-n} d\psi = (ab)^n \int [a^2 - (a^2 - b^2) \cos^2 \phi]^{(1-3n)/2} d\phi$$

which can be calculated numerically fairly easily but is not expressible in tabulated functions for n between 0 and 1 unless $n = \frac{1}{3}$ when it is $(ab)^n \phi$ or $n = \frac{2}{3}$ when it is an elliptic integral.

Formulae for the string path

The actual path may be of importance and it is usually possible to express the co-ordinates of this path using ψ as a parameter. Thus, since $\cos \zeta = dz/ds = \text{constant}$, we see, by integration, that, along the path,

$$(z - z_0) = (s - s_0) \cos \zeta \quad (17)$$

while it is well known that

$$s = \int \rho d\psi \quad (18)$$

Hence equations (12) and (17) enable (x, y, z) along the string path, to be expressed in terms of ψ.

3. STRING STATIONARY, CYLINDER MOVING PARALLEL TO ITS AXIS

Or the cylinder can be considered to be stationary and the string to have everywhere the same velocity parallel to the cylinder axis. In all these cases friction acts parallel to the cylinder axis OZ.

It is shown below that:

(iv) $N = (T \sin^2 \zeta)/\rho$;

(v) $T \sin \zeta = \text{constant} = K$, say;

(vi) $K^{1-n} \int_{\zeta_0}^{\zeta_1} \text{cosec}^{1+n} \zeta d\zeta = a \int_{\psi_0}^{\psi_1} \rho^{1-n} d\psi$.

Proof. Result (iv) has been shown to be universally true in Section 2. Again, if the projections of forces on an element on the plane OXY are considered it can be seen, in the case of forces in the direction of the tangent to the cross-section, that

$$d(T \sin \zeta) = 0 \quad (19)$$

since friction acts entirely in the OZ direction. Hence result (v) follows. Considering components parallel to OZ it can be seen that

$$d(T dz/ds)/ds + aN^n = 0 \quad (20)$$

and, since $dz/ds = \cos \zeta$, from results (iv) and (v) above and from equation (20), it can be seen that

$$\sin \zeta \left[d(K \cot \zeta)/d\psi \right] + a\rho^{1-n} (K \sin \zeta)^n = 0 \quad (21)$$

and integration of this proves result (vi).

In using formula result (vi) the following result is helpful:

$$n \int \text{cosec}^{1+n} \zeta d\zeta = \text{constant} - \cos \zeta \, \text{cosec}^n \zeta - (1 - n) S_{1-n}(\zeta) \quad (22)$$

where $S_m(\zeta)$ is as defined in Section 2(*d*) and is tabulated in the table.

The integral $\int \rho^{1-n} d\psi$ can be evaluated by the methods given in Section 2.

String path

No simple formula for this path can be found for a cylinder of general cross-section except in the case of the circular cylinder. Now

$$dz/ds \equiv \cos \zeta;$$

hence it follows that

$$z = \int (\cos \zeta) ds = \int (\cos \zeta) \rho d\psi \ .$$

From equation (21), substituting for $d\psi$

$$z = (K^{1-n}/a) \int \rho^n \, \text{cosec}^{2+n} \zeta \cos \zeta d\zeta$$

which in the case of a circular cylinder, when $\rho = r = \text{constant}$, gives

$$z - z_0 = \left\{ (K^{1-n} r^n)/[(1 + n)a] \right\} (\text{cosec}^{1+n} \zeta_0 - \text{cosec}^{1+n} \zeta)$$

REFERENCES

(1) MACK, C. *Brit. J. Appl. Phys.*, **4**, p. 145 (1953).

(2) BOWDEN, F. P., and YOUNG, J. E. *Proc. Roy. Soc. A*, pp. 208, 444 (1951).

(3) HOWELL, H. G. *J. Text. Inst.*, **44**, p. *T*359 (1953).

(4) LINCOLN, B. *Brit. J. Appl. Phys.*, **3**, p. 260 (1952).

(5) BAIRD, M. E., and MIESZKIS, K. W. *J. Text. Inst.*, **46**, p. *P*101 (1955).

(6) CHAPMAN, J. A., PASCOE, H. W., and TABOR, D. *J. Text. Inst.*, **46**, p. *P*3 (1955).

(7) LYNE, D. G. *J. Text. Inst.*, **46**, p. *P*112 (1955).

(8) RUBENSTEIN, C. Private communication.

(9) EDWARDS, J. *Differential Calculus*, 3rd Ed., paragraphs 322 and 325 (London: Macmillan and Co. Ltd., 1929).

Space-charge limited current in insulating oil

By Tadashi Satō, Shigeo Nagao, D.Sc., and Yotsuo Toriyama, D.Eng., Engineering Faculty, Tōhoku University, Sendai, Japan

[*Paper first received* 23 *February*, 1955, *and in final form* 19 *March*, 1956]

In order to analyse the pre-breakdown phenomena in insulating oil, a hot tungsten filament emitting an abundance of electrons in a vacuum was employed as cathode. The gap between the electrodes was therefore only partly occupied by the liquid. Currents measured with various voltages and depths of oil were explained on the basis of space-charge limitation in the oil, and the mobility of the negative ion in transformer oil formed by the attachment of electrons to oil molecules was found to be 1×10^{-4} cm/s per V/cm.

In order to analyse pre-breakdown phenomena in insulating oil, a hot tungsten filament emitting an abundance of electrons in a vacuum was employed as cathode. The gap between the electrodes was therefore only partly occupied by the liquid. The mechanism of electric conduction was investigated with a specially constructed discharge tube as shown in Fig. 1. Thermionic electrons emitted from the tungsten filament are accelerated by the electric field through the vacuum and reach the surface of the liquid without serious hindrance. As a specimen, commercial transformer oil filtered free of dust particles by means of sintered glass filters was used. Fig. 2 shows typical current-voltage characteristics with unidirectional stress. It should be noted that the currents are considerably larger than those observed in normal cases of cold-cathode conduction in oil. The results show good reproducibility when the pressure (1 to 2×10^{-3} mm of mercury) remains constant. From these results, particularly the dependence of current on depth of oil, it may be reasonable to consider that the currents depend mainly upon the field strength in the oil, not upon that in the vacuum space. Thus the major part of the voltage is impressed across the oil. This assumption may be proved by an auxiliary measurement of current–voltage characteristics under the same pressure with oil removed from the whole gap. The result is shown in Fig. 3 and it is obvious that the voltages are very much smaller than those required in the presence of oil.

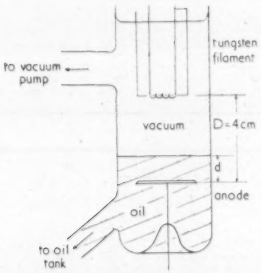

Fig. 1. The discharge tube. The depth d of the oil is accurately controllable. Diameter of anode = 3 cm

Thus we assume that negative ions formed by the attachment of electrons to liquid molecules accumulate near the surface of the oil and give rise to ionic conduction. The problem is thus one of space-charge limited conduction by

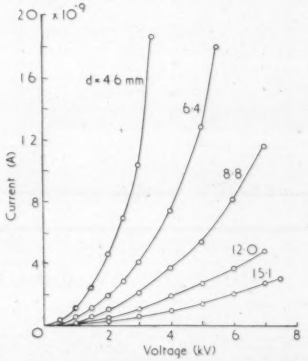

Fig. 2. Current–voltage characteristics with oil depth d as parameter. (Pressure above oil = 2×10^{-3} mm of mercury)

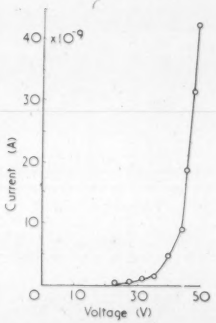

Fig. 3. Current–voltage characteristics with oil removed from gap. (Pressure = 2×10^{-3} mm of mercury)

negative ions. The currents therefore obey the following equation[1]

$$j = 9\epsilon\mu V^2/32\pi d^3 \qquad (1)$$

where j is the current density, ϵ the dielectric constant of the oil, μ the ionic mobility, d the oil depth and V the applied voltage. In this equation the mobility is assumed independent of the field strength and the slight voltage drop in the vacuum is neglected as already explained. Fig. 4 shows the application of equation (1) to our measurements. Currents are shown as ordinates and values of V^2/d^3 as abscissae. It may be that the characteristic curves are satisfactorily represented by equation (1) if the slight voltage drop in the vacuum space, the heating of the oil surface by the hot filament and other experimental errors are taken into consideration. Experimental evidence for our assumption of space-charge limited conduction is thus obtained and the ionic mobility can be evaluated from the slopes of the curves in Fig. 4 as follows:

$$\mu = 0{\cdot}6 \text{ to } 1{\cdot}1 \times 10^{-4} \text{ cm/s per V/cm} \qquad (2)$$

The value of the mobility agrees fairly well with those of previous workers,[2] but we considered it worth while to

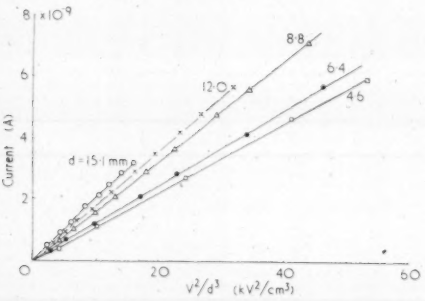

Fig. 4. Results of application of equation (1) to the current–voltage characteristics (Fig. 2)

perform an independent measurement of the mobility. The circuit for this measurement is shown in Fig. 5. The measurement procedure was to apply to the tungsten filament a negative rectangular voltage pulse V_1 of duration t_1 followed by a positive pulse V_2 with duration t_2. The charge accumulated in the condenser C was measured by an electrometer E.

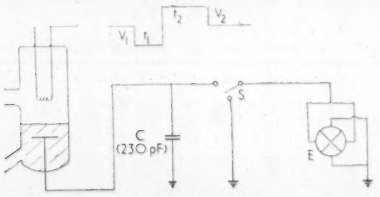

Fig. 5. Circuit for the direct measurement of ionic mobility

The object of the second voltage pulse is to remove residual ions in the oil, thus avoiding induced charges on the anode. In our case, because of the asymmetric distribution of electric field in oil and vacuum, the product of the voltage drop V_2' in oil and the pulse duration t_2 were chosen to be slightly greater than V_1, t_1 and V_2' is assumed to be given by

$$V_2' = V_2 d/[\epsilon D - (\epsilon - 1)d] \qquad (3)$$

Here D is the total gap length. Fig. 6 shows the results of the measurement. Since the transit time t_0 of the negative ion is related to the oil depth d as follows:

$$d = t_0 \mu V/d$$

we obtain

$$\mu = 1{\cdot}1 \times 10^{-4} \text{ cm/s per V/cm} \qquad (4)$$

The agreement of the above value with that obtained from equation (2) also supports the assumption of space-charge limited conduction by negative ions in this case.

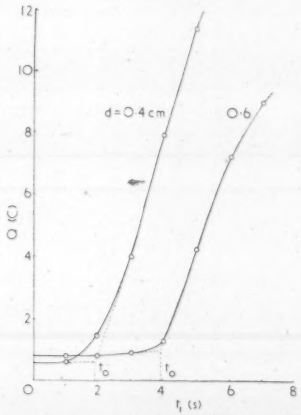

Fig. 6. Results of direct measurement of mobility. The charge Q accumulated by condenser C is plotted against the duration of the negative pulse t_1. The transit times are shown by the intercepts t_0. (Pressure above oil = $2{\cdot}2 \times 10^{-3}$ mm of mercury, $V_1 = 850$ V, $t_2 = 10$ s)

The above experimental evidence suggests that electrons introduced into an insulating oil form negative ions in the presence of field strengths of about 10^{-4} V/cm, that conduction by these ions can take place under conditions of space-charge limitation and that these effects form the basis of a new method of estimating the mobility of such ions.

REFERENCES

(1) Bragg, J. K., Sharbaugh, A. H., and Crowe, R. W. *J. Appl. Phys.*, **25**, p. 382 (1954).

(2) Whitehead, J. B. *Physics*, **6**, p. 380 (1935).
Adamczewsky. *Ann. Phys.* [*Paris*], **8**, p. 309 (1937).

The vibration of segmented beams

By J. P. ELLINGTON, B.Sc., University of Nottingham

[*Paper received* 20 *January*, 1956]

The frequency equations and normal modes are obtained for the flexural oscillations of a light beam carrying equal and equally-spaced concentrated masses. The mass distribution in the "lumped mass" approximation to a continuous beam is discussed.

1. INTRODUCTION

The vibrations of a continuous elastic system can often be conveniently studied by replacing the given system by a number of concentrated or "lumped" masses connected by massless elastic restoring elements, thereby reducing the number of degrees of freedom to a finite value and allowing numerical methods to be used. In certain simple cases, such as the longitudinal or torsional oscillation of a light uniform shaft carrying equal and equally-spaced masses or inertias, it is possible to obtain exact solutions for the frequencies and displacements of the lumped system,[1] but the corresponding case of flexural oscillation does not appear to have been so solved.[2] The problem is not only of interest in helping to assess the errors inherent in the "lumped mass" approximation to a continuous system, but in estimating the frequencies of actually segmented beams which can occur in bridge deckings, trusses or certain stiffened box beams.

In the following study only pure bending is considered, rotary inertia and shearing being neglected, although these latter effects may be appreciable in the higher order modes of vibration.[3] The bending moments and deflexions at the loaded points are taken as unknowns and then the continuity and equilibrium conditions furnish equations which can be solved by the methods of the calculus of finite differences. Substitution in the end conditions then leads to the frequency equation and normal modes.

2. THE DIFFERENCE EQUATIONS

Consider now a long uniform beam, of modulus of elasticity E, and second moment of area I, carrying a number of point loads, each of mass m, spaced at equal distances L. Supposing the beam is vibrating in a sinusoidal manner at a natural circular frequency ω, let the deflexion from the equilibrium position and bending moment at the rth mass be Y_r and M_r.

Then, the slope at the ends of the element connecting the rth and $(r+1)$th masses is given by

$$\theta_r = (1/L)(Y_{r+1} - Y_r) - (L/6EI)(2M_r + M_{r+1})$$

and $$\theta_{r+1} = (1/L)(Y_{r+1} - Y_r) + (L/6EI)(2M_{r+1} + M_r) \quad (1)$$

The shear force which is constant over the element is

$$S_{r,r+1} = S_{r+1,r} = (1/L)(M_{r+1} - M_r) \quad (2)$$

The positive directions for all quantities are as shown in Fig. 1.

From equation (1), for continuity of the beam at the $(r+1)$th mass,

$$\theta_{r+1} = (1/L)(Y_{r+2} - Y_{r+1}) - (L/6EI)(2M_{r+1} + M_{r+2}) = (1/L)(Y_{r+1} - Y_r) + (L/6EI)(2M_{r+1} + M_r)$$

and for equilibrium,

$$S_{r+1,r+2} - S_{r+1,r} = (1/L)(M_{r+2} - 2M_{r+1} + M_r) = m\omega^2 Y_{r+1}$$

These latter two equations are a pair of homogeneous, second order, linear difference equations[4] in the unknowns Y_r and M_r, and using the finite difference "shifting" operator E, defined by $E^x Y_r = Y_{r+x}$, they may be written in operational form as

$$(L^2/6EI)(E-1)^2 M_r + (L^2/EI)EM_r - (E-1)^2 Y_r = 0 \quad (3)$$

and $$(E-1)^2 M_r - m\omega^2 LEY_r = 0 \quad (4)$$

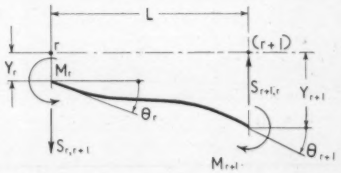

Fig. 1. Sign convention for positive forces, couples and deflexions

For a solution, assume

$$M_r = A\exp(\phi r), \quad \text{and} \quad Y_r = A\mu\exp(\phi r) \quad (5)$$

where A is a disposable constant and ϕ and μ are to be determined. Noting that

$$(E-1)^2\exp(\phi r) = [\exp(\phi) - 1]^2\exp(\phi r)$$

substitution in equation (4) gives

$$\mu = \frac{1}{m\omega^2 L}\frac{[\exp(\phi)-1]^2}{\exp\phi} = \frac{2}{m\omega^2 L}(\cosh\phi - 1) \quad (6)$$

Equation (3) then becomes

$$\frac{L^2}{6EI}[\exp(\phi)-1]^2 + \frac{L^2}{EI}\exp(\phi) - \mu[\exp(\phi)-1]^2 = 0$$

or, $$\cosh^2\phi - \left(2 + \frac{m\omega^2 L^3}{12EI}\right)\cosh\phi + \left(1 - \frac{m\omega^2 L^3}{6EI}\right) = 0$$

Writing $m\omega^2 L^3/24EI = K$,

$$\cosh\phi_{1,2} = (1+K) \pm \sqrt{(K^2 + 6K)} \quad (7)$$

This is the characteristic equation giving a total of four roots, there being a positive and negative value of ϕ associated with each $\cosh\phi$, whilst to each pair of roots there is a corresponding value of μ.

Taking the positive sign in equation (7) it will be seen that the value of $\cosh\phi_1$ is always greater than unity and hence the corresponding roots are real, say $\pm\lambda$. However, taking the negative sign, and noting that the maximum

possible value of K in a free vibration is 2, the value of $\cosh \phi_2$ lies between 1 and -1, and hence gives imaginary roots, say $\pm i\gamma$.

The general solution to the difference equation is then,

$$M_r = A \cosh \lambda r + B \sinh \lambda r + C \cos \gamma r + D \sin \gamma r \quad (8)$$

and

$$Y_r = \mu_1(A \cosh \lambda r + B \sinh \lambda r) + \mu_2(C \cos \gamma r + D \sin \gamma r) \quad (9)$$

where $\left.\begin{matrix}\cosh \lambda \\ \cos \gamma\end{matrix}\right\} = 1 + K \pm \sqrt{(K^2 + 6K)} \quad (10)$

and $$\mu_{1,2} = (2/m\omega^2 L)\left\{\begin{matrix}\cosh \lambda \\ \cos \gamma\end{matrix} - 1\right\} \quad (11)$$

3. THE SIMPLY-SUPPORTED BEAM

(*a*) *Supports distance L from a load.* Consider a beam carrying N masses with simple supports at points O and $(N + 1)$, as shown in Fig. 2(*a*). The end conditions are then that the deflexion and bending moment at each support is zero.

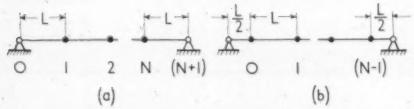

Fig. 2. Arrangement of masses on simply-supported segmented beam

Thus, from equations (8) and (9), at

$$r = 0,\ A + C = 0 \quad \text{and} \quad \mu_1 A + \mu_2 C = 0$$

but from equation (11), $\mu_1 \neq \mu_2$, unless K is zero, so that

$$A = C = 0$$

At

$$r = (N + 1),\ B \sinh \lambda (N + 1) + D \sin \gamma (N + 1) = 0$$

and

$$\mu_1 B \sinh \lambda (N + 1) + \mu_2 D \sin \gamma (N + 1) = 0$$

These equations are satisfied, if $B = 0$, and

$$\sin \gamma (N + 1) = 0, \quad \text{or} \quad \gamma = p\pi/(N + 1),$$

where p is an integer.

From equation (10),

$$K = (\cos \gamma - 1)^2/(4 + 2 \cos \gamma)$$

Therefore $$\frac{m\omega^2 L^3}{24EI} = \frac{\{\cos[p\pi/(N + 1)] - 1\}^2}{4 + 2 \cos[p\pi/(N + 1)]} \quad (12)$$

Permissible values of p for non-trivial solutions are $p = 1, 2 \ldots N$. If $p = (N + 1)$ then $\sin \gamma r$ is always zero and there is no motion, whilst the values $p = (N + 2)$, $(N + 3)$, . . . merely repeat the values of ω given by $p = N, (N - 1), \ldots$

(*b*) *Supports distance L/2 from a load.* In this case consider a beam carrying N masses, with the supports at a distance $L/2$ from the Oth and $(N - 1)$th masses, as shown in Fig. 2(*b*). Now since the simple supports give the same end conditions as a node, the beam may be regarded as a portion of an infinite beam so that,

$$Y_0 = -Y_{-1} \quad \text{and} \quad M_0 = -M_{-1}$$

also, $$Y_{N-1} = -Y_N \quad \text{and} \quad M_{N-1} = -M_N$$

Therefore

$$0 = \mu_1[A(1 + \cosh \lambda) - B \sinh \lambda] + \\ + \mu_2[C(1 + \cos \gamma) - D \sin \gamma]$$

$$0 = A(1 + \cosh \lambda) - B \sinh \lambda + C(1 + \cos \gamma) - D \sin \gamma$$

Again, for a non-trivial solution $\mu_1 \neq \mu_2$.

Therefore $$0 = A(1 + \cosh \lambda) - B \sinh \lambda \quad (13)$$

and $$0 = C(1 + \cos \gamma) - D \sin \gamma \quad (14)$$

Also,

$$0 = \mu_1 \cosh \tfrac{1}{2}\lambda [A \cosh \lambda (N - \tfrac{1}{2}) + B \sinh \lambda (N - \tfrac{1}{2})] + \\ + \mu_2 \cos \tfrac{1}{2}\gamma [C \cos \gamma (N - \tfrac{1}{2}) + D \sin \gamma (N - \tfrac{1}{2})]$$

and

$$0 = \cosh \tfrac{1}{2}\lambda [A \cosh \lambda (N - \tfrac{1}{2}) + B \sinh \lambda (N - \tfrac{1}{2})] + \\ + \cos \tfrac{1}{2}\gamma [C \cos \gamma (N - \tfrac{1}{2}) + D \sin \gamma (N - \tfrac{1}{2})]$$

Hence $$0 = A \cosh \lambda (N - \tfrac{1}{2}) + B \sinh \lambda (N - \tfrac{1}{2}) \quad (15)$$

and $$0 = C \cos \gamma (N - \tfrac{1}{2}) + D \sin \gamma (N - \tfrac{1}{2}) \quad (16)$$

From equations (13) and (15) $A = B = 0$, whilst from equations (14) and (16), unless C and D are zero, then

$$0 = (1 + \cos \gamma) \sin \gamma (N - \tfrac{1}{2}) + \sin \gamma \cos \gamma (N - \tfrac{1}{2}) = \\ = 2 \sin \gamma N \cos \gamma/2$$

Thus, $$\gamma = p\pi/N \quad (p = 1, 2, \ldots N)$$

and $$\frac{m\omega^2 L^3}{24EI} = \frac{[\cos(p\pi/N) - 1]^2}{4 + 2 \cos(p\pi/N)} \quad (17)$$

The modal shape from, say, equation (14) is

$$Y_r = C \sin (p\pi/N)(r + \tfrac{1}{2})$$

4. THE FREE-FREE BEAM

With the free-free beam and encastré beam, it is convenient to consider a beam carrying an odd number of masses, thereby allowing an origin to be taken at the centre of the beam so that the symmetric and asymmetric modes may be considered separately.

(i) *Symmetric modes*

With a symmetric mode the deflexions and moments on either side of the origin are equal, or,

$$Y_1 = Y_{-1} \quad \text{and} \quad M_1 = M_{-1}$$

Therefore $$\mu_1 B \sinh \lambda + \mu_2 D \sin \gamma = 0$$

and $$B \sinh \lambda + D \sin \gamma = 0$$

Thus, as $\mu_1 \neq \mu_2$,

$$B = D = 0 \quad (18)$$

(ii) *Asymmetric modes*

Here, the centre of the beam is a node, the central deflexion and bending moment being zero.

$$Y_0 = 0 \quad \text{and} \quad M_0 = 0,$$

or, $$\mu_1 A + \mu_2 C = 0 \quad \text{and} \quad A + C = 0$$

Thus, $$A = C = 0 \quad (19)$$

(*a*) *Masses $\frac{1}{2}m$ at each end.* The beam, in this case, is taken as carrying $(2N+1)$ equally spaced masses, with the Nth, or end, loads of mass $\frac{1}{2}m$. The bending moment at the end of the beam is zero, so that,

$$M_N = 0 = A\cosh\lambda N + B\sinh\lambda N + C\cos\gamma N + D\sin\gamma N \quad (20)$$

For equilibrium of the Nth mass,

$$M_{N-1} - (m\omega^2 L/2)\,Y_N = 0$$

or, since $m\omega^2 L\mu_{1,2} = 2\left\{\begin{matrix}\cosh\lambda \\ \cos\ \gamma\end{matrix} - 1\right\}$,

$$0 = \sinh\lambda\,(A\sinh\lambda N + B\cosh\lambda N) + \sin\gamma\,(-C\sin\gamma N + D\cos\gamma N) \quad (21)$$

In a symmetric mode,

$$B = D = 0$$

or,
$$0 = \sin\gamma\tan\gamma N + \sinh\lambda\tanh\lambda N \quad (22)$$

and
$$Y_r = A\left[(\cosh\lambda - 1)\frac{\cosh\ \lambda r}{\cosh\lambda N} - (\cos\gamma - 1)\frac{\cos\ \gamma r}{\cos\gamma N}\right] \quad (23)$$

In an asymmetric mode,

$$A = C = 0$$

or,
$$0 = \sin\gamma\cot\gamma N - \sinh\lambda\coth\lambda N \quad (24)$$

and
$$Y_r = B\left[(\cosh\lambda - 1)\frac{\sinh\ \lambda r}{\sinh\lambda N} - (\cos\gamma - 1)\frac{\sin\ \gamma r}{\sin\gamma N}\right] \quad (25)$$

The frequency equations (22) and (24) are most readily solved by plotting the above expressions over an assigned range of values of K.

(*b*) *Masses m at each end.* Here, for equilibrium at $r = N$,

$$M_{N-1} - m\omega^2 L\,Y_N = 0$$

or,

$$0 = A\cosh\lambda(N+1) + B\sinh\lambda(N+1) + C\cos\gamma(N+1) + D\sin\gamma(N+1) \quad (26)$$

Hence from equations (20) and (26), in a symmetric mode,

$$\frac{\cos\gamma(N+1)}{\cos\gamma N} - \frac{\cosh\lambda(N+1)}{\cosh\lambda N} = 0 \quad (27)$$

and in an asymmetric mode,

$$\frac{\sin\gamma(N+1)}{\sin\gamma N} - \frac{\sinh\lambda(N+1)}{\sinh\lambda N} = 0 \quad (28)$$

The modal shapes are also given by the expressions (23) and (25).

5. THE BUILT-IN BEAM

Again, a beam carrying an odd number of masses, $(2N+1)$, is considered, the origin being taken at the centre of the beam with position and direction fixed ends at $r = \pm(N+1)$.

Since the deflexion and slope are zero at each end,

$$Y_N = 0 = (\cosh\lambda - 1)\,[A\cosh\lambda(N+1) + B\sinh\lambda(N+1)] + (\cos\gamma - 1)\,[C\cos\gamma(N+1) + D\sin\gamma(N+1)] \quad (29)$$

From equation (1)

$$\theta_{N+1} = 0 = -(Y_N/L) + (L/6EI)(2M_{N+1} + M_N)$$

Noting from the characteristic equation (7)

$$\frac{6EI}{L^2}\mu_1 = \frac{\cosh\lambda + 2}{\cosh\lambda - 1} \quad \text{and} \quad \frac{6EI}{L^2}\mu_2 = \frac{\cos\gamma + 2}{\cos\gamma - 1} \quad (30)$$

the zero slope condition becomes

$$0 = A\left[2\cosh\lambda(N+1) - \frac{3\cosh\lambda N}{(\cosh\lambda - 1)}\right] + B\left[2\sinh\lambda(N+1) - \frac{3\sinh\lambda N}{(\cosh\lambda - 1)}\right] + \text{similar terms in } \gamma.$$

Then writing $\cosh\lambda N = \cosh[\lambda(N+1) - \lambda]$, etc., and expanding in the above equation, and using equations (29) and (30)

$$0 = [\sinh\lambda/(\cosh\lambda - 1)][A\sinh\lambda(N+1) + B\cosh\lambda(N+1)] + [\sin\gamma/(\cos\gamma - 1)][-C\sin\gamma(N+1) + D\cos\gamma(N+1)] \quad (31)$$

Thus, in a symmetric mode with $B = D = 0$ the frequency equation is

$$0 = \frac{\sinh\lambda\tanh\lambda(N+1)}{(\cosh\lambda - 1)^2} + \frac{\sin\gamma\tan\gamma(N+1)}{(\cos\gamma - 1)^2} \quad (32)$$

and
$$Y_r = A\left[\frac{\cosh\lambda r}{\cosh\lambda(N+1)} - \frac{\cos\gamma r}{\cos\gamma(N+1)}\right] \quad (33)$$

Similarly, for an asymmetric mode,

$$0 = \frac{\sinh\lambda\coth\lambda(N+1)}{(\cosh\lambda - 1)^2} - \frac{\sin\gamma\cot\gamma(N+1)}{(\cos\gamma - 1)^2} \quad (34)$$

and
$$Y_r = B\left[\frac{\sinh\lambda r}{\sinh\lambda(N+1)} - \frac{\sin\gamma r}{\sin\gamma(N+1)}\right] \quad (35)$$

6. THE CANTILEVER

The cantilever is taken as carrying N masses, with a mass $\frac{1}{2}m$ at the free-end and the support at $r = N$.

Then, at the free end,

$$M_0 = 0 \quad \text{and} \quad 2M_1 - m\omega^2 L\,Y_0 = 0$$

Therefore

$$C = -A \quad \text{and} \quad D = -(B\sinh\lambda/\sin\gamma)$$

At the fixed end, using equations (29) and (31)

$$0 = A\left[\cosh\lambda N - \frac{(\cos\gamma - 1)}{(\cosh\lambda - 1)}\cos\gamma N\right] + B\left[\sinh\lambda N - \frac{(\cos\gamma - 1)}{(\cosh\lambda - 1)}\frac{\sinh\lambda}{\sin\gamma}\sin\gamma N\right]$$

and
$$0 = A\left[\sinh\lambda N + \frac{(\cosh\lambda - 1)}{(\cos\gamma - 1)}\frac{\sin\gamma}{\sinh\lambda}\sin\gamma N\right] + B\left[\cosh\lambda N - \frac{(\cosh\lambda - 1)}{(\cos\gamma - 1)}\cos\gamma N\right]$$

Eliminating A and B gives the frequency equation,

$$0 = 2 - \cosh\lambda N\cos\gamma N\left(\frac{\mu_1}{\mu_2} + \frac{\mu_2}{\mu_1}\right) + \sinh\lambda N\sin\gamma N\left(\frac{\mu_2\sinh\lambda}{\mu_1\sin\gamma} - \frac{\mu_1\sin\gamma}{\mu_2\sinh\lambda}\right) \quad (36)$$

where μ_1/μ_2 has been written for $(\cosh\lambda - 1)/(\cos\gamma - 1)$.

7. APPROXIMATE SOLUTIONS

Table 1. *Comparison of values of* λ *and* γ *from equation* (10),

$$\left.\begin{matrix}\cosh\lambda\\ \cos\gamma\end{matrix}\right\} = 1 + K \pm \sqrt{(K^2 + 6K)}$$

K	λ	γ	γ/λ
0·005	0·5886	0·5886	1·0000
0·010	0·7000	0·7000	1·0000
0·050	1·0470	1·0472	1·0002
0·10	1·2454	1·2461	1·0006
0·50	1·8642	1·8784	1·0076
1·00	2·2174	2·2729	1·0250
1·50	2·4528	2·5944	1·0577
2·00	2·6338	3·1416	1·1928

Table 1 gives values λ and γ calculated from equation (10), and it can be seen that over a large range of values of K, λ and γ are equal, the difference between them being only 0·76% at $K = 0{\cdot}5$, and 2·5% at $K = 1$.

Hence, when K is less than unity, as will be the case for beams with a moderate number of segments in their graver modes, the work involved in solving the frequency equations can be reduced by taking λ and γ as equal.

8. THE UNIFORM CONTINUOUS BEAM

If the number of segments in the beam is sufficiently greater than the order of mode of vibration, so that $\sqrt{K}$ is an extremely small quantity, then the characteristic equation (7) can be written as,

$$\cosh\phi_{1,2} = 1 \pm \sqrt{(6K)}$$

Thus ϕ is also a small quantity and $\cosh\phi$ can be written as $(1 + \frac{1}{2}\phi^2)$, so that there are four roots

$$\phi = \pm\sqrt[4]{(24K)} \quad \text{and} \quad \pm i\sqrt[4]{(24K)}$$

Equations (8)–(11) then become

$$M_r = A\cosh\beta r + B\sinh\beta r + C\cos\beta r + D\sin\beta r \quad (37)$$

and

$$Y_r = \mu(A\cosh\beta r + B\sinh\beta r - C\cos\beta r - D\sin\beta r) \quad (38)$$

where

$$\beta^4 = 24K = m\omega^2L^3/EI \quad (39)$$

and

$$\mu = \beta^2/m\omega^2L \quad (40)$$

These equations agree with the Bernoulli–Euler equations for the vibrations of a uniform continuous beam and may be used for deriving frequency equations and modes. Alternatively taking, say, the case described in Section 4(*a*), a free-free beam, since λ and γ are very small and equal, $\sinh\lambda = \sin\gamma$, and the frequency equations for the symmetric and asymmetric modes are,

$$\tan\beta N + \tanh\beta N = 0$$

$$\tan\beta N - \tanh\beta N = 0$$

If σ is the mass per unit length of the continuous beam, and l its overall length,

$$\sigma = m/L \quad \text{and} \quad l = 2NL$$

so that $\beta N = \frac{1}{2}l(\sigma\omega^2/EI)^{\frac{1}{4}}$.

Multiplying the two previous equations together then gives the well-known result for the continuous free-free beam,

$$\cos l(\sigma\omega^2/EI)^{\frac{1}{4}} = \operatorname{sech} l(\sigma\omega^2/EI)^{\frac{1}{4}}$$

The question now arises, when, in order to render the problem amenable to computational methods, a continuous structure is replaced by a segmented one, in what way should the mass of the structure be distributed? Taking a continuous beam regarded as divided into a convenient number of sections two possibilities occur; the mass of each section can be placed at the centre of the section, or, alternatively, the mass can be divided into halves, with one half at each end of the section. The results obtained from these two possibilities must be compared on the basis of the number of degrees of freedom of the system and not on the number of sections, since, say, in the case of the free-free beam divided into n sections the central mass distribution gives n masses, whilst the end mass distribution gives $(n + 1)$.

To consider some particular cases take first of all a continuous simply supported beam divided into equal sections so that there are N vibrating masses. If σ is the mass per unit length, and the overall length l, then from equations (12) and (17), with end mass distribution,

$$\alpha_E = \frac{\sigma\omega^2l^4}{EI} = \frac{12(N+1)^4\{\cos[p\pi/(N+1)] - 1\}^2}{2 + \cos[p\pi/(N+1)]} \quad (41)$$

and with central mass distribution,

$$\alpha_C = \frac{\sigma\omega^2l^4}{EI} = \frac{12N^4[\cos(p\pi/N) - 1]^2}{2 + \cos(p\pi/N)} \quad (42)$$

The correct frequency parameter is $\alpha = (p\pi)^4$, and the results given by equations (41) and (42) are compared in Table 2.

Table 2. *Simply supported beam*

Number of masses	*Fundamental* $\alpha = 97{\cdot}409$		*Simply supported beam. First overtone* $\alpha = 1558{\cdot}84$	
	α_E/α	α_C/α	α_E/α	α_C/α
1	0·9855	0·4928	—	—
2	0·9979	0·9855	0·9356	0·4928
3	0·9994	0·9979	0·9855	0·9355
4	0·9997	0·9994	0·9951	0·9855

It can be seen that for a given number of *sections* these results are identical, and that when the number of sections n is much larger than p,

$$\frac{\sigma\omega^2l^4}{EI} \simeq (p\pi)^4 - \frac{1}{720}\frac{(p\pi)^8}{n^4}$$

or, the error in the frequency parameter ultimately becomes inversely proportional to the fourth power of the number of segments.

Table 3, obtained from Section 4, gives results for the free-free beam. In this case inspection shows that the error in the frequency parameter eventually becomes inversely

Table 3. *Free-free beam*

Number of masses	*Fundamental* $\alpha = 500{\cdot}55$		*First overtone* $\alpha = 3803{\cdot}53$	
	α_E/α	α_C/α	α_E/α	α_C/α
3	0·3836	1·4564	—	—
5	0·7142	1·1373	0·6058	1·2324
7	0·8507	1·0669	0·7723	1·1151
9	0·9107	1·0404	0·8575	1·0678

proportional to the square of the number of masses. A similar result for the segmented cantilever has been given by Duncan.[2]

The difference in the degree of convergence between these cases may be explained in that only the simply supported beam satisfies all the end conditions of the uniform beam, the modal shapes agreeing exactly.

From Table 2 it can be seen that for a fairly uniform simply supported beam both mass distributions underestimate the natural frequency of the actual beam, with the end mass distribution giving the better approximation. Similar conclusions can be drawn for the beam encastré at each end.

With the free-free beam, Table 3, and the cantilever beam, the central mass distribution gives the highest and, generally, the more accurate estimate of the actual frequency.

ACKNOWLEDGEMENT

The author would like to express his gratitude to Dr. H. McCallion for his helpful advice and encouragement.

REFERENCES

(1) KÁRMÁN, T. V., and BIOT, M. A. *Mathematical Methods in Engineering* (New York: McGraw-Hill Book Co. Inc., 1940).
(2) DUNCAN, W. J. *Quart. J. Mech. Appl. Math.*, **5**, p. 97 (1952).
(3) TRAILL-NASH, R. W., and COLLAR, A. R. *Quart. J. Mech. Appl. Math.*, **6**, p. 186 (1953).
(4) MILNE-THOMSON, L. M. *The Calculus of Finite Differences* (London: Macmillan and Co. Ltd., 1951).

Applications of a transformer analogue computer

By J. R. BARKER, Ph.D., A.Inst.P., Electrical Engineering Dept., Imperial College of Science and Technology, London

[*Paper first received* 9 *January, and in final form* 11 *April*, 1956]

The Blackburn analyser is a versatile transformer analogue computer well known among electrical-power engineers as an a.c. network analyser. This paper shows that it can be used to solve many algebraic problems involving real or complex numbers. Among these are the extraction of the latent roots of matrices, the location of the zeros of polynomials, and the solution of linear and non-linear simultaneous equations.

The Imperial College transformer analogue computer, based on Blackburn's principle,[1] was primarily designed for the solution of steady state a.c. network problems, and for the solution of simultaneous linear equations with complex coefficients. A detailed description of its principles and applications as a network analyser (particularly for power-network problems) has been given elsewhere.[2,3] It has since been used for studies of circuits containing valves and transistors operating under linear conditions and for the solution of differential equations by means of networks. (Michaelson[4] has given a mathematical account of the use of network analysers in solving differential equations.) This paper describes how a Blackburn analyser can be used to solve some mathematical problems, occurring in physics and engineering, which are not directly related to its function as a network analyser. These are:

(i) linear algebra with real or complex numbers: solution of simultaneous equations; multiplication and inversion of matrices; solution of secular (=latent-root or eigenvalue) equations;

(ii) non-linear algebra: evaluation of polynomials for real and complex values of the variable, and the location of their zeros; solution of simultaneous algebraic equations involving products, quotients and powers of the unknowns;

(iii) examination of simultaneous inequalities for consistency.

Doubtless, further applications will become apparent in the future, but it seems timely to review what has already been achieved because several of these Blackburn analysers are now being planned or built in this country.

PRINCIPLES OF THE ANALYSER

The analyser consists of: (i) a set of identical voltage transformers whose ratios can be varied by decade switches; each transformer has a simple valve circuit associated with it, in a feedback connexion, so that the performance closely approximates that of an "ideal transformer"; (ii) a 75 c/s oscillator providing constant output voltage at nearly zero output impedance, for energizing the transformers; and (iii) equipment for selecting and measuring the voltage on any transformer winding. For further details, see Refs. 2 and 3.

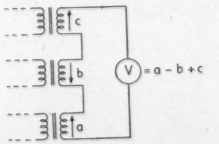

Fig. 1. Addition and subtraction

Details of Blackburn's original analyser have not been published.

The analyser can perform addition and subtraction of numbers represented by voltages, and multiplication and division of numbers represented, in turn, by voltages and transformer ratios; as shown in Figs. 1 and 2, the results appear as voltages. It is possible to combine these two ideas and to carry out many complicated algebraic operations.

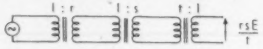

Fig. 2. Multiplication and division

Blackburn's principal achievement was to show how addition and multiplication could be carried out with *complex* numbers. Thus, for the two triple wound transformers connected as in Fig. 3, the voltages and transformer ratios satisfy the equations:

$$x = ay - a'y' \qquad x' = a'y + ay' \tag{1}$$

These are recognizable as, respectively, the real and imaginary parts of the complex number equation

$$\boldsymbol{X} = \boldsymbol{AY} \tag{2}$$

where $\boldsymbol{X} = x + jx'$, $\boldsymbol{A} = a + ja'$, $\boldsymbol{Y} = y + jy'$ and $j = \sqrt{-1}$. The arrangement is therefore an analogue multiplier in Cartesian form.

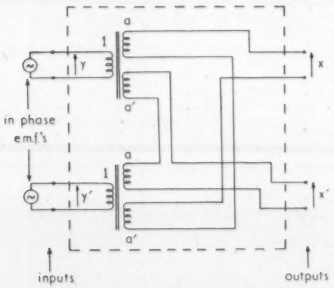

Fig. 3. A complex multiplier

To add complex numbers, each of which is now specified by two voltages, it is merely necessary to add the real parts by connecting them in series, and similarly to add the imaginary parts. To produce the complex number $\boldsymbol{AYZ}$, the two output voltages on the right of Fig. 3 are put into the left-hand (input) side of a similar transformer arrangement set to ratios $1 : z : z'$ (instead of $1 : a : a'$) where $z + jz' = \boldsymbol{Z}$.

Referring to Fig. 3, the windings marked 1 consist of 1000 turns; those marked with letters can be varied in unit steps from 0 to 999 turns so that complex numbers with Cartesian components in the range 0 to 0·999 can be accommodated. Negative signs are obtained by reversing the appropriate windings by switches. Complex numbers with real and/or imaginary parts greater than unity can be represented, on the convenient scale of 1000 turns per unit, if the inputs and outputs of Fig. 3 are exchanged (left for right) and the *reciprocal* of the complex number is set on the dials. Thus the whole range of complex numbers is attainable.

PRODUCTION OF INTERCONNEXION DIAGRAMS

As an example, the function $\boldsymbol{Y} = \boldsymbol{AX} + \boldsymbol{BZ}$ can be generated as a voltage by the network of Fig. 4, where each box is a complex multiplier unit such as is enclosed by the dotted lines of Fig. 3. If *real* numbers were being used, the network generating the function $y = ax + bz$ would be that of Fig. 5. Then, on comparing Figs. 4 and 5, it is evidently

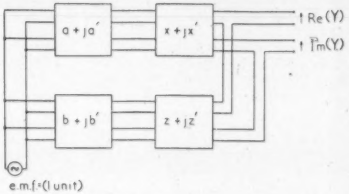

Fig. 4. Generation of $\boldsymbol{Y} = \boldsymbol{AX} + \boldsymbol{BZ}$

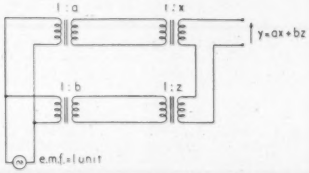

Fig. 5. Generation of $y = ax + bz$

only necessary to work out a connexion scheme which satisfies corresponding real-number equations. This connexion scheme is carried out with the upper (real) inputs and upper outputs of the "boxes" and is then rapidly copied on the lower (imaginary) inputs and lower outputs. In the rest of this paper, therefore, as in practical applications of the analyser, it is only necessary to formulate the transformer network for real number calculations on the lines of Fig. 5.

LINEAR ALGEBRA

Simultaneous linear equations. The method of solution will be explained for the case of two equations, which have to be solved for x_1 and x_2:

$$ax_1 + bx_2 = y_1 \tag{3a}$$
$$cx_1 + dx_2 = y_2 \tag{3b}$$

In the network of Fig. 6, the voltages round the shaded loops satisfy the equations, and the voltages x_1 and x_2 in equation (3*a*) are forced to be the same as those in equation (3*b*) by the constraints imposed by the connexions at the right-hand

side of Fig. 6. The simultaneous solution of the equations is thus automatically ensured. The voltages x_1 and x_2 can be measured and, in favourable cases, give the solution with an error of only 1 in 500. The extension to complex coefficients has already been explained, and the case of more than two equations is readily solved on the same lines. The number of complex multiplier units needed for n simultaneous

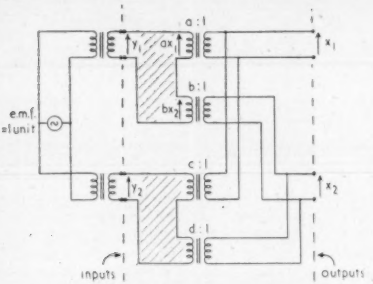

Fig. 6. Simultaneous equations

equations is $n^2 + n$; the present analyser has 32 units so the maximum value of n is 5.

Mallock's well-known simultaneous equation solver[5] uses n transformers with n windings each, for n equations in *real* numbers. This computer cannot be applied to such a wide range of problems as Blackburn's.

Inversion of matrices. The analyser can invert $n \times n$ matrices, where n does not exceed 5 in this case. To give a simple example, the matrix of coefficients in equations (3), namely $\begin{pmatrix} a & b \\ c & d \end{pmatrix}$, is inverted just as in hand computation[6] by solving the simultaneous equations with the right-hand sides y_1, y_2 first equal to 1, 0 and then to 0, 1. If the solutions are α, β and γ, δ respectively, the inverse matrix is $\begin{pmatrix} \alpha & \gamma \\ \beta & \delta \end{pmatrix}$ and this can be interpreted by stating that equations (3) have been transformed into

$$\begin{aligned} \alpha y_1 + \gamma y_2 &= x_1 \\ \beta y_1 + \delta y_2 &= x_2 \end{aligned}$$

Multiplication of matrices. Banks and Parton[7] have shown how matrix products, and their inverses, can be computed with the analyser. Consider the matrix $\boldsymbol{A} = \begin{pmatrix} a & b \\ c & d \end{pmatrix}$ belonging to equations (3), and $\boldsymbol{A}' = \begin{pmatrix} a' & b' \\ c' & d' \end{pmatrix}$ which belongs to equations (4) below.

$$\begin{aligned} a'z_1 + b'z_2 &= x_1 \\ c'z_1 + d'z_2 &= x_2 \end{aligned} \qquad (4)$$

Now $\boldsymbol{AA'Z} = \boldsymbol{AX} = \boldsymbol{Y}$, so that the matrix product $\boldsymbol{AA'}$ is the array of coefficients $\begin{pmatrix} p & q \\ r & s \end{pmatrix}$ belonging to equations (5) which relate $\boldsymbol{Z}$ and $\boldsymbol{Y}$:

$$\begin{aligned} pz_1 + qz_2 &= y_1 \\ rz_1 + sz_2 &= y_2 \end{aligned} \qquad (5)$$

These relations between the y's and the z's become available on the analyser if the outputs x_1, x_2 of Fig. 6 are fed into the inputs of another set of similarly connected transformers (the components to the left of the left-hand dotted line on Fig. 6 not being needed on the second set); the transformer ratios of the second set are made $a' : b' : c' : d' : 1$ instead of $a : b : c : d : 1$ If now, using equations (5) (which apply to the double set of transformers) and the ideas of the previous paragraph, the values of y_1, y_2 are set in turn to 1, 0 and then to 0, 1, the measured values of z_1, z_2 which are the output voltages of the second set of transformers will be the elements of the matrix *inverse* to $\begin{pmatrix} p & q \\ r & s \end{pmatrix}$. This is itself a useful result, but it is also possible to obtain p, q, r and s directly as follows. The compound network is excited at its extreme right-hand (instead of left-hand) side by voltages z_1, z_2 which are in turn 1, 0 and then 0, 1. By equations (5), the voltages y_1, y_2 measured at the normal input positions on open loop (i.e. at the left-hand dotted line of Fig. 6) will be the elements p, r and then q, s. The other matrix product $\boldsymbol{A'A}$ can be evaluated by exchanging the order of the matrices on the two sets of transformers.

All these ideas can be extended to matrices of higher order, and also to triple matrix products, with some limitations on accuracy.

Secular equations. Simultaneous equations of the type

$$\begin{aligned} (a_{11} - \lambda)x_1 + a_{12}x_2 &= 0 \\ a_{21}x_1 + (a_{22} - \lambda)x_2 &= 0 \end{aligned} \qquad (6)$$

are of frequent occurrence in vibrational problems and have to be solved for λ and x_2/x_1. The natural frequency and the damping of each mode of vibration can be found from the values of λ (which are generally complex numbers). Equations 6 are satisfied by two different values of λ and of x_2/x_1.

In the transformer assembly of Fig. 7, the voltages round loops A and B satisfy equations (6) provided that the two

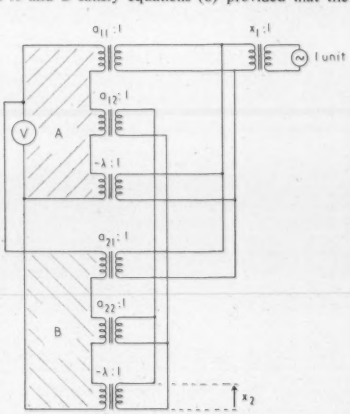

Fig. 7. Secular equations

transformers of ratio λ : 1 have been adjusted together until the voltmeter V reads zero. This voltage V, when dealing with a complex number problem, is really *two* in-phase voltages representing the Cartesian components of the unbalance; the one representing the imaginary component is

advanced 90° in phase in the measuring equipment, added to the real part, and the modulus displayed on a meter; λ is varied until this modulus vanishes. Voltage x_1 has to be set to a convenient value so that no transformers are saturated and voltage x_2 is within the range of the measuring equipment; there are two values of λ for which $|V|$ vanishes.

To show the accuracy attainable, the "eigenvalues" λ and "eigenvectors" (x_1, x_2) of the complex number matrix

$$\begin{pmatrix} a_{11} = 0{\cdot}500 + 0{\cdot}300j & a_{12} = -1{\cdot}000 + 0{\cdot}600j \\ a_{21} = 0{\cdot}200 + 1{\cdot}000j & a_{22} = 0{\cdot}700 - 0{\cdot}500j \end{pmatrix}$$

were measured and compared with computed values:

	Measured	*Computed*
λ	$0{\cdot}153 + 0{\cdot}971j$	$0{\cdot}1525 + 0{\cdot}9725j$
x_2/x_1	$0{\cdot}553 - 0{\cdot}342j$	$0{\cdot}5522 - 0{\cdot}3412j$
λ	$(0{\cdot}423 + 0{\cdot}476j)^{-1}$	$1{\cdot}0475 - 1{\cdot}1725j$
x_2/x_1	$-1{\cdot}060 + 0{\cdot}846j$	$-1{\cdot}0522 + 0{\cdot}8412j$

The second value of λ has real and imaginary parts greater than unity so that its reciprocal was obtained from the analyser dials: $(0{\cdot}423 + 0{\cdot}476j)^{-1} = 1{\cdot}043 - 1{\cdot}174j$.

The method can be used for n equations of the type being considered, when $n^2 + n + 2$ complex multiplier units are required (one unit, not shown in Fig. 7, is used to step-up the voltage applied to the meter in the last stages of adjustment to zero). Ryder[8] has shown how to solve secular equations with the Mallock type of transformer computer.

NON-LINEAR ALGEBRA

Evaluation of polynomial functions and the location of their zeros. A polynomial

$$f(z) = z^n + a_{n-1}z^{n-1} + \ldots + a_1 z + a_0$$

can be generated by the transformer assembly of Fig. 8. Using complex multiplier units, $f(z)$ can be generated and measured even when z and the coefficients are complex numbers. By adjusting the ratios of all the z-transformers together, so as to scan the complex z-plane in a systematic manner, both the real and complex zeros of $f(z)$ can be located in a reasonable time, a time which could, however, be much reduced if ganged complex multiplier units were available. (Such units would be useful for many other problems, e.g. solution of secular equations.) When the coefficients a_i are all real, the complex roots, if any, occur in conjugate pairs so that only the upper half of the z-plane needs scanning. This is done in four sections:

(i) real part of z in the range (0, 1)
(ii) real part of z in the range (0, −1)
(iii) real part of z^{-1} in the range (0, 1)
(iv) real part of z^{-1} in the range (0, −1).

In all four cases, the imaginary part of the variable indicated is taken through the range (0, 1), but real zeros are sought before complex ones. A suitable interval for the scan seems to be 0·2 in both real and imaginary parts, so that there are thirty-six readings of $|f(z)|$ in each region, although eleven of them are common to other regions. The readings of $|f(z)|$ are taken only to two significant figures, direct from a voltmeter, and are recorded on a diagram of the z-plane. It takes about twenty minutes to produce each of the four diagrams and about five minutes to refine the position of each roughly-indicated zero. (These figures refer to a fifth or sixth degree polynomial. If ganged complex-multipliers

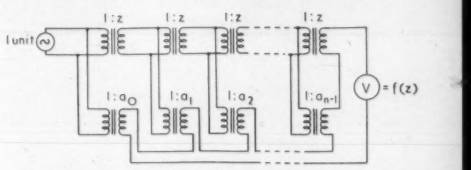

Fig. 8. Generation of polynomial function

were available, the process would be much quicker.) The total number of units needed for an n^{th} degree equation is $2n + 1$, the extra one being used to step-up the voltage to the meter in order to increase the sensitivity when near a zero.

The following polynomial equation has been solved on the analyser:

$$z^6 + 0{\cdot}730z^5 + 0{\cdot}751z^4 + 0{\cdot}207z^3 + 0{\cdot}153z^2 + 0{\cdot}048z + 0{\cdot}822 = 0$$

The six roots, which are all complex, were found in the first two regions examined, thus taking considerably less than an hour. From each pair of roots $p \pm jq$, the corresponding quadratic factors $z^2 - 2pz + p^2 + q^2$ were calculated, and these were refined (on a hand calculating machine) by one application of Bairstow's process (Ref. 6, p. 205) so that their accuracy before refinement could be judged:

roots found	*quadratic factor*	*refined quadratic factor*
$0{\cdot}647 + 0{\cdot}531j$	$z^2 - 1{\cdot}294z + 0{\cdot}700$	$z^2 - 1{\cdot}2925z + 0{\cdot}7005$
$(-0{\cdot}130 + 0{\cdot}939j)^{-1}$	$z^2 + 0{\cdot}290z + 1{\cdot}113$	$z^2 + 0{\cdot}2865z + 1{\cdot}1125$
$(-0{\cdot}822 + 0{\cdot}519j)^{-1}$	$z^2 + 1{\cdot}740z + 1{\cdot}058$	$z^2 + 1{\cdot}7364z + 1{\cdot}0547$

Simultaneous non-linear algebraic equations. Consider the equation

$$\frac{\alpha}{f^2} = \frac{A}{1 + (f/f_c)^2} + B$$

which expresses the variation of absorption coefficient α with frequency f for plane ultrasonic waves in a medium exhibiting a relaxation phenomenon in the vicinity of a frequency f_c and involves real numbers only. The values of A, B and f_c are characteristic of the medium and have to be found from measurements of α/f^2 and f. Thus, altering the notation so that the unknowns become x, y and z,

$$a_i = \frac{x}{1 + (b_i/y)} + z \quad \text{where } i = 1, 2, 3, \ldots$$

The analyser can be used to solve three such equations for x, y and z. If more than three equations were available, combinations of three at a time could be solved and the best values of x, y and z obtained by intelligent averaging. Mallock,[5] however, gives some information as to how "least squares" solutions might be obtained.

The equations are now rearranged into a form which leads to the transformer assembly of Fig. 9:

$$a_i(1 + b_i y^{-1}) - z(1 + b_i y^{-1}) = x \quad \text{where } i = 1, 2 \text{ or } 3.$$

The transformers of ratio marked $1 : (-z)$ are varied together until the voltmeter reads zero; this adjustment of three transformers takes about five minutes. The voltages marked (2) and (3) must be equal because of the connexions; they become equal to (1) when z has been adjusted so that $V = 0$. Then, since the equations must be satisfied by the voltages on the analyser, voltages (1), (2) and (3) equal $-x$, y^{-1} equals the voltage so marked on the figure, and z is read off the transformer ratio dials.

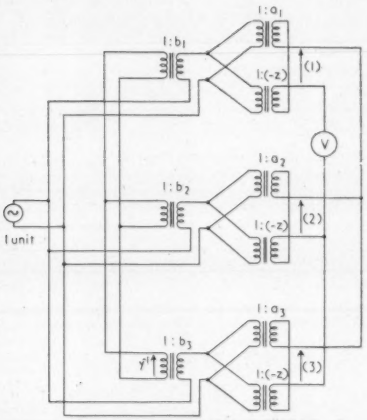

Fig. 9. Non-linear simultaneous equations

Fig. 9 is not the only transformer assembly on which the equations are satisfied. It was chosen because it is simple to adjust to balance as only one of the unknowns is a transformer ratio, consequently x and y^{-1} appear *automatically* at their proper values when z has been adjusted.

It is possible, and useful, to measure the effects of small changes in a_i and b_i on the solution.

ALGEBRAIC INEQUALITIES

Ryder[8] has shown how to use transformers to discover whether a set of linear inequalities are consistent. That is, for example, to discover whether values of x_1 and x_2 exist for which the following inequalities are satisfied:

$$\begin{aligned} a_{11}x_1 + a_{12}x_2 &\geqslant b_1 \\ a_{21}x_1 + a_{22}x_2 &\geqslant b_2 \\ a_{31}x_1 + a_{32}x_2 &\geqslant b_3 \end{aligned}$$

This problem, and variations of it, can arise when seeking optimum decisions in engineering designs, in economics and in military strategy. There would seem to be no difficulty in solving such problems on a Blackburn analyser.

CONCLUSIONS

In addition to its major function as a steady state a.c. network analyser, the analyser has a quite surprising versatility, and without doubt, problems other than those discussed here will be brought within its range. Its accuracy is—generally speaking—comparable with that of far more specialized computers, and its versatility is greater than that of other types of transformer analogue computer.

Its utility could be improved by (*a*) providing different socket arrangements on the complex multipliers for network analysis and for the problems discussed in this paper, and (*b*) providing six or eight complex multiplier units which are ganged together.

ACKNOWLEDGEMENTS

The author's thanks are due to Mr. M. W. Humphrey Davies (who made the analyser available) for his interest and encouragement, to Dr. M. K. E. Ismail who taught the author how to use the analyser, and to Mr. P. Aylett and other colleagues for useful suggestions and discussions. The author's work on computing is assisted by a grant from the Central Research Funds of the University of London.

REFERENCES

(1) BLACKBURN, C. L. British Patent Nos. 476164 and 476165 (1937).

(2) HUMPHREY DAVIES, M. W., and SLEMON, G. R. S. *Proc. Instn Elect. Engrs*, **100** (II), pp. 469–486 (1953).

(3) ISMAIL, M. K. E. Ph.D. thesis. (University of London, 1955.)

(4) MICHAELSON, S. *The Numerical Solution of Differential Equations by means of Equivalent Networks.* Technical report, V/T 107 (London: Electrical Research Association, 1951).

(5) MALLOCK, R. R. M. *Proc. Roy. Soc. A*, **140**, pp. 457–483 (1933).

(6) HARTREE, D. R. *Numerical Analysis*, p. 162 (London: Oxford University Press, 1955).

(7) BANKS, J. H., and PARTON, K. C. Private communication.

(8) RYDER, F. L. *J. Franklin Inst.*, **259**, pp. 427–439 (1955).

Correspondence

Note on discharges from a flat thermionic cathode

In a previous paper[1] an account has been given of the initiation and appearance of discharges from a hot cylindrical cathode through mercury vapour at a low pressure (about 10^{-3} mm of mercury). Fairly full information is also available about similar discharges from a flat cathode in several gases at low pressure.[2,3] The present note describes some observations, made incidental to the first investigation,[1] on discharges from flat cathodes at rather higher pressure (0·1–1·0 mm of mercury) in argon. These have shown that the visual appearances preceding striking of the arc with this electrode geometry are similar to those for a cylindrical cathode at low pressure, and that, after plasma has formed, it may have an internal structure of the still imperfectly understood type reported by Druyvesteyn and Warmolz[4] for cylindrical cathodes in the higher pressure range.

The cathode used was an indirectly heated, oxide-coated disk, 8 mm in diameter, parallel to and 3 cm distant from a plane anode 15 mm in diameter. The inter-electrode space could be explored by a movable cylindrical Langmuir probe 3 mm long and 0·1 mm in diameter. The discharge was passed diametrically across a long Pyrex tube 5 cm in diameter. Arc and probe circuits were conventional. The argon was taken from a commercial glass cylinder.

The discharges started in a similar manner to discharges in mercury vapour at lower pressure.[1] On increasing the potential difference between cathode and anode from a low value, nothing was seen in the gas until slightly above the ionization potential of argon, 15·7 V. A faint blue glow then appeared on the anode and spread towards the cathode as the voltage was increased. When it touched the cathode the arc struck. Probe characteristics taken before striking could not be analysed. Those taken after striking were of regular Langmuir form, with the slight rounding sometimes found at these relatively high pressures. After striking, the space potential was close to that of the anode.

The appearance of the discharge in this mode was interesting. The plasma consisted of two sections, a brilliant one near the cathode and a less intense one near the anode, with quite sharp demarcation between them. For a typical discharge at a pressure of 0·9 mm of mercury, with tube voltage 22 V and tube current 30 mA, the more intense plasma stretched from the cathode about one-third of the way towards the anode. The boundary between the two parts approached the anode as the tube current was increased. Neither space potential nor electron temperature showed an abrupt change at the junction.

These observations confirm that the higher pressure phenomena discovered by Druyvesteyn and Warmolz[4] are not dependent on the use of a cylindrical system. It is possible that they are connected with plasma electron oscillations, but direct proof of this is lacking. The exact relation of this form of discharge to the modes investigated by Malter, Johnson and Webster,[5] Pengelly and Wright,[6] and very recently Kok[7] is also not at present clear.

Queen's University of Belfast, Belfast. N. R. DALY, K. G. EMELEUS

REFERENCES

(1) DALY, N. R., and EMELEUS, K. G. *Brit. J. Appl. Phys.*, **6**, p. 370 (1955).
(2) ALLEN, T. K., BAILEY, R. A., and EMELEUS, K. G. *Brit. J. Appl. Phys.*, **6**, p. 320 (1955).
(3) ALLEN, T. K. *Proc. Phys. Soc.* [*London*], *A*, **68**, p. 696 (1955).
(4) DRUYVESTEYN, M. J., and WARMOLZ, N. *Physica*, **4**, p. 51 (1937).
(5) MALTER, L., JOHNSON, E. O., and WEBSTER, W. M. *R.C.A. Rev.*, **12**, p. 415 (1951).
(6) PENGELLY, A. E., and WRIGHT, D. A. *Brit. J. Appl. Phys.*, **5**, p. 391 (1954).
(7) KOK, J. A. *Appl. Sci. Res.*, *B*, **5**, p. 445 (1956).

A photographic method of obtaining stress trajectories

I read with particular interest Mr. A. R. Morris's paper published on p. 59 of the February issue of this *Journal*. It is always a pleasure to see that someone else finds the same idea worth attention which one's self thought to be of value. This is the case with the method of photographing a pattern of tangents to the stress trajectories by superimposing photographs of isoclinics through a properly oriented rectangular grid. I developed and used this method in my early photoelastic work in 1943, at the Technical University, Budapest.

I presented the idea at the annual meeting of the Society for Experimental Stress Analysis, held in New York on 1 December, 1949, in a paper entitled *Contribution to the calculation of stresses from photoelastic values* and it was published by that Society in 1951.*

University of Washington, Seattle, U.S.A. D. VASARHELYI

At the time when my paper was published, I had no knowledge that such a method had been used anywhere else. Professor Vasarhelyi must be regarded as the originator of the method. Nevertheless, I trust that readers will find the practical details in my paper of some use to them.

National Physical Laboratory, Pretoria, South Africa. A. R. MORRIS

* VASARHELYI, D. *Proc. Soc. Exper. Stress Anal.*, **9**, p. 27 (1951).

New books

Small-angle scattering of X-rays. By A. GUINIER and G. FOURNET. Translated by C. B. WALKER. With a bibliography by K. L. YUDOWITCH. (London: Chapman and Hall Ltd., 1956.) Pp. xi + 268. Price 60*s*.

Guinier and Fournet are acknowledged masters of their respective parts of the investigation of the small-angle scattering of X-rays, and the appearance of this book is very welcome. The four main sections are: general theory (78 pp.), experimental equipment (43 pp.), methods of interpretation and applications (91 pp.), and the bibliography (43 pp.). To deal with the last first, the bibliography originally appeared as a publication of the American Crystallographic Association in 1952. It has now been enlarged from about 400 entries to over 550, and will be of the greatest value to anyone working in the field.

The general theory attempts to cover too much in the space allowed for it, and in places it is too condensed to be easily understood. Perhaps it is best to regard these parts as annotations to the bibliography. The section on equipment is wholly admirable, and that on methods of interpretation gives a reasoned account of the difficulties of unambiguous interpretation and of the conclusions that may safely be drawn. All who are crystallographers, and many who are not, will find the section on applications fascinating.

The book is well produced, and one is not conscious of reading a translation. A. J. C. WILSON

Kovar. By Dr. W. ESPE. (Füssen: C. F. Winter'sche Verlagshandlung, 1956.) Pp. 84. Price DM. 6.40.

Kovar, Fermico and Nilo K are among the names which different suppliers have given to the range of iron–nickel–cobalt alloys used so extensively for making glass-to-metal seals. This pamphlet is addressed to those who would themselves use the alloys for this purpose. In it is collected much useful information including valuable data for alloys and glasses in use in Great Britain and the United States as well as on the Continent. A wide variety of seals is illustrated and their preparation described. Matters such as the methods of joining Kovar to other metals and the degassing of the alloy are well dealt with, often in tabular form. The manufacture, forming and physical metallurgy of the alloys, topics of interest rather than importance to the man for whom this booklet is intended, are outlined. G. A. GEACH

Mesons and fields, Vol 1. Fields. By S. S. SCHWEBER, H. A. BETHE and F. DE HOFFMANN. (Illinois: Row, Peterson and Company, 1956.) Pp. xvi + 449. Price $8.

In Volume 1 of *Mesons and fields* Professor S. S. Schweber has joined Professor H. A. Bethe and Dr. F. de Hoffmann in a clear introductory account of modern field theory which gives a suitable introduction to Volume 2 on mesons [see the review in *Brit. J. Appl. Phys.*, **7**, p. 81 (1956)], and to recent work in quantum electrodynamics and meson theory.

The first chapter is concerned with one-particle relativistic wave-equations and should be standard knowledge for all postgraduate students in theoretical physics, even the non-specialists in field theory. However, one would have enjoyed a more thorough discussion of spinors: even a brief reference to Watanabe's modern presentation of Cartan's fundamental work would be welcome. As presented, all difficulties of time reversal are ignored and even under the restriction to the connected Lorentz group a clear explanation of exponentiation (p. 25) is not given. In this chapter, too, a greater emphasis of the usefulness of certain representations, e.g. that of Yennie and Ravenhall, together with the Foldy transformation, would help the beginner in field theory. These topics would have gone well with the equivalence theorem and the Dyson transformation which are given a thorough treatment in the appendix, though the importance of Foldy's transformation in configuration space, of which Professor Schweber is an authority, could justify its appearance in the main text together with Wigner's work on the Dirac position operators. While discussing the subject of canonical transformations one should say that the authors give a clear presentation of the different quantum mechanical pictures during their introduction to the Dyson *S*-matrix theory in Chapter 2b, but very little on time-independent transformations such as that of Möller and Rosenfeld or the Bloch–Nordsiek treatment of the infra-red divergences in quantum electrodynamics. In the section on *S*-matrix theory the adiabatic hypothesis appears as mysterious as ever: no mention is made of Möller–Belinfante's arguments concerning the non-existence of the limit of $U(t, t_0)$.

Sections 8 and 9 give a delightful account of the Feynman theory for the positron–electron field. One could have wished that Feynman's Lagrangian formulation of quantum mechanics was used as the starting-point for the introduction to field theory in the next section. The authors apologize for this omission in their survey of recent developments which close the book.

The later sections discuss a few physical applications of the formalism from the scattering of neutral π-mesons by a nucleon to the Lamb shift. (Rutherford and Möller scattering are treated earlier as examples of the Feynman theory.) The main thesis of these sections is to present the theory of the renormalization programme as applied to the ultra-violet divergences. Here is good, if heavier, reading but the text neither reaches the most recent developments (e.g. use of the principle of causality) nor do all the equations remain precise. E. A. POWER

Handbook of chemistry and physics. 37th Ed. Edited by C. D. Hodgman in association with R. C. Weast and S. M. Selby and in collaboration with many chemists and physicists. Pp. xxii + 3156 on India paper. (Cleveland: Chemical Rubber Publishing Co., 1955.) Price £5.

This well-known monumental handbook first appeared about forty years ago and has been revised and enlarged at frequent intervals ever since; this alone is ample commendation of its value and importance. Among new tables that have been added in this edition are oxidation potentials, formulae for calculating titration data, ionization potentials, viscosity conversion factors, dielectric constants of water, dipole moments, activity coefficients, crystal ionic radii of elements, and allowable carrying capacities of conductors. Some new definitions have also been added. Much of the information has been revised including the data on gravimetric factors, dissociation constants of acids and bases, industrial organic compounds, half-wave potentials for polarographic analysis, physical constants for ozone and oxygen, properties of plastics, photographic formulae, velocity of light, and properties of dielectrics. As examples of the up-to-dateness of this volume the inclusion of tables giving the specific heat of heavy water, the cross-sections of thermal neutrons and X-ray diffraction data may be quoted. The editors state that

care has been taken to use only data "which can be considered reliable." The work is divided into the following sections: mathematical tables (333 pages), properties and physical constants (1148 pages), general chemical tables (271 pages), specific gravity and properties of matter (216 pages), heat (227 pages), hygrometric and barometric tables (23 pages), sound (4 pages), electricity and magnetism (153 pages), light (278 pages), quantities and units (156 pages), miscellaneous (149 pages), and the volume ends with a good index.

H. R. LANG

Proceedings of conference on effects of radiation on dielectric materials. (Washington: Naval Research Laboratory, 1956.) Pp. v + 169. Price $4.25.

This is a collection of twenty-one short papers which were read at a conference held in Washington, in December 1954, by scientists from various U.S. laboratories. The conference had two purposes, to exchange information about the programmes and progress of these laboratories, and to discuss general aspects of this widespread field by bringing together diverse viewpoints of chemists, physicists and engineers. Several of the papers are written in a rather casual style, as if they were printed records of the authors' lecture notes. A few are developed in considerable detail, but one or two others are no more than abstracts of the lecture. Roughly one-half of them deal with organic and polymer materials, and one-quarter with ionic, valence, and refractory materials. There are also a few general papers which discuss the physics and chemistry of radiation damage, compare the relative behaviours of metallic, ionic, valence and organic materials, and advise on the best types of high-energy machines for studying radiation damage. The book contains much technical information on the performance of electrical insulating materials under conditions of pile irradiation, and as such should be particularly valuable to reactor designers.

A. H. COTTRELL

Creep and fracture of metals at high temperatures. (London: H.M. Stationery Office, 1956.) Pp. iv + 420. Price 30*s*.

A symposium on the creep and fracture of metals at high temperatures was held at the National Physical Laboratory in 1954 and the twenty-two papers presented on that occasion have now been published, together with a record of the discussion. In the main, the papers contain few new experimental results; the majority of the contributions are either critical reviews of specific branches of this complex subject or theoretical papers aimed at a basic understanding of the various phenomena.

Apart from an introductory paper by N. P. Allen, the various contributions are contained in four separate sections. The first section on the deformation processes in simple materials contains papers relating to the behaviour of both single crystal and polycrystalline material. A theoretical interpretation of creep in simple materials is attempted and the relationship between grain boundary movement, slip and polyganization is discussed. The effects of alloying elements in solid solution and precipitation processes on the creep behaviour of complex materials is the theme of the papers in section two. It is shown that a partial understanding of the effects of alloying on creep behaviour is now possible at least in simple alloy systems. Two of the three papers on the theory of fracture deal with the properties of grain boundaries and grain boundary films, and the remaining paper in this section discusses fracture in relation to the behaviour of dislocations and vacancies. The final section on tertiary creep and fracture is mainly concerned with complex engineering materials and it is apparent that the mechanisms involved are not as yet understood.

The report as a whole presents a comprehensive review of our knowledge on the mechanism of the creep and fracture of metals at elevated temperatures and, as an examination of the list of authors will show, the papers have been written by recognized authorities in their various fields. The delay between the presentation of these papers at the symposium and their subsequent publication is regrettable, but now they have appeared in print they will be studied with interest by all those connected with this important subject.

D. A. ROBINS

Control of nuclear reactors and power plants. By M. A. SCHULTZ. (London: McGraw-Hill Publishing Co. Ltd., 1956.) Pp. viii + 313. Price 52*s*. 6*d*.

This is the first book to be published on the control of nuclear reactors and the author has approached the subject from the viewpoint of servo-engineering. It includes chapters on reactor physics and discusses in detail the solution of the various kinetic equations which explain the operation of a nuclear reactor, but the bulk of the volume is concerned with the problems of the control engineer, e.g. automatic reactor control, reactor control mechanisms, control of nuclear power plants, etc. Special attention is given to operating control problems during start-up, power-level operation and shut-down. There is also a chapter on simulators which discusses both the design of simulators and the use which may be made of these machines in solving control and other problems.

The text is clear and the subject-matter well presented. It is a book which can be recommended. Little is included in the book on instrumentation, or how the limitations in the instrumentation affects the design of the control mechanism, or the philosophy of reactor plant safety. There is room for a companion volume dealing with these important matters.

DENIS TAYLOR

Vierpoltheorie und Frequenztransformation. By T. LAURENT. (Berlin: Springer-Verlag, 1956.) Pp. xii + 299. Price DM34.50.

It is good to see a German edition of Professor Laurent's work on electric network theory, for this will make it available to a much wider audience than hitherto, the only previous edition being, to the writer's knowledge, in Swedish. Furthermore, considerable care has been taken by the author to correct a number of errors which had appeared in the earlier version.

Professor Laurent is well known in the world of electric network theory, especially for his work on transformations. Much of this he has published in the journals, in English, though unfortunately not in journals of wide circulation, as normally read by the more practical kind of working engineer. His work may be regarded as truly academic, dealing with basic conceptions and methods of analysis; it represents the type of approach which leads to real understanding of the mathematical core of network theory. As presented in the book, the subject is started at the beginning and would appeal to practical telephone engineers and circuit designers who may have taken an elementary course on communication

circuits, telephony, "electronics," transmission theory, etc., but who now want deeper insight into network theory. At the same time, the (conformal) transformation theory, as it is presented, forms a set of ideas essential to anyone engaged in research into the properties of linear networks.

At research level, the work has many obvious analogous applications to acoustics and mechanics; it would seem to the writer that there are interpretations to be found also in optics.

The latter part of the book is concerned with the theory of filters and transmission circuits, balancing and equalizing, matching, amplifying and other aspects of telephony which are of an analytical nature. The whole work is reasonably well indexed, but includes a somewhat restricted list of references.

COLIN CHERRY

Wool research, Vol. 2. Physical properties. (Leeds: Wool Industries Research Association, 1956.) Pp. vi + 234. Price 30*s*.

This book deals with the more fundamental work of the association on the physical properties of wool fibres and fabrics. Other volumes in this series have covered physical problems encountered directly in the various processes of the industry and in the testing of its products. All aspects of water absorption and transmission, thermal insulation, and air permeability, are involved in problems of cloth finishing and in studies of the warmth and other physiological effects of clothing, and the protection it affords against wind and rain. About half the book has been allotted to these subjects and their applications, but this is amply justified by their importance, the accepted authority of the association in this field, and the breadth and quality of the treatment. The rest of the book contains chapters on elastic properties, electrical properties, friction, and colour and optical properties. Inevitably, these chapters are less connected than the earlier part of the book, but individually they are of the same high standard.

The book is based largely on papers published by the association, but the material has been re-written with the object of producing a book acceptable to both the textile technologist and the textile scientist. This object should have been achieved, for the material has been admirably co-ordinated and condensed, and the type and layout make for easy reading. Those who doubt the value of basic research in a long-established industry might well study the relations between theory, laboratory experiment, and practical application shown in this and other books in the series.

J. POLLITT

Radium therapy—its physical aspects and extensions with radioactive isotopes. 2nd. ed. By C. W. WILSON. (London: Baillière, Tindall and Cox, Ltd., 1956.) Pp. ix + 286. Price 37*s*. 6*d*.

Radium therapy—its physical aspects was published in 1948 and since that time has become a standard textbook for use by post-graduate students of radiology. It was inevitable that the author should consider revising it in the light of the many additions to the armoury of the radium therapist made possible by the production of radioactive isotopes in the atomic reactor.

The chapter headings and general scope of the book follow closely the pattern set in the earlier edition. Following a description of the properties and medical applications of radium, there is a new chapter dealing with most of the important radio-isotopes used in radium therapy. It is a pity, however, that radioactive iodine is omitted, owing to the author's rather restricted definition of radiotherapy, and the opportunity thus lost of covering all aspects of therapy with radioactive materials.

The chapters on the interaction of high-voltage radiation and matter, and the methods and theory of γ-ray dosimetry, remain largely unchanged although the section on apparatus for dosage measurement has been thoroughly revised. Cavitary and interstitial therapy are allotted a chapter apiece and the section on γ-ray teletherapy has been much expanded to allow for the extensive changes in technique made possible by the production of kilocurie sources. The book concludes with a concise account of the hazards of radiation and methods of protection, and a collection of data in tabular form of everyday use to the practising radium therapist and, indeed, the hospital physicist.

This is in every way a well-produced book and may be thoroughly recommended. The fact that the price is only twice that of the first edition is surprising in these days of continually rising costs.

W. A. LANGMEAD

Advances in electronics and electron physics. Vol. 7. Edited by L. MARTON. (New York: Academic Press Inc., 1956.) Pp. x + 527. Price $11.50.

It is not surprising that a substantial part of this volume is devoted to solid-state phenomena. This subject, with its many aspects, is at present attracting a tremendous amount of effort in research, development and application. It is fitting, therefore, to find papers in which the physics, electrical properties and other characteristics are surveyed.

"The physics of semiconductor materials" is discussed by E. Burstein and P. H. Egli. The basic properties, characterizing a semiconductor, are related to the structure and type of chemical binding of the solid: from a consideration of these it is possible to establish which crystals will be of interest and the properties to be expected of them. H. Brooks in "Theory of the electrical properties of germanium and silicon" reports on the progress that has been made in determining the energy-level structure of the valence-type semiconductors, germanium and silicon.

When slow electrons impinge upon solid surfaces the resulting energy distribution after reflexion shows a kind of line spectrum due to energy losses occurring in certain characteristic values. These are reviewed by L. Marton, L. B. Leder and H. Mendlowitz in "Characteristic energy losses of electrons in solids." G. K. Wehner, in "Sputtering by ion bombardment," is concerned with the physics of the sputtering action and the effects of various parameters on the resulting characteristics of the bombarded target. New experimental techniques for studying discharges in gases employ microwave or pulsed signals acting as "probes" of such a nature that the discharge is sensibly undisturbed. Studies of this nature comprise the review by L. Goldstein on "Electrical discharge in gases and modern electronics."

"Observational radio astronomy" is a subject which will demand further reports in the future as more data is collected. J. P. Wild deals with some results already obtained and with the aerial systems devised in the constant endeavour to obtain better resolving power. A. W. Vance, E. C. Hutter, J. Lehmann and M. L. Wadlin review advances in "Analog computers" that have occurred in the past five years.

A. J. MADDOCK

Notes and comments

The Institute of Physics

At the Annual General Meeting of The Institute of Physics held in London on 16 July, 1956, Mr. O. W. Humphreys (the Director of the General Electric Co. Ltd. in charge of research) was elected President, Dr. B. P. Dudding was elected a Vice-President, Dr. J. Taylor, Honorary Treasurer and Professor F. A. Vick, Honorary Secretary. The two new Ordinary Members of the Board elected were Dr. L. R. G. Treloar and Mr. G. W. Warren. Sir George Paget Thomson was elected to Honorary Fellowship in recognition of his contributions to physics and his services to physicists.

The Report for 1955, which was adopted at the meeting, shows that during the year the total membership passed 5000; 726 applications for election or transfer to the various grades were considered compared with 579 the previous year. Representatives of the Institute visited seven technical colleges, which had applied for recognition or a continuance of recognition by the Institute. The Institute's recently established Graduateship examination was taken in four centres by 54 candidates of whom only 11 satisfied the examiners. The number of candidates for the final examination for National Certificates in Applied Physics was 309 at the Ordinary level and 82 for the Higher Certificate. These figures compare with 206 and 75 respectively in 1954. The Board has continued to comment upon and support proposals for the development of facilities for higher technical education. It accepted an invitation from the Ministry of Education to nominate a member to one of the two Boards of Studies set up to advise the newly appointed National Council for Diplomas in Technology. Arising from concern felt at the increasing evidence of declining numbers of advanced students in the physics departments of several well-equipped technical colleges, the Board decided to institute an inquiry into the availability of places for students of physics in the universities and larger technical colleges of the country. A report on the findings was published and comments on it were made in the scientific and technical press.

The Report records the continued increase in circulation of both the *Journal of Scientific Instruments* and the *British Journal of Applied Physics*, the fourth Supplement of which was devoted to the proceedings of a conference on "Luminescence with particular reference to solid inorganic phosphors."

Two volumes in the "Physics in Industry" series were published during the year. They were the ¼-million-word book entitled *X-ray Diffraction by Polycrystalline Materials* to which 31 members of the Institute's X-ray Analysis Group contributed. The other volume was entitled *Physics of Fibres*. Three small books were added to the "Student Monograph" series, namely *Theory of Lenses*, *Humidity* and *Errors of Observation and their Treatment*.

The sentence in the Report, "The permanent Officers have again dealt with a regular flow of inquiries on professional matters and the Board expresses its thanks to the several Fellows who have assisted them with expert advice," is a modest record of work of a confidential nature carried out towards the "elevation of the profession of physicist" which is one of the Institute's objects. Another activity on behalf of physicists and their dependants, referred to in the Report, is the Benevolent Fund.

The Institute was one of the constituent bodies which during the year founded the (permanent) British Nuclear Energy Conference; the Board welcomed this opportunity of further collaboration with the engineering institutions.

Nearly one hundred meetings were held during the year by the Institute's Branches and specialist Groups in the United Kingdom, among which was the inaugural meeting of the Liverpool and North Wales Branch. Some of the meetings took the form of two- or three-day conferences. The Australian Branch staged an exhibition of scientific instruments and apparatus in Sydney in November, and held several meetings.

As usual the brief reports from the Institute's representatives on outside bodies demonstrate the wide interests and many activities with which the Institute is associated.

Symposium on magnetic resonance

A symposium on magnetic resonance is being arranged by the Liverpool and North Wales Branch of The Institute of Physics at the University College of North Wales, Bangor, on 26 and 27 September, 1956. Lectures will be given by Dr. B. Bleaney (Clarendon Laboratory, University of Oxford) on free atom resonance, Dr. J. G. Powles (Queen Mary College, London) on spin echo techniques, Dr. R. E. Richards (Department of Physical Chemistry, University of Oxford) on magnets, and Professor E. R. Andrew (University College of North Wales, Bangor) on nuclear magnetic resonance work and other research at Bangor.

The formation of a subject group to provide occasional meetings will be considered at this symposium.

Further particulars of the symposium may be obtained from Professor E. R. Andrew, Physics Department, University College of North Wales, Bangor, Caernarvonshire. Accommodation will be available for a limited number in the Hall of Residence for Men Students.

Erratum

In the paper entitled "The Eberhard effect in X-ray powder photographs" by T. W. Baker, published in the April issue of this *Journal*, the illustrations used for Figs. 1 and 3 should be transposed while the legends remain unchanged.

THIS JOURNAL is produced monthly by The Institute of Physics, in London. It deals with all branches of applied physics (including theory and technique).
All rights reserved. Responsibility for the statements contained herein attaches only to the writers.
EDITORIAL MATTER. Communications concerning editorial matter should be addressed to the Editor, The Institute of Physics, 47 Belgrave Square, London, S.W.1. (*Telephone:* Sloane 9806.) Prospective authors are invited to prepare their scripts in accordance with the *Notes on the preparation of contributions*. (Price 2s. 6d. including postage.)
REPRODUCTION. The Institute of Physics is a signatory to The Royal Society's Fair Copying Declaration. Details may be obtained upon application from The Royal Society, London, W.1.
ADVERTISEMENTS. Communications concerning advertisements should be addressed to the agents, Messrs. Walter Judd Ltd., 47 Gresham Street, London, E.C.2. (*Telephone:* Monarch 7644.)
CLAIMS FOR MISSING JOURNALS. Claims from regular subscribers to this *Journal* for missing numbers will only be considered if received within 60 days of the date of mailing plus normal outward time of transit and time for lodging the claim. Losses attributable to failure to notify a change of address or to similar omissions will not be considered.
SUBSCRIPTION RATES. A new volume commences each January. The charge is £4 per volume ($11.50 U.S.A.), including index (post paid), payable in advance. Single parts, so far as available, may be purchased at 8s. each ($1.15 U.S.A.), post paid, cash with order. Orders should be sent to The Institute of Physics, 47 Belgrave Square, London, S.W.1, or to any bookseller.

Crystallography and the phase rule*

By PROF. A. R. UBBELOHDE, D.Sc., F.R.S., Imperial College of Science and Technology, London

Classical thermodynamics provides powerful methods for correlating various thermal parameters of a system. However, anomalies are found in the classical theory particularly for condensed phases, such as solids or liquids. A detailed study of the structure of such phases by what may be broadly termed crystallographic methods has thrown much light on the classical anomalies. The present review surveys various structural changes such as crystal lattice transformations or melting that produce increases of entropy and thus can favour thermodynamic transitions in solids.

Particular attention is directed towards the structural elucidation of the following anomalies.

(i) Pre-transition and pre-melting phenomena. In many cases these can now be attributed to gradual structural changes within a crystal of the same kind as the discontinuous jump at a transition.

(ii) The occurrence of smeared or continuous thermodynamic transitions, which are sometimes described as transitions of "higher order." These can often now be attributed to the coexistence of regions of two slightly different structures or sub-units within a hybrid single crystal. Reference is made to some of the techniques of study that have been used to investigate such coexistence.

(iii) The occurrence of hysteresis around a thermodynamic transition. This can arise from the same coexistence phenomena that lead to smeared thermodynamic transitions.

Precision studies on single crystals of the kinds described seem likely to throw much light on thermodynamic transitions in solids.

The classical phase rule can be summarized by the statement that the free energy G of a "phase" is completely determined by pressure, temperature, volume and composition. It makes no comment on structure,

$$G = f(p, V, T, n_1, n_2 \ldots)$$

By means of this powerful generalization of the laws of thermodynamics, ignorance about the detailed structure of matter was circumvented to a remarkable degree by skilful use of the geometry of surfaces.(1) But, of course, very much more can be done with thermodynamics by combining it with information about the detailed structure of matter.

Three main themes for discussion are all related to the basic problem of the transformation from one phase into another. These are:

(1) the mechanisms of entropy increase in transformations of condensed phases;

(2) the structural interpretation of pre-transition phenomena generally;

(3) the coexistence of sub-crystalline regions or domains around a transformation point.

In the classical phase rule, two "phases" are regarded as completely independent and the G surfaces cross if equilibrium can be set up between them. Probably this statement is still quite adequate for liquid/gas or solid/gas transitions, but special problems arise in solid/liquid or solid/solid transitions, i.e. between "condensed" phases where the structure of the phase is of dominant importance and the difference between the specific volumes may be small. It is here that various methods of determining the structures of condensed phases are proving so important for the thermodynamics of solids. Of these, X-ray crystallography has been most exploited, and probably has most information to yield. However, for the present purpose any method for studying the order and regularity of arrangement of molecular units in condensed phases may yield supporting information usefully included under the title "crystallography."

In this connexion it is perhaps useful to summarize the variety of structural studies that have been applied to investigate say a Δ transformation. These include applications of X-rays using monochromatic, Laue and divergent beam methods, neutron diffraction, optical microscopy, and in favourable cases measurements of ultra-violet, infra-red and microwave absorption spectra, Raman spectra, measurements of nuclear magnetic resonance, particularly for compounds containing hydrogen, and studies of electrical conductance, dielectric capacity and dielectric relaxation.

MECHANISMS OF ENTROPY INCREASE IN PHASE TRANSITIONS

One major objective of crystallography is to explain why phase transitions occur, in terms of the structure of the crystals whose thermal transformation is under discussion. Study of the definition of free energy in terms of heat content and entropy $G = H - TS$ has led to the recognition of a large number of transitions which can be explained in terms of an increase of entropy of some kind.

Vibrational entropy in a discontinuous phase transition: grey tin → white tin

One important source of entropy increase is associated with the vibrations of the constituents of the crystal. The problem can be stated in its simplest terms, when the units of structure are atoms, as in the phase relationships between grey tin and white tin.

Fig. 1 illustrates the trends of the thermodynamic functions G, H and S from absolute zero upwards, for the two crystal structures.(2) The specific heat of white tin lies above that for grey tin throughout this range of temperatures so that the difference in vibrational entropy between the two forms

* Based on an evening discourse delivered to the X-ray Analysis Group of The Institute of Physics on 18 November, 1955.

rises steadily. At 292° K and atmospheric pressure the difference in heat contents ΔH for the process

$$Sn_{grey} \rightarrow Sn_{white} \ldots \Delta H = 522 \text{ cal/g. atom}$$

is just balanced by the entropy difference so that the difference in free energy $\Delta G = \Delta H - T\Delta S$ sinks to zero; 292° K is the transformation temperature. In this instance a knowledge of the two crystal structures throws considerable light on why the thermodynamic transition occurs. Grey tin has a cubic structure, with co-ordination number 4 and a distance between nearest neighbours of 2·80 Å. White tin has a tetragonal structure, with four nearest neighbours at 3·016 Å forming a flattened tetrahedron and two nearest neighbours at 3·175 Å.[3]

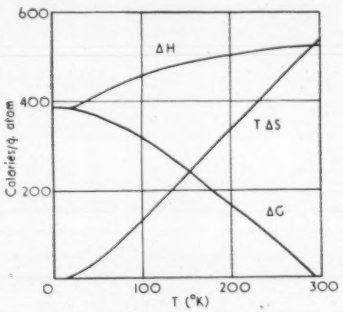

[Reproduced from *Thermodynamics of Alloys*[2]]

Fig. 1. Plots of thermodynamic functions for the change from grey tin to white tin

On balance the heat content term favours the cubic form but the entropy term favours the tetragonal form. The crystal lattice of grey tin has a lower potential energy than white tin, but the force constants for atomic vibrations are also greater.[4] Since the atomic masses are the same in both crystals, amplitudes of vibration must be greater at the same temperature in the less firmly bound white tin. At a sufficiently high temperature the less firmly bound structure is more stable because of the higher vibrational entropy of this form.

This opposing influence of vibrational entropy and heat content on the stability of polymorphic modifications of crystals is quite general and has extensive applications. It makes vibrational studies in polymorphs of obvious interest. In particular, studies of intensities of X-ray reflexions in relation to phase transitions should yield much information about the thermodynamics of solids in relation to their crystal structure. Much of this work still remains to be done, however.

At this point brief mention may also be made of certain other aspects of the comparatively unexplored variations of intensities of X-ray reflexions with temperature, particularly in the neighbourhood of a transition. The well-known formula for the variation of intensity with temperature $I = I_0 \exp(-2M)$ where $M = 8\pi^2(\overline{u_x^2}\sin^2\theta)/\lambda^2$ has not been applied at all extensively, save in the case of simple structures where the mean square displacement from the ideal lattice plane $\overline{u_x^2}$ can be correlated with the vibrations of the crystal lattice. It is known, however, that $\overline{u_x^2}$ assumes abnormally large values for certain crystal planes in the neighbourhood of certain thermodynamic transitions; the corresponding randomizations of structure are of great interest for interpreting phase rule relationships. One kind of randomization takes the form of increasing amplitudes of vibration, as in the change from grey tin to white tin; it has been suggested that such effects as the abnormally rapid fading of intensities of certain X-ray reflexions in the transition.[5]

$$\underset{\text{co-ordination No. 8}}{CsCl} \overset{469^\circ C}{\rightleftharpoons} \underset{\text{co-ordination No. 6}}{CsCl}$$

arise from other forms of structural randomization, such as co-operative positional defects[6] in the crystals. These co-operative defects can be due to the coexistence of substructures in the neighbourhood of a thermodynamic transition, discussed below. Presumably the rapid increase[7] of intensity of specific reflexions such as (222) in the transformation α quartz $\overset{575^\circ C}{\rightleftharpoons}$ β quartz arises from thermal peculiarities of certain structure factors, though this warrants further investigation.

Other forms of entropy increase

In other mechanisms of entropy increase, groups of atoms in a crystal such as the anion $(NO_3)^-$ or the cation $(NH_4)^+$ randomize their orientation in the crystal lattice. This randomization is sometimes called "rotation"; normal crystallographic methods do not, however, give information about kinetic aspects, i.e. whether the molecules occupy any given orientation for very short periods of time only, so that they are truly rotating, or whether they undergo jumps of orientation from time to time from one potential minimum to another on the crystal lattice. This kind of information can only be obtained from crystal parameters involving time as a variable; important methods for the study of thermal transitions in solids include observations on relaxation times, as in measurements of dielectric constants at various frequencies, especially when the units of structure are polar; information about rotation can also be obtained from absorption-spectrum measurements.

In addition to many examples of randomization of orientation of non-spherical molecules, crystallographic methods have revealed a few instances of transformations linked with randomization of lattice positions in the solid. Such instances have proved highly suggestive for current interpretations of melting. One interesting example is the progressive randomization of position of the cations in crystals of Ag_2HgI_4 and of AgI as the temperature rises, rising to a peak at the respective Δ points. Crystallographic studies[8,9] indicate that in AgI the framework of the large I' anions remains substantially the same above and below the transition. At temperatures well below the transition the small Ag^+ cations occupy only one set of interstices between the I' anions; above it, alternative interstices are equally well occupied at random. In some ways this change from an ordered arrangement to a random arrangement of cations resembles the melting of a crystal. Such a resemblance is illustrated by the high conductance of the crystal above the transition. At around 146° C the specific conductance of solid AgI decreases fairly abruptly to $1{\cdot}3\ \Omega^{-1}\ cm^{-1}$.[9] This value is of the same order as in many ionic melts (NaCl has $K = 3{\cdot}5\ \Omega^{-1}\ cm^{-1}$ at 850° C) and indicates movement of the Ag^+ from one position to another in the crystal, about as free as in an actual melt.

THE STRUCTURAL INTERPRETATION OF PRETRANSITION PHENOMENA AND OF CONTINUOUS TRANSITIONS

In the examples quoted and in many other cases thermodynamic methods of study, such as measurements of heat content or of specific volume, have indicated certain obvious peculiarities that do not fit in readily with the classical phase rule. These peculiarities include the following.

(*a*) Transitions of "higher order" in solids, in which the normal phase rule appears to break down or to be "smeared." If sections of the free energy surfaces for each of two phases by the planes P = constant and T = constant are considered, the classical phase rule requires a clean intersection without any compromise and a sharp angle between the tangents to the curves since

$$\left(\frac{\partial G_1}{\partial T}\right)_P - \left(\frac{\partial G_2}{\partial T}\right)_P = S_2 - S_1$$

$$\left(\frac{\partial G_1}{\partial P}\right)_T - \left(\frac{\partial G_2}{\partial P}\right)_T = V_1 - V_2$$

In actuality, fully smeared transformations have no sharp discontinuous changes of entropy or volume. First derivatives such as

$$C_P = T\left(\frac{\partial S}{\partial T}\right)_P \quad \text{or} \quad \alpha = \frac{1}{V}\left(\frac{\partial V}{\partial T}\right)_P$$

may show discontinuities, or at least steep maxima. In less markedly anomalous cases there still is a discontinuous jump of thermodynamic parameters at the transformation point from one phase to another, but on either side of this jump the phases exhibit "pre-transition" phenomena and begin to approximate to the other phase. Mathematical implications of such continuous transformations have received very considerable discussion by Ehrenfest, von Laue and later workers.[10] This article is concerned particularly with certain structural implications. The descriptions[11] "discontinuous transformation" and "continuous transformation" seem preferable for a number of reasons to the older terminology "transformations of the first order," "transformations of the second order," etc.; attempts to define the "order" of a transformation imply mathematical characteristics of the free-energy surfaces that may not have real physical counterparts, as is discussed below.

(*b*) So far as the resolving power of present experimental methods can go, hysteresis is observed in many but apparently not all continuous phase transitions; within a hysteresis cycle no unique structural equilibrium can be defined. Partial equilibrium prevails with respect to certain kinds of fluctuations such as those maintaining uniformity of temperature.[12]

(*c*) There are also certain phase rule difficulties in regard to the relative stabilities of different crystal surfaces which will not be detailed here. Special interest attaches to the problem "when can a single crystal be regarded as synonymous with the classical expression 'solid phase'?" Even disregarding any contributions to the free energy from the free surfaces exposed, single crystals have specific axes and the statistical foundations of the phase rule appear to require random occurrence of such axes; in this sense a polycrystalline assembly may be the only valid example of a "solid phase."

Occurrence of anomalous transformations in crystals

Continuous transformations, or pre-transition phenomena associated with discontinuous transformations are found in many types of solids. Structural studies have thrown new light on what is happening, and have raised fresh problems of their own.

Before examining some detailed examples, two general conclusions can be stated on the basis of evidence so far obtained. Crystallographically, it seems safe to say that a smeared transition *never* occurs unless the structure of the two "states" of the solid well above and well below the transition is closely related; often the similarity is so close that very precise methods are necessary to detect any difference—for example in the case of X-ray reflexions very precise intensity measurements, and very precise spacing measurements with sharp focusing are called for, as in the ammonium chloride transition to be mentioned below. Where there is a discontinuous transformation the prominence of any pre-transition phenomena associated with it often depends on the degree of similarity of structures between the two phases.

A second general statement is that the concept of some kind of regions or domains in "single crystals" seems likely to prove particularly suggestive in linking up thermodynamic and crystallographic studies. As is well-known, domains were first suggested to account for some of the phenomena of paramagnetic ⇌ ferro-magnetic transitions; the significance of the concept for other transformations in crystals has arisen independently of the special peculiarities associated with polar domains in ferro-magnetism. Below the transition temperature a ferro-magnetic crystal in the absence of a strong external field breaks up into coexistent domains which are oppositely magnetized; the free energy is lessened by this means. Problems about the boundary regions between contiguous surfaces of such domains, and about the equilibrium sizes of such domains, take a rather special form for the ferro-magnetic crystal, because the interaction forces are long range and of a special nature. It has been estimated that the Bloch wall separating two ferro-magnetic domains is several hundred layers of atoms thick; the size of individual ferro-magnetic domains can be such that they can readily be made visible under the microscope. For other kinds of transitions in crystals not involving magnetic forces of interaction regions or domains may be much smaller and the "walls" separating them may be thinner. A general structural question is whether every transition that is anomalous from the standpoint of the classical phase rule involves a dividing up of single crystals into domains or regions that can be distinguished in some way? It may prove generally true that in the immediate proximity of the transition temperature on one side or other of an anomalous transition the nominal crystal structure is strictly only an average structure. Classical crystallography might describe this average structure by saying that what appears to be a single crystal of fairly high symmetry is in fact a pseudomorphic assemblage of regions of lower symmetry. But the words "pseudomorphic assemblage" do not describe all the particulars which may emerge from a study of instances of coexistence of regions or domains, and from an examination of conditions for such coexistence within a "single crystal." A second related problem is to determine what happens when a "single crystal" is taken round a thermal cycle that includes an anomalous phase rule transition. The problem is to determine whether the crystal axes persist in a continuous transition or whether some randomization and break-up occurs.

Some of the thermodynamic problems arising out of these general structural questions can be brought into clearer focus in terms of specific examples of crystallographic studies.

Pre-melting and crystal structure

Crystallographic studies have given direct information about certain processes of randomization such as eventually lead to melting, which would otherwise be rather obscure from the standpoint of the phase rule. As is well known, structural crystallographic methods have shown that the average close-packing in the molten state of the vast majority of liquids is close to that in the solids, but that the long range order which is characteristic of the crystal does not persist in the melt.[13]

In what is now generally termed "pre-melting"[14] there are trends in the G curves; their direction changes more steeply as the melting temperature is approached, as if the phase "knew" melting was going to take place. Such behaviour is quite unexplained on the classical phase rule, according to which the two G surfaces are quite distinct and unrelated, so that a sharp transition should occur at the section of the G surfaces. Analogous "pre-transition" changes of trend are frequently observed for transitions other than melting.

Very marked pre-melting has been observed, for example, in crystalline paraffins.[14,15] In the melts of molecules of this class a tendency to roughly parallel alinement of the chain molecules has been observed by X-ray methods.[16] The consequent similarity in structure between solid and melt probably explains the comparatively marked pre-melting observed. X-ray crystallographic studies[17] show that the unit cell rapidly changes its dimensions as the melting point is approached. For normal $C_{23}H_{48}$ the change is such as to approach hexagonal close packing of the polymethylene chains just below the melting point. It seems highly likely that in this case the structural change accompanying pre-melting involves increased randomization of orientation of the paraffin molecules about their long axes. So far as can be determined by X-ray crystallography, this change is continuous for $C_{23}H_{48}$ but includes a discontinuous jump in the solid for $C_{29}H_{60}$.

Domain formation in other transformations in solids

Many other instances of pre-melting phenomena have been reported[18] but their structural implications have not usually been worked out to give crystallographic information comparable to what is available even for the paraffins. Largely for technical reasons, the experiments required are often less difficult below the melting temperature, for transformations in solids. A certain amount of information about the possible role of domains has been sought even from X-ray photographs of powders. For example, a transformation of great theoretical importance is the order-disorder transformation in certain stoicheometric alloys such as CuAu. As is well known, these alloys show continuous transitions having the general thermodynamic characteristics already mentioned. A typical specific heat curve[19] can serve to illustrate this point. Crystallographic studies on the polycrystalline alloys show that above the transition peak at T_c° C the alloy consists of Cu and Au atoms arranged at random on a lattice which is cubic close-packed. Below this temperature, additional powder lines appear of a so-called super-lattice, in which the Cu atoms occupy preferred positions as do the Au atoms. As the temperature is lowered, these additional superstructure lines gradually become stronger. It would be important to establish experimentally whether this gradual increase of intensity below T_c arises from cellular regions of highly ordered CuAu coexisting with regions of disordered alloy and gradually absorbing them, or whether the average degree of order is more or less uniform on a *micro-scale*, as is assumed in most of the current statistical theories. Powder methods have not given a clear answer to this problem. To test this question further X-ray measurements have been made on single crystals of CuZn and Cu_3Au held at various temperatures below their respective T_c values.[20] For CuZn, $T_c = 465$° C for the change b.c.c. (disordered) → ordered. For Cu_3Au, $T_c = 394$° C. In the range of these experiments, no splitting or broadening of selected reflexions could be established, which supports the "uniform single crystal" model. However, the temperature controls available were not sufficiently accurate to permit work within 5° C of the transformation temperatures; in the region which is highly important thermodynamically, close to the transformation peak T_c, the problem of coexistence of micro-regions as against a smooth spread of disorder is still unresolved.

Precision micro-thermostats are essential in this kind of work. One example[21] developed for single crystal work in our laboratories permits the use of temperatures to $\pm\frac{1}{20}$° C instead of the more usual ± 5° but order/disorder in metal alloys has not yet been re-investigated by its means. More recently, from precision studies of widths of X-ray reflexions it has been claimed that micro-regions are layered at random in CuAu so as to give statistical symmetry above 408° C[22]; further work seems to be required to clear up the question for this kind of transformation in solids. The discovery of hysteresis in physical or mechanical properties such as Young's modulus for an order-disorder transformation in the alloy[23] would help to establish ways of distinguishing regions or domains at least near T_c, for reasons connected with the origin of hysteresis discussed below.

Other metal crystals which appear to exhibit coexistence of two substructures over a range of temperatures around a transformation point include rhodium ($T_c \simeq 1200$° C) and possibly manganese.[24] There is also evidence of coexistence in the grey tin ⇌ white tin transition[4] and in other metal transitions.[50]

Clearer examples may now be considered where the nature of the co-operative forces in solids appears to favour a temperature range for coexistence of more highly ordered and disordered regions in the solid, rather than a uniform gradual increase of disorder.

In discussing phenomena associated with the coexistence around a transition temperature of regions of two structures which are closely related, some refinement of the term "domain" seems advisable. Based on experimental studies the terms "sub-crystalline units" and "hybrid single crystal" have been proposed[11] to describe an association of sub-units which fulfils the characteristics of a single crystal on average. Every sub-unit has a structure and orientation closely related to the average structure; but the sub-units are distinguishable by sufficiently refined methods. The pseudo-single crystal in which these sub-units are present is, in fact, a hybrid; provided the differences between the sub-units do not exceed the breaking strength of the pseudo-single crystal, the hybrid behaves in many respects like a true single crystal. As the temperature moves away from the transformation point, distinguishable sub-units disappear; apart from possible internal scars and co-operative defects[6] the hybrid single crystal becomes identical in every way with the conventional concept of a single crystal.

Various kinds of minor differences between distinguishable sub-units can be foreseen, but only two types of differentiation have so far been reported in practice.

(i) The sub-units may all have the same symmetry, but may be arranged so as to average the orientation of polar axes in a hybrid crystal. The coexistence pattern then involves

arrangements that can be symbolized (1+) (1−), etc. This appears to be the case, for example, in ferro-electric ⇌ para-electric transitions below the transition temperature in the absence of an external field.

(ii) The sub-units may differ slightly in lattice spacing, involving the coexistence pattern (1) (2) in the hybrid crystal. Combinations of (i) and (ii) are likely to occur in the immediate neighbourhood of the peak transformation temperature, but no clear evidence has yet been advanced.

A rather different crystallographic description of phase transformations has been proposed by M. J. Buerger.[25]

COEXISTENCE OF SUB-CRYSTALLINE UNITS IN A HYBRID SINGLE CRYSTAL

In order to reveal the coexistence of sub-units in a hybrid crystal lattice, it is highly advantageous to work with what appears as a single crystal well above or well below the transition. When powder methods are used, these always involve averaging over different crystallites, so that clear evidence about the coexistence of sub-regions and the growth of one sub-region at the expense of the other can seldom be obtained. Thus in the case of a transition in MnO at 115·9° K the coexistence of regions with lattice spacings $a = 4{\cdot}4260$ Å and $a' = 4{\cdot}4160$ Å but the same general crystal structure has been postulated[26] on the basis of powder X-ray diagrams. The evidence is somewhat inconclusive, but both lattice constants appear side by side in a specimen where thermal equilibrium was certainly established between about 115·9° K and about 80° K. Above 115·9° K only a persists, below 80° K only a'.

Observations on single crystals are technically more difficult, but have proved much more informative in certain cases. When the units of structure in the crystal can develop a co-operative ferro-electric field below a transition temperature, the low temperature form 2 of the crystal is polar; it can happen that the difference of lattice spacing and arrangement of units of structure between form 2 and the non-polar high temperature form 1 is quite small. In such a case polar and non-polar regions may coexist over a narrow range of temperatures, and regions of opposite polarity (2+) (2−) can pack together without shattering the hybrid crystal. Such coexistence of regions of slightly lower crystal symmetry leads to the phenomenon of "split-reflexions." For example, if a single crystal of Rochelle salt is photographed below the transition at 18° C a split of the reflexions in the 0 12 6 direction has been reported.[27] When the hybrid single crystal is viewed in other directions in which the projections of form 1 and form 2 are more nearly similar the split merges. This can be interpreted if the orthorhombic unit cell 1 of high temperature Rochelle salt transforms into a monoclinic pseudo-orthorhombic unit cell 2, with random choice of which right angles in the unit cell increase or decrease slightly. In other examples of the ferro-electric ⇌ para-electric transition, coexistence of sub-units of form 2 is found with alternative choices in the transformation from form 1, as illustrated in Fig. 2 for KH_2PO_4. With such pseudo-single crystals, the coexistence of sub-units may be apparent using monochromatic X-rays, but angular relationships between the sub-units can better be followed by Laue photographs. In the case of KH_2PO_4 such Laue photographs indicate (Fig. 3) that the options are chosen positive or negative relative to a common framework; other methods of selection are conceivable for other transformations, as from austenite to martensite.[28] Since coexistence of sub-units was originally demonstrated by X-rays for hybrid single crystals of Rochelle salt and of the acid phosphates[11,27,29] and for ammonium chloride[30] the phenomenon has been reported in a rapidly growing number of examples extending over a variety of structures. Other examples of ferro-electric ⇌ para-electric crystals in which X-ray methods have been used to exhibit coexistence of sub-structures include a range of titanates of the general formula $M^{2+}[TiO_3]^{=}$. Thus as barium titanate is cooled from 0 to −160° C there is a complicated sequence of transformations between hybrid single crystals containing different coexistent sub-units.[31] It has been verified in a number of ferro-electric hybrid crystals that when a sufficiently strong external electric field is applied in the appropriate direction, all the sub-units assume the most favourable polarity so that the splits disappear.

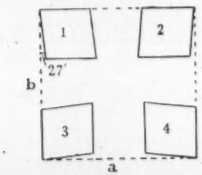

[Reproduced from *Proceedings of the Royal Society*]

Fig. 2. Alternative options for the formation of sub-units in tetragonal KH_2PO_4 on cooling

In the examples quoted of the coexistence of sub-units of opposite polarity in a hybrid single crystal, the difference of angle between alternative orientations is too small to permit convenient testing of the persistence of crystal axes, when a hybrid crystal is taken through a series of thermal cycles. When the temperature of the hybrid crystal is raised 2 ⇄ 1 well above the transition temperature, the sub-units merge into a single crystal as stated above; but any small jump of orientation in space of form 1 with respect to the former polar axes in form 2 is difficult to establish. Persistence of crystal axes can be more readily tested crystallographically in some other types of transformation, such as those involving a rotational transition. In KNO_3 the "rotational" transition with a peak at 128° C associated with the triangular

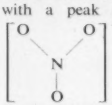

ion involves a change from a trigonal (calcite) structure at low temperatures to an orthorhombic pseudo-hexagonal (aragonite) structure at high temperatures. This makes it possible to start with crystal 1, and in a thermal cycle to test:

(*a*) whether all the possible alternative orientations of the less symmetrical sub-units appear on cooling the more symmetrical form;

(*b*) whether a single crystal reappears with the same crystal axes as before, on re-heating the low temperature hybrid above the transformation temperature.

Actually since the transition temperature with this particular crystal is well above room temperature it is technically more convenient to invert the thermal cycle. Though the conclusions are somewhat less direct in consequence, it does appear that there is a very substantial degree of persistence of axes

in a cyclic thermal transformation in KNO_3.[32] The influence of the crystal surfaces (external or internal) may be decisive in this persistence.

It has been reported that a single crystal of the high temperature form of $K_2[LiAlF_6]$ slowly undergoes transformation to a single crystal of the low temperature form, but the persistence of crystal axes in thermal cycles does not appear to have been studied.[33]

Another well-known example is the Δ transformation in sodium nitrate. Thermodynamic studies[34] show a marked "anomaly" in the specific heat extending over many degrees. Thermal expansion measurements[34] show that during this process the *c* axis of the crystals rapidly increases. Detailed intensity measurements of X-ray reflexions[35] from this and

In NH_4Cl there is a jump in lattice spacing from 3·8540 Å in structure 2 to 3·8480 Å in structure 1 with a peak transition temperature at −30·8° C. Coexistence of sub-units of crystal with each of these spacings, in a hybrid single crystal, has been verified[30] in the transition region. As the temperature is changed from −30·8° C in either direction, one form absorbs the other.

These two forms almost certainly differ in the degree of "rotational" randomization of the tetrahedral $(NH_4)^+$ cation, but since both have (pseudo) cubic symmetry rather special methods would have to be devised to test for persistence of axes in a thermal cycle.

Hybrid crystals also appear to be formed on cooling the complex salt $Ni(NO_3)_2.6NH_3$[36] but single crystal studies

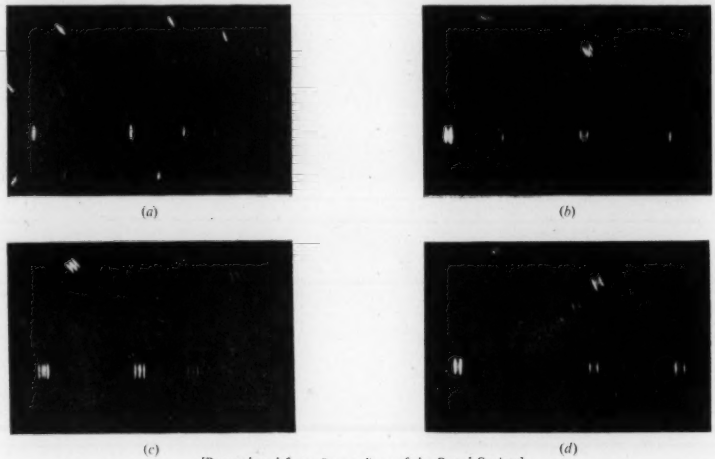

(*a*) (*b*) (*c*) (*d*)

[Reproduced from *Proceedings of the Royal Society*]

Fig. 3. (*a*) Laue photograph of KH_2PO_4 crystal above the transition around 123° K. (*b*, *c*) Laue photographs of other orientations of KH_2PO_4 below 123° K showing split reflexions. (*d*) Split of the same reflexions on cooling below 123° K, due to coexistence of sub-units

other nitrates confirm that above the transition temperature the nitrate groups "rotate" about an axis normal to the plane containing the 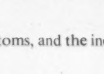 atoms, and the increased space requirements explain the observed anomalous thermal expansion. The specific heat measurements indicate prolonged "pre-transition" effects; occupancy of the alternative orientations for the NO_3^- ions must begin well below the peak transformation temperature.

Up to the present, X-ray intensity measurements have been mainly carried out on powder specimens of these nitrates, and are not sufficiently precise to determine whether orientational randomization occurs in co-operative sub-units or as a smooth statistical process as the temperature gradually rises. It seems safe to anticipate randomization of orientation in co-operative sub-units.

are still wanting. Facts reported for the rotational transition in NaCN[37] indicate persistence of axes and the coexistence of cubic and rhombohedral sub-units around the transformation temperature; single crystals apparently do not break up in thermal cycles through the transformation region.

Internal dislocations may persist as scars throughout all these transformations, and such scars may determine the growth of one type of sub-unit at the expense of the other; scars are likewise found to be important in thermal transformation cycles in $BaTiO_3$.[38]

Crystal scars or co-operative defects in the neighbourhood of a thermal transformation have not as yet received much specific study. One indication of their presence could be a marked discrepancy between the lattice expansion as determined by X-rays, and the volume occupancy determined by macro-techniques.[39] Though this discrepancy could be due to isolated crystal defects, its reported magnitude suggests the intervention of co-operative defects. Caution in the assessment of some of the reported results seems advisable.[40]

The development of a large "internal surface energy" associated with the coexistence of sub-units near a thermal transition in a crystal has an important influence on many other properties of the crystal that are structure sensitive. For example, the electrical conductance usually shows an anomalous rise, due to the production of numerous "low-energy" paths at the boundaries between micro regions.[41] Corresponding anomalies may be expected in internal friction and related mechanical properties of the solids near a transformation temperature.

Hybrid crystals seem likely to prove an important concept in thermodynamics of the solid state in a number of ways. Once the concept of sub-crystalline randomization at a level intermediate between the atomic and the polycrystalline is established, it becomes possible to bring quite a variety of sub-crystalline vagaries into accord with a modified phase rule. As one example, there is the so-called "one dimensional polymorphism" arising out of the stacking of layers of cubic or hexagonal close-packed spherical units in random sequence hcc'hchcc'hchc . . . Here the mean square amplitude of random variation forms an analogue to the size of the sub-crystalline regions in three dimensional hybrid crystals. This kind of hybridization can be significant in solids such as ZnS or SiC[42] in cobalt[42] in graphite[43] and probably in many other cases. Coexistent layered regions with the closely related anorthite and albite structures have been reported in plagioclase felspar.[45] Sub-structure formation has likewise been reported in metallic tin but its nature does not yet seem clear.[24,4]

Contributions to the crystal potential energy are generally predominantly determined by nearest neighbour interactions; crystal energy changes for randomization of units with respect to neighbouring units on a sub-crystalline scale are not likely to be large; this makes the comparatively small entropy increases associated with such randomization effective even at quite low temperatures. The free energy of different kinds of stacking will be much the same, and this favours the observed indeterminacy of structure.

In conclusion, a return may be made to some more formal consequences of crystallographic smeared transitions for the phase rule. Though such studies are still in their beginnings, in selected cases they serve to show the following.

(i) When a "gradual" transformation or "premonitory effects" are inferred from thermodynamic evidence, crystallographic studies generally indicate a gradual change of structural features such as the positional order or the regularity of orientation of units of structure in the lattice.

(ii) If the crystal structure above and below the transformation process or "phase change" is sufficiently similar, *regions* (sub-units) of the solid of structure 1 and structure 2 may *coexist* side by side in what remains apparently a single crystal, over a range of temperatures. Coexistence of (1+) and (1−) or (2+) and (2−) may also occur. Each of these regions of sub-structure in the hybrid "single crystal" will be in a state of strain, and the atoms or other units of structure in the "walls" separating the regions will be in states of exceptional misfit possessing what can be described as internal surface energy. As a consequence, the free energy will need two additional parameters[12] of strain ξ and internal surface energy η to describe it, when this state 1 is present as a "sub-structure" or region within a hybrid single crystal.

i.e. $$G_1 = f_1(p, V, T, \xi_{12}, \eta_{12})$$

and similarly for state 2

$$G_2 = f_2(p, V, T, \xi_{21}, \eta_{21})$$

Until the mechanical strain is so great that it exceeds the breaking strain of the crystal, or until the local internal surface energy η exceeds the activation energy required for migration of the units of structure with consequent self-annealing, sub-units 1 and 2 or (+) and (−) will coexist side by side in a crystal hybrid. This coexistence over a region of temperatures of two closely similar structures genetically related has some very important consequences for the phase rule. Generally a coexistence (1) (2) leads to "premonitory changes" in G. If there are premonitory phenomena, this means that slopes such as $(\partial G_2/\partial T)_p$ begin to curl round towards the value $(\partial G_1/\partial T)_p$ faster as the transition is approached. If the $2 \rightarrow 1$ transition is itself thermodynamically continuous, so that there is no sharp latent heat intake or volume change at any one temperature, this is usually stated to mean that the G curves for 2 and 1 "touch" instead of intersecting at a sharp angle. There has been considerable discussion about the "order of contact" of two G curves which could represent the kind of continuous behaviour actually observed. According to Justi and V. Laue, cf. Ref. (10), this contact is of the second order, but other alternatives have been proposed. The structural evidence now presented in outline suggests that the notion of mathematical contact between two curves is not always appropriate to the phase rule presentation. Over the range of temperatures where structures (+) and (−) or (1) and (2) coexist as sub-crystalline regions, the free energy of either hybrid crystal can in fact assume a small range of values even at constant temperature and pressure. This range is determined by the experimentally realizable ranges of ξ and η. This means that G_2 and/or G_1 in this region should be represented by a "thickened" surface whose thickness extends over the range of variation determined by the mechanical and other properties of the hybrid crystals. Such thickening is equivalent to a certain indeterminacy in G_2 and G_1. Intersection between surfaces thickened in this way simulates true *contact* between surfaces[46] (see

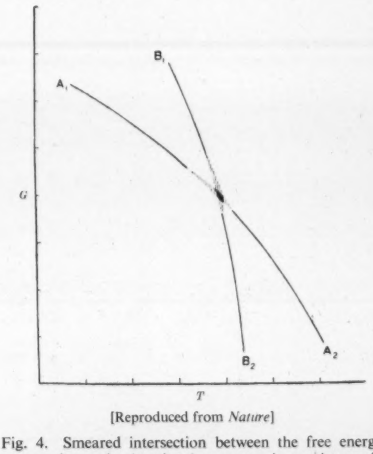

[Reproduced from *Nature*]

Fig. 4. Smeared intersection between the free energy curves of two closely related structures in coexistence in a hybrid crystal. (The angle between the curves has been exaggerated for clarity)

Fig. 4). Outside the range of temperatures where two sub-structures can coexist the free energy surfaces shrink again to mathematically true surfaces whose thickness is determined merely by probable thermal fluctuations in G.

Indeterminacy in the values of G in a region of coexistence of two sub-structures may be anticipated for many important "continuous" transitions where this has not yet been explored crystallographically. In some cases the crystallographic measurements are likely to require rather unconventional techniques; for example, in the transition in solid methane where X-rays do not readily reveal the positions of the hydrogen atoms, neutron diffraction may give new information. In the case of the Δ transition in liquid helium, if there are sub-regions of differing density this could in principle be detectable, though other forms of indeterminacy of G could arise for quantum reasons. Another aspect of indeterminacy in the G curves, to which crystallographic methods have not yet been applied systematically, involves the phenomenon of hysteresis. In many transitions of the types described, thermodynamic parameters are not completely reversible in the region of the transition. For example, the specific volume of NH_4Cl follows a well-defined hysteresis loop[47] (see Fig. 5). A probable explanation is that states of strain and surface energy of sub-regions of 2, produced spontaneously within structure 1, at first differ appreciably from states of strain and surface energy of 2 when sub-regions of 1 begin to appear in it. Since there is a small difference of specific volume between (1) and (2), hysteresis is to be anticipated.[47] If $v_2 > v_1$, hybrid 1 containing a small proportion of sub-units of 2 would be in a state of compression whilst sub-units of 1 environed by hybrid (2) would be in a state of tension. Precision measurements of the two lattice spacings in the region of coexistence are needed to determine whether hysteresis is mainly due to compression and tension energy ξ, or whether it involves substantial dislocation energy η at internal "walls" as well. With the limited structural information yet available certain observations on hysteresis are at present rather baffling. For example, it is not difficult to understand why reduction of the crystallite size should reduce the width of the hysteresis loop in the transition in NH_4Cl at $-30{\cdot}6^\circ$ C[48] since the methods used to obtain reduction in size almost certainly lead to the incorporation of a greater proportion of crystal defects from which strains can be released at lower threshold values. But why substitution of deuterium for hydrogen should reduce[48] the width of the hysteresis loop, for 100% D, in the transition at $-23{\cdot}4^\circ$ C, calls for a more recondite explanation.

Crystallographic methods based on the concept of sub-units have been developed in certain cases to study the rate of transformation within a hybrid single crystal. For example, the phase transition at a ferro-electric $\rightleftharpoons$ para-electric transformation temperature has been studied on "single crystals"[49] observed between crossed Nicol prisms. Nucleation of transformation $1 \rightleftharpoons 2$ appears to proceed from specific imperfections and in a specific crystal the transformation proceeded at about 2 cm/min with a wall thickness between sub-regions of about 24 Å at 0° C and 43 Å at 20° C. This is much thinner than ferro-magnetic domain walls which may extend over 1000 Å, and throws suggestive light on the nature of the co-operative interaction in the two cases.

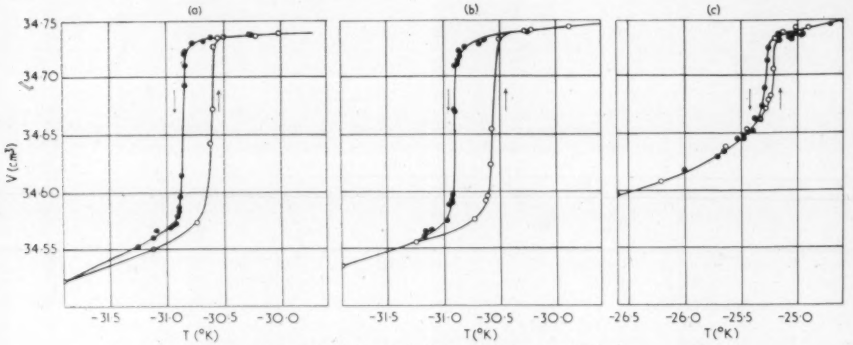

[Reproduced from *Proceedings of the Royal Society*]

Fig. 5. (*a*) Hysteresis for the Δ point transition in NH_4Cl, *small crystals*. (*b*) Hysteresis for the Δ point transition in NH_4Cl, *sublimed crystals*. (*c*) Hysteresis in ND_3HCl, *small crystals*

To sum up, the interaction between crystallography and phase rule studies depends on the development of high precision measurements on single crystals through the various thermal transformations these can undergo. The results seem likely to inspire major developments in theories of the solid state.

REFERENCES

(1) FINDLAY, A. *The Phase Rule and its Applications*, 8th Ed. (London: Longmans, Green and Co., Ltd., 1938), records historical facts about the phase rule.
(2) LUMSDEN, J. *Thermodynamics of Alloys*, p. 94 (London: Institute of Metals, 1952).
(3) WELLS, A. F. *Structural Inorganic Chemistry*, 2nd Ed., p. 674 (London: Oxford University Press, 1950).
(4) PRASAD, S. C., and WOOSTER, W. A. *Acta Cryst.*, **9**, p. 35 (1956).
(5) MENARY, J. W., UBBELOHDE, A. R., and WOODWARD, I. *Proc. Roy. Soc. A*, **208**, p. 158 (1951).

(6) OLDHAM, J. W. H., and UBBELOHDE, A. R. *Proc. Roy. Soc. A*, **176**, p. 50 (1940).

(7) GIBBS, R. E. *Proc. Roy. Soc. A*, **107**, p. 561 (1925).

(8) STROCK, L. W. *Z. Phys. Chem. B*, **25**, p. 441 (1934); *Z. Phys. Chem. B*, **31**, p. 132 (1935).
KETELAAR, J. A. *Z. Krist. A*, **87**, p. 436 (1934); *Z. Phys. Chem. B*, **26**, p. 327 (1934).

(9) HELMHOLZ, L. *J. Chem. Phys.*, **3**, p. 740 (1935); for specific heat determinations cf. Lieser, K. H. *Z. Phys. Chem.*, **2**, p. 238 (1954).

(10) Many of the references are reviewed by JAFFRAY, J. *Ann. Phys.* [*Paris*], **3**, p. 5 (1948).

(11) UBBELOHDE, A. R., and WOODWARD, I. *Nature* [*London*], **155**, p. 170 (1945); **156**, p. 20 (1946): *Proc. Roy. Soc. A*, **185**, p. 448 (1946); *A*, **188**, p. 357 (1947).

(12) UBBELOHDE, A. R. *Proc. Roy. Soc. A*, **159**, p. 301 (1937); *Trans Faraday Soc.*, **33**, p. 1203 (1937).

(13) References are reviewed, e.g., by UBBELOHDE, A. R. *Ann. Rep. Chem. Soc.*, **37**, p. 167 (1940); *Quart. Rev. Chem. Soc.*, **4**, p. 356 (1950).

(14) UBBELOHDE, A. R. *Trans Faraday Soc.*, **34**, p. 289 (1938).

(15) HOOK, A. VAN, and SILVER, L. *J. Chem. Phys.*, **10**, p. 686 (1942).

(16) STEWART, G. W. *Chem. Rev.*, **6**, p. 483 (1929).
STEWART, G. W., and EDWARDS, R. E. *Phys. Rev.*, **35**, p. 726 (1930), cf. other evidence discussed in STEWART, G. W. *Phys. Rev.*, **38**, p. 1575 (1931).
MCCOUBREY, J. C., and UBBELOHDE, A. R. *Quart. Rev. Chem. Soc.*, **5**, p. 364 (1951).

(17) MÜLLER, A. *Proc. Roy. Soc. A*, **138**, p. 514 (1932).

(18) e.g. DOUGLAS, T. B., and DEVER, J. L. *J. Amer., Chem. Soc.*, **76**, p. 4826 (1954).
CARPENTER, L. G. *J. Chem. Phys.*, **21**, p. 2244 (1953).
LAWSON, A. W. *Phys. Rev.*, **78**, p. 185 (1950).
CHRISTY, R. W., and LAWSON, A. W. *J. Chem. Phys.*, **19**, p. 517 (1951).

(19) COWLEY, J. W. *J. Appl. Phys.*, **21**, p. 24 (1950).

(20) KEATING, D. T., and WARREN, B. E. *J. Appl. Phys.*, **22**, p. 286 (1951).

(21) MCKEOWN, P. J. *J. Sci. Instrum.*, **31**, p. 271 (1954).

(22) ROBERTS, B. W. *Acta Met.*, **2**, p. 597 (1954).

(23) Such hysteresis is described by SIEGEL, S. *Symposium on Phase Transformations*, p. 379 (New York: John Wiley and Sons Inc., 1951).
Various properties are reviewed by NIX, F. C., and SHOCKLEY, W. *Rev. Mod. Phys.*, **10**, p. 1 (1938); LIPSON, H. *Progr. Met. Phys.*, **2**, p. 1 (1950).

(24) ARLMAN, J. J., and KRONIG, R. *Physica*, **10**, p. 795 (1943).

(25) BUERGER, M. J. *Symposium on Phase Transformations in Solids*, p. 183 (New York: John Wiley and Sons Inc., 1951).

(26) RUHEMANN, M. and B. *Low Temperature Physics*, p. 176 (London: Cambridge University Press, 1937).
cf. TOMBS, N. C., and ROOKSBY, H. P. *Nature* [*London*], **165**, p. 442 (1950).

(27) UBBELOHDE, A. R., and WOODWARD, I. *Proc. Roy. Soc. A*, **185**, p. 448 (1946).

(28) GAY, P., and HIRSCH, P. B. *Acta Cryst.*, **4**, p. 284 (1951).

(29) UBBELOHDE, A. R., and WOODWARD, I. *Proc. Roy. Soc. A*, **188**, p. 358 (1947).

(30) DINICHERT, P. *Helv. Chim. Acta.*, **17**, p. 338 (1944).

(31) HULM, J. K. *Nature* [*London*], **160**, p. 127 (1947).
KAY, H. F., and RHODES, R. G. *Nature* [*London*], p. 126 (1947).
MEGAW, H. D. *Proc. Roy. Soc. A*, **189**, p. 261 (1947).
RHODES, R. G. *Acta Cryst.*, **4**, p. 105 (1951).
BLATTNER, H., KANZIG, W., MERZ, W., and SUTTER, H. *Helv. Phys. A*, **21**, p. 207 (1948).

(32) KENNEDY, S. W., UBBELOHDE, A. R., and WOODWARD, I. *Proc. Roy. Soc. A*, **219**, p. 305 (1953).

(33) WINKLER, H. F. *Acta Cryst.*, **7**, p. 33 (1954).

(34) KRACEK, F. C. *J. Amer. Chem. Soc.*, **53**, p. 2609 (1931).
KRACEK, F. C., POSNJAK, E., and HENDRICKS, S. B. *J. Amer. Chem. Soc.*, **53**, p. 3339 (1931).
MIEKK-OJA, H. *Ann. Acad. Sci. Fenn. Helsinki Ser. A*, **1**, *Math. Phys. No.* 7 (1941).

(35) FINBAK, C., and HASSEL, O. *Z. Phys. Chem. B*, **35**, p. 25 (1937); *B*, **37**, pp. 75, 468 (1937).
TAHVONEN, P. E. *Ann. Acad. Sci. Fennicae A*, **1**, *Math. Phys.*, **44**, p. 20 (1947).
KETELAAR, J. A., and STRIJK, B. *Receuil Trav. Chim. Pays-Bas*, **64**, p. 174 (1945).

(36) YU, S. H. *Nature* [*London*], **150**, p. 347 (1942).

(37) BIJVOET, J. M., and VERWEEL, H. J. *Receuil Trav. Chim. Pays-Bas*, **54**, p. 631 (1935).
VERWEEL, H. J., and BIJVOET, J. M. *Z. Krist*, **100**, p. 201 (1938).

(38) KANZIG, W., and MAIKOFF, N. *Helv. Phys. Acta*, **24**, p. 343 (1951).

(39) For $NaNO_3$ cf. SAINI, H., and MERCIER, A. *Helv. Phys. Acta*, **7**, p. 257 (1934).

(40) For alkali halides cf. CONNELL, L. F., and MARTIN, J. H. *Acta. Cryst.*, **4**, p. 75 (1951).

(41) DAVIS, W. J., ROGERS, S. E., and UBBELOHDE, A. R. *Proc. Roy. Soc. A*, **220**, p. 14 (1953).
HARPUR, W. W., and UBBELOHDE, A. R. *Proc. Roy. Soc. A*, **232**, p. 310 (1955).
PLESTER, D. W, ROGERS S. E., and UBBELOHDE, A. R. *Proc. Roy. Soc. A*, **235**, p. 469 (1956).

(42) SCHNEER, C. J. *Acta Cryst.*, **8**, p. 279 (1954).

(43) EDWARDS, O. S., and LIPSON, H. *Proc. Roy. Soc. A*, **180**, p. 268 (1941).
WILSON, A. J. C. *Proc. Roy. Soc. A*, **180**, p. 277 (1941).

(44) LIPSON, H., and STOKES, A. R. *Proc. Roy. Soc. A*, **181**, p. 101 (1942).

(45) CHAO, S. H., and TAYLOR, W. H. *Proc. Roy. Soc. A*, **176**, p. 76 (1940).

(46) UBBELOHDE, A. R. *Nature* [*London*], **169**, p. 832 (1952).

(47) THOMAS, D. G., and STAVELEY, L. A. K. *J. Chem. Soc.*, p. 1420 (1951).

(48) THOMAS, D. G., and STAVELEY, L. A. K. *J. Chem. Soc.*, p. 2572 (1951).
THOMAS, D. G., STAVELEY, L. A. K., and CULLIS, A. F. *J. Chem. Soc.*, p. 1727 (1952).

(49) MITSUI, J., and FURUICHI, J. *Phys. Rev.*, **90**, p. 193 (1953).
MITSUI, J., and FURUICHI, J. *Phys. Rev.*, **95**, p. 558 (1954).

(50) JAEGER, F. M. *Proc. Ned. Akad. Wet. Amsterdam*, **43**, pp. 762, 815 (1940).

Preparation of scattering foils of uranium by evaporation of the metal in high vacuum

By K. K. DAMODARAN, M.A., Ph.D.,* Physics Department, University College, London

[*Paper received* 23 *March*, 1956]

Scattering foils of uranium were prepared by evaporating uranium in high vacuum and depositing it on thin backing foils of aluminium. The average thickness of each foil was determined by direct weighing. The variation in thickness of each of the foils was measured by counting the α- and β-radiations emitted by uranium from the various parts of the foil, using a Geiger–Müller counter.

Thin foils of heavy elements, such as uranium and thorium, are often required for scattering experiments but are not available commercially. In a scattering experiment the monitoring of the thickness and the determination of the purity of uranium in the foils are very important. The present work was carried out in connexion with an experiment on the scattering of fast electrons by heavy nuclei.†

Many different types of heater were tried for the evaporation of uranium without much success. (Open helical tungsten wire coils, close-wound conical tungsten wire baskets, flat tungsten strips, flat tungsten strip folded to form a crucible, boat-shaped tungsten strip, ceramic crucibles formed on tungsten wire baskets and cylindrical graphite crucibles heated in a tungsten spiral were all tried.) In most cases, the filament broke off when the uranium melted and wetted the heater. When a graphite crucible was tried, it was found that the molten uranium wetted the sides of the crucible and the evaporation did not proceed. Molybdenum and tantalum heaters were also tried without much success.

In the end, the most successful heater was found to be a bare tungsten filament consisting of three strands of 1 mm thick tungsten wire. Three parallel strands of 1 mm thick tungsten wire were clamped horizontally between copper terminals by means of iron clamps so that the three strands formed a flat bridge of length 4 cm and width about 4 mm. A thin flat rectangular strip of uranium, of length and breadth nearly equal to those of the tungsten heater, was placed on the heater. A thin aluminium foil (thickness 0·18 mg/cm^2, length about 6 cm and breadth about 4·5 cm) was sandwiched between two rectangular copper plates, mounted horizontally on a copper block resting on the aluminium base of the chamber, the copper plates being about 5 cm below the tungsten heater. The upper copper plate was provided with a rectangular hole (2·67 × 1·40 cm or 2·60 × 2·25 cm) so that a rectangular area at the centre of the aluminium foil was exposed to the tungsten heater. The copper plates were so placed that the rectangular area of the exposed foil was symmetrical with respect to the heater. The heater and the copper terminals were surrounded by two concentric radiation shields of nickel.

Evaporation was carried out by passing a current of about 150 A through the tungsten heater, at pressures less than 10^{-3} mm of mercury; the heater became white hot. (The pressure was below 10^{-4} mm of mercury before the current was passed and during the process of evaporation the pressure went up to about 10^{-3} mm of mercury.) Uranium was deposited on the exposed rectangular area of the aluminium foil. It was necessary to pass the current for fifteen minutes to get about 1·5 μ thickness of deposit on the foil. At the end of the process, the current was gradually decreased to zero so that neither the foil carrying the uranium deposit nor the tungsten heater broke due to sudden cooling. The method of mounting the aluminium foil ensured good thermal contact with the water-cooled aluminium base of the chamber. In spite of the precautions, the foil or the heater or both were sometimes found to be broken after the evaporation. However, five uranium foils were made by this method. One was used as a thin scattering foil and two others were combined to form a thick foil, because it was found to be very difficult to get a thick uranium deposit in a single evaporation process, owing to the excessive heating of the chamber when the evaporation was continued for more than about fifteen minutes.

MEASUREMENT OF THICKNESS OF THE URANIUM FOILS

The average thickness of the uranium deposit on each of the foils was determined by weighing. The scattering foils were then carefully mounted on aluminium frames by a little shellac dissolved in alcohol. The variation in thickness of the uranium deposit was determined by counting the α- and β-particles emitted from them. The aluminium frame was mounted on the mechanical traverse of a travelling microscope so that the plane of the foil was vertical and the longer side of the rectangular area of the uranium deposit was horizontal and was parallel to the horizontal traverse of the microscope. A square hole of side about 4·5 mm was cut at the centre of a 1·2 mm thick lead sheet which was mounted between the foil and a Geiger–Müller counter tube (type E.H.M.2S by the General Electric Co. Ltd.) with a very thin mica window (thickness 2·3 mg/cm^2). The uranium foil with the aluminium mount could be moved by means of the traverse so that any part of the deposit could be brought against the hole in the lead sheet. The counting rate corresponding to the part of the foil immediately behind the hole in the lead sheet was measured. For the thin scattering foil, the area of the uranium deposit was divided in this way into eighteen cells as shown in Fig. 1. The average counting rate per unit area

* Now Research Fellow at the Physics Department, University of Birmingham.

† DAMODARAN, K. K., and CURR, R. M. *Proc. Phys. Soc. A [London]*, **69**, p. 196 (1956).

for a foil, the mean thickness of which was known by weighing, was thus obtained and the mean thickness of the deposit at any cell area could then be determined from the observed number of counts above the background corresponding to that cell. The results of these measurements are shown in the table.

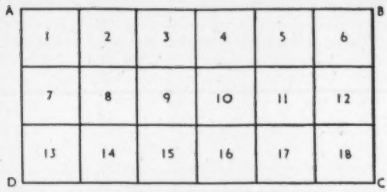

Fig. 1. Thin uranium foil divided into eighteen cells with their numbers marked

Determination of the variation in thickness over the thin uranium foil (Fig. 1)

(Background counts in 6 min = 105)

Cell number	*Number of counts in 6 min less the background*	*Mean thickness over the cell* (mg/cm²)	*Probable error* (%)
1	271	1·89	5
2	370	2·58	4
3	458	3·20	4
4	443	3·09	4
5	387	2·70	4
6	298	2·08	5
7	309	2·16	5
8	444	3·10	4
9	526	3·67	3
10	512	3·57	4
11	470	3·28	4
12	399	2·78	4
13	271	1·89	5
14	363	2·53	4
15	456	3·18	4
16	450	3·14	4
17	386	2·69	4
18	333	2·32	5

Mean thickness of the foil (by weighing) = 2·77 mg/cm²
Mean counting rate (above background) per cell over the whole foil = 397

As seen from the table, the uranium deposit is thickest at the central part of each of the foils and thinner towards the edges. This is reasonable because, during the evaporation, the central part of the foil was nearer to the heater than the edges. Fig. 2 gives the distribution of thickness of the uranium deposit over the thin foil. These curves are drawn with the mean thickness over each cell (the cell number being indicated) against the distance of the centre of the cell from one side of the foil. Similar results were obtained with the thick foil.

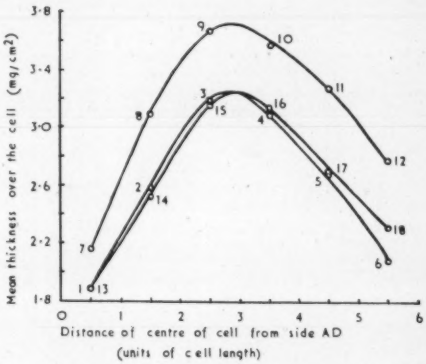

Fig. 2. Distribution of thickness over the thin foil

CHEMICAL ANALYSIS OF THE URANIUM FOILS

Two of the five uranium foils, all of which had been prepared almost under similar conditions, were chemically analysed by Mr. A. V. Winter under the supervision of the late Prof. H. Terry of the Chemistry Department. From the analysis of one of the two foils, it was found that the purity of uranium in the uranium deposit made by evaporation was 91·4%. By the analysis of the other foil, it was found that the impurities mainly consisted of silica. There were also about 0·22% of iron and about 0·1% of tungsten present.

ACKNOWLEDGEMENTS

The author has great pleasure in expressing his sincere thanks to Dr. E. H. S. Burhop for his guidance and encouragement during the course of the work, to Mr. R. M. Curr and Dr. C. Henderson for many valuable suggestions, to the late Prof. H. Terry for the chemical analysis and to the Atomic Energy Research Establishment, Harwell, for supplying the uranium. The author is also indebted to the S.N.D.P. Yogam and the Management of the Sree Narayana College, Travancore-Cochin, India, and to the University of Travancore for financial assistance.

The viscosity of mixtures of gases at high temperatures

By M. J. KENNEY, M.Sc., Grad.Inst.P., R. J. SARJANT and Prof. M. W. THRING, F.Inst.P., University of Sheffield

[*Paper received* 19 *January*, 1956]

An accurate knowledge of the high temperature viscosity of mixtures of gases, such as the products of fuel combustion, is desirable for heat transfer calculations. The viscosities of mixtures of carbon dioxide and nitrogen were determined up to 900° C by a method in which the rate of fall of gas pressure in a closed, heated container is observed over a short period during which the gas is flowing out to the atmosphere along a heated capillary tube. A comparison is made between the experimental values obtained and those calculated for similar gas mixtures on the basis of a modern theory of transport coefficients. This comparison shows that it is possible to calculate the viscosities of gas mixtures at high temperatures with an accuracy of at least 2%.

In heat transfer calculations for boilers, jet engines and gas turbines it is necessary to know the viscosity of the waste gases at high temperatures. At present there are comparatively few experimental data available on this subject, although there have been many formulae proposed (both theoretical and empirical) for calculating the viscosity over a wide range of temperatures.

An apparatus which has been used to determine the viscosity of mixtures of gases up to temperatures of approximately 900° C is described in this paper. A discussion is given of the most suitable method for calculating the viscosity of mixtures of gases, the composition of which resembles that of waste gases.

The many and varied methods available[36] for the determination of the viscosity of gases were examined with a view to finding that most suitable for use at high temperatures. Eventually the method chosen was the capillary flow method because of the proven accuracy of the theory and the relative simplicity of the apparatus.

APPARATUS

The apparatus[1] was designed so that the gas is heated to the operating temperature in the same furnace as the capillary tube, thus overcoming an objection to the capillary flow method that the gas entering the tube was not at the temperature of the tube.

The present viscometer (Fig. 1) is based on the design of Edwards[2] and consists of a reservoir made from Firth Brown Immaculate 5 steel and a capillary tube drawn from Henry Wiggin Inconel tubing.

The capillary tube was wound on to a refractory former which had a spiral grove cut into it, and was secured with several pieces of wire. This former was supported by a hollow cylinder of Immaculate 5 sheet which was welded to an Immaculate 5 rod projecting from the reservoir. A cone and socket joint was used to join the capillary tube to the reservoir, while connected at the far end of the tube was a length of wider bore Inconel tubing, to which was attached a wide bore glass tap. At the centre of the other end of the reservoir an Immaculate 5 tube was welded serving as a gas inlet line, a vacuum tapping and a pressure tapping. A manometer was attached to this tube by means of one arm of a T-piece; the other arm of the T-piece was connected to a two-way tap. The tap served to connect the reservoir with either the vacuum or the gas supply.

The manometer was of the constant volume type having one short and one long limb. It was constructed mainly of wide bore tubing to ensure that surface tension effects should be negligible. The short arm of the manometer was connected to the reservoir by means of narrow bore tubing to make the "dead-space" as small as possible. A zero mark near the top of the short arm was illiminated by a small car bulb placed behind a ground-glass screen; the heating effect of the bulb on the liquid in the manometer was negligible. The manometric height was read with the aid of a straight edge on a metal slider fitted around both the manometer tube

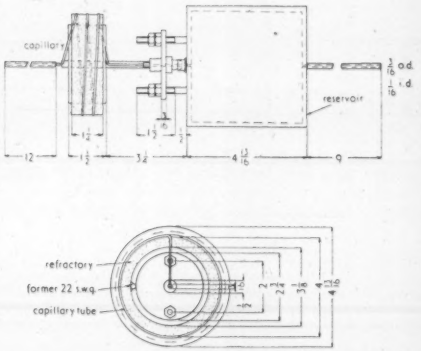

Fig. 1. Design of viscometer (all dimensions in inches)

The dimensions of the capillary tube are:

length	42·5 in.
o.d.	0·0625 in.
i.d.	0·02 in.

and the meter rule: this enabled the height of the liquid to be measured quite readily to 0·5 mm. A micrometer screw adjustment of the liquid reservoir was used to bring the liquid back accurately to the constant volume mark. Coloured paraffin of density 0·78 g/ml. at 20° C was used as the manometric fluid.

Air used for calibrating the apparatus was dried by passing it through calcium chloride, concentrated sulphuric acid and silica gel, and was freed from carbon dioxide by means of Sofnolite.

The gas mixtures were made in a large gas holder from standard commercial cylinders of nitrogen and carbon dioxide. The gas holder was of the wet type and had a film of vacuum oil on the surface of the water to minimize adsorption of gases.

Flow times of the gas from the viscometer were measured with a $\frac{1}{5}$ s stop-watch which was accurate to $\pm\frac{1}{10}$ s.

An electrically-heated furnace, constructed of insulating bricks held in an angle-iron framework by sheets of aluminium, was used to heat the viscometer. The furnace was constructed in two halves, the heating chamber being in the shape of a cylinder 9 in. in diameter and 12 in. in length. Heating was provided by coils of Nichrome wire sunk into the sides and ends of the cylinder and covered with a layer of refractory cement. A steady temperature was maintained by the use of a Sunvic energy régulator and the mains input was fed to the heaters *via* a Variac transformer.

Chromel-alumel thermocouples used to measure temperatures were connected *via* a selector switch to a potentiometer. Two thermocouples were fitted to the capillary former and two others were at the side and at the top of the furnace.

EXPERIMENTAL PROCEDURE

The reservoir was detached from the capillary and thoroughly washed and dried to remove any loose particles of scale, etc. The capillary tube was then inserted into the reservoir by means of the cone and socket joint and fixed into position by bolting to the reservoir. A layer of Autostick was used to block any very small leaks which may have been present around the joint.

Calibration of the viscometer was carried out using dry air and air free from carbon dioxide; the value for the viscosity at the calibration temperature was found from the N.B.S.–N.A.C.A. tables of thermal properties of gases.[37] The method of calibration was as follows.

The viscometer was evacuated by means of a vacuum pump, taps *B*, *C* and *E* being closed and taps *A* and *D* open (Fig. 2). After some time the tap *A* was turned so that air

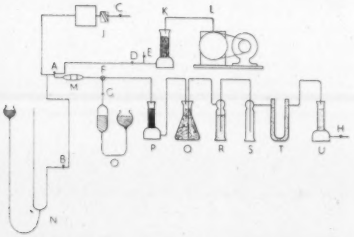

Fig. 2. Flow diagram for calibration runs

came in through the drying agents into the reservoir. The flow rate was kept low. Tap *F* was then turned so that the compressor (which had previously been filled with dry air) was connected to the viscometer. The reservoir of the compressor was then lifted and the mercury compressed the air into the viscometer. Small dust particles which would tend to block the capillary tube were removed by filtering the air through a sintered glass disk.

In order to fill the small space between the viscometer and the top of the liquid in the manometer with purified air, the paraffin in the manometer was brought as near to the tap *B* as possible in the initial evacuation. The compressed air in the reservoir was then allowed to push the paraffin back to the index mark on the manometer by opening tap *B* after the apparatus had been filled with air.

The viscometer was evacuated and filled several times prior to a determination to ensure that only dry air free from carbon dioxide was in the reservoir.

The pressure of the gas in the reservoir was then measured by closing tap *A* and opening tap *B*, and the height of the paraffin was adjusted so that the meniscus was at the zero mark on the pressure side of the manometer. Any excess air was allowed to flow out by opening tap *C* for a short time until the required pressure was obtained in the apparatus.

The tap *B* was then closed; tap *C* at the end of the capillary tube was opened and simultaneously a stop-watch started. A record was made during the determination of the air and the paraffin temperatures. At the end of a suitable time the tap *C* was closed and the stop-watch stopped. Immediately after the determination or, if there was time, during the determination the barometer pressure was read. The paraffin reservoir was lowered during the run to the position it was anticipated it would be at the end of the run when the pressure was remeasured.

The tap *B* was carefully opened and after allowing about one minute for the pressure inside the apparatus to even out, the paraffin was readjusted to the zero mark and the final pressure of the gas in the reservoir obtained. These readings enabled a calibration constant for the apparatus to be determined.

For a hot run the furnace was switched on several hours prior to a determination being carried out. When the temperature was steady (as indicated by the thermocouples) the apparatus was evacuated and filled with gas in a manner similar to that described previously. The gas was left in the viscometer for at least one hour prior to the pressure reading being taken. If the gas had been insufficiently heated the paraffin level in the pressure side of the manometer would be continually falling and when this happened a further period was allowed for the gas to heat up to the required temperature.

During a hot run pieces of asbestos board were fixed in front of and at a small distance away from the back and front of the furnace. These prevented any heat from the outside of the furnace reaching the manometer and also prevented the tap grease being softened.

For gas mixture runs, the purification of the gas was carried out by leaving only the drying agents in circuit, the Sofnolite being removed. A three-way tap was inserted in the gas line between the filter and tap *F*. A vacuum line was attached at this point and a large volume of gas drawn through the drying agents to purge them of the gas which had previously been in them. Gas analyses were made during the purging to indicate when the lines were free from foreign gases.

The viscometer was evacuated and tap *F* closed so that the inlet side of the apparatus was cut off from the viscometer. Tap *A* was turned through 180° and the gas in the filter section of the line removed; the tap was then turned to its original position. Tap *F* was opened so that gas filled this section of tubing and the process repeated several times. Finally gas was put into the viscometer in the normal way, care being taken to remove all foreign gases from both the gas compressor and the manometer. The actual measuring procedure was then carried out as for the determination on air.

When Inconel is heated to high temperatures a thin film of scale is formed; obviously the calibration constant of the viscometer would alter during the course of a series of hot runs unless this diminution in the size of the bore of the capillary tube was allowed for. Fortunately the need for the application of this correction was minimized by heating

the viscometer to 820° C for approximately 100 hours, at the same time periodically passing air through the capillary tube. It was found that with Inconel a scale was formed which after prolonged heating at high temperatures only increased in thickness very slightly and, in fact, during the whole course of the experiments the calibration factor altered by approximately 1%.

THEORY

Consider the viscometer in its simplest form as a vessel of volume V having attached to it a capillary tube of internal radius r and length L. Meyers transpirational formula[3] (based on the differential equations of Stokes[4] for flow of a gaseous medium subject to frictional forces) gives for the mass of gas flowing through a tube of radius r, in a short time dt:

$$dmR\theta = -(\pi r^4/16\eta_0 L)(P^2 - P_0^2)\,dt \qquad (1)$$

where the pressure of the gas in the viscometer at any instant is P, the external pressure P_0, and the mass of gas in the viscometer is m at time t; R is the gas constant, θ the absolute temperature and η_0 is the coefficient of viscosity of the gas at θ° K.

Assuming that the gas under consideration obeys Boyles law:

$$PV = mR\theta \quad \text{or} \quad VdP = dmR\theta \qquad (2)$$

By substitution of equation (2) into equation (1)

$$VdP = -(\pi r^4/16L\eta_0)(P^2 - P_0^2)\,dt$$

Now if $(P_1 + P_0)$ and $(P_2 + P_0)$ are the initial and final pressures respectively of the gas in the viscometer and t is the total time of flow, then:

$$-\int_{P_1+P_0}^{P_2+P_0} \frac{dP}{P^2 - P_0^2} = \frac{\pi r^4 t}{16LV\eta_0}$$

On integration this gives:

$$\frac{1}{2P_0}\log e\left[\frac{(P_2 + 2P_0)P_1}{(P_1 + 2P_0)P_2}\right] = \frac{\pi r^4 t}{16LV\eta_0} \qquad (3)$$

and by substituting $2{\cdot}303\log_{10} x$ for $\log_e x$ one obtains:

$$\frac{1}{P_0}\log_{10}\left[\frac{(2P_0 + P_2)P_1}{(2P_0 + P_1)P_2}\right] = \frac{\pi r^4 t}{18{\cdot}424LV\eta_0} \qquad (4)$$

Equation (4) is the basic formula used in this series of determinations; several corrections have, however, to be applied and these will now be considered.

Volume correction. At the beginning of a determination, tap B is closed and this means that the gas inside the manometer is at a pressure $(P_1 + P_0)$; at the end of a determination, the tap B is opened and the gas at a pressure of $(P_1 + P_0)$ will mix with that in the reservoir at a pressure $(P_2 + P_0)$, thus causing an increase in the overall pressure in the system. At the instant of closing the tap C the gas in the outlet end of the tube will be at atmospheric pressure. A flow of gas will therefore take place and the resultant pressure of the gas in the outlet tube will be greater than that in the reservoir at the instant the tap C was closed.

Consider the viscometer as being in the three sections as in Fig. 3. The pressure in each part of the apparatus at the end of a run, before and after opening the tap B connecting the reservoir and the manometer, are as given in Fig. 3.

Then by application of the gas laws:

$$(P_1 + P_A)\frac{V_1}{T_A} + (P_2 + P_1)\frac{V_2}{T_F} + \frac{P_A V_3}{T_3} = (P + P_A)\left(\frac{V_1}{T_A} + \frac{V_2}{T_F} + \frac{V_3}{T_3}\right)$$

Hence $$\frac{P_1 V_1}{T_A} + \frac{P_2 V_2}{T_F} = \frac{PV_1}{T_A} + \frac{PV_2}{T_F} + \frac{PV_3}{T_3}$$

giving finally:

$$P_2 = \frac{V_1 T_F}{T_A V_2}(P - P_1) + P\left(1 + \frac{V_3 T_F}{T_3 V_2}\right) \qquad (5)$$

Slip correction. In the derivation of the formula for calculating the coefficient of viscosity of gases using the apparatus described previously, it has been assumed that the layer of gas at the wall of the capillary tube is at rest.

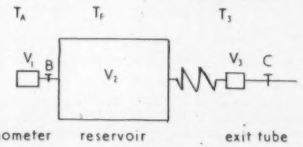

Fig. 3. Viscometer represented as three sections. The pressure in each part being

	manometer	*reservoir*	*exit tube*
immediately after a run	P_1	P_2	P_A
after tap B has been opened	P	P	P

Experiments[3,5,6] have shown that slip does occur. An allowance can be made for this in the calculations by assuming the effective radius of the capillary tube to be $(r + \epsilon)$ where ϵ is called the depth of slip. This is equivalent to multiplying equation (4) by

$$[1 + (4\epsilon/r)] \qquad (6)$$

It has been shown[7,8] that $\epsilon = 1{\cdot}41\lambda$ where λ is the mean free path of the gas.

Thus equation (6) becomes

$$[1 + (5{\cdot}64\lambda/r)] \qquad (7)$$

Thermal expansion correction. When the apparatus is heated both the reservoir and the capillary tube expand, and allowance must be made in the basic formula (4) for this expansion.

Let α_a = temperature coefficient of linear expansion of the metal of the capillary and α_r = temperature coefficient of linear expansion of the metal of the reservoir.

The suffixes 0 and t will be used to denote the property at 0° C and t° C respectively.

Then $$\frac{r_t^4}{V_t L_t} = \frac{r_0^4(1 + \alpha_a t)^4}{V_0(1 + 3\alpha_r t)L_0(1 + \alpha_a t)} \qquad (8)$$

THE EFFECT OF COILING

It has been shown[9] that the resistance to the flow of fluids in curved pipes is greater than that in straight pipes of similar dimensions. Dean[10] showed that, for laminar flow, the ratio of the coefficient of pressure change in a curved tube to that in a straight tube of the same dimensions is given by a function of:

$$D = Re\sqrt{(d/D)} \qquad (9)$$

Where D = Deans number, Re = Reynolds number, d = internal diameter of the tube, and D = mean diameter of the coil. When D is less than 11·6 then there is no appreciable difference between the flow in straight and the flow in curved tubes.

Equation (4) was derived on the assumption that the flow in the capillary tube is laminar. The criterion for laminar flow is that the Reynolds number should be less than 2000. The present experiments were carried out at Reynolds numbers well below 2000, thus ensuring that the flow was laminar. It was also arranged that the Deans number during a determination should be less than 11·6 and so no correction was needed for the coiling effect. The equation used in the calculations was thus:

$$\frac{1}{P_0}\log_{10}\left[\frac{(P_2+2P_0)P_1}{(P_1+2P_0)P_2}\right]=\frac{\pi r^4 t}{18\cdot424LV\eta_0}\xi E \qquad (10)$$

Where ξ is the slip correction factor and E is the thermal expansion factor.

As the term $\pi r^4/18\cdot424LV$ is independent of temperature, it may be represented by a constant Δ.

Rewriting equation (10) and replacing $\left[\frac{(P_2+2P_0)P_1}{(P_1+2P_0)P_2}\right]$ by $f(P)$

$$\eta_1=\frac{t_1P_0\Delta}{\log f_1(P)}\xi_1E_1 \quad \text{for a temperature } T_1 \qquad (11)$$

By carrying out a determination on air at room temperature (the viscosity of which is known accurately), the value of Δ may be calculated by use of equation (11). If the viscosity coefficient of any gas is required at another temperature, the values of t, P_0 and $f(P)$ are determined and ξ and E calculated, then, by substitution of these values in equation (11) and by knowing Δ, the value of η may be found.

EXPERIMENTAL RESULTS

The viscosities of three mixtures of gases were determined at temperatures up to about 900° C. Table 1 gives the values obtained while Table 2 gives the composition of the gas mixtures A, B and C as determined by analysis. The values of the slip correction factor, and of the thermal expansion factor for gas A are given in Table 3. It is estimated that the maximum possible error for these determinations is 2%.

Table 1. *Viscosities*

Gas mixture A		*Gas mixture B*		*Gas mixture C*	
Temperature (°C)	*Viscosity* ($\eta \times 10^7$ g cm^{-1} s^{-1})	*Temperature* (°C)	*Viscosity* ($\eta \times 10^7$ g cm^{-1} s^{-1})	*Temperature* (°C)	*Viscosity* ($\eta \times 10^7$ g cm^{-1} s^{-1})
44	1844	32	1763	18·2	1703
288	2723	275·5	2733	130	2169
414	3121	464	3220	223	2489
540·5	3536	631·5	3805	358	2901
754·5	4184	766	4111	538	3477
887·5	4516	861	4413	659	3823
				774	4187
				873	4374

Table 2. *Gas mixture compositions*

	Percentage by volume		
Gas	*Carbon dioxide*	*Oxygen*	*Nitrogen*
A	10·62	0·73	88·65
B	15·0	0·5	84·5
C	19·82	0·64	79·54

Table 3. *Values of slip correction and thermal expansion factors for gas A*

Temperature (°K)	*Uncorrected viscosity* ($\eta \times 10^7$ g cm^{-1} s^{-1})	*Slip correction factor* ξ	*Thermal expansion factor* E	*Corrected viscosity* ($\eta \times 10^7$ g cm^{-1} s^{-1})
317	1843	1·0009	0·9999	1844
561	2721	1·0015	0·9991	2723
687	3122	1·0019	0·9977	3121
813·5	3542	1·0023	0·9960	3536
1027·5	4174	1·0029	0·9995	4184
1160·5	4511	1·0033	0·9979	4516

In order to compare values of the coefficient of viscosity obtained in this series of experiments with those of other workers, a series of experiments were carried out on air at various temperatures. The values obtained are given in Table 4 and a graph (Fig. 4) is given comparing these results and those of other workers.

Table 4. *Coefficient of viscosity of air*

Temperature (°C)	*Viscosity* ($\eta \times 10^7$ g cm^{-1} s^{-1})
143·5	2320
307·5	2981
417	3257
513	3528
639	3949
732	4223
775	4355
891	4536

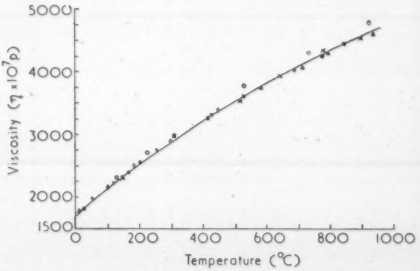

Fig. 4. Viscosity/temperature relationship for air

× = experimental values
△ = Vasilesco[33]
○ = Rammler and Breitling[25]
▽ = Shilling and Laxon[34]
● = Trautz and Ludwig[35]
◇ = Edwards[2]

CALCULATION OF THE VISCOSITY OF GAS MIXTURES

Numerous formulae[11-26] have been prepared for calculating the viscosity of both single gases and mixtures of gases, together with the effect of temperature on the viscosity.

One of the simplest formulae proposed is that due to Sutherland.[27]

$$\eta=\eta_0\left(\frac{273\cdot2+C}{T+C}\right)\left(\frac{T}{273\cdot2}\right)^{3/2} \qquad (12)$$

where η_0 = coefficient of viscosity at 0° C, η = coefficient of viscosity at T° K, and C = Sutherland's constant.

The constant C is usually determined experimentally but it can be related to various molecular quantities.

Rewriting equation (12) one can obtain:

$$T = (KT^{3/2}/\eta) - C \qquad (13)$$

By plotting a graph of $T^{3/2}/\eta$ against T for a gas, the value of Sutherland's constant may be obtained from the intercept of the line providing that C remains constant with temperature.

Figs. 5, 6 and 7 show the Sutherland plots for the present series of determinations and illustrate that for these gases C

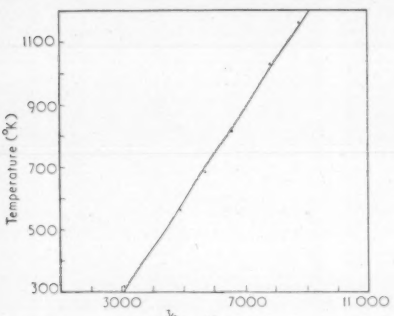

Fig. 5. Sutherland plot for gas mixture A

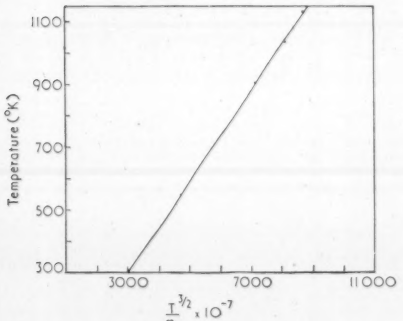

Fig. 6. Sutherland plot for gas mixture B

is constant over the temperature range considered. Furthermore, it is possible to calculate the viscosities of other gas mixtures of similar type by use of the Sutherlands equation providing the viscosity of the mixture is known at two different temperatures.

The present results agree best with Hirschfelder's formula[28, 29] which is outlined below.

Hirschfelder's method is based on the solution of the Boltzmann equation[30] for the molecular distribution, as carried out by Chapman[31] and Enskog.[32] This solution permits the coefficient of viscosity to be expressed in terms of a set of double integrals $\Omega^{(l,s)}$ which involve explicitly the dynamics of a binary collision and hence the intermolecular force law.

The results obtained by this method are applicable at low pressures (about atmospheric pressure) and strictly apply only to monatomic gases. In actual practice, however, it is found that the results may be applied to polyatomic molecules for the calculation of gas viscosities.

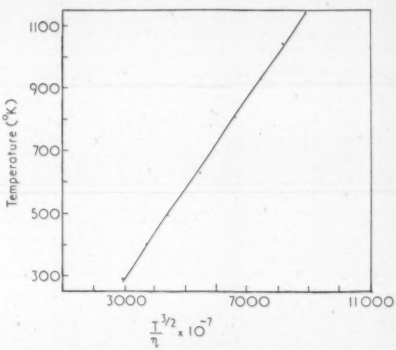

Fig. 7. Sutherland plot for gas mixture C

For a pure non-polar gas the first approximation to the coefficient of viscosity is given by:

$$[\eta]_1 \times 10^7 = 266{\cdot}93\sqrt{(MT)}/\sigma^2\Omega^{(2,2)*} \qquad (14)$$

where $[\eta]_1$ = first approximation to the coefficient of viscosity, M = molecular weight of the gas, T = absolute temperature, and $\Omega^{(2,2)*}$ = the collision integral for T^* made dimensionless by dividing by suitable combinations of ϵ and σ where ϵ and σ are parameters characteristic of the chemical species involved. $T^* = kT/\epsilon$ where k = Boltzmann constant.

Tables are available[28, 29] giving values of σ and ϵ for various substances and also giving values of $\Omega^{(2,2)*}$ for various values of T^*.

For the binary mixtures considered in this paper the formulae used were as given below:

$$\frac{1}{[\eta_{MIXT}]_1} = \frac{X_{\eta}}{1 + Z_{\eta}}$$

where $[\eta_{MIXT}]_1$ is the first approximation to the coefficient of viscosity of the gaseous mixture, and X_{η}, Y_{η} and Z_{η} are as defined below.

$$X_{\eta} = \frac{x_1^2}{[\eta_1]_1^2} + \frac{2x_1x_2}{[\eta_{12}]_1} + \frac{x_2^2}{[\eta_2]_1^2}$$

$$Y_{\eta} = \frac{3}{5}A_{12}^*\left[\frac{x_1^2}{[\eta_1]_1}\left(\frac{M_1}{M_2}\right) + \right.$$

$$\left. + \frac{2x_1x_2}{[\eta_{12}]_1}\left(\left[\frac{(M_1+M_2)^2}{4M_1M_2}\right]\left\{\frac{[\eta_{12}]_1^2}{[\eta_1]_1[\eta_2]_1}\right\}\right) + \frac{x_2^2}{[\eta_2]_1}\left(\frac{M_2}{M_1}\right)\right]$$

$$Z_{\eta} = \frac{3}{5}A_{12}^*\left[x_1^2\left(\frac{M_1}{M_2}\right) + 2x_1x_2\left(\left[\frac{(M_1+M_2)^2}{4M_1M_2}\right]\right.\right.$$

$$\left.\left.\left\{\frac{[\eta_{12}]_1}{[\eta_1]_1} + \frac{[\eta_{12}]_1}{[\eta_2]_1}\right\} - 1\right) + x_2^2\left(\frac{M_2}{M_1}\right)\right]$$

$[\eta_{12}]_1$ is a further parameter and is defined as follows:

$$[\eta_{12}]_1 \times 10^7 = \frac{266{\cdot}93\sqrt{[M_1M_2T/(M_1+M_2)]}}{\sigma_{12}^2\Omega_{12}^{(2,2)*}}$$

Where M_1 and M_2 are the molecular weights of the two components, σ_{12} and $\Omega_{12}^{(2,2)*}$ are collision integrals similar to those described previously, but applying in this case to the binary mixture, and $A_{1,2}^*$ is a function of T^* and is related to the diffusion coefficient. x_1 and x_2 are the mole fractions of components 1 and 2.

The values obtained by calculations based on this method (on the basis of mixtures of carbon dioxide and nitrogen only) are given in Table 5 together with the deviation from the experimental results. It will be seen that this method of calculation gives values which agree with those obtained experimentally with an accuracy of about 1%.

Table 5. *Deviation of calculated from experimental viscosities*

Gas A			*Gas B*			*Gas C*		
Temperature (°C)	*Calculated viscosity* ($\eta_1 \times 10^7$ g cm^{-1} s^{-1})	*Deviation* (%)	*Temperature* (°C)	*Calculated viscosity* ($\eta_1 \times 10^7$ g cm^{-1} s^{-1})	*Deviation* (%)	*Temperature* (°C)	*Calculated viscosity* ($\eta_1 \times 10^7$ g cm^{-1} s^{-1})	*Deviation* (%)
44	1829	−0·82	32	1764	−0·06	18·2	1688	−0·88
288	2748	+0·92	275·5	2626	−0·26	223	2517	+1·12
754·5	4062	−2·9	766	4089	−2·9	774	4121	−1·6

Thus, the present work supports the contention that the Hirschfelder method may be used to calculate accurately the viscosity of gas mixtures without any experimental data for the viscosity of the gas mixture. Furthermore, the values obtained are accurate over a wide temperature range.

CONCLUSIONS

The conclusions which may be reached as a result of this work may be summarized as follows.

It is possible by use of the apparatus described to measure the viscosities of gases up to 1000° C with an accuracy of at least 2%.

The viscosities of various mixtures of carbon dioxide and nitrogen were determined up to about 900° C and the values so obtained were shown to obey Sutherlands law. If the viscosity of a gas mixture (of similar composition to those described here) is known at two differing temperatures then it is possible to obtain from these values a value for Sutherlands constant. The values for the viscosity at higher temperatures may then be calculated using Sutherlands law.

The comparison of the experimental values with those calculated by means of Hirschfelder's formula show that it is possible to calculate the viscosity of gas mixtures accurately for a large temperature range with no experimental values for the gas mixture concerned.

ACKNOWLEDGEMENTS

One of the authors (M. J. K.) wishes to thank the British Coal Utilisation Research Association who sponsored this work.

REFERENCES

(1) KENNEY. *M.Sc. Thesis* (University of Sheffield, 1955).
(2) EDWARDS. *Proc. Roy. Soc. A*, **117**, p. 245 (1927).
(3) MEYER. *Pogg. Ann.*, **127**, pp. 253, 353 (1866).
(4) STOKES. *Trans Camb. Phil. Soc.*, **8**, pp. 107, 287 (1845).
(5) HELMHOLTZ and PIOTROWSKI. *Wein. Ber.*, **40**, p. 607 (1860).
(6) KNUDT and WARBURG. *Pogg. Ann.*, **155**, p. 337 (1875).
(7) KNUDSEN. *Ann. Phys.* [*Leipzig*], **28**, p. 75 (1909).
(8) CHAPMAN. *Phil. Trans A*, **216**, p. 279 (1915).
(9) EUSTICE. *Proc. Roy. Soc. A*, **84**, p. 107 (1910); **85**, p. 119 (1911).
(10) DEAN. *Phil. Mag.*, **3**, p. 912 (1927); **4**, p. 208 (1927).
(11) GRAHAM. *Phil. Trans*, **136**, p. 573 (1846).
(12) MEYER. *Ann. Phys.* [*Leipzig*], **113**, p. 383 (1861).
(13) SUTHERLAND. *Phil. Mag.*, **40**, p. 421 (1895).
(14) SCHUDEL. *Schweiz. Ver. Gas. Wasserfach Monats. Bull.*, **22**, pp. 112, 131 (1942).
(15) BUDDENBURG and WILKE. *Industr. Engng Chem.*, **41**, p. 1345 (1949).
(16) WILKE. *J. Chem. Phys.*, **18**, p. 517 (1950).
(17) PULUJ. *Wien Ber.*, **79** (II), pp. 97, 745 (1879).
(18) OMNES. *Comm. Phys. Lab. Univ. Leiden*, No. 12 (1894).
(19) LEFEVRE. *Amer. Soc. Mech. Engrs*, Paper 53-A-192 (1953).
(20) WHALLEY. *Canad. J. Chem.*, **32**, p. 485 (1954).
(21) UYEHARA and WATSON. *Nat. Petroleum News* (*Tech. Section*), **36**, pp. 714–722 (1944).
(22) MANN. *Gas Wasserfach.*, **73**, p. 570 (1930).
(23) ZIPPERER. *Gas Wasserfach.*, **74**, p. 1101 (1931).
(24) HERNING and ZIPPERER. *Gas Wasserfach.*, **79**, pp. 49, 69 (1936).
(25) RAMMLER and BREITLING. *Die. Warme.*, **38**, p. 620 (1937).
(26) WESTMORELAND. *National Advisory Committee for Aeronautics Technical note* 3180 (June 1954).
(27) SUTHERLAND. *Phil. Mag.*, **36**, p. 507 (1893).
(28) HIRSCHFELDER, BIRD and CURTISS. *Trans Amer. Soc. Mech. Engrs*, **76**, p. 1031 (1954).
(29) HIRSCHFELDER, BIRD and CURTISS. *The Molecular Theory of Gases and Liquids* (New York: John Wiley and Sons, 1954).
(30) BOLTZMANN. *Vorlesungen über Gas Theorie*. 3rd ed. Vol. I, Chaps. 1 and 2. (Leipzig: J. A. Barch, 1923.)
(31) CHAPMAN. *Phil. Trans A*, **216**, p. 279 (1916); **217**, p. 115 (1917).
(32) ENSKOG. *Dissertation* (University of Uppsala, 1917).
(33) VASILESCO. *Ann. Phys.* [*Paris*], **20**, pp. 137, 292 (1945).
(34) SHILLING and LAXON. *Phil. Mag.*, **10**, p. 721 (1930).
(35) TRAUTZ and LUDEWIGS. *Ann. Phys.* [*Paris*], **3**, p. 409 (1929).
(36) KENNEY. *University of Sheffield Fuel Society J.*, **7**, p. 51 (1956).
(37) MOREY. *Thermal Properties of gases*. National Advisory Committee for Aeronautics—National Bureau of Standards. Table 2.39 (1950).

Focal properties and chromatic and spherical aberrations of the three-electrode electron lens

By G. D. ARCHARD, A.Inst.P., Research Laboratory, Associated Electrical Industries Ltd., Aldermaston, Berkshire

[*Paper received* 24 *May*, 1956]

Published theoretical and experimental values of the *focal lengths* of simple three-electrode electron lenses are compared and found to be in general agreement. These are presented in the form of graphs which show directly the dependence of focal length on lens geometry and voltage ratio. Analogous graphs are derived for *spherical* and *chromatic* aberrations in the form of the ratios C_S/S and C_C/S (S being the separation of adjacent electrodes), and the general relation between the various curves is discussed.

INTRODUCTION

Whereas the important properties of magnetic electron lenses have already been adequately presented in a collected and generalized form,[1] this cannot as yet be said of electrostatic lenses. Although many papers on electrostatic lenses have been published, most of these have dealt with their focal properties, and very often the results have not been expressed in a form immediately applicable to the design of electron-optical systems. The aim of the present paper is to present the focal properties, spherical and chromatic aberrations of simple three-aperture lenses in the form of comprehensive data related to the lens dimensions and applied potentials.

Regenstreif[2] has presented a complete theory of the three-electrode lens (schematically depicted in Fig. 1), based on

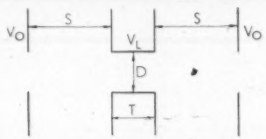

Fig. 1. Simplified form of three electrode lens

certain simplifying assumptions regarding its potential distribution. Focal lengths deduced from this theory agree closely with experimental values of Heise and Rang,[3] and calculations of the distortion produced by lenses with thick central electrodes agree with experimental results of Heise.[4] Some doubts were cast on the theory by experiments of Lippert and Pohlit,[5] but the form in which these workers presented their results may have given an exaggerated view of the discrepancies; when their experimental values of focal length are directly compared with those of Heise and Rang, the differences do not appear formidable.

However, a further check seems desirable, and to this end the theory of Glaser and Schiske[6] has been consulted. This relates to a bell-shaped potential distribution approximating to that of a three-electrode lens with *thin* central electrode (for which Glaser and Schiske's parameter κ^2 may be approximately identified with $1 - x$, where x is Regenstreif's parameter, equal to the ratio of the potential in the centre of the lens to that in the centres of the outer apertures). By a simple modification, the theory can be extended to simulate the cases of lenses with *thick* central electrodes (approximated by a region of constant potential separating two half-bell shaped potential distributions). Focal lengths obtained from the modified theory show close agreement with the experimental results quoted and with the theory of Regenstreif, as well as with an experimental result of Liebmann[7] (his "lens No. 14") which coincided with earlier calculations of Ramberg[8] carried out by numerical ray-tracing.

FOCAL LENGTHS

Sufficient confidence is established in the theoretical expressions for focal lengths by the considerations of the preceding section to justify the plotting of Fig. 2, in which S, D and T have the same meanings as in Fig. 1, while f represents focal length, V_0 the accelerating voltage, and V_L the voltage on the central electrode. Fig. 2 gives the relative focal length f/S for a range of geometries S/D, T/D and a range of voltage ratios V_L/V_0. The dotted parts of the curves correspond to the condition in which the focus occurs inside the lens—this would make it impossible to use the lens as an objective lens in an electron microscope.

As a weak lens approximation, Regenstreif's formula (47) may be applied. This involves the evaluation of the parameter x from a knowledge of dimensions and voltages [his equations (196) to (198)], merely replacing z_2 by $(S + T/2)$, z_1 by $T/2$, R_1 and R_2 by $D/2$, V_1 by V_L and V_2 by V_0. It may, however, be useful to set down a simplified form approximately valid for $0{\cdot}7 \leqslant V_L/V_0 \leqslant 1$ and $0{\cdot}6 \leqslant S/D \leqslant 2{\cdot}0$; this is:

$$f \simeq \frac{8}{3}(S + T/2)\left[\frac{1 + 2S/D - T/2D}{2S/D}\right]^2 /(1 - V_L/V_0)^2$$

SPHERICAL ABERRATION

The confidence thus established in Regenstreif's theory in respect of focal lengths may reasonably be extended to his expressions for aberrations. Regenstreif gives an expression for the displacement Δr of a non-paraxial ray from the paraxial focus as a function of r_0 (height at which ray enters lens) and other quantities depending on parameter x. By expanding the functions containing r_0 and neglecting terms above second order, an expression may be obtained for C_S/f^3 (which is nearly the same as $\Delta r/r_0^3$) where C_S is the third order coefficient of spherical aberration.

The intermediate steps involve cumbersome equations which will not here be reproduced; they take different forms for the cases $x \ll 1$, $x > 1$. (The condition $x > 1$ means that the central electrode is at a higher potential than the outer electrodes.) Evaluation of the expressions shows that the aberration for, say, $x = a$ is generally of the same order as that for $x = 1/a$, and it is therefore sufficient to consider values of C_S/f^3 corresponding to the condition more usually found in practice, namely, $x < 1$. Thus, Fig. 3 gives the relative spherical aberration C_S/S in terms of lens geometry and voltage ratio. If Figs. 2 and 3 are taken together, similar

curves may be plotted for C_S/f. These show that the value of V_L/V_0 for which C_S/f is a minimum is the same as that for which f/S is a minimum (S/D and T/D being kept constant), and the minimum value of C_S/f is independent of S/D and T/D, being approximately equal to 3.

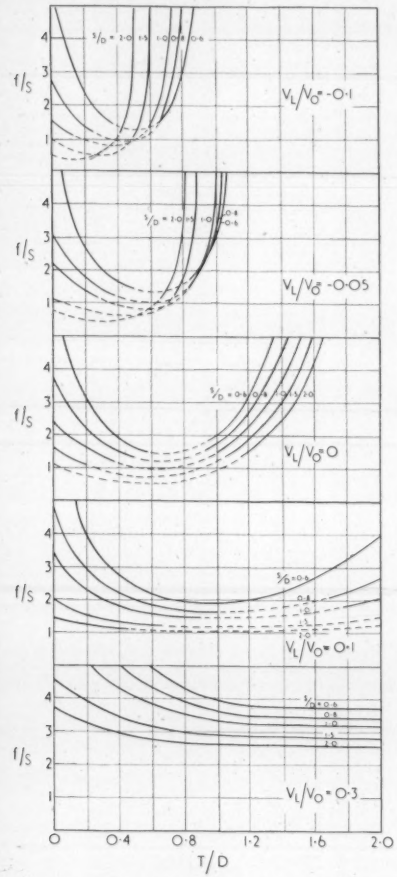

Fig. 2. Relative focal length f/S as a function of dimensions T/D, S/D and voltage ratio V_L/V_0. Dotted lines mean focus occurs inside lens

Liebmann's lens No. 14 (referred to in the previous section) was approximately characterized by $D/(2S + T) = 0{\cdot}7$, $T/(2S + T) = 0{\cdot}2$. In the following table, comparison is made between the theoretical and experimental values of C_S/f for this lens. Seeliger[9] also, in an investigation covering a series of einzel lenses, failed to obtain values of C_S/f lower than 3. These facts provide experimental support for the curves of Fig. 3.

V_L/V_0	0·3	0·2	0·1	0·0	−0·1
$C_S(expt.)/f$	72	29	15	8	5
$C_S(theor.)/f$	68	30	14	7	4

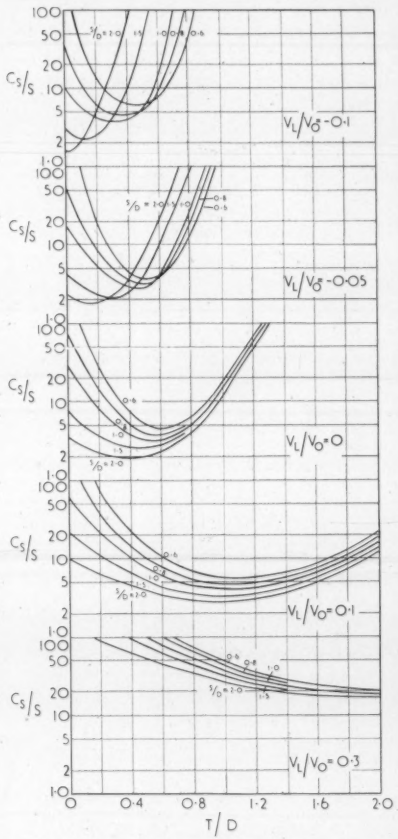

Fig. 3. Relative spherical aberration C_S/S as a function of dimensions T/D, S/D and voltage ratio V_L/V_0

Figs. 2 and 3, or the C_S/f curves which may be derived from them, show that considerable changes in C_S/f can be caused by small changes of geometry or voltage ratio. From a practical point of view, this means that, after the geometry has been chosen and the lens built, a fine adjustment of voltage ratio may be used to bring about the condition of

minimum spherical aberration, which coincides with the condition of maximum lens strength. As a weak lens approximation, the following expression may be used:

$$C_S/f^3 \simeq 3{\cdot}5/(S + T/2)^2$$

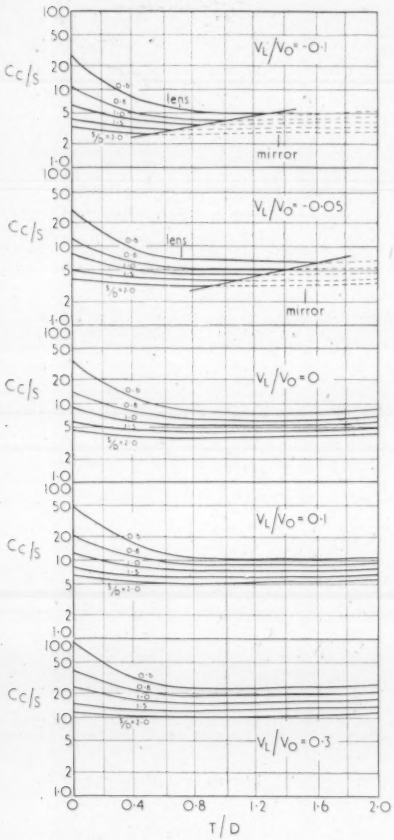

Fig. 4. Relative chromatic aberration C_C/S as a function of dimensions T/D, S/D and voltage ratio V_L/V_0

CHROMATIC ABERRATION

Regenstreif's theory provides a simple relation (deduced from work of Recknagel[10]) for the chromatic aberration constant of the three-electrode lens [his equation (50)]. It is expressed in terms of the parameter x. The values of C_C/S so deduced are plotted in Fig. 4. It will be noted in this case that there is a continuous transition from lens to mirror (shown by dotted lines): the dividing line corresponds to the values of T/D for which f/S becomes infinite in Fig. 2.

Fig. 4 may be taken in conjunction with Fig. 2 to produce curves of C_C/f. The maximum value of C_C/f in all these curves is approximately 6. The asymptotic value of C_C/f for weak lenses is 2. The latter is precisely confirmed by Glaser and Schiske's theory (Fig. 7 of their 1954 paper). Moreover, when the relation $\kappa^2 \simeq 1 - x$ (mentioned in the first section) is employed, the two theories also show fair agreement for strong lenses ($x \ll 1$).

CONCLUSIONS

The sets of curves given in Fig. 2, 3, 4, represent the focal lengths and spherical and chromatic aberration constants of simple three-electrode electrostatic lenses of a range of geometrical parameters and voltage ratios likely to be used in practice. Important general tendencies are:

1. Maximum lens strength and minimum spherical aberration may be obtained for negative, zero, or positive values of V_L/V_0, depending on the geometry.

2. The minimum value of C_S/f occurs at the same value of V_L/V_0 as does the maximum value of S/f, and is independent of geometry.

3. In general, an increase of $D/(2S + T)$ can be compensated by a suitable increase of V_L/V_0. Thus, if a lens were built with slightly incorrect geometry, the desired properties could be restored by an appropriate adjustment of voltage ratio.

ACKNOWLEDGEMENTS

The author wishes to thank Mr. M. E. Haine, the late Dr. G. Liebmann and Mr. T. Mulvey for much helpful comment, and Dr. T. E. Allibone, Director of the Laboratory, for permission to publish this paper.

REFERENCES

(1) LIEBMANN, G. *Proc. Phys. Soc.* [*London*] *B*, **68**, p. 737 (1955).

(2) REGENSTREIF, E. *Ann. Radioélectricité*, **6**, pp. 51, 114 (1951).

(3) HEISE, F., and RANG, O. *Optik*, **5**, p. 201 (1949).

(4) HEISE, F. *Optik*, **5**, p. 479 (1949).

(5) LIPPERT, W., and POHLIT, W. *Optik*, **9**, p. 456 (1952); **10**, p. 447 (1953); **11**, p. 181 (1954).

(6) GLASER, W., and SCHISKE, P. *Optik*, **11**, pp. 422, 445 (1954); **12**, p. 233 (1955).

(7) LIEBMANN, G. *Proc. Phys. Soc.* [*London*] *B*, **62**, p. 213 (1949).

(8) RAMBERG, E. G. *J. Appl. Phys.*, **13**, p. 582 (1942).

(9) SEELIGER, R. *Optik*, **4**, p. 258 (1948).

(10) RECKNAGEL, A. *Jb. All. Elekt. Ges.*, **7**, p. 15 (1940).

The accuracy of particle size determination by cumulative sedimentation methods

By J. K. DONOGHUE, B.Sc., A.Inst.P., Simon-Carves Ltd., Stockport

[*Paper received* 5 *March*, 1956]

Cumulative methods of particle size analysis are sometimes alleged to be inaccurate because it is necessary to differentiate the sedimentation curve in order to evaluate the size distribution. By considering a hypothetical distribution it has been shown that, provided sufficient points are obtained to enable the sedimentation curve to be plotted accurately, this differentiation does not give rise to errors. Comparative tests with the microscope and sedimentation balance on two samples composed of spherical particles confirm this conclusion.

The sedimentation methods which are used to determine the size distribution in finely-divided materials are of two types. The first type, in which the changes of concentration at a particular level in a settling suspension are measured, is called incremental. Examples are the pipette, diver, hydrometer and photoextinction methods. The second type, called cumulative, involves the measurement of the changes in the overall concentration of the suspension, usually by a sedimentation balance or a manometric method. With the first type the fractional concentration at a chosen depth gives directly the weight fraction of those particles smaller than the size which would just fall from the surface to that depth in a given time from the commencement of settling. In the second type, however, a weight-deposited *versus* time curve is obtained which must be differentiated before the size distribution can be evaluated. This curve is usually known as the sedimentation curve. Heywood,[1] and Jarrett and Heywood,[2] have criticized cumulative methods because of the need for differentiation, on the grounds that sudden but slight discontinuities in the frequency distribution curve cannot be detected. There are, however, certain advantages which make their use worth while provided that doubts concerning their accuracy can be resolved.

ADVANTAGES OF CUMULATIVE METHODS

For satisfactory sedimentation analysis certain criteria must be satisfied: the dimensions of the vessel must be sufficiently large for the wall effect to be negligible; the concentration of the suspension must be very low so that the particles do not interfere one with another whilst settling and so that the tendency for agglomeration is reduced; the measuring device must not affect the settling of the suspension; the rate of fall of the particles should be such that Stokes' law can be applied directly to the evaluation of size.

With the exception of the photoextinction method all incremental methods fail to satisfy one or more of these conditions. With the pipette, diver and hydrometer the settling of the suspension is obviously disturbed and the concentration used (at least 1% by weight) causes interference between particles during settling and may also lead to agglomeration. The pipette method involves evaporation to dryness and therefore necessitates the use of volatile liquids. As these are usually of low viscosity the upper limit of the particle size range of a particular material to which the method can be applied is reduced. Viscous liquids may be used with divers but this necessitates the use of a different set of divers for each different liquid. Although the photoextinction method is not restricted to volatile liquids and may be used with very low concentrations it has one serious disadvantage. The extinction coefficient, by which is understood the ratio of the amount of light cut off by a particle to the amount predicted by geometrical optics, is not independent of particle size and the evaluation of a size distribution from the experimental data is thus somewhat complicated.

Turning to the cumulative methods, the manometric method is suspect partly because it is difficult to measure accurately the small pressures produced by low concentrations and partly because the return of clear liquid from a side arm causes convection in the suspension. The sedimentation balance, however, is free from these defects. Owing to the great sensitivity of the method a very low concentration may be used and, as there is no need to restrict the viscosity of the liquid, a wider range of sizes may be covered. The only factor that could cause interference with the settling is the movement of the balance pan and this can be arranged to be very slight indeed. A further advantage is that it is unnecessary to make an accurate determination of the initial concentration.

For the reasons stated above it was felt that an examination of the sedimentation balance method was desirable. Two aspects are considered: the errors involved in differentiating the sedimentation curve and the performance of the instrument in sizing a sample of known size distribution.

DIFFERENTIATION OF THE SEDIMENTATION CURVE

The fractional weight p, deposited in time t, is composed of two fractions. These are (*a*) the whole of the portion w of the material of size greater than or equal to that size which would just fall the full height of suspension in the time t, and (*b*) a proportion of the material of smaller size. Oden,[3] whose method of evaluation is the most widely used, showed that this latter fraction is equal to $t(dp/dt)$. Thus

$$p = w + t(dp/dt) \qquad (1)$$

The evaluation of values of w is carried out by plotting p against t and drawing tangents to the curve at different values of t. The intercept of the tangent on the p-axis is quite clearly equal to w for that particular value of t.

Nissan[4] pointed out that errors could arise in the plotting of the original curve as well as in the drawing of tangents. In order to determine the magnitude of the errors associated with these processes he took a set of data on the settling of a kaolin clay suspension and evaluated w in three ways. These were, firstly the tangent intercept method, secondly a method which involved plotting the sedimentation curve and calculating w by successive approximations, and thirdly by fitting a polynomial to the original data, a method requiring no drawing whatever. This last method was used as a standard against which to compare the graphical methods

which were shown to be a few per cent in error. As much error was associated with the original plotting of the sedimentation curve as with the tangent drawing.

A simpler approach than this is to take a hypothetical size distribution such as that shown in Fig. 1, and represented as a

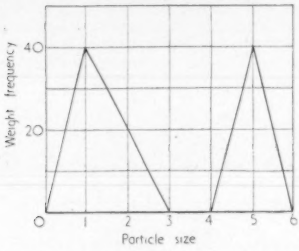

Fig. 1. Hypothetical frequency distribution (arbitrary units)

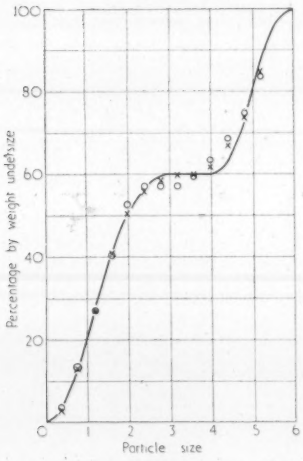

Fig. 2. Cumulative distribution curve (particle size in arbitrary units)

○ = evaluated with times increasing by a factor of 2.
× = evaluated with times increasing by a factor of $\sqrt{2}$.

weight-undersize curve in Fig. 2. Heywood[1] has shown how a sedimentation curve may be derived from such a distribution. This curve, Fig. 3, is that which would be obtained with an ideal instrument and enables a check to be made on the accuracy of graphical differentiation. The analysis may be carried out by the method of tangential intercepts, one tangent being shown as an illustration, but it will be seen that the accuracy with which the tangents can be drawn, particularly at low values of t is not very high. It is preferable to use the method proposed by Gaudin, Schuhmann and Schlechter[5] who pointed out that equation (1) could be rewritten:

$$p = w + dp/d(\log_e t) \qquad (2)$$

If the sedimentation curve is plotted as p *versus* $\log_e t$ differentiation is much easier. Evaluation of w is carried out by plotting values of the differential on the same scale as

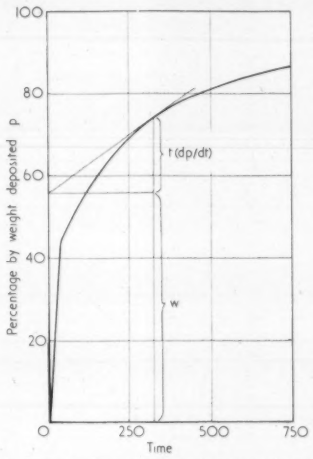

Fig. 3. Percentage by weight deposited *versus* time (arbitrary units)

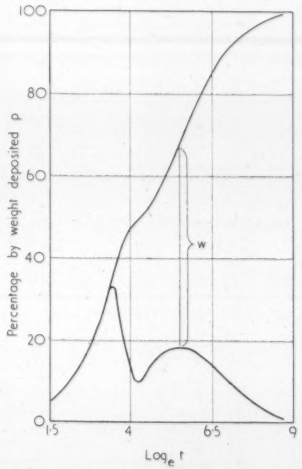

Fig. 4. Percentage by weight deposited *versus* $\log_e t$

the p *versus* $\log_e t$ curve. The value of w for a particular value of t is equal to the difference in the ordinates of the two curves at that time. This method is illustrated in Fig. 4.

In order that the test of accuracy should be a strict one it is desirable that only as many points should be used in plotting the sedimentation curve as would be obtained in a normal experiment. Nissan's data were obtained with times increasing by a factor of 2 whereas the present practice in this laboratory is to use a factor of $\sqrt{2}$. The analysis was, therefore, carried out twice with values of p taken at times corresponding to these factors. The results are compared with the original distribution in Fig. 2. It will be seen that the results for a time factor of 2 are considerably in error, whereas those for the $\sqrt{2}$ factor are quite accurate. If even greater accuracy were desired a time factor of $\sqrt[3]{2}$ could be used.

The accuracy of the method of evaluation having been established it is necessary to show that no errors are introduced by the apparatus used. For these tests an instrument of the type described by Bostock[6] was used.

TESTS ON APPARATUS

In order to test any apparatus it is necessary to have a standard powder whose size distribution is known. Such a standard is difficult to achieve since the only method by which a size distribution may be obtained in absolute terms is by the use of the microscope, and the difficulties associated with microscope counting are well known. In addition, a microscope analysis is only directly comparable with a sedimentation test when the particles are spherical.

In spite of these difficulties it was felt that the only true test of the sedimentation balance was a comparison with a microscope count; a sample of glass spheres was therefore prepared by blowing powdered glass through an oxy-hydrogen flame. To test the ability of the method to distinguish a slight discontinuity in the distribution a fraction of the particles in the middle of the size range was removed by means of a centrifugal air elutriator. This material was used for both microscope and sedimentation tests. The problem of taking the very small sample required for the microscope was solved in the following manner. The bulk sample was reduced by quartering to the quantity (0·5 g) required for the sedimentation test and this material was mixed on a watch-glass with a few drops of ethylene glycol until a thick paste was formed. A small drop of this paste was transferred by means of a glass rod to a microscope slide and carefully rubbed out. The whole of the sample on the slide was counted into various size grades by means of a cross-hatch eyepiece graticule which also permitted the projected area of the occasional non-spherical particle to be estimated.

Sedimentation tests were carried out both in water and in mixtures of ethylene glycol and water. Values of p were determined at frequent intervals of time so that the plotting of the sedimentation curve could be carried out as accurately as possible.

The results of the two methods of analysis are compared in Fig. 5. It will be seen that the agreement is very good over most of the size range and the slight discontinuity has, in fact, been detected. As a further test, and to demonstrate the adaptability of the method, comparative analyses were carried out on a sample of methyl methacrylate spheres of a rather larger size than the glass ones. The results are shown in Fig. 6 and it will again be noticed that the agreement is remarkably good. To keep the falling speed of the particles to an acceptable value the sedimentation test was carried out in a mixture of kerosine and liquid paraffin at a viscosity of 0·047 P determined at 25·4° C.

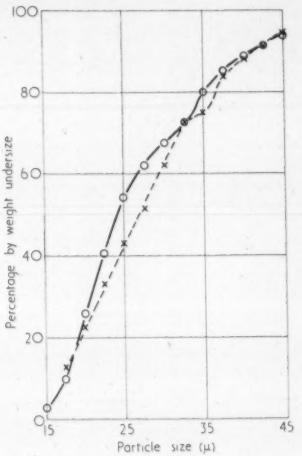

Fig. 5. Size distribution of glass spheres

○ = microscope.
× = sedimentation.

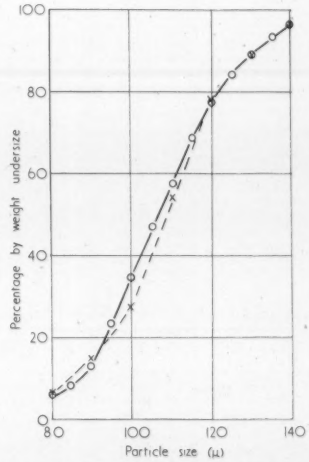

Fig. 6. Size distribution of methacrylate spheres

○ = microscope.
× = sedimentation.

CONCLUSIONS

It has been demonstrated that, provided sufficient experimental points are obtained to enable the sedimentation curve to be plotted accurately, cumulative sedimentation methods are, in fact, sufficiently accurate and in view of their many advantages could profitably be more widely used. It is suggested that for accurate work values of p, the weight fraction deposited, should be determined at times increasing by a factor of not more than $\sqrt{2}$.

ACKNOWLEDGEMENTS

This paper is published by permission of Dr. W. Rheinallt Thomas, Director of Research, and the Management Board, Simon-Carves Ltd. Thanks are due to Mr. W. Bostock for much helpful advice.

REFERENCES

(1) HEYWOOD, H. *Symposium on Recent Developments in Mineral Dressing*, p. 31 (London: Institute of Mining and Metallurgy, 1952).
(2) JARRETT, B. A., and HEYWOOD, H. *Brit. J. Appl. Phys., Suppl. No.* 3, **5**, p. *S* 21 (1954).
(3) ODEN, S. *Proc. Roy. Soc. Edinburgh*, **36**, p. 219 (1915).
(4) NISSAN, A. H. *Disc. Faraday Soc.* (11), p. 15 (1951).
(5) GAUDIN, A. M., SCHUHMANN, R., and SCHLECHTER, A. W. *J. Phys. Chem.*, **46**, p. 903 (1942).
(6) BOSTOCK, W. *J. Sci. Instrum.*, **29**, p. 209 (1952).

Uniform-field breakdown in air

By R. F. SAXE, Ph.D., Queen Mary College, University of London

[*Paper received* 5 *January*, 1956]

Experiments on the breakdown processes in a uniform-field gap at the minimum d.c. breakdown voltage in air at atmospheric pressure are described. It is shown that the breakdown processes consist of two phases, (1) a diffuse glow completely bridging the gap, followed by (2) a filamentary channel moving from the cathode to the anode, and bridging a 0·77 cm gap in about 3×10^{-9} s in a 13 Ω coaxial system. Spectrograms of the stages of the discharge are also given. These experimental results are in disagreement with both the Townsend and the Streamer theories.

The mechanism of the breakdown of a uniform-field gap in air at the minimum breakdown voltage has been the subject of considerable theoretical study, the results of which are summarized in Ref. (1). The two main theories to explain this breakdown are the Townsend theory and the Streamer theory. The detection by Llewellyn Jones and Parker[2] of the effect of a γ mechanism in air (for values of pd in the range $250 < pd < 760$ mm of mercury cm approximately) has given strength to the suggestion that the breakdown is the natural consequence of the build-up current due to the Townsend processes. It is the author's contention, however, that while the Townsend processes are a necessary condition, they are not a sufficient condition to explain the breakdown of such a gap.[3] If the circuit contains a high value of series resistance, then it would appear that a breakdown is not possible on Townsend processes alone. In order that no misunderstanding should arise, the definition of breakdown which will be employed in this paper is "the sudden collapse of voltage on the gap to a small value" since it is this collapse of voltage by which the instant of breakdown is usually detected.[4] The "attainment of the Townsend criterion" will not be considered as a definition of breakdown here as no experimental demonstration of the attainment has, as yet, been provided.

Previous investigations of the final stages of the breakdown of uniform-field, or nearly uniform-field gaps were performed by three methods:

(1) the removal of the voltage before the discharge develops completely across the gap (suppressed discharge);
(2) short-exposure photography; and
(3) cloud-chamber investigations.

With the possible exception of the work by Dunnington[5] and by White,[6] this work suffers from the disadvantage that it was not performed at the minimum breakdown voltage, the breakdown being caused either by the application of a transient overvoltage or by the application of an intense flash of ultra-violet light. The processes so observed may not, therefore, be considered as necessarily characteristic of those which occur in the breakdown of a uniform-field gap at minimum breakdown voltage. The Streamer theory, which is based on these experimental results, may not therefore be considered as necessarily applicable to the breakdown at minimum breakdown voltage.

From the work of Llewellyn Jones and Parker,[2] the average current at any voltage below breakdown may be calculated, while considerable information exists about the main spark channel. However, the transition from the condition of high applied voltage and small current flow to the condition of the low impedance channel joining the electrodes has not been adequately investigated hitherto. This paper is concerned with an experimental investigation of this transition.

EXPERIMENTAL

The use of the image tube to study the movement of the visible manifestations of the breakdown processes has previously been described[7] but will be briefly repeated here for completeness. A coaxial system is formed from two brass cylinders of diameter 7·6 cm and 8·9 cm separated by a polythene tube P of dielectric constant ε. The centre conductor is made in two sections with a spark gap between them as shown in Fig. 1. The discharges in the experiments to be described take place between two nickel-plated, uniform-field electrodes, the plane portion of the electrodes being approximately 1·5 cm diameter. The gap length used is $0{\cdot}7_7$ cm in air at atmospheric pressure ($pd \simeq 585$ mm of mercury cm).

Section A of the coaxial system is charged to a voltage V

through a high (500 MΩ) resistor, R, and when a complete discharge occurs across the gap a voltage transient of amplitude $V/2$ and duration $2T$, where $T (= L\sqrt{\varepsilon}/c)$ is the time of travel of a wave along section A of the coaxial system, is propagated along section B. The end of section B remote from the spark gap is matched by resistors to prevent reflexion of the transient, and the image tube I is connected across the matching resistor z. The outer conductor of the coaxial system is pierced as indicated in Fig. 1 to allow the discharge to be observed, and to allow the gap to be irradiated.

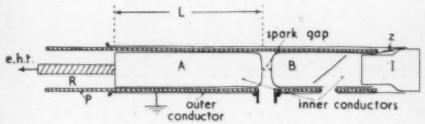

Fig. 1. Spark-gap circuit

For observation of the breakdown processes by the image tube, the charged length of line, A, is such that a wave travels along it in $2{\cdot}75 \times 10^{-9}$ s, so that ideally the image tube is subjected to a transient of duration $5{\cdot}5 \times 10^{-9}$ s. This duration of transient is such that the main spark channel completely bridges the gap on every occasion (see later). The various stages of the breakdown are then observed by delaying the arrival of the optical transient relative to that of the electrical transient, at the image tube, by a known amount, as described in Ref. (7).

The study of the breakdown processes by the method of suppression of the applied voltage is performed using the same coaxial system as that used for the image tube shutter. Variation of the length of the charged section of the line enables the duration of the voltage transient to be varied. If the length of the charged section of the line is reduced sufficiently, the discharge is unable to form a spark channel completely bridging the electrodes (see below) and the resulting "partial" discharge may then be photographed by normal means without the use of a short-exposure shutter. This photography is performed by means of an ordinary camera using a glass, f: 5·6 lens and Ilford Pan F film developed for 12 min in developer type ID11 at 20° C.

It must be emphasized that in both cases, i.e. the observation by the image tube and the observation by suppressed discharge, the breakdown is the breakdown of a uniform field gap at the minimum d.c. breakdown voltage.

The whole coaxial system is enclosed in a glass envelope which is evacuated to 0·02 mm of mercury. Air is then admitted through a liquid air trap to eliminate moisture. The envelope also contains phosphorus pentoxide. The voltage supply is stabilized to better than 0·1% and it is found in practice that the breakdown voltage of the gap for a short sequence is reproducible to about 0·1%. Over a large number of breakdowns a slow conditioning effect is observed.[8]

Some of the photographs reproduced in the paper are out of focus due to the discharge's position occurring at random over the plane surfaces of the electrodes. However, more than one discharge is shown for each condition and in most cases at least one is approximately in focus. Even when badly out of focus, the photograph shows most of the interesting features. The human eye is not unduly troubled by this positional variation and is able to observe readily.

No photographs of the discharge viewed by means of the

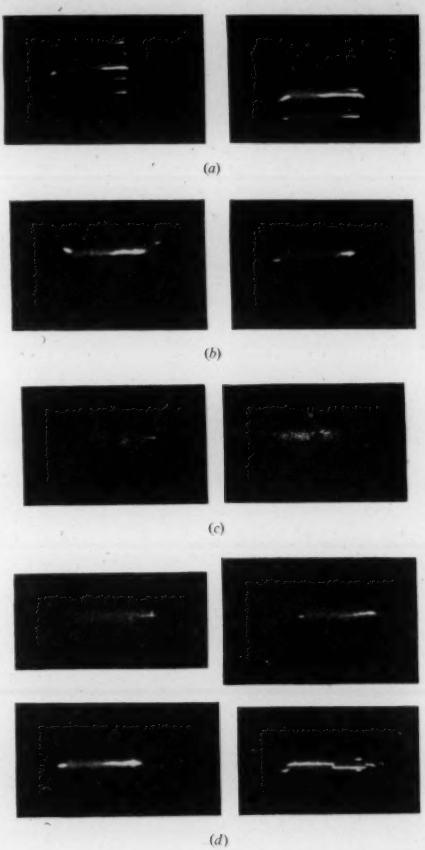

Fig. 2. Photographs obtained by methods of suppressed discharges

(*a*) In each case, more than one discharge is shown due to the rapid recharge of the line. The discharge with the shortest "filamentary channel" is the first discharge. The cathode is to the right. The "length" of the changed section of the line is approximately equivalent to 9×10^{-10} s. The "filamentary channels" appearing on the left of the photographs are due to reflexions from the electrode surfaces, which are vertical.

(*b*) "Length" $= 15 \times 10^{-10}$ s.
The "filamentary channels" appearing on the left of the photographs are due to reflexions from the electrode surface.

(*c*) "Length" $= 21 \times 10^{-10}$ s.
It will be noticed that the right-hand photograph shows two channels developing simultaneously.

(*d*) "Length" $= 37{\cdot}5 \times 10^{-10}$ s.
It will be noticed that more than one channel may be seen in some of the photographs; reflexion from the electrode surfaces may also be seen.

image tube are reproduced as the out-of-focus trouble is aggravated in this case by the need to use wide aperture lenses. As a result, the observation of a large number of discharges is necessary in order to see one in focus. The photography of such a large number of discharges was deemed inexpedient.

Spectra are obtained by using a Hilger quartz spectrograph recording on Ilford long-range spectrum emulsion developed for 10 min in developer type ID33 at 18° C.

RESULTS

Observation of the d.c. breakdown of a uniform-field gap in a 13 Ω coaxial system between nickel electrodes (plane surfaces 1·5 cm diameter, gap length approximately $0{\cdot}7_7$ cm) at minimum breakdown voltage in air at atmospheric pressure by means of the image tube shutter, shows that:

(1) at about 3×10^{-9} s before breakdown is complete, a highly luminous, comparatively filamentary channel commences to form at the cathode;
(2) this channel advances towards the anode at a high velocity (not less than about 2×10^8 cm/s), finally bridging the gap;
(3) when the gap has been completely bridged by the "filamentary channel," the stage known as the spark channel is reached and the complete channel becomes brighter as the current flow is maintained;
(4) prior to the commencement of the growth of the channel from the cathode, a diffuse glow of relatively low intensity is observed. The glow may be observed at least 2×10^{-9} s before the channel from the cathode commences;
(5) the diffuse glow appears to increase in brilliance as the filamentary discharge grows.

These stages of the discharge may also be observed by the method of suppressed discharges described above. Representative photographs obtained in this way are shown in Figs. 2(*a–d*). It will be seen that these photographs bear out the evidence obtained by the use of the image tube shutter,

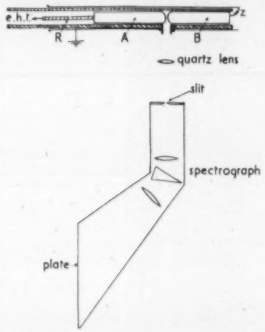

Fig. 3. Method for obtaining spectra of the discharge

and that they are complicated by optical reflexions from the electrode surfaces.

It will be noticed that each "breakdown" in Fig. 2(*a*) consists of more than one discharge path. This is due to the formation of more than one discharge before the voltage may be reduced. In the first discharge, the "filamentary channel"

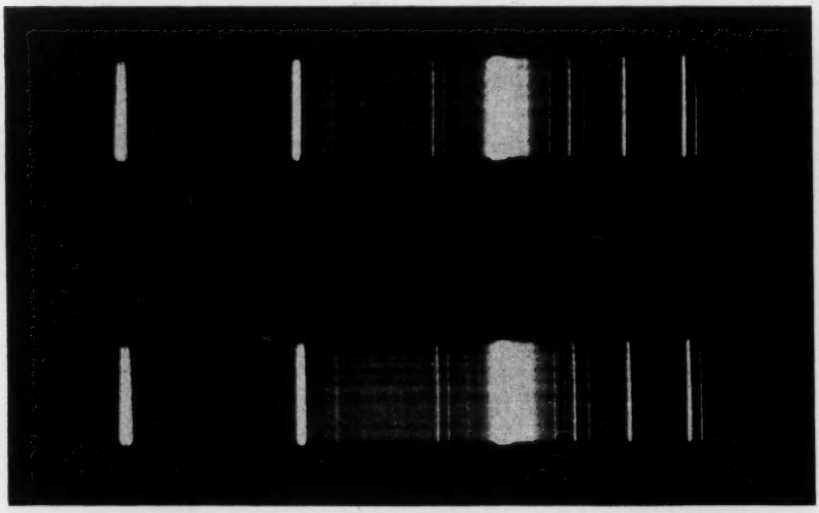

Fig. 4. Spectrum of the "glow" near anode in 13 Ω system. (Mercury comparison spectrum)

is short; in subsequent discharges it is longer, due presumably to the subsequent discharges being affected by the products of the first discharge. It will also be noticed that the length of the filamentary channel exhibits a considerable variation in each of Figs. 2(*a–d*). In Fig. 5, this variation causes the gap to be completely bridged in some instances by the "filamentary channel."

The use of a lens of wider aperture and the use of a faster emulsion shows that the glow is more extensive than is shown in Figs. 2(*a–d*), where the aperture and emulsion are chosen to show both stages at once. The sequence shown in Figs. 2(*a–d*) is not influenced by the presence or absence of ultra-violet irradiation. In the presence of irradiation the time between successive discharges is more uniform than in the absence of irradiation.

The spectra of the various stages of the breakdown process are obtained by imaging the required portion of the gap on to the slit of the spectrograph by means of a quartz lens. The

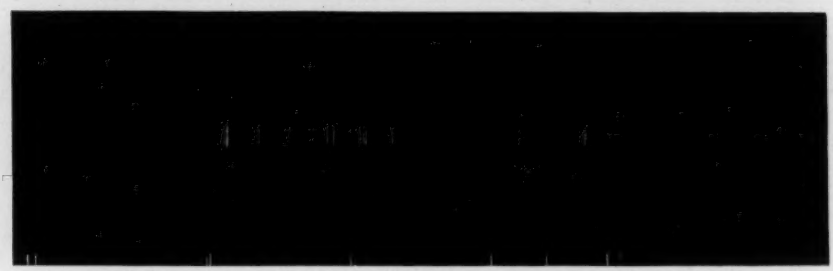

Fig. 5. Spectrum of the "filamentary channel" when part-way across the gap from the cathode in a 13 Ω system. (Mercury comparison spectrum)

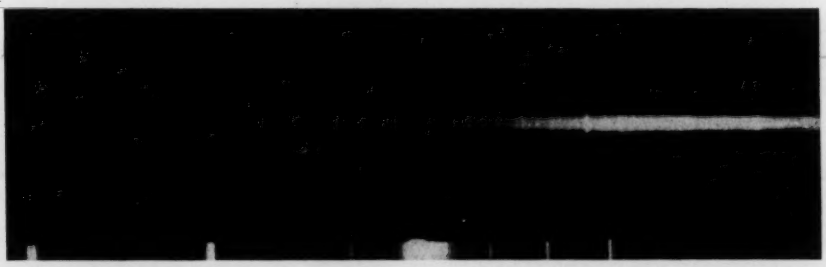

Fig. 6. Spectrum of the discharge when the gap is completely bridged by the "filamentary channel" and current has flowed for a further 2×10^{-9} s approximately in a 13 Ω system. (Mercury comparison spectrum)

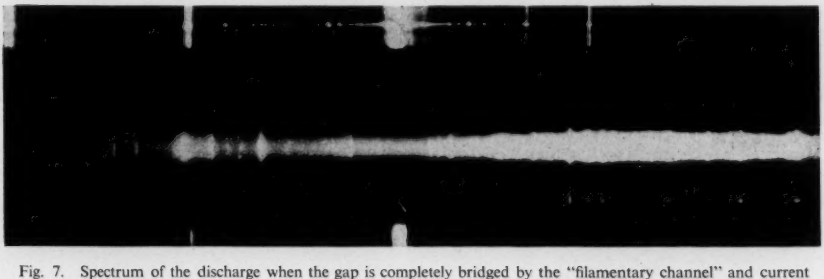

Fig. 7. Spectrum of the discharge when the gap is completely bridged by the "filamentary channel" and current has flowed for a further 150×10^{-9} s approximately in a 70 Ω system. (Mercury comparison spectrum)

slit of the spectrograph is arranged to be parallel to the electrodes as shown in Fig. 3. The spectra of:

(1) the glow (approximately one quarter of the gap length from the anode),

(2) the luminous filamentary channel when partway across the gap from the cathode, and

(3) the channel which has bridged the gap completely and in which current has flowed for a further 2×10^{-9} s approximately,

are shown in Figs. 4–6, all discharges being in a 13 Ω system.

The spectrum of the discharge in a 70 Ω system in which current has flowed for approximately 150×10^{-9} s after the gap has been completely bridged is shown in Fig. 7. Figs. 4–7 are the result of approximately 7000, 2000, 1200 and 800 discharges respectively.

It will be seen that the spectrum of Fig. 4 shows only the second positive bands of nitrogen, while Figs. 5–7 show in addition many other lines and a continuum.

DISCUSSION

The experimental results described above show that the breakdown process consists of at least two phases. Firstly, a diffuse glow is observed stretching across the whole gap and then a filamentary channel grows within this glow from the cathode towards the anode, finally bridging the whole gap and then growing in brilliance as current continues to flow in it.

Neither of the two theories at present extant, the Townsend theory and the Streamer theory, may be seriously considered to be applicable here since the former is incapable of explaining the breakdown of a gap in a circuit containing a high impedance (500 MΩ charging resistor) and the latter is based on experimental evidence obtained under different experimental conditions from those to which this paper refers. Further, the former theory in no way attempts to explain the manner in which a filamentary spark channel is formed from processes which can be shown to result in a diffuse discharge.[3]

The experimental results outlined in the previous section seem at first glance to suggest that a "streamer" grows from cathode to anode to complete the breakdown. However, a more careful analysis suggests that the definition and characteristics of the "streamer" need to be stated before the method of breakdown of a uniform-field gap in terms of a "streamer" may be given.

The spectroscopic evidence quoted above shows that the light from the diffuse blue glow which precedes the filamentary channel consists of the second positive bands of nitrogen. The excitation function for these bands has been investigated by Langstroth,[9] who showed that the bands are emitted by molecules bombarded by electrons of energy 13 eV or more. The velocity of an electron of energy of 13 eV is approximately 2×10^8 cm/s and such an electron could cross a $0{\cdot}7_7$ cm gap in approximately 3×10^{-9} s if unimpeded.

The spectrum of the light from the more filamentary second stage of the discharge is more complex, showing many lines, in addition to the second positive system of nitrogen, and also a continuum. The spectrum of the light emitted from a discharge in which current has passed for some time after the gap has been completely bridged is similar to that of the second stage of the discharge, apart from being more intense.

There is, therefore, no evidence to suggest that there is any basic difference between the second stage of the discharge and the spark channel.

Further, it is of interest to note that:

(1) the measured velocity of the second stage of the discharge is no greater than, and is in the same direction as the apparent velocity of the electrons in the first stage of the discharge;

and

(2) the observed behaviour of the breakdown processes are similar to those reported by White[6] for hydrogen and nitrogen for gaps of less than $0{\cdot}3_5$ cm.

It is, therefore, suggested that while the avalanche-streamer-spark channel sequence may hold for a gap subjected to a large overvoltage, the evidence presented above shows that a different sequence obtains at minimum breakdown voltage. There is no evidence at present to suggest a differentiation between the "filamentary channel" and the spark channel.

The velocity of the electrons in the first (diffuse) stage of the discharge (2×10^8 cm/s) is considerably greater than the velocity which has been assumed hitherto ($1{\cdot}3 \times 10^7$ cm/s). This discrepancy suggests that mobility theory is not applicable to these conditions, and it also tends to affect the calculations of formative time lag.[3,4,10]

Observation of the breakdown processes in a 70 Ω coaxial system suggests that the velocity of propagation of the "filamentary channel" is dependent on the impedance of the associated circuit. Previous theoretical work on the breakdown process has tended to ignore the possible effect of the external circuit on the rate of growth of current in the gap. Since earlier experimental work has been done using ordinary circuits containing considerable inductance, the effect of the circuit may have been dominant.

ACKNOWLEDGEMENTS

This work was commenced during the author's tenure of an I.C.I. Research Fellowship, which is gratefully acknowledged, and was made possible by a grant from the University of London Central Research Fund which is also gratefully acknowledged.

The author also wishes to thank Prof. W. J. John, in whose laboratories this work was performed, and the Mullard Valve Co. for the generous facilities provided.

REFERENCES

(1) Meek, J. M., and Craggs, J. D. *Electrical Breakdown of Gases* (London: Oxford University Press, 1953).
(2) Llewellyn Jones, F., and Parker, A. B. *Proc. Roy. Soc., A*, **213**, p. 185 (1952).
(3) Saxe, R. F. *Nature [London]*, **175**, p. 82 (1955).
(4) See, for example, Fisher, L. H., and Bederson, B. *Phys. Rev.*, **81**, p. 109 (1951).
(5) Dunnington, F. G. *Phys. Rev.*, **38**, p. 1535 (1931).
(6) White, H. J. *Phys. Rev.*, **46**, p. 99 (1934).
(7) Saxe, R. F., and Chippendale, R. A. *Brit. J. Appl. Phys.*, **6**, p. 336 (1955).
(8) Saxe, R. F., and Lewis, T. J. *Brit. J. Appl. Phys.*, **6**, p. 211 (1955).
(9) Langstroth, G. O. *Proc. Roy. Soc., A*, **146**, p. 166 (1934).
(10) Dutton, J., Haydon, S. C., and Llewellyn Jones, F. *Brit. J. Appl. Phys.*, **4**, p. 170 (1953).

New books

Progress in nuclear energy: Series 1. Physics and mathematics. Vol. 1. Edited by R. A. CHARPIE, D. J. HUGHES, D. J. LITTLER and S. HOROWITZ. (London: Pergamon Press Ltd., 1956.) Pp. x + 398. Price 84*s*.

Eight series of volumes are to be published under the title "Progress in nuclear energy" and are intended to co-ordinate and to review the enormous amount of detailed information on fission and neutron physics presented at the 1955 Geneva Conference on Peaceful Uses of Atomic Energy. This volume is the first of Series 1. It well reflects the outstanding theme of that conference, namely the truly international character of scientific progress as a whole and of the development of nuclear energy in particular. Most of the results discussed in this volume were made public for the first time at Geneva and the average physicist can hardly fail to be impressed by the accounts given of the many beautiful experiments made by groups of workers to whom no facility was denied.

The articles differ in readability: the first two (by J. A. Harvey and J. E. Sanders and by P. A. Egelstaff and D. J. Hughes) present very clearly the properties of fissionable nuclei and in the following chapter H. A. Bethe briefly discusses these results in the light of statistical nuclear theory. L. Cranberg and others contribute an excellent article on the techniques and results of neutron cross-section and energy measurements. This is followed by detailed accounts of the interaction of neutrons with ^{135}Xe (S. Bernstein and E. C. Smith) and with a large number of other elements (R. L. Macklin and H. S. Pomerance). The interesting and highly important phenomenon of delayed neutron emission in fission is reviewed by G. R. Keepin. The remaining articles are rather severely technical; they describe calculations and experiments on a number of critical assemblies, including fast reactors, and will be chiefly of interest to the specialist reader. The agreement between theory and experiment is generally impressive. The volume has been rapidly but carefully produced and will be valued by many as part of the record of a remarkable human achievement. W. E. BURCHAM

Meteorological results of the *Balaena* expedition, 1946–47. (Geophysical Memoirs No. 94.) By H. H. LAMB. (London: H.M. Stationery Office, 1956.) Price 8*s*. 6*d*.

Mr. Lamb was appointed to give meteorological advice to the floating factory *Balaena* on her Antarctic whale-hunting cruise in 1946–47. The *Balaena* carried two amphibian aircraft for whale-spotting and ice reconnaissance and it was for these operations particularly that the meteorologist was needed. Operating mainly in the Indian Ocean sector of the Antarctic between about 60° S and 65° S, Mr. Lamb prepared daily synoptic charts for the southern ocean using observations from distant ships and those made from the *Balaena* and its associated whale-catchers. Pilot balloon ascents and aircraft soundings of temperature were made from the *Balaena*.

The memoir describes the nature of the weather systems of the southern ocean and makes the point that the Antarctic continent is not the seat of a semi-permanent cold anticyclone as has sometimes been inferred in the past. Appendices provide the surface weather observations (one entry: "mirage rendered moonrise unrecognisable"), observations of ocean waves, pilot balloon winds and aircraft soundings.

P. A. SHEPPARD

Symposium on non-destructive testing of materials and structures. Vols. 1 and 2. (Paris: Rilem, 12 Rue Brancion, Paris 15.) Vol. 1. Pp. 208; Vol. 2. Pp. 191. Price 2200*f*.

These volumes, available in either English or French, form a comprehensive report on the research currently being conducted to establish non-destructive testing methods for concrete, and one or two papers deal with similar methods for testing stones and soils. The first 300 pages are devoted to the sonic methods, namely longitudinal or transverse vibration of specimens and stress wave velocity measurement by pulse techniques. Surface hardness methods by the ball test and sclerometer techniques, and the uses of radioactive isotopes are discussed in the remaining 100 pages. The papers presented come from laboratories in Japan, U.S.A., South America and South Africa as well as from those in most European countries. The English of many papers is faulty and this occasionally makes the meaning obscure. The reviewer feels, however, that English readers are fortunate to have so many informative papers collected in two volumes.

Less excusable than faulty English is the number of misprints which occur, particularly in the mathematical formulae of theoretical papers. These are usually obvious enough but this is of no help in the instance where an entire figure is missing (page 290), the space being followed by a discussion commencing, "Unfortunately, the table is not very clear . . ."

Introductions are provided to the three sections of the report. That to Section A on sonic methods contains a tabulated summary, which is useful in view of the mass of information presented on the relationships between the compressive, flexural or rupture strengths of specimens, and the dynamic moduli or wave velocities, under a great diversity of conditions. The effects of different cements, aggregates, constituent ratios, moisture contents, curing conditions and ages of concretes are all dealt with while cyclic loading or freezing and thawing, corrosion and fire damage are also investigated by some authors. Some theoretical explanations are attempted and very many empirical relationships are given.

Many of the papers on the pulse technique are devoted to the testing of specimens, as opposed to that of placed concrete. From this it is evident that the pulse techniques cannot yet be employed for completely non-destructive testing, and they are in such an active state of development at present that it has been impossible for anyone to come to decisive conclusions. However, paper A17 by Mr. R. Jones gives an excellent all-round picture of pulse techniques as applied to concrete testing. The fundamental difficulties associated with vibration testing are well described in two papers, A3 and A4, which point to the need for some international agreement on specimen dimensions and apparatus.

Section B on the ball test and sclerometer comprises nine very lucid papers which suggest that these methods have great promise. Most of Section C lies in one comprehensive paper by Mr. J. P. Fackler, which succeeds in adapting the theories of nuclear physics for practical testing applications. The uses of γ-rays from isotope sources, for measurements of density and moisture content, are discussed.

An introduction to the complete report is given by M. L'Hermite, who makes some penetrating remarks on the

sonic methods. It might have been emphasized, however, that these methods are not yet fully developed to the status of non-destructive tests and that auxiliary determinations of density or Poisson's ratio are sometimes necessary.

Although the editors have arranged the papers in such a way as to provide some introduction to each method for the uninitiated, these volumes will be of use mainly to the person engaged in research in this field. As M. L'Hermite says, "He will find in them matter for reflection and, it is hoped, the source of new research . . ." W. R. BUCHAN

The theory of games and linear programming. By S. VAJDA. (London: Methuen and Co. Ltd., 1956.) Pp. 106. Price 8*s*. 6*d*.

The player of games, the general planning a military strategy, and the industrialist trying to make the most economical use of his employees are all grappling with the one problem which forms the subject of this book. Mathematically it is the problem of finding a solution of some linear algebraic equations for which a given linear combination of the variables takes either a maximum or a minimum value. The author uses graphical methods to help the reader understand the basic concepts of linear programming, of which the theory of games forms a special case. The subject is then developed algebraically from first principles, and quite recent developments are included. Many examples are worked in detail. In all, this comprehensive though necessarily condensed account provides a welcome introduction to a new subject, which has practical applications in widely differing fields.

J. CRANK

Resonance in organic chemistry. By G. W. WHELAND. (New York: J. Wiley and Sons, Inc.; London: Chapman and Hall Ltd., 1955.) Pp. xiii + 846. Price 120*s*.

This book, which is a greatly enlarged successor to Professor Wheland's *Theory of resonance* published in 1944, is addressed primarily to chemists, and probably more than half of it is of little concern to others. Nevertheless physicists may well be interested in the pedagogic methods used to present an essentially mathematical subject to an audience which cannot be presumed to have extensive mathematical equipment, and they can hardly fail to be impressed by the record of great advances which have been made by the application of the concept of resonance guided by chemical intuition, in many cases to systems far beyond the reach of precise calculation.

The word resonance is derived from the analogy between a system of coupled mechanical oscillators and a system of electrons and nuclei, and in its most fundamental form the concept of resonance lies at the root of wave-mechanical ideas about valency, so that it is of the utmost importance that chemists should understand it fully. Professor Wheland has clearly given much thought to the presentation of these fundamental ideas, and has dealt fully with a number of points which every teacher will recognize as stumbling blocks for beginners, but which are not often adequately treated in textbooks. In contrast to physical resonance for example, resonance in chemistry (as I have recently had to write in red letters on more than one essay) is *not* a phenomenon, and the "resonance frequency" cannot be measured experimentally. Professor Wheland rightly insists on these points from the outset and by his insistence should help many students to greater clarity of thought about the fundamentals of quantum chemistry.

In the more restricted sense the term resonance is used to account for the electronic distributions in those numerous molecules which cannot satisfactorily be described by any one classical formula but must be regarded as being in some way hybrids of two or more (non-existent) classical structures. The bulk of Professor Wheland's book is devoted to the development, in masterly fashion, of the idea of resonance in this restricted sense and its application to organic chemistry. The table of bond lengths, which was a valuable feature of the first edition, has been expanded to a hundred pages and there is a new 150-page chapter on the mathematical basis of resonance. Although, as Professor Wheland says, this last chapter is written "as simply as possible and without any attempt to achieve rigor" [*sic*], it is to be feared that it will give many students of chemistry cold feet. E. G. Cox

Les aérosols. By A. P. AVY. (Paris: Dunod, 1956.) Pp. x + 292. Price 2700 *f*.

This book is divided into two sections; rather more than half describes the general properties of particles, with the rest devoted to practical problems which involve aerosols. The first section is broken down into two chapters dealing respectively with the behaviour of individual particles and the physics of clouds of particles. The last section treats industrial hygiene, filtration and military aerosols in separate chapters and ends with a general chapter about meteorology, therapeutic aerosols, disinfection, insecticides, dust explosions and unsolved problems.

It will be apparent from this wide range of coverage that little detail can be given about any one subject. This, the paucity of references, and the absence of a classified bibliography and index reduce the value of the book to the reader who is given no aid if he wishes to study some matter in greater detail. This is rather a pity because the very brief surveys given build up an interesting picture of the science of aerosols, especially in the first section. The information given is, however, so very meagre, besides being at times out of date or misleading, as in the cases of rate of fall and light scattering, that one wishes that rather less had been attempted with rather more attention given to the results of modern critical reviews and research.

The book is well illustrated and a number of points with which the author has presumably been particularly concerned are of interest to the more knowledgeable reader who will skim rapidly through the bulk of the text. C. N. DAVIES

Nuclear and radiochemistry. By G. FRIEDLANDER and J. KENNEDY. (New York: John Wiley and Sons, Inc.; London: Chapman and Hall Ltd., 1956.) Pp. ix + 467. Price 60*s*.

This book is "written from the chemist's viewpoint," and the active nuclear physicist is hardly likely to find much of importance to him in it. To many others, however, who try to maintain a broad understanding of the subject, this book may well prove stimulating and attractive. Some chapters, mainly those concerned with radiochemical techniques, are just detailed enough to whet the appetite for the other man's speciality, and ordinary physicists will surely leave the chapter on statistical considerations in counting experiments until they have immediate occasion to use it. But when this is said there remains much straightforward nuclear physics of the kind that can be developed with little mathematics, and most of this extremely well presented. The discussion on an early page of the importance to the initial studies of the natural radioactive series of the gaseous emanations is typical of the clarity and economy with which historical matter is presented.

For the general reader the final chapter, into which are

compressed thermonuclear processes in astrophysics (nevertheless including the He → Be → C synthesis in very hot stars) cosmic rays, unstable nuclear particles, cosmochronology and the genesis of the elements, will be far too short.

There is, chapter by chapter, an excellent reading reference list together with abundant numerical exercises for the serious minded. This is a conspicuously interesting book.

J. G. WILSON

Atomkraft. By Dr.-Ing. Dr.-Ing.E.h. F. MÜNZINGER. (Berlin: Springer-Verlag, 1955.) Pp. vi + 94. Price DM. 10.50.

This book is written for power station designers and engineers as an introduction to reactor technology. The detailed discussion of types of reactors forms a large section of the book but unfortunately as a result of the Geneva conference, which took place while the book was in the press, this material is now largely out of date.

The author deals at length with steam turbines and other ancillary equipment with which a potential reader should be familiar, while the introduction to reactor principles is quite inadequate. The reader can derive from this section no concept of criticality or of the role of neutron leakage in reactor design, and no mention is made of the four-factor formula. Little has been written on reactor control and reactor kinetics and this leads on p. 20 to the misleading use of the words "fast" and "slow" for "prompt" and "delayed." The book also contains some errors; for example on p. 11 the dimensions of the BEPO fuel elements are incorrect.

The reviewer can envisage no class of reader for whom the book would be satisfactory. For English-speaking readers more adequate material is available while for German readers seeking an introduction to the field the book is entirely lacking in the necessary background of reactor physics which would make the later considerations intelligible. K. C. HINES

International electrotechnical vocabulary. (Electronics.) 2nd Ed. (London: British Standards Institution, 1956.) Pp. ix + 157. Price 24*s*.

This important work should be readily available to all those who use electronics which is here defined as "that branch of science and technology which deals with the study of the phenomena of conduction of electricity in a vacuum, in a gas, and in semi-conductors, and with the utilisation of devices based on these phenomena." The international electrotechnical vocabulary (2nd edition) has 22 groups to be published in separate parts of which this is the second. The definitions are given in French and English and the terms are also translated into German, Spanish, Italian, Dutch, Polish and Swedish and for ready reference might usefully be printed on different coloured papers. The indexes are in these eight languages. The first draft of this vocabulary was considered in 1951 at an international meeting and many comments and amendments have since been received; some of these have been incorporated, but in such a difficult task it is almost impossible to satisfy all interests. "The present edition," says the preface, "can only be regarded as forming a basis for more mature consideration of its contents, after publication, by the National Committees which are invited to propose additional terms, with their definitions. Although the co-operation of experts, selected for their specialist knowledge, has been enlisted as far as possible in the preparation of this edition, it would be advisable that it be examined in its present state by scientists and, particularly, by senior members of the teaching profession."

Again quoting the preface, "The definitions have been drawn up with the object of striking a correct balance between absolute precision and simplicity. The principal object of the vocabulary is to provide definitions which are sufficiently clear so that each term can be understood with the same meaning by all electrical engineers and it does not, therefore, constitute a treatise on electrical engineering. Thus it may sometimes be felt that the definitions are not sufficiently precise, do not include all cases, do not take account of certain exceptions or are not identical with those which may be found in other publications designed with other objects and for other readers. Such imperfections, which will be eliminated as far as possible in later editions, are inevitable and must be accepted in the interest of simplicity and clarity."

A few test terms were all readily found in the vocabulary and the committees and individuals concerned who prepared this work are to be congratulated on their achievement and will, I hope, be encouraged to continue what must be a rather troublesome and time consuming task.

H. R. LANG

Molecular vibrations. By E. B. WILSON, Jr., J. C. DECIUS, and P. C. CROSS (London: McGraw-Hill Book Co. Ltd.). Pp. xi + 388. Price 64*s*.

In a sub-title the book is called "The theory of infra-red and Raman vibrational spectra." It is strictly theoretical. Actual molecules of specific substances are only referred to in the text when they serve as examples of the methods of calculation described. The treatment of specific molecules is dealt with by Herzberg in *Infra-red and Raman spectra of polyatomic molecules* (New York: D. van Nostrand Co. Inc., 1945) and, fortunately, the authors of the present book have followed the conventions used by Herzberg. The reader does not need to have a considerable mathematical background to begin this book, for he is led through the mathematics required as the theories are consistently developed. The mathematical treatments are, in addition, conveniently summarized and extended in twenty-six appendices. For a first reading, or for those whose interest is mainly in the qualitative assignment of frequencies by the application of symmetry conditions, the text is clearly annotated so that large sections may be omitted.

An introductory portion describes the problem and defines terms used, giving elementary explanations of the main phenomena in classical, quantum and wave-mechanical language. This leads to the statement of internal co-ordinates, the setting up of the secular equation and the determination of normal co-ordinates. Symmetry considerations are then introduced, and sufficient description is given of group theory to be able to understand its importance in this connexion, and further to be able to apply it to molecular vibration problems generally. Various potential functions are treated, and matrix theory is explained sufficiently to use it.

The benzene molecule is taken in a special chapter, as an example of vibrational analysis, and various points covered in the book are brought out. It is curious that, in considering this subject, no reference is given to the very important and exhaustive paper by Ingold and others in the *Journal of the Chemical Society*, p. 222 (1946), especially as references later in time than this are given.

The book is written by acknowledged experts in the field, yet in an understandable way, and cannot be too warmly recommended to those who handle infra-red and Raman spectra and feel in need of a consistent text which describes the theory. A. C. MENZIES

Notes and comments

Elections to The Institute of Physics

The following elections have been made by the Board of The Institute of Physics.

Fellows: C. Davies, W. S. Elliott, G. De V. Gipps, H. G. Jerrard, J. M. Valentine.

Associates: K. J. Bobin, P. F. Burden, J. A. Brand, K. G. Carr, W. E. Carr, J. P. Carter, J. G. Clouston, M. V. Cowin, J. F. Croft, P. B. Curtis, G. E. Darwin, P. U. A. Grossman, E. R. Harrison, H. D. Harwood, D. Hughes, I. MacPherson, M. McChesney, J. D. McKee, I. L. Muter, N. Ochert, A. C. Pawson, J. V. Ramsay, G. H. Rees, J. R. Rowbotham, R. F. Saxe, A. M. Short, J. J. Singh, J. G. Speight, L. K. Street, T. N. Swindon, I. M. Templeton, D. A. Tidman, M. W. J. Tulett, A. H. Ward.

Twenty-six Graduates, six Students and two Subscribers were also elected.

British Chemical Engineering

A monthly journal under the Editorship of Mr. W. E. Dick and devoted to the techniques of chemical engineering applied to industry has been added to the technical journals owned and produced by Heywood and Co. Ltd. The first issue consists of sixty pages of text measuring $10\frac{1}{2} \times 8\frac{1}{4}$ in. Besides a leader, there are eleven articles and various trade items, including book reviews. Mr. Barker's article on the potentialities of viscosity control for industrial processes is the one most likely to interest readers of this journal. The new periodical is nicely produced, although we do not see that anything is gained by using a coloured background for some figures.

The annual subscriptions to the new periodical (£1 10*s.* 0*d.* including postage) should be sent to any newsagent or direct to the publishers at Drury House, Russell Street, Drury Lane, London, W.C.2.

Proceedings of the ninth international congress of refrigeration

The proceedings have now been published of the ninth international congress of refrigeration which was held in Paris in September 1955. The 215 papers are contained in two volumes and also split into seven separate books each containing the papers of one or more commissions.

The papers of Commissions 1 and 2 are issued together in one of the volumes. The papers presented to Commission 1 covered scientific and technological problems concerning very low temperatures and included the following: the heat transfer coefficient to boiling oxygen; a helium–hydrogen liquefier; production of pure nitrogen; the temperature scale below 20° K. Commission 2 embraced papers on heat and mass transfer in an air cooler under frosting conditions; measurement of the thermal conductivity of heat insulators at low temperatures; the temperature reverse phenomenon in a vortex tube; properties and charts of moist air.

Both volumes are obtainable from the Comité Du IXth Congress International Du Froid, 177 Boulevard Malesherbes, Paris 17e. The price of the volume containing the papers of Commissions 1 and 2 is 2500 francs; both volumes containing papers of the nine commissions can be obtained for 10 000 francs.

Quality Control and Applied Statistics Abstracts

The publication has been commenced of monthly loose-leaf abstracts covering the international literature on quality control, operations research and industrial applications of statistical methods of all kinds. The Editors of this abstract service are Dr. Robert S. Titchen, Division of Defense Laboratories, M.I.T. (Navy Department, Washington, D.C.); Mr. Arnold J. Rosenthal, Celanese Corporation, Summit, N.J.; Mr. Bruce Bollerman, Electronic Tube Coil Company, Orange, N.J., and Mr. Frank Nistico, General Electric Company, Cincinnati, Ohio.

The subscription to *Quality Control and Applied Statistics Abstracts* is $60.00 per volume and one annual volume will consist of about 1000 pages in twelve issues. Further details may be obtained from Interscience Publishers, Inc., 250 Fifth Avenue, New York 1, N.Y., U.S.A.

Journal of Scientific Instruments

Contents of the September issue

ORIGINAL CONTRIBUTIONS

Papers

A portable temperature-chlorinity bridge for estuarine investigations and sea water analysis. By B. V. Hamon.

The measurement of film thickness with a pneumatic hypodermic needle mechanism. By N. Stolow.

A semi-conducting antimony bolometer. By E. J. Gillham.

A photoelectric microscope for the measurement of linear scales. By J. S. Clark and A. H. Cook.

On preparing plastic copies of diffraction gratings—an extension to the Merton–N.P.L. process.

A microwave thermistor calorimeter. By M. J. Smith and J. R. M. Vaughan.

An instrument for measuring absorptivities for solar radiation. By H. Tabor and I. T. Steinberger.

Laboratory and workshop notes

A d.c. arc chamber for radioactive materials. By F. T. Birks and R. P. Thorne.

A gas introductor for a vacuum system. By H. A. Wyllie.

A method for comparing ultrasonic velocities in solids and liquids using a spectrometer. By G. M. Sreekantath and A. O. Mathai.

A modified flap-type vacuum valve. By H. M. Buck.

Adhesives for galvanometer mirrors. By N. W. Sullivan.

A microwave amplitude stabilizer. By S. J. Fray and M. F. Kimmitt.

NOTES AND NEWS

Correspondence

A simple bridge circuit for the accurate measurement of pulse impedance. From J. B. Gunn.

Temperature controller for an electric furnace. From R. W. Christy.

New instruments, materials and tools

Notes and comments

THIS JOURNAL is produced monthly by The Institute of Physics, in London. It deals with all branches of applied physics (including theory and technique).

All rights reserved. Responsibility for the statements contained herein attaches only to the writers.

EDITORIAL MATTER. Communications concerning editorial matter should be addressed to the Editor, The Institute of Physics, 47 Belgrave Square, London, S.W.1. (*Telephone:* Sloane 9806.) Prospective authors are invited to prepare their scripts in accordance with the *Notes on the preparation of contributions.* (Price 2*s.* 6*d.* including postage.)

REPRODUCTION. The Institute of Physics is a signatory to The Royal Society's Fair Copying Declaration. Details may be obtained upon application from The Royal Society, London, W.1.

ADVERTISEMENTS. Communications concerning advertisements should be addressed to the agents, Messrs. Walter Judd Ltd., 47 Gresham Street, London, E.C.2. (*Telephone:* Monarch 7644.)

CLAIMS FOR MISSING JOURNALS. Claims from regular subscribers to this *Journal* for missing numbers will only be considered if received within 60 days of the date of mailing plus normal outward time of transit and time for lodging the claim. Losses attributable to failure to notify a change of address or to similar omissions will not be considered.

SUBSCRIPTION RATES. A new volume commences each January. The charge is £4 per volume ($11 50 U.S.A.), including index (post paid), payable in advance. Single parts, so far as available, may be purchased at 8*s.* each ($1.15 U.S.A.), post paid, cash with order. Orders should be sent to The Institute of Physics, 47 Belgrave Square, London, S.W.1, or to any bookseller.

Reactions occurring during decomposition of alkaline earth carbonates on tungsten

By M. A. CAYLESS, B.Sc., A.R.C.S., A.Inst.P., and B. N. WATTS, B.Sc., A.Inst.P.,
The British Thomson-Houston Co. Ltd., Rugby

[*Paper received* 21 *March*, 1956]

Analysis of the gases evolved during decomposition of alkaline earth carbonates on tungsten coiled cathodes shows that carbon dioxide, carbon monoxide and hydrogen are the principal gases evolved. The ratio of carbon dioxide to carbon monoxide is found to be markedly dependent on the decomposition schedule, varying widely with temperature and speed of exhaust. It is shown that the carbon monoxide is produced during the formation of a basic tungstate interface of the type $(Ba, Sr, Ca)_3 WO_6$. The chemical reactions involved are discussed and it is shown that none of these reach equilibrium during normal decomposition schedules. The rate of formation of free barium in the completed cathode is determined by the amount of interface produced during breakdown.

This investigation was an attempt to elucidate some of the reactions occurring during the breakdown and activation of an oxide cathode on a tungsten substrate. Such cathodes are usually formed by coating a tungsten wire or spiral with a mixture of alkaline earth carbonates. These are subsequently converted to oxides by heat treatment after assembly and exhaust of the valve or lamp.

During this process a variety of reactions can occur between the carbonates, the tungsten and the evolved gases. One result of these reactions is the formation of a basic tungstate interface on the surface of the tungsten. It is only recently that interest has been shown in these reactions and even then of very limited extent. Rooksby and Steward[1] have identified various interface compounds which are formed on heating alkaline earth carbonates with tungsten in a vacuum, whilst Hughes, Coppola and Evans[2] have investigated the reactions of barium oxide and carbonate with tungsten.

In the present investigation, analyses of the gases evolved during the breakdown and activation processes have been carried out. These results have been used to study the reactions occurring and how they may be modified by changes in the processing schedules.

EXPERIMENTAL

The cathodes used were coiled-coil filaments of 0·003 in. tungsten wire. The coating was a mixture of barium, strontium and calcium carbonates in the proportions by weight of 5 : 3 : 2. These powders were made into a suspension using nitrocellulose in amyl acetate adjusted to a suitable viscosity.

The coating was applied by dipping the coils into the suspension so that the primary coil was filled, but not the secondary. The cathodes were then mounted on nickel supports in 10 × 3·5 cm diameter hard glass bulbs and sealed to the exhaust system, usually by a short exhaust stem of 3·5 mm bore. The test bulbs were then exhausted and baked at 500° C for thirty minutes. The breakdown of the carbonates was carried out by passing heating currents through the tungsten coils, the gases evolved during this operation being passed to a gas analysis apparatus. This apparatus and the method of analysis has been described by one of the authors in an earlier paper.[3]

The results shown in Tables 1 to 3 for two cathodes are typical of the large number tested. Cathode No. 1 was decomposed by passing a heating current of 0·6 A and No. 2 using 0·5 A. These heating currents correspond to steady temperatures of 1250 and 1070° C respectively. All temperatures quoted in this paper are uncorrected brightness temperatures measured with an optical pyrometer. These heating currents are in the range normally used for the breakdown and activation of this type of cathode. The evolution of gas from an uncoated but otherwise identical tungsten spiral is also given for comparison. The method of analysis used gives only a minimum value for the quantity of water present. There is also uncertainty as to whether a small amount of free oxygen may have been present in any of these cases, but

Table 1. *Total gas evolved*

Cathode No.	Type	Heating current (A)	Total time (s)	Steady brightness temp. (°C)	Total quantities (μl.)					
					CO_2	CO	H_2	H_2O (approx.)	O_2 (max.)	N_2 (residue)
1	coated	0·6	240	1250	177	36·5	6·1	0·3	0·6	1·4
2	coated	0·5	360	1070	182	37·0	8·2	0·3	0·5	3·0
3	plain	0·6	660	1450	0·1	0·35	2·8	0·5	0·16	0·15

Table 2. *Gas evolved on first heating*

Cathode No.	Type	Heating current (A)	Heating time (s)	Steady brightness temp. (°C)	Quantities evolved (μl.)					
					CO_2	CO	H_2	H_2O (approx.)	O_2 (max.)	N_2 (residue)
1	coated	0·6	10	1250	176	33·1	1·3	0·2	0·5	1·2
2	coated	0·5	10	1070	176	30·5	2·9	0·25	0·2	2·5
3	plain	0·6	60	1450	0·05	0·15	1·4	0·45	0·1	0·1

Table 3. *Proportion evolved on first heating*

Cathode No.	Type	Heating current (A)	Heating time (s)	Gas evolved initially (%)			
				CO_2	CO	H_2	N_2
1	coated	0·6	10	99·5	90·5	21	86
2	coated	0·5	10	96·5	82·5	35	83
3	plain	0·6	60	50	43	50	66

it is considered unlikely: the figures quoted are the maximum amounts which could have been present.

It is clear from these results that almost the whole of the evolution of carbon dioxide takes place in the first few seconds of heating. There is also considerable evolution of carbon monoxide over a slightly longer period. Hydrogen is the third major constituent of the evolved gases, and is liberated at a fairly steady rate over an appreciable period.

Table 3 shows the proportion of each gas evolved during the initial heating period, and in Fig. 1 the rate of evolution of each gas is shown against heating time. It will be seen

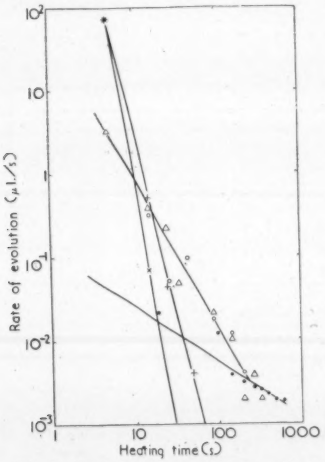

Fig. 1. Evolution of gas on decomposition

× = carbon dioxide from cathode decomposed at 1250° C.
+ = carbon dioxide from cathode decomposed at 1070° C.
○ = carbon monoxide plus hydrogen from cathode decomposed at 1250° C.
△ = carbon monoxide plus hydrogen from cathode decomposed at 1070° C.
● = hydrogen from tungsten coil heated to 1450° C. (Brightness temperatures)

that after the initial ten seconds the evolution of carbon dioxide has almost ceased. After twenty seconds heating the principal gases coming off are carbon monoxide and hydrogen in the ratio of about 10 : 1. This evolution is practically the same at each temperature and continues for 100–150 seconds; after this time only a slowly decreasing evolution of hydrogen continues.

Comparison of the hydrogen evolution from coated and uncoated filaments demonstrates that this slow evolution of hydrogen results from the outgassing of the tungsten, which is annealed in hydrogen during manufacture. A somewhat larger quantity of hydrogen evolved during the earlier stages of breakdown of coated filaments (see Table 1) was shown to be evolved from the decomposition of the nitrocellulose binder. Any carbon oxides from this source were not detectable against the large quantities from the breakdown of the carbonates.

CHEMICAL REACTIONS

It has been shown[1,2] that the reactions to be expected on heating tungsten filaments coated with alkaline earth carbonates are:

$$RCO_3 \rightleftharpoons RO + CO_2 \quad (1)$$

$$3RCO_3 + W \rightleftharpoons R_3WO_6 + 3CO \quad (2)$$

$$6RO + W \rightleftharpoons R_3WO_6 + 3R \quad (3)$$

where R may be Ba, Sr, Ca, or various molecular combinations of these; Rooksby and Steward have identified Ba_2SrWO_6, Ba_2CaWO_6 and $BaSrCaWO_6$.

The equilibrium pressures of carbon dioxide at various temperatures for reaction (1) have been calculated by the method of Rittner.[4] At 1000° K the equilibrium pressures over the separate carbonates are:

$BaCO_3$: 7×10^{-3} mm
$SrCO_3$: 0·3 mm
$CaCO_3$: 170 mm

Hughes, Coppola and Evans[2] have shown that for barium carbonate in contact with tungsten, reaction (2) begins to occur with appreciable speed above about 600° C, while reaction (1) does not begin until 800–900° C. With a normal type of breakdown schedule, therefore, both reactions will occur together. The exact proportion of each occurring will depend on many factors, such as the rate of temperature rise, the particle size of the carbonates and the intimacy of their contact with the tungsten.

At activation temperatures above 800° C, i.e. when reaction (1) can occur to an appreciable extent, the following reaction will also occur:

$$3RO + 3CO_2 + W \rightleftharpoons R3WO_6 + 3CO \quad (4)$$

possibly in the sequence:

$$3CO_2 + W \rightleftharpoons 3CO + WO_3$$
$$WO_3 + 3RO \rightleftharpoons R_3WO_6$$

Other reactions leading to the formation of the tungstates RWO_4 have been suggested but, as shown later, the authors do not believe that these occur to any appreciable extent. The reactions occurring during the breakdown of alkaline earth carbonates on tungsten may then be written schematically as below:

$$\begin{array}{ccccc} 3RCO_3 & & \rightleftharpoons & & 3CO_2 + 3RO \\ + & & & & + \\ W & & & W & W \\ \downarrow & & & & \downarrow \\ 3CO & & 3CO & & 3CO \\ + & + & & & + \\ R_3WO_6 & & \rightleftharpoons & & 3RO + WO_3 \end{array}$$

The subsequent activation of the cathode, which is

responsible for its electron emissive properties, is the production of free barium by the "activation reaction"

$$6BaO + W \rightleftharpoons Ba_3WO_6 + 3Ba \qquad (5)$$

The production of free strontium and calcium is usually considered to be negligible.

The extent to which reaction (5) can occur is governed by (*a*) the amount of barium oxide available, and (*b*) the intimacy of contact of the barium oxide with the tungsten base. These factors are both controlled by the extent to which reactions (1), (2) and (4) have occurred during breakdown, the amount of barium oxide being controlled by the relative speeds of the competing reactions (1) and (2), and the formation of the interface being governed by the reactions (2) and (4).

RESULTS

By determination of the ratio of carbon monoxide to carbon dioxide in the total gas evolved, the relative extent to which the various reactions have occurred may be assessed. This also allows an estimate to be made of the interface formed during decomposition, since carbon monoxide is only evolved in those reactions leading to interface formation.

Fig. 2 illustrates the dependence of carbon monoxide evolution and hence interface formation, on the heating schedule and pumping arrangement. It is clear that rapid heating to high temperatures and low pumping speed are very favourable to interface formation. The very marked dependence on pumping speed, and hence on gas pressure, demonstrates that much of this formation is due to the reaction (4) with gaseous carbon dioxide.

In pumping arrangement (iv), Fig. 2, the same exhaust tube was used as in arrangement (ii), but the whole bulb was immersed in liquid air, thus removing all the carbon dioxide immediately upon formation so that reaction (4) cannot occur. Under these conditions more carbon monoxide is evolved using the lower temperature heating schedules, thus demonstrating that reaction (2) occurs, the slower schedules enabling it to proceed for a longer time, with the consequent evolution of carbon monoxide, before reaction (1) begins. This agrees with the observations of Hughes, Coppola and Evans[2] that reaction (2) occurs at lower temperatures than reaction (1).

A further experiment was carried out which demonstrated that the absence of appreciable amounts of carbon monoxide after decomposing by schedules *F* to *H*, using pumping arrangement (iv), is not because carbon monoxide is first formed by reaction (2) and subsequently converted to carbon dioxide by reversal of reaction (4). After decomposition the bulb was evacuated, then filled with pure carbon monoxide to a few millimetres of mercury pressure, and the filament heated to 1340° C whilst the bulb was immersed in liquid

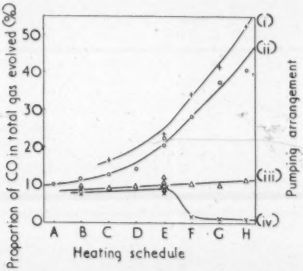

Fig. 2. Carbon monoxide evolved on decomposition

Heating schedules

Schedule	*Heating current for successive 5 s intervals* (A)										*Heating current* (A)	*Steady brightness temp.* (°C)
A	0·1	0·2	0·25	0·3	0·35	0·5	0·45	0·5	0·55	0·6	0·3	710
B	0·2	0·3	0·4	0·5	0·6						0·4	990
C	0·4	0·5	0·6								0·5	1070
D	0·5	0·5	0·6								0·6	1250
E	0·6	0·6	0·6								0·65	1340
F	0·65	0·65	0·65								0·7	1430
G	0·7	0·7	0·7								0·75	1520
H	0·75	0·75	0·75									

Pumping arrangements

Arrangement	*Description*	*Bulb volume* (cm³)	*Pumping connexion*	*Approx. max. pressure attained*	*Approx. pressure at end of* 15 s
(i)	sealed off	266	none	4 mm	4 mm
(ii)	slow pumping	100	3·5 mm diameter exhaust stem	1 mm	15 μ
(iii)	fast pumping	100	20 mm diameter pumping line	50–100 μ	0·1 μ
(iv)	liquid air immersed	200	3·5 mm diameter exhaust stem	very small	very small

air. Only about 1% of the carbon monoxide was converted to carbon dioxide per minute, a negligible rate of conversion.

Further experiments were carried out by heating filaments in a sealed-off system of 400 cm^3 volume. This system included a small freezing tip and an inclined oil manometer for rapid pressure determinations. Each filament was heated for repeated periods by a current producing a given steady temperature. After each period the pressure was measured, together with the drop in pressure on immersing the tip in liquid air. The gas remaining after immersing the tip is taken to be carbon monoxide.

The results of these experiments are shown in Fig. 3 where the percentage of carbon monoxide is plotted against total

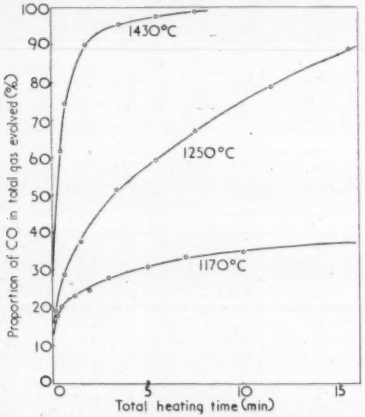

Fig. 3. Conversion of carbon dioxide into monoxide by an oxide-coated tungsten cathode

The cathode was in a bulb of 400 cm^3 volume and the total gas pressure was 1·5 mm of mercury. The steady brightness temperature of the cathode is shown.

heating time. It is immediately clear from these results that equilibrium conditions for these reactions are never reached during a normal schedule, which involves heating to 1200–1400° C for about one minute. The variations in the amounts of carbon monoxide observed in the previous experiments must therefore be due to the different speeds of reaction.

If heating is continued the reactions go to completion, at least at temperatures over 1200° C. After a few minutes the reaction rates become exponential, which suggests that they are then mainly governed by diffusion processes. Thus the speed of reaction is determined largely by the time taken for the reactants to come together.

IDENTIFICATION OF THE INTERFACE

To provide some confirmation of the interpretation of these results a number of cathodes were broken down at 1250° C for thirty seconds and the coating, together with the interface, stripped off by stretching out the coils. X-ray diffraction analysis of this mixture showed a mixed tungstate (Ba, Sr, Ca)$_3$ WO_6, in addition to the mixed oxide. No trace of (Ba, Sr, Ca)WO_4 was detected. Diffraction photographs taken 15, 60 and 100 minutes after removing the cathode from its vacuum envelope showed no change due to hydrolysis. When, however, the oxide was removed by dissolving in dilute acetic acid, the residue was found to be entirely (Ba, Sr, Ca)WO_4, hydrolysis having occurred.

Three further cathodes were broken down in a closed bulb of 266 cm^3 using heating schedules *B*, *E* and *H* (Fig. 2). The amount of carbon monoxide evolved was measured in each case and then each cathode was taken out, the coating removed, and the interface separated and weighed as (Ba, Sr, Ca)WO_4 by a microchemical technique, using dilute (1 in 5) acetic acid to remove the oxide. Table 4 shows the

Table 4. *Interface weights*

Schedule	*RWO_4 calculated from* CO (mg)	*RWO_4 weighe* (mg)
B(i)	0·20	0·06
E(i)	0·41	0·16
H(i)	0·71	0·35

weights of (Ba, Sr, Ca)WO_4 obtained, compared with those to be expected from the corresponding quantity of carbon monoxide.

Since it was not possible to strip the interface completely from the tungsten, and some was inevitably lost during manipulation, the agreement shown provides a reasonable confirmation of the present interpretation of the reactions.

CONCLUSIONS

It has been shown that on breaking down mixed alkaline earth carbonates on a tungsten substrate the main gases evolved are carbon dioxide, carbon monoxide and hydrogen. The hydrogen is evolved from the tungsten and plays no part in the chemical reactions occurring on decomposition of the carbonates. The carbon monoxide evolved is the result of the formation of a basic tungstate interface layer. This interface may be formed by either of reactions (2) or (4).

At decomposition temperatures below about 1250° C reaction (2) occurs to an appreciable extent and the formation of interface is largely independent of pumping speeds. At higher decomposition temperatures reaction (1) proceeds so rapidly that reaction (2) is almost entirely suppressed. Interface formation is then by reaction (4), and is markedly dependent on the rate of removal of the gaseous reaction products.

The formation of large amounts of interface during decomposition of the carbonates impedes the activation of the cathode by retarding reaction (5), the amount of free barium formed by reaction (5) being the prime factor in determining the electron emissive properties of the cathode.

It has also been shown that the various reactions which occur during decomposition do not reach equilibrium under normal heating and exhaust schedules. The final condition of the cathode depends entirely, therefore, on the rates at which the different reactions occur. This once again emphasizes the importance of matching the heating and exhaust conditions during cathode decomposition in order to obtain optimum cathode characteristics.

REFERENCES

(1) Rooksby, H. P., and Steward, E. G. *J. Appl. Phys.*, **22**, p. 358 (1951).
(2) Hughes, R. C., Coppola, P. P., and Evans, H. T. *J. Appl. Phys.*, **23**, p. 635 (1952).
(3) Cayless, M. A. *Brit. J. Appl. Phys.*, **7**, p. 13 (1956).
(4) Rittner, E. S. *Philips Res. Rep.*, **8**, p. 184 (1953).

The dynamic magnetostriction of nickel-cobalt alloys

By C. A. CLARK, Ph.D., A.Inst.P., The Mond Nickel Co., Ltd., Birmingham, 16

[*Paper received* 18 *April*, 1956]

The magnetostrictive properties of binary nickel–cobalt alloys in the range 0–23% cobalt are discussed, with particular reference to the use of these materials for transducers. Measurements, at various polarizing fields, of the electromechanical coupling coefficient, reversible permeability and Young's modulus are described. Various criteria which govern the choice of magnetic materials for ultrasonic transducers are discussed and it is shown that two alloys, containing respectively about 4·4 and 18·4% cobalt, give good performance as transducer materials.

The use of magnetostrictive materials in transducers has increased considerably in recent years: applications include echo-sounders, drilling equipment, ultrasonic cleaning equipment, the ultrasonic soldering iron and delay lines.

The requirements for magnetostrictive transducer materials are a high rate of change of Joule magnetostriction with magnetic field, good mechanical properties (to enable the core to withstand the induced stresses), and, in many applications, good corrosion-resistance. In order to reduce the eddy currents, metallic materials for such applications should be readily obtainable in the form of thin laminations, and for transducers rated at high powers it is also an advantage for the magnetic core to possess a high Curie temperature, so that some internal heating can be tolerated without adversely affecting the magnetostrictive properties.

In the present work the magnetic properties necessary for high alternating magnetostriction are considered and criteria by which the quality of materials for ultrasonic transmitters can be assessed are discussed. The dynamic magnetostrictive properties of binary nickel–cobalt alloys are then considered in relation to theoretical predictions.

THE PRODUCTION OF MAGNETOSTRICTION

In an annealed ferromagnetic material it may be assumed that the domain magnetization vectors are alined as far as possible along preferred crystallographic directions, subject to the limitation that the magnetic induction must be continuous. When a small magnetic field is applied it is probable that the initial stage of magnetization occurs by movement of 180° domain boundaries. This process does not require appreciable work against the forces of magnetic anisotropy or against magnetostrictive stress. The absence of magnetostrictive strain near the initial part of the magnetization curve has been confirmed experimentally for several nickel–iron alloys by McKeehan and Cioffi.[1]

When the applied magnetic field is increased a different process of magnetization occurs; the domain walls move in such a way that the magnetization lies in that easy direction of magnetization which is nearest to the direction of the magnetic field. Since, in general, this process involves a change of alinement of the magnetization vectors, magnetostrictive length-changes will result.

Above the "knee" of the magnetization curve, magnetization by domain boundary movement no longer predominates since the magnetization is rotated out of easy directions of magnetization, so as to be parallel to the applied field. The approach to magnetic saturation is accompanied by magnetostriction, but since it is also opposed by magnetic crystal anisotropy, magnetostrictive transducers are less efficient when operated at this part of the magnetization curve.

In practice, therefore, it is found that when annealed laminations are used in transducers, there exists an optimum magnetic polarization at which the efficiency of transformation of magnetic to mechanical energy is at a maximum.

If the mechanism of magnetization described above is substantially correct, it follows that in order to increase the reversible magnetostriction it would be necessary either to orientate the grains, so that an easy direction of magnetization would be parallel to the applied field, or, by suitable alloying additions, to reduce the magnetic crystal anisotropy.

In most types of laminated core it is difficult to obtain suitable grain orientation along the entire magnetic circuit; it was accordingly decided to investigate initially the effect, on the magnetostrictive properties of nickel, of reducing its magnetic anisotropy. It is obvious that in transducer applications, any alloying addition which reduces the anisotropy must not simultaneously reduce the magnitude of the linear magnetostriction to an appreciable extent. From a review of relevant literature it seemed that from these considerations, the only binary nickel alloys likely to possess dynamic magnetostrictive properties better than those of nickel were the alloys with cobalt.

The linear magnetostriction of nickel–cobalt alloys has been measured by several workers, including Masumoto,[2] Masiyama[3] and Yamamoto and Miyasawa.[4] The published data are reasonably consistent, bearing in mind that the magnitude of the effect depends on the impurities present, processing technique, previous heat-treatment, and magnetic history. According to Masumoto, the saturation magnetostriction changes almost linearly from about -42×10^{-6} for pure nickel to about -22×10^{-6} for 20% cobalt–nickel. A review of the data on the magnetic anisotropy constant is given by Yamamoto,[5] who concluded that for the face-centred cubic alloys the anisotropy constant is zero at about 5 and 19·5% cobalt.

Preliminary work by Hinton and Round[6] showed that a 4% cobalt–nickel alloy possessed a larger electromechanical coupling coefficient than nickel or 10% cobalt–nickel, which is in agreement with the above hypothesis. It was therefore decided to make a more detailed investigation on alloys containing up to 23% cobalt.

EXPERIMENTAL TECHNIQUE

The tests were carried out on sixteen nickel–cobalt alloys made from raw materials of commercial purity. In addition, an alloy containing 49·5% iron, 1% tungsten, balance cobalt, was made by powder metallurgy for comparison purposes. All the alloys were processed to 0·006 in. thick strip; the chemical analyses of the strip are given Table 1.

The alloy strip was stamped into ring laminations having an outer diameter of 5 cm and an inner diameter of 4 cm, and these were annealed in dry hydrogen for one hour at 750° C. The iron–cobalt–tungsten alloy was very brittle after being processed to 0·006 in. thick strip, but ring

Table 1. *Composition of the alloys tested*

(weight %: balance substantially nickel)

Cobalt	*Iron*	*Tungsten*	*Carbon*	*Sulphur*
<0·1	0·64	N.D.	N.D.	N.D.
2·3	0·040	N.D.	0·03	0·004
2·6	0·036	N.D.	0·04	0·003
3·7	0·085	N.D.	0·01	N.D.
4·1	0·05	N.D.	0·02	0·006
5·8	0·071	N.D.	0·04	0·006
6·5	0·11	N.D.	N.D.	N.D.
8·3	0·22	N.D.	N.D.	N.D.
10·0	0·07	N.D.	N.D.	0·009
13·7	0·058	N.D.	0·02	0·005
15·3	0·078	N.D.	0·05	0·007
15·7	0·065	N.D.	0·02	0·007
17·8	0·079	N.D.	0·03	N.D.
19·7	0·088	N.D.	0·04	N.D.
21·2	0·064	N.D.	0·03	0·005
23·1	0·12	N.D.	N.D.	N.D.
49·5	49·5	1·0	—	—

N.D. = not determined.

laminations were obtained without difficulty and these were annealed in the same way as the nickel–cobalt rings.

The test cores for each alloy consisted of thirty annealed rings fitting loosely into a polystyrene former on which were wound excitation and polarizing windings, each consisting of 120 turns of copper wire. The polarizing winding was connected, through an ammeter and rheostats, to a direct current supply, so that measurements of the reversible magnetic properties could be made with various degrees of steady magnetization in the core. Prior to making impedance measurements a steady magnetic field of 40 oersteds was produced in the toroid for a few seconds and was then removed, the core thus being brought to remanence.

The excitation winding, in parallel with a 1 μF variable condenser and in series with a milliammeter and an air-cored ballast coil, was connected in one arm of an equal-ratio inductance bridge. The current in the *X*-arm of the bridge was maintained constant at 14 mA and the ballast coil possessed sufficient inductance to ensure that the reactance of the *X*-arm did not become negative over the range of frequency required in the experiments.

The input current to the bridge was supplied by a decade oscillator by means of which the frequency could be varied at intervals of 10 c/s over the range 0–110 kc/s and a heterodyne amplifier detector giving a beat frequency of 1 kc/s was used as the bridge detector. The oscillator and detector were isolated from the bridge by balanced and screened transformers.

Fig. 1 shows the components in the X-arm of the bridge; L, C and R are the electrical equivalent of the transducer, L_0 is the inductance of the excitation winding, R_0 represents the electrical and magnetic losses, and C_0 is the variable condenser. To determine the electromechanical coupling coefficient, the bridge was first balanced at suitable increments of frequency over the frequency range of about 20 to 50 kc/s, with the terminals MN shorted. The short circuit was then removed and the bridge rebalanced over the same frequency range. The difference in the settings for the two conditions gave the effective resistance and reactance across MN, as a function of frequency. The curve showing variation of effective resistance with frequency possessed the typical *M*-shape as shown for one alloy in Fig. 2. When the variable capacitance was correctly chosen this curve was symmetrical. The coupling coefficient K can be calculated[7] from the frequency interval 2Δ between the two maxima and the resonance frequency f_0 given by the minimum in the curve.

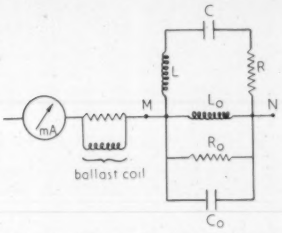

Fig. 1. Circuit diagram showing the *X*-arm of the inductance bridge

For transducers operating into air, as in the present experiments, the electromechanical coupling coefficient K is given to a close approximation by the equation:

$$K^2 = L_0/(L + L_0) = 4\,\Delta^2/(f_0^2 + 4\,\Delta^2) \qquad (1)$$

The measurements on each core were repeated for various polarizing fields, in order to determine the maximum value of the electromechanical coupling coefficient as the magnetization of the core was increased above remanence. The

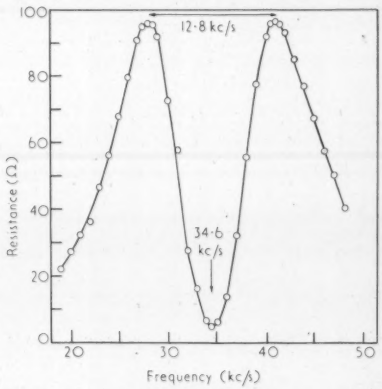

Fig. 2. The resistance-frequency curve for 13·7% cobalt–nickel alloy. The polarizing field is 7·5 oersteds

incremental permeability at resonance was calculated from the value of the capacitance required to tune the electrical circuit at the mechanical resonance frequency. The variation of the electromechanical coupling coefficient and incremental permeability with polarizing field is shown for a 4% cobalt–nickel alloy in Fig. 3. It is seen that, under these experimental conditions, variations from the optimum value of the polarizing field by about ±3 oersteds are not critical. The value of 2Δ could be estimated to about ±0·5 kc/s,

which was equivalent to an accuracy of about ±0·015 in the electromechanical coupling coefficient. The accuracy of determination of the reversible permeability was about ±5%.

The ballistic method was used to obtain the d.c. magnetic properties including coercive force, initial and maximum

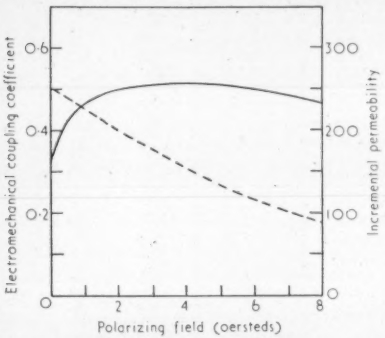

Fig. 3. Coupling coefficient and incremental permeability for 4% cobalt–nickel alloy

——— electromechanical coupling coefficient.
– – – incremental permeability at the resonance frequency.

permeability, and incremental permeability at remanence for a reversal of 0·2 oersteds. The thickness of the strip was obtained by weighing thirty rings for each alloy and assuming a density of 8·90 for the nickel–cobalt alloys and 8·20 for the iron–cobalt–tungsten alloy. The estimated accuracies for the magnetic field and the magnetic induction are about ±1% and ±2%, respectively.

THE MAGNETOSTRICTION EQUATIONS

In estimating the value of the nickel–cobalt alloys for transducer applications an extension of the thermodynamic treatment given by Sussman and Ehrlich,[8] from whose paper equations (2) to (14) are taken, is used.

The shape S and magnetic induction B of a ferromagnetic material may be expressed as functions of the applied field H and the applied stress P in the form

$$dH = \left(\frac{\partial H}{\partial B}\right)_S dB + \left(\frac{\partial H}{\partial S}\right)_B dS \qquad (2)$$

and

$$dP = \left(\frac{\partial P}{\partial B}\right)_S dB + \left(\frac{\partial P}{\partial S}\right)_B dS \qquad (3)$$

In addition, the following partial derivatives are used in this treatment:

$(\partial P/\partial B)_S = -\lambda$ = magnetostriction constant (4)

$(\partial B/\partial P)_H = \Lambda$ = stress sensitivity (5)

$(\partial P/\partial S)_B = E_B$ = Young's modulus at constant induction (6)

$(\partial P/\partial S)_H = E_H$ = Young's modulus at constant field (7)

$(\partial B/\partial H)_S = \mu_S$ = reversible permeability at constant shape (8)

$(\partial B/\partial H)_P = \mu_P$ = reversible permeability at constant stress (9)

Two other relations which may be derived from the thermodynamic equations of magnetostriction are:

$$(\partial P/\partial B)_S = (1/4\pi)(\partial H/\partial S)_B \qquad (10)$$

and

$$\Lambda = 4\pi\lambda\mu_P/E_B \qquad (11)$$

Manipulation of equations (2) to (11) gives

$$dH = (1/\mu_S)dB - 4\pi\lambda dS \qquad (12)$$

and

$$dP = -\lambda dB + E_B dS \qquad (13)$$

Eliminating dB between equations (12) and (13) leads to:

$$E_H = E_B\left(1 - \frac{4\pi\lambda^2\mu_S}{E_B}\right) \qquad (14)$$

and

$$\frac{1}{l}\left(\frac{\partial l}{\partial H}\right)_P = \lambda\mu_S \Big/ \left[E_B\left(1 - \frac{4\pi\lambda^2\mu_S}{E_B}\right)\right] \qquad (15)$$

where l is the length of the specimen. Similarly, by eliminating dS between equations (12) and (13) it follows that:

$$\frac{1}{\mu_P} = \frac{1}{\mu_S}\left(1 - \frac{4\pi\lambda^2\mu_S}{E_B}\right) \qquad (16)$$

and

$$\Lambda = \frac{4\pi\lambda\mu_S/E_B}{(1 - 4\pi\lambda^2\mu_S/E_B)} \qquad (17)$$

For the cases of no losses and no radiation it is readily shown that K^2 represents the ratio of converted stored energy ($\frac{1}{2}E_H S^2$) to input stored energy ($B^2/8\pi\mu_P$). The electromechanical coupling coefficient is therefore a suitable criterion for materials for transducers used in ultrasonic transmitters. In transmitters $dP = 0$, and equation (13) may be integrated to give $S = \lambda B/E_B$ so that the ratio of mechanical to magnetic stored energy is:

$$K^2 = \frac{4\pi E_H S^2\mu_P}{B^2} = \frac{4\pi E_H\lambda^2\mu_P}{E_B^2} = \frac{4\pi\lambda^2\mu_S}{E_B} \qquad (18)$$

Equations (14) and (16) can therefore be rewritten:

$$E_H = E_B(1 - K^2) \qquad (19)$$

$$\mu_s = \mu_P(1 - K^2) \qquad (20)$$

In ultrasonic receivers a high induced electromotive force in the electrical winding is required. Since this is proportional to the rate of change of magnetic flux, the stress-sensitivity provides a suitable criterion for materials for use in receiving transducers. Using equations (11), (18), (19) and (20) it is readily shown that:

$$\Lambda = K\sqrt{(4\pi\mu_P/E_H)} \qquad (21)$$

From this equation the stress-sensitivity can be computed from the quantities K, μ_P and E_H, obtained from impedance measurements. It is seen that in a particular alloy system the composition giving maximum stress-sensitivity does not necessarily coincide with the composition associated with maximum electromechanical coupling coefficient.

From equations (15), (18), (19), (20) and (21) it follows that

$$\frac{1}{l}\left(\frac{\partial l}{\partial H}\right)_P = \frac{\Lambda}{4\pi} = \frac{K}{4\pi}\sqrt{\left(\frac{4\pi\mu_P}{E_H}\right)} \qquad (22)$$

In principle the coupling coefficient at zero frequency can

be calculated from equation (22), since $(1/I)(\partial I/\partial H)_P$, E_H and μ_P can be measured under magnetostatic conditions.

A knowledge of the magnetostriction constant is sometimes required, and this may be calculated from the following equation:

$$\lambda = \frac{K}{1 - K^2}\sqrt{\left(\frac{E_H}{4\pi\mu_P}\right)} \qquad (23)$$

DISCUSSION

Sufficient alloys were tested ballistically to confirm the general variation in magnetic properties observed by Yamamoto.[5] The curve of initial permeability *versus* cobalt content contained two maxima of 660 and 1450, at approximately 4 and 18% cobalt, respectively, compared with the maximum values of about 880 and 1450 reported by Yamamoto as occurring, respectively, at 5 and 15% cobalt. According to Yamamoto, variation of maximum permeability with cobalt content indicated maximum values of about 6500 and 10 300 at 6 and 12% cobalt respectively, whereas the present experiments give maxima of 3000 and 4300 at cobalt contents of 4·5 and 16% respectively. The larger values of maximum permeability reported by Yamamoto probably result from the higher annealing temperature and more prolonged heat treatment applied to his alloy, namely, two hours in a vacuum at 1000° C. In Fig. 4 the magnetic

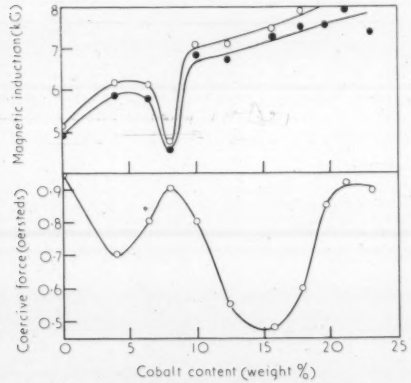

Fig. 4. Magnetic induction at 10 and 15 oersteds and coercive force as a function of the cobalt content

○ magnetic induction at 15 oersteds.
● magnetic induction at 10 oersteds.

induction at 10 and 15 oersteds, and the coercive force, are plotted as functions of the cobalt content. At about 8·5% cobalt, magnetic induction passes through a minimum and coercive force through a maximum value, effects which are possibly associated with the fact that the magnetic crystal anisotropy constant is at a maximum positive value at about this composition.

The maximum values of the coupling coefficient are shown in Fig. 5, as a function of the cobalt content. Maxima of 0·51 and 0·42 are obtained at 4 and 18% cobalt, respectively, compared with 0·30 for nickel. The coupling coefficient at remanence shows a similar variation with cobalt content, although the scatter in the experimental points is much higher. This is attributed to partial demagnetization by the alternating field, which is comparable with the coercive force,

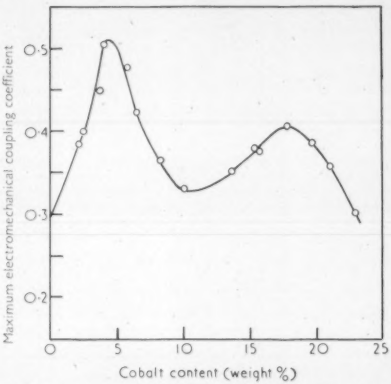

Fig. 5. Electromechanical coupling coefficients determined in the optimum polarizing field

causing reduced magnetostriction. It is clear that for transformation of electrical to mechanical energy 4 and 18% cobalt–nickel alloys are better than nickel by factors of three and two respectively. The coupling coefficient of the iron–cobalt–tungsten alloy was 0·31 at remanence: this was the highest value found for this alloy.

Young's modulus was calculated from the approximate equation:

$$E_H = \pi^2 d^2 f_0^2 \rho \qquad (24)$$

where ρ is the density, and d is the mean diameter. From Fig. 6 it is seen that the modulus of elasticity passes through minima at approximately 4 and 18% cobalt and that for all the alloys it increases with magnetization. This increase of Young's modulus with magnetization is primarily a result of the well-known ΔE effect. Thus, if a ferromagnetic material is subjected to applied stress, the resulting strain is a combination of the usual elastic strain together with a magnetostrictive strain produced by rotation of domain magnetization. If, however, by means of a magnetic field, the domain magnetization vectors are previously alined parallel to the applied stress, the measured Young's modulus results solely from the elastic strain. According to Döring,[9] a magnetic material possessing small internal stresses should possess a large ΔE effect when the magnetic anisotropy constant is small. The variation of Young's modulus with cobalt content is thus in qualitative agreement with theory. The values of Young's modulus for nickel are in good agreement with published results and justify the use of equation (24) for the calculations. The effective modulus of elasticity also depends on the degree of eddy-current shielding. At very high frequencies, for example, almost the whole of the lamination would be at constant induction, and the difference between the moduli at constant induction and constant field is given by Brown[10] as:

$$E_B - E_H = \frac{E_B E_H}{4\pi\mu}\left(\frac{\partial B}{\partial P}\right)^2 \qquad (25)$$

Since $(\partial B/\partial P)$ is the stress-sensitivity, it is seen, by using equation (21), that Brown's equation is identical with equation (19), which can be rearranged to give

$$E_B - E_H = E_B K^2 = \frac{E_B E_H}{4\pi\mu_P}\Lambda^2 \qquad (26)$$

In practice the effective modulus of elasticity in magnetostriction oscillators will be intermediate between E_B and E_H.

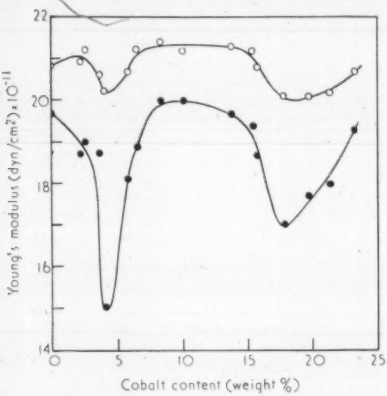

Fig. 6. Young's modulus as a function of the cobalt content

○ values for optimum polarizing field.
• values at remanence.

Numerical values of stress-sensitivity in the optimum polarizing field have been calculated from equation (21) and in Fig. 7 are plotted as a function of the cobalt content. The dotted curve indicates theoretical values of maximum stress-sensitivity, derived from the equation:

$$\Lambda_m = 0{\cdot}77\lambda_S B_S/K_1 \qquad (27)$$

where λ_s is the saturation magnetostriction, B_s the saturation induction and K_1 the anisotropy constant. This equation was obtained by Bozorth and Williams[11] from domain theory, and, in applying it to the nickel–cobalt system, values

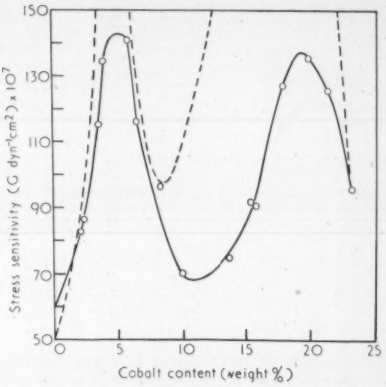

Fig. 7. Stress-sensitivities for polarized nickel–cobalt alloys

○ experimental results.
– – – calculated results.

of λ_s were taken from Masumoto,[2] of B_s from Bozorth[12] and of K_1 from Yamamoto.[5] In view of the approximations involved in applying equations (21) and (27), the agreement, particularly at low cobalt contents, is satisfactory. In addition, the value of Λ_m for nickel is in good agreement with that determined by Bozorth and Williams.[11] The optimum compositions for maximum stress sensitivity are at 5 and 19% cobalt–nickel alloys, respectively, i.e. the cobalt levels are somewhat higher than in the alloys giving the maximum coupling coefficients. It follows from these results that for use in receiving transducers the 5 and 19% cobalt–nickel alloys are about equal in value and possess stress-sensitivities more than twice as large as that for nickel.

The important dynamic magnetostrictive properties of

Table 2. *Magnetic properties of transducer materials*

		nickel–zinc ferrite* A	nickel–zinc ferrite* B	nickel–zinc ferrite* C	35%† cobalt, 0·5% chromium, balance iron	49·5% iron, 1% tungsten, balance cobalt	nickel	4% cobalt–nickel	18% cobalt–nickel
Electromechanical coupling coefficient	at remanence	0·055	0·049	0·067	0·14	0·31	0·23	0·34	0·23
Stress sensitivity $\times 10^7$, $G\ dyn^{-1}\ cm^2$		34	21	20	26	83	72	148	121
Magnetostriction constant $\times 10^{-3}$, $dyn\ G^{-1}\ cm^{-2}$		0·89	1·14	2·35	5·1	11·9	7·8	8·3	4·6
Reversible permeability		430	170	70	123	160	160	250	390
Electromechanical coupling coefficient	polarized				0·17		0·30	0·59	0·46
Stress sensitivity $\times 10^7$, $G\ dyn^{-1}\ cm^2$					36	as	61	135	127
Magnetostriction constant $\times 10^{-3}$, $dyn\ G^{-1}\ cm^{-2}$					8·0	above	16·7	32·3	18·7
Reversible permeability					75		70	130	150

* Taken from Popper.[13]
† Calculated from results by Sussman and Ehrlich.[8]

nickel, 4% cobalt–nickel alloy, 18% cobalt–nickel alloy and the iron–cobalt–tungsten alloy are given in Table 2. Also included are data for an alloy containing approximately 35% cobalt, 0·5% chromium, balance iron, the properties of which have been calculated from the results of Sussman and Ehrlich,[8] and the properties at remanence for three nickel–zinc ferrites (after Popper).[13] It is clear that the 4 and 18% cobalt–nickel alloys possess better dynamic magnetostriction properties than many other magnetostrictive materials, and should be suitable as transducer materials in ultrasonic transmitters and receivers. An additional advantage of the cobalt–nickel alloys compared with nickel, is their higher Curie temperatures, which permits operation of the magnetic core, if necessary, at a higher temperature without seriously affecting its magnetostrictive properties: the 4 and 18% cobalt–nickel alloys possess Curie temperatures of about 410 and 570° C, respectively, compared with 360° C for nickel.

Finally, the important marine applications of magnetostrictive transducers made it desirable to ascertain the reaction of various magnetostrictive alloys to salt water, and in particular to observe whether the addition of cobalt to nickel affected its resistance to corrosion by this medium. Specimens of nickel, 4% cobalt–nickel, 18% cobalt–nickel, 42% nickel–iron and the iron–cobalt–tungsten alloy, all in the form of 0·006 in. thick strip, were freely exposed in the annealed condition to aerated 3½% sodium chloride solution and loss of weight determined after 136 days' exposure. The results of these tests are given in Table 3, where it will be noted that the addition of cobalt to nickel improves rather than impairs resistance to corrosion by this medium, and that nickel and the two cobalt–nickel alloys are much more resistant to attack than the iron–cobalt–tungsten and 42% nickel–iron alloys.

Table 3. *The resistance of magnetostrictive alloys to corrosion by aerated 3½% sodium chloride solution at room temperature*

Material	*Loss in weight after 136 days' exposure* (mg/dm²)	*Type of attack*
nickel	6·3	slight uniform attack.
4% cobalt–nickel alloy	3·2	extremely slight localized corrosion.
18% cobalt–nickel alloy	1·8	extremely slight localized corrosion.
iron–cobalt–tungsten alloy	540	severe local attack resulting in perforation of the strip.
42% nickel–iron alloy	775	severe local attack, resulting in perforation of the strip.

CONCLUSIONS

The dynamic magnetostriction properties of binary nickel–cobalt alloys in the composition range 0–23% cobalt are in qualitative agreement with theory. Alloys containing approximately 4·4 and 18·4% cobalt would be suitable for both transmitting and receiving ultrasonic transducers, and for these applications are superior to the other magnetostrictive materials examined including nickel. Additional advantages of the 4 and 18% cobalt–nickel alloys are the higher Curie temperatures compared with that of nickel, the ease of processing to thin strip, and the good resistance to corrosion by salt water.

ACKNOWLEDGEMENTS

The author is indebted to The Mond Nickel Co. Ltd., for permission to publish this paper.

REFERENCES

(1) McKeehan, L. W., and Cioffi, P. P. *Phys. Rev.*, **28,** p. 146 (1926).
(2) Masumoto, H. *Sci. Rep. Tôhoku Univ.*, **16,** p. 321 (1927).
(3) Masiyama, Y. *Sci. Rep. Tôhoku Univ.*, **22,** p. 338 (1933).
(4) Yamamoto, M., and Miyasawa, R. *Sci. Rep. Tôhoku Univ.*, **5,** p. 22 (1953).
(5) Yamamoto, M. *Sci. Rep. Tôhoku Univ.*, **4,** p. 14 (1952).
(6) Hinton, K. G., and Round, H. J. Brit. Patent Specification 733,255.
(7) Round, H. J. *Wireless Engr*, **29,** p. 101 (1952).
(8) Sussman, H., and Ehrlich, S. L. *J. Acoust. Soc. Amer.*, **22,** p. 499 (1950).
(9) Döring, W. *Z. Phys.*, **114,** p. 579 (1939).
(10) Brown, W. F., Jr. *Phys. Rev.*, **50,** p. 1165 (1936).
(11) Bozorth, R. M., and Williams, H. J. *Rev. Mod. Phys.*, **17,** p. 72 (1945).
(12) Bozorth, R. M. *Ferromagnetism*, p. 279 (New York: D. Van Nostrand Co., 1951).
(13) Popper, P. *Soft Magnetic Materials for Communications*, p. 322. Ed. by Richards, C. E., and Lynch, A. C. (London: Pergamon Press Ltd., 1953).

The use of the stereoscopic tilt device of the electron microscope in unit-cell determinations

By J. A. GARD, B.Sc., A.R.I.C., Chemistry Department, University of Aberdeen

[*Paper received* 2 *March*, 1956]

An improved method is detailed, making use of electron diffraction of individual crystals in the electron microscope, for determination of the unit-cell dimension most nearly parallel to the electron beam. A series of diffraction patterns is recorded from a crystal tilted through known angles by the device normally used for making stereomicrographs. One of these patterns serves as a datum, for location on each of the others of the centre of its almost circular Laue zones. A new method is described for calibration of the instrument without using additional apparatus; all the factors which vary with the electron-beam potential can then be derived from a single diffraction pattern of a standard substance. A graph has also been prepared to allow correction of errors in calculation due to large angles between the "third-row" axis and the electron beam. The improvement in accuracy due to the procedure is illustrated by results obtained using crystals of known unit-cells.

The use of the three-stage electron microscope in the preparation of transmission electron-diffraction patterns of crystallites has been described by le Poole,[1] Challice,[2] Brown and Clark,[3] Rymer,[4] and Wilman.[5] The technique has two main applications, firstly, for identification of minor constituents in non-homogeneous specimens such as are common in hydrothermal preparations, and secondly, to provide sufficient information about the unit-cell to enable X-ray powder diffraction patterns of low symmetry to be indexed. Two of the unit-cell dimensions can often readily be determined with good accuracy, but estimation of the third is much less certain, as it is derived from consideration of the almost circular Laue zones[3,6] into which the electron diffraction pattern is divided. The breadth of these zones allows considerable tolerance in location of their common centre, which is normally estimated by inspection using a pair of dividers, and a wide range of results may be obtained from crystals of the same species. The wavelength of the electron beam and the effective camera length must be independently known, and both vary with the potential of the beam. The camera length cannot be measured directly, and determination of the wavelength requires special apparatus, such as a high-voltage meter, or a simple electron-diffraction camera using the same high-voltage source, in which a pattern of a standard substance is recorded simultaneously with that of the test crystal.[7]

This paper is concerned principally with improving the accuracy and convenience with which the third unit-cell dimension may be measured. A procedure is described by which the centres of sets of Laue zones from a crystallite may be located; the specimen tilting device normally used for the preparation of stereomicrographs is employed to tilt the crystal through definite angles. Descriptions are included of methods for calibration of all the factors required in the calculation of results.

The following review of the conditions governing the general form of transmission electron-diffraction patterns from single crystals will clarify the reasons for the procedures which were adopted.

GENERAL FORM OF SINGLE-CRYSTAL TRANSMISSION PATTERNS

In the electron microscope, a diffraction pattern is first obtained at the back focal plane of the objective lens, and is then imaged by the other two lenses,[4] so its general form is identical with that produced in a simple electron-diffraction camera of the same effective camera length. For simplicity, therefore, the latter system will be considered.

The thin crystals suitable for electron diffraction often lie on the supporting film with a main cleavage face approximately normal to the electron beam; this plane may be regarded provisionally as one face of the unit-cell. As the electron-beam wavelength is short, and its associated angles of diffraction small, the pattern consists of a regular network of spots, from which two unit-cell dimensions, and the angle between their directions, can be directly determined. The instrument must be frequently calibrated with a pattern from a standard material, which may be incorporated in the specimen.[5] To complete the definition of the unit-cell it is necessary to measure the third axis, which is usually part of the row of lattice points most nearly parallel to the beam, and to determine its orientation with respect to the other two. As already indicated, the spacing of this third row of lattice points may be calculated from the radii of the concentric, almost circular Laue zones into which the network is divided.[3,6] The common centre of the zones lies at the point where the plane of the diffraction pattern is intersected by the axis of the row of lattice points. The two general cases, in which the axis is exactly parallel and at an angle ϕ to the electron beam, are illustrated in Figs. 1(*a*) and (*b*) respectively.

When the angle ϕ is small, so that the form of the pattern approximates to that of Fig. 1(*a*), the centre of the zones may be located by inspection, but the zones are too few and too broad for accurate measurement of their radii. When the angle ϕ is progressively increased the centre of the zones moves in a straight line away from the direct beam; the zero order zone becomes circular, passing through the direct beam spot, and on both sides appear zones of higher orders, becoming narrower and more numerous as ϕ increases. The loci of the zone maxima become clearer, but because the area covered by the recording plate is small, location of their centre by inspection becomes less certain. If the angle of tilt ϕ and the effective camera length were known, however, the zone centre could be located with certainty, and the zone radii measured with greater accuracy.

Calculation of the third-row spacing from the radii of the Laue zones has been described by Pinsker.[6] With the electron beam and the l-th order zone at angles ϕ and ψ, respectively, to the c-axis of the crystal,

$$c = \lambda l / |\cos\psi - \cos\phi| \qquad (1)$$

where λ is the wavelength of the electron beam and l is the order of the zone (0, 1, 2, etc.).

It is much more convenient to use the radii of the zones in the calculation of c. For small angles, equation (1) may be written

$$c = \lambda l/[2|\sin^2(\phi/2) - \sin^2(\psi/2)|] \simeq 2\lambda l/[(\phi + \psi)|\phi - \psi|] \simeq (2\lambda L^2)l/[(r_0 + r_l)|r_0 - r_l|] \quad (2)$$

where r_0 and r_l are radii of the zero and l-th order zones, respectively, and L the effective camera length.

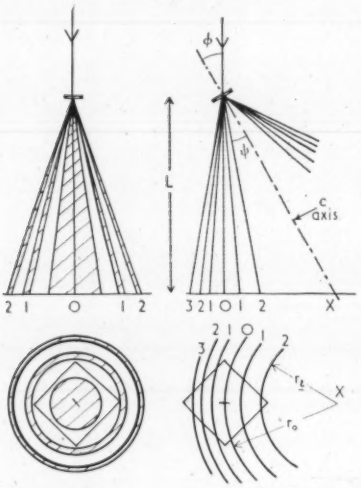

Fig. 1. Laue zones arising as cones from the c-axis of a crystal, with the c-axis (*a*) parallel to, and (*b*) at an angle ϕ to the electron beam

If the angles ϕ and ψ are large, a correction must be applied to give the true value of c. Thus:

$$\frac{\text{true } c}{\text{calculated } c} = \frac{[2\tan\phi + \tan(\phi - \psi)]\tan|\phi - \psi|}{2|\cos\psi - \cos\phi|} = F_\phi \quad (3)$$

In the section of a diffraction pattern covered by the recording plate in the Metropolitan-Vickers type EM-3 microscope, $|\phi - \psi|$ does not exceed 5°. Substituting this value in equation (3), a graph (Fig. 2) has been drawn showing the variation with ϕ of the ratio (F_ϕ) of the true and "calculated" values for c. The tolerance in measurement of the zone radii probably does not justify the use of the correction when ϕ is less than 10°. Equation (2) may now be written

$$c = F_\phi(2\lambda L^2)l/[(r_0 + r_l)|r_0 - r_l|] \quad (4)$$

It follows that for accurate measurement of the radii of the zones, $\tan\phi$ and L are required, while for calculation of c, the factor $(2\lambda L^2)$ must be known. Methods for calibration of these quantities will be described later in the text. Where extreme accuracy is not required, use may be made of the facts that an error in location of the centre of the zones does not appreciably alter the values obtained for $|r_0 - r_l|$, and that as ϕ increases, the mean value of $(r_0 + r_l)$ approaches $2r_0$, or $2L\tan\phi$. This leads to the approximation

$$c \simeq F_\phi(\lambda L)l/[|r_0 - r_l|\tan\phi] \quad (5)$$

For many purposes, it is sufficient to assume that L is constant for each nominal cathode-voltage setting, at a

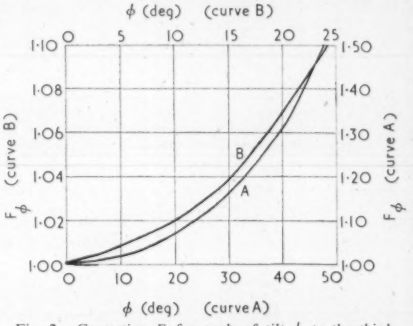

Fig. 2. Correction F_ϕ for angle of tilt ϕ, to the third-row spacing calculated from the approximate equation (2)

value of L'. The latter may be derived from a typical measurement of λL and the nominal cathode voltage. Separate calibration of λ and L is then evaded. At 80 kV, for example, $L' = (\text{typical } \lambda L)/0{\cdot}0433$.

Equation (4) may now be written

$$c \simeq 2F_\phi(\lambda L)L'l/[(r'_0 + r'_l)|r'_0 - r'_l|] \quad (6)$$

where r'_0 and r'_l are the radii of the corresponding zones when their centre is located using $L'\tan\phi$; $|r'_0 - r'_l|$ is almost identical with $|r_0 - r_l|$.

The orientation of the third unit-cell axis presents a difficult problem which is usually incapable of solution by single-crystal electron diffraction alone, but some factors can assist in finding the approximate orientation. When the specimen grid is normal to the electron beam, a high degree of symmetry is indicated in crystals of lamellar habit, if they frequently give identical diffraction patterns, of which the zero-order zone is nearly central. The third axis is normal to the other two, or nearly so, and the form of the unit-cell can be decided from the appearance of the network of spots. In other cases, a rough estimate of the orientation may sometimes be made from the angle of tilt necessary to give a diffraction pattern with the zero-order zone central; the examination of such crystals is less tedious when they have a distinctly fibrous or prismatic habit. In all cases, comparison of electron and X-ray diffraction data can be profitable, as the former gives unit-cell dimensions, and the latter d-spacings between lattice planes; these measurements are not identical in crystals of low symmetry. Electron diffraction of the mineral okenite,[8] for example, indicated the form of one unit-cell face, and comparison with X-ray fibre data enabled the other unit-cell dimension and the approximate monoclinic angle β to be estimated. The X-ray pattern was completely indexed, and the unit-cell accurately defined.

The electron-diffraction pattern may also be regarded as a section of the reciprocal lattice, and the reflexions allocated indices corresponding to the appropriate crystal planes.

Comparison of adjacent Laue zones indicates whether the unit-cell is primitive or not, as in the latter case there are characteristic systematic absences of reflexions. As an example, the diffraction patterns from lamellar crystals of synthetic potash felspar[9] shown in Figs. 3(*a*)–(*d*) indicate a *c*-face-centred monoclinic unit-cell, with (010) in the plane of the supporting film. In the c^* direction, the rows of spots in the odd order zones lie halfway between those in the even order zones, as reflexions with $(h + k)$ odd are missing.

Crystals with poor growth or cleavage commonly give electron-diffraction patterns in which an identical cross-grating of spots appears to be displaced from one zone to the next by a simple fraction of the distance between the rows of spots. The row of lattice points giving rise to the zones is clearly not along a primitive unit-cell axis, and the number of such cells spanned by adjacent points in this row is obtained from the fractional displacement. Patterns of this type are often too complex for easy analysis, and a search

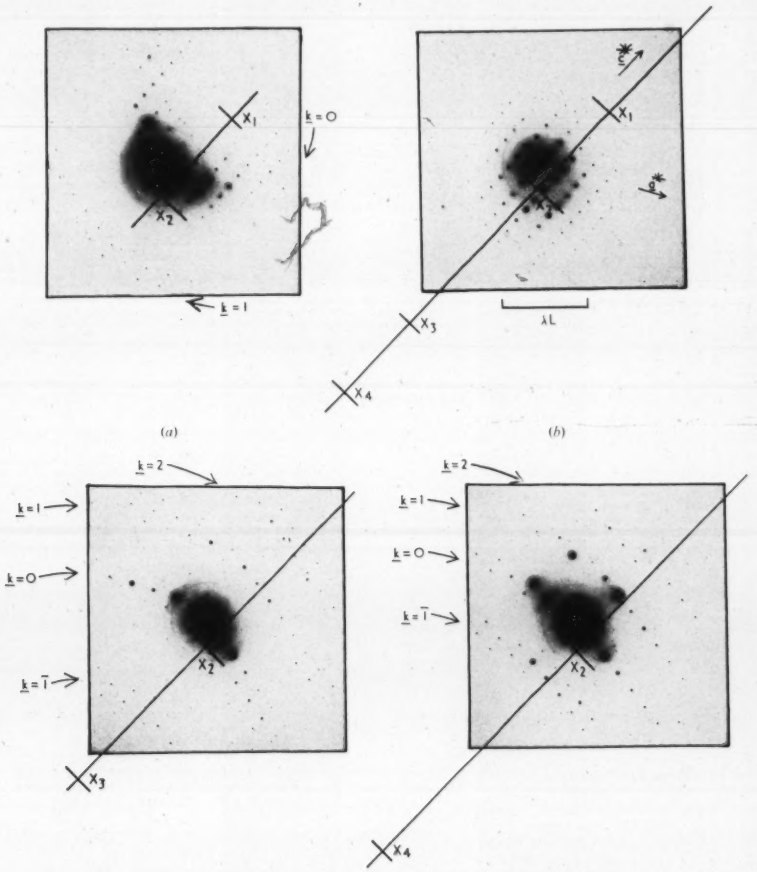

Fig. 3. A series of diffraction patterns from a (010) lamellar crystal of potash felspar, tilted to four consecutive positions. The angles of tilt from the datum position are (*a*) $-\tan^{-1} 0{\cdot}0472$, (*b*) datum, (*c*) $+\tan^{-1} 0{\cdot}0850$, (*d*) $+\tan^{-1} 0{\cdot}1287$. (*b*) shows the locus of the centres of Laue zones as the crystal is tilted; the calculated positions of the four recorded patterns are shown

for crystals with simpler orientations is usually advisable. A comparatively simple example, which will be referred to later, is shown in Fig. 4. The principal Laue zone axis is at the intersection of (010) and (30$\bar{1}$) planes of a prismatic crystal of synthetic potash felspar,[9] which has its (001) face on the supporting film. The relation of the Laue zone axis to the unit-cell is shown in Fig. 5(*a*). The cross-grating is used to record a series of electron-diffraction patterns of a crystal tilted through different angles. Each pattern carries a set of concentric Laue zones, and all the centres lie on the straight line formed where the plane traversed by the third-row axis intersects the plane of the recording plate (Fig. 6). The direction of this line depends on the orientation of the tilt axis, and also on the rotation of the image by the magnetic

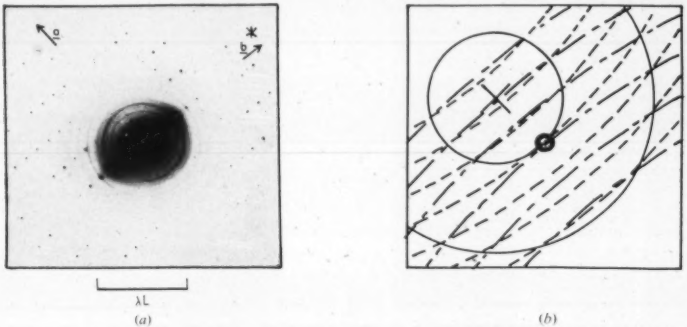

Fig. 4. (*a*) One of a series of four diffraction patterns of a crystal of potash felspar lying on (001). The specimen grid was normal to the electron beam
(*b*) Loci of the three sets of zones on Fig. 4(*a*) arising from the axes shown in Fig. 5(*a*). The crystal is in the second position of Fig. 5(*b*)

Zones from axis I ——————————
axis II — — — — — — — —
axis III —— - —— - —— - ——

displaced along one row of spots by exactly one-third of the distance between them, indicating that there are three unit-cells between lattice points on the Laue zone axis.

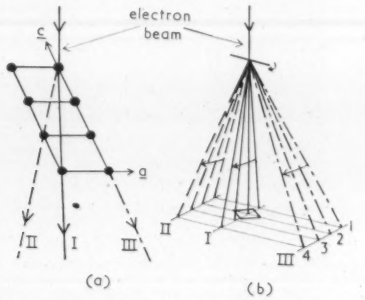

Fig. 5. Axes giving rise to the zones shown in Fig. 4, and their relation to the unit-cell of potash felspar. Axis I spans three unit-cells

POSITION OF THE CENTRES OF LAUE ZONES

In most three-stage electron microscopes, there is some arrangement for tilting the plane of the specimen about one axis for the purpose of recording stereomicrographs, without breaking the vacuum of the instrument. The device may be lenses. This rotation is equal to half the angle between a corresponding row of spots on two diffraction patterns recorded from the same crystal, with the imaging lens currents in turn normal and all reversed. It is reduced to a minimum

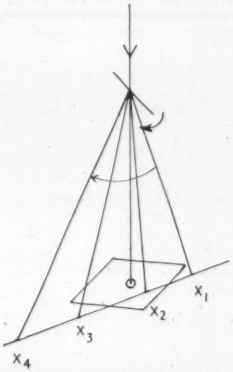

Fig. 6. Positions of the centres of Laue zones from a crystal tilted through known angles. One of the angles is selected so that the zero-order zone of the pattern is as nearly central as possible. Its centre, X_2, forms the datum for location of the zone centres of the other patterns.

when the rotations due to the objective and intermediate lenses are in the same sense, and opposite to that of the projector lens, the setting which is, incidentally, most favourable to high resolving power.

If one of the tilt angles is selected so that the zero order zone of the diffraction pattern is nearly central [X_2 in Fig. 6 and Fig. 3(*b*)], it can serve as a datum for the other patterns. The distance of each zone centre from that of the datum is the product of the effective camera length and the tangent of the angle of tilt from the datum. The method of measurement of the angles of tilt must vary in different electron microscopes. An optical method for calibration of the tilt mechanism of the Metropolitan-Vickers type EM-3 instrument is described elsewhere,[10] which, with modification, could be applied to other types of specimen stage.

ROUTINE CALIBRATION OF THE INSTRUMENT FACTORS

It has already been shown that an approximate value for the effective camera length L', is normally adequate for estimation of the third-row spacing, when the angle of inclination of this axis to the electron beam is known. It is occasionally preferable to use the more accurate equation (4) in place of equation (6), in which case it is necessary to know the absolute values of L and $2\lambda L^2$, both of which vary with the electron-beam potential V. For measurement of the two lattice dimensions in the plane of the substrate, frequent calibration of the "camera constant" λL is necessary. This is calculated from the ring diffraction pattern of a standard substance such as graphite,[5] which may be deposited on the film together with the test specimen, and the two patterns recorded simultaneously. It was thought that if the factors L and $2\lambda L^2$ could be related to λL, all the instrumental factors could be calibrated by recording a single diffraction pattern.

Consideration of the imaging system of the three-stage electron microscope (Fig. 7) suggests that this should be possible. A diffraction pattern is first formed at the back focal plane of the objective lens,[1,4] and may be imaged by the intermediate lens at the focal plane of the projector lens. A magnified pattern is then projected by the latter on the viewing screen. Any change of the beam potential V alters the focal lengths of all the lenses, as they are proportional to V, but it is necessary to restore those of the objective and intermediate lenses to their initial values in order to retain an image of the pattern on the screen [Fig. 7(*b*)]. This means that after adjustment of the lens currents, λL is inversely proportional to the focal length of the projector lens f_p, i.e. to the beam potential V as the pole pieces of this lens are saturated during normal operation. This gives rise to the following relationships.

$$\lambda L = k_1/f_p = k_2/V$$

where k_1 and k_2 are constants, and f_p the projector lens focal length.

But $\lambda = (150/V)^{\frac{1}{2}}$ (de Broglie[11])

Therefore: $\lambda L = (k_2/150)\lambda^2$

$$L^2 = (k_2/150)\lambda L$$

$$L = k(\lambda L)^{\frac{1}{2}} \qquad (7)$$

where $k = (k_2/150)^{\frac{1}{2}} = \text{constant}.$

$$2\lambda L^2 = 2(\lambda L)L.$$

Substituting equation (7) for L,

$$2\lambda L^2 = 2k(\lambda L)^{\frac{1}{2}} \qquad (8)$$

From equation (7) $k = (L/\lambda)^{\frac{1}{2}}$ (9)

To test the validity of this hypothesis, and to evaluate the constant k, some means of comparing λL with λ at various gun voltages was necessary. As a high-voltage meter was not available, and in any case a more direct means of comparison was preferable, the microscope was temporarily converted to a simple electron-diffraction camera. The imaging lenses were replaced by a brass cylinder sealed between the specimen and viewing chambers. A specimen grid carrying magnesium oxide smoke was inserted in the stage, and its diffraction pattern recorded at the nominal 40, 60, and 80 kV settings of the cathode voltage, using the condenser lens to focus the rings on the plate. The distance from specimen to plate was accurately measured, and the wavelengths of the beam calculated from the ring diameters. The electron microscope was reassembled immediately, and diffraction patterns from the same specimen again recorded at the 40, 60, and 80 kV settings. As the whole experiment was done on the same day, and the stabilizer batteries were new, it may reasonably be assumed that there was no appreciable change in the cathode voltages. The experimental values for λ and λL, and values of L and $k[=(L/\lambda)^{\frac{1}{2}}]$ derived from them, are given in Table 1.

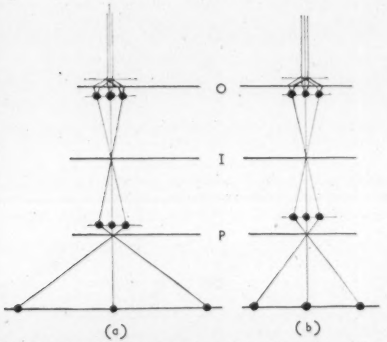

Fig. 7. The effect of cathode voltage V on λL. λL is shown to be inversely proportional to the focal length of the final projector lens. Thus $\lambda L = \text{constant}/V$

Table 1. *Calibration of the constant* $(\lambda L)^{\frac{1}{2}}$

Nominal voltage (kV)	40	60	80
λ(Å)	0·0589	0·0482	0·0418
λL (mm)	53·6	37·0	27·2
L (mm)	911	767	651
$(L/\lambda)^{\frac{1}{2}} = k$	124·3	126·1	124·6

The term $(L/\lambda)^{\frac{1}{2}}$ was thus shown to be practically constant over a very wide range of cathode voltage, at a value of $125 \pm 1\%$ in this particular microscope. The normal variation in cathode voltage due to deterioration of the stabilizer batteries is comparatively small. Equations (8) and (9) become, for this value for k:

$$L = 125(\lambda L)^{\frac{1}{2}} \qquad (10)$$

$$2\lambda L^2 = 250\,(\lambda L)^{\frac{1}{2}} \qquad (11)$$

It is probable that the value of k will vary considerably in

different microscopes, but once it has been determined in the manner described, calibration of λL alone is necessary.

In the calculations and experiment described above, only the effect of variation in cathode voltage was studied. For several reasons the height of a crystal above the objective lens may differ slightly from one specimen to another. Considerations similar to those leading to equation (5) suggest that the overall error is not serious, provided that the camera constant is calibrated with an internal standard. This was confirmed by an experiment in which two series of patterns were recorded from the same crystal; the specimen cartridge was clamped (*a*) in the normal position, and (*b*) much higher in the tilt block. In spite of the fact that the ratio of objective focal lengths was as high as 1·35, the estimated lattice spacing was within 1% of the true value in both series.

PROCEDURE FOR MEASUREMENT OF THE RADII OF LAUE ZONES

Practical details of the procedure will now be described. A series of diffraction patterns is recorded from a crystal tilted through known angles, as described earlier in the text, so that the zero order zone of the datum pattern is nearly central. The distance of the zone centre from the datum ($L \tan \phi$) is calculated for each pattern. The datum plate is placed in the centre of an illuminated viewing screen, and a large sheet of tracing cloth is stretched over it. The positions of the direct electron beam spot, the edges of the plate, and the estimated centre of the zero-order zone, are marked on the cloth. The latter point forms the datum, and a straight line is drawn through it [Fig. 3(*b*)] in a direction determined by that of the tilt axis and the rotation due to the lenses. The first plate is replaced by another, which is fixed on the cloth in a similar position with two lengths of cellulose tape. A vernier caliper gauge with needle points is most convenient for measuring the zone radii. One point is located in a centre-punch mark on a piece of brass, which is fixed to the cloth with cellulose tape at the calculated position of the zone centre. The gauge is adjusted to measure the radii of the zone maxima in turn. The procedure is repeated for each plate, the radii tabulated, and the lattice spacings calculated. It is sometimes possible to adjust the datum point to give better overall agreement.

EXPERIMENTAL EVALUATION OF ACCURACY

In order to estimate the accuracy obtainable when the described procedure is followed, the third-row spacing was determined of crystals with known unit-cells. During examination of these and other crystals, it was observed that, in general, accuracy improved with increase of: (*a*) the thickness of the crystal, (*b*) the length of the dimension giving rise to the zones, and (*c*) the angle of tilt from the datum position.

The overall accuracy cannot therefore be clearly defined, but it is usually between 1 and 5% on a mean of results from four or more crystals of the same species. A better measure of the value of the procedure is given by comparison of results obtained with and without its use. A number of patterns with clearly defined zones were selected from series made using the procedure. On these, maximum and minimum apparent values for the third-row spacing were obtained, using the extremes of zone-centre positions which could be located by inspection. Comparison of mean results from flakes of muscovite and from lamellar synthetic potash felspar[9] are given in Table 2, which demonstrates clearly the improvement in accuracy due to the procedure.

Table 2. *Improvement in accuracy due to the procedure*

	Muscovite c (Å)	*Potash felspar* b (Å)
True value	20·04	12·90
(i)		
Result	20·9 ± 0·7	12·75 ± 0·2
Error (%)	+4·0	−1·2
(ii)		
Minimum	14·65	8·5
Maximum	23·65	13·9
Error (%)	−27 to +18	−34 to +7·8

(i) Results obtained using the tilt procedure.
(ii) Results obtained using inspection.

An independent check on the general principles of the procedure and the calibration of the instrument was afforded by a set of four patterns, one of which is shown in Fig. 4; from the prismatic crystal of potash felspar[9] already referred to. The crystal was about 3000 Å thick, so it was assumed to be free from distortion. The (001) planes of the crystal were normal to the beam, and the *a*-axis almost coincided with the axis of tilt. Close inspection revealed that each pattern could be regarded as three intersecting sets of Laue zones arising from different rows of lattice points in the (010) plane (Fig. 5). The position of the centre of each Laue zone was calculated from the geometrical arrangement of the unit-cell; the radii of each set of zones were measured, and the lattice spacings calculated. Correction of the results by reference to the graph in Fig. 2 was necessary. The results are compared with the corresponding spacings obtained from the unit-cell of orthoclase felspar (i.e. *c*-centred monoclinic: $a = 8{\cdot}45$, $b = 12{\cdot}90$, $c = 7{\cdot}15$ Å, $\beta = 116°$) in Table 3, below.

Table 3. *Estimated spacings along three axes of a* (001) *crystal of potash felspar*

Axis	I	II	III
Angle to I	0°	12°27′	23°9′
True spacing (Å)	19·30	13·07	7·15
Estimated spacing (Å)	19·3	13·0	7·07
Error (%)	0	−0·5	−1·1

Axis I is at the intersection of (010) and (30$\bar{1}$).
Axis II is at the intersection of (010) and (20$\bar{1}$)
Axis III is at the intersection of (010) and (100).

The excellent agreement between the estimated and the true values for the spacings, in a case where the effective angles of tilt are decided by the unit-cell of the crystal, confirms the reliability of the procedure.

DISCUSSION

It has been demonstrated that the accuracy with which the radii of Laue zones are measured, and with which the third-row spacing is calculated, may be improved considerably by use of the procedures described in the text. They are applicable in principle to any type of tilt mechanism capable of calibration. They have now been used on a large number of crystal species, and have given much assistance in identification of unknown crystals and in elucidation of unit-cells. The most successful applications have been to crystals of thin lamellär or prismatic habit having the third row of the lattice almost normal to their principal face. Since control of the tilt is limited in the existing specimen stage, certain types of crystal cannot be suitably oriented. Flakes of poor cleavage rarely lie with an easily recognizable plane normal

to the electron beam, while crystals of low symmetry seldom have a row of lattice points sufficiently near to it to give well-defined Laue zones. In such cases a more flexible control of orientation would be advantageous. Brown and Clark[3] have already expressed the need for a specimen stage allowing rotation of the specimen about three mutually perpendicular axes during normal operation. The mechanical requirements for such a stage conflict with those permitting the highest resolving power. A stage suitable for electron diffraction should therefore be readily capable of alternation with the existing stage, in order to allow the potentialities of the instrument to be fully realized.

ACKNOWLEDGEMENTS

The author wishes to thank Prof. R. M. Barrer, of Imperial College, London University, and Dr. H. F. W. Taylor, of Aberdeen University, for their continued interest in this work, and for their helpful advice.

REFERENCES

(1) LE POOLE, J. B. *Philips Tech. Rev.*, **9**, p. 33 (1947).
(2) CHALLICE, C. E. *Proc. Phys. Soc.* [*London*] *B*, **63**, p. 59 (1950).
(3) BROWN, J. F., and CLARK, D. *Acta Cryst.*, **5**, p. 615 (1952).
(4) RYMER, T. B. *Brit. J. Appl. Phys.*, **4**, p. 297 (1953).
(5) MATTHEWS, H. I., and WILMAN, H. *Brit. J. Appl. Phys.*, **6**, p. 277 (1955).
(6) PINSKER, Z. G. *Electron Diffraction*, pp. 80–88 (London: Butterworths Scientific Publications, 1953).
(7) YAMAGUCHI, S. *Rev. Sci. Instrum.*, **26**, p. 89 (1955).
(8) GARD, J. A., and TAYLOR, H. F. W. *Min. Mag.*, **31**, p. 5 (1956).
(9) GARD, J. A., BARRER, R. M., and BAYNHAM, J. *J. Chem. Soc.*, p. 2480 (1955).
(10) GARD, J. A. *J. Sci. Instrum.*, **33**, p. 307 (1956).
(11) DE BROGLIE, L. *Dissertation* (Paris: Masson, 1924); *Ann. Phys.* [*Paris*], **3**, p. 22 (1925).

A possible source of error in the interpretation of electron diffraction patterns

By G. D. ARCHARD, A.Inst.P., Associated Electrical Industries Ltd., Aldermaston, Berks

[*Paper received* 2 *March*, 1956]

It is shown that a slight degree of preferred orientation of the crystallites in an electron diffraction specimen may be represented as the combination of two types of orientation which produce different kinds of distortion in the diffraction pattern. Unless special precautions are taken, these may lead to erroneous values of the Bragg angles deduced from ring radii.

It is well known that, when the crystallites comprising the specimen in an electron diffraction camera have a strongly preferred orientation, the diffraction pattern consists of discrete arcs rather than the complete rings which obtain when the orientation is random. At an intermediate stage ("partial orientation"), it may be impossible to detect any arc formation by eye, but careful measurement will show that the diameter of the ring is a function of azimuth. It appears unlikely that a specimen will ever possess completely random orientation, and it therefore becomes important, when accuracy better than 0·1 % is envisaged, to know whether the diameters of the rings which suffer from a slight degree of orientation correspond to the true Bragg angles.

Two kinds of orientation, which may reasonably be expected to affect a polycrystalline specimen, may be described as type *a* and type *b* (Figs. 1 and 2). In type *a* orientation, a particular axis in the crystallite tends to settle at as great an angle as possible to an axis fixed in space (i.e. perpendicular to it). In type *b* orientation, a particular axis in the crystallite tends to lie as nearly as possible parallel to an axis fixed in space. In general, types *b* and *a* tendencies may exist together, but, for simplicity, they will at first be considered separately.

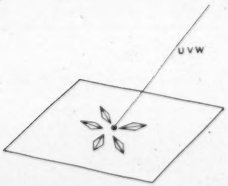

Fig. 1. Type *a* orientation. Most crystals have long axes in a plane perpendicular to a line with direction cosines *uvw*,

TYPE A ORIENTATION

Consider a rectangular system of axes set up in an electron diffraction camera, the negative *z* axis corresponding to the direction of the electron beam. In the camera, imagine a

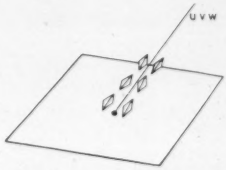

Fig. 2. Type *b* orientation. Most crystals have long axes parallel to a line with direction cosines *uvw*

crystallite (the "reference" crystallite), the normal to the (*hkl*) plane of which has direction cosines (*uvw*) with respect to the camera axes. Consider also a similar crystallite, the normal to the (*hkl*) plane of which has direction cosines:

$$\cos\mu\cos\lambda, \quad \cos\mu\sin\lambda, \quad \sin\mu$$

This means that the electron beam strikes the (*hkl*) plane in the second crystallite at glancing angle μ, and that its plane of incidence lies at an azimuth λ, measured from the *x* axis.

The angle between the (hkl) planes of the two crystallites is thus given by:

$$\cos\theta = u\cos\mu\cos\lambda + v\cos\mu\sin\lambda + w\sin\mu \qquad (1)$$

Now suppose that, owing to some directional bias in the preparation of a polycrystalline specimen, the normals to the (hkl) planes of the majority of the crystallites lie approximately at right-angles to that of the reference crystallite, that is, that there exists a preferential orientation given by $\theta = \pi/2$. This may be visualized by analogy with a thin metal disk, on which a straight line is drawn, falling through a viscous liquid; the disk will tend to fall with its faces horizontal, so that the straight line drawn on it remains approximately at right angles to the direction of gravity, but has no marked tendency to settle in any particular azimuth.

This kind of orientation may reasonably be represented by the probability function:

$$P(\theta)d\Omega = A\exp(\kappa\sin\theta)d\Omega \qquad (2)$$

where κ is fairly large compared with unity (see Appendix) and $d\Omega$ is the elementary solid angle. Thus the probability is at a minimum for $\theta = 0$, and at a maximum for $\theta = \pi/2$ (θ is limited to the range $0 \leqslant \theta \leqslant \pi/2$, so there is no question of a change of sign).

Reflexions arise only from lattice planes presented at angles not too far removed from the Bragg angle, so that, when orientation is random, the intensity distribution measured radially across a diffraction ring has the approximate form:

$$I(\mu) = \exp\left[-(\mu-\mu_0)^2/2\sigma^2\right] \qquad (3)$$

When the orientation probability is given by equation (2), however, the diffraction ring arising from the plane in question has the intensity distribution:

$$I(\mu) = \exp\left[-(\mu-\mu_0)^2/2\sigma^2 + \kappa\sin\theta\right] \qquad (4)$$

in which $\theta = \theta(\mu\lambda)$ is given by equation (1). The peak of the intensity contour (with reference to which measurements of ring radii are ordinarily made) no longer occupies a position corresponding to the exact Bragg angle μ_0, but may be located by differentiating the right-hand side of equation (4) with respect to μ, and equating the result to zero. Thus:

$$\mu_{peak} - \mu_0 = \frac{\sigma^2\kappa[p\cos(\lambda-\lambda_0)\cos\mu + w\sin\mu][p\cos(\lambda-\lambda_0)\sin\mu - w\cos\mu]}{\{1-[p\cos(\lambda-\lambda_0)\cos\mu + w\sin\mu]^2\}^{1/2}} \qquad (5)$$

wherein $p = u\sec\lambda_0 = v\operatorname{cosec}\lambda_0$.

This represents an azimuth-dependent deviation of the measured position of the diffraction ring from the position which it would occupy in the absence of preferred orientation. As, in electron diffraction, μ is usually small, the terms in $\sin\mu$ on the right-hand side of equation (5) may be omitted, and $\cos\mu$ may be set equal to unity. If the square root in equation (5) be expanded, the result is:

$$\mu_{peak} - \mu_0 \simeq -\sigma^2\kappa w p[\cos(\lambda-\lambda_0) + \tfrac{1}{2}p^2\cos^3(\lambda-\lambda_0) + \tfrac{3}{8}p^4\cos^5(\lambda-\lambda_0) + \ldots] \qquad (6)$$

The power series can be converted into a Fourier series containing only *odd harmonics* of $(\lambda - \lambda_0)$ by elementary methods. These Fourier components would be detected if an harmonic analysis were made of the ring. All the harmonics would have the same value of λ_0 (which may be called the "particular azimuth" of the ring). Equation (6) also indicates that the average radius of the ring (determined by measuring diameters at many regularly spaced azimuths) corresponds to the exact Bragg angle μ_0.

Now consider the crystallites macrocosmically, as irregular polyhedra. If many such polyhedra are thrown on to a plane which is horizontal except for small random undulations, most of them rest on one of their faces, so that *some* face is always nearly horizontal, as the two-dimensional analogue in Fig. 3 shows. The relation of the crystallites to their supporting membrane is unlikely to be as simple as this, but, even if there were only a slight tendency for it to be so, there would exist a certain orientating influence with respect to *each* exterior face.

Let the whole mass of crystallites be divided into groups:

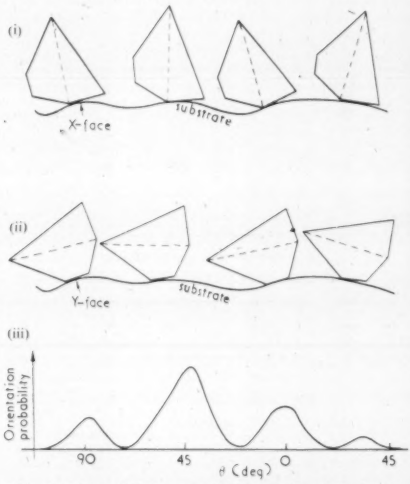

Fig. 3. Curve (iii) shows probability of dotted line in (i) and (ii) being inclined at θ° to horizontal

one group containing all those which rest upon a face such as X (so that the normals to all lattice planes perpendicular to an X face tend to be horizontal, i.e. have type a orientation with respect to the vertical); another group containing all those which rest upon a face such as Y, and so on. If now attention be fixed on the X group, it is apparent that only the lattice planes perpendicular (or nearly perpendicular) to an X face will give observable diffraction rings (assuming that the electron beam impinges approximately vertically). By virtue of the tendency of the X faces to lie nearly horizontal, these planes will have type a orientation with respect to the corresponding planes in a reference crystal which has its X face vertical. Consequently they will have odd harmonics and particular azimuths. It is not difficult to see that the angle between two such particular azimuths will be equal to the angle between the corresponding lattice planes. If, however, the specimen is tilted, so that the electron beam no longer falls on the crystals approximately perpendicular to the plane on which the faces rest, this angular property will

be lost, since, for example, the number of crystals with indices *hkl* in a position to reflect may now exceed the corresponding number of crystals with indices *khl* (indices being assigned with respect to the external form of each crystal so that they are not necessarily commutable even for cubic lattices).

Quite independently, the group of crystallites resting on faces such as *Y* will give rise to rings having odd harmonics and particular azimuths, for the lattice planes perpendicular to face *Y*. There will not necessarily be a simple relationship between the particular azimuths of lattice planes belonging to different groups. Also, the more complicated lattice planes, lying skew with respect to the external faces of the crystallites, may not show particular azimuths at all.

EXPERIMENTAL CORRELATION

Butler[1] made harmonic analyses of a number of electron diffraction photographs of gold leaf and alkali halides. After the removal of first and second harmonics, which were shown to be produced largely by the instrument,[2,3] there remained a number of higher harmonics. These were predominantly of *odd* order [compare equation (6)]. All the harmonics pertaining to a specified ring contained (within the limits of experimental error) the same "particular azimuth." The particular azimuths pertaining to different rings were usually related to one another in a manner typified by the following example:

Gold leaf. Particular azimuth of (220) taken as zero.
Particular azimuths of (111) (002) ($\bar{1}\bar{1}3$) were, respectively: 30°, 89°, 105°.
Angles between these planes and (220) were, respectively: 35°, 90°, 115°.

In the case of another gold specimen, the (113) ring appeared to have a particular azimuth intermediate between those which would have been predicted for ($\bar{1}\bar{1}3$) and (113), considered separately. Another specimen was tilted so that the plane of the substrate no longer remained approximately perpendicular to the electron beam. Particular azimuths were found, but they did not possess the former inter-azimuth property.

TYPE B ORIENTATION

Pure type *b* orientation follows the same lines as type *a* orientation, save that the probability function of equation (2) is replaced by

$$P(\theta)d\Omega = A \exp(\kappa \cos\theta)d\Omega \qquad (7)$$

The deviation of the peak of the diffraction line from that corresponding to the true Bragg angle then becomes:

$$\mu_{peak} - \mu_0 = \sigma^2\kappa[p \cos(\lambda - \lambda_0) \sin\mu - w \cos\mu] \qquad (8)$$

Here, the azimuth-dependent term is small, since it contains $\sin\mu$. As it also involves only the first harmonic of $(\lambda - \lambda_0)$, it would almost certainly be submerged by instrumental effects. The remaining term, $\sigma^2\kappa w\cos\mu$, is important, for it represents an increase or decrease in the radius of the ring, which is constant for all azimuths. That is, the ring may appear perfectly circular, *but it may not yield the correct Bragg angle*. It is, moreover, difficult to see how this error could be quantitatively determined, since the orientation function is only described qualitatively.

It is conceivable that both types *a* and *b* tendencies may exist simultaneously, and their effects will then be superimposed; this may be shown formally by using a probability function of the form:

$$P(\theta) = A \exp[\kappa \cos(\theta - \theta^*)] \qquad (9)$$

Particular azimuths will be found, together with odd harmonics, but it will still be impossible to remove the type *b* part of the discrepancy by averaging the ring diameters for many azimuths, since a term analagous to $\sigma^2\kappa w \cos\mu$, constant for all azimuths, remains.

This constant term depends on four factors: σ^2 (which represents the breadth of the line, narrow lines show less discrepancies), κ (which represents the degree of randomness, the more random the orientation the better), w (which represents the particular direction with respect to which the orientation is of type *a* or type *b*, w is zero if this direction is perpendicular to the electron beam), and $\cos\theta^*$ (which represents the proportion of type *b* tendency). Of these, the most susceptible to control seems to be w.

CONCLUSIONS

Partial orientation of the crystallites in an electron diffraction specimen may be represented by the combination of two tendencies, in which, respectively, a particular axis of each crystallite lies preferentially in a fixed plane (type *a* orientation), or in a fixed direction (type *b* orientation). Type *a* orientation yields diffraction ring shapes characterized by a series of odd harmonic terms containing "particular azimuths" peculiar to each ring. Certain simple relations may exist between the particular azimuths of different rings. By measuring ring radii at many azimuths, the effects of the harmonic terms may be averaged out. Type *b* orientation yields a constant term which cannot be removed by averaging, and which may therefore lead to erroneous values of Bragg angles.

ACKNOWLEDGEMENTS

The author wishes to thank Dr. T. B. Rymer for making available experimental information and for helpful comment, Mr. M. E. Haine, Mr. A. E. Ennos, and Dr. J. S. Halliday for helpful comment, and Dr. T. E. Allibone, Director of this laboratory for permission to publish this note.

REFERENCES

(1) BUTLER, C. C. *Ph.D. Thesis*, University of Reading (1946).
(2) RYMER, T. B., and BUTLER, C. C. *Phil. Mag.*, **36**, pp. 515, 821 (1945).
(3) RYMER, T. B., and BUTLER, C. C. *Proc. Phys. Soc. [London]*, **59**, p. 541 (1947).

APPENDIX

The author is indebted to Dr. T. B. Rymer for the following commentary on the numerical values involved. Bearing in mind dynamical interaction effects,* the quantity σ may be taken to be of the order of 10^{-2}. The measured amplitude of the third harmonic on a typical photograph corresponded to a value of $\mu_{peak} - \mu_0 = 5{\cdot}10^{-4}$. The quantity wp^3 in equation (6) would be of the order of 1/3. Thus from equation (6):

$$\kappa = 30$$

Hence the function $P(\theta)$ of equation (2) falls to half its peak value when θ deviates about 12° from the 90° which corresponds to the maximum. This seems a reasonable value for the width of the probability function.

* RYMER, T. B. *Brit. J. Appl. Phys.*, **4**, p. 297 (1953).

The flow of air through beds of charcoal

By W. M. Jones, D.Phil., A.Inst.P., Physics Department, University College of Wales, Aberystwyth

[*Paper first received* 25 *January, and in final form* 19 *March*, 1956]

It is shown experimentally that the flow of air through beds of irregular porous granules of charcoal may be correlated with that through beds of solid spheres by using the usual equations for flow through granular beds. The envelope specific volumes of the charcoal granules are found with mercury after impregnating the granules with paraffin wax, and the envelope specific surface areas of the granules are deduced from measurements of the projected area and shape of the granules, according to the procedure laid down by Heywood.[4]

The resistance of beds of solid spheres to the flow of fluids through them may be expressed in terms of the diameter, length, and porosity of the bed, the viscosity, density, and velocity of flow of the fluid, and the diameter of the spheres making up the bed. If the spheres are not all of the same diameter, a mean effective diameter can be calculated provided the distribution of diameters among the spheres is known; if the particles are not spheres, but are all of the same shape, a mean effective diameter can be calculated provided the surface area, volume and linear dimensions of each particle be known. (Rose, p. 114, and Mott, p. 242 of Ref. 1.) When the particles are irregular it has been suggested that the calculation of the resistance to flow of a bed may be attempted through taking Heywood's projected area as basis and that comparisons should be made with those of single disks (Mott[1]). In attempting to solve a problem connected with the flow of air through beds of charcoal the author was able to test this last point of view experimentally and found that Heywood's projected area is indeed a satisfactory basis for comparison, but that a simpler approach could be made to the problem by regarding the granular bed as a bundle of capillaries thus deriving, after Carman, an equation for the resistance to flow which is very similar to Kozeny's well-known equation.

This paper is concerned with, firstly, briefly reviewing the theoretical approach to a granular bed regarded as a bundle of capillaries, secondly, describing the experiments and presenting the results, and lastly, discussing the results in the light of previous work.

THEORETICAL

The simplest model to adopt of a porous bed is that of a bundle of identical circular capillaries. Then if there are n such capillaries of radius r and equivalent length l_e threading a cylindrical granular bed, of circular cross-section, the volume of the voids in the bed is

$$n'\pi r^2 l_e = (\epsilon\pi D^2 l)/4$$

where ϵ is the porosity of the bed, D its diameter, and l its length. Putting l_e/l equal to $\sqrt{2}$,[2]

$$\epsilon = (4\sqrt{2}n'r^2)/D^2 \qquad (1)$$

The surface area of the capillaries is

$$2n'\pi r l_e = [(S\pi D^2 l)/4] + \pi D l$$

where S is the envelope surface area of the particles in 1 cm^3 of bed, and hence

$$S + (4/D) = (8\sqrt{2}n'r)/D^2 \qquad (2)$$

From equations (1) and (2),

$$r = 2\epsilon/[S + (4/D)] \qquad (3)$$

The velocity at which fluid flows through a capillary is $u_m = V/n'\pi r^2$, where V is the volume rate of flow of fluid through the bed. Hence, from equation (1),

$$u_m = (4V\sqrt{2})/\pi D^2\epsilon = (u\sqrt{2})/\epsilon \qquad (4)$$

where u is the velocity of flow of fluid into, or out of, the bed. Proceeding now as in the case of tubes the friction factor λ for a fluid of density ρ is given by

$$\lambda = \frac{2\Delta p r g}{l_e \rho u_m^2} = \frac{\sqrt{2}\Delta p \epsilon^3 g}{l\rho u^2[S + (4/D)]} \qquad (5)$$

and the Reynolds number R_e by

$$R_e = \frac{r u_m \rho}{\eta} = \frac{2\sqrt{2}u\rho}{[S + (4/D)]\eta} \qquad (6)$$

When $\log \lambda$ is plotted as a function of $\log R_e$ for tubes, a single straight line of slope 45° is obtained in the region of streamline flow and a single straight line of slope $\tan^{-1}\frac{1}{4}$ in the region of turbulent flow, for all tubes. The portion of the curve corresponding to the transition region between streamline and turbulent flow usually varies in character from tube to tube.

The aim of experimenters working on flow through granular beds must be to represent the flow through all such beds by one curve such as that obtained for tubes. As explained above, this aim has been realized already for beds of solid spheres and beds of solid particles of some other shapes and it is the purpose of this paper to show that by using the equations (5) and (6) this can be accomplished with beds of irregular porous particles.

EXPERIMENTAL

To apply equations (5) and (6) the quantities u, Δp, ϵ and S must be measured for different values of l and D. Also, since air is a compressible fluid, ρ must be known at the region where u is measured; the region immediately below the bed (i.e. on the low-pressure side) was chosen for the measurement of u, and the density ρ below the bed was calculated from the known total pressure in that region.

The granular beds were made up from samples of charcoal, to be described, by pouring the charcoal into cylindrical containers through crossed gauzes, to give reproducible packing. Gauze or filter pads held the charcoal in position. Ordinary laboratory air was drawn through the bed by a mechanical pump, the rate of flow through the bed being adjusted by a stout screw-clip on rubber tubing attached to a buffer volume between the pump and the bed.

The velocity of flow was determined from the volume flow recorded by a rotameter type flowmeter; readings on the flowmeter were corrected for changes of temperature and pressure in the flowmeter and the calibration of the flowmeter was checked.

The pressure drop Δp across the granular bed was measured

with a water manometer, except when Δp was less than 4 cm of water when an aniline-sodium carbonate manometer was used. Any pressure drop occurring in the tubing and in the container of the bed was allowed for from blank experiments. The kinetic energy correction was negligible in all cases. Unless results determined with increasing rates of flow agreed with those determined with decreasing rates of flow the results were ignored until the discrepancy was removed. As a final check on the experimental procedure in determining the flow some experiments were done with straight tubes of known dimensions and the results compared with those of previous workers; the agreement was within the experimental error.

To find ϵ, the envelope volume V_ϵ of the particles per gramme must be found, then ϵ can be determined from the weight and volume of the bed. The difficulty in determining V_ϵ by the usual technique of enveloping the particles in mercury in an evacuated container is that the particles are porous and mercury can penetrate some of the pores. An attempt was therefore made to seal such pores by immersing the charcoal in molten paraffin wax and then superficially drying the paraffin from the charcoal by rolling the charcoal over filter papers at about 65° C. The object of the "drying" was to clean the paraffin from the outside of the charcoal whilst retaining the paraffin in the pores. The envelope volume was then determined with mercury, after cooling. The results were erratic, probably due to too much paraffin being removed in some cases and too little in others, but the results were smoothed out by plotting ϵ as a function of D_m/D, where D_m is the mean sieve size of the particles making up the bed, and drawing the best straight line through the collection of points. [That ϵ should vary linearly with D_m/D has been established experimentally (Ref. 1, p. 249.) Also, when the porosity (ϵ^1) was determined with mercury but with no wax in the pores it was found that ϵ^1 varied linearly with D_m/D for a given sample of charcoal thus justifying the use of a linear relationship between ϵ and D_m/D.] Values of ϵ and V_ϵ were then taken from this straight line.

To find S, the envelope surface area S_0 of a unit weight of granules was found and S determined from the weight of unit volume of the bed. To find S_0 the following procedure was adopted. The specific projected area A of the charcoal settled in its most stable position was found from measurements with an apparatus very similar to that used by Beirne and Hutcheon.[3] The number of particles per gramme, N, was found by counting the number of particles in a known weight manually. (About 200 particles of sample 24 to about 1 000 particles of sample 29 were counted, the number counted increasing with the decreasing size of particle. To estimate N for sample 30, an apparently uniform layer of particles, as judged by eye, was spread on a sheet of graph paper and the number in a known fraction of this counted; the charcoal covering the whole sheet of graph paper was weighed.) The average length, L, of a particle and its breadth, B, were determined from microscopic measurements on fifty particles. Hence, the following could be calculated:

d_p, the mean projected diameter, from $d_p^2 = 4A/\pi N$;
k, Heywood's volume constant, from $k = V_\epsilon/Nd_p^3$;
n, the elongation index, from $n = L/B$;
f, Heywood's surface coefficient,[4] from $f = 1{\cdot}57 + Ck^{4/3}[(n+1)/n^{\frac{1}{3}}]$;
S_0, the specific surface determined optically,[4] from $S_0 = Nfd_p^2$.

In the equation used to determine f the quantity C was put equal to 3·1 since examination of the charcoal granules suggested they belonged to Heywood's group of angular particles.[4]

RESULTS

Seven samples of charcoal (Table 1) were used for the flow experiments. Using these seven samples about twenty charcoal beds were made up (Table 2). One bed (No. 23) was made from lead shot in the B.S.S. range 8 to 10, for the direct comparison of flow through beds of irregular porous granules with that through beds of solid spheres. Assuming no error arises in measuring average quantities because of the size of the sample of charcoal used in the measurements, the probable errors in the quantities quoted in Tables 1 and 2 can be estimated from the accuracy of observation and the number of observations; these errors are given at the heads of the columns in Tables 1 and 2. (D_m was determined with calibrated sieves.) In estimating the error in S_0 it is assumed that the value 3·1 used for C in the above formula is correct; should the value be 3·3 then a further error of 3% is introduced into S_0, this being an absolute error as distinct from an experimental error.

The results of the flow experiments are summarized in the figure where $\log \lambda$ is plotted as a function of $\log R_e$. The size of the circles is an indication of the experimental accuracy. The points representing all the results, including those for lead shot, fall on to a narrow band, with the central line of the band appearing to depart from linearity when $R_e \simeq 0{\cdot}5$. The linear portion of the line has a slope of 45° and shows λ to be related to R_e through the equation $\lambda = 9/R_e$.

Table 1. *Description of the samples of charcoal*

Sample No.	*B.S.S. range*	$N \pm \frac{1}{2}\%$ (g^{-1})	$A \pm 1\frac{1}{2}\%$ (cm^2g^{-1})	$V_\epsilon \pm 2\%$ (cm^3g^{-1})	D_m (*cm*)	$d_p \pm \frac{1}{2}\%$ (*cm*)	$k \pm 3\%$	$\frac{L}{2\ to\ 4\%}$ (*cm*)	$\frac{B}{2\ to\ 4\%}$ (*cm*)	$\frac{n}{3\ to\ 5\frac{1}{2}\%}$	$S_0 \pm 3\%$ (cm^2g^{-1})
24	− 7 + 8	230	12·4	1·51	0·223	0·262	0·37	0·377	0·265	1·42	52·3
25	− 8 +10	288	13·0	1·57	0·187	0·240	0·39	0·373	0·233	1·60	59·1
26	−10 +12	566	17·3	1·49	0·154	0·197	0·39	0·268	0·188	1·42	76·6
27	−12 +14	1030	21·1	1·66	0·131	0·162	0·39	0·227	0·159	1·43	93·5
28	−14 +16	1715	26·0	1·48	0·110	0·139	0·32	0·171	0·132	1·30	99·7
29	−16 +18	2560	29·9	1·47	0·093	0·122	0·31	0·160	0·123	1·30	119·2
30	−52 +60	$3{\cdot}6 \times 10^5$	143	1·57	0·027	0·023	0·36	0·051	0·034	1·60	630·0

Table 2. *Description of the beds of charcoal*

No. of bed	D (cm)	l (cm)	Charcoal sample No.	$\epsilon \pm 2\%$	$S \pm 3\%$ (cm^{-1})
2	2·00	6·34	25	0·382	23·3
3	2·00	6·34	24	0·392	21·2
4	2·00	6·34	26	0·372	28·5
5	2·00	6·34	27	0·366	35·6
6	2·00	6·34	28	0·358	43·0
7	2·00	6·34	29	0·354	52·5
8	2·00	6·34	26 and 27*	0·323	32·0
9	2·00	6·34	24 and 29*	0·317	40·0
10	2·00	6·34	24–29 inclusive*	0·363	34·0
11	2·00	6·34	30	0·464	292
13	2·00	6·34	30 and 24†	0·258	123
14	5·75	2·8	25	0·402	22·5
15	5·75	5·4	25	0·370	24·6
16	5·75	8·2	25	0·382	23·2
17	5·75	5·6	27	0·334	37·4
18	5·75	5·5	29	0·369	51·1
19	9·57	3·42	25	0·340	23·6
20	9·57	3·28	27	0·335	41·6
21	9·57	3·31	29	0·333	56·5
23	2·00	6·34	lead shot	0·395	19·6

* Equal weights of each constituent.
† Approximately 1 of sample 30 to 3 of sample 24, by weight.

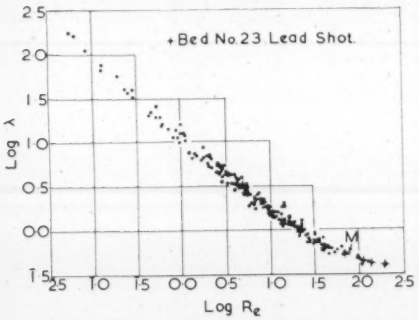

Curve showing the relationship between the friction factor and Reynolds number for beds of charcoal granules

(Crown copyright reserved)

DISCUSSION OF THE RESULTS

In comparing the results with those of previous workers it is convenient to refer to the reviews of Rose and Mott in Ref. 1 since they describe previous work from different points of view, although both regard the granular bed as a collection of particles rather than as a collection of tubes. Mott's approach results in equations for λ and R_e which are similar to equations (5) and (6), except for a numerical constant. Taking account of the different numerical constant and considering a point on the middle of the curve from Mott's collection of results for spheres, the point M on the figure is obtained, in exact agreement with the results presented here for irregular porous particles. Other points are similarly situated. Rose's dimensional approach includes several empirical factors depending on the conditions of the experiment, but considering the comparison which Rose makes between his results and those of Mott it may be seen that his results too could be represented on the curve of the figure.

From considerations such as those above it is seen that flow through beds of irregular porous particles may be correlated with that through beds of solid spheres, by regarding the beds either as a bundle of capillaries or as a collection of particles. This is a satisfactory conclusion to be able to draw from the work, but before concluding this discussion one or two other features should perhaps be emphasized.

A typical feature of flow through granular beds is the early onset of turbulence and the extent of the transition region. In flow through tubes streamline flow persists up to a Reynolds number of about 1 000, then the transition region occupies but a relatively small portion of the curve of log λ as a function of log R_e; in flow through beds turbulence begins when Reynolds number is about unity but is not complete until Reynolds number is about 1 000. On the capillary model of granular beds the early onset of turbulence and the extent of the transition region is to be expected, since the capillaries through a bed are not straight capillaries and regions of turbulence will be set up at the elbows at comparatively low rates of flow these being increasingly numerous as flow rates increase (Ref. 1, p. 70); also, the capillaries are not smooth capillaries and turbulence will be set up by the spikes at the walls of the capillaries (Ref. 1, p. 65).

On the basis of the particle view of the bed the early onset of turbulence is to be expected, since it is well known that in fluid flow around a particle the flow is streamline only for $R_e < 1$ or so.

Another feature of the curves of log λ as a function of log R_e is the onset of turbulence for the different beds. Some beds show streamline flow for higher Reynolds numbers than others. (This property is not apparent from the figure since no distinction is made on the figure between the results from the different beds; but it should be mentioned that the spread of the points in the transition region is partly due to flow in different beds deviating from streamline flow at different Reynolds numbers.) This is consistent with results on tubes and with the expectation of different properties of the pores in the different beds, but it should also be remembered that the choice of a number for l_c/l also affects the values of R_e at which turbulence is observed to begin.

Where mixtures of particles occur the distribution of size and the surface area of the different sizes are known and are accounted for in calculating the surface area of the charcoal beds. It is interesting to see what results are obtained if the distribution of size is ignored and S_0 is found directly from N, A and V_ϵ for such beds of mixed particles. From the practical point of view it is encouraging to find that little difference is found in the value of S_0, whichever method is used, provided there is a smooth distribution of particle size among the different sizes in the range chosen (e.g. bed No. 10). If however there is a mixture of only two sizes and these are markedly different (e.g., bed No. 13) the value of S_0 found by merely observing N, A and V_ϵ for the mixture is grossly in error.

Finally the converse problem of finding V_ϵ and S_0 from flow experiments may be tackled by the trial-and-error method provided N, A and n are measured in addition to the flow, the value of V_ϵ, and hence S_0, consistent with these

then being chosen so that a point representing the flow lies on the central curve of the figure.

ACKNOWLEDGEMENTS

Part of this work was done while the writer was engaged as a Vacation Consultant at C.D.E.E., Porton; thanks are due to Dr. F. A. P. Maggs of C.D.E.E. for many helpful discussions, and to Prof. R. M. Davies of University College, Aberystwyth, for advice on the presentation of this paper.

REFERENCES

(1) *Some Aspects of Fluid Flow* (London: Edward Arnold and Co., 1951).
(2) HATFIELD, M. R. *Industr. Engng Chem.*, **31**, p.1419 (1939).
(3) BEIRNE, T., and HUTCHEON, J. *Brit. J. Appl. Phys., Suppl.* 3, **5**, p. S76 (1954).
(4) HEYWOOD, H. *Symposium on Particle Size Analysis*, Supplement to *Trans Instn Chem. Eng.*, **25**, p. 14 (1947).

A replica technique for particle surfaces

By J. MARRIOTT, Ph.D., Grad.Inst.P., Research Laboratory, Imperial Smelting Corporation Ltd., Avonmouth

[*Paper received* 4 *April*, 1956]

Difficulty is often experienced in the interpretation of electron micrographs of pigments as surface detail cannot normally be observed. A simple technique for the preparation of shadowed carbon replicas of zinc sulphide and lithopone is described. The use of a selective leaching agent permitting differentiation of the zinc sulphide and barium sulphate in lithopone is demonstrated.

The application of the electron microscope to the examination of pigments has developed considerably over the past few years as a result of increasing interest in the particle size distribution and particle shape. There is, however, great difficulty in interpreting photographs of certain types of pigment because surface detail of the particles cannot be seen. For example, clusters of small particles are often mistaken for irregular single particles. Similarly, when the pigment has more than one component these cannot be identified unless there is a marked difference in particle shape. Lithopone—a mixture of barium sulphate and zinc sulphide—is an example of this type of pigment.

A replica technique has been developed to reveal the surface detail of particles. The technique is easy to carry out and, with suitable modifications, can be used to distinguish between different chemical compounds in the pigment.

THE METHOD

The replica is made by evaporating carbon on to the pigment particles which have been shadowed with gold-palladium and the particles are then dissolved from the carbon film. Details of the various stages are as follows.

(1) A microscope slide is cleaned with a few drops of Teepol solution (10% with water) by rubbing with filter paper until no interference colours appear when the slide is breathed on. A dispersion is made by gently rubbing the pigment on a glass plate in amyl acetate with a palette knife. A drop is then spread with a glass rod on the clean slide. This method of dispersion, though less effective than those involving the milling of the pigment in linseed oil or a 15% solution of nitrocellulose in dibutyl phthalate,[1] is adequate for replica work since flocculation is easily recognized.

(2) The particles on the slide are shadowed by the oblique evaporation of gold-palladium in the usual way. In addition to the shadows cast on the slide by the particles themselves, surface irregularities are also shadowed but this is normally not observed owing to the opacity of the particles to electrons.

(3) A thin layer of carbon, about 100 Å thick, is evaporated normally on to the slide in a vacuum as described by Bradley.[2]

(4) For ease of handling, the film on the slide is cut into squares of about 4 mm side using a sharp blade. The composite film, holding the pigment particles, is stripped by slowly lowering the slide at an angle of about thirty degrees through a water surface in the usual manner. The ease of stripping appears to depend on the degree of dispersion of the pigment on the slide and, if difficulty is encountered at this stage, a more dilute dispersion should be used.

(5) Squares of the film are then transferred by means of a silver gauze (about 60 B.S.S.) to the surface of acid to dissolve the pigment. The concentration and temperature should be chosen so that the reaction does not proceed violently as rapid evolution of gas ruptures the carbon film round the particles. After washing on several changes of distilled water, the films are lifted from the water surface on specimen grids supported by the wire gauze and finally dried.

For replicas of zinc sulphide and lithopone, concentrated hydrochloric acid diluted 1 : 1 with water is satisfactory. The pigment is dissolved completely in half an hour at a

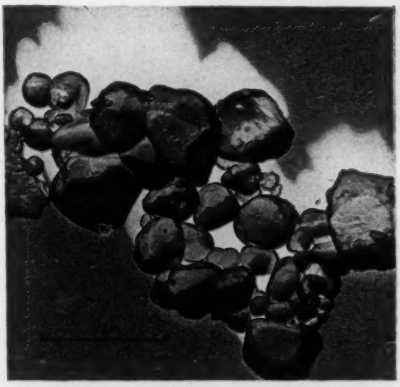

Fig. 1. Replica of calcined zinc sulphide particles, shadowed (×2) with gold palladium

temperature of 60–70° C. An electron micrograph of calcined zinc sulphide treated in this way is shown in Fig. 1, whilst that of a precipitated zinc sulphide having a similar particle size but a much larger surface area is shown in Fig. 2. The porosity of the precipitated material is immediately apparent.

Fig. 2. Replica of zinc sulphide particles prepared by slow precipitation, shadowed (×2) with gold palladium

If it is desired to distinguish between separate components of a mixed pigment, only one is dissolved from the film by a suitable leaching agent. A leaching solution consisting of 50 ml. of concentrated hydrochloric acid, 10 ml. of concentrated sulphuric acid and 50 ml. of water at a temperature of 60–70° C dissolves zinc sulphide completely in half an hour, leaving barium sulphate unaffected and permits differentiation between the two components in lithopone. Fig. 3 illustrates this aspect of the technique; the barium sulphate appears as black particles among the replicas of the zinc sulphide particles.

This technique may be applied quite generally if suitable leaching agents can be prepared for the materials under investigation. Carbon films are remarkably resistant to acid attack but, in some cases, it may be necessary to employ a different shadowing metal. In this connexion, platinum was used by Comer and Turley[3] in the preparation of surface replicas of massive clay samples when the clay was subsequently dissolved in hydrofluoric acid.

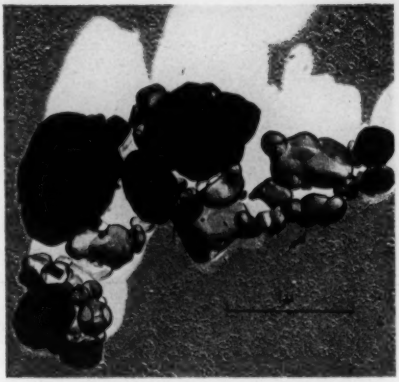

Fig. 3. Replica of zinc sulphide in lithopone; the barium sulphate appears as opaque particles. Shadowed (×2) with gold palladium

CONCLUSIONS

The use of this simple carbon replica technique extends the range of application of the electron microscope in the study of pigments. The technique, with slight modifications, may also be applied generally where knowledge of the surface characteristics is important.

ACKNOWLEDGEMENTS

The author wishes to express his thanks to the Directors of The Imperial Smelting Corporation Ltd. for permission to publish this paper.

REFERENCES

(1) DRUMMOND, D. G. (Ed.). *The Practice of Electron Microscopy* (London: Royal Microscopical Society, 1950).

(2) BRADLEY, D. E. *Brit. J. Appl. Phys.*, **5**, pp. 65, 96 (1954).

(3) COMER, J. J., and TURLEY, J. W. *J. Appl. Phys.*, **26**, p. 346 (1955).

Defects in germanium crystals grown from the melt

By E. Billig, D.Sc., M.I.E.E., F.Inst.P., Associated Electrical Industries Ltd., Aldermaston, Berks

[*Paper received* 15 *March*, 1956]

Thermal stresses arising from differential shrinkage as the crystal cools down from the freezing point to room temperature are considered as a major source of structural defects. The distribution of etch pits over various parts of a crystal has been studied and correlation has been obtained with the lifetime of minority carriers and with transistor action.

It has long been known that crystals grown from the melt are considerably less perfect in their texture than those grown from the vapour phase. Even if the most obvious reason for this—the constraint of the solidifying crystal by the crucible wall—is avoided, as, for instance, in the crystal-"pulling" technique after Czochralski[1] which is now generally practised in the preparation of large mono-crystalline ingots of silicon, germanium and other semi-conductors, a large number of defects are still observed on occasion. One of the reasons which has recently been discussed in detail[2] is due to the mechanical stresses which arise in the crystal as it cools down to room temperature. The stresses set up by differential thermal shrinkage, though quite small, may still be sufficient to cause plastic deformation, resulting in slip along the preferred glide planes in those parts of the crystal which are close to the melt.

Fig. 1(*a*) shows a section through the axis of a mono-crystalline ingot of high-purity germanium after suitable etch treatment. The ingot had been grown along a [1$\bar{1}$0] direction and cut along its length so as to expose a (111) plane. After grinding the surface with carborundum papers of increasing fineness up to 600 grade, and chemically polishing to remove all distorted material, an aqueous, alkaline, solution of potassium ferricyanide was applied so as to produce etch pits

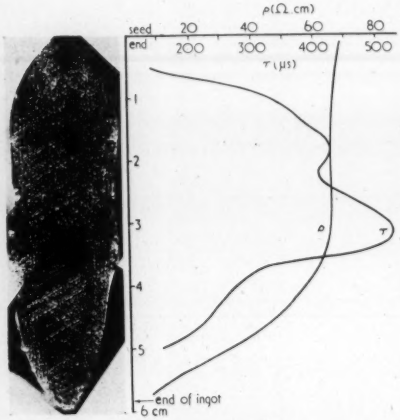

(*a*) (*b*)

Fig. 1. (*a*) Variation of carrier lifetime and electrical resistivity along germanium ingot P. 152. (*b*) Resistivity (ρ) and lifetime (τ) of germanium ingot P. 152 grown in [1$\bar{1}$0] direction

at the sites of dislocations. The high density of pits at both the starting and finishing end of the ingot are just what would be expected if the defects were indeed caused by thermal stresses. On the other hand, the pit concentration is also higher near the surface of the ingot—at its "skin"—than near the centre. These pits at the "skin" run in streaks at rather irregular intervals; they are presumed to be triggered off by slight unevennesses in the temperature distribution during or immediately after the growth process: slip would then most likely start at the intersection of the liquid/solid interface with the surface of the ingot, and propagate back into the solid crystal along a glide plane as far as this is still plastic, say 5 mm above the interface. Such a mechanism would also explain the etch pattern frequently observed on the cross-section of an ingot perpendicular to the growth axis. The concentration of pits there has approximately radial symmetry, but quite often an annular area of low pit density would separate a high-concentration area in the centre from a similar one near the surface.

It is generally assumed that every etch pit corresponds to the intersection of a dislocation line with the etched surface,[3] and recent electrical and optical measurements on such ingots (germanium and silicon) carried out at this Laboratory tend to confirm this assumption. The distribution of the lifetime of holes along the axis of the *n*-type ingot shown in Fig. 1(*a*) was measured by the photoconductivity decay technique,[4] and is plotted in Fig. 1(*b*). It is seen that the local variations in lifetime follow the distribution of etch pits quite closely, even in detail. The electrical resistivity, on the other hand, also plotted in Fig. 1(*b*), seems to be practically independent of dislocations, at least to first approximation. The resistivity remains at a constant high level near the start of the ingot, in spite of the high density of etch pits and the low lifetime there. Towards the end of the ingot, the resistivity drops in the usual way, due to the accumulation of impurities caused by segregation during the growth process.

Further evidence for the existence of strained regions near the skin of these pulled ingots has been obtained by the following various techniques.

(i) Under mechanical stress, crystals of silicon exhibit optical birefringence in direct proportion to the stress.[5] Thin slices cut from a silicon ingot produced by the pulling technique were exposed to polarized infra-red light; strong birefringence was observed near the edge of the slice, i.e. at the skin of the ingot, but was almost absent near the centre.

(ii) Transistor action in similar slices of germanium has been measured between two point contacts acting as emitter and collector respectively. The current multiplication factor α has been found to be quite constant over the large central area of the slice, but to be much reduced near the edge. (Resistivity has been found to be uniform over the whole surface of these disks so that the observed fall in α cannot be attributed to any change of resistivity towards the edges.)

(iii) The uneven distribution of stresses might also account for the fact that junction transistors prepared from one and the same slice of germanium under almost identical conditions frequently show a considerable spread in their electrical characteristics, although the impurity distribution is quite uniform over the slice.

ACKNOWLEDGEMENTS

I wish to thank several of my colleagues at this Laboratory for their help: Mr. J. B. Willis for preparing the germanium ingot shown in Fig. 1 and for measuring the electrical conductivity; Mr. M. S. Ridout for measuring the lifetime; and Dr. P. D. Fochs for establishing the infra-red birefringence pattern.

Thanks are due to Dr. T. E. Allibone for permission to publish this paper.

REFERENCES

(1) CZOCHRALSKI, J. V. *Z. Phys. Chem.*, **92**, p. 219 (1917).
(2) BILLIG, E. *Proc. Roy. Soc.*, **A235**, p. 37 (1956).
(3) VOGEL, F. L., JR. *Acta Met.*, **3**, p. 245 (1955).
(4) HAYNES, J. R., and HORNBECK, J. A. *Phys. Rev.*, **90**, p. 152 (1952).
(5) DASH, W. C. *Bull. Amer. Phys. Soc.*, **30**, p. *F*. 11 (1955).

The properties of high-pressure steady-state discharges in hydrogen

By W. A. GAMBLING, B.Sc., Ph.D., A.M.I.E.E.,* and H. EDELS, B.Sc.(Tech.), Ph.D., A.M.I.E.E., Department of Electrical Engineering, University of Liverpool

[*Paper received* 27 *March*, 1956]

The results of a large number of measurements of total voltage, voltage gradient, current density and excitation temperature over a range of current, pressure, gap length and electrode condition for high-pressure steady-state discharges in hydrogen are given. Tungsten and copper electrodes were used as these are typical refractory and non-refractory materials respectively. The results show that in the absence of metal vapour the cathode and column regions are quite independent, the state of one not affecting that of the other. With increasing current a change from the glow to an arc column occurs at a critical value of the gas temperature. At short gaps the column transition current is modified by heat transfer with the electrodes. With tungsten electrodes, increase in current causes a continuous transition between glow and arc at the cathode which is due to thermionic emission. With copper electrodes the cathode transition is discontinuous, erratic and independent of cathode temperature, being a function rather of the surface condition.

It is known[1,2] that a glow discharge can be maintained at pressures up to and above one atmosphere, and a previous paper[3] gives complete electrical characteristics for a high-pressure glow in free air. The results given[3] show that the zero-length voltage of the discharge is independent of current for both copper and tungsten electrodes and has the value associated with the cathode-fall voltage at low pressures, thus enabling the cathode-fall voltage to be measured at high pressures. Further results[3] indicate that the electrical properties of the high-pressure glow column are similar to those of an arc column operating at the same current. Investigations in air are difficult owing to the appearance with tungsten electrodes of an oxide cone[3] and the production of oxides on the electrode surfaces and in the gas, resulting in glow-to-arc transitions at comparatively low currents. By operating in hydrogen these difficulties are overcome and in addition it is possible to obtain the excitation temperatures of the discharge from the emitted Balmer series radiation.

A considerable number of investigations have been made by the authors on the high-pressure glow and glow-to-arc transitions in hydrogen with electrodes of tungsten, a typical thermionically emitting material, and copper, a non-thermionic material. From these investigations it is possible to state the general properties of the high-pressure glow, and in particular to show that the constricted column which can be produced from the glow in hydrogen is a true arc column.

APPARATUS AND EXPERIMENTAL TECHNIQUE

In order to maintain the stability of the high-pressure glow which has a high voltage gradient, a voltage source of 1500 V was used. Voltage gradient measurements were obtained by observation of a magnified image of the gap and in some cases by photographic recording of the discharge. The photographs also provided current density measurements. The excitation temperature measurements were made using a Hilger quartz monochromator in conjunction with a highly-stabilized and cooled photomultiplier, calibrated with a standard tungsten filament lamp.

In all the investigations great care was taken to ensure the cleanliness and full deoxidation of the electrode surfaces by prolonged operation in hydrogen. The hydrogen used contained less than 1 part in 10^5 of oxygen and 2 parts in 10^4 water vapour.

VISUAL OBSERVATIONS ON THE DISCHARGE

Visual observation of the hydrogen high-pressure glow and the changes produced by variation of current, pressure and gap length indicates some important properties of the discharge which, it will be shown later, has clearly defined electrical and optical characteristics. Observation indicates that the column characteristics are in the main independent of the electrode material, being simply gas dependent, whereas great differences are apparent at the cathode with different cathode materials. It is thus possible to discuss the column and cathode regions separately.

The discharge column. With both water-cooled copper and large diameter (i.e. cool) tungsten electrodes the following effects are observed in the discharge column. With an electrode separation of more than 3 mm at atmospheric pressure and at low currents, the column is pink and diffuse and is terminated at the cathode end by a number of striations. As the current is increased the column diameter increases

* Now at Department of Electrical Engineering, University of British Columbia.

slowly. Above about 1 A, increase in current causes the diameter to decrease and produces an increased luminosity at the centre. Ultimately a critical current is reached, of the order of 1·5 A, when a sudden contraction occurs resulting in the formation of a bright red concentrated column with a diameter of the order of 0·3 mm. Further increase in current results in an increase in both luminosity and diameter of this concentrated column. If the gas pressure is increased or reduced the whole of the above process may be repeated with, however, the corresponding phases of the process occurring at lower and higher currents respectively.

The transition between the two types of column can also be produced by variation in the electrode separation, and in this case the direction of the transition depends on the temperature of the electrodes. Thus at constant current with small diameter (i.e. hot) tungsten electrodes a reduction in gap length can produce a change from the diffuse to the constricted column, whilst with water-cooled copper electrodes, reduction in electrode separation produces a change from the constricted to the diffuse column. These changes are not caused by electrode vapour, but by the input of energy into the gap from the hot tungsten electrodes, and the loss of energy from the gap into the cooled copper, and is in agreement with the conception, derived from detailed investigations, that the column constriction is essentially governed by thermal conditions.

The discharge cathode region. At low currents the visual properties of the cathode region are similar for both copper and tungsten electrodes, comprising the blue negative glow next to the cathode followed by the Faraday dark space. With copper and large diameter tungsten electrodes the current may be increased to values greater than that at which the constricted column forms, with little change at the cathode other than an expansion of the negative glow and a slight extension of the constructed column into the Faraday dark space.

With copper electrodes further current increase eventually causes a sudden transition to occur at the cathode resulting in the disappearance of the cathode glow phenomena and the formation of an arc cathode spot as the termination of the now elongated column. The current at which the cathodic transition occurs is found to depend greatly on the electrode and gas purity and was of the order of 4 A in these experiments. In spite of cathode cooling, copper vapour enters the column when an arc cathode spot is formed so that the column becomes green and its diameter increases. The discharge is now very unstable so that no accurate measurements are possible with it. This discharge burns in a mixture of copper vapour and hydrogen and is no longer a true hydrogen arc. It should be emphasized that the results with copper electrodes given in this paper refer to the discharge with the cathode regions in the glow state, i.e. to currents less than 4 A.

With tungsten electrodes, increase in current causes the cathode temperature to rise until, at a current which depends on the electrode diameter, the cathode becomes white hot and the negative glow is no longer visible. The anode remains comparatively cold. If the current is increased sufficiently a transition to an arc-type cathode spot is observed, the overall radiant emission from the cathode decreases greatly so that it appears to be cold, and a small spherical red luminous region appears close to the cathode. At pressures less than 1 atm there is a dark space between this luminous region and the constricted column, and below $\frac{1}{4}$ atm striations appear between the dark space and the column. As the current is further increased the cathode becomes increasingly hot, the red luminous sphere being no longer visible; the temperature of the anode also increases rapidly until both the electrodes appear white hot. In this condition the transition at the cathode is complete. Spectroscopic examination shows that over the whole current range studied, 0·5 to 10 A, a negligible amount of electrode material enters the discharge when tungsten electrodes are used, so that the discharge burns in almost pure hydrogen.

ELECTRICAL AND OPTICAL CHARACTERISTICS

The visual observations may be explained by reference to the electrical and optical characteristics of the discharge which are typified by the results at 1 atm pressure shown on Figs. 1 to 4. The curves are to a large extent self-explanatory

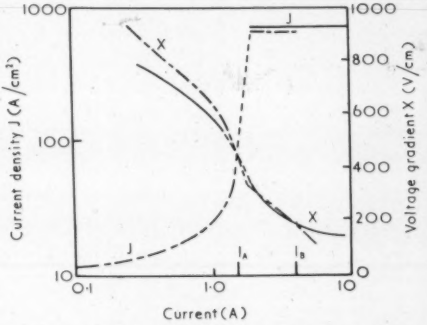

Fig. 1. Current density (J) and voltage gradient (X) measured in the positive column
——— = tungsten; — — — — — = copper.

but it should be noted that the excitation temperatures of Fig. 2 are obtained from the relative intensities of the first three Balmer lines $H\alpha$, $H\beta$ and $H\gamma$.[4]

Examining the figures it will be seen that a discontinuity exists at I_A in the column characteristic (Fig. 1) which is also reflected in the total discharge voltage curves (Fig. 3). It

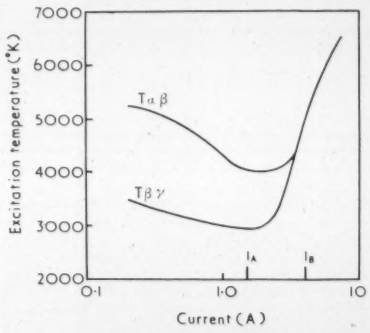

Fig. 2. Excitation temperatures in the positive column

was found that this discontinuity occurs simultaneously with the observed sudden column constriction. One further characteristic discontinuity exists at I_B as shown in Fig. 3

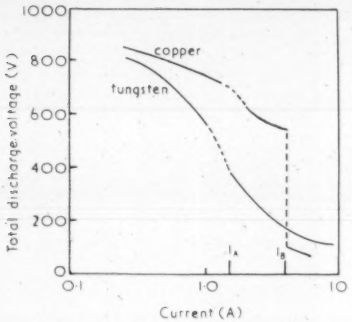

Fig. 3. Variation of total discharge voltage with current

and represents the cathode glow-to-arc transition on copper electrodes. Referring now to Fig. 1 it will be observed that the column characteristics are closely similar for both copper and tungsten electrodes confirming the important observation that in the absence of metal vapour the column may be studied independently of the electrodes. However, if only small diameter tungsten electrodes are used, the heat generated at the cathode affects the column voltage gradient slightly as shown. At the constriction current value I_A it is seen that the voltage gradient falls whilst the current density rises markedly. However, after this discontinuity no further sudden changes are obtained with tungsten electrodes up to the highest currents reached when the discharge exists in a state which is usually accepted as being a normal arc. It is thus apparent that for currents greater than I_A the column is in the arc form and since the constricted column which is obtained with copper electrodes (at currents between I_A and I_B) has almost identical properties then it too must be an arc-type column. This view is confirmed by consideration of the excitation temperature curves of Fig. 2, which indicate, moreover, the possible attainment for $i > I_B$ of thermal equilibrium in the column, a property normally associated with arc columns. Fig. 2 reveals the interesting fact that a minimum in the temperature curves is obtained at the column constriction value. The experiments show further that this minimum is always coincident with column constriction even when variation of pressure alters the constriction current value I_A. The results also show that for $i < I_A$ the excitation temperature diverges, whilst for $i > I_A$ a gradual convergence to equilibrium is obtained. Since the column gas temperature must approach ambient values at zero current, it is clear that the excitation temperatures indicate electronic excitation at low currents. As the current is increased the gas temperature will increase, and it seems likely that at the constriction current I_A a critical gas temperature is reached which allows the process of column contraction to take place.

Fig. 3 gives the total discharge voltage characteristics for copper and tungsten and it will be seen that the column constriction produces, as expected, a discontinuity in the discharge voltage curves for both electrode materials. The column constriction is thus the cause of one of the transitions observed by Suits,[5] although there appears to be no evidence of the further transitions which he reported. Apart from the column constriction effect upon the voltage curves, Fig. 3 shows that the different electrode materials produce markedly different curves. Since the column characteristics are the same for both copper and tungsten (Fig. 1) it is clear that differences must exist in the cathode region voltage variation. This is confirmed by the deduced measurements of cathode-fall voltages which may be obtained from the voltage-length characteristics of Figs. 4(*a*) and (*b*). With

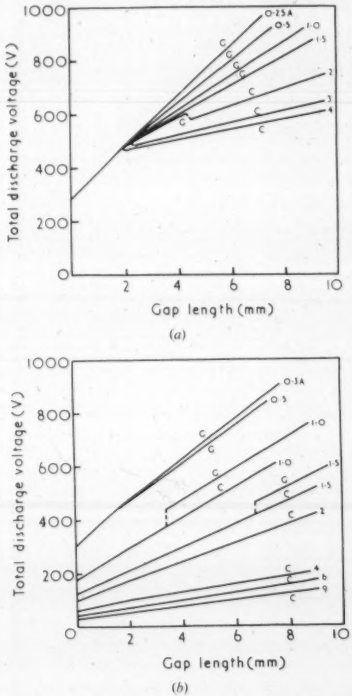

Fig. 4.(*a*) Voltage-length characteristics with copper electrodes. (*b*) Voltage-length characteristics with tungsten electrodes

G, glow column; *C*, constricted column.

copper electrodes [Fig. 4(*a*)] the characteristics merge over a wide current range for gap lengths less than 2 mm. Thus the zero-length voltage, which corresponds closely to the cathode-fall voltage,[3] has the value 285 ± 3 V and is independent of current. The total voltage characteristics between I_A and I_B will therefore vary gradually with variation in column gradient until a current I_B is reached at which a sudden cathodic transition to the arc state occurs. This transition is characterized by the large decrease in cathode-fall voltage from the glow value of 285 V to that of the arc of about 15 V. The

transition current I_B is not accurately reproducible, but depends greatly on the cathode surface condition. With tungsten, however, a pure cathodic glow state can only be obtained at low currents and with sufficiently large electrode masses to ensure no appreciable electrode temperature rise. In this condition, as shown by Fig. 4(*b*), a cathode-fall voltage of 300 ± 5 V is indicated. The results show, however, that the cathode-fall voltage (zero-length value) decreases with increase in current thus producing, as shown by Fig. 3, a gradual but rapid fall in total voltage which continues through the discontinuity at I_A into the full arc state. It will be appreciated that the gradual zero-length voltage variation indicates the existence of a continuous glow-to-arc cathodic transition with tungsten electrodes, a process which is adequately explained in terms of the growth of thermionic emission.[6] The authors' experiments show that by increasing the electrode mass higher currents are required to promote the continuous transition, and this is further evidence in favour of a process based on thermionic emission.

Figs. 4(*a*) and (*b*) also show the effect of gap variation on the column constriction. Thus with copper electrodes, Fig. 4(*a*) shows that above a certain minimum current, increase in electrode separation eventually results in a sudden fall in the discharge voltage, as shown by the discontinuity in the curve. This change in the characteristic is caused by the formation of the constricted column. At higher current it will be seen that the constriction forms at progressively smaller gaps. It is to be noted that the discontinuities in the curves are entirely consistent and repeatable. With tungsten electrodes, Fig. 4(*b*) shows that exactly reverse effects are obtained, namely, that column constriction is caused by gap reduction. The dependence of column constriction on gap separation is easily explicable if it is assumed that a minimum critical gas temperature is necessary before constriction can occur. Thus with water-cooled copper electrodes reduction in gap spacing will allow a greater cooling of the column and hence a higher current will be necessary before constriction can occur. However, with tungsten electrodes, which operate at higher temperatures, energy can be fed from the electrodes into the column and gap reduction causes an increased gas column temperature, thus inducing the column constriction.

It is of interest to note here that measurements of the cathode current density with copper electrodes show that the similarity relationships may be applied to the cathode-fall region, if the column does not exist in its constricted form. Further experiments have shown[7] that discontinuous cathodic transitions similar to those obtained with copper electrodes may also be obtained with contaminated or irregular tungsten electrodes. It is interesting to note that in these cases of induced cathodic transition by contamination it is possible to obtain at low currents a discharge having a typical diffuse glow column with an arc cathode spot.

CONCLUSIONS

From the experimental and visual evidence given it is possible to state and explain the main properties of the high-pressure glow and arc discharges in hydrogen. Thus it is clear that if the diffuse column which exists at low currents is defined as a glow discharge column, then it is possible to define the column which exists after constriction as an arc column. Although the column constriction has been observed before,[8,9] the authors have now shown that it is always coincident with a minimum in the excitation temperature curves and is therefore most probably formed at a critical gas temperature value. The voltage gradient, current density and excitation temperature characteristics of the constricted column are continuous with those associated with the column of the hydrogen arc. Furthermore, the measurements show that with increasing current after constriction the column approaches a condition of thermal equilibrium, a property normally associated with high-pressure arc columns. It has also been shown that the constricted column is largely independent of electrode material, but that the constriction current value is influenced by the heat transfer with the electrodes. This thermal dependence of the constriction appears to be strong evidence in favour of the thermal theory of arc column formation as given by Höcker and Finkelnburg[10] and King.[11]

Although the existence of the constricted column has an effect on the cathode current density, experiments show that the cathode region phenomena are largely independent of the column conditions. It has been shown that at current values for which no appreciable electrode temperature increase occurs, both tungsten and copper electrodes behave similarly, exhibiting a constant cathode-fall voltage. With increasing electrode temperature, tungsten electrodes exhibit a continuous and reversible glow-to-arc cathodic transition, satisfactorily explained in terms of thermionic emission. With copper electrodes, however, increase in electrode temperature up to the boiling point does not necessarily produce a cathodic transition, even though the column has well established arc characteristics. Ultimately a transition to an arc cathode state occurs but in an uncontrollable and discontinuous form. Experiments[7] have indicated that the presence of cathodic surface irregularities and contamination are important in inducing transition.

These experiments have shown that the high-pressure hydrogen discharge may exist in all of the four combinations of glow and arc states of cathode and column. It is to be expected, moreover, that these combined states will exist for discharges in gases other than hydrogen to which the thermal theory may be applied, and in which the contaminating effects of oxidation may be prevented. It would appear therefore that future investigators should define discharges under observation in terms of the states existent both at the cathode and in the column.

ACKNOWLEDGEMENTS

The authors wish to express their appreciation of the interest shown in this work by Professor J. M. Meek and Professor J. D. Craggs.

REFERENCES

(1) Thoma, H., and Heer, L. *Z. Techn. Phys.*, **13**, p. 464 (1932).
(2) Von Engel, A., Seeliger, R., and Steenbeck, M. *Z. Phys.*, **85**, p. 144 (1933).
(3) Gambling, W. A., and Edels, H. *Brit. J. Appl. Phys.*, **5**, p. 36 (1954).
(4) Edels, H., and Craggs, J. D. *Proc. Phys. Soc.* [*London*] *A*, **64**, p. 562 (1951).
(5) Suits, C. G. *J. Appl. Phys.*, **10**, p. 648 (1939).
(6) Von Engel, A., and Steenbeck, M. *Elektrische Gasentladungen*, Vol. 2 (Berlin: Springer-Verlag, 1934).
(7) Price, W. L., Gambling, W. A., and Edels, H. *Nature* [*London*], **176**, p. 28 (1955).
(8) Fan, H. Y. *Phys. Rev.*, **55**, p. 769 (1939).
(9) Bruce, C. E. R. *Nature* [*London*], **161**, p. 521 (1948).
(10) Höcker, K. H., and Finkelnburg, W. *Z. Naturforsch*, **1**, p. 305 (1946).
(11) King, L. A. *Nature* [*London*], **174**, p. 1008 (1954).

Correspondence

Large increase of light sensitivity at low temperatures for certain types of X-ray film

During the course of some experiments on the X-ray diffraction by crystals at varying temperatures the question arose whether the X-ray film used (Industrial G by Ilford, Ltd.) had a coefficient of expansion that ought to be taken into account, since the film temperature was not quite constant.

In order to measure the coefficient of expansion a millimetre scale was photographed on to the film, using the light from an enlarging lantern, the film being kept first at room temperature, 15° C, and then at about −85° C. The actual coefficient of expansion was found to be of the order of 0·005% per °C over this range, but the (to us) unexpected observation was made that for an exposure time of upwards of 5 s the blackening was very much greater for the low temperature than for room temperature.

Subsequent experiments were made at five different temperatures from about 50° C down to −95° C using first a scale and then an intensity step wedge and it was found that the blackening, under otherwise similar conditions, increased as the temperature decreased, within that range. Wetting the film did not affect the result. (This was tested because the film, in warming up, did sometimes tend to become covered with a film of ice.) The actual ratio of blackenings was dependent upon the exposure time and light intensity. For a bright light and 1/60 s exposure the ratio was nearer to unity than for a low intensity and a 40 s exposure. For equal exposure times the ratio was greater for a low intensity light. To give an example, a 40 s exposure to light coming first through a step wedge, and then through a 0·38 mm diameter pin-hole in an enlarger, to produce areas of uniform density 6×7 mm^2 in size, gave the following density match:

$$\begin{cases} 15^\circ \text{ C, light passed through step of density } 0{\cdot}08. \\ -95^\circ \text{ C, light passed through step of density } 1{\cdot}34. \end{cases}$$

No other type of film showed this effect so strongly, although Industrial B (Ilford) and, for exposure times of 40 s or more, Industrex (Kodak) did show some increase of blackening at low temperatures. Strongly light-sensitive films, on the other hand, showed decreased blackening for lowered temperatures, other conditions remaining the same.

It is clear from Mees's *Theory of the Photographic Process* (New York: The MacMillan Co., 1954) that, although the whole matter of sensitivity and the failure of the reciprocity law is a complicated one, depending on time of exposure, intensity of light and wavelength, and that a considerable loss of sensitivity usually occurs at low temperatures, there are cases in which there is a gain of speed. The present observations disclose so large an effect, however, that they seem worth recording, although we do not ourselves intend to pursue the investigation further.

It may be worth mentioning also that we found practically no change of sensitivity of Industrial G film to X-rays of ordinary diffraction wavelengths, within the range of temperatures mentioned above. The greatly enhanced sensitivity of Industrial G film to weak visible light at low temperatures suggested the possibility of developing intensifying screens for low temperature use. However, films such as Red Seal, which already provide an extremely fast combination when used with suitable intensifying screens, become less sensitive both to light and to X-rays at low temperatures, while the Industrial G emulsion appears to have been made deliberately insensitive to light under normal conditions, and the gain at low temperatures as observed, although large, is not sufficient to offset this insensitiveness.

Department of Chemistry, University College, London.
KATHLEEN LONSDALE
H. JUDITH GRENVILLE-WELLS

Arc initiation in hydrogen

In a paper by Edels[1] a method has been described for initiating an arc discharge between fixed electrodes. In this technique the arc source is connected through a filter circuit to the gap, to which is also connected an impulse generator. Operation of the impulse generator gives a spark breakdown of the gap, and with the correct circuit conditions the arc source follows through and establishes an arc discharge. It was noted in the paper, however, that initiation in hydrogen was difficult. Our more recent investigations have clarified some of the causes of this difficulty in initiation.

Experiment showed that with both copper and tungsten electrodes in an oxidized condition, or with gases with small admixtures of oxygen, initiation in hydrogen was obtained without difficulty. However, with arc operation the electrodes rapidly become deoxidized and further arc initiation is often impossible; this is in agreement with the work of Price, Gambling and Edels.[2] In order to obtain initiation for tungsten and copper under oxygen and oxide-free conditions the apparatus was modified to give an initial high arc current pulse. This was achieved by short circuiting, with a contactor, a portion of the arc series resistor and subsequently opening the contactor after arc establishment. It was found that with tungsten electrodes this method was satisfactory so long as the initial high arc pulse was sufficient to produce a high temperature at the cathode and thus ensure thermionic emission. With copper electrodes satisfactory operation was achieved, but with the present lack of understanding of the cold cathode arc mechanism it is not possible to describe the process of initiation. It is of interest to note that initiation with carbon electrodes was obtained without the production of an initial high arc pulse. This is understandable since carbon has a relatively low thermal conductivity and an arc spot can therefore be formed with lower energy inputs from the arc source.

Further experiments showed that even after complete arc initiation in hydrogen the arc on many occasions was unstable and finally ceased. Investigation showed that large oscillations in the current occurred in the unstable arc condition. We believe that this is a reflexion of the violent or rapid changes in the hydrogen arc column position and length which have been previously cited by Suits.[3]

Department of Electrical Engineering, The University of Liverpool.
F. W. CRAWFORD
H. EDELS

REFERENCES

(1) EDELS, H. *Brit. J. Appl. Phys.*, **2**, p. 171 (1951).
(2) PRICE, W. L., GAMBLING, W. A., and EDELS, H. *Nature [London]*, **176**, p. 28 (1955).
(3) SUITS, C. G. *J. Appl. Phys.*, **10**, p. 648 (1939).

New books

Survey in mechanics. The G. I. Taylor 70th Anniversary Volume. Edited by G. K. BATCHELOR and R. M. DAVIES. (London: Cambridge University Press, 1956.) Pp. 475. Price 50*s*.

Many years ago, the reviewer had occasion to study G. I. Taylor's work on the stability of fluid flow between rotating cylinders: this investigation, with its remarkable agreement between mathematical analysis and experiment, was felt to depict the true goal of an applied mathematician. It is now easier to understand the feelings then engendered, when Prof. Southwell says in his biographical note "there have always been blended in G.I. the mathematician's power of abstruse thought and the artist's gift of perception."

The editors of this commemorative volume have endeavoured to cover fields of knowledge which Sir Geoffrey Taylor has made his own and have set out to provide authoritative accounts that will be read. They have succeeded. Each chapter provides an appreciation of what has been done and of what are the difficulties ahead. This is particularly evident in the concise discussions of plastic deformation of metals by R. Hill and of dislocations in crystalline solids by N. F. Mott, which also serve to bring out the early contributions of G. I. Taylor. Those concerned with stress waves in solids will find in R. M. Davies's chapter a useful, compact and yet comprehensive survey.

The remaining two-thirds of the book are concerned with fluid flow. H. B. Squire gives an account of the elegant investigations on rotating fluids. The articles are of a uniform high quality and it is invidious to pick out any for special mention: but W. R. Lane and H. L. Green, in their discussion of the mechanics of drops and bubbles and with their emphasis on basic physical principles, provide an exposition of work not readily accessible elsewhere. This is followed by F. Ursell's critical résumé of wave generation by wind and a long study by M. J. Lighthill of viscosity effects in sound waves of finite amplitude. As might be expected in such a volume, there follow two chapters on turbulence; G. K. Batchelor and A. A. Townsend treat turbulent diffusion in a particularly well integrated manner and T. H. Ellison, in his chapter on atmospheric turbulence, reviews present, mainly empirical, knowledge. The book concludes with an account by K. S. M. Davidson of the mechanics of sailing ships and yachts.

The book is a worthy addition to the Cambridge Monographs on Mechanics and Applied Mathematics and may be recommended to the non-specialist, to engineers desirous of knowing what his scientific colleagues have to offer, and to the specialist who wishes to have an expert exposition of the present position in his subject. R. L. BROWN

Statistical mechanics of irreversible change. By R. T. COX. (Baltimore: Johns Hopkins Press: London: Oxford University Press, 1955.) Pp. viii + 130. Price 40*s*.

It is the task of the kinetic theory of matter to give account of the macroscopic mechanical and thermal properties of material bodies in equilibrium and in non-equilibrium. But this task can be carried out only for definite molecular models of such bodies, and it is in general so difficult that only fairly simple models, like those of gases, can be dealt with in practice. On the other hand, classical statistical mechanics is capable of dealing with any kind of material system, irrespective of its mechanism, but only in a state of thermodynamic equilibrium, and it is in particular possible to derive the theorems of phenomenological thermodynamics on a statistical mechanical basis.

This book presents, in a comprehensive form, a new development in the field of statistical mechanics to which its author has contributed a great deal. It aims at giving an equally general theory of non-equilibrium processes in material systems, in particular of the various types of transport phenomena, whose main feature is their irreversibility, and also at laying the statistical-mechanical foundations to the thermodynamics of irreversible processes.

The theory, although making use of the quantum-mechanical concept of transition probabilities between discrete quantum states, is essentially based on classical Boltzmann statistics, and the validity of its application to "degenerate" systems like liquid helium and electrons in metals is doubtful. But otherwise the method appears to be remarkably versatile, and the author has succeeded in presenting the matter rigorously and yet in a way which is fairly easy to follow. The book can be warmly recommended to all workers in the field of statistical physics. R. FÜRTH

Microstructures of diamond surfaces. 1st Ed. By Prof. S. TOLANSKY. (London: N.A.G. Press Ltd., 1955.) Pp. xii + 67. Price 40*s*.

Those to whom the study of diamond is of importance will be indebted to Prof. Tolansky for the appearance of this book. The author makes no claim to have written a comprehensive treatise on the surfaces of diamond but to have recorded the results of optical studies carried out by himself and his collaborators in his own laboratory on the microtopographical structure of diamond surfaces. The optical techniques used by the author and described in Chapter 2 will commend themselves to investigators in this field. The large number of illustrations are exceedingly well produced from remarkable pictures, many being taken at very high magnification. The chapters in the monograph dealing with diamond surfaces are both interesting and informative and the method used for artificially etching diamond surfaces is described in detail. From a study of the etched pits in the surface of diamond the author has formed very interesting conclusions on the growth of diamond.

The book is well written and produced, and will find a welcome place on many book-shelves. R. E. LEEDS

Hydro-dynamics. By H. L. DRYDEN, F. D. MURNAGHAN, H. BATEMAN. (New York: Dover Publications, Inc., 1956.) Pp. 634. Price $2.50.

The subject of hydrodynamics is of interest to specialists in so many of the pure and applied sciences that it is in some danger of disintegrating. Any attempt, therefore, to collect within a single volume the most significant developments of the subject, regardless of their special origin and applications, is warmly to be welcomed. The Committee on Hydrodynamics of the Division of Physical Sciences of the National Research Council of the U.S.A. has made such an attempt, and the book under review is an unabridged and unaltered republication of the report of that committee.

Recognizing "the lack of agreement in most cases between the results of classical fluid dynamics and experiment" the committee has attempted a survey of "the general field of experimental aerodynamics in such a manner as to outline

the types of flow susceptible to theoretical treatment and to indicate the general nature of the experimental data available for checking results of the new theoretical methods." In doing so they have covered the early literature of the subject and particularly those aspects of it of primary interest to engineers very thoroughly; nearly three thousand literature references are, in fact, given in the book. Copious as are these references, however, it should be noted that none is more recent than 1931. This limitation may be due to the delay which has occurred between the preparation of the report and its publication this year in book form, but whatever its cause it certainly restricts considerably the usefulness of the book.

Furthermore, the coverage of the book, which the publishers describe as "encyclopaedic," is also limited by its almost complete lack of reference to work done in this field by physical chemists, biophysicists, and physiologists. Again, the treatment of the subject leaves much to be desired, especially since the work is now presented in book form. Although the book contains well over six hundred pages, only twenty-three illustrations, all line diagrams, are included, and of these sixteen are concentrated within forty pages of the text. The rest of the text, in spite of the fact that a large part of it is devoted to experimental apparatus, methods and results, is for all practical purposes, unillustrated. Some of the diagrams are, moreover, extremely badly drawn and not only in the sense that they exhibit poor draughtsmanship but also that they fail to give a clear picture of the author's intentions. One diagram, Fig. 3 on page 373, for example, consists of nothing but three lines, two of which, one presumes, are co-ordinate axes. Another diagram, Fig. 2 on page 105, relates apparently to some un-named liquid for which there is a quite appreciable flow at zero stress.

Although two misprints occur on the inside of the front cover, the book is, on the whole, free from errors of this kind, and errors of the more serious type, such as the inconsistent definitions of apparent viscosity given on pages 105 and 123, are also few.

The copious use of undefined terms, the general reliance of the authors on references to other books and papers, and the comparative absence of illustration, make this book quite unsuitable for use by any reader who is not already fairly familiar with the subject, and most readers who are somewhat familiar with its contents will look for something more up to date. The book can, nonetheless, be recommended to any, and especially engineers, who, having some previous knowledge of the subject and wishing to make a close study of some aspect of it, are prepared to supplement their reading by reference not only to the books and papers mentioned in the text but also to the many other papers since published.

This book certainly represents the most thorough survey of the literature of the subject prior to 1932 of which the reviewer is aware, and for this reason alone it can be recommended for reference purposes. It is to be hoped, however, that it will soon be followed by an even more comprehensive review of the literature to date. T. V. STARKEY

Methods of mathematical physics (3rd Ed.). By SIR HAROLD and LADY JEFFREYS. (London: Cambridge University Press, 1956.) Pp. 714. Price 84*s*.

This third edition of a book which is the most important single book on the applied mathematician's or theoretical physicist's shelves is produced six years after the second and ten years after the original.

The changes made in the third edition are less extensive than those incorporated in the second. The most substantial are in Chapter 1 which now, in the treatment of covering theorems and Riemann and Stieltjes integrals, compares very favourably with the original and also includes (regrettably as a note) an elementary proof by Besicovitch of the theorem of bounded convergence for Riemann integrals. If these changes were not an excellent end in themselves one might be forgiven a fleeting suspicion that they were aimed at producing a book as ubiquitous as the elliptic functions of Chapter 25.

Other changes incorporated arise in the derivation of Poisson's equation (and a discussion of the restrictions on the density) in Chapter 6, a more detailed discussion for complex arguments of the Airy integral in 17·07, of asymptotic solutions of Green's type for complex argument in 17·13, 17·131 and the analytical continuation of solutions of the confluent hypergeometric equation in 23.05.

In short, the alterations are not extensive enough to "date" the earlier editions unduly but the authors are to be congratulated on their alterations which are all improvements. For my part, I would have preferred to see one further alteration, this time in the definition of the Bessel function K (x). I cannot convince myself that the superiority of Heaviside's definition offsets the sheer volume of results available on Macdonald's definition, and conversion factors can be so trying on the temper. L. HOWARTH

Theory of combustion instability in liquid propellent rocket motors. By LUIGI CROCCO and SIN-I CHENG. (Published for and on behalf of The Advisory Group for Aeronautical Research and Development, North Atlantic Treaty Organization by Butterworths Scientific Publications, 1956.) Pp. viii + 200. Price 37*s*. 6*d*.

This book, the first on this subject, should prove valuable to the specialist engaged on rocket propulsion and it may also be useful to those who take a general interest in combustion. It provides a sound theoretical introduction to the problem and is mainly compiled from published papers, many of them by the two authors of the book, although it does contain some additional information.

In Chapter 1 various possible mechanisms of unstable combustion are considered. The well-known, low-frequency or "chugging" type is discussed in terms of a combustion time lag, instability being either intrinsic or arising from a varying injection rate. For the equally familiar high-frequency or "screaming" type it is necessary to consider both a time lag and a corresponding space lag and instability is identified with the various possible acoustic modes of oscillation within the chamber. Of the mechanisms possible for intermediate frequencies discussed, one based on variable entropy, is particularly interesting. Oscillating conditions produce oscillations in mixture ratio and consequently the temperature and entropy of the products will oscillate too. This entropy excess or deficiency moves down the chamber with the products until it reaches the nozzle where it produces a pressure wave which travels back up the chamber, thus providing a closed loop.

Chapters 2 and 3 (and Appendixes) are devoted to detailed analysis of the low- and high-frequency mechanisms, linear effects only being considered, treated by the method of small perturbations. Non-linear effects are at present little understood and their analytical treatment has not yet been attempted. In Chapter 4 the limited amount of experimental evidence available is shown to be in agreement with the theoretical deductions. A. C. MERRINGTON

Notes and comments

Non-metallic materials for use at extreme temperatures

There is a growing national need for non-metallic materials of many types capable of maintaining their efficiency over an increasingly wide temperature range, and the development of such materials is a matter of urgent importance. Many types of materials needed for structural and functional purposes are required to function over a range from approximately −65° C to +350° C or even higher. They include lubricants, hydraulic fluids, heat exchange media, paints, adhesives, rubbers, fibres, plastics and solid non-metallic structural materials. In some cases the structural materials need to have special additional characteristics such as good optical and electrical properties whilst in other cases, for example, where a rubber is in contact with a fluid, the higher temperatures create a need for increased chemical stability. At all levels in the physical, inorganic, organic and organo-metallic fields, work is required ranging from fundamental theoretical considerations to practical preparatory investigations. Such topics as fluorocarbon and silicone chemistry already absorb considerable effort, both academic and industrial, but there is scope for additional work not only in those fields but, particularly, in less developed areas.

This problem is one of the main considerations of the Ministry of Supply and Admiralty Joint-Services Materials (Non-Metallic) Advisory Board and anyone who is interested in the possibility of helping in the matter should apply to any of the following who are members of the Advisory Board: Prof. G. Gee, Prof. W. T. Astbury, Prof. R. M. Barrer, Dr. J. W. Barrett, Prof. H. V. A. Briscoe, Prof. F. H. Garner, Mr. R. B. Richards, Dr. L. R. G. Treloar, or to one of the three Executive Officers: Dr. E. N. Dodd, Department of Engineering and Materials Research, Royal Naval Scientific Service, Sanctuary Buildings, 20 Great Smith Street, London, S.W.1, Mr. H. Warburton Hall, Directorate of Materials and Explosives Research and Development, Ministry of Supply, Shell Mex House, Strand, London, W.C.2, and Mr. W. Hardy, Directorate of Materials Research and Development (Air), Ministry of Supply, St. Giles Court, St. Giles Street, London, W.C.1.

Terminology of internal defects in castings as revealed by radiography

A new British Standard, initiated by the Non-destructive Testing Group of The Institute of Physics, rationalizes the terminology of defects in castings. The purpose of this standard is to enable the interpretation of casting radiographs to be understood without ambiguity of terminology, by those interested in the radiographic inspection of castings. The terms have as far as possible been chosen to correlate the definitions with their metallurgical or foundry origin. The aim has been to select those terms which will be applicable to all the metals normally used in castings. The defects listed have been classified into five groups of associated types with sub-divisions. A separate section is included relating to diffraction mottling, which arises from purely crystallographic causes, and should not be regarded as a defect.

The terms and definitions used in the standard are illustrated by radiographs, which have been selected not only to show the salient features of the defects, but also because of their suitability for reproduction by half-tone blocks. These illustrations are intended solely to be complementary to the definitions of the defects, and not as criteria of their severity. Some of the radiographs have been supplemented by macrographs or micrographs to help in the appreciation of the nature of the defects.

Copies of this standard, price 12*s.* 6*d.*, may be obtained from the British Standards Institution, Sales Branch, 2 Park Street, London, W.1.

Radioactive products

The Radiochemical Centre, Amersham, Buckinghamshire, has issued a loose-leaf catalogue of radioactive products in which materials of similar function are grouped as follows: processed isotopes (in simple chemical form and of high specific activity); labelled compounds (carbon 14, iodine 131, phosphorus 32, sulphur 35, etc.); radiation sources (beta and gamma emitters for industrial and medical use); natural radioelements (and radium appliances).

The lists are not comprehensive, but they include most of the materials in regular production. Users are recommended to choose these items, wherever possible, on the grounds of economy and ready availability but the Centre welcomes inquiries for materials not listed. It is also willing to advise potential users on the most suitable product for their particular purpose.

Radioactive products and irradiation services offered directly by the Atomic Energy Research Establishment at Harwell are not included in this list, and a separate catalogue of them is obtainable on request from the Isotope Division at Harwell.

International ferrite convention

The scope of the international convention on ferrites (29 October–2 November, 1956), which is being organized in London by The Institution of Electrical Engineers, will include the theory, preparation and properties of ferrites, microwave, square loop and carrier frequency applications and their use in radio and television. About sixty papers dealing with ferrites and their applications in electrical engineering will be presented and discussed. An introductory lecture will be given by Dr. Willis Jackson.

Further information can be obtained from The Secretary, The Institution of Electrical Engineers, Savoy Place, London, W.C.2.

Metallurgical Reviews

The Institute of Metals has commenced publication of its new quarterly under the title *Metallurgical Reviews* containing critical and interpretative reviews written for the non-specialist. The field to be covered is: refining and properties of commercially pure metals; production and properties of very pure metals; metal physics; metallography; powder metallurgy; secondary metals; mechanical properties and methods of testing; materials for special purposes; corrosion, protection, cleaning, and finishing; metallurgical analysis; non-destructive testing; melting and solidification, including all aspects of foundry work; metallurgical engineering, including working and heat-treatment; joining; miscellaneous subjects not included above.

The first issue is produced to the high standard one has come to expect of the Institute's publications and runs to 155 pages of text measuring $8\frac{1}{2} \times 5\frac{1}{2}$ in. The articles contained in it are "Metallurgical aspects of microradiography" by J. J. Trillat, "Mechanical properties in relation to design requirements" by C. Richard Soderberg, "The principles of continuous casting of metals" by D. M. Lewis and J. Savage,

"The preparation and properties of high-purity iron" by B. E. Hopkins.

The annual subscription rate is £2 2*s*. 0*d*. and the publishers' address is The Institute of Metals, 17 Belgrave Square, London, S.W.1.

The Story of The Thermal Syndicate Ltd.

To mark this firm's jubilee an illustrated volume has been produced in which the fascinating story is told of Mr. (later Sir) Richard Paget's visit to Lord Rayleigh's laboratory in 1902 when he first saw fused quartz. As a result, and with his characteristic courage and drive, he helped to establish a new industry in this country. It tells too of the parallel establishment of the industry through the work of Mr. W. A. Shenstone (a master at Clifton College) and others at about the same time, with the support of Johnson, Matthey and Co. Ltd. These two enterprises amalgamated in 1917 to form the firm whose products need no introduction to readers of this *Journal*.

This little volume is a valuable historical record of a British enterprise of the first half of the century. We wish the firm continued success in the coming years.

Heat bibliography

A limited number of copies of *Heat Bibliography* 1948–1952 are still available free of charge from the Heat Division of the Mechanical Engineering Research Laboratory, East Kilbride, Glasgow. The references have been collected in a variety of ways, the most important being by seeing the actual paper in the original journal, by noting an abstract in an abstracting journal, and by selection on the basis of title only from a bibliography or from a journal specializing in reprinting lists of contents of other journals. In these last two cases the source of the abstract, etc., has also been noted. Titles of papers in languages other than English have been translated; the original title is not given but the language is stated. Judging from the list of contents and the number of pages (414) the scope covered is extensive.

Co-operative Electrical Research

The British Electrical and Allied Industries Research Association has commenced publication of a house journal with the title *Co-operative Electrical Research*. It is intended to issue two numbers per year and include articles written by members of the staff and others closely associated with the work of the association. These articles will review various aspects of the association's activities and emphasize the effect of these on the practical problems facing the electrical and allied industries. The journal is meant to appeal to those in executive positions in these industries, who have a broad but not necessarily a specialized knowledge of the subjects and have neither the time nor the need to study them in great detail.

The first issue has 40 pages (10 × 8 in.) and includes the following contributions: E.R.A. and the electricity supply industry, by C. W. Marshall; Short-circuit forces in transformers, by H. M. Lacey; Recent research on insulating materials, by C. G. Garton; Insulation co-ordination in high voltage transmission systems, by A. Morris Thomas; The development of the light wood pole line and the Electrical Research Association, by H. W. Grimmitt; The early E.R.A. researches on circuit breaking, by L. Gosland; and Radio interference, by W. Nethercot.

All communications should be addressed to The Editor, Thorncroft Manor, Dorking Road, Leatherhead, Surrey. The price of each issue is 2*s*. 6*d*. (plus 3*d*. postage).

Erratum

In the table on page 91 of the paper entitled "The estimation of the specific surface of a soil from mechanical analysis data," by J. R. H. Coutts, which was published in Vol. 6 (1955) of this Journal:

for $4{\cdot}13 \times 10^5$ *read* $4{\cdot}13 \times 10^6$
for $3{\cdot}64 \times 10^5$ *read* $3{\cdot}64 \times 10^6$
for $1{\cdot}27 \times 10^5$ *read* $1{\cdot}22 \times 10^6$
for $0{\cdot}41 \times 10^5$ *read* $0{\cdot}38 \times 10^6$

Journal of Scientific Instruments

Contents of the October issue

SPECIAL ARTICLE

Fine measurements. By J. R. Adams.

ORIGINAL CONTRIBUTIONS

Papers

A radioactive ionization gauge and its application to the measurement of latent heat of vaporization. By J. H. Beynon and G. R. Nicholson.
An alinement and co-ordinate system for nuclear emulsion stacks. By E. Silverstein and W. Slater.
A miniature eight-channel pressure recorder. By H. M. Nelson and G. A. Parker.
A high-temperature micro-thermostat for X-ray studies on single crystals of appreciable vapour pressure. By P. J. A. McKeown.
The application of pneumatic gauging to high precision linear measurement. By J. C. Evans and I. G. Morgan.
A simple scanning mechanism for X-ray diffraction. By G. W. Smith and R. M. Hinde.
A simple vacuum leak detector using a radio-frequency mass spectrometer. By P. F. Varadi and L. G. Sebestyén.
An instrument for the continuous measurement of shrinkage of textile yarns. By R. A. E. Ellis, K. W. Hillier and A. B. Thompson.
A portable instrument for respirable dust sampling. By R. J. Hamilton.

Laboratory and workshop notes

Preparation and maintenance of spherical metal electrodes in hydrogen. By J. O'M. Bockris, B. E. Conway and W. Mehl.
Conical ground joint extractor. By S. G. Yorke.
A simple demountable vacuum seal for electrical connexions. By N. Fuschillo and J. Gilvey.
A micromanometer designed for recording. By G. W. E. Robertson.
An indium foil counter for the measurement of neutron flux. By D. H. Peirson and F. C. Lovelace.

NOTES AND NEWS

Correspondence

The use of octal numbers for recording binary-coded information. From G. W. Hutchinson.
Solarization technique for interferograms. From C. E. Arregger.

New instruments, materials and tools

Notes and comments

THIS JOURNAL is produced monthly by The Institute of Physics, in London. It deals with all branches of applied physics (including theory and technique).
All rights reserved. Responsibility for the statements contained herein attaches only to the writers.
EDITORIAL MATTER. Communications concerning editorial matter should be addressed to the Editor, The Institute of Physics, 47 Belgrave Square, London, S.W.1. (*Telephone*: Sloane 9806.) Prospective authors are invited to prepare their scripts in accordance with the *Notes on the preparation of contributions*. (Price 2*s*. 6*d*. including postage.)
REPRODUCTION. The Institute of Physics is a signatory to The Royal Society's Fair Copying Declaration. Details may be obtained upon application from The Royal Society, London, W.1.
ADVERTISEMENTS. Communications concerning advertisements should be addressed to the agents, Messrs. Walter Judd Ltd., 47 Gresham Street, London, E.C.2. (*Telephone*: Monarch 7644.)
CLAIMS FOR MISSING JOURNALS. Claims from regular subscribers to this *Journal* for missing numbers will only be considered if received within 60 days of the date of mailing plus normal outward time of transit and time for lodging the claim. Losses attributable to failure to notify a change of address or to similar omissions will not be considered.
SUBSCRIPTION RATES. A new volume commences each January. The charge is £4 per volume ($11.50 U.S.A.), including index (post paid), payable in advance. Single parts, so far as available, may be purchased at 8*s*. each ($1.15 U.S.A.), post paid, cash with order. Orders should be sent to The Institute of Physics, 47 Belgrave Square, London, S.W.1, or to any bookseller.

Summarized proceedings of a conference on the structures of semi-crystalline and non-crystalline materials—London, November 1955

The annual Autumn Conference of the X-ray Analysis Group of The Institute of Physics was held in London on 18 and 19 November, 1955. The three sessions dealt respectively with coals, cokes and carbons; with glasses, liquids and disordered structures; and with non-biological fibres.

STRUCTURE OF COALS, COKES AND CARBONS

The first paper, given by Dr. R. E. FRANKLIN (Birkbeck College, London), consisted of a summary of her published work[1–4] on the classification of carbons as graphitizing and non-graphitizing. She first defined these and related terms, and expressed the hope that other authors would follow her definitions, particularly with regard to the term graphitic which has, in the past, been used to cover a wide range of meanings.

In all carbons there are small ordered regions in which the atoms are arranged on an hexagonal network similar to that in the layer-planes of graphite. But in the less ordered carbons these planar groups, although they may be parallel to and equidistant from neighbouring groups, are in random orientation about an axis perpendicular to their planes, as first described by Biscoe and Warren.[5] Such carbons are said to have a non-graphitic structure. The non-graphitizing carbons are non-graphitic carbons which, on heating to temperatures up to 3000° C, show no homogeneous development of the three-dimensional structure of graphite. In the graphitizing carbons, the three-dimensional structure of graphite develops continuously and homogeneously in the temperature range 1700–3000° C. Graphitizing carbons in which the true graphite structure is partially developed are referred to as graphitic carbons. The apparent interlayer spacing in graphitic carbons is intermediate between the value 3·44 Å found in the non-graphitic carbons and the 3·354 Å of graphite, and is a measure of the degree of graphitization.

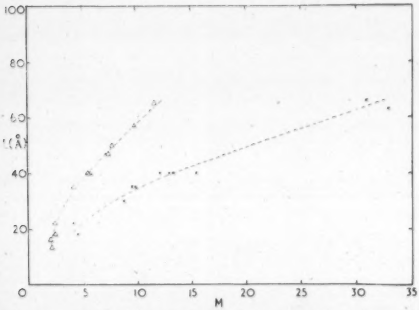

[Reproduced from *Proceedings of the Royal Society*]

Fig. 1. Relationship between the layer diameter L and the number M of layers per parallel group for graphitizing (X) and non-graphitizing (Δ) carbons

Dr. Franklin described how graphitizing and non-graphitizing carbons may be distinguished by means of either their physical properties, their chemical properties, or their structural characteristics. Graphitizing carbons are soft, non-porous and readily react with Brodie's reagent to form graphitic acid. Non-graphitizing carbons are hard and porous, and do not form graphitic acid.[6] The two classes of carbons are very sharply distinguished when the diameter of the planar ordered groups L is plotted against M, the mean number of such planar groups stacked parallel to one another (Fig. 1).

From the paucity of carbons showing characteristics intermediate between the graphitizing and non-graphitizing, Dr. Franklin deduces that lateral growth of the ordered layer-planes in carbons is essentially a two-stage process.[4] The first stage, the coming together and uniting of two coplanar ordered layer-planes, is the rate-controlling factor in the graphitizing carbons. The second stage is the atom-by-atom rearrangement of one of the two united groups so that its hexagonal network takes up the same orientation as that of the other group. This is the rate-controlling process in the graphitizing carbons.

Mr. H. W. DAVIDSON (General Electric Co. Ltd., Wembley) asked if Dr. Franklin had succeeded in accommodating the family of carbon blacks in her account of graphitization. From extensive measurements carried out by Dr. E. G. Steward of the G.E.C. Research Laboratories it was clear that the carbon blacks must be regarded as non-graphitizing, i.e. they failed to achieve three-dimensional register of the layer-planes after heat treatments at 2800° C.

It was not clear from Dr. Franklin's remarks why the carbon blacks should be non-graphitizing. The blacks showed no marked internal porosity, as was now well established by comparison of surface area measurements by electron micrography and nitrogen adsorption. Moreover, their helium densities (about 1·8 g/cm^3) did not reach the low value of, for instance, Saran charcoal. Further, their method of preparation did not involve any raw material deficient in hydrogen. Finally, experience with quite a wide range of blacks had, so far, failed to reveal the "islands of highly graphitized material" to be expected from Dr. Franklin's account.

In reply, Dr. Franklin expressed the belief that particle size is an important factor. On heating carbon blacks, strong inter-particle chemical bonds are probably formed and prevent a merging of the particles. Crystallite growth can therefore only occur in each particle independently, and small particle size will thus impose a restriction. At higher temperatures, when inter-particle cross-links break down, the

crystallites in neighbouring particles will be unfavourably oriented with respect to one another, so that little further crystallite growth will occur.

Dr. G. E. Bacon (Atomic Energy Research Establishment, Harwell) pointed out that the converse process to graphitization is observed in the progressive disruption of the graphite structure by neutron bombardment. Interstitial carbon atoms produce a steady increase of interlayer spacing with the amount of irradiation. However, the main framework of the structure is maintained certainly up to expansions of about 10% and the original dimensions and structural perfection can be regained by annealing at 1500° C.

In the next paper, Mr. R. Diamond (Cavendish Laboratory, Cambridge) described the use of the method of least squares to estimate molecular size distributions in carbons, some examples being given from carbonized coals.

The principle of the method is to calculate exactly the X-ray scattering from randomly oriented aromatic molecules of particular sizes, and then to fit a linear combination of such curves to the observed intensity curve for a particular specimen. The coefficients in such a combination then provide an estimate of the molecular size distribution.

The theoretical intensity curves were obtained by the use of the Debye radial distribution function

$$A(s) = \sum_r \frac{N(r)}{n} \frac{\sin 2\pi rs}{2\pi rs}$$

in which $A(s)$ is the intensity in atomic units scattered at an angle 2θ; $s = 2 \sin \theta/\lambda$ and λ is the wavelength; $N(r)$ is the number of inter-atomic vectors of length r irrespective of direction, and n is the number of atoms in the molecule. The theoretical intensity in electron units is then given by

$$B(s) = f^2 A(s) + C(s)$$

in which f is the atomic scattering factor for carbon and $C(s)$ is the Compton scattering. The quantities B may then be arranged in a matrix in which one suffix denotes the s value and the other the size group. Using a prime to denote a transpose, $\boldsymbol{I}$ to denote a column matrix containing the observed intensities and $\boldsymbol{\mu}$ to denote a column matrix containing the coefficients for each size group, we have

$$\boldsymbol{I} = \boldsymbol{B}'\boldsymbol{\mu} + \boldsymbol{\nu}$$

in which $\boldsymbol{\nu}$ contains the residual errors. The condition for solution is

$$\boldsymbol{\nu}\,\boldsymbol{B} = 0$$

i.e. the residual errors shall contain no component of any of the theoretical intensities. Hence

$$\boldsymbol{BI} = \boldsymbol{BB}'\boldsymbol{\mu}$$

and $\boldsymbol{BB}'$ is a symmetrical square which is best inverted by rotation into diagonal form by a unitary orthogon matrix $\boldsymbol{A}$, whence

$$\boldsymbol{\mu} = \boldsymbol{HI} = \boldsymbol{A}'\boldsymbol{Z}(\boldsymbol{ABB}'\boldsymbol{A}')\boldsymbol{ABI}$$

The problem is only soluble if the various functions $B(s)$ are linearly independent. As this is only just the case, the square matrix $\boldsymbol{Z}$ (having ones or zeros on the diagonal and zeros elsewhere) is necessary to exclude from the matrix $\boldsymbol{\mu}$ components which are due to one or more types of unresolvable ripple on the intensity curve which give rise to nearly vanishing eigenvalues on the diagonal of $\boldsymbol{ABB}'\boldsymbol{A}'$. If this is not done implausible results may be given in which the populations of neighbouring size groups are shown with opposite sign, and it is deemed justified to compromise the "least squares" criterion to the criterion of "least total square error consistent with the absence of strong fine scale modulation in the resulting histogram of molecular sizes," the increment in $\Sigma\nu^2$ being minute.

The method is analogous to Fourier inversion, the rows of the matrix $\boldsymbol{AB}$ being orthogonal functions resembling and being used in place of cosines.

Fig. 2 shows the development of a histogram for a coal heated to 300° C. The function of $\boldsymbol{Z}$ is to halt the process at the stage in the dotted box, further detail being unreliable.

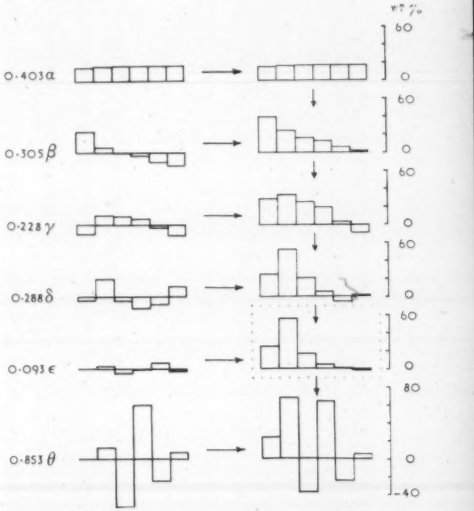

Fig. 2. The histogram is built up by the addition of scalar multiples of components of the types shown on the left. Each component adds a finer degree of detail, and is less accurate than the preceding one

A series of results for a coking coal carbonized *in vacuo* is shown in Fig. 3. The first two columns correspond to independent determinations from the same specimen, whilst the third column is the average of the first two set on a scale such that 100% corresponds to the mass of the specimen before heating, evaporation losses being shown on the curve to the right. Evaporation of small molecules and edge groups takes place up to 500° C, and is followed by polymerization at higher temperatures to form larger layers. The work will be published in detail in *Acta Crystallographica*.

Dr. L. Cartz (Cavendish Laboratory, Cambridge) described the use of the matrix method of Diamond to fit theoretical to experimental scattering curves for a series of coals. Discrepancies between the experimental and the fitted theoretical curves were considered and histograms of layer diameters were shown for the vitrain series of coals, and for their extractable part in ethylene diamine solution.

The fitting of the theoretical curves was carried out in the neighbourhood of the (11) band (in the region of $s = 0{\cdot}66$

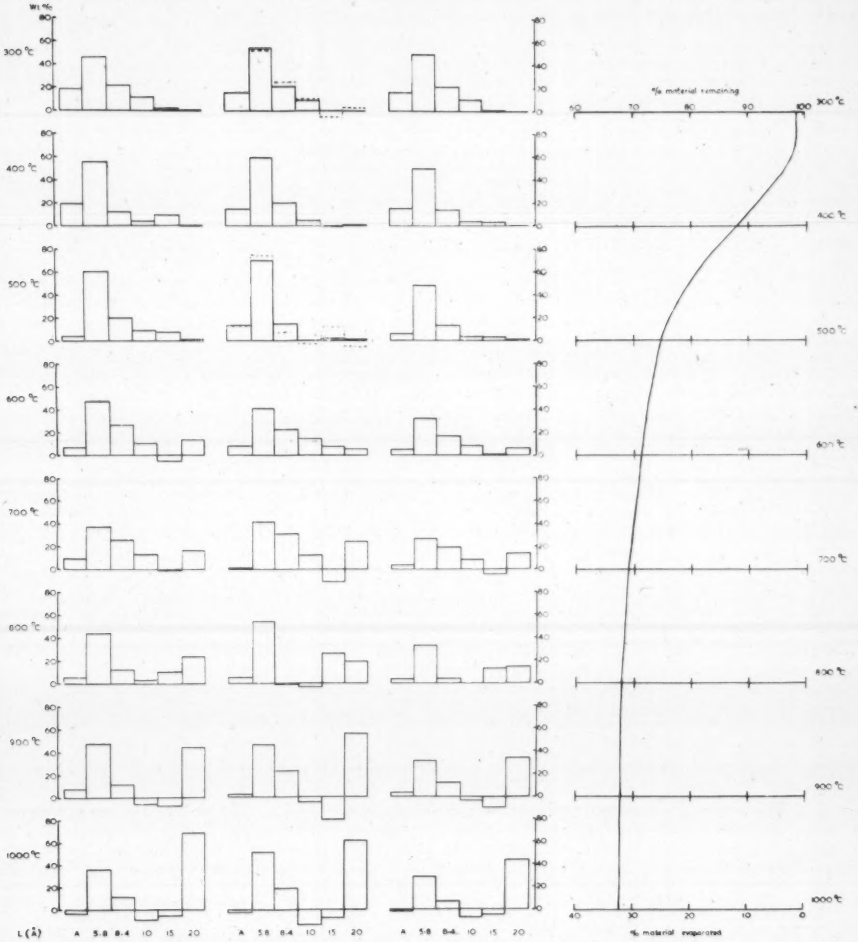

Fig. 3. Molecular size distributions for a coking vitrain carbonized at various temperatures *in vacuo*; L is a nominal layer diameter in Ångstrom units

to 0·96 on Fig. 4 where $s = 2 \sin \theta/\lambda$); discrepancies were observed at higher values of s and in the neighbourhood of the (10) band ($s \simeq 0{\cdot}5$). The agreement at higher values of s was considered as affected by (*a*) the texture of the monochromatizing crystal being other than mosaic, and (*b*) the possibility that the data available for the Compton scattering of carbon are inaccurate.

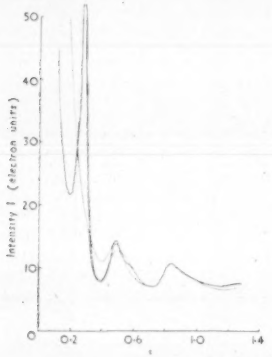

Fig. 4. Discrepancies are observed between the theoretical curve (dashes) and the experimental curve (full line)

(*a*) for $s > 1{\cdot}0$;
(*b*) in the neighbourhood of the (10) band at $s \simeq 0{\cdot}4 - 0{\cdot}6$. This is due to the (00 *l*) variation of intensity. A trial fitting of a (00 *l*) variation is given by the dotted line.

The region of the (10) band is affected by the (00 *l*) band, owing to the intermolecular interference effects, for the layers tend to stack parallel to each other; the theoretical curves of Diamond assume only intramolecular interference effects. From the difference between the experimental and the theoretical curves, the (00 *l*) band can be resolved from that due to the structure of the layers. This explanation was confirmed by good agreement between the observed and an evaluated (00 *l*) band. In Fig. 4, a trial fitting has been made by adding to the previously calculated theoretical curves a (00 *l*) variation due to 25% of the layers single and 75% in groups of four, with $d = 3{\cdot}50$ Å and $\mu = 0{\cdot}10$.

The histograms of layer diameters for the vitrain series of coals (Fig. 5) show that the layers contain about four rings for coals up to 89% carbon content, above which the layers are increasingly large, containing at 94% carbon content about nine to ten rings in good agreement with the observations of Hirsch.[7] The amorphous term of the histogram decreases fairly linearly with increase of carbon content, being about 30% for a coal of 80% carbon, and 9% for an anthracite of 94% carbon: in the interpretation, no allowance was made for the presence of non-carbon atoms in the coal. The mean value of the layer diameters is the most accurate part of the measurement, whereas the distribution is particularly sensitive to errors in the observed (20) band, which is superimposed on the (11) tail.

A series of coal extracts of the vitrains using ethylene diamine solution was examined. In general, the extracted material showed a histogram similar to that of the original coal, so that the solutions of the coal obtained with ethylene diamine appear to be truly representative of the coal as a whole. This was not true, however, for a coal of 89% carbon content, the extract of which gave a low-angle scattering pattern quite different both from that of the parent coal and from those of the other extracts.

In answer to various questions concerning the possible origin of the observed discrepancy between observed and theoretical scattering curves at high angles, Dr. Cartz stated that fluorescent radiation could not be responsible because closely similar results were obtained with CuKα and MoKα radiation, that mineral inclusions gave no Debye–Scherrer rings and left less than 1% ash, and that the corrections for absorption by the specimen were negligible. While errors in the correction for Compton scattering might account for discrepancies in the scattering curves, they would not influence the size distribution deduced. Although the presence of large quantities of non-carbon atoms in coals might possibly be an important factor, one coal after treatment at 1000° C for three hours *in vacuo* did not show any reduction in the high-angle discrepancies.

In answer to Dr. H. P. STADLER (King's College, Newcastle-upon-Tyne), Dr. Cartz said that he had examined the coal-like coprecipitate of pyranthrone, isodibenzanthrone and 1′ : 2′ : 6′ : 7′—dibenzpyrene—7 : 14—quinone from sulphuric acid solution. If no change in structure occurred on precipitation, the scattering curve would be expected to be similar to the theoretical curve for pyranthrone, which corresponds in size to the mean of the three molecules used. However, the observed curve for the coprecipitate differed considerably from the theoretical curve for pyranthrone.

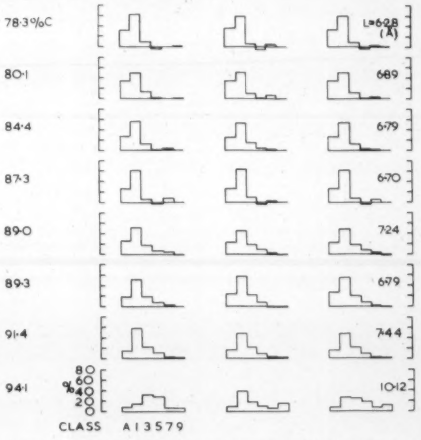

Fig. 5. Histograms of layer diameters for the vitrain series of coals

Class *A*—"amorphous carbon"; the carbon atoms are assumed to scatter the X-rays independently.

1	5·8 Å	nominal layer diameters
3	8·5 Å	
5	10 Å	
7	15 Å	
9	20 Å	

GLASSES, LIQUIDS AND DISORDERED STRUCTURES

Prof. R. W. Douglas (University of Sheffield) reviewed studies of the structures and physical properties of glasses. Warren's[8,9] work on X-ray scattering by vitreous silica led him to the idea of a continuous network of silicon–oxygen tetrahedra with a short-range order resembling that of cristobalite but without its crystalline long-range order; sodium–silicate glasses were then interpreted in terms of a similar network of SiO_4 tetrahedra with the sodium ions in the interstices. Additional evidence for this picture is provided by specific heat data, by electrical conductivity measurements, and recently by infra-red spectroscopy.

Boric-oxide glasses were interpreted by Warren in terms of a continuous network of BO_3 triangles. The much lower viscosity of these glasses than that of the silica glasses (in spite of the lower strength[10] of the Si–O bond compared with the B–O) appears to be due to the significant amount of water present in the boron glasses: infra-red absorption spectra[11] show peaks due to O–H bonds. In the sodium–borate glasses it is shown by infra-red spectroscopy[12] that BO_4 tetrahedra exist in addition to BO_3 triangles, their

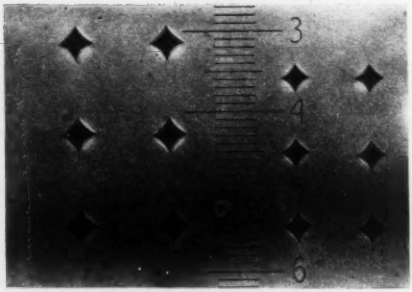

[Reproduced from *Journal of the Society of Glass Technology*]

Fig. 6. Photograph of a typical set of diamond pyramid indentations made, under loads of 100 g and 70 g, in a soda–lime–silica glass. One small division of the graticule corresponds to a distance of about 5 μ

number increasing with the sodium–oxide content until this reaches 10–15% (approximately one sodium to five borons). Above this point, additional sodium atoms appear to prefer interstitial positions, and the trend of the physical properties with composition changes. In these glasses it is thought that each BO_4 group tries to surround itself with BO_3 triangles; in sodium–borosilicate glasses, however, BO_4 tetrahedra are probably surrounded by silicon tetrahedra, and the critical composition is one sodium atom per boron atom. Ainsworth[13,14] has demonstrated the existence of this critical composition by measurements of the diamond pyramid hardness of sodium–borosilicate glasses (Fig. 6).

Prof. Douglas then discussed some of the consequences of the pseudo-liquid structure of glasses. The apparent change with time of certain physical properties (e.g. density[15]) can be explained if the glass is considered to be a viscous liquid. To any temperature there corresponds an equilibrium atomic distribution function, but at temperatures just above the solid phase, the time required after a temperature change for the glass to reach the new equilibrium distribution may be considerable. The results obtained, for example, in measurements of densities at various temperatures[16] therefore depend on the total time spent by the glass at each temperature. Prof. Douglas concluded with a hope that X-ray diffraction might in the future be able to shed much more light on the long-range order in glasses, particularly in "non-ideal" glasses which at present are little understood.

Opening the discussion on Prof. Douglas's paper, Dr. A. E. J. Vickers (Thermal Syndicate Ltd., Wallsend-on-Tyne) described some of the difficulties in the preparation of fused quartz. Plates of quartz, after heating to fusion point, may show the properties of glass in the direction perpendicular to the plate surface and crystalline properties parallel to it. Small crystals of quartz are sometimes found dispersed within these plates. Dr. Vickers felt that in a study of glass structure as many methods of investigation as possible should be brought to bear on the problem. Mr. H. P. Rooksby (General Electric Co. Ltd., Wembley) thought that a convention was needed in the use of the terms "fused quartz" and "fused silica." Dr. P. B. Hirsch (Cavendish Laboratory, Cambridge) mentioned recent measurements by Prof. E. Orowan of the diamond pyramid hardness of glass with very fine diamond indenters: these showed that the apparent strength of the glass increases as the dimensions of the indenter are reduced, and the measured strengths correspond to Griffith cracks of length of the order of 100 Å only. Recent work on low-angle X-ray scattering from glasses[17] also indicates density variations on this scale. In reply, Prof. Douglas said that very small diamond indenters had also been used in the work which he had reported, the aim being to avoid fracture of the glass.

Dr. R. L. Gordon (Safety in Mines Research Establishment, Sheffield) presented a paper by Mr. O. G. Griffin, Mr. G. W. Harris, Dr. G. Nagelschmidt and himself on peculiarities in the surface layers of ground quartz particles. Studies[18] of accurately sized samples of quartz with particle sizes in the range 0·2–20 μ by X-ray diffraction had shown that the intensity diffracted into a given line (usually the $10\bar{1}2$ reflexion, $d = 1{\cdot}81$ Å) varied considerably with the particle size of the sample, smaller samples showing lower diffracted intensities (Fig. 7). The measurements were made by means of a counter diffractometer[19] or, if sufficient sample

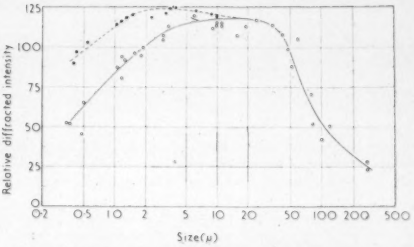

Fig. 7. Peak line intensities of the $11\bar{2}2$ reflexion ($d = 1{\cdot}81$ Å) from quartz powder as a function of the particle diameter. (The fall in intensity at larger particle diameters is due to extinction)

○ = quartz untreated
● = quartz treated with HF

was not available for this, by a photographic internal standard method.[20,21] Normally, peak line intensities rather than integrated intensities were measured; but the fall in peak intensity for small particles could not be entirely accounted for by particle-size or strain line-broadening, although a small amount of broadening did occur at the smallest particle sizes. Etching of the powder samples with hydrofluoric acid was successful in every case in raising the diffracted intensity; for the finest samples, however, the etched powder did not give as high an intensity as an etched, coarse sample. Similar effects have been reported[22,23] in differential thermal analysis of quartz powders; in this the height of the thermal transformation peak appears to be even more sensitive to the size of the powder than the intensity of X-ray diffraction, and the peak becomes noticeably broader with decrease in particle size.

The effects are qualitatively interpreted in terms of a disturbed layer at the surface of each particle. Estimates of the layer thickness, assuming that an entirely amorphous layer surrounds a perfectly crystalline core, are of the order of 1000 Å; this agrees well with estimates made from the differential thermal analysis data,[22] but is an order of magnitude greater than the thickness of the "high-solubility" layer on quartz particles deduced from measurements of solubility,[24] which has been estimated to be of the order of 100 Å. The concept of a perfectly amorphous layer surrounding a perfectly crystalline core is physically unattractive, and it seems much more likely that a continuous increase of crystallinity takes place towards the centre of the particle. It does not seem possible, on the existing evidence, to choose between drastic deformation of the crystal lattice and the breaking-up of the surface into small crystallites as the mechanism of damage. The most striking feature of the results is probably the extreme constancy of the X-ray intensities at a given particle size, whatever the origin and method of preparation of the sample.

In the discussion on this paper, Dr. A. E. J. VICKERS mentioned that the bulk quartz from which one group of samples had been prepared had been supplied by his firm; it had in fact been not ground but shattered by sudden cooling. Prof. J. D. BERNAL (Birkbeck College, London) emphasized the tendency of free oxygen ions at a surface to attach to themselves hydrogen from the atmosphere; fresh quartz surfaces might be expected to behave in this way. He mentioned also the possibility of residual fluorine at such surfaces as a result of the etching treatment. Dr. Gordon confirmed that this took place, and that it had been responsible for the accidental death of a number of experimental rats. Dr. P. B. HIRSCH referred to earlier work on ground quartz surfaces,[25,26] which showed only crystalline reflexions. He wondered if electron diffraction might give more definite information about the nature of the disturbed layer. Dr. J. W. MIDGLEY (Imperial College of Science and Technology, London) developed this theme, suggesting the use of electron beams of different wavelength (and thus of different penetrating power) to study the surface properties. A suitable electron diffraction camera had been developed at Imperial College by Finch, Lewis and Webb.[27] Dr. W. A. WOOSTER (Department of Mineralogy and Petrology, University of Cambridge) wondered if fruitful results might be obtained from a study of the diffuse scattering near the Bragg maxima: and perhaps from piezoelectric resonance measurements. Experiments on compression of a quartz surface with a steel ball had shown that the deformation took place by twinning.

Dr. W. MAY (Koninklijke/Shell Laboratorium, Amsterdam), presenting a paper by Dr. H. B. M. WOLTERS and himself, described a camera designed to record diffraction patterns from liquids. The specimen consists of a fine smooth jet of liquid as in the earlier cameras of Katzoff[28] and of Morgan and Warren;[29] but whereas these workers used an open circulating system, the present camera (Fig. 8) is entirely closed to the atmosphere, enabling the use of volatile liquids and of high or low temperatures. The liquid is pumped up into the reservoir immediately over the jet by air pressure; the necessary pressure is produced by moving the level of oil in the reservoir (to the left of Fig. 8) up and down by means of a motor-driven bellows, while the valves, also shown in Fig. 8 (steel spheres coated with glass), prevent back-flow. The camera is of the conventional type, of diameter 57·3 mm, and is helium-filled to prevent air-scatter. (Hydrogen is

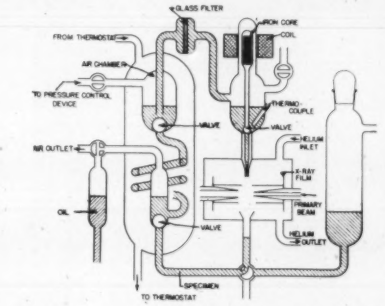

Fig. 8. Diagram of X-ray camera and associated liquid circulation system for obtaining diffraction patterns of liquids

avoided since it presents obvious dangers and because it is believed to attack the X-ray film.) A plane lithium–fluoride monochromator is mounted on the camera. Dr. May showed patterns obtained with this camera and discussed briefly the results obtained for AgI_2^- ions in acetone, and for Hg^{++} and $HgCl_4^{--}$ ions in water. (The interpretation of these diagrams[30] had been carried out by other workers in the authors' laboratory.)

Dr. P. B. HIRSCH congratulated Dr. May and Dr. Wolters on the design of their camera. Discussing the derivation of radial distributions, he mentioned two notable difficulties: cut-off errors, which were apparent in some of the radial distribution curves shown by Dr. May; and the theoretical values of the Compton scattering, which he thought were unreliable and in need of recalculation.

Mme J. LONGUET-ESCARD (Laboratoire Central des Services Chimiques de l'Etat, Paris), in a paper by herself and M. J. MÉRING, described an investigation into some abnormal spacings which are observed in freshly precipitated colloidal nickel hydroxide, $Ni(OH)_2$. The colloidal particles are positively charged due to an excess of nickel cations adsorbed on their (001) faces; these are balanced by anions, for example Cl^-, of the original solution.[31] In settling, the particles tend to stick together along their (001) faces, imprisoning between these faces a double ionic layer (Ni^+, Cl^-); non-rational reflexions result. The thickness of the trapped layer could not be determined from the formula derived by Hendricks and Teller,[32] since the stacking

distribution of the particles does not follow a law of constant probability as required by this formula. It could, however, be estimated indirectly by trial and error using a modification of the formula due to Landau;[33] and a direct determination was obtained from a Fourier transform of the (00 *l*) intensity distribution. Values for the layer thickness of about 12·5 Å were obtained by both methods. The thickness of the layer appears to depend on the nature of the anion and on the state of hydration.

Dr. P. B. HIRSCH said that a similar technique to that used by Mme Longuet-Escard and M. Méring had been employed by himself and his collaborators[34] in the determination of the inter-layer spacings and distributions of layers in groups of parallel layers in coals. Dr. H. P. STADLER asked whether the authors had observed similar effects due to cations. He and Dr. BRIGGS at King's College, Newcastle, had found that a sharp line at about 9·5 Å resulted from the presence of small amounts of cations. M. Méring replied that similar effects had been observed for F^- anions, but that they had not studied the effect of cations.

Dr. K. DORNBERGER-SCHIFF (Deutsche Akademie der Wissenschaften, Berlin) discussed formal methods for the treatment of one-dimensional positional disorder in layer structures. Systematic treatment of disordered structures is unsatisfactory if attempted with the aid of concepts (e.g. unit cell, space group) which are appropriate to ordered structures. Other concepts are needed instead, for example the symmetry group of the single layer, the "stacking vectors" (vectors bringing one layer into coincidence with a neighbour), etc. Such concepts permit the application of Fourier transform techniques and the deduction, from the distribution of sharp spots and diffuse streaks in reciprocal space, of information both on the intra-layer structure and on the packing of the layers. The layer symmetry is indicated by the intensities of the sharp spots and by systematic absences of both spots and streaks; the method of stacking may be deduced from the distribution of spots and from the variation of intensity along the streaks. *Periodic* stacking results in an ordered structure; some of the reflexions from such structures are equivalent to the sharp spots of the disordered case, and have the symmetry of the single layer, whilst others correspond to parts of the diffuse streaks: these may have a lower symmetry than the "layer-spots." Such cases of periodic stacking will in general show systematic non-space-group absences.

The evening discourse was given by Prof. A. R. Ubbelohde who spoke on "Crystallography and the phase rule." As it was published in full in the September issue of this *Journal* (pp. 313–21) it is not summarized here.

NON-BIOLOGICAL FIBRES

Dr. L. BROWN (Courtaulds Ltd., Coventry) described a preliminary investigation of the polymer with the repeating unit

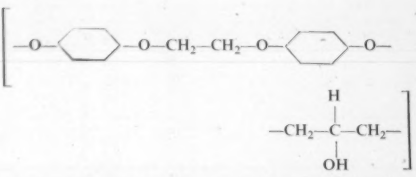

which is prepared from 4–4′ dihydroxydiphenoxyethane and epichlorhydrin in the presence of sodium hydroxide,[35] and which can be made into fibres by melt spinning[36] (it melts at about 216° C). A fibre photograph [Fig. 9(*a*)] shows a high degree of crystallinity and orientation, with, however, sufficient disorientation for three meridional reflexions at 13·8, 6·9 and 4·6 Å to appear, corresponding to even orders of a cell 27·6 Å long. Stretching the sample by 10% at room temperature and photographing it under tension [Fig. 9(*b*)] results in a 5% increase of the repeat distance along the fibre axis to 29 Å; other changes in the pattern include the disappearance of the weak equatorial reflexions, a movement of the layer line reflexions towards the equator, and changes in intensity as well as in position of the three meridional reflexions. The extension of the unit cell is completely reversible, but in the fibres themselves some degree of permanent set occurs.

A second spun sample, with rather higher amorphous content (so that greater stretching was possible), showed a

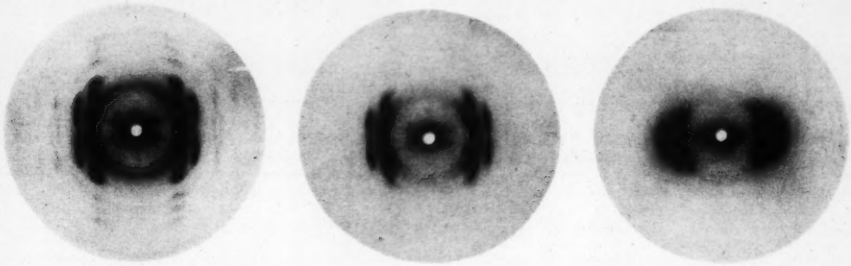

(*a*) (*b*) (*c*)

Fig. 9. Diffraction patterns of the synthetic fibre discussed by Dr. L. Brown

(*a*) A fibre prepared for structural examination.
(*b*) The fibre stretched by about 10%, photographed at room temperature.
(*c*) A fibre with greater amorphous content, stretched by about 35%.

fibre-axis repeat before stretching of 29·4 Å, and a repeat of 31 Å at 10% extension. At an extension of 35% the crystalline pattern disappeared [Fig. 9(*c*)], leaving only a diffuse reflexion spreading across the equator and a streak across the meridian at 16 Å. Heating this sample at temperatures up to 180° C under tension yields a reasonably well-resolved crystalline pattern; still better resolution of the (*hkl*) reflexions along the row lines is obtained by heating at 180° C without tension.

Undrawn quenched fibres give only a broad amorphous ring; no crystalline pattern appears on stretching, nor if the fibres are allowed to relax at room temperature (when they contract in length by about 10%). Heating without tension at 180° C now results in a further contraction of about 30% and the highly crystalline pattern of Fig. 9(*a*) is obtained.

These data may be explained in terms of a unit cell containing two molecular units, strongly kinked and arranged around a two-fold axis parallel to the fibre axis. The planes of the benzene rings are inclined at about 40° to this axis. The unit cell is at least monoclinic and possibly orthogonal; a tentative rectangular unit cell has $a = 10{\cdot}8$, $b = 4{\cdot}8$, $c = 27{\cdot}6$ Å, and contains four polymer repeating units. The high degree of order suggests that the bonding is almost entirely by Van der Waals forces.[37,38]

Dr. E. R. Howells (Imperial Chemical Industries Ltd., Welwyn) described an investigation carried out by Mr. C. W. Bunn and himself, part of which had been previously reported,[39] on some straight-chain fluorocarbons, in particular "Fluon" (polytetra fluoroethylene). Polythene, the hydrocarbon analogue of Fluon, has a chain repeat length of 2·54 Å;[40] Fluon itself, however, shows a repeat distance of 16·8 Å, indicating a departure from planarity of the carbon backbone. If the chain is assumed to be helical, the Bessel-function analysis of Cochran, Crick and Vand[41] shows that only a six-turn helix fits the observed layer-line intensities. It seems clear that this arrangement is adopted by the chain for stereochemical reasons.

The molecular shape is more nearly cylindrical than that of polythene; it is thought that this fact is responsible for the remarkable transition which takes place at room temperature: a 1% change in volume is observed at 20° C, with a further, smaller, increase at 30° C. The transition may be shown, by comparison with similar effects in perfluorocetane, $C_{16}F_{34}$, to result from some feature of the fluorocarbon chain itself rather than from some property of the high polymer. The effect is apparently due to a bodily rotation of the molecules about their axes, with no associated change in the molecular configuration; this is suggested by the X-ray diagrams and partially confirmed by nuclear magnetic resonance work on Fluon by Dr. J. A. S. Smith in the Chemistry Department, University of Leeds. The occurrence of the transition so far below the melting point (327° C) is probably due to the energy barriers to molecular rotation in the fluorocarbon structure being lower than in the corresponding hydrocarbons. A quantitative study of the X-ray intensities indicates a reduction of the F–C–F angle from the tetrahedral value to about 104°; this is confirmed by the nuclear magnetic resonance data, and in turns confirms the theoretical predictions of Coulson.[42]

Replying to a query by Mr. H. S. Peiser (Hadfields Ltd., Sheffield) about the relation between the structure and the physical properties of Fluon, Mr. C. W. Bunn said that the most striking property of the polymer was its remarkably low coefficient of friction, which has found application in the coating of skis, to give considerable increases in speed, and in the fabrication of self-lubricating bearings. It was natural to suppose that this property is connected with the streamlined profile of the molecules; these might be thought of as microscopic roller bearings! The observed rise in coefficient of friction above the transition range (20–30° C) may possibly be accounted for by molecular friction. It appears that below room temperature only some two-thirds of the molecules rotate (which they may do in pairs, in the manner of gear wheels, compatibly); whereas above room temperature all the molecules rotate with a consequent increase in molecular friction.

Dr. A. Keller (University of Bristol) discussed certain orientation phenomena in synthetic crystalline polymers. In polymers which are macroscopically unoriented, a considerable degree of orientation may exist on the microscopic scale; this has been studied, in polyhexamethylene adipamide and sebacamide, polyethylene and polyethylene teraphthalate, by a micro-X-ray technique due to Herbst.[43] Individual crystallites of the polymers form submicroscopic fibrous aggregates or fibrils, which themselves form larger structures, or "spherulites," within which they are radially oriented.[44–46] The spherulites are easily recognized (Fig. 10) under the

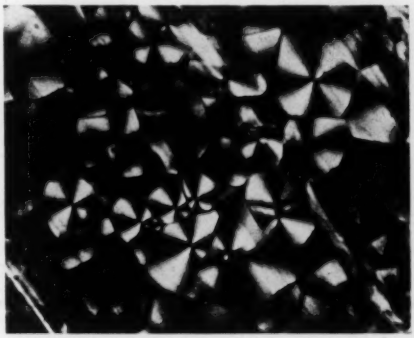

Fig. 10. Spherulitic structure in a section of polyhexamethylene adipamide (nylon 6,6). Crossed Nicols; magnification about ×200

microscope between crossed Nicol prisms. The intensity distribution along the Debye–Scherrer rings of the micro-X-ray diagrams indicates that the molecules within individual crystallites lie predominantly perpendicular to the radius of the spherulite (i.e. to the axis of the fibrils). The exact structure of the fibrils is not clear; but a helical model is proposed[47,48] to account for the perpendicular orientation of the molecules.

The existence of these spontaneously oriented regions can manifest itself when a crystalline or crystallizing polymer is artificially oriented. In such cases a number of uniaxial orientations has been observed which are unusual in that the molecular chains are oriented preferentially in directions other than that corresponding to the external orienting influence. This is unexpected as a result of simple molecular considerations; but if it is considered that the fibrous units which form spontaneously during crystallization can grow in preferential directions even under the influence of external orientation, and that once formed they can be deformed in a

preferential manner, these apparently anomalous orientation effects all follow readily from one and the same picture.

In the discussion on Dr. Keller's paper, Mr. H. S. PEISER touched on the general relation between the microscopic and macroscopic orientation textures of fibrous polymers and between these and their physical properties. Dr. Keller's particular contribution had been to draw attention to the often forgotten "locational" effects, by which the orientation of a crystallite was influenced not only by the macro-texture but also by the orientation of neighbouring crystallites. Prof. J. D. BERNAL drew attention to a similarity between Dr. Keller's spherulites and those observed (though on a larger scale) by Robinson[49] in solutions of poly-γ-benzyl-L-glutamate. He preferred to think of the spherulites as a special kind of spherical crystallite, rather than as an aggregate of crystallites. In reply to Prof. Bernal's enquiry about the orientation conditions at the surfaces of the spherulites, Dr. Keller said that no surface structure had been observed. The surfaces were surprisingly smooth, pointing to highly co-ordinated growth of the fibrils within the spherulites: on this basis a spherulite as a whole might well be regarded as a special type of crystal. He thought that there was a fundamental distinction between the spherulites of liquid crystals as studied by Robinson and those of solid polymers: the former are in equilibrium with the surrounding isotropic medium, while the latter are not and will continue to grow at the expense of the surrounding medium. There might, however, be some property common to the two types of system.

Dr. E. J. W. WHITTAKER (Ferodo Ltd., Chapel-en-le-Frith) took as the starting point of his paper "A classification of cylindrical lattices" the minerals such as chrysotile,[50–52] halloysite[53] and garnierite[54] whose morphology suggests the use of some form of cylindrical lattice. The structure of chrysotile, determined from X-ray fibre diagrams, indicates that the individual layers are stacked in just such a way as would be expected if they were cylindrical.[55–58] The description of minerals of this kind in terms of, for example, "orthorhombic" or "monoclinic" lattices may be useful;[59–61] but a logical description and classification of such lattices is desirable. Dr. Whittaker defined a cylindrical lattice[62] as a set of congruent two-dimensional lattices inscribed on a set of cylindrically curved surfaces and mutually ordered with respect to the cylinder axis, there being equal and uniform spacings between each successive pair of such surfaces. He used this definition to develop the cylindrical analogues of orthorhombic, monoclinic and anorthic lattices; the corresponding slightly imperfect (because slightly strained) helical lattices; the regular spiral lattices; and the corresponding helical spiral lattices. Centred lattices are also possible; the centring may be either conventional, for a rectangular lattice, or by means of one or more sets of similar lattice layers intercalated between the original layers. The distribution of matter associated with each lattice point cannot conform to a three-dimensional space group, but two projections of such a distribution may be defined which constitute regular two-dimensional repeating patterns and can therefore be treated in terms of two-dimensional space-groups.

Dr. D. E. C. CORBRIDGE (Albright and Wilson Ltd., Oldbury, Birmingham), in a paper titled "Some long-chain inorganic ions," dealt with the structures of the fibrous insoluble metaphosphates termed "Kurrol salts."[63] The existence of long chains in these salts was demonstrated in the structure of rubidium phosphate $(RbPO_3)_n$, which had been worked out by three-dimensional methods.[64] In this the monoclinic unit cell contains continuous chains of composition $(PO_3)_n^{n-}$ which spiral around the screw axes with a repeat pattern every two PO_3 units. Similar arrangements are indicated for the potassium and caesium salts;[65] these, like the rubidium compound, have characteristic fibre axes of 4·2–4·5 Å. Work is in progress on the sodium salt, which appears to have a chain structure with a rather longer fibre axis (6·02 Å) and a repeat pattern every four units. The results so far obtained, however, disagree with those reported by Plieth and Wurster[66] except for the length of the *b*-axis.

It is interesting to compare this type of chain with those in anhydrous sodium metasilicate, Na_2SiO_3,[67] and in the asbestos form of sulphur trioxide $(SO_3)_n$.[68] In each the chain axis lies parallel to the shortest unit-cell axis; the crystals develop their fibrous character in this direction, the pattern repeating every two XO_3 units, and two-fold screw axes of symmetry coincide with the chain axis.

The mode of polymerization of the tetrahedral XO_4 groups (where X = Si, P or S) is a sharing of corner oxygen atoms with adjacent tetrahedra; the maximum number of corners which can be shared is four in silicates, three in phosphates and two in sulphates. A number of types of chain can be formulated according to this principle. Examples of several of them have already been found in the silicate series, and some may also exist in the phosphate series. Double chains of the amphibole and felspar types may also have analogues among the phosphates; more complex "super-chains" may be possible in both series.

Prof. E. G. COX (University of Leeds), opening the discussion on the papers by Dr. Whittaker and by Dr. Corbridge, remarked that current discussions of cylindrical and spiral lattices have a lineage which goes back at least as far as Bravais. The phenomenon of phyllotaxis (the arrangement of leaves on the stems of plants), observed quantitatively by de Candolle, led to a paper by A. and L. Bravais[69] on the mathematics of spiral lattices. The crystallo-chemical relationships of silicon and phosphorus, of which Dr. Corbridge had given a very useful survey, were worthy of further study and likely to prove as interesting as those of carbon and nitrogen. Too much reliance, however, should not be placed on the details of some of the earlier silicate structure determinations. He added that, although infinite chain molecules often had two-fold screw-axis symmetry, where two such molecules were related by a centre or plane of symmetry they were not necessarily enantiomorphous, since two-fold screw axes were not themselves enantiomorphous; consideration of the detailed structure of the molecules concerned was necessary to decide this.

Mr. J. R. S. WARING (Imperial Chemical Industries Ltd., Manchester) suggested that Dr. Whittaker's treatment of cylindrical lattices might be extended to the general case of curved lattices in three-dimensional space, which would have obvious applications in the study of the spherulites discussed earlier by Dr. Keller. Dr. K. DORNBERGER-SCHIFF referred to the discrepancy between the results of Dr. Corbridge and those of Plieth and Wurster for the lattice constants and space group of sodium metaphosphate. Plieth and Wurster had, she said, examined a twinned crystal but had not interpreted their results accordingly; a recent investigation in her laboratory on an untwinned crystal indicated two unit cells, each bigger than that deduced by Plieth and Wurster.

R. E. FRANKLIN
R. L. GORDON

REFERENCES

(1) FRANKLIN, R. E. *Acta Cryst.*, **3**, p. 107 (1950).
(2) FRANKLIN, R. E. *Acta Cryst.*, **4**, p. 253 (1951).

(3) FRANKLIN, R. E. *Proc. Roy. Soc. A*, **209**, p. 196 (1951).

(4) FRANKLIN, R. E. *Brennstoff-Chemie*, **34**, p. 359 (1953).

(5) BISCOE, J., and WARREN, B. E. *J. Appl. Phys.*, **13**, p. 364 (1942).

(6) MAIRE, J. *C.R. Acad. Sci.* [*Paris*], **232**, p. 61 (1951).

(7) HIRSCH, P. B. *Proc. Roy. Soc. A*, **226**, p. 143 (1954).

(8) WARREN, B. E., and BISCOE, J. *J. Amer. Ceram. Soc.*, **21**, p. 259 (1938).

(9) BISCOE, J., DRUESNE, M. A. A., and WARREN, B. E. *J. Amer. Ceram. Soc.*, **24**, p. 100 (1941).

(10) FAJANS, K., and BARBER, S. W. *J. Amer. Ceram. Soc.*, **74**, p. 2761 (1952).

(11) ANDERSON, S., BOHON, R. L., and KIMPTON, D. D. *J. Amer. Ceram. Soc.*, **38**, p. 370 (1955).

(12) JELLYMAN, P. E., and PROCTOR, J. P. *J. Soc. Glass Technol.*, **39**, p. 173 (1955).

(13) AINSWORTH, L. *J. Soc. Glass Technol.*, **38**, p. 479 (1954).

(14) AINSWORTH, L. *J. Soc. Glass Technol.*, **38**, p. 501 (1954).

(15) DOUGLAS, R. W., and ISARD, J. O. *J. Soc. Glass Technol.*, **35**, p. 206 (1951).

(16) DOUGLAS, R. W., and JONES, G. A. *J. Soc. Glass Technol.*, **32**, p. 309 (1948).

(17) HOFFMAN, L. C., and STATTON, W. O. *Nature* [*London*], **176**, p. 561 (1955).

(18) GORDON, R. L., and HARRIS, G. W. *Nature* [*London*], **175**, p. 1135 (1955).

(19) GORDON, R. L., and HARRIS, G. W. *Safety Mines Res. Establ. Res. Rep.* No. 138 (1956).

(20) GORDON, R. L., GRIFFIN, O. G., and NAGELSCHMIDT, G. *Safety Mines Res. Establ. Res. Rep.* No. 52 (1952).

(21) GRIFFIN, O. G. *Safety Mines Res. Establ. Res. Rep.* No. 103 (1955).

(22) DEMPSTER, P. B., and RITCHIE, P. D. *J. Appl. Chem.*, **3**, p. 182 (1953).

(23) LE BOUFFANT, L. Private communication (1956).

(24) DEMPSTER, P. B., and RITCHIE, P. D. *Nature* [*London*], **169**, p. 538 (1952).

(25) ARMSTRONG, E. J. *Bell Syst. Tech. J.*, **25**, p. 136 (1946).

(26) GAY, P., HIRSCH, P. B., and KELLAR, J. N. *Acta Cryst.*, **5**, p. 7 (1952).

(27) FINCH, G. I., LEWIS, H. C., and WEBB, D. P. D. *Proc. Phys. Soc.* [*London*] *B*, **66**, p. 949 (1953).

(28) KATZOFF, S. *J. Chem. Phys.*, **2**, p. 841 (1934).

(29) MORGAN, J., and WARREN, B. E. *J. Chem. Phys.*, **6**, p. 666 (1938).

(30) *Proceedings of the International Conference on Co-ordination Compounds, Amsterdam* (1955). To be published.

(31) BAGNO, O., and LONGUET-ESCARD, J. *J. Chim. Phys.*, **51**, p. 434 (1954).

(32) HENDRICKS, S. B., and TELLER, E. *J. Chem. Phys.*, **10**, p. 147 (1942).

(33) LANDAU, L. *Phys. Z. Sowjet.*, **12**, p. 579 (1937).

(34) HIRSCH, P. B. *Proc. Roy. Soc. A*, **226**, p. 143 (1954).

(35) REEDER, F. Unpublished work.

(36) RAKOWSKI, L. Unpublished work.

(37) BAMFORD, C. H., BROWN, L., ELLIOT, A., HANBY, W. E., and TROTTER, I. F. *Nature* [*London*], **173**, p. 27 (1954).

(38) BROWN, L., and TROTTER, I. F. *Trans Faraday Soc.* To be published.

(39) BUNN, C. W., and HOWELLS, E. R. *Nature* [*London*], **174**, p. 549 (1954).

(40) BUNN, C. W. *Trans Faraday Soc.*, **35**, p. 482 (1939).

(41) COCHRAN, W., CRICK, F. H. C., and VAND, V. *Acta Cryst.*, **5**, p. 581 (1952).

(42) COULSON, C. A. *Contribution à l'étude de la structure moléculaire*. Vol. Commém. Victor Henri 1947/48, p. 15 (Liège: Desoer, 1948).

(43) HERBST, M. *Z. Elektrochem.*, **54**, p. 318 (1950).

(44) KELLER, A. *J. Polym. Sci.*, **17**, p. 291 (1955).

(45) KELLER, A. *J. Polym. Sci.*, **17**, p. 351 (1955).

(46) KELLER, A., and WARING, J. R. S. *J. Polym. Sci.*, **17**, p. 447 (1955).

(47) KELLER, A. *J. Polym. Sci.*, **11**, p. 567 (1953).

(48) KELLER, A. *J. Polym. Sci.*, **15**, p. 31 (1955).

(49) ROBINSON, C. *Trans Faraday Soc.*, **50**, p. 1012 (1954).

(50) TURKEVITCH, J., and HILLIER, J. *Analyt. Chem.*, **21**, p. 475 (1949).

(51) BATES, T. F., SAND, L. B., and MINK, J. F. *Science*, **111**, p. 512 (1950).

(52) NOLL, W., and KIRCHER, H. *Neues Jahrbuch Mineral. Monatsch.*, p. 219 (1951).

(53) BATES, T. F., HILDEBRAND, F. A., and SWINEFORD, A. *Amer. Min.*, **35**, p. 463 (1950).

(54) NOLL, W., and KIRCHER, H. *Naturwissenschaften*, **39**, p. 233 (1952).

(55) ARUJA, E. *Ph.D. thesis* (University of Cambridge, 1943).

(56) WHITTAKER, E. J. W. *Acta Cryst.*, **6**, p. 747 (1953).

(57) JAGODZINSKI, H., and KUNZE, G. *Neues Jahrbuch Mineral. Monatsch.*, p. 113 (1954).

(58) WHITTAKER, E. J. W. *Acta Cryst.*, **8**, p. 261 (1955).

(59) WHITTAKER, E. J. W. *Acta Cryst.*, **4**, p. 187 (1951).

(60) PADUROW, N. N. *Acta Cryst.*, **3**, p. 200 (1950).

(61) WHITTAKER, E. J. W. *Acta Cryst.*, **5**, p. 143 (1952).

(62) WHITTAKER, E. J. W. *Acta Cryst.*, **8**, p. 571 (1955).

(63) TOPLEY, B. *Quart. Revs. Chem. Soc.* [*London*], **3**, p. 345 (1949).

(64) CORBRIDGE, D. E. C. *Acta Cryst.*, **9**, p. 308 (1956).

(65) CORBRIDGE, D. E. C. *Acta Cryst.*, **8**, p. 520 (1955).

(66) PLIETH, K., and WURSTER, C. *Z. Anorg. Chem.*, **267**, p. 49 (1951).

(67) GRUND, A., and PIZY, M. *Acta Cryst.*, **5**, p. 857 (1952).

(68) WESTRIK, R., and MACGILLAVRY, C. H. *Acta Cryst.*, **7**, p. 764 (1954).

(69) BRAVAIS, A., and BRAVAIS, L. *Ann. Sci. Nat.* (2), **1**, p. 42 (1877).

The suppression of screen grid emission by carbon*

By J. A. CHAMPION, M.Sc., Grad. Inst.P., M.-O. Valve Co. Ltd., at the G.E.C. Research Laboratories, Wembley

The screen grid emission level which obtains in a receiving valve in which there is no suppression is shown to be of the same magnitude as that of a thin activated layer of barium oxide. It is further shown that the mechanism by which carbon suppresses screen grid emission is by the chemical reduction of deposited barium oxide to barium which evaporates. Below 900° C this reduction proceeds at a negligible rate and is only sufficient to activate the grid film. At 950° C the emission decays to a negligibly small value after a few minutes.

During the processing and life of a radio valve, material is evaporated from the oxide-coated cathode and settles on the other parts of the valve. In particular, some settles on the grids. If these grids become heated, either by radiation from the cathode or by electron bombardment, they themselves emit thermionically. Such emission, known as grid emission, if excessive, is harmful from the point of view of the performance of the valve.

Previous work[1-3] has been mainly concerned with the suppression of emission from control grids; such grids are usually heated only by radiation from the cathode and to the relatively low temperature of 300–400° C. Screen grid emission is of importance when considerable power has to be dissipated in the screen grid of tetrode or pentode valves. An example of this is a valve in a line time base circuit in a television set, where if screen grid emission exceeds a certain amount, the circuit will not function satisfactorily.

For screen grid emission not to be detrimental in the application mentioned, it must be less than about 100 μA, which corresponds to about 0·1 mA . cm^{-2} for a typical valve screen grid. If untreated molybdenum were to be used the screen grid dissipation, and therefore the output, would have to be limited to about a fifth of that which would be possible with a valve having a screen grid operating for example at 700° C. From an untreated molybdenum grid at a temperature of about 700° C the emission may, however, well be of the order of 10 mA . cm^{-2} and the usual methods for emission suppression are not applicable at this temperature.

Considering now the source of this emission, it must be remembered that during the processing of a valve the oxide-coated cathode is run at a temperature in the region of 1100° C. At this temperature both barium and barium oxide will be evaporated and deposited on to the grids, thus thermionically activating them. The rate of evaporation of barium during this stage will be limited by the rate at which it is produced by the reaction of barium oxide with the core material of the cathode. Some of the free barium evolved from the cathode will be subsequently oxidized by the gas present during the processing and by any oxide films on the grid wires. Experimental results have been given by Jenkins and Newton[4] which show that the amount of free barium evaporated from a cathode during activation is only a small fraction of the known total amount of barium contained in the deposits found on the electrodes. In practice it is also found that the emission from such a layer on a grid can greatly exceed that which would be expected from a monolayer of pure barium; this confirms the theory that the layer is a mixture of barium oxide and barium.

Emission from control grids of receiving valves may be suppressed by plating the material of the grid wires, for example, molybdenum, with gold. This has been described by Baker.[1] A paper by Noga and Okada[2] has also described the use of gold and one by Arizumi and Narita[3] mentions the use of silver and carbon in addition to gold. It is inadvisable, however, to use gold-plated molybdenum for the winding wire of screen grids since, although there is evidence that gold will sufficiently suppress grid emission, there is considerable likelihood of the gold evaporating in sufficient quantities to poison the emission from the cathode within a relatively short space of time. If the valve is one in which the screen grid wires are alined with those of the control grid, then displacement of a single turn can expose it to the electron beam; if this happens a considerable rise in temperature will result in an even more copious evaporation of gold.

Carbon is a natural material to be considered as a surface layer for screen grid winding wires because it has a high thermal emissivity, so that for a given power dissipation the grid will operate at a lower temperature.

It is found, however, under certain circumstances that the reduction in screen grid emission by carbon coating is greater than can be accounted for by a reduction in temperature. This paper describes an investigation into the mechanism of this reduction of grid emission, which makes carbon a very useful grid emission suppressor for high-temperature applications.

VALVE USED FOR FIRST SERIES OF EXPERIMENTS

In the first of two series of experiments, an assembly was used in which either barium or barium oxide could be evaporated on to a carbon-coated molybdenum strip and on to a tungsten wire. The strip and wire could be independently heated electrically and the thermionic emission drawn to a surrounding nickel anode. It was decided to use a tungsten wire as a control as such a wire may be heated to a higher temperature, and so cleaned more thoroughly, then a molybdenum wire, and because more data was available for thin films on tungsten (see, for example, the work of Becker[5]). Experiments are, however, described later in this paper which show that the thermionic properties of thin films of barium and barium oxide on tungsten differ little from those of similar films on molybdenum.

The actual design of the valves is shown in Fig. 1, from which it may be seen that four elements are mounted on a

* G.E.C. Communication No. 678.

valve pinch and surrounded by an anode. The four elements are

A, a "batalum" getter, consisting of a reaction mixture of barium orthotitanate and beryllium deposited on a molybdenum strip, to provide a source of barium,

B, a spiral of platinum wire sprayed with a barium carbonate suspension, to provide a source of barium oxide,

C, a strip of molybdenum 1 mm wide, coated with a colloidal suspension of graphite,

D, a tungsten wire 0·1 mm diameter.

It was so arranged that any of the four elements could be heated by passing an electric current through them. Suitable slots were provided in the nickel anode so that any of the elements could be observed with an optical pyrometer. Unless otherwise stated, all temperatures quoted for the tungsten wire include a correction for its spectral emissivity. Those for the carbon-coated molybdenum are luminance temperatures, as given by an optical pyrometer, but will be very near to the black body temperatures owing to the high spectral emissivity of carbon. A "Kic" (Kemet iron-clad) getter loop which releases barium on heating was also fixed to the bottom of the assembly.

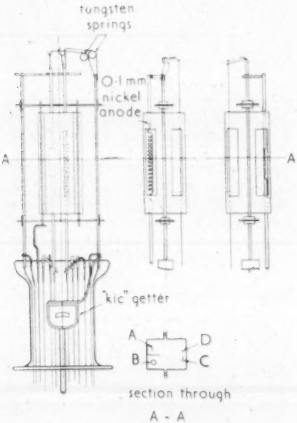

Fig. 1. Valve assembly used in first series of experiments

A, Batalum getter; *B*, Platinum spiral sprayed with barium carbonate; *C*, Carbon-coated molybdenum strip 1 mm wide; *D*, Tungsten wire 0·1 mm diameter.

After evacuating and baking the valve on a mercury diffusion pump with liquid air trap the anode and "Kic" getter were outgassed by eddy current heating. Next the "batalum" getter was outgassed and the barium carbonate on the platinum spiral converted to the oxide, both by electrical heating. The graphite-coated molybdenum strip was outgassed by heating to a temperature of 650° C for 1 min and the tungsten wire heated to about 2300° C for 2 min in order to clean it. Finally the barium was evaporated from the getter loop by eddy current heating and the valve sealed off from the pump.

In order that the temperature of the molybdenum strip and tungsten wire would be known during subsequent experiments, temperature-current graphs were constructed for both these elements using an optical background pyrometer. Plots were obtained which were linear to a good approximation, so that it was considered justifiable to extrapolate back for temperatures below the visible region.

In all the evaporation experiments to be described the receptors were cold.

EVAPORATION OF BARIUM

In order to find the maximum emission level that could be obtained when barium alone was evaporated, the batalum getter was electrically heated with a current of 3·5 A for discreet intervals of time, say 2 min, between which the emission from both the tungsten wire and the carbon-coated molybdenum strip were measured. The effective area of the tungsten wire on to which barium was evaporated was about 0·03 cm^2 and of the carbon-coated molybdenum about 0·2 cm^2. In order to measure the emission, I_a–V_a curves were plotted for values of V_a up to about 200 V, and the curve above the saturation point extrapolated back to the I_a-axis in order to take account of any electrical leak.

It was found that the emission from the tungsten wire when measured at a temperature of 700° C reached a maximum, corresponding to a monolayer of barium,[5] after about 35 min of evaporation. The value of the maximum emission was 2·5 mA.cm^{-2}. The rate of increase of emission from the carbon-coated molybdenum, when measured at 700° C became very small after about 80 min, at which time

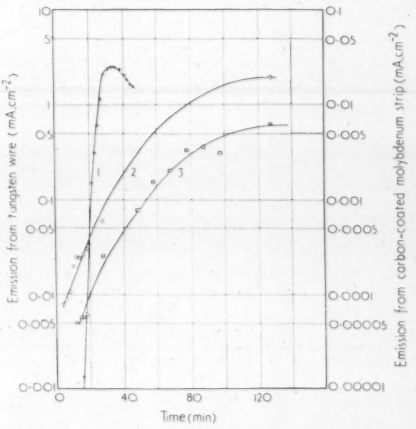

Fig. 2. Emission from tungsten wire and carbon-coated molybdenum as a function of the time for which barium has been evaporated on to them

Curve 1: Tungsten wire, 700° C; Curve 2: Carbon-coated molybdenum strip, 700° C; Curve 3: Carbon-coated molybdenum strip, 670° C.

the emission was 0·01 mA.cm^{-2}. Evaporation was continued for a total time of 120 min after which the emission was 0·02 mA.cm^{-2}. The results are plotted in Fig. 2. It will be seen therefore that the emission from barium on a carbon-coated grid would be well under the dangerous limit.

If we calculate what the emission should be from a monolayer of barium on clean tungsten at 973° K (700° C) from the Richardson equation

$$I = AT^2 \exp(-\phi/kT)$$

taking $A = 1{\cdot}5$ A.cm^{-2}.°C^{-2} and $\phi = 1{\cdot}6$ eV we get $I = 6$ mA.cm^{-2}, which gives reasonably good agreement with the value of 2·5 mA.cm^{-2} found in practice and referred to in an earlier paragraph.

Before the barium oxide experiments were performed the barium was removed from the carbon-coated molybdenum by heating to as high a temperature as practicable (*circa* 1100° C) for 20 min, after which time the emission measured at 700° C had fallen to a few millimicroamperes. The barium was evaporated from the tungsten by flashing it again at 2300° C.

EVAPORATION OF BARIUM OXIDE

The platinum spiral was heated to a temperature of about 1100° C and the emission from the carbon-coated molybdenum and from the tungsten wire was measured at 700° C at intervals throughout a period of 60 min. The effective areas on to which evaporation took place were approximately the same as in the case of the barium. During this time it was found that the emission from both elements increased approximately exponentially with time. When evaporation was finally stopped the emission measured at 700° C from the tungsten wire had reached 1 mA.cm^{-2} and that from the carbon-coated molybdenum 20 mA.cm^{-2}. It was noticed in the case of the molybdenum that the emission continued to increase while the emission measurements were made. The final thickness of barium oxide deposit, as estimated from interference fringes formed was of the order of 10^{-5} cm. It has been deduced from measurements of evaporated material, that a layer of the same order of thickness is deposited on screen grids during the processing of valves.

For measurements involving rapidly changing emission with time, it was not practicable to plot I_a–V_a curves at each stage. Instead the emission for a fixed anode potential (200 V) was read. For the same reason, during experiments on deactivation at high temperature the barium was measured at the high temperature only, apart from an initial observation at 700° C, and at one or two subsequent points, for comparison purposes.

The carbon-coated molybdenum strip was heated to 1000° C: the emission against time relationship is given by Curve 1 of Fig. 3. Initially the emission at 700° C was about 20 mA.cm^{-2}, after 36 min it was about 0·2 μA.cm^{-2} and finally after 100 min it was about 0·1 μA.cm^{-2}. The tungsten wire was heated to 900° C for 25 min and then at 1000° C; the emission obtained from the wire is shown by Curves 1 and 2 in Fig. 4. The emission at 700° C was originally about 1 mA.cm^{-2}, after 37 min it was about 0·3 mA.cm^{-2} and after 153 min 0·3 μA.cm^{-2}.

The whole procedure, of evaporating the same amount of barium oxide and afterwards observing the change of emission with time, was repeated for a fixed temperature of 950° C. The emission-time curve obtained from the tungsten wire at this temperature is shown by Curve 3 in Fig. 4. From this it may be seen that the emission increased considerably as a result of the wire being heated. The emission at 700° C was measured after 115 min and found to be about 30 mA.cm^{-2}.

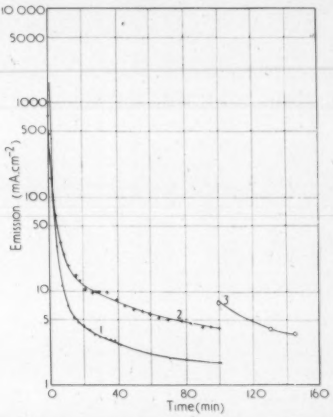

Fig. 3. Change of emission with time from carbon-coated molybdenum strip when heated to different temperatures after barium oxide had been evaporated on to it

Curve 1: Strip heated to 1000° C; Curve 2: Strip heated to 950° C; Curve 3: Continuation of Curve 2, temperature increased to 1000° C.

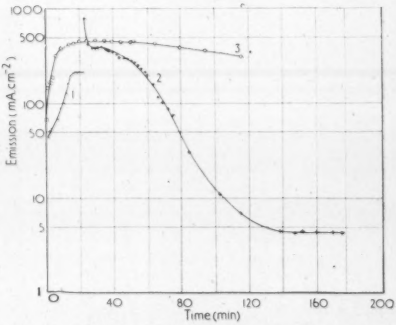

Fig. 4. Change of emission with time from tungsten wire when heated to different temperatures after barium oxide had been evaporated on to it

Curve 1: Wire heated to 900° C; Curve 2: Continuation of Curve 1, temperature increased to 1000° C; Curve 3: Wire heated to 950° C.

The emission from the carbon-coated molybdenum strip, however, fell rapidly as shown in Curves 2 and 3 in Fig. 3; after 100 min the emission was measured at 700° C and found to be about 100 μA.cm^{-2}.

***

Fig. 3 indicates that there is a rapid decay of emission for temperatures of 950° C and above. Further experiments were therefore carried out for temperatures below this. Fig. 5 shows the emission, in this case measured at 700° C, when the carbon-coated molybdenum strip, on to which the

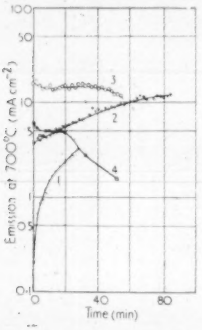

Fig. 5. Change of emission with time from carbon-coated molybdenum strip at 700° C, having had barium oxide evaporated on to it, when heated to various successive temperatures

Curve 1: 750° C; Curve 2: 800° C; Curve 3: 850° C; Curve 4: 900° C.

same amount of barium oxide as before had been evaporated, was heated in successive experiments to temperatures of 750° C, 800° C, 850° C and 900° C. From these curves it is seen that below 850° C continuous activation took place, while at 900° C a slow decay was obtained.

COMPARISON OF TUNGSTEN AND MOLYBDENUM

Further experiments were carried out in order to compare the thermionic emission from barium and barium oxide films on tungsten with that from similar films on molybdenum. The valve used differed little from that shown in Fig. 1, except that the carbon-coated molybdenum strip was replaced by a molybdenum wire of 0·1 mm diameter. The valve was processed in a similar manner to the earlier type; the molybdenum wire being cleaned by heating to as high a temperature as possible without excessive evaporation taking place.

With the wires cold, barium was evaporated on to them and the emission at 700° C measured at equal intervals of time. The variation of emission with time of deposition of barium on to the tungsten wire was similar to that shown in Fig. 2. The emission from the barium on molybdenum reached a less well-defined maximum but the optimum emission occurred after the same time of deposition and was the same for a given wire temperature within the accuracy permitted by the temperature measurement. It was found in another experiment that if the tungsten wire was cleaned less thoroughly, then it behaved in very much the same way as the molybdenum wire, confirming that it is necessary to have a thoroughly clean wire before a well-defined peak in the emission-thickness of deposit curve can be obtained.

Evaporation of barium oxide on the cleaned wires gave results for both wires similar to those reported above for tungsten within the experimental error. A layer of barium oxide of thickness of the order of 10^{-5} cm was deposited on each wire and then heated to 900° C. The emission at 900° C from each wire increased with time by a factor of about ten before becoming stable, but it was noticed that the time taken for the molybdenum wire to reach a stable emission was about five times that for the tungsten wire. The stable values of emission at 900° C and at 700° C for each wire were similar within the limits of experimental error.

SECOND SERIES OF EXPERIMENTS

For these experiments a suspension of one part by weight of carbon black and three parts by weight of barium carbonate in a binder were sprayed on to the middle 5 or 6 mm of a strip of shot-blasted platinum 3·0 cm × 1·3 mm × 0·1 mm. The strip was sprayed to a coating weight of approximately 0·5 mg. After spraying, the platinum strip was mounted on a B7G valve base and a nickel rod of 0·5 mm diameter was mounted about 2 mm in front of the coating. The base was sealed into a glass envelope in an atmosphere of nitrogen.

The system was exhausted and baked in a similar manner to the first type of valve. The coating was outgassed by passing a current of 6 A through the platinum strip for two minutes, during which time the strip reached a luminance temperature of 850° C. After this there was no visible evidence of any deposit having formed on either the nickel rod or on the glass envelope. The current was increased to 6·5 A, which corresponded to a luminance temperature of the coating of 900° C, and after 2 min there seemed to be some indication that a film was forming on the nickel rod. The heating was continued for a further 8 min. After this time it appeared that a dark film was beginning to form on the rod. The current was increased to 6·8 A giving a luminance temperature of 940° C, when it was obvious that the film was forming much more rapidly. After 10 min had elapsed the thickness of the dark deposit was such that two complete interference fringes could be seen under white light. At this stage the envelope was sealed off. If we assume that the average thickness of the deposit is 5×10^{-5} cm, the area of the deposit 5 mm × 0·5 mm and take the density of the deposit to be 3·5 g.cm^{-3} (i.e. that of barium) the weight of the deposit works out to be 4 μg.

Confirmation that the deposit was barium and not the oxide was given by the fact that the interference fringes disappeared immediately upon opening the envelope and the deposit became invisible.

The amount of barium contained in the deposit was determined by dissolving the film in distilled water and measuring the conductivity of the resultant solution of barium hydroxide. This method of determination gave the weight of barium as 3·8μg. This is in surprisingly good agreement with the figure of 4 μg estimated above assuming the deposit to be entirely composed of barium.

Further confirmation that the metallic radical of the deposit which had been dissolved was barium was obtained by a chemical spot test applied to the solution after evaporating to a small volume.

DISCUSSION

From the first series of experiments it may be seen that, if pure barium is evaporated on to clean tungsten, clean

molybdenum or carbon-coated molybdenum, the maximum emission obtainable is much lower than the screen grid emission encountered in receiving valves having no suppression. Measurements on evaporated layers of barium oxide on tungsten or molybdenum and on carbon-coated molybdenum show, however, that the high screen-grid emission level which often obtains in practice is consistent with barium oxide together with some barium having been deposited on to the grids during processing. It has been shown that at temperatures of 950° C and above, the emission from a deposited layer of barium oxide on carbon-coated molybdenum decays to a negligibly small value in a few minutes. Below 900° C there is actually a rise in emission with time, corresponding to activation of the layer. On the other hand, where tungsten, on to which barium oxide has been evaporated, is heated, the decay of emission is very gradual, even at 1000° C.

When the emission from the barium oxide on carbon-coated molybdenum at 1000° C is plotted against time on a log–log scale, as has been done in Fig. 6, it is seen that a

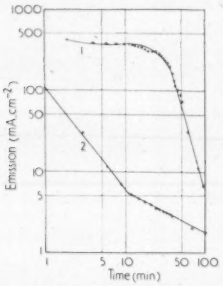

Fig. 6. Change of emission with time from carbon-coated molybdenum strip and from tungsten wire when heated to 1000° C after barium oxide had been evaporated on to them

Curve 1: Tungsten wire; Curve 2: Carbon-coated molybdenum strip.

straight line is obtained for approximately the first 10 min, after which time there is an abrupt change in slope to a straight line of smaller negative gradient. This type of curve was not obtained for a barium oxide film on tungsten (see also Fig. 6). It is suggested that during the first part of the curve barium oxide is being reduced to barium by the carbon, according to the equation

$$BaO + C = Ba + CO,$$

and that the emission is from an activated barium oxide layer of steadily reducing thickness. It is thought that the change in slope of the curve marks the end point of the above reaction, and that further decay in emission past this point is due to evaporation of the remaining free barium. According to the above hypothesis, the emission at the point where there is an abrupt change in slope should equal that from a monolayer of barium; in fact, they are equal to within an order of magnitude.

The second series of experiments, in which it was shown that at temperatures above 900° C barium is evaporated from a mixture of carbon and barium oxide, seems to confirm the above theory.

During the life of a relatively well-aged and gas-free valve, where the running temperature of the cathode is about 700° C, the main constituent being evaporated is free barium. From the results shown in Fig. 2 it is seen that this should not be sufficient to produce an undesirable high emission from the screen grid at its usual operating temperature of 600–700° C.

It may be seen from this work that the mechanism by which carbon suppresses grid emission is entirely different from that of gold. Gold on the surface of a grid wire will tend to dissolve any barium evaporated on to it and so prevent proper activation of any barium oxide, and also prevents the initial formation of barium oxide due to reaction of barium with an oxidized grid wire. Carbon on the other hand suppresses screen grid emission by virtue of being a good reducing agent.

Possible alternatives to carbon which might suppress grid emission by reducing any oxide deposits include titanium, zirconium, tantalum, silicon and thorium, but such materials would necessarily be more expensive than carbon. A possible advantage of these materials is that the reducing reaction does not produce gas, but this is at the expense of leaving a layer of barium compound on the surface of the grid wire, for example barium titanate or silicate whose emission might be dangerously high.

ACKNOWLEDGEMENT

In conclusion, the author wishes to thank M.-O. Valve Co. Ltd., on whose behalf this work was carried out, for permission to publish this paper.

REFERENCES

(1) BAKER, B. O. *Brit. J. Appl. Phys.*, **4**, p. 311 (1953).

(2) NOGA, K., and OKADA, Y. *J. Phys. Soc. Japan.*, **4**, p. 360 (1949).

(3) ARIZUMI, T., and NARITA, S. *J. Phys. Soc. Japan*, **4**, p. 300 (1949).

(4) JENKINS, R. O., and NEWTON, R. H. C. *J. Sci. Instrum.*, **26**, p. 172 (1949).

(5) BECKER, J. A. *Trans Faraday Soc.*, **28**, p. 151 (1932).

Multiplicity in the anode marks of sparks

By J. M. Somerville, M.A., D.Sc., F.Inst.P., and C. T. Grainger, M.Sc., The University of New England, Armidale, New South Wales, Australia

[*Paper first received* 15 *March, and in final form* 4 *June*, 1956]

The conditions which lead to multiplicity in the mark left on the anode by a spark of short duration in air have been studied. The anode surface condition is important in determining multiplicity and was controlled in this investigation by depositing various numbers of layers of barium stearate on clean palladium, aluminium and tin anodes. The nature of the mark is determined in the first few tenths of a microsecond of the life of the spark and depends chiefly on the number of "contaminating" layers on the anode, on the rate of rise of current in the spark and on the breakdown voltage of the spark gap.

It has been found[1] that the mark left on the anode surface by a transient arc passing between electrodes in air at atmospheric pressure may be multiple, particularly when the duration of the arc is reduced to the order of a microsecond. (Since all discharges discussed in this paper are of duration so short that stability is never approached, it will be more appropriate to refer to the discharges as sparks than arcs.) The phenomenon is a striking one and the mark may consist of a hundred or more small separate spots instead of the single spot characteristic of arcs of longer duration. It was suggested[1] that the significant parameter controlling multiplicity might well be the rate of rise of current in the spark rather than its duration, but the equipment then used did not allow the rate of rise of current to be varied independently of other factors. It was the object of this investigation to determine whether the rate of rise of current is the chief or only factor determining multiplicity, and if not, to determine the influence of other factors.

EXPERIMENTAL APPARATUS

A number of pulse-forming artificial lines were constructed which were designed to allow several factors to be varied independently of the others so that their influence on the occurrence of multiplicity could be studied separately.

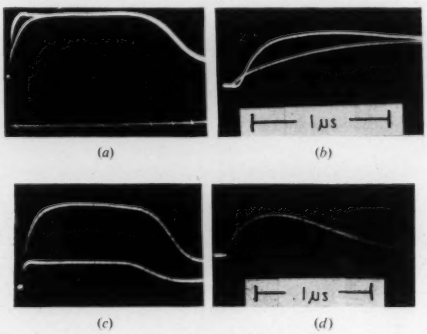

(*a*) (*b*)

(*c*) (*d*)

Fig. 1. Oscillograms of current pulses

(*a*) Pulses *A* (slow rising) and *C* (fast rising) superposed; 1 μs time markers.
(*b*) Pulses *A* and *C* (leading edges only).
(*c*) Pulses *C* and *D* (high current).
(*d*) Pulses *E* and *F* superposed.

Oscillograms of the current pulses produced by these lines are shown in Fig. 1.

Pulses *A* and *C* differ only in rate of rise of current and are produced by the line shown in Fig. 2. The four inductances L_1–L_4 and the four condensers C_1–C_4 make up a conventional

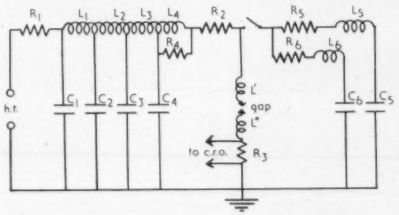

Fig. 2. Pulse-forming artificial line used for generating current pulses *A* and *C*

pulse-forming line with a characteristic impedance R_2 of 50 Ω, a pulse duration of about 8 μs and a rise time (10% to 90%) of about 1 μs. This line generates the "slow-rising" pulse *A*. In order to reduce the rise time, an additional short, rapidly rising pulse may be fed into the spark. This is formed by two *L*, *R*, *C* combinations L_5, R_5, C_5 and L_6, R_6, C_6 which are adjusted to achieve a smooth join with the slow-rising pulse. With these combinations in circuit the "fast-rising" pulse *C* is formed with a rise time of about 0·2 μs. Due to non-linearity in the rise of pulse *A*, the mean rate of rise over the first 0·2 μs of pulse *C* is approximately 2·5 times that of pulse *A*. The small inductances L' and L'' and the resistance R_4 serve to suppress high frequency transients (about 100 Mc/s) which otherwise appear across the gap. The duration of either pulse may be reduced simply by removing one or more of the sections L_1C_1, L_2C_2, L_3C_3. In this way the pulse length may be made approximately 2, 4, 6 or 8 μs, independently of the rise time. This line thus allows either rise time or pulse duration to be changed independently of any other quantity. The peak current in pulses *A* and *C* is equal to $9 \times 10^{-3} V_0$ amperes where V_0 is the voltage to which the line is charged.

Pulse *D* is generated by a line, the characteristic impedance of which is about one third that of the line generating pulse *C*. When these two lines are charged to the same potential difference and discharged, two current pulses of equal duration are generated in which the current rises at the same rate for about 0·2 μs, after which that in pulse *C* levels off while that in pulse *D* continues to rise until it is three times

that in pulse C. The peak current in pulse D is $2{\cdot}7 \times 10^{-2} V_0$ amperes.

Pulses E and F, shown superposed and not really distinguishable in Fig. 1(d), are two current pulses, identical in shape, generated by discharging two simple L, R, C circuits through the gap. The difference between them lies in the fact that the circuits forming pulses E and F generate identical current pulses when their respective condensers are charged to potential differences in the ratio 2·4 to 1. The peak currents in pulses E and F are respectively $1{\cdot}2 \times 10^{-2} V_0$, and $2{\cdot}9 \times 10^{-2} V_0$ amperes.

EXPERIMENTAL PROCEDURE

The spark was passed between a cathode in the form of a rounded wire and a horizontal plane anode. The spark was struck by charging the appropriate pulse-forming line to the required potential difference, usually between 1000 and 5000 V, and then moving the cathode towards the anode until breakdown took place. Breakdown thus took place under "static" conditions as opposed to "impulse" or "over-volted" conditions.

When systematic observations of multiplicity were begun it very soon became apparent that the condition of the anode surface played a major role. If the anode was very clean, then no mark at all appeared on high melting-point anodes such as palladium, while on low melting-point anodes such as tin, a single relatively large spot appeared. If, however, either anode was coated with a thin grease film by, for example, rubbing it with a finger, then multiplicity as described earlier was observed.

Since a clean anode showed no multiplicity it was evident that systematic results would not be attained unless the anode was "contaminated" in a carefully controlled manner. This was done by taking a clean anode surface and depositing

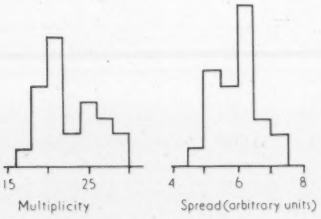

Fig. 3. Histograms of two typical sets of observations of multiplicity and spread of anode marks

on it a number of layers of barium stearate by means of the Langmuir–Blodgett process,[2] each layer being $2{\cdot}44 \times 10^{-7}$ cm thick.

The use of these layers resulted in much greater consistency and reproducibility in the results. Throughout the observations of anode marks, two quantities were measured, namely (i) the "multiplicity" M of the mark, which is simply the number of separate spots forming the mark (where two or more spots have obviously melted together, each is counted separately) and (ii) the "spread" S of the mark, which is the diameter of the smallest circle which will enclose all the spots of the mark. Typical distributions of values of these two quantities are shown in the histograms of Fig. 3.

RESULTS OF OBSERVATIONS

The results of observations of the influence on multiplicity and spread of the various variable factors which could be controlled are given below.

(i) *The influence of spark duration.* The effect on the appearance of the anode mark of varying the spark duration has been described in an earlier publication[3] where it was shown that after 2 μs (the minimum spark duration used) no change takes place in either the multiplicity or spread of the anode mark. The observations suggested strongly that during the initial period of rapid expansion of the spark channel the central spots of the mark are created first but are subsequently abandoned by the current within about 1 μs, after which, for several microseconds, the current flows chiefly or solely in the outer ring of spots. During this time, therefore, the current distribution in the spark channel near the anode has a hollow character which is consistent with observations of the distribution of light intensity in the channels of similar sparks in hydrogen described by Craig and Craggs.[4]

Since the only changes occurring in the mark after 2 μs are due to increased melting at the anode surface, which ultimately obscures the original fine structure, it is best to confine observation to the marks left by sparks of short duration. Consequently the majority of the observations described below were made using pulses not exceeding 2 μs in duration.

(ii) *Influence of anode surface condition and material.* As Fig. 4 shows, with increasing numbers of layers of barium

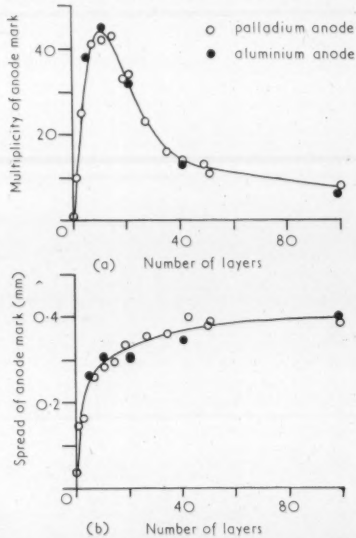

Fig. 4. Showing the dependence of (a) multiplicity and (b) spread of the anode mark on the number of layers of barium stearate present on anodes of palladium and aluminium. Current pulse E, maximum current 48 A

stearate on the anode the multiplicity rose to a maximum at about twenty layers, thereafter decreasing steadily, while the spread rose sharply at first up to about ten layers after which the rate of rise of the spread was much lower. The graphs show points corresponding to both palladium and aluminium anodes, the two sets of points for the different metals falling substantially on the same curve. Other comparisons between anodes of aluminium, palladium and tin showed that, when more than about thirty layers were present, values of multiplicity were independent of the anode material to within the experimental error. Below this number of layers the multiplicity may depend on the anode material. This is shown in Fig. 5(*a*) in which (amongst other data discussed below) values of multiplicity are given corresponding to marks made by pulse *C* under the same conditions on palladium and tin anodes. On the low melting-point tin anode some of the spots had melted together when only a few layers were present. Consequently the measured multiplicity was lower than the original number of spots, and significant estimates of the original number of spots

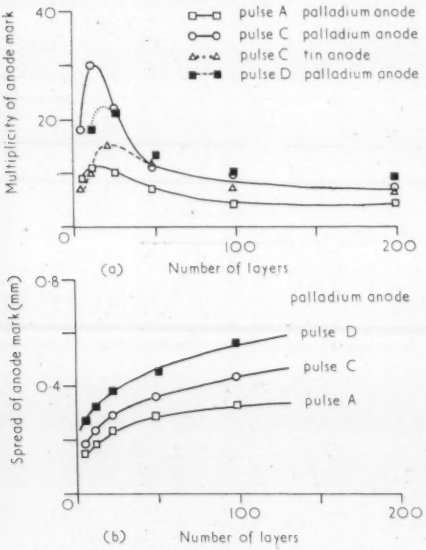

Fig. 5. Showing the dependence of (*a*) multiplicity and (*b*) spread of the anode mark on the number of layers of barium stearate present on anodes of various materials. Current pulses *A* and *C* duration shortened to 2 μs, maximum current 36 A; pulse *D*, shortened to 2μs, maximum current 108 A

were not possible with tin unless the number of layers exceeded thirty. For this reason no significance is attached to the maximum in the observed multiplicity on low melting point anodes.

For a different reason the maximum is not significant for high melting point anodes either. In this case, as the number of layers decreases, the conducting channels through the film become so numerous that most of them do not carry sufficient energy to the anode to cause melting and, in the limit, on a clean anode no mark at all is left. If, therefore, we introduce the concept of "true multiplicity," defined as the number of conducting channels to the anode, it seems reasonable to suppose that the true multiplicity falls steadily from an infinite value on a perfectly clean anode, corresponding to a continuous current distribution, to the measured values, independent of anode material, achieved when the number of layers exceeds about thirty.

The anodes were only roughly polished, but the presence of the scratches left by a fine abrasive powder had no influence on the distribution of the spots of the mark. Even much deeper scratches or blemishes, if present before the layers were applied, had no effect. On the other hand, however, scratches made after the application of the layers had a marked effect, the spots being concentrated along the scratch.

(iii) *Influence of rate of rise of current.* Comparison of the curves of Fig. 5(*a*) and (*b*) for the two pulses *A* and *C* shows that both the multiplicity and the spread produced on a palladium anode by the fast rising pulse *C* were notably greater than those produced by the slow rising pulse *A*. This occurred under all circumstances and, other things being equal, pulse *C* always gave greater multiplicity and spread than pulse *A*.

(iv) *Influence of peak current.* In Fig. 5(*a*) points giving the multiplicity produced by pulse *D* on a palladium anode are shown. It is seen that, for the larger number of layers, the multiplicity produced by pulse *D* was perhaps just significantly greater than that produced by pulse *C* while, for a small number of layers, the greater melting caused by the higher current in pulse *D* made the spots in the mark of *D* run together to give a lower measured multiplicity.

In Fig. 5(*b*) it is seen that the spread produced by pulse *D* was considerably greater than that produced by pulse *C*. This difference, however, is largely due to the presence in the mark of pulse *D* of a few outlying spots at a considerable distance from the others as shown in Fig. 6. It is reasonable to assume that these outlying spots were formed after pulse *D* diverged from pulse *C*.

(v) *Influence of spark length and breakdown potential.* Observations were made of multiplicity and spread in the marks produced by pulses from lines *E* and *F* charged in the ratio 2·4 : 1 so that they gave practically identical current pulses. Since breakdown took place under static conditions, the electrode separation was greater for pulse *E* than for pulse *F*. It was found that the multiplicity produced by pulse *E* was slightly and probably just significantly greater than that produced by pulse *F*. The spread, on the other hand, was quite significantly greater for *E* than for *F*.

(vi) *Influence of line voltage.* If we vary the voltage V_0 to which the pulse-forming line is charged before the spark is struck we are no longer altering only one factor at a time, but are changing the rate of rise of current, peak current and arc channel length simultaneously. Nevertheless, it proves instructive to do so. Fig. 7 shows multiplicity as a function of line voltage for lines *A*, *C*, *E* and *F* discharged to a palladium anode covered with forty-one layers of barium stearate. This number of layers was chosen because it is greater than the number at which any dependence on anode material has been observed. It is seen that, for each line, multiplicity is proportional to line voltage to within the experimental error. Since the rate of rise of current is proportional to the line

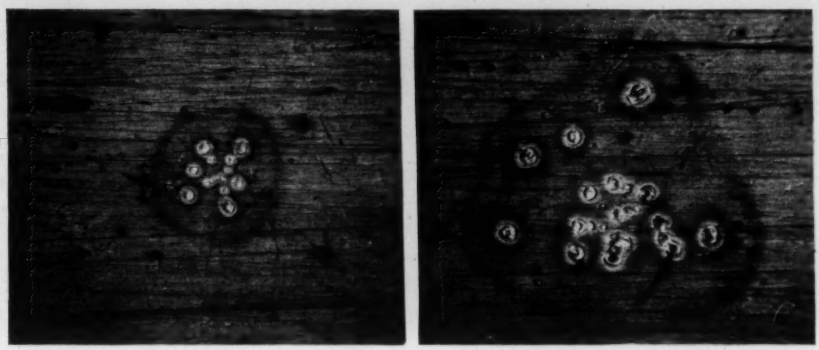

(*a*) (*b*)

Fig. 6. Marks left on a palladium anode coated with forty-one layers of barium stearate by (*a*) current pulse *C*, 2 μs duration, maximum current 36 A, and (*b*) current pulse *D*, 2 μs duration, maximum current 108 A

voltage we may write for each line, $M = kdI/dt$. If we use the straight line best fitting the points, in conjunction with the mean rate of rise of current over the first 0·2 μs, to determine the factor of proportionality k for each of the pulse forming lines, we obtain the following values of k: line *A*, $k = 1{\cdot}6 \times 10^{-7}$; line *C*, $1{\cdot}4 \times 10^{-7}$; line *E*, $1{\cdot}6 \times 10^{-7}$; line *F*, $1{\cdot}3 \times 10^{-7}$ spots s A^{-1}. We are therefore justified in concluding that not only is rate of rise of current the chief factor determining multiplicity (for a given surface condition), but, to a first approximation, the multiplicity is proportional to the rate of rise of current for all four lines and all voltages.

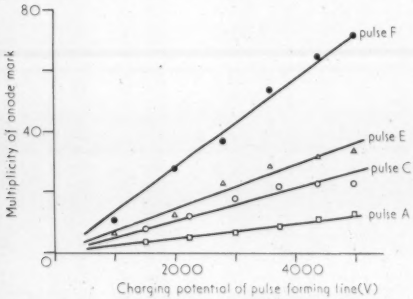

Fig. 7. Graphs of anode mark multiplicity against pulse-forming line charging voltage for various current pulses, using a palladium anode coated with forty-one layers of barium stearate

A somewhat similar situation exists with regard to the spread, as Fig. 8 shows. However, if we follow the same procedure given above and write $S = k_1 dI/dt$, the values of k_1 for the lines *A*, *C*, *E* and *F* respectively are 2·7, 1·5, 1·35 and 0·81 in arbitrary units. If instead, we write $S = k_2\sqrt{(V_0 dI/dt)}$, which of course still preserves the proportionality between S and V_0, then the values of k_2 for *A*, *C*, *E* and *F* are respectively $4{\cdot}3 \times 10^{-8}$, $3{\cdot}8 \times 10^{-8}$, $3{\cdot}9 \times 10^{-8}$ and $3{\cdot}8 \times 10^{-8}$ cm.s$^{\frac{1}{2}}$.W$^{-\frac{1}{2}}$. Consequently, to a first approximation, the spread is proportional to $\sqrt{(V_0 dI/dt)}$.

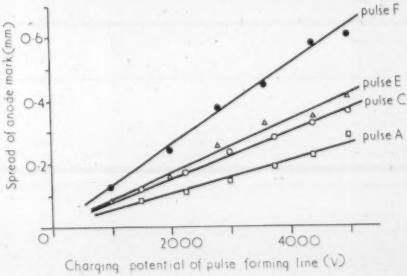

Fig. 8. Graphs of anode mark spread against pulse-forming line charging voltage for various current pulses, using a palladium anode coated with forty-one layers of barium stearate

DISCUSSION

It is clear that the nature of the anode mark is determined during the early stages of the development of the spark. An upper limit to the time of development of the mark is set by the observations of sparks of varying durations which showed[3] that no change in the number or disposition of the spots takes place after 2 μs. For an indication of a lower limit to the development time of the mark we may look to the comparison between the marks left by pulses *C* and *D*. The currents in these pulses are almost identical for the first 0·2 μs, after which they diverge. As we have seen, there were differences in the spread of the marks produced by *C* and *D*, caused chiefly by an additional outer ring of spots in

the mark of D, and there was probably a just significant corresponding difference in multiplicity. This shows that events occurring after the first 0·2 μs could affect the mark.

It seems then, that the nature of the anode mark is determined in the first 0·2 to 2 μs of the life of the spark, with the probability that most of its development takes place in the first two or three tenths of a microsecond. Judging from the measurements of Higham and Meek,[5] these times are rather less than those required for the full development of the spark channel but are of the order of magnitude of the period of maximum rate of channel expansion up to the time of separation of the shock wave[6,7] and of the major collapse in voltage across the gap.[8] The spread of the mark is less than the diameter of the final luminous channel and photographs of the arc show a contraction at the anode which appears to be greater on a clean anode than on an anode covered with a large number of layers (Fig. 9).

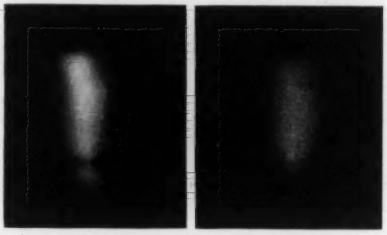

(*a*) (*b*)

Fig. 9. Photographs of a spark carrying current pulse E (maximum current 48 A) to (*a*) a clean palladium anode, (*b*) a palladium anode coated with 200 layers of barium stearate. The anode is the lower electrode and the reflexion in it of part of the spark channel is visible. Camera shutter open for whole duration of spark

Since the structure of the anode mark is determined during a period when the spark channel is in a highly unstable state one can scarcely hope to describe its development in detail. In what follows a general picture of the process which seems to be consistent with the observations is suggested.

After the first break through of the anode film, the current in the spark will rise rapidly and presumably an instantaneous anode fall will develop which may, in the initial stages, be some hundreds of volts.[8] One of the functions of the potential distribution achieved near the anode at this stage must be the "focusing" of electrons approaching the anode so that most of them pass through the hole in the anode film. The distribution of positive ions in the neighbourhood of the spot will play a major role in determining this potential distribution. However, as Drabkina[6] has shown theoretically and Gegechkori[7] and Boyle[9] have demonstrated experimentally, a zone of high gas density travels outwards behind the shock wave, leaving a region of low density behind at the centre. Thus a large proportion of the atoms and ions forming the initial channel will be carried out behind the shock front. This is likely to make the focusing action difficult to maintain and electrons will reach the surface of the anode film in considerable quantities. When sufficient charge accumulates to cause breakdown of the film, there will be a redistribution of potential in the neighbourhood of the breakthrough which will tend to draw electrons from the column into the anode through it. If the instantaneous anode fall necessary to draw the current through the new spot or ring of spots is substantially less than that required to draw it through the old spot, as may well be the case if the plasma electron density is greater in the vicinity of the new spot, then presumably the old spot will be abandoned. As the channel continues to expand similar processes cause the abandonment of the first ring of spots in favour of a second, and so on. [Somewhat analagous cases of discrete spot formation due to the motion of a plasma (at a very much slower rate than in the channel expansion above) over a contaminated electrode surface have been observed at the cathode by Dunkerly and Schaefer[10] and at the anode in this laboratory[11] and by Winson and Lee (see Ref. 10).]

On this picture one would expect the multiplicity to decrease as the film thickness increases and it becomes more difficult to break down. This is observed to happen once the film thickness becomes great enough for reliable measurements of multiplicity to be made. Consistent also is the fact that for a large number of layers (more than a hundred) the central spots of the mark are no longer smaller than the outer spots, showing that the current passed through them for a longer time, corresponding to the longer time required to establish alternative spots.

Some observations which were made of *cathode* spots are relevant here. We reversed the electrodes and studied cathode marks made under the conditions described above. The behaviour at the cathode was quite different from that at the anode, the mark being single or very occasionally double. This was to be expected because, if we adapt the above picture to the cathode it is positive ions which must accumulate on the film to cause it to break down, and, in the times involved, which are of the order of 10^{-7} s, positive ion motion in the electric field or by diffusion will be small.

We have seen that the state of the anode surface has a major influence on the nature of the anode mark. If the anode surface state is fixed, then the multiplicity appears to depend chiefly on the initial value of dI/dt, while the spread depends on $V_0 dI/dt$. If the gap length, and hence V_0, are fixed and the current initially rises at a steady rate, then dI/dt is the only variable determining the initial nature of the discharge. Consequently, if the nature of the mark is determined during this initial stage one would expect that for a given gap length it would depend on dI/dt alone.

When the gap length is varied, then, under conditions of static breakdown, V_0 varies with it. Any attempt to separate gap length and V_0 as independent variables would involve impulse breakdown. We are at present studying mark formation under such conditions.

ACKNOWLEDGEMENTS

Our thanks are due to Mr. G. Cowling for assistance with some of the measurements. The work has been made possible by the support of the Electrical Research Board of Australia which has provided funds for equipment and for the salary of one of us (C.T.G.).

REFERENCES

(1) Somerville, Blevin and Fletcher. *Proc. Phys. Soc. [London] B*, **65**, p. 963 (1952).

(2) Langmuir: *Proc. Roy. Soc. A*, **170**, p. 1 (1939).

(3) SOMERVILLE and GRAINGER. *Brit. J. Appl. Phys.*, **7**, p. 109 (1956). See also SOMERVILLE and FLETCHER on p. 419 of this issue.
(4) CRAIG and CRAGGS. *Proc. Phys. Soc.* [*London*] *B*, **66**, p. 500 (1953).
(5) HIGHAM and MEEK. *Proc. Phys. Soc.* [*London*] *B*, **63**, p. 649 (1950).
(6) DRABKINA. *J. Exp. Theor. Phys. USSR*, **21**, p. 473 (1951).
(7) GEGECHKORI. *J. Exp. Theor. Phys. USSR*, **21**, p. 493 (1951).
(8) ABRAMSON and GEGECHKORI. *J. Exp. Theor. Phys. USSR*, **21**, p. 484 (1951).
(9) BOYLE. *J. Appl. Phys.*, **26**, p. 584 (1955).
(10) DUNKERLEY and SCHAEFER. *J. Appl. Phys.*, **26**, p. 1384 (1955).
(11) BLEVIN. *M.Sc. thesis* (The University of Sydney, 1952).

The frequency of vibration and the elastic stability of a fixed-free strip

By R. F. S. HEARMON, F.Inst.P., Forest Products Research Laboratory, Princes Risborough, Bucks

[*Paper received* 18 *April*, 1956]

The suggestion that critical buckling loads can be found by estimating the load at which the frequency of vibration becomes zero is subjected to experimental test on fixed-free strips of boxwood, brass and steel. The results show good agreement between the load at zero frequency and the critical load calculated from the Euler formula.

The effect of an end thrust P on the frequency of lateral vibrations of a beam pinned at both ends is well known.[1] The relationship can be written

$$(\omega/\omega_0)^2 = 1 - (P/P_{cr}), \tag{1}$$

where ω is the angular frequency under an end compression P, ω_0 is the angular frequency when $P = 0$, and P_{cr} is the critical buckling load. Evidently $(\omega/\omega_0)^2 = 0$ when $P = P_{cr}$, and Lurie[2] has recently generalized this result to suggest that the buckling load of more complicated linear systems could be approximately determined by measuring the frequency as a function of load, and extrapolating to zero frequency. In his paper, experimental measurements were reported for rigid-joint rectangular frames and trusses with good results, and on thin flat plates which showed non-linear effects; experimental measurements have also been made on stiffened panels by Johnson and Goldhammer.[3] However, the expression (1) does not appear to have been tested on beams carrying concentrated masses, or on systems in which the end thrust is provided by gravitational forces. The purpose of the present paper is to report measurements made on fixed-free struts carrying end masses. The theoretical buckling loads can be calculated for this case, serving as a check for the experimental work.

THEORY

In an earlier paper[4] results were reported for the flexural vibration frequency of strips clamped at one end, with the other end free and vertically below the point of clamping. A number of masses were attached in sequence to the free end of the strip and the frequency of vibration of the system corresponding to each attached mass was measured by timing the vibrations with a stop watch. Under these circumstances the stress in the strip is tensile and the question of instability does not arise. The present experiments were carried out with the loaded free end vertically above the fixed end. The strip is therefore in compression and as the load is increased, the strip will eventually become elastically unstable.

In the earlier paper[4] Rayleigh's method was applied to obtain an approximate expression for the frequency. Ellington[5] has pointed out that the Rayleigh method yields an upper limit to the frequency; he has calculated a lower limit and has given an equation for the frequency which lies between the two limits and which he suggests is a better approximation to the true value. Nevertheless, for present purposes, the expression derived earlier [equation (10) of Ref. 4] will be used because it leads to better agreement both with the Euler theory and with experiment [compare equation (4) and Table 2 below]. Applied to the case of a strip with the free end vertically above the fixed end, this expression can be written

$$\omega^2 l/g = (3EI/mgl^2) - 1{\cdot}2, \tag{2}$$

where E = Young's modulus,
I = moment of inertia of cross-section,
l = length of strip,
m = attached mass,
g = gravitational acceleration,

and the mass of the strip and rotatory inertia effects are ignored. If $\omega = 0$, and identifying $(mg)_{\omega=0}$ with P_{cr},

$$(mg)_{\omega=0} = P_{cr} = \frac{3}{1{\cdot}2}\frac{EI}{l^2} = 2{\cdot}5\frac{EI}{l^2}, \tag{3}$$

compared with the Euler value for the critical load of a fixed-free strut[6]

$$P_{cr} = \pi^2 EI/4l^2 = 2{\cdot}468(EI/l^2). \tag{4}$$

The difference between equations (3) and (4) is not significant and can be explained on the basis of approximations introduced into the derivation of equation (3). A treatment essentially the same as the above was given by Balinkin[7] in 1936, but owing to an unnecessary additional assumption, his result differed appreciably from equations (3) and (4).

Equation (2) can be transformed into

$$(\omega/\omega_0)^2 = 1 - (mgl^2/2{\cdot}5EI), \tag{5}$$

where

$$\omega_0^2 = 3EI/ml^3. \tag{6}$$

Since, however, $mg = P$ and $P_{cr} = 2{\cdot}5EI/l^2$, equation (5) can also be written

$$(\omega/\omega_0)^2 = 1 - (P/P_{cr}),$$

which is identical with equation (1). If the mass of the strip and rotatory inertia effects cannot be ignored, approximate allowance for both can be made in vibration experiments[8] by replacing m with M as given by the equation

$$M = \frac{m}{1 - (9i^2/4l^2)} + \frac{33m_0l}{140}, \qquad (7)$$

where i is the radius of gyration of the load about the neutral axis of the strip and m_0 is the mass of the strip per unit length. where W is the weight of the strip. Comparing equation (8) with the Euler expression (4), we get

$$P_{cr} = 2{\cdot}468\ W/7{\cdot}84 = 0{\cdot}315\ \mathrm{W},$$

i.e. the effect of the weight of the strip is the same as the effect of a compressive load $0{\cdot}315\ W$ applied to a massless strip. In the absence of rotary inertia effects, the use of M instead of m is equivalent to replacing the above factor $0{\cdot}315$ by $33/140 = 0{\cdot}236$. The occurrence of rotatory inertia effects will tend to increase the second factor somewhat and, moreover, the exact factor to use when an external compressive load is superimposed on the weight of the strip does not appear to be known. In these circumstances, it was considered adequate to use M as abscissa. This procedure

Table 1. *Attached masses and frequency ratios*

	Boxwood $E = 1{\cdot}47 \times 10^{11}$ dyn/cm²; $I = 2{\cdot}28 \times 10^{-2}$ cm⁴								*Steel* $E = 20{\cdot}3 \times 10^{11}$ dyn/cm²; $I = 8{\cdot}50 \times 10^{-4}$ cm⁴			
	$l = 65$ cm		$l = 55$ cm		$l = 45$ cm		$l = 40$ cm		$l = 45$ cm		$l = 40$ cm	
m	M	$(\omega/\omega_0)^2$	M	$(\omega/\omega_0)^2$	M	$(\omega/\omega_0)^2$	M	$(\omega/\omega_0)^2$	M	$(\omega/\omega_0)^2$	M	$(\omega/\omega_0)^2$
283·2	299·2	0·8724	297·1	0·8924	295·4	0·9142	294·6	0·9654	317·8	0·7806	314·6	0·8226
873·0	890·6	0·5648	889·3	0·6707	888·7	0·7537	888·8	0·8196	911·2	0·5050	908·8	0·5961
1456·4	1476	0·2847	1475	0·4718	1476	0·6346	1477	0·7360	1498	0·2478	1497	0·4005
2037·7			2059	0·2656	2060	0·4836	2062	0·6080			2082	0·1780
2614·8					2641	0·3668	2644	0·5143				
3190·4							3224	0·3927				
3763·2							3801	0·3005				

	Brass $E = 8{\cdot}95 \times 10^{11}$ dyn/cm²; $I = 7{\cdot}52 \times 10^{-3}$ cm⁴									
	$l = 80$ cm		$l = 70$ cm		$l = 60$ cm		$l = 50$ cm		$l = 40$cm	
m	M	$(\omega/\omega_0)^2$	M	$(\omega/\omega_0)^2$	M	$(\omega/\omega_0)^2$	M	$(\omega/\omega_0)^2$	M	$(\omega/\omega_0)^2$
283·7	415	0·7712	399	0·8212	383	0·8500	367	0·8804		
872·5	1005	0·5500	989	0·6498	973	0·7227	958	0·7875	944	0·8225
1455·8	1589	0·3398	1573	0·4941	1558	0·6145	1543	0·7192	1532	0·7818
2037·0	2171	0·1167	2155	0·3214	2141	0·4876	2127	0·6263	2117	0·7208
2614·1					2720	0·3754	2707	0·5549	2699	0·6796
3189·7					3297	0·2480	3286	0·4610	3279	0·6228
3762·8					3873	0·1346	3861	0·3893	3856	0·5774
4328·6							4430	0·2979	4426	0·5123
4890·0									4992	0·4716
5448·1									5554	0·4115
5999·2									6110	0·3708

RESULTS

Experiments were carried out by timing the vibrations at a series of values of m. The technique was the same as that used previously,[4] except that the free end of strip was above the fixed end. The values of ω were worked out from the observations and the ratio $(\omega/\omega_0)^2$ calculated, using equation (6) for ω_0^2 with M substituted for m. The ratio was then plotted against M in grammes, and the value of M for $(\omega/\omega_0) = 0$ read off from the graph. This value was then compared with P_{cr}/g, with P_{cr} calculated from equation (4). The experimental results are given in Table 1; the values of E and I are taken from Ref. (4).

The justification for the use of M as abscissa rather than m is that even when unloaded, there will be some stress in the strip due to its own weight. It can be shown[9] that the maximum length of an unloaded fixed-free strip consistent with stability is given by

$$l^2 = 7{\cdot}84\ EI/W, \qquad (8)$$

at least makes some allowance for the weight of the strip, whereas if m were used, no allowance would be made at all.

Typical graphs of $(\omega/\omega_0)^2$ plotted against M are given in Figs. 1, 2 and 3. The boxwood results (Fig. 1) are very satisfactory. As predicted by equation (1), the points lie very close to a straight line which passes through the point $M = 0$, $(\omega/\omega_0)^2 = 1$ and these features apply to all the boxwood results.

The brass and steel results (Figs. 2 and 3) also give straight lines which, however, do not pass exactly through the point 0, 1. The explanation for this disagreement with theory is not known, but it may possibly be connected with the deviation of the actual boundary conditions from those assumed in deriving the theoretical results.

The comparison between the observed intercepts at $(\omega/\omega_0)^2 = 0$ and the values calculated from equation (4) is given in Table 2.

The agreement is satisfactory throughout. On the boxwood the difference (observed minus calculated) is variable in

Table 2. *Critical loads*

Boxwood			Brass			Steel		
Length (cm)	Load (g)		Length (cm)	Load (g)		Length (cm)	Load (g)	
	Obs.	Calc.		Obs.	Calc.		Obs.	Calc.
40	5400	5270	40	10200	10580	40	2580	2712
45	4050	4163	50	6475	6770	45	2060	2143
55	2790	2785	60	4520	4703			
65	2090	1994	70	3320	3455			
			80	2500	2645			

sign; three out of the four differences are positive, but only one of them exceeds 4% of the calculated value. On the brass and the steel the difference is always negative, but only one of the differences exceeds 5%. It would, therefore, be possible to predict the critical load of a fixed-free strip with reasonable accuracy from frequency measurements alone.

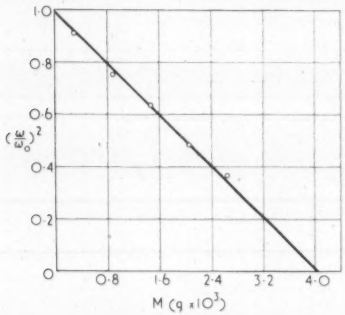

Fig. 1. Plot of frequency ratio squared against applied load for boxwood

$l = 45$ cm; intercept = 4050 g; $\pi^2 EI/4l^2 g = 4163$ g.

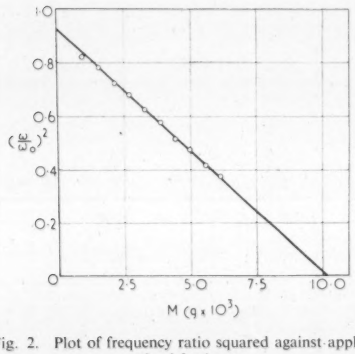

Fig. 2. Plot of frequency ratio squared against applied load for brass

$l = 40$ cm; intercept = 10200 g; $\pi^2 EI/4l^2 g = 10580$ g.

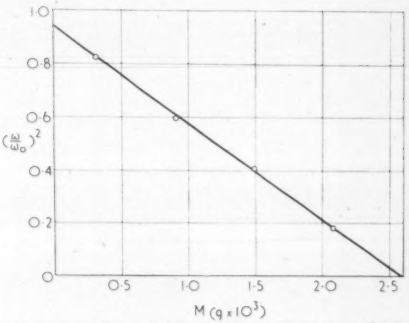

Fig. 3. Plot of frequency ratio squared against applied load for steel

$l = 40$ cm; intercept = 2580 g; $\pi^2 EI/4l^2 g = 2712$ g.

ACKNOWLEDGEMENTS

This paper is published by permission of the Department of Scientific and Industrial Research. Acknowledgement is also made to Associate Professor H. Lurie, California Institute of Technology, for helpful correspondence and suggestions.

REFERENCES

(1) TIMOSHENKO, S., and YOUNG, D. H. *Vibration Problems in Engineering*, 3rd ed., pp. 374–375. (New York and London: McGraw Hill Book Co. Inc., 1955.)

(2) LURIE, H. *J. Appl. Mech.*, **19**, p. 195 (1952).

(3) JOHNSON, E. E., and GOLDHAMMER, B. F. *Proc. Soc. Exp. Stress Anal.*, **11** (1), p. 221 (1953).

(4) HEARMON, R. F. S., and ADAMS, E. H. *Brit. J. Appl. Phys.*, **6**, p. 280 (1955).

(5) ELLINGTON, J. P. *Brit. J. Appl. Phys.*, **6**, p. 451 (1955).

(6) TIMOSHENKO, S. *Theory of Elastic Stability*, 1st ed., pp. 64–66 (New York and London: McGraw Hill Book Co. Inc., 1936).

(7) BALINKIN, I. A. *Phil. Mag.*, **21**, p. 283 (1936).

(8) RAYLEIGH, LORD. *Theory of Sound.* (London: Macmillan and Co. Ltd., 1877).

(9) LOVE, A. E. H. *The Mathematical Theory of Elasticity*, 4th ed., p. 425 (Cambridge: University Press, 1927).

The fusing of wires with heavy surge currents

By A. E. Barrington, B.Sc., Ph.D., A.M.I.E.E., Queen Mary College, University of London

[*Paper received* 2 *May*, 1956]

The behaviour of wires fused by means of a high-frequency discharge yielding peak-current densities of 100–200 kA/mm² is investigated. From records of electrical transients it is estimated that complete melting does not occur prior to break-up. The nature of the arc discharge following break-up is shown to depend on the length and the material of the wires when exploded in air, but independent of these when exploded in vacuum. As a consequence of these experiments, results obtained by earlier investigators are examined critically.

The fusing of wires with heavy surge currents has been studied by several investigators. Early experimenters[1,2,3] were concerned with the high temperatures attainable by this means, subsequent workers have given greater attention to the process of disintegration of the wires. In order to gain a better understanding of the phenomena leading to break-up, it is desirable to obtain an estimate of the energy supplied to the wire, but published data are not conclusive. Furthermore, the conditions for current flow to continue after disintegration are not completely understood. Some of the results of an investigation of wires fused in air and in vacuum may therefore be of interest, particularly, since only few records of electrical transients have been reproduced in the literature, some of which show marked differences when compared with those obtained by the writer. In view of present researches in the production of high temperatures, the behaviour of wires subsequent to break-up, which greatly depends on the material of the wires, may also be significant.

EXPERIMENTAL EQUIPMENT

The wires were fused by discharging ten 1 μF condensers connected in parallel which could be charged from a variable d.c. power supply to a maximum voltage of 10 kV, and discharged by triggering the mid-electrode of a three-electrode gap. Transient current and voltage were recorded with a single-sweep cathode-ray oscillograph, suitable deflecting voltages being obtained by means of a coaxial current shunt and a high-voltage capacitance divider respectively. The natural period of oscillation of the discharge circuit was 44 μs and peak currents exceeding 10 kA could be obtained.

THE PROCESS OF DISINTEGRATION

Much information is available as to the behaviour of wires under heavy overload in d.c. and a.c. power systems,[4] and it is generally agreed that even under the most severe conditions complete vaporization does not occur prior to break-up. Provided the current density is greater than 1 kA/mm² uniform melting does not occur,[5] since, owing to surface tension effects, the wire assumes a shape approximating to an unduloid (a solid of revolution the generating curve of which is of sinusoidal form). Increased heating then results in the portions of smaller cross-section and, under the influence of electromagnetic forces due to the current in the wire, the unduloid breaks up into a large number of globules. This occurs when the energy dissipated in the wire is approximately equal to the heat required to raise it to its melting temperature (liquid state),[5,6] but in many cases only a portion of the latent heat of fusion is sufficient.[4,5]

Some difference of opinion, however, seems to exist as to the precise nature of break-up, when wires are fused under conditions where current peaks of some thousand amp may be attained in only a few microseconds. Duvoisin and Brownlee,[7] Bellaschi[8] and Miller[9] conclude that the electrical energy just sufficient to disrupt the wire is substantially equal to that required to raise it to its melting temperature. Karsten[10] states that the amount of heat is less than half the energy to melt it completely. Lapple,[11] Foitzik,[12] Wrana[13] and Gantenbein[14] claim that with sufficiently high current densities complete vaporization occurs.

Since experiments of this nature are usually carried out by discharging a bank of condensers, the energy dissipated in the wire can be estimated from the decrease of voltage during the period prior to break-up if the losses in the discharge circuit are small. A more precise measure of the energy may be obtained if the current waveshape is known, by considering the area under the current-squared time curve.[8] Gibson[15] has treated this problem in greater detail and has given current-squared time integrals depending on the physical properties of the wires which are calculated for (*a*), the period of heating the wire to melting temperature, (*b*), the period during which the latent heat of fusion is supplied, (*c*), the period during which the liquid metal is raised to its vaporization temperature.

This method can only be applied if accurate current oscillograms are available and great care must be taken in the design of current measuring equipment. A major source of error is introduced if the inductance of the current shunt is not kept sufficiently low, as can be seen from oscillograms published by Wrana[13] which are very similar to those obtained by the writer during preliminary tests when a shunt was used having appreciable inductance. A sinusoidal current produces a voltage across such a shunt, which is the

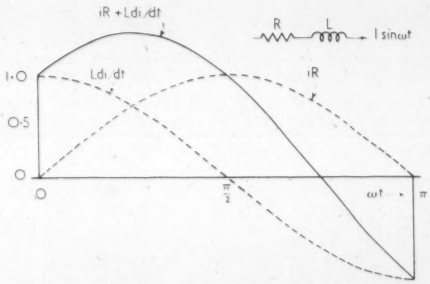

Fig. 1. Effect of inductance of current measuring shunt ($\omega L = R$)

sum of resistive and reactive voltage drops as shown in Fig. 1. Incorrect matching of the feeder to the oscillograph, on the other hand, causes undesirable reflexions, which may introduce distortions of the kind shown on records reproduced by Baligin.[16] A typical current oscillogram obtained by the writer with the coaxial current shunt mentioned previously is shown for comparison in Fig. 2.

In view of the likely errors in Wrana's oscillograms, it is doubtful whether some of his calculations are justified; in particular, his estimates of the energy required for disintegration based on the current-squared time integral are suspect. Values of energy dissipated prior to break-up have been calculated by the writer from a large number of records, both by means of the current-squared timed integral and the decrease of energy stored by the condenser bank; some of these are given in Tables 1 and 2. It has been pointed out that the process of disintegration is largely independent of the size of wire and its surroundings if fusion takes place within 0·1 s.[5] This was confirmed by tests of wires fused in vacuum described in greater detail in the following section, results of which are included in the tables.

Table 1. *Energy dissipated (from current-squared time integrals)*

	Copper		*Aluminium*		*Silver*
	Air	*Vacuum*	*Air*	*Vacuum*	*Vacuum*
Break-up time (μs)	7·5	7·5	4·0	5·0	2·1
Current density at break-up (kA mm^2)	186	193	150	129	68
Current-squared time integrals $\times 10^{-8}$					
(*a*) to heat to m.p.[15]	8·63		2·53		5·91
(*b*) to melt completely[15]	1·33		0·60		1·02
(*c*) from records	8·9	9·3	3·0	2·7	6·8
Percentage molten	20	50	78	28	87

Table 2. *Energy dissipated (from decrease of condenser voltage)*

	Copper		*Aluminium*	
	Air	*Vacuum*	*Air*	*Vacuum*
Break-up time (μs)	8·9	6·7	4·9	4·0
Energy dissipated (J)				
(*a*) to heat to m.p.	61		27	
(*b*) to melt completely	21·2		15·5	
(*c*) from records	95	75	44	41
Percentage molten	100	66	100	90

The trend of the data obtained indicates that complete melting is unlikely to take place, particularly, since energy values based on decrease of condenser voltages include losses in the remainder of the circuit (terminal contact resistances, copper links, current shunt, arc drop in three-electrode trigger gap).

THE TRANSIENT VOLTAGE

As a consequence of the results given above, Wrana's assumption that, on break-up, the wire is replaced suddenly by an insulating column of metal vapour, does not seem justified. It is more likely that globule formation takes place in the manner described previously and that the gaps between globules are bridged by short arcs which lead to vaporization of the remaining molten metal particles. If, however, the inductance of the discharge circuit is very low, the induced voltage tending to maintain current flow cannot build up to a value large enough to sustain the chain of short arcs until complete vaporization of the intervening metallic globules leads to the establishment of a single arc.[5] Current flow is therefore interrupted (Fig. 2). This is a phenomenon not usually met with in the case of fuses operating in power systems where there is generally sufficient inductance, and other means must therefore be found to achieve current interruption. The magnitudes of transient voltage obtained with wires fused by means of a condenser discharge are very much greater than those obtained with wires of equal dimensions under heavy overload conditions at power frequencies.[4] However, Suits[17] has shown that a finite time interval of the order of 10^{-4} s is required for the establishment of thermal equilibrium of an arc column. Since the formation of multiple break-up occurs within 10^{-6} s, thermal equilibrium is unlikely to be established and most of the necessary ionization can be brought about only by electron collisions, requiring much higher voltages.

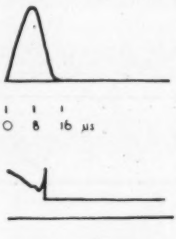

Fig. 2. Oscillogram of current (upper trace) and voltage (lower trace) of copper wire (length 24 cm, cross-section 0·059 mm^2) fused in air. Peak current 11·3 kA, transient voltage 7·7 kV

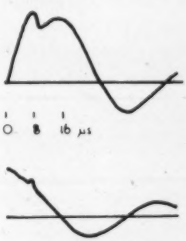

Fig. 3. Oscillogram of current (upper trace) and voltage (lower trace) of copper wire (length 24 cm, cross-section 0·059 mm^2) fused in vacuum. Peak current 11 kA

To obtain further evidence of the manner of break-up, wires were fused in a test vessel evacuated to a pressure of 10^{-4} mm of mercury. Here, records of electrical transients (Fig. 3) are strikingly different compared with those obtained at atmospheric pressure. Similar results in an a.c. power system have already been reported elsewhere,[4] and the conclusions reached will therefore be summarized only briefly. As a consequence of surface evaporation due to the increasing temperature of the wire, some metal vapour is present in the test vessel prior to break-up.[18] On formation of the first globule and its associated arc this vapour is ionized and a low-pressure arc discharge then by-passes the remaining solid or liquid portions of the wire. The transient voltage is therefore greatly reduced and conduction is maintained until the condensers are discharged. It is unlikely that conduction takes place along the walls of the test vessel, since, on completion of the test, the vessels could withstand an applied voltage of 10 kV without passing any current. Baligin's assumption,[16] based on a similar test of copper wires, that conduction is due to a layer of condensed metal vapour on the walls does not, therefore, seem justified.

RE-STRIKING PHENOMENA

It was shown in Fig. 2 that, following disintegration of the wire in air, current flow ceases and that the voltage on the condensers then remains at a constant reduced level. Provided this is of sufficient magnitude it is liable to cause immediate breakdown of the gap between the clamping terminals.[13] There is, however, another type of re-striking which may occur under certain conditions after a quiescent period lasting several microseconds. According to Baligin,[16] this is due to an oscillatory process, where, as a consequence of the electrical explosion, ions are first thrown out laterally from the discharge space, causing current interruption. Re-ignition occurs on the reverse movement towards the discharge channel. Recent work on expanding gases[19] has, in fact, shown the existence of shock waves during the first few microseconds following short-duration spark discharges at atmospheric pressure; conditions in the present case may well be similar. It is observed, however, that re-striking to a marked degree depends on the material of the wire. Thus, the behaviour of an aluminium wire of a length equal to that of the copper wire mentioned above is demonstrated in Fig. 4, where re-striking occurs after about 16 μs. If the wire is shortened, there is no quiescent period (Fig. 5). Records of

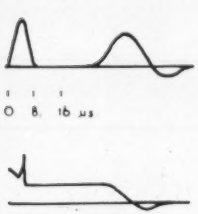

Fig. 4. Oscillogram of current (upper trace) and voltage (lower trace) of aluminium wire (length 24 cm, cross-section 0·059 mm^2) fused in air. Peak current 7·3 kA, transient voltage 10·4 kV

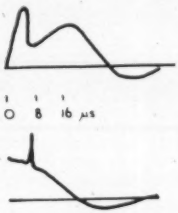

Fig. 5. Oscillogram of current (upper trace) and voltage (lower trace) of aluminium wire (length 16 cm, cross-section 0·059 mm^2) fused in air. Peak current 8·8 kA, transient voltage 10·8 kV

these phenomena have been reproduced previously by Wrana[13] and Baligin,[16] but in both cases serious distortions are present due to imperfect recording equipment and they compare unfavourably with the above oscillograms. Wrana concluded that re-striking depends on the calorific value of the material of the wire, since, owing to oxidation of the metallic vapour, its temperature may be raised sufficiently to bring about thermal ionization causing re-striking. This seems to be supported by the above results for aluminium (calorific value 6970 cal/g) and copper (540 cal/g). The behaviour of wires of a given material was in all cases remarkably consistent, as is shown by the above traces of current and voltage which owing to limitations of the recording apparatus had to be obtained separately.

In order to confirm the theory of thermal ionization by oxidation more conclusively, experiments would have to be carried out in the absence of oxygen. Tests in vacuum are not suitable since, as was seen in the previous section, phenomena of a different nature then occur. Thus, an aluminium wire fused in vacuum (Fig. 6) behaves in the same manner as the copper wire (Fig. 3). There remains the possibility of tests in an inert atmosphere (neon, argon), but unless a sufficiently large test vessel is available, shock waves may give rise to undesirable effects.

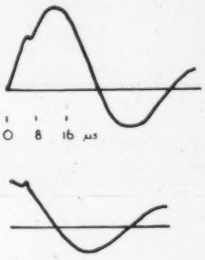

Fig. 6. Oscillogram of current (upper trace) and voltage (lower trace) of aluminium wire (length 24 cm, cross-section 0·059 mm^2) fused in vacuum. Peak current 12·4 kA

CONCLUSIONS

From observations based on current and voltage oscillograms, the process of disintegration of wires fused with heavy surge currents seems to be similar to that of wires under heavy-current overload in power systems where the rate of rise of current is very much smaller. Re-striking phenomena have also been examined and the results obtained support Wrana's theory of thermal ionization depending on the physical properties of the material of the wire.

ACKNOWLEDGEMENTS

Thanks are due to Prof. W. J. John and Dr. T. J. Lewis for much helpful discussion and advice. The experimental work described forms part of a Ph.D. thesis and is published with permission of the University of London.

REFERENCES

(1) ANDERSON, J. A. *Astrophys. J.*, **51**, p. 37 (1920).
(2) SMITH, S. *Astrophys. J.*, **61**, p. 186 (1925).
(3) ANDERSON, J. A., and SMITH, S. *Astrophys. J.*, **64**, p. 295 (1926).
(4) BARRINGTON, A. E. *Engineer*, **198**, p. 187 (1954).
(5) BAXTER, H. W. *Electric Fuses*, Chapters IX, X (London: E. Arnold and Co., 1950).
(6) FORREST, J. S. *Brit. J. Appl. Phys.*, **1**, p. 10 (1950).
(7) DUVOISIN, E. M., and BROWNLEE, T. *Gen. Elect. Rev.*, **35**, p. 260 (1932).
(8) BELLASCHI, P. L. *Elect. Engng*, **53**, p. 86 (1934).
(9) MILLER, J. L. *E.R.A. Report*, Ref. S/T 61 (1950).
(10) KARSTEN, O. *Tekn. T.*, **77**, p. 239 (1947).
(11) LAPPLE, H. *Elektrotech. Z.* [*ETZ*], **58**, p. 369 (1937).
(12) FOITZIK, R. *Elektrotech. Z.* [*ETZ*], **60**, p. 89 (1939).
(13) WRANA, J. *Arch. Elektrotech.*, **33**, p. 656 (1939).
(14) GANTENBEIN, A. *International Conference on Large High-Tension Systems* [*CIGRE*], **1**, Paper 131 (Paris: *Conférence Internationale des Grounds Réseaux Électriques à Haute Tension*, 1939).
(15) GIBSON, J. W. *J. Instn. Elect. Engrs*, **88**, p. 2 (1941).
(16) BALIGIN, I. E. *Elektrichestvo*, No. 4, p. 70 (1949); E.R.A. Translation, Ref. Trans./IB 973 (1949).
(17) SUITS, C. G. *Gen. Elect. Rev.*, **39**, p. 194 (1936).
(18) ESPE, W., and KNOLL, M. *Werkstoffe der Hochvakuumtechnik*, p. 358 (Berlin: Springer, 1936).
(19) OLSEN, H. L., EDMONSON, R. B., and GAYHART, E. L. *J. Appl. Phys.*, **23**, p. 1157 (1952).

The electric strength of hydrocarbon gases

By A. E. D. Heylen, B.Sc., and T. J. Lewis, M.Sc., Ph.D., Department of Electrical Engineering, Queen Mary College, London

[*Paper received* 11 *June*, 1956]

Careful measurements of the static electric strengths of a number of pure hydrocarbon gases over a range of pressure and spark-gap spacings, including the Paschen minimum are reported. A relationship between strength and molecular structure is found which, if unsaturated compounds such as ethylene, acetylene and butadiene are included, is not so simple as hitherto reported. The possible correlation of electric strength with the ultra-violet spectra and Ramsauer cross-sections of these gases is discussed briefly.

Pulse discharges which occur readily in these gases at fields below the breakdown value are attributed to the exceedingly small secondary ionization coefficients (γ).

Accurate determinations of the electric strengths of pure hydrocarbon gases are useful in investigating the processes of breakdown in gases since the effect of certain molecular properties may be studied systematically. Series of hydrocarbon gases such as the paraffins or the olefins are available in which the molecular properties vary gradually through a series. In addition to this valuable property, certain features present in one series may be entirely absent in another. For example, in the paraffin series the molecular weight and chain length increase uniformly through the series and single bonds only are present, whereas the olefins, which also increase uniformly, contain double bonds in addition to single ones. Thus it should be possible to correlate the electric strength of these hydrocarbon gases with definite molecular properties, furnishing thereby evidence for particular processes of breakdown in molecular gases in a way which is not possible for monatomic or diatomic gases. Although halogen-substituted hydrocarbons have been tested extensively[1] the emphasis has been on engineering applications since these gases are electro-negative and have high electric strengths. The reactive nature of such gases introduces difficulties when explaining their behaviour under stress.

The object of the work to be reported here was to measure the electric strengths of a number of hydrocarbon gases over a wide range of *pd* (pressure $\times$ electrode separation) extending the measurements of Crowe and Devins[2] to lower *pd* values including the Paschen minimum and including some olefin gases not previously tested. This work is of an exploratory nature and ultimately it is hoped to extend the measurements into pressure and temperature ranges near the critical points. In this region, since the gas densities are then comparable with those of the corresponding liquids, important information concerning mechanisms applicable to breakdown in liquids should be obtained. The relationship between electric strength and molecular structure in liquids has already received attention.[3,4]

EXPERIMENTAL PROCEDURE

The electrode system for the breakdown measurements consisted of two parallel plate electrodes of 2 cm diameter having accurate Rogowski profiles producing a uniform field over an area of diameter 1 cm at the maximum gap of 5 mm. These electrodes are smaller than those frequently used for such measurements but it was essential to reduce the test cell volume to a minimum in order to economize in the use of gases. The electrodes were mounted on a rigid frame of glass rods and a micrometer for gap adjustment as well as a levelling device for the electrodes, were provided. The whole electrode assembly, after adjustment to a standard gap of 3·175 mm, was placed in a vacuum tight glass test cell, electrical connexion to the electrodes being made through tungsten seals in the glass. Before introducing the gas to be tested, a vacuum of 5×10^{-5} mm of mercury was obtained in the test cell and the leakage rate during tests was such that contamination of the gas sample was less than 1 part in 10^4 even at pressures of 1 mm of mercury near the Paschen minimum. The pressure in the cell was measured by means of a differential manometer used as a null device in conjunction with mercury and oil manometers except for pressures less than 25 mm of mercury in which range the differential manometer, calibrated against the oil manometer, was used alone. Since hydrocarbons are efficient solvents, care was taken to keep the system free of grease by employing bellows-type vacuum valves in positions where contact with the gases was unavoidable.

The voltage supply for the experiments was fully stabilized and capable of fine control so that the breakdown voltage could be approached very slowly. The static breakdown voltage V_s was measured at the spark gap by calibrated high-stability resistors and a micro-ammeter with an overall error of less than 0·5%.

A problem peculiar to hydrocarbon gases is the comparatively heavy deposition of discharge products following a spark particularly for the unsaturated gases. These dissociation products not only reduce the gas purity but also spoil the electrode surfaces and cause a variation in the subsequent breakdown voltages. These deposits have been reduced very considerably be employing a spark-quenching or diverting device using the principles outlined by Saxe and Lewis[5] and following a design by House.[6] This device was especially valuable for measurements near the V_s *versus pd* minimum since stable cathode conditions could be maintained during a series of measurements involving as many as twenty sparks. Oscillographic measurements showed that the spark discharge could be extinguished in less than 1 μs, most of the discharge energy being that stored in the self-capacitance of the test gap and therefore not capable of diversion.

For reasons to be discussed below, discharges in the form of discrete current pulses occurred readily in hydrocarbon gases at voltages well below V_s. These were monitored qualitatively using a capacitance potential divider across the gap in conjunction with a cathode-ray oscilloscope and appeared to be initiated by photo-electrons from the cathode If the pulse activity was excessive a lowering of the sparking potential V_s occurred, this reduction being as much as 30% with strong ultra-violet illumination. By monitoring with a cathode-ray oscilloscope, the incident illumination could be adjusted to prevent lowering of V_s, but at the same time permitting sufficient pulses to avoid overvoltage on the gap.

All the gases tested were of the highest possible purity as checked by the National Bureau of Standards. They were provided in ampoules which were sealed to the vacuum system and broken under vacuum to ensure the minimum of contamination.

Aluminium electrodes were used exclusively for the tests since experience showed that their surfaces could be obtained readily in a stable condition as indicated by consistent pulse activity and breakdown voltage especially near the V_s *versus pd* minimum. Similar conclusions were also reached by Badareu and Constantinescu[7,8] when investigating certain aromatic hydrocarbons. The electrodes were highly polished, washed free of grease in pure n-hexane and inserted in the test cell. The system was then pumped out for two days before each test. No attempts were made to outgas them thoroughly and for this reason results obtained in the immediate neighbourhood of the Paschen minimum ($pd \sim 1$ cm $\times$ mm of mercury) were not so accurate as those obtained at higher values of *pd* where cathode effects are not important. Apart from the small range near $pd = 1$, precise measurements of V_s were possible and in most cases one breakdown at each *pd* value was sufficient to determine V_s. Adequate warning of imminent breakdown was always given by a marked increase of pulse activity which was so sensitive that V_s could be approached very gradually.

RESULTS

Preliminary measurements were made with nitrogen and hydrogen to check the reliability of the apparatus and the procedure adopted. V_s *versus pd* characteristics in close agreement with those given by Ehrenkrantz[9] and Llewellyn Jones and Henderson[10] respectively were obtained and it was concluded that the procedure was reliable.

Fig. 1 shows the characteristics of the normal paraffins methane–pentane together with certain isomers and also the results obtained for nitrogen. It should be noted that linear plots are obtained in the *pd* range above about $pd = 30$

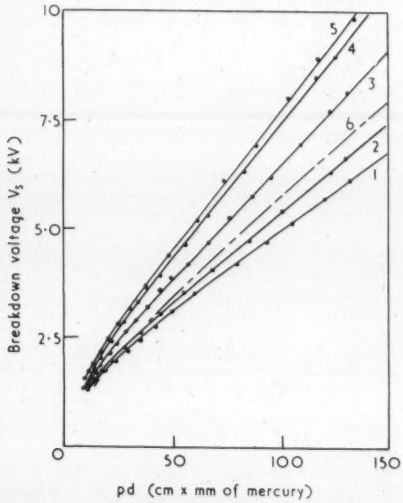

Fig. 1. Breakdown characteristics of the paraffins

1, methane; 2, ethane; 3, propane; 4, n-butane; 5, iso-butane; 6, nitrogen.

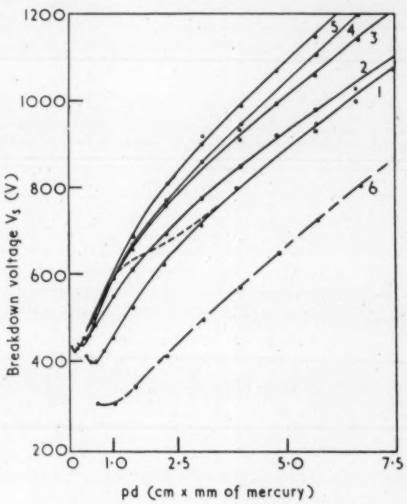

Fig. 2. The breakdown minimum for the paraffins

1, methane; 2, ethane; 3, propane; 4, n-butane; 5, iso-butane; 6, nitrogen.

The effect of illumination is shown by the dotted curve for n-butane, which merges into that for methane when excessive illumination is present.

(Paschen's law was also obeyed in this range). At smaller values of *pd* departures from linearity occurred (Fig. 2) and the effect was accentuated as the minimum was approached. This effect is greater than that found with nitrogen. As stated already, results near the minimum depend on cathode conditions to a large extent but it is believed that the characteristics do represent general trends in this region. Over the whole *pd* range there is a regular increase in strength as the chain length or rather as the number of carbon atoms in the molecule increases since isomers are not greatly different from the normal forms. The minimum V_s also increases with the number of carbon atoms and moves to smaller *pd* values (i.e. larger V_s/pd values).

The importance of using a minimum of gap illumination for breakdown studies in these hydrocarbons is well illustrated by the typical result for butane in Fig. 2. Even if normal laboratory illumination by fluorescent lamps is used, V_s for butane is lowered so much as to merge into that for methane at $pd \simeq 3{\cdot}5$. Pre-breakdown pulse activity was excessive and it is likely that a space charge was set up sufficient to depress V_s. This explanation might account for the unusual results obtained for methane by Crowe and Devins[2] in

which the methane characteristic lies across that for ethane in the range where $pd \sim 10$ cm × mm of mercury.

Characteristics for several olefins which contain the carbon–carbon double bond as well as the single bond and for acetylene which has a triple carbon–carbon bond are given in Figs. 3 and 4. The general shape of the curves is

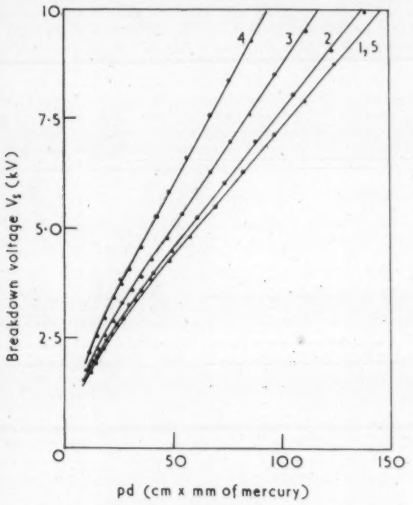

Fig. 3. Breakdown characteristics of unsaturated hydrocarbons

1, ethylene; 2, propylene; 3, butene-1; 4, butadiene; 5, acetylene.

similar to that for the paraffins but a significant increase of strength results from the introduction of a double or triple bond as can be seen by a comparison of ethane, ethylene and acetylene ($CH_3 - CH_3$, $CH_2 = CH_2$, $CH \equiv CH$). The presence of two double bonds as in butadiene ($CH_2 = CH - CH = CH_2$) produces an even greater strength.

DISCUSSION

A considerable amount of further work will be required before a comprehensive theory of the influence of molecular structure on breakdown can be advanced and at present it is wise to restrict any discussion to general tendencies. The reasons for this lack of precision are firstly the limited range of molecular structures studied and secondly the theory of the breakdown process into which the molecular properties of the gas enter in a complex form. If, as previously,[2] the Townsend criterion of breakdown is assumed for the hydrocarbons, then at the breakdown voltage V_s

$$\gamma \exp(\alpha d) = 1 \qquad (1)$$

where α and γ are the usual first and second Townsend coefficients. Now α is a function involving both the scattering cross-sections of the gas molecules for electrons and the ionization potential V_i, the precise form of which has received much attention in the past. For the present argument, following Crowe and Devins,[2] we may write that at breakdown

$$\alpha = AV_s d^{-1} \exp(-Bpd/V_s) \qquad (2)$$

in which A and B are constants characteristic of the gas, B involving the elastic and inelastic scattering cross-sections

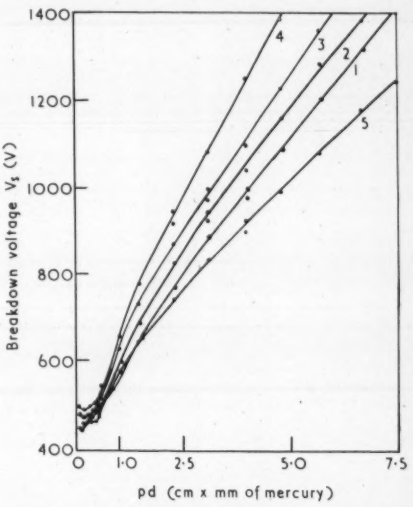

Fig. 4. The breakdown minimum for some unsaturated hydrocarbons

1, ethylene; 2, propylene; 3, butane-1; 4, butadiene; 5, acetylene.

and the excitation and ionization potentials. Combination of equations (1) and (2) gives

$$\frac{pd}{V_s} = \frac{\ln V_s}{B} + \frac{\ln[A/\ln(\gamma^{-1})]}{B} \qquad (3)$$

and the slope of the pdV_s^{-1} *versus* $\ln V_s$ plot should yield the value of B provided that γ remains sensibly constant. Equation (3) establishes a link between molecular properties and electric strength. The plot for ethane, which is typical, is shown in Fig. 5 and only when V_s/pd is large near the V_s minimum does the curve depart from linearity. In this region γ variations become more important as discussed below.

If the various assumptions made by Crowe, Bragg and Devins[11] are employed, the simple relationship $B \propto QV_i^{3/2}$ can be derived in which Q is dimensionally that of a collision cross-section. Noting the regular increase in strength for the paraffins as the number of CH bonds in the molecule is increased, it is also plausible to write $Q \propto n$ where n is the number of CH bonds. The carbon skeleton of the molecule is neglected, being largely screened and not effective in causing scattering of slow electrons. On this basis, Fig. 6

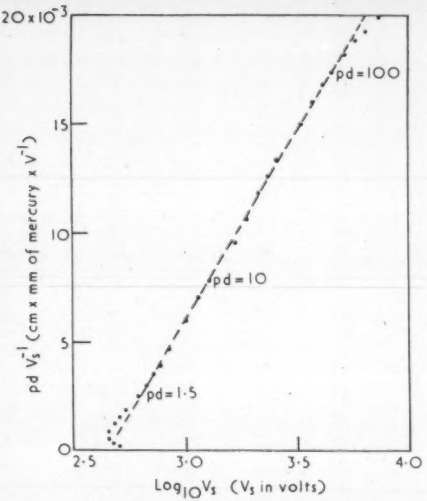

Fig. 5. Relationship between pdV_s^{-1} and log V_s for n-ethane. The slope of the dotted line determines the molecular parameter B^{-1}

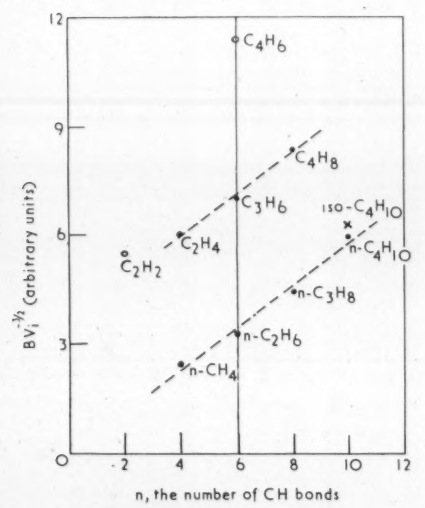

Fig. 6. Relationship between $BV_i^{-3/2}$ and n for single- and multiple-bonded hydrocarbons

shows a strong correlation for the paraffins including some isomers, but introduction of double or triple bonds causes a large vertical shift of the characteristic. It is concluded that unsaturated molecules include scattering centres different from those in the saturated compounds. Inelastic scattering in these cases probably involves displacement of the π-electrons of the multiple bonds in addition to displacement of σ bonding electrons which are present alone in the saturated hydrocarbons. Literature on total collision cross-sections and an extensive bibliography on the absorption spectra of these hydrocarbons exists already. Absorption occurs in both the near and far ultra-violet and various spectral bands can be associated with transitions due to electronic excitations in the π or σ orbitals, including dissociative and ionizing transitions at energies of approximately 4 eV and 10 eV respectively. Absorption bands in the near ultra-violet region which appear for the olefins but are absent in the paraffins may explain why the former are stronger electrically.

The absorption spectra of these molecules also help to explain the pulse activity before breakdown already described above. Dissociation following excitation occurs readily in these gases[12] and it has been concluded that the life-time of the excited state is very small so that a secondary photon has a very small probability of being emitted. As a further consequence of the short life-time, secondary electron emission by positive-ion action at the cathode is also weak. It may be expected that γ will be very much smaller than for gases such as nitrogen and a γ as small as 10^{-9} has been reported for the ring hydrocarbons, benzene, toluene and cyclohexane[13] in the range of V_s/pd 225 to 3000. Values of γ equal to those normally accepted for gases such as nitrogen (10^{-4}) are reached only at large V_s/pd in the neighbourhood of the V_s/pd minimum. It is now clear why the onset of detectable pulses did not occur at the minimum but at smaller values of V_s/pd and also why the presence of excess photoelectrons from the cathode could lower V_s by space charge effects. As equation (1) shows, large values of α giving large avalanches are possible without the breakdown condition being reached when γ is small.

CONCLUSIONS

The present measurements provide precise data on V_s for a range of hydrocarbons and extend the earlier measurements by Crowe and Devins to the important Paschen minimum. The preliminary results for double and triple bond gases indicate that the simple picture suggested by these authors[11] will require generalizing. Work is proceeding on this and it is hoped that more direct correlations between V_s and the ultra-violet spectra and Ramsauer cross-sections of a wide range of molecular gases will be possible. The extremely low values of γ found in such gases should provide opportunity for interesting studies of the pre-breakdown conditions, especially statistical studies concerned with avalanche and pulse formation. Although such gases are commonly used as quenching agents in Geiger tubes, they have seldom been investigated alone. A knowledge of the breakdown mechanisms in these gases, especially if they can be extended to greater densities, will also be valuable in establishing the corresponding processes in dielectric liquids.

ACKNOWLEDGEMENTS

The authors wish to thank Prof. W. J. John in whose laboratories the work was carried out. They also wish to acknowledge the awards of a grant by the Department of

Scientific and Industrial Research, and a Turner and Newall Fellowship by the University of London to the authors respectively.

REFERENCES

(1) McCormick, N. R., and Craggs, J. D. *Brit. J. Appl. Phys.*, **5**, p. 171 (1954).
(2) Crowe, R. W., and Devins, J. C. *Annual Report, Conference on Electrical Insulation*, p. 4 (Washington: National Academy of Sciences, National Research Council, 1953).
(3) Crowe, R. W., Sharbaugh, A. H., and Bragg, J. K. *J. Appl. Phys.*, **25**, p. 1480 (1954).
(4) Lewis, T. J. *J. Appl. Phys.*, **27**, p. 645 (1956).
(5) Saxe, R. F., and Lewis, T. J. *Brit. J. Appl. Phys.*, **6**, p. 211 (1955).
(6) House, H. *Dielectric breakdown of organic liquids* (Ph.D. thesis, London University, 1955).
(7) Badareu, E., and Constantinescu, L. *Bull. Soc. Roumaine Phys.*, **39**, p. 45 (1938).
(8) Constantinescu, L. *Bull. Soc. Roumaine Phys.*, **41**, p. 73 (1940).
(9) Ehrenkrantz, F. *Phys. Rev.*, **55**, p. 219 (1939).
(10) Llewellyn Jones, F., and Henderson, J. P. *Phil. Mag.*, **28**, p. 185 (1939).
(11) Crowe, R. W., Bragg, J. K., and Devins, J. C. *J. Appl. Phys.*, **26**, p. 1121 (1955).
(12) Korff, S. A., and Present, R. D. *Phys. Rev.*, **65**, p. 274 (1944).
(13) Valeriu-Petrescu, M. *Bull. Soc. Roumaine Phys.*, **44**, p. 3 (1943).

Reduction of counting time in low activity assays

By H. A. Hughes, B.Sc., A.R.C.S., A.Inst.P., Physics Department, Western General Hospital, Edinburgh, 4

[*Paper first received* 18 *June, and in final form* 20 *July*, 1956]

Modification of a counting system can result in a reduction in background and sample counting rates. Such an arrangement will decrease the minimum counting time necessary to achieve a given fractional deviation in the net counting rate only under certain conditions. A method is described of determining these conditions. The application of this principle is exemplified in the use of a pulse amplitude analyser with a scintillation counter.

A criterion in the diagnostic use of radioactive isotopes in medicine is that the energy absorbed by the patient shall be reduced as far as possible below a certain limit. The minimum quantity which can be administered is governed by the time available to make either *in vivo* measurements or sample assays to a given accuracy, the deciding factor for a given detector being the background counting rate. A certain reduction in background rate can be accomplished by the use of increased shielding around the detecting element and anti-coincidence counting arrangements, without affecting the sample counting rate. Further modifications may be made to a counting system, which reduce both sample and background counting rates, and it is of interest to determine the conditions under which a definite reduction in counting time results. Apart from the obvious choice of different types and sizes of detector, an important example of the latter type of modification is the use of a pulse amplitude analyser with a scintillation counter.

CONDITIONS FOR REDUCTION OF COUNTING TIME

Thomas[1] has derived expressions for relative factors of merit for counters assuming either that the time spent in counting sample plus background is made equal to the time spent in counting background alone, or that the counts measured in each case are made equal.

However, it may be shown[2] that if a time T has to be divided into a time t for counting background and a time $(T - t)$ for counting sample plus background, then a minimum value of the standard deviation in the net counting rate results if t is given by

$$t = T[\sqrt{(R + 1)} - 1]/R \qquad (1)$$

where R is the ratio of the sample counting rate a to the background rate b. The minimum value of T for a given fractional standard deviation in a also results under these conditions and is given by

$$T_{min} = (b\Delta^2)^{-1}[\sqrt{(R + 1)} + 1]^2/R^2 \qquad (2)$$

If the background rate can be reduced from b to nb by a modification of the counting system, then a reduction in T_{min} will result provided that the corresponding ratio of sample to background rate is greater than mR where m is given by

$$nm^2 = [\sqrt{(mR + 1)} + 1]^2/[\sqrt{(R + 1)} + 1]^2 \qquad (3)$$

It follows that the new sample rate must be greater than nma. The figure shows the quantity mn plotted against R for various values of n.

The curves in the figure can be used as follows. The value of n and nm are determined by counting background and sample rates under the two conditions to be compared. The corresponding value of R is then read off on the appropriate

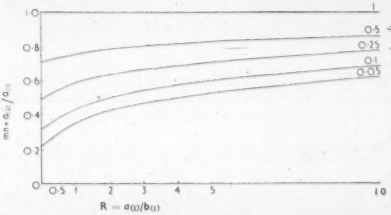

Curves for comparison of merits of two counting systems. System 2 will only be preferable for measurements involving values of R lower than that corresponding to the measured values of n and nm

curve. Then for any smaller value of R the minimum counting time will be decreased. The fractional reduction in T_{min} approaches a limiting value of $(m^2n)^{-1}$ as R approaches zero.

APPLICATION TO USE OF A PULSE AMPLITUDE ANALYSER AND SCINTILLATION COUNTER

The use of analysers in assay work[3,4] and in *in vivo* studies[4,5] has been reported. It is to be expected that a useful reduction in counting time would arise from such an instrument when a monochromatic source is counted by a crystal which absorbs a large fraction of the radiation emitted. These conditions are also necessary in γ-ray spectroscopy.[6] A well-type crystal is thus indicated. No such crystal was available for test, but measurements were made on an Ekco type N550 scintillation sample counter, an instrument frequently used in assay work. Pulse spectra were obtained for ^{131}I and ^{51}Cr with a Dynatron type N/101 pulse analyser. A comparison of counting rates using a single discriminator setting recommended by the makers, and with a suitable channel width covering the 0·364 MeV peak in the case of ^{131}I, and the 0·33 MeV peak with ^{51}Cr, was made. The table shows the results, systems 1 and 2 referring to a single discriminator setting, and the use of a pulse analyser respectively.

Comparison of relative values of integral and differential bias techniques

	Background rate System 1 b(c/s)	*Fractional reduction in b System 2 n*	*Fractional reduction in a System 2 mn*	*Value of R for equal counting times (from graph) R_{max}*	*Max. fractional reduction in T_{min}*
^{131}I	0·9	0·25	0·57	0·71	0·77
^{51}Cr	0·9	0·3	0·73	4·5	0·56

The relatively complex spectrum of ^{131}I somewhat restricts the value of the pulse analysis technique; however the limiting activity is of the same order as that obtained from blood plasma taken during thyroid function tests.[7] For ^{51}Cr a higher value of R_{max} results from the detection of only 0·33 MeV quanta, and the small fraction of the total disintegrations giving rise to these quanta account for the corresponding relatively high value of limiting activity.

ACKNOWLEDGEMENT

The author wishes to thank Dr. C. A. Murison for his helpful criticism of this paper.

REFERENCES

(1) THOMAS, A. *Nucleonics*, **6**, (2), p. 50 (1950).
(2) TAYLOR, D. *The Measurement of Radio Isotopes*, 1st ed., p. 58 (London: Methuen and Co. Ltd., 1951).
(3) ARNOLD, J. R. *Science*, **119**, p. 155 (1954).
(4) FRANCIS, J. E., BELL, P. R., and HARRIS, C. C. *Nucleonics*, **13**, (11), p. 82 (1955).
(5) ALLEN, H. C., RISSER, J. R., and GREENE, J. A., in *Radioisotope Conference 1954*, Vol. 1, p. 76 (London: Butterworth Scientific Publications, 1954).
(6) BELL, P. R., in *Beta- and Gamma-Ray Spectroscopy*, 1st ed., p. 132, K. Siegbahn (Ed.) (Amsterdam: North-Holland Publishing Co., 1955).
(7) HUGHES, H. A., and MILLER, R. M. *Brit. Med. J.*, **1**, p. 493 (1956).

The tensile strengths of viscous liquids under dynamic loading

By T. H. BULL, B.Sc., Ph.D., Imperial Chemical Industries Ltd., Akers Research Laboratories, Welwyn, Herts

[*Paper received* 18 *April*, 1956]

Under similar conditions of transient loading the cavitation thresholds of syrup and olive oil are 130×10^6 dyne/cm^2 and 29×10^6 dyne/cm^2 respectively. For fluids with a viscosity (η) in the range 0·01 to 400 P the cavitation threshold pressure P_c is given by the empirical relation $P_c = k\eta^{0\cdot2}$. This result can be interpreted on the basis of the growth of cavitation nuclei in viscous liquids subjected to transient stresses.

In a previous paper[1] some experiments were described relating to the tensile strengths, or cavitation thresholds, of liquids under dynamic loading. From the results of these experiments a tentative suggestion was put forward that the viscosity of a liquid markedly affects its experimentally observed cavitation threshold under dynamic loading. In order to test further this hypothesis the dynamic cavitation thresholds of both a concentrated sugar solution (syrup) and olive oil have been measured using the electrical pressure bar technique described in the paper mentioned above.

EXPERIMENTAL

The apparatus was similar to that fully described in the earlier paper. Briefly, the liquid under test was contained in a vertical thick-walled steel cylinder 18 in. long, and with a nominal bore of 1 in. The upper end of the cylinder was open, while into the lower end was sealed a silver-steel rod, 4 ft long, which made a good sliding fit into the cylinder. An electric detonator fired at the lower end of the steel rod caused a compression wave to travel up the rod and into the liquid. On reaching the free surface of the liquid the compression wave was reflected as a wave of tension, which travelled back down through the liquid provided the liquid was not cavitated.

The pressure changes in the liquid as the waves of compression and tension travelled through it were measured with a silver-steel electrical pressure bar, 3 ft long and $\frac{1}{4}$ in. diameter, sealed into the side of the cylinder at its mid-point. The face of the pressure bar in contact with the liquid was machined flush with the bore of the cylinder. The stress waves set up in the pressure bar, due to the pressure changes in the liquid, were recorded with a $\frac{1}{2}$ in. parallel-plate condenser microphone. The output of the condenser microphone feed unit was amplified and displayed on a double-gun, high-speed, cathode-ray oscilloscope.

RESULTS

The procedure adopted in all the experiments was similar. The face of the pressure bar in contact with the liquid was lined up flush with the inner face of the cylinder. The cylinder was filled with a test liquid to a known height above the end of the pressure bar and allowed to reach temperature equilibrium with the surroundings. The separation between the free end of the bar and the insulated plate of the condenser microphone was adjusted with slip gauges. The detonator was fired and the output of the condenser feed unit, suitably amplified, recorded upon the oscilloscope screen. This was repeated for various depths of liquid in the cylinder.

Fig. 1 is an enlargement of the traces recorded on the oscilloscope screen in the first series of experiments using

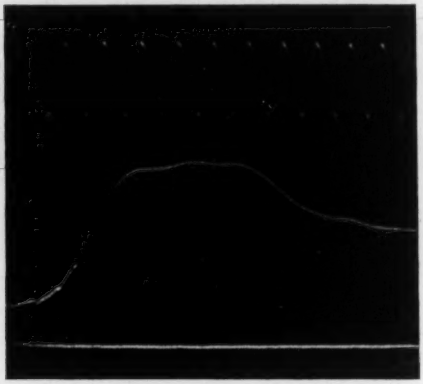

Fig. 1. Oscillogram of pressure pulses in syrup

upper trace: 100 kc/s timing wave
middle trace: amplified output of condenser microphone
lower trace: datum line

syrup. The depth of syrup above the pressure bar was 5·2 cm. The upper trace is a 100 kc/s timing wave, increasing time being measured from left to right. The middle trace shows the variation of amplified voltage output of the condenser feed unit. The lower trace is a datum line photographed separately after the two upper traces had been obtained.

The centre trace gives a measure of the displacement x of the end of the pressure bar with time t. The variation of pressure p below the free surface of the liquid is given by

$$p = \tfrac{1}{2}\rho c \frac{dx}{dt} \qquad (1)$$

where ρ is the density of the pressure bar and c is the velocity of propagation of a plane compression pulse in the bar. Applying equation (1) to the displacement-time curve, the variation of p with t is given in Fig. 2. The pressure pulse A is the wave of compression passing up through the liquid. This is followed by a few oscillations due to distortion in the measuring bar. Pulse B is a wave of tension passing down through the liquid brought about by the reflexion of A at the free surface. The peak amplitudes of the incident and reflected waves are about 50×10^6 dyne/cm^2 and 24×10^6 dyne/cm^2 respectively.

For this series of experiments the variation of the peak amplitude of the reflected wave with distance below the free surface is given by curve (1) of Fig. 3. At 1·7 cm below the free surface the peak amplitude is numerically equal to that of the initial wave of compression, indicating that the transient tensile stress applied to the liquid was insufficient to cause a detectable cavitated state. The wave of tension is attenuated by viscous forces as it travels through the liquid.

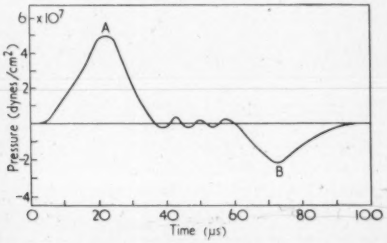

Fig. 2. Variation of pressure with time at pressure bar

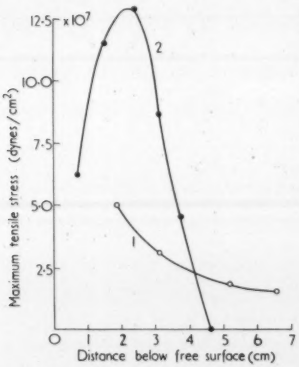

Fig. 3. Variation of peak pressure amplitude of reflected wave with distance below the free surface

In order to apply a larger transient compression wave, and hence a larger tensile stress to the liquid, the silver-steel firing rod was replaced by a rod of Perspex of similar dimensions, the acoustic impedance match between Perspex and syrup being much more favourable than that between steel and syrup.

A repetition of the experiments described above showed that the peak amplitude of the compression pulse reaching the free surface was about 320×10^6 dyne/cm^2. The variation of the peak amplitude of the tensile stress (using the Perspex firing rod) with distance below the free surface is given by curve (2) of Fig. 3. The maximum value of the tensile stress was approximately 130×10^6 dyne/cm^2. No

tensile stress was observed at distances greater than 4·2 cm below the free surface.

For tests with olive oil the silver-steel firing rod was used. The maximum value of dynamic tensile stress set up in olive oil was 29×10^6 dyne/cm^2 at 24·5° C.

The viscosities of syrup, glycerol and olive oil were determined, at the appropriate temperature, using a falling ball viscometer. The viscosity of water was obtained from the International Critical Tables.

Fig. 4 is a logarithmic plot of the cavitation pressure P_c against viscosity η, the results of the experiments being combined with those given in the earlier paper. Within the

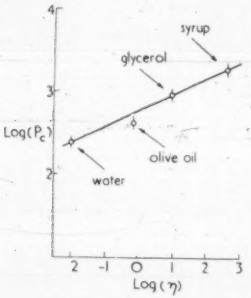

Fig. 4. Logarithmic plot of cavitation pressure P_c against viscosity η for various liquids

limits of experimental error it will be seen that the relation between P_c and η over a range of η from 0·01 to 400 P is given empirically by $P_c = k\eta^{0.2}$, k being a constant. No simple correlation was found between P_c and such properties of the liquids as vapour pressure, surface tension or density.

DISCUSSION

In order to interpret the results given here it is necessary to look qualitatively into the growth of cavities in liquids under tension.

Since no efforts were made to degas the test liquids it is reasonable to assume that each sample of liquid contained either air or vapour-filled cavities, or unwetted nuclei of solid material, or both; these will be referred to generally as cavitation nuclei. When the stress in a liquid becomes tensile these nuclei may grow. The factors which govern the inception of growth are the size of the initial cavity, surface tension, viscosity and inertia forces, and the amplitude and duration of the applied stress. For liquids of low viscosity the growth is retarded mainly by inertia forces.

A device for measuring the transient stress in a liquid also gives a measure of the strain. If the strain is destroyed the stress returns to its equilibrium value prior to stressing; the strain in a liquid subjected to a tensile stress can obviously be destroyed by the growth of cavities. A pressure device thus gives a measure of the transient tensile stress necessary to enable cavities to grow to a size sufficient to destroy the strain set up by that stress. The magnitude of the dynamic tensile stress a liquid may withstand, as measured in the experiments described here, is therefore governed by the rate at which cavitation nuclei enlarge, and hence is dependent on those properties of the liquid which control the growth of nuclei.

The surface tensions, compressibilities and densities of the liquids used in this investigation are all of the same order of magnitude. If it is assumed that the number and size of the original nuclei in the liquids are about the same then the factor which determines the rate of growth of the nuclei is the viscosity of the liquids.

A theoretical treatment of the growth of a spherical cavity in a viscous fluid under tension has been given by Poritsky,(2) assuming that the fluid is incompressible and that a constant pressure exists within the cavity. Unfortunately the theory is so complex as to require separate numerical integrations in order to determine the growth of a particular cavity for a particular set of initial conditions. Nevertheless it is evident that for small bubbles the initial growth is retarded primarily by viscous forces.

Dr. F. C. Roesler(3) has pointed out that the theory of cavity growth in its initial stages can be greatly simplified by disregarding inertia effects. He finds that the radius R of a cavity as it grows from an initial radius R_0 is given approximately by

$$R = R_0(1 + e^{pt/4\eta}) \text{ for small values of } pt/4\eta$$

where t is the time after the application of stress p and η the viscosity of the liquid. For small values of $pt/4\eta$ the inertia and surface tension are relatively unimportant. Consider now cavities with similar values of R_0 in liquids of differing viscosity. When under tension, the requirement that the cavity growth rate in all the liquids shall be similar is that $p \propto \eta$.

The maximum size of the cavities existing in the experiments here was much larger than those in the régime covered by the above equation if we assume $R_0 \sim 10^{-5}$ cm. Thus the expression above is not strictly applicable to these results, but serves to indicate that, on theoretical grounds, viscosity is the most important factor in retarding the initial growth of cavitation nuclei.

CONCLUSIONS

Over the range of viscosities from 0·01 to 400 P the measured cavitation threshold P_c of an undegassed liquid under dynamic loading is related to the viscosity η of the liquid by the empirical expression $P_c \propto \eta^{0.2}$. The dynamic stress in a liquid is relieved by the growth of cavitation nuclei. Theory predicts that the growth of these nuclei is impeded by viscous forces during the initial stages of growth.

ACKNOWLEDGEMENTS

The author wishes to thank Dr. F. C. Roesler and Dr. H. Kolsky for valuable discussions.

REFERENCES

(1) Bull, T. H. *Phil. Mag.*, 8, **1**, No. 2, p. 153 (1956).

(2) Poritsky, H. *Proc. First U.S. Nat. Congr. Appl. Mech.*, p. 813 (1951).

(3) Roesler, F. C. Private communication.

Correspondence

A photoelastic method of two-dimensional separation of stresses along a line of symmetry by using the isochromatic fringes only

The paper by Dr. S. P. Christodoulides, published on pp. 190–4 of the May 1956 issue of this *Journal*, was quite interesting. However, the author's conclusion "that the radius of curvature is the same for any of the curves: the orthogonal to the isoclinics, the isochromatics, and one of the principal stress trajectories at any point on a line of symmetry" is incorrect. One can think of several simple cases which show that this statement is not valid. Consider, for example, a circular disk under diametral loads. The radii of curvature of the stress trajectories and the isochromatics are not equal along either axis of symmetry of the disk. (See Figs. 124 and 125, Jessop and Harris.*) A second illustration is offered by the simply supported beam under a central concentrated load, where the radii of curvature of the isochromatics and stress trajectories are clearly different along the vertical axis of symmetry. (Figs. 143 and 144, Jessop and Harris.*)

The author's error seems to be in the interpretation of equations (18) and (20). For the case in which the isochromatics are taken as the s-curves and for a line of symmetry, he shows in equation (20) that

$$\frac{\partial P}{\partial n} + (P - Q)\frac{\partial \alpha}{\partial s} = 0$$

From Fig. 3,

$$\alpha = \theta - \phi \qquad (1)$$

so that

$$\frac{\partial \alpha}{\partial s} = \frac{\partial \theta}{\partial s} - \frac{\partial \phi}{\partial s} \qquad (2)$$

On the line of symmetry, $\alpha = \theta$ from our equation (1), but $\partial\alpha/\partial s$ is given by equation (2). The curvature of the stress trajectories orthogonal to the axis of symmetry is $\partial\alpha/\partial s$ and its values do not depend on the particular choice of the orthogonal s-curves, whereas $\partial\theta/\partial s$ and $\partial\phi/\partial s$ depend on the choice of the s-curves. When the isochromatics are taken as the s-curves, $\partial\theta/\partial s$ is the curvature of the isochromatics. The author's statement "that $\partial s/\partial\alpha = \partial s/\partial\theta =$ the radius of curvature of the isochromatics" is incorrect since $\partial\phi/\partial s$ is not zero in our equation (2). The value of $\partial\phi/\partial s$ is zero only when the stress trajectories orthogonal to the axis of symmetry are chosen as the s-curves. Thus, for the line of symmetry, equation (20) is the Lamé–Maxwell equation in which $\partial\alpha/\partial s$ is the curvature of the orthogonal stress trajectories, not the curvature of the isochromatics.

In a similar manner, it can be shown that the radii of curvature of the principal stress trajectories and the orthogonal curves to the isoclinics are different for points on a line of symmetry.

As a consequence of the error in the interpretation of equations (18) and (20) the method of stress determination based on measuring the radii of curvature of the isochromatics as proposed by the author is not valid. The computations for the numerical example on p. 193 are therefore in error. In addition, there are some errors resulting from a confusion of sign convention. It is known both from theory and experiment that for a tension bar containing a central hole both principal stresses on the transverse axis of symmetry are tensile. Therefore, the stresses shown in Fig. 9 cannot possibly be correct.

General Engineering Laboratory, General Electric Company, Schenectady, 5, New York, U.S.A.

P. D. Flynn,
R. Guernsey, Jr.

Dr. P. D. Flynn and Dr. R. Guernsey, Jr., are quite correct in their criticisms. As they have pointed out, an error occurred in the interpretation of equations (18) and (20) where the rate of change of the angle ϕ was by mistake taken equal to zero on the line of symmetry. This error was the result of faulty reasoning from the conditions of symmetry existing on the axis, from which symmetry in ϕ (i.e. $\theta - \alpha$), was assumed instead of $|\phi|$.

The quantities $\partial\phi/\partial n$ or $\partial\phi/\partial s$ can be small, but cannot be ignored in the step by step integration, and the error actually invalidates the method of separation of stresses suggested.

I thank Dr. Flynn and Dr. Guernsey for pointing out this mistake.

University College, London.

S. P. Christodoulides*

* Now at Ove Arup and Partners, London, W.1.

Ring conduction in the early stages of sparks

In a recent letter[1] it was shown that a study of the marks left by brief sparks on an anode covered by a thin contaminating film of a substance like barium stearate could give information about the variation with time of the current

Kerr-cell shutter photograph (exposure about 2 μs) of an 80 A spark to a plane tin anode, 40 μs after initiation of the spark. The photograph was taken looking down obliquely at the anode. The diameter of the luminous ring is about 0·04 cm

* Jessop, H. T., and Harris, F. C. *Photoelasticity* (London: Cleaver-Hume Press Ltd., 1949).

distribution at the anode. Using this technique it was found that, about 1 μs after the initiation of the spark, all or most of the current leaves the anode in a ring and that this state of affairs persists for perhaps 10 or 20 μs, after which a more uniform current distribution probably prevails.

On looking over some old records we came across four photographs of sparks taken during the course of an earlier investigation[2] some four years ago. The figure shows one of these photographs, all of which are similar. It confirms in a striking way the existence of an active ring at the anode, already deduced from the study of anode marks. At the time when the photograph was taken the significance of the anode surface condition was not realized and this particular anode must have had, by chance, the right degree of contamination to show the ring clearly.

The photograph shows a central luminous channel suggesting that much of the current may have moved back to the centre, as previously suggested.[1] It is not possible to say whether the ring is still passing current or not; it may be still incandescent after earlier use.

University of New England,
Armidale,
New South Wales,
Australia.

J. M. SOMERVILLE
N. H. FLETCHER*

REFERENCES

(1) SOMERVILLE and GRAINGER. *Brit. J. Appl. Phys.*, **7**, p. 109 (1956).

(2) SOMERVILLE, BLEVIN and FLETCHER. *Proc. Phys. Soc. [London] B*, **65**, p. 963 (1952).

* Now at Division of Radiophysics, Commonwealth Scientific and Industrial Research Organization, Sydney.

New books

Abstracts of the literature on semiconducting and luminescent materials and their applications. Compiled by Battelle Memorial Institute. (New York: J. Wiley and Sons Inc.; London: Chapman and Hall Ltd., 1956.) Pp. viii + 200. Price 40*s*.

The comments made by Prof. Garlick on the 1953 issue of these abstracts (*Brit. J. Appl. Phys.*, **6**, p. 453, 1955) apply with little change to the 1954 volume. The time lag seems to be shorter, but the latest papers are well over a year old. The use of abstract journals as sources for some of the material must have aggravated this delay.

Though printed from typescript in a not very durable loose-leaf form, these abstracts look opulent with their good paper, wide margins, and lines of full page width. In the more essential feature of completeness of cover the position is not entirely satisfactory. This is particularly the case for the patent literature, not perhaps the scientist's favourite reading, but which is often a source of new information. In 765 abstracts about 33 patents are mentioned, and of these only one is British, the rest are mostly American or Japanese, and several are hardly worth inclusion. There is also some untidiness in the classification. Thus electroluminescence references occur under the main heading "Sulphides," and also under a sub-section of "Fluorescence and phosphorescence"; but it would be difficult to suggest a completely logical arrangement. On the whole this is a valuable compilation of good abstracts for the worker who tries to remain aware of recent literature, not a little of which is in inaccessible journals.

S. T. HENDERSON

Theory of sound, Vols. 1 and 2. By LORD RAYLEIGH. (New York: Dover Publications Inc., 1956.) Pp. xlii + 480 (Vol. 1); xvi + 504 (Vol. 2). Price $3.90 per set (paper bound).

Dover Publications of New York have in recent years adopted the admirable policy of making available a series of reprints of classics of the mathematical and physical sciences. These have included works such as Agricola's *De re metallica*, Descartes's *Geometry*, Galileo's *Dialogues*, Clerk Maxwell's *Scientific papers*, Newton's *Opticks* and Helmholtz's *Sensations of tone*. The volumes are well produced, often having been photostated from the originals, and are available in cloth or in a cheaper paper bound edition. Now comes the famous *Theory of sound* in two volumes by Lord Rayleigh, the original edition of which appeared in 1877–8 (Macmillan and Co. Ltd.). A revised and enlarged edition was issued in 1894 (Vol. 1), and 1896 (Vol. 2). Since then there have been English reprintings in 1926 and 1929 and an American reprinting in 1945, the latter being greatly enriched with an historical introduction of 32 pages, comprising a brief biography of Lord Rayleigh, a survey of the history of acoustics, and an excellent bibliography, contributed by Robert Bruce Lindsay, Hazard Professor of Physics in Brown University. The present reissue is the same as that of 1945, together with the historical introduction.

Until the advent of popular radio and reproduction of sound some thirty years ago, from which originated modern acoustical engineering, the science of acoustics was the cinderella of physics.

Despite attempts to draw illustrations of acoustical phenomena from the art of music—not very successfully it must be admitted since they commanded little respect from musicians—the majority of the textbooks of pre-radio days were arid in the extreme. An extensive discussion of the mechanics of vibration, some reference to measurements of the velocity of sound by very crude methods, an unimaginative, purely numerical, treatment of the tuning of keyboard instruments ignoring almost entirely the artistic needs of the musician, a dubious theory of the action of organ pipes which was negatived every day in the work of practical organ builders, and a questionable discussion of the mode of action of other musical instruments, constituted the core of the subject.

One would have looked in vain for the terms *transients* and *formants*; there would be no reference to the sensitivity characteristics of the ear that are so important in both speech and music, while very few authors referred at all to the acoustical properties of auditoriums though Sabine had done his (now) classical work twenty years previously.

The importance of acoustics in the modern world through developments in the fields of telephony, the radio transmission and recording of sounds, the "measurement" of sound, and the design of concert halls, has emphasized the connexions of the subject with psychology on the one hand and electricity on the other. Great advances in sensory

psychology arising from the work of numerous experimenters in England, Germany and America have enabled us to understand more clearly the conditions of hearing with consequent applications to interpretation in musical performance, while electricity provides the acoustical engineer with his measuring instruments and many of the means by which he achieves his practical effects.

If, therefore, the pre-radio (that is, approximately pre-1930) books are so deficient, the question may be asked why reissue an old Victorian textbook? The reason is that Rayleigh's treatise on sound, unlike most other similar works, was largely based upon the author's original researches which provide a wonderfully apt background for all subsequent developments. As Lindsay has so clearly indicated in his introduction, there are few indeed of today's applications that do not owe something to Rayleigh's suggestive foresight and the results of his experiments.

On the conclusion of the mathematical tripos examination at Cambridge in 1865, when Lord Rayleigh was Senior Wrangler, it was reported that his worked papers were set out with such elegance and lucidity that they could have been published immediately with but little revision. The treatise on sound possesses these same characteristics to the full whether in the presentation of mathematical reasoning or in the description of experimental findings; it is well entitled to its place as a classic of physics and, to quote Lindsay, it is safe to predict that for a long time to come it "will be a *vade mecum* for both the pure and applied acoustician."

H. LOWERY

Molecular beams. By N. F. RAMSEY. (London: Oxford University Press, 1956.) Pp. xii + 466. Price 75*s*.

The great advances in molecular beam techniques during the last twenty years, which have yielded a wealth of information about molecules, atoms and nuclei, have been largely concentrated at a few universities, and the results have been published in highly specialized papers. A review of the subject is therefore long overdue, and although this need has recently been met to some extent by the excellent Methuen monograph of Dr. K. F. Smith the fuller treatment by Prof. N. F. Ramsey is no less welcome. The whole field, in both its practical and theoretical aspects is now covered for the first time, and by an author who has himself made brilliant contributions.

The technique developed rapidly from the relatively simple deflexion method as used in the celebrated Stern–Gerlach experiment to the wonderfully precise magnetic resonance method; and it is a valuable feature of the book that separate sections are devoted to detailed descriptions of the design and operation of the apparatus. A warning is also given that the peak of a resonance curve does not always denote the true resonant frequency; and it might perhaps have been useful if the description of the various pitfalls had been extended and related to the different types of resonance and methods of measurement. The opening chapters give a general historical account of the method, and describe the kinetics of a gas in a high vacuum with the formation and the shape of the beam. This is followed by an analysis of the interaction of a nucleus with atomic and molecular fields, and in this analysis, as with the other mathematical sections, it is noteworthy that the stages in the argument can be followed by the non-mathematical reader. Expressions are derived for the effective magnetic moment of an atom in an external magnetic field and for its deflexion in a non-uniform field. The deflexions give information concerning nuclear moments and spins, and the early experiments are described before the more powerful resonance method is considered. The measured quantities in this method are not deflexions but frequencies, fields, and the dimensions of the apparatus, and many comparative results can be expressed in terms of frequencies alone, so that the accuracy obtained is limited only by the sharpness of the resonance. The many applications are dealt with in detail, particular attention being given to the important improvement gained by using separated exciting fields, the calculation of the probability of transitions being extended to this case; and to the work on the atomic fine structure and the Lamb shift of the hydrogen lines.

A study of Prof. Ramsey's book will be essential to anyone wishing to learn about this new and important branch of physics as well as to the actual worker in the field.

L. ESSEN

Physics of fully ionized gases. By L. SPITZER, Jr. (New York: Interscience Publishers Inc., 1956.) Pp. 105. Price $1.75 (paper), $3.50 (hard cover).

In the types of electrical discharges with which physicists have long been familiar (e.g. gas discharge lamps, cold cathode tubes, mercury arc rectifiers, Geiger counters) the current density is so low that only a fraction of the gas molecules present are ionized. The electron, and so the ion concentration is small compared with that of the neutral particles. To a certain extent, this complicates the treatment of the kinetics of the assemblies. In recent years, however, considerable interest has been directed to the case of gases which are almost completely ionized. While there is an increasing interest in such cases in the field of electronics, they are also of importance in theoretical astro-physics. The appearance of this monograph by Lyman Spitzer, Jr, of Princeton University Observatory, is thus greatly to be welcomed, and it can be said at once that it is an excellent book.

The case of hydrogen is particularly interesting. As the author points out in his preface, this gas is the most abundant element in the stars and in space, and, further, atoms which are ionized are also stripped. Helium, the next most abundant nucleus, is in the sun mostly stripped of its two orbital electrons. Again, in discharges in the laboratory, certain plasma oscillations are independent of the neutral particle concentration and of the bound electrons in the ionized atom. Hence, analysis of the behaviour of a gas composed simply of electrons and pure nuclei is likely to be important as well as interesting. The advantages of this simplification are considerable, because one can ignore those phenomena which often make detailed analysis of ordinary low-pressure discharges practically intractable, namely electron attachment, associated recombination, excitation and de-excitation of molecules, as well as wall and electrode phenomena. Quantum-mechanical effects can thus be ignored apart from weak interaction with the radiation field, and encounters between the charged particles treated simply on the basis of the inverse square law. On the other hand, the motions of the particles are thus more complicated than in the case of ordinary discharges, because of coupling with the electromagnetic forces.

The author treats the subject in five chapters entitled Motion of a particle; Macroscopic motion, Principles; Problems; Waves in a plasma; and Encounters between charged particles.

The treatment everywhere is clear and concise, the formulation of the mathematics being modern and very clear. To avoid breaking the continuity, treatment of the Boltzmann

equation suitable for the present subject is given in an appendix. When it is realized that all this is done in just about 100 pages, the author is to be highly congratulated. The book can indeed serve as an object lesson to anyone who may tend to confuse size and weight with quality. This book can be very strongly recommended.

F. LLEWELLYN JONES

X-rays; their origin, dosage and practical application. 7th ed. By W. E. SCHALL. (Bristol: John Wright and Sons Ltd., 1956.) Pp. vii + 331. Price 42*s*.

There can be but few scientific or technological textbooks that attain the distinctions of a seventh edition and useful service as standard texts for more than thirty years in a rapidly expanding subject. This book has achieved these merits through its author's rare insight into the interests of those on whose practical skill, knowledge and reliability depends the operation of equipment and methods in our progressing scientific age. For in the training of technologists a middle course should be steered between the dangers of encouraging unintelligent button-pushing and too profound scientific appreciation.

The reviewer feels this book strikes the right balance. Throughout the author has chosen and explained his topics well. Furthermore, the claim seems justified that the book caters for all radiographers whether they be concerned with diagnostic, therapeutic or industrial applications. Those concerned with routine X-ray diffraction tests would benefit equally.

The book is well produced and therefore a pleasure to read, particularly owing to excellent figures and plates. There are, however, some striking exceptions, notably Fig. 169 on which the writing can barely be read. A uniform presentation of circuit diagrams would be helpful (e.g. compare Figs. 95 and 100).

The reviewer regrets the omission of literature references. Mention of original papers may be out of place, but encouragement for looking up the writings of other authors in wider and more specialized fields is so fundamental in the training of scientists and technologists that suggestions for further reading should have been included.

Nevertheless, further generations of radiographers will yet praise and thank author and publisher for this fine and useful volume.

H. S. PEISER

Transistor electronics. By A. W. LO, R. O. ENDRES, J. ZAWELS, F. D. WALDHAUER and C. CHENG. (New York: Prentice-Hall Inc.; London: Bailey Bros. and Swinfen Ltd., 1955.) Pp. xii + 521. Price 96*s*.

So many meanings are given to "electronics" that the only way of discerning the contents of a book on the subject is to look through the pages. "Transistor circuits" might have been a more appropriate title for this book, although it probably contains sufficient on semiconductor physics to justify the somewhat broader title.

Anyone who has taught or studied transistor circuits will realize the importance of introducing the correct amount of physics at appropriate places. In this book the first chapter contains enough transistor physics for the reader to be able to follow the next chapters which deal with low-frequency amplifier circuits. High-frequency operation is then discussed and, in order that it can be better understood, another chapter on physics is added. The circuit engineer is much more likely to appreciate the value of physics when it is introduced gradually in this way; he is more likely to go to the trouble of understanding it, thereby becoming a better engineer.

The main circuit aspects considered are amplifiers, oscillators, modulation and demodulation, and pulse circuits. The presentation is logical and a wealth of subject-matter is included. However, little or no attention is given to a number of topics that are particularly important to anyone using transistors; neutralization of feedback effects in amplifiers, the application of negative feedback, and the thermal stability of power amplifiers are examples. The reader is also confronted with yet another graphical symbol for the transistor.

Many will find this a useful guide to circuit design. Senior students and lecturers, at those few colleges that treat transistor circuits seriously, will also find it useful. Nevertheless, its high price may limit the number of engineers and physicists who would benefit from having a comprehensive book of this type in their private libraries.

D. D. JONES

Engineering fluid mechanics. By C. JAEGER. (Glasgow: Blackie and Son Ltd., 1956.) Pp. vii + 529. Price 60*s*.

The above textbook is by an author who has had considerable teaching experience and a distinguished research record in applied hydraulics. It contains much that is Dr. Jaeger's original work. The bibliographical references, copiously given, are very useful for they give the reader an historical description of the growth of the subject, and of the workers who have been responsible for its development.

The English translation of the original work has possibly not been given a fitting title as its scope is by no means as comprehensive as that suggested. As stated on the fly-leaf and in the preface, the book is concerned with water supply and transmission for hydraulic power installations. In the introductory chapter physical principles, basic to the study of hydraulics, are discussed. There is an account of the relevant hydrodynamic equations followed by a few applications to engineering problems. The topics dealt with in detail are flow in open channels, theory of surge tanks, and ground water flow. The water hammer phenomenon in pipe lines receives quite an extensive treatment. Allievi was perhaps the leading pioneer in this field and his investigations are amply described. It may be noted, however, that he did not consider frictional flow. Methods were later devised by Bergeron and Schnyder in which a rough allowance was made for frictional losses; but their treatment is known to be mathematically unsatisfactory, involving serious error.

There are no set questions in any part of the book, the apparent reason being to cut down size to a minimum. This feature, disfavoured by many in this country, is fairly common practice on the Continent, and it may easily be rectified by the teacher.

The book is not intended primarily for the undergraduate reader, nevertheless university degree syllabuses have demanded a fuller treatment of the above-mentioned sections than is usually given in general textbooks. This authoritative work will consequently be welcomed by those interested in this branch of engineering, and it will rightly find a place on the shelves of college libraries.

C. DAVIES

Notes on applied science No. 11. Wind effects on bridges and other flexible structures. (London: H.M. Stationery Office, 1955.) Pp. iv + 14. Price 1*s*. 6*d*.

This monograph, prepared by the National Physical Laboratory, discusses the effects of wind loading on structures, principally suspension bridges; the dynamic effects of wind loading on suspension bridges have been studied and much

discussed since the spectacular failure of the Tacoma Narrows bridge in 1940.

These effects are discussed mainly in relation to the work, done at the N.P.L. and elsewhere, on a model of the proposed Severn bridge by R. A. Frazer and his team.

E. K. FRANKL

Progress in semiconductors. Edited by A. F. GIBSON, P. AIGRAIN and R. E. BURGESS. (London: Heywood and Co. Ltd., 1956.) Pp. vii + 220. Price 50*s*.

The appearance of an annual progress report on semiconductor research will be welcome news to those—and there must be many—who have been struggling with the almost impossible task of "keeping up with the literature" in this field. In this first volume of the new series, several authors deal with recent advances in silicon (fundamentals as well as technology), with the use of germanium filaments in semiconductor research, with the theory of the Seebeck effect, with the electrical properties of several important phosphors (including a brief discussion of electro-luminescence), with transistor design for high-frequency operation, with the photo-magneto-electric effect and with the effect of external fields on surface properties. A progress report of this kind can fulfil an extraordinarily useful function. To do so, the various contributions must offer to the reader so much more than a series of classified abstracts and, what is equally important, distinctly less than a comprehensive treatise. They must have the character of considered digests and reviews, and should not themselves be research communications of the kind normally published in journals. On the basis of this criterion, most of the contributions in this volume satisfy their purpose well. The book is attractively produced and will be of interest to the ever increasing circle of readers who are active in this field.

H. K. HENISCH

The electrolytic and chemical polishing of metals, in research and industry. By W. J. MCG. TEGART. (London: Pergamon Press Ltd., 1956.) Pp. x + 129. Price 30*s*.

This book had its origin in a report prepared some time ago in the Division of Tribophysics of the Commonwealth Scientific and Industrial Research Organization in Melbourne. It aims to be the first comprehensive survey of the subject to be published, covering the theoretical aspects of chemical and electrolytic polishing and the application of such processes in both research and industry. This claim is unduly wide to be adequately met by so slim a volume. Unfortunately, the treatment of theoretical aspects and the chapters on industrial polishing are unlikely either to satisfy the specialists or to attract the general reader.

The book can be recommended, however, for its useful collection of recipes, to those laboratory workers who may from time to time wish to prepare electropolished metal surfaces for investigational work.

G. L. J. BAILEY

Proceedings of the eleventh general assembly of the International Scientific Radio Union (U.R.S.I.), Vol. 10, Part 2, **Radio and Troposphere.** (Union Radio-Scientifique Internationale, 42 Rue des Minimes, Brussels.) Pp. 90. Price 14*s*. 9*d*.

The radio sounding of the upper atmosphere has been, of course, for many years a classic instance of the importance of applying laboratory and industrial techniques in the study of natural and cosmic phenomena. The reports of U.R.S.I. have already afforded surveys of interest, in geophysics based on radio reflexion, and in emissions from astronomical sources. The present volume of *Radio and Troposphere*, discusses the case of the propagation of radio waves through those portions of the lower and middle atmosphere which have usually been regarded as the province of the meteorologist. Apart from its importance to specialists, it is a good thing for physicists in all kinds of laboratories to realize that these problems of refractive index and scattering in radio wavelengths can now be valuably pursued at all heights above the earth's surface.

MARTIN JOHNSON

Theoretische Metallkunde. By U. DEHLINGER. (Berlin: Springer-Verlag, 1955.) Pp. iv + 250. Price DM 27.

The text of the present book occupies 208 pages in which the author reviews the crystal structures and electron theories of metals and alloys, together with heats of formation, electrical, magnetic and optical properties, and applications of thermodynamics to various problems. Diffusion, nucleation, and precipitation are also considered, together with lattice imperfections, surface effects, and relaxation processes. The text is followed by 26 pages of tables of theoretical functions and physical data, and by eight pages with suggestions for further reading.

The wide range of subjects considered in such a short space has necessitated extreme condensation, and, unfortunately, this has sometimes been done so that the simple and fundamental principles are not revealed clearly. The book is hardly one to recommend for the beginner, but the reader with previous knowledge of the subject will find that the book provides a useful review in which the emphasis and general approach are sometimes very different from those of most British or American authors, and for this reason the book is well worth reading.

W. HUME-ROTHERY

Flow of gases through porous media. By P. C. CARMAN. (London: Butterworths Scientific Publications, 1956.) Pp. ix + 182. Price 30*s*.

This book deals mainly with the viscous flow of gases in fine-pored media. By the latter are meant consolidated or unconsolidated structures possessing fine capillary networks. The permeability of glasses or high polymers to gases is thus outside the scope of the book. The Kozeny approach is used throughout, the porous medium being idealized, for the sake of analysis, as an equivalent parallel capillary model. This model has been frequently used in flow studies and its usefulness and limitations are closely analysed. The transition regions to Knudsen and turbulent flow are also discussed but in less detail. On the whole the case for the Kozeny theory is well presented but one feels that more attention could have justifiably been paid to the transient state of flow which is all too briefly discussed. An interesting chapter is included on the application of permeability measurements to the calculation of surface areas, a detailed comparison being made with the sorption technique. The chapter on the separation of gas mixtures is mainly of a qualitative nature but serves to illustrate further the applications of flow measurements. An up-to-date review of the surface diffusion of adsorbed molecules is marred by an error in Fig. 18, p. 121: E_1 and E_2, and E_{a1} and E_{a2} should be interchanged respectively; also for "decrease" on the penultimate line of the same page read "increase." Overall there are relatively few printing errors, and the author is to be congratulated for giving a clear account of progress in this field in which he has done much research himself. The book is recommended to all those interested in problems of gas flow in porous media.

J. A. BARRIE

Notes and comments

Elections to The Institute of Physics

The following elections have been made by the Board of The Institute of Physics.

Fellows: B. C. Abbott, C. E. Arreger, J. B. Dick, P. W. Mummery, B. N. Watts.

Associates: S. G. G. Aston, K. D. Barritt, K. M. Beazley, J. Blitz, G. R. Boulding, D. O. Bullas, W. Burnside, P. B. Carter, K. J. Close, R. F. Coe, F. C. W. Colmer, T. C. Common, R. H. Davies, M. De, A. S. Douglas, J. Gilbert, A. Gray, G. Y. Haig, B. I. H. Hall, F. W. Harrison, P. W. Hoare, T. A. Holbeche, J. T. Jefferies, P. Johnson, B. E. Jones, T. B. Kent, W. A. Langton, J. H. Leck, C. H. Leigh-Dugmore, W. J. Legon, J. G. Moreley, G. H. Parks, I. J. W. Pothecary, K. Pringle, D. A. Secomb, K. G. Stephens, A. F. Taylor, R. G. S. Taylor, R. J. Tracey, F. L. Ward, P. G. Walker, J. Wartnaby, J. W. Watts, A. N. D. Young.

Forty-seven Graduates, eight Students and five Subscribers were also elected.

Electrical Energy

We have received the first issue of a new monthly periodical called *Electrical Energy*, which is intended "for the professional electrical engineer engaged in research, development, design and manufacture." It is owned and produced by the proprietors of *The Engineer* and *Electronic Engineering*, and has the same Managing Editor (Mr. H. G. Foster) as the latter periodical. The articles will cover the whole field of electrical engineering and will include such topical subjects as servo mechanisms, remote control by electrical methods, automation, the electrical aspects of nuclear power generation, electrical traction, magnetic amplifiers, aeronautical and marine electrical engineering. Regular features will include news items of technical and topical interest, reviews of books on electrical engineering subjects, notices of meetings of institutions and professional bodies and letters to the Editor.

The thirty-two-page issue before us measures $8\frac{1}{2} \times 11\frac{3}{4}$ in. and is well produced, as one would expect of a periodical with such strong backing. We wish our latest contemporary all success. The subscription rate is £1 16*s.* and the publishers are Morgan Brothers (Publishers) Ltd., 28 Essex Street, London, W.C.2.

British Standards Institution

The Annual Report of the British Standards Institution for the year ended 31 March, 1956, again records an increase in membership and activities. The first section of the report, which serves as a general introduction, includes references to the progress made in the study of fuel efficiency, the completion of the first British Standard concerned with smoke abatement, and preliminary steps taken in the preparation of standards required for the development of nuclear energy.

The main body of the report contains a detailed review of the standards projects completed and in hand in the Institution's four main divisions: building, chemical, engineering and textiles (and in the industries outside the scope of these four), and the work carried out under the Council for Codes Practice.

The international section of the report contains an account of the B.S.I.'s increasing contribution to the work of the International Organization for Standardization (ISO) and the Electrotechnical Commission (I.E.C.). Among the diverse undertakings were discussions on medical gas cylinders, the revision and extension of the well-known classification of insulating materials, work on tests for chemicals, discussions on unification of screw threads, recommendations on ball and roller bearings, proposals for common names for pest control chemicals, etc.

Other aspects of international co-operation in standardization included a conference of the ABC countries (America, Britain and Canada) to secure closer unification of basic engineering standards; B.S.I.'s participation in the work of the European Productivity Agency and preparation for next year's Commonwealth Standards Conference in Delhi.

Erratum

The review of the book *Proceedings of conference on effects of radiation on dielectric materials* published on p. 310 of the August issue of this *Journal* should have indicated that copies can be obtained from the Office of Technical Services, Department of Commerce, Washington 25, D.C., U.S.A., quoting PB number 111863.

Journal of Scientific Instruments

Contents of the November issue

ORIGINAL CONTRIBUTIONS

Papers

An automatic electromechanical stressing unit for creep and fatigue testing. By A. J. Kennedy and R. F. Slade.
An electrostatic null detector. By J. Hart and A. G. Mungall.
An electrical indicator for a mercury U-tube manometer. By A. E. Hawkins.
Eight-channel recording on $\frac{1}{4}$ in. magnetic tape with a stationary-tape playback. By J. C. Barton.
Simple equipment for a small low temperature laboratory. By R. F. Broom and A. C. Rose-Innes.
An instrument for the measurement of salinity in estuaries. By E. G. Sandels.
A fast coincidence system for the measurement of short lifetimes. By G. Jones and J. B. Warren.
Dynamometer for tensile testing of high polymers. By A. R. Payne and J. F. Smith.
An electronic analogue of the saturated vapour pressure curve of water. By R. J. Taylor.
An all-glass reference electrode for molten salt systems. By J. O'M. Bockris, G. J. Hills, D. Inman and L. Young.
A heart pulse amplifier and ratemeter. By D. G. Wyatt.

Laboratory and workshop notes

A window material for high temperature X-ray cameras. By A. G. Provan, B. A. Shaw and G. I. Williams.
On internally metallizing a betatron toroid by vacuum deposition. By K. R. Allen, F. Ashworth and G. Siddall.
A simple rotary film evaporator. By B. B. Marsh and P. M. Nottingham.
An improved design of radio-frequency ion source. By H. R. Allan and N. Sarma.
A secondary microwave attenuator. By H. A. Prime.
Regulator for maintaining a constant gas flow through a restriction of variable resistance. By E. F. Keen and P. L. Palmer.
An apparatus for the production of controlled lesions in biological tissue without stimulation. By G. E. Kaufer.
The output resistance of a switch-dial potential divider. By R. W. Williams.
A method of storing mechanically fragile specimens for examination. By C. A. Tremlett.

NOTES AND NEWS

New books
New instruments, materials and tools
Notes and comments

THIS JOURNAL is produced monthly by The Institute of Physics, in London. It deals with all branches of applied physics (including theory and technique). All rights reserved. Responsibility for the statements contained herein attaches only to the writers.

EDITORIAL MATTER. Communications concerning editorial matter should be addressed to the Editor, The Institute of Physics, 47 Belgrave Square, London, S.W.1. (*Telephone:* Sloane 9806.) Prospective authors are invited to prepare their scripts in accordance with the *Notes on the preparation of contributions*. (Price 2*s.* 6*d.* including postage.)

REPRODUCTION. The Institute of Physics is a signatory to The Royal Society's Fair Copying Declaration. Details may be obtained upon application from The Royal Society, London, W.1.

ADVERTISEMENTS. Communications concerning advertisements should be addressed to the agents, Messrs. Walter Judd Ltd., 47 Gresham Street, London, E.C.2. (*Telephone:* Monarch 7644.)

CLAIMS FOR MISSING JOURNALS. Claims from regular subscribers to this *Journal* for missing numbers will only be considered if received within 60 days of the date of mailing plus normal outward time of transit and time for lodging the claim. Losses attributable to failure to notify a change of address or to similar omissions will not be considered.

SUBSCRIPTION RATES. A new volume commences each January. The charge is £4 per volume ($11.50 U.S.A.), including index (post paid), payable in advance. Single parts, so far as available, may be purchased at 8*s.* each ($1.15 U.S.A.), post paid, cash with order. Orders should be sent to The Institute of Physics, 47 Belgrave Square, London, S.W.1, or to any bookseller.

Summarized proceedings of a conference on low temperature crystallography—Oxford, April 1956

A joint conference of the X-ray Analysis Group of The Institute of Physics, and the Low Temperature Group of the Physical Society, was held at the Clarendon Laboratory, Oxford, on 12 and 13 April, 1956. The theme included the study of structure and associated properties at low temperature, phase transitions, specific heat, thermal vibrations and absorption spectra, in both theoretical and experimental aspects.

FIRST SESSION: PHYSICAL PROBLEMS IN LOW TEMPERATURE CRYSTALLOGRAPHY

The first session of the conference was devoted to "Physical problems in low temperature crystallography," and was held under the Chairmanship of DR. K. MENDELSSOHN (Clarendon Laboratory, Oxford).

An introductory talk on the relationship of X-ray analysis to low temperatures was given by PROF. SIR FRANCIS SIMON (Clarendon Laboratory, Oxford). The third law of thermodynamics stated that a system in equilibrium tended to a state of perfect order as the absolute zero of temperature was approached. This state of order was destroyed as the temperature was raised.

For many practical purposes, liquid air was often considered to provide a low temperature, but in any experiment it was necessary to enquire carefully whether a given temperature T was "high" or "low." The magnitude of some characteristic interaction energy must be known and if kT was small compared to this then T was "low." Thus for diamond, 1000° K was a low temperature; for many nuclear orientation effects, 0·1° K was a high temperature.

Prof. Simon then enumerated some problems which could be attacked by a combination of X-rays and low temperatures. Historically the first problem to be investigated was the structure of the solid inert gases, which because of their comparatively simple interaction forces were of great importance theoretically. This work was begun over thirty years ago. Keesom and his collaborators contributed largely to this work and by 1937 solid helium had been studied down to the region of 1·5° K by Dr. K. W. Taconis (who was present at this Conference).

Another important line of investigation was the study of crystallographic transitions, which could often take place at surprisingly low temperatures. Specific heat anomalies often provided the first clue that such transitions had occurred, and in sodium an anomaly had been reported in one specimen at 0·8° K. Prof. C. S. Barrett's careful studies of the alkali metals was outstanding in revealing the extreme complication of the transitions which could occur in metals sometimes referred to by physicists as simple. Another type of transition which could be investigated by thermal as well as X-ray methods was the internal transition, in which disorder could be stored at high temperatures by the rotation of molecules or by the disorientation of magnetic or electric dipoles. A further possibility was made manifest by the study some years ago of the transition in liquid helium at 2·18° K, which showed that kinds of disorder other than geometrical disorder could exist.

Real crystals were never perfect in their structure and the imperfections could travel even at low temperatures; X-rays could provide much useful information on the perfection of crystals. Low temperature physicists were only just beginning to realize the importance of checking that their specimens were pure and free from imperfections before making entropy measurements on them.

Often the main motive for which X-ray crystallographers cooled their specimens was that with the decrease of amplitude of thermal vibration, the lines become more pronounced. But in addition a quantitative study of the scattering could provide a good deal of data about the vibration spectra of solids, the elucidation of which is one of the most important problems in solid state physics. In this connexion it was important to remember that zero-point motion behaves like thermal agitation in its effect on X-rays.

DR. M. BLACKMAN (Imperial College of Science and Technology, London) then spoke on theoretical aspects of the effect of temperature on the reflexion of X-rays. His main topic was the general relation between the intensity of the Bragg reflexions and the distribution function for the frequencies of the lattice vibrations. As for monatomic cubic crystals, the relation is established in two stages, the first relating the intensity of a Bragg reflexion with the mean square amplitudes of atomic vibration, and the second relating the amplitudes with the frequency distribution. For general crystals the intensity of X-ray scattering is proportional to

$$I = |L \sum_k f_k \exp(-M_{kq})|^2$$

where L is the Laue factor, f_k the scattering factor of the kth particle in the unit cell for the particular reciprocal vector, and

$$M_{kq} = 8\pi^2(\sin^2\theta/\lambda^2)\overline{u_{kq}^2}$$

with $\overline{u_{kq}^2}$ the mean square amplitude of oscillation of this particle parallel to the reciprocal vector. For general crystals one can show that the mean square displacements of the atoms can be represented as ellipsoids. Dr. Blackman then gave the general relation between the mean square amplitudes and the vibration spectrum as

$$\sum_k m_k(\overline{u_{kx}^2} + \overline{u_{ky}^2} + \overline{u_{kz}^2}) = \frac{3g}{4\pi} \frac{\int \rho(\nu)\bar{\varepsilon}(\nu)\nu^{-2}d\nu}{\int \rho(\nu)d\nu}$$

where m_k is the mass of the kth particle in the cell, $u_{kx} \ldots$, are the displacements with respect to Cartesian axes, g is the number of particles in the cell, $\rho(\nu)$ is the distribution function for the frequencies, and $\bar{\varepsilon}(\nu)$ is the mean energy of an oscillator of frequency ν at the temperature T. The results derived from the theoretical vibration spectra for sodium chloride and potassium chloride using this formula

agreed fairly closely with the X-ray results, though the comparisons were not entirely satisfactory.

In reply to a question from PROF. W. N. LIPSCOMB (University of Minnesota, U.S.A.) on anharmonicity, Dr. Blackman said that if the thermal terms in an extended Debye–Waller theory involved fourth as well as second order tensors, then the two carbon atoms in the (rhombodhedral) diamond cell would produce different scattering effects. Specific heat data on crystals suggested that anharmonic effects would not play a part until $T > \Theta_D$; measurements below $T = \Theta_D/3$ should be completely safe.

The next paper was read by DR. D. W. J. CRUICKSHANK (School of Chemistry, University of Leeds) on a theoretical study of the variation of vibration amplitudes with temperature in some molecular crystals. The speaker first remarked that the variation with temperature of the amplitude of oscillation of an atom in a monatomic cubic crystal is well known,[1] and can be expressed in terms of the Debye characteristic temperature Θ_D of the "acoustic" lattice vibrations. Conversely, if the amplitude is known at one T, Θ_D may be calculated, and hence the amplitude estimated for any other T.

For crystals composed of rigid molecules, account must be taken of the lattice waves involving rotational oscillations of the molecules. These waves belong to "optic" branches, and the amplitudes of angular oscillation about any axis may be estimated approximately assuming an Einstein oscillator. Account must also be taken of the extra translational and rotational "optic" branches occurring when there is more than one molecule in the unit cell.

Dr. Cruickshank then derived the various characteristic temperatures of benzene and anthracene from the r.m.s. amplitudes of the translational and rotational oscillations determined by three-dimensional Fourier anisotropic thermal parameter refinements, some of the rotational Θ's being checked with the lattice frequencies determined in Raman investigations.[2] The temperature dependence of the translational and rotational oscillations in benzene and anthracene were then calculated. A typical result was that the r.m.s. amplitude of angular oscillation about the hexad axis in benzene known[3] to be 7·9° at 270° K, was estimated to fall to 4·6° at 90° K, 2·9° at 25° K and 2·7° at 0° K. The full results showed that for studying fine details of electron density by X-ray crystallography substantial advantages (over working near room temperature) may be obtained by using liquid nitrogen as a coolant (giving say 90° K), that further substantial advantages accrue from using liquid hydrogen (giving say 25° K), but that there is little point in working at still lower temperatures for structures such as these.

In discussion, DR. S. C. ABRAHAMS (University of Glasgow) drew attention to a paper by Kozhin and Kitaigorodski[4] which reports intensities for naphthalene at 20° C and at −195° C, and gives the corresponding atomic positions.

PROF. DAME KATHLEEN LONSDALE (University College, London) next spoke on the determination of Debye factors by intensity measurements at low temperatures. She said that it was important to distinguish between the Debye factor B_j^T for an anisotropically vibrating atom j at temperature T° K and the Debye factor B_{hkl}^T for the diffraction from the hkl planes at temperature T. B_j^T may be expressed in terms of the amplitudes and orientations of the atomic vibrations, and then $f_j^T = f_j^R \exp(-B_j^T \sin^2\theta/\lambda^2)$, where f_j^R is the atomic scattering factor for the atom at rest. B_{hkl}^T may be obtained in two independent ways:

(1) $B_{hkl}^T = (\lambda^2/\sin^2\theta) \ln (F^R/F^T)$,

where $F^R = \Sigma f_j^R \exp[2\pi i(hx_j + ky_j + lz_j)]$,

and $F^T = \Sigma f_j^R \exp[-B_j^T \sin^2/\lambda^2 + 2\pi i(hx + ky_j + lz_j)]$

In this case the values of B_j^T, $x_j y_j z_j$ for each kind of atom are determined by a structure refinement at the one temperature T, and F^R and F^T are both calculated for the given hkl. Except for a monatomic structure, B_{hkl}^T will vary from one hkl to another, even in a cubic crystal.

(2) If, however, measurements of intensity are made at different temperatures, it is possible to plot a curve of F^T *versus* T for each hkl and to extrapolate to 0° K, within limits. Then

$$(B_{hkl}^T - B_{hkl}^0) = (\lambda^2/\sin^2\theta) \ln (F^0/F^T)$$

where B_{hkl}^0 is the "Debye factor due to zero point energy."

Dr. R. E. Gilbert has made these measurements for urea for a number of reflexions of intermediate intensity, and has compared the values of $(B_{hkl}^T - B_{hkl}^0)$ with B_{hkl}^T values obtained by the first method, using the data given by Vaughan and Donohue for the urea structure at 293° K. The agreement is surprisingly good: better than it should be, in fact, for when the second method is used there may well be changes in the atomic parameters as well as a scaling down of thermal vibration amplitudes as the temperature is lowered. For urea, there seems to be little change of atomic parameters, though the B_{hkl}^T values calculated by the first method seem to be fairly sensitive to co-ordinate changes and to changes in the B_j^T equations.

Prof. Lonsdale concluded by stressing the importance of structure refinements at more than one temperature, so that accurate data may be provided for studies in crystal physics at various temperatures.

In answer to a question from DR. J. D. DUNITZ (Royal Institution, London) it was made clear that if the fractional atomic parameters in urea do not change appreciably at low temperatures, this must mean some change in intramolecular bond lengths (and, after all, even diamond does have a coefficient of expansion). Most of the very anisotropic expansion of urea, however, is due to a change of the H-bond lengths with temperature.

DR. L. COUTURE (Laboratories de Bellevue, France) mentioned that the molecular external vibrations of urea had been classified after a Raman spectra single crystal investigation.[5]

Referring to both Dr. Cruickshank's and Prof. Lonsdale's papers PROF. E. G. COX (School of Chemistry, University of Leeds) remarked that there were some advantages in measuring urea, anthracene, etc., rather than sodium chloride, etc., to test fundamental theories of thermal motion, because (*a*) these substances gave more X-ray reflexions, and (*b*) other methods such as nuclear magnetic resonance, can be applied to them to give independent checks.

After this, PROF. C. S. BARRETT (Institute for the Study of Metals, University of Chicago) described his work on the body-centred cubic metals. He began by remarking that he had come to distrust all such "simple" metals and alloys: there was a strong possibility that any one might be unstable and undergo transitions at low temperatures!

The cryostat for the diffraction studies (constructed by Drs. Long, Meyer, Walker and Barrett) is illustrated in Fig. 1. The container (1), holding 2 litres of liquid helium (or hydrogen or nitrogen) cooled the specimen by conduction through the bar (9). The specimen was surrounded by the shield (10) at

helium temperatures and the shield (5) which was connected to the annular space (2) containing 3 litres of liquid nitrogen. The specimen could be changed by opening the O-ring joint between (3) and (4) and the conical joint (7). The vacuum pumps were disconnected at the O-ring joint (15) and the valve (14) to permit rotation of the cryostat during a diffraction experiment. The containers were refilled after 24 hours' operation at nitrogen temperatures or 3 to 8 hours' operation at helium temperatures. The cryostat was mounted on a precision X-ray spectrometer, with appropriate counter-weights, position adjustment, X-ray tube, stabilized power supply, counter and recorder. An attachment for cold-working the specimens at low temperatures, by scraping the surfaces *in vacuo*, was also provided.[6]

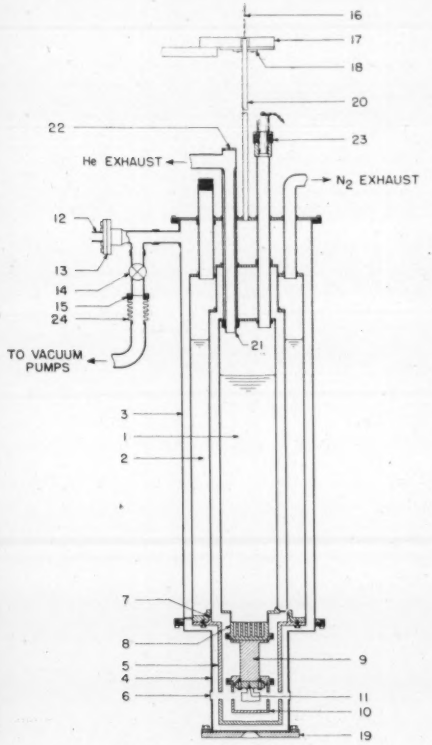

Fig. 1. Cryostat for diffraction studies

With this equipment the transformation (body-centred cubic to hexagonal close-packed) in lithium and its alloys with magnesium had been confirmed. In lithium the change started at about 70° K and about one-third was transformed; the transformation temperature was raised by cold working. Improved determinations of the unit cell dimensions had been made.[7] Sodium was found to transform partially at temperatures below 36° K to a faulted close-packed hexagonal structure of nearly ideal axial ratio (a structure like that of lithium and its alloys), but unlike lithium it did not further transform to face-centred cubic during cold work at 5° K. Specific heat anomalies had been variously reported at 7, 3 and 0·8° K.

Potassium, rubidium, caesium, barium and europium showed no transformation down to 5° K with or without cold work.[8] Beta brass—even in the so-called stable range of composition—transformed with cold work.[9]

In reply to DR. K. MENDELSSOHN it was explained that metals often undercooled a little before transformation; cold work, however, substituted for temperature agitation, with the result that the transformation temperature was raised by cold work.

PROF. SIMON reiterated that it was important for low temperature physicists to define the physical state of their materials. If a phase were undercooled to a region where it was unstable though crystalline, entropy measurements would be hardly affected because the third law was obeyed. But if the transformation were sluggish, then the smeared-out heat of transformation, the specific heat of the stable phase and the (larger) specific heat of the unstable phase all contributed to the measured "specific heat." Many "anomalies" were due to the evolution of the heat of transformation. It was also important that the container for the specimen could alter the transformation because of cold work produced by differential contraction on cooling. Prof. Barrett confirmed this last point from his own experience.

DR. M. BLACKMAN said that the transformation in lithium, with the large changes in Debye Θ to be expected, might have an important bearing on the specific heat measurements. DR. P. L. SMITH (Clarendon Laboratory, Oxford) reported that there was no difference in the measured specific heat below 4° K between specimens of lithium cooled quickly or slowly; possibly even the slowest cooling had been too quick. Prof. Barrett said that there was no evidence of transformation while the temperature was held constant but only while the temperature was changing.

Dr. Blackman pointed out that Zener had suggested that the large value of the shear modulus ($C_{11} - C_{12}$) in some alkali metals might give rise to transformations. The fact that potassium did not transform on cooling showed however that elastic anisotropy was not a particularly good criterion for the possibility of transformation since sodium and potassium had very similar anisotropies.

Prof. Barrett asked whether discussions of entropy changes could shed light on these transformations, in view of the very small preference for the cubic over the hexagonal structure. Prof. Simon answered that in the transition in solid helium (at 14° K under 1500 atm pressure) only a very small entropy change was involved yet the transformation was perfectly reversible. This was strange, since one would have expected the entropy change to have been much greater because of the large number of stacking faults that were no doubt present.

DR. W. B. PEARSON (National Research Council, Ottawa, Canada) then described his work with E. G. EELES on the expansion coefficients of the solid rare gases. The variation of the Grüneisen constant γ with temperature could yield much data on the vibration spectra of these simple solids.[10] However, the interesting region of temperature was that below 0·3 Θ, and a relative accuracy of 1 part in 40 000 in the lattice spacings had to be maintained down to

the lowest temperature if the measurements were to be of any use at all. The Debye-Scherrer method was used throughout.

Three cameras were described. That illustrated in Fig. 2 was the simplest since the Unicam 19 cm diameter casette was at room temperature, which made it easy to reload the film without disturbing the specimen. The substance under examination was mounted on a copper post, down which cold was conducted to cool the specimen. Room temperature radiation was absorbed by cellophane windows and, provided the powder specimen was packed tightly enough (without preferred orientation of the grains), its thermal conductivity was adequate to deal with the heat influx. The copper-constantan thermocouple was calibrated *in situ* down to 5° K. An automatic arrangement speeded up the rotation and shut off the X-ray beam when the radiation shields intervened; the direction of rotation was reversed after every revolution to prevent tangling of the thermocouple leads. The Dewar vessel held 1½ litres of liquid helium which lasted 3½ hours. The specimen was surrounded by shields at a different (lower) temperature.

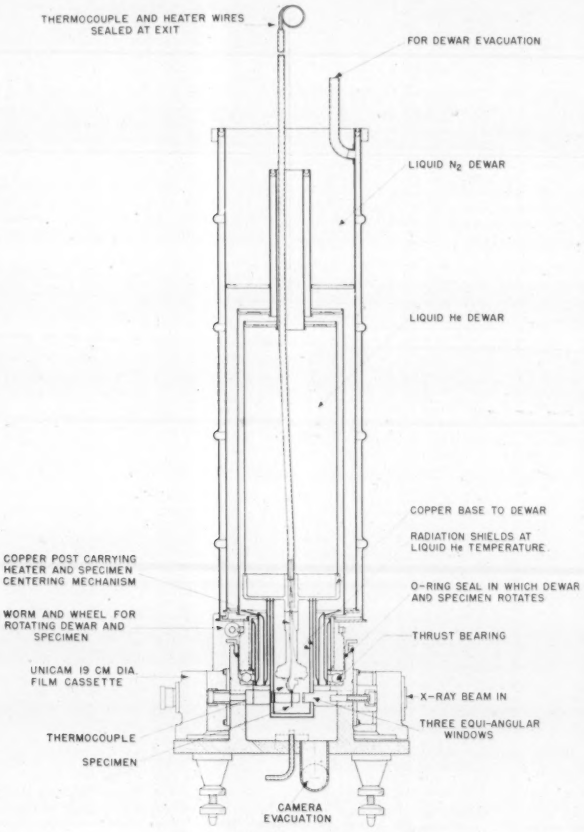
THERMOCOUPLE AND HEATER WIRES SEALED AT EXIT
FOR DEWAR EVACUATION
LIQUID N_2 DEWAR
LIQUID He DEWAR
COPPER BASE TO DEWAR
RADIATION SHIELDS AT LIQUID He TEMPERATURE
COPPER POST CARRYING HEATER AND SPECIMEN CENTERING MECHANISM
O-RING SEAL IN WHICH DEWAR AND SPECIMEN ROTATES
WORM AND WHEEL FOR ROTATING DEWAR AND SPECIMEN
THRUST BEARING
UNICAM 19 CM DIA. FILM CASSETTE
X-RAY BEAM IN
THREE EQUI-ANGULAR WINDOWS
THERMOCOUPLE
SPECIMEN
CAMERA EVACUATION

Fig. 2. Low-temperature camera

A second camera used the same casette, base and rotation mechanism, but cooling was by gas flow. The range from room temperature down to 35° K could be covered using different gases passed in through the vacuum-jacketed syphon.

The specimen was inside a vacuum-jacketed enclosure and it was possible to use a loosely packed powder specimen in a glass capillary.

A third model was the most satisfactory from the thermal point of view, because the camera body formed an isothermal enclosure round the specimen which was in turn cooled by radiation and through contact gas; loose powders could be used. It was important to note that the sensitivity of X-ray film exposed at 4° K was not greatly different from that at room temperature, while the low scattering power of liquid helium allowed the camera to be filled with liquid. However, the X-ray precision was likely to be less than in the previous models, because although the camera dimensions were obtained through the use of a Strumanis-type mounting the accuracy depended on the contraction of the film being uniform. About 2½ litres of liquid helium gave an excellent picture of copper in 2 hours or less.

A fourth camera for examining the structure of metals strained *in situ* had already been described.[11]

In reply to DR. K. MENDELSSOHN, Dr. Pearson said that calibration of copper-constantan thermocouples could be done satisfactorily if the reading between 273 and 4·2° K was taken as the reference; an accuracy of ±0·5° could be attained in the region where the e.m.f. varied rapidly with temperature.

The lecturer agreed with DR. OLGA KENNARD (National Institute for Medical Research, London) that the use of proportional counters might have had advantages, and in reply to DR. U. W. ARNDT (Royal Institution, London) he stated that no work had yet been done using microcameras and microfocusing.

SECOND SESSION: X-RAY METHODS AND MEASUREMENTS AT LOW TEMPERATURES

The second session of the conference, on "X-ray methods and measurements at low temperatures," was chaired by PROF. C. S. BARRETT, and was opened with an introductory survey by PROF. W. N. LIPSCOMB (University of Minnesota, U.S.A.).

Prof. Lipscomb began with a review of the history of single crystal studies carried out at low temperatures. He pointed out that the subject was not at all of very recent origin, some of the first work at reduced temperature having been conducted over twenty-five years ago (benzene, at −22° C: Cox,[12]; ice: Barnes[13]). Special mention was made of the work of Ruhemann who, in 1932, studied single crystals of nitrogen, cooled within a capillary by a stream of hydrogen.[14] Cooling by means of a stream of cold gas was first used by McKeehan and Cioffi in 1922.[15] This technique has been greatly developed and employed for a large number of structural investigations, especially by Kaufman, Fankuchen and co-workers at Brooklyn,[16] and Collins, Lipscomb and the group at Minnesota.[17] In this way over thirty different substances have been crystallized at low temperatures in Minnesota, for example, and the method is being employed by many other workers. Low temperature studies on single crystals have been reported from countries as widely separated as France, Britain, The Netherlands and Japan. At the present time the main lines for advance would seem to be the study of low compounds, improvement in accuracy and precision, and extension of structural work to the range below −190° C.

Turning to experimental techniques, Prof. Lipscomb described the way in which a liquid (or gas) can be induced to form a single crystal inside a glass capillary: by freezing, melting until all but a fragment is liquid, and then cooling very slowly till the growth of this fragment fills the entire space. Impurities, he remarked, usually facilitate this step. Maintenance of the crystal commonly requires a rate of consumption of liquid nitrogen of about 4 litres per hour for a temperature of −180° C, or two thirds of a litre per hour for temperatures of the order of −50° C. Complete *hkl* data can be collected from a single crystal, especially if a precession camera is used. Details were given of the work on B_5H_{11}.[18]

Recent Dutch X-ray work at low temperatures was then described by DR. AAFJE VOS (Laboratorium von Anorganische en Fysische Chemie, Groningen, The Netherlands).

Surveying work done in Amsterdam, she reported that the use of temperatures of about −150° C was now routine procedure for organic substances. As an example of the appreciable gain in resolution which can be obtained with low temperatures, she mentioned a projection of phthalic acid in which atoms only 0·7 Å apart were completely resolved. She then described work on the molecular compound of trinitrobenzene and benzene, carried out by Prof. C. H. MacGillavry and others. On rather over-exposed pictures taken at room temperature, a diffuse background was observed which disappeared completely at low temperatures. This diffuse scattering could be explained by assuming a large thermal motion of individual molecules—probably the benzene molecules—without appreciable lattice coupling.

In a survey of work done in Groningen, Miss Vos showed the results obtained in the three-dimensional structure determination of 1,8-diphenyl-1,3,5,7-octatetraene, at −100° C.[19] The use of the low temperature enabled carbon—carbon bond lengths to be obtained with standard deviations as low as 0·004 Å. She also mentioned the low temperature work on the crystal of $N(C_2H_5)_4I_7$, in which the correct formula had been found to be $N(C_2H_5)_4.2I_2.I_3$.[20] In this investigation the crystal was cooled by dripping liquid nitrogen from a Dewar vessel, having a Dewar outlet tube, directly on to the capillary within which the crystal was mounted. Crystal temperatures as low as 160° C were readily obtained, while the consumption of liquid nitrogen was less than ½ litre per hour.

In a paper on recent low temperature crystallographic work in France, DR. A. J. RICHARD (Kodak-Pathé, Paris) described two techniques which have been developed.

Structural studies to −50° C: the technique developed by Bouttier and Luzzati[21] comprised three stages. (*a*) Crystals were grown by means of carefully controlled external cooling of a short, wide-necked, Pyrex tube containing the liquid of required composition. Cooling was accomplished by electrically controlled boiling of liquid nitrogen. When crystallization had progressed to the desired degree any remaining liquid was removed by pipette. These crystals could be preserved indefinitely by placing the Pyrex tube in a Dewar vessel containing dry ice. (*b*) The crystal was then placed on a cylindrical metal block, partially immersed in liquid nitrogen where it could be examined conveniently, cut if necessary, fastened with silicon grease to an aluminium wire, and then transported to the goniometer head of the Weissenberg camera. (*c*) The crystal was maintained at low temperature in the camera by placing it in a jet of cold nitrogen gas which passed down the camera axis. The cold jet was obtained by electrically controlled boiling of liquid nitrogen in a Dewar flask mounted on the equi-inclination turn-table.

Structural studies to −160° C: the apparatus designed for this work is shown in Fig. 3; its operation is essentially similar to the method of Kaufman and Fankuchen.[16,22] Special features are: (*a*) the liquid nitrogen is boiled by current from a battery source to ensure stable operation, as well as

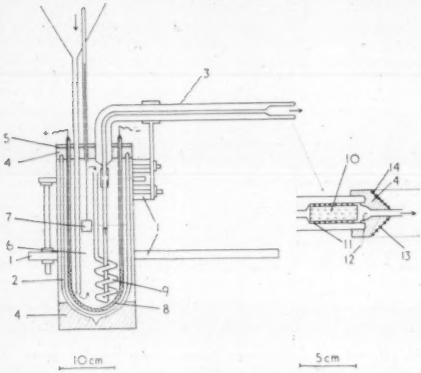

Fig. 3. Apparatus for diffraction studies at controlled low temperatures

(1), steel holder; (2), Dewar vessel; (3), Dewar tube; (4), cork; (5), paraffin wax and Vaseline; (6), liquid nitrogen; (7), level indicator; (8), heating coil in Pyrex tube; (9), copper coil (temperature stabilizer); (10), copper block, temperature regulation; (11), heating coil, temperature regulation; (12), thermocouple; (13), heating coil (to avoid ice condensation); (14), cellophane screen.

to avoid power breakdowns, which would result in the loss of the crystal; (*b*) sensitive control of the temperature is provided, for varying the speed of crystallization. Before flowing over the capillary the cold nitrogen gas is passed through a heating element of appropriate capacity, to give the jet a very stable temperature; (*c*) ice formation is eliminated by having an electric resistance coil placed at the outlet of the camera.

Using this second low temperature technique, it was possible to obtain any temperature between −160 and +20° C, with a maximum liquid nitrogen consumption of ½ litre per hour. The temperature variation for several hours continuous operation is no more than 5° C, and, for any hour, it does not vary by more than 1° C. During crystallization the temperature can be adjusted to a tenth of a degree, and can also be varied as slowly as desired. The progress of crystallization can be viewed through a polarizing microscope, and the speed adjusted by varying the current in the heating element.

These low temperature techniques were employed in the following structural studies, undertaken in the Kodak-Pathé Laboratory: nitric acid,[21] and its monohydrate,[23] and its trihydrate[24]; mono-, di-, tetra,[25] penta- and hepta-hydrates[26] of sodium hydroxide; sulphuric acid and several compounds of the tertiary system N_2O_5–SO_3–H_2O[27]; salicylic aldehyde[28]; acetaldehyde.[29]

The possibility of extension of crystallographic studies on single crystals to temperatures below the range obtainable with liquid nitrogen, was the subject of a paper by Dr. J. H. Robertson (University of Leeds). He pointed out that gas-stream cooling is superior to other methods, from the point of view of the X-ray crystallographer, especially for single crystal work. This is because the crystal can be bathed in the X-ray beam, isolated from all but the minimum support. A stream of gas produces negligible disturbance of the specimen and negligible fogging of the diffraction record, as compared with liquid cooling; also there is the possibility of variation and control of the temperature over a considerable range. Further, in contrast with conduction cooling, thermal gradients in the specimen are avoided.

Hydrogen gas, it was claimed, compares well with nitrogen gas as a coolant. Even at 20° K it still has a thermal conductivity over twice that of nitrogen gas at 80° K, and the heat capacity, at this temperature, is three times that of nitrogen gas, when expressed in terms of calories per unit volume per degree. Heat exchange by radiation can be shown to be negligibly greater when the specimen is a 20° K than when at 80° K. The chief difficulty encountered in practice, when attempting to achieve these low temperatures, is the leakage of heat to the cold gas stream before it reaches the specimen.

A simple form of cryostat was designed and constructed at Leeds, consisting of a large Dewar vessel with a Dewar tube exit passing through its base. The refrigerant, boiling gently, evolves gas which is led first through a metal spiral in the liquid before passing downwards through the exit tube. The jet of gas at the specimen is, consequently, almost as cold as the liquid itself. With liquid nitrogen, a temperature of 83° K was achieved, with a consumption as low as 1/7 litre per hour. Using liquid hydrogen as refrigerant, the temperature achieved was below 24° K. When hydrogen was used, it was necessary to employ hydrogen also for the surrounding warm dry sheath protecting the specimen from atmospheric humidity, which was technically more difficult than the use of nitrogen for this purpose. The consumption of liquid hydrogen for maintaining temperatures in the region of 24° K was of the order of ¼ litre per hour.

In reply to a question by Dr. W. Cochran (Cavendish Laboratory, Cambridge), Dr. Robertson said that there was no difficulty in refilling the apparatus while it was running. Dr. K. Mendelssohn, referring to the remarks in the paper about the heat capacity of hydrogen gas, drew attention to the point that when discussing the methods of cooling, one should compare the available enthalpies rather than the heat capacities per degree. Gas cooling would indeed be economical and effective if the specimen temperature were to be held well above the boiling point of the coolant, but for experiments close to the boiling point, liquid cooling has the great advantage of making use of the large latent heat of vaporization, compared with which the heat content of the vapour is negligible.

As another means of economizing in coolant, Prof. Dame Kathleen Lonsdale suggested the improving of film sensitivity, or the use of intensifying screens. With Dr. H. J. Grenville-Wells, she had found that, for Industrial G, blackening produced by ordinary light was much greater at low temperatures (−95° C), the reversal of the usual effect with photographic film. The effect was dependent on exposure time, the contrast being less for 1/60 second exposures to a strong light, and increasing markedly for longer exposures to weaker light. This appeared very hopeful for low temperature X-ray work, for which fluorescent screens could be used; unfortunately, however, Industrial G (or B) film has been deliberately made light-insensitive, unlike Industrial A (Red Seal) which is intended for use with

fluorescent screens, but which does not show an increase of blackening at low temperatures. Nevertheless, Prof. Lonsdale felt that the possibilities of using screens for intensifying X-ray photographs both at room and low temperatures needed to be investigated more thoroughly. Incidentally, she found that Industrial G is equally sensitive to CuK_α radiation at both temperatures, 20° and −95° C.

Dr. E. Mendoza (University of Bristol) drew attention to the fact that when a tube containing gas had a strong temperature gradient maintained down it, the gas could easily be excited into violent longitudinal oscillations of low frequency; these could cause big heat leakages leading to unreproducible results. Their apparent absence from all the gas cooling devices described was surprising; possibly the high velocity of the gas flow stopped them. Dr. W. B. Pearson confirmed that in some of his cameras troublesome oscillations had occurred.

In the evening discourse following this session, Prof. J. D. Bernal (Birkbeck College, London) gave a masterly survey of molecular crystals, designed to bring this very mixed, but important group into some sort of order. Prof. Bernal argued that the time was ripe for a detailed classification; he presented a scheme for this, based on the types of intermolecular forces involved and the differing shapes of molecules, and illustrated his lecture with a wealth of examples.

THIRD SESSION: MISCELLANEOUS CONTRIBUTIONS

The third session was chaired by Mr. H. P. Rooksby (G.E.C. Research Laboratories, Wembley), and the first paper was given by Dr. M. H. Francombe (also of G.E.C. Research Laboratories, Wembley).

Dr. Francombe spoke on the application of low temperature powder photography to studies of magnetic and dielectric phenomena, in particular to ferromagnetic and antiferromagnetic transitions, which usually involved small distortions from cubic symmetry, and to ferroelectric transitions. It was desired to take 19 cm powder photographs at temperatures down to 90° K. With the conventional liquid cooling technique, in which a stream of the liquid dripped on to the specimen from a fine nickel tube, a good deal of low-angle scattering occurred; this led to difficulties with ferroelectrics where superlattice lines at low angles were of interest. A gas cooling device was therefore developed[30] which obviated these and in which, moreover, the film remained at room temperature thus avoiding distortions in the film and enabling small line shifts due to small changes in structure to be identified.

The lecturer described several investigations among which was the recent work[31] on spinel-type solid solutions of magnetite (Fe_3O_4) and ferrous chromite ($FeCr_2O_4$). The addition of the chromite to the magnetite removed the rhombohedral type of low temperature deformation previously reported for pure polycrystalline Fe_3O_4, or perhaps lowered the transition temperature below 90° K. For compositions containing more chromium, e.g. $Fe_{2.0}Cr_{1.0}O_4$, a new tetragonal-type structure deformation was detected at 90° K. The magnitude of this effect increased with chromium content, until for $Fe_{1.8}Cr_{1.2}O_4$ the tetragonal axial ratio reached a value of $c/a = 1{\cdot}005$. Photographs taken at various temperatures between 20 and −140° C showed that the transition occurred at about −60° C. A pronounced low-temperature distortion had also been observed in pure ferrous chromite.

Reference was also made to low-temperature X-ray powder work carried out on ferroelectric compounds such as the fluorite-type $Cd_2Nb_2O_7$, perovskite-type $PbTiO_3$ and sodium niobate solid solutions.

Dr. W. B. Pearson asked whether it was yet possible to predict what sort of deformation would be associated with ferromagnetic or antiferromagnetic transitions; but Dr. Francombe said that not enough information had yet been collected.

Dr. W. M. Neier (Swiss Federal Institute, Zürich) said that a low temperature camera for the study of transitions should allow the easy exchange of the film without removing the cryostat and should permit the taking of a whole series of photographs at slightly differing temperatures without disturbance. Such a powder camera had been described by Känzig and others[32]; this could be adapted to take rotation and oscillation photographs with single crystals down to liquid nitrogen temperatures.

Dr. W. Parrish (Philips Laboratories, New York, U.S.A.) emphasized that the counter diffractometer was much better suited than film methods to the study of low temperature transitions and deformations because the line profiles could be accurately measured; all measurements might be made with the specimen temperature maintained or varied at will and there was no problem of cooling the film or of angular calibration of the pattern. Moreover, the measurements could be made quantitative, the resolution and dispersion being greater than that even in the 19 cm camera. When scintillation or proportional counters were used, the peak-to-background ratio was much greater than with film or Geiger counter detection. Dr. S. C. Abrahams (University of Glasgow) reiterated that for the small changes associated with ferromagnetic phase changes, diffractometer techniques could be superior to photographic methods.

Prof. C. H. Shaw (Ohio State University, U.S.A.) then described work on the structure of liquid helium above and below the lambda-point; these experiments had been carried out in collaboration with Dr. W. L. Gordon and Prof. J. G. Daunt. In dealing with a liquid with such a low scattering power one could possibly use an intense source of X-rays in conjunction with a conventional detector; but it was preferable to use a standard source and a sensitive detector with a low background count, paying great attention to statistics. In the present work a Machlett A2 copper anode tube was used as a source and a proportional counter with differential pulse height discriminator as detector. An X-ray differential filter monochromatized the beam.[33] The X-ray intensity had to be kept constant to 1/10% for several hours. In a typical experiment the scattered intensity at large angles gave about 400 counts per minute compared with a background of about four counts per minute. To get significant results an accuracy of better than 1% was necessary, and hence each point demanded several minutes' observation.

The sample was contained in a tube ¼ in. diameter made of 0·010 in. beryllium, which could support high vacuum; the temperature was controlled by a helium bath in good thermal contact. The scattering angle ranged from 1·5 to 90°. Measurements were taken on gaseous helium at 4·2° K and on liquid helium at 4·2, 2·4 and 1·4° K, the last two temperatures being chosen because the number densities were equal. After correction for instrumental geometry, the scattering from gaseous helium agreed with that calculated from Hartree wave functions to better than 2%. The liquid structure factor could then be obtained directly from the measurements of gaseous and liquid scattering, after applying

the several corrections necessary. The results showed that the liquid structure factor was unity for angles from 65 to 90°. There were slight differences in the main peak (at about 28°) when the measurements at different temperatures were compared. Fig. 4 shows the excess radial atomic density derived in the usual way[34] on the assumption that the liquid structure factor remained unity to larger angles. There was a gradual change of correlation number from ten to eight as the temperature was decreased.

Some measurements had also been carried out on the scattering from tungsten as a function of temperature; the agreement with the Debye-Waller curve was poor. A maximum in the value of Θ was indicated both by these results and by specific heat measurements.

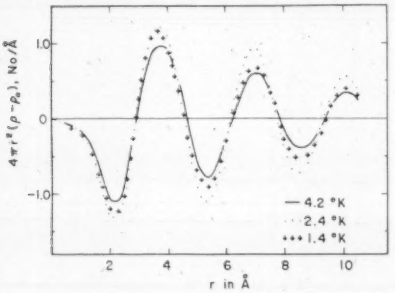

Fig. 4. Excess radial atomic density for helium

In the discussion which followed this paper Dr. M. Blackman pointed out that a restriction was placed on the graph of Θ against temperature, namely that the value at absolute zero must correspond to that deduced from low temperature elastic data. In any case, the maximum in Θ was difficult to explain theoretically. In reply to a question from Dr. K. Mendelssohn, Dr. Shaw said that they hoped to be able to carry out measurements on ^{3}He in the future.

In the next talk, Dr. J. A. S. Smith (School of Chemistry, University of Leeds) spoke on nuclear magnetic resonance experiments at low temperatures as an aid to structure analysis. The speaker distinguished between two sorts of resonance experiments, one involving nuclear resonance absorption and the other free nuclear precession. Experimentally, the former was more suited to solid state studies at low temperatures. The principle of the method was to measure the energy absorbed by the sample, placed in a homogeneous magnetic field, from a superimposed radio-frequency field of the resonance frequency. In solids at low temperatures, the local magnetic fields of neighbouring nuclei generally gave rise to broad absorption lines, often with marked fine structure. As the temperature was raised, the resonance line frequently narrowed over a small range of temperature. For molecular crystals this behaviour was explained by reorientation of the molecules in the crystal; when the frequency of the motions equalled the frequency width of the line, the observed narrowing would be expected to occur. One example of this was benzene, in which the line-width transition between 100 and 120° K has been attributed to reorientation of the molecules about their six-fold axes.[35] In the X-ray measurements,[3] the anisotropy of the temperature factor indicated that the molecular oscillation of largest amplitude occurred about this axis.

Below the transition temperature, the broadening of the resonance line and its shape have been used to obtain information on molecular structure. One example was solid hydrogen at 1·16° K, in which the predicted absorption curve consisting of two maxima was well resolved, and led to the conclusion that the internuclear distance was slightly smaller in the solid than it was in the gas.[36] A rather similar curve, but more poorly resolved, was given by $MoO_3.2H_2O$ at 77° K (S. Maričić and J. A. S. Smith); on allowing the sample to warm up to room temperature, a "spike" appeared at the centre of the line, suggesting the presence of a small percentage of disordered water molecules in the lattice.

In the discussion, Dr. G. Donnay (Geophysical Laboratory, Carnegie Institution, Washington, U.S.A.) mentioned the case of Torbernite, $Cu(UO_2)_2(PO_4)_2.8H_2O$, in which an attempt to determine the point group symmetry of Cu^{++} by a magnetic resonance determination (Prof. M. H. L. Pryce) led to an ambiguous result because of electron exchange between the copper ions despite the fact that these were about 8 Å apart. Dr. A. H. Cooke (Clarendon Laboratory, Oxford) indicated that this was a possible limitation in paramagnetic resonance studies, but was unlikely to occur in nuclear resonance. In reply to a question by Dr. H. Megaw (Cavendish Laboratory, Cambridge), Dr. Smith continued the discussion of proton resonance in $MoO_3.2H_2O$ and $MoO_3.H_2O$; at 77° K, both spectra were very similar to that of $MgCl_2.6H_2O$[37] and were consistent with the presence of H_2O groups with much the same inter-proton distance as found in other hydrates by nuclear resonance studies (see, for example, Ref. 38). On raising the temperature of both hydrates to 293° K, a narrow line appeared superimposed on the broad curve observed at 77° K. Such behaviour would be consistent with the presence in both hydrates at this temperature of disordered water molecules, to the extent of about 10% of the total water of hydration present.

Miss M. Leela (University College, London) spoke on diamagnetic anisotropy of crystals and molecules at low temperatures. Measurements of diamagnetic susceptibilities of single crystals of organic substances, when corrected for relative molecular orientations, give data from which the projected areas of electron orbits in various directions can be obtained. By this method, the existence of molecular orbitals in conjugated compounds was confirmed some years ago. In graphite, at room temperatures, the $(\overline{r^2})^{\frac{1}{2}}$ for the π electron orbits was shown to be about 7·8 Å, increasing considerably at low temperatures.

Ordinarily one would not expect any change of diamagnetism with temperature, but since a large increase does occur for graphite, it is of interest to see whether a similar increase occurs for other conjugated molecules. Measurement shows an increase of crystalline diamagnetic *anisotropy* for benzyl, $(C_6H_5.CO)_2$, but no increase of *absolute* susceptibility at low temperatures (down to −134° C). This implies a change of molecular orientation rather than of the area of the molecular orbitals. A similar increase of anisotropy is observed for phthalic acid, but although X-ray structure analyses have been made at 20 and −150° C, the atomic co-ordinates are not known sufficiently accurately to be able to say with certainty whether this increase is accounted for by a change of molecular orientation or not.

In the case of urea no change of orientation is possible,

and no change of diamagnetic anisotropy is found, in spite of a considerable diminution of thermal agitation of the molecule. Further measurements of diamagnetic susceptibilities, combined with *accurate* atomic co-ordinates and thermal parameters at various temperatures, are very desirable in this field.

A paper by B. S. Figgins, G. O. Jones and D. P. Riley (Queen Mary College, London) on the measurement of lattice parameters and thermal expansion at low temperatures was then read by Prof. Jones. This work had the ultimate object of making accurate measurements on the solidified inert gases, and hence providing an independent line of attack upon certain problems of lattice dynamics.

The X-ray method has several advantages for the study of thermal expansion; it determines the size of the unit cell directly, it is an absolute method, and, when the film is kept at room temperature throughout, it is immune to errors arising indirectly from temperature gradients in the apparatus. For use with the solidified inert gases it has the added advantage that it does not require complex manipulation of the specimen.

Measurements were made of the lattice parameter of aluminium (which has the same structure as solid argon and roughly similar X-ray scattering and absorption characteristics) between 20 and 125° K. A modified Hilger and Watts 19 cm camera was used in the van Arkel mounting, in order to take Debye-Scherrer photographs, without rotation, of a polycrystalline specimen. Eleven lines of high Bragg angle were considered, using the extrapolation function of Nelson and Riley.[39] For accurate control of temperature, the specimen, thermally fixed to a block of copper surrounded by a series of appropriately slotted radiation shields, was mounted in the vacuum of a liquid hydrogen cryostat.

The standard deviation of the averaged results at a given temperature (taking several films at each temperature) was about 0·00002 Å. The ultimate sensitivity in the determination of values of $\Delta a/a$ (where a is the lattice parameter) was then about 1 in 2×10^5. This accuracy, though very high, was insufficient for an accurate estimate of the very low values of expansivity in the neighbourhood of 20–30° K. When the results were plotted over a range of temperatures, however, they could be compared with the predictions of the Grüneisen theory, and they appeared to represent a tendency for the Grüneisen γ to increase at these lowest temperatures.

A further paper on this subject was given by Dr. Dobbs (Queen Mary College, London). He pointed out that the back-reflexion method of measuring lattice parameters from fine-grained material is simple and requires only two length measurements at each temperature. It had, therefore, been used, together with a suitable apparatus for forming the solid specimen, to measure the lattice parameter of krypton from 77 to 105° K.

A spiral-exit glass Dewar vessel, as used by Lonsdale and Smith,[40] had a 3 mm copper tube inserted in it. This tube was surrounded by a vacuum enclosure with a 0·3 mm thick, wide-angled Perspex window in it which allowed unfiltered copper radiation from a Phillips tube to irradiate a small portion of the tube, which was fitted with a flat-faced aluminium collar. After evacuation and cooling of this flat surface with liquid nitrogen or liquid oxygen from the Dewar vessel, krypton gas could be condensed directly on to the cooled flat and formed a thin, compact, transparent layer at a suitable rate of flow of the gas. The window allowed back-reflexions with Bragg angles of 65 to 85° to be photographed at a specimen to film distance of about 7 cm. Only 0·3 litre per hour of cooling liquid was required to maintain the low temperatures.

With krypton, the temperature of the surface was measured from its known vapour pressure[41] and exposures of one hour gave three doublet reflexions at Bragg angles of about 67, 72 and 74°. These were indexed, using an approximate lattice parameter from existing measurements[42,43] as the (444), (711/551) and (640) lines. The latter two pairs of lines were used to obtain a mean lattice parameter (a); the maximum error was about 1 in 5000, mainly due to the difficulty of obtaining intense, sharp rings from the solid krypton. A smooth curve through the measurements showed the following variation of lattice parameter (a) with temperature (T):—

a (Å):	5·7353	5·7497	5·7653	5·7821
T (° K):	75	85	95	105

This corresponds to a volume expansivity of $8 \cdot 2 \times 10^{-4}$/°C at 90° K. An extrapolation of the lattice parameter curve, with zero expansivity at 0° K, gave an estimated closest interatomic distance of 4·02 ± 0·01 Å at 0° K.

The camera is suitable in its present form for pure solidified gases and is being adapted by Mr. Heastie at Queen Mary College for measurements on alloys of the heavier inert gas substances.

In reply to Prof. Simon, Dr. Dobbs added that the krypton gas was supplied in sealed glass cylinders by the British Oxygen Co. as 99–100% pure, the balance being xenon. When Mr. Heastie had measured the lattice parameters of alloys of krypton and xenon, it would be possible to estimate the error in the krypton lattice parameter due to this impurity, but it was probably less than 0·1%.

Answering a query by Dr. Pearson as to whether accuracy can really be as high as one part in 10^5, Dr. Riley emphasized that the extrapolation technique was capable of minimizing to a quite remarkable degree all the errors which had been mentioned. He quoted results obtained for the lattice parameter of aluminium, at 25° C, by a variety of different observers, as follows:

Figgins, Jones and Riley	(1956)	4·049 63 Å
Ievins and Straumanis	(1936)	4·049 63
Smakula and Kalnajs	(1955)	4·049 60
Jette and Foote	(1935)	4·049 58
van Bergen	(1941)	4·049 58
Wilson	(1941)	4·049 53

(Note: all results include the correction for refraction and refer to a scale of length defined by $\lambda(\mathrm{CuK}\alpha_1) = 1 \cdot 540\,51$ Å; results at the nearest observed temperature are corrected to values at 25° C by allowing for thermal expansion.)

In this connexion, Dr. Parrish commented that accurate parameter determinations with the counter diffractometer are made by measuring the centre of gravity of the entire profile of several high order lines. The centre of gravity is preferred to the peak position because corrections for geometrical abberations have been calculated for the former but not for the latter, except in a restricted angular range. This also makes it possible to determine lattice parameters from even weak broad lines which would be very difficult with film or peak measurements. Dr. Grenville-Wells (University College, London) then added that for most ordinary photographic observations of thermal expansion, it is convenient to use multiple exposure cameras, so that spectra at different temperatures are recorded on the same

film. Film-shrinkage errors are minimized, and time is saved.

In the final paper of the conference, MME L. COUTURE (Centre National de Recherche Scientifique, Bellevue) described optical studies carried out by herself, P. JACQUINOT and I. TSUJIKAWA, on the low temperature phase changes exhibited by some of the chrome alums. The specimens were inside a cryostat filled with liquid nitrogen, hydrogen or helium, with glass windows. Between crossed nicols, birefringent domains could often be seen. Absorption spectra, produced by electronic transitions between the ground and excited levels, were studied in the red region, around 15000 cm^{-1}.

The upper levels were sensitive to the electric fields exerted on the Cr^{+++} ions; if the ions were in non-equivalent positions the lines were split. The Zeeman effect allowed a distinction to be made between absorption lines arising from different electronic transitions of the one Cr^{+++} ions and between transitions of the same type made by ions differently perturbed by the crystalline field. The accuracy of measurement of the splitting was some 150 times lower than that by paramagnetic resonance; but since the latter could only measure the (much smaller) splitting of the ground level, the optical measurements were of significance and could usefully supplement the others.

At ordinary temperatures the chrome alums possessed four equivalent ions per unit cell[44]; this was designated phase I. Cr–NH_4–alum (I), stable above 81° K, the absorption spectrum of which (Fig. 5*a*) showed two intense and narrow lines, possessed two non-equivalent families of Cr^{+++} ions. Cr–K alum in phase II comprised three such families (Fig. 6*c*)

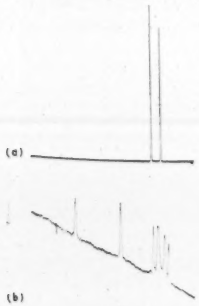

Fig. 5. Absorption spectra

(*a*) Cr–NH_4–alum (I), 20° K, rapid cooling.
(*b*) Cr–NH_4–alum (II), 20° K, slow cooling.

—the four other weak lines in the spectrum showed a different Zeeman effect and might have arisen from the lifting of a selection rule because of the lowered symmetry of the crystalline field. The spectra of Cr–NH_4–alum (II) (Fig. 5*b*) and of (Cr, Al)–Na–alum (II) also comprised seven narrow lines but their Zeeman effect had not yet been studied.

It was known that Cr–NH_4–alum (I) could persist at temperatures below the transition point;[45] Cr–K–alum, which exhibits a progressive substitution of one phase by the other, taking place over a wide range of temperature,[46] had also been found to have a retardation of phase change. Figs. 6*b* and 6*c* show the absorption spectra after rapid and slow cooling, the first of these resembling Fig. 6*a* which was obtained at 77° K. The width of the lines may be due to perturbations of the levels of the Cr^{+++} ions caused by inhomogeneities in the crystalline field due to the presence of two solid phases.

Fig. 6. Absorption spectra

(*a*) Cr–K–alum (I, II), 77° K.
(*b*) Cr–K–alum (I, II), 20° K, rapid cooling.
(*c*) Cr–K–alum (II), 20° K, slow cooling.

It would be desirable to know the structures of these different low temperature phases. Comparable phase changes were common among hydrated crystals[47] and, moreover, the varying rapidity of cooling could produce one or other of the phases or a mixture of the two as in Cr–K–alum. Such phenomena might explain a number of discrepancies[46] or anomalies;[48] and finally, in experiments on diluted crystals the phase changes might be influenced by the dilution itself. Mme Couture recalled van Vleck's aphorism that each crystal within a family presented a surprise.

DR. A. H. COOKE asked what constituted "quick" and "slow" cooling—for many low temperature magnetic experiments it was important to know this. Mme Couture replied that pouring liquid hydrogen on to the crystal would constitute "quick" cooling, the drop of temperature from 100 to 20° K taking place in a few seconds; if this interval were increased to a few minutes the cooling could be called "slow." DR. D. BIJL (St. Andrew's University) said that in his work on the thermal conductivity of Cr–K alum at liquid helium temperatures (which could be altered by the rate of cooling) he had found that it needed at least one hour to cool from 100 to 20° K before the cooling was "slow."

PROF. H. LIPSON (College of Technology, Manchester) said that when he and Beevers had studied the structure of the alums some twenty years ago, they had done so just for the fun of it, and now the alums were proving even more

exciting than they had thought; it was perhaps a pity that nowadays so much attention was being directed to such a dull-sounding subject as the expansion coefficient of solid argon! In reply, the low temperature physicists present maintained a dignified silence.

DR. HELEN MEGAW (Cavendish Laboratory, Cambridge), commenting on the elegance of Mme Couture's work, said that the variety of structures which could occur at low temperatures, all derived from the same high-symmetry structure, reminded her of the situation in ferroelectrics. There, for example, KH_2PO_4 and $NH_4H_2PO_4$ had different low temperature forms derived by slight distortions from the same high temperature form. It was becoming clear that this behaviour was not a peculiarity of a limited class of ferroelectrics, but was widespread.

Closing the conference, MR. H. P. ROOKSBY, Chairman of the X-ray Analysis Group of The Institute of Physics, remarked on the keen interest that had been shown in the subject of the papers, and expressed the hope that this would not be the last joint conference of this kind.

D. W. J. CRUICKSHANK
E. MENDOZA
J. H. ROBERTSON

REFERENCES

(1) JAMES, R. W. *The Optical Principles of the Diffraction of X-rays* (London: G. Bell and Sons Ltd., 1948).

(2) FRUHLING, A. *Ann Phys.* [*Paris*], **6**, p. 401 (1951).

(3) COX, E. G., CRUICKSHANK, D. W. J., and SMITH, J. A. S. *Nature* [*London*], **175**, p. 766 (1955).

(4) KOZHIN, V. M., and KITAIGORODSKI, A. I. *Zh. Fiz. Khim.*, **29**, p. 1897 (1955).

(5) COUTURE, L. *C.R. Acad. Sci.* [*Paris*] **229**, p. 495 (1949).

(6) BARRETT, C. S. *Acta Cryst.*, **9**, p. 671 (1956).

(7) BARRETT, C. S. *Acta Metallurgica*, **4**, p. 528 (1956).

(8) BARRETT, C. S. *J. Chem. Phys.*, to be published; *J. Inst. Metals*, **84**, p. 43 (1955).

(9) BARRETT, C. S. *Symposium on Transformations* (London: Institute of Metals, to be published).

(10) BARRON, T. H. K. *Phil. Mag.*, **46**, p. 720 (1955).

(11) PEARSON, W. B. *Canad. J. Phys.*, **33**, p. 473 (1955).

(12) COX, E. G. *Nature* [*London*], **122**, p. 401 (1928).

(13) BARNES, W. H. *Proc. Roy. Soc., A*, **125**, p. 670 (1929).

(14) RUHEMANN, M. *Z. Phys.*, **76**, p. 368 (1932).

(15) MCKEEHEN, L. W., and CIOFFI, P. *Phys. Rev.*, **19**, p. 444 (1922).

(16) KAUFMAN, H. S., and FANKUCHEN, I. *Rev. Sci. Instrum.*, **20**, p. 733 (1949).

(17) ABRAHAMS, S. C., COLLINS, R. L., LIPSCOMB, W. N., and REED, T. B. *Rev. Sci. Instrum.*, **21**, p. 396 (1950).

(18) LAVINE, L. R., and LIPSCOMB, W. N. *J. Chem. Phys.*, **22**, p. 614 (1954).

(19) DRENTH, W., and WIEBENGA, E. H. *Acta Cryst.*, **8**, p. 755 (1955).

(20) HAVINGA, E. E., and WIEBENGA, E. H. *Proc. Acad. Sci. Amst., B*, **58**, p. 412 (1955).

(21) LUZZATI, V. *Acta Cryst.*, **4**, p. 120 (1950).

(22) POST, B., SCHWARTZ, R. S., and FANKUCHEN, I. *Rev. Sci. Instrum.*, **22**, p. 218 (1951).

(23) LUZZATI, V. *Acta Cryst.*, **4**, p. 239 (1950).

(24) LUZZATI, V. *Acta Cryst.*, **6**, p. 152 (1952).

(25) HEMILY, P. W. *C.R. Acad. Sci.* [*Paris*], **234**, p. 2009 (1952); *Memorial Services Chimiques*, **38**, p. 21 (1953).

(26) HEMILY, P. W. *C.R. Acad. Sci.* [*Paris*], **236**, p. 1579 (1953).

(27) PASCARD, R. To be published.

(28) BOURRE-MALADIERE, Mme P. *C.R. Acad. Sci.* [*Paris*], **237**, p. 825 (1953).

(29) RICHARD, A. J. *Thesis* (Nancy, 1955).

(30) FRANCOMBE, M. H. *J. Sci. Instrum.*, to be published.

(31) FRANCOMBE, M. H., and ROOKSBY, H. P. *Nature* [*London*], **178**, p. 586 (1956).

(32) JACCARD, C., KÄNZIG, W., and PETER, M. *Helv. Phys. Acta*, **26**, p. 521 (1953).

(33) SOULES, J. A., GORDON, W. L., and SHAW, C. H. *Rev. Sci. Instrum.*, **27**, p. 12 (1956).

(34) GINGRICH, N. S. *Rev. Mod. Phys.*, **15**, p. 90 (1943).

(35) ANDREW, E. R., and EADES, R. G. *Proc. Roy. Soc. A*, **218**, p. 537 (1953).

(36) REIF, F., and PURCELL, E. M. *Phys. Rev.*, **91**, p. 631 (1953).

(37) SIDEI, T., and YANO, S. *J. Chem. Phys.*, **23**, p. 1554 (1955).

(38) WERTZ, J. E. *Chem. Rev.*, **55**, p. 829 (1955).

(39) NELSON, J. B., and RILEY, D. P. *Proc. Phys. Soc.* [*London*], **57**, p. 160 (1945).

(40) LONSDALE, K., and SMITH, H. *J. Sci. Instrum.*, **18**, p. 133 (1941).

(41) KEESOM, W. H. *Physica*, **2**, p. 669 (1935).

(42) NATTA, G., and NASINI, A. *Atti. Accad. Linci. Rendi.*, **12** (6), p. 141 (1930).

(43) RUHEMANN, B., and SIMON, F. E. *Z. Phys. Chem., B*, **15**, p. 389 (1912).

(44) LIPSON, H., and BEEVERS, C. A. *Proc. Roy. Soc., A*, **148**, p. 664 (1935).

(45) KRAUS, D. L., and NUTTING, G. C. *J. Chem. Phys.*, **9**, p. 133 (1941).

(46) BLEANEY, B. *Proc. Roy. Soc., A*, **204**, p. 203 (1950); BIJL, D. *Physica*, **14**, p. 684 (1948).

(47) See, for example, TSUJIKAWA, I., and COUTURE, L. *J. Phys. Rad.*, **16**, p. 430 (1955).

(48) KRAMERS, H. A. BIJL, D., and GORTER, C. J. *Physica*, **16**, p. 65 (1950).

A photoelastic method employing scattered light for the solution of plane stress problems

By W. SHELSON, Ph.D., The Hydro-Electric Power Commission of Ontario, Toronto, and I. W. SMITH, M.A.Sc., University of Toronto, Canada

[*Paper received* 24 *May*, 1956]

A new photoelastic method for the determination of the individual principal stresses in two-dimensional problems is described. The method is based on the combined use of three retardation fringe patterns—a standard isochromatic pattern and two perpendicular scattered light patterns.

For the separation of the principal stresses in plane stress problems, there are many possible approaches. A recent paper[1] lists fourteen analytical, graphical and experimental methods which are available. All these methods are time-consuming and tedious, although some of the point-by-point methods are satisfactory when results at a limited number of points in the model are required.

A new method for the separation of the principal stresses in two-dimensional problems is here outlined. This method, although formulated independently by one of the authors, was first proposed by Drucker and Mindlin[2] without experimental verification. This method will, in many instances, provide an easier and sometimes more accurate solution in the determination of the principal stresses. To facilitate reference to this method, it is referred to herein as the "combined method for plane stress."

COMBINED METHOD FOR PLANE STRESS

Consider any small element in a two-dimensional model acted on by forces in the plane of the model. At this position in the model, there are only three components of stress σ_x, σ_y and τ_{xy} as shown in Fig. 1. If the model is placed in a standard transmission polariscope, the isochromatics supply directly the values of the difference of the principal stresses, i.e. $(\sigma_1 - \sigma_2)$.

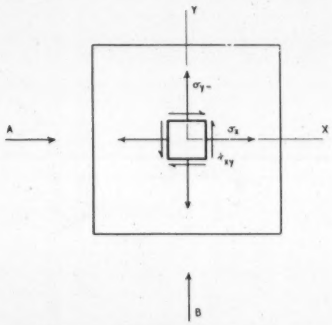

Fig. 1. Stress components of plane stress

To obtain further information, the model is examined in a scattered light polariscope with the polarized light projected through the edge of the model from the direction *A*. The only stresses which will produce a photoelastic effect are the principal stresses in the wave-front of the beam. In this case, the only effective principal stress is σ_y. Thus the distance between scalifs (scattered light fringes) obtained in the scattered light polariscope is inversely proportional to σ_y and quite unaffected by σ_x or τ_{xy}. Similarly, if the model is oriented so that a pattern of scalifs is obtained with the light projected from the *B*-direction, values of the stress component σ_x are obtained. The sum $(\sigma_x + \sigma_y)$ may then be obtained from two patterns of scalifs in the manner just described.

It is known from the transformation equations[3] that $(\sigma_x + \sigma_y)$ is invariant and therefore:

$$(\sigma_x + \sigma_y) = (\sigma_1 + \sigma_2)$$

Thus the three fringe patterns provide the following data:

$$(\sigma_1 - \sigma_2) \quad \text{and} \quad (\sigma_1 + \sigma_2)$$

The values of the principal stresses are therefore determined. In the foregoing, a possible difficulty arises regarding the sign of $(\sigma_1 + \sigma_2)$. But knowing that σ_1 is greater than σ_2 and knowing the sign of $(\sigma_1 - \sigma_2)$, this difficulty is easily resolved.

EXPERIMENTAL PROCEDURE

To establish the feasibility of the method, the problem of an elastic disk subjected to concentrated loads along a diameter was chosen. This particular problem in classical elasticity was selected because the theoretical solution is known and the expressions for the stresses are of a relatively simple form. The ease of machining the disk and applying the load were also factors in the choice.

The disk was machined from a bar of Fosterite (manufactured by Westinghouse Electric Corp.), the properties of which have been described by Leven.[4] The dimensions of the disk were 1·500 in. in diameter and 0·250 in. thick. Two perpendicular diametral lines were scribed on the face of the disk to assist in the subsequent photoelastic measurements. Two tiny grooves were located at the loading points to maintain stability as well as the direction of loading. The load was applied as shown in Fig. 2, with pins at the points of contact to approximate a concentrated load. The use of a sharp edge at the point of loading as in the theoretical case would have fractured the

model. Since by St. Venant's principle the stress distribution throughout the disk except in the neighbourhood of the load is identical for both cases, it is still valid to consider the theoretical solution applicable.

The frozen stress technique* was employed in this study although the fringe patterns could have been obtained while the loads were acting. This latter course would have required a more elaborate loading jig designed so that it would not interfere with the photographic work. The loading cycle for

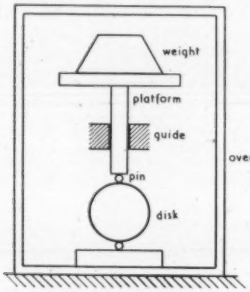

Fig. 2. Experimental set-up for stressing disk

the fixation technique was carried out in an oven designed for photoelastic investigations, the load being applied at 70° C and maintained for thirty minutes before commencement of the cooling part of the cycle. Both the heating and cooling periods were of long duration, four and twelve hours respectively, to ensure a uniform temperature within the model to prevent the inclusion of thermal stresses.

After preparation of the frozen stress model, isochromatic and scalif photographs were made of the stress distribution in the disk. The photographs were taken on Kodak Super Ortho Press Film, with slit widths for the scalif patterns varying from 0·01 to 0·03 in. It is hoped that details of the photoelastic equipment employed may be described in a future paper since some of it is of new design and may be of interest to photoelasticians.

PHOTOELASTIC FRINGE PATTERNS

The isochromatic fringe pattern obtained from the disk, Fig. 3, is generally similar to the pattern that would be obtained under direct load at room temperature. However, it will be noted that in the region of the applied load, the deformations are considerable; the fringe pattern in these regions does not then correspond to the pattern based on elastic theory. The hole near the bottom of the model, visible in the photograph, was drilled after freezing to aid in mounting the disk on the model location jig for scalif photographs. Since the isochromatic pattern for a disk under diametral load has been exhaustively treated,[5] there is no need here to comment further on the isochromatics.

Figs. 4 and 5 are representative scalif photographs of loaded disks while the scalifs of Figs. 6 and 7 were used for measurement and comparison with the theoretical results. In the first of each set of photographs, the sheet of polarized light was projected along the direction of the applied loads

Fig. 3. Isochromatic pattern for disk

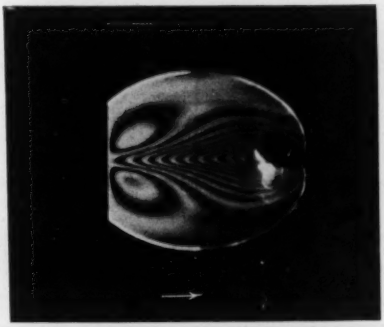

Fig. 4. Scattered light fringes for σ_x for disk. Arrow indicates direction of light

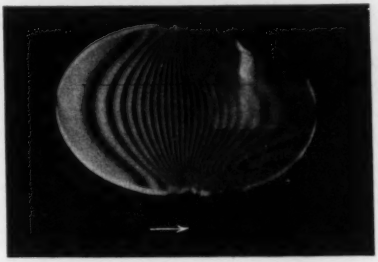

Fig. 5. Scattered light fringes for σ_y for disk. Arrow indicates direction of light

(i.e. the y-axis) resulting in fringe spacing proportional to σ_x; in the second photograph of each set, the light was projected along a direction perpendicular to the line of action of the

* Stresses may be fixed in a model by allowing it to cool from an elevated temperature while under load.

applied loads (i.e. the x-axis) producing scalifs proportional to σ_y.

To assist in obtaining better scalif patterns of σ_x within the disk, portions of the frozen stress models were machined away. Otherwise, the light entering through the point of loading would be subject to the very high stresses of this region; any slight differences in stress here result in unsymmetrical fringes which make comparison with the theoretical patterns more difficult. The effect is quite noticeable in the scalifs for σ_y where the fringes on the right do not correspond in position to those on the left. When obtaining scalif patterns, it is always advisable to have the light proceed from a region of low stress to a region of high stress. It is then easier to estimate the trend of the stress pattern.

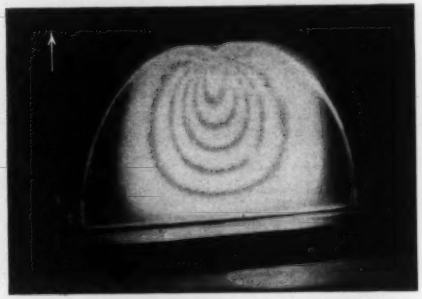

Fig. 6. Scattered light fringes for σ_x for disk. Arrow indicates direction of light

Fig. 7. Scattered light fringes for σ_y for disk. Arrow indicates direction of light

COMPARISON OF THEORETICAL AND EXPERIMENTAL STRESS PATTERNS

The scalif photographs, Figs. 6 and 7, and the corresponding theoretical fringe patterns, Figs. 8 and 9, demonstrate the validity of the scattered light method as a means for isolating directional stresses; in this instance, σ_x and σ_y. The correspondence of the patterns tends, however, to diverge as the point of loading is approached. This is due to the excessive deformations near the load and probably, in addition, to the existence of stresses exceeding the proportional limit in this region. On the whole, the agreement appears to be adequate.

An interesting feature of the scalif pattern for σ_x is the line $x = 0$. Along this line, the horizontal stress is known to be constant upon the basis of the theoretical solution. This deduction is convincingly confirmed by Fig. 4 where the fringe spacing along this diameter is constant for almost the entire length.

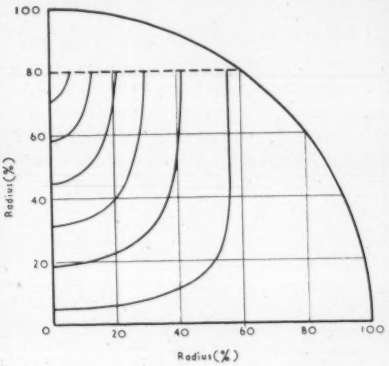

Fig. 8. Theoretical scattered light fringes for disk (σ_x)

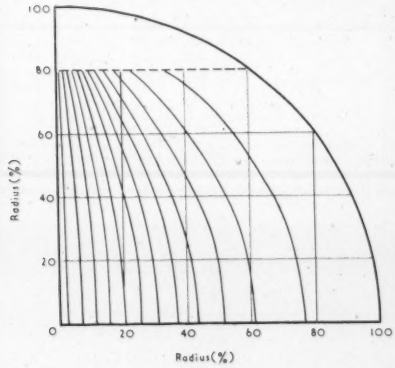

Fig. 9. Theoretical scattered light fringes for disk (σ_y)

ACCURACY OF EXPERIMENTAL DATA

As an indication of the accuracy attainable by the scattered light method, the experimental values of σ_x and σ_y along $y = 0$, and σ_y along $y = 0{\cdot}5$ radius, have been computed and plotted against the theoretical values in Figs. 10 to 12. The stresses were obtained by assuming that the stress

represented by a fringe spacing was the stress at the mid-point between the fringes. Along the horizontal diameter, the accuracy is relatively good at the higher stress levels but diminishes as the stress falls toward the edge. The error

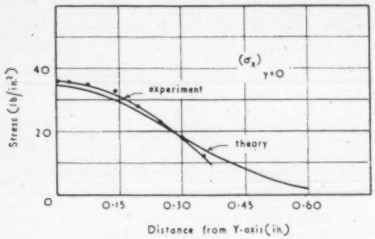

Fig. 10. Comparison of theoretical and experimental values of σ_x along horizontal axis $y = 0$

appears to reach about 4% for σ_y and 6% for σ_z at the most highly stressed points, but increases rapidly with reduction in the stress level. The increase in relative error at lower stress levels is due primarily to the fact that the fringe spacing does not directly correspond to the stresses, although it is a function of stress and distance. The form of the curve of stress *versus* distance can vary considerably between fringes in regions of low stress, while in highly stressed regions the closeness of the fringes reduces to a large extent the possible error in assuming the straight line relation. Thus for increased

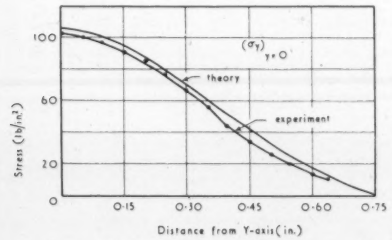

Fig. 11. Comparison of theoretical and experimental values of σ_y along horizontal axis $y = 0$

accuracy in the use of scalifs, it appears necessary that photometric values of intensity of scalif patterns be obtained to increase the effective number of contours that may be plotted or that materials with higher photoelastic fringe constants be employed.

The curves of σ_y for $y = 0{\cdot}5$ radius, Fig. 12, indicate a greater divergence between experiment and theory. It seems probable that this difference is not due primarily to difficulties of measurement, but to the fact that the stress situation in the model does not entirely correspond to the elastic case. This result provides evidence of the inadequate information that may ensue from the use of frozen stress models with large deformations in the region under study.

Along $y = 0$, a line of symmetry, the stress components σ_x and σ_y are the principal stresses since there are no shearing stresses; and Figs. 10 and 11 provide the complete solution of the stresses for this path. Hence, the scalifs alone may be used in this manner to solve completely and most easily the principal stresses along a line of symmetry in plane stress models.

No attempt was made to carry to completion over the entire disk the combined method for plane stress. The comparisons shown demonstrate the inherent feasibility of the method. However, the low fringe constant of the material as well as

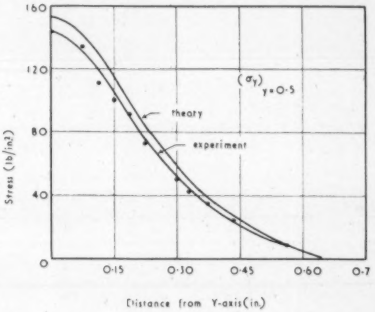

Fig. 12. Comparison of theoretical and experimental values of σ_y along horizontal line $y = 0{\cdot}5$ radius

the large deformations do not permit high accuracy in this case. Practicability of the method would be greatly enhanced by the development of a plastic with a high stress-optic coefficient so that instead of measuring the distance between fringes, the number of fringes per unit distance (up to, say, twenty fringes per millimetre in the elastic range) could be counted.

ACKNOWLEDGEMENTS

The authors wish to acknowledge financial assistance from the School of Engineering Research, Shell Oil Co. of Canada, Ltd., and Babcock–Wilcox and Goldie–McCulloch Ltd. Acknowledgement is also made of assistance from the Computation Centre of the University of Toronto, say, in particular Dr. H. Gellman, in the construction of the theoretical scalif patterns.

REFERENCES

(1) FRANKL, E. K. *J. Roy. Aero. Soc.*, **50**, pp. 974–85 (1946).

(2) DRUCKER, D. C., and MINDLIN, R. D. *J. Appl. Phys.*, **11**, p. 732 (1940).

(3) LOVE, A. E. H. *A Treatise on the Mathematical Theory of Elasticity*, p. 80 (New York: Dover Publications Inc., 1944).

(4) LEVEN, M. M. *Proc. Soc. Exper. Stress Anal.*, **6**, pp. 106–10 (1948).

(5) FROCHT, M. M. *Photoelasticity*, Vol. 2 (New York: J. Wiley and Sons Inc., 1948).

Flying spot counting and sizing of non-uniform particles

By H. W. Loeb, Ph.D., A.Inst.P., Hivac Ltd., Harrow, Middlesex

[*Paper received* 29 *May*, 1956]

A modified scanning principle involving a variable speed of scan is described which permits the extension of applicability of flying spot methods to particles, such as bubbles or droplets, characterized by a non-uniform degree of interception of the scanning beam.

The flying spot principle has in recent years been proposed[1,2] as a means for the automatic evaluation of particle fields. A number of instruments have been described which represent an application of this principle in one form or another.[3,4,5] Basically, the utilization of such methods involves the comparison of signals derived from the scanning of adjacent lines and the processing of such signals into information relating to the number of particles exceeding a chosen minimum dimension in the direction of scan. The occurrence of an interception of the scanning light beam is detected by means of a photosensitive device, the output of which, if necessary after amplification, operates a suitable discriminator circuit. The primary signals are thus essentially of the on/off type. If such methods are applied to particles which present a non-uniform degree of interception over their area, difficulties are encountered when the difference in interception between some portions of the particle and the background becomes too small to permit the electronic circuit to discriminate between the two. For this reason conventional flying spot counting and sizing methods are not suitable with particles which consist of an outer intercepting region surrounding a central non- or slightly intercepting region. Particles of this type which are commonly encountered consist of droplets of liquids, globules of or bubbles within a transparent medium as well as photographic records thereof. By virtue of their optical properties such particles present the appearance of a ring rather than that of a disk to the intercepting beam, so that over some regions of them two pulses instead of one are generated when the scanning spot passes across.

A modified method of operation of the scanning equipment makes it possible to overcome these difficulties. Whereas normally a single pulse (*N*-pulse) is derived from each act of interception in such a manner that the beginning of the pulse represents the passing-on of the beam to the particle and the end of the pulse signifies its passing-off, in the modified method[6] a second pulse (inhibitor pulse) is generated, the duration of which is equal to a pre-selected constant fraction, $1/a$, of the duration of the *N*-pulse. Each inhibitor pulse, delayed by exactly one line scan period, is then used to suppress throughout its duration the generation of passing-off signals. Provided the value of a is chosen suitably with respect to the particle geometry, this arrangement will enable the apparatus to "ignore" the non-intercepting portion of each particle. Fig. 1 illustrates the response obtained by this means if a ring shaped particle is being scanned. The particle is first encountered during the scan *GH* which gives rise to *N*-pulse shown at (*b*) of duration T_n. At the same time the inhibitor pulse n_{inh} of duration T_n/a, shown at (*c*) is generated by means to be described below. During the following scan, *JM*, the central non-intercepting area is encountered which would normally give rise to passing off signals at *K* and *M*. By the action of the delayed n_{inh} pulse, however, the signal at *K* is suppressed and the $(n+1)$'th *N*-pulse of duration T_{n+1} is identical with one which would have been obtained had the non-intercepting region *KL* been absent. A new inhibitor pulse is generated of duration $(T_{n+1})/a$, which in turn converts the following pulse into one corresponding to an intercept *NQ*. In this manner all information relating to the non-uniformity of the particles will have been eliminated from the series of *N*-pulses obtained, which can then be processed and analysed by the methods evolved for conventional scanning equipment.

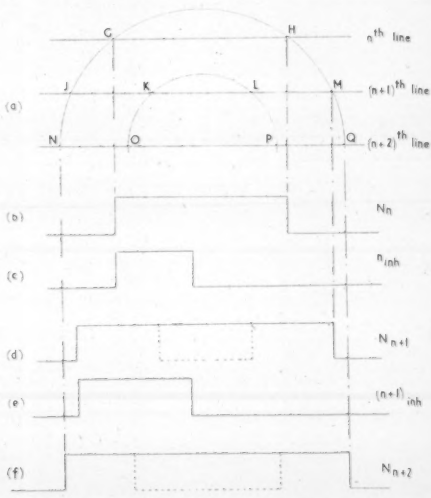

Fig. 1. Pulse shapes obtained during scan of non-uniform particle. Full curves: pulses from which non-uniformity information has been eliminated by the action of inhibitor pulses n_{inh}, $(n+1)_{inh}$; dotted curves: pulse shapes obtained without inhibitor action

The essential feature of the modified method lies in the apparent anticipation of T_n implied by the condition that $T_{inh}/T_n = 1/a < 1$. This requirement is fulfilled in the manner indicated in Fig. 2 by a velocity modulation of the scanning process. While in the established methods a constant scanning speed, say V, is maintained throughout, so that an intercept of length $AB = x$ will yield a *N*-pulse of duration x/V, in the modified method here reported the scanning speed equals V only as long as no particle is encountered but is increased to a value aV upon receipt of a passing-on signal. The intercept x is thus traversed in an interval x/aV, after which the passing-off signal is obtained. The latter causes the scan to be arrested at *B* for a period equal to $(x/V) - (x/aV)$, after which normal scanning with speed V

is resumed. The scanning beam thus proceeds from *B* at the same instant at which it would have passed *B* had no interception occurred at *A*; nevertheless the "anticipation" of the length *AB* had been completed at a time *x*/*aV* after the scan had reached *A*. The latter interval is the required inhibitor pulse, while the sum of inhibitor pulse and period of arrested scan yield the normal *N*-pulse of duration *x*/*V*. Details of a deflexion modulator circuit suitable for the above purpose have been described elsewhere.[6] It is of interest to note that all delay actions required, i.e. those involved in particle identification by the comparison of adjacent lines as well as those arising in conjunction with the inhibitor mechanism here described, can be obtained from a single delay device.

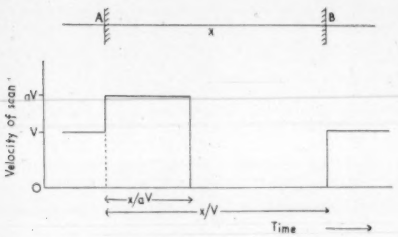

Fig. 2. Changes in velocity of scan during traversal of an intercepting region *AB*

REFERENCES

(1) YOUNG, J. Z., and ROBERTS, F. *Nature* [*London*], **167,** p. 231 (1951).
(2) WALTON, H. S. *Nature* [*London*], **169,** p. 518 (1952).
(3) ROBERTS, F., and YOUNG, J. Z. *Proc. Instn Elect. Engrs*, **99,** IIIA, p. 747 (1952).
(4) DELL, H. A. *Brit. J. Appl. Phys.*, **5,** Suppl. 3, p. S156 (1954).
(5) TAYLOR, W. K. *Brit. J. Appl. Phys.*, **5,** Suppl. 3, p. S173 (1954).
(6) British Patent Appl. 20154/55.

The elastic properties of dilute aqueous gels

By L. J. HASTEWELL, Ph.D., and R. ROSCOE, Ph.D., A.Inst.P., Physics Department, King's College, Newcastle upon Tyne

[*Paper first received* 16 *April, and in final form* 9 *July*, 1956]

A study of elastic behaviour under shear stress below the yield value has been made on seven different gels covering a wide range of chemical constitution. The static rigidity of a gelatine gel was found to increase with temperature in accordance with the kinetic theory of elasticity for long-chain polymers, and a similar variation was found in the case of a bentonite gel. This suggests that even when the material dispersed in a gel consists of discrete particles a loose chain structure is formed which is mechanically similar to that existing in a polymer gel. The theory of elastic loss for solid cross-linked polymers developed by Kirkwood would thus appear to be applicable to these gels. This has been tested by a series of measurements on the dynamic rigidity and dynamic viscosity of all seven gels together with observations of their creep and static rigidity. In four cases the results are consistent with this theory, but in the others it appears that the spectrum of retardation times is broader than the theoretical spectrum.

Each of the aqueous dispersions used in this work may be properly described as a *gel* on the ground that it shows the essential characteristics of a solid. That is to say, when it is deformed by a shear stress less than a certain critical value (known as the *yield stress*) and the stress is then removed, it eventually returns to its undeformed condition. Many weak gels appear at first sight to be liquids and even careful observations may fail to reveal the solid characteristics if the stress range is too limited. Thus Hastewell and Ritson[1] have found that an aqueous gel of gum tragacanth (1·83 g/100 cm^3) behaves as an elastic liquid in the stress range 0·5–8·0 dyn/cm^2, but Bergen and Patterson[2] have found a similar gel to possess a yield point just below this range. The present authors[3] have shown that an oscillating float apparatus devised by McDowell and Usher[4] provides a sensitive method of detecting the presence of a yield point.

This work is concerned only with the solid properties of gels, that is to say, with the elasticity and elastic retardation effects under shear stresses below the yield value; and it is further restricted in that measurements have only been made under conditions of simple shear. No attempt has been made to investigate effects occurring as a result of volume changes such as are produced during the passage of a longitudinal sound wave, nor is consideration given here to the flow which takes place in gels when the yield stress is exceeded. It must be mentioned, however, that certain gels take time to re-set after being subjected to stress in excess of the yield value. Thus, in investigating solid properties, it is always necessary to ascertain that the gel has reached a steady condition since the last occasion on which the yield stress was exceeded. For example, in working with bentonite gels it is found that a rest period of at least half an hour must be allowed after filling an apparatus before making observations.

MATERIALS USED

Since the investigation was concerned with general behaviour and no correlation was sought with the exact constitution of the gels, commercial materials were used in their preparation, details of which are given below. After preparation the gels were kept at temperatures between 15 and 18° C and, except where otherwise stated, measurements were made between temperatures of 17 and 19° C.

Gelatine. The principal constituent of this material is gelatin. The molecules of the latter substance are polypeptide chains. The British Gelatine and Glue Research Association have very kindly specified the commercial material used as follows: "The isoelectric point is at pH 5 which means that the gelatine has been produced by an alkali process. Its properties at a nominal concentration of 6¼% (weight of air dried gelatine per weight of solution), actual concentration 5·45% w/w, were: rigidity, after maturing eighteen hours at 10° C and measured at 10° C, 48 500 dyn/cm^2 (this is equivalent to a commercial grading of 160 g Bloom); the viscosity of the same solution, measured at 40° C, was 3·6 cP; the ash was 1·8%; and the pH of the solution as made up was 6." The gel used in the present work (1 g/100 cm^3) was made by dissolving the solid in distilled water kept at 70° C for two minutes after which it was cooled to 18° C.

Rice starch, gum tragacanth, agar. The molecules of the principal constituents of these materials are polysaccharide chains. The rice starch gel was prepared as follows: a thick paste made with cold water was diluted to 10 g/100 cm^3 before heating to 85° C in ten minutes, and then allowed to cool to 18° C before further dilution to 2 g/100 cm^3. In the case of gum tragacanth, a uniform dispersion (1 g/100 cm^3) was obtained by simply allowing the solid to swell in water at 15–18° C for a period of three weeks. In order to make the agar gel (0·25 g/100 cm^3) the solid was heated in water at 85° C for five minutes and the solution was then cooled to 18° C.

Sodium stearate, $CH_3(CH_2)_{16}.COONa$. The material used had an ash content of 16·5%. The gel (0·33 g/100 cm^3) was prepared by heating the powder in distilled water for two minutes at 65° C and then cooling to 18° C.

Benzopurpurine 4B. This is the sodium salt of ditolyl–disazo–bis–α–napthylamine–4–sulphonic acid ($C_{34}H_{26}N_6O_6S_2Na_2$). The gel (1 g/100 cm^3) was prepared by heating the powder in distilled water for ten minutes at 98° C, making up the volume to the required amount and cooling to 18° C.

Bentonite. The principal constituent of this clay is the mineral montmorillonite $Al_2O_3 . CaO . 5SiO_2$ in the form of sub-microscopic particles which are believed to have the form of flat plates. Larger particles of impurities such as quartz or feldspar are also present in commercial materials such as that used in the present work. The gels were prepared by allowing the powder to swell in the requisite volume of distilled water (to which sodium chromate or potassium dichromate had been added) for three weeks at 15–18° C with occasional shaking. The gel principally used contained 3 g of bentonite and 0·08 g of sodium chromate in 100 cm^3.

GENERAL ELASTIC PROPERTIES

Great similarity exists between the elastic properties of all the gels investigated, in spite of the wide diversity of constitution. In every case a considerable amount of deformation can take place before the yield point is reached and, under static conditions, the shear strain is directly proportional to the shear stress except when the yield point is approached. This is illustrated in Fig. 1 by some measurements made with an apparatus in which the gel was contained in a fixed cylindrical vessel, a coaxial cylinder hanging in this vessel from a torsion wire. Stress was applied by rotating the torsion head and the amount of shear was determined from the rotation of the cylinder.

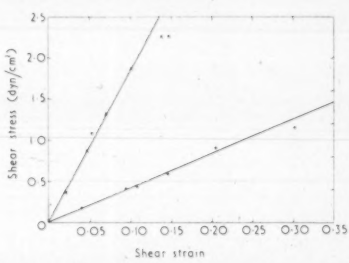

Fig. 1. Static stress-strain relationship. × = bentonite (2·61 g/100 cm^3) with potassium dichromate (0·17 g/100 cm^3). + = rice starch (2·5 g/100 cm^3)

The elastic deformation is subject to retardation. Thus a sudden application of stress does not produce an immediate strain but a creep which proceeds at a decreasing rate. Also, free oscillations of the material are subject to internal damping. If the gels were to consist of separate interpenetrating phases of elastic solid and viscous liquid, retardation effects would be expected to arise simply on account of the viscosity of the liquid phase. Since the solid material only amounts to a few per cent of the whole volume in these gels, the shear stress (S) would be given to a good approximation by the expression

$$S = G_0\sigma + \eta_0 \frac{d\sigma}{dt} \qquad (1)$$

where σ is the amount of shear. The first term in this expression would represent the elastic resistance of the solid structure to shear, and the second the viscous resistance of the liquid phase; G_0 would represent the rigidity of the elastic structure and the second constant η_0 would be nearly equal to the viscosity coefficient of the liquid phase. It has been noticed, however, that low-frequency dynamic measurements of the apparent value of η_0 for weak aqueous gels (such as those made by Bungenberg de Jong and his collaborators[5] upon gelatin) come out much higher than the value of the viscosity of water.

In their previous paper the authors[3] have shown how measurements of the frequency and decrement of the oscillations of a float embedded in a gel can give values for two quantities: the dynamic rigidity G and dynamic viscosity η

Table 1. *Frequency dependence of G and η. Measurements at* 18° C

Ge	Concentration (g/100 cm^3)	Frequency 0·7–1·1 c/s		Frequency 50 kc/s			
				Observed		Calculated	
		G (dyn/cm^2)	τ_c (P)	G	τ_c	G	τ_c
Rice-starch	2·00	2·76	0·27	5000	0·02	1350	0·02
Bentonite with sodium chromate (0·08 g/100 cm^3)	3·00	8·2	0·24	<2000	0·04	1050	0·02
Gum tragacanth	1·00	6·0	0·6	5000	0·02	3500	0·07

of the gel. If the material were to obey equation (1) these quantities would be independent of the frequency of the oscillations and equal respectively to G_0 and η_0. Results of such measurements on three gels made at frequencies of about 1 c/s are shown in the third and fourth columns of Table 1, and it is to be noted that as usual the values of η are much greater than the viscosity of water (0·01 poise). In the fifth and sixth columns are shown values of G and η made at 50 kc/s. These are from some unpublished work by Pryor,[6] who employed a torsionally oscillating transducer following the method of McSkimin.[7] The gels used for the two sets of measurements were made from the same materials. The low frequency results for starch and gum tragacanth are actually interpolated values since measurements were not made at the same concentrations as used for the high frequency measurements. It can be seen from Table 1 that, instead of remaining constant in accord with the two-phase hypothesis, the values of η decrease with frequency while those of G (at any rate in two cases) increase.

Finally, it is to be noticed that if the gels obeyed equation (1), the deformation under constant stress would increase with time in proportion to $1 - \exp(-t/\tau)$ where the "retardation time" τ is equal to η_0/G_0. The observed creep curves can never be fitted by such an exponential formula since the initial deformation is very rapid and is followed by a long period of slow deformation (Fig. 2). A satisfactory theory

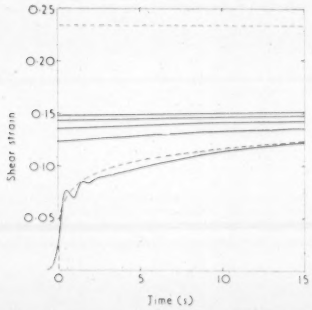

Fig. 2. Creep curve for an agar gel (0·25 g/100 cm^3) under a shear stress of 1·50 dyn/cm^2. The upper lines represent the creep during successive intervals of 15 s. The initial fluctuations are due to mechanical oscillation of the apparatus resulting from the sudden application of stress

must account for the form of these curves in addition to providing an explanation of the high deformability of the solid structure, the high values of η obtained from low frequency measurements and the frequency variation of G and η.

EXPLANATION OF STATIC BEHAVIOUR

In the case of gelatine, there is little difficulty in explaining the high deformability of the gel structure. The gelatin chain molecules are supposed to form a three-dimensional network, the junctions being provided by secondary bonds and possibly also by chain entanglements. It is further assumed that the sections of chain between junction points are normally maintained in a randomly coiled form by the bombardment of the surrounding molecules. Such a structure could evidently undergo large deformations without rupture and should behave in accordance with the kinetic theory of rubber-like elasticity. Thus resistance to deformation should arise principally from the resultant decrease in configurational entropy, and on this account the static rigidity is to be expected to increase with temperature. An increase in internal energy on deformation is also to be expected, and this would contribute to the rigidity, but such a contribution may be small as in the case of vulcanized rubber.

A detailed discussion of the gelatin network has been given by Ferry[8] who has noted that the part of the rigidity which is due to change in configurational entropy should be proportional to the absolute temperature. He quotes his own measurements,[9] however, which indicate that the rigidity decreases rapidly with temperature. This he explains by supposing that a network dissociation masks the expected increase in rigidity with rising temperature. On the other hand, it has been found with the gelatine used in the present work that the static rigidity of the gel does in fact increase with increasing temperature. In order to demonstrate this effect, a freshly prepared gelatine solution is poured into a cylindrical vessel in which a coaxial cylinder hangs from a weak torsion wire. The gelatine is allowed twenty-four hours in which to set, and stress is then applied by rotating the torsion head through a large angle, but care is taken to ensure that the stress is well below the yield value. The shear strain undergone by the gel is proportional to the small rotation of the cylinder which is measured by means of a galvanometer lamp, mirror and scale. The system is left untouched for fifteen hours at 18° C, after which creep is undetectable. The vessel is then surrounded by a can of iced water and the cylinder proceeds to turn through a small angle in the same sense as the torsion in the wire. After an hour at the low temperature further motion is almost undetectable and the can of iced water is replaced by one containing water at 18° C. The cylinder at once proceeds to return towards its original orientation, against the torsion of the wire, showing that the rigidity increases with increasing temperature. The same effect can be observed by simply heating the suspension a few degrees above the room temperature of 18° C, but since the yield stress decreases with increasing temperature, plastic flow may take place at the higher temperature so that the retraction effect is obscured.

Since a weak torsion wire is used in this experiment, the small rotation of the cylinder leaves the stress on the gel almost unaltered, so the final deformation attained at any temperature is an inverse measure of the rigidity. The temperature coefficient of the rigidity can thus be estimated, but an accurate determination is scarcely possible because long periods must be allowed for the deformation to creep towards its final value and during such periods the progressive change in the properties of the gel (which occurs continuously from the time of preparation) may be quite substantial. For a gel containing 1 g/100 cm^3 of gelatine, the temperature coefficient of rigidity was found to be 0·011 ± 0·004 per ° C at 10° C, while the theoretical value corresponding to proportionality with absolute temperature is 0·003 5 per ° C.

The discrepancy between this result and that obtained by Ferry may arise from the fact that his measurements were made by a dynamic method at frequencies between 320 and 630 c/s. It is to be expected that such measurements would give values appreciably in excess of the static values on account of elastic retardation effects. Such effects decrease with increasing temperature, so that the effect of increasing tem-

perature might well be a nett reduction in dynamic rigidity. On the other hand, Ferry states that there is an absence of dispersion in his rigidity measurements and he considers that they can be taken as identical with those obtained by static methods. The possibility that the discrepancy arises from the widely different samples of gelatine used must therefore be kept in mind.

It should be mentioned in passing that Gray[10] has found that when gelatine gels are kept strained for long periods the stress suddenly starts to fall exponentially to zero from its previously constant value. No such relaxation effects have been observed in the present work except when a crack has developed at the surface of the gel. Such cracks rapidly deepen and run round until the suspension is divided into two parts adhering respectively to the cylinder and vessel.

Dry bentonite powders consist of minute mineral plates so that bentonite gels represent the opposite extreme of constitution to gels of long-chain molecules such as those of gelatine. It has often been assumed that the forces between bentonite particles in suspension must have a very long range in order to account for the deformability of the structure which they build up. It is scarcely to be expected that the rigidity of such a structure would increase with temperature, but the static rigidity of a bentonite gel has in fact been found to increase in this way. This has been shown by the same method as for gelatine. The gel was allowed to re-set for an hour after being poured into the cylindrical vessel and stress was then applied for seven hours before the temperature was altered. As this gel does not break down at a low temperature like gelatine gels, it was found possible to alternate the temperature between 10 and 40° C with half-hour intervals at each temperature. The deformation of the gel started to decrease as soon as the temperature was raised and to increase when it was lowered. For a gel containing 3 g/100 cm^3 of bentonite with 0·08 g/100 cm^3 of sodium chromate, the temperature coefficient of the rigidity was found to be 0·0014 ± 0·0006 per °C at 25° C, a value considerably lower than that for gelatine but still of the same order as the theoretical value of 0·0034 per °C for a long-chain network.

The simplest interpretation of this observation is that the particles in a bentonite gel link up into loose chains which are coiled as a result of thermal bombardment, the structure being thus mechanically similar to that existing in gels of long-chain molecules. The high deformability of the structure is also explained by this hypothesis, without recourse to the assumption of long-range forces. Similar observations of the effect of temperature on rigidity could not be made on dilute gels of gum tragacanth because of the low yield stress, but observations were made on the four remaining gels. The rice starch gel was investigated in just the same way as the gelatine gel, and it was also found to show a positive temperature coefficient. A peculiar effect was exhibited, however, by the gels of agar, benzopurpurine and sodium stearate. In these cases, when the temperature was lowered the deformation of the gel proceeded to increase for about two minutes after which it started to decrease, and the opposite effects occurred when the temperature was raised.

The results on agar, benzopurpurine and sodium stearate suggest that change in temperature produces a slow change in the structure of the gel. In all cases investigated, however, the immediate effect of an increase in temperature is an increase in rigidity. It is therefore reasonable to suppose that in every case the gel structure consists of a network of chains and that the rigidity arises principally from the decrease in configurational entropy which occurs when the chains are uncoiled.

EXPLANATION OF DYNAMIC BEHAVIOUR

The dynamic behaviour of the gels can now be considered in the light of the kinetic theory suggested in the previous section. Retardation effects are seen to arise as a result of the transient resistance encountered by the chains as they uncoil under the influence of stress. A theory of the dielectric loss of solid long-chain polymers has been developed by Kirkwood and Fuoss[11] on the assumption that a moving chain element encounters a resistance in a direction at right angles to its length proportional to its velocity in that direction, and the theory has been adapted by Kirkwood[12] to account for elastic retardation effects in these materials. The assumption of proportionality between resistance and velocity appears to be rather crude in the original application of the theory to solid polymers. On the other hand, it would seem to be quite reasonable when applied to gels which only contain a few per cent of solid material so that the chains are largely surrounded by molecules of liquid. According to this theory, the material should possess a continuous spectrum of retardation times (τ) instead of the single retardation time ($\tau = \eta_0/G_0$) possessed by a material obeying equation (1). This spectrum may be represented by a normalized distribution function $F(\tau)$ such that $F(\tau)d\tau/G_0$ represents the fraction of the elastic compliance of the material which has retardation times between τ and $\tau + d\tau$, G_0 now standing for the static rigidity of the material. Kirkwood's theory gives the form of the distribution function as

$$F(\tau) = \frac{\tau_0}{(\tau_0 + \tau)^2} \tag{2}$$

where τ_0 is a constant.

Now if alternating stress were applied to a material obeying equation (1), the relation between strain and stress would be of the form

$$\sigma = \left[\frac{1}{G_0(1 + \omega^2\tau^2)} - \frac{i}{G_0}\frac{\omega\tau}{(1 + \omega^2\tau^2)}\right]S \tag{3}$$

when complex representation is used for the sinusoidally varying quantities σ and S. If, on the other hand, the elastic compliance has a spectrum of values, this relation has the modified form

$$\sigma = \left[\frac{1}{G_0}\int_0^\infty \frac{F(\tau)d\tau}{1 + \omega^2\tau^2} - \frac{i}{G_0}\int_0^\infty \frac{\omega\tau F(\tau)d\tau}{1 + \omega^2\tau^2}\right]S$$

$$= [J_1(\omega) + iJ_2(\omega)]S \tag{4}$$

where $J_1(\omega)$ and $J_2(\omega)$ are respectively the real and imaginary parts of the complex compliance at a frequency $\omega/2\pi$. Equation (4) can be re-written in the form

$$S = \left[\frac{J_1(\omega)}{J_1^2(\omega) + J_2^2(\omega)} - \frac{iJ_2(\omega)}{J_1^2(\omega) + J_2^2(\omega)}\right]\sigma \tag{5}$$

If the material obeyed equation (1), the term in the bracket would be simply $G_0 + i\eta_0\omega$, so in the general case the dynamic rigidity G and dynamic viscosity η are defined as

$$G = \frac{J_1(\omega)}{J_1^2(\omega) + J_2^2(\omega)}, \quad \eta = \frac{1}{\omega}\frac{-J_2(\omega)}{J_1^2(\omega) + J_2^2(\omega)} \tag{6}$$

For a material having a distribution of retardation times of the Kirkwood type, the following expressions for $J_1(\omega)$ and $J_2(\omega)$ are obtained by inserting the expression for $F(\tau)$

given by equation (2) in the integral expressions for $J_1(\omega)$ and $J_2(\omega)$ given by equation (4):

$$G_0 J_1(\omega) = \left(\frac{\pi}{2}\omega\tau_0 - 1\right)\left(1 - \frac{1}{\omega^2\tau_0^2}\right) - 2(\ln \omega\tau_0 - 1),$$

$$-\omega\tau_0 G_0 J_2(\omega) = 2\left(\frac{\pi}{2}\omega\tau_0 - 1\right) + (\omega^2\tau_0^2 - 1)(\ln \omega\tau_0 - 1) \qquad (7)$$

When these expressions for $J_1(\omega)$ and $J_2(\omega)$ are inserted in (6), it is found that G increases from the value G_0 without limit as ω increases. On the other hand η increases without limit as ω decreases, but approaches zero as ω becomes very great. The theory thus explains why the values of η obtained by low frequency measurements are often greatly in excess of the viscosity of the liquid phase, and also accounts quantitatively for the observed type of variation of G and η with frequency.

On this theory there are only two constants (G_0 and τ_0) defining the properties of the gel, both of which can be determined from a pair of observations of G and η at a single frequency $\omega/2\pi$. The calculation is most easily made by means of the theoretical graphs of G/G_0 and $G/\eta\omega$ plotted against $\omega\tau_0$, which are shown as the curves marked "2" in Figs. 3 and 4. Using the observed value of $G/\eta\omega$, the value

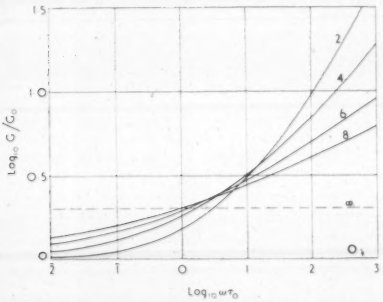

Fig. 3. Relationships between G/G_0 and $\omega\tau_0$ for materials having retardation-time spectra of the form given by equation (10). The values of β are marked against the curves

of $\omega\tau_0$ is read off from the second graph and the value of τ_0 is thus obtained. Then this value of τ_0 is used to obtain G/G_0 from the first graph, whence G_0 is obtained using the known value of G. Values of G_0 and τ_0 thus calculated from the low frequency data of Table 1 have been used to calculate values of G and η at 50 kc/s for comparison with Pryor's data in the fifth and sixth columns of Table 1. These figures, shown in the last two columns of the table, are of the same order of magnitude as the observations. Pryor does not claim more than 50% accuracy for his observations, so the agreement is nearly satisfactory when it is remembered that his observations were made at 50 000 times the frequency of the low-frequency observations.

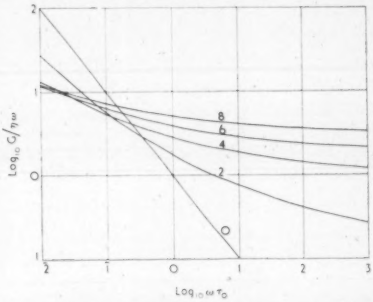

Fig. 4. Relationships between $G/\eta\omega$ and $\omega\tau_0$ for materials having retardation-time spectra of the form given by equation (10). The values of β are marked against the curves

For a material having the Kirkwood distribution of retardation times, the relation between shear strain and time under the application of constant stress from time $t = 0$ onwards is given by

$$\sigma = \frac{S}{G_0}\frac{\gamma t}{\tau_0}\exp(\gamma t/\tau_0)\left[-Ei\left(-\frac{\gamma t}{\tau_0}\right)\right] \qquad (8)$$

where $\gamma = 1{\cdot}781$ and the function $Ei(-x)$ has been tabulated by Jahnke and Emde.[13] When plotted, this expression gives a creep curve of the general type observed; that is to say the final period of slow creep is much more extended than with an exponential law.

FURTHER COMPARISON OF THEORY AND OBSERVATION

Another method of testing the validity of the Kirkwood distribution function consists in comparing the observed value of the static rigidity G_0 with the value calculated from a pair of observations of G and η made at a frequency $\omega/2\pi$ using the graphical method described above. This has been done for four gels and the results are shown in Table 2. It is difficult to make accurate observations on G_0 by subjecting the gels to constant stress because of the long duration of the final stage of the creep process, but reasonably good estimates have been made for the first three suspensions. In the case of agar, however, the creep was so prolonged that the final

Table 2. *Comparison of observed values of G_0 with values calculated from dynamic data assuming a Kirkwood distribution function*

Gel	*Concentration* (g/100 cm³)	ω (s^{-1})	τ_0 (*P*)	G (dyn/cm²)	*Calculated* G_0 (dyn/cm²)	*Observed* G_0 (dyn/cm²)
Gelatine	1·0	15·6	0·47	39	35	37
Benzopurpurine	1·0	2·8	0·35	1·44	0·87	0·49
Sodium stearate	0·33	21·3	1·0	74	62	24
Agar	0·25	13·3	1·0	29	21	(8·5)

value of the strain could only be determined by fitting a creep curve of the type given by equation (8) to the observations. The corresponding value of G_0 is therefore shown in brackets.

These figures show that the Kirkwood distribution function is not applicable in the last three cases, and further consideration shows that no other single-constant function could represent the behaviour of all four gels and the three considered previously. An empirical two-constant modification of the Kirkwood function has been constructed, however, which gives an adequate representation of all the observations. This has only been done to illustrate the diversity which must exist in the actual distribution functions, and no special significance should be attached to the exact form of function chosen. If u is written for $\ln(\tau/\tau_0)$, the Kirkwood distribution function (2) can be re-written as

$$F(\tau)d\tau = f(u)du = \tfrac{1}{4}\,\mathrm{sech}^2\,(u/2)\,du \qquad (9)$$

Thus when the logarithmic variable u (which varies from $-\infty$ to $+\infty$) is used, the distribution function $f(u)$ is symmetrical about the origin and the peak has a fixed width at half-value. A normalized function of the same form but of variable width is given by

$$f(u)du = \frac{1}{2\beta}\,\mathrm{sech}^2\,(u/\beta)du \qquad (10)$$

where β is a numerical parameter proportional to the peak width. It is to be noted that if $\beta = 0$ the material has a single retardation time τ_0 and obeys equation (1), while if $\beta = 2$ it has a Kirkwood distribution of retardation times. Distribution functions with various values of β are shown in Fig. 5. The function (10), which involves two constants

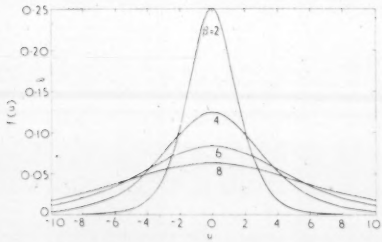

Fig. 5. Retardation-time spectra of the form given by equation (10)

β and τ_0 (the latter only appearing explicitly when $u = \ln(\tau/\tau_0)$ is substituted in the equation), is adopted for the present purposes. Computed values of G/G_0 and $G/\eta\omega$ are shown plotted against $\omega\tau_0$ in Figs. 3 and 4, the values of β being marked against the curves. With the help of these curves, the constants G_0, β and τ_0 for a particular gel can be calculated from an observation of G_0 and a pair of observations of G and η at a frequency $\omega/2\pi$. The observations shown in Table 2 thus give values of β for the gelatine, benzopurpurine and sodium stearate gels of 2, 3 and 7 respectively.

In the case of the agar gel, a method of trial and error has to be used to find the values of the constants G_0, β and τ_0 which give values of G and η close to the observed values and also a creep curve fitting that shown in Fig. 2. The creep curve corresponding to the distribution function (10) is very closely given by the approximation

$$\sigma = \frac{S}{G_0}\left[1 + \left(\frac{\gamma t}{\tau_0}\right)^{-2/\beta}\right]^{-1} \qquad (11)$$

for values of β greater than 4. It is found that reasonable agreement is only obtained with constants in the neighbourhood of $G_0 = 6{\cdot}4$ dyn/cm^2, $\beta = 7$, $\tau_0 = 18$ s. These give calculated values of $G = 34$ dyn/cm^2 and $\eta = 0{\cdot}91$ P at $\omega = 13{\cdot}3\ \mathrm{s}^{-1}$ as compared with the observed values $G = 29$ dyn/cm^2 and $\eta = 1{\cdot}0$ P. They also give the calculated creep curve shown by the broken line in Fig. 2. The agreement with the upper sections of the observed curve is too close for the two to be shown separately. The horizontal broken line at the top of the figure represents the calculated asymptotic value of the strain.

It is of interest to consider here the measurements made by Bungenberg de Jong and his collaborators[5] on gels of purified gelatin. Observations were made on the time period and decrement of the rotational oscillations performed by gels contained in glass spheres. The motion was produced by rotating the sphere and then stopping it suddenly, and the subsequent oscillations of the gel were followed by observing the motion of small air bubbles. The theory of the oscillations was worked out only for certain simple cases, including that of a material obeying equation (1). It is to be noted, however, that the system used is covered by the theory of the oscillating float of arbitrary form given by the present authors,[3] since it can be regarded as the limiting case of a float of very small size in a vessel of spherical shape. For the oscillating float it has been shown that the dynamic rigidity G and viscosity η at the frequency of the oscillations $\omega/2\pi$ are given closely by

$$G = M(\alpha^2 + \omega^2),\ \eta = 2M\alpha \qquad (12)$$

provided the decrement of the oscillations is not very high. In these expressions, α is the exponential decay factor of the oscillations and M is a constant depending on the geometry of the float and vessel, the moment of inertia of the float and the density of the gel. In general, M has to be determined by measuring the exponential decay factor of the non-oscillatory motion obtained when a calibrating Newtonian liquid (of the same density as the gel and of known viscosity η') is used in the apparatus, this decay factor being equal to η'/M. In the case of the spherical vessel without float, however, no calibration is necessary as the decay factor with a Newtonian liquid is known to be[14] $20{\cdot}2\ \eta'/\rho R^2$, where ρ is the density of the liquid and R the radius of the vessel. The value of M is therefore $0{\cdot}049\,5\ \rho R^2$ where ρ is the density of the gel.

In Bungenberg de Jong's experiments different frequencies of oscillation were obtained by the use of spheres of different sizes, and the results for a particular gel (containing $0{\cdot}7$ g/100 cm^3; six days after preparation) are shown by the points plotted in Fig. 6. The logarithmic decrement Λ (between successive swings in the same sense) which is plotted on the second graph, is equal to αT or $2\pi\alpha/\omega$. Since α was very small compared to ω in these experiments, equation (12) thus gives Λ as equal to $\pi\eta\omega/G$ and the time period T (shown on the first graph) as $2\pi\sqrt{(M/G)}$. If the gel obeyed equation (1), η and G would be constants; and as M is proportional to R^2, T would be proportional to R and hence Λ would be proportional to R^{-1}. It was noted, however, that the latter relation (shown by the broken curve on the second graph) is not in agreement with the observations.

On the other hand, the results can be fitted by assuming the gel to have a distribution of retardation times of the form (10) with a suitable value of β. The best choice of constants is found to be $G_0 = 42$ dyn/cm^2, $\beta = 3$, $\tau_0 = 0{\cdot}000\,29$ s. With these values, the relations between T and R and between Λ and R have been calculated, using the graphs of Figs. 3 and 4, and are shown by the full lines in Fig. 6.

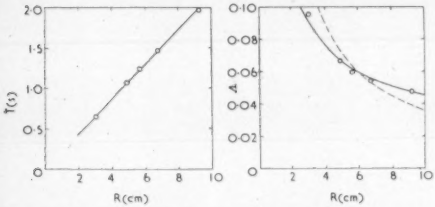

Fig. 6. Measurements of time period of oscillation T and logarithmic decrement Λ of a gelatin gel in spheres of radius R (Ref. 5), with calculated curves

DISCUSSION OF THE RETARDATION-TIME SPECTRUM

No special significance is to be attached to the exact values of the constants for the various gels given in Table 3. There is a certain amount of latitude in the choice of these constants because of the experimental error in the observations, so the best integral values of the spectrum width β have been adopted. Good agreement could have been obtained in some cases by using values of β differing by half a unit from these, with corresponding alterations in the mean retardation time τ_0 which in some cases would amount to changes by a factor as large as 5. Furthermore, it must be remembered that as the properties of aqueous gels depend critically upon the presence of electrolytes, widely varying values for the constants are to be expected when using gels made from different batches of commercial materials. The results for the first four gels in Table 3 are in accord with the Kirkwood distribution of retardation times which rests on a theoretical basis. In order to account for the results in other cases, however, it has been necessary to make an arbitrary modification of the Kirkwood distribution function, and the results of observation are not sufficiently extensive to give a real empirical justification for the form of the modified function. It may, nevertheless, be concluded that the spectrum of retardation times is considerably broader than the Kirkwood spectrum in these cases. It is perhaps significant that, in the investigations on change of rigidity with temperature, anomalous effects were found in the case of three gels (agar, benzopurpurine and sodium stearate) all of which have wide distributions of retardation times.

The spectrum corresponding to distribution functions of the adopted type (10) are very similar to those given by Wiechert's "log-normal" distribution function which has often been used to give an empirical representation of dielectric loss phenomena. This function has the form

$$F(\tau)d\tau = f(u)du = \frac{b}{\sqrt{\pi}} \exp(-b^2u^2)du \qquad (13)$$

where $u = \ln(\tau/\tau_0)$ as before and b is a constant. The log-normal distribution falls off more rapidly at large values of u, however, and consequently does not account for the extremely high values of G observed at high frequencies (Table 1).

Table 3. *Collected values for the constants of different gels*

Gel	*Concentration* (g/100 cm^3)	G_0 (dyn/cm^2)	β	τ_0 (s)
Gelatine	1·0	37	2	0·007 0
Bentonite with sodium chromate (0·08 g/100 cm^3)	3·0	7·5	2	0·018
Rice starch	2·0	2·1	2	0·12
Gum tragacanth	1·0	3·9	2	0·19
Gelatin (measurements by Bungenburg de Jong)	0·7	42	3	0·000 29
Benzopurpurine	1·0	0·49	3	2·3
Sodium stearate	0·33	24	7	0·66
Agar	0·25	6·4	7	17·8

REFERENCES

(1) HASTEWELL, L. J., and RITSON, F. J. U. *J. Sci. Instrum.*, **29**, p. 20 (1952).

(2) BERGEN, J. T., and PATTERSON, W. *J. Appl. Phys.*, **24**, p. 712 (1953).

(3) HASTEWELL, L. J., and ROSCOE, R. *J. Sci. Instrum.*, **32**, p. 96 (1955).

(4) MCDOWELL, C. M., and USHER, F. L. *Proc. Roy. Soc., A*, **131**, p. 409 (1931).

(5) BUNGENBERG DE JONG, H. G., VAN DEN BERG, H. J., and VERHAGEN, H. J. *Proc. K. Ned. Akad. Wet., B*, **55**, p. 1 (1952).

(6) PRYOR, A. W. *Ph.D. Thesis* (University of Durham, 1953).

(7) MCSKIMIN, H. J. *J. Acoust. Soc. Amer.*, **24**, p. 355 (1952).

(8) FERRY, J. D. *Advances in Protein Chemistry*, Vol. 4, p. 1 (New York: Academic Press Inc., 1948).

(9) FERRY, J. D. *J. Amer. Chem. Soc.*, **70**, p. 2244 (1948).

(10) GRAY, V. R. *Nature [London]*, **164**, p. 584 (1949).

(11) KIRKWOOD, J., and FUOSS, R. *J. Chem. Phys.*, **9**, p. 329 (1941).

(12) KIRKWOOD, J. *J. Chem. Phys.*, **14**, p. 51 (1946).

(13) JAHNKE, E., and EMDE, F. *Tables of Functions*, 4th ed., p. 6 (New York: Dover Publications, 1945).

(14) LAMB, H. *Hydrodynamics*, 6th ed., p. 637 (Cambridge: University Press, 1932).

Viscosity and action

By T. V. STARKEY, B.Sc., Ph.D., F.Inst.P., The Technical College of Monmouthshire, Crumlin, Mon.

[*Paper received* 27 *August*, 1956]

Hamilton's principle is used to show that for the laminar flow of a given volume of liquid through a tube the product of the energy dissipated and the time is a minimum. This condition requires a parabolic velocity distribution in laminar flow through tubes. It is also shown that the non-turbulent flow of a fluid showing shear dependence is not laminar, and that it resembles in many fundamental respects the turbulent flow of a Newtonian liquid. These results follow from the recognition of apparent viscosity as a direct measure of the action per unit volume associated with a given change in the configuration of the elements of which the fluid may be imagined to consist.

1. INTRODUCTION

It was observed in a previous paper[1] that the dimensions of viscosity are the same as those of action per unit volume, and it was shown there that, by assuming simple proportionality between the apparent viscosity and the action per unit volume of a suspension flowing non-turbulently through a given tube, relations between specific viscosity and the dimensions and concentration of the suspended particles, similar to those obtained by Einstein and others, could be easily derived.

In the present paper the results of a more detailed study of the relation between viscosity and action are set out, and the conclusions reached are made the basis of a theoretical investigation into the conditions governing the nature of the flow of Newtonian liquids in tubes. The significance to be attached to measurements of the apparent viscosity of non-Newtonian liquids is also considered in the light of these same conclusions.

2. APPLICATION OF HAMILTON'S PRINCIPLE

The recognition of viscosity as a measure under given flow conditions of the action per unit volume associated with changes in the relative positions of the component parts of a liquid during shear suggests the applicability of Hamilton's principle to problems of viscous flow. It is, therefore, proposed initially to derive an expression of this principle in a form suitable for use in a study of the streamline flow of a Newtonian liquid through a tube.

Hamilton's principle relates to the action involved in a change in the configuration of a system of particles and states that of all possible paths those followed are such that the change is effected with least (or greatest) action. Jeans[2] has considered the general application of this principle (including its application to non-conservative systems) and states it mathematically in the following form:

$$\int_0^{\gamma} [\delta T - (\delta W)]dt = 0 \qquad (1)$$

where $-(\delta W)$ is the work done in moving the system from the configuration defined by co-ordinates θ_1, θ_2, etc., to that represented by $\theta_1 + \delta\theta_1$, $\theta_2 + \delta\theta_2$, etc., δT being the corresponding gain in the kinetic energy of the system and γ the time occupied by the complete change in its configuration.

The configuration change contemplated in the present problem is that resulting from the motions of the particles of which the liquid may be imagined to consist during the flow of a given volume of liquid through the tube. For the sake of simplicity it will be assumed that the velocities of all of these particles remain constant during the change and that the term δT in equation (1) can, therefore, be neglected. This simplification is similar to that resulting from the neglect of the kinetic energy correction to Poisseuille's law. Under these conditions Hamilton's principle can be stated thus:

$$\int_0^{\gamma} (\delta W)dt = 0 \qquad (2)$$

In the present problem the work δW done in any given elementary change in the configuration is constant. Equation (2) can, therefore, be rewritten in the form

$$(\delta W)\int_0^{\gamma} dt = \gamma(\delta W) = 0$$

or, since the time occupied by a given change in the configuration is constant,

$$\delta(W\gamma) = 0 \qquad (3)$$

In its present application, Hamilton's least action requirement is, therefore, satisfied if the product of the total work done and the total time occupied in effecting the flow of a given volume of the liquid through the tube is a minimum.

3. STREAMLINE FLOW AND LEAST ACTION

Rayleigh[3] has shown for a Newtonian liquid under laminar shear between a pair of coaxial cylinders of which one rotates, that of all distributions of angular velocity satisfying the boundary condition the actual distribution gives the least dissipation of energy. Since the time of shear is the same for all coaxial cylindrical elements of which the liquid can be imagined to consist, this is equivalent to the statement that Hamilton's principle holds in this case.

It is now proposed to show for the laminar flow of a Newtonian fluid through a tube, that of all distributions of linear velocity satisfying the boundary condition a parabolic distribution alone satisfies the requirement of least action. Such a distribution is, of course, known to occur under the conditions visualized.

Thus, let v denote the velocity of the liquid at a distance r from the axis of the tube, and, let

$$v = a + br + cr^2 + \text{etc.} \qquad (4)$$

where a, b, c, etc., are constant coefficients.

For no slip to occur at the wall of the tube $v = 0$ when $r = R$, R being the internal radius of the tube.

Therefore $\quad a = -(bR + cR^2 + \text{etc.})$

Also, from the symmetry of the system, $dv/dr = 0$ when $r = 0$.

Therefore $\quad b = 0$

Equation (4), therefore, reduces to

$$v = c(r^2 - R^2) + d(r^3 - R^3) + \text{etc.} \quad (5)$$

Applying Hamilton's principle in the form derived in Section 2

$$W\gamma = 2\pi P\gamma^2 \int_0^R [cr(r^2 - R^2) + dr(r^3 - R^3) + \text{etc.}]dr$$

where P is the pressure difference between the ends of the tube.

i.e. $$W\gamma = -2\pi P\gamma^2[(cR^4/4) + (3dR^5/10) + \text{etc.}] \quad (6)$$

But $W\gamma$ must be positive and finite for all positive and finite values of P, γ and R consistent with the conditions assumed. Therefore, the series on the right-hand side of equation (6) must be finite and the coefficients c, d, etc., must be negative or zero. The least positive value of $W\gamma$, therefore, occurs when $d = e = \text{etc.} = 0$.

The velocity distribution for least action is, therefore, given by:

$$v = c(r^2 - R^2) \quad (7)$$

But when $r = 0$, $v = v_m$ where v_m is the maximum value of v.

Therefore $$c = -v_m/R^2$$

The distribution is, therefore, given by:

$$v = v_m(1 - r^2/R^2) \quad (8)$$

It is important to note that in deriving this result the fluid has been assumed to be Newtonian and, therefore, homogeneous in the sense that δW in equation (2) has been assumed to be constant. In deriving equation (6) it has further been assumed that the flow is laminar, this term being used here to imply that the viscous forces responsible for the dissipation of energy are everywhere parallel to the tube axis.

4. THE COEFFICIENT OF APPARENT VISCOSITY

In Section 3 of a previous paper[1] it was assumed that the coefficient of viscosity, whether real or apparent, is a direct measure of the action per unit volume within a fluid flowing under given conditions through a given tube. It is proposed now to examine this assumption in detail and with reference in the first instance to the laminar flow of Newtonian liquids but later of non-Newtonian fluids also.

Using the same notation as in previous sections and denoting the total energy dissipated per second by W_1,

$$W_1 = (\pi P^2/2\eta l) \int_0^R (R^2 - r^2)r\, dr$$

where l is the length of the tube and η the coefficient of viscosity of the liquid assumed here to be Newtonian. This equation follows from the use of the expression

$$v = P(R^2 - r^2)/4\eta l$$

for the velocity at a distance r from the tube axis. That is,

$$W_1 = \pi P^2 R^4/8\eta l \quad (9)$$

If V_1 denotes the volume of fluid emerging from the tube per second, then, since $V_1 = P\pi R^4/8\eta l$,

$$W_1 = PV_1 \quad (10)$$

from equation (9).

Therefore, $W\gamma = W_1\gamma^2 = PV_1\gamma^2$, and, since the volume emerging in γ seconds is $V_1\gamma$, the action, A, per unit volume of liquid emerging is given by:

$$A = P\gamma \quad (11)$$

From Poisseuille's law, therefore,

$$A = (8lV/\pi R^4)\eta \quad (12)$$

where V the volume of liquid emerging in γ seconds, defines the total change considered in the configuration of the system.

As suggested by equation (12) the absolute determination of η by a capillary viscometer involves basically the measurement of the action per unit volume when a given volume of liquid is passed through a given capillary tube. Again the relative viscosity of two Newtonian fluids is determined by passing equal volumes of the fluids in turn through the same capillary tube and measuring the actions per unit volume or factors proportional to them, in the two cases. The relative viscosity is simply the ratio of these actions or factors.

In determining the coefficient of apparent viscosity of a non-Newtonian fluid, equal volumes of it and a Newtonian fluid of known viscosity are passed in turn through the same capillary tube, and the ratio of the actions per unit volume determined as in the measurement of relative viscosity.

This method of measuring a coefficient of apparent viscosity, and, by implication, of defining that term, assumes that the ratio of the actions per unit volume of the two fluids is the same as the ratio of their intrinsic viscous properties as measured by their coefficients of viscosity, since V, l and R in equation (12) are all constant under the conditions of the experiment. Moreover, since Poisseuille's law has been used in the derivation of this equation, it further assumes that the flow is laminar in the non-Newtonian as well as in the Newtonian fluid, and in the sense in which this term is used in Section 3 of this paper. Let us consider these assumptions in greater detail, and let us take a suspensoid sol as an example of the non-Newtonian fluid.

During the passage of such a sol through a tube the suspended particles are known to rotate; the relative motions of elements of the fluid in which the particles are suspended cannot, therefore, be everywhere parallel to the axis of the tube. The flow, in consequence, cannot in this case be laminar. Furthermore, the introduction additionally of viscous forces in directions not parallel to the tube axis will increase the action per unit volume. The value of this under any given conditions is, therefore, a function of the flow pattern under those conditions as well as of such intrinsic viscous properties as the fluid possesses, and the value obtained for the apparent viscosity will depend on the precise form of this pattern.

The increase in the action per unit volume consequent upon the introduction of particles in suspension in a Newtonian fluid leads, therefore, to an increase in the measured value of the coefficient of viscosity, an increase which itself grows as the concentration of the particles is increased. The measured value of the viscosity of a suspension is, therefore, always greater than that of the suspension liquid alone and increases with increased concentration.

5. TURBULENT FLOW

The turbulent flow of a Newtonian liquid resembles in many fundamental respects the steady flow of a suspensoid sol. Thus, the flow is not laminar nor is the distribution of linear velocities parabolic in either case. Again, the apparent

viscosity of the turbulent liquid is greater than for the same liquid in laminar flow and increases with the degree of turbulence.

The irregularities normally observed in the pressure-rate of flow curves when turbulence first starts to develop are readily accounted for in terms of the spasmodic flow of vortices through the tube. The introduction of such vortices temporarily increases the action of the liquid by introducing additionally viscous forces not parallel to the tube axis and brings about a corresponding temporary reduction in dV_1/dP. In the same way dV_1/dP can be temporarily diminished by the introduction of particles in suspension in a laminarly flowing Newtonian liquid.

6. GENERAL OBSERVATIONS

The recognition of apparent viscosity as a direct measure of the total action per unit volume associated with a given change in the configuration of the elements of the liquid under given conditions, and of total action as the scalar sum of the component actions under the same conditions, allows an extremely simple approach to be adopted in the solution of otherwise extremely complicated hydrodynamic problems. The simplicity of this approach, which results largely from the substitution of scalar for vector mathematics, is illustrated in the derivation of Einstein's law in one of the papers already referred to.[1] The recognition additionally of the applicability of Hamilton's principle to such problems, as illustrated by the analysis used in a paper on the laminar flow of streams of suspended particles,[4] should yield solutions to a number of problems which hitherto have proved intractable.

REFERENCES

(1) Starkey, T. V. *Brit. J. Appl. Phys.*, **6**, p. 34 (1955).
(2) Jeans, J. H. *The Mathematical Theory of Electricity and Magnetism*, 5th ed., p. 492 (London: Cambridge University Press, 1951).
(3) Rayleigh, Lord. *Phil. Mag.*, **26**, p. 776 (1913).
(4) Starkey, T. V. *Brit. J. Appl. Phys.*, **7**, p. 52 (1956).

Vibrations of an end-loaded strip

By H. S. C. Chen, M.S., Ph.D., Johns Hopkins University, Baltimore, Maryland, U.S.A.

[*Paper first received* 12 *January, and in final form* 31 *May*, 1956]

The problem of an end-loaded strip, vibrating in a vertical plane, has been solved under the usual condition that the mass of the strip is neglected. The deflexion curve is derived first from statical considerations. Frequency is then calculated on the basis of energy relations. Agreement with experiments of Hearmon and Adams seems to be better than previous results.

The problem of an end-loaded strip vibrating in a vertical plane, as shown in the figure, has been worked by Balinkin,[1] Davies[2] and Hearmon.[3] Recently, Hearmon and Adams[4] gave a solution which is an improvement over the others. They assumed an expression for the deflexion curve involving two constants. Employing the Ritz modification of the Rayleigh method, they minimized the frequency, and obtained an expression for $\omega\sqrt{l/g}$, which gives good agreement with their experimental values. They also determined the shape of the deflexion curve from measurements on double-exposure photographs of the vibrating strip, and compared it with their equation. The agreement is fair, except that most of the experimental points in the middle region lie above the theoretical curve.

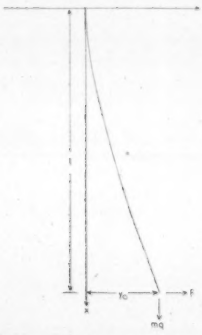

End-loaded strip vibrating in a vertical plane

It seems to the author that to a first approximation the shape of the deflexion curve may be calculated as a static problem. Instead of minimizing the frequency, one sets up the condition for statical equilibrium, and solves for the deflexion curve. Effect of strip mass and rotary inertia may be taken into account by using a corrected value of load mass, as in Hearmon and Adams's paper. An expression for frequency of the strip is then derived from the deflexion curve by energy considerations.

THE DEFLEXION CURVE

When the strip is displaced from the vertical position, a certain force is required, say F. Thus at any section of the strip, the bending moment consists of two terms, one due to the force F and the other due to the end-load mg, if we neglect the mass of the strip itself. The usual beam formula becomes

$$\frac{d^2y}{dx^2} = \frac{1}{EI}\left[F(l-x) - mg(y_0 - y)\right] \qquad (1)$$

Rewriting, we get

$$\frac{d^2y}{dx^2} - \frac{mg}{EI}y = \frac{1}{EI}\left[F(l-x) - mgy_0\right] \qquad (2)$$

This is a differential equation with constant coefficients; its solution is given by

$$y = A\exp(\beta x) + B\exp(-\beta x) + y_0 - \frac{F}{mg}(l-x) \qquad (3)$$

where $\beta = \sqrt{(mg/EI)}$. The constants A, B and F/mg are to be evaluated by imposing the boundary conditions,

$$y = 0,\ x = 0;\quad y = y_0,\ x = l;\quad y' = 0,\ x = 0 \qquad (4)$$

Performing the substitutions, one obtains

$$\left.\begin{aligned} A &= \frac{y_0 \exp(-\beta l)}{[\exp(\beta l) - \exp(-\beta l)] - \beta l[\exp(\beta l) + \exp(-\beta l)]} \\ B &= \frac{-y_0 \exp(\beta l)}{[\exp(\beta l) - \exp(-\beta l)] - \beta l[\exp(\beta l) + \exp(-\beta l)]} \\ F/mg &= \frac{-\beta y_0[\exp(\beta l) + \exp(-\beta l)]}{[\exp(\beta l) - \exp(-\beta l)] - \beta l[\exp(\beta l) + \exp(-\beta l)]} \end{aligned}\right\} \quad (5)$$

To see how equation (3) compares with equation (22) in the paper by Hearmon and Adams, numerical computations are made for the boxwood strip, for which their Fig. 4 is drawn. After one introduces $u = x/l$ and $v = y/y_0$, one obtains from equation (3), with the substitution of equation (5), and using the corrected mass of 3760 g,

$$v = -0{\cdot}000\,851 \exp(3{\cdot}15\,u) + 0{\cdot}4635 \exp(-3{\cdot}15\,u) + 1{\cdot}4627\,u - 0{\cdot}4627 \quad (6)$$

Whereas Hearmon and Adams gave

$$v = 1{\cdot}82\,u^2 - 0{\cdot}92\,u^3 + 0{\cdot}10\,u^4 \quad (7)$$

If one uses the uncorrected mass of 3733 g, one gets the following

$$v = -0{\cdot}000\,874 \exp(3{\cdot}139\,u) + 0{\cdot}4658 \exp(-3{\cdot}139\,u + 1{\cdot}4649\,u - 0{\cdot}4649 \quad (8)$$

Table 1 gives a comparison between experimental values[5] and theoretical values calculated from equations (6), (7) and (8).

Table 1. *Calculated and experimental values for the deflexion curve*

	Values of v		
Values of u	*H. and A.'s solution equation (7)*	*Experimental*	*Present solution equations (6) or (8)*
0·091	0·014	0·016	0·017
0·182	0·055	0·066	0·063
0·273	0·117	0·137	0·131
0·364	0·199	0·225	0·214
0·455	0·294	0·314	0·310
0·546	0·402	0·414	0·414
0·637	0·517	0·528	0·525
0·728	0·638	0·646	0·639
0·820	0·762	0·758	0·760
0·910	0·882	0·875	0·880

It is to be noticed that values calculated from equations (6) and (8) are equal, differing only in the fourth decimal. It means that no matter what value, uncorrected or corrected, of the load mass is used, the shape of the deflexion curve comes out to be the same. The second point to be noticed is that values so calculated are closer to the experimental values than those calculated from the equation of Hearmon and Adams.

Table 2. *Calculated and experimental values for frequency of vibration*

			Values of $\omega\sqrt{(l/g)}$		
m	M	*Observed*	*Equation (11) using M*	*Equation (11) using m*	*Hearmon and Adams*
873	896·2	1·57	1·564	1·575	1·57
2038	2062	1·32	1·313	1·316	1·32
3190	3217	1·23	1·232	1·233	1·24
4329	4357	1·19	1·190	1·190	1·20
5448	5477	1·17	1·164	1·165	1·17
5998	6029	1·16	1·155	1·155	1·16

FREQUENCY OF VIBRATION

Starting with equation (3), one next proceeds to calculate the elastic and the gravitational potential energies. The elastic potential energy is given by

$$V_1 = \frac{EI}{2}\int_0^l \left(\frac{d^2y}{dx^2}\right)^2 dx = \tfrac{1}{2}EI\beta^4[2ABl + \frac{1}{2\beta}(B^2 - A^2)] \quad (9)$$

The gravitational potential energy is given by

$$V_2 = \frac{mg}{2}\int_0^l \left(\frac{dy}{dx}\right)^2 dx = \frac{mg}{2}\left\{\left[\left(\frac{F}{mg}\right)^2 - 2AB\beta^2\right] - 2\frac{F}{mg}(A + B) + \frac{\beta}{2}(B^2 - A^2)\right\} \quad (10)$$

Equating the sum $V_1 + V_2$ to the maximum kinetic energy $\frac{m}{2}y_0^2\omega^2$ one arrives at the expression

$$\omega\sqrt{\left(\frac{l}{g}\right)} = \left\{\frac{\beta l[\exp(\beta l) + \exp(-\beta l)]}{\beta l[\exp(\beta l) + \exp(-\beta l)] - [\exp(\beta l) - \exp(-\beta l)]}\right\}^{\frac{1}{2}} \quad (11)$$

To test the validity of equation (11), computations are made for the case of the boxwood strip 95 cm long. Table 2 compares the values of $\omega\sqrt{(l/g)}$ from equation (11), using corrected and uncorrected values of mass with experimental values and the values of Hearmon and Adams.

As a matter of fact, for most of the cases in Table 2 βl is large enough so that $\exp(-\beta l)$ is negligible in comparison with $\exp(\beta l)$ and equation (11) reduces to

$$\omega\sqrt{(l/g)} = \left(\frac{\beta l}{\beta l - 1}\right)^{\frac{1}{2}} \quad (12)$$

Calculations from equation (12) give the values 1·69, 1·32, 1·23, 1·19, 1·17 and 1·16 respectively. All except the first agree with the experimental values.

It is reassuring to note that in the case of frequency there is a difference, depending on whether the uncorrected or the corrected value of the mass is used, as it should be. Of course, when the percentage difference between the two values of the mass gets small, the frequency difference becomes negligible. In fact, this is also the case with the deflexion curve. Here, where $m = 3733$ g and $M = 3760$ g, the difference is not noticeable. If one uses this method to determine the Young's modulus of the material, since the period can be measured easily to 0·1%, a good value of the Young's modulus should be possible.

ACKNOWLEDGEMENTS

This work was carried out while the author was on leave from the Drexel Institute, Philadelphia, during the tenure of a faculty fellowship awarded by the Fund for the Advancement of Education.

REFERENCES

(1) BALINKIN, I. A. *Phil. Mag.*, **21**, p. 283 (1936).
(2) DAVIES, R. M. *Phil. Mag.*, **22**, p. 892 (1936); **23**, pp. 464, 563 (1937).
(3) HEARMON, R. F. S. *Elasticity of Wood and Plywood*, Special Rep. for Prod. Res., London, No. 7 (London: H.M. Stationery Office, 1948).
(4) HEARMON, R. F. S., and ADAMS, E. H. *Brit. J. Appl. Phys.*, **6**, p. 280 (1955).
(5) HEARMON, R. F. S. Private communication.

Correspondence

The application of the centripetal effect in air to the design of a pump

Second-order effects in the flow of fluids as predicted by Reiner[1] on theoretical grounds, and first demonstrated shortly after that by Weissenberg,[2] are now well known for very viscous and elastic liquids such as solutions of rubber, cellulose and starch and generally in concentrated colloidal and high polymer solutions with a more or less complex structure. When such a liquid is sheared between a rotating plate and a fixed one parallel and coaxial with it, the liquid is drawn *inwards* against the action of the centrifugal forces, the whole arrangement forming a centripetal pump. This effect, which is one of several comprised under the designation "Weissenberg effects," has not previously been reported for low viscosity liquids, but we have recently observed[3] that the effect is also present in air. The object of this letter is to call attention to this effect and to describe briefly how it can be employed to make a centripetal pump.

The adjustment of the gap between stator and rotor is made by means of a micrometer screw M with a pitch of 0·5 mm. The scale E is graduated in hundredths of a millimetre, and each division is large enough to estimate sub-divisions; the zero pointer Z is adjustable. The screw is pressed against the pillar P by means of two additional springs, not shown in the figure. A grooveless thrust bearing reduces friction and abrasion.

If three orthogonal axes x, y, z are imagined as attached to bracket K, so that the x-axis is parallel to the rotor axis, then in order to have the rotor and stator in parallel planes their relative position must be adjustable around the y and x axes. This is achieved by means of the arrangement shown in the figure where the bracket K, and the sheet springs holder H are fixed on two perpendicular parts of the chassis C by screws. The screw holes are slightly wider than the screws which permit adjustment perpendicular to the screw axes, as required.

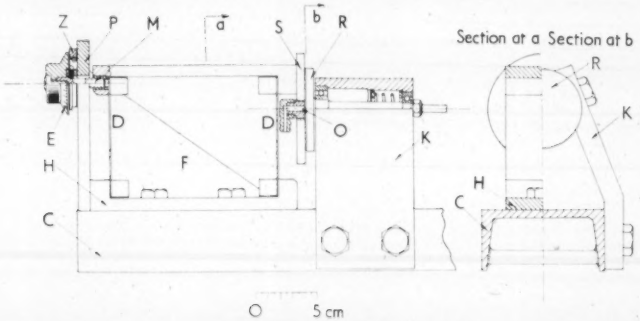

Design for a centripetal air pump

The plane rotor R revolves opposite a plane stator S, and the gap between them can be reduced from 0·75 mm to 0·015 mm with a tolerance of 0·002 mm. The rotor can be given speeds of up to 10 000 rev/min. It has two bearings; one is fixed while the other is pressed on by a spring. The distance between the bearings is large enough to reduce the influence of their radial inaccuracies on the position of the rotor plane to a negligible amount. The stator can be displaced axially. To keep it parallel while displacing it, two broad sheet springs D, D are employed which enable it to be moved free of backlash.

Let d be the deflexion of the springs, l their length, and r their radius of curvature; r will be smallest near their ends where

$$\frac{1}{r} = \frac{12d}{l^2}$$

The maximum deflexion in our machine is 0·5 mm and the total free length of each spring is 85 mm. Substituting in the above equation we get $r = 1200$ mm.

In order to avoid vibrations, especially in the axial direction, the bracket K is very rigid; and the lowest vibrating speed perpendicular to the shaft axis of the whole rotor assembly is 50 000 vibrations per minute; this is far enough from the highest speed of the rotor, which is less than 10 000 rev/min. In order to avoid vibrations of the pillar P, two triangular steel plates F are fastened to it. The stator has an opening O in its centre which can be connected by means of a nipple to rubber tubing leading to a manometer or a flowmeter.

When the rotor is given a speed of about 7000 rev/min and with the maximum gap, the manometer registers a suction of about 1 cm of water. When the gap is reduced to about 0·02 mm, this suction turns into a pressure which becomes more than half an atmosphere. It is proposed to use the machine to verify Maxwell's theory,[4] according to which air is an elastoviscous fluid with a time of relaxation of $1{\cdot}961 \times 10^{-10}$ s.

We acknowledge with thanks the help of Mr. Ayalon who built the apparatus. Its use as a pump is the subject of a

patent application, and the work has been sponsored in part by the U.S.A. Air Research and Development Command.

Israel Institute of Technology, Haifa.
B. POPPER
M. REINER

REFERENCES

(1) REINER, M. *Amer. J. Math.*, **67**, p. 350 (1945).
(2) WEISSENBERG, K. *Nature [London]*, **159**, p. 310 (1947).
(3) BLOTT, J. F. T., and REINER, M. (Awaiting publication.)
(4) MAXWELL, J. CLERK. *Phil. Mag.*, **35**, pp. 129, 185 (1868).

Corner fractures in explosively loaded thin-walled steel cylinders

Conical surfaces of fracture (corner fracture) are often generated near the corner formed by the intersection of two free surfaces of an impulsively loaded body. The fracture takes place as a result of a highly localized stress concentration that develops when a transient compressional wave enters the corner. Such fracture surfaces have been described by Poncelet[1,2] in his investigation on the comminution of brittle solids, by Kolsky and others[3,4] and Christie[5] in their investigation of fractures produced by transient waves in plastics and by Schardin[6] in his studies of fractures in thin glass plates. Evans[7] has reported the occurrence of such fractures in steel targets by firing contact explosive charges. The generation of such fracture surfaces in thick-walled metallic cylinders have been presented by Rinehart and Pearson[8] and by Starr and Savitt.[9] The occurrence of such fractures in different materials has been reviewed by Rinehart and Pearson.[10] The present note describes the generation of such fractures in a thin-walled cylinder. The direction of emission of the "hub" fragments is discussed. The scabbing of fragments is also described.

Cylinders were machined from solid round commercial steel bars and annealed. All cylinders were made 6 in. long, 1 to 2 in. internal diameter and $\frac{1}{4}$ to $1\frac{1}{2}$ in. wall thickness. They were each mounted in a vertical position with the base at a certain convenient height from the top face of an ice box. The ice box was fabricated from armour plates having slanting walls and with a massive circular block of steel at the centre. The outer surfaces of the cylinders were free from any restraint. Composition P.E. (plastic explosive) No. 2 was the explosive. The charge was boostered by a pellet of pressed tetryl and initiated by an A.S.A. (azide, styphnate and aluminium)/tetryl electric detonator. The lay-out of the equipment for firing is shown in Fig. 1. Almost all the fragments collected in the ice box showed conical surfaces of fracture and obviously these must have arisen from the base of the cylinder. It seems that each hub breaks into several fragments with the fractures extending radially through the hub. The surface of a hub fragment which was in contact with the detonating gases becomes more curved as the wall thickness of the cylinder decreases. Photographs of cross-sectional views of the hub fragments are reproduced in Fig. 2. The angle of fracture, α, cannot be measured accurately in the hub fragments arising from the cylinders of wall less than $\frac{1}{4}$ in. and is about 45 to 52°. For cylinders having wall thicknesses ranging from 1 to $1\frac{1}{2}$ in., it was often possible to put all the hub fragments together to make the complete hub. The percentage recovery of the hub fragments was sufficiently high in cylinders of wall thicknesses from $\frac{3}{8}$ to 1 in., but very poor in cylinders of $\frac{1}{4}$ in. wall, as these hub fragments further broke into tiny fragments. The angle of fracture, α, in copper and brass thin-walled ($\frac{3}{8}$ and $\frac{1}{2}$ in.) cylinders was about 60 to 66°.

In another set of experiments, the cylinders (6 in. long × 2 in. inner diameter × $\frac{1}{8}$ or $\frac{1}{4}$ in. wall thickness) were mounted in a vertical position with the base at a certain convenient height from a mild steel "witness-plate." On firing, the cylinder broke into fragments. Some of the fragments on

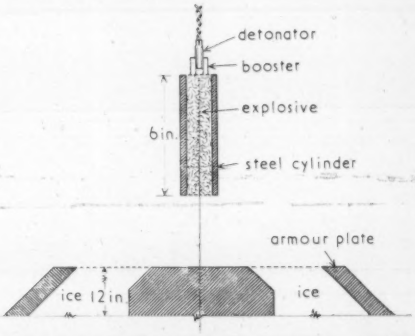

Fig. 1. Lay-out of the equipment before firing for collection of the hub fragments in an ice box

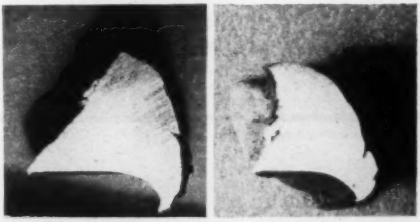

Fig. 2. Cross-sections of the hub fragments from thin-walled steel cylinders; (*a*) $\frac{1}{4}$ in. wall cylinder (× 2); (*b*) $\frac{1}{4}$ in. wall cylinder (×4)

striking a "witness-plate" produced a fragmentation pattern. A typical fragmentation pattern, which consists of a ring, is shown in Fig. 3. A simple analysis of its geometry indicates that each fragment is emitted along a line that makes an angle of 45° to the normal to the inner surface of the cylinder.

Corner fracturing plus subsequent expansion seems to be the plausible explanation for the end fragments that are emitted at 45° to the normal inner surface. It seems that the events that take place are as follows: (i) when detonation of the explosive reaches the end of the cylinder, a corner fracture is produced, (ii) the surface in contact with the detonating gases becomes curved, (iii) since the pressures resulting from the detonation gases are everywhere normal to the surface, it results in imparting the ring of material a forward component of velocity, (iv) each hub breaks into

several fragments with the fractures extending radially through the hub and (v) the hub fragments are then blown apart by the action of the detonating gases. If these hub fragments happen to strike a "witness-plate," these produce a fragmentation pattern (Fig. 3). The duration of all these events is quite short, however, lasting only a few microseconds.

It is felt that the ring of fragments emitted at 45° to the normal inner surface is certainly the same ring that Clark[11] observed in his studies of flash radiography of "ring type" charges, and corner fracturing plus subsequent expansion now seems a more logical explanation.

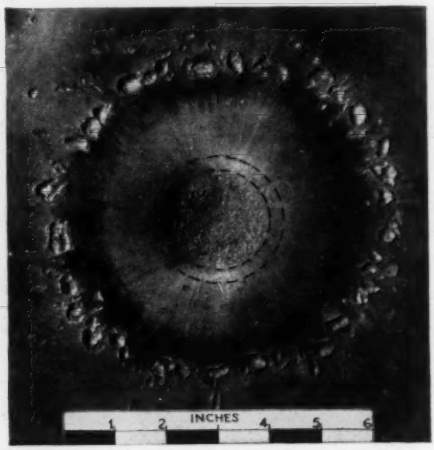

Fig. 3. Typical fragmentation pattern on a mild steel "witness-plate" on firing a cylinder (6 in. long, 2 in. internal diameter and $\frac{1}{4}$ in. wall) having its base at a height of 2 in. from the witness-plate. The dotted lines show the projected area of the steel cylinder normal to the witness-plate

In another set of experiments, the cylinders (6 in. long × 2 in. inner diameter × $\frac{1}{2}$ to 1 in. wall thickness) were fired and fragments recovered in wet sawdust bags. It seemed that the outer surfaces of the fragments, which had arisen from the initiating end of the cylinder, had scabbed. Fig. 4 shows a cross-sectional view of a fragment that had scabbed. The scabbing of fragments was not described by Mott,[12] and Pearson and Rinehart.[13]

The author is grateful to Prof. D. S. Kothari, Scientific Adviser to the Ministry of Defence, for his encouragement and interest throughout the course of this investigation. Thanks are due to Dr. John S. Rinehart, Astrophysical Observatory, Massachusetts, U.S.A., for stimulating correspondence on this subject.

Defence Science Laboratory,
Ministry of Defence,
New Delhi, India.

SAMPOORAN SINGH

Fig. 4. Photograph of cross-sectional view of a fragment that had scabbed (*AB* is the scabbed surface)

REFERENCES

(1) PONCELET, E. F. *Amer. Inst. Min. Met. Engrs.*, Tech. Pub. No. 1684 (1944).

(2) PONCELET, E. F. *La Fracture, Verres et Refractaires* (Paris: 1951).

(3) KOLSKY, H., and SHEARMAN, A. C. *Research*, **2**, p. 384 (1949).

(4) CHRISTIE, D. G., and KOLSKY, H. *Trans Soc. Glass Technology*, **36**, p. 65 (1952).

(5) CHRISTIE, D. G. *Trans Soc. Glass Technology*, **36**, p. 74 (1952).

(6) SCHARDIN, V. H. *Glastechnische Berichte*, **23**, pp. 1, 67, 325 (1950).

(7) EVANS, W. M. *Research*, **5**, p. 502 (1952).

(8) RINEHART, J. S., and PEARSON, J. *J. Appl. Phys.*, **23**, p. 685 (1952).

(9) STARR, L., and SAVITT, J. *Phys. Rev.*, **86**, p. 600 (1952).

(10) RINEHART, J. S., and PEARSON, J. *Behaviour of Metals under Impulsive Loads*, p. 131 (Cleveland: American Society for Metals, 1954).

(11) CLARK, J. C. *J. Appl. Phys.*, **20**, p. 363 (1949).

(12) MOTT, N. F. *Proc. Roy. Soc., A*, **189**, p. 300 (1947).

(13) PEARSON, J., and RINEHART, J. S. *J. Appl. Phys.*, **23**, p. 434 (1952).

New books

Ionized gases. By A. VON ENGEL. (Oxford: Clarendon Press, 1955.) Pp. x + 281. Price 42*s*.

This book is based on a course of undergraduate lectures which has clearly set the range and selection of topics from a subject which is now vast. Attention is accordingly concentrated on fundamental processes and concepts.

After a brief historical survey the subject is introduced by a chapter on conduction in feebly ionized gases describing the movement of charged particles under conditions of minimum interaction. Like every other chapter it calls the reader's attention to the numerical magnitudes involved, a worth-while and sometimes salutory feature.

Chapters 3 to 7 deal with production of charged particles, mobility, diffusion, recombination and ionization in an electric field. In these only the features which can be treated by elementary mathematics are given in any detail, but the results of wave mechanical or other more advanced analyses are fully described, often in illuminating terms. Comparison between theory and experiment and the shortcomings of both are emphasized. Chapters 8 and 9 deal with the glow and arc discharges respectively. Both these are essentially introductions, but the author seems less happy with the latter.

The book should be of real value to research workers because it is up to date, gives a carefully selected list of references and is thoroughly critical. It is profusely illustrated, and presents much valuable information in the form of curves and tables. The printing and format are up to the customary high standard of the Clarendon Press.

A. M. CASSIE

Temperature: its measurement and control in science and industry. Vol. 2. (London: Chapman and Hall Ltd.; New York: Reinhold Publishing Corp., 1956.) Pp. x + 467. Price 96*s*.

In 1941 the American Institute of Physics sponsored the publication of a book entitled *Temperature: its measurement and control in science and industry* which was based on the second symposium on temperature which had been held in New York two years earlier. This book became, and still remains, an indispensable reference work for all who are concerned with the measurement of temperature. The third symposium was held in Washington in 1954, and its proceedings have now been published as a second volume under the same title.

Volume 1 contained 126 papers and covered an extremely wide field; Volume 2 comprises 24 papers and the scope has been narrowed considerably. Indeed, the title is now somewhat misleading, since only one paper (*Temperature measurement in engineering* by H. J. Hoge) relates to industrial applications, while temperature control is not considered at all. Nevertheless, Volume 2 provides a valuable supplement to Volume 1.

About half the papers are concerned with standard scales of temperature and the techniques required for their realization, while the remainder are divided fairly evenly between techniques for special applications and purely theoretical papers on the concept of temperature and on transient phenomena.

While the United States are responsible for two-thirds of the papers, Europe and the United Kingdom are well represented, and the authors have been well chosen to provide an authoritative survey of the field. For example, the contributions concerned with very low temperatures come from Sir Francis Simon in this country, from R. B. Scott and R. P. Hudson of the National Bureau of Standards and William E. Keller of the University of California in the United States, and from H. van Dijk and D. de Klerk of the Kamerlingh Onnes Laboratory in the Netherlands.

Papers directly concerned with the International Temperature Scale are contributed by the national standardizing laboratories of Canada, Germany, the United Kingdom and the United States. Notable among these is the first published description of a new type of gas thermometer devised by Moser and Otto at the Physikalisch-Technische Bundesanstalt for measurements at high temperatures.

Among the more theoretical papers, Cecilia Payne-Gaposchkin's account of astrophysical temperatures provides some striking examples of the difficulties which arise with non-equilibrium conditions, while W. Lochte-Holtgreven describes the experimental techniques for producing extremely high temperatures (up to 50 000° K) in the electric arc.

J. AINGER HALL

A textbook of sound. 3rd Ed. (revised). By A. B. WOOD, O.B.E., D.Sc., F.Inst.P. (London: G. Bell and Sons Ltd., 1955.) Pp. xvi + 610. Price 42*s*.

This book was originally published in 1930, and a second and revised edition was published in 1941; it is the third edition containing further revisions which is the subject of this review. The choice of title and the author's preface indicates that the book is written primarily for university students, but in the newer sections extensive references are given to recent work, especially in applied acoustics.

The purpose of a textbook is to provide the student with a formal grounding in the fundamentals of the subject; to describe and analyse the principal methods and instruments of measurement; and perhaps to relate the fundamental studies to the technical needs of the day. This is the course followed by Dr. Wood, who deals in the first three sections with the theory of vibration, vibrating systems and sources of sound, and with the transmission of sound. As in most British books on sound, the theoretical treatment tends to be dominated by the majestic shadow of Rayleigh's *Theory of sound*, but the treatment of the third section is fresh and original and reflects Dr. Wood's own considerable researches on underwater acoustics.

It is in the last two sections, dealing with measurement and technical applications, that the difficulty of presenting an adequate account in one volume becomes apparent. Conventional modern methods of measurement are not clearly distinguished from methods having now only historical interest. A similar difficulty is apparent in the section concerned with technical applications, which gives quite inadequate consideration to many of the commonplaces of present-day applied acoustics, such as noise, ultrasonics, or the transmission of sound through partitions. A fuller treatment of these two latter sections is really necessary in order to reflect the great technical advances in acoustics during the last twenty-five years. However, the value of the book lies in the discussion of all the major acoustical topics within the scope of a single volume which remains a useful introduction to the student, or to the physicist or engineer beginning the study of sound.

A. T. PICKLES

Notes and comments

Nuclear Engineering

A new monthly periodical entitled *Nuclear Engineering* "has been designed to meet the requirements both of potential users of nuclear energy and of the manufacturers of plant and equipment." Judged by the first issues this new journal under the Editorship of Mr. E. N. Shaw promises to maintain the high standard of the firm's other periodicals.

Matters which will receive attention are: power supplies and economics; public health; nuclear fuel supply; nuclear reactor fuels; nuclear reactors; chemical processing; radiation shielding; supply and treatment of special materials; heat transfer; isotopes; nuclear engineering education and training; special techniques of nuclear engineering. Regular features will include: news of contracts; industry and trade; patents; new equipment and processes; lectures and courses; movements of personnel.

The annual subscription rate is 42*s.* including postage, and single copies are 3*s.* 6*d.* The publishers are The Temple Press, Bowling Green Lane, London, E.C.1.

Journal of Fluid Mechanics

A new periodical has been established to publish "theoretical and experimental investigations of all aspects of the mechanics of fluids and is to be in six parts per volume" under the title *Journal of Fluid Mechanics*. The first issue contains the following papers: The slender elliptic cone as a model for non-linear supersonic flow theory, by M. D. van Dyke; On the collision of drops in turbulent clouds, by P. G. Saffman and J. S. Turner; Drift, by M. J. Lighthill; On the thrust due to an air jet flowing from a wing placed in a wind tunnel, by L. C. Woods; Vibrational relaxation in oxygen and nitrogen, by V. Blackman; Long waves on a rotating earth in the presence of a semi-infinite boundary, by J. Crease; The laminar boundary layer on oscillating plates and cylinders, by M. B. Glauert; Diffraction of a weak shock with vortex generation, by Nicholas Rott.

The new journal, which is printed and published by Taylor and Francis Ltd., of Red Lion Court, Fleet Street, London, E.C.4, is edited by Dr. G. K. Batchelor of the Cavendish Laboratory, Cambridge.

The subscription price per volume is £5 10*s.* 0*d* ($16.50 in U.S.A., Canada).

Fourth general assembly and international congress of the International Union of Crystallography

The International Union of Crystallography has accepted the invitation of the National Research Council of Canada to hold its Fourth General Assembly and International Congress in Canada from the 10th July to the 17th July, 1957, followed by two Symposia on the 18th and 19th. At the Congress papers will be presented on all aspects of crystallographic research; the subjects of the Symposia will be "Physical techniques of crystallographic interest" and "Electron diffraction." The meetings are being held in Montreal.

Copies of a brochure giving details may be obtained from the Secretaries of the national committees of the member countries of the Union; from the General Secretary of the Union, Dr. D. W. Smits, Laboratorium voor Anorganische en Fysische Chemie, Bloemsingel 10, Groningen, The Netherlands; or from the Secretary of the Canadian Committee, Dr. W. H. Barnes, Division of Physics, National Research Council, Ottawa 2, Ontario, Canada (envelope to be clearly marked "Personal"); or from the Chairman of the Programme Committee, Dr. W. N. Lipscomb, School of Chemistry, University of Minnesota, Minneapolis, U.S.A.

Journal of Scientific Instruments

Contents of the December issue

SPECIAL ARTICLE

Some principles of measurement and control. By J. F. Coales.

ORIGINAL CONTRIBUTIONS

Papers

A new vacuum plate-camera of large capacity. By L. N. D. Lucas and P. B. Sewell.
An automatic analyser of uranium content in process streams. By H. Bisby, L. H. Brown and D. R. Chapman.
On the reduction of the dark current of photomultipliers. By Zs. Náray.
A Kösters-type interferometer. By C. F. Bruce.
A simple direction-sensitive phototransistor circuit for use in optical pulse-counting systems. By W. T. Bane and D. L. A. Barber.
A simple method for the measurement of high resistance values. By A. E. Hawkins.
Precision measurement of small radii of curvature. By R. N. Wilson.
An improved ionization gauge control circuit. By P. Hariharan and M. S. Bhalla.
A double-beam microspectrometer. By G. H. Haggis.
Temperature cycle controller. By J. C. Barnes.
Measurement of the optical density of smoke in a chimney. By A. Littlewood.
A mechanical Gardner mobilometer. By J. E. Roberts, A. J. Taylor and D. E. Woods.
The generation of accurate cylinders. By D. A. Davies.

Laboratory and workshop notes

The magnifying powers of optical instruments. By D. A. Richards.
The adaption of a metallurgical microscope to the "light profile" method. By H. Mykura.
A note on joining tungsten wire to other metals. By K. F. Chackett, P. Reasbeck and D. G. Tuck.
A reversible message register. By C. J. Sumner.
Quantitative application of the Foucault test to objective lenses. By P. Hariharan.
Device for measurement of tangents. By A. R. King.

NOTES AND NEWS

Correspondence

Fringe spacing in interference microscopes. From J. W. Gates.
Temperature and pressure measurement in an over-compression cloud chamber. From D. W. Hadley, J. C. Bower and J. Walker.

New instruments, materials and tools

Manufacturers' publications

Notes and comments

THIS JOURNAL is produced monthly by The Institute of Physics, in London.

It deals with all branches of applied physics (including theory and technique). All rights reserved. Responsibility for the statements contained herein attaches only to the writers.

EDITORIAL MATTER. Communications concerning editorial matter should be addressed to the Editor, The Institute of Physics, 47 Belgrave Square, London, S.W.1. (*Telephone*: Sloane 9806.) Prospective authors are invited to prepare their scripts in accordance with the *Notes on the preparation of contributions*. (Price 2*s.* 6*d.* including postage.)

REPRODUCTION. The Institute of Physics is a signatory to The Royal Society's Fair Copying Declaration. Details may be obtained upon application from The Royal Society, London, W.1.

ADVERTISEMENTS. Communications concerning advertisements should be addressed to the agents, Messrs. Walter Judd Ltd., 47 Gresham Street, London, E.C.2. (*Telephone*: Monarch 7644.)

CLAIMS FOR MISSING JOURNALS. Claims from regular subscribers to this *Journal* for missing numbers will only be considered if received within 60 days of the date of mailing plus normal outward time of transit and time for lodging the claim. Losses attributable to failure to notify a change of address or to similar omissions will not be considered.

SUBSCRIPTION RATES. A new volume commences each January. The charge is £4 per volume ($11.50 U.S.A.), including index (post paid), payable in advance. Single parts, so far as available, may be purchased at 8*s.* each ($1.15 U.S.A.), post paid, cash with order. Orders should be sent to The Institute of Physics, 47 Belgrave Square, London, S.W.1, or to any bookseller.

BLANK
PAGE